FUSE

Volume 16, December 2025

Fungal Systematics and Evolution

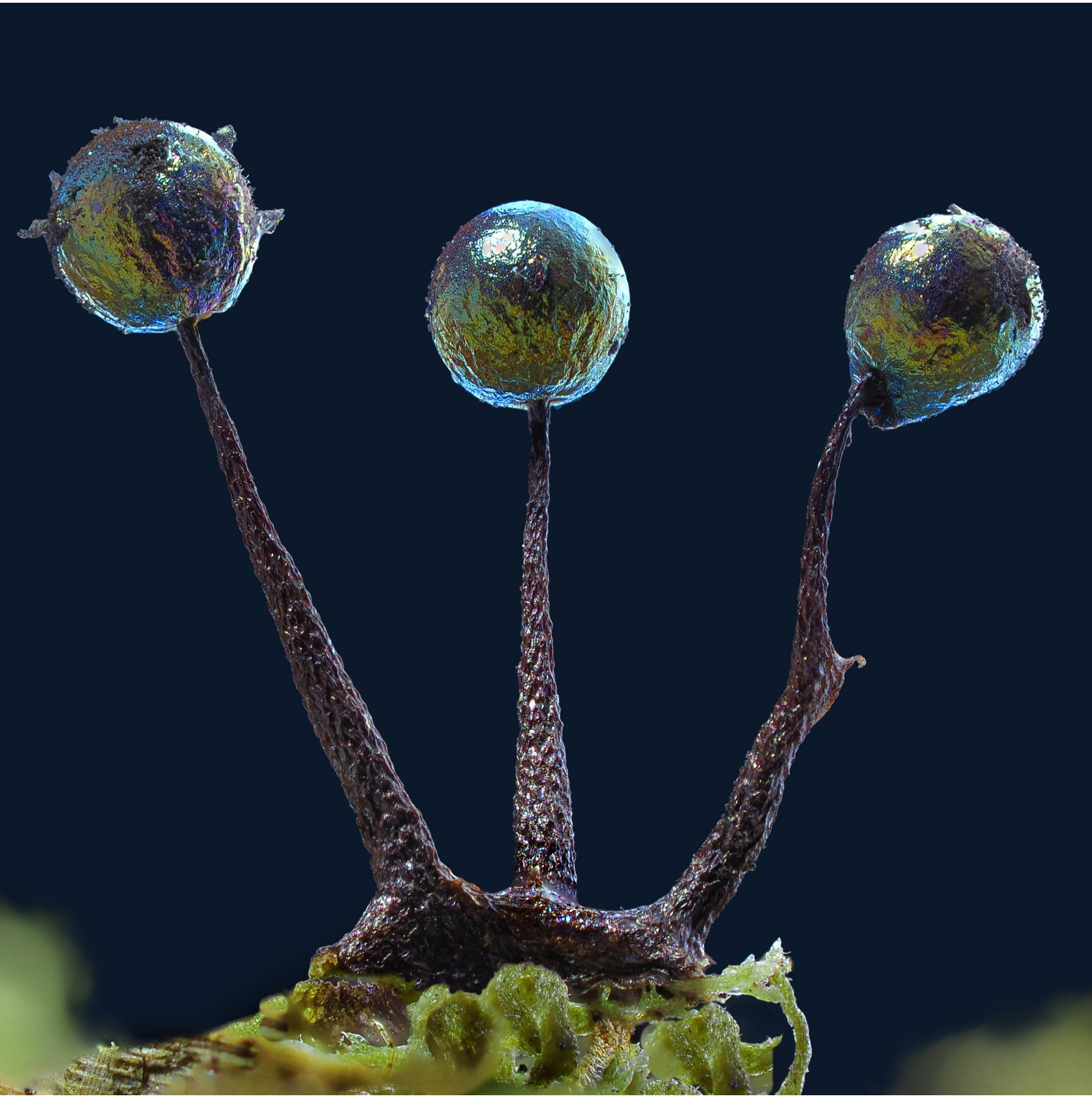

WESTERDIJK FUNGAL BIO DIVERSITY INSTITUTE

Cover: Sporocarps of *Lamproderma columbinum* (photo credit: Dmytro Leontyev).

EDITORIAL BOARD

Editor-in-Chief

Prof. dr P.W. Crous, Westerdijk Fungal Biodiversity Institute, Uppsalalaan 8, 3584 CT Utrecht, The Netherlands. E-mail: p.crous@wi.knaw.nl

Senior Editors

Prof. dr U. Braun, Martin-Luther-Universität, Institut für Biologie, Geobotanik und Botanischer Garten, Herbarium, Neuwerk 21, D-06099 Halle, Germany; e-mail: uwe.braun@botanik.uni-halle.de
Dr J.Z. Groenewald, Westerdijk Fungal Biodiversity Institute, Uppsalalaan 8, 3584 CT Utrecht, The Netherlands; e-mail: e.groenewald@wi.knaw.nl
Prof. dr M. Thines, Goethe University Frankfurt am Main, Faculty of Biosciences, Institute of Ecology, Evolution and Diversity, Max-von-Laue-Str. 9, D-60438 Frankfurt am Main, Germany; e-mail: Marco.Thines@senckenberg.de
Dr A.J.L. Phillips, Department of Botany, Faculty of Science, University of Lisbon, 1749-016 Lisbon, Portugal; e-mail: alan.jl.phillips@gmail.com

Layout Editor

K.F. Luijsterburg, Westerdijk Fungal Biodiversity Institute, Uppsalalaan 8, 3584 CT Utrecht, The Netherlands; e-mail: K.Luijsterburg@wi.knaw.nl

Graphic Design Editor

M. Vermaas, Westerdijk Fungal Biodiversity Institute, Uppsalalaan 8, 3584 CT Utrecht, The Netherlands; e-mail: m.vermaas@wi.knaw.nl

Associate Editors

Prof. dr A.M. Al-Sadi, Department of Crop Sciences, College of Agricultural and Marine Sciences, Sultan Qaboos University, P.O. Box 34, Al-Khod 123, Sultanate of Oman; e-mail: alsadiam@gmail.com
Prof. dr M. Arzanlou, Plant Protection Department, Agriculture Faculty, University of Tabriz, P.O. Box: 5166614766, Tabriz, Iran; e-mail: arzanlou@hotmail.com
Prof. dr T.I. Burgess, School of Biological Sciences and Biotechnology, Murdoch University, Perth, 6150, Australia; e-mail: tburgess@murdoch.edu.au
Prof. dr L. Cai, State Key Laboratory of Mycology, Institute of Microbiology, Chinese Academy of Sciences, No. 3 Park 1, Beichen West Road, Chaoyang District, Beijing, 100101, China; e-mail: cail@im.ac.cn
Prof. dr L. Carris, Associate Professor, Department of Plant Pathology, Washington State University, Pullman, WA 99164-6340, USA; e-mail: carris@mail.wsu.edu
Dr C. Decock, MUCL, Croix du Sud 2 bte L7.05.06, B-1348 Louvain-la-Neuve, Belgium; e-mail: cony.decock@uclouvain.be
Dr X.L. Fan, The Key Laboratory for Silviculture and Conservation of Ministry of Education, Beijing Forestry University, Beijing 100083, China; e-mail: xinleifan@bjfu.edu.cn
Dr D. Gramaje, Instituto de Ciencias de la Vid y del Vino (ICVV), Consejo Superior de Investigaciones Científicas - Universidad de la Rioja - Gobierno de La Rioja, Ctra. Mendavia-Logroño NA 134, Km. 90, 26071 Logroño, Spain; e-mail: david.gramaje@icvv.es
Dr V. Guarnaccia, Department of Agriculture, Forestry and Food Sciences (DiSAFA), University of Torino, via Paolo Braccini 2, 10095 Grugliasco, TO, Italy., Italy; e-mail: vladimiro.guarnaccia@unito.it
Dr J. Houbraken, Westerdijk Fungal Biodiversity Institute, Uppsalalaan 8, 3584 CT Utrecht, The Netherlands; e-mail: j.houbraken@wi.knaw.nl
Dr R. Jeewon, Department of Health Sciences, Faculty of Science, University of Mauritius, Reduit, Mauritius; e-mail: r.jeewon@uom.ac.mu
Dr F. Liu, State Key Laboratory of Mycology, Institute of Microbiology, Chinese Academy of Sciences, No. 3 Park 1, Beichen West Road, Chaoyang District, Beijing, 100101, China; liufang@im.ac.cn
Dr L. Mostert, Department of Plant Pathology, University of Stellenbosch, P. Bag X1, Matieland 7602, South Africa; e-mail: lmost@sun.ac.za
Prof. dr A.J.L. Phillips, University of Lisbon, Faculty of Sciences, Biosystems and Integrative Sciences Institute (BioISI), Campo Grande, 1749-016 Lisbon, Portugal; e-mail: alan.jl.phillips@gmail.com
Dr H.D.T. Nguyen, Agriculture and Agri-Food Canada, K.W. Neatby Building, 960 Carling Ave., Ottawa, ON, Canada, K1A 0C9; e-mail: Hai.Nguyen@agr.gc.ca
Dr M. Piątek, Department of Mycology, W. Szafer Institute of Botany, Polish Academy of Sciences, Lubicz 46, PL-31-512 Kraków, Poland; e-mail: m.piatek@botany.pl
Prof. dr H.-D. Shin, Division of Environmental Science and Ecological Engineering, Korea University, Seoul 02841, Korea; e-mail: hdshin@korea.ac.kr
Prof. dr B. Summerell, Royal Botanic Gardens and Domain Trust, Mrs. Macquaries Road, Sydney, NSW 2000, Australia; e-mail: Brett.Summerell@rbgsyd.nsw.gov.au
Dr J.B. Tanney, Pacific Forestry Centre, Canadian Forest Service, Natural Resources Canada, 506 Burnside Rd W, Victoria, BC V8Z 1MS, Canada; e-mail jtanney@lakeheadu.ca
Prof. dr P. Taylor, Faculty of Veterinary and Agricultural Sciences, University of Melbourne, VIC, 3010, Australia; e-mail: paulwjt@unimelb.edu.au
Dr A.D. van Diepeningen, Business Unit Biointeractions and Plant Health, Wageningen University and Research, Wageningen, the Netherlands; e-mail: anne.vandiepeningen@wur.nl
Prof. dr C.M. Visagie, Forestry and Agricultural Research Institute (FABI), University of Pretoria, Pretoria 0002, South Africa; e-mail: cobus.visagie@up.ac.za
Prof. dr M.J. Wingfield, Forestry and Agricultural Research Institute (FABI), University of Pretoria, Pretoria 0002, South Africa; e-mail: mike.wingfield@up.ac.za
Prof. dr R. Zare, Agricultural Research, Education and Extension Organization, Tehrãn, Iran; e-mail: simplicillium@yahoo.com

© 2025 Westerdijk Fungal Biodiversity Institute

SCOPE AND AIMS

SCOPE
All aspects of systematics and evolution of fungi.

AIMS
Fungal Systematics and Evolution is an international, peer-reviewed, open-access, full colour, fast-track journal. Papers will include reviews, research articles, methodology papers, taxonomic monographs, and the description of fungi. The journal strongly supports good practice policies, and requires voucher specimens to be deposited in a fungarium, cultures in long-term genetic resource collection, sequences in GenBank, alignments in TreeBASE, and taxonomic novelties in MycoBank.

ABOUT FUNGAL SYSTEMATICS AND EVOLUTION
Fungal Systematics and Evolution has an OPEN ACCESS publishing policy. All manuscripts will undergo peer review before acceptance, and will be published as quickly as possible following acceptance. There are no page charges or length restrictions, or fees for colour plates. The official journal language is English. All content submitted to Fungal Systematics and Evolution is checked for plagiarism.

Fungal Systematics and Evolution is licensed under a Creative Commons Attribution-NonCommercial-ShareAlike 4.0 International License.

PUBLISHED BY
Westerdijk Fungal Biodiversity Institute, Uppsalalaan 8, 3584 CT Utrecht, The Netherlands.



All articles are copyright of Westerdijk Fungal Biodiversity Institute.

FREQUENCY
Twice per year (June and December).

ISSN: 2589-3823
E-ISSN: 2589-3831

CONTENTS

Research papers

Larsson K-H, Spirin V, Ryvarden L, Larsson E. Reclassification of eleven corticioid basidiomycetes with nine typifications 1

Hussain S, Al-Kharousi M, Al-Maqbali D, Al-Owaisi AA, Velazhahan R, Al-Sadi AM, Al-Yahya'ei MN. Phylogeny of the genus *Volvariella* with the description of one new species and two new records from Oman 29

Van der Vyver LS, De Bruin W, Siyoum N, Nsibo DL, Groenewald JZ, Crous PW, Korsten L. Exploring *Neopestalotiopsis* diversity associated with Blueberry leaf and twig blight in South African nurseries 41

Nascimento SS, Ferro LO, Silva EA, Felipe MTC, Souza-Motta CM, Bezerra JDP. Introducing two new genera, *Paivomyces gen. nov*. and *Pseudoselenophoma gen. nov.*, in *Saccotheciaceae* (*Dothideales*) 55

Marincowitz S, Pham NQ, Wingfield BD, Wingfield MJ. Microfungi associated with dying quiver trees (*Aloidendron dichotomum*) in South Africa .. 71

Pham NQ, Marincowitz S, Crous PW, Wingfield MJ. Diversity of soil-borne *Gliocladiopsis* from Indonesia, Malaysia and Vietnam 81

Leontyev D, Ishchenko Y, Leontieva M, Yatsiuk I, Shchepin O, Song W-L, Chen SL, Moroz E, Schnittler M. Expanding *Lycogala*: twenty-four new species, their morphology and phylogenetic relationships 93

Bailey J, Miller ST, Castlebury LA. *Hemileia ritscheliae*, a new species of rust fungus on *Aristolochia* sp. collected from Uganda in 1943 147

Sá CEVA, Souza-Motta CM, Tiago PV, Machado AR. Diversity of fungicolous fungi associated with *Camarotella* spp. (*Phyllachorales*, *Sordariomycetes*) on *Cocos nucifera* in Brazil, including *Fusicolla parasitica sp. nov.* (*Nectriaceae*) 155

Manz C, Ortiz-Suárez A, Adamčíková K, Looney B, Noffsinger CR, Caboň M, Hampe F, Piepenbring M, Hofmann T, Buyck B, Parra-Aldana CA, Adamčík S, Corrales A. Recent taxonomic discoveries suggest a host-symbiont co-migration of *Russula* subsect. *Castanopsidum* with *Fagaceae* in the Americas 181

Singh G, Kumari P, Rajwar S, Yadav S, Mall S, Kumar S, Singh R. *Uwebraunomyces*, a novel genus of the family *Mycosphaerellaceae* 197

Möller EJ, Timdal E, Haugan R, Bendiksby M. Integrative taxonomy and genus delimitation in the *Rhizocarpaceae* (lichenized *Ascomycota*) 215

Kreth L-S, Groenewald JZ, Braun U, Götz M. Phylogeny and taxonomy of *Cercospora malkoffii* (*Mycosphaerellaceae*) 233

Lima-Santos SJ, Araújo JPM, Feitosa RM, Mendes-Pereira T, Elliot SL, Evans HC. There is gold in the graveyard: a new lineage of zombie-ant fungi in the genus *Ophiocordyceps* (*Ophiocordycipitaceae*: *Hypocreales*) from Minas Gerais, Brazil 243

Miller ST, Salgado-Salazar CS, Munck I, Castlebury LA. Two novel species of *Pestalotiopsis* on *Picea* and *Tsuga* from temperate forests in the United States 265

Guard FE, Dearnaley J, Lebel T. Purple Pinwheel and more: The *Marasmius haematocephalus* complex (*Marasmiaceae*) in Australia 283

Thorn RG, Consiglio G, Setti L, Kekki T, Daigneault BC, O'Neill EST. The sexual morph of *Hohenbuehelia* subreniformis (*Pleurotaceae*) discovered in Finland 307

© 2025 Westerdijk Fungal Biodiversity Institute

© 2025 Westerdijk Fungal Biodiversity Institute

FUSE

Fungal Systematics and Evolution

VOLUME 16
DECEMBER 2025
PAGES 1–27

doi.org/10.3114/fuse.2025.16.1

Reclassification of eleven corticioid basidiomycetes with nine typifications

K.-H. Larsson[1,2*], V. Spirin[3,4], L. Ryvarden[1], E. Larsson[2,4]

[1]Natural History Museum, University of Oslo, P.O. Box 1172, Blindern, 0318 Oslo, Norway
[2]Gothenburg Global Biodiversity Centre, P.O. Box 463, 40530 Göteborg, Sweden
[3]Botany Unit (Mycology), Finnish Museum of Natural History, P.O. Box 7 FI-00014 University of Helsinki, Finland
[4]University of Gothenburg, Dep. of Biological and Environmental Sciences, P.O. Box 463, 40530 Göteborg, Sweden

*Corresponding author: k.h.larsson@nhm.uio.no

Key words:
ITS
new taxa
phylogeny
taxonomy
typifications
28S

Abstract: Several species of wood-inhabiting resupinate basidiomycetes are reclassified following examination of type material and sequencing of recent collections. *Grandinia ocellata* is considered the correct name for *Phlebia livida* subsp. *tuberculata* and transferred to *Mycoacia*. *Peniophora avellanea* is an older name for *Phlebia margaritae* and the species moved into *Lopharia*. *Radulum pendulum* is identified as the oldest name for the species most commonly called *Phlebia albida*. *Grandinia tuberculata*, type species for *Stereophlebia*, is accepted as a synonym to *Radulum pendulum* and the combination *Stereophlebia pendula* introduced. *Phlebia canadensis* is accepted as an older name for *Quasiphlebia densa* and the combination *Quasiphlebia canadensis* proposed. Other new combinations proposed are *Cytidiella pallidolivens*, *Hydnophlebia flavicans*, *Hyphodermella pallidovirens*, *Meruliopsis rubicunda*, *Parvodontia gloeocystidiata*, *Phaeophlebiopsis roumeguerei*, and *Rhizochaete galactites*. *Hyphodermella albostraminea* is considered to be a synonym of *Hyphodermella pallidovirens*. *Ceriporia pseudocystidiata* is considered to be a synonym of *Meruliopsis rubicunda*. *Meruliopsis faginea* is considered to be a synonym of *Meruliopsis albostraminea*. Typifications are suggested for *Corticium seriale* subsp. *pallidolivens*, *Kneiffia avellanea*, *Corticium roumeguerei*, *Peniophora moelleriana*, *Grandinia ocellata*, *Corticium lividum*, *Thelephora viscosa* var. *uvida*, and *Radulum pendulum*.

Citation: Larsson K-H, Spirin V, Ryvarden L, Larsson E (2025). Reclassification of eleven corticioid basidiomycetes with nine typifications. *Fungal Systematics and Evolution* **16**: 1–27. doi: 10.3114/fuse.2025.16.1
Received: 24 November 2024; **Accepted:** 5 March 2025; **Effectively published online:** 28 March 2025
Corresponding editor: P.W. Crous

INTRODUCTION

Corticioid basidiomycetes develop morphologically simple, effused basidiomata that usually extend over a substrate, normally decaying wood, without defined borders (Fig. 1). Before fungal taxonomy got access to molecular methods, the classification of corticioid fungi into natural entities was considered challenging and most species were lumped into the admittedly artificial family *Corticiaceae* (Donk 1964). Radical changes followed from the molecular revolution and corticioid fungi have so far been distributed over more than 10 orders and many more families. This reorganization is very much an ongoing process, mainly driven by access to sequences from species not earlier examined. During the preparation of an identification handbook for European corticioid basidiomycetes (Larsson & Ryvarden 2021) several misplaced species were encountered and new combinations therefore deemed necessary. Most suggested transfers are based on evidence from both morphology and molecular data.

MATERIALS AND METHODS

Specimens were studied in a Zeiss Axioskop 2 equipped with phase contrast lenses. Preparations were placed in 2 % KOH, Melzer's solution, and Cotton Blue (0.3 %) in lactic acid (80 %). Measurements were made digitally with a Zeiss Er5c video camera and Zen Blue software (Zeiss Inc.). When possible, 20 basidiospores each from at least two specimens were measured. For spore measurements 5 % extreme values from both ends of variation are given in parentheses. If an extreme value consists of more than 5 % of the measurements, the parenthesis is omitted. The following abbreviations are used; L = mean length, W = mean width, Q = mean length / width ratio.

DNA was extracted from herbarium specimens using DNeasy plant mini kit (Qiagen, Hilden), following manufacturer's recommendations. The PCR amplifications were carried out using Ready-To-Go™ PCR beads (Amersham Pharmacia Biotech, Uppsala). Primers used to amplify the complete ITS region and the 5´end of the nuclear LSU region were ITS1F and ITS4B (Gardes & Bruns 1993), and LR0R and LR7 (Hopple & Vilgalys 1999), respectively. Amplified products were purified using Qiaquick spin columns (Qiagen, Hilden). Primers used for sequencing were ITS1, ITS4 (White *et al*. 1990), LR5, LR3R (Hopple & Vilgalys 1999), and CTB6 (Garbelotto *et al*. 1997). Sequencing was done by a commercial service provider (Macrogen Europe, Amsterdam), Sequences were assembled using Sequencher v. 5.2.4 (Gene Codes, Ann Arbor).

Through this study 43 ITS sequences and 28 LSU sequences are made public. For the phylogenetic analyses our new

Fungal Systematics and Evolution is licensed under a Creative Commons Attribution-NonCommercial-NoDerivatives 4.0 International License

© 2025 Westerdijk Fungal Biodiversity Institute



Fig. 1. A. *Hyphodermella pallidovirens* (Photo E. Martini). **B.** *Lopharia avellanea* (Photo V. Spirin). **C.** *Meruliopsis rubicundus* (Photo A. Singer). **D.** *Mycoacia ocellata* (Photo L. Zibarová). **E.** *Mycoacia livida* (Photo B.E. Andersen). **F.** *Phaeophlebiopsis roumeguerei* (Photo L. Goodwin). **G.** *Rhizochaete galactites* (Photo V. Spirin). **H.** *Stereophlebia pendula* (Photo M. Kulju).

© 2025 Westerdijk Fungal Biodiversity Institute

Table 1. Sequences from specimens used for morphological studies, phylogenetic analyses, and for typification. GenBank accession numbers in bold-face refer to sequences generated for this study. n/a means no sequence was available. Em-dash means that the gene was not used in any analyses.

Species	Voucher	ITS	LSU	Origin	Reference
Allophlebia ludoviciana	O:110341	MT974603	MT982120	Brazil	Lira *et al.* (2022)
	O:110340	MT974604	MT982121	Ecuador	Lira *et al.* (2022)
Bjerkandera adusta	CFMR:HHB-12826	KP134983	KP135198	USA	Floudas & Hibbett (2015)
Ceriporia pseudocystidiata	KUC:20131001-47	KJ668566	—	South Korea	Jang *et al.* (2015)
Ceriporia tarda	BJFC:Dai 10226	JX623945	—	China	Jia *et al.* (2014)
Ceriporia viridans	H:VS 3843	KX236480	—	Russia	Spirin *et al.* (2016)
	H:OM 11701	KX752600	—	Netherlands	Miettinen et al. (2016)
	H:VS 5909	KX236481	—	Finland	Spirin *et al.* (2016)
Ceriporiopsis fimbriata	BJFC:Dai 11672	KJ698633	KJ698637	China	Zhao *et al.* (2015)
Ceriporiopsis gilvescens	O: A Bernicchia	**OR822132**	**OR822132**	Italy	This study
Ceriporiopsis guidella	O:262837	FJ496687	FJ496722	Italy	Tomsovsky *et al.* (2010)
Ceriporiopsis lagerheimii	BJFC:Dai 12304	KX161647	KX161651	China	Zhao *et al.* (2017)
Cremeoderma unicum	GB:KHL 11786	EU118657	EU118657	Sweden	Larsson (2007)
Crustodontia chrysocreas	CFMR:HHB-6333	KP135358	KP135263	USA	Floudas & Hibbett (2015)
Dentocorticium portoricense	CFMR:HHB-19632	**OR822100**	**OR822100**	USA	This study
	CFMR:He 2161	MF626356	MF626380	USA	Liu *et al.* (2018)
	CFMR:He 2202	MF626357	MF626381	USA	Liu *et al.* (2018)
Dentocorticium sulphurellum	CFMR:FP-11801	JN165018	AF261539	USA	Justo & Hibbett (2011); Moncalvo *et al.* (2002)
	CFMR:T 609	JN165015	JN164815	Canada	Justo & Hibbett (2011); Moncalvo *et al.* (2002)
Dentocorticium taiwanianum	BJFC:He 4615	MF626362	MF626386	China	Liu *et al.* (2018)
	BJFC:He 3383	MF626361	MF626385	China	Liu *et al.* (2018)
	TNM:Wu 9907-1	MF626363	MF626387	China	Liu *et al.* (2018)
Dentocorticium ussuricum	BJFC:He 3278	MF626358	MF626382	China	Liu *et al.* (2018)
	BJFC:He 3322	MF626360	MF626384	China	Liu *et al.* (2018)
	BJFC:He 3294	MF626359	MF626383	China	Liu *et al.* (2018)
Donkia pulcherrima	O:Hausknecht & Kovac	KX752591	KX752591	Austria	Miettinen *et al.* (2016)
Geesterania carneola	SP:446234	KY175000	KY175000	Brazil	Westphalen *et al.* (2018)
Geesterania davidiae	SP:446193	KY174998	KY174998	Brazil	Westphalen *et al.* (2018)
Gelatinofungus brunneus	TNM:GC 1703-31	LC387339	LC387344	Taiwan	Chen *et al.* (2021)
Gelatoporia subvermispora	H:HK 20823	FN907911	FN907911	Russia	Miettinen & Larsson (2010)

© 2025 Westerdijk Fungal Biodiversity Institute

Table 1. (Continued)

Species	Voucher	ITS	LSU	Origin	Reference
Gloeoporus guerreroanus	ICN:139059	MG572754	—	Brazil	Jung *et al.* (2018)
Hapalopilus rutilans	JV 0206/2 (Vlasak herb.)	KX752623	KX752623	Sweden	Miettinen *et al.* (2016)
Hydnophanerochaete odontoidea	TNM:GC 1308-45	LC363486	LC363492	China	Chen *et al.* (2018)
Hydnophlebia alachuana	CFMR:FP-103881-Sp	KP135341	KP135201	USA	Floudas & Hibbett (2015)
Hydnophlebia aurantia	TNM:F33329	MZ636982	MZ637143	Taiwan	Chen *et al.* (2021)
	TNM:F33330	MZ636983	MZ637144	Taiwan	Chen *et al.* (2021)
Hydnophlebia canariensis	MA:MA-Fungi 86622	KF483012	KF528103	Canary Isl.	Telleria *et al.* (2017)
	MA:MA-Fungi 86623	KF483013	KF528104	Canary Isl.	Telleria *et al.* (2017)
Hydnophlebia chrysorhiza	CFMR:FD-282	KP135338	KP135217	USA	Floudas & Hibbett (2015)
Hydnophlebia crocata	TNM:F33298	MZ636985	MZ637146	China	Chen *et al.* (2021)
	TNM:F33297	MZ636984	MZ637145	China	Chen *et al.* (2021)
Hydnophlebia flavicans	GB:Moreno & Illana 12690	**OR822101**	**OR822101**	Spain	This study
Hydnophlebia gorgonea	MA:MA Fungi 86659	KF483049	KF528140	Cape Verde	Telleria *et al.* (2017)
	MA:MA Fungi 86658	KF483048	KF528139	Cape Verde	Telleria *et al.* (2017)
Hydnophlebia meloi	MA:MA Fungi 86654	KF483044	KF528135	Cape Verde	Telleria *et al.* (2017)
Hydnophlebia omnivora	CFMR:ME-497	KP135332	KP135218	USA	Floudas & Hibbett (2015)
	CFMR:KKN-112	KP135334	KP136216	USA	Floudas & Hibbett (2015)
Hydnophlebia sp.	BJFC:He 4003	MK860725	MK860738	China	Liu *et al.* (2020)
Hydnophlebia subchrysorhiza	BJFC:Cui 16185	MK860722	MK860739	China	Liu *et al.* (2020)
Hyhodermella corrugata	MA:MA-Fungi 61395	FN600380	JN939584	France	Telleria *et al.* (2010)
Hyphodermella pallidostraminea	LE:286968	OK138912	OK138911	Russia	Crous *et al.* (2021)
Hyphodermella pallidovirens	GB:KHL 15122	**OR822115**	**OR822115**	Norway	This study
	GB:EM 12656	**OR822116**	n/a	Switzerland	This study
	H:VS15797	**PQ066114**	n/a	Austria	This study
Hyphodermella rosae	CFMR:FP-150552	KP134978	KP135223	USA	Floudas & Hibbett (2015)
Hyphodermella sp.	GB:KHL 12623	**OR822117**	**OR822117**	Costa Rica	This study
Lopharia avellanea	GB:EL19-10	**OR822098**	**OR822098**	Spain	This study
	H:VS15422	**OR822099**	n/a	France	This study
Lopharia ayresii	GB:KHL 12549	**OR822097**	**OR822097**	Costa Rica	This study
	BJFC:He 20120724-4	MF626352	MF626375	China	Liu *et al.* (2018)
	BJFC:He 2778	MF626353	MF626376	China	Liu *et al.* (2018)

© 2025 Westerdijk Fungal Biodiversity Institute

Table 1. (Continued)

Species	Voucher	ITS	LSU	Origin	Reference
Lopharia cinerascens	CFMR:He 2188	MF626350	MF626373	USA	Liu *et al.* (2018)
	CFMR:He 2228	MF626351	MF626374	USA	Liu *et al.* (2018)
	CBS:485.62	MH858220	MH869821	USA	Vu *et al.* (2019)
	CBS:125884	MH864085	MH875543	New Zealand	Vu *et al.* (2019)
	PDD:95857	JQ694103	n/a	New Zealand	Unpublished
	?:A42	KC414245	n/a	n/a	Unpublished
	CFMR:FP-105043-sp	JN165019	JN165019	USA	Justo & Hibbett (2011)
	H:OM 16670.2	KY948709	n/a	USA	Justo *et al.* (2017)
	O:D276	**OR822096**	**OR822096**	Brazil	This study
Lopharia erubescens	URM:93246	MK993641	MK993636	Brazil	Xavier de Lima *et al.* (2020)
Lopharia mirabilis	BJFC:Dai 5147	MF626342	MF626365	China	Liu *et al.* (2018)
	BJFC:Dai 14978	MF626345	MF626368	China	Liu *et al.* (2018)
	BJFC:Yuan 2532	MF626343	MF626366	China	Liu *et al.* (2018)
	O:Parihar & Tiwari 121	**OR822095**	**OR822095**	India	This study
	BJFC:Dai 5598	MF626341	MF626364	China	Liu *et al.* (2018)
	BJFC:Dai13722	MF626346	MF626369	China	Liu *et al.* (2018)
	BJFC:He 4558	MF626344	MF626367	China	Liu *et al.* (2018)
Lopharia resupinata	BJFC:He 4401	n/a	MF626377	China	Liu *et al.* (2018)
Lopharia sinensis	BJFC:He 2510	MF626348	MF626371	China	Liu *et al.* (2018)
	BJFC:He 2428	MF626347	MF626370	China	Liu *et al.* (2018)
	BJFC:He 2424	MF626349	MF626372	China	Liu *et al.* (2018)
Luteochaete subglobosa	TNM:F30796	MZ636995	MZ637156	Taiwan	Chen *et al.* (2021)
Luteoporia albomarginata	BJFC:Dai 15229	KU598873	KU598879	China	Wu *et al.* (2016)
	BJFC:Dai 15240	KU598874	KU598879	China	Wu *et al.* (2016)
Luteoporia lutea	TNM:F28925	MZ636998	MZ637158	Taiwan	Chen *et al.* (2021)
Luteoporia straminea	SWFC:CLZhao 18947	MW732407	MW724799	China	Zhao *et al.* (2023)
Meruliopsis albomellea	BJFC:Dai 15205	KX494574	—	China	Yuan *et al.* (2017)
	BJFC:Dai 15223	KX494575	—	China	Yuan *et al.* (2017)
Meruliopsis albostraminea	GB:KHL 13798	**OR822130**	**OR822130**	France	This study
Meruliopsis crassitunicata	BJFC:Dai 10833	JX623935	—	n/a	Jia *et al.* (2014)
	TNM:CHWC 1506-46	LC427010	—	Taiwan	Chen *et al.* (2020)

© 2025 Westerdijk Fungal Biodiversity Institute

Table 1. (Continued)

Species	Voucher	ITS	LSU	Origin	Reference
Meruliopsis cystidiata	NYBG:776308	MG572749	—	Brazil	Jung *et al.* (2018)
Meruliopsis faginea	LE:F-334408	MW673659	—	Russia	Crous *et al.* (2021)
Meruliopsis hirtella	CFMR:FD-497	KP135054	—	USA	Floudas & Hibbett (2015)
	CFMR:DLL 2009-033	JQ673110	—	USA	Brazee *et al.* (2012)
	CFMR:HHB-4788	KP135053	—	USA	Floudas & Hibbett (2015)
Meruliopsis leptocystidiata	TNM:Wu 1708-15	LC427012	—	China	Chen *et al.* (2020)
	TNM:Wu 1708-43	LC427013	—	China	Chen *et al.* (2020)
Meruliopsis marginata	BJFC:Cui 6878	JX623943	—	China	Jia *et al.* (2014)
Meruliopsis nanlingensis	SWFC:CLZhao 6889	OM955801	—	China	Unpublished
	BJFC:Li 1568	JX623937	—	China	Jia *et al.* (2014)
	BJFC:Dai 8173	JX623942	—	China	Jia *et al.* (2014)
Meruliopsis parvispora	TNM:Wu 1209-58	LC427017	—	Taiwan	Chen *et al.* (2020)
	TNM:Wu 1207-3	LC427016	—	Taiwan	Chen *et al.* (2020)
	TNM:CHWC 1505-129	LC427015	—	Taiwan	Chen *et al.* (2020)
Meruliopsis pseudocystidiata	BJFC:Li 1704	JX623944	—	China	Jia *et al.* (2014)
	TNM:WEI 17-078	LC427019	—	Taiwan	Chen *et al.* (2020)
Meruliopsis rubicunda	GB:VS 4951	**OR822128**	—	Russia	This study
	SWFC:CLZhao 7682	OM955808	—	China	Unpublished
	GB:G Norstedt 081011	**OR822129**	—	Sweden	This study
Meruliopsis sp.	PERTH:8690804	MT537012	—	Australia	Unpublished
	PERTH:08944830	MT537109	—	Australia	Unpublished
	PERTH:8945039	MT537118	—	Australia	Unpublished
	CFMR:HHB-9594	KP135056	—	USA	Floudas & Hibbett (2015)
	CFMR:FD-278	KP135057	—	USA	Floudas & Hibbett (2015)
	CFMR:HHB-10729	KP135051	—	USA	Floudas & Hibbett (2015)
	CFMR:L-9778-sp	KP135052	—	USA	Floudas & Hibbett (2015)
	UC:2023018	KP814205	—	USA	Rosenthal *et al.* (2017)
Meruliopsis taxicola	GB:GB-0237349	EU118648	—	Sweden	Larsson (2007)
	DAOM:16560	MH856432	—	Canada	Vu *et al.* (2019)
	K(M):167914	MZ159419	—	England	Unpublished
Meruliopsis variegata	BJFC:Li 1780	JX623936	—	China	Jia *et al.* (2014)

© 2025 Westerdijk Fungal Biodiversity Institute

Table 1. (Continued)

Species	Voucher	ITS	LSU	Origin	Reference
Meruliopsis violacea	LE:247365	KF856503	—	Russia	Zmitrovich & Malysheva (2014)
Mycoacia livida	GB:KHL11705	**PQ636985**	—	Finland	This study
	GB:GB-0069572	HQ153414	—	Sweden	Ghobad-Nejhad & Hallenberg (2012)
Mycoacia ocellata	GB:KHL13967	**PQ066115**	n/a	Sweden	This study
	O:PM 354-11	**PQ636983**	**PQ636983**	Norway	This study
	O:PM 311-12	**PQ636984**	**PQ636984**	Norway	This study
	GB:VS 5285	**PQ636982**	—	Russia	This study
Mycoaciella bispora	GB:EL 13-99	**OR822104**	**OR822104**	Estonia	This study
Odoria alborubescens	BRNU:627479	JQ821319	JQ821318	Czech Rep.	Dvorak *et al.* (2014)
Oxychaete cervinogilva	H:Schigel 5216	KX752596	KX752596	Australia	Miettinen *et al.* (2016)
Phaeophlebiopsis caribbeana	CFMR:HHB-6990	KP135415	KP135243	USA	Floudas & Hibbett (2015)
Phaeophlebiopsis himalayensis	TNM:F29973	MZ637013	MZ637174	Taiwan	Chen *et al.* (2021)
Phaeophlebiopsis peniophoroides	CFMR:FP-150577	KP135417	KP135273	Hawaii	Floudas & Hibbett (2015)
Phaeophlebiopsis ravenelii	GB:GB-0161379	MZ637015	GQ470675	Canary Isl.	Chen *et al.* (2021); Wu *et al.* (2010)
Phaeophlebiopsis roumeguerei	GB:KHL 13759	**OR822122**	**OR822122**	France	This study
Phanerina mellea	H:OM 11393	KX752602	KX752602	Indonesia	Miettinen *et al.* (2016)
Phanerochaete alnea	GB:KHL 12054	**OR822121**	**OR822121**	Norway	This study
Phanerochaete arizonica	CFMR:RLG-10248	KP135170	KP135239	USA	Floudas & Hibbett (2015)
Phanerochaete australis	CFMR:HHB-7105	KP135081	KP135240	USA	Floudas & Hibbett (2015)
Phanerochaete burtii	CFMR:HHB-4618-Sp	KP135117	KP135241	USA	Floudas & Hibbett (2015)
Phanerochaete chrysosporium	CFMR:HHB-6251	KP135094	KP135246	USA	Floudas & Hibbett (2015)
Phanerochaete cumulodentata	GB:KHL 13765	**OR822119**	**OR822119**	France	This study
Phanerochaete laevis	GB:KHL 11839	**OR822118**	**OR822118**	Sweden	This study
Phanerochaete magnoliae	CFMR:HHB-9829	KP135089	KP135237	USA	Floudas & Hibbett (2015)
Phanerochaete sordida	LE:209918	KP994377	KP994383	Finland	Volobuev *et al.* (2015)
Phanerochaete velutina	GB:KHL 11926	**OR822120**	**OR822120**	Sweden	This study
Phlebia albida	GB:GB-0181539	AF141616	AF141616	Greenland	Parmasto & Hallenberg (2000)
Phlebia caspica	GB:EM 13525	**OR822134**	n/a	France	This study
Phlebia cf. bresadolae	CFMR:RLG-10795sp	KY948785	KY948857	USA	Justo *et al.* (2017)
Phlebia chrysocreas	not known	LN611115	LN611115	not known	Kuuskeri *et al.* (2015)
	not known	LN611114	LN611114	not known	Kuuskeri *et al.* (2015)

© 2025 Westerdijk Fungal Biodiversity Institute

Table 1. (Continued)

Species	Voucher	ITS	LSU	Origin	Reference
Phlebia formosana	TNM:F30406	MZ637033	MZ637237	Taiwan	Chen *et al.* (2021)
Phlebia margaritae	TUF:124409	KX826788	n/a	Italy	Saitta *et al.* (2017)
Phlebia sp.	TNM:F31277	MZ637038	MZ637241	Taiwan	Chen *et al.* (2021)
	CFMR:HHB-12357	MZ637065	MZ637264	USA	Chen *et al.* (2021)
	not known	LN611130	LN611130	Sweden	Kuuskeri *et al.* (2015)
Phlebia subochracea	GB:KGN 162-95	EU118656	EU118656	Sweden	Larsson (2007)
Phlebia uda	GB:KHL 13157	**OR822103**	**OR822103**	Estonia	This study
Phlebiodontia acanthocystis	CFMR:FP-150571	KY948767	KY948844	Hawaii	Justo *et al.* (2017)
Phlebiodontia fissurata	SWFC:CLZhao 2900	MW732402	MW724794	China	Zhao *et al.* (2023)
	GB:EM 13468	**OR822135**	n/a	Switzerland	This study
Phlebiodontia rajchenbergii	SP:MCW 636-18	OP265192	OP265190	Brazil	Motato-Vasquez *et al.* (2022)
Phlebiodontia sp.	O:LR 46383	**OR822136**	**OR822136**	Brazil	This study
Phlebiodontia subochracea	GB:RGC 160804A1	**OR822102**	**OR822102**	Sweden	This study
Phlebiopsis castanea	H:VS 5295	KX752610	KX752610	Russia	Miettinen *et al.* (2016)
Phlebiopsis crassa	CFMR:KKN-86	KP135394	KP135215	USA	Floudas & Hibbett (2015)
Phlebiopsis flavidoalba	CFMR:FD-263	KP135402	KP135271	USA	Floudas & Hibbett (2015)
Phlebiopsis gigantea	CFMR:FP-70857	KP135390	KP135272	USA	Floudas & Hibbett (2015)
Phlebiopsis sp.	CFMR:FP-102937	KP135391	KP135270	Puerto Rico	Floudas & Hibbett (2015)
Phlebiporia bubalina	BJFC:Dai 13168	KC782526	KC782528	China	Jia *et al.* (2014)
Pirex concentricus	OSC:41587-sp	KP134984	KP135275	USA	Floudas & Hibbett (2015)
Porostereum spadiceum	GB:KHL 13438	**OR822131**	**OR822131**	Germany	This study
Quasiphlebia densa	TNM:F14971	MZ637067	MZ637266	Taiwan	Chen *et al.* (2021)
	TNM:F31834	MZ637066	MZ637265	Taiwan	Chen *et al.* (2021)
Quasiphlebia canadensis	O:PM 343-11	**PQ013065**	**PQ013065**	Norway	This study
	GB:GB-0095231	**PQ013064**	**PQ013064**	Sweden	This study
Rhizochaete americana	CFMR:FP-102188	KP135409	KP135277	USA	Floudas & Hibbett (2015)
Rhizochaete belizensis	CFMR:FP-150712	KP135408	KP135280	Belize	Floudas & Hibbett (2015)
Rhizochaete borneensis	TNM:F31080	MZ637070	MZ637270	Taiwan	Chen *et al.* (2021)
Rhizochaete brunnea	BAFC:34528	AY219389	AY219389	Argentina	Greslebin *et al.* (2004)
Rhizochaete chinensis	TNM:Wu 0910-45	LC387335	MF110294	China	Chen *et al.* (2018); Wu *et al.* (2018)
Rhizochaete filamentosa	CFMR:HHB-3169	KP135410	KP135278	USA	Floudas & Hibbett (2015)

© 2025 Westerdijk Fungal Biodiversity Institute

Table 1. (Continued)

Species	Voucher	ITS	LSU	Origin	Reference
Rhizochaete flava	CFMR:PR-1141	KY273030	KY273033	Puerto Rico	Nakasone *et al.* (2017)
Rhizochaete fouquieriae	CFMR:KKN-121	AY219390	AV219390	USA	Greslebin *et al. (*2004)
Rhizochaete galactites	GB:Hjm 18924	**OR822124**	**OR822124**	Sweden	This study
	H:VS 11261	**OR822125**	n/a	Russia	This study
	H:VS 12070	**OR822126**	n/a	Russia	This study
Rhizochaete lutea	TNM:F21760	MZ637072	GQ470651	Taiwan	Chen *et al. (*2021); Wu *et al. (*2010)
Rhizochaete radicata	CFMR:FD-123	KP135407	KP135279	USA	Floudas & Hibbett (2015)
Rhizochaete sulphurina	GB:SPG 745	**OR822127**	**OR822127**	Spain	This study
Rhizochaete sulphurosa	URM:87190	KT003522	KT003519	Brazil	Chikowski *et al.* (2016)
Rhizochaete violascens	GB:GB-0161553	**OR822123**	**OR822123**	Sweden	This study
Riopa metamorphosa	H:VS 2395	KX752601	KX752601	Russia	Miettinen *et al. (*2016)
Scopuloides hydnoides	GB:KHL 11916	EU118665	EU118665	Sweden	Larsson (2007)
Scopuloides sp.	GB:KHL 12320	**OR822105**	**OR822105**	USA	This study
Stereophlebia pendula	GB:KHL 15159	**PQ013066**	**PQ013066**	Spain	This study
	GB:EL 29-11	**PQ013067**	**PQ013067**	Spain	This study
	H:6200339	**PQ013069**	n/a	Finland	This study
	H:6200089	**PQ013071**	n/a	Finland	This study
	H:7047608	**PQ013072**	n/a	USA	This study
	H:7068342	**PQ013070**	n/a	Russia	This study
	OULU:Kulju 78/21	**PQ013068**	n/a	Finland	This study
Terana caerulea	CFMR:FP-104073	KP134980	KP135276	USA	Floudas & Hibbett (2015)

© 2025 Westerdijk Fungal Biodiversity Institute

sequences were complemented by sequences downloaded from GenBank (Table 1). Four sequence datasets were compiled using the AliView editor (Larsson 2014). Sampling for the *Hydnophlebia* dataset was guided by the phylogenetic analyses in Chen *et al*. (2021) and Lira *et al*. (2022) and includes a subset of species from *Meruliaceae*. Two *Scopuloides* species were selected as outgroup. Sampling for the *Lopharia* dataset follows Liu *et al*. (2018) with *Gelatoporia subvermispora* added as outgroup (Justo *et al*. 2017). The *Phanerochaetaceae* dataset is modelled after Chen *et al*. (2021) and has *Bjerkandera adusta* and *Porostereum spadiceum* included as outgroup. The *Meruliopsis* ITS dataset has *Ceriporia viridans* as outgroup (Chen *et al*. 2020).

Sequences were aligned through MAFFT (Katoh & Standley 2013) as implemented on the EMBL-EBI server (Madeira *et al*. 2022) with default settings. Ambiguously aligned regions were removed using GBlocks v. 0.91b with relaxed settings (Talavera & Castresana 2007), available on the phylogeny.fr server (Dereeper *et al*. 2008).

The Maximum Likelihood (ML) analysis were conducted with IQ-TREE (Nguyen *et al*. 2015) using the online server at http://iqtree.cibiv.univie.ac.at/ (Trifinopoulos *et al*. 2016). ITS1, 5.8S, ITS2 and 28S were treated as separate partitions (Chernomor *et al*. 2016). The best-fitting substitution model was estimated automatically using ModelFinder implemented on the IQ-TREE server (Kalyaanamoorthy *et al*. 2017). Branch support was estimated through the SH-aLRT test (Guindon *et al*. 2010) and through ultrafast bootstrap (UB) (Hoang *et al*. 2018), both of which are available on the IQ-TREE server.

Bayesian Inference (BI) was calculated using MrBayes v. 3.2 (Ronquist *et al*. 2012) implemented on the CIPRES Science Gateway server v. 3.3 (Miller *et al*. 2010) and utilizing the BEAGLE library (Ayres *et al*. 2012). The same partitions as in the ML analyses were used. Substitution models were selected with MrModeltest2 (Nylander 2004). Analyses were run for 5 M generations, sampling trees every 1000th generation. Other program settings were the default ones.
The original and Gblocks-curated alignments for the phylogenetic trees are uploaded to Figshare (https://doi.org/10.6084/m9.figshare.28560074).

RESULTS

The aligned and end-trimmed *Hydnophlebia* dataset had 1720 nucleotide sites. After curation with GBlocks, 1495 sites remained for the analyses. MrModeltest suggested the K80 model for the ITS region and GTR+I+G for the LSU region. Maximum Likelihood and BI analyses produced essentially the same topology. Figure 2 shows the ML tree with branch support from SH-aLRT (≥ 80 %), UB (≥ 95 %), and BI pp values (≥ 0.95), respectively. The analyses recovered *Hydnophlebia* with strong support and the clade includes an *Odonticium flavicans* sequence in a sister taxon position to *Hydnophlebia alachuana*.

The aligned and end-trimmed *Phanerochaetaceae* dataset consisted of 2078 nucleotide sites. After curation with GBlocks, 1429 sites remained for the analyses. MrModeltest selected SYM+G for ITS1 and GTR + G for 5.8S, ITS2, and LSU. Maximum Likelihood and BI analyses produced essentially the same topology. Figure 3 shows the ML tree with branch support as indicated above. The *Hyphodermella* clade is strongly supported and includes three sequences of *Corticium pallidovirens* that are identical to the type sequence for *Hyphodermella pallidostraminea*. The *Quasiphlebia* clade is also strongly supported and includes three sequences from Norway and Sweden that are identified as *Phlebia canadensis*. These three sequences differ from the type of *Quasiphlebia densa* at two nucleotide positions in ITS2 and one position in LSU. The *Stereophlebia* clade received strong support and is recovered as a sister group to *Gelatinofungus brunneus*. The *Rhizochaete* clade is strongly supported by SH-aLRT but unsupported by UB and BI. The clade includes *Phanerochaete galactites* but its relation to other species remains unclear. The *Phaeophlebiopsis* clade is strongly supported and includes *Peniophora roumeguerei*.

The aligned and end-trimmed *Lopharia* dataset had 1482 nucleotide sites. After curation with GBlocks, 1370 sites remained. MrModeltest suggested SYM+G for ITS1, K80 for 5.8S, GTR+G for ITS2, and GTR+I+G for LSU. The ML and BI analyses produced essentially the same topology. Figure 4 shows the ML tree with branch support threshold values as indicated above. *Lopharia* was recovered as strongly supported by SH-aLRT and BI analyses and weakly supported by UB (87%). The clade included *Peniophora avellanea*, which occurred as a sister taxon to *Lopharia erubescens*.

The aligned and end-trimmed *Meruliopsis* ITS dataset consisted of 670 character sites. After curation with GBlocks, 479 sites remained for the analyses. MrModeltest selected HKY+G for ITS1, K80 for 5.8S, and GTR+G for ITS2. The ML and BI analyses produced essentially the same topology. Figure 5 shows the ML tree with branch support as indicated above. One sequence of *Meruliopsis albostraminea* proved to be identical to the type specimen of *Meruliopsis faginea*. They were recovered well separated from three American sequences of *Meruliopsis hirtella*. Three sequences of *Meruliopsis rubicunda* were found identical to the type of *Ceriporia pseudocystidiata*. The four formed a strongly supported sister clade relationship with *Meruliopsis* sp. from North America.

Taxonomy

Cytidiella pallidolivens (Bourdot & Galzin) K.H. Larss. & Ryvarden, ***comb. nov.*** MycoBank MB 857615. Fig. 6.
Basionym: *Corticium seriale* subsp. *pallidolivens* Bourdot & Galzin, *Bull. Soc. Mycol. Fr*. **27**: 254. 1911.
Synonyms: *Corticium pallidolivens* (Bourdot & Galzin) Bourdot & Galzin, *Hyménomyc. de France* (Sceaux): 222. 1928.
Phlebia pallidolivens (Bourdot & Galzin) Parmasto, *Eesti NSV Tead. Akad. Toim., Biol. seer* **16**: 391. 1967.

Typus: **France**, Aveyron, Millau, Le Causse Noir, on *Pinus sylvestris*, 23 Mar. 1907, *A. Galzin* (**lectotype** of *Corticium seriale* subsp. *pallidolivens*, designated here, PC Bourdot 5508, MBT 10024806; **isolectotype** GB, studied).

Additional material studied: **Spain**, Catalonia, Lerida, N. of Lles, on still attached *Pinus* branch, 18 Nov. 1986, *N. Hallenberg* 10123, GB-0181215.

© 2025 Westerdijk Fungal Biodiversity Institute

Description: *Basidiomata* resupinate, effused, closely adnate, at first orbicular, then confluent, soft ceraceous when fresh, firm after drying, membranous, hymenium smooth or with blunt warts, dirty yellow to brick-red, liver-coloured or even chestnut brown, margin paler than hymenium, byssoid to finely fimbriate, subiculum whitish. *Hyphal system* monomitic, hyphae with clamps, in the subiculum parallel, densely arranged, 2.5–6 µm wide, thin-walled to slightly thick-walled, sometimes somewhat gelatinized, in the subhymenium thin-walled, 2–3 µm, frequently branched and with a fine-grained incrustation. Crush preparations in Melzer receive golden yellow oil-drops, probably from dissolution of the incrustation seen in the subhymenium. *Basidia* narrowly clavate 25–40 × 4.5–6 µm, with four sterigmata and a basal clamp. *Basidiospores* narrowly elliptical to almost cylindrical, (6.2–)6.3–7.8(–8.2) × (2.8–)2.9–3.6(–3.7) µm, L = 7.0 µm, W = 3.2 µm, L/W = 2.2, adaxially sometimes slightly concave, some spores weakly sigmoid, thin-walled, smooth, without reaction in Melzer's or Cotton Blue.

Ecology and distribution: On decaying coniferous wood, especially *Pinus* sp. but also *Abies* sp. Frequently on dead but still attached branches. With certainty known from France and Spain. It is reported from pine wood in Austria, Russia, and Canada but we have not studied any specimens. Other reports (see gbif.org) seem to derive from angiosperm wood and are most likely not this species.

Notes: In an early attempt to place *Phlebia albida* in a phylogenetic context, Nakasone (1996) used a culture derived from a Spanish specimen collected on a still attached branch of *Pinus* sp. (host erroneously given as *Populus* by Nakasone). The sequence was recovered in the vicinity of *Phlebia albomellea* and this position has been retained in subsequent studies that used the same culture (e.g. Justo *et al*. 2017). Following the resurrection of *Cytidiella* as the correct place for *Phlebia albomellea* (Larsson 2007), also *Phlebia nitidula* and *Phlebia albida* have been moved to that genus (Zmitrovich 2018, Chen *et al*. 2021).

Phlebia albida is a species growing on a variety of angiosperm trees. This casts doubts on the identity of the pine-dwelling Spanish specimen. A restudy showed that it has been misidentified. The material consists of an effused basidioma having a smooth to slightly tuberculate hymenium with a reddish colour. A search in the literature brought up the name *Corticium pallidolivens* and comparison with authentic material revealed that the Spanish specimen belongs to this species. *Corticium pallidolivens* was collected frequently by Galzin in pine forest in southern France but has rarely been reported during the last hundred years. As indicated by published phylogenetic analyses where sequences from the misidentified specimen have been included, the species should be moved to *Cytidiella* (Chen *et al*. 2021). The identity and correct classification of *Phlebia albida* are discussed below under *Stereophlebia pendula*.

Hydnophlebia flavicans (Bres.) K.H. Larss. & Ryvarden, ***comb. nov.*** MycoBank MB 857616.
Basionym: *Hydnum flavicans* Bres., *Atti Acad. Agiato Rovereto* **3**(1): 95. 1897.
Synonyms: *Odonticium flavicans* (Bres.) Nakasone, *Cryptog. Mycol.* **29**(3): 245. 2008.
Odonticium monfraguense M.N. Blanco, G. Moreno & Manjón, *Cryptog. Mycol.* **10**(2): 137. 1989.

Typus: **Slovakia**, Prencow, na háj, on *Quercus*, 2 Dec. 1890, *A. Kmet* (**lectotype** of *Hydnum flavicans*, S F15525). **Hungary**, on *Quercus*, 12 Feb. 1912, *A. Kmet* (**epitype** S F15531, studied).

Additional materials examined: **Italy**, Sicily, Palermo, Altopiano Batia, St. Mauro Castelverde, on *Quercus suber*, 29 Jan. 2000, *A. Saitta* (A. Bernicchia 7201), O. **Spain**, Cáceres, Monfragüe Nat. Park, Las Cansinas, La Bazagona, on *Quercus suber*, 26 Apr. 1990, *G. Moreno & C. Illana*, GB, dupl. ex. HAH 12690.

Illustration: Michel & Duhem (2003; as *Odonticium monfraguense*).

Description: *Basidiomata* resupinate, closely adnate, effused, ceraceous when fresh, compact and rather hard when dried, hymenium densely hydnoid, pale yellow to pale orange, becoming brownish orange or pale cinnamon, spines cylindrical or slightly flattened, up to 10 mm long, 3–4 per mm, single or fused, margin narrow and pale yellow. *Hyphal system* monomitic, septa without clamps, hyphae in the thin subiculum 3–5 µm wide, irregular, much branched, thick-walled, partly pale brownish, hyphae in aculeal trama 3.5–5 µm, straight, parallel, thick-walled, apically thin-walled and with obtuse apices, subhymenium very thin, composed of thin-walled, 2–3 µm wide, richly branched, densely united hyphae. *Cystidia* scattered to rare, fusiform, 25–30 × 4–5(–7) µm, apically obtuse, thin-walled, projecting for about half their length. *Basidia* clavate, 14–18 × 4–4.5 µm, with four sterigmata. *Basidiospores* elliptical, (3.3–)3.4–4.5(–4.9) × 2.1–2.8(–2.9) µm, L = 3.9 µm, W = 2.35 µm, Q = 1.64 thin-walled, smooth, without reaction in Melzer's or Cotton Blue.

Ecology and distribution: On bark and wood of *Quercus*, especially *Q. suber*. Apparently, a rare species. The lectotype was collected in Slovakia and the epitype in Hungary. All recent collections are from Portugal, Spain, France, and Italy.

Notes: This species has usually been placed in *Odonticium* because of its hydnoid hymenium and the simple-septate hyphae (Manjón *et al*. 1989, Nakasone 2008). However, the type of *Odonticium*, *O. romellii*, belongs in *Hymenochaetales* while *Hydnum flavicans* belongs in *Polyporales*. Molecular data (Fig. 2) confirm that its proper place is in *Hydnophlebia*.

Hyphodermella pallidovirens (Bourdot & Galzin) K.H. Larss. & Spirin, ***comb. nov.*** MycoBank MB 857617. Figs 1A, 7.
Basionym: *Corticium pallidovirens* Bourdot & Galzin, *Hyménomyc. de France*: 215. 1928.
Synonyms: *Corticium pallidovirens* Bourdot & Litsch., *Öst. bot. Z.* **77**(2): 123. 1928, nom. illeg., a homonym of *C. pallidovirens* Bourdot & Galzin. *Typus*: **Austria**, Tirol, "Wäldchen bei Stams in Oberinntal", on branches of *Corylus avellana* and *Alnus incana*, 6 Jun. 1926, *V. Litschauer* (**lectotype** W 16376)
Phlebia viridesalebrosa J. Erikss. & Hjortstam, *Cortic. N. Eur*. **6**: 1127. 1981. *Typus*: **Austria**, Tirol, "Wäldchen bei Stams in Oberinntal", on branches of *Corylus avellana* and *Alnus incana*, 6 Jun. 1926, *V. Litschauer* (**lectotype** W 16376)
Hyphodermella pallidostraminea Bukharova & Volobuev, *Persoonia* **47**: 323. 2021.

© 2025 Westerdijk Fungal Biodiversity Institute

Typus: **Austria**, Tirol, "Wäldchen bei Stams in Oberinntal", on branches of *Corylus avellana* and *Alnus incana*, 6 Jun. 1926, *V. Litschauer* (**lectotype** of *Corticium pallidovirens* PC Bourdot 34284, studied).

Additional materials examined: **Austria**, Niederösterreich, Perchtoldsdorf, Naturpark Föhrenberge, on *Corylus avellana*, 10 Sep. 2022, *V. Spirin* 15797, H. **France**, Aveyron, Castelnau-Pégayrols, Le Trou d'Enfer, on rotten branches of *Buxus sempervirens*, May 1923, *A. Galzin* 27295 (Bourdot 33957), PC. **Norway**, Oslo, Hovedøya, on frondose wood, 22 Sep. 2011, *K.H. Larsson* 15122, GB. **Switzerland**, Ticino, Cevio, Conzorzio, on deciduous wood, 25 Aug. 2015, *E. Martini* 12656, GB.

Description: *Basidiomata* resupinate, effused, closely adnate, thin, crustaceous, hymenium smooth, mostly continuous or slightly cracked when dry, a bit shiny, greyish white with a glaucous or yellowish cast, margin not differentiated, thinning out or pruinose. *Hyphal system* monomitic, hyphae without clamps, in the thin subiculum 3–6(–8) µm wide, mostly thin-walled but some hyphae next to the substrate with thickened walls, partly irregular, partly parallel, closely united into a dense structure, in the subhymenium thin-walled, 3–4 µm wide, crystals common throughout the hyphal structure. *Cystidia* absent. *Basidia* clavate, usually with a slight median constriction and then subutriform, 18–27 × 5–7 µm, with four sterigmata. *Basidiospores* elliptical, (4.9–)5.0–5.7(–5.9) × (3.0–)3.1–3.6 µm, L = 5.35 µm, W = 3.4 µm, Q = 1.59 smooth, thin-walled, with homogenous contents, without reaction in Melzer's or Cotton Blue.

Ecology and distribution: On decaying branches and stems of angiosperm trees and bushes, on both bark and wood. Very rare and in Europe recorded only from Austria, Switzerland, Italy, France, and Norway. Recently collected in the Russian Far East (as *Hyphodermella pallidostraminea*).

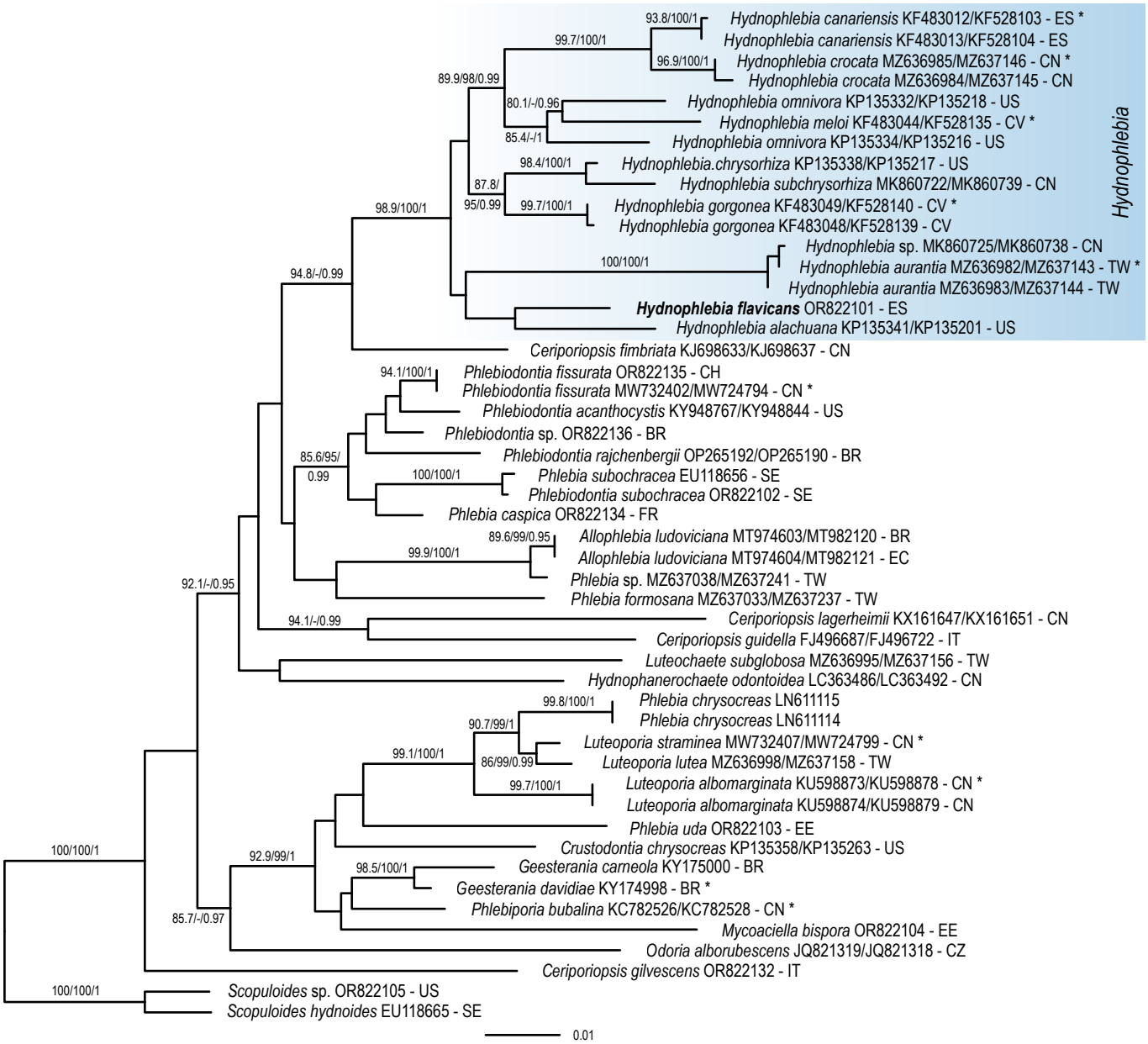

Fig. 2. Maximum likelihood tree for a part of *Meruliaceae* using ITS and LSU sequences. Focal taxa are highlighted. Support values from SH-aLRT (≥ 80), ultrafast boostrap (≥ 95) and Bayesian inference (≥ 0.95) are indicated on branches. Type sequences are marked with *.

© 2025 Westerdijk Fungal Biodiversity Institute

Notes: Eriksson *et al*. (1981) treated this species in remarks to *Phlebia lilascens* and concluded that *Corticium pallidovirens* Bourdot & Galzin and *Corticium pallidovirens* Bourdot & Litsch. were different species. Hence, they introduced *Phlebia viridesalebrosa* in order to validate the latter homonym. Hjortstam (1987) later changed his mind and regarded the two species as synonyms. Wu (1990) came to the same conclusion and we concur.

Molecular phylogenetic analyses recover *Corticium pallidovirens* in *Hyphodermella* with strong support (Fig. 3). *Hyphodermella* was originally described as a genus with odontioid hymenium with the hymenial spines consisting

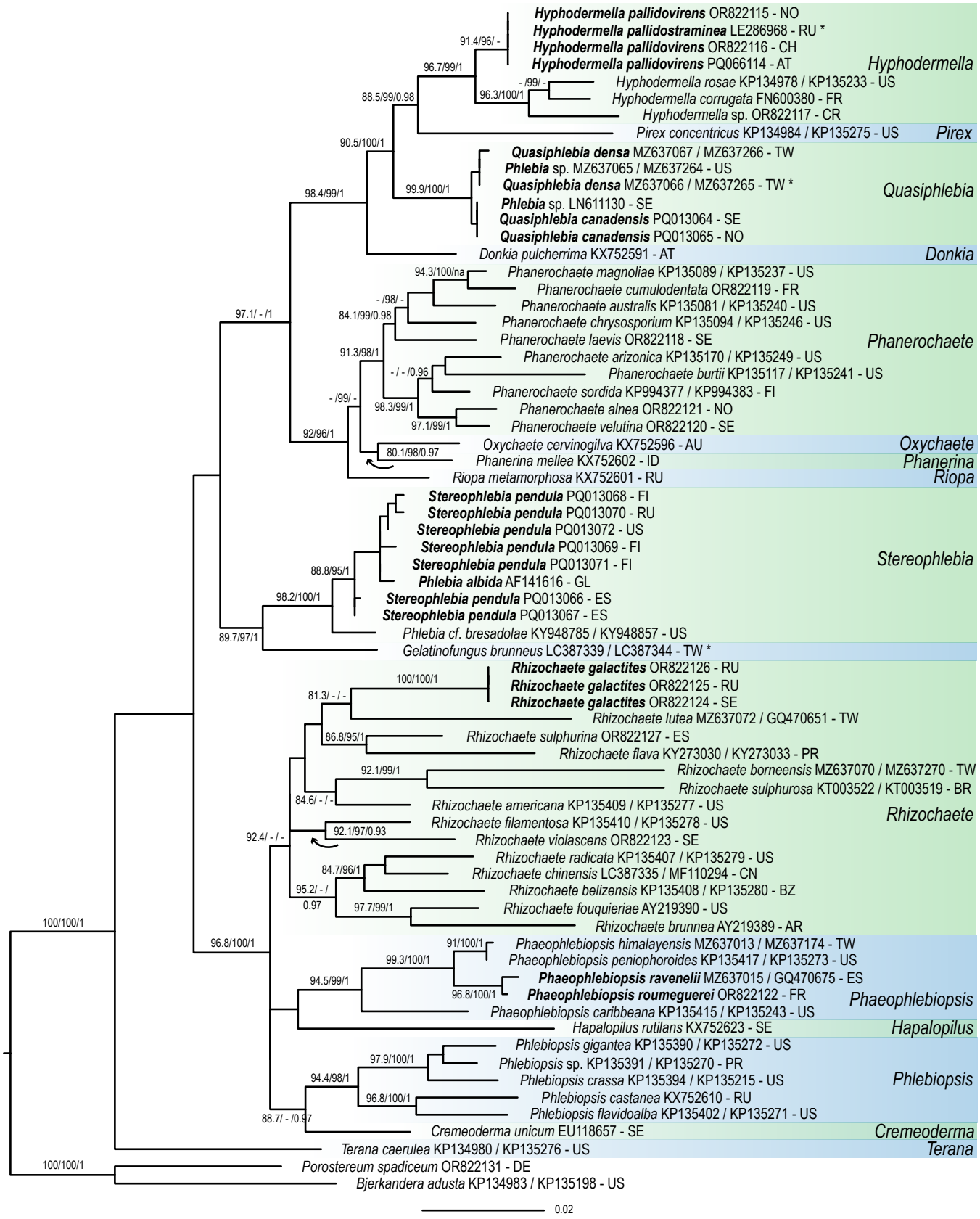

Fig. 3. Maximum likelihood tree for *Phanerochaetaceae* using ITS and LSU sequences. Focal taxa are highlighted. Support values from SH-aLRT (≥ 80), ultrafast boostrap (≥ 95) and Bayesian inference (≥ 0.95) are indicated on branches. Type sequences are marked with *.

© 2025 Westerdijk Fungal Biodiversity Institute

of bundles of encrusted hyphae. The genus was initially monotypic. Later additions have introduced species with smooth to tuberculate and poroid hymenial configurations (Zhao *et al*. 2017, Wang & Zhao 2020, Wang *et al*. 2021). However, recent phylogenetic analyses indicate that not all of these additions belong in the genus (Chen *et al*. 2021). *Hyphodermella pallidovirens* has a strictly smooth hymenium with no tendencies to form encrusted bundles of hyphae like the type species.

Lopharia avellanea (Bres.) K.H. Larss. & E. Larss., ***comb. nov.*** MycoBank MB857618. Fig. 1B.
Basionym: *Kneiffia avellanea* Bres., *Ann. Mycol.* **1**: 102. 1903.
Synonym: *Phlebia margaritae* Duhem & H. Michel, *Cryptog. Mycol*. **28**: 30. 2007.

Typus: **Poland**, on branches of *Ulmus*, leg. *Eichler* (**lectotype** of *Kneiffia avellanea*, designated here, S F15745, MBT 10024814, studied).

Additional materials examined: **France**, Aveyron, Millau, Dourbie, on *Quercus pubescens*, 10 May 2022, *V. Spirin* 15422, H. **Poland**, on branches of Ulmus, Jul.-Aug. 1900, *B. Eichler*, S F15745, **lectotype** of *Kneiffia avellanea*, GB **isolectotype**. **Spain**, Huesca, Caspe, 14 km N of Caspe on road A2410 Caspe – Peñalba, on *Quercus ilex*, 7 Apr. 2010, *E. Larsson* EL19-10, GB.

Illustration: Duhem & Michel (2007; as *Phlebia margaritae*).

Description: *Basidiomata* resupinate, effused, closely adnate, thin to moderately thick, rather soft, ceraceous, by age becoming more and more rimose, hymenium smooth, when dried minutely porose, velutinous from emerging cystidia, pale chamois to greyish pink or violaceous, margin thinning out or developed as white, byssoid mycelium. *Hyphal system* monomitic, septa with clamps, subiculum rather compact, composed of 2–4(–5) µm wide, frequently branched and somewhat irregular generative hyphae and 0.5–2 µm wide, somewhat thick-walled micro-binding hyphae with short narrow side-branches, mainly visible along the margin or in cracks in the hymenium. Some hyphae are minutely encrusted. Subhymenial hyphae thin-walled, richly branched, 2–3 µm wide, forming a vertically arranged dense tissue where individual hyphae are difficult to observe. *Cystidia* abundant, conical, thick-walled, densely encrusted, mostly 50–80 × 10–

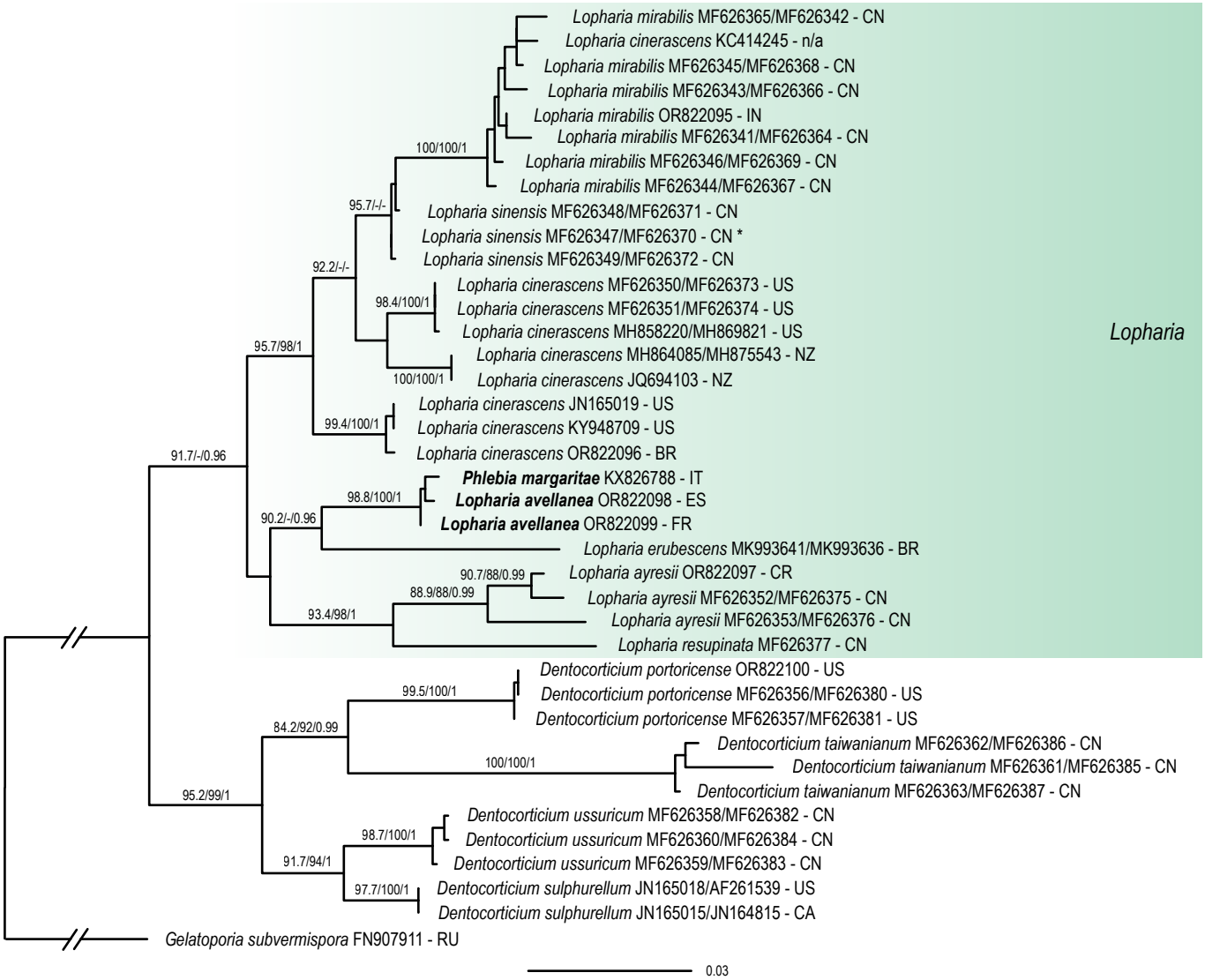

Fig. 4. Maximum likelihood tree for *Lopharia* using ITS and LSU sequences. Focal taxa are highlighted. Support values from SH-aLRT (≥ 80), ultrafast boostrap (≥ 95) and Bayesian inference (> 0.95) are indicated on branches. Type sequences are marked with *.

© 2025 Westerdijk Fungal Biodiversity Institute

15 µm, older ones slightly yellowish, initially broadly club-shaped and thin-walled, developing in the hymenium from generative hyphae, in the beginning strongly projecting, becoming embedded when the basidioma thickens. *Basidia* narrowly clavate to subcylindrical, 25–40 × 3–5 µm, distinctly widened at apex when sterigmata develop, with four rather straight sterigmata. *Basidiospores* cylindrical, more or less allantoid, (5.9–)6.0–7.3(–7.9) × (2.1–)2.3–3.4(–3.9) µm, L = 6.85 µm, W = 2.8 µm, Q = 2.29, thin-walled, with one-to-many oil-drops, without reaction in Melzer's or Cotton Blue.

Ecology and distribution: On trunks and branches of angiosperm wood. A rare species, so far found in France, Italy, Iran, Poland and Spain.

Notes: Bresadola (1903) compared his new species to *Peniophora cinerea* and Höhnel & Litschauer (1908) moved it to *Peniophora*. Both Höhnel & Litschauer (1908) and Eriksson *et al*. (1978: 985) suggested that it could be related to *Peniophora* (*Hyphoderma*, *Peniophorella*) *pubera*. According to notes in the type envelope, Burdsall studied the material and concurred with Bresadola about its place in *Peniophora* sensu stricto.

Phylogenetic analyses firmly place the species in *Lopharia* (Fig. 4). This genus was originally regarded as dimitic (Hjortstam & Ryvarden 1990) but the concept was changed when the monomitic species *Peniophora ayresii* was added to the genus (Hjortstam 1995). Recently, more monomitic species have been included and the genus definition emended (Liu *et al.* 2018). *Phlebia margaritae* was described as dimitic because the subiculum contains skeleto-binding hyphae (here called micro-binding hyphae) (Duhem & Michel 2007). However, in our opinion a presence of micro-binding hyphae should not qualify for a classification as dimitic.

The Spanish specimen is paler and with less violaceous tints than the types of *Phlebia margaritae* and *Kneiffia avellanea*. It is also older, which is seen by the thicker, strongly cracked basidioma. The Polish specimen is thin and probably young. In all other respects the studied material is homogenous.

There are three specimens in the Bresadola herbarium in Stockholm (herb S, F15744, F15745, F78491). They all bear the same label data and are apparently pieces of a single specimen from Poland seen by Bresadola. One of them (F15745) also has annotations on microscopic details and pencil drawings of cystidia and spores and is here selected as lectotype.

Meruliopsis rubicunda (Litsch.) Spirin & K.H. Larss. ***comb. nov.*** MycoBank MB 857619. Fig. 1C.

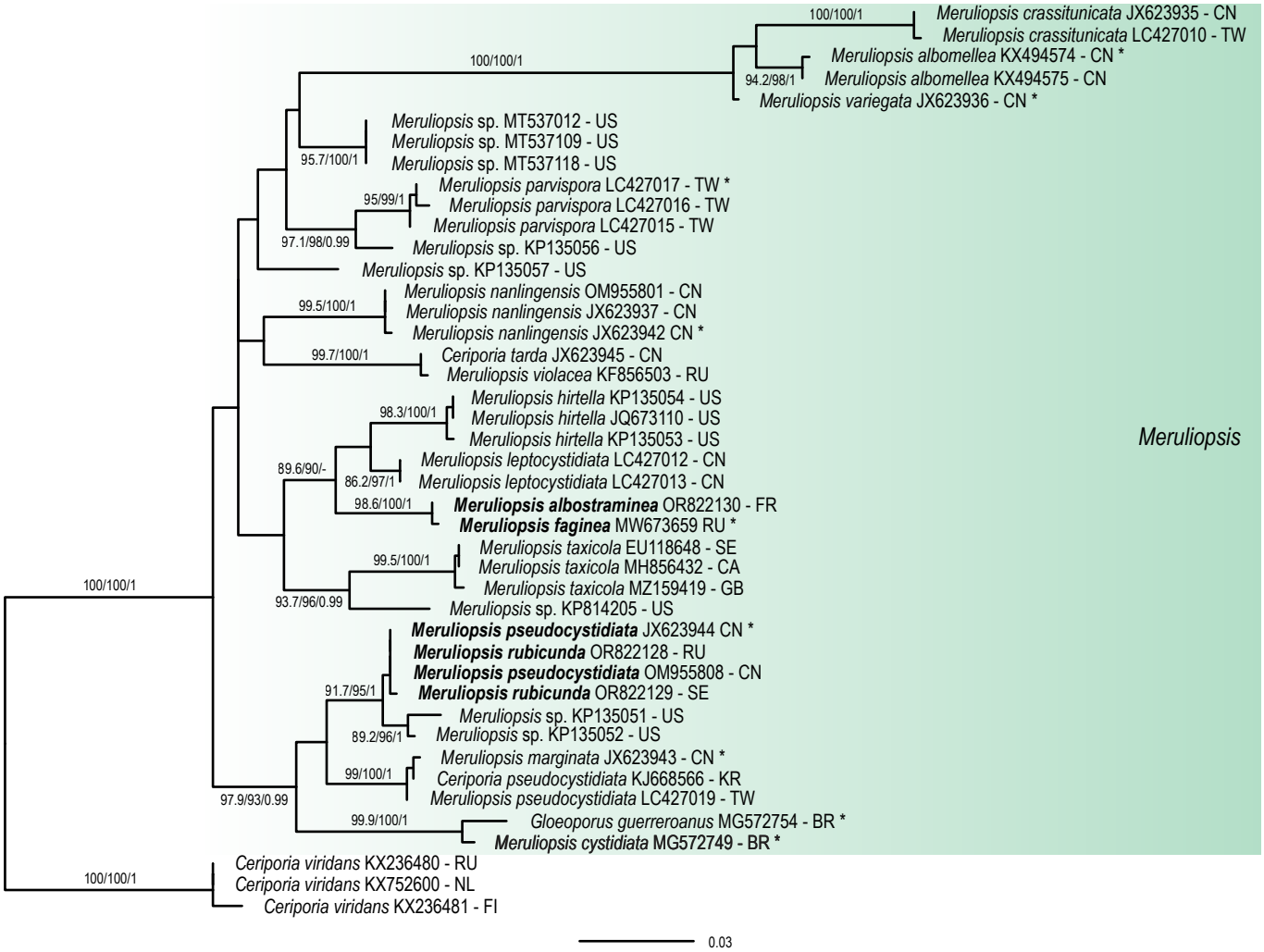

Fig. 5. Maximum likelihood tree for *Meruliopsis* using ITS sequences. Focal taxa are highlighted. Support values from SH-aLRT (≥ 80), ultrafast boostrap (≥ 95) and Bayesian inference (≥ 0.95) are indicated on branches. Type sequences are marked with *.

© 2025 Westerdijk Fungal Biodiversity Institute

Basionym: *Merulius rubicundus* Litsch., *Bull. Trimest. Soc. Mycol. Fr.* **49**: 293. 1934.
Synonyms: *Ceraceomerulius rubicundus* (Litsch.) J. Eriksson & Ryvarden, *Cortic. N. Eur*. **2**: 197. 1973.
Ceriporia pseudocystidiata B.S. Jia & Y.C. Dai, *Mycol. Prog.* **13**: 86. 2013.
Meruliopsis pseudocystidiata (B.S. Jia & Y.C. Dai) C.C. Chen & Sheng H. Wu, *Mycologia* **112**: 78. 2020.

Typus: **Russia**, Khakassia, Sayan Mts., on *Alnus* (?), 15 Jul. 1932, *Krawtzew* (**holotype** of *Merulius rubicundus* PRM 618737, studied).

Additional materials examined: *Meruliopsis albostraminea*. **Armenia**, Kaphan, Tsav, on *Sambucus ebulus*, 2 Oct. 1962, *E. Parmasto*, TAAM 16280, **holotype** of *Byssomerulius armeniacus*. **France**, Pyrenées-Orientales, Sorède, E of Lavaill, on *Erica arborea*, 5 Nov. 2008, *H. Michel*, (KHL13798), GB. **Portugal**, Bemfica, on *Eucalyptus globulus*, *C. Torrend* 344, S F15976, BPI, **isolectotype** of *Merulius albostramineus* — *Meruliopsis rubicunda*. **Russia**, Khabarovsk Reg., Khabarovsk Dist., Malyi Niran, on fallen decorticated hard log of *Pinus koraiensis*, 6 Aug. 2012, *V. Spirin* 4951, H, GB. **Sweden**, Norrbotten, Överkalix, Lansjärv, Storberget, on conifer wood, 11 Oct. 2008, *G. Norstedt*, GB — *Merulius armeniacus*. **USA**, Idaho, *Abies grandis*, *J.R. Weir* 15306, BPI, **holotype**.

Illustration: Eriksson & Ryvarden (1973; as *Ceraceomerulius rubicundus*).

Description: *Basidiomata* effused, resupinate, membranous, rather soft, ab. 0.5 mm thick, hymenium reticulately wrinkled to folded or semiporoid, whitish to pale pinkish orange or pale reddish, margin fibrillose, white, subiculum white. *Hyphal system* monomitic, hyphae without clamps, in the subiculum loosely interwoven, 3–5 µm wide, partly encrusted, in the subhymenium densely united, frequently branched, 2.5–4 µm wide. *Cystidia* cylindrical to narrowly clavate, obtuse, 30–40 × 5–6 µm, thin-walled, apically sparsely encrusted, developing in the hymenium and slightly projecting. *Basidia* narrowly clavate, 18–25 × 4–5 µm, with four sterigmata. *Basidiospores* subcylindrical to allantoid, (4.4–)4.8–6.3(–6.6) × (1.7–)1.8–2.3(–2.7) µm, L = 5.4 µm, W = 2.0 µm, Q = 2.72 smooth, thin-walled, without reaction in Melzer's or Cotton Blue.

Ecology and distribution: On decaying wood of conifers. The host tree on the label of *Merulius rubicundus* type is indicated as *'Alnus* (?)', which is likely a misidentification. Belonging to the boreal forest region throughout Eurasia and conifer forests in the Central European mountains.

Notes: Ginns (1971) studied original material of *Merulius albostramineus* (in BPI and S) and *Merulius rubicundus* (PRM) and concluded that they were conspecific. His interpretation has gained wide acceptance. We restudied the same specimens and noticed clear differences in spore morphology; thus, we must reject the synonymy suggested by Ginns (1971).

Ginns (1976) suggested that *Merulius armeniacus*, *M. atropurpureus*, and *M. purpurascens* are synonyms of *Meruliopsis rubicunda* (by Ginns called *Ceraceomerulius albostramineus*). Since *Merulius armeniacus* is older than *M. rubicundus* we studied the type (BPI). The material is heavily grazed by insects and rather collapsed. The hymenium is subporoid and vinaceous brown. Subicular hyphae are rather

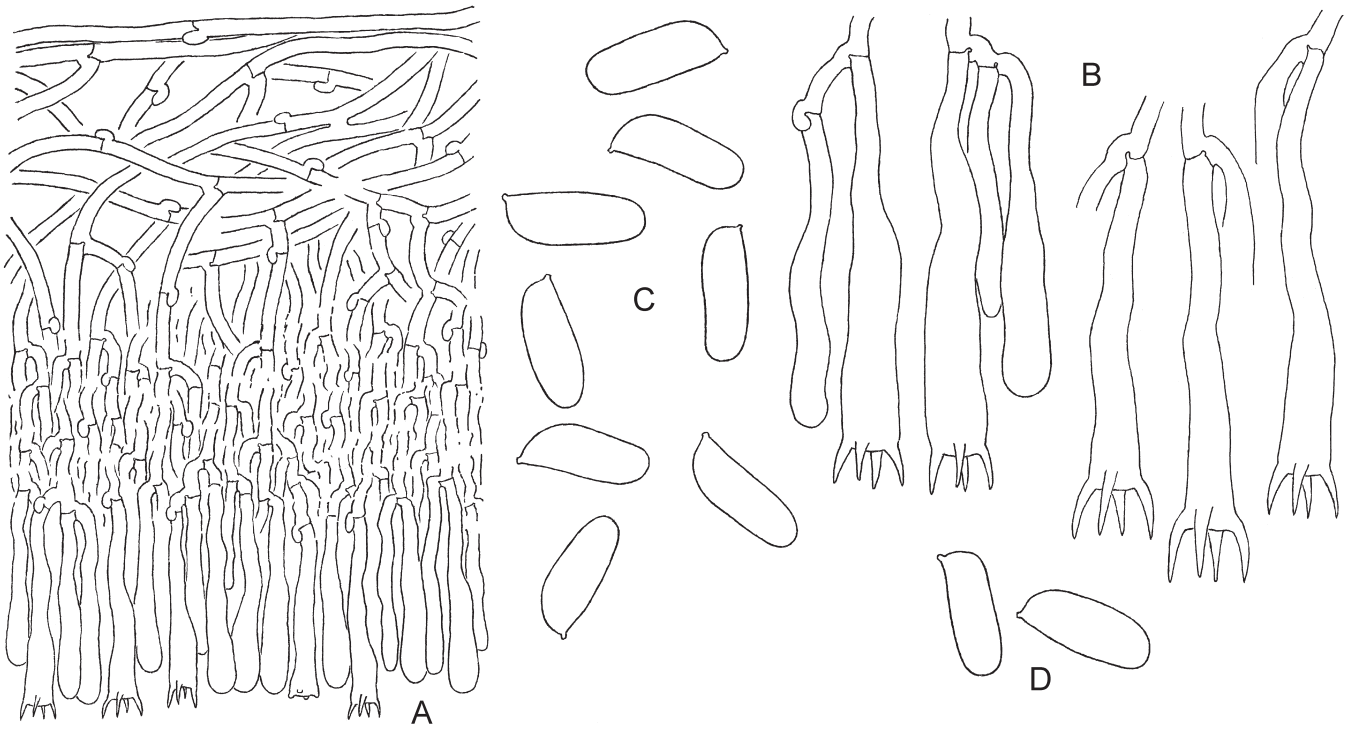

Fig. 6. *Cytidiella pallidolivens*. **A.** Section through basidioma. **B.** Basidia and basidioles. **C, D.** Basidiospores. A–C from N. Hallenberg 10123 (GB); D from Bourdot 5508 (GB).

© 2025 Westerdijk Fungal Biodiversity Institute

straight and 3–4 µm wide, while subhymenial elements are not discernible. The whole tissue is filled with a golden yellow encrustation. No rehydrated basidiospores were observed. We find these characters incompatible with *Meruliopsis rubicunda* and reject the synonymy. *Merulius atropurpureus* could be the same as *M. armeniacus*, which is also suggested by Ginns (1971). Hjortstam (1995) studied the type of *M. purpurascens* and compared it with *Meruliopsis taxicola*. He found that both cystidia and basidiospores differed from those of *M. rubicunda*.

Meruliopsis albostraminea is typified with material collected by Torrend in Portugal. This species differs from *M. rubicunda* through a cream-coloured hymenium without the orange pinkish cast typical for the latter species. Moreover, basidiospores are elliptical and never allantoid. Its distribution in Europe is throughout the Mediterranean region and eastwards to the lowlands at the Caspian Sea. Since the publications by Ginns (1971, 1976), the true *M. albostraminea* has been called *M. hirtella* (Burt) Ginns. Burt's species is morphologically similar to *M. albostraminea*. However, ITS sequences of North American specimens identified as *M. albostraminea* sensu Ginns or *Meruliopsis* sp. all differ from sequences from *M. albostraminea* s.s. as well as from *M. rubicunda*. Therefore, we conclude that *M. hirtella* and *M. albostraminea* are different species and that *M. hirtella* likely is absent from Europe. The recently published *Meruliopsis faginea* from the Caucasus is a synonym of *M. albostraminea* as confirmed through DNA sequences. Another, much older synonym of *M. albostraminea* from the Caucasian area, is *Byssomerulius armeniacus*.

Meruliopsis pseudocystidiata is a synonym of *M. rubicunda*. The published ITS sequence of the type specimen is identical to European sequences from material identified as *Meruliopsis rubicunda*. We have not studied the type but both description and illustration from the protologue leave no doubt about the synonymy.

Mycoacia ocellata (Fr.) K.H. Larss. & Spirin, ***comb. nov.*** MycoBank MB 857620. Figs 1D, 8.

Basionym: *Grandinia ocellata* Fr., *Epicrisis Systematis Mycologici*: 527. 1838.
Synonyms: *Phlebia livida* subsp. *tuberculata* Hallenb. & E. Larss., *Mycol. Res.* **97**: 353. 1993.
Phlebia tuberculata (Hallenb. & E. Larss.) Ghob.-Nejh., *Mycol. Progr.* **11**: 32. 2012, nom. illeg., not *Phlebia tuberculata* (Berk. & M.A. Curtis) Ţura *et al.*, *Biodiversity of the Heterobasidiomycetes and non-gilled Hymenomycetes (former Aphyllophorales) of Israel*: 446. 2011.
Mycoacia neotuberculata S.H. He *et al.*, *Mycology*, in press. https://doi.org/10.1080/21501203.2024.2443216

Typus: **Sweden**, Halland, Kvibille parish, Biskopstorp Nature Reserve, on decaying wood of *Fagus sylvatica*, 17 Sep. 2009, *K.H. Larsson* 13967 (**neotype** of *Grandinia ocellata*, designated here, GB GB-0207712, MBT 10024820). ITS GenBank accession PQ066115.

Additional materials examined: **France**, Essonne, Soisy-sur-Seine, Forêt de Sénart, on *Tilia cordata*, 11 Nov. 2021, *V. Spirin* 15277, H. **Norway**, Vestfold, Tønsberg, Askehaug, on *Fagus sylvatica* log, 17 Dec. 2011, *P. Marstad* 354-11, O; Vestfold, Sandefjord, Kile, on *Fagus sylvatica*, 25 Nov. 2012, *P. Marstad* 311-12, O. **Romania**, Arad Co., Bârzava, Runcu Groşi, on *Fagus sylvatica*, 15 Sep. 2021, *V. Spirin* 15054, H; Brasov, Padurea Bogatii, deciduous wood, 22 Oct. 1985, *N. Hallenberg* 9350, GB-0069567. **Russia**, Khabarovsk Reg., Khabarovsk Dist., Ulika, on *Tilia amurensis*, 15 Aug. 2012, *V. Spirin* 5285, GB, H. **Spain**, Lerida. S. of Las Bordas, *Fagus* log, 13 Nov. 1986, *N. Hallenberg* 9958, GB-0069561.

Description: *Basidiomata* effused, resupinate, closely adnate, corneous, hymenium smooth to grandinioid or irregularly tuberculate, hymenial spines usually pointed, when fresh mostly bluish to violaceous, when dried more brownish, hymenial spines often with a whitish tip, margin thinning out, sterile margin lacking. *Hyphal system* monomitic, septa with clamps, subiculum clearly differentiated, composed of parallel, agglutinated, thick-walled, 3–4 µm wide hyphae

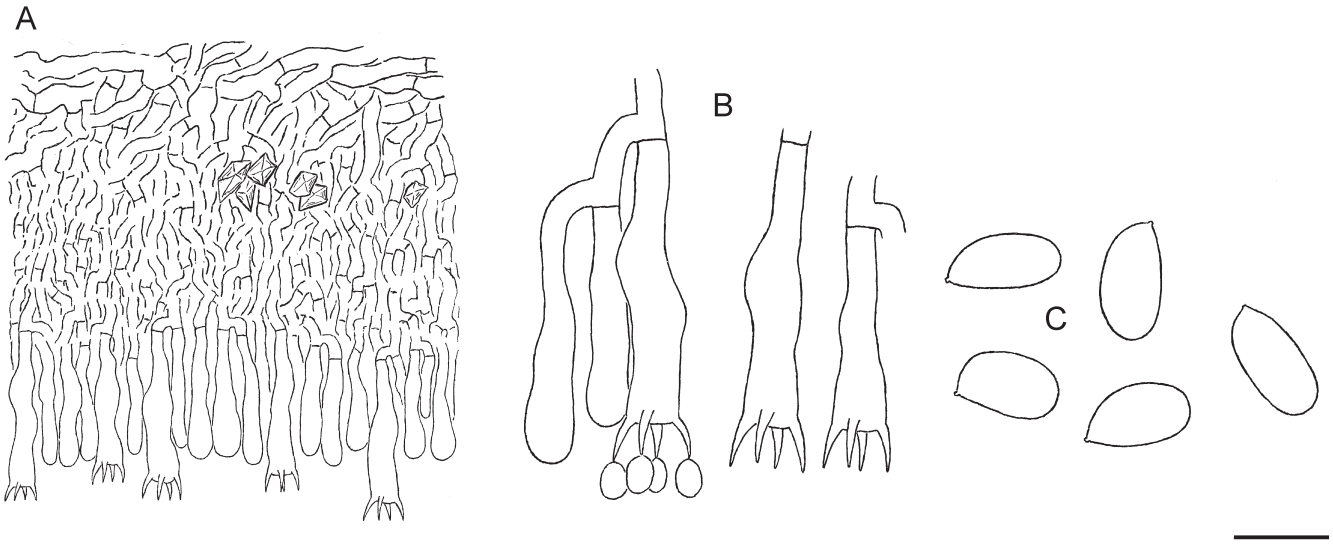

Fig. 7. *Hyphodermella pallidovirens* [E. Martini 12656 (GB)]. **A.** Section through basidioma. **B.** Basidia and basidioles. **C.** Basidiospores. Scale bars: A = 20 µm; B = 10 µm; C = 5 µm.

© 2025 Westerdijk Fungal Biodiversity Institute

growing horizontally, subhymenium formed by thin-walled, ab. 2 µm wide, rather short-celled and strongly tortuous hyphae in a dense tissue where individual hyphae and hyphal direction is difficult to observe. *Cystidia* few or sometimes lacking, narrowly fusoid with a long, thin apex, 40–50 × 3–4 µm, thin-walled, developing from subhymenial hyphae and projecting up to half the length. Simple, hypha-like hyphidia common among the basidia. *Basidia* narrowly clavate 20–30 × 3.5–4.5 µm, with four sterigmata. *Basidiospores* cylindrical, (3.7–)3.8–5.4(–5.6) × (1.5–)1.6–2.0(–2.1) µm, L = 4.3, W = 1.8, Q = 2.4, adaxial side often slightly concave with a bend close to apiculus, thin-walled, without reaction in Melzer's or Cotton Blue.

Ecology and distribution: On angiosperm trees, in Northern Europe mostly on *Fagus* (see also notes below). With a nemoral to South boreal distribution in Europe. It is known through sequences from several Asian countries and also from Australia. Not yet reported from North America.

Notes: Hallenberg and co-workers studied the taxonomy of *Phlebia livida* (Hallenberg 1988, 1991, Hallenberg & Larsson 1991, 1993, Ghobad-Nejhad & Hallenberg 2012). They concluded that the species in Europe consists of two well-separated populations, one preferably growing on conifers, and the other mainly found on angiosperm trees. Since *Phlebia livida* by typification is connected to the conifer-dwelling taxon, the angiosperm taxon was described as new, first as a subspecies, *Phlebia livida* subsp. *tuberculata* (Hallenberg & Larsson 1993), then, after a re-evaluation using DNA sequences, raised to species level as *Phlebia tuberculata* (Ghobad-Nejhad & Hallenberg 2012). Unfortunately, *Phlebia tuberculata* (Hallenb. & E. Larss.) Ghob.-Nejh. is a later homonym of *Phlebia tuberculata* (Berk. & M.A. Curtis) Tura *et al.* (Tura *et al*. 2011). This has left *P. livida* subsp. *tuberculata* without a name when treated as a species. Recently, Li *et al*. (2025) introduced *Mycoacia neotuberculata* as a *nomen novum* to replace the illegitimate name *Phlebia tuberculata*. As we show below, there is an old name available that should have been used instead; thus, *Mycoacia neotuberculata* is superfluous.

Name databases (Index Fungorum, MycoBank) suggest several names as synonyms of *Phlebia livida*, i.e. *Corticium viscosum* Pers. (1800), nom. sanct., *Grandinia ocellata* Fr. (1838), *Corticium uvidum* (Fr.) Fr. (1838), *Xerocarpus cacao* P. Karst. (1890), and *Sebacina peritricha* Bourdot & Galzin (1909). Below, the availability of each of these names is discussed.

No original material of *Corticium viscosum* is known. Persoon (1800) underlines that the fungus is sticky, especially when touched. It is effused and smooth with but a few papillae and Persoon discusses if they just reflect irregularities in the substrate. When dried, the fungus becomes strongly cracked (*diminuiter*) and sordid blackish (*sordide fuscescit*). When moving the species to *Thelephora* (Persoon 1801), Persoon slightly changed the description and adds that it is subgelatinous and that the colour of the (fresh?) fungus is greyish whitish or pale (lavender) blue.

In the sanctioning works *Thelephora viscosa* is treated twice. First Fries (1821) merely repeated the text by Persoon, giving the remark that the species is very similar to *Thelephora livida*. However, when Fries returned to the subject in Elenchus Fungorum (Fries 1828), he expressed a different opinion. He now wrote that *T. viscosa* is completely different (*omnino diversa*) from *T. livida*, although easily confused. We conclude that neither the original description nor the descriptions in the sanctioning works provide strong evidence for a synonymy with *Thelephora livida*. Thus, the identity of *Corticium viscosum* remains unknown, and we suggest it is best treated as a nomen dubium.

Grandinia ocellata is a species Fries found on *Fagus*. He described the colour as *lividus* and the hymenium as covered with granules whose white tips resemble pearls (*granulis confertis, subconicis obtusis … Granula terminata apiculo subtilissimo albido, … quasi ocellata*). Lundell & Nannfeldt (1941) regarded *Grandinia ocellata* as a synonym of *Corticium lividum* and we agree. The details of the protologue clearly connect the species to *Phlebia livida* subsp. *tuberculata*.

Fries (1828) introduced *Corticium uvidum* in Elenchus Fungorum as a variety to *Thelephora viscosa* (as β *uvida*). Thus, it is only sanctioned at variety level. In 1838, Fries placed the species next to *Corticium comedens* (=*Vuilleminia comedens*). He remarked that the fungus grows on both sides

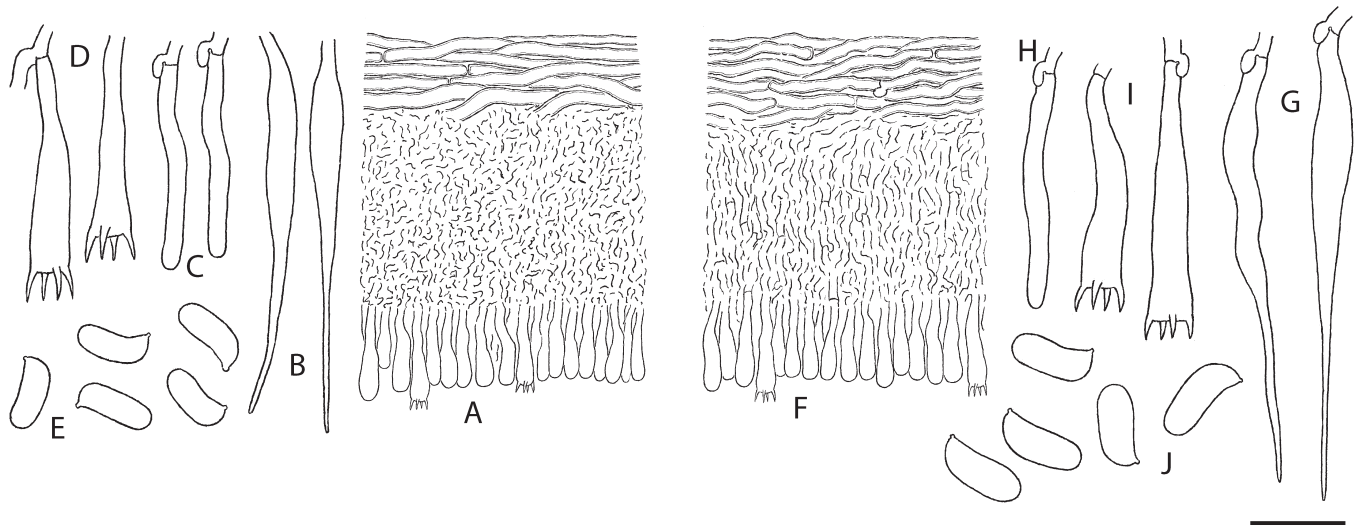

Fig. 8. *Mycoacia ocellata* (A–E) and *M. livida* (F–J). **A, F.** Section through basidioma. **B, G.** Cystidia. **C, H.** Hymenial hyphidia. **D, I.** Basidia. **E, J.** Basidiospores. A–E from neotype; F–J from K. Hjortstam 4371 (GB). Scale bars: A, F = 20 µm; B–D, G–I = 10 µm; E, J = 5 µm.

© 2025 Westerdijk Fungal Biodiversity Institute

of *Fagus* branches, and is rosy-lilac but fading. The basidiocarp is described as widely effused, very thin, tremellaceous, very smooth, moist, and when old disappearing (*tritum fugax*). These characters do not immediately recall *Phlebia livida* subsp. *tuberculata*. However, the UPS herbarium preserves a specimen with the name *Corticium uvidum* in Fries' handwriting that was collected in Femsjö, SW Sweden. The basidioma is rather dark and completely smooth. Microscopy reveals that the species belongs to *Phlebia livida* sensu lato, as already pointed out by Lundell & Nannfeldt (1947). Furthermore, as discussed below, a subhymenial structure with thin-walled, mainly ascending hyphae and plenty of resinous exudates when mounted in Cotton Blue makes it possible to identify the specimen as *Phlebia livida* subsp. *livida*. The specimen is here selected as neotype for *Thelephora viscosa* var. *uvida* (see below).

The type of *Xerocarpus cacao* is well preserved and differs clearly from *Phlebia livida* by a less agglutinated context, presence of irregular, short-celled, rather wide subicular hyphae, and by somewhat wider and less pointed cystidia. These characters place *X. cacao* in the vicinity of *Phlebia subserialis*.

Finally, our study of type material of *Sebacina peritricha* (PC) shows that the species belongs in *Auriculariales*. This leaves us with *Grandinia ocellata* as the best alternative when naming *Phlebia livida* subsp. *tuberculata* at species level.

Phlebia livida is not closely related to the type of *Phlebia*, *P. radiata*, and has therefore twice been placed in other genera. First *Phlebia livida* was made the type of the new genus *Lilaceophlebia* (Spirin & Zmitrovich 2004). Later *Phlebia livida* was instead moved to *Mycoacia* (Zmitrovich 2018). Both arrangements are supported in phylogenetic analyses based on nuclear ribosomal sequences (Justo *et al*. 2017, Chen *et al*. 2021). If the wider concept for *Mycoacia* suggested by Zmitrovich (2018) is accepted, an unfortunate result is that *Ceriporiopsis*, typified by *C. gilvescens*, becomes a synonym of *Mycoacia*. However, currently we prefer this solution since most necessary combinations in *Mycoacia* are already in place. Consequently, we here introduce *Mycoacia ocellata* to replace the invalid name *Phlebia tuberculata* (Hallenb. & E. Larss.) Ghob.-Nejh.

Ghobad-Nejhad & Hallenberg (2012) stated that *Mycoacia livida* and *Mycoacia ocellata* can only be separated macroscopically. They point to differences in colour and in the hymenial ornamentation that is pointed in *M. ocellata*, never so in *M. livida*. They also mention that old basidiomata of *M. livida* may become detached from the substrate. We can only partly agree with these observations. Hymenial ornamentation is not always pointed in *M. ocellata*, and juvenile and senescent specimens can be almost smooth, without any sign of pointed emergences; in addition, some older specimens of the species (especially dried ones) are as dark as those of *M. livida*. This makes it often impossible to separate the two taxa macroscopically, but there are several microscopical features that could aid in identification. First, the basidiospores of *M. ocellata* are on average slightly narrower and often shorter than in subsp. *livida*, on average 4.3 × 1.8 µm vs 4.4 × 2.0 µm, respectively. The differences are tiny, however, and it is necessary to measure several specimens and at least twenty spores per specimen. Second, when mounted in Cotton Blue an amorphous resinous exudate is present among hymenial cells and subhymenial hyphae in *M. livida*, usually observable as large, yellowish, grainy bodies. The same substance is present in *M. ocellata*, but to a much lesser extent and only as small droplets. Third, subhymenial hyphae of *M. livida* are normally thin-walled, rather long-celled and as a rule with a clear tendency for vertical orientation (Fig. 8). In *M. ocellata*, subhymenial hyphae have a variable wall thickness, are short-celled and strongly tortuous, making the tissue look almost pseudoparenchymatic (Fig. 8). The detaching margin in old basidiomata of subsp. *livida* is an additional useful character for identification.

Basidioma substrate is the most important information for separating *Mycoacia livida* and *M. ocellata*. Ghobad-Nejhad & Hallenberg (2012) report one case where *M. livida* was collected on hardwood. Unfortunately, we were not able to locate this specimen. They also report one case of *M. ocellata* collected on *Abies*. We studied this specimen and found the substrate to be *Fagus*. We conclude that even if not clearly demonstrated, rare cases of host jumping cannot be excluded.

We have seen specimens of *Mycoacia ocellata* misidentified as *Phlebiodontia caspica*. When fully developed, *P. caspica* is regularly hydnoid, but young basidiomata may appear strongly tuberculate as in specimens of *M. ocellata*. Microscopically *P. caspica* develops numerous cystidia whereas in *M. ocellata* cystidia are typically few or even absent. Above all, the two species differ in spore morphology, being suballantoid in *M. ocellata* and narrowly elliptical in *P. caspica*.

Mycoacia livida (Pers.) Zmitr., *Folia Cryptog. Petropolitana* **6**: 101. 2018. Figs 1E, 8.
Basionym: *Corticium lividum* Pers., *Observ. Mycol.* **1**: 38 (1796), nom. sanct. [Fries, *Syst. Mycol*. **1**: 447. 1821, as *Thelephora*].
Synonyms: *Thelephora viscosa* var. *uvida* Fr., nom. sanct. [Fries, *Elench. Fung.* **1**: 218. 1828]. *Typus*: **Sweden**, Småland, Femsjö, leg. E. Fries (**neotype**, designated here, UPS F-003107, MBT 10024861, studied).
Phlebia livida (Pers.) Bres., *Atti Acad. Agiato Rovereto* **3**: 105. 1897.
Lilaceophlebia livida (Pers.) Spirin & Zmitr., *Nov. sist. Niz. Rast.* **37**: 179. 2004.

Typus: **Sweden**, Småland, Femsjö, *E. Fries* (**neotype** of *Corticium lividum* UPS F-002613, designated by Eriksson *et al*. 1981, as **lectotype**, studied). **Sweden**, Småland, Femsjö, on *Picea abies* log, 3 Oct. 1984, *N. Hallenberg* 8658 (**epitype**, designated here, GB-0069572, MBT 10024815). ITS GenBank accession HQ153414.

Additional materials examined: **Finland**, Pohjois-Häme, Pyhä-Häkki Nat. Park, on *Picea abies* trunk, 21 Aug. 1986, *N. Hallenberg* 9543, GB-0069566. **Russia**, Khabarovsk Reg., Verkhnebureinskii Dist., Dublikan Nat. Res., on *Picea ajanensis*, 21 Aug. 2015, *V. Spirin* 7717, H; Nizhny Novgorod Reg., Sharanga Dist., Kilemary Nat. Res., on *Picea abies*, 25 Aug. 2019, *V. Spirin* 13055, H. **Sweden**, Dalsland, Ör, W of lake Örsjön, on *Pinus sylvestris*, 3 Nov. 1972, *K.H. Larsson & K. Hjortstam* 6029, GB-0115280; Ångermanland, Junsele, Kortinghöjden, on *Picea abies*, 22 Sep. 1970, *K. Hjortstam* 4371, GB-0115291.

© 2025 Westerdijk Fungal Biodiversity Institute

Parvodontia gloeocystidiata (Gorjón & Saitta) K.H. Larss., ***comb. nov*.** MycoBank MB 857621. Fig. 9.
Basionym: *Leptocorticium gloeocystidiatum* Gorjón & Saitta, *Mycosphere* **5**(3): 407. 2014.

Typus: **Italy**, Sicily, Messina, Portella Scarno, on dead wood of *Fagus sylvatica*, 14 Apr. 2012, *A. Saitta* 483 (**holotype** SALA; **isotype** GB, studied).

Description: *Basidiomata* resupinate, effused, adnate, soft ceraceous, hymenium smooth to sparingly grandinioid, ochraceous, margin not differentiated. *Hyphal system* dimitic, generative hyphae with clamps, subiculum dominated by branching, 1–1.5 µm wide skeletal hyphae, generative hyphae 2–3 µm, thin-walled, subhymenium dense with ab. 2 µm wide, thin-walled hyphae, difficult to observe. *Cystidia* none, but a few, slightly branching hyphidia present in the hymenium. *Gloeocystidia* numerous, present throughout the basidioma, irregular to cylindrical, frequently with constrictions and often apically moniliform, 15–35 × 5–8.5 µm, some gloeocystidia with weakly yellowish and refractive contents. *Basidia* clavate 15–20 × 3–4 µm, with four sterigmata and a basal clamp. *Basidiospores* elliptical, 4–5 × 2.5–3 µm (few spores measured), smooth, thin-walled, without reaction in Melzer's or Cotton Blue.

Ecology and distribution: The type was collected on decaying wood of *Fagus*. Only known from the type locality in Italy.

Notes: *Parvodontia* was introduced with *P. luteocystidia* as the only species (Hjortstam & Ryvarden 2004). Later, three more species were added, viz. *P. albocrustacea* from Brazil (Baltazar *et al*. 2016), *P. austrosinensis* from China (Li *et al*. 2022), and *P. relampaga* from Southeast USA (Paez *et al*. 2024). All species have gloeocystidia with more or less yellowish contents and small elliptical basidiospores. The type species and *P. albocrustacea* are monomitic while the other two species have skeletal hyphae that are branched in *P. austrosinensis* and unbranched in *P. relampaga*. *Parvodontia gloeocystidiata* shares with *P. austrosinensis* the presence of skeletal hyphae but gloeocystidia are thin-walled in the former and thick-walled in the latter. As indicated by Gorjón & Saitta (2014), the placement in *Leptocorticium* was provisional in absence of molecular data.

Phaeophlebiopsis roumeguerei (Bres.) K.H. Larss. & Ryvarden, ***comb. nov*.** MycoBank MB 857622. Fig. 1F.
Basionym: *Corticium roumeguerei* Bres., *Fung. Trident*. **2**(8–10): 36. 1892.
Synonyms: *Peniophora moelleriana* Bres. ex Sacc., *Bol. Soc. Broteriana*, sér. **1**(11): 13. 1893. *Typus*: **Portugal**, Coimbra, Coimbra, Choupal National Forest, on *Eucalyptus globulus*, Feb. 1891, *A. Möller* (**holotype**, designated here, S F15831, MBT 10024921, studied).
Kneiffia subascondita Bres., *Ann. Mycol.* **1**: 102. 1903.

Typus: **France**, Haute-Garonne, Toulouse, winter 1878, *C. Roumeguère* Fungi Selecti Gallici 506 (**lectotype** of *Corticium roumeguerei*, designated here, S F204886, MBT 10024908, studied).

Additional materials examined: **France**, Pyrenées orientales, Argèles-sur-Mer, Forêt dominicile des Albères, La Vallée Heureuse, along track to Ribera del Tallot d'en Bac, on frondose wood, 3 Nov. 2008, *K.H. Larsson* 13759, GB. **Italy**, Tuscany, Florence, Boboli Gardens, on frondose wood, Sep. 1890, *U. Martelli*, paratype of *Corticium roumeguerei*, S F204885. **Portugal**, Minho, Parque Nacional de Peneda-Geres, Terras de Bouro, Camp de Geres, via Romana, on deciduous wood, 1 May 1989, *K. Hjortstam* 17087, GB. **Spain**, Canary Islands, Tenerife, Anaga Mountains, along road Las Mercedes – Bailadero, on *Erica*, 7 Mar. 1989, *N. Hallenberg* 10963, GB-0161379.

Illustration: Eriksson *et al*. (1981; as *Phlebiopsis roumeguerei*).

Description: *Basidiomata* resupinate, closely adnate, effused and sometimes large, varying in thickness, up to 1 mm or even more, hymenium pale whitish to dark ochraceous or with a reddish tint, in old basidiomata densely cracked, margin abrupt. *Hyphal system* monomitic, hyphae 2–4 µm, with thin walls in the hymenial part, otherwise somewhat thick-walled, densely interwoven but the hyphal direction is mainly vertical, subhymenium stratified, subiculum hardly

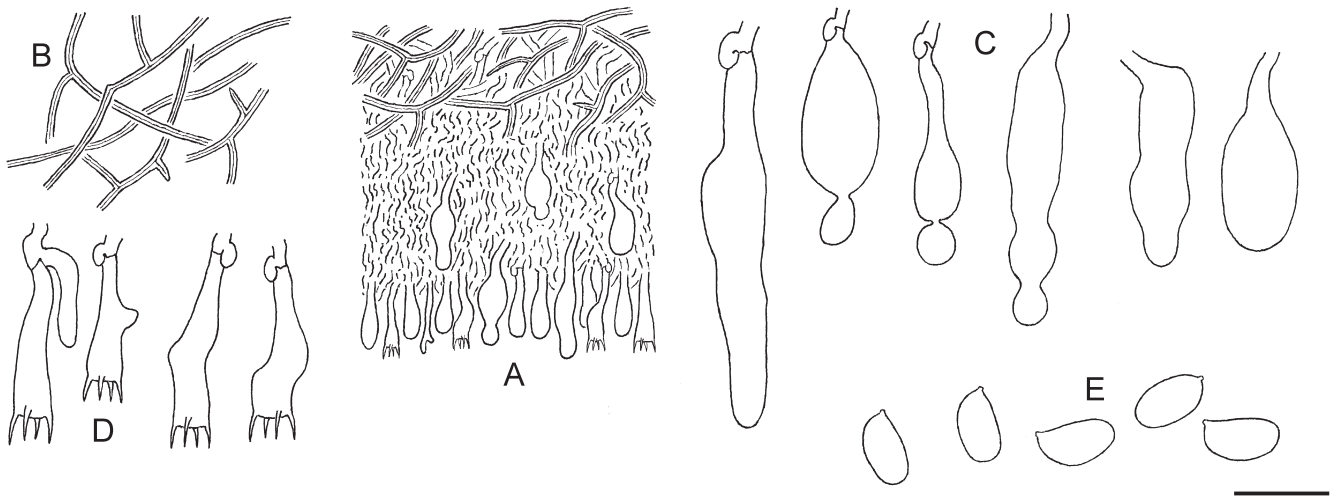

Fig. 9. *Parvodontia gloeocystidiata* [isotype (GB)]. **A.** Skeletal hyphae from subiculum. **B.** Section through basidioma. **C.** Gloeocystidia. **D.** Basidia. **E.** Basidiospores. Scale bars A, B = 20 µm; C, D = 10 µm; E = 5 µm.

© 2025 Westerdijk Fungal Biodiversity Institute

discernible. *Cystidia* numerous, conical, (50–)70–100 × 10–15 µm, apically encrusted, projecting to half the length, thick-walled with a central capillary lumen, basally smooth, with somewhat thickened walls. *Basidia* narrowly clavate, 18–22(–30) × 4–5 µm, apically widened, with four sterigmata. *Basidiospores* oblong to narrowly elliptical, (4.2–)4.3–5.6(–5.8) × (2.0–)2.4–3.4(–3.8) µm, L = 5.0 µm, W = 2.9 µm, Q = 1.75, adaxial side straight or slightly concave, smooth, thin-walled, without reaction in Melzer's or Cotton Blue.

Ecology and distribution: On decayed wood of broadleaved trees, on twigs, branches as well as on trunks. Known with certainty from South and West Europe and from Canary Islands.

Notes: This species is often treated as a younger synonym of *Peniophora ravenelii*, described from South Carolina, United States. According to the original description, *P. ravenelii* has decidedly shorter cystidia. Cooke (1879) reported the cystidium length as 30–35 µm; similarly, Burt (1925) gives measurements as 30–40 µm. In contrast, *P. roumeguerei* has cystidia that measure (50–)70–100 µm. DNA sequences from American specimens identified as *P. ravenelii* do not match any sequences from European material. Chen *et al*. (2021) and Zhao *et al.* (2021) showed that *P. ravenelii* clusters in the *Phaeophlebiopsis* clade. They used two sequences generated from specimens collected from Canary Islands and France, respectively. We studied the specimen from Canary Islands and found that it has the long cystidia typical for *P. roumeguerei*. As pointed out by Floudas & Hibbett (2015), the identity of *Peniophora ravenelii* remains unclear.

Quasiphlebia canadensis (W.B. Cooke) K.H. Larss., ***comb. nov.*** MycoBank MB 857623. Fig. 10.
Basionym: *Phlebia canadensis* W.B. Cooke, *Mycologia* **48**(3): 398. 1956.
Synonym: *Quasiphlebia densa* C.C. Chen & Sheng H. Wu, *Fungal Diversity* **111**: 391. 2021.

Typus: **Canada**, Ontario, Lake Timagami, Long Point, on *Acer spicatum*, 16 Aug. 1939, *H.S. Jackson* (**holotype** TRTC 18156, studied).

Additional materials examined: **Norway**, Akershus, Oslo, Sørkedalen, Kjellertjern, on angiosperm wood, 30 Sep. 1983, *K.H. Larsson* 4460, GB; Sogn og Fjordane, Luster, Mørkris, on *Corylus avellana*, 29 May 1979, *J-H. Støverud* 791/99, O-F-120446; Vestfold, Sandefjord, Råstad, on *Salix* sp., 10 Dec.

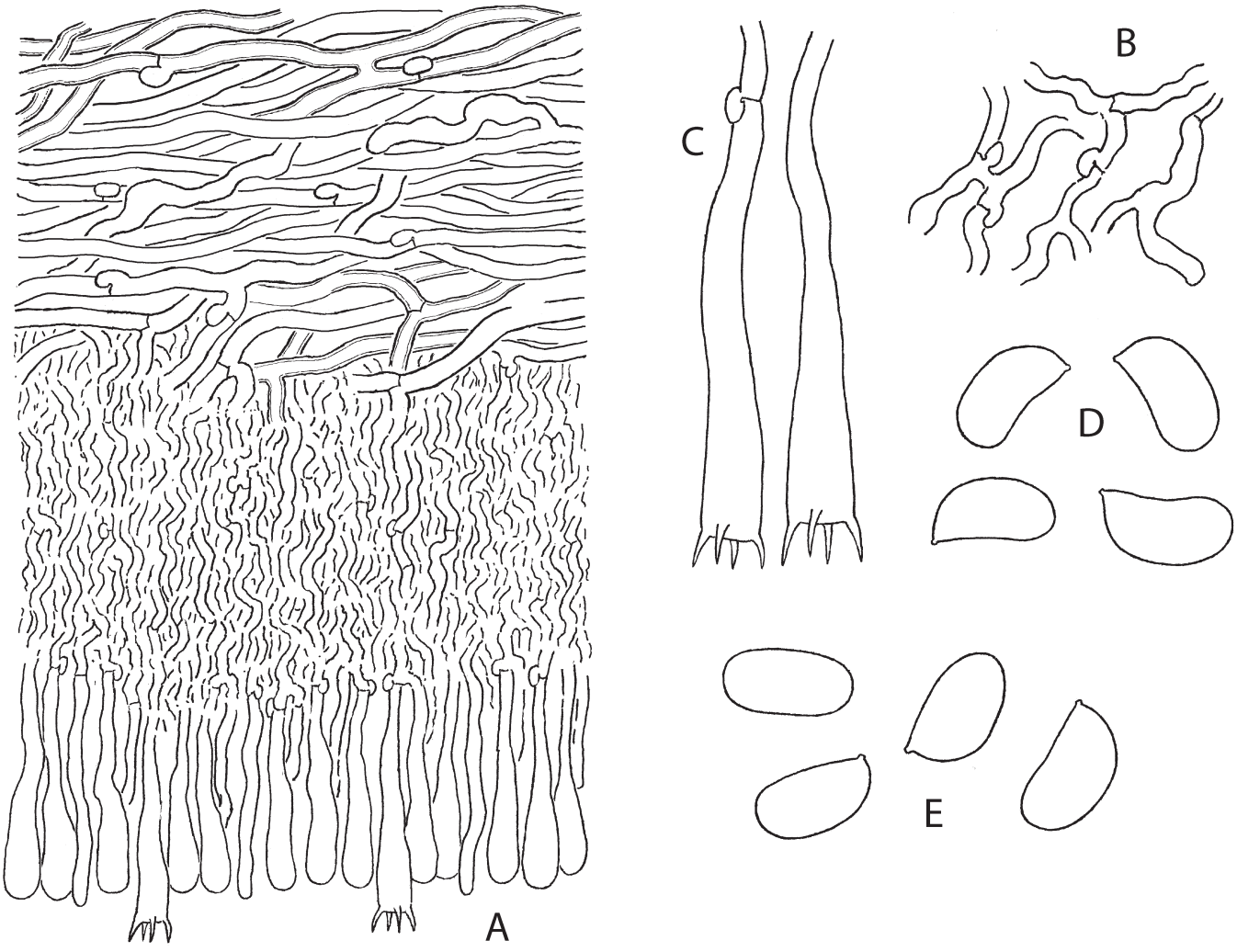

Fig. 10. *Quasiphlebia canadensis*. **A.** Section through basidioma. **B.** Subicular hyphae. **C.** Basidia. **D, E.** Basidiospores. A–D from P. Marstad 343-11 (O); E from isotype of *Phlebia canadensis* (GB). Scale bars: A, B = 20 µm; C = 10 µm; D, E = 5 µm.

© 2025 Westerdijk Fungal Biodiversity Institute

2011, *P. Marstad* 343-11, O. **Sweden**, Dalarna, Garpenberg, Hässlen, on *Corylus avellana*, 8 Sep. 1968, *I. Nordin* 4572, GB-0087227; Lappland, Torne Lappmark, Jukkasjärvi, Abisko, at Nissanjokk, on *Salix* sp., 3 Aug. 1928, *J.A. Nannfeldt* 1547, GB-0114826; ibid., Tornehamn, E of Ruonajaurats, on *Betula tortuosa*, 22 Aug. 1960, *J. Eriksson* 4430, GB-0206024; Norrbotten, Nedertorneå, Kurkisviken, on *Alnus incana*, 26 Aug. 1960, *J. Eriksson* 9330, GB-0095232; Skåne, Sturup, close to Ekholmssjön, on *Ulmus glabra*, 3 Apr. 2004, *S. Svensson* SSE04004, GB-0095231.

Description: *Basidiomata* resupinate, effused, closely adnate, firm ceraceous, hymenium smooth to tuberculate, often with radiating ridges, especially in marginal areas, orange reddish to violaceous or pale brown to brown, margin fimbriate, sometimes somewhat elevated. *Hyphal system* monomitic, all septa with clamps, subicular hyphae firm-walled, distinct, winding and somewhat irregular, 3–5(–6) µm wide, extending horizontally over the substrate, forming a dense but not agglutinated, white tissue, often with coarse crystals present, subhymenium composed of densely united, thin-walled, richly branched 2–2.5 µm wide hyphae, individual hyphae difficult to observe. *Hyphidia*, or rather hyphal ends, common in the hymenium, 30–40 × 2–2.5 µm, thin-walled, apically sometimes hooked or even branched. *Basidia* narrowly clavate, 30–40 × 5–6 µm, with four sterigmata and a basal clamp, soon collapsing after spore discharge. *Basidiospores* elliptical, often with a slightly concave adaxial side and then almost reniform, (4.0–)4.3–5.1(–5.4) × (2.2–)2.5–2.8(–3.2) µm, L = 4.5 µm, W = 2.6 µm, Q = 1.75, smooth, thin-walled, without reaction in Melzer's or Cotton Blue.

Ecology and distribution: On decaying wood of a variety of broadleaved trees. Reported from *Acer*, *Alnus*, *Betula*, *Corylus*, *Quercus*, *Salix*, *Ulmus*, and unidentified angiosperms. Described from Canada and reported from USA, Taiwan, Norway and Sweden. Probably widespread but often misidentified as *Phlebia albida* (see *Stereophlebia pendula* below).

Notes: *Phlebia canadensis* has mostly been treated as a synonym to *Phlebia albida* (Eriksson *et al*. 1981, Ginns & Lefebvre 1993), although the smaller basidiospores were noticed. However, Nakasone (1996) did not accept this synonymy. Despite the striking morphological similarity of *P. albida* (= *Stereophlebia pendula*, see below) and *Quasiphlebia canadensis* these two species are not closely related. *Quasiphlebia canadensis* is firmly placed within the *Donkia* subclade in *Phanerochaetaceae* whereas *Phlebia albida* belongs to a different subclade together with *Gelatinofungus brunneus*.

European specimens of *Quasiphlebia canadensis* differ by one substitution and one deletion in ITS2 region from Asian and American specimens. We consider these differences to be a geographically structured infraspecific variation.

Rhizochaete galactites (Bourdot & Galzin) K.H. Larss. & Spirin, ***comb. nov.*** MycoBank MB 857624. Fig. 1G.
Basionym: *Corticium rhodoleucum* subsp. *galactites* Bourdot & Galzin, *Hyménomyc. de France*: 189. 1928.
Synonym: *Phanerochaete galactites* (Bourdot & Galzin) J. Erikss. & Ryvarden, *Cort. N. Europe* **5**: 1005. 1978.

Materials examined. **France**, Allier, Château-Charles, on *Pinus* sp., 23 Aug. 1905, *H. Bourdot* 5107, PC; Aveyron, Vinnac, on *Pinus* sp., 29 Nov. 1912, *A. Galzin* (Bourdot 9210, UPS F-1033348); *ibid*., Bourdot 9211, UPS F-1033413. **Russia**, Nizhny Novgorod Reg., Lukoyanov Dist., Razino, on *Pinus sylvestris*, 30 Jul. 2017, *V. Spirin* 11261, H; *ibid*. 27 Jul. 2018, *V. Spirin* 12070, H. **Sweden**, Öland, N. Möckleby par., S of Dörby, close to the shooting range, on *Pinus sylvestris*, 20 Sep. 2005, *K. Hjortstam* 18924, GB-0112026.

Illustration: Eriksson *et al*. (1978; as *Phanerochaete galactites*).

Description: *Basidiomata* resupinate, effused, loosely attached to the substrate and more or less detachable, membranous, 0.1–0.4 mm thick, hymenium smooth, soft and tender when alive, when dried brittle and cracking,

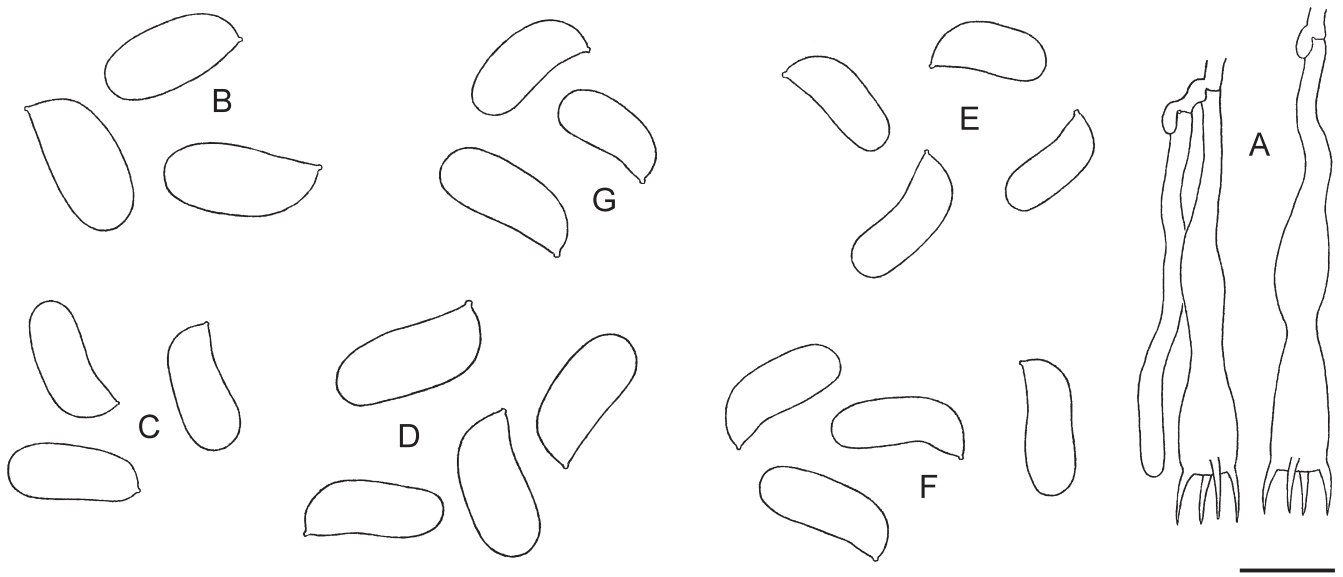

Fig. 11. *Stereophlebia pendula*. **A.** Basidia and hyphidium. **B–G.** Basidiospores. A from O. Miettinen 24536 (H); B from K.H. Larsson 15159 (GB); C from *Grandinia tuberculata*, type (K); D from *Radulum pallidum*, type (K); E from *Stereum subcostatum*, isolectotype (GB); F from *Stereophlebia pendula*, epitype (H); G from O. Miettinen 24536 (H). Scale bars: A = 10 µm; B–G = 5 µm.

© 2025 Westerdijk Fungal Biodiversity Institute

showing the white subiculum, hymenium at first white then turning cream-coloured or finally more or less ochraceous to isabelline, margin variable but usually more or less fibrillose, hyphal cords present in subiculum and extending beyond the basidioma margin, also emerging from the margin itself. *Hyphal system* monomitic, subicular hyphae mostly 3–5(–7) µm wide, narrower ones thin-walled, wider hyphae somewhat thick-walled, wider hyphae with occasional clamps, but no clamp whorls, hyphal cords up to 0.5 mm wide, with 3–15(–20) µm wide hyphae, sometimes embedded in an oily matter, subhymenial hyphae 2–3 µm, thin-walled, richly branched, crystals often present in old specimens, hyphal cords extending from the basidioma margin do not contain clamped or very wide hyphae. *Cystidia* few, or seemingly absent, cylindrical, blunt, mostly 30–45 × 6–10 µm, covered by fine-grained crystals, encrusted part 15–40 µm, thin-walled, embedded or projecting, easily crushed in microscope preparations and then only visible as lumps of crystals. *Basidia* subclavate, 25–30 × 4–5 µm, with four sterigmata. *Basidiospores* narrowly elliptical to subcylindrical, (4.2–)4.3–5.3 × (2.0–)2.1–2.5(–2.7) µm, L = 4.6 µm, W = 2.3 µm, Q = 2.01, adaxial side slightly convex, straight or somewhat concave, smooth, thin-walled, without reaction in Melzer's or Cotton Blue.

Ecology and distribution: On decaying wood on the ground. Most specimens have been collected on *Pinus* spp. but it is also reported from *Juniperus*, *Abies*, *Populus*, and *Quercus*. Scattered throughout Europe and always rare. Originally described from France and perhaps more common in West Europe.

Notes: Eriksson *et al*. (1978) observed that it was not always possible to find cystidia. In the original material they studied, for example in the selected lectotype (Bourdot 5108, herb PC), no cystidia were found, whereas in Scandinavian specimens cystidia could usually be demonstrated. Burdsall (1985) accepted only acystidiate specimens in *Phanerochaete galactites* and placed specimens with cystidia in *P. subiculosa*. Burdsall (1985) cited Bourdot 9211 among the collections of *P. subiculosa* he had examined, while Bourdot 9210 from the same date and place was cited as *P. galactites*. We studied both collections and conclude that they are conspecific and belong to *P. galactites*. Most likely, *P. subiculosa* is not a member of the European funga.

Stereophlebia pendula (Fr.) K.H. Larss., ***comb. nov.*** MycoBank MB 857629. Figs 1H, 11.
Basionym: *Radulum pendulum* Fr., *Elench. Fung*. **1**: 149. 1828. nom. sanct. [Fries, op. cit.].
Synonyms: *Grandinia tuberculata* Berk. & M.A. Curtis, *Hooker's J. Bot. Kew Gard. Misc*. **1**: 237. 1849. *Typus*: **USA**, South Carolina, on *Carya*, *Curtis* 1111 (**holotype** K, studied).
Phlebia albida H. Post, in Fries, *Monogr. Hymenomyc. Suec.* (Upsaliae) **2**(2): 280. 1863. *Typus*: **Sweden**, Östergötland, Skedevi, Rejmyra, on wood, 5 Nov. 1862, *H. von Post* (**lectotype** S F15542, selected by Eriksson *et al.* 1981).
Radulum pallidum Berk. & M.A. Curtis, *Grevillea* **1**(no. 10): 145. 1873. *Typus*: **USA**, South Carolina, on bark of *Carya*, No. 2599 (**holotype** K, studied).
Stereum subcostatum P. Karst., *Hedwigia* **20**: 178. 1881. *Typus*: **Finland**, Mustiala, in ramos dejectos arbor. frond., 10 Oct. 1881, *P.A. Karsten* (**lectotype** H; **isolectotype** GB, studied).

Typus: **Sweden**. Östergötland, Skedevi par., Rejmyra, 30 Oct. 1862, drawn by von Post and P. Åkerlund, "*direxit et approbavit* E. Fries" (**neotype** of *Radulum pendulum*, designated here, S S1142, https://herbarium.nrm.se/specimens/S1142, MBT 10024833). **Finland**, Inari Lappin, Inari, Muotkatunturin erämaa, Soavveljávrecopma, on *Betula pubescens*, 27 Aug. 2020, *O. Miettinen* 23860.2 (**epitype** designated here, H 6200339, MBT 10024834). ITS GenBank accession PQ013071.

Additional materials examined: **Denmark**, Greenland, Narssarssuaq valley, on branch of *Betula*, Aug. 1991, *V. Mukhin*, GB-0181519. **Finland**, Oulun Pohjanmaa, Oulu, Metsokangas, on *Betula* sp., 30 Oct. 2021, *M. Kulju* 78/21, OULU; Uusimaa, Helsinki, Haltiala, on fallen *Betula* branch, 2 Jan. 2021, *O. Miettinen* 24536, H 6200089. **Russia**. Nizhny Novgorod Reg., Lukoyanov Dist., Razino, on *Tilia cordata*, 30 Jul. 2019, *V. Spirin* 12778, H 7068342. **Spain**, Madrid, Ontigola, SE of Aranjues, on *Salsola vermicularis*, 4 Mar. 2011, *E. Larsson* 29-11, GB; Madrid, Pioz, on angiosperm wood, 31 Oct. 2011, *K.H. Larsson* 15159. **USA**, Washington, Pend Oreille County, Slate Creek, on *Corylus cornuta*, 15 Oct. 2014, *V. Spirin* 8566, H 7047608.

Description: *Basidiomata* resupinate, effused to effused-reflexed, membranous, hymenium smooth to tuberculate, sometimes with radiating ridges near the margin, cream to ochraceous to pale orange reddish, pileus surface smooth with adpressed hyphae, white, margin white, finely fimbriate. *Hyphal system* monomitic, septa with clamps, subicular hyphae firm-walled to thick-walled, distinct, 3–5.5 µm, rather straight, uniform, often with a grainy incrustation, subhymenial hyphae thin-walled, richly branched, 2–3.5(–5) µm, rather densely united. *Hyphidia* or hyphal ends common in hymenium, of hyphal width, mostly tapering towards apex, 20–40 × 2.5–3.5 µm. *Basidia* narrowly clavate, 35–40 × 5–6 µm, with four sturdy sterigmata up to 7 µm long, with a basal clamp. *Basidiospores* narrowly elliptical to cylindrical, often slightly bent near apiculus, (5.6–)5.7–7.1(–7.4) × (2.5–)2.7–3.3(–3.5) µm, L = 6.3 µm, W = 3,0 µm, Q = 2.15. smooth, thin-walled, without reaction in Melzer's or Cotton Blue.

Ecology and distribution: On angiosperm wood, often on thin branches and twigs, observed on many different tree species, also on bushes like *Salsola vermicularis*. Found from Mediterranean steppe-vegetation to alpine *Betula* forest and *Salix* thickets. Recorded in many regions of the Northern Hemisphere but seemingly with an uneven presence.

Notes: A surprisingly variable species and therefore often misidentified. *Phlebia albida* was introduced by Fries (1863), who attributed the species to Hampus von Post, a Swedish botanist, chemist and geologist that contributed many fungal specimens to Fries. A specimen collected by von Post in 1862 is selected as lectotype (Eriksson *et al*. 1981, Nakasone 1996). Several names have been suggested as synonyms of *P. albida* (Nakasone 1996). Of these synonyms, for which

© 2025 Westerdijk Fungal Biodiversity Institute

type specimens are preserved, the oldest is *Grandinia tuberculata*. Using this epithet the species has recently been referred to a separate genus as *Stereophlebia tuberculata*, however, without discussing the suggested synonomy with *Phlebia albida* (Zmitrovich 2018).

Basidiomata of *Phlebia albida* have a variable configuration and a variable colour and also show variation in spore morphology. They can be completely effused but also develop more or less distinct pilei. The hymenium can be smooth, radially veined or more or less strongly tuberculate. Hymenium colour varies from cream to ochraceous or orange-red. The micromorphology is fairly simple with a monomitic hyphal system, clamped hyphae, narrowly clavate basidia, and cylindrical, thin-walled, smooth basidiospores. Spores are mostly cylindrical with a more or less distinct bend close to apiculus. However, two Spanish specimens have elliptical spores (Fig. 11). Their ITS sequence differs slightly, why it is possible that further studies of other markers will reveal them as a separate species.

In his sanctioning work Fries (1828) described *Radulum pendulum*, a name that was interpreted as a synonym of *Phlebia albida* (Bresadola 1903, Bourdot & Galzin 1928, Boidin 1958). There is no authentic material of *R. pendulum* and for this reason the name was treated as a nomen dubium (Nakasone 1996). However, the lack of type material has not prevented Friesian names from being given a modern interpretation, especially when it is possible to follow a tradition.

Fries (1828) describes a fungus that breaks through the bark on *Alnus* twigs and develops narrow, azonate, pubescent pilei. The species has a soft coriaceous consistency and a tuberculate hymenium with a milk-white colour, eventually becoming rimose. The context is soft and white and tubercles sometimes grow to the size of a teeth. Fries compares his new species with *Thelephora hirsuta* (≡ *Stereum hirsutum*) but points to the erumpent growth as a difference.

Because his species concept is based primarily on macroscopic characters, Fries (1863) introduced the new species *Phlebia albida* for a collection by von Post (the lectotype) that was entirely resupinate without a pileus.

According to the nomenclatural rules a type should first of all be selected among original materials. In the case of *Phlebia albida*, the protologue refers to an icon preserved in the Stockholm herbarium that was drawn from a specimen collected in November 1861 from Rejmyra where von Post lived. Although the specimen selected as lectotype was not mentioned in the protologue, it was collected and annotated by von Post in 1862 before the publication of the species in 1863. It can reasonably be regarded as original material and is preferrable as type compared to the icon.

In the case of *Radulum pendulum* we choose the icon in herb. S as neotype since it is the only material that is connected to Fries. We supplement this neotype with an epitype based on a recently collected and sequenced specimen from Finland.

Conflict of interest: The authors declare that they have no conflict of interest.

REFERENCES

Ayres DL, Darling A, Zwickl DJ, *et al*. (2012). BEAGLE: an application programming interface and high-performance computing library for statistical phylogenetics. *Systematic Biology* **61**: 170–173. https://doi.org/10.1093/sysbio/syr100

Baltazar JM, da Silveira RMB, Rajchenberg M (2016). Type studies of J. Rick's corticioid homobasidiomycetes (*Agaricomycetes, Basidiomycota*) housed in the Herbarium Anchieta (PACA). *Phytotaxa* **255**: 101–132. https://doi.org/10.11646/phytotaxa.255.2.1

Boidin J (1958). Essai biotaxonomique sur les hydnés résupinés et les corticiés. *Revue Mycologique. (Paris), Mémoire hors-série* **6**: 1–388.

Bourdot H, Galzin A (1909). Hyménomycètes de France. (I. Hétérobasidiés). *Bulletin de la Société Mycologique de France* **25**: 15–36.

Bourdot H, Galzin A (1928). *Hyménomycètes de France*. Sceaux.

Brazee NJ, Lindner DL, Fraver S, *et al.* (2012). Wood-inhabiting, polyporoid fungi in aspen-dominated forests managed for biomass in the US Lake States. *Fungal Ecology* **5**: 600–609. https://doi.org/10.1016/j.funeco.2012.03.002

Bresadola G (1903). Fungi polonici a cl. viro B. Eichler lecti. *Annales Mycologici* **1**: 65–96.

Burdsall HH (1985). A contribution to the taxonomy of the genus *Phanerochaete* (*Corticiaceae, Aphyllophorales*). *Mycologia Memoir* **10**: 1–165.

Burt EA (1925). The *Thelephoraceae* of North America XIV. *Annals of the Missouri Botanical Garden* **12**: 213–357.

Chen CC, Chen CY, Lim YW, *et al.* (2020). Phylogeny and taxonomy of *Ceriporia* and other related taxa and description of three new species. *Mycologia* **112**: 64–82. https://doi.org/10.1080/00275514.2019.1664097

Chen CC, Chen CY, Wu SH. (2021). Species diversity, taxonomy and multigene phylogeny of phlebioid clade (*Phanerochaetaceae*, *Irpicaceae*, *Meruliaceae*) of *Polyporales*. *Fungal Diversity* **111**: 337–442. https://doi.org/10.1007/s13225-021-00490-w

Chen CC, Wu SH, Chen CY (2018) *Hydnophanerochaete* and *Odontoefibula*, two new genera of phanerochaetoid fungi (*Polyporales, Basidiomycota*) from East Asia. *MycoKeys* **39**: 75–96. https://doi.org/10.3897/mycokeys.39.28010

Chernomor O, von Haeseler A, Minh BQ (2016). Terrace aware data structure for phylogenomic inference from supermatrices. *Systematic Biology* **65**: 997–1008. https://doi.org/10.1093/sysbio/syw037

Chikowski RS, Larsson K-H, Gibertoni TB (2016). Three new combinations in *Rhizochaete* (*Agaricomycetes*, *Fungi*) and a new record to the Brazilian Amazonia. *Nova Hedwigia* **102**: 185–196. https://doi.org/10.1127/nova_hedwigia/2015/0298

Cooke MC (1879). On *Peniophora*. *Grevillea* **8**(no 45): 17–21.

Crous PW, Osieck ER, Jurjevi Ž, *et al.* (2021). Fungal Planet description sheets: 1284–1382. *Persoonia* **47**: 178–384. https://doi.org/10.3767/persoonia.2021.47.06

Dereeper A, Guignon V, Blanc G, *et al.* (2008). Phylogeny.fr: robust phylogenetic analysis for the non-specialist. *Nucleic Acids Research* **36**, issue suppl_2, 1: W465–469. https://doi.org/10.1093/nar/gkn180

Donk MA (1964). A conspectus of the families of *Aphyllophorales*. *Persoonia* **3**: 199–324.

© 2025 Westerdijk Fungal Biodiversity Institute

Duhem B, Michel H (2007). Une espèce nouvelle de *Phlebia* possédant des fibres arboriformes. *Cryptogamie, Mycologie* **28**: 29–38.

Dvorák D, Beták J, Tomsovský M (2014). *Aurantioporus alborubescens* (*Basidiomycota*, *Polyporales*) – first record in the Carpathians and notes on its systematic position. *Czech Mycology* **66**: 71–84.

Eriksson J, Hjortstam K, Ryvarden L (1978). *Corticiaceae of North Europe*, vol. 5. Fungiflora, Oslo.

Eriksson J, Hjortstam K, Ryvarden L (1981). *Corticiaceae of North Europe*, vol. 6. Fungiflora, Oslo.

Eriksson J, Ryvarden L (1973). *Corticiaceae of North Europe*, vol. 2. Fungiflora, Oslo.

Floudas D, Hibbett DS (2015). Revisiting the taxonomy of *Phanerochaete* (*Polyporales, Basidiomycota*) using a four gene dataset and extensive ITS sampling. *Fungal Biology* **119**: 679–719. https://doi.org/10.1016/j.funbio.2015.04.003

Fries E (1821). *Systema Mycologicum*, vol. 1. Lund (Lundae).

Fries E (1828). *Elenchus Fungorum*, vol. 1. Greifswald (Gryphiswaldiae).

Fries E (1838). *Epicrisis Systematis Mycologici*. Lund (Lundae).

Fries E (1863) *Monographia Hymenomycetum Sueciae* **2**: 1–355. Uppsala (Upsaliae).

Garbelotto MM, Lee HK, Slaughter G, *et al.* (1997). Heterokaryosis is not required for virulence of *Heterobasidion annosum*. *Mycologia* **89**: 92–102. https://doi.org/10.1080/00275514.1997.12026759

Gardes M, Bruns TD (1993). ITS primers with enhanced specificity for basidiomycetes - application to the identification of mycorrhizae and rusts. *Molecular Ecology* **2**: 113–118. https://doi.org/10.1111/j.1365-294X.1993.tb00005.x

Ghobad-Nejhad M, Hallenberg N (2012). Multiple evidence for recognition of *Phlebia tuberculata*, a more widespread segregate of *Phlebia livida* (*Polyporales*, *Basidiomycota*). *Mycological Progress* **11**: 27–35. https://doi.org/10.1007/s11557-010-0722-1

Ginns JH (1971). The genus *Merulius* V. Taxa proposed by Bresadola, Bourdot & Galzin, Hennings, Rick, and others. *Mycologia* **63**: 800–818.

Ginns JH (1976). *Merulius*: s.s. and s.l., taxonomic disposition and identification of species. *Canadian Journal of Botany* **54**: 100–167.

Greslebin AG, Nakasone KK, Rajchenberg M. (2004). *Rhizochaete*, a new genus of phanerochaetoid fungi. *Mycologia* **96**: 260–271. https://doi.org/10.1080/15572536.2005.11832976

Guindon S, Dufayard J-F, Lefort V, *et al.* (2010). New algorithms and methods to estimate maximum-likelihood phylogenies: Assessing the performance of PhyML 3.0. *Systematic Biology* **59**: 307–321. https://doi.org/10.1093/sysbio/syq010

Hallenberg N (1988). Species delimitation in *Corticiaceae* (*Basidiomycetes*). *Mycotaxon* **31**: 445–465.

Hallenberg N (1991). Pairing tests with species of *Aphyllophorales* (*Basidiomycetes*) from two phytogeographically isolated areas. *Mycotaxon* **42**: 355–386.

Hallenberg N, Larsson E (1991). Differences in cultural characters and electrophoretic patterns among sibling species in four different species complexes (*Corticiaceae*, *Basidiomycetes*). *Mycologia* **83**: 131–141. https://doi.org/10.1080/00275514.1991.12025989

Hallenberg N, Larsson E (1993). On taxonomy of *Phlebia livida*. *Mycological Research* **97**: 351–354. https://doi.org/10.1016/S0953-7562(09)81135-0

Hjortstam K (1987). A check-list to genera and species of corticioid fungi (*Hymenomycetes*). *Windahlia* **17**: 55–85.

Hjortstam K (1995). Two new genera and some new combinations of corticioid fungi (*Basidiomycotina*, *Aphyllophorales*) from tropical and subtropical areas. *Mycotaxon* **54**: 183–193.

Hjortstam K, Ryvarden L (1990). *Lopharia* and *Porostereum* (*Corticiaceae*). *Synopsis Fungorum* **4**: 1–68.

Hjortstam K, Ryvarden L (2004). Some new tropical genera and species of corticioid fungi (*Basidiomycotina, Aphyllophorales*). *Synopsis Fungorum* **18**: 20–32.

Hoang DT, Chernomor O, von Haeseler A, *et al.* (2018). UFBoot2: Improving the ultrafast bootstrap approximation. *Molecular Biology and Evolution* **35**: 518–522. https://doi.org/10.1093/molbev/msx281

Hopple Jr JS, Vilgalys R (1999). Phylogenetic relationships in the mushroom genus *Coprinus* and dark-spored allies based on sequence data from the nuclear gene coding for the large ribosomal subunit RNA: divergent domains, outgroups, and monophyly. *Molecular Phylogenetics and Evolution* **13**: 1–19. https://doi.org/10.1006/mpev.1999.0634

Höhnel F von, Litschauer V (1908). Beiträge zur Kenntnis der Corticieen III. *Sitzungsberichten der kaiserliche Akademie der Wissenschaften in Wien, Mathem.-Naturw. Klasse* **117**(1): 1082–1124.

Jang Y, Jang S, Min M, *et al.* (2015). Comparison of the diversity of Basidiomycetes from dead wood of the manchurian fir (*Abies holophylla*) as evaluated by fruiting body collection, mycelial isolation, and 454 sequencing. *Microbial Ecology* **70**: 634–645. https://doi.org/10.1007/s00248-015-0616-5

Jia BS, Zhou LW, Cui BK, *et al.* (2014). Taxonomy and phylogeny of *Ceriporia* (*Polyporales*, *Basidiomycota*) with an emphasis of Chinese collections. *Mycological Progress* **13**: 81–93. https://doi.org/10.1007/s11557-013-0895-5

Jung PE, Lee H, Wu S-H, *et al.* (2018). Revision of the taxonomic status of the genus *Gloeoporus* (*Polyporales*, *Basidiomycota*) reveals two new species. *Mycological Progress* **17**: 855–863. https://doi.org/10.1007/s11557-018-1400-y

Justo A, Hibbett DS (2011). Phylogenetic classification of *Trametes* (*Basidiomycota*, *Polyporales*) based on a five-marker dataset. *Taxon* **60**: 1567–1583. https://doi.org/10.1002/tax.606003

Justo A, Miettinen O, Floudas D, *et al.* (2017). A revised family-level classification of the *Polyporales* (*Basidiomycota*). *Fungal Biology* **121**: 798–824. https://doi.org/10.1016/j.funbio.2017.05.010

Kalyaanamoorthy S, Minh BQ, Wong TKF, *et al.* (2017). ModelFinder: Fast model selection for accurate phylogenetic estimates. *Nature Methods* **14**: 587–589. https://doi.org/10.1038/nmeth.4285

Katoh K. Standley DM (2013). MAFFT multiple sequence alignment software version 7: improvements in performance and usability. *Molecular Biology and Evolution* **30**(4): 772–780. https://doi.org/10.1093/molbev/mst010

Kuuskeri J, Mäkelä MR, Isotalo J, *et al.* (2015). Lignocellulose-converting enzyme activity profiles correlate with molecular systematics and phylogeny grouping in the incoherent genus *Phlebia* (*Polyporales*, *Basidiomycota*). *BMC Microbiology* 15: 217. https://doi.org/10.1186/s12866-015-0538-x

Larsson A (2014). AliView: a fast and lightweight alignment viewer and editor for large datasets. *Bioinformatics* **30**: 3276–3278. https://doi.org/10.1093/bioinformatics/btu531

Larsson K-H (2007). Re-thinking the classification of corticioid fungi. *Mycological Research* **111**: 1040–1063. https://doi.org/10.1016/j.mycres.2007.08.001

© 2025 Westerdijk Fungal Biodiversity Institute

Larsson K-H, Ryvarden L (2021). Corticioid fungi of Europe vol 1. *Synopsis Fungorum* **43**: 1–266.

Li Y, Cao Y, Nakasone KK, *et al.* (2025). Species diversity, taxonomy, multi-gene phylogeny and divergence times of *Meruliaceae* (*Polyporales*, *Basidiomycota*). *Mycology*, https://doi.org/10.1080/21501203.2024.2443216.

Li Y, Nakasone KK, Chen CC, *et al*. (2022) Taxonomy and phylogeny of *Cystostereaceae* (*Agaricales, Basidiomycota*): A new genus, five new species, and three new combinations. *Journal of Fungi* **8**(11): 1229. https://doi.org/10.3390/jof8111229

Lira CS, Chikowski RS, de Lima VX, *et al.* (2022). *Allophlebia*, a new genus to accommodate *Phlebia ludoviciana* (*Agaricomycetes*, *Polyporales*). *Mycological Progress* **21**(4): 47–58. https://doi.org/10.1007/s11557-022-01781-5

Liu DM, Xu YL, Li Y, *et al.* (2020). Two new species of *Hydnophlebia* (*Meruliaceae*, *Polyporales*) from China based on morphological and molecular evidence. *Phytotaxa* **477**: 35–46. https://doi.org/10.11646/phytotaxa.477.1.2

Liu S-L, Nakasone KK, Wu S-H, *et al.* (2018). Taxonomy and phylogeny of *Lopharia* s.s., *Dendrodontia*, *Dentocorticium* and *Fuscocerrena* (*Basidiomycota*, *Polyporales*). *MycoKeys* **32**: 25–48. https://doi.org/10.3897/mycokeys.32.23641

Lundell S, Nannfeldt JA (1941). *Fungi exsiccati suecici, praestertim upsaliensis*, Fasc. XX1–XX11: 1–51. Uppsala.

Lundell S, Nannfeldt JA (1947). *Fungi exsiccati suecici, praestertim upsaliensis*, Fasc. XX1X–XXX: 1–61. Uppsala.

Madeira F, Pearce M, Tivey ARN, *et al.* (2022). Search and sequence analysis tools services from EMBL-EBI in 2022. *Nucleic Acids Research* **50**(W1): W276–W279. https://doi.org/10.1093/nar/gkac240

Manjón JL, Blanco MN, Moreno G (1989). *Odonticium monfraguense sp. nov. Corticiaceae*. *Cryptogamie, Mycologie* **10**: 135–140.

Michel H, Duhem B (2003). Qu'est-ce que l'*Acia squalina* Fr. sensu Bourdot? *Cryptogamie, Mycologie* **24**: 327–338.

Miettinen O, Larsson K-H (2010). *Sidera*, a new genus in *Hymenochaetales* with poroid and hydnoid species. *Mycological Progress* **10**: 131–141. https://doi.org/10.1007/s11557-010-0682-5

Miettinen O, Spirin V, Vlasák J *et al.* (2016). Polypores and genus concepts in *Phanerochaetaceae* (*Polyporales, Basidiomycota*). *MycoKeys* **17**: 1–46. https://doi.org/10.3897/mycokeys.17.10153

Miller MA, Pfeiffer W, Schwartz T (2010). Creating the CIPRES Science Gateway for inference of large phylogenetic trees. 2010 Gateway Computing Environments Workshop (GCE), New Orleans, LA: 1–8. https://doi.org/10.1109/GCE.2010.5676129

Moncalvo JM, Vilgalys R, Redhead SA, *et al.* (2002). One hundred seventeen clades of euagarics. *Molecular Phylogenetics and Evolution* **23**: 357–400. https://doi.org/10.1016/S1055-7903(02)00027-1

Motato-Vásquez V, Westphalen M, Gugliotta A (2022). *Phlebiodontia rajchenbergii gen. et sp. nov.* (*Polyporales*, *Meruliaceae*) from the Brazilian Atlantic Forest based on morphological and molecular evidence. *Lilloa* **59**(suppl.): 305–330. https://doi.org/10.30550/j.lil/2022.59.S/2022.09.26

Nakasone KK (1996). Morphological and molecular studies on *Auriculariopsis albomellea* and *Phlebia albida* and a reassessment of *A. ampla*. *Mycologia* **88**: 762–775. https://doi.org/10.1080/00275514.1996.12026714

Nakasone KK (2008). Type studies of corticioid Hymenomycetes described by Bresadola. *Cryptogamie, Mycologie* **29**: 231–257.

Nakasone KK, Draeger KR, Ortiz-Santana B (2017). A contribution to the taxonomy of *Rhizochaete* (*Polyporales*, *Basidiomycota*). *Cryptogamie, Mycologie* **38**: 81–99. https://doi.org/10.7872/crym/v38.iss1.2017.81

Nguyen L-T, Schmidt HA, von Haeseler A, *et al.* (2015). IQ-TREE: A fast and effective stochastic algorithm for estimating maximum-likelihood phylogenies. *Molecular Biology and Evolution* **32**: 268–274. https://doi.org/10.1093/molbev/msu300

Nylander JAA (2004). *MrModeltest* v2. Program distributed by the author. Evolutionary Biology Centre, Uppsala University, Sweden.

Paez CA, Smith JA, Nakasone KK, *et al.* (2024). *Parvodontia relampaga sp. nov.*: A *Cystostereaceae* fungal pathogen that is the causal agent of relampago blight of woody plants in Florida, USA. *Fungal Biology* **128**: 1758–1770. https://doi.org/10.1016/j.funbio.2024.03.002

Parmasto E, Hallenberg N (2000). A taxonomic study of phlebioid fungi (*Basidiomycota*). *Nordic Journal of Botany* **20**: 105–118. https://doi.org/10.1111/j.1756-1051.2000.tb00740.x

Persoon CH (1800). *Observationes Mycologicae*, vol. 2. Leipzig and Luzern (Lipsiae et Lucernae).

Persoon CH (1801). *Synopsis Methodica Fungorum*, vol. 2. Göttingen (Gottingae).

Ronquist F, Teslenko M, van der Mark P, *et al.* (2012). MrBayes 3.2: Efficient Bayesian phylogenetic inference and model choice across a large model space. *Systematic Biology* **61**: 539–542. https://doi.org/10.1093/sysbio/sys029

Rosenthal LM, Larsson KH, Branco S, *et al*. (2017). Survey of corticioid fungi in North American pinaceous forests reveals hyperdiversity, underpopulated sequence databases, and species that are potentially ectomycorrhizal. *Mycologia* **109**: 115–127. https://doi.org/10.1080/00275514.2017.1281677

Saitta A, Losi C, Ambrosio E (2017). First record of *Phlebia margaritae* (*Polyporales*, *Basidiomycota*) in Italy. *Nova Hedwigia* **105**: 37–41. https://doi.org/10.1127/nova_hedwigia/2017/0398

Spirin V, Vlasák J, Rivoire B, *et al.* (2016). Studies in the *Ceriporia purpurea* group (*Polyporales*, *Basidiomycota*), with notes on similar *Ceriporia* species. *Cryptogamie, Mycologie* **37**: 421–435. https://doi.org/10.7872/crym/v37.iss4.2016.421

Spirin VA, Zmitrovich IV (2004). A contribution to the taxonomy of corticioid fungi. *Merulius* Fr., *Phlebia* Fr., and related genera (in Russian). *Novosti Sistematiki Nizshikh Rastenii* **37**: 166–188.

Talavera G, Castresana J. (2007). Improvement of phylogenies after removing divergent and ambiguously aligned blocks from protein sequence alignments. *Systematic Biology* **56**: 564–577. https://doi.org/10.1080/10635150701472164

Telleria MT, Dueñas M, Melo I, *et al.* (2010). Morphological and molecular studies of *Hyphodermella* in the Western Mediterranean area. *Mycological Progress* **9**: 585–596. https://doi.org/10.1007/s11557-010-0666-5

Telleria MT, Dueñas M, Martín MP (2017). Three new species of *Hydnophlebia* (*Polyporales*, *Basidiomycota*) from the Macaronesian Islands. *MycoKeys* **27**: 39–64. https://doi.org/10.3897/mycokeys.27.14866

Tomšovský M, Menkis A, Vasaitis R (2010). Phylogenetic relationships in European *Ceriporiopsis* species inferred from nuclear and mitochondrial ribosomal DNA sequences. *Fungal Biology* **114**: 350–358. https://doi.org/10.1016/j.funbio.2010.02.004

© 2025 Westerdijk Fungal Biodiversity Institute

Trifinopoulos J, Nguyen L-T, von Haeseler A, *et al.* (2016). W-IQ-TREE: a fast online phylogenetic tool for maximum likelihood analysis. *Nucleic Acids Research* **44**: W232–W235. https://doi.org/10.1093/nar/gkw256

Tura D, Zmitrovich IV, Wasser SP, *et al*. (2011). *Biodiversity of the Heterobasidiomycetes and non-gilled Hymenomycetes (former Aphyllophorales) of Israel*. Gantner Verlag, Ruggell.

Volobuev S, Okun M. Ordynets A, *et al.* (2015). The *Phanerochaete sordida* group (*Polyporales*, *Basidiomycota*) in temperate Eurasia, with a note on *Phanerochaete pallida*. *Mycological Progress* **14**: 80. https://doi.org/10.1007/s11557-015-1097-0

Vu D, Groenewald M, de Vries M, *et al.* (2019). Large-scale generation and analysis of filamentous fungal DNA barcodes boosts coverage for kingdom fungi and reveals thresholds for fungal species and higher taxon delimitation. *Studies in Mycology* **92**: 135–154. https://doi.org/10.1016/j.simyco.2018.05.001

Wang H, Zhao C-L (2020). *Hyphodermella aurantiaca sp. nova* (*Polyporales*, *Basidiomycota*) as evidenced by morphological characters and phylogenetic analyses. *Annales Botanici Fennici* **58**: 61–68. https://doi.org/10.5735/085.058.0110

Wang H, Gu Z-R, Zhao C-L (2021). *Hyphodermella zixishanensis* (*Polyporales*, *Basidiomycota*), a new species with reddish hymenial surface. *Nordic Journal of Botany* **39**(8): 03329. https://doi.org/10.1111/njb.03329

Westphalen MC, Rajchenberg M, Tomšovský M, *et al.* (2018). A re-evaluation of Neotropical *Junghuhnia* s.lat. (*Polyporales*, *Basidiomycota*) based on morphological and multigene analyses. *Persoonia* **41**: 130–141. https://doi.org/10.3767/persoonia.2018.41.07

White TJ, Bruns TD, Lee S, *et al.* (1990). Amplification and direct sequencing of fungal ribosomal RNA genes for phylogenetics. In: *PCR protocols: A guide to methods and applications* (Innis MA, Gelfand DH, Sinisky JJ, *et al*., eds). Academic Press, USA: 315–322.

Wu F, Yuan Y, Chen JJ, *et al.* (2016). *Luteoporia albomarginata gen. et sp. nov.* (*Meruliaceae*, *Basidiomycota*) from tropical China. *Phytotaxa* **263**: 31–41. https://doi.org/10.11646/phytotaxa.263.1.3

Wu SH (1990). The *Corticiaceae* (*Basidiomycetes*) subfamilies *Phlebioideae*, *Phanerochaetoideae* and *Hyphodermoideae* in Taiwan. *Acta Botanica Fennica* **142**: 1–123.

Wu SH, Nilsson HR, Chen CT, *et al.* (2010). The white-rotting genus *Phanerochaete* is polyphyletic and distributed throughout the phlebioid clade of the *Polyporales* (*Basidiomycota*). *Fungal Diversity* **42**: 107–118. https://doi.org/10.1007/s13225-010-0031-7

Wu SH, Wang DM, Chen YP (2018). *Purpureocorticium microsporum* (*Basidiomycota*) *gen. et sp. nov*. from East Asia. *Mycological Progress* **17**: 357–364. https://doi.org/10.1007/s11557-017-1362-5

Xavier de Lima V, Lira CS, Chikowski RS, *et al.* (2020). Additions to neotropical stereoid fungi (*Polyporales*, *Basidiomycota*): one new species of *Lopharia* and one new combination in *Phlebiopsis*. *Mycological Progress* **19**: 31–40. https://doi.org/10.1007/s11557-019-01538-7

Yuan Y, Ji XH, Wu F, *et al.* (2017). *Ceriporia albomellea* (*Phanerochaetaceae*, *Basidiomycota*), a new species from tropical China based on morphological and molecular evidences. *Phytotaxa* **298**: 20–28. https://doi.org/10.11646/phytotaxa.298.1.2

Zhao C-L, Liu S-L, Ren G-J, *et al.* (2017). Three species of wood-decaying fungi in *Polyporales* new to China. *Mycotaxon* **132**: 29–42. https://doi.org/10.5248/132.29

Zhao C-L, Qu MH, Huang RX, *et al.* (2023). Multi-gene phylogeny and taxonomy of the wood-rotting fungal genus *Phlebia* sensu lato (*Polyporales*, *Basidiomycota*). *Journal of Fungi* **9**: 320. https://doi.org/10.3390/jof9030320

Zhao C-L, Ren GJ, Wu F (2017). A new species of *Hyphodermella* (*Polyporales*, *Basidiomycota*) with a poroid hymenophore. *Mycoscience* **58**: 452–456. https://doi.org/10.1016/j.myc.2017.06.007

Zhao C-L, Wu F, Liu H-X, *et al.* (2015). A phylogenetic and taxonomic study on *Ceriporiopsis* s. str. (*Polyporales*) in China. *Nova Hedwigia* **101**: 403–417. https://doi.org/10.1127/nova_hedwigia/2015/0282

Zhao Y-N, He S-H, Nakasone KK, *et al.* (2021). Global phylogeny and taxonomy of the wood-decaying fungal genus *Phlebiopsis* (*Polyporales*, *Basidiomycota*). *Frontiers in Microbiology* **12**: 622460. https://doi.org/10.3389/fmicb.2021.622460

Zhu XT, Li YC, Wu G, *et al.* (2014). The genus *Imleria* (*Boletaceae*) in East Asia. *Phytotaxa* **191**: 81–98. https://doi.org/10.11646/phytotaxa.191.1.5

Zmitrovich IV (2018). Conspectus systematis Polyporacearum v. 1.0. *Folia Cryptogamica Petropolitana* **6**: 3–145.

Zmitrovich, IV, Malysheva VF (2014). Studies on *Oxyporus*. I. Segregation of *Emmia* and general topology of phylogenetic tree. *Mikologiya i Fitopatologiya* **48**(3): 161–171.

© 2025 Westerdijk Fungal Biodiversity Institute

© 2025 Westerdijk Fungal Biodiversity Institute

FUSE

Fungal Systematics and Evolution

VOLUME 16
DECEMBER 2025
PAGES 29–39

doi.org/10.3114/fuse.2025.16.2

Phylogeny of the genus *Volvariella* with the description of one new species and two new records from Oman

S. Hussain[1,2,3], M. Al-Kharousi[2], D. Al-Maqbali[2], A.A. Al-Owaisi[2], R. Velazhahan[1], A.M. Al-Sadi[1,4*], M.N. Al-Yahya'ei[2*]

[1]Department of Plant Sciences, College of Agricultural and Marine Sciences, Sultan Qaboos University, PO Box 34, AlKhoud 123, Sultanate of Oman
[2]Oman Animal and Plant Genetic Resources Center (Mawarid), Ministry of Higher Education, Research and Innovation, P.O. Box 515, AlKhoud 123, Muscat, Sultanate of Oman
[3]Center for Environmental Studies and Research (CESAR), Sultan Qaboos University, P.O. Box 34, AlKhoud 123, Muscat, Sultanate of Oman
[4]College of Agriculture, University of Al Dhaid, Sharjah P.O. Box 27272, United Arab Emirates

*Corresponding authors: Abdullah M. Al-Sadi, alsadi@squ.edu.om; Mohamed N. Al-Yahya'ei, mohamed.alyahyaei@moheri.gov.om

Key words:
Arabian Peninsula
new taxon
Pluteineae
taxonomy
Volvariellaceae

Abstract: In the present study, a newly found species of *Volvariella* from Oman is described and named *V. darbatica*. Evidence for this decision is based on morphology and multigene phylogeny. *Volvariella darbatica* is characterized by small-sized basidiomata, pale pinkish to pale brownish pileus, and ellipsoid to ovoid basidiospores measuring 5.0–6.0 × 4.0–4.5 µm. Colour photographs of basidiomata and illustrations of anatomical characters are provided, along with the phylogenetic trees of the genus *Volvariella* and the suborder *Pluteineae* (where family *Volvariellaceae* is nested). Morphological similarities with closely related species are discussed. Furthermore, we also report the presence of *Volvariella cubensis* and *V. sathei* in Oman, extending the distribution of these species. *Volvariella sathei* was previously known only from its type locality in India.

Citation: Hussain S, Al-Kharousi M, Al-Maqbali D, Al-Owaisi AA, Velazhahan R, Al-Sadi AM, Al-Yahya'ei MN (2025). Phylogeny of the genus *Volvariella* with the description of one new species and two new records from Oman. *Fungal Systematics and Evolution* **16**: 29–39. doi: 10.3114/fuse.2025.16.2
Received: 4 June 2024; **Accepted:** 17 March 2025; **Effectively published online:** 28 March 2025
Corresponding editor: P.W. Crous

INTRODUCTION

The genus *Volvariella* was introduced by Spegazzini (1899). The name refers to the presence of a volva (wrapper, covering or integument) at the base of the stipe of these mushrooms. *Volvariella* is characterized by a pileostipitate basidiome, small to medium-sized (rarely large-sized), with a fibrillose to strigose pileus surface, free lamellae, brownish-rose spore print, smooth stipe with no annulus, and the presence of a volva at the base of the stipe. Microscopically, species of *Volvariella* have smooth basidiospores smaller than < 11 µm in length, which are also in-amyloid, non-dextrinoid, and lack a germ-pore, 4-spored basidia, presence of both cheilo- and pleurocystidia, inversely arranged hyphae in lamellae, absence of clamp connections, and a non-gelatinous pileipellis (Orton 1986, Boekhout 1990, Kirk *et al*. 2008, Justo *et al*. 2011, Vizzini *et al*. 2024).

There are nearly 125 described species in the genus, with *Volvariella argentina* being the type species (Malysheva *et al*. 2019, Chattopadhyay *et al*. 2022, Kumla *et al*. 2022, Haqnawaz *et al*. 2023, Caballero *et al.* 2025, Jabeen *et al*. 2025). However, databases like Index Fungorum (https://www.indexfungorum.org/; accessed on 7 May 2024) and MycoBank (https://www.mycobank.org/; accessed on 7 February 2025), report 166 and 168 names associated with *Volvariella*, respectively. Some of the names mentioned in these databases are illegitimate or invalid, and include names widely accepted as heterotypic synonyms or infraspecific names. Ecologically, species of the genus occur as saprotrophs on wood, woody debris, and on soil, spread over the eastern and western hemispheres in tropical, subtropical, and temperate climates, with no reports from artic or alpine regions (Shaffer 1957, Boekhout 1990).

Species of *Volvariella* were classified into two sections, namely sect. *Macrosporae* and sect. *Volvariella* by Contu (1998). This classification was based on basidiospore size, with species in *Macrosporae* having spores larger than 11 µm in length, and those in sect. *Volvariella* having spores generally smaller than 11 µm. Later, species in sect. *Macrosporae* were moved to the independent genus *Volvopluteus* (Justo *et al*. 2011). *Volvopluteus* differs from *Volvariella* by its smooth cap surface, basidiospores longer than 11 µm in length, and the presence of a gelatinous matrix in the pileipellis. Phylogenetically, *Volvopluteus* is more closely related to *Pluteus* in *Pluteaceae* (Vizzini *et al*. 2024). The systematic position of *Volvariella* was controversial for a long time, being placed in *Amanitaceae* (Lee *et al.* 1959), *Agariaceae* (Lee 1973), and finally transferred to *Pluteaceae* (Singer 1986). Later, *Volvariella* was thought to have a closer relationship with *Cantharocybe* and *Cuphophyllus* in the family *Hygrophoraceae* (Justo *et al*. 2011). As a result of the uncertainty, the genus was treated as incertae sedis by other authors (Niego *et al*. 2021, Kumla *et al.* 2022). In a recent study of *Agaricales* based on a 6-gene phylogeny, species of *Volvariella* formed a separate lineage inside the suborder *Pluteineae*, and a new family

Fungal Systematics and Evolution is licensed under a Creative Commons Attribution-NonCommercial-NoDerivatives 4.0 International License

© 2025 Westerdijk Fungal Biodiversity Institute

Volvariellaceae was coined for it (Vizzini *et al*. 2024).

The present study is a continuation of mushroom exploration research in Oman. Oman is situated on the southeast coast of the Arabian Peninsula's. The samples were collected in Dhofar region of Oman, which experiences a yearly monsoon rain season from June to September, about 100–400 mm in these months (Bookhagen *et al.* 2005. Kwarteng *et al*. 2009). Research on mushroom diversity in the Sultanate of Oman has started only very recently, and only nine species have been reported from the entire country so far (Al-Kharousi *et al*. 2022a, b, Hussain *et al*. 2022a, b, 2024a–c). In the present work, several collections of *Volvariella* from Oman are studied. Upon morphological and phylogenetic analyses, these collections contain one new species and two new records of *Volvariella* from Oman, which are subsequently treated below.

MATERIALS AND METHODS

Sampling and morphological characterization

Basidiocarps were found in August and September, during the rainy season of the years 2022 and 2023. The specimens were found on logs, tree trunks, and soil in Wadi Darbat and Wadi Jarzeez, located in Dhofar region, southern Oman, and photographed in their natural habitat. Macromorphological characters such as size, shape, and colour of basidiocarps were recorded based on fresh materials. Basidiocarps were then dried in a fruit dehydrator set to 45 °C, sealed in zipper bags, and subjected to -80 °C for 2 wk to prepare them for long term preservation.

For microscopic studies, a thin section of the lamellae, pileus covering, and volva were mounted on glass slides, stained with 5 % aqueous KOH, and further stained with 1 % aqueous Congo red for better contrast. Different microscopic structures such as basidiospores, basidia, cystidia, pileipellis, volval structure, etc. were examined under a compound microscope (ECLIPSE Ni-U, Nikon Co., Ltd., Japan). For basidiospores, at least 50 spores were measured at 1000×, and measurements are presented as: (a–)b–c(–d) × (e–)f–g(–h), [, Qm, n] where b–c and f–g include the spore length and width respectively between the 5th and the 95th percentile, (a) and (d) the extreme values of spore lengths recorded, (e) and (h) the extreme values of spores width recorded, the mean of length and width of basidiospores with ± SD (standard deviation) respectively, Qm the mean of Q coefficient (length/width ratio), n is the total number of basidiospores measured (Nawaz *et al*. 2024). All the samples are preserved at the Oman Animal and Plant Genetic Resources Center (Mawarid), Muscat, Oman.

DNA extraction, amplification, and sequencing

The X-AMP DNA extraction kit (Dubuque, Iowa, USA) was employed following the manufacturer's instructions to isolate genomic DNA from dried materials. Three DNA regions were amplified, including the nuclear ribosomal DNA internal transcribed spacer regions (ITS1-5.8S-ITS2 = ITS), the D1/D2 domain of the large subunit nrDNA (28S), and a portion of the translation elongation factor 1 alpha gene (*TEF-1α*). For amplification of these regions, the primer combinations employed were: ITS1F/ITS4 for ITS (White *et al.* 1990, Gardes & Bruns 1993), LR0R/LR5 for 28S (Vilgalys & Hester 1990, White *et al.* 1990), and EF1-983/EF1-1567R for *TEF-1α* (Rehner & Buckley 2005), respectively. The PCR optimization was according to Hussain *et al.* (2024a) and the PCR amplicons were sent to Macrogen Inc. © (Seoul, Republic of Korea) for purification and sequencing in both directions using the same amplification primers. The two reads were assembled using BioEdit v. 7.0.9 (Hall 1999) and the consensus sequences were deposited at GenBank.

Sequence alignment and phylogenetic analyses

Phylogenetic analyses were performed on two different datasets. First, a combined ITS-28S-*TEF-1α* dataset was constructed using sequences from 39 specimens of the suborder *Plutineae* (including *Lepista panaeolus* KUN-HKAS 105370 from suborder *Tricholomatineae* as the outgroup taxon) following Vizzini *et al*. (2024) – see Vizzini *et al*. (2024) for GenBank accession numbers of included sequences. This dataset mainly shows that the two species *V. darbatica* and *V. sathei* (the 3rd *V. cubensis* not included in the combined dataset) found in Oman belong to genus *Volvariella*. Second, the ITS dataset with 71 sequences of *Volvariella* plus the outgroup taxon *Cantharocybe virosa* (SDBR-CMUNK0280), was assembled to study the evolutionary relationships between species in the genus *Volvariella* (Caballero *et al.* 2025). Both datasets were constructed with sequences employed in recent phylogenetic studies of *Volvariella* and *Plutineae* (Malysheva *et al*. 2019, Chattopadhyay *et al*. 2022, Kumla *et al*. 2022, Haqnawaz *et al*. 2023, Vizzini *et al*. 2024, Caballero *et al*. 2025). The assembled datasets were aligned using MAFFT v. 7 (Katoh *et al*. 2019), and manually inspected and adjusted in BioEdit v. 7.0.9 (Hall 1999), and ClustalX v. 2.1 (Larkin *et al*. 2007), respectively. Files of the ITS and the combined ITS-28S-*TEF-1α* alignments are available online at the figshare platform (doi: 10.6084/m9.figshare.25911064).

Two different phylogenetic analyses were run, maximum likelihood (ML) and Bayesian Inference (BI). The ML analysis was executed in RAxML v. 8.2.12 (Stamatakis 2014) specifying a GTRGAMMAI model for all partitions and 1000 rapid bootstrap (BS) replicates, implemented in the CIPRES Science Gateway (https://www.phylo.org/portal2/; Miller *et al*. 2010). The BI analysis was done using BEAST v. 1.8.2 (Drummond *et al.* 2012). A Birth-Death Incomplete Sampling model was specified (Stadler 2009). Four runs were performed, each with 10 M generations. The *log* files were loaded in Tracer v. 1.6 (Rambaut *et al*. 2014) to check the values of effective sample size (ESS) for all parameters; all of these were found to be well over 200. In LogCombiner v. 1.8.2, the tree files were merged, and TreeAnnotator v. 1.8.2 was used to create a maximum clade credibility (MCC) tree (Drummond & Rambaut 2007). Statistical support values were considered significant when the ML bootstrap (BS) percentage was ≥ 70 %, and BI posterior probabilities (PPs) were ≥ 0.95. FigTree v. 1.4.2 (Rambaut 2012) was used to visualize the phylogenetic tree, which were subsequently annotated using Adobe Illustrator CC2019.

© 2025 Westerdijk Fungal Biodiversity Institute

RESULTS

Phylogenetic analyses

The combined ITS-28S-*TEF-1α* dataset of 39 specimens of *Pluteineae* consisted of 1710 characters, including 996 constant sites, 601 parsimony informative sites, and 113 parsimony uninformative sites. The alignment included sequences of 38 specimens from representative species of the suborder *Plutineae*. There were nine species of *Amanitaceae*, eight of *Pluteaceae*, nine of *Volvariellaceae*, two of *Limnoperdaceae*, and 10 of *Melanoleucaceae*. Since both ML and BI analyses produced phylogenetic trees with similar topologies, only the ML is depicted (Fig. 1) with annotated with both BS and PP values.

The final ITS dataset of *Volvariella* consisted of 71 sequences with an alignment length of 589 characters, including 181 constant sites, 346 parsimony informative sites, and 62 uninformative sites. The dataset contained 70 different specimens of the genus *Volvariella* along with the outgroup taxon *Cantharocybe virosa* (SDBR-CMUNK0280). Phylogenetic trees resulting from the ML and BI methods were topologically similar, so only the ML tree was reproduced (Fig. 2), annotated with support values from both analyses. Species of *Volvariella* grouped into three major clades with good statistical support. The basal clade (V–I; V stands for *Volvariella*) consisted of *Volvariella bombycina*, *V. diplasia*, *V. orientalis*, and *V. volvacea*. The common morphological feature among these species is their large-sized basidiocarps. The second clade (V-II) contained *V. bilobata*, *V. niveosulcata*, *V. perciliata* and *V. pulla*. There is no common morphological feature among these species; however, brown colouration of the cap is common in *V. bilobata* and *V. pulla* (Malysheva *et al*. 2019, Chattopadhyay *et al*. 2022). Most of the species included in this study fall in the third clade (V-III). Species in V-III shared small to medium-sized basidiomata. The new species *Volvariella darbatica* formed an independent lineage in clade V-III with two conspecific sequences, deposited in GenBank as *Volvariella* sp. (KY636377 from Pakistan, MK018839 from USA). The closely related species to *Volvariella darbatica* are: *V. cubensis*, *V. morozovae*, *V. nullicystidiata*, *V. ptilotricha*, *V. taylorii*, *V. cordispora*, and *V. izmirensis*. Collection DRB2-23-001 was found to be phylogenetically similar to *V. cubensis* ARF-4948 from the

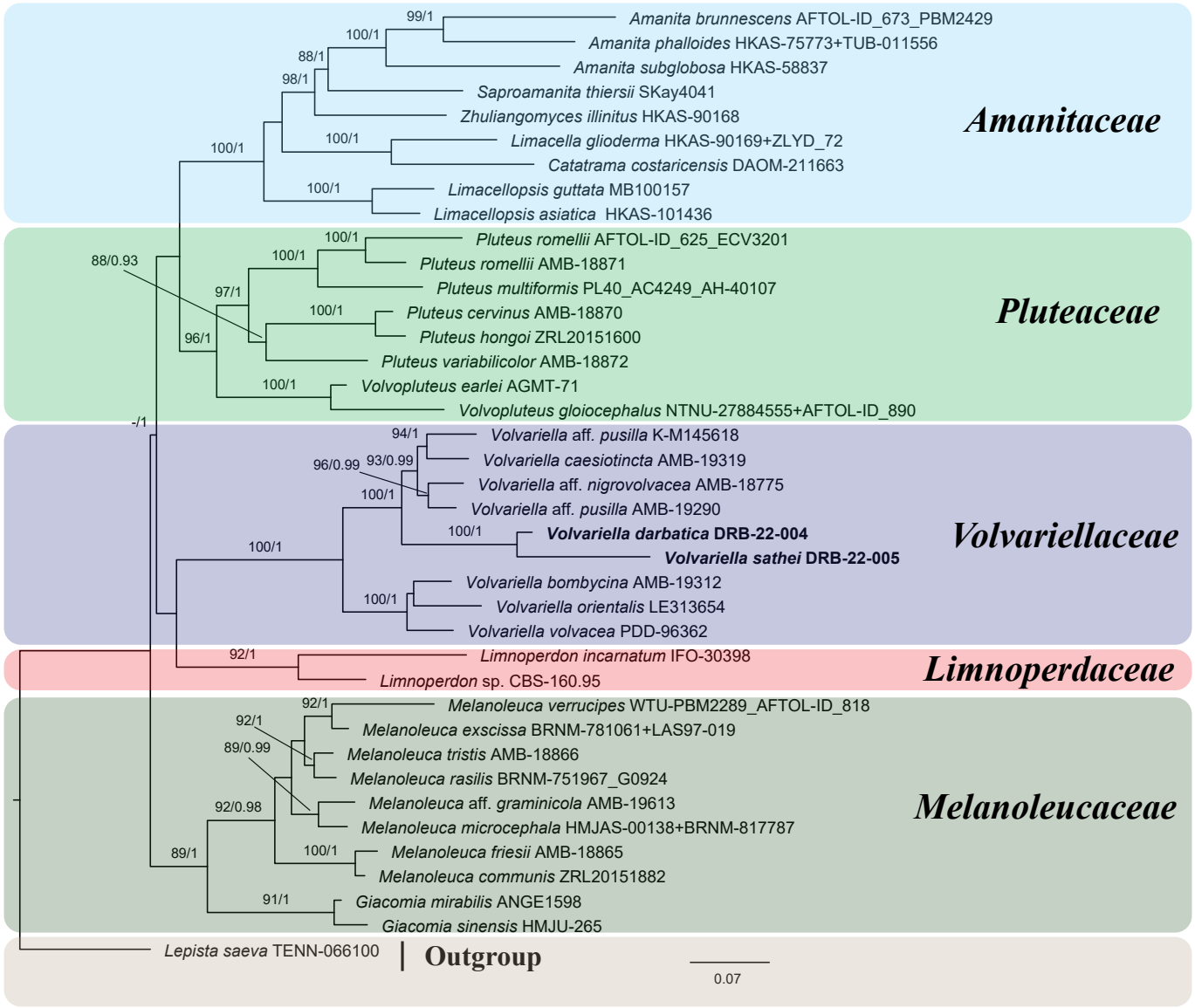

Fig. 1. Phylogeny of suborder *Plutineae* based on multigene sequence data, individual family in the suborder recovered with excellent statistical support; values above the nodes represent maximum likelihood bootstrap and Bayesian posterior probabilities.

© 2025 Westerdijk Fungal Biodiversity Institute

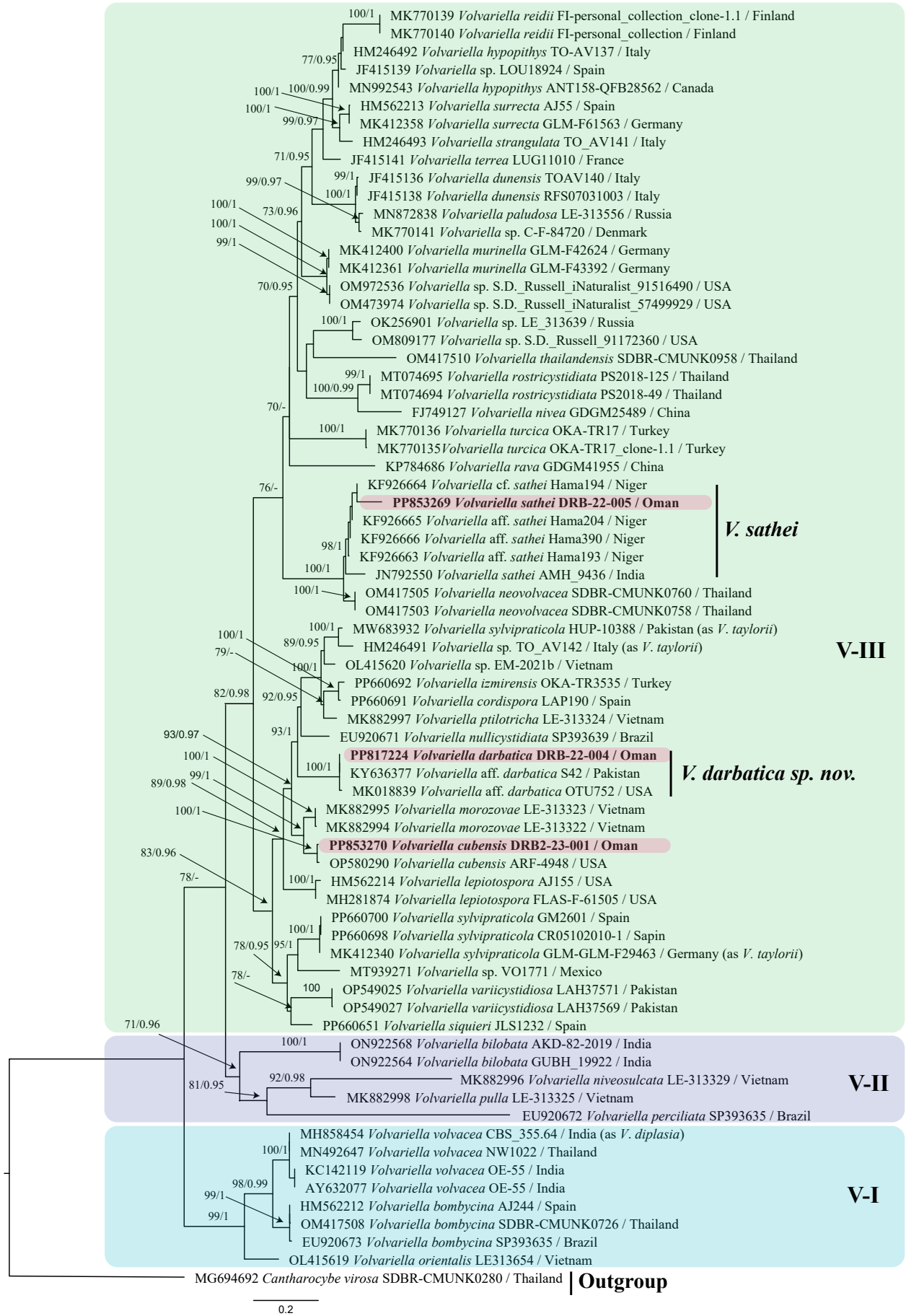

Fig. 2. The ML phylogeny of *Volvariella* based on 71 ITS sequences including the outgroup taxon *Cantharocybe virosa* (SDBR-CMUNK0280). Text on each leaf arranged in order as GenBank accession, species name, specimen's voucher, and country of origin. Above the nodes are the values of bootstrap percentages (BS) and Bayesian Posterior Probabilities (PPs). The BS values ≥ 70 % and PPs ≥ 0.95 are shown. Species of the genus are recovered in three major clades with excellent to moderate phylogenetic support; the pink highlighted taxa in clades V–III are the specimens studied during this study.

© 2025 Westerdijk Fungal Biodiversity Institute

USA. Similarly, the specimen DRB-22-005 grouped with *Volvariella sathei*, being related also to *V. neovolvacea*. The specimen DRB-22-005 seems phylogenetically different but morphologically identical to *V. sathei*.

Taxonomy

Volvariella darbatica S. Hussain, A. Al-Owaisi, Al-Sadi & Al-Yahya'ei, ***sp. nov.*** MycoBank MB 854048. Figs 3A–C, 4.

Etymology: The specific epithet "*darbatica*" refers to the locality Darbat, a tourist spot in Dhofar region, southern Oman, where the holotype was collected.

Typus: **Oman**, Dhofar, Wadi Darbat, 250 m a.s.l., grassland, in soil, 9 Aug. 2022, *S. Hussain* & *Al-Yahya'ei*, DRB-22-004 (**holotype** Mawarid DRB-22-004). GenBank accessions: ITS = PP817224, 28S = PP813713, *TEF-1α* = PP826251.

Description: Basidiomata small-sized. *Pileus* 30–40 mm diam., plano-convex to convex, pale pinkish to creamy, centre pale brownish to greyish brown, slightly umbonate at the centre, surface silky fibrillose to hairy, the fibrils aggregate into squamules that arrange in radial lines when wet, with crenate margins fringed with silky fibrils; non-hygrophanous, not viscid, membranous. *Lamellae* free, subdistant, broad to slightly ventricose, pinkish to pale pink, edge entire and concolourous to lamellae, with 0–1 layer of lamellulae. *Stipe* 40–50 × 2–3 mm, central, equal, white, smooth. *Annulus* absent. *Volva* thin, membranous, saccate, greyish brown, irregularly lobed, outer surface smooth. *Odour* and *taste* not recorded. *Basidiospores* (4.7–)5.0–6.0(–6.2) × (4.2–) 4.5–5.0 (–5.2) µm, (= 5.5 ± 0.23 × 4.8 ± 0.24 µm, Qm = 1.3, n = 50), in front view broadly ellipsoid to ovoid, in side view ellipsoid to broadly ellipsoid, hyaline in KOH, thick-walled, smooth, germ-pore absent. *Basidia* 22.0–26.0 × 7.5–9.5 µm, clavate to broadly cylindrical, hyaline in KOH, 4-spored. *Cheilocystidia* 50.0–62.0 × 20.0–28.0 µm, clavate to broadly fusiform, thin-walled, hyaline in KOH. *Pleurocystidia* 50.0–62.0 × 20.0–28.0 µm, ellipsoid to clavate or utriform, thin-walled, hyaline. *Lamellar trama* convergent, consisting of thin walled, hyaline hyphae, measuring 7.0–12.0 µm diam. *Pileipellis* a cutis, consisting of short, cylindrical elements, each 15.0–18.0 µm diam., terminal elements with rounded ends, each measuring 50.0–75.0 × 15.0–18.0 µm, hyaline to pale in KOH. *Volva* is arranged as an irregular trichoderm, made up of branched hyphae with terminal elements clavate to cylindrical or subglobose, greyish brown in KOH, measuring 22.0–40.0 × 11.0–22.0 µm. *Clamp connection* absent in all tissues.

Habitat and distribution: Saprobic on soil and woody debris. Solitary or dispersed in small groups among herbaceous plants. Distributed in West Asia (Oman), South Asia (Pakistan) and North America (USA).

Additional materials examined: **Oman**, Dhofar, Wadi Jarzeez, on woody debris under herbaceous plants, 5 Sep. 2023, *S. Hussain* & *M. Al-Jahwari*, JRZ2-23-021 (Mawarid JRZ2-23-021); ibid., JRZ2-23-023 (Mawarid JRZ2-23-023).

Notes: *Volvariella darbatica* is characterized by its small-sized and slender basidiomata with pale creamy to pale brownish and fibrillose pileus, greyish brown and membranous volva, and its small (5.0–6.0 × 4.5–5.0 µm) and broadly ellipsoid to ovoid basidiospores. On the basis of the BI and ML analyses of the ITS region, the most similar species to *Volvariella darbatica* are: *V. cubensis*, *V. morozovae*, *V. ptilotricha*, and *V. taylorii*. *Volvariella cubensis* is a neotropical species, distributed in South America, Central America and South Asia (Shaffer 1957, Pegler 1983, Wartchow 2009, Farook *et al*. 2013, Hernández-Del Valle *et al*. 2019). In the present study the distribution of *V. cubensis* is further extended to West Asia (Oman). This species has huge basidiomata very different from that of *V. darbatica*, with a pileus up to 116 mm diam., an olive grey colouration of fibrils, and larger basidiospores (5.5–7.5 × 4.5–6 µm; Hernández-Del Valle *et al*. 2019). *Volvariella ptilotricha* is a recently described species, only known from the type locality in Vietnam, characterized by its remarkably small basidiomata with a pileus about 5–15 mm diam., fibrillose cap surface, fibrils sandy grey to brownish, and olive grey volva (Malysheva *et al*. 2019). *Volvariella morozovae* is another small-sized species only reported from Vietnam, which differs from *V. darbatica* by its greyish to blackish fibrillose pileus surface (Crous *et al*. 2017, Malysheva *et al*. 2019). *Volvariella izmirensis* is a recently reported species from Turkey, characterized by small to medium-sized basidiomata, with whitish pileus with cinereous centre, golden brown to ochre brown saccate volva, mainly narrow fusiform to fusiform pleurocystidia with an elongated neck, and larger basidiospores measuring 6.8–9.5 × 4.2–5.4 µm (Caballero *et al.* 2025). *Volvariella cordispora* is another small-sized species, characterized by whitish pileus with pale brown veil remnants at the centre, and a characteristic heart-shaped basidiospores (Caballero *et al.* 2025). *Volvariella taylorii* is a medium-sized, greyish coloured species, with saccate volva and large cystidia, found in coastal region, widely distributed species in Europe (Boekhout 1990). Several studies have reported this species outside Europe, such as from North and South America (Shaffer 1957), and Asia (Seok *et al*. 2002, Khan *et al*. 2021). In most of these reports the species reported as *V. taylorii* turned out to be a different species following molecular phylogenetic analysis (Caballero *et al.* 2025). For example, a collection HUP-10388 (GenBank accession MW683932) which was recently reported from Pakistan as *V. taylorii* (Khan *et al*. 2021) is actually *V. sylvipraticola* (Caballero *et al.* 2025). This could be the reason that specimens of *V. taylorii* cluster in different clades in the phylogeny of *Volvariella*.

Volvariella sathei Senthil. *et al.*, *Mycotaxon* **119**: 470. 2012. Figs 3D–E, 5.

Description: *Basidiomata* medium to large-sized. *Pileus* 60–90 mm diam., convex to hemispheric, yellowish brown to whitish, surface covered with shiny yellowish fibrils, with radial striations towards the margin, margins thin, slightly eroded. *Lamellae* free, broad to ventricose, pinkish to pinkish brown, crowded, with 0–3 layers of lamellulae. *Stipe* 70–100 × 7–10 mm, central, equal, cylindrical, solid, surface creamy to white, glabrous. *Annulus* absent. *Volva* free,

© 2025 Westerdijk Fungal Biodiversity Institute



Fig. 3. Basidiomata of *Volvariella* species. **A–C.** *Volvariella darbatica* (holotype DRB-22-004), arrows in **B** represent the radially arranged fibrils. **D–E.** *Volvariella sathei* (DRB-22-005). **F–H.** *Volvariella cubensis* (DRB2-23-001). Scale bars = 20 mm.

© 2025 Westerdijk Fungal Biodiversity Institute

irregularly lobed, thick, inner surface white and glabrous, outer surface greyish and glabrous. *Odour* pleasant when fresh, pungent when dry, *taste* not recorded. *Basidiospores* (5.5–)6.0–7.0(–7.5) × (5.2–)5.5–6.5(–7.0) µm, [= 6.5 ± 0.26 × 4.8 ± 0.25 µm, Qm = 1.1, n = 50], in face view subglobose to rounded triangular or heart-shape, in side view broadly obovoid to broadly pyriform, hyaline in KOH, slightly thick-walled, germ-pore absent, apiculus visible. *Basidia* 22.0–33.0 × 7.0–10.0 µm, clavate to cylindrical, 4-spored. *Cheilocystidia* 66.0–96.0 × 18.0–38.0 µm, narrowly fusiform to fusiform, abundant, hyaline in KOH, smooth. *Pleurocystidia* 76.0–110.0 × 25.0–54.0 µm, broadly fusiform to broadly utriform, hyaline in KOH. *Lamellar trama* convergent, consisting of thin-walled hyaline, 5.0–18.0 µm diam hyphae. *Pileipellis* a cutis, consisting of thin-walled hyphae 7.5–11 µm diam., rarely branched, pale yellowish in KOH. *Volva* arranged as a cutis composed of unbranched hyaline hyphae, up to 15 µm diam., with terminal elements cylindrical to clavate, each measuring 90–160 × 12–15 µm. *Clamp connections* absent from all tissues.

Habitat and distribution: *Volvariella sathei* is a rare subtropical species, previously known only from the type locality, Pune, Maharashtra State, India (Senthilarasu *et al*. 2012). This is the second report of this species outside of India. However, *V*. cf. *sathei*, a similar taxon has been reported from Niger, Africa (Daniëls *et al*. 2015).

Material examined: **Oman**, Dhofar, Wadi Darbat, 250 m a.s.l., on soil under grasses, 9 Aug. 2022, *S. Hussain* & *Al-Yahya'ei*, DRB-22-005 (Mawarid DRB-22-005). GenBank accessions: ITS = PP853269, 28S = PP820531.

Notes: *Volvariella sathei* is a medium to large-sized mushroom in the *Volvariellaceae*. The genus contains some important edible species, such as *Volvariella volvacea* which is called paddy straw mushroom. However, the edibility of *Volvariella sathei* has not been tested, it is therefore recommended not to consume it. It is extremely important to investigate the nutritional and biochemical properties of this mushroom to avoid poisonings.

Volvariella cubensis (Murrill) Shaffer, *Mycologia* **49**: 564. 1957. Figs 3F–H, 6.

Description: *Basidiomata* medium to large sized. *Pileus* 60 mm in diam., convex to hemispheric with umbonate centre, covered with radially arranged silky fibrils, fibrils pale greyish towards the periphery, dark greyish at centre, with entire margins. *Lamellae* free, cream to pinkish, broad, crowded with 0–2 layers of lamellulae, lamellar edge even. *Stipe* 55 × 5 mm, central, broader towards the base, whitish, smooth. *Annulus* absent. *Volva* fleshy, irregularly lobed, smooth, greyish brown. *Odour* and *taste* not recorded. *Basidiospores* (5.5–)6.0–7.0(–7.5) × (3.5–)4.0–4.5(–5.0) µm, (= 6.5 ± 0.28 × 4.3 ± 0.20 µm, Qm = 1.5, n = 55), in front view broadly ellipsoid to amygdaliform or ovoid, in side view ellipsoid, hyaline to light green in KOH, smooth, thick-walled, apiculus visible, germ-pore absent. *Basidia* 15.5–22.0 × 7.5–10.0 µm, cylindrical to clavate, hyaline in KOH, 2- to 4-spored.

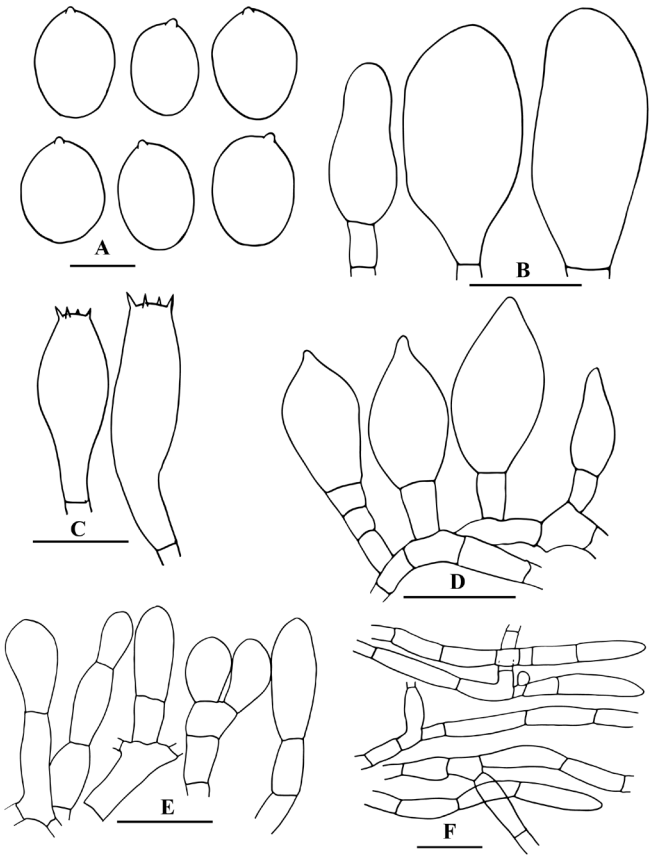

Fig. 4. Illustrations of anatomical features of *Volvariella darbatica* (holotype DRB-22-004). **A.** Basidiospores. **B.** Pleurocystidia. **C.** Basidia. **D.** Cheilocystidia. **E.** Volva elements. **F.** Pileipellis. Scale bars: A = 5 µm; B–D = 20 µm; E, F = 30 µm.

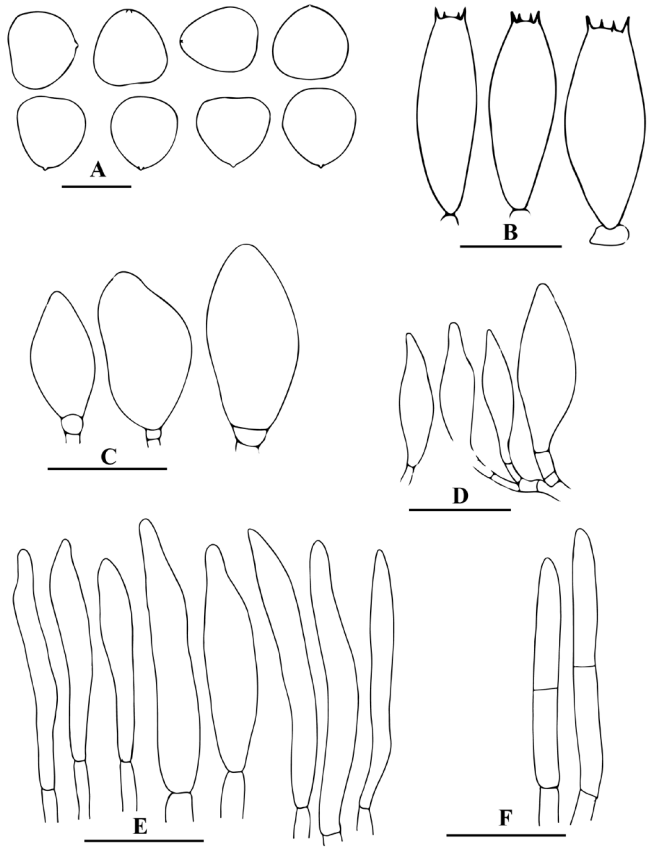

Fig. 5. Illustrations of anatomical features of *Volvariella sathei* (DRB-22-005). **A.** Basidiospores. **B.** Basidia. **C.** Pleurocystidia. **D.** Cheilocystidia. **E.** Pileipellis. **F.** Volva elements. Scale bars: A = 5 µm; B–D = 20 µm; E, F = 40 µm.

© 2025 Westerdijk Fungal Biodiversity Institute

Cheilocystidia 37.0–50.0 × 13.0–20.0 µm, utriform to broadly utriform, hyaline in KOH, thin-walled. *Pleurocystidia* 45.0–75.0 × 15–23.5 µm, utriform to clavate, hyaline in KOH, thin-walled. *Lamellar trama* convergent, consisting of thin-walled hyaline hyphae measuring 7–10 µm diam. *Pileipellis* an intricate trichoderm to irregular trichoderm, rarely branched, consisting of cylindrical elements with up to 15 µm in diam., terminal elements cylindrical to clavate, pale greyish in KOH, measuring 40.0–76.0 × 11.5–17.5 µm. *Volva* is arranged as trichoderm, consisting of branched hyphae, pale greyish to pale brownish in KOH, terminal elements clavate to fusiform with rounded end, measuring 47.5–69.0 × 14.5–18.0 µm. *Clamp connection* absent in all tissues.

Habitat and distribution: *Volvariella cubensis* is a rarely reported species, distributed in South America, Central America, and India (Shaffer 1957, Pegler 1983, Wartchow 2009, Farook *et al*. 2013, Hernández-Del Valle *et al*. 2019). In the present study, the known distribution of the species is extended to include West Asia, the Arabian Peninsula.

Material examined: **Oman**, Dhofar, Wadi Darbat, 250 m a.s.l., on trunk of *Ficus* tree, 2 Sep. 2023, *S. Hussain* & *Al-Jahwari*, DRB2-23-001 (Mawarid DRB2-23-001). GenBank accession: ITS = PP853270.

Notes: *Volvariella cubensis* is a medium to large-sized mushroom, characterized by greyish silky fibrillose pileus surface. The specimen we studied is morphologically similar to the published descriptions of *Volvariella cubensis* (Shaffer 1957, Pegler 1983, Wartchow 2009, Farook *et al*. 2013, Hernández-Del Valle *et al*. 2019). Using ML phylogenetic analysis of the ITS region, the sequence obtained from the Omani collection seems identical to other identified as *V. cubensis* (GenBank OP580290).

DISCUSSION

Volvariella is an important mushroom genus present in tropical, subtropical, and temperate regions (Shaffer 1957, Pegler 1977, Kirk *et al*. 2008, Li *et al*. 2009, Niego *et al*. 2021). Currently, the species identification of *Volvariella* is based on both morphological characters of basidiomata and molecular phylogenetic analyses of different DNA regions, including ITS, 28S, and *TEF-1α* (Justo & Castro 2010, Justo *et al*. 2011, He *et al*. 2019, Malysheva *et al*. 2019, Niego *et al*. 2021, Kumla *et al.* 2022). Morphologically, species of *Volvariella* are characterized by pluteoid basidiomata (free lamellae, context of the pileus discontinuous with context of the stipe, stipe usually longer than pileus), pinkish brown

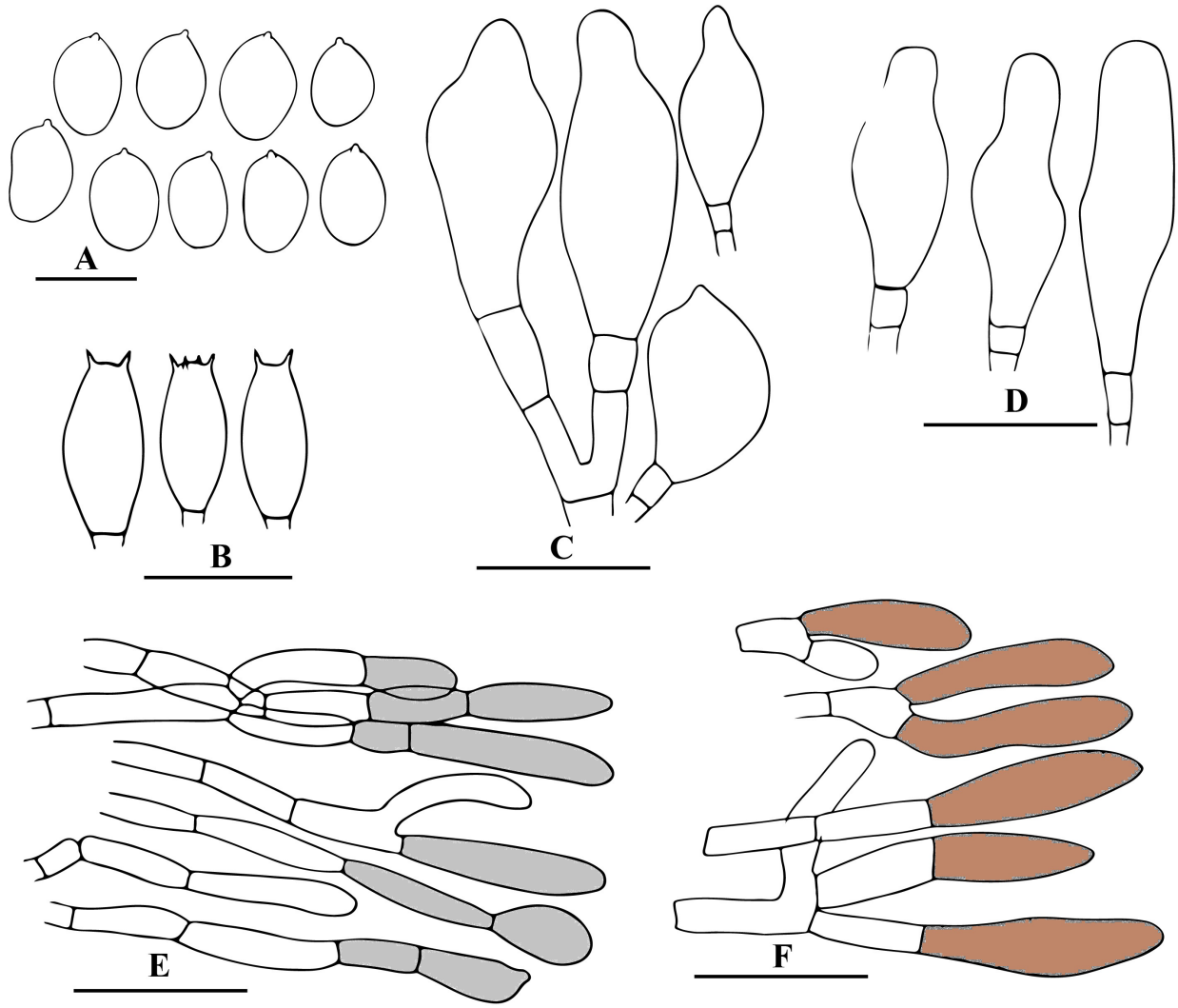

Fig. 6. Illustrations of anatomical features of *Volvariella cubensis* (DRB2-23-001). **A.** Basidiospores. **B.** Basidia. **C.** Cheilocystidia. **D.** Pleurocystidia. **E.** Pileipellis. **F.** Volva elements. Scale bars: A = 5 µm; B–D = 20 µm; E, F = 40 µm.

© 2025 Westerdijk Fungal Biodiversity Institute

spore-print, and a saccate volva at the stipe base (Justo *et al*. 2011, Caballero *et al.* 2025). The taxonomic keys of the genus are mainly based on colour of basidiomata, size of pileus, lignicolous/terrestrial habitat, and basidiospore morphology (Shaffer 1957, Caballero *et al.* 2025). In the present study, we reported one new species and two first records of *Volvariella* species from Oman. *Volvariella darbatica* is a terrestrial species sporulating under grasses, characterized by a small-sized basidiomata, whitish to creamy fibrillose pileus surface, brownish membranous volva, and broadly ellipsoid to ovoid basidiospores (5.0–6.0 × 4.0–4.5 µm). There are several species in the genus with similar morphology and related habitat. For example, *V. cordispora* is a small-sized species with whitish basidiomata, sprouting under disturbed habitat, with globose to heart-shaped basidiospores measuring 5.0–8.1 × 3.8–5.2 µm (Caballero *et al.* 2025). *Volvariella alba* is a small-sized, whitish species, with volva (15 mm in length) almost half of the size of stipe (20–30 mm in length), and was recently reported from Southern Pakistan on soils with a deserted habitat (Jabeen *et al*. 2025). *Volvariella pusilla* is a European species found mostly in lawns and gardens, and occasionally in forest floor, basidiomata small-sized, whitish, with 2–3 lobed membranaceous, saccate volva (Caballero *et al.* 2025). *Volvariella reidii* is small-sized, whitish at the young stage, pale pinkish at the old stage, found on the forest floor of gymnosperms (Heinemann 1978). *Volvariella globifera*, a recently reported species from Spain, with whitish, small-sized basidiomata, with broadly ellipsoid to oblong basidiospores (4.6–7.3 × 3.3–4.6 µm), sporulates on sandy soil under *Cupressus macrocarpa* (Caballero *et al.* 2025). *Volvariella pilosipilea* might be the smallest species in the genus with a pileus diameter of 6–11 mm, both cap and volva are delicate, whitish and translucent (Caballero *et al.* 2025).

Some species of *Volvariella* are sporulating in association with other mushrooms. *Volvariella terrea* is a small to medium-sized species, characterized by having a tomentose-lanose pileus surface, growing under broad-leaved trees, with ellipsoid to cylindrical basidiospores measuring 5.9–9.9 × 3.8–5.6 µm (Caballero *et al.* 2025).

The two species *Volvariella neovolvacea* and *V. sathei* share a clade with strong phylogenetic support. Both are phylogenetically closely related, but morphologically easily distinguishable. *Volvariella sathei* is a whitish, medium to large-sized species, found on soil under trees with grasses, basidiospores globose to subglobose, measuring 6.0–6.5 × 5.0–5.5 µm (Senthilarasu *et al*. 2012, Daniëls *et al*. 2015). *Volvariella neovolvacea* is a recently reported species from Thailand, growing on soil in grasslands, with medium-sized basidiomata, brownish orange to greyish brown pileus, ellipsoid to broadly ellipsoid basidiospores, measuring 6.7–7.5 × 5.2–5.5 µm (Kumla *et al*. 2022).

The systematic position of *Volvariella* has changed multiple times. Due to the presence of a volva it was included in *Amanitaceae* (Lee *et al.* 1959), while the pinkish spore-print was the basis to transfer it to *Agariaceae* (Lee 1973), and finally, it was placed in *Pluteaceae* based on its morphology similarity to *Pluteus* (Singer 1986). Molecular phylogenetic analyses suggested that *Volvariella* is related to *Cantharocybe* and *Cuphophyllus* in the family *Hygrophoraceae* (Justo *et al*. 2011). Other studies failed to place *Volvariella* in any family and treated it as incertae sedis (Niego *et al*. 2021, Kumla *et al.* 2022). Recently, an updated phylogeny of *Agaricales* was constructed with six genes, where *Volvariella* was placed in a newly erected family *Volvariellaceae* in the suborder *Pluteineae* (Vizzini *et al*. 2024). The present results confirm that *Volvariella* does not belong to the other families of *Pluteineae*, a result found in many previous studies.

ACKNOWLEDGEMENTS

We express our gratitude to B. Al Quyudhi, S. Al Balushi, and M. Al Hinai for their indispensable assistance during the Dhofar Region foray, which was crucial to the accomplishment of our research. Additionally, we are grateful to M. Al Jahwari and A. Qattan for their leadership and assistance during the project.

Conflict of interest: The authors declare that they have no conflict of interest.

REFERENCES

Al-Kharousi M, Hussain S, Al-Muharabi MA, *et al*. (2022a). The genus *Xanthagaricus*: an updated global species distribution and phylogeny with the description of two new species from Oman. *Journal of Fungi* **8**: 173. https://doi.org/10.3390/jof8020173

Al-Kharousi M, Hussain S, Al-Muharabi MA, *et al*. (2022b). Notes on the genus *Micropsalliota* (*Agaricales*, *Basidiomycota*) and the description of a new species from Southern Oman. *Phytotaxa* **543**: 113–126. https://doi.org/10.11646/phytotaxa.543.2.2

Boekhout T (1990). *Volvariella*. In: *Flora agaricina neerlandica* (Bas C, Kuyper ThW, Noordeloos ME, Vellinga EC, eds.), Vol. 2. Rotterdam, the Netherlands: AA Balkema.

Bookhagen B, Thiede RC, Strecker MR (2005). Abnormal monsoon years and their control on erosion and sediment flux in the high, arid northwest Himalaya. *Earth and Planetary Science Letters* **231**: 131–146. https://doi.org/10.1016/j.epsl.2004.11.014

Caballero F, Justo A, Parra LA, *et al*. (2025). Taxonomic and phylogenetic overview of the genus *Volvariella* (*Volvariellaceae*), with a focus on European species. *Phytotaxa* **680**: 1–85. https://doi.org/10.11646/phytotaxa.680.1.1

Chattopadhyay P, Talukdar M, Beypih J, *et al*. (2022). A new species of *Volvariella* (*Agaricales*, *Basidiomycota*) from West Bengal, India. *Phytotaxa* **567**: 36–48. https://doi.org/10.11646/phytotaxa.567.1.3

Contu M (1998). Studi sulle *Pluteaceae* della Sardegna. I. *Volvariella cookei* spec. nov., una nuova specie della sezione *Macrosporae*. *Micologia Italiana* **27**(3): 37–41.

Crous PW, Wingfield MJ, Burgess TI, *et al*. (2017). Fungal Planet description sheets: 625–715. *Persoonia* **39**: 270–467. https://doi.org/10.3767/persoonia.2017.39.11

Daniëls PP, Hama O, Fernández A, *et al*. (2015). First records of some Asian macromycetes in Africa. *Mycotaxon* **130**: 337–359. https://doi.org/10.5248/130.337

Drummond AJ, Rambaut A (2007). BEAST: Bayesian evolutionary analysis by sampling trees. *BMC Evolutionary Biology* **7**: 214. https://doi.org/10.1186/1471-2148-7-214

Drummond AJ, Suchard MA, Xie D, *et al.* (2012). Bayesian phylogenetics with BEAUti and the BEAST 1.7. *Molecular Biology and Evolution* **29**: 1969–1973. https://doi.org/10.1093/molbev/mss075

© 2025 Westerdijk Fungal Biodiversity Institute

Farook VA, Khan SS, Manimohan P (2012). A checklist of agarics (gilled mushrooms) of Kerala State, India. *Mycosphere* **4**: 97–131. https://doi.org/10.5943/mycosphere/4/1/6

Gardes M, Bruns TD (1993). ITS primers with enhanced specificity for basidiomycetes-application to the identification of mycorrhizae and rusts. *Molecular Ecology* **2**: 113–118. https://doi.org/10.1111/j.1365-294X.1993.tb00005.x

Hall TA (1999). BioEdit: a user-friendly biological sequence alignment editor and analysis program for Windows 95/98/NT. *Nucleic Acids Symposium Series* **41**: 95–98.

Haqnawaz M, Khan Z, Niazi AR, *et al.* (2023). *Volvariella variicystidiosa sp. nov*. (*Agaricaceae*, *Basidiomycota*) from Punjab, Pakistan. *Phytotaxa* **578**: 189–198. https://doi.org/10.11646/phytotaxa.578.2.5

He MQ, Zhao RL, Hyde KD, *et al*. (2019). Notes, outline and divergence times of *Basidiomycota*. *Fungal Diversity* **99**: 105–367. https://doi.org/10.1007/s13225-019-00435-4

Heinemann P. (1978). *Volvariella insignis sp. nov*. *et V. reidii nom. nov*. *Bulletin du Jardin Botanique National de Belgique* **48**: 239.

Hernández-Del Valle JF, de la Fuente JI, García-Jiménez J (2019). First record of *Volvariella cubensis* (Murrill) Shaffer (*Agaricales*, *Basidiomycota*) from Mexico. *Check List* **15**: 985–989. https://doi.org/10.15560/15.5.985

Hussain S, Al-Kharousi M, Al-Maqbali DA, *et al*. (2024a). Two new species of *Hymenagaricus* (*Agaricales*, *Agaricaceae*) from Oman, based on morphology and molecular phylogeny. *MycoKeys* **105**: 1–19. https://doi.org/10.3897/mycokeys.105.113591

Hussain S, Al-Kharousi M, Al-Muharabi MA, *et al*. (2022a). Phylogeny of *Agaricus* subgenus *Pseudochitonia* with the description of a new section and a new species from Oman. *Mycological Progress* **21**: 72. https://doi.org/10.1007/s11557-022-01819-8

Hussain S, Al-Kharousi M, Al-Muharabi MA, *et al*. (2022b). Phylogeny, distribution and time divergence of *Fuscoporia* (*Hymenochaetaceae*, *Basidiomycota*) with the description of a new species from Dhofar region, southern part of Oman. *Phytotaxa* **570**: 150–164. https://doi.org/10.11646/phytotaxa.570.2.3

Hussain S, Al-Kharousi M, Al-Owaisi AA, *et al.* (2024b). The genus *Termitomyces*: outline, phylogeny, and divergence times estimation with description of a new edible species from Arabian Peninsula. *Sydowia* **76**: 185–198. https://doi.org/10.12905/0380.sydowia76-2024-0185

Hussain S, Al-Kharousi M, Al-Maqbali DA, *et al.* (2024c). Notes on the ecology and distribution of species of the genera of *Bondarzewiaceae* (*Russulales* and *Basidiomycota*) with an emphasis on *Amylosporus*. *Journal of Fungi* **10**: 625. https://doi.org/10.3390/jof10090625

Jabeen S, Ijaz H, Ullah S, *et al*. (2025). New and noteworthy *Volvariella* spp. (*Volvariellaceae*) from Pakistan. *Phytotaxa* **691**: 151–172. https://doi.org/10.11646/phytotaxa.691.2.3

Justo A, Castro M (2010). The genus *Volveriella* in Spain: *V. dunensis comb. & stat. nov.* and observations on *V. earlei*. *Mycotaxon* **112**: 261–270. https://doi.org/10.5248/112.261

Justo A, Vizzini A, Minnis AM, *et al*. (2011). Phylogeny of the *Pluteaceae* (*Agaricales*, *Basidiomycota*): taxonomy and character evolution. *Fungal Biology* **115**: 1–20. https://doi.org/10.1016/j.funbio.2010.09.012

Katoh K, Rozewicki J, Yamada KD (2019). MAFFT online service: multiple sequence alignment, interactive sequence choice and visualization. *Briefings in Bioinformatics* **20**: 1160–1166. https://doi.org/10.1093/bib/bbx108

Khan MB, Ishaq M, Fiaz M, *et al*. (2021). A new record of *Pluteaceae* (*Agaricales*) from Pakistan. *Studies in Fungi* **6**: 514–518. https://doi.org/10.5943/sif/6/1/41

Kirk PM, Cannon PF, Minter DW, *et al*. (2008). *Ainsworth & Bisby's Dictionary of the Fungi*. 10th edn. CAB International, Wallingford, UK.

Kumla J, Suwannarach N, Wannathes N, *et al*. (2022). Survey of *Volvariella* (*Agaricales*, *Basidiomycota*) including two new species, *V. neovolvacea* and *V. thailandensis*, from Northern Thailand. *Diversity* **14**(3): 161. https://doi.org/10.3390/d14030161

Kwarteng AY, Dorvlo AS, Vijaya Kumar GT. (2009). Analysis of a 27-year rainfall data (1977–2003) in the Sultanate of Oman. *International Journal of Climatology* **29**: 605–617. https://doi.org/10.1002/joc.1727

Larkin MA, Blackshields G, Brown NP, *et al.* (2007). Clustal W and Clustal X version 2.0. *Bioinformatics* **23**: 2947–2948. https://doi.org/10.1093/bioinformatics/btm404

Lee JY (1973). The list of the fungi of Korea. *Korean Journal of Mycology* **1**: 35–43.

Lee JY, Lee YW, Lim J (1959). *Coloured Illustrations of Fungi of Korea*. Baemunkak, Seoul, Korea.

Li TH, Chen XL, Shen YH, *et al*. (2009). A white species of *Volvariella* (*Basidiomycota*, *Agaricales*) from southern China. *Mycotaxon* **109**: 255–261. https://doi.org/10.5248/109.255

Malysheva E, Malysheva V, Alexandrova A, *et al*. (2019). Observations on *Pluteaceae* in Vietnam. 1. New species and new records of *Volvariella*. *Phytotaxa* **408**: 233–254. https://doi.org/10.11646/phytotaxa.408.4.1

Miller MA, Pfeiffer W, Schwartz T (2010). Creating the CIPRES science gateway for inference of large phylogenetic trees. *Proceedings of the 2010 Gateway Computing Environments Workshop (GCE)*. IEEE: Manhattan, NY, USA: 1–8. https://doi.org/10.1109/GCE.2010.5676129

Nawaz R, Murad W, Irshad M, *et al*. (2024). *Agaricus* subgenus *Pseudochitonia* in Malakand, Pakistan: An updated phylogeny and description of three new species. *Mycologia* **116**: 577–600. https://doi.org/10.1080/00275514.2024.2334473

Niego AGT, Sysouphanthong P, Thongklang N, *et al*. (2021). A new species of *Volvariella* and the first record of *Volvariella pulla* (*Agaricales*: Incertae sedis) from Thailand. *Phytotaxa* **480**: 237–250. http://dx.doi.org/10.11646/phytotaxa.480.3.3

Orton PD (1986). *British fungus flora-agarics and boleti*: *Pluteaceae*. Royal Botanic Garden, Edinburgh, UK.

Pegler DN (1977). A preliminary agaric flora of East Africa. *Kew Bulletin Additional Series* **6**: 1–615.

Pegler DN (1983). *Agaric flora of the Lesser Antilles*. Kew bulletin additional series. Royal Botanic Gardens, Kew.

Rambaut A (2012). FigTree v. 131. Available from: http://treebioedacuk/software/figtree/ (accessed on 30 December 2022).

Rambaut A, Suchard MA, Xie D, *et al.* (2014). *TRACER v 1.6*. Computer program and documentation distributed by the authors. Available from: http://beast.bio.ed.ac.uk/Tracer (accessed 16 December 2022).

Rehner SA, Buckley E (2005). A *Beauveria* phylogeny inferred from nuclear ITS and *EF1-α* sequences: Evidence for cryptic diversification and links to *Cordyceps* teleomorphs. *Mycologia* **97**: 84–98. http://dx.doi.org/10.3852/mycologia.97.1.84

Senthilarasu G, Sharma R, Singh S (2012). A new species of *Volvariella* from India. *Mycotaxon* **119**: 467–476. http://dx.doi.org/10.5248/119.467

© 2025 Westerdijk Fungal Biodiversity Institute

Seok SJ, Kim YS, Weon HY, *et al*. (2002). Taxonomic study on *Volvariella* in Korea. *Mycobiology* **30**: 183–192. http://dx.doi.org/110.4489/MYCO.2002.30.4.183

Shaffer RL (1957). *Volvariella* in North America. *Mycologia* **49**: 545–579.

Singer R (1986). *The Agaricales in Modern Taxonomy*. 4th edn. Koeltz Scientific Books, Koenigstein, Germany.

Spegazzini C (1898). *Fungi Argentini*: novi v. critici.

Stadler T (2009). On incomplete sampling under birth-death models and connections to the sampling-based coalescent. *Journal of Theoretical Biology* **261**: 58–66. https://doi.org/10.1016/j.jtbi.2009.07.018

Stamatakis A (2014). RAxML version 8: a tool for phylogenetic analysis and post-analysis of large phylogenies. *Bioinformatics* **30**: 1312–1313. https://doi.org/10.1093/bioinformatics/btu033

Vilgalys R, Hester M (1990). Rapid genetic identification and mapping of enzymatically amplified ribosomal DNA from several *Cryptococcus* species. *Journal of Bacteriology* **172**: 4238–4246. https://doi.org/10.1128/jb.172.8.4238-4246.1990

Vizzini A, Alvarado P, Consiglio G, *et al*. (2024). Family matters inside the order *Agaricales*: systematic reorganization and classification of incertae sedis clitocyboid, pleurotoid and tricholomatoid taxa based on an updated 6-gene phylogeny. *Studies in Mycology* **107**: 67–148. https://doi.org/10.3114/sim.2024.107.02

Wartchow F (2009). *Volvariella cubensis*: a rare neotropical agaric new to South America. *Mycotaxon* **107**: 181–187. https://doi.org/10.5248/107.181

White TJ, Bruns TD, Lee S, *et al.* (1990). Amplification and direct sequencing of fungal ribosomal RNA genes for phylogenetics. In: *PCR protocols: A guide to methods and applications* (Innis MA, Gelfand DH, Sinisky JJ, *et al*., eds). Academic Press, USA: 315–322. https://doi.org/10.1016/B978-0-12-372180-8.50042-1

© 2025 Westerdijk Fungal Biodiversity Institute

© 2025 Westerdijk Fungal Biodiversity Institute

FUSE

Fungal Systematics and Evolution

VOLUME 16
DECEMBER 2025
PAGES 41–53

doi.org/10.3114/fuse.2025.16.3

Exploring *Neopestalotiopsis* diversity associated with Blueberry leaf and twig blight in South African nurseries

L.S. Van der Vyver[1], W. De Bruin[1], N. Siyoum[1], D.L. Nsibo[1,3], J.Z. Groenewald[2], P.W. Crous[2,3], L. Korsten[1*]

[1]Department of Plant and Soil Sciences, University of Pretoria, Pretoria, South Africa
[2]Westerdijk Fungal Biodiversity Institute, Uppsalalaan 8 3584 CT, Utrecht, The Netherlands
[3]Forestry and Agricultural Biotechnology Institute (FABI), University of Pretoria, South Africa

*Corresponding author: lise.korsten@up.ac.za

Key words:
Neopestalotiopsis
nursery
phylogeny
South Africa
taxonomy
Vaccinium corymbosum

Abstract: New blueberry plantings in South Africa have increased dramatically since the year 2000, exceeding the global expansion rate. The crop is, however, impacted by several economically important fungal pathogens. Lesser-known fungi such as pestalotioid species can cause leaf and twig blight, and have the potential to become a global threat to blueberry production and expansion. This study aimed to assess the presence of such fungal species in blueberry nurseries in South Africa due to the industry's exponential growth and mass introduction of new cultivars. Symptomatic leaf and twig samples were collected from six propagation nurseries, resulting in 180 pestalotioid isolates, of which a subset of 48 isolates were selected for molecular characterisation using multi-locus sequence analysis of the internal transcribed spacer region (ITS), partial translation elongation factor 1-α (*TEF1*) and partial β-tubulin (*TUB2*) gene regions. Phylogenetic analyses were performed using Maximum Likelihood, Maximum Parsimony and Bayesian Inference methods. Based on the phylogenetic analyses, all isolates clustered with three previously described species of *Neopestalotiopsis*, namely *N. rosae*, *N. hispanica* and *N. longiappendiculata.* Of these, 32 isolates were identified as *N. rosae,* followed by *N. hispanica* (12) and *N. longiappendiculata* (4). To the best of our knowledge, this is the first report of these species in South Africa. Based on phylogenetic analysis and morphological comparisons, we further recommend that *N. vaccinii* be considered a synonym of *N. hispanica.*

Citation: Van der Vyver LS, De Bruin W, Siyoum N, Nsibo DL, Groenewald JZ, Crous PW, Korsten L (2025). Exploring *Neopestalotiopsis* diversity associated with Blueberry leaf and twig blight in South African nurseries. *Fungal Systematics and Evolution* **16**: 41–53. doi: 10.3114/fuse.2025.16.3
Received: 4 February 2025; **Accepted:** 5 March 2025; **Effectively published online:** 13 May 2025
Corresponding editor: A.J.L. Phillips

INTRODUCTION

Blueberries (*Vaccinium corymbosum*) belong to the family *Ericaceae* and are perennial shrubs that bear tasty and highly nutritious fruits (Milivojevic *et al.* 2012). These nutrient-dense fruits are rich in vitamins, fibre and antioxidants such as flavonoids and phenolic acids (Krishna *et al.* 2023). Due to their nutritional value, global demand has increased, leading to a 5.12 % rise (from 1,769530 to 1,860080 tons) between 2021 and 2022. America was the leading producer during this time, contributing 920080 tons. In South Africa, blueberry production grew by 17.31 % (from 26000 to 30500 tons) between 2022 and 2023, with most growth in the Western Cape Province (Pienaar *et al.* 2019, IBO 2023).

Blueberry cultivation in South Africa is primarily divided between shade netting and open-field production, with 17 % of blueberries grown under plastic covers (Pienaar *et al.* 2019). The two main varieties grown are the southern highbush (SHB) and the northern highbush (NHB). Due to limited chilling hours, SHB is predominantly grown in the southern coastal regions, whereas NHB is grown in the central areas of South Africa (Retamales & Hancock 2018). To ensure the healthy growth and expansion of the industry, it is therefore essential to assess which potential fungal pathogens occur in nursery material. This knowledge is critical for the development and implementation of effective disease-management strategies.

Leaf and twig blight symptoms have been observed in some newly planted blueberry fields and other production regions and nurseries in South Africa. These types of symptoms are generally caused by *Botrytis cinerea*, *Alternaria alternata* and *Botryosphaeria dothidea* (Milholland 1972, Wright *et al.* 2004, Rivera *et al.* 2013). Other fungi that can affect blueberry plants pre- and post- harvest are *Colletotrichum gloeosporioides*, *Diaporthe vaccinii* and *Pucciniastrum minimum*, leading to fruit decay, twig blight and leaf rust (Hartung 1981, Cardinaals *et al.* 2018, Anderson 2022). While most of these pathogens are economically important, there is also a need to characterise lesser-known pathogens, such as pestalotioid fungi, which can be overlooked when investigating causal agents of leaf and twig blight. These fungal species are known to be plant pathogens and can pose a major concern in a rapidly expanding industry. Some of these species can under conditions of high humidity, long periods of leaf wetness and wounding cause symptoms similar to other well-known blueberry leaf diseases (Belisário *et al.* 2020).

Fungal Systematics and Evolution is licensed under a Creative Commons Attribution-NonCommercial-NoDerivatives 4.0 International License

© 2025 Westerdijk Fungal Biodiversity Institute

Pestalotioid fungi have also been reported to cause blueberry canker and twig dieback (Borrero *et al.* 2018), strawberry fruit rot (Baggio *et al.* 2021), tea leaf blight (Shahriar *et al.* 2021) and blueberry leaf spot (Zheng *et al.* 2023) in Spain, Florida, Malaysia and China, respectively. *Pestalotiopsis* was first described by Steyaert (1949) and later revised by Guba (1961). However, a molecular-based phylogenetic evaluation of these species was conducted by Hu *et al.* (2007). While the diversity of *Pestalotiopsis* was assessed using culture morphology and molecular methods using the ITS region, species identification became possible only after incorporating sequence data from the partial β-tubulin gene region (*TUB2*) into phylogenetic analyses (Hu *et al.* 2007). Subsequently, Maharachchikumbura *et al.* (2012) evaluated 10 genes and identified ITS, partial translation elongation factor 1-α (*TEF1*) and *TUB2* as suitable for identifying *Pestalotiopsis* species. This led to their further classification in 2014, dividing *Pestalotiopsis* into three genera: *Pestalotiopsis*, *Neopestalotiopsis* and *Pseudopestalotiopsis*, distinguished through phylogenetic analyses and colouration of conidial median cells (Maharachchikumbura *et al.* 2014). The aforementioned genera include endophytes (Gideon *et al.* 2018), saprophytes (Liu *et al.* 2008) and phytopathogenic species (Crous *et al.* 2011). To date, only *N. natalensis* has been documented in South Africa on *Acacia mollissima* (black wattle) (Maharachchikumbura *et al.* 2014). Phytopathogenic pestalotioid species such as *Pestalotiopsis neglecta* (Espinoza *et al.* 2008), *N. clavispora* (Borrero *et al.* 2018, Lee *et al.* 2019, Jevremović *et al.* 2022), *N. rosae* (Rodríguez-Gálvez *et al.* 2020) and *N. vaccinii* (Santos *et al.* 2021) have been reported on blueberries from Chile, Spain, Korea, Serbia, Peru and Portugal, respectively. The presence of pestalotioid fungi in blueberry nurseries of South Africa is currently unknown, an aspect which this study aimed to address.

MATERIALS AND METHODS

Sample collection and fungal isolation

In 2023, symptomatic blueberry leaves and twigs were collected from six propagation nurseries across the northern and southern production regions of South Africa. One nursery was located in Gauteng Province, while the remaining five were situated in Western Cape Province. Leaves and twigs were removed with pruning shears that had been surface-sterilised with 70 % ethanol. Samples were individually stored in paper bags and transported in a cooler box to the Plant Pathology laboratories of the University of Pretoria and stored overnight at 4 °C for immediate processing. Fungal isolation was performed according to the method described by Liu *et al.* (2015). Leaf and twig samples were surface sterilised with 70 % ethanol and 1 % sodium hypochlorite for 1 min each and then rinsed three times in sterile distilled water. Samples were dried on sterile paper towels in laminar flow cabinets. Leaf tissue from the margin of the diseased areas was aseptically removed (5 mm^2), placed onto half-strength potato dextrose agar (PDA) and incubated at 25 °C in the dark. After five d, 180 *Neopestalotiopsis* fungal colonies were sub-cultured from the margin of the colony onto full-strength PDA and incubated at 25 °C in the dark. To obtain pure cultures, representative isolates were purified by hyphal tipping onto full-strength PDA plates and incubated at 25 °C in the dark. Based on their cultural morphology, 48 of the 180 isolates were selected as group representatives for identification.

Culture preparation and morphological analysis

The cultural characteristics and conidiomata of the 48 isolates were observed in cultures grown on PDA at 25 °C in darkness for five days, then at 20 °C under a 12 h light/dark cycle for an additional 7 d. Digital images of all structures were recorded with an Axiocam 105 colour camera mounted on a Zeiss Axioskop 2 plus compound microscope with differential interference contrast illumination. Conidiomatal morphology was examined using a Keyence VHX-7000 digital dissecting microscope. Microscope preparations were mounted in a 20 % glycerol solution. A Nikon Eclipse E200 compound microscope was used to make 30 measurements of each structure. Conidial length was measured from the base of the apical appendages to the base of the basal cell and conidial width was measured across the widest conidial segment. The length and width values were reported as one standard deviation (SD) above and below the mean, with extreme measurements shown in parentheses, followed by the mean ± SD. All other measurements were provided as the full range, from the lowest to the highest extremes. Colony colours were determined using a mycological colour chart (Rayner 1970). Cultures with an (ex-)type status are indicated with a superscript T throughout the text.

DNA extraction, PCR amplification and sequencing

Genomic DNA was extracted from 7–14-d-old cultures using a Quick-DNA Fungal/Bacterial Miniprep Kit (Zymo Research, USA) following the manufacturer's instructions. Extracted DNA was stored at -20 °C until further use. The internal transcribed spacer (ITS) regions and intervening 5.8S nrRNA gene of the nrDNA was amplified with the primers ITS1 (5'-TCCGTAGGTGAACCTGCGG-3') and ITS4 (5'-TCCTCCGCTTATTGATATGC-3') (White *et al.* 1990). The partial β-tubulin (*TUB2*) gene was amplified with the primers Bt2a (5'-GGTAACCAAATCGGTGCTGCTTTC-3') and Bt2b (5'-ACCCTCAGTGTAGTGACCCTTGGC-3') (Glass & Donaldson 1995). The partial translation elongation factor 1-α (*TEF1*) gene was amplified with the primers EF1-728F (5'- CATCGAGAAGTTCGAGAAGG-3') and EF1-986R (5'-TACTTGAAGGAACCCTTACC-3') (Carbone & Kohn 1999). The PCR mixture consisted of 12.5 µL DreamTaq Green PCR Master Mix (2×) (Thermo Scientific, Germany), 0.25 µL (2 µm) of each forward and reverse primer, 11 µL of PCR grade ddH2O and 1 µL of template DNA. Thermocycling conditions for the amplification of ITS and *TUB2* were as follows: initial denaturation at 95 °C for 2 min; followed by 35 cycles of 94 °C for 30 s, 57 °C for 45 s and 72 °C for 90 s; and a final extension at 72 °C for 7 min. Part of the *TEF1* gene was amplified as described by Udayanga *et al.* (2012). Initial denaturation was performed at 95 °C for 5 min, followed by 40 cycles at 95 °C for 30 s, 58 °C for 50 s and 72 °C for 60 s and a final elongation at 72 °C for 10 min. Thermocycling was performed using Mastercycler Pro Thermocycler S (Eppendorf, Germany).

© 2025 Westerdijk Fungal Biodiversity Institute

The amplified PCR products were purified using a Smarted Nucleic Acid Kit (Stratec, Germany), according to the manufacturer's guidelines. The purified amplicon was further amplified with a BigDye Terminator v. 3.1 Cycle Sequencing Kit (Thermo Scientific, Germany). The PCR mixture consisted of 0.5 µL of BigDye Terminator v. 3.1 Ready Reaction Mix, 1 µL (2 µm) forward or reverse primers, 2.5 µL of 5× sequencing Buffer, 4 µL of ddH2O and 2 µL of purified amplicon DNA to serve as a template. Terminator thermocycling conditions for all amplicons were as follows: initial denaturation at 96 °C for 1 min, followed by 25 cycles at 96 °C for 10 s, 50 °C for 5 s and 60 °C for 4 min. The resulting product was precipitated with ethanol before submission to the University of Pretoria's Sanger Sequencing facility at the Faculty of Natural and Agriculture sciences using an ABI3500xL Genetic analyser Applied Biosystems, ThermoFisher Scientific, USA).

Phylogenetic analyses

The DNA sequences of ITS, *TUB2* and *TEF1* were used for phylogenetic analyses. Additional sequences that served as reference data were obtained from GenBank (www.ncbi.nlm.nih.gov/genbank/) and are listed in Table 1. A total of 118 strains were selected for phylogenetic analysis, of which 48 were isolated in this study and 70 served as reference strains, including one outgroup taxon. Sequences were aligned with MAFFT v. 7 (https://mafft.cbrc.jp/alignment/server/index.html). The resulting alignment was manual improvement using Mesquite v. 3.81. (Maddison & Maddison 2023) and MEGA v. 11.0.13 (Tamura *et al.* 2021). Multi-locus phylogenetic analysis was performed using Maximum Likelihood (ML), Maximum Parsimony (MP) and Bayesian inference (BI). Inference of the ML partitioned alignment was achieved using RAxML v. 8.2.10 (Stamatakis 2014). One thousand rapid bootstraps were used to determine the support values for the optimal ML tree. The "-m GTRGAMMA" parameter was used in the RAxML analysis to estimate and optimise unique alpha-shaped parameters, GTR rates and empirical base frequencies for each partition. A final optimised likelihood score was used by the software to select the final tree among suboptimal trees. The MP was performed using PAUP (Phylogenetic Analysis Using Parsimony) v. 4.0a. build 169 (Swofford 2003). Trees were inferred using the heuristic search option with 1000 random sequence additions and TBR branch swapping. A total of 1000 bootstrap replications were used to evaluate the robustness of the equally most parsimonious trees. Optimal nucleotide substitution models were determined prior to the Bayesian analysis using MrModeltest v. 2.4 (Nylander 2004) in conjunction with PAUP. The BI analyses were done with MrBayes v. 3.3.7a (Rodríguez-Gálvez *et al.* 2020). Four Markov Chain Monte Carlo chains ran simultaneously over a maximum of 1000 M generations, terminating when the standard deviation of split frequencies reached 0.01 with a burn-in factor of 0.25. Trees were sampled every 10 generations and the trees were summarised and posterior probability values were calculated from the trees remaining after removal of the burn-in trees. The alignment and phylogenetic trees were deposited at www.figshare.com (doi: 10.6084/m9.figshare.28302329).

Congruence between single locus and concatenated trees were assessed based on overall topography by visualisation in FigTree v. 1.4.4 (http://tree.bio.ed.ac.uk/software/figtree/) and modified in the Inkscape Project (https://inkscape.org).

RESULTS

Phylogenetic analyses

The resulting concatenation of the three-locus alignment contained a total of 1288 nucleotide positions, including gaps (ITS: 549, *TEF1*: 318, and *TUB2*: 421). The best ML tree was obtained with an optimised likelihood of -4390,954206 (Fig. 1). The MP analysis determined 881 characters to be constant, 281 to be variable characters and 126 to be parsimony-informative characters. The heuristic analysis revealed 1000 equally most parsimonious trees with 749 steps (CI = 0.656, RI = 0.762, RC = 0.499, HI = 0.344). MrModelTest selected the following best-fit models for the different partitions for the Bayesian analysis: for ITS, the HKY+I model includes a proportion of invariable sites; for *TEF1*, the HKY+G model applies a gamma distribution for rate variation; and for *TUB2*, the GTR+G model uses gamma-distributed rates. Dirichlet (1,1,1,1) state frequency distribution was determined to be suitable for the MrBayes analyses across all partitions. The BI analysis ran until the standard deviation of split frequencies reached 0.01 after 62,600000 generations. A total of 12,520002 trees were saved, 75 % of which were used to calculate the 50 % majority rule consensus tree and the posterior probabilities. The ML, MP and BI phylogenetic trees showed similar species-level topologies.

Of the 48 isolates used in the present study, 32 isolates formed a poorly supported cluster with *N. rosae* (CBS 101057^{T}), with ML bootstrapping (MLB), MP bootstrapping (MPB) and BI posterior probability (PP) support values of 59/-/0.52. The Pairwise comparison (blast2) between the novel sequences in the clade and the ex-type sequences of *N. rosae* (CBS 101057^{T}) were highly similar across all gene regions. On ITS: 99 % (over 476/492 nt including one gap), *TEF1*: 100 % (over 244/276 nt) and *TUB2*: 100 % (over 405/405 nt).

An additional 12 isolates clustered with *N. hispanica* (CBS 147686^{T}) and *N. vaccinii* (CAA1059^{T}) with moderate support values of 86/87/0.77 (MLB/MPB/PP). The microscopic morphologies of *N. hispanica* (CBS 147686^{T}) and *N. vaccinii* (CAA1059^{T}) were compared together with an isolate from our study that clustered in the same clade (Table 2), as described by Diogo *et al.* (2021) and Santos *et al.* (2021). One of our isolates, BBFC0176, resembled *N. hispanica* in all parameters. However, when comparing *N. hispanica* to *N. vaccinii*, the length of the conidia, basal appendage, apical appendage and number of apical appendages did not correlate. When considering the concatenated alignment, the *TEF* and *TUB2* gene regions were identical with the only differences between *N. hispanica* (CBS 147686^{T}) and *N. vaccinii* (CAA1059^{T}) being a single nucleotide deletion in the ITS region. Pairwise comparisons (blast2) between the novel sequences generated in this study to the ex-type sequences of *N. hispanica* (CBS 147686^{T}) revealed a high degree of similarity across all gene regions. On ITS: 99 % (over 474/475 nt including one gap and 473/476 including two gaps), *TEF1*: 100 % (over 251/259 nt) and *TUB2*: 100 % (over 354/397 nt).

The remaining four isolates clustered with *N.*

© 2025 Westerdijk Fungal Biodiversity Institute



Fig. 1. Maximum-likelihood phylogram tree generated by RAxML-based analysis of the concatenated (ITS+*TEF1+TUB2*) alignment. Maximum-likelihood bootstrapping (MLB), maximum-parsimony bootstrapping (MPB) above 50 % and Bayesian inference posterior probabilities (PP) above 0.5 (MLB/MPB/PP) are shown. Isolates from the current study isolated from blueberry are printed in red with identified/synonymised taxa in respective superscripts. Reference (ex-)type strains indicated by superscript T. The tree is rooted to *Pestalotiopsis diversiseta* (MFLUCC 12-0297^{T}).

© 2025 Westerdijk Fungal Biodiversity Institute

Table 1. GenBank accession numbers of isolates used in this study for the phylogenetic analyses of *Neopestalotiopsis* species.

Species	Strain[1]	GenBank Accession number		
		ITS	***TEF1***	***TUB2***
Neopestalotiopsis acrostichi	MFLUCC 17-1754 [T]	MK764272	MK764316	MK764338
N. alpapicalis	MFLUCC 17-2544 [T]	MK357772	MK463547	MK463545
N. aotearoa	CBS 367.54 [T]	KM199369	KM199526	KM199454
N. asiatica	MFLUCC 12-0286 [T]	JX398983	JX399049	JX399018
N. australis	CBS 114159 [T]	KM199348	KM199537	KM199432
N. brachiate	MFLUCC 17-1555 [T]	MK764274	MK764318	MK764340
N. brasiliensis	COAD 2166 [T]	MG686469	MG692402	MG692400
N. camelliae-oleiferae	CSUFTCC81 [T]	OK493585	OK507955	OK562360
N. cavernicola	KUMCC 20-0269 [T]	MW545802	MW550735	MW557596
N. chrysea	MFLUCC 12-0261 [T]	JX398985	JX399051	JX399020
N. clavispora	MFLUCC 12-0281 [T]	JX398979	JX399045	JX399014
N. coffea-arabicae	HGUP4015 [T]	KF412647	KF412644	KF412641
N. cubana	CBS 600.96 [T]	KM199347	KM199521	KM199438
N. dendrobii	MFLUCC 14-0106 [T]	MK993571	MK975829	MK975835
N. drenthii	BRIP 72263a [T]	MZ303786	MZ344171	MZ312679
N. egyptiaca	CBS 140162 [T]	KP943747	KP943748	KP943746
N. eucalypticola	CBS 264.37 [T]	KM199376	KM199551	KM199431
N. eucalyptorum	CBS 147684 [T]	MW794108	MW805397	MW802841
N. foedans	CGMCC 3.9123 [T]	JX398987	JX399053	JX399022
N. formicarum	CBS 362.72[T]	KM199358	KM199517	KM199455
N. fragariae	ZHKUCC 22-0115	ON651146	ON685197	ON685199
N. guajavae	FMB0026 [T]	MF783085	MH460868	MH460871
N. guajavicola	FMB0129 [T]	MH209245	MH460870	MH460873
N. hadrolaeliae	VIC 47180 [T]	MK454709	MK465122	MK465120
N. haikouensis	SAUCC212271 [T]	OK087294	OK104877	OK104870
N. hispanica	CBS 147686 [T]	MW794107	MW805399	MW802840
	BBFC0104	**PV018578**	**PV033977**	**PV033929**
	BBFC0151	**PV018579**	**PV033978**	**PV033930**
	BBFC0152	**PV018580**	**PV033979**	**PV033931**
	BBFC0176	**PV018581**	**PV033980**	**PV033932**
	BBFC0222	**PV018582**	**PV033981**	**PV033933**
	BBFC0229	**PV018583**	**PV033982**	**PV033934**
	BBFC0235	**PV018584**	**PV033983**	**PV033935**
	BBFC0241	**PV018585**	**PV033984**	**PV033936**
	BBFC0243	**PV018586**	**PV033985**	**PV033937**
	BBFC0250	**PV018587**	**PV033986**	**PV033938**
	BBFC0265	**PV018588**	**PV033987**	**PV033939**
	BBFC0273	**PV018589**	**PV033988**	**PV033940**
N. honoluluana	CBS 114495 [T]	NR_145245	KM199548	KM199457
N. hydeana	MFLUCC 20-0132 [T]	MW266069	MW251129	MW251119
N. hypericin	KUNCC 22-12597 [T]	OP498010	OP713768	OP765908
N. iberica	CBS 147688 [T]	MW794111	MW805402	MW802844
N. javaensis	CBS 257.31 [T]	KM199357	KM199543	KM199437
N. longiappendiculata	CBS 147690[T]	MW794112	MW805404	MW802845
	BBFC0259	**PV018590**	**PV033989**	**PV033941**
	BBFC0266	**PV018591**	**PV033990**	**PV033942**
	BBFC0268	**PV018592**	**PV033991**	**PV033943**

© 2025 Westerdijk Fungal Biodiversity Institute

Table 1. (Continued).

Species	Strain[1]	GenBank Accession number		
		ITS	***TEF1***	***TUB2***
	BBFC0300	**PV018593**	**PV033992**	**PV033944**
N. lusitanica	MEAN 1317 [T]	MW794110	MW805406	MW802843
N. maddoxii	BRIP 72266a [T]	MZ303782	MZ344167	MZ312675
N. mesopotamica	CBS 336.86 [T]	KM199362	KM199555	KM199441
N. mianyangensis	CGMCC 3.23554[T]	OP546681	OP723490	OP672161
N. musae	MFLUCC 15-0776 [T]	NR_156311	KX789685	KX789686
N. nebuloides	BRIP 66617 [T]	MK966338	MK977633	MK977632
N. olumideae	BRIP 72273a [T]	MZ303790	MZ344175	MZ312683
N. paeoniae-suffruticosae	CGMCC 3.23555[T]	OP082292	OP204794	OP235980
N. perukae	FMB0127 [T]	MH209077	MH523647	MH460876
N. petila	MFLUCC 17-1738 [T]	MK764275	MK764319	MK764341
N. phangngaensis	MFLUCC 18-0119 [T]	MH388354	MH388390	MH412721
N. photiniae	MFLUCC 22-0129 [T]	OP498008	OP753368	OP752131
N. protearum	CBS 114178 [T]	JN712498	KM199542	KM199463
N. psidii	FMB0028 [T]	MF783082	MH460874	MH477870
N. rhizophorae	MFLUCC 17-1550 [T]	MK764277	MK764321	MK764343
N. rhododendi	MFLUCC 22-0130[T]	OP497995	OP753370	OP762671
N. rhododendri	GUCC 21504[T]	MW979577	MW980444	MW980443
N. rhododendricola	KUN-HKAS-123204 [T]	OK283069	OK274148	OK274147
N. rosae	CBS 101057 [T]	KM199359	KM199523	KM199429
	BBFC0122	**PV018594**	**PV033993**	**PV033945**
	BBFC0131	**PV018595**	**PV033994**	**PV033946**
	BBFC0135	**PV018596**	**PV033995**	**PV033947**
	BBFC0175	**PV018597**	**PV033996**	**PV033948**
	BBFC0177	**PV018598**	**PV033997**	**PV033949**
	BBFC0178	**PV018599**	**PV033998**	**PV033950**
	BBFC0179	**PV018600**	**PV033999**	**PV033951**
	BBFC0180	**PV018601**	**PV034000**	**PV033952**
	BBFC0181	**PV018602**	**PV034001**	**PV033953**
	BBFC0186	**PV018603**	**PV034002**	**PV033954**
	BBFC0187	**PV018604**	**PV034003**	**PV033955**
	BBFC0188	**PV018605**	**PV034004**	**PV033956**
	BBFC0189	**PV018606**	**PV034005**	**PV033957**
	BBFC0199	**PV018607**	**PV034006**	**PV033958**
	BBFC0201	**PV018608**	**PV034007**	**PV033959**
	BBFC0202	**PV018609**	**PV034008**	**PV033960**
	BBFC0205	**PV018610**	**PV034009**	**PV033961**
	BBFC0206	**PV018611**	**PV034010**	**PV033962**
	BBFC0207	**PV018612**	**PV034011**	**PV033963**
	BBFC0208	**PV018613**	**PV034012**	**PV033964**
	BBFC0209	**PV018614**	**PV034013**	**PV033965**
	BBFC0217	**PV018615**	**PV034014**	**PV033966**
	BBFC0223	**PV018616**	**PV034015**	**PV033967**
	BBFC0245	**PV018617**	**PV034016**	**PV033968**
	BBFC0249	**PV018618**	**PV034017**	**PV033969**
	BBFC0251	**PV018619**	**PV034018**	**PV033970**
	BBFC0255	**PV018620**	**PV034019**	**PV033971**

© 2025 Westerdijk Fungal Biodiversity Institute

Table 1. (Continued).

Species	Strain[1]	GenBank Accession number		
		ITS	*TEF1*	*TUB2*
	BBFC0256	**PV018621**	**PV034020**	**PV033972**
	BBFC0261	**PV018622**	**PV034021**	**PV033973**
	BBFC0262	**PV018623**	**PV034022**	**PV033974**
	BBFC0267	**PV018624**	**PV034023**	**PV033975**
	BBFC0298	**PV018625**	**PV034024**	**PV033976**
N. rosicola	CFCC 51992 ^{T}	KY885239	KY885243	KY885245
N. samarangensis	MFLUCC 12-0233 ^{T}	JQ968609	JQ968611	JQ968610
N. saprophytica	MFLUCC 12-0282 ^{T}	KM199345	KM199538	KM199433
N. sichuanensis	SM15-1C^{T}	MW166232	MW199751	MW218525
N. siciliana	CBS 149117 ^{T}	ON117813	ON107273	ON209162
N. sonneratae	MFLUCC 17-1745 ^{T}	MK764279	MK764323	MK764345
N. subepidermalis	CFCC 55160 ^{T}	OK560699	OM622425	OM117690
N. suphanburiensis	MFLUCC 22-0126- ^{T}	OP497994	OP753372	OP752135
N. surinamensis	CBS 450.74 ^{T}	KM199351	KM199518	KM199465
N. terricola	CGMCC 3.23553^{T}	OP082294	OP204796	OP235982
N. thailandica	MFLUCC 17-1730 ^{T}	MK764281	MK764325	MK764347
N. umbrinospora	MFLUCC 12-0285 ^{T}	JX398984	JX399050	JX399019
N. vaccinii	CAA1059 ^{T}	MW969747	MW959099	MW934610
N. vacciniicola	CAA1055 ^{T}	MW969749	MW959101	MW934612
N. vheenae	BRIP 72293a ^{T}	MZ303792	MZ344177	MZ312685
N. vitis	MFLUCC 15-1265 ^{T}	KU140694	KU140676	KU140685
N. zakeelii	BRIP 72282a ^{T}	MZ303789	MZ344174	MZ312682
N. zimbabwana	CBS 111495 ^{T}	JX556231	KM199545	KM199456
Outgroup: *Pestalotiopsis diversiseta*	MFLUCC 12–0287 ^{T}	JX399009	JX399073	JX399040

[1]CBS: Culture Collection of the Westerdijk Fungal Biodiversity Institute, Utrecht, The Netherlands; CGMCC: China General Microbial Culture Collection Center (China); MFLUCC: Mae Fah Luang University Culture Collection, Chiang Rai, Thailand; BRIP: Queensland Plant Pathology Herbarium, Brisbane, Queensland, Australia; FMB: Department of Plant Pathology, University of Agriculture Faiasalabad, Jail Road, Faisalabad, Punjab, Pakistan; CAA: Personal Culture Collection Artur Alves, Department of Biology, University of Aveiro; ZHKUCC: Uppsala University Culture Collection, Sweden.
Isolates and sequences from the current study printed in bold.
Reference (ex)-type strains indicated by supescript T.

Table 2. Microscopic morphological comparison of *N. hispanica* (CBS 147686^{T}), *N. vaccinii* (CAA1059^{T}) and isolate BBFC0176.

Morphology (µm)	*N. vaccinii* (CAA1059^{T})	*N. hispanica* (CBS 147686^{T})	Isolate BBFC0176
Conidiogenous cells length	(1.3–)14.1–19.9(–25.8)	7–14.7	7-20.5
Conidiogenous cells width	(2.1–)2.7–3.0(–3.7)	2.4–4.1	3.2-5.9
Conidia length	(11.0–)13.4–13.8(–15.2)	(21.5–)24.4–25.3(–27.1)	(20.1–) 20.8-26.7 – (27.9)
Conidia width	(4.9–)6.3–6.6(–7.5)	(5.9–)7.2–7.8(–8.7)	(6.1–) 6.2-7.9 (–8.3)
Basal cell	(2.2–)2.9–3.6(–6.3)	3.3–5.5	3.5–6.6
Apical cell	(2.4–)3.7–4.3(–5.1)	2.8–6.2	2.5-4.7
Basal appendage	1.7–6.6	5.1–15.5	2-9.8
Apical appendage	8.9–25.3	(30.7–)19.5–22.6(–30.7)	(16.9–) 17-27.4 (–41.4)
Appendage number	2–3	3–4	3–4

© 2025 Westerdijk Fungal Biodiversity Institute

longiappendiculata (MEAN 1315[T]) with high support values, 89/90/1 (MLB/MPB/PP). Pairwise comparison (blast2) between novel sequences generated in this study to the ex-type sequence of *N. longiappendiculata* (MEAN 1315[T]) revealed high similarity across all gene regions. On ITS: 100 % (over 481/492 nt), *TEF1*: 100 % (over 259/259 nt) and *TUB2*: 99 % (over 404/405 nt).

Taxonomy

Neopestalotiopsis hispanica E. Diogo *et al.*, *Mycol. Progr.* **20**: 1448. 2021. Fig. 2.
Synonym: *Neopestalotiopsis vaccinii* J. Santos *et al.*, *Eur. J. Pl. Path.* **162**: 549. 2021.

Pycnidial conidiomata (BBFC0176) on PDA, globose, semi-immersed, black, 183–527 µm; exuding globose, black, glistening conidial masses. *Conidiophores* indistinct, often reduced to conidiogenous cells. *Conidiogenous cells* discrete, cylindrical, hyaline, smooth-walled, simple, proliferating percurrently, tapering towards a truncated apex, 5.9–19.0 × 2.4–7.0 µm. *Conidia* fusoid, ellipsoid, straight or slightly curved with 4 septa (21.2–)21.7–27.2(–28.6) × (5.6–)5.7–7.9(–7.9) µm, $\bar{x}$ ± SD = 24.3 ± 1.8 × 6.6 ± 0.6 µm; basal cell; conic with truncated base, hyaline, rugose and thin-walled, 2.9–6.3 µm, with a single, tubular, unbranched, centric basal appendage 1.6–8 µm long; three median cells doliiform 15–17.7 µm long, $\bar{x}$ ± SD = 16.2 ± 0.8 µm, wall rugose, versicoloured, with septa darker than the rest of the cell; second cell from base pale brown, 3.4–6 µm long; third cell honey brown, 4.4–6.6 µm long; fourth cell brown, 4.4–6.4 µm long; apical cell 3.3–5.6 µm long, hyaline cylindrical, thin with smooth walls; 3–4 apical appendages, inserted each in upper half of apical cell, unbranched, filiform, (19.5–)20.8–38.6(–39.1) long, $\bar{x}$ ± SD = 30.8 ± 7.2 µm.

Culture characteristics: On PDA cultures reached 56 mm diam. after 7 d at 25 °C with irregular margins, pale-yellow,

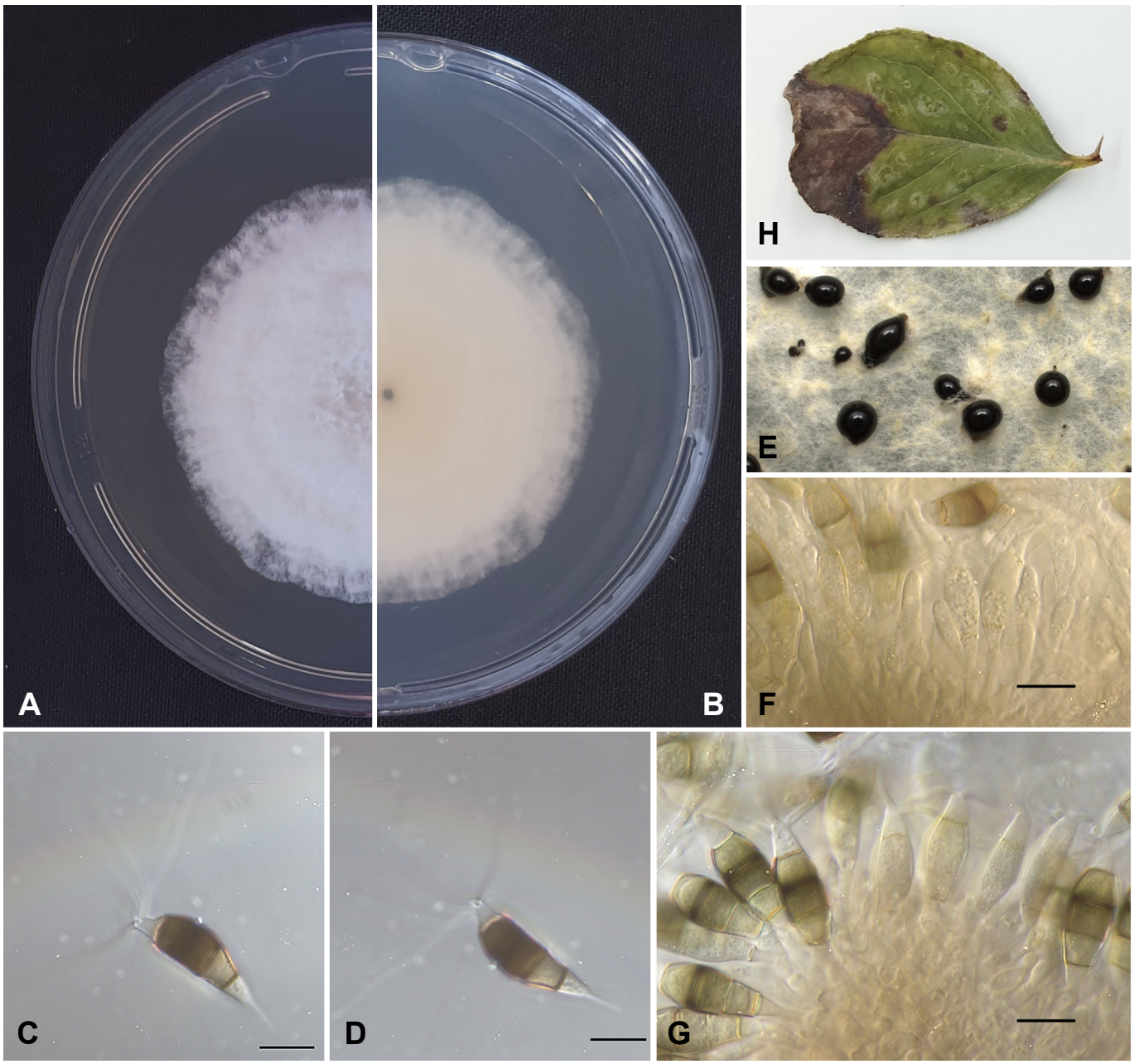

Fig. 2. Morphology of *Neopestalotiopsis hispanica* (BBFC0176) isolated from *Vaccinium corymbosum*. **A.** Upper culture surface. **B.** Reverse culture surface on PDA after 7 d at 25 °C. **C, D.** Conidia. **E.** Conidiomata on PDA. **F, G.** Conidiogenous cells. **H.** Sampled leaf. Scale bars = 10 µm.

© 2025 Westerdijk Fungal Biodiversity Institute

with aerial mycelium conidiomata prevalent on mycelium margins (Fig. 2).

Neopestalotiopsis longiappendiculata E. Diogo *et al*., *Mycol. Progr*. **20**: 1450. 2021. Fig. 3.

Pycnidial conidiomata (BBFC0266) on PDA, globose, semi-immersed, black, 272−357 µm; exuding globose, black, glistening conidial masses. *Conidiophores* indistinct, often reduced to conidiogenous cells. *Conidiogenous cells* discrete, cylindrical, hyaline, smooth-walled, simple, proliferating percurrently, tapering towards a truncated apex, 10.6−17.5 × 3.1−7.8 µm. *Conidia* fusoid, ellipsoid, straight or slightly curved with four septa (17.3−)17.5−25.9(−26.5) × (5.9−)6.1−7.8(−8.0) µm, $\bar{x}$ ± SD = 21.1 ± 2.2 × 7 ± 0.5 µm; basal cell; conic with truncated base, hyaline, rugose and thin-walled, 2.1−5.3 µm, with a single, tubular, unbranched, centric basal appendage 1.7−11.4 µm long; three median cells doliiform (11.7–)12–17.3(–17.8) µm long, $\bar{x}$ ± SD = 14.2 ± 1.5 µm, wall rugose, versicoloured, with septa darker than the rest of the cell; second cell from base pale brown, 2.8–6.2 µm long; third cell honey brown, 3.6–5.9 µm long; fourth cell brown, 4.1–6.1 µm long; apical cell 2.9–5.2 µm long, hyaline cylindrical, thin with smooth walls; 3–4 apical appendages, inserted each in upper half of apical cell, unbranched, filiform, (12.2−)12.7−23.9(−24.3) long, $\bar{x}$ ± SD = 19.1 ± 3.2 µm.

Culture characteristics: On PDA cultures reached 32 mm diam. after 7 d at 25 °C with irregular margins, pale yellow, with aerial mycelium conidiomata prevalent on mycelium margins (Fig. 3).

Neopestalotiopsis rosae Maharachch. *et al.*, *Stud. Mycol*. **79**: 147. 2014. Fig. 4.

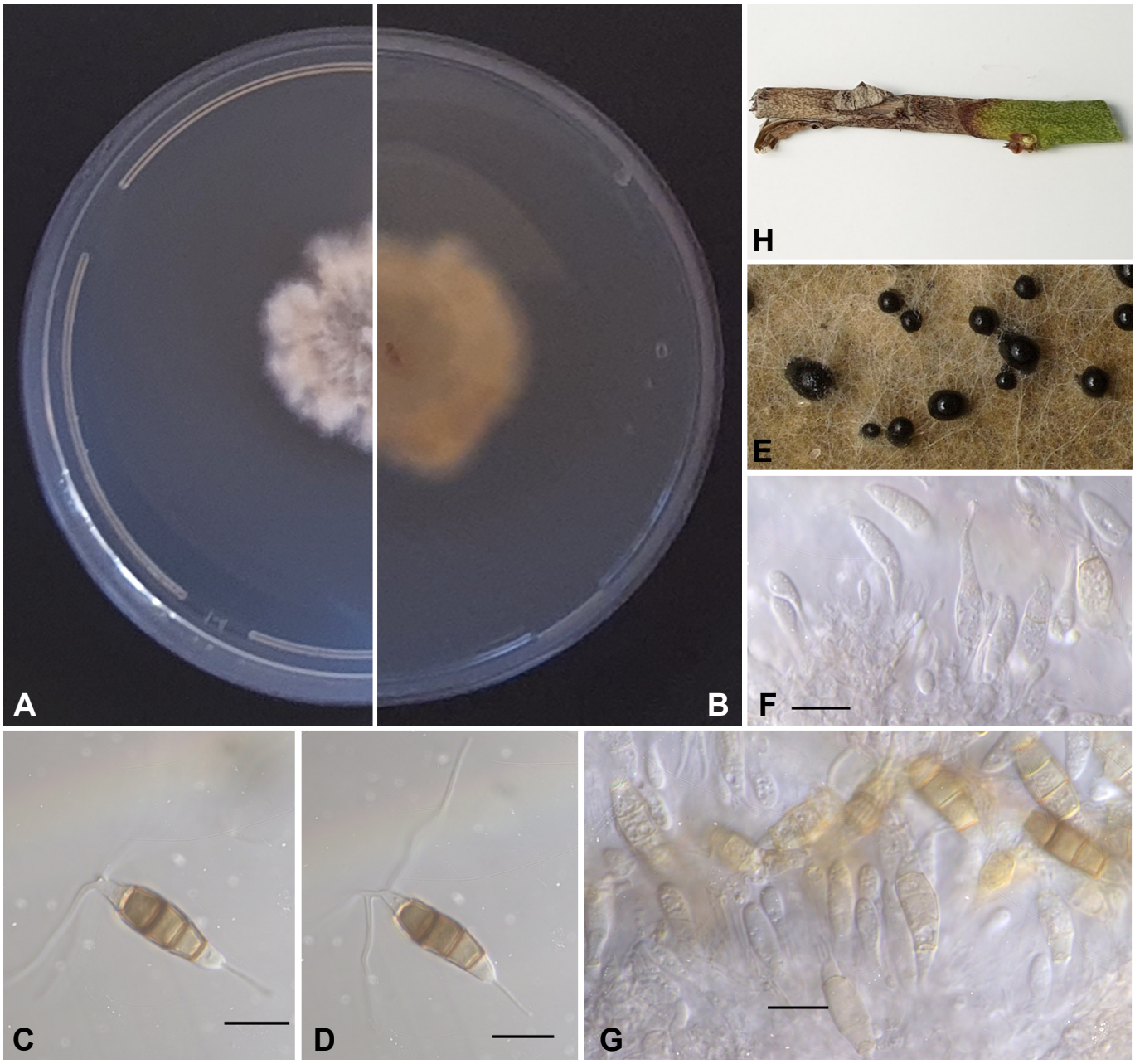

Fig. 3. Morphology of *Neopestalotiopsis longiappendiculata* (BBFC0266) isolated from *Vaccinium corymbosum*. **A.** Upper culture surface. **B.** Reverse culture surface on PDA after 7 d at 25 °C. **C, D.** Conidia. **E.** Conidiomata on PDA. **F, G.** Conidiogenous cells. **H.** Sampled twig. Scale bars = 10 µm.

© 2025 Westerdijk Fungal Biodiversity Institute

Pycnidial conidiomata (BBFC0178) on PDA, globose, semi-immersed, black, 236–527 µm; exuding globose, black, glistening conidial masses. *Conidiophores* indistinct, often reduced to conidiogenous cells. *Conidiogenous cells* discrete, cylindrical, hyaline, smooth-walled, simple, proliferating percurrently, tapering towards a truncated apex, 7.0–20.5 × 3.2–5.9 µm. *Conidia* fusoid, ellipsoid, straight or slightly curved with 4 septa (20.1–)20.8–26.7(–27.9) × (6.1–)6.2–7.9(–8.3) µm, $\bar{x}$ ± SD = 23.5 ± 1.9 × 6.9 ± 0.6 µm; basal cell; conic with truncated base, hyaline, rugose and thin-walled, 2.8–5.3 µm, with a single, tubular, unbranched, centric basal appendage 2.0–9.8 µm long; three median cells doliiform (13.2–)13.9–16.9(–16.9) µm long, $\bar{x}$ ± SD = 15.5 ± 0.9 µm, wall rugose, versicoloured, with septa darker than the rest of the cell; second cell from base pale brown, 3.5–6.6 µm long; third cell honey brown, 4.2–6.6 µm long; fourth cell brown, 3.9–6.1 µm long; apical cell 2.5–4.7 µm long, hyaline cylindrical, thin with smooth walls; 3–5 apical appendages, inserted each in upper half of apical cell, unbranched, filiform, (16.9–)17.0–27.4(–41.4) long, $\bar{x}$ ± SD = 23.3 ± 3 µm.

Culture characteristics: On PDA cultures reached 59 mm diam. after 7 d at 25 °C with irregular margins, pale-yellow, with aerial mycelium conidiomata prevalent on clearly visible concentric mycelium (Fig. 4).

DISCUSSION

In this study, 48 *Neopestalotiopsis* isolates from six nurseries in South Africa were identified through molecular characterisation using multi-locus phylogenetic analyses of ITS, *TEF1* and *TUB2* genes. The resulting ML, MP and BI phylogenetic trees showed similar species-level topology when compared to previous studies (Maharachchikumbura

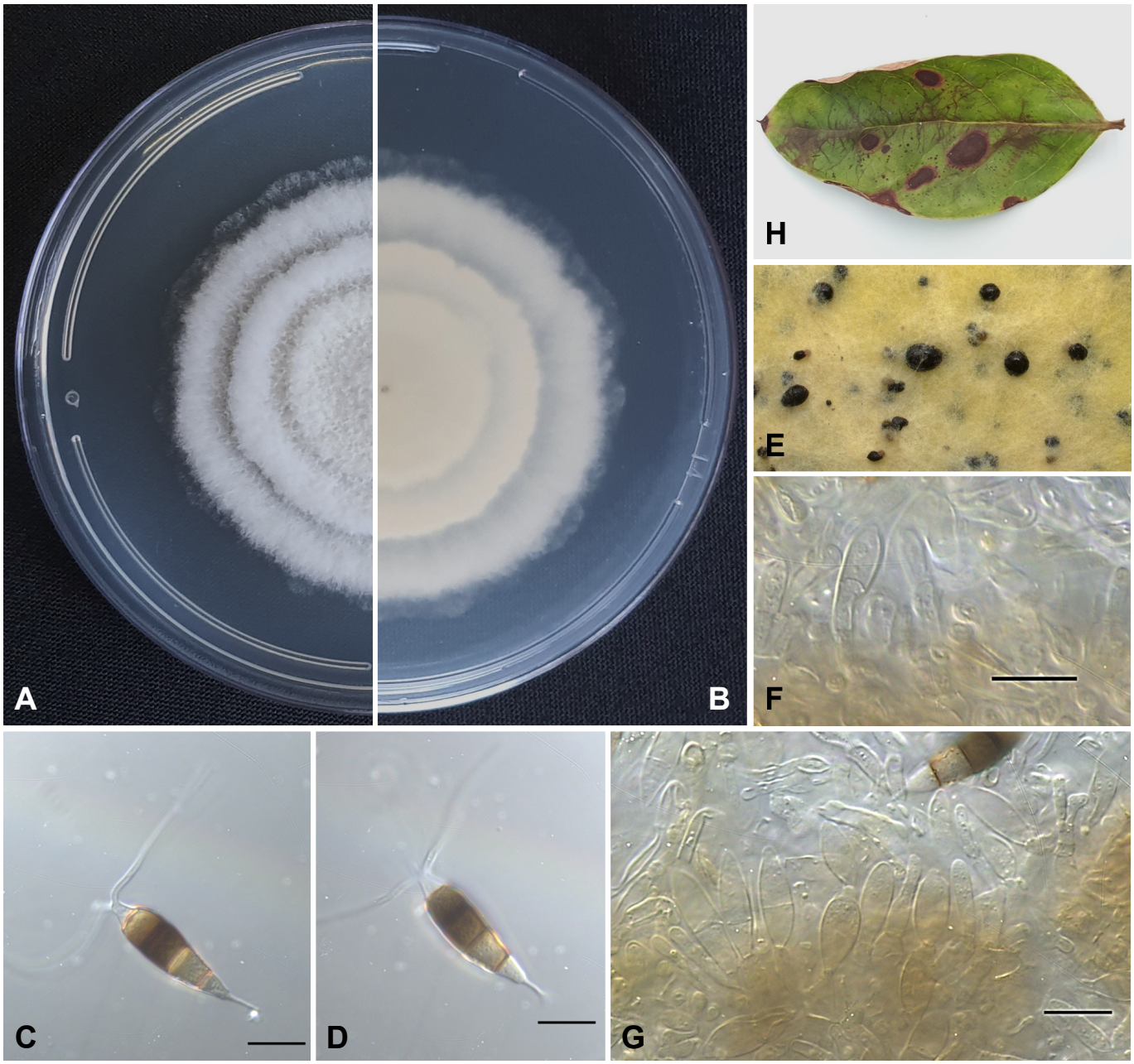

Fig. 4. Morphology of *Neopestalotiopsis rosae* (BBFC0178) isolated from *Vaccinium corymbosum*. **A.** Upper culture surface. **B.** Reverse culture surface on PDA after 7 d at 25 °C. **C, D.** Conidia. **E.** Conidiomata on PDA. **F, G.** Conidiogenous cells. **H.** Sampled leaf. Scale bars = 10 µm.

© 2025 Westerdijk Fungal Biodiversity Institute

et al. 2014, Solarte *et al.* 2018, Darapanit *et al.* 2021, Santos *et al.* 2021). *Neopestalotiopsis rosae* was the most abundant (59 %), followed by *N. hispanica* (29 %) and *N. longiappendiculata* (12 %). A related study conducted in Portugal investigated twig-associated pestalotioid fungi in blueberry orchards and identified species of *Pestalotiopsis* and *Neopestalotiopsis* (Santos *et al.* 2021). No species of *Pestalotiopsis* were found in the current study from blighted twigs or leaves, only species of *Neopestalotiopsis.*

Since its initial description by Guba (1961), *N. rosae* has emerged globally as a significant plant pathogen that causes various diseases in a range of plant species. It has been identified as the causal agent of blueberry dieback and stem blight in Peru (Rodríguez-Gálvez *et al.* 2020), strawberry root rot, fruit rot and leaf spot in Mexico (Rebollar-Alviter *et al.* 2020), pomegranate leaf and fruit spot in Florida (Xavier *et al.* 2020), avocado dieback and stem blight in Italy (Fiorenza *et al.* 2022) and leaf and fruit spot of pecan in China (Gao *et al.* 2022). During 2019–2020, strawberry production in Florida (USA) suffered losses due to *N. rosae*, causing leaf and fruit spots and ultimately reducing the vigour of the affected plants. The outbreak affected 18 commercial farms, leading to the estimated destruction of 80 ha of strawberry production fields to prevent the spread to unaffected areas. A strawberry nursery selling infected plant material was suggested as the source of the outbreak (Baggio *et al.* 2021).

Neopestalotiopsis rosae was identified as a pathogen on the blueberry varieties 'Biloxi' and 'Duke' in studies by (Rodríguez-Gálvez *et al.* 2020, Santos *et al.* 2021). Pathogenicity trials conducted on the 'Duke' variety showed that both *N. rosae* and *N. vaccinii* produced significant lesions on the stems, with *N. rosae* resulting in considerably larger lesions compared to *N. vaccinii*. Additionally, *N. rosae* further retarded the growth of inoculated blueberry plants more than any other tested species of *Neopestalotiopsis* (Santos *et al.* 2021). Based on its history in strawberry nursery settings and blueberry orchards, *N. rosae* can become a serious threat to blueberry nursery and orchard production in South Africa.

Neopestalotiopsis rosae differs from *N. javaensis* by having longer conidial appendages and at the molecular level by 2 nt in ITS and 5 nt in *TEF1.* These characteristics are often used to confirm identity as these species are very closely related (Maharachchikumbura *et al.* 2014, Diogo *et al.* 2021). In our study, the BI phylogeny was unable to differentiate between these species. However, the maximum likelihood phylogenetic tree generated by RAxML successfully did so, supported by apical appendage measurements. This is possibly due to the limited nucleotide substitution models available when using RAxML. This highlights the importance of utilising ML, MP and BI instead of relying on only one or the other. Furthermore, the primer sets used for the amplification of the three gene regions in the current study only partially overlap (ITS: 95.4 %; *TEF1*: 55.9 %; *TUB2*: 55.2 %) with the study done by (Maharachchikumbura *et al.* 2014).

A total of 12 isolates from our study formed a well-supported clade with *N. vaccinii* (CAA1059^{T}) and *N. hispanica* (CBS 147686^{T}). *Neopestalotiopsis vaccinii* has only been reported in association with blueberries, isolated from twig dieback, twig blight and necrotic leaf symptoms in blueberry orchards of Portugal (Santos *et al.* 2021). *Neopestalotiopsis hispanica*, on the other hand, has only been described on *Eucalyptus globulus*, which was found in stem girdling and dieback tissue from a nursery in Portugal (Diogo *et al.* 2021). Due to the absence of sufficient taxonomical and molecular features to confidently distinguish *N. vaccinii* and *N. hispanica*, we regard them as synonymous. The name *N. hispanica* should be used, as it was published first (8 Nov. 2021 versus 22 Nov. 2021) in accordance with the International Code of Nomenclature for algae, fungi and plants (Turland *et al.* 2018), and therefore has priority.

Lastly, four isolates from our study formed a well-supported clade with *N. longiappendiculata* (CBS 147690^{T}), which was also first isolated from *Eucalyptus globulus* tissue in the aforementioned study in Portugal (Diogo *et al.* 2021). Furthermore, *N. longiappendiculata* was also found to cause grey blight on leaves of *Camellia* spp. in China (Wang *et al.* 2022). Our finding expands the host range of *N. longiappendiculata*, marking its first documented occurrence on blueberry.

This study is the first to record the presence of *N. rosae* and *N. hispanica* in symptomatic blueberry leaves and twigs in South African nurseries, while *N. longiappendiculata* was identified exclusively on symptomatic twigs. We recommend that future studies investigate the pathogenicity of all three species of *Neopestalotiopsis* on blueberry varieties to determine if they warrant a more effective prevention of introduction and control strategy as part of a plant improvement programme.

ACKNOWLEDGEMENTS

The authors are grateful to the nurseries for their willingness to participate in this study investigating present species of *Neopestalotiopsis* in South Africa. This research was supported by the South African berry industry, Berries ZA.

Conflict of interest: The authors declare that they have no conflict of interest.

REFERENCES

Anderson J (2022). *Pucciniastrum minimum* (blueberry leaf rust). In: CABI Compendium Wallingford, UK: CAB International. https://doi.org/10.1079/cabicompendium.11863

Baggio JS, Forcelini BB, Wang N-Y*, et al.* (2021). Outbreak of leaf spot and fruit rot in Florida strawberry caused by *Neopestalotiopsis* spp. *Plant Disease* **105**: 305–315. https://doi.org/10.1094/PDIS-06-20-1290-RE

Belisário R, Aucique-Pérez CE, Abreu LM*, et al.* (2020). Infection by *Neopestalotiopsis* spp. occurs on unwounded eucalyptus leaves and is favoured by long periods of leaf wetness. *Plant Pathology* **69**: 194–204. https://doi.org/10.1111/ppa.13132

Borrero C, Castaño R, Avilés M (2018). First report of *Pestalotiopsis clavispora* (*Neopestalotiopsis clavispora*) causing canker and twig dieback on blueberry bushes in Spain. *Plant Disease* **102**: 1178. https://doi.org/10.1094/PDIS-10-17-1529-PDN

Carbone I, Kohn LM (1999). A method for designing primer sets for speciation studies in filamentous ascomycetes. *Mycologia* **91**: 553–556. https://doi.org/10.1111/ppa.13132

Cardinaals J, Wenneker M, Voogd JGB*, et al.* (2018). Pathogenicity

© 2025 Westerdijk Fungal Biodiversity Institute

of *Diaporthe* spp. on two blueberry cultivars (*Vaccinium corymbosum*). *EPPO Bulletin* **48**: 128–134. https://doi.org/10.1111/epp.12451

Crous PW, Summerell BA, Swart L, *et al.* (2011). Fungal pathogens of *Proteaceae*. *Persoonia* **27**: 20–45. https://doi.org/10.3767/003158511X606239

Darapanit A, Boonyuen N, Leesutthiphonchai W, *et al.* (2021). Identification, pathogenicity and effects of plant extracts on *Neopestalotiopsis* and *Pseudopestalotiopsis* causing fruit diseases. *Scientific Reports* **11**: 1–11. http://doi.org/10.1038/s41598-021-02113-5

Diogo E, Gonçalves CI, Silva AC, *et al.* (2021). Five new species of *Neopestalotiopsis* associated with diseased *Eucalyptus* spp. in Portugal. *Mycological Progress* **20**: 1441–1456. http://doi.org/10.1007/s11557-021-01741-5

Espinoza JG, Briceño EX, Keith LM, *et al.* (2008). Canker and twig dieback of blueberry caused by *Pestalotiopsis* spp. and a *Truncatella* sp. in Chile. *Plant Disease* **92**: 1407–1414. http://doi.org/10.1094/PDIS-92-10-1407

Fiorenza A, Gusella G, Aiello D, *et al.* (2022). *Neopestalotiopsis siciliana sp. nov*. and *N. rosae* causing stem lesion and dieback on avocado plants in Italy. *Journal of Fungi* **8**: 562. http://doi.org/10.3390/jof8060562

Gao Y, Zhai FY, Zhang YB, *et al.* (2022). *Neopestalotiopsis rosae* causing black spot on leaf and fruit of *Pecan* (*Carya illinoinensis*) in China. *Plant Disease* **106**: 1995. http://doi.org/10.1094/PDIS-07-21-1541-PDN

Gideon OA, Jones OM, Bakare AG, *et al.* (2018). Metabolites from endophytic fungus; *Pestalotiopsis clavispora* isolated from *Phoenix reclinata* leaf. *Future Journal of Pharmaceutical Sciences* **4**: 273–275. https://doi.org/10.1016/j.fjps.2018.10.001

Glass NL, Donaldson GC (1995). Development of primer sets designed for use with the PCR to amplify conserved genes from filamentous ascomycetes. *Applied and Environmental Microbiology* **61**: 1323–1330. http://doi.org/10.1128/aem.61.4.1323-1330.1995

Guba EF (1961). *Monograph of Monochaetia and Pestalotia*. Harvard University Press, Cambridge, Mass.

Hartung JS (1981). Epidemiological studies of blueberry anthracnose disease caused by *Colletotrichum gloeosporioides*. *Phytopathology* **71**: 449. https://doi.org/10.1094/Phyto-71-449

Hu H, Jeewon R, Zhou D, *et al.* (2007). Phylogenetic diversity of endophytic *Pestalotiopsis* species in *Pinus armandii* and *Ribes* spp.: evidence from rDNA and β-tubulin gene phylogenies. *Fungal Diversity* **24**: 1–22.

IBO (2023). International Blueberry Organisation. *Global State of the Blueberry Industry Report*. California, United States of America. https://www.internationalblueberry.org/2023-report

Jevremović D, Vasić T, Živković S, *et al.* (2022). *Neopestalotiopsis clavispora:* a causal agent of twig dieback on highbush blueberries in Serbia. *Journal of Plant Diseases and Protection* **129**: 1277–1283. http://doi.org./10.1007/s41348-022-00610-x

Krishna P, Pandey G, Thomas R, *et al.* (2023). Improving blueberry fruit nutritional quality through physiological and genetic interventions: A review of current research and future directions. *Antioxidants* **12**: 810. https://doi.org/10.3390/antiox12040810

Lee Y, Kim GH, Kim Y, *et al.* (2019). First report of twig dieback caused by *Neopestalotiopsis clavispora* on blueberry in Korea. *Plant Disease* **103**: 1022. http://doi.org/10.1094/PDIS-10-18-1734-PDN

Liu F, Weir BS, Damm U, *et al.* (2015). Unravelling *Colletotrichum* species associated with *Camellia*: employing ApMat and GS loci to resolve species in the *C. gloeosporioides* complex. *Persoonia* **35**: 63–86. http://doi.org/10.3767/003158515X687597

Liu L, Liu S, Jiang L, *et al.* (2008). Chloropupukeananin, the first chlorinated pupukeanane derivative, and its precursors from *Pestalotiopsis fici*. *Organic Letters* **10**: 1397–1400. http://doi.org/10.1021/ol800136t

Maddison WP, Maddison DR (2023). *Mesquite: a modular system for evolutionary analysis*. Version 3.81. http://www.mesquiteproject.org.

Maharachchikumbura SSN, Guo L-D, Cai L, *et al.* (2012) A multi-locus backbone tree for *Pestalotiopsis*, with a polyphasic characterization of 14 new species. *Fungal Diversity* **56**: 95–129. https://doi.org/10.1007/s13225-012-0198-1

Maharachchikumbura SSN, Hyde KD, Groenewald JZ, *et al.* (2014). *Pestalotiopsis* revisited. *Studies in Mycology* **79**: 121–186. http://doi.org/10.1016/j.simyco.2014.09.005

Milholland R (1972). Histopathology and pathogenicity of *Botryosphaeria dothidea* on blueberry stems. *Phytopathology* **62**: 654–660. http://doi.org/10.1094/Phyto-62-654

Milivojevic J, Maksimovic V, Maksimovic JD, *et al.* (2012). A comparison of major taste-and health-related compounds of *Vaccinium* berries. *Turkish Journal of Biology* **36**: 738–745. http://doi.org/10.3906/biy-1206-39

Nylander JAA (2004). *MrModeltest V2.* Program distributed by the author. Evolutionary Biology Centre, Uppsala University.

Pienaar L, Mzwanele L, Philips S (2019). *The economic contribution of the South African blueberry industry.* https://www.berriesza.co.za/wp-content/uploads/2021/01/BlueberryIndustryReport_2019FINAL.pdf.

Rayner RW (1970). *A mycological colour chart*. Commonwealth Mycological Institute; British Mycological Society, Kew, England.

Rebollar-Alviter A, Silva-Rojas HV, Fuentes-Aragón D, *et al.* (2020). An emerging strawberry fungal disease associated with root rot, crown rot and leaf spot caused by *Neopestalotiopsis rosae* in Mexico. *Plant Disease* **104**: 2054–2059. http://doi.org/10.1094/PDIS-11-19-2493-SC

Retamales JB, Hancock JF (2018). Blueberries. 2nd edn. In: *Crop production science in horticulture*. CABI, Wallingford, United Kingdom. https://doi.org/10.1079/9781780647265.0000

Rivera SA, Zoffoli JP, Latorre BA (2013). Infection risk and critical period for the postharvest control of gray mold (*Botrytis cinerea*) on blueberry in Chile. *Plant Disease* **97**: 1069–1074. https://doi.org/10.1094/PDIS-12-12-1112-RE

Rodríguez-Gálvez E, Hilário S, Lopes A, *et al.* (2020). Diversity and pathogenicity of *Lasiodiplodia* and *Neopestalotiopsis* species associated with stem blight and dieback of blueberry plants in Peru. *European Journal of Plant Pathology* **157**: 89–102. http://doi.org/10.1007/s10658-020-01983-1

Santos J, Hilário S, Pinto G, *et al.* (2021). Diversity and pathogenicity of pestalotioid fungi associated with blueberry plants in Portugal, with description of three novel species of *Neopestalotiopsis*. *European Journal of Plant Pathology* **162**: 539–555. http://doi.org/10.1007/s10658-021-02419-0

Shahriar SA, Nur-Shakirah AO, Mohd MH (2021). *Neopestalotiopsis clavispora* and *Pseudopestalotiopsis camelliae-sinensis* causing grey blight disease of tea (*Camellia sinensis*) in Malaysia. *European Journal of Plant Pathology* **162**: 709–724. http://doi.org/10.1007/s10658-021-02433-2

Solarte F, Muñoz CG, Maharachchikumbura SSN, *et al.* (2018). Diversity of *Neopestalotiopsis* and *Pestalotiopsis* spp., causal agents of guava scab in Colombia. *Plant Disease* **102**: 49–59.

© 2025 Westerdijk Fungal Biodiversity Institute

http://doi.org/10.1094/PDIS-01-17-0068-RE

Stamatakis A (2014). RAxML Version 8: a tool for phylogenetic analysis and post-analysis of large phylogenies. *Bioinformatics* **30**: 1312–1313. http://doi.org/10.1093/bioinformatics/btu033

Steyaert RL (1949). Contribution à l'étude monographique de *Pestalotia* de Not. et *Monochaetia* Sacc. (*Truncatella gen. nov*. et *Pestalotiopsis gen. nov*.). *Bulletin Jardin Botanic Éat Bruxelles* **39**: 285–354. https://doi.org/10.2307/3666710

Swofford D (2003). *PAUP*: Phylogenetic analysis using parsimony (* and other methods).* Version 4 Sinauer Associates, Sunderlands, Massachusetts.

Tamura K, Stecher G, Kumar S*, et al.* (2021). MEGA11: Molecular Evolutionary Genetics Analysis Version 11. *Molecular Biology and Evolution* **38**: 3022–3027. http://doi.org/10.1093/molbev/msab120

Turland NJ, Wiersema JH, Barrie FR*, et al.* (2018). *International Code of Nomenclature for algae, fungi, and plants (Shenzhen Code) adopted by the Nineteenth International Botanical Congress Shenzhen, China, July 2017. Regnum Vegetabile 159. Glashütten.*, Koeltz botanical books. https://doi.org/10.12705/Code.2018

Udayanga D, Liu X, Crous PW*, et al.* (2012). A multi-locus phylogenetic evaluation of *Diaporthe* (*Phomopsis*). *Fungal Diversity* **56**: 157–171. http://doi.org/10.1007/s13225-012-0190-9

Wang Q-T, Cheng Y-H, Zhuo L*, et al.* (2022). *Neopestalotiopsis longiappendiculata* as the agent of grey blight disease of *Camellia* spp. *Journal of Phytopathology* **170**: 770–777. http://doi.org/10.1111/jph.13139

White TJ, Bruns T, Lee S, *et al*. (1990). Amplification and direct sequencing of fungal ribosomal RNA genes for phylogenetics. In: *PCR protocols: a guide to methods and applications* (Innis MA, Gelfand DH, Sninsky JJ, *et al*., eds). *Academic Press, Inc*., New York, USA: 315–322. https://doi.org/10.1016/B978-0-12-372180-8.50042-1

Wright ER, Rivera MC, Esperón J*, et al.* (2004). Alternaria leaf spot, twig blight, and fruit rot of highbush blueberry in Argentina. *Plant Disease* **88**: 1383. https://doi.org/10.1094/PDIS.2004.88.12.1383B

Xavier K, Yu X, Vallad GE (2020). First report of *Neopestalotiopsis rosae* causing foliar and fruit spots on pomegranate in Florida. *Plant Disease* **105**: 504. http://doi.org/10.1094/PDIS-06-20-1282-PDN

Zheng X, Liu X, Li X*, et al.* (2023). *Pestalotiopsis* species associated with blueberry leaf spots and stem cankers in Sichuan Province of China. *Plant Disease* **107**: 149–156. https://doi.org/10.1094/PDIS-07-21-1550-RE

© 2025 Westerdijk Fungal Biodiversity Institute

© 2025 Westerdijk Fungal Biodiversity Institute

FUSE

Fungal Systematics and Evolution

VOLUME 16
DECEMBER 2025
PAGES 55–69

doi.org/10.3114/fuse.2025.16.4

Introducing two new genera, *Paivomyces gen. nov.* and *Pseudoselenophoma gen. nov.*, in *Saccotheciaceae* (*Dothideales*)

S.S. Nascimento[1,2#], L.O. Ferro[1,2#], E.A. Silva[1,2], C.S. Oliveira[3,4], M.T.C. Felipe[1,2], C.M. Souza-Motta[1,2], J.D.P. Bezerra[2,3,4*]

[1]Departamento de Micologia Prof. Chaves Batista, Universidade Federal de Pernambuco, Av. Prof. Moraes Rego, s/n, Centro de Biociências, Cidade Universitária, CEP: 50670-901, Recife, PE, Brazil
[2]Programa de Pós-Graduação em Biologia de Fungos, Departamento de Micologia Prof. Chaves Batista, Universidade Federal de Pernambuco, Av. Prof. Moraes Rego, s/n, Centro de Biociências, Cidade Universitária, CEP: 50670-901, Recife, PE, Brazil
[3]Laboratório de Micologia, Departamento de Biociências e Tecnologia, Instituto de Patologia Tropical e Saúde Pública, Universidade Federal de Goiás, Rua 235, s/n, Setor Universitário, CEP: 74605-050, Goiânia, GO, Brazil
[4]Programa de Pós-Graduação em Biologia da Relação Parasito-Hospedeiro, Instituto de Patologia Tropical e Saúde Pública, Universidade Federal de Goiás, Rua 235, s/n, Setor Universitário, CEP: 74605-050, Goiânia, GO, Brazil

[#] These authors contributed equally

*Corresponding author: jadsonbezerra@ufg.br

Key words:
aureobasidium-like
Fabaceae
endophytes
fungal taxonomy
new taxa

Abstract: Members of the family *Saccotheciaceae* are found in various environments and have different lifestyles. While exploring *Mimosa tenuiflora*-associated endophytic fungi in the Caatinga dry forest in Brazil, the isolates were initially identified as aureobasidium-like fungi. Based on morphological features and phylogenetic analyses using ITS, LSU, *tub2*, *rpb2*, and *tef1* gene sequences, these endophytes were placed within a distinct clade in *Saccotheciaceae*, differing from the genera currently accepted in the family. Here, we describe a new genus, *Paivomyces gen. nov.* (including *Paivomyces mimosae sp. nov.*). Additionally, during our phylogenetic analyses, we observed that *Selenophoma australiensis*, described from leaves of *Eucalyptus mineata* in Australia, could be treated as a unique lineage among the genera in the family *Saccotheciaceae*. Herein, we introduce *Pseudoselenophoma gen. nov.* (including *Pseudoselenophoma australiensis comb. nov.*) to accommodate the species. Our findings improve our understanding of the fungal diversity in the Caatinga dry forest in Brazil and clarify the phylogenetic lineages of *Saccotheciaceae*.

Citation: Nascimento SS, Ferro LO, Silva EA, Felipe MTC, Souza-Motta CM, Bezerra JDP (2025). Introducing two new genera, *Paivomyces gen. nov*. and *Pseudoselenophoma gen. nov.*, in *Saccotheciaceae* (*Dothideales*). *Fungal Systematics and Evolution* **16**: 55–69. doi: 10.3114/fuse.2025.16.4.
Received: 21 January 2025; **Accepted:** 26 March 2025; **Effectively published online:** 13 May 2025
Corresponding editor: P.W. Crous

INTRODUCTION

Bonorden (1864) introduced the family *Saccotheciaceae* (*Dothideales*, *Dothideomycetes*, *Ascomycota*) to accommodate the genus *Saccothecium*. Currently, the genera *Aureobasidium*, *Banningia*, *Columnosphaeria*, *Kabatiella*, *Moringomyces*, *Pseudoseptoria*, *Pseudosydowia*, *Saccothecium*, and *Selenophoma* are included in *Saccotheciaceae* (Hyde *et al.* 2024). However, the genera in *Saccotheciaceae* were previously placed in *Aureobasidiaceae* (Thambugala *et al.* 2014), which was later synonymised under *Saccotheciaceae* because of its morphological features and phylogenetic placement (Liu *et al.* 2015). *Aureobasidium*, *Kabatiella*, and *Selenophoma* represent the genera with the largest number of species according to the Index Fungorum and MycoBank databases (accessed in January 2025). Morphologically, both sexual and asexual reproduction are known for the taxa in this family. In the sexual morph, they may have black ascomata that vary from immersed to erumpent, with globose to subglobose shapes. The asexual morphs are classified as coelomycetes or hyphomycetes, with coelomycetes having dark brown conidiomata, solitary or aggregated, and hyphomycetes with the presence or the absence of hyaline, or slightly pigmented stroma (Hongsanan *et al.* 2020). The family has undergone classification changes owing to phylogenetic relationships (Liu *et al.* 2015), and Calabon *et al.* (2023) recently presented an updated classification of *Saccotheciaceae* showing marine *Aureobasidium* species.

Saccotheciaceae members are mostly found as saprophytes (Pande 2008, Peterson *et al.* 2013) in several environments and on different substrates, such as healthy leaves (Quaedvlieg *et al.* 2013), soil (Wu *et al.* 2023), and have been reported to be human opportunistic pathogens (Chan *et al.* 2011). Studies have also shown that species of this family are endophytes (Saber *et al.* 2023), with *Aureobasidium* being the most common genus (Arzanlou & Khodaei 2012, Saber *et al.* 2023). However, most genera included in *Saccotheciaceae*, except *Aureobasidium* (Silva *et al.* 2024), have not previously been reported as endophytes in the Caatinga (dry forest), an exclusive Brazilian biome

Fungal Systematics and Evolution is licensed under a Creative Commons Attribution-NonCommercial-NoDerivatives 4.0 International License

© 2025 Westerdijk Fungal Biodiversity Institute

covering approximately 10 % of the country (MMA 2022). Like other biomes in Brazil, the Caatinga is a forest with high anthropogenic influence and unsustainable impact, increasing its degradation and desertification (Aquino *et al.* 2021). In this forest, we have identified several endophytic fungi of native and cultivated plant species (e.g., Bezerra *et al.* 2017a, Barbosa *et al.* 2020, Oliveira *et al.* 2021), and new fungal taxa have been introduced based on Caatinga endophytes. Some examples are *Diaporthe caatingaensis*, isolated from *Tacinga inamoena* (Crous *et al.* 2016), the genus *Bezerromyces* (*Bezerromycetaceae*, *Tubeufiales*) (Bezerra *et al.* 2017a), *Toxicocladosporium* species from cacti (Bezerra *et al.* 2017b), *Quambalaria fabacearum* from *Mimosa tenuiflora* (*Fabaceae*) (Bezerra *et al.* 2018), *Pseudoplagiostoma myracrodruonis* from *Myracrodruon urundeuva* (current name: *Astronium urundeuva*; *Anacardiaceae*) (Bezerra *et al.* 2019), *Leptosillia* species from *M. tenuiflora* (*Fabaceae*) (Silva *et al.* 2021), *Cladophialophora* species from *Tillandsia catimbauensis* (Nascimento *et al.* 2021), and recently *Endophytium* (*Endophytiaceae*, *Endophytiales*, *Dothideomycetes*) was introduced for isolates obtained from cacti (Barreto *et al.* 2024), seven new *Diaporthe* species were described from *Anacardium occidentale* (*Anacardiaceae*), *Miconia* sp. (*Melastomataceae*), and *Brosimum gaudichaudii* (*Moraceae*) (Ferro *et al.* 2024a), and *Aureobasidium caatingaense* and *A. santateresinhaense* from *Anadenanthera colubrina* (*Fabaceae*) (Silva *et al.* 2024).

Our studies describing new taxa showed that the Brazilian Caatinga (dry forest) can be treated as a hotspot for fungal diversity. While studying *M. tenuiflora*-associated endophytic fungi in the Caatinga forest of Brazil, the isolates were morphologically identified as aureobasidium-like. After analysis of the ITS and LSU rDNA, *tub2*, *rpb2*, and *tef1* sequences, these strains were placed in a unique lineage phylogenetically distinct from other genera accepted in *Saccotheciaceae*. Therefore, this study aimed to introduce a new genus based on its morphology, multi-locus phylogeny, and ecology/lifestyle. Furthermore, our phylogenetic analyses revealed that *Selenophoma australiensis* (from type material CBS 124776) could be treated as a unique lineage in the family and is introduced here as a new genus in *Saccotheciaceae*.

MATERIAL AND METHODS

Fungal isolates

Endophytes were isolated from branches of *Mimosa tenuiflora* (*Fabaceae*, *Mimosoideae*) during the dry season of April 2013 and collected in the Fazenda Tamanduá (Tamanduá Farm), a private conservation area (RPPN) of the Brazilian Caatinga (dry forest), in the municipality of Santa Teresinha, state of Paraíba, Brazil (07º02'20"S, 37º26'43"W). Details of the study site, plant processing, and fungal isolation have been described by Bezerra *et al.* (2013) and Oliveira *et al.* (2020). Collections were registered in the Ministério do Meio Ambiente (MMA)/Instituto Chico Mendes de Conservação da Biodiversidade (ICMBio) (number: 40331-1) and the study in the Sistema Nacional de Gestão do Patrimônio Genético (SisGen)/MMA/Conselho de Gestão do Patrimônio Genético (CGen) (number: ACD07BF).

Morphological analyses

Isolates were grown on potato dextrose agar (PDA) (Crous *et al.* 2009), malt extract agar (MEA) (Samson *et al.* 2010), Czapek Yeast Autolysate agar (CYA) (Pitt 1979), Dichloran 18 % glycerol agar (DG18) (Hocking & Pitt 1980), and malt extract yeast extract 40 % glucose (MY40G) (Palacios-Cabrera *et al.* 2005), and incubated in dark at 25 °C. The PDA plates were also incubated at 30 and 35 °C. Colony size and morphological features (e.g., texture, colour, pigmentation, and margin appearance) were visualised after 14 d on PDA, MEA, CYA, DG18, and MY40G. Colony colour was evaluated using Rayner's colour chart (Rayner 1970). Reproductive structures were visualised after 60 d on PDA, and conidiogenous cells and conidia were analysed. Microscopic slides were prepared with lactic acid (85 %). A LEICA® DM500 compound microscope equipped with Flexacam C3 cameras was used to capture digital images using NIS-Elements AR v. 4.20 software. The photos and plates were prepared in Adobe® Photoshop CC 2015.

Isolates are deposited in the URM culture collection (*Micoteca URM Profa. Maria Auxiliadora Cavalcanti*) and slide preparations (holotype) in the HURM herbarium (*Herbário URM Pe. Camille Torrend*), both located at the Universidade Federal de Pernambuco, Recife, Brazil. In addition, isolates are deposited in the working collection FCCUFG (*Coleção de Culturas de Fungos da Universidade Federal de Goiás*) housed at the Laboratório de Micologia (LabMicol) of the Instituto de Patologia Tropical e Saúde Pública (IPTSP), Universidade Federal de Goiás, Goiânia, Brazil.

DNA extraction, PCR amplification, and sequencing

The Wizard® SV Genomic DNA Purification System kit (Promega Corp., Madison, WI, USA) was used for genomic DNA extraction according to the manufacturer's instructions. We analysed the rDNA internal transcription spacer (ITS) and intervening 5.8S nRNA gene, the nuclear ribosomal RNA large subunit (LSU) gene, the β-tubulin (*tub2*) gene, the RNA polymerase II second largest subunit (*rpb2*) gene, and the translation elongation factor 1-α (*tef1*) gene, using primers ITS4/ITS5 (White *et al.* 1990), LR0R/LR5 (Vilgalys & Hester 1990, Rehner & Samuels 1994), Bt2a/Bt2b (Glass & Donaldson 1995), RPB2-5F/RPB2-7cR (Liu *et al.* 1999), and EF-728F/EF2 and EF-983F/EF-2218R (Carbone & Kohn 1999, O'Donnell *et al.* 1998, Rehner & Buckley 2005), respectively. Amplification, sequencing, and sequence editing were performed according to Ferro *et al.* (2024b). The sequences obtained in this study were deposited in GenBank (Table 1).

Phylogenetic analyses

Phylogenetic analyses were performed using the sequences generated in this study and reference sequences of all genera included in *Saccotheciaceae* following recent publications (e.g., Humphries *et al.* 2017, Wijayawardene *et al.* 2020). Alignments were performed individually using the MAFFT v. 7 online interfaces (Katoh & Standley 2013; http://mafft.cbrc.jp/alignment/server) and manually edited using MEGA v. 7.0 (Kumar *et al.* 2016). First, we performed a maximum likelihood (ML) analysis for each gene (ITS and LSU rDNA) and the combined matrix to determine the phylogenetic

© 2025 Westerdijk Fungal Biodiversity Institute

Table 1. GenBank accession numbers of sequences used in this study. Sequences in **boldface** were obtained during this study. Ex-type strains are marked with (T).

Species	Strain	Host/substrate	Country	GenBank numbers				
				ITS	LSU	*tub2*	*rpb2*	*tef1*
Aureobasidium iranianum	CCTU 268^{T}	Stems of *Bambusa*	Iran	NR_137598	NG_057049	–	–	–
Aureobasidium leucospermi	CBS 130593^{T}	Leaves of *Leucospermum conocarpodendron*	Indonesia	NR_156246	NG_058566	–	KT693970	–
Aureobasidium lini	CBS 125.21^{T}	Leaves of *Linum usitatissimum*	United Kingdom	MH854694	MH866211	FJ157873	KT693984	–
Aureobasidium namibiae	CBS 147.97	From dolomitic marble	Africa	AJ244231	NG_056961	FJ157863	KT693973	XM_013574385
Aureobasidium proteae	CBS 114273 = CPC 2824^{T}	Leaves of *Protea* sp.	South Africa	JN712491	JN712557	–	–	–
Aureobasidium pullulans	CBS 584.75^{T}	From fruit of *Vitis vinifera*	France	NR_144909	NG_055734	FJ157869	KT693976	–
Aureobasidium thailandense	NRRL 58539^{T}	Leaves of *Cerbera Odollam*	Thailand	NR_147337	–	–	–	–
Aureobasidium tremulum	UN 1^{T}	From Petri dish as contaminant	India	MK503657	MK503660	–	–	–
Banningia maryelizabethiae	BRIP 64084b^{T}	Branch of *Corymbia citriodora*	Australia	NR_191310	–	–	–	–
Columnosphaeria fagi	CBS 171.93	Dead leaves of *Arctostaphylos uva-ursi*	Switzerland	MH861759	MH873458	–	KT693980	–
Dothidea sambuci	AFTOL-ID 274^{T}	Dead corticate twigs of *Sambuci nigrae*	Austria	NR_111220	NG_027611	–	DQ522854	DQ497606
Dothiora agapanthi	CPC 20600^{T}	Leaves of *Agapanthus* sp.	South Africa	NR_155055	NG_059132	KU728617	–	–
Dothiora aloidendri	CBS 146775^{T}	Leaves of *Aloidendron dichotomum*	South Africa	NR_171992	NG_074489	–	–	–
Dothiora cannabinae	CBS 737.71^{T}	Dead branches of *Daphne cannabina*	India	NR_144904	NG_068997	–	–	–
Dothiora prunorum	CBS 933.72^{T}	From fruit of *Prunus domestica*	Great Britain	NR_138366	NG_070590	–	–	–
Dothiora pyrenophora	CBS 142621 = CPC 30632^{T}	Twig of *Sorbus aucuparia*	Germany	KY929146	KY929179	KY929210	–	–
Endoconidioma euphorbiae	CBS 146776 = CPC 38551^{T}	Leaves of *Euphorbia mauritanica*	South Africa	MW175350	MW175390	–	–	–

© 2025 Westerdijk Fungal Biodiversity Institute

Table 1. (continued)

Species	Strain	Host/substrate	Country	GenBank numbers				
				ITS	LSU	*tub2*	*rpb2*	*tef1*
Endoconidioma populi	UAMH 10297^{T}	Twigs of *Populus tremuloides*	Canada	NR_121303	NG_059198	–	–	–
Hormonema carpetanum	ATCC 74360	Leaves of *Juniperus communis*	Spain	AF182375	MF611880	–	MF611881	MF611882
Hormonema macrosporum	CBS 536.94^{T}	*Rutilus rutilus*	Russia	NR_145340	NG_064169	–	–	–
Hormonema schizolunatum	CBS 707.95^{T}	Leaves of *Salvia canariensis*	Spain	NR_175111	MH874183	–	–	–
Muellerites juniperi	CBS 339.73	Leaves of *Juniperus nana*	Switzerland	–	MH877745	–	–	–
Neocelosporium corymbiae	CPC 39297 = CBS 147080^{T}	Stems of *Corymbia variegata*	Australia	NR_173062	NG_076748	–	–	–
Neocelosporium eucalypti	CPC 34468 = CBS 145086^{T}	Leaves of *Eucalyptus cyanophylla*	Australia	NR_164293	NG_066297	–	–	–
Paivomyces mimosae sp. nov.	**URM 9011 = FCCUFG 153**	**Endophyte from leaves of *Mimosa tenuiflora***	**Brazil**	**PQ811695**	**PQ826408**	**–**	**–**	**–**
	URM 9012 = FCCUFG 156^{T}	**Endophyte from leaves of *Mimosa tenuiflora***	**Brazil**	**PQ811698**	**PQ826411**	**PQ855593**	**PQ855598**	**PQ855602**
	FCCUFG 154	**Endophyte from leaves of *Mimosa tenuiflora***	**Brazil**	**PQ811696**	**PQ826409**	**PQ855592**	**–**	**–**
	FCCUFG 155	**Endophyte from leaves of *Mimosa tenuiflora***	**Brazil**	**PQ811697**	**PQ826410**	**–**	**PQ855597**	**–**
	FCCUFG 157	**Endophyte from leaves of *Mimosa tenuiflora***	**Brazil**	**PQ811699**	**PQ826412**	**PQ855594**	**PQ855599**	**PQ855603**
Pringsheimia chamaecyparidis	CBS 746.71^{T}	Twig of *Chamaecyparis lawsoniana*	France	MH860328	MH872083	–	–	–
Pringsheimia smilacis	CBS 873.71	Dead branches of *Smilax aspera*	India	AJ244257	FJ150970	–	–	–
Pseudoselenophoma australiensis comb. nov.	CBS 124776 = CPC 14582^{T}	Leaves of *Eucalyptus mineata*	Australia	NR_156527	NG_057833	**PQ855595**	**PQ855600**	**PQ855604**
	CPC 14583	Leaves of *Eucalyptus mineata*	Australia	**PQ811700**	–	**PQ855596**	**PQ855601**	**PQ855605**

© 2025 Westerdijk Fungal Biodiversity Institute

Table 1. (continued)

Species	Strain	Host/substrate	Country	GenBank numbers				
				ITS	LSU	*tub2*	*rpb2*	*tef1*
Pseudoseptoria collariana	CBS 135104^{T}	Leaves of bamboo	Iran	NR_156560	KF251721	KF252707	–	–
Pseudoseptoria donacis	CBS 313.68	Leaves of *Phragmites australis*	Netherlands	MH859141	MH877798	–	–	–
Pseudoseptoria obscura	CBS 135103	Leaves of bamboo	Iran	KF251219	KF251722	KF252708	–	–
Pseudosydowia backhousiae	BRIP 28243^{T}	Leaves of *Backhousia citriodora*	Australia	MW443073	–	–	–	–
Pseudosydowia eucalypti	CBS 131832	Leaves of *Eucalyptus* sp.	Australia	MH865934	MH877368	–	–	–
	CPC 14028	Leaves of *Eucalyptus* sp.	Southern Africa	GQ303296	–	–	–	–
Pseudosydowia eucalyptorum	CBS 145546^{T}	Leaves of *Eucalyptus* sp.	Australia	NR_165231	NG_067893	–	–	–
Pseudosydowia indooroopillyensis	BRIP 28248^{T}	Leaves of *Eucalyptus* sp.	Australia	MW443076	MW443081	–	–	–
Pseudosydowia louisecottisiae	BRIP 28159^{T}	Leaves of *Eucalyptus* sp.	Australia	NR_173227	MW443079	–	–	–
Pseudosydowia phantasmae	CBS 146830^{T} = CPC 38883	Leaves of *Moringa ovalifolia*	Africa	NR_171999	NG_074499	–	–	–
Pseudosydowia queenslandica	BRIP 28249^{T}	Leaves of *Eucalyptus* sp.	Australia	NR_173230	MW443082	–	–	–
Saccothecium australianum	BRIP 72385d^{T}	Leaves of *Grevillea decora*	Australia	OR452101	OR452104	–	–	–
Saccothecium rubi	MFLUCC 14-1171^{T}	Dead spines of *Rubus ulmifolius*	Italy	NR_148096	NG_059644	–	–	–
Saccothecium sepincola	MFLU 14-0276	Twigs of *Cornus sanguinea*	Italy	KM388546	KM388554	–	–	–
Saccothecium widdringtoniae	CBS 149071 = CPC 42458^{T}	Twigs of *Widdringtonia wallichii*	South Africa	ON603785	ON603805	–	ON605625	ON605633
Selenophoma juncea	CF285463	Endophytes from leaves of *Salsola oppositifolia*	Spain	KU295578	–	–	–	–
Selenophoma linicola	CBS 468.48^{T}	On *Linum usitatissimum*	Canada	MH856436	MH867982	–	–	–
Selenophoma mahoniae	CBS 388.92	Leaves of *Mahonia repens*	United States	KT693746	FJ150943	–	KT693987	–

© 2025 Westerdijk Fungal Biodiversity Institute

Table 1. (continued)

Species	Strain	Host/substrate	Country	GenBank numbers				
				ITS	LSU	*tub2*	*rpb2*	*tef1*
Sydowia japonica	FFPRI 411084	*Cryptomeria japonica*	Japan	JQ814700	–	–	–	–
Sydowia polyspora	CBS 116.29	Branches of *Calluna vulgaris*	Germany	NR_160075	NG_057801	–	–	–
Zalaria alba	DAOMC 250847^{T}	House dust	Canada	NR_153465	NG_060009	KX579117	KX579105	–
Zalaria obscura	DAOMC 250849^{T}	House dust	Canada	NR_153466	NG_060010	KX579118	KX579106	–
Phaeosclera dematioides (outgroup)	CBS 157.81^{T}	Pith of *Pinus contorta*	Canada	MH857756	NG_057860	–	–	GU349047

placement of our isolates among the genera within *Saccotheciaceae*. Furthermore, we constructed a combined dataset (ITS, LSU, *rpb2*, *tub2*, and *tef1*) with only strains/isolates containing sequences of at least one specified protein-coding marker, along with the ITS and LSU nrDNA sequences. The ML analysis was performed using RAxML-HPC BlackBox v. 8.2.12 (Stamatakis 2014) using default system options with 1000 bootstrap replicates in the CIPRES Science Gateway (Miller *et al.* 2010) and IQ-TREE v. 1.6.12 software (Nguyen *et al.* 2015) involving 5000 replications and the ultrafast bootstrap (UFboot2) method to calculate branch support (Hoang *et al.* 2018). ModelFinder (Kalyaanamoorthy *et al.* 2017), included in IQ-TREE v. 1.6.12, was used to determine the partitioning strategy and models based on the Akaike information criterion (AICc). The concatenated data set was also analysed based on Bayesian inference (BI) conducted using MrBayes v. 3.2.7a (Ronquist *et al.* 2012) in the CIPRES Science Gateway (Miller *et al.* 2010, http://www.phylo.org/), using the same models and partitions as in the ML analysis (IQ-TREE). The BI analysis was conducted with 50 M generations and 25 % burn-in value, with chains sampled every 1000 generations. The trees obtained were visualised using FigTree v. 1.4.4 (Rambaut 2012) and subsequently edited. Posterior probability BI (BPP) and bootstrap ML (RAxML-BS and IQ-TREE-BS) ≥ 0.95 and 70 %, respectively, are shown near nodes. The final combined alignments were deposited in Figshare (doi: 10.6084/m9.figshare.28200014).

RESULTS

Phylogeny

The ITS, LSU, *tub2*, *rpb2*, and *tef1* gene sequences of our isolates were compared with the sequence data in GenBank using the BLASTn search tool, which indicated that they were related to genera in *Saccotheciaceae* (e.g., *Aureobasidium*, *Pseudosydowia*, and *Selenophoma*). The combined matrix of ITS and LSU comprised sequences from 56 strains, including the outgroup *Phaeosclera dematioides* (CBS 157.81), and 1592 characters, including gaps (654 characters for ITS and 938 for LSU), of which 1064 were conserved, 501 variable, and 325 parsimony-informative. For the ML analysis, the best tree score and final optimization likelihood value was −ln = −9843.732201 and the estimated base frequency were: A = 0.254699, C = 0.226779, G = 0.278235, and T = 0.240287, with substitution rates of AC = 1.775502, AG = 1.871284, AT = 2.215471, CG = 0.679930, CT = 5.205799, and GT = 1.000000 and the distribution shape parameter gamma: α = 0.430374. For BI, the average standard deviation of the split frequencies was 0.001100 after 50 million generations. The combined matrix of ITS, LSU, *tub2*, *rpb2*, and *tef1* had sequences from 56 strains and 3890 characters including gaps (654 characters for ITS, 938 for LSU, 485 for *tub2*, 664 for *rpb2*, and 1149 for *tef1*), of which 2635 were conserved, 1205 variable, and 844 parsimony-informative. The best-scoring ML tree with a final optimization likelihood value was −ln = −19645.714678 and the estimated base frequency were: A = 0.246000, C = 0.248510, G = 0.272910, and T = 0.232581, with substitution rates of AC = 1.523374, AG = 2.235797, AT = 1.659177, CG = 0.810446, CT = 6.148495, and GT = 1.000000 and the distribution shape parameter gamma: α = 0.478754. For BI,

© 2025 Westerdijk Fungal Biodiversity Institute

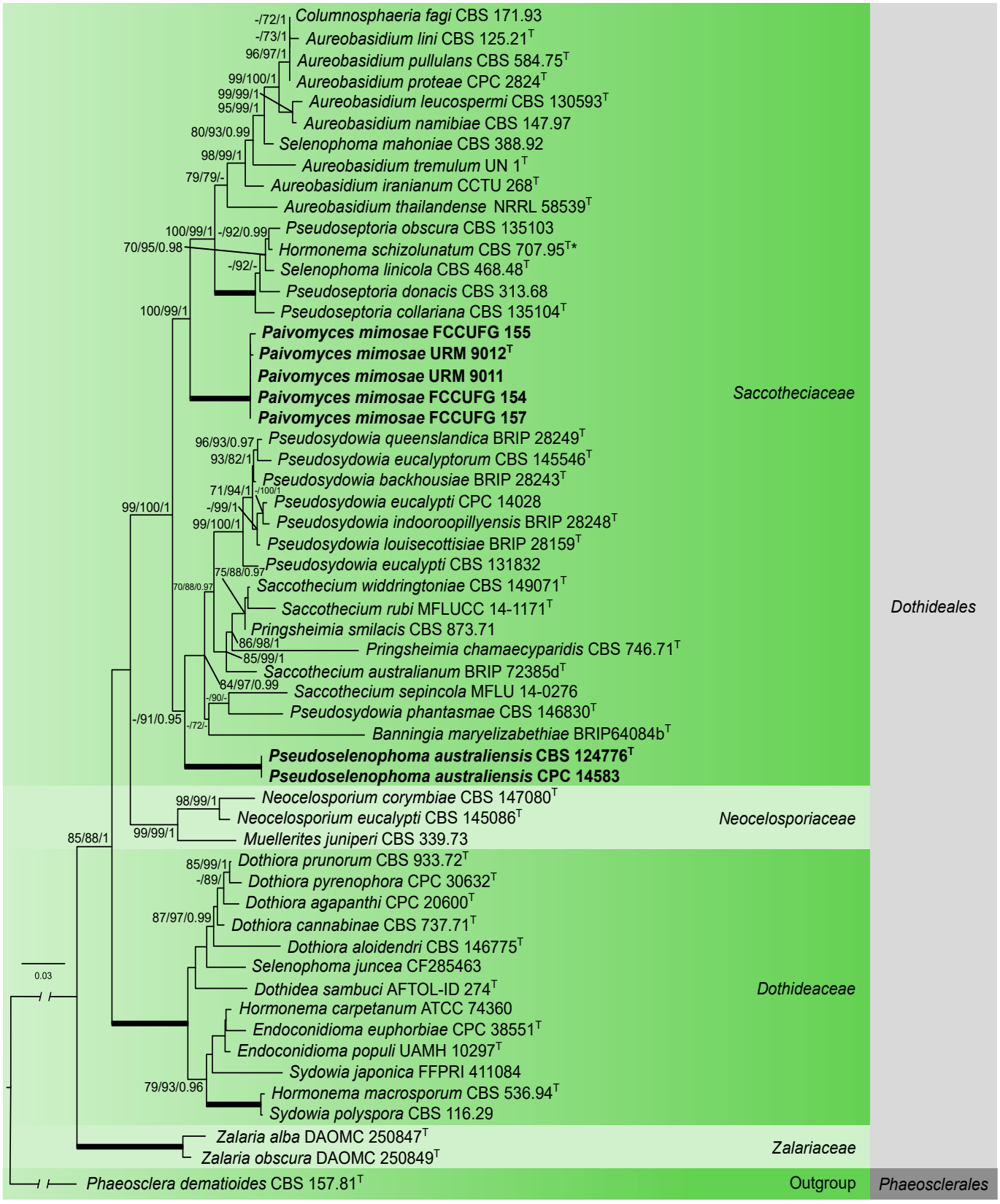

Fig. 1. Maximum Likelihood (ML) phylogenetic tree of the combined ITS and LSU sequences of the new genus *Paivomyces* and related taxa in *Saccotheciaceae* (*Dothideales*). New taxa are in **boldface**. Thickened branches indicate full statistical support in all analyses. Confidence values for ML-BS and IQ-TREE-BS ≥ 70 % (UFboot2/RAxML) and BPP ≥ 0.95 are included near the nodes, and the (-) indicates statistical support below the threshold values. Ex-type strains are marked with (T). Species classified in *Dothideaceae* are marked with an asterisk (*). The tree was rooted to *Phaeosclera dematioides* (CBS 157.81) (*Phaeosclerales*, *Dothideomycetes*).

© 2025 Westerdijk Fungal Biodiversity Institute

the average standard deviation of the split frequencies was 0.001153 after 50 M generations. The models used for IQ-TREE ML and BI were SYM + I + G for ITS and LSU, GTR + I + G for *rpb2*, and GTR + G for *tub2* and *tef1*. The GTR+I+G model was used for RAxML-HPC.

We conducted combined (ITS–LSU and ITS–LSU–*tub2*–*rpb2*–*tef1*) and individual phylogenetic analyses of each gene; our isolates (URM 9011 = FCCUFG 153, URM 9012 = FCCUFG 156, FCCUFG 154, FCCUFG 155, and FCCUFG 157) and *Pseudoselenophoma* (*P.*) *australiensis comb. nov.* (CBS 124776 = CPC 14582 and CPC 14583) formed unique lineages among the *Saccotheciaceae*. In the combined ITS–LSU matrix (Fig. 1), our sequences formed a unique lineage (ML-BS = 100 %, IQ-TREE-BS = 100 % and BPP = 1) related to a clade having species of *Aureobasidium*, *Selenophoma*, and *Pseudosydowia*. *Pseudoselenophoma australiensis comb. nov.* sequences were also placed in a unique and well-supported lineage (ML-BS = 100 %, IQ-TREE-BS = 100 % and BPP = 1) related to a clade having species of *Pseudosydowia*, *Saccothecium*, *Pringsheimia* and *Banningia*. In the five-gene matrix inference (ITS–LSU–*tub2*–*rpb2*–*tef1*), sequences from our isolates were placed in a unique, well-supported lineage (ML-BS = 100 %, IQ-TREE-BS = 100 % and BPP = 1) near *P. australiensis comb. nov.* (ML-BS = 100 %, IQ-TREE-BS = 100 % and BPP = 1), which were connected by a low-supported node (ML-BS = < 70 %, IQ-TREE-BS = < 70 % and BPP = < 0.95) to sequences from *Aureobasidium*, *Selenophoma*, *Columnosphaeria*, *Pseudoseptoria* and *Hormonema* (ML-BS = 96 %, IQ-TREE-BS = 95 % and BPP = < 0.95) as related taxa in *Saccotheciaceae* (Fig. 2).

In the ML ITS tree (Suppl. Fig. S1), our isolates were phylogenetically placed as a well-supported (ML-BS = 100 % and IQ-TREE-BS=100 %) and unique lineage in *Saccotheciaceae* distant from the other genera of the family, and related to a clade (ML-BS = < 70 % and IQ-TREE-BS = 89 %) with species of *Aureobasidium*, *Selenophoma*, and *Pseudosydowia* (ML-BS = 94 % and IQ-TREE-BS = 97 %). *Pseudoselenophoma australiensis comb. nov.* was also placed as a unique lineage (ML-BS = 100 % and IQ-TREE-BS = 100 %) and related to a clade (ML-BS = < 70 % and IQ-TREE-BS = 86 %) having species of *Pseudosydowia*, *Saccothecium*, *Pringsheimia* and *Banningia* (ML = 73 % and IQ-TREE-BS = 98 %). In the LSU tree (Suppl. Fig. S2), the clade containing our isolates (ML-BS = 100 %, IQ-TREE-BS = 100 %) was phylogenetically related as in the ITS tree. *Pseudoselenophoma australiensis comb. nov.* CBS 124776 has the same phylogenetic placement as described above. In the *tub2* tree (Suppl. Fig. S3), the clade of our isolates (ML-BS = 100 % and IQ-TREE-BS = 100 %) was phylogenetically related (ML = 74 % and IQ-TREE-BS = < 70 %) to the clade of *Pseudoseptoria* species (ML-BS = 100 % and IQ-TREE-BS = 100 %). In the *rpb2* tree (Suppl. Fig. S4), our isolates were well-supported (ML-BS = 100 % and IQ-TREE-BS = 100 %) and phylogenetically related to *Saccothecium widdringtoniae* CBS 149071 (ML = < 70 % and IQ-TREE-BS = < 70 %). *Pseudoselenophoma australiensis comb. nov.* CBS 124776 was well-supported (ML-BS = 100 % and IQ-TREE-BS = 100 %) and placed between *Saccothecium widdringtoniae* CBS 149071 and *Zalaria* species. In the *tef1* tree (Suppl. Fig. S5), our isolates formed a well-supported lineage (ML-BS = 100 % and IQ-TREE-BS = 97 %) related to *Saccothecium widdringtoniae* CBS 149071 (ML = < 70 % and IQ-TREE-BS = < 70 %), and *P. australiensis comb. nov.* CBS 124776 (ML = 100 % and IQ-TREE-BS = 97 %) was placed in a single lineage phylogenetically related to *Aureobasidium namibiae* CBS 14797.

Based on the morphological features and phylogenetic inferences presented above, two new genera, *Paivomyces gen. nov.* (including *Paivomyces mimosae sp. nov.*) and *Pseudoselenophoma gen. nov.* (including *Pseudoselenophoma australiensis comb. nov.*) are here introduced in *Saccotheciaceae*.

Taxonomy

Paivomyces S.S. Nascimento, L.O. Ferro, Souza-Motta & J.D.P. Bezerra, ***gen. nov.*** MycoBank MB 857815.

Etymology: Named in honour of Prof. Dr Laura Mesquita Paiva, a mycologist of the Departamento de Micologia (Universidade Federal de Pernambuco, Recife, Brazil), for her dedication to teaching several students about the mystery of fungal life and kindling our love for fungi.

Hyphae hyaline when young, becoming brown to dark brown with age, smooth, toruloid, and occasionally covered with a mucilage-like sheath. *Conidiogenous cells* enteroblastic, globose to subglobose, apically verrucose, often with an inconspicuous solitary collarette, become dark brown over time. *Conidia* enteroblastic, globose to subglobose, smooth, guttulate, hyaline when young, brown to dark brown with age. *Chlamydospores* occasionally observed, globose to subglobose, intercalary and terminal, and brown to dark brown. *Hyphal coils* occasionally observed. *Hyphopodia-like* structures occasionally observed, elongate, smooth, and brown. *Sexual* morphs not observed.

Type species: *Paivomyces mimosae* S.S. Nascimento *et al.*

Paivomyces mimosae S.S. Nascimento, L.O. Ferro, Souza-Motta & J.D.P. Bezerra, ***sp. nov.*** MycoBank MB 857816. Fig. 3.

Etymology: Named in reference to the host genus *Mimosa*, from which the fungus was first isolated.

Hyphae septate, branched, toluroid, smooth, hyaline when young and becoming brown to dark brown with age, mucilage-like sheath occasionally present, 2.5–6 µm wide. *Conidiogenous cells* enteroblastic, globose to subglobose, apically verrucose, often with an inconspicuous collarette, solitary and grouped in chains, dark brown, (7.5–)10–12.5(–16) × (6–)8–11(–12) µm (av. 11 × 8.5 µm). *Conidia* enteroblastic, globose to subglobose, smooth, guttulate, hyaline when young, brown to dark brown with age, (10–)13–14(–17.5) × (9–)11–14(–17.5) µm (av. 14 × 13 µm). *Chlamydospores* occasionally observed, globose to subglobose, intercalary and terminal, and brown to dark brown. *Hyphal coils* occasionally observed. *Hyphopodia-like* structures occasionally observed, elongate, smooth, and brown. *Sexual morph* not observed.

Culture characteristics: Colonies on PDA measuring 45 mm diam. after 14 d, velvety, slightly furrowed, mostly flat but elevated at the centre, exudates present, olive greenish at the centre and white margins with wavy edges; reverse smoke

© 2025 Westerdijk Fungal Biodiversity Institute

grey and white margins. Colonies on MEA, measuring 48 mm diam. after 14 d, glistening with aerial mycelia resembling a black yeast-like fungus, fuscous black to sepia, white wavy margins, and reverse amber to hazel. Colonies on CYA, DG18, and MY40G measuring 25, 20, and 16 mm diam. after 14 d, respectively. Colony growth on PDA was observed at 25 and 30 °C, and no growth was observed at 35 °C.

Typus: **Brazil**, Paraíba state, Santa Teresinha municipality, RPPN Fazenda Tamanduá (07º02'20"S, 37º26'43"W), isolated

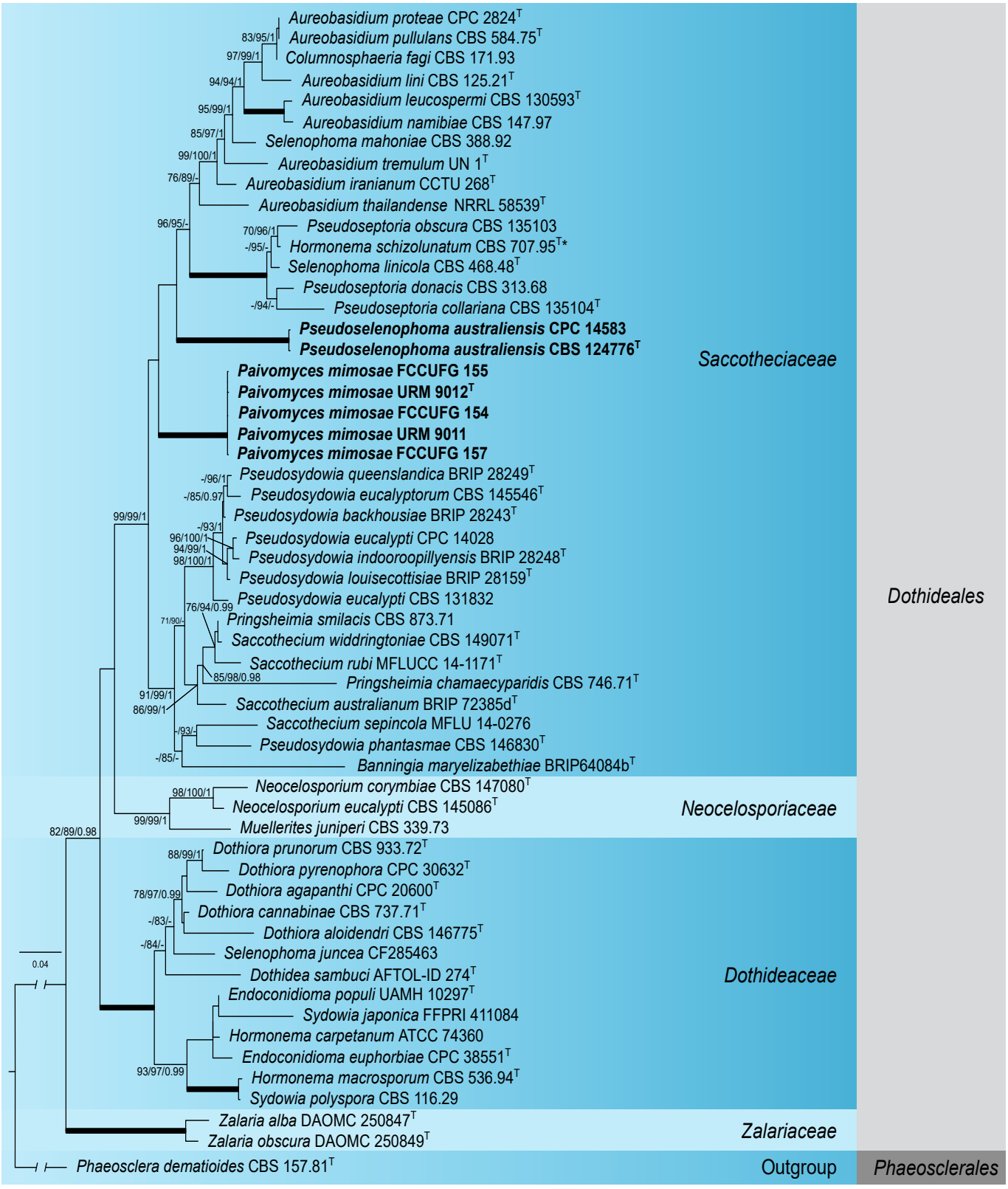

Fig. 2. Maximum Likelihood (ML) phylogenetic tree of the combined ITS, LSU, *tub2*, *rpb2*, and *tef1* sequences of the new genus *Paivomyces* and related taxa in *Saccotheciaceae* (*Dothideales*). New taxa are in **boldface**. Thickened branches indicate full statistical support in all analyses. Confidence values for ML-BS and IQ-TREE-BS ≥ 70 % (UFboot2/RAxML) and BPP ≥ 0.95 are included near the nodes, and the (-) indicates statistical support below the threshold values. Ex-type strains are marked with (T). Species classified in *Dothideaceae* are marked with an asterisk (*). The tree was rooted to *Phaeosclera dematioides* (CBS 157.81) (*Phaeosclerales*, *Dothideomycetes*).

© 2025 Westerdijk Fungal Biodiversity Institute



Fig. 3. *Paivomyces mimosae* URM 9012. **A.** Colonies on PDA after 14 d at 25 °C in the dark (surface and reverse). **B.** Colonies on MEA after 14 d at 25 °C in the dark (surface and reverse). **C.** Hyphae and conidiogenous cells. **D–F.** Hyphae and conidiogenous cells producing young conidia. **G, H.** Details of old conidia attached to conidiogenous cells. **I.** Hyphae, conidiogenous cells, and hyphopodia-like structures. **J.** Details of hyphal coils. Scale bars = 10 µm.

© 2025 Westerdijk Fungal Biodiversity Institute

as an endophyte from branches of *Mimosa tenuiflora* (*Fabaceae*), 4 Apr. 2013, *J.D.P. Bezerra* (**holotype** HURM 95896, **isotypes** HURM 95897 and HURM 95898, culture ex-holotype URM 9012 = FCCUFG 156).

Additional specimens examined: **Brazil**, Paraíba state, Santa Teresinha municipality, Fazenda Tamanduá (07º02'20"S, 37º26'43"W), isolated as endophytes from branches of *Mimosa tenuiflora*, 4 Jun. 2013, *J.D.P. Bezerra* (living cultures URM 9011 = FCCUFG 153, FCCUFG 154, FCCUFG 155, and FCCUFG 157).

Notes: Brazilian isolates exhibited distinct morphological differences from those of other species described in the *Saccotheciaceae*. Morphologically, the main features include enteroblastic conidiogenous cells. Phylogenetically, the new genus is related to a clade that includes members of *Pseudosydowia* (*Pss.*), mostly isolated from leaves (*e.g.*, *Pss. eucalypti*, Thambugala *et al.* 2014), *Pss. eucalyptorum* (Crous *et al.* 2019), *Pss. indooroopillyensis*, *Pss. louisecottisiae*, and *Pss. queenslandica* (Crous *et al.* 2021) isolated from *Eucalyptus* sp. (*Myrtaceae*); *Pss. backhousiae* (Crous *et al.* 2021) isolated from leaves of *Backhousia citriodora* (*Myrtaceae*); *Pss. phantasmae* (Crous *et al.* 2022a) isolated from *Moringa ovalifolia* (*Moringaceae*); *Pringsheimia* (*Pr.*) (e.g., *Pr. chamaecyparidis*, Vu *et al.* 2019) isolated from dead branches of *Chamaecyparis lawsoniana* (*Cupressaceae*) and *Pr. smilacis* (Vu *et al.* 2019) isolated from dead branches of *Smilax parvifolia* (*Smilacaceae*); and *Saccothecium* (*Sa.*) (e.g., *Sa. australianum* (Tan *et al.* 2023) isolated from *Grevillea decora* (*Proteaceae*), *Sa. rubi* (Li *et al.* 2016) isolated from dead spines of *Rubus ulmifolius* (*Rosaceae*), *Sa. sepincola* (Thambugala *et al.* 2014) isolated from the twigs of *Cornus sanguinea* (*Cornaceae*), and *Sa. widdringtoniae* (Crous *et al.* 2022b) isolated from twigs of *Widdringtonia wallichii* (*Cupressaceae*). *Paivomyces* (*Pa.*) can be differentiated from *P. australiensis comb. nov.* by producing pycnidia, endoconidia, and arthroconidia that are absent in *Paivomyces* (Cheewangkoon *et al.* 2009).

Pseudoselenophoma S. S. Nascimento, L. O. Ferro, Souza-Motta & J. D. P. Bezerra, ***gen. nov.*** MycoBank MB 857817.

Etymology: Named in reference to *Selenophoma*.

Two asexual morphotypes, selenophoma-like and hormonema-like. *Selenophoma-like*: *Conidiomata* pycnidial, dark brown, subepidermal to erumpent, and globose. *Pycnidial wall* consists of 2–3 layers of medium to dark brown textura angularis, thick-walled. *Conidiophores* non-uniform, short, barrel-shaped or subovoid, simple, medium brown, thick-walled, composed of 1–3 cells, tapering toward conidiogenous cells, and occasionally reduced to conidiogenous cells. *Conidiogenous cells* subglobose, obpyriform or obovoid, and phialidic, with apical periclinal thickening. *Conidia* aseptate, hyaline, ellipsoidal to obovoid, thin-walled, guttulate. *Hormonema-like*: *Mycelium* immersed and superficial; hyphae hyaline, thin-walled, smooth to slightly verruculose, loosely septate; brown hyphae (type 1) thick-walled, slightly verruculose, densely septate mostly constricted at septa, phialides integrated in hyphal cells, producing hyaline, aseptate conidia; and brown hyphae (type 2), thin-walled, smooth, loosely septate, not constricted at septa, producing endoconidia. *Conidiogenous cells* undifferentiated from creeping hyphae, intercalary or terminal on brown hyphae, producing 1–2 conidia basipetally, with prominent loci and visible collarettes after conidial secession. *Conidia* produced synchronously, along hyphae and on short lateral branches, aseptate, hyaline, ellipsoid to obovoid, smooth, truncate base, slightly thick-walled, turning brown and thick-walled when mature, occasionally becoming 1-medianly septate, slightly constricted at the septum. *Arthroconidia* ellipsoid, medium brown, thick-walled, medially septate, or with slightly longer basal cell, conspicuously constricted at septum, with broadly rounded ends; sometimes producing secondary conidia via microcyclic conidiation. *Endoconidia* produced in thick- and thin-walled hyphae, septate, ellipsoidal, constricted at the septa, and thick-walled. *Chlamydospores* multiseptate, brown, composed of subglobose cells, thick-walled, constricted at the septa, and irregular in shape (based on Cheewangkoon *et al.* 2009).

Type species: *Pseudoselenophoma australiensis* (Cheewangkoon & Crous) S.S. Nascimento *et al.*

Pseudoselenophoma australiensis (Cheewangkoon & Crous) S.S. Nascimento, L.O. Ferro, Souza-Motta & J.D.P. Bezerra, ***comb. nov.*** MycoBank MB 857818.
Basionym: *Selenophoma australiensis* Cheewangkoon & Crous, *Persoonia* **23**: 77. 2009.

Description and illustration: See Cheewangkoon *et al.* (2009).

Typus: **Australia**, Northern Territory, Edith Falls, 14°05'20"S, 14°05'20"E, on *Eucalyptus mineata*, 22 Sep. 2007, coll. *B.A. Summerell*, isol. *P.W. Crous* (**holotype** CBS H-20294, culture ex-type CBS 124776 = CPC 14582).

Additional specimen examined: **Australia**, Northern Territory, Edith Falls, 14°05'20"S, 132°05'12"E, on *Eucalyptus mineata*, 22 Sep. 2007, coll. *B.A. Summerell*, isol. *P.W. Crous* (living culture CPC 14583).

Notes: *Selenophoma australiensis* was originally described from *Eucalyptus mineata* leaves in Australia (Cheewangkoon *et al.* 2009). The authors tentatively included this isolate in *Selenophoma* due to "considerable confusion surrounds the delimitation of *Aureobasidium* and *Hormonema*, complicating species identification in these genera" and because of "a similar yeast synanamorph as observed in *S. eucalypti*" (Crous *et al.* 1995, Cheewangkoon *et al.* 2009). Currently, *S. eucalypti* is placed in *Pseudosydowia* (Thambugala *et al.* 2014), a genus whose morphological characteristics are similar to those of *Aureobasidium* and *Hormonema* species (de Hoog & Yurlova 1994, Crous *et al.* 1995, 2003, Bills *et al.* 2004, Zalar *et al.* 2008). The absence of DNA sequences from the type species of *Selenophoma* (*S. catananches*), along with the replacement of species of this genus with other genera, was also important information for our decision to treat *P. australiensis comb. nov.* as the type species of *Pseudoselenophoma gen. nov.* introduced into *Saccotheciaceae*. Furthermore, our analyses are important for clarifying the phylogenetic position of the taxa in this family.

© 2025 Westerdijk Fungal Biodiversity Institute

DISCUSSION

We analysed endophytic fungal isolates from the Caatinga forest in Brazil based on morphological and multi-locus phylogenetic analyses. We introduced a new genus, *Paivomyces* (including *Pa. mimosae sp. nov.*), a unique lineage among the members of *Saccotheciaceae*. During our phylogenetic analyses, we observed that *S. australiensis* was positioned in a clade distinct from the other species treated as *Selenophoma* and differed from the other genera in the family. Based on this analysis and the morphological features, we introduced a new genus, *Pseudoselenophoma* (including *P. australiensis comb. nov.*), to clarify the position of this species in *Saccotheciaceae*. Currently, the family *Saccotheciaceae* has nine accepted genera (Hyde *et al.* 2024), and here, we expand this number to 11 with the descriptions of *Paivomyces gen. nov.* and *Pseudoselenophoma gen. nov.* Our phylogenetic analyses included representative taxa of *Saccotheciaceae*, *Dothideadeae*, *Neocelosporiaceae*, and *Zalariaceae* in *Dothideales* (*Dothideomycetes*). Except for the genus *Aureobasidium*, the species of *Saccotheciaceae* are poorly described; thus, building a robust database for phylogenetic analyses is challenging (Hirooka *et al.* 2013, Quaedvlieg *et al.* 2013, Silva *et al.* 2024). Phylogenetic inferences from our study revealed that sequences identified as *Selenophoma* and *Pseudosydowia* were placed in different clades (e.g., Cheewangkoon *et al.* 2009, Thambugala *et al.* 2014, Crous *et al.* 2022a, b), highlighting the current challenges in consolidating its taxonomy. The description of these two new genera is important for clarifying the phylogenetic relationships among the members of this family, as has been done for *Aureobasidium* and *Hormonema* (Crous *et al.* 2015, Crous *et al.* 2020, Haelewaters *et al.* 2021).

Selenophoma was introduced by Maire (1906); most species of this genus which have been identified before the 2000s are based on morphological differentiation without much access to molecular tools for appropriate phylogenetic analyses (Crous *et al.* 1995, Cheewangkoon *et al.* 2009). In our phylogenetic analyses of *Saccotheciaceae* and related families, *Paivomyces mimosae sp. nov.* and *Pseudoselenophoma australiensis comb. nov.*, are positioned in different clades, reinforcing their separation from other genera within *Saccotheciaceae*. Phylogenetically, in the ITS and LSU matrix, *P. australiensis* is positioned in a unique and distinct clade from *Pa. mimosae*; in the ITS, LSU, *rpb2*, *tub2*, and *tef1* matrices, these species remain in distinct but close clades. Morphologically, both species exhibit hyaline and dematiaceous structures with age, *P. australiensis* presents conidiomata, conidiophores, and conidia, unlike *Pa. mimosae*, which presents hyphae toluroid and enteroblastic conidiogenous cells, often with an inconspicuous collarette.

An example of reclassification in *Saccotheciaceae* is the species *Sphaerulina eucalypti*, isolated from *Eucalyptus* leaves in Southern Africa (Verwoerd & Du Plessis 1931), which was relocated into *Selenophoma eucalypti* (Crous *et al.* 1995) and later to *Sydowia eucalypti* (Crous 2003). Currently, it is classified as *Pseudosydowia eucalypti* (Thambugala *et al.* 2014). This reclassification exemplifies the importance of new taxonomic and phylogenetic analyses, which can provide a precise understanding of evolutionary relationships and enhance our knowledge of the members of *Saccotheciaceae*. Species of this family occur in diverse environments. For example, *Aureobasidium* species are found in various organic materials, demonstrating the importance of studying their ecology in different ecosystems (Wu *et al.* 2023). Similarly, Quaedvlieg *et al.* (2013) described two species of *Pseudoseptoria* from bamboo leaves in Iran, and *Aureobasidium iranianum* was isolated as an endophyte from bamboo stems in Iran (Arzanlou & Khodaei 2012). Recently, two new species of *Aureobasidium* were introduced as endophytes of *A. colubrina* (*Fabaceae*) in Brazil (Silva *et al.* 2024). These findings demonstrate the different lifestyles of related *Saccotheciaceae* genera (Saber *et al.* 2023).

The description of *Paivomyces* and *Pseudoselenophoma* as new genera in *Saccotheciaceae* provides insights into this family's unique lineage and expands the taxonomic information on these understudied taxa in *Dothideales*. Fungal isolates from tropical forests with different lifestyles are important for a broad understanding of fungal diversity and highlighting their contribution to the phylogenetic analyses of taxa in *Saccotheciaceae*.

ACKNOWLEDGEMENTS

We thank the Conselho Nacional de Desenvolvimento Científico e Tecnológico (CNPq, process numbers 130148/2023-7, 404989/2021-7, 303939/2022-2, and 151166/2024-2), the Fundação Coordenação de Aperfeiçoamento de Pessoal de Nível Superior (CAPES, finance code 001; 88881.986045/2024-01), and the Fundação de Amparo à Pesquisa do Estado de Goiás (FAPEG, process number 202310267000226). C.M. Souza-Motta has a fellowship from the CNPq and J.D.P. Bezerra from CNPq and FAPEG. We also would like to thank Ewald Groenewald, Pedro Crous, and Mieke Starink-Willemse for helping us obtaining new DNA sequences from CPC strains and the teams of the Laboratório de Micologia Ambiental (UFPE), the Micoteca URM (UFPE), and the Laboratório de Micologia (LabMicol, IPTSP/UFG) for their help during this study.

Conflict of interest: The authors declare no conflict of interest.

REFERENCES

Aquino DN, Andrade EMAM, Tavares ETSF, *et al.* (2021). Impacto de secas e antropização na dinâmica da cobertura florestal em fragmento do domínio fitogeográfico da Caatinga. *Revista Brasileira de Geografia Física* **14**: 1675–1689. https://doi.org/10.26848/rbgf.v14.3.p1675-1689

Arzanlou M, Khodaei S (2012). *Aureobasidium iranianum*, a new species on bamboo from Iran. *Mycosphere* **3**: 404–408. https://doi.org/10.5943/mycosphere/3/4/2

Barbosa RN, Bezerra JDP, Santos ACS, *et al.* (2020). Brazilian tropical dry forest (Caatinga) in the spotlight: an overview of species of *Aspergillus*, *Penicillium* and *Talaromyces* (*Eurotiales*) and the description of *P. vascosobrinhous sp. nov. Acta Botanica Brasilica* **34**: 409–429. https://doi.org/10.1590/0102-33062019abb0411

Barreto GG, Souza-Motta CM, Silva GA, *et al.* (2024). Meristematic and meristematic-like fungi in *Dothideomycetes*. *Fungal Systematics and Evolution* **14**: 77–88. https://doi.org/10.3114/fuse.2024.14.05

© 2025 Westerdijk Fungal Biodiversity Institute

Bezerra JDP, Oliveira RJV, Paiva LM, *et al.* (2017a). *Bezerromycetales* and *Wiesneriomycetales ord. nov.* (class *Dothideomycetes*), with two novel genera to accommodate endophytic fungi from Brazilian cactus. *Mycological Progress* **16**: 297–309. https://doi.org/10.1007/s11557-016-1254-0

Bezerra, JDP, Sandoval-Denis M, Paiva LM, *et al.* (2017b). New endophytic *Toxicocladosporium* species from cacti in Brazil, and description of *Neocladosporium gen. nov*. *IMA Fungus* **8**: 77–97. https://doi.org/10.5598/imafungus.2017.08.01.06

Bezerra JDP, Machado AR, Firmino AL, *et al.* (2018). Mycological diversity description I. *Acta Botanica Brasilica* **32**: 656–666. https://doi.org/10.1590/0102-33062018abb0154

Bezerra JDP, Pádua APSL, Oliveira TGL, *et al.* (2019). *Pseudoplagiostoma myracrodruonis* (*Pseudoplagiostomataceae*, *Diaporthales*): a new endophytic species from Brazil. *Mycological Progress* **18**: 1329–1339. https://doi.org/10.1007/s11557-019-01531-0

Bills GF, Collado J, Ruibal C, *et al.* (2004). *Hormonema carpetanum sp. nov.*, a new lineage of dothideaceous black yeasts from Spain. *Studies in Mycology* **50**: 149–157.

Bonorden HF (1864). Abhandlungen aus dem Gebiete der Mykologie (Vol. 1). Schmidt.

Carbone I, Kohn LM (1999). A method for designing primer sets for speciation studies in filamentous ascomycetes. *Mycologia* **91**: 553–556. https://doi.org/10.1080/00275514.1999.12061051

Calabon MS, Jones EG, Pang KL, *et al.* (2023). Updates on the classification and numbers of marine fungi. *Botanica Marina* **66**: 213–238. https://doi.org/10.1515/bot-2023-0032

Cheewangkoon R, Groenewald JZ, Summerell BA, *et al.* (2009). *Myrtaceae*, a cache of fungal biodiversity. *Persoonia* **23**: 55–85. https://doi.org/10.3767/003158509X474752

Chan GF, Puad MSA, Chin CF, *et al.* (2011). Emergence of *Aureobasidium pullulans* as human fungal pathogen and molecular assay for future medical diagnosis. *Folia Microbiologica* **56**: 459–467. https://doi.org/10.1007/s12223-011-0070-9

Crous PW, Lennox CL, Sutton BC (1995). *Selenophoma eucalypti* and *Stigmina robbenensis sp. nov.* from *Eucalyptus* leaves on Robben Island. *Mycological Research* **99**: 648–652. https://doi.org/10.1016/S0953-7562(09)80521-2

Crous PW, Groenewald JZ, Wingfield MJ, *et al.* (2003). The value of ascospore septation in separating *Mycosphaerella* from *Sphaerulina* in the *Dothideales*: a Saccardoan myth? *Sydowia* **55**: 136–152.

Crous PW, Verkley GJM, Groenewald JZ, *et al.* (2009). *Fungal Biodiversity* [CBS Laboratory Manual Series 1]. Utrecht: CBS-KNAW Fungal Biodiversity Centre.

Crous PW, Wingfield MJ, Guarro J, *et al.* (2015). Fungal Planet description sheets: 320–370. *Persoonia* **34**: 167–266. https://doi.org/10.3767/003158515X688433

Crous PW, Wingfield MJ, Burgess TI, *et al.* (2016). Fungal Planet description sheets: 469–557. *Persoonia* **37**: 218–403. https://doi.org/10.3767/003158516X694499

Crous PW, Carnegie AJ, Wingfield MJ, *et al.* (2019). Fungal Planet description sheets: 868–950. *Persoonia* **42**: 291–473. https://doi.org/10.3767/persoonia.2019.42.11

Crous PW, Cowan DA, Maggs-Kölling G, *et al.* (2020). Fungal Planet description sheets: 1112–1181. *Persoonia* **45**: 251–409. https://doi.org/10.3767/persoonia.2020.45.10

Crous PW, Cowan DA, Maggs-Kölling G, *et al.* (2021). Fungal Planet description sheets: 1182–1283. *Persoonia* **46**: 313–528. https://doi.org/10.3767/persoonia.2021.46.11

Crous PW, Begoude BAD, Boers J, *et al.* (2022a). New and Interesting Fungi. 5. *Fungal Systematics and Evolution* **10**: 19–90. https://doi.org/10.3114/fuse.2022.10.02

Crous PW, Boers J, Holdom D, *et al.* (2022b). Fungal Planet description sheets: 1383–1435. *Persoonia* **48**: 261–371. https://doi.org/10.3767/persoonia.2022.48.08

De Hoog GS, Yurlova NA (1994). Conidiogenesis, nutritional physiology and taxonomy of *Aureobasidium* and *Hormonema*. *Antonie van Leeuwenhoek* **65**: 41–54. https://doi.org/10.1007/BF00878278

Ferro LO, Bezerra JDP, da Silva TM, *et al.* (2024a). Endophytic *Diaporthe* species from Brazil. *Fungal Systematics and Evolution* **14**: 251–269. https://doi.org/10.3114/fuse.2024.14.16

Ferro LO, Da Silva AC, Nascimento SS, *et al.* (2024b). *Cytospora anacardii* (*Cytosporaceae, Diaporthales*): A new endophytic species from *Anacardium occidentale* of the Brazilian savanna. *Phytotaxa* **669**: 25–35. https://doi.org/10.11646/phytotaxa.669.1.3

Glass NL, Donaldson GC (1995). Development of primer sets designed for use with the PCR to amplify conserved genes from filamentous ascomycetes. *Applied and Environmental Microbiology* **61**: 1323–1330. https://doi.org/10.1128/aem.61.4.1323-1330.1995

Haelewaters D, Urbina H, Brown S, *et al.* (2021). Isolation and molecular characterization of the romaine lettuce phylloplane mycobiome. *Journal of Fungi* **7**: 277. https://doi.org/10.3390/jof7040277

Hirooka Y, Masuya H, Akiba M, *et al.* (2013). *Sydowia japonica*, a new name for *Leptosphaerulina japonica* based on morphological and molecular data. *Mycological Progress* **12**: 173–183. https://doi.org/10.1007/s11557-012-0823-0

Hoang DT, Chernomor O, Von Haeseler A, *et al.* (2018). UFBoot2: improving the ultrafast bootstrap approximation. *Molecular Biology and Evolution* **35**: 518–522. https://doi.org/10.1093/molbev/msx281

Hocking AD, Pitt JI (1980). Dichloran-glycerol medium for enumeration of xerophilic fungi from low-moisture foods. *Applied and Environmental Microbiology* **39**: 488–492. https://doi.org/10.1128/aem.39.3.488-492.1980

Hongsanan S, Hyde KD, Phookamsak R, *et al.* (2020). Refined families of *Dothideomycetes*: *Dothideomycetidae* and *Pleosporomycetidae*. *Mycosphere* **11**: 1553–2107. https://doi.org/10.5943/mycosphere/11/1/13

Humphries Z, Seifert KA, Hirooka Y, *et al.* (2017). A new family and genus in *Dothideales* for Aureobasidium-like species isolated from house dust. *IMA Fungus* **8**: 299–315. https://doi.org/10.5598/imafungus.2017.08.02.05

Hyde KD, Noorabadi MT, Thiyagaraja V, *et al.* (2024). The 2024 Outline of *Fungi* and fungus-like taxa. *Mycosphere* **15**: 5146–6239. https://doi.org/10.5943/mycosphere/15/1/25

Kalyaanamoorthy S, Minh BQ, Wong TK, *et al.* (2017). ModelFinder: fast model selection for accurate phylogenetic estimates. *Nature Methods* **14**: 587–589. https://doi.org/10.1038/nmeth.4285

Katoh K, Standley DM (2013). MAFFT multiple sequence alignment software version 7: Improvements in performance and usability. *Molecular Biology and Evolution* **30**: 772–780. https://doi.org/10.1093/molbev/mst010

Kumar A, Birnbaum MD, Patel DM, *et al.* (2016). Posttranslational arginylation enzyme Ate1 affects DNA mutagenesis by regulating stress response. *Cell Death & Disease* **7**: 2378–2378. https://doi.org/10.1038/cddis.2016.284

© 2025 Westerdijk Fungal Biodiversity Institute

Li GJ, Hyde KD, Zhao RL *et al.* (2016). Fungal diversity notes 253–366: taxonomic and phylogenetic contributions to fungal taxa. *Fungal Diversity* **78**: 1–237. https://doi.org/10.1007/s13225-016-0366-9

Liu YJ, Whelen S, Hall BD (1999). Phylogenetic relationships among ascomycetes: evidence from an RNA polymerse II subunit. *Molecular Biology and Evolution* **16**: 1799–1808. https://doi.org/10.1093/oxfordjournals.molbev.a026092

Liu JK, Hyde KD, Jones EG, *et al.* (2015). Fungal diversity notes 1–110: taxonomic and phylogenetic contributions to fungal species. *Fungal Diversity* **72**: 1–197. https://doi.org/10.1007/s13225-015-0324-y

MMA home page (2022). Ministério do Meio Ambiente. Caatinga. https://www.gov.br/mma/pt-br/assuntos/ecossistemas-1/biomas/caatinga.

Maire MR (1906). Contributions a l'etude de la flore mycologique de 1' A frique du Nord. *Bulletin de la Société Botanique de France* **53**: 180–215.

Miller MA, Pfeiffer W, Schwartz T (2010). Creating the CIPRES Science Gateway for inference of large phylogenetic trees. *Proceeding Gateway Computing Environments Workshop* **14**: 1–8. https://doi.org/10.1109/GCE.2010.5676129

Nascimento SS, Ferro LO, Freire KTLS, *et al.* (2021). *Cladophialophora bromeliacearum* (*Herpotrichiellaceae*, *Chaetothyriales*), a novel endophytic species from the Brazilian tropical dry forest. *Phytotaxa* **509**: 211–224. https://doi.org/10.11646/phytotaxa.509.2.4

Nguyen LT, Schmidt HA, Von Haeseler A, *et al.* (2015). IQ-TREE: a fast and effective stochastic algorithm for estimating maximum-likelihood phylogenies. *Molecular Biology and Evolution* **32**: 268–274. https://doi.org/10.1093/molbev/msu300

O'Donnell K, Kistler HC, Cigelnik E, *et al.* (1998). Multiple evolutionary origins of the fungus causing Panama disease of banana: concordant evidence from nuclear and mitochondrial gene genealogies. *Proceedings of the National Academy of Sciences* **95**: 2044–2049. https://doi.org/10.1073/pnas.95.5.2044

Oliveira TGL, Bezerra JDP, Silva IRD, *et al.* (2021). Diversity of endophytic fungi in the leaflets and branches of *Poincianella pyramidalis*, an endemic species of Brazilian tropical dry forest. *Acta Botanica Brasilica* **34**: 755–764. https://doi.org/10.1590/0102-33062020abb0253

Palacios-Cabrera H, Taniwaki MH, Hashimoto JM, *et al.* (2005). Growth of *Aspergillus ochraceus*, *A. carbonarius* and *A. niger* on culture media at different water activities and temperatures. *Brazilian Journal of Microbiology* **36**: 24–28. https://doi.org/10.1590/S1517-83822005000100005

Pande A (2008). *Ascomycetes of peninsular India*. Scientific Publishers.

Peterson SW, Manitchotpisit P, Leathers TD (2013). *Aureobasidium thailandense sp. nov*. isolated from leaves and wooden surfaces. *International Journal of Systematic and Evolutionary Microbiology* **63**: 790–795. https://doi.org/10.1099/ijs.0.047613-0

Pitt JI (1979). The genus *Penicillium* and its teleomorphic states *Eupenicillium* and *Talaromyces.* Academic Press, London.

Quaedvlieg WGJM, Verkley GJM, Shin HD, *et al.* (2013). Sizing up *Septoria*. *Studies in Mycology* **75**: 307–390. https://doi.org/10.3114/sim0017

Rambaut A (2012). FigTree v. 1.4.0. Institute of Evolutionary Biology, University of Edinburgh, Edinburgh. http://tree.bio.ed.ac.uk/software/figtree/.

Rayner RW (1970). *A mycological colour chart*. Commonwealth Mycological Institute and British Mycological Society. Kew, Surrey, UK.

Rehner SA, Samuels GJ (1994). Taxonomy and phylogeny of *Gliocladium* analysed from nuclear large subunit ribosomal DNA sequences. *Mycological Research* **98**: 625–634. https://doi.org/10.1016/S0953-7562(09)80409-7

Rehner S, Buckley E (2005). A *Beauveria* phylogeny inferred from nuclear ITS and *EF1-α* sequences: evidence for cryptic diversification and links to *Cordyceps* teleomorphs. *Mycology* **97**: 84–98. https://doi.org/10.1080/15572536.2006.11832842

Ronquist F, Teslenko M, Van Der Mark P, *et al.* (2012). MrBayes 3.2: efficient Bayesian phylogenetic inference and model choice across a large model space. *Systematic Biology* **61**: 539–542. https://doi.org/10.1093/sysbio/sys029

Saber WI, Al-Askar AA, Ghoneem KM (2023). Exclusive biosynthesis of pullulan using taguchi's approach and decision tree learning algorithm by a novel endophytic *Aureobasidium pullulans* strain. *Polymers* **15**: 1419. https://doi.org/10.3390/polym15061419

Samson RA, Houbraken J, Thrane U, *et al.* (2010). *Food and Indoor Fungi*. [CBS Laboratory Manual series no. 2.] Utrecht: CBS-KNAW Fungal Biodiversity Centre.

Silva AV, Oliveira TGL, Souza-Motta CM, *et al.* (2021). *Leptosillia mimosae* (*Leptosilliaceae*, *Xylariales*), a new endophytic species from the Caatinga dry forest in Brazil. *Nova Hedwigia* **113**: 507–530. https://doi.org/10.1127/nova_hedwigia/2021/0653

Silva AC, Ferro LO, Alves VCS *et al.* (2024). Phylogenetic evidence revealed new *Aureobasidium* species (*Saccotheciaceae*, *Dothideales*) from Brazil. *Mycological Progress* **23**: 70. https://doi.org/10.1007/s11557-024-02009-4

Stamatakis A (2014). RAxML version 8: a tool for phylogenetic analysis and post-analysis of large phylogenies. *Bioinformatics* **30**: 1312–1313. https://doi.org/10.1093/bioinformatics/btu033

Thambugala KM, Ariyawansa HA, Li YM, *et al.* (2014). *Dothideales*. *Fungal Diversity* **68**: 105–158. https://doi.org/10.1007/s13225-014-0303-8

Tan YP, Shivas RG (2023). *Index of Australian Fungi* **11**: 1–11. https://doi.org/10.5281/zenodo.8252565

Verwoerd L (1931). Descriptions of some new species of South African fungi and of species not previously recorded in south Africa-iii. *South African Journal of Science* **28**: 290–297.

Vilgalys R, Hester M (1990). Rapid genetic identification and mapping of enzymatically amplified ribosomal DNA from several *Cryptococcus* species. *Journal of Bacteriology* **172**: 4238–4246. https://doi.org/10.1128/jb.172.8.4238-4246.1990

Vu D, Groenewald M, Vries M, *et al.* (2019). Large-scale generation and analysis of filamentous fungal DNA barcodes boosts coverage for kingdom fungi and reveals thresholds for fungal species and higher taxon delimitation. *Studies in Mycology* **92**: 135–154. https://doi.org/10.1016/j.simyco.2018.05.001

White TJ, Bruns T, Lee S, *et al.* (1990). Amplification and direct sequencing of fungal ribosomal RNA genes for phylogenetics. In: *PCR protocols: a guide to methods and applications* (Innes MA, Gelfand DH, Sninsky JJ, *et al.*, eds). Academic Press, USA: 315–322.

Wijayawardene NN, Hyde KD, Dai DQ, *et al.* (2020). Outline of *Fungi* and fungus-like taxa – 2021. *Mycosphere* **11**: 1060–1456. 1060–1456. https://doi.org/10.5943/mycosphere/11/1/8

© 2025 Westerdijk Fungal Biodiversity Institute

Wu F, Feng Z, Wang M, *et al.* (2023). Proposal of four new *Aureobasidium* species for exopolysaccharide production. *Journal of Fungi* **9**: 447. https://doi.org/10.3390/jof9040447

Zalar P, Gostinčar C, De Hoog GS, *et al.* (2008). Redefinition of *Aureobasidium pullulans* and its varieties. *Studies in Mycology* **61**: 21–38. https://doi.org/10.3114/sim.2008.61.02

Supplementary Material: http://fuse-journal.org/

Fig. S1. Maximum Likelihood (ML) phylogenetic tree of the representative ITS sequences of the species related to *Paivomyces gen. nov*. New taxa are in **boldface**. Confidence values for ML-BS and IQ-TREE-BS ≥ 70 % (UFboot2/RAxML) are included near the nodes, and the (-) indicates statistical support below the threshold values. Ex-type strains are marked with (T). The tree was rooted to *Phaeosclera dematioides* (CBS 157.81) (*Phaeosclerales*, *Dothideomycetes*).

Fig. S2. Maximum Likelihood (ML) phylogenetic tree of the representative LSU sequences of the species related to *Paivomyces gen. nov*. New taxa are in **boldface**. Confidence values for ML-BS and IQ-TREE-BS ≥ 70 % (UFboot2/RAxML) are included near the nodes and the (-) indicates statistical support below the threshold values. Ex-type strains are marked with (T). The tree was rooted to *Phaeosclera dematioides* (CBS 157.81) (*Phaeosclerales*, *Dothideomycetes*).

Fig. S3. Maximum Likelihood (ML) phylogenetic tree of the representative *tub2* sequences of the species related to *Paivomyces gen. nov*. New taxa are in **boldface**. Confidence values for ML-BS and IQ-TREE-BS ≥ 70 % (UFboot2/RAxML) are included near the nodes and the (-) indicates statistical support below the threshold values. Ex-type strains are marked with (T). The tree was rooted to *Dothiora pyrenophora* (CPC 30632) (*Dothideales*, *Dothideomycetes*).

Fig. S4. Maximum Likelihood (ML) phylogenetic tree of the representative *rpb2* sequences of the species related to *Paivomyces gen. nov*. New taxa are in **boldface**. Confidence values for ML-BS and IQ-TREE-BS ≥ 70 % (UFboot2/RAxML) are included near the nodes and the (-) indicates statistical support below the threshold values. Ex-type strains are marked with (T). The tree was rooted to *Dothidea sambuci* (AFTOL-ID 274) (*Dothideales*, *Dothideomycetes*).

Fig. S5. Maximum Likelihood (ML) phylogenetic tree of the representative *tef1* sequences of the species related to *Paivomyces gen. nov*. New taxa are in **boldface**. Confidence values for ML-BS and IQ-TREE-BS ≥ 70 % (UFboot2/RAxML) are included near the nodes and the (-) indicates statistical support below the threshold values. Ex-type strains are marked with (T). The tree was rooted to *Phaeosclera dematioides* (CBS 157.81) (*Phaeosclerales*, *Dothideomycetes*).

© 2025 Westerdijk Fungal Biodiversity Institute

© 2025 Westerdijk Fungal Biodiversity Institute

FUSE

Fungal Systematics and Evolution

VOLUME 16
DECEMBER 2025
PAGES 71–80

doi.org/10.3114/fuse.2025.16.5

Microfungi associated with dying quiver trees (*Aloidendron dichotomum*) in South Africa

S. Marincowitz[1*], N.Q. Pham[1], B.D. Wingfield[1], M.J. Wingfield[1]

[1]Department of Biochemistry, Genetics and Microbiology, Forestry and Agricultural Biotechnology Institute (FABI), University of Pretoria, Private Bag X20, Pretoria 0028, South Africa

*Corresponding author: seonju.marincowitz@fabi.up.ac.za

Key words:
Aloe
Botryosphaeriaceae
new taxa
Thermoascaceae
Togniniaceae

Abstract: Quiver trees *(Aloidendron dichotomum)* are large iconic succulent plants found in arid areas of southern Africa. These trees have been observed suffering from die-back symptoms for many years. Various environmental and abiotic factors have been investigated as possible causes of the symptoms. However, biotic causes, especially microfungi that commonly cause die-backs in trees, have never been considered. During a routine disease survey, symptomatic stems and roots of the dying trees were collected in the Cape Province, South Africa. Isolations were made from tissues at the leading edges of the lesions on symptomatic stems and roots, and the resulting fungi were identified using morphological characteristics and DNA sequence data of four loci (LSU, SSU, ITS and β-tubulin). Five species were identified: *Paecilomyces formosus*, *Phaeoacremonium* (*Pm.*) *parasiticum*, *Pm. luteum*, *Xylogone sphaerospora*, and the newly described *Coniophoma aloidendri gen. et sp. nov*. Three species, *Pm. parasiticum* and *C. aloidendri* from this study and *Alanphillipsia* (*Ala.*) *aloes* were tested for their pathogenicity on *A. dichotomum* plants in a greenhouse trial. All three species gave rise to lesions significantly different in size from the controls. The *Pm. parasiticum* strains showed larger necrotic lesions than *C. aloidendri* and *Ala. aloes*. However, none of the isolated fungi were aggressive or are known as primary pathogens, and the cause of the die-back on symptomatic trees remains to be determined.

Citation: Marincowitz S, Pham NQ, Wingfield BD, Wingfield MJ (2025). Microfungi associated with dying quiver trees (*Aloidendron dichotomum*) in South Africa. *Fungal Systematics and Evolution* **16**: 71–80. doi: 10.3114/fuse.2025.16.5.
Received: 13 January 2025; **Accepted:** 26 March 2025; **Effectively published online:** 21 May 2025
Corresponding editor: P.W. Crous

INTRODUCTION

Aloidendron dichotomum, also known as the quiver tree, is one of five indigenous *Aloidendron* spp. found in southern Africa. *Aloidendron* (*Asphodelaceae*) was segregated from the larger genus *Aloe* to accommodate the tree aloe species (Grace *et al.* 2013, Smith *et al.* 2019). Quiver trees are commonly featured in iconic scenes of southern Africa as giant succulent trees against the backdrop of rocky and arid landscapes (Fig. 1). They are mainly found in the Northern Cape region of South Africa and parts of southern Namibia (Smith & Van Wyk 2008) (Fig. 2). They grow rapidly for the first 50 years, reaching up to nine meters in height under optimal conditions, then mature for another 150 years without a considerable increase in volume, followed by 50 years of senescence (Kaleme 2003). A high moisture content in their stems and leaves can support various mammals, birds and insects (Midgley *et al.* 1997). *Aloidendron dichotomum* is currently listed as 'vulnerable' in the IUCN Red List of Threatened Species (Foden *et al.* 2022).

The decline of quiver trees has been observed in their natural habitat for decades, and various investigations have been conducted to determine its cause. Global warming, geographical effects of climate change, and various emission scenarios suggest climate change as the most probable explanation for the decline (Foden 2002, Foden *et al.* 2007, 2022, Guo *et al.* 2011, Van der Merwe & Geldenhuys 2017), although there is some debate regarding this explanation (Jack *et al.* 2016). The possible role of fungal pathogens in the mortality of the *A. dichotomum* population has been considered, but without any clear result (Foden *et al.* 2007).

Roux *et al.* (2009) surveyed more than 300 symptomatic *A. dichotomum* trees in Goegap Nature Reserve (Northern Cape Province), specifically considering the possibility of a fungal disease. They found high levels of insect infestation and animal damage but no evidence of biotic pathogens. Various microfungi including *Alanphillipsia aloes*, *Dothiora aloidendri*, *Fusarium pharetrum*, *Hantamomyces aloidendri*, *Lapidomyces aloidendricola*, *Neophaeococcomyces aloes*, *Neoscytalidium dimidiatum*, *Phoma aloes* and *Staurosphaeria aloe* have been isolated from dying quiver trees in taxonomic studies (Crous *et al.* 2006, 2013, 2015, 2020, 2021, Lombard *et al.* 2019), but these have not been tested for their pathogenicity. During a routine disease survey in the areas where *A. dichotomum* grows naturally, many dying trees were found with lesions that might be attributed to the disease. The aim of this study was thus to isolate fungi from these lesions and to conduct pathogenicity tests with those most commonly isolated.

Fungal Systematics and Evolution is licensed under a Creative Commons Attribution-NonCommercial-NoDerivatives 4.0 International License

© 2025 Westerdijk Fungal Biodiversity Institute

MATERIALS AND METHODS

Fungal isolation from diseased tissues

Stems and roots with necrotic lesions were collected from six dying *A. dichotomum* trees near Nieuwoudtville, Cape Province, South Africa, in 2020 (Fig. 2). The samples were retained in paper bags under refrigerated conditions and transferred to the laboratory for further investigation. Microscopes (Nikon SMZ 18 or Nikon Eclipse N*i*, Tokyo, Japan) were used to examine the samples for visible fungal structures on the symptomatic tissues. Small pieces of tissue (less than 3 mm in diam.) were cut from the interface between the lesions and healthy tissues and placed on 2 % malt extract agar (MEA: 20 g Biolab malt extract, 20 g Difco agar, 1 L water) supplemented with streptomycin (100 mg/L). The isolates were incubated at room temperature until fungal growth developed.

Fungal hyphae growing from the diseased tissue pieces were transferred onto fresh 2 % MEA to obtain pure cultures. These cultures were then incubated at 23 °C in the dark until they could be grouped based on colony characteristics. One or two isolates representing each fungal morphotype were selected for identification based on DNA sequence data.

For morphological identification of the putative new taxon, isolates were grown on water agar (WA: 20 g Difco agar, 1 L water) with sterilised toothpicks placed on the agar surface to induce the production of fruiting structures. Fruiting structures were mounted on microscope slides, and up to fifty measurements were made for characteristic structures. Dimensions were recorded as minimum–maximum (average ± standard deviation). Images were captured using Nikon DS-Ri2 cameras mounted on the microscopes. All the measurements and image-taking were done using an imaging program (NIS Elements, Tokyo, Japan).

The optimum temperature for growth and culture characteristics for the putative new taxon were studied on 2 % MEA. Plugs (5 mm diam.) of actively growing mycelium were placed at the centres of 90-mm-diam. Petri dishes containing MEA. The Petri dishes were incubated at six temperatures, 10–35 °C at 5° intervals, with five replicates at each temperature. Two colony diameters perpendicular to each other were recorded after 15 d, and the averages were used to calculate the growth rate. Colours were named after the ISCC-NBS system. Cultures were deposited in the culture collection (CMW) at the Forestry and Agricultural Biotechnology Institute (FABI), University of Pretoria, South Africa. The ex-type culture of the new taxon was deposited

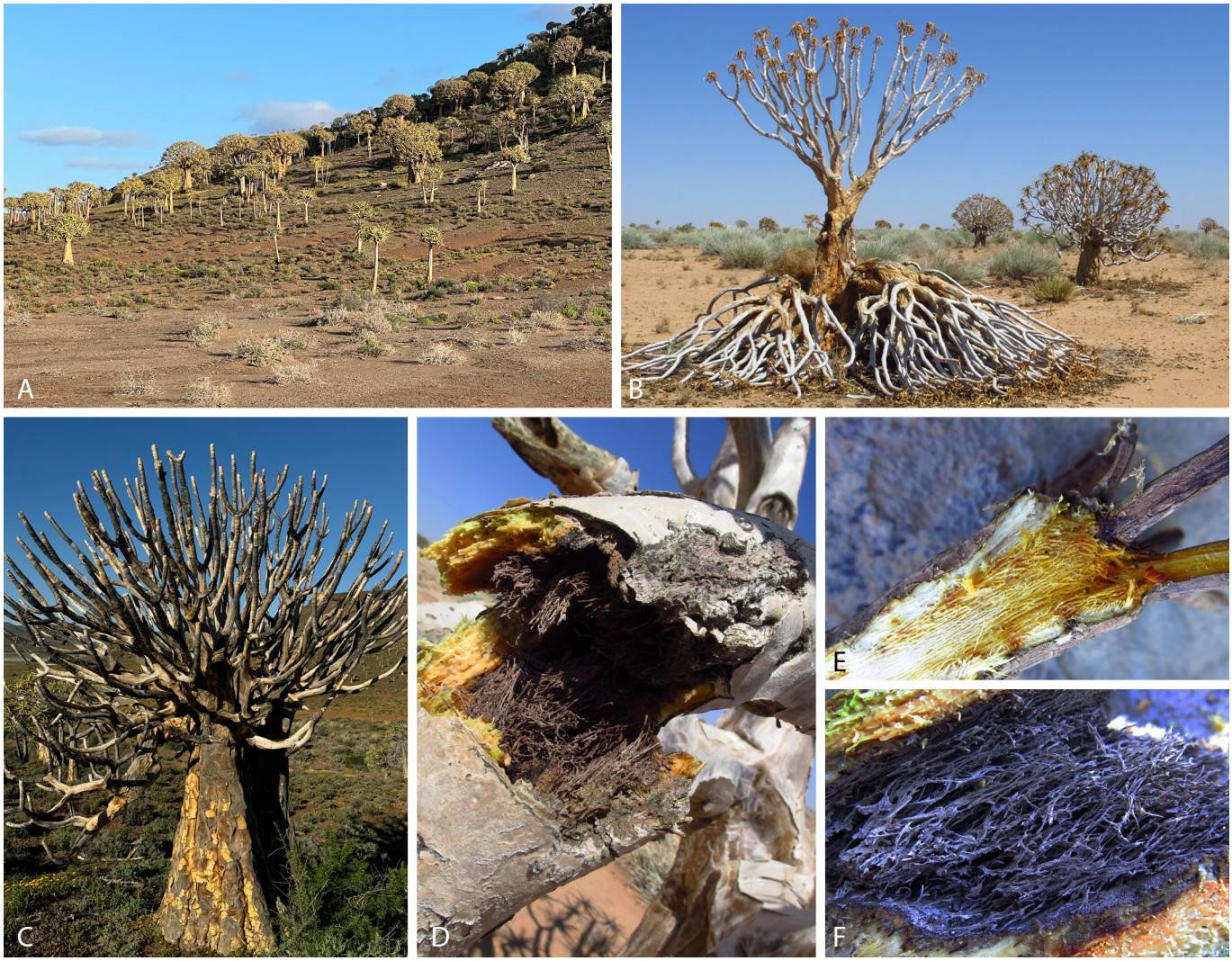

Fig. 1. Quiver trees, *Aloidendron dichotomum*, in the field. **A.** Healthy trees and trees showing die-back symptoms dispersed in a natural habitat. **B, C.** Trees with die-back symptoms. **D–F.** Inside symptomatic stems.

© 2025 Westerdijk Fungal Biodiversity Institute

in the culture collection of Innovation Africa (CMW-IA) based at the University of Pretoria (https://fabi.up.ac.za), and herbarium specimens were deposited in the H.G.W.J. Schweickerdt herbarium (PRU), University of Pretoria, South Africa.

Sequencing and phylogenetic analyses

Fungal strains were grown on 2 % MEA for 7 d at 25 °C and subsequently used for DNA extraction. Mycelium was gently removed from the medium surface using sterile needles and transferred to 1.5 mL Eppendorf tubes. DNA extraction was performed using the Prepman® Ultra Sample Preparation Reagent (Thermo Fisher Scientific, Waltham, MA, USA) according to the manufacturer's recommended protocols. The internal transcribed spacer (ITS) 1 and 2, including the 5.8S rRNA region, was amplified using primers ITS1F and ITS4 (White *et al.* 1990, Gardes & Bruns 1993); the nuclear large subunit (LSU) of rRNA with primers LR0R and LR5 (Vilgalys & Hester 1990, Rehner & Samuels 1994); and the nuclear small subunit (SSU) of rRNA with primers NS1 and NS4 (White *et al.* 1990). Part of the β-tubulin (*TUB2*) gene region was amplified using primers BT2a and BT2b (Glass & Donaldson 1995) as an additional barcoding gene. PCR reactions were conducted utilising an Applied Biosystems ProFlex PCR System (Thermo Fisher Scientific, Waltham, MA, USA). The amplified fragments were cleaned using the ExoSAP-IT™ PCR Product Cleanup Reagent (Thermo Fisher Scientific, Waltham, MA, USA) and sequenced in both directions using an ABI PRISM™ 3100 DNA sequencer (Applied Biosystems, USA) at the sequencing facility of the Faculty of Natural and Agricultural Sciences, University of Pretoria, South Africa.

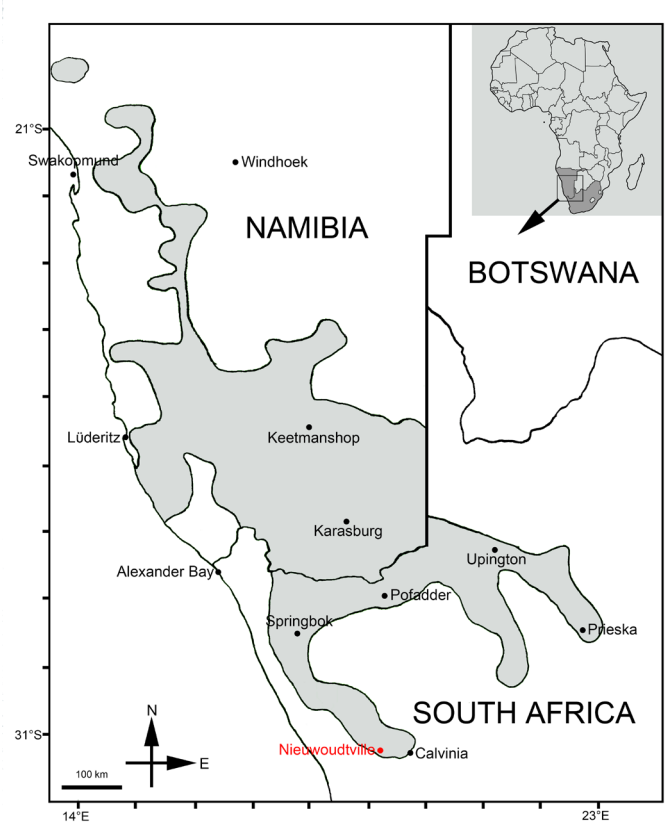

Fig. 2. Distribution and natural habitats of *Aloidendron dichotomum* (shaded) and the location where the samples were collected (Nieuwoudtville, red dot) (map adapted from Jack *et al.* 2016).

Geneious Prime v. 2022.1.1 (https://www.geneious.com) was utilised to assemble and edit the raw sequences. All the sequences generated in this study were submitted to GenBank (http://www.ncbi.nlm.nih.gov) (Table S1).

Preliminary identification was conducted using ITS sequences to perform a nucleotide BLAST search against the NCBI GenBank database (http://www.ncbi.nlm.nih.gov). This information was used to develop datasets for further phylogenetic analysis. Sequences of species related to this study were retrieved from GenBank (Table S1). The sequences were aligned using MAFFT v. 7 (Katoh & Standley 2013) and manually inspected using MEGA v. 7 (Kumar *et al.* 2016). The appropriate model was determined using jModeltest v. 1.2.5 (Posada 2008). Bayesian inference (BI) analysis was performed using MrBayes v. 3.2.6 (Ronquist *et al.* 2012) on the CIPRES Science Gateway v. 3.3. Four Markov chain Monte Carlo (MCMC) chains were initiated from a random starting tree for five million generations, and trees were sampled every 100th generation. The initial 25 % of sampled trees were eliminated as burn-in, and the remaining trees were used to determine the posterior probabilities. Maximum-likelihood (ML) analysis was conducted using RAxML v. 8.2.4 (Stamatakis 2014) on the CIPRES Science Gateway v. 3.3 (Miller *et al.* 2010), with the default GTR substitution matrix and 1000 rapid bootstraps. The final consensus trees were viewed utilising MEGA v. 7 (Kumar *et al.* 2016).

Pathogenicity trials

Three species, each including two strains, were selected for a pathogenicity test on *A. dichotomum* plants: Two of the species, *Phaeoacremonium parasiticum* (CMW 56378, 56380) and the new taxon (CMW 56381, 56376), were from the present study, and the third species, *Alanphillipsia aloe* (CMW 56344, 56346), previously isolated from dying *Euphorbia mauritanica* in 2020 (Marincowitz *et al.* 2023), was retrieved from the culture collection (CMW).

Toothpicks were submerged in 2 % malt broth and autoclaved twice at a two-day interval. They were then placed on the surface of half-strength potato dextrose agar (PDA: 19.5 g Difco Potato Dextrose Agar, 1 L water). Discs of the fungal isolates to serve as inoculum were placed alongside the toothpicks and allowed to grow and penetrate the wood tissue.

Well-established young *A. dichotomum* plants with approximately five vertical rows of leaves were maintained in a greenhouse at 25 °C for 3 mo before inoculation. Six isolates, three of each test species and a negative control, were inoculated on the stems of 15 plants. Colonised or sterile (control) toothpicks were inserted into the stems of the plants to reach approximately the mid-point of the stem tissue. The inoculated plants were watered regularly and monitored for the development of disease symptoms.

Eight weeks after inoculation, the treated plants were split in half to expose the entire length of the toothpick inoculum. The toothpicks were removed, and the areas of discoloured tissue were traced with a marker using a transparent plastic sheet. The trial was conducted only once, as it was difficult to obtain plants that are not commonly propagated commercially. The traces of the infected areas were scanned using a scanner (Epson Perfection V700 photo, China) and measured using Adobe Photoshop 2021 (Adobe

© 2025 Westerdijk Fungal Biodiversity Institute

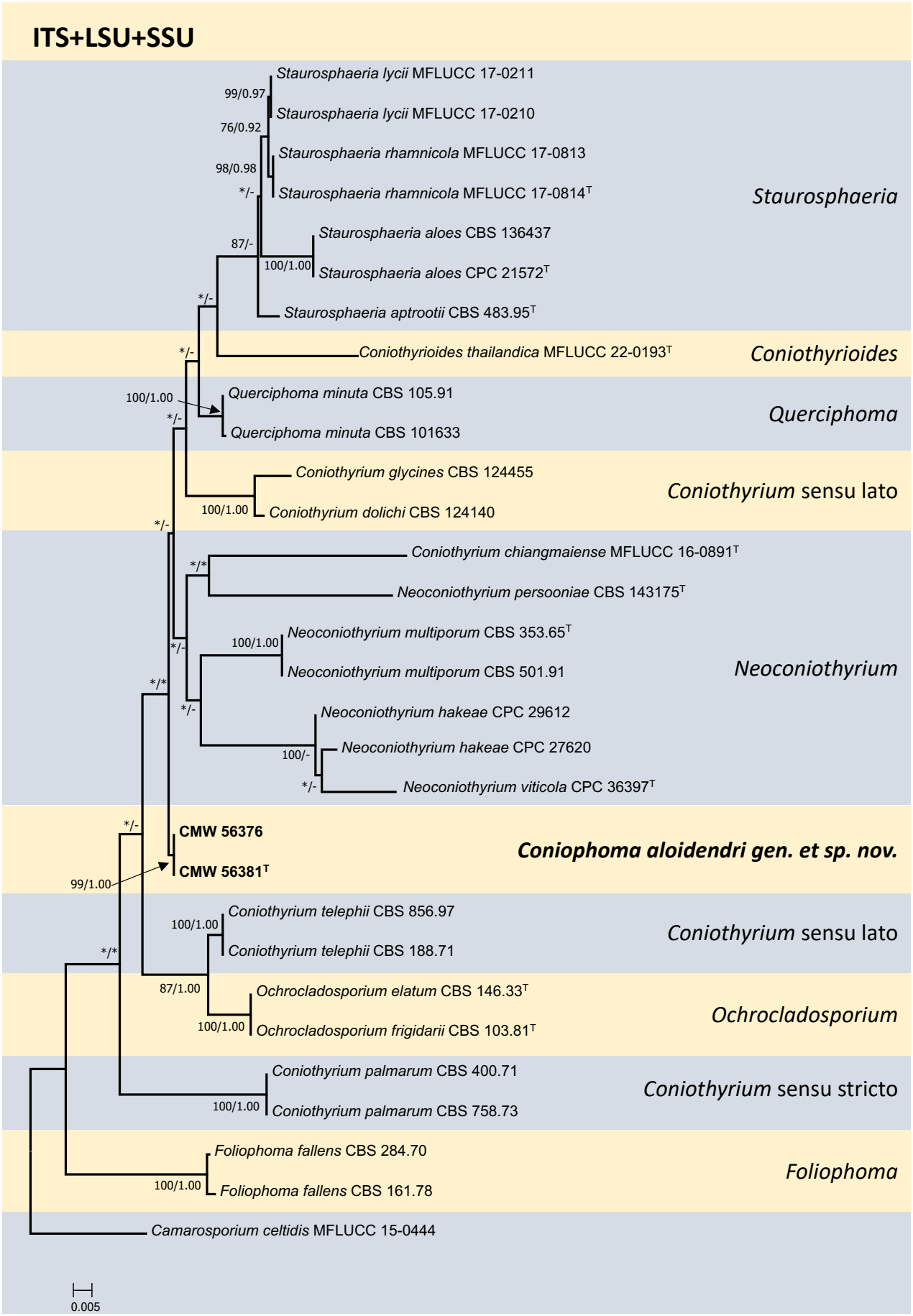

Fig. 3. Phylogenetic tree based on a maximum likelihood (ML) analysis of a combined DNA data set of ITS, LSU and SSU sequences for *Coniothyriaceae* species. The isolates sequenced in this study are presented in **boldface**. Bootstrap support values ≥ 70 % for ML analyses and posterior probabilities values ≥ 0.9 obtained from Bayesian inference (BI) are indicated at the nodes as ML/BI. Bootstrap support values < 70 % or probability values < 0.9 are marked with "*", and nodes lacking support values are marked with "–". Isolates representing ex-type material are marked with "T". *Camarosporium celtidis* (MFLUCC 15-0444*)* represents the outgroup.

© 2025 Westerdijk Fungal Biodiversity Institute

Systems Incorporated). The data for the diseased areas were analysed statistically using R software v. 4.2.1 (R Core Team 2020) by performing a One-way analysis of variance test and Games-Howell post hoc test for pairwise comparisons. To meet Koch's postulates, small pieces of tissue surrounding the toothpicks were then placed on 2 % MEA to allow for re-isolation of the inoculated fungi. A subset of these isolates was identified based on sequences of the ITS region.

RESULTS

Isolations from diseased tissues

Seventeen fungal strains were isolated from diseased stems and roots of dying quiver trees, with five originating from root samples and 12 from stems. The fungal strains were grown from the small pieces of tissue cut from the border of the lesions and healthy tissues. They were classified into five groups based on colony morphology. No visible fungal fruiting structures were found on the lesions of diseased plant parts.

Sequencing and phylogenetic analyses

Representative strains from each colony morph were sequenced and identified into five species based on BLAST results of ITS and/or *TUB2* sequence data (Supplementary data S1). The collection comprised two strains of *Paecilomyces formosus* (represented by CMW 56375; ITS PV405791, *TUB2* PV420379) from stems, five strains of *Phaeoacremonium parasiticum* (CMW 56380, 56382, 56378, 56384; ITS PV405792, *TUB2* PV420380) from roots and stems, two strains of *Pm. luteum* (CMW 56379; ITS PV405793, *TUB2* PV420381) from stems, and four strains of *Xylogone sphaerospora* (CMW 56383, 56385; ITS PV405794) from roots.

Two strains, CMW 56376 and CMW 56381, represented the fifth colony morph. They included two isolates clustered within the *Coniothyriaceae*, apart from other taxa, based on initial BLAST searches of the ITS sequences. The ML and BI analyses were performed based on the concatenated sequences of three loci (ITS, LSU and SSU). This concatenated dataset consisted of 29 ingroup taxa and 2362 characters, including alignment gaps. *Camarosporium celtidis* (MFLUCC 15-0444) was used as the outgroup taxon. Concatenated sequence alignments were deposited in Figshare (doi: 10.6084/m9.figshare.28532144). The TIM2+I+G models were selected for the ITS and LSU region, respectively, and TPM3uf+I for the SSU region. The ML and BI analyses generated phylogenetic trees with concordant topologies, revealing similar phylogenetic relationships among taxa. The ML tree with bootstrap support values for the ML and the posterior probabilities obtained from the BI is presented in Fig. 3. The two strains clustering in *Coniothyriaceae* represented a new lineage (ML/BI = 99/1.00), introduced here as a novel genus in *Coniothyriaceae*.

Taxonomy

Coniophoma N.Q. Pham, Marinc. & M.J. Wingf. ***gen. nov.*** MB 857753.

Etymology: The name 'Conio' is derived from its taxonomic affinity to the *Coniothyriaceae* and '*phoma*' from its morphological similarity to *Phoma*.

Conidiomata pycnidial, sub-globose to globose, brown. *Conidiophores* blastic, lining along peridial surface, simple, reduced to conidiogenous cells. *Conidiogenous cells* ampulliform. *Conidia* hyaline, oval to oblong, aseptate. *Sexual morph* not observed.

Type species: *Coniophoma aloidendri* N.Q. Pham, Marinc. & M.J. Wingf.

Coniophoma aloidendri N.Q. Pham, Marinc. & M.J. Wingf., ***sp. nov.*** MB 857754. Fig. 4.

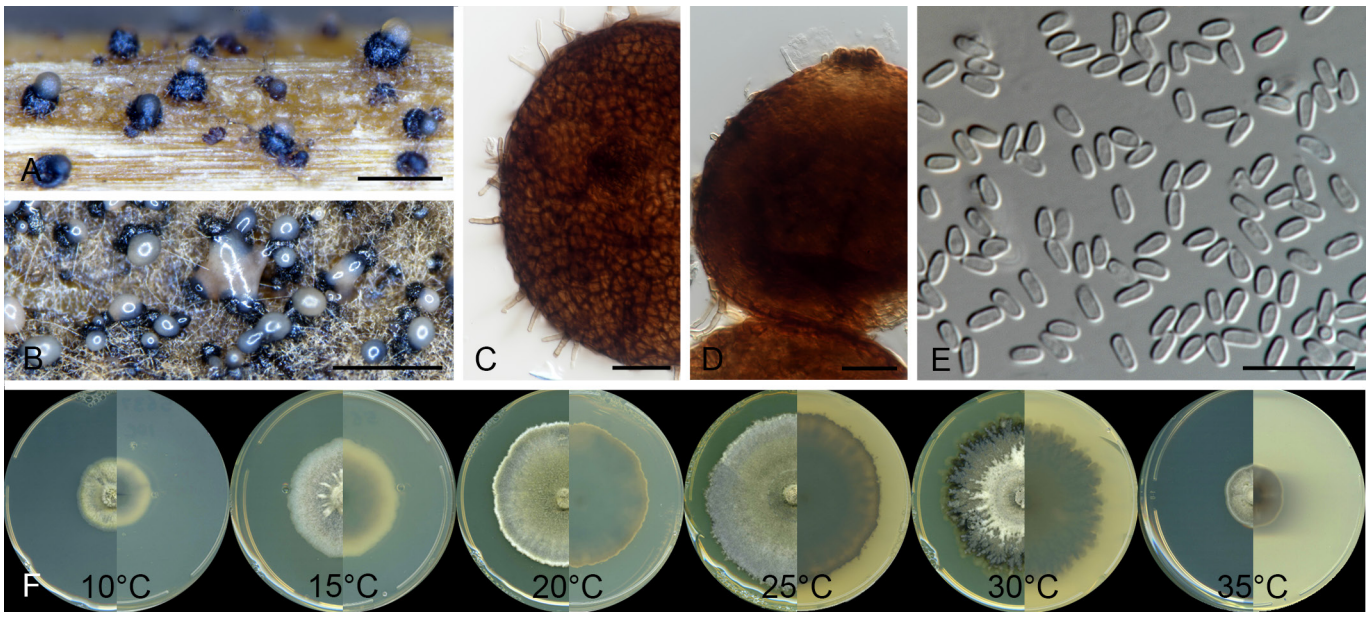

Fig. 4. Micrograph of *Coniophoma aloidendri gen. et sp. nov.* (CMW-IA 48, CMW 56381). **A, B.** Pycnidia formed on a toothpick (A) and WA (B). **C.** Pycnidium covered with hyphae. **D.** Pycnidium with prominent ostiole. **E.** Conidia. **F.** Cultures on 2 % MEA kept in the dark for 29 d (left: above, right: reverse). Scale bars: A = 250 µm; B = 500 µm; C, D = 25 µm; E = 10 µm.

© 2025 Westerdijk Fungal Biodiversity Institute

Etymology: The name refers to *Aloidendron*, the host on which it occurs.

Diagnosis: Closely related to *Neoconiothyrium* but differs in having aseptate, hyaline conidia.

Typus: **South Africa**, Northern Cape Province, Nieuwoudtville, isolated from stem tissue of dying *Aloidendron dichotomum*, Aug. 2020. *M.J. Wingfield* [**holotype** PRU(M) 4619, dried culture; ex-holotype culture CMW-IA 48 = CMW 56381]. GenBank: ITS = PV405790; LSU = PV405796; SSU = PV405798.

Conidiomata formed on toothpicks or WA, pycnidial, sub-globose to globose, papillate, 69–183 × 66–186 (132.5 ± 30.44 × 121.6 ± 30.24) µm, pycnidial walls pseudoparenchymatous. *Conidiophores* lining along inside peridial walls, reduced to conidiogenous cells. *Conidiogenous cells* hyaline, ampulliform, 4–5 × 2.5–3.5 µm. *Conidia* hyaline, oval to oblong, mostly straight, aseptate, at times tapering to base and upper region swollen, exudating conidial mass creamy, 3–4 × 1–2 (3.3 ± 0.32 × 1.5 ± 0.15) µm.

Culture characteristics: Optimum growth temperature on 2 % MEA in the dark at 25 °C showing 3.1 mm/d, followed by 30 °C (2.4 mm/d), 20 °C (2.3 mm/d), 15 °C (1.41 mm/d) and 10 °C and 35 °C (0.6 mm/d). Cultures (29-d-old) sterile: *shape* circular (10–35 °C); *margins* entire (10–20, 35 °C), erose (20–30 °C); *elevation* flat (10–35 °C); *texture* velvety (10–35 °C); *colour* above yellowish white, yellowish grey with medium grey patches (10 °C), yellowish grey background with dark greyish reddish brown radial patches (15 °C), light yellow background with olive grey centre and purplish grey patches (20 °C), moderate yellow, brownish grey or olive grey in concentric areas (25 °C), dark reddish brown background with moderate yellow centre and pale yellow edges (30 °C), moderate yellow to olive grey or dark reddish brown (35 °C); *density* medium dense (10–30 °C), dense (35 °C); *pigmentation* on media absent.

Additional materials examined: **South Africa**, Northern Cape Province, Nieuwoudtville, isolated from stem tissue of dying *Aloidendron dichotomum,* Aug. 2020, *M.J. Wingfield*, fungarium PRU(M) 4617; culture CMW-IA 47 = CMW 56376. GenBank: ITS = PV405789; LSU = PV405795; SSU = PV405797.; ibid., fungarium PRU(M) 4618; culture CMW-IA 2602 = CMW 56377.

Notes: The strains of *Coniophoma aloidendri* formed a distinct lineage within a clade containing members of the *Coniothyriaceae*, i.e. coelomycete genera such as *Coniothyrium* s. str., *Coniothyrium* s. lat., *Coniothyrioides*, *Foliophoma*, *Neoconiothyrium*, *Querciphoma*, *Staurosphaeria*, and a hyphomycete genus *Ochrocladosporium.* Other than *Staurosphaeria*, only asexual morphs are known for these genera. High morphological variability in the family makes morphological delineation of genera difficult. However, *Coniophoma* can still be distinguished from other genera by its colourless aseptate conidia on simple blastic conidiogenous cells. In contrast, *Coniothyrioides* produces ellipsoidal to ovoid conidia that become pale to dark brown at maturity (Wijesinghe *et al.* 2023), *Coniothyrium* s. str. has brown conidia, *Neoconiothyrium* hyaline to medium brown conidia and ellipsoidal to sub-clavate conidia (Crous *et al.* 2017). *Querciphoma* has broadly ellipsoid conidia turning into brown with maturity (Crous & Kirk 2017), *Ochrocladosporium* has pale brown conidia and ramoconidia and is hyphomycetous (Crous *et al.* 2007), *Staurosphaeria* has red-brown macroconidia and hyaline globose to ellipsoidal microconidia (Wanasinghe *et al.* 2017), and *Foliophoma* has hyaline, aseptate, broadly ellipsoidal conidia produced in eustromatic conidiomata (Crous & Groenewald 2017). The members of *Coniothyrium* s. lat. such as *C. glycines*, *C. dolichi* and *C. telephii* are known to produce dark pycnidial setae (De Gruyter *et al.* 2013).

Pathogenicity

Eight weeks after inoculation, the *A. dichotomum* plants inoculated with six fungal strains of three fungi, *Ala. aloes*, *C. aloidendri* and *Pm. parasiticum*, showed distinct lesions on their stems. All the infected stems developed sepia to dark brown lesions around the inoculation points. Stems inoculated with clean toothpicks were used as controls and produced no lesions. Mean lesion areas caused by all six

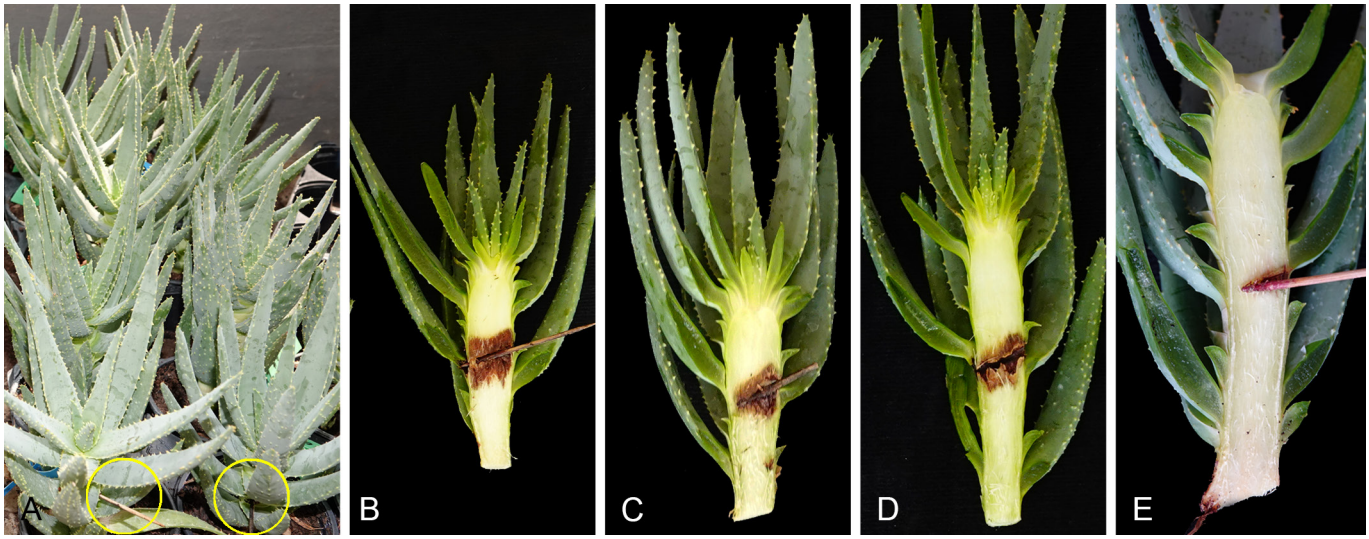

Fig. 5. Pathogenicity test on *Aloidendron dicotomum*. **A.** Seedlings inoculated with toothpick cultures (yellow circles). **B–D.** Lesions developed in 8-wk-old inoculated plants. **B.** *Phaeoacremonium parasiticum* (CMW 56378). **C.** *Coniophoma aloidendri* (CMW-IA 48, CMW 56381). **D.** *Alanphillipsia aloes* (CMW 56344). **E.** Control.

© 2025 Westerdijk Fungal Biodiversity Institute

strains were significantly larger than the controls ($p < 0.05$) (Figs 5, 6). Two strains of *Pm. parasiticum* produced lesions significantly larger than those associated with *Ala. aloes* ($p < 0.05$) and *C. aloidendri* (Fig. 6). The inoculated fungi were easily re-isolated from the resulting lesions but never from the controls.

DISCUSSION

Five species of fungi were isolated from the edges of necrotic lesions of the stems and roots of dying *A. dichotomum* trees in this study. Among these, four species, *Paecilomyces formosus*, *Phaeoacremonium parasiticum*, *Pm. luteum* and *Xylogone sphaerospora* are reported from this tree for the first time. A fifth fungus represented a new species in a previously undescribed genus, described here as *Coniophoma aloidendri*. This study has increased the number of fungi known from *A. dichotomum* to fourteen. Nine previously reported species from these trees include *Alanphillipsia aloes* (*Botryosphaeriales*, Crous *et al.* 2013), *Dothiora aloidendri* (*Dothiorales*, Crous *et al.* 2020), *Hantamomyces aloidendri* (*Hypocreales*, Crous *et al.* 2020), *Lapidomyces aloidendricola* (*Capnodiales*, Crous *et al.* 2021), *Fusarium pharetrum* (*Hypocreales*, Lombard *et al.* 2019), *Neophaeococcomyces aloes* (*Chaetothyriales*, Crous *et al.* 2013, 2015), *Phoma aloes* (*Pleosporales*, Crous *et al.* 2013), *Staurosphaeria aloes* (*Pleosporales*, Crous *et al.* 2013), and *Neoscytalidium dimidiatum* (*Botryosphaeriales*, Crous *et al.* 2006).

Paecilomyces formosus was isolated less frequently than other species in this study and consequently excluded from the pathogenicity test. This is a common fungus known from various environmental samples, including soil, indoor air, and house dust (Samson 1974, Samson *et al.* 2004). It is also known to infect patients with underlying conditions (Sprute *et al.* 2021) and to cause diseases in woody plants, as well as post-harvest rot (Biango-Daniels & Hodge 2018). More recently, *P. formosus* has been reported in Iran, causing die-back of pistachio (*Pistacia vera*) in orchards (Heidarian *et al.* 2018, Sabernasab *et al.* 2019) and as a common endophyte on pistachio trees (Kavehnia *et al.* 2023). *Paecilomyces formosus* was initially considered a member of a species complex comprising three cryptic species (Samson *et al.* 2009, Heidarian *et al.* 2018), which has recently been resolved using whole-genome sequences (Urquhart & Idnurm 2023). The present study adds an unusual habitat for this fungus in South Africa. If it is isolated more consistently from *A. dichotomum* in the future, it would be useful to consider its pathogenicity on these trees.

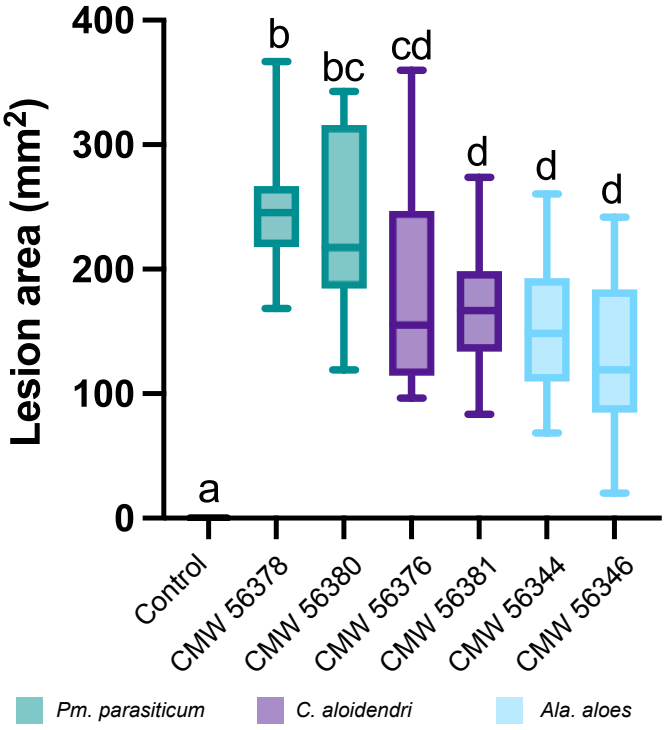

Fig. 6. Boxplots indicating lesion area resulting from the pathogenicity test of *Aloidendron dichotomum* inoculated with six different isolates and the control. Vertical bars represent the standard error of the means. Bars with different letters indicate statistical significance at $P \leq 0.05$.

Two *Phaeoacremonium* species, *Pm. parasiticum* and *Pm. luteum* were isolated in this study. *Phaeoacremonium parasiticum* was isolated from both stem and root samples more frequently than *Pm. luteum*, which was isolated only from stem tissues. *Phaeoacremonium* species occur on diverse substrates, including human tissue, woody plants, soil, and bark beetles (Crous *et al.* 2006, Gramaje *et al.* 2014). Several *Phaeoacremonium* species contribute to the notorious Petri and esca diseases of grapevines (Crous *et al.* 1996, Mostert *et al.* 2006) or cause subcutaneous phaeohyphomycosis in immunocompromised individuals (Mostert *et al.* 2005). Sixteen *Phaeoacremonium* species have been recorded from woody plants in South Africa, the best-known of which is *Pm. parasiticum* that has been isolated from necrotic wood tissue of apricot trees (*Prunus armeniaca*) and grapevines (*Vitis vinifera*) (Mostert *et al.* 2006, Damm *et al.* 2008, Cloete *et al.* 2011). *Phaeoacremonium parasiticum* strains isolated in this study gave rise to larger lesions, and it could be considered a possible candidate contributing to the decline of these trees.

Phaeoacremonium luteum was first reported from pruning wounds of tropical sandalwood (*Santalum album*) in Australia and was amongst five other species of the same genus isolated from wounds (Gramaje *et al.* 2014). Its name was derived from the yellow pigmentation on the media, which was absent in our strains. This is the first report of the fungus from South Africa.

Xylogone sphaerospora was frequently isolated in this study, occurring only on root tissues. The genus *Xylogone* belongs to the *Leotiomycetes* and is one of only two species in the genus. *Xylogone sphaerospora*, the type species, was initially reported from stored pulpwood chips in Sweden (von Arx & Nilsson 1969). The second species, *X. ganodermophthora,* was described from the basidiomycete fungus *Ganoderma lucidum* cultivated in Korea, which causes destructive yellow rot on the basidiocarps and associated wood logs (Kang *et al.* 2010). This is the first report of the fungus from the Southern Hemisphere.

Alanphillipsia aloes was first isolated from *A. dichotomum* in 2012 (Crous *et al.* 2013) and was recently re-isolated from *Euphorbia mauritanica* (*Euphorbiaceae*) in 2020 (Marincowitz *et al.* 2023). Both isolations were from necrotic lesions on the host plants. The genus was established to accommodate *Ala. aloes* (Crous *et al.* 2013), and five species have been added to the genus from *Aloidendron* and *Euphorbia* spp. in South Africa since its introduction (Crous

© 2025 Westerdijk Fungal Biodiversity Institute

et al. 2013, 2014). Botryosphaeriaceous fungi are known to exist asymptomatically in host plants and cause diseases in the presence of environmental or biological stress (Slippers & Wingfield 2007, Mehl *et al.* 2013). The fungus was included in this study due to its previous occurrence on *A. dichotomum* and its association with disease in these and other plants. Interestingly, this was the least pathogenic of the three fungal species tested in this study. Its role in causing disease on *A. dichotomum* appears to be minimal, but under stress conditions, it could contribute to decline, consistent with its known opportunistic biology.

Quiver trees such as *A. dichotomum* have a long lifespan and occupy large habitats, extending over approximately 200,000 km^2 in the arid western regions of the Northern Cape in South Africa and south-central Namibia (Smith & Van Wyk 2008). Our samples were collected from a limited number of dying trees at one location. The results must be viewed as preliminary and are insufficient to attribute the death of *A. dichotomum* to the isolated fungi. However, they provide some insight into the role that fungi may play in the decline of these trees and suggest that a single plant pathogen is unlikely to be the sole cause. Based on this preliminary evidence and the earlier survey by Roux *et al.* (2009), we support the view raised in various previous studies (Foden *et al.* 2007, Guo *et al.* 2011, Jack *et al.* 2016, Van der Merwe & Geldenhuys 2017) that abiotic stress is likely an important factor to consider in the decline of these trees. Nonetheless, further studies on fungi and their potential role in contributing to this problem would be worthwhile.

ACKNOWLEDGEMENTS

We acknowledge funding from the DSI/NRF Chair in Fungal Genomics held by BDW and the Harry Oppenheimer Fellowship Award of the Oppenheimer Memorial Trust to MJW. We are also grateful to Dr Jason Samson for assistance in locating *A. dichotomum* plants used in the pathogenicity trials and Dr Konstanze Bensch at MycoBank for help naming the new taxon.

Conflict of interest: The authors declare that there is no conflict of interest.

REFERENCES

Biango-Daniels MN, Hodge KT (2018). Paecilomyces rot: A new apple disease. *Plant Disease* **102**: 1581–1587. https://doi.org/10.1094/PDIS-12-17-1896-RE

Cloete M, Fourie PH, Damm U, *et al.* (2011). Fungi associated with die-back symptoms of apple and pear trees, a possible inoculum source of grapevine trunk disease pathogens. *Phytopathologia Mediterranea* **50**: S176–S190. https://doi.org/10.2307/26458720

Crous PW, Braun U, Schubert K, *et al.* (2007). Delimiting *Cladosporium* from morphologically similar genera. *Studies in Mycology* **58**: 33–56. https://doi.org/10.3114/sim.2007.58.02

Crous PW, Cowan DA, Maggs-Kölling G, *et al.* (2020). Fungal Planet description sheets: 1112–1181. *Persoonia* **45**: 251–409. https://doi.org/10.3767/persoonia.2020.45.10

Crous PW, Cowan DA, Maggs-Kölling G, *et al.* (2021). Fungal Planet description sheets: 1182–1283. *Persoonia* **46**: 313–528. https://doi.org/10.3767/persoonia.2021.46.11

Crous PW, Gams W, Wingfield MJ, *et al.* (1996). *Phaeoacrremonium gen. nov*. associated with wilt and decline diseases of woody hosts and human infections. *Mycologia* **88**: 786–796. https://doi.org/10.1080/00275514.1996.12026716

Crous PW, Groenewald JZ (2017). The Genera of Fungi – G 4: *Camarosporium* and *Dothiora*. *IMA Fungus* **8**: 131–152. https://doi.org/10.5598/imafungus.2017.08.01.10

Crous PW, Kirk PW (2017). Nomenclatural novelties. *Index Fungorum* **336**: 1.

Crous PW, Slippers B, Wingfield MJ, *et al.* (2006). Phylogenetic lineages in the *Botryosphaeriaceae*. *Studies in Mycology* **55**: 235–254. https://doi.org/10.3114/sim.55.1.235

Crous PW, Wingfield MJ, Burgess TI, *et al.* (2016). Fungal Planet description sheets: 469–557. *Persoonia* **37**: 218–403. https://doi.org/10.3767/003158516X694499

Crous PW, Wingfield MJ, Burgess TI, *et al.* (2017). Fungal Planet description sheets: 625–715. *Persoonia* **39**: 270–467. https://doi.org/10.3767/persoonia.2017.39.11

Crous PW, Wingfield MJ, Guarro J, *et al.* (2013) Fungal Planet description sheets: 154–213. *Persoonia* **31**: 188–296. https://doi.org/10.3767/003158513X675925

Crous PW, Wingfield MJ, Le Roux JJ, *et al.* (2015). Fungal Planet description sheets: 371–399. *Persoonia* **35**: 264–327. https://doi.org/10.3767/003158515X690269

Crous PW, Wingfield MJ, Lombard L, *et al.* (2019). Fungal Planet description sheets: 951–1041. *Persoonia* **43**: 223–425. https://doi.org/10.3767/persoonia.2019.43.06

Crous PW, Wingfield MJ, Schumacher RK, *et al.* (2014) Fungal Planet description sheets: 281–319. *Persoonia* **33**: 212–289. https://doi.org/10.3767/003158514X685680

Damm U, Mostert L, Crous PW, *et al.* (2008). Novel Phaeoacremonium species associated with necrotic wood of Prunus trees. *Persoonia* **20**: 87–102. https://doi.org/10.3767/003158508X324227

De Gruyter J, Aveskamp MM, Woudenberg JH, *et al.* (2009). Molecular phylogeny of *Phoma* and allied anamorph genera: towards a reclassification of the *Phoma* complex. *Mycological Research* **113**:508–519. https://doi.org/10.1016/j.mycres.2009.01.002

De Gruyter J, Woudenberg JH, Aveskamp MM, *et al.* (2013). Redisposition of Phoma-like anamorphs in *Pleosporales*. *Studies in Mycology* **75**: 1–36. https://doi.org/10.3114/sim0004

Foden WB (2002). *A demographic study of Aloe dichotoma in the succulent karoo: are the effects of climate change already apparent?* M.Sc. thesis, University of Cape Town, South Africa.

Foden WB, Midgley GF, Hughes G, *et al.* (2007). A changing climate is eroding the geographical range of the Namib Desert tree *Aloe* through population declines and dispersal lags. *Diversity and Distributions* **13**: 645–653. https://doi.org/10.1111/j.1472-4642.2007.00391.x

Foden W, Raimondo D, Eastment C, *et al.* (2022). *Aloidendron dichotomum*. The IUCN Red List of Threatened Species 2022: e.T140661836A140666503.

Gardes M, Bruns TD (1993). ITS primers with enhanced specificity for basidiomycetes–application to the identification of mycorrhizae and rusts. *Molecular Ecology* **2**: 113–118. https://doi.org/10.1111/j.1365-294X.1993.tb00005.x

Glass NL, Donaldson GC (1995). Development of primer sets designed for use with the PCR to amplify conserved genes from filamentous ascomycetes. *Applied and Environmental Microbiology* **61**: 1323–1330. https://doi.org/10.1128/

© 2025 Westerdijk Fungal Biodiversity Institute

aem.61.4.1323-1330.1995

Grace OM, Klopper R, Smith GF, *et al.* (2013). A revised generic classification for *Aloe* (*Xanthorrhoeaceae* subfam. *Asphodeloideae*). *Phytotaxa* **76**: 7–14. https://doi.org/10.11646/phytotaxa.76.1.2

Gramaje D, León M, Pérez-Sierra A, *et al.* (2014). New *Phaeocremonium* species isolated from sandalwood trees in Western Australia. *IMA Fungus* **5**: 67–77. https://doi.org/10.5598/imafungus.2014.05.01.08

Guo D, Guo R, Cui Y, *et al.* (2011). Climate change impact on quiver trees in arid Namibia and South Africa. In: *Climate Change – Geophysical Foundations and Ecological Effects* (Blanco J, Kheradmand H, eds), Intech Open. https://doi.org/10.5772/23999

Heidarian R, Fotouhifar KB, Debets AJM, *et al.* (2018). Phylogeny of *Paecilomyces*, the causal agent of pistachio and some other trees dieback disease in Iran. *PLoS ONE* **13**: e0200794. https://doi.org/10.1371/journal.pone.0200794

Jack SL, Hoffman MT, Rohde RF, *et al.* (2016). Climate change sentinel or false prophet? The case of *Aloe dichotoma*. *Diversity and Distribution* **22**: 745–757. https://doi.org/10.1111/ddi.12438

Kaleme PK (2003) *Regional differences in the long-term population dynamics of a succulent tree Aloe dichotoma in the semi-arid karoo, as revealed by repeat photography*. M.Sc. Thesis, University of Cape Town, Cape Town, South Africa.

Kang H-J, Sigler L, Lee J, *et al.* (2010). *Xylogone ganodermophthora sp. nov.*, an ascomycetous pathogen causing yellow rot on cultivated mushroom *Ganoderma lucidum* in Korea. *Mycologia* **102**: 1167–1184. https://doi.org/10.3852/09-304

Katoh K, Standley DM (2013). MAFFT multiple sequence alignment software version 7: improvements in performance and usability. *Molecular Biology and Evolution* **30**: 772–780. DOI: https://doi.org/10.1093/molbev/mst010

Kavehnia A, Samsampour D, Seyahooei MA (2023). Isolation and morphological and molecular identification of important endophyte fungi of *Pistacia mutica* in Hormozgan province and their effect on increasing salt stress tolerance of California Wonder 3 pepper seedlings. *Journal of Plant Production Research* **39**: 41–64.

Kumar S, Stecher G, Tamura K (2016). MEGA7: Molecular Evolutionary Genetics Analysis version 7.0 for bigger datasets. *Molecular Biology and Evolution* **33**: 1870–1874. https://doi.org/10.1093/molbev/msw054

Lombard L, Sandoval-Denis M, Lamprecht SC, *et al.* (2019). Epitypification of *Fusarium oxysporum* - clearing the taxonomic chaos. *Persoonia* **43**: 1–47. https://doi.org/10.3767/persoonia.2019.43.01

Marincowitz S, Pham NQ, Wingfield BD, *et al.* (2023). Microfungi associated with dying *Euphorbia mauritanica* in South Africa and their relative pathogenicity. *Fungal Systematics and Evolution* **12**: 59–71. https://doi.org/10.3114/fuse.2023.12.04

Midgley JJ, Cowling RM, Hendricks H, *et al.* (1997). Population ecology of tree succulents (*Aloe* and *Pachypodium*) in the arid western Cape: decline of keystone species. *Biodiversity and Conservation* **6**: 869–876.

Mehl JW, Slippers B, Roux J, *et al.* (2013). Cankers and other diseases caused by the *Botryosphaeriaceae*. In: *Infectious Forest Diseases* (Gonthier P, Nicolotti G, eds). CAB International. Oxon, UK: 298–317. https://doi.org/10.1079/9781780640402.0298

Miller MA, Pfeiffer W, Schwartz T (2010). Creating the CIPRES Science Gateway for inference of large phylogenetic trees. In: *Proceedings of the Gateway Computing Environments Workshop (GCE),* 14 Nov. 2010. New Orleans, Louisiana: 1–8. https://doi.org/10.1109/GCE.2010.5676129

Mostert L, Groenewald JZ, Summerbell RC, *et al.* (2006). Taxonomy and pathology of *Togninia* (*Diaporthales*) and its *Phaeoacremoinum* anamorphs. *Studies in Mycology* **54**: 1–113. https://doi.org/10.3114/sim.54.1.1

Mostert L, Groenewald, JZ, Summerbell RC, *et al.* (2005). Species of *Phaeoacremonium* associated with infections in humans and environmental reservoirs in infected woody plants. *Journal of Clinical Microbiology* **43**: 1752–1767. https://doi.org/10.1128/jcm.43.4.1752-1767.2005

Posada D (2008). jModelTest: phylogenetic model averaging. *Molecular Biology and Evolution* **25**: 1253–1256. DOI: https://doi.org/10.1093/molbev/msn083

R Core Team (2020). *R: A language and environment for statistical computing*. R Foundation for Statistical Computing, Vienna, Austria. https://www.R-project.org/.

Rehner SA, Samuels GJ (1994). Taxonomy and phylogeny of *Gliocladium* analysed from nuclear large subunit ribosomal DNA sequences. *Mycological Research* **98**: 625–634. https://doi.org/10.1016/S0953-7562(09)80409-7

Ronquist F, Teslenko M, Van der Mark P, *et al.* (2012). MrBayes 3.2: efficient Bayesian phylogenetic inference and model choice across a large model space. *Systematic Biology* **61**: 539–542. https://doi.org/10.1093/sysbio/sys029

Roux J, Van Rooyen G, Uys N (2009). Results of a disease investigation of *Aloe dichotomum* in Goegap Nature Reserve, South Africa. *South African Journal of Botany* **75**: 418–419. http://dx.doi.org/10.1016/j.sajb.2009.02.100 (abstract).

Sabernasab M, Jamali S, Marefat A, *et al.* (2019). Molecular and pathogenic characteristics of *Paecilomyces formosus*, a new causal agent of oak tree dieback in Iran. *Forest Science* **65**: 743–750. https://doi.org/10.1093/forsci/fxz045

Stamatakis A (2014). RAxML version 8: a tool for phylogenetic analysis and post-analysis of large phylogenies. *Bioinformatics* **30**: 1312–1313. https://doi.org/10.1093/bioinformatics/btu033

Slippers B, Wingfield MJ. (2007). *Botryosphaeriaceae* as endophytes and latent pathogens of woody plants: diversity, ecology and impact. *Fungal Biology Reviews* **21**: 90–106. https://doi.org/10.1016/j.fbr.2007.06.002

Samson RA (1974). *Paecilomyces* and some allied hyphomycetes. *Studies in Mycology* **6**: 1–119.

Samson RA, Hoekstra ES, Frisvad JC (2004). *Introduction to food and airborne fungi*, 7th ed. Centraalbureau voor Schimmelcultures, Utrecht, Netherlands.

Samson RA, Houbraken J, Varga J, *et al.* (2009). Polyphasic taxonomy of the heat resistant ascomycete genus *Byssochlamys* and its *Paecilomyces* anamorphs. *Persoonia* **22**: 14–27. https://doi.org/10.3767/003158509X418925

Smith GF, Van Wyk B (2008). *Aloes in Southern Africa*. Struik Nature, Cape Town.

Smith GF, Klopper RR, Grace OM (2019). *Aloidendron* (*Asphodelaceae* subfam. *Alooideae*) consists of six species, not seven: *Aloe sabaea* is a true aloe. *Phytotaxa* **416**: 88–90. https://doi.org/10.11646/phytotaxa.416.1.11

Sprute R, Salmanton-García J, Sal E, *et al.* (2021). Characterization and outcome of invasive infections due to *Paecilomyces variotii*: Analysis of patients from the FungiScope (R) registry and literature reports. *Journal of Antimicrobial Chemotherapy* **76**: 765–774. https://doi.org/10.1093/jac/dkaa481

Thambugala KM, Wanasinghe DN, Phillips AJL, *et al.* (2017).

© 2025 Westerdijk Fungal Biodiversity Institute

Mycosphere notes 1–50: grass (*Poaceae*) inhabiting *Dothideomycetes*. *Mycosphere* **8**: 697–796. https://doi.org/10.5943/mycosphere/8/4/13

Urquhart AS, Idnurm A (2023). A polyphasic approach including whole genome sequencing reveals *Paecilomyces paravariotti* sp. nov. as a cryptic sister species to *P. varriotii*. *Journal of Fungi* **9**: 285. https://doi.org/10.3390/jof9030285

Vilgalys R, Hester M (1990). Rapid genetic identification and mapping of enzymatically amplified ribosomal DNA from several *Cryptococcus* species. *Journal of Bacteriology* **172**: 4238–4246. https://doi.org/10.1128/jb.172.8.4238-4246.1990

Van der Merwe H, Geldenhuys C (2017). Proposed long-term monitoring protocol and applications for *Aloidendron dichotomum* populations. *South African Journal of Botany* **109**: 253–262. https://doi.org/10.1016/j.sajb.2017.01.008

Von Arx JA, Nilsson T (1969). *Xylogone sphaerospora*, a new ascomycete from stored pulpwood chips. *Svensk Botanisk Tidskrift* **63**: 345–349.

Wanasinghe DN, Hyde KD, Jeewon R, *et al.* (2017). Phylogenetic revision of *Camarosporium* (*Pleosporinae*, *Dothideomycetes*) and allied genera. *Studies in Mycology* **87**: 207–256. https://doi.org/10.1016/j.simyco.2017.08.001

White TJ, Bruns T, Lee S, *et al.* (1990). Amplification and direct sequencing of fungal ribosomal RNA genes for phylogenetics. In: *PCR protocols: a guide to methods and applications* (Innis MA, Gelfand DH, Sninsky JJ, *et al.*, eds), Academic Press, San Diego, California, USA: 315–322.

Wijesinghe SN, Calabon MA, Xiao Y, *et al.* (2023). A novel coniothyrium-like genus in *Coniothyriaceae* (*Pleosporales*) from salt marsh ecosystems in Thailand. *Studies in Fungi* **8**: 1–10. https://doi.org/10.48130/SIF-2023-0006

Supplementary Material: http://fuse-journal.org/

Data S1. Blast results of the different species treated in this study.

Table S1. Meta data and GenBank accession numbers of the strains used in the phylogenetic analyses.

© 2025 Westerdijk Fungal Biodiversity Institute

FUSE

Fungal Systematics and Evolution

VOLUME 16
DECEMBER 2025
PAGES 81–92

doi.org/10.3114/fuse.2025.16.6

Diversity of soil-borne *Gliocladiopsis* from Indonesia, Malaysia and Vietnam

N.Q. Pham [1], S. Marincowitz[1*], P.W. Crous[1,2], M.J. Wingfield[1]

[1]Department of Biochemistry, Genetics and Microbiology, Forestry and Agricultural Biotechnology Institute (FABI), University of Pretoria, Pretoria, South Africa
[2]Westerdijk Fungal Biodiversity Institute, Uppsalalaan 8, 3584 CT Utrecht, The Netherlands

[*]Corresponding author: seonju.marincowitz@fabi.up.ac.za

Key words:
fungal diversity
new taxon
Southeast Asia

Abstract: *Gliocladiopsis* comprises a diverse group of soil-borne fungi predominantly found in tropical and subtropical regions of the world. This study investigated *Gliocladiopsis* strains collected from soil samples across three Southeast Asian countries, namely, Indonesia, Malaysia and Vietnam. Morphological characteristics and multi-gene phylogenetic analyses based on four loci (ITS, *TEF1, TUB2*, and *HIS3*) were used to identify the strains. Eleven *Gliocladiopsis* spp., including a novel taxon, *Gliocladiopsis vietnamensis sp. nov*., were identified. The six species, *G. curvata*, *G. forsbergii*, *G. guangdongensis*, *G. irregularis*, *G. whileyi* and *G. wuhanensis*, are newly reported in Vietnam, *G. curvata* in Malaysia, and *G. mexicana* in Indonesia. This study has significantly expanded the known diversity of *Gliocladiopsis* in Southeast Asia. The results also suggest that Southeast Asia is a biodiversity hotspot for this genus, highlighting the importance of further research to explore fungal diversity in understudied tropical and subtropical ecosystems.

Citation: Pham NQ, Marincowitz S, Crous PW, Wingfield MJ (2025). Diversity of soil-borne *Gliocladiopsis* from Indonesia, Malaysia and Vietnam. *Fungal Systematics and Evolution* **16**: 81–92. doi: 10.3114/fuse.2025.16.6.
Received: 26 February 2025; **Accepted:** 5 March 2025; **Effectively published online:** 21 May 2025
Corresponding editor: M. Arzanlou

INTRODUCTION

The genus *Gliocladiopsis* was established by Saksena (1954) based on *G. sagariensis* from a soil sample from Ghatera forests in Sagar, India. The name was chosen to reflect its similarity to *Gliocladium* in having slimy spore droplets. Saksena (1954) also noted a resemblance of the genus to *Cylindrocladium* (*Cm.*) and *Penicillium* in having conidiophores terminating in penicillate branches and, in the case of *Cylindrocladium*, cylindrical conidia. *Gliocladiopsis* spp. are characterised by having penicillate (rarely subverticillate) conidiophores, (0–)1-septate cylindrical conidia resembling the conidial morph of *Calonectria* (*Cylindrocladium*) but without stipe extensions terminating in terminal vesicles, and pale yellow spore droplets at the tips of the conidiogenous apparatuses (Crous & Wingfield 1993, Crous 2002, Lombard & Crous 2012). In some species, globose and brown chlamydospore chains have been observed in culture (Crous 2002).

Gliocladiopsis has undergone a number of taxonomic treatments since its first description. Saksena (1954) initially assigned *Gliocladiopsis* to the *Moniliaceae*, an obsolete family accommodating numerous unrelated hyphomycetes. Later, Agnihothrudu (1959), after studying the ex-types of *G. sagariensis* and *Cylindrocarpon* (*Cp.*) *tenue*, reduced the monotypic *Gliocladiopsis* to synonymy with *Cylindrocarpon*, and treated *G. sagariensis* as a heterotypic synonym of *Cp. tenue* (Bugnicourt 1939). Independently, Barron (1968) considered *Gliocladiopsis* as a synonym of *Cylindrocladium.* Crous & Wingfield (1993) later resurrected *Gliocladiopsis* as a separate genus based on *G. sagariensis* as a type species and established *G. tenuis* for *Cp. tenue.* The placement of *Gliocladiopsis* within the *Nectriaceae* was confirmed using multi-gene phylogenetic analyses (Lombard & Crous 2012, Lombard *et al.* 2015). *Gliocladiopsis* has been linked to the sexual genus *Glionectria* (Schoch *et al.* 2000, Crous 2002), but following the "One Fungus = One Name" convention (Hawksworth 2011), the older asexual genus name *Gliocladiopsis* was chosen over the lesser-known *Glionectria* (Rossman *et al.* 2013).

Lombard & Crous (2012) provided the most comprehensive monograph for *Gliocladiopsis* spp., using the combination of morphological characters and sequence data from the 28S large subunit (LSU) and internal transcribed spacer (ITS) region of the ribosomal DNA, β-tubulin (*TUB2*), histone H3 (*HIS3*), and translation elongation factor 1-α (*TEF1*). They accepted *G. sagariensis* as the type species and confirmed the taxonomic status of nine *Gliocladiopsis* spp. known from culture. To date, 20 *Gliocladiopsis* spp. are recognised (Lombard & Crous 2012, Parkinson *et al.* 2017a, Liu & Cai 2013, Hyde *et al.* 2018, Zhai *et al.* 2019, Gordillo & Decock 2019, Perera *et al.* 2020, 2023).

Gliocladiopsis species are predominantly found in tropical and subtropical regions and are commonly associated with plant litter, soil and rhizosphere (Crous 2002, Lombard & Crous 2012). Although they are generally soil-borne, some species have been found in aquatic habitats (Liu & Cai 2003, Gordillo & Decock 2019, Hyde *et al.* 2019), and others have been isolated as endophytes from asymptomatic plant tissues (Li *et al.* 2008, Refaei *et al.* 2011, Hidayat *et al.* 2016). Most of these species have never been experimentally tested for pathogenicity, and they are generally regarded as saprobes (Crous 2002, Lombard &

Fungal Systematics and Evolution is licensed under a Creative Commons Attribution-NonCommercial-NoDerivatives 4.0 International License

© 2025 Westerdijk Fungal Biodiversity Institute

Table 1. Collection details and GenBank accessions of isolates included in the phylogenetic analyses.

Species	Isolate numbers	Substrate	Locality	GenBank accession				Reference
				TUB2	*HIS3*	ITS	*TEF1*	
Gliocladiopsis aquaticus	MFLUCC 17-1811^{T}	submerged wood	Thailand	MG574421	MG734182	MG543924	N/A	Hyde *et al*. (2018)
G. aquaticus	MFLUCC 17-2028	submerged wood	Thailand	MG574422	MG734183	MG543925	N/A	Hyde *et al*. (2018)
G. curvata	CBS 978.73	N/A	Brazil	JQ666119	JQ666009	JQ666043	JQ666085	Lombard & Crous (2012)
	CBS 194.80	*Persea americana*	Ecuador	JQ666120	JQ666010	JQ666044	JQ666086	Lombard & Crous (2012)
	CBS 110840 = MUCL 38873 = CPC 855	green house	Belgium	JQ666121	JQ666011	JQ666045	JQ666087	Lombard & Crous (2012)
	CBS 111194 = CPC 1354	soil	Mauritius	JQ666122	JQ666012	JQ666046	JQ666088	Lombard & Crous (2012)
	CBS 111195 = CPC 1355	soil	Mauritius	JQ666123	JQ666013	JQ666047	JQ666089	Lombard & Crous (2012)
	CBS 111196 = CPC 1356	soil	Mauritius	JQ666124	JQ666014	JQ666048	JQ666090	Lombard & Crous (2012)
	CBS 111421 = CPC 1652	soil	Ecuador	JQ666125	JQ666015	JQ666049	JQ666091	Lombard & Crous (2012)
	CBS 112365^{T} = CPC 10491 = Lynfield 791-B	*Archontophoenix purpurea*	New Zealand	JQ666126	JQ666016	JQ666050	JQ666092	Lombard & Crous (2012)
	CBS 112935 = CPC 4574	*Syzygium aromaticum*	Indonesia	JQ666127	JQ666017	JQ666051	JQ666093	Lombard & Crous (2012)
	CBS 114464 = CPC 1656	soil	Ecuador	JQ666128	JQ666018	JQ666052	JQ666094	Lombard & Crous (2012)
	CBS 115688 = IFO 9133 = CPC 539 = NBRC 9133	N/A	Japan	JQ666129	JQ666019	JQ666053	JQ666095	Lombard & Crous (2012)
	CMW 47217	soil associated with *Acacia* hybrid	Cuc Phuong National Park, Ninh Binh, Vietnam	PV420432	PV420382	PV405799	PV434096	This study
	CMW 47331	soil associated with *Acacia mangium*	Son Duong, Tuyen Quang, Vietnam	PV420433	PV420383	PV405800	PV434097	This study
	CMW 48247	soil associated with *Eucalyptus* sp.	Aek Nauli, North Sumatra, Indonesia	PV420434	PV420384	PV405801	PV434098	This study
	CMW 48275	soil associated with *Eucalyptus urophylla*	Tawau, Sabah, Malaysia	PV420435	PV420385	PV405802	PV434099	This study
G. ecuadoriensis	MUCL 54740^{T}	rhizosphere of *Polybotrya* sp.	Ecuador	KX611501	KX671146	KX671139	KX671131	Gordillo & Decock (2019)
G. elghollii	CBS 206.94	*Chamaedorea elegans*	USA	JQ666130	JQ666020	JQ666054	JQ666096	Lombard & Crous (2012)
	CBS 116104^{T} = CPC 636 = P93-2051	*Chamaedorea elegans*	USA	JQ666131	JQ666021	JQ666055	JQ666097	Lombard & Crous (2012)
G. forsbergii	BRIP 60984	*Grevillea* sp.	Australia	KX274036	KX274053	KX274070	N/A	Parkinson *et al.* (2017a)
	BRIP 61349a^{T}	*Persea americana*	Australia	KX274037	KX274054	KX274071	N/A	Parkinson *et al.* (2017a)

© 2025 Westerdijk Fungal Biodiversity Institute

Table 1. (continued).

Species	Isolate numbers	Substrate	Locality	GenBank accession				Reference
				*TUB*2	*HIS*3	ITS	*TEF*1	
	CMW 47195	soil associated with *Acacia* hybrid	Tuyen Quang, Vietnam	PV420436	PV420386	PV405803	PV434100	This study
	CMW 47287	soil associated with *Acacia* hybrid	Cuc Phuong National Park, Ninh Binh, Vietnam	PV420437	PV420387	PV405804	PV434101	This study
	CMW 47292	soil associated with *Acacia* hybrid	Cuc Phuong National Park, Ninh Binh, Vietnam	PV420438	PV420388	PV405805	PV434102	This study
G. guangdongensis	LC 1340^{T}	submerged wood	China	KC776124	KC776120	KC776122	KC776118	Liu & Cai (2013)
	LC 1349	submerged wood	China	KC776125	KC776121	KC776123	KC776119	Liu & Cai (2013)
	CMW 47386 = CBS 144576	soil associated with *Camellia* sp.	Tam Dao, Vinh Phuc, Vietnam	PV420439	PV420389	PV405806	PV434103	This study
	CMW 47388 = CBS 144577	soil associated with *Camellia* sp.	Tam Dao, Vinh Phuc, Vietnam	PV420440	PV420390	PV405807	PV434104	This study
	CMW 47397 = CBS 144578	soil associated with *Camellia* sp.	Tam Dao, Vinh Phuc, Vietnam	PV420441	PV420391	PV405808	PV434105	This study
	CMW 47398	soil associated with *Camellia* sp.	Tam Dao, Vinh Phuc, Vietnam	PV420442	PV420392	PV405809	PV434106	This study
G. hennebertii	MUCL 54818^{T}	rhirosphere of *Costus scaber*	Ecuador	KX611502	N/A	KX671140	KX671132	Gordillo & Decock (2019)
G. indonesiensis	CBS 116090^{T} = CPC 715	soil	Indonesia	JQ666132	JQ666022	JQ666056	JQ666098	Lombard & Crous (2012)
	CMW 48255	soil associated with *Eucalyptus* sp.	Aek Nauli, North Sumatra, Indonesia	PV420443	PV420393	PV405810	PV434107	This study
	CMW 48258	soil associated with *Eucalyptus* sp.	Aek Nauli, North Sumatra, Indonesia	PV420444	PV420394	PV405811	PV434108	This study
G. irregularis	CBS 755.97^{T} = CPC 718	soil	Indonesia	JQ666133	JQ666023	AF220977	JQ666099	Lombard & Crous (2012)
	CBS 111142 = CPC 1279	*Araucaria* sp.	Malaysia	JQ666134	JQ666024	JQ666057	JQ666100	Lombard & Crous (2012)
	CBS 111176 = CPC 1280	*Araucaria* sp.	Malaysia	JQ666135	JQ666025	JQ666058	JQ666101	Lombard & Crous (2012)
	CBS 114667 = 1278	*Araucaria* sp.	Malaysia	JQ666136	JQ666026	JQ666059	JQ666102	Lombard & Crous (2012)
	CBS 116086 = CPC 716	soil	Indonesia	JQ666152	JQ666042	JQ666072	JQ666118	Lombard & Crous (2012)
	CMW 47170 = CBS 144564	soil associated with *Acacia auriculiformis*	Do Luong, Nghe An, Vietnam	PV420445	PV420395	PV405812	PV434109	This study
	CMW 47177	soil associated with *Acacia auriculiformis*	Do Luong, Nghe An, Vietnam	PV420446	PV420396	PV405813	PV434110	This study
	CMW 47189 = CBS 144570	soil associated with *Acacia* hybrid	Quang Tri, Vietnam	PV420447	PV420397	PV405814	PV434111	This study

© 2025 Westerdijk Fungal Biodiversity Institute

Table 1. (continued).

Species	Isolate numbers	Substrate	Locality	GenBank accession				Reference
				*TUB*2	*HIS*3	ITS	*TEF*1	
	CMW 47328 = CBS 144571	soil associated with *Acacia mangium*	Tan Huong, Yen Bai, Vietnam	PV420448	PV420398	PV405815	PV434112	This study
	CMW 47345	soil associated with *Acacia mangium*	Dai Lai, Vinh Phuc, Vietnam	PV420449	PV420399	PV405816	PV434113	This study
	CMW 47346 = CBS 144565	soil associated with *Camellia* sp.	Thanh Son, Phu Tho, Vietnam	PV420450	PV420400	PV405817	PV434114	This study
	CMW 47383 = CBS 144572	soil associated with *Camellia* sp.	Tam Dao, Vinh Phuc, Vietnam	PV420451	PV420401	PV405818	PV434115	This study
	CMW 47390	soil associated with *Camellia* sp.	Tam Dao, Vinh Phuc, Vietnam	PV420452	PV420402	PV405819	PV434116	This study
	CMW 47415 = CBS 144566	soil associated with *Eucalyptus urophylla*	Nghia Dan, Nghe An, Vietnam	PV420453	PV420403	PV405820	PV434117	This study
	CMW 47431	soil associated with *Eucalyptus* hybrid	Bac Tu Liem, Hanoi, Vietnam	PV420454	PV420404	PV405821	PV434118	This study
	CMW 47518	soil associated with *Pinus* sp.	Do Luong, Nghe An, Vietnam	PV420455	PV420405	PV405822	PV434119	This study
	CMW 47520	soil associated with *Pinus* sp.	Do Luong, Nghe An, Vietnam	PV420456	PV420406	PV405823	PV434120	This study
	CMW 47521	soil associated with *Pinus* sp.	Do Luong, Nghe An, Vietnam	N/A	PV420407	PV405824	PV434121	This study
	CMW 47524	soil associated with *Pinus* sp.	Do Luong, Nghe An, Vietnam	PV420457	PV420408	PV405825	PV434122	This study
	CMW 47528	soil associated with *Cinnamomum cassia*	Mau A, Yen Bai, Vietnam	PV420458	PV420409	PV405826	PV434123	This study
	CMW 47529 = CBS 144567	Soil associated with *Cinnamomum cassia*	Mau A, Yen Bai, Vietnam	PV420459	PV420410	PV405827	PV434124	This study
	CMW 47533	soil associated with *Cinnamomum cassia*	Mau A, Yen Bai, Vietnam	PV420460	PV420411	PV405828	PV434125	This study
	CMW 47535	soil associated with *Cinnamomum cassia*	Mau A, Yen Bai, Vietnam	PV420461	PV420412	PV405829	PV434126	This study
	CMW 47537	Soil in natural forest	Anh Son, Nghe An, Vietnam	PV420462	PV420413	PV405830	PV434127	This study
	CMW 47555	soil associated with *Castanea* sp.	Van Ban, Lao Cai, Vietnam	PV420463	PV420414	PV405831	PV434128	This study
	CMW 49939	soil in natural forest	Bu Gia Map National Park, Binh Phuoc, Vietnam	PV420464	PV420415	PV405832	PV434129	This study

© 2025 Westerdijk Fungal Biodiversity Institute

Table 1. (continued).

Species	Isolate numbers	Substrate	Locality	GenBank accession				Reference
				TUB2	*HIS3*	ITS	*TEF1*	
	CMW 48272	soil associated with *Acacia mangium*	Tawau, Sabah, Malaysia	PV420465	PV420416	PV405833	PV434130	This study
G. mexicana	CBS 110938^{T} = CPC 964	soil	Mexico	JQ666137	JQ666027	JQ666060	JQ666103	Lombard & Crous (2012)
	CBS 111131 = CPC965	soil	Mexico	JQ666138	JQ666028	JQ666061	JQ666104	Lombard & Crous (2012)
	CMW 48270	soil associated with *Eucalyptus* sp.	Aek Nauli, North Sumatra, Indonesia	PV420466	PV420417	PV405834	PV434131	This study
	CMW 48250	soil associated with *Eucalyptus* sp.	Aek Nauli, North Sumatra, Indonesia	PV420467	PV420418	PV405835	PV434132	This study
G. peggii	BRIP 60983^{T}	*Persea americana*	Australia	KX274038	KX274065	KX274083	N/A	Parkinson *et al.* (2017a)
	BRIP 60987	*Persea americana*	Australia	KX274040	KX274062	KX274074	N/A	Parkinson *et al.* (2017a)
G. pseudotenuis	CBS 114763 = CPC 4575	*Vanilla* sp.	Indonesia	JQ666139	JQ666029	JQ666062	JQ666105	Lombard & Crous (2012)
	CBS 116074^{T} = CPC 706	soil	China	JQ666140	JQ666030	AF220981	JQ666106	Lombard & Crous (2012)
G. sagariensis	CBS 199.55^{T}	soil	India	JQ666141	JQ666031	JQ666063	JQ666107	Lombard & Crous (2012)
G. siamensis	MFLUCC 18-0576T	decaying stem	Thailand	ON364481	ON364457	ON361571	N/A	Perera *et al.* (2023)
G. singaporiensis	MUCL 48728T	submerged leaf litter	Singapore	KX611500	N/A	KX671138	KX671130	Gordillo & Decock (2019)
G. sumatrensis	CBS 754.97^{T} = CPC 1353	soil	Indonesia	JQ666142	JQ666032	JQ666064	JQ666108	Lombard & Crous (2012)
	CBS 111198 = CPC 1352	soil	Indonesia	JQ666143	JQ666033	JQ666065	JQ666109	Lombard & Crous (2012)
	CBS 111213	soil	Indonesia	JQ666144	JQ666034	JQ666066	JQ666110	Lombard & Crous (2012)
	CBS 111368 = CPC 1351	soil	Indonesia	JQ666145	JQ666035	AF220978	JQ666111	Lombard & Crous (2012)
	CMW 48262	soil associated with *Eucalyptus* sp.	Aek Nauli, North Sumatra, Indonesia	PV420468	PV420419	PV405836	PV434133	This study
	CMW 48267	soil associated with *Eucalyptus* sp.	Aek Nauli, North Sumatra, Indonesia	PV420469	PV420420	PV405837	PV434134	This study
G. swieteniae	MFLUCC 17-2616^{T}	*Swietenia mahagoni*	Thailand	MT212214	MT212194	MT215501	N/A	Perera *et al.* (2020)
G. tenuis	CBS 111961 = CPC 2910	*Coffee* sp.	Vietnam	JQ666146	JQ666036	JQ666067	JQ666112	Lombard & Crous (2012)
	CBS 111964 = CPC 2909	*Coffee* sp.	Vietnam	JQ666147	JQ666037	JQ666068	JQ666113	Lombard & Crous (2012)
	CBS 114147 = CPC 2912	soil	Vietnam	JQ666148	JQ666038	JQ666069	JQ666114	Lombard & Crous (2012)
	CBS 114148 = CPC 2911	soil	Vietnam	JQ666149	JQ666039	JQ666070	JQ666115	Lombard & Crous (2012)
	IMI 68205^{T} = CPC 2403	*Indigofera* sp.	Indonesia	JQ666150	JQ666040	AF220979	JQ666116	Lombard & Crous (2012)
	CMW 49920	soil associated with *Hevea brasiliensis*	Duong Minh Chau, Tay Ninh, Vietnam	PV420470	PV420421	PV405838	PV434135	This study

© 2025 Westerdijk Fungal Biodiversity Institute

Table 1. (continued).

Species	Isolate numbers	Substrate	Locality	GenBank accession				Reference
				TUB2	*HIS3*	ITS	*TEF1*	
	CMW 49927	soil associated with *Hevea brasiliensis*	Long Thanh, Dong Nai, Vietnam	PV420471	PV420422	PV405839	PV434136	This study
	CMW 49916	soil associated with *Hevea brasiliensis*	Duong Minh Chau, Tay Ninh, Vietnam	PV420472	PV420423	PV405840	PV434137	This study
G. vietnamensis	**CMW 47402 = CBS 144585**	soil associated with *Eucalyptus urophylla*	Son Duong, Tuyen Quang, Vietnam	PV420473	PV420424	PV405841	PV434138	This study
	CMW 49944 = CBS 144586	soil associated with *Alnus nepalensis*	Hoang Lien National Park, Lao Cai, Vietnam	PV420474	PV420425	PV405842	PV434139	This study
	CMW 49945^{T} = CBS 144587	soil associated with *Alnus nepalensis*	Hoang Lien National Park, Lao Cai, Vietnam	PV420475	PV420426	PV405843	PV434140	This study
	CMW 49947	soil associated with *Alnus nepalensis*	Hoang Lien National Park, Lao Cai, Vietnam	PV420476	PV420427	PV405844	PV434141	This study
G. whileyi	BRIP 61430^{T}	*Persea americana*	Australia	KX274052	KX274069	KX274086	N/A	Parkinson *et al.* (2017a)
	CMW 47392	soil associated with *Camellia* sp.	Tam Dao, Vinh Phuc, Vietnam	PV420477	PV420428	PV405845	PV434142	This study
G. wuhanensis	HEAC17307^{T}	soil	China	MH169602	MH255786	MH024520	N/A	Zhai *et al.* (2019)
	CMW 47540 = CBS 144579	soil in natural forest	Nhu Xuan, Thanh Hoa, Vietnam	PV420478	PV420429	PV405846	PV434143	This study
	CMW 47541 = CBS 144580	soil in natural forest	Nhu Xuan, Thanh Hoa, Vietnam	PV420479	PV420430	PV405847	PV434144	This study
	CMW 49936 = CBS 144581	soil in natural forest	Bu Gia Map Natural Park, Binh Phuoc, Vietnam	PV420480	PV420431	PV405848	PV434145	This study
Gliocladiopsis sp. 1	CBS 111038 = CPC 1157	soil	Colombia	JQ666151	JQ666041	JQ666071	JQ666117	Lombard & Crous (2012)
Penicillifer pulcher	CBS 560.67^{T} = ATCC 18931 = MUCL 11607	soil	The Netherlands	KM231998	KM231456	KM231742	KM231862	Lombard *et al.* (2015)

Note: N/A represents information that is not available. Isolates obtained in this study are indicated in **bold**. ^{T} denotes ex-type strain.
ATCC, American Type Culture Collection, VA, USA; **BRIP**, Biosecurity Queensland Plant Pathology Herbarium, Department of Agriculture and Fisheries, Dutton Park, Australia; **CBS**, the culture collection of Westerdijk Fungal Biodiversity Institute, Utrecht, the Netherlands; **CMW**, the culture collection of the Forestry and Agricultural Biotechnology Institute (FABI), University of Pretoria, Pretoria, South Africa; **CPC**, Pedro Crous working collection housed at Westerdijk Fungal Biodiversity Institute; **HEAC**, the Herbarium of Henan Agricultural University, Zhengzhou, China; **IMI**, International Mycological Institute, CABI-Bioscience, Egham, Bakeham Lane, UK; **LC**, Herbarium of Microbiology, Academia Sinica, Taipei, Taiwan; **MFLUCC,** Mae Fah Luang University culture collection, Chiang Rai, Thailand; **MUCL**, Mycotheque, Laboratoire de Mycologie Systematique st Appliqee, l'Universite, Louvain-la-Neuve, Belgium.
ITS, internal transcribed spacer regions 1 and 2 including the 5.8S region of ribosomal RNA; ***HIS3***, histone H3; ***TEF1***, translation elongation factor 1-alpha; ***TUB2***, β-tubulin.

© 2025 Westerdijk Fungal Biodiversity Institute

Crous 2012). In this study, we used the combination of multi-gene phylogenetic inference and morphological observations to identify a collection of isolates resembling *Gliocladiopsis* species from soil samples collected in Indonesia, Malaysia and Vietnam.

MATERIALS AND METHODS

Sampling and fungal isolations

Surveys were conducted in various forestry plantations, nurseries and natural forests across 13 Vietnamese provinces (Binh Phuoc, Dong Nai, Hanoi, Lao Cai, Nghe An, Ninh Binh, Phu Tho, Quang Tri, Tay Ninh, Thanh Hoa, Tuyen Quang, Vinh Phuc and Yen Bai), Indonesia (North Sumatra) and Malaysia (Sabah). Soil samples were placed in plastic bags and transferred to the laboratory for fungal isolations. The collected samples were baited with germinating *Medicago sativa* (alfalfa) seeds following the method described by Crous (2002). Gliocladiopsis-like spore masses were located under a dissecting microscope and transferred using a sterile hypodermic needle directly onto Petri dishes containing 2 % (w/v) malt extract agar (MEA; Biolab, Midrand, South Africa) supplemented with 1 % streptomycin sulphate (Sigma-Aldrich).

Primary isolations were incubated for 3–7 d at 25 °C for fungal growth. Single hyphal tips cut from young fungal colonies were transferred to fresh MEA plates to obtain pure cultures. These isolates were deposited in the research culture collection (CMW) of the Forestry and Agricultural Biotechnology Institute (FABI), University of Pretoria, South Africa, and the publicly accessible culture collection (CMW-IA) of the Innovation Africa at the University of Pretoria, and the culture collection (CBS) of the Westerdijk Fungal Biodiversity Institute, Utrecht, The Netherlands. Dried cultures representing the holotype of the novel taxon were deposited in the H.G.W.J. Schweickerdt herbarium (PRU), University of Pretoria, South Africa.

DNA sequencing and phylogenetic analyses

DNA was extracted from 7-d-old pure fungal cultures grown on MEA, using Prepman® Ultra Sample Preparation Reagent (Thermo Fisher Scientific, Waltham, MA, USA), following the protocols suggested by the manufacturer. Four loci, namely, ITS, *TEF1*, *TUB2* and *HIS3*, were amplified using the set of primers as described by Pham *et al.* (2018). The PCR amplification were conducted using an Applied Biosystems ProFlex PCR System (Thermo Fisher Scientific, Waltham, MA, USA) following the preparation described by Pham *et al.* (2018). Amplified fragments were cleaned using ExoSAP-IT™ PCR Product Cleanup Reagent (Thermo Fisher Scientific, Waltham, MA, USA). Amplicons were sequenced in both directions using an ABI PRISM™ 3100 DNA sequencer (Applied Biosystems, USA) at the Sequencing Facility of the Faculty of Natural and Agricultural Sciences, University of Pretoria. Geneious Prime v. 2025.0.3 (https://www.geneious.com) was used to assemble and edit the raw sequences. All sequences generated in this study were deposited in GenBank (http://www.ncbi.nlm.nih.gov).

Representative sequences of *Gliocladiopsis* spp. published previously were obtained from GenBank to compare with sequences generated in this study (Table 1). Alignments of all sequences were assembled using MAFFT v. 7 (http://mafft.cbrc.jp/alignment/server/) (Katoh & Standley 2013), then confirmed manually in MEGA v. 7 (Kumar *et al.* 2016) where necessary. Maximum likelihood (ML) and Bayesian inference

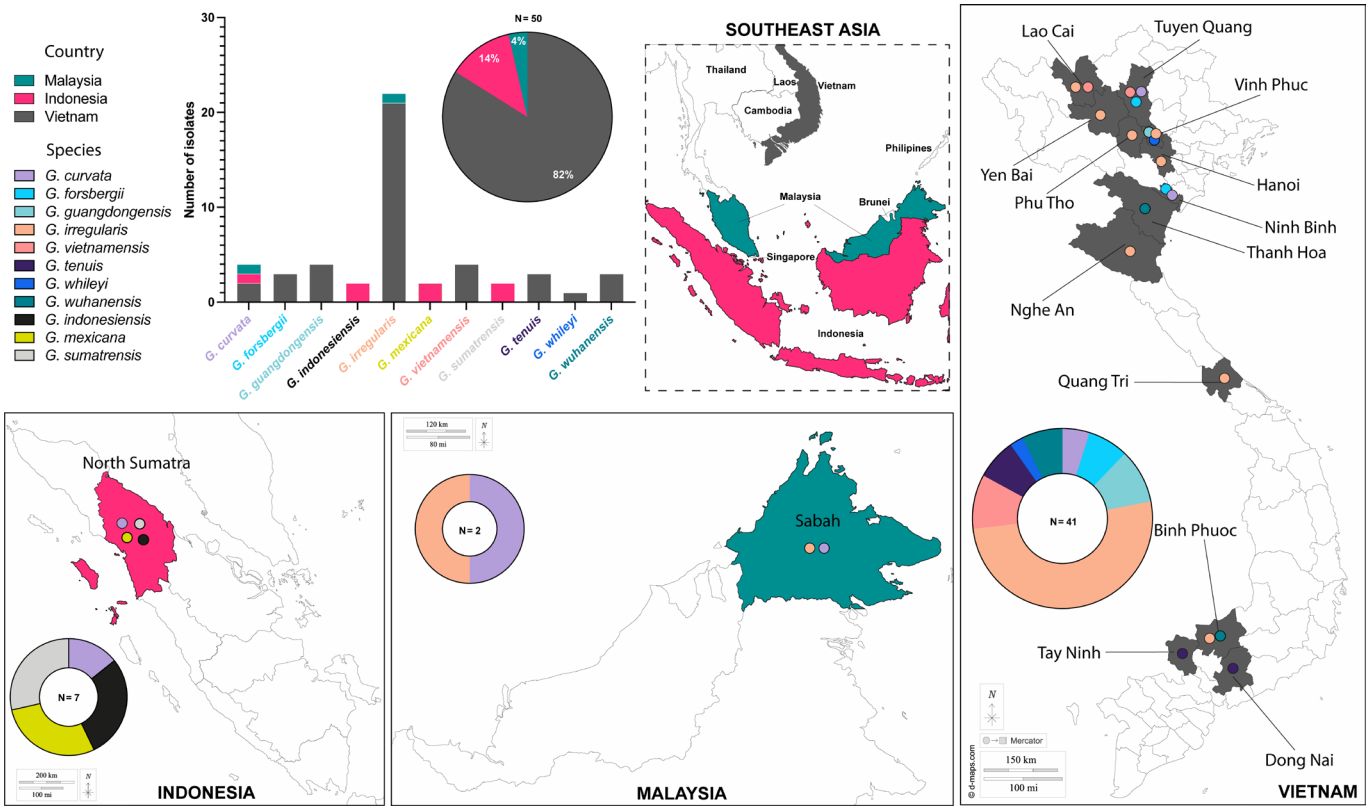

Fig. 1. Geographic location of the sampling sites in Vietnam, Indonesia and Malaysia and the diversity of *Gliocladiopsis* spp. isolated in each region.

© 2025 Westerdijk Fungal Biodiversity Institute

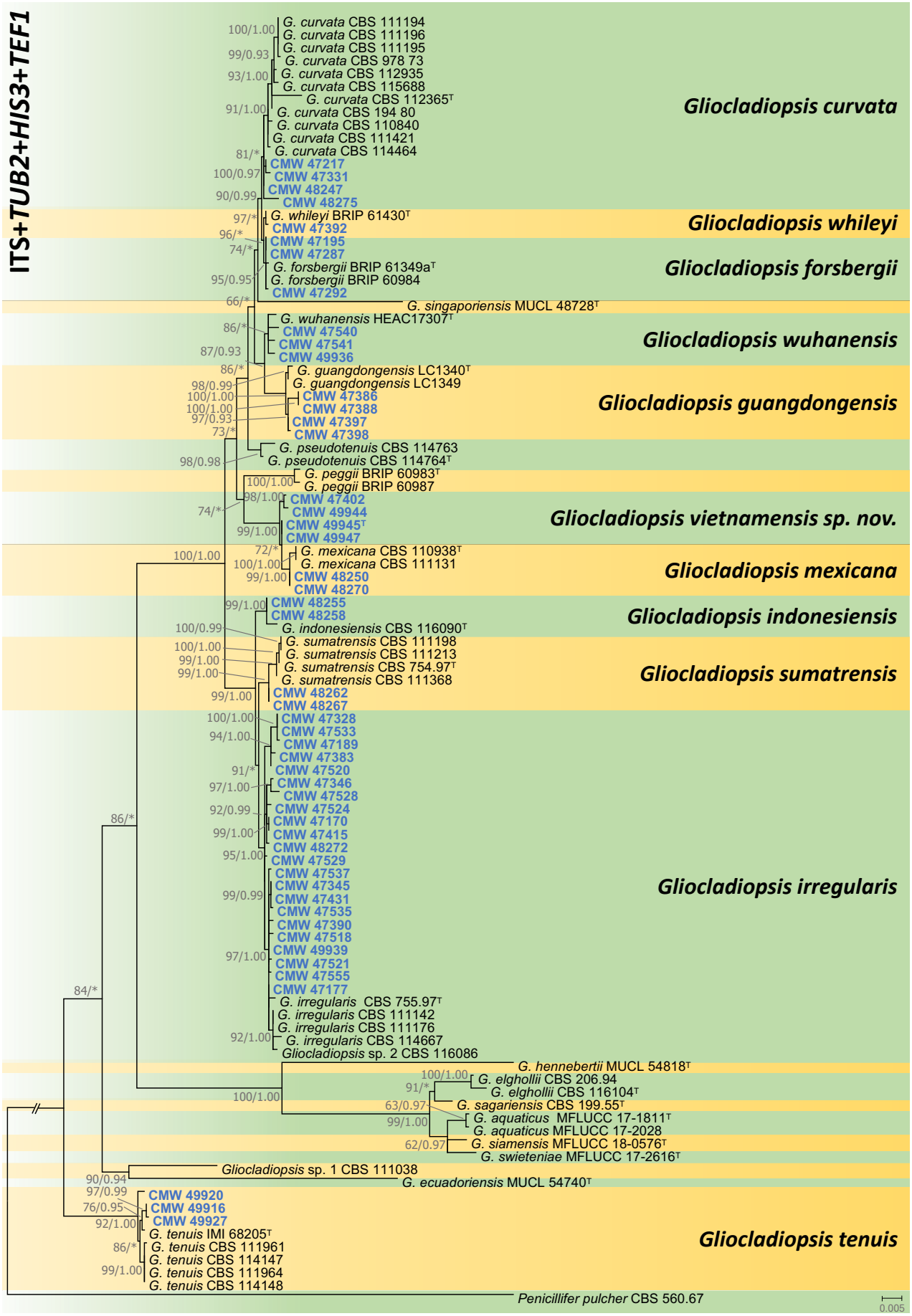

Fig. 2. Phylogenetic tree based on maximum likelihood (ML) analysis of a combined DNA dataset of ITS, *TUB2*, *HIS3*, and *TEF1* sequences for *Gliocladiopsis* spp. Bootstrap support values ≥ 60 % for ML analyses and posterior probabilities values ≥ 0.90 obtained from Bayesian inference (BI) are indicated at the nodes as ML/BI. Bootstrap support values < 60 % or probabilities values < 0.90 are marked with "*". Isolates representing ex-type material are marked with "T" and novel isolates from this study are in blue. *Penicillifer pulcher* (isolate CBS 560.67) represents the outgroup.

© 2025 Westerdijk Fungal Biodiversity Institute

(BI) analyses were performed on the combined dataset of four regions. For ML, analyses were conducted using W-IQ-TREE with an optimal substitution model automatically determined and 1000 ultrafast bootstraps (Trifinopoulos *et al.* 2016). For BI, analyses were performed using MrBayes v. 3.2.6 (Ronquist *et al.* 2012) on the CIPRES Science Gateway v. 3.3. Four Markov chain Monte Carlo (MCMC) chains were run from a random starting tree for five million generations, and trees were sampled every 100th generation. The first 25 % of trees sampled were eliminated as burn-in, and the remaining trees were used to determine the posterior probabilities. *Penicillifer pulcher* (CBS 560.67) was used as the outgroup taxon. The resulting trees were visualised using MEGA v. 7 (Kumar *et al.* 2016).

Microscopy and morphological characteristics

The isolates were grown on synthetic nutrient-poor agar (SNA; Nirenburg 1981) to study morphological characteristics. The conidiophores were initially mounted in water and later replaced with 85 % lactic acid for further observation and preservation. Nikon microscopes (Eclipse Ni, SMZ 18, Nikon, Tokyo, Japan) were used to study microscopic features. Images were captured with a Nikon DS-Ri2 camera mounted on the microscopes, and characteristic structures were measured utilising the NIS-Elements BR program. Twenty-five to 50 measurements of all taxonomically relevant characteristics were made whenever possible. The dimensions of the structures are presented as ranges other than those where an average is included. Colony characteristics were observed for cultures on 2 % MEA incubated in the dark in 7 d and were described using Rayner's colour charts (Rayner 1970). Colony growth was determined on MEA at temperatures ranging from 10–35 °C at 5 ° intervals with five replicate plates for each temperature. Two measurements of colony diameter were taken for cultures grown for 7 d, and averages were computed.

RESULTS

Fungal isolates

Collectively, 50 cultures having a morphology typical of *Gliocladiopsis* spp. were isolated from 84 soil samples collected in Vietnam, eight from Indonesia, and six from Malaysia. Of these, 41 isolates (82 %) were from Vietnam, seven (14 %) from Indonesia and two (4 %) from Malaysia (Fig. 1). Twenty-two isolates (44 %) were of a single species, and of these, 21 were from Vietnam (Fig. 1). The remaining 19 isolates represented a maximum of four isolates of any one species. Only one species occurred in all three countries. Three species were found only in Indonesia, and five were found only in Vietnam (Fig. 1).

Phylogenetics analyses

Amplicons of approximately 520 bp were generated for the ITS region, 450 bp for the *TUB2*, 470 bp for the *HIS3*, and 500 bp for the *TEF1*. The combined sequence dataset used in the phylogenetic analyses included 99 ingroup taxa and 2023 characters, including gaps. The ML and BI analyses generated phylogenetic trees with concordant topologies, revealing similar phylogenetic relationships among taxa. The ML tree with bootstrap support values and the posterior probabilities obtained from BI are presented in Fig. 2. Isolates obtained from this study resided in 11 different clades. Of these, most isolates (22) grouped in a well-supported clade (ML/BI = 95/1.00) with the ex-type and representative isolates of *G. irregularis*. The remaining isolates grouped with *G. curvata* (four isolates), *G. whileyi* (one isolate), *G. forsbergii* (three isolates), *G. wuhanensis* (three isolates), *G. guangdongensis* (four isolates), *G. mexicana* (two isolates), *G. indonesiensis* (two isolates), *G. sumatrensis* (two isolates) and *G. tenuis* (three isolates). Four isolates (CMW 47402, CMW 49944, CMW 49945, CMW 49947) resided in a cluster distinct from the most closely related species *G. mexicana*, and are thus described as a novel taxon.

Taxonomy

Gliocladiopsis vietnamensis N.Q. Pham, Marinc. & M.J. Wingf., ***sp. nov***. MB 858515. Fig. 3.

Etymology: The name refers to Vietnam, where the species was first discovered.

Diagnosis: Morphologically similar to *G. mexicana* but can be differentiated from *G. mexicana* by ITS (2 bp), *TUB2* (1 bp), *HIS*3 (2 bp), and *TEF1* (5 bp) sequences.

Typus: **Vietnam**, Lao Cai Province, Hoang Lien National Park, from soil associated with *Alnus nepalensis*, 1 Sep. 2013, *N.Q. Pham, Q.N. Dang & T.Q. Pham* [**holotype** specimen PRU(M) 4633; ex-holotype culture CBS 144587 = CMW 49945 = CMW-IA 7117]. GenBank: PV420475 (*TUB2*); PV420426 (*HIS3*); PV405843 (ITS); PV434140 (*TEF1*).

Description: *Sexual morph* not observed. *Conidiophores* penicilliate, upright, simple. *Conidiogenous apparatus* often consisting of a layer of conidiogenous cells or branching in 2–3 tiers; 1° branches 6–25.5 × 1–5 µm; 2° branches 5–20.5 × 1–4 µm. *Conidiogenous cells* hyaline, cylindrical, phialidic, tapering towards the apex, 6–22 × 1–3.5 µm. *Conidia* hyaline, cylindrical, straight or curved, medianly 1-septate, 13–23 × 2.5–4 µm (avg. 17 × 3 µm).

Colony characteristics: On MEA after 7 d, colonies buff on the surface, ochreous becoming paler toward the margin in reverse, margin entire, elevation flat. Optimal growth temperature at 25 °C reaching 37.9 mm in 7 d, followed by 20 °C (24.5 mm), 30 °C (22.9 mm), 15 °C (11.2 mm), and no growth at 10 °C and 35 °C.

Distribution: Vietnam (Tuyen Quang and Lao Cai Province)

Additional materials examined: **Vietnam**, Tuyen Quang Province, Son Duong, from soil collected in an *Eucalyptus urophylla* plantation, 1 Nov. 2013, *N.Q. Pham & T.Q. Pham*, culture CBS 144585 = CMW 47402, GenBank: PV420473 (*TUB2*); PV420424 (*HIS3*); PV405841 (ITS); PV434138(*TEF1*); Lao Cai Province, Hoang Lien National Park, from soil associated with *Alnus nepalensis*, 1 Sep. 2013, *N.Q. Pham,*

© 2025 Westerdijk Fungal Biodiversity Institute

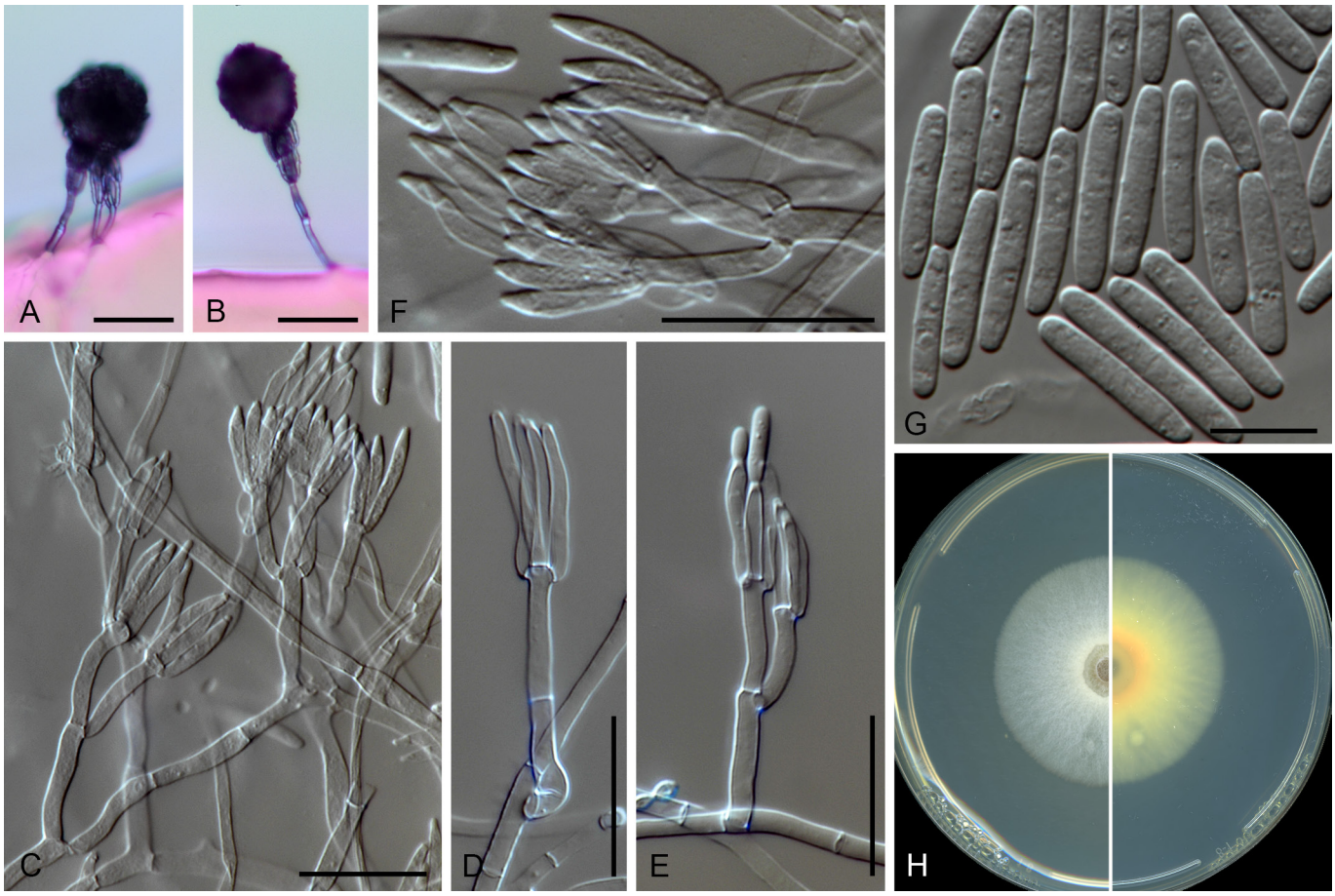

Fig. 3. Microscopic features of *Gliocladiopsis vietnamensis* (ex-holotype CBS 144587 = CMW 49945 = CMW-IA 7117). **A, B.** Conidiophores on SNA. **C–E.** Conidiophores. **F.** Conidiogenous cells. **G.** Conidia. **H.** Culture grown on PDA for 7 d at 25 °C in the dark (left, above; right, reverse). Scale bars: A, B = 50 µm; C–F = 25 µm; G = 10 µm.

N.Q. Dang & T.Q. Pham, PRU(M) 4632, culture CBS 144586 = CMW 49944 = CMW-IA 7116, GenBank: PV420474 (*TUB2*); PV420425 (*HIS3*); PV405842 (ITS); PV434139(*TEF1*).

Notes: *Gliocladiopsis vietnamensis* is phylogenetically closely related to *G. mexicana*. They are morphologically similar in not having tertiary branches (rarely found in *G. mexicana*) and in having similar conidial dimensions (15–21 × 2–4 µm for *G. mexicana*, 13–23 × 2.5–4 µm for *G. vietnamensis*) (Lombard & Crous 2012). The colony colour of *G. mexicana* was described as sayal brown to sepia in reverse, whereas *G. vietnamensis* cultures are buff to ochreous in reverse.

Gliocladiopsis mexicana was first reported from soil samples in Mexico in 1994 (Lombard & Crous 2012). This study added two strains (CMW 48250, 48270) of the species, which were isolated from Indonesian soil samples. *Gliocladiopsis peggii* is a sister taxon to *G. vietnamensis* and *G. mexicana* and is morphologically similar. However, unlike the other two from soil samples, it was isolated from necrotic roots of avocado and necrotic stem lesions on *Grevillea* sp. (Parkinson *et al.* 2017a).

DISCUSSION

This study represents the largest collection of *Gliocladiopsis* isolates from Southeast Asia that has ever been subjected to DNA sequence analyses. Based on morphological characteristics and phylogenetic analyses of four loci (ITS, *TUB2, HIS3,* and *TEF1*), 11 *Gliocladiopsis* spp. were identified from soils collected from different regions of Indonesia, Malaysia and Vietnam. These included 10 of the 20 previously described species in the genus, namely, *G. curvata*, *G. guangdongensis*, *G. indonesiensis*, *G. irregularis*, *G. forsbergii*, *G. mexicana*, *G. sumatraensis*, *G. tenuis*, *G. whileyi*, and *G. wuhanensis.* In addition, a new species was discovered, described in this study as *G. vietnamensis*.

Six species, namely, *G. curvata*, *G. forsbergii*, *G. guangdongensis*, *G. irregularis*, *G. whileyi*, and *G. wuhanensis,* are reported for the first time from Vietnam. *Gliocladiopsis curvata* is reported for the first time in Malaysia. *Gliocladiopsis mexicana*, previously known only in Mexico, was also recovered from soils in Indonesia. This increases the number of known *Gliocladiopsis* spp. in Southeast Asia to 15 (Crous 2002, Hyde *et al.* 2008, Lombard & Crous 2012, Gordillo & Decock 2019, Perera *et al.* 2020, 2023), suggesting that this region represents a biodiverse hotspot for soil-borne *Gliocladiopsis* spp. The identification of a relatively high number of species from a relatively small number of isolates, exclusively from soils collected in areas not previously examined, also suggests that many more *Gliocladiopsis* species await discovery, especially in the tropics and the Southern Hemisphere.

Gliocladiopsis irregularis was one of the most commonly isolated species (44 %) in this study. This species was found to have a broad distribution across Vietnam, encompassing eight provinces, as well as in Sabah, Malaysia. Although *G. irregularis* had previously been reported from Indonesia

© 2025 Westerdijk Fungal Biodiversity Institute

(Crous 2002, Lombard & Crous 2012), we did not isolate this species from North Sumatra. *Gliocladiopsis irregularis* was recovered from soils associated with a wide range of planted tree species, *i.e.*, *Acacia*, *Camellia*, *Eucalyptus*, *Pinus* and *Cinnamomum* spp., as well as from native and largely undisturbed forests. Given its common occurrence and wide distribution, it seems probable that *G. irregularis* is native to this area. However, further studies, including those at a population genetics level, would be required to resolve that question.

All *Gliocladiopsis* species identified in this study were isolated exclusively from baited soils and could not be directly linked to disease symptoms. Their isolation from germinating alfalfa seedlings and thus green tissues used in baiting suggests some level of pathogenicity; however, their role, even as weak plant pathogens, remains to be determined. To date, the only species that has been experimentally tested for pathogenicity is *G. peggii*, which has been found to be non-pathogenic (Parkinson *et al.* 2017b) and, in some cases, even promotes plant growth (Dann *et al.* 2012). Clearly, a much deeper understanding of the biology, particularly their ecological role in the rhizosphere, is needed for species of *Gliocladiopsis*.

ACKNOWLEDGEMENTS

We thank M.R.B.A. Rauf for his assistance with surveys in Malaysia. T.Q. Pham and Q.N. Dang are thanked for assisting in sample collection and fungal isolation in Vietnam, and K. Bensch at MycoBank for helping with the nomenclature of the new taxon. We acknowledge the financial support from the Forest Protection Research Centre (FPRC), Vietnam Academy of Forest Sciences (VAFS), Vietnam, members of the Tree Protection Co-operative Programme (TPCP), and the DST/NRF Centre of Excellence in Plant Health Biotechnology (CPHB), South Africa.

Conflict of Interest: The authors declare no conflicts of interest.

REFERENCES

Agnihothrudu V (1959). Notes on fungi from North-East India. *Transactions of the British Mycological Society* **42**: 458–462.

Barron GL (1968). *The genera of Hyphomycetes from soil*. The Williams & Wilkins Company, USA.

Bugnicourt F (1939). Les *Fusarium* et *Cylindrocarpon* de l'Indochine. *Encyclopédie Mycologique* **11**: 1–206.

Crous PW (2002). *Taxonomy and pathology of Cylindrocladium (Calonectria) and allied genera*. APS Press, USA.

Crous PW, Wingfield MJ (1993). A re-evaluation of *Cylindrocladiella*, and a comparison with morphologically similar genera. *Mycological Research* **97**: 433–448. https://doi.org/10.1016/S0953-7562(09)80131-7

Dann EK, Cooke AW, Forsberg LI, *et al.* (2012). Pathogenicity studies in avocado with three nectriaceous fungi, *Calonectria ilicicola*, *Gliocladiopsis* sp. and *Ilyonectria liriodendri*. *Plant Pathology* **61**: 896–902. https://doi.org/10.1111/j.1365-3059.2011.02579.x

Gordillo A, Decock C (2019). Multigene phylogenetic and morphological evidence for seven new species of *Aquanectria* and *Gliocladiopsis* (*Ascomycota*, *Hypocreales*) from tropical areas. *Mycologia* **111**: 299–318. https://doi.org/10.1080/00275514.2018.1548863

Hawksworth DL (2011). A new dawn for the naming of fungi: impacts of decisions made in Melbourne in July 2011 on the future publication and regulation of fungal names. *MycoKeys* **1**: 7–20. https://doi.org/10.5598/imafungus.2011.02.02.06

Hidayat I, Radiastuti N, Rahayu G, *et al.* (2016). Endophytic fungal diversity from *Cinchona calisaya* based on phylogenetic analysis of the ITS ribosomal DNA sequence data. *Current Research in Environmental & Applied Mycology* **6**: 132–142. https://doi.org/10.5943/cream/6/2/7

Hyde KD, Chaiwan N, Norphanphoun C., *et al.* (2018). Mycosphere notes 169–224. *Mycosphere* **9**: 271–430.

Katoh K, Standley DM (2013). MAFFT multiple sequence alignment software version 7: improvements in performance and usability. *Molecular Biology and Evolution* **30**: 772–780. https://doi.org/10.1093/molbev/mst010

Kumar S, Stecher G, Tamura K (2016). MEGA7: Molecular Evolutionary Genetics Analysis version 7.0 for bigger datasets. *Molecular Biology and Evolution* **33**: 1870–1874. https://doi.org/10.1093/molbev/msw054

Li J, Zhao J, Xu L, *et al.* (2008). Endophytic fungi from rhizomes of *Paris polyphylla* var. *yunnanensis*. *World Journal of Microbiology and Biotechnology* **24**: 733–737. https://doi.org/10.1007/s11274-007-9531-3

Liu F, Cai L (2013). A novel species of *Gliocladiopsis* from freshwater habitat in China. *Cryptogamie, Mycologie* **34**: 233–241. https://doi.org/10.7872/crym.v34.iss2.2013.233

Lombard L, Crous PW (2012). Phylogeny and taxonomy of the genus *Gliocladiopsis*. *Persoonia* **28**: 25–33. https://doi.org/10.3767/003158512X635056

Lombard L, van der Merwe NA, Groenewald JZ, *et al.* (2015). Generic concepts in *Nectriaceae*. *Studies in Mycology* **80**: 189–245. https://doi.org/10.1016/j.simyco.2014.12.002

Nirenberg HI (1981). A simplified method for identifying *Fusarium* spp. occurring on wheat. *Canadian Journal of Botany* **59**: 1599–1609.

Parkinson LE, Shivas RG, Dann EK (2017a). Novel species of *Gliocladiopsis* (*Nectriaceae*, *Hypocreales*, *Ascomycota*) from avocado roots (*Persea americana*) in Australia. *Mycoscience* **58**: 95–102. https://doi.org/10.1016/j.myc.2016.10.004

Parkinson LE, Shivas RG, Dann EK (2017b). Pathogenicity of nectriaceous fungi on avocado in Australia. *Phytopathology* **107**: 1479–1485. https://doi.org/10.1094/PHYTO-03-17-0084-R

Perera RH, Hyde KD, Jones EBG, *et al.* (2023). Profile of *Bionectriaceae*, *Calcarisporiaceae*, *Hypocreaceae*, *Nectriaceae*, *Tilachlidiaceae*, *Ijuhyaceae fam. nov.*, *Stromatonectriaceae fam. nov.* and *Xanthonectriaceae fam. nov*. *Fungal Diversity* **118**: 95–271. https://doi.org/10.1007/s13225-022-00512-1

Perera RH, Hyde KD, Maharachchikumbura SSN, *et al.* (2020). Fungi on wild seeds and fruits. *Mycosphere* **11**: 2108–2480. https://doi.org/10.5943/mycosphere/11/1/14

Pham NQ, Barnes I, Chen SF, *et al.* (2018). New species of *Cylindrocladiella* from plantation soils in South-East Asia. *MycoKeys* **32**: 1–24. https://doi.org/10.3897/mycokeys.32.23754

Rayner RW (1970). *A Mycological Colour Chart*. Commonwealth Mycological Institute: British Mycological Society. Kew, Surrey, UK.

Refaei J, Jones EBG, Sakayaroj J, *et al.* (2011). Endophytic fungi from *Rafflesia cantleyi*: species diversity and antimicrobial activity.

© 2025 Westerdijk Fungal Biodiversity Institute

Mycosphere **2**: 429–447.

Ronquist FMT, Van der Mark P, *et al.* (2012). MrBayes 3.2: efficient Bayesian phylogenetic inference and model choice across a large model space. *Systematic Biology* **61**: 539–542. https://doi.org/10.1093/sysbio/sys029

Rossman, A.Y., Seifert, K.A., Samuels, G.J. *et al.* (2013). Genera in *Bionectriaceae*, *Hypocreaceae*, and *Nectriaceae* (*Hypocreales*) proposed for acceptance or rejection. *IMA Fungus* **4**: 41–51. https://doi.org/10.5598/imafungus.2013.04.01.05

Saksena SB (1954). A new genus of *Moniliaceae*. *Mycologia* **46**: 660–666. https://www.jstor.org/stable/4547875

Schoch CL, Crous PW, Wingfield MJ, *et al.* (2000). Phylogeny of *Calonectria* and selected hypocrealean genera with cylindrical macroconidia. *Studies in Mycology* **45**: 45–62.

Trifinopoulos J, Nguyen LT, von Haeseler A, *et al.* (2016). W-IQ-TREE: a fast online phylogenetic tool for maximum likelihood analysis. *Nucleic Acids Research* **44**: W232–W235. https://doi.org/10.1093/nar/gkw256

Zhai NP, Sun ZQ, Zhang YL, *et al.* (2019). *Gliocladiopsis wuhanensis sp. nov*. from China. *Mycotaxon* **134**: 313–319. https//doi.org/10.5248/134.313

© 2025 Westerdijk Fungal Biodiversity Institute

FUSE

Fungal Systematics and Evolution

VOLUME 16
DECEMBER 2025
PAGES 93–146

doi.org/10.3114/fuse.2025.16.7

Expanding *Lycogala*: twenty-four new species, their morphology and phylogenetic relationships

D. Leontyev[1,2*], Y. Ishchenko[3], M. Leontieva[2], I. Yatsiuk[4,5], O. Shchepin[2], W.-L. Song[6], S.L. Chen[6], E. Moroz[3], M. Schnittler[2]

[1]H.S. Skovoroda Kharkiv National Pedagogical University, Alchevskih 29, Kharkiv 61002 Ukraine
[2]Institute of Botany and Landscape Ecology, University Greifswald, Soldmannstr. 15, Greifswald D-17487, Germany
[3]Independent researcher
[4]Estonian University of Life Sciences, Kreutzwaldi 52, Tartu 51006, Estonia
[5]Institute of Ecology & Earth Sciences, University of Tartu, Vanemuise 46, 51014 Tartu, Estonia
[6]School of Life Sciences, Nanjing Normal University, Xianlin Campus, No. 163 of Xianlin Avenue, Qixia District, Nanjing 210023, China

*Corresponding author: alwisiamorula@gmail.com

Key words:
ASAP analysis
myxomycetes
new taxa
phylogeny
reproductive isolation
ribogroup
species delimitation
systematics

Abstract: The genus *Lycogala* was historically considered a small, morphologically uniform group of myxomycetes, with its classification remaining largely unchanged for most of the 20th century. However, recent molecular studies have revealed exceptional cryptic diversity within the genus, challenging its traditional species delimitations. This study continues the taxonomic reassessment of *Lycogala*, integrating three-gene phylogenies and morphological analyses of 716 specimens from four continents. A total of 706 nucSSU, 273 mtSSU, and 130 *COI* sequences were analysed to delimit species within the genus using recombination test and distance-based delimitation. As a result, 716 specimens were assigned to 93 nucSSU ribogroups, which were further grouped into 63 putative morphological species. Of these, only 20 had been formally described prior to this study. Herein, we describe an additional 24 species, significantly expanding the known diversity of the genus. Phylogenetic analyses suggest the division of *Lycogala* into five major clades, which correspond to distinct morphological traits, supporting the proposal of five new sections within the genus. The study also confirms that *L. epidendrum* s. str. exhibits significant genetic polymorphism, with at least 29 subgroups detected. However, species delimitation within *L. epidendrum* remains challenging due to conflicting results from genetic markers and the presence of recombined genotypes. The study underscores the necessity of integrating molecular and morphological approaches for resolving *Lycogala* taxonomy and highlights the potential for further discoveries in myxomycete diversity.

Citation: Leontyev D, Ishchenko Y, Leontieva M, Yatsiuk I, Shchepin O, Song W-L, Chen SL, Moroz E, Schnittler M (2025). Expanding *Lycogala*: twenty-four new species, their morphology and phylogenetic relationships. *Fungal Systematics and Evolution* **16**: 93–146. doi: 10.3114/fuse.2025.16.7.
Received: 21 January 2025; **Accepted:** 8 April 2025; **Effectively published online:** 4 July 2025
Corresponding editor: P.W. Crous

INTRODUCTION

The genus *Lycogala* is one of the earliest myxomycete taxa discovered, with four 'classical' species formally described in the 18th–19th centuries. By the early 20th century, taxonomists had nearly lost interest in this genus due to its relatively simple morphology and low variability. All *Lycogala* species form sessile sporocarps (misinterpreted as aethalia for a long time, see McHugh & Reid 2008), coloured in dull shades of brown and grey, lacking stalks, columellae, or a distinct hypothallus (except for *L. flavofuscum*). Ornamentation of spores and capillitium show little variation within the genus. As a result, no significant progress in the taxonomy of *Lycogala* was observed throughout the 20th and early 21st centuries. In 2022, the genus included only seven recognized species, among which the abovementioned four 'classical' taxa (*L. conicum*, *L. flavofuscum*, *L. epidendrum*, and *L. exiguum*) were consistently referenced in literature, while the rest were known mainly from their original descriptions. The 'classical' species were distinguished mostly by macroscopic traits, such as the size and shape of the sporocarps, reducing the need for detailed microscopic examination of collected material. Many authors chose not to collect herbarium specimens of *Lycogala*, merely recording them in field notes (Leontyev *et al.* 2023a).

Everything changed with the critical revision of the genus *Lycogala* based on molecular and morphological data (Leontyev *et al.* 2022). It was demonstrated that the peridium (the protective covering of the fruiting bodies) exhibits in this genus an exceptional structural diversity, and that patterns in its structure correlate with barcoding data from the 18S rDNA (nucSSU) marker. Subsequently, it became clear that groups of specimens with similar structure of the peridium display characteristics of distinct species, as evidenced by a barcode gap and reproductive isolation tests (Leontyev *et al.*

Fungal Systematics and Evolution is licensed under a Creative Commons Attribution-NonCommercial-NoDerivatives 4.0 International License

© 2025 Westerdijk Fungal Biodiversity Institute

2023a). The number of putative species identified through molecular methods exceeded all expectations: the 2022 study reported 45 species, and the 2023 study identified 66, with mathematical predictions suggesting the total number could exceed 100. This is the highest number of species ever detected during a critical revision of a myxomycete taxon. Nearly all undescribed species discovered in these studies were identified in herbarium collections labelled as *L. epidendrum*, meaning that uncovering the hidden diversity of *Lycogala* essentially amounted to studying the *L. epidendrum* agg. This taxon, long considered as one of the most mundane representatives of the myxomycetes, was revealed to be a highly complex group comprising dozens of unknown species.

In 2023, descriptions of 15 new species within *L. epidendrum* agg., primarily from Europe, were published (Leontyev *et al.* 2023b). The authors identified novel diagnostic criteria for species delimitation, including the pigmentation of immature fruiting bodies, the colour of fresh spore mass, the shape and mutual arrangement of peridial vesicles, and the presence of crystalline and oily deposits within them. Traits such as capillitium and spore ornamentation, traditionally given greater importance in myxomycete taxonomy, appeared to be less useful for *Lycogala*. New species partitioning was supported by nucSSU and cytochrome oxidase subunit I gene (*COI*) phylogenies. However, only the first genetic marker, nucSSU, could be used to barcode all samples. The *COI* sequences were obtained for approximately one-third of the collections due to limited primer specificity.

The discovery of new *Lycogala* species sparked interest in the scientific community. Between 2023 and 2025, regional biodiversity surveys were published for countries such as Belarus, China, Norway, and Ukraine, reporting new occurrences of the recently described taxa (Johannesen & Vetlesen 2024, Leontyev *et al.* 2024, Song *et al.* 2024, Yatsiuk *et al.* 2024). Data on occurrences of these species also appeared on platforms like GBIF and iNaturalist. Additional morphological observations were published as well, including the first documentation of immature fruiting bodies of *L. fossiculatum* (Johannesen & Vetlesen 2024). The species *L. alisaulianovae* was found to exhibit a unique blue colouration of the contents of immature sporocarps, a feature unprecedented in *Reticulariaceae* and rare among bright-spored myxomycetes in general (Johannesen & Vetlesen 2024).

The authors of new species understood that they were describing only a fraction of the revealed diversity. However, the differences between *Lycogala* species are often subtle, while intraspecific polymorphism, on the contrary, can be considerable. For this reason, the authors opted against a 'turbo-taxonomic' approach in favour of an integrative methodology (Riedel *et al.* 2013), and chose to follow the Good Taxonomic Practice rules developed for myxomycetes (Schnittler *et al.* 2025). In this paper, we present a continuation of our work, based on a three-gene phylogeny and morphological analysis of over 700 *Lycogala* specimens collected from Europe, Asia, America, and Australia.

MATERIALS AND METHODS

Collections

The material examined in this study consisted of 716 specimens of *Lycogala*, including 714 studied directly and two involved as a published DNA sequence (Table S1). Analysed specimens and sequences originate from 22 countries and eight macro regions: Europe (473), North Asia (13), South-East Asia (50), East Asia (74), Australia (54), North America (32), Central America (19), and South America (1) (Fig. 1).



Fig. 1. Distribution map for all *Lycogala* specimens involved in this study, created in GPSVisualizer, www.gpsvisualizer.com.

© 2025 Westerdijk Fungal Biodiversity Institute

Type collections of the species, described here, are kept in following collections: CWP (Herbarium of the H.S. Skovoroda Kharkiv National Pedagogical University, Kharkiv, Ukraine), TNSM (National Museum of Nature and Science, Tsukuba, Japan), MCCNNU (Microbial Cultures Centre of Nanjing Normal University, Nanjing, China) and HFNNU (Herbarium of Fungi of Nanjing Normal University, Nanjing, China). Type specimens marked with acronyms IY, JuKl, PMcD and sc are kept in the myxomycete section of the Herbarium of the University of Greifswald, Germany (GFW). All collections involved in the study are listed in Table S1.

Morphological study

Microscopic characters were studied with a Keyence VHX 7000 digital microscope (view in reflected light, RL) and a Leica DM2500 microscope in conjunction with a Flexacam C1 camera (view in natural and polarized transmitted light, TL and PL, respectively). Measurements of microscopic structures were carried out with the application Leica LAS X. Scanning electron microscopy was carried out with a Zeiss Evo LS10 device in the Institute of Microbiology, University of Greifswald.

To study variation in sporocarp size, nearly all available sporocarps were measured for every specimen. Thirty spores, 15 capillitium threads and, on average, 50 peridial vesicles were measured for at least two specimens from each ribogroup (groups of similar ribosomal haplotypes). Measurements of spores included ornamentation. The range of variation in size is given in descriptions as (minimum–) 25 % quartile – 75 % quartile (–maximum) for sporocarps, vesicles, and capillitium, while spore size is shown as (minimum–) Mean−SD – Mean+SD (–maximum). Quantitative values are rounded to two significant digits (three for values over 100), down if closer to the lower bound, up if closer to the upper bound, and the last digit was adjusted to 0 or 5. Raw measurement data are provided in Table S2.

Microscopic slides with peridium pieces were prepared using pure lactic acid as a mounting medium. Microscopy of spores and capillitium was carried out in lactic acid mixed with Methyl blue, as described before (Leontyev *et al.* 2023b). Microphotographs of capillitium and spores were processed with the program Sharpen AI (Topaz Labs, Dallas, Texas, US) to enhance visibility of the surface ornamentation.

Microphotographs not included in the figures of newly described species, along with photographic materials of previously described species and putative taxa not yet formally described (~6000 photographs), are available in the database on Zenodo (https://zenodo.org/records/14963023).

DNA studies

Here and after for the mtSSU gene we do not use the term 12S rDNA, since in myxomycetes the corresponding rRNA molecule has a variable weight (17S in dark-spored myxomycetes, see Jones *et al.* 1990, and unknown in bright-spored). For consistency, we also use the term nucSSU instead of 18S rDNA. Genomic DNA was obtained from spores and amplified following a protocol described earlier (Leontyev *et al.* 2023a). For the amplification of mtSSU sequences we used the primers and PCR protocol developed for *Trichiales* (García-Cunchillos *et al.* 2022). Purified PCR products were sequenced by Macrogen Europe (Netherlands). From one to four sequences were obtained for each specimen and each marker gene, using different primer pairs and forward or reverse primer of each pair. As a result, for this study we obtained 1109 DNA sequences (706 nucSSU, 273 mtSSU, 130 *COI*), including 631 sequences published here for the first time (301 nucSSU, 278 mtSSU, 52 *COI*) (Files S1–S3). Newly obtained sequences were deposited in NCBI GenBank under accession numbers PQ633663−PQ633955, PQ685819−PQ685961 (nucSSU), PQ633386−PQ633662 (mtSSU), and PQ628450−PQ628501, PQ728318−PQ728402 (*COI*). NCBI GenBank codes for all molecular barcodes are provided in Table S1. The first author obtained 698 partial sequences of nucSSU and 116 of cytochrome oxidase subunit I gene (*COI*), including 301 nucSSU, 278 mtSSU, 53 *COI* sequences published in this study for the first time. M. Leontieva obtained 278 mtSSU sequences. W.-L. Song and S.L. Chen obtained for this study 16 nucSSU and 16 COI sequences.

Phylogenetic analysis

All obtained chromatograms were checked and edited in Chromas v. 2.6.6 (https://technelysium.com.au/wp/chromas/) and collected in fasta files using BioEdit v. 7.2.5 (Hall 1999). Sequence sets were aligned in MAFFT webserver (Katoh *et al.* 2019) using the E-INS-I iterative strategy. Resulting alignments include 1582 (nucSSU), 452 (mtSSU), and 601 (*COI*) positions.

For the construction of the Maximum likelihood (ML) phylogenetic trees for each marker gene, the IQ-TREE webserver was used (Trifinopoulos *et al.* 2016). The best evolutionary model selected by ModelFinder (Kalyaanamoorthy *et al.* 2017) as implemented in IQ-TREE was GTR+F+I+G4 for nucSSU and mtSSU, while GTR+F+G4, TPM3+F+G4, and GTR+F+I+G4 were selected for the first, second, and third codon positions of the *COI* gene, respectively. Three types of branch support statistics were employed to evaluate the reliability of trees, including Felsenstein bootstrap with 200 pseudo replicates (Hoang *et al.* 2018), approximate Bayes test and Shimodaira-Hasegawa approximate likelihood ratio test (SH-aLRT). Trees were rooted and edited in FigTree v. 1.4.4 (Rambaut 2018).

For the three-gene phylogenetic analysis, sequence data from 191 specimens of *Lycogala* were selected, and additional 12 specimens of bright- and dark-spored myxomycetes were used as an outgroup. Two representative specimens per every nucSSU ribogroup were selected if possible (i.e. if the ribogroup was not represented by a singleton), with preference to those specimens for which sequences of other genes were also available. Sequences were concatenated using MEGA software (Tamura *et al.* 2021). To remove unalignable parts of sequences (helices), GBlocks (Castresana, 2000) software was used, with the block length and minimum number of sequences for a flank position tweaked to allow less stringent block selection (-b2 = b1+20; -b4 = 8); the rest of parameters were left as default. The concatenated alignment 1442 bp long was partitioned as follows: nucSSU 1–525; mtSSU 526–841; and *COI* 842–1442, with a separate partition assigned for each codon position.

Bayesian inference was performed on the same alignment with MrBayes v. 3.2.7a (Ronquist *et al.* 2012).

© 2025 Westerdijk Fungal Biodiversity Institute

Reversible model jump (NST = MIXED) was applied to explore all possible GTR-models with unlinked rates of reversible substitutions, stationary state frequencies, shape of gamma distribution and proportion of variable sites across partitions. Gamma-distributed rate heterogeneity across sites and a proportion of invariable sites were permitted. Four runs with 20 M generations were done starting with a random tree and utilizing four MCMC chains, with stop rule deactivated. Trees were sampled every 1000 generations, and 25 % fraction was discarded as burn-in. Results of the Bayesian analysis were examined in Tracer v. 1.7.1 (Rambaut *et al.* 2018). The analysis ended with convergence of parameters (combined ESS > 2000). However, topological convergence was not reached after this number of generations (ASDSF = 0.028). It resulted in the consensus tree with polytomies at deeper nodes. The analysis was repeated on the full (not trimmed) concatenated alignment with 2603 positions. After 20 M generations mixing was poor and neither parameter nor topology convergence was reached (combined ESS for many key parameters < 100, ASDF = 0.12). An additional 15 M generations did not improve convergence. Similarly, tuning the temperature of heated chains, simplification of partitioning and evolutionary models have not made any significant improvements to analyses. Overall, the Bayesian interference pointed at disagreements in topologies between employed genes.

The maximum likelihood single-gene trees were used to infer a species tree under the multi-species coalescent model (Rannala & Yang 2003) using wASTRAL v. 1.20.3.7 (Zhang & Mirarab 2022). The analysis was done with the default weighting mode ("hybrid"), 30 initial rounds of placements, 30 rounds of subsampling per exploration step and branch local posterior probability values (Sayyari & Mirarab 2016) written to the final species tree. Multiple sequenced individuals from the same putative or described species were marked to belong to one species.

Species delimitation

Preliminary species delimitation was carried out separately for each marker gene using the Assemble Species by Automatic Partitioning (ASAP, Puillandre *et al.* 2021) algorithm employing the Kimura (K80) 2.0 distance model. Five best scores were calculated for each marker.

The reproductive isolation was tested by checking correspondence between nucSSU, mtSSU and *COI* groups in specimens for which more than one marker was obtained (see explanation in Leontyev *et al.* 2023a). Each sequence variant (haplotype) of every gene was assigned a unique numeric code. The combined file was then put through the GUI python program LineChart (Shchepin *et al.* 2021), which visualizes the combinations of haplotypes that were observed in the studied individuals. Groups of connected haplotypes – those that appear as linked nodes on the recombination diagram – are considered as freely recombining.

RESULTS

Molecular delimitation of species

The nucSSU gene is widely used for molecular barcoding and species delimitation in myxomycetes (Leontyev & Schnittler 2017, 2022). The obtained 706 partial sequences of this gene were analysed by ASAP to provide the preliminary distance-based species delimitation scheme. Five best score partitions grouped our sequences in 83–107 putative species (Fig. S1). The lowest (best) score was obtained for the partition with 97 species hypotheses, designated here as ribogroups. With this partition, the Chao1 index predicts that the total number of ribogroups within *Lycogala* may reach 183. In the nucSSU phylogeny (see File S1), nearly all 97 ASAP-delimited ribogroups form monophyletic branches and correspond well to preliminary delineated morphological species. The partial exception is *L. epidendrum* s. str., an extremely variable taxon (Leontyev *et al.* 2023a), which the ASAP proposed to separate into five species (01j, 01n, 01o, 01q and the rest of subgroups). However, in the present paper we considered all *L. epidendrum* as a single ribogroup, taking into account that (i) subgroups 01n and 01q are not separated phylogenetically from the rest of the species, as seen from the nucSSU phylogeny, and (ii) that the delimitation of *L. epidendrum* subgroups strongly varies in ASAP analyses and single-gene trees based on other markers (see below). After fusion of all *L. epidendrum* groups, the total number of ribogroups assigned for the genus *Lycogala* reached 93. The numbering of ribogroups used in previous publications (Leontyev *et al.* 2023a, b) has been retained wherever possible.

The ASAP delimitation of mtSSU was carried out for 273 sequences, which represent 59 nucSSU-based ribogroups. The five best score partitions grouped our sequences in 75–89 putative species, with the lowest score obtained for 77 species (Fig. S2). Among them, 16 are sub-branches of *L. epidendrum* s. str. All others are congruent to the nucSSU ribogroups with minor modifications: rg08, 37, 47 are split in two, while related rg54 and 80 are merged into one.

The ASAP delimitation of *COI* was carried out for 130 sequences, which represent 31 nucSSU-based ribogroups. The five best score partitions grouped our sequences in 24–33 putative species, with the lowest score for 32 species (Fig. S3). Among them, three are sub-branches of *L. epidendrum* s. str. that are poorly represented in our *COI* alignment, and the rest corroborate *nucSSU* ribogroups, with one exception of related rg15 and 91, forming a single group in the *COI* delimitation.

The recombination test by LineChart revealed no evidence of recombination between ribogroups (Figs S4, S5). In all cases, specimens that belong to different nucSSU ribogroups also belong to different mtSSU and *COI* groups. This provides evidence that ASAP-based species hypotheses correspond to groups with mutually exclusive allele sets. For non-singleton ribogroups, intricate within-group connections are typical. Within *L. epidendrum* s. str., most of nucSSU phylogeny-based subgroups show an isolation from each other, but with a number of exceptions: within-group connections are found for clusters b1+b2+h+v+w, c+p, and d+i.

The species hypotheses, based on the recombination test results and the ASAP delimitations for three marker genes, are summarized in Fig. 2.

© 2025 Westerdijk Fungal Biodiversity Institute

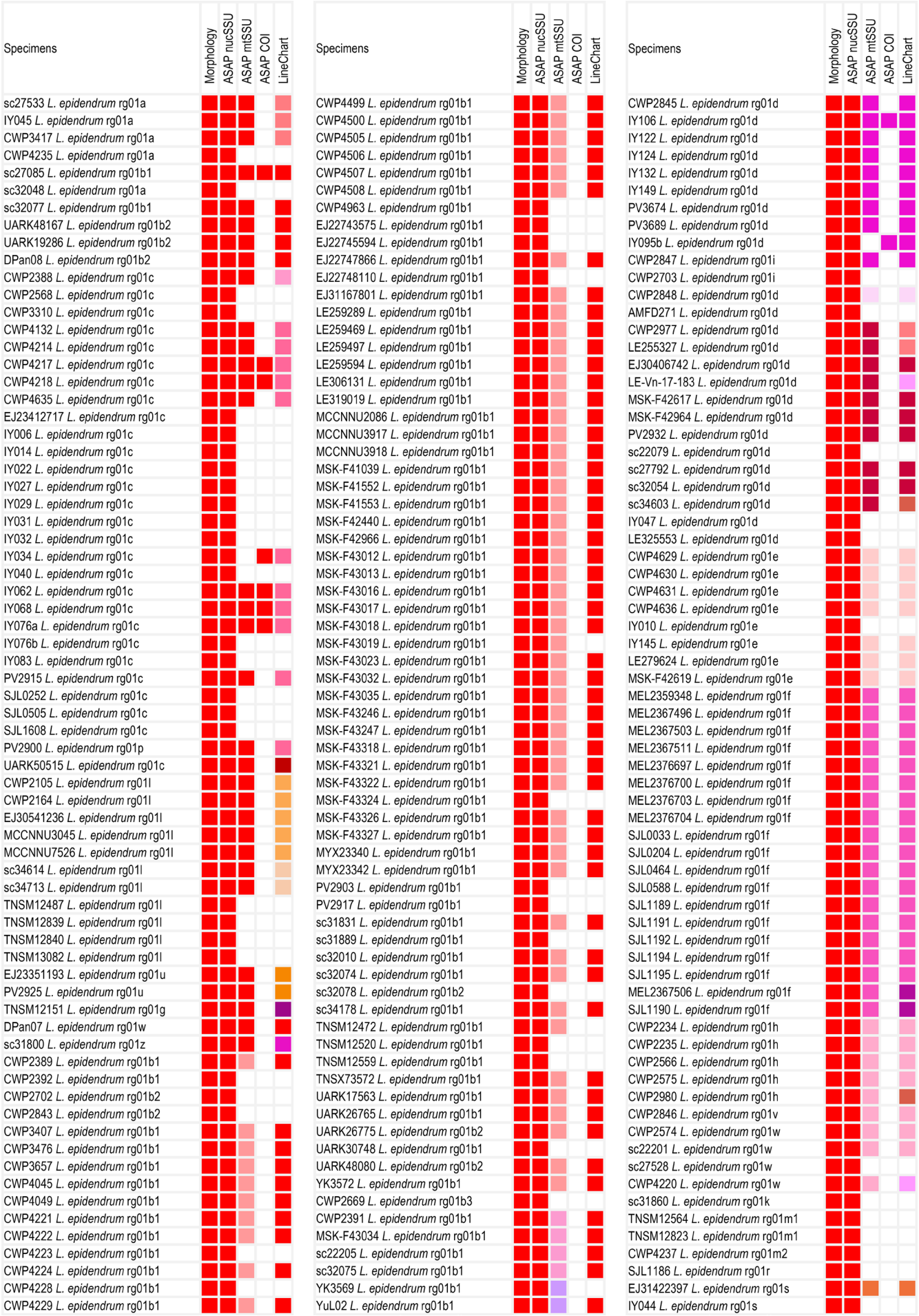

Fig. 2. Species delimitation in the genus *Lycogala* based on morphology, ASAP analysis of three marker genes, and recombination test in LineChart. In the first four columns, each colour represents a distinct species hypothesis. In the recombination test, colours indicate groups of specimens sharing common alleles (haplotypes) for any marker gene.

© 2025 Westerdijk Fungal Biodiversity Institute

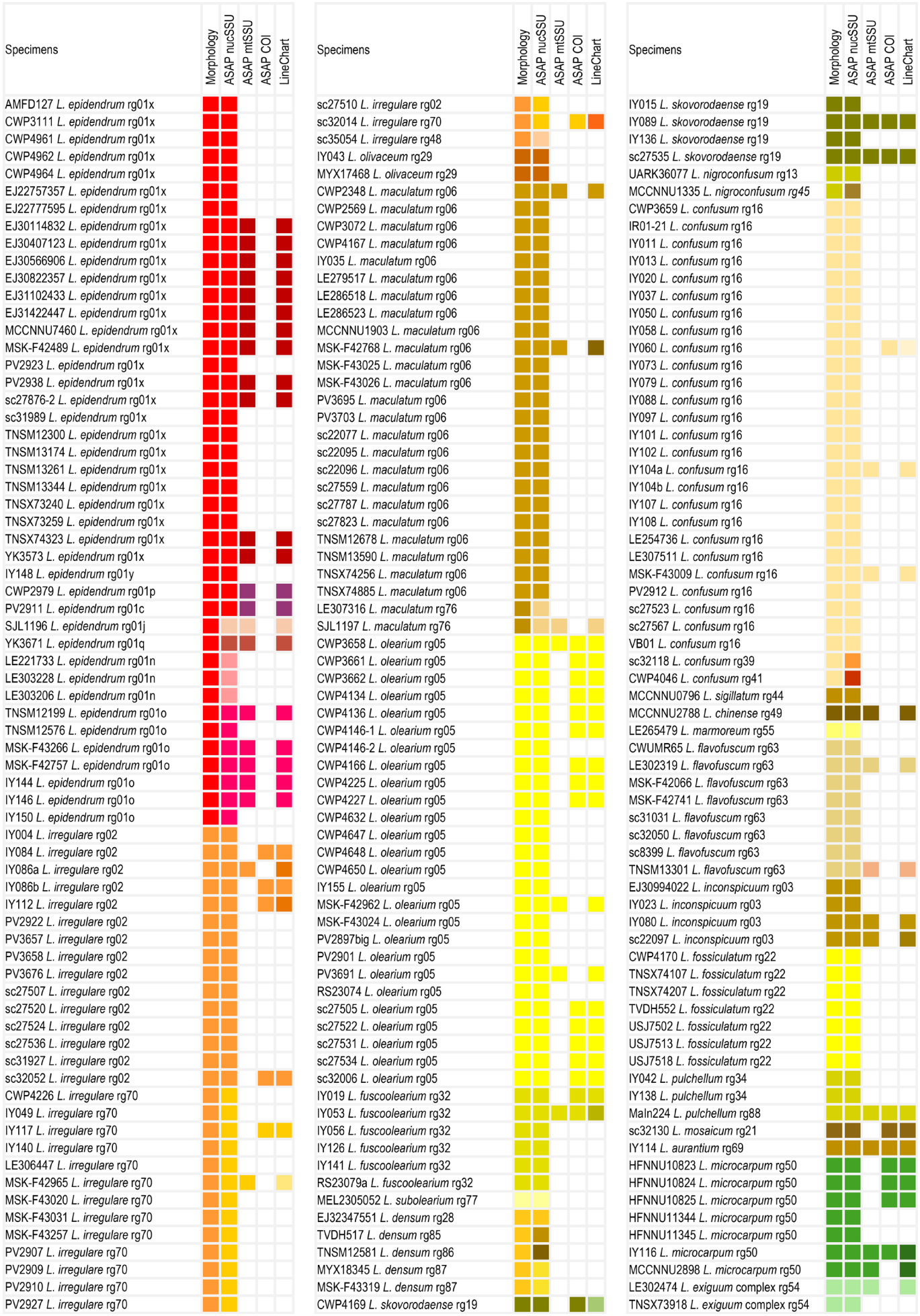

Fig. 2. (Continued).

© 2025 Westerdijk Fungal Biodiversity Institute

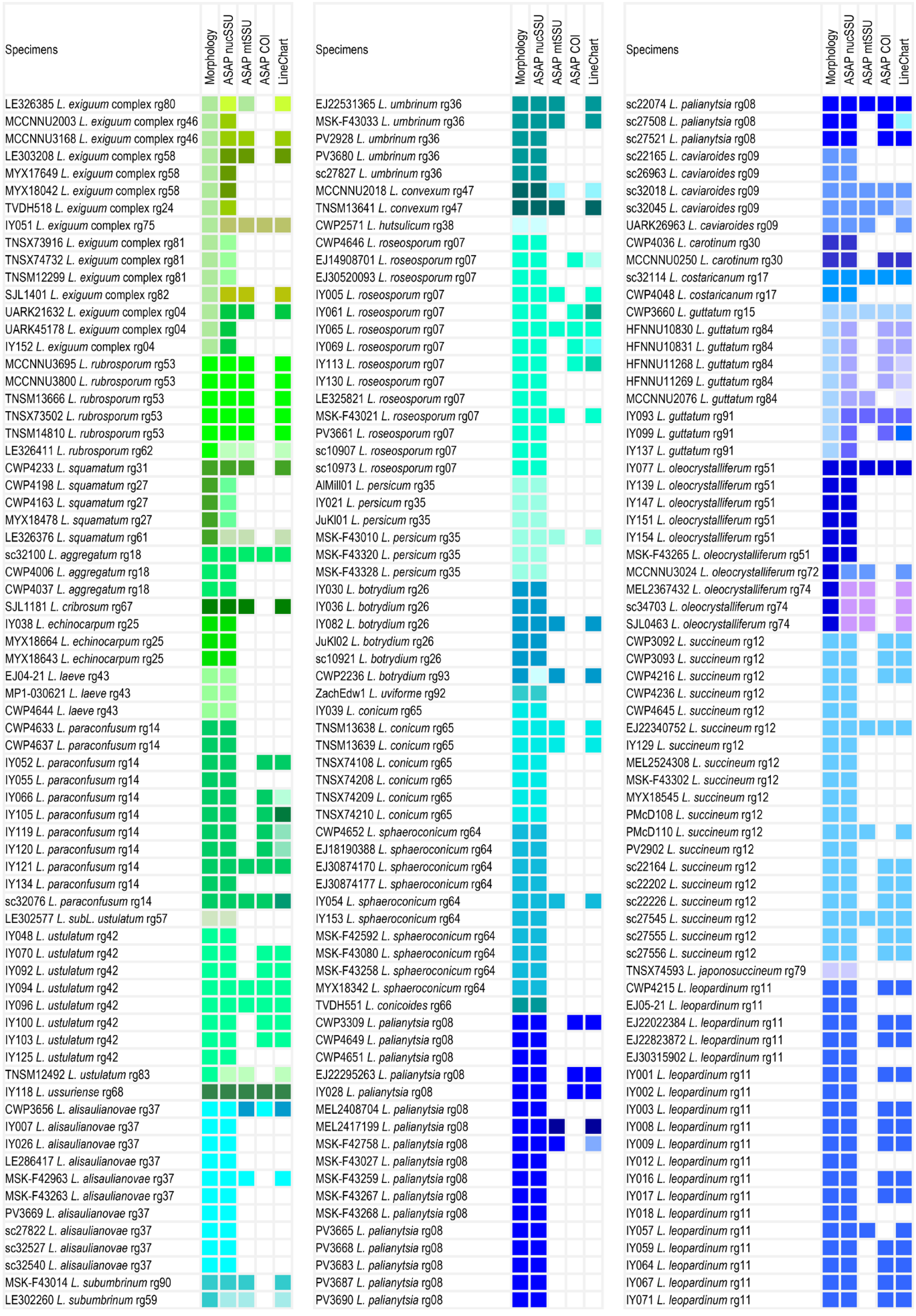

Fig. 2. (Continued).

© 2025 Westerdijk Fungal Biodiversity Institute

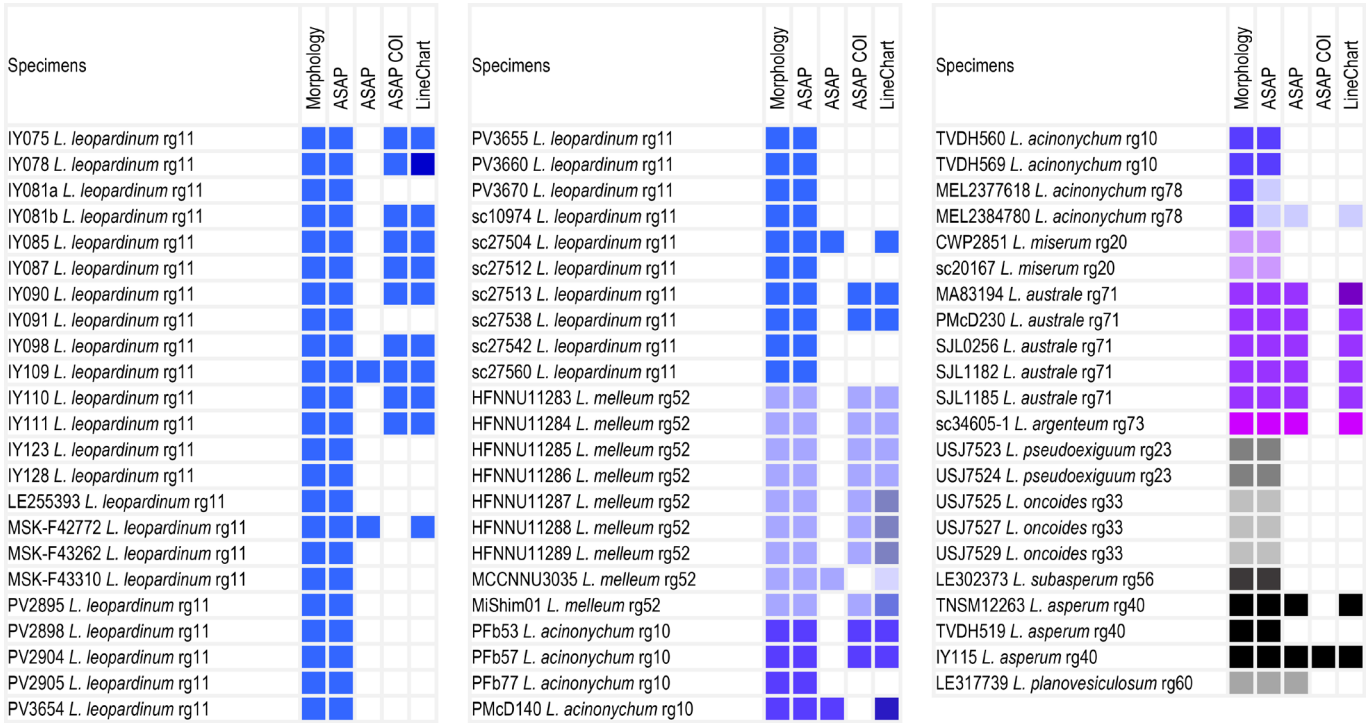

Fig. 2. (Continued).

Morphological delimitation of species

Morphological examination of barcoded specimens allowed, in some cases, the grouping of related ribogroups into provisional morphological species complexes, including *Lycogala botrydium* (rg26, 93), *L. densum sp. nov.* (rg28, 85–87), *L. guttatum sp. nov.* (rg15, 84, 91), *L. irregulare* (rg02, 48, 70), *L. oleocrystalliferum sp. nov*. (rg52, 72, 74), *L. pulchellum sp. nov.* (rg54, 88), *L. rubrosporum sp. nov.* (rg53, 62), *L. squamatum sp. nov.* (rg27, 31, 61), and *L. ustulatum sp. nov.* (rg42, 83).

As a result of integrating molecular and morphological data, the 92 identified ribogroups were grouped into 63 morphological species. Of these, five were described before 2023, 15 were described in 2023 (Leontyev *et al.* 2023b), 24 are described in this study (Figs 5–7, 9–29), and an additional 18 remain undescribed, primarily due to insufficient data. A complete database of macro- and microphotographs taken for all these species, including the undescribed ones, is available on Zenodo (https://zenodo.org/records/14963023).

Deep phylogeny and delimitation of sections

A three-gene ML phylogeny based on 191 most representative specimens (Fig. 3) has shown that most of 63 putative species of *Lycogala* form five major clades (I–V), which, however, receive rather low support: I: 35.3/0.656/48, II: 85.2/0.92/8, III: 72.4/0.54/8, IV: 97.6/1/27, and V: 31.8/0.676/9 (SH-aLRT/aB/BS). Five species were not included into these groups and formed a staircase-like series of basal branches. A very similar grouping of species in five branches was obtained in a coalescent species tree (CST) (Fig. 4), based on single-gene trees (Figs S6–S8). In its unrooted version, all 63 species branch within five clades. The composition of these branches corresponds well with the ML phylogeny; exceptions include positions of *L. botrydium* (IV in ML / V in CST), *L. pulchellum* (II/IV), *L. oncoides* (basal clade/I), and several undescribed taxa. The statistical support values for branches in the coalescent tree are 0.67, 0.83, 0.67, 0.82, 0.83 for the clades I–V, respectively. Bayesian inference could not resolve deep branches of the genus *Lycogala* (Fig. S9). However, it reconstructed the clade I (support 0.83), II (0.82), most of V (0.53), and two main sub-branches of clades III (0.80, 0.53) and IV (1, 0.53).

Although branch supports do not allow for reliable conclusions about deeper phylogenetic relationships within the genus *Lycogala*, species included in the five reconstructed clades share a set of morphological characteristics, mainly related to the spatial arrangement and contents of peridial vesicles. Given that the present study identifies already 44 species within *Lycogala* (excluding several problematic taxa, see Lado 2005–2025), to facilitate orientation in this large genus we suggest to divide it into five sections.

TAXONOMY

Lycogala Adans., *Fam. pl*. **2**:7. 1763.

Lycogala* sect. *Lycogala

Diagnosis: Section unites species with solitary peridial vesicles, rather irregular in shape and variable in size, with both oil and crystals absent.

Description: *Sporocarps* large, grouped, often deformed from mutual pressure. *Vesicles* under RL hardly visible, faint or distinct (*L. maculatum*); greyish patches of dried slime often present. Vesicles under TL loosely or densely (*L. maculatum*) distributed, solitary, variable in size, irregular in shape, light brownish to brown. *Oil* and *crystals* in vesicles absent or nearly absent. *Capillitium* ornamented with bracelets. Fresh *spore mass* coloured in pale colours: beige, dull pinkish.

© 2025 Westerdijk Fungal Biodiversity Institute

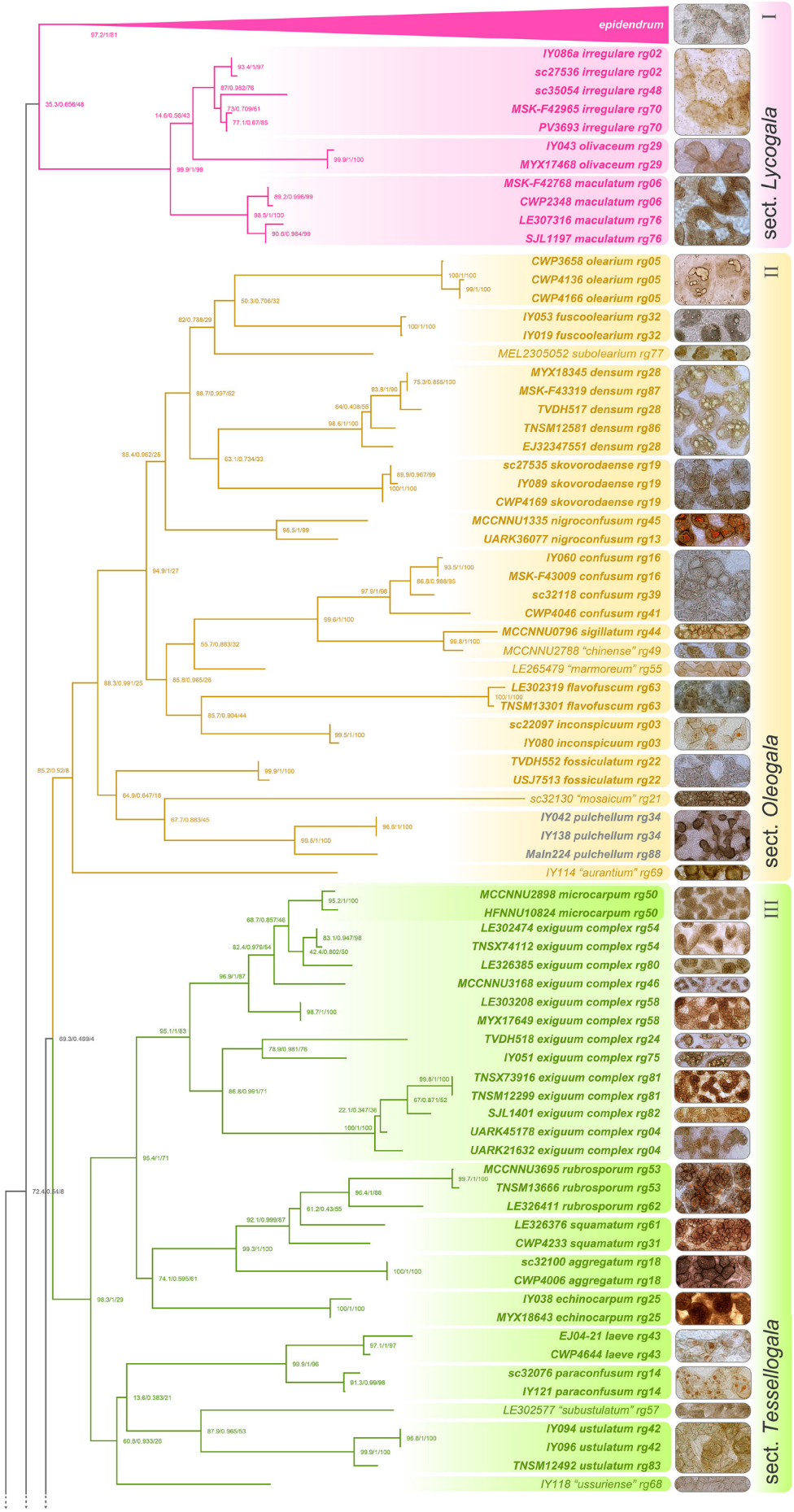

Fig. 3. Three-gene maximum likelihood phylogeny of the 191 representative specimens of *Lycogala*, based on 191 nucSSU, 118 mtSSU and 44 *COI* sequences. Branch support is shown as follows: Shimodara-Hasegawa SH-aLRT test / Approximate Bayes test / non-parametric (Felsenstein) bootstrap test (200 pseudoreplicates). Microphotographs show the typical microscopic appearance of the peridium for every morphospecies in transmitted light.

© 2025 Westerdijk Fungal Biodiversity Institute

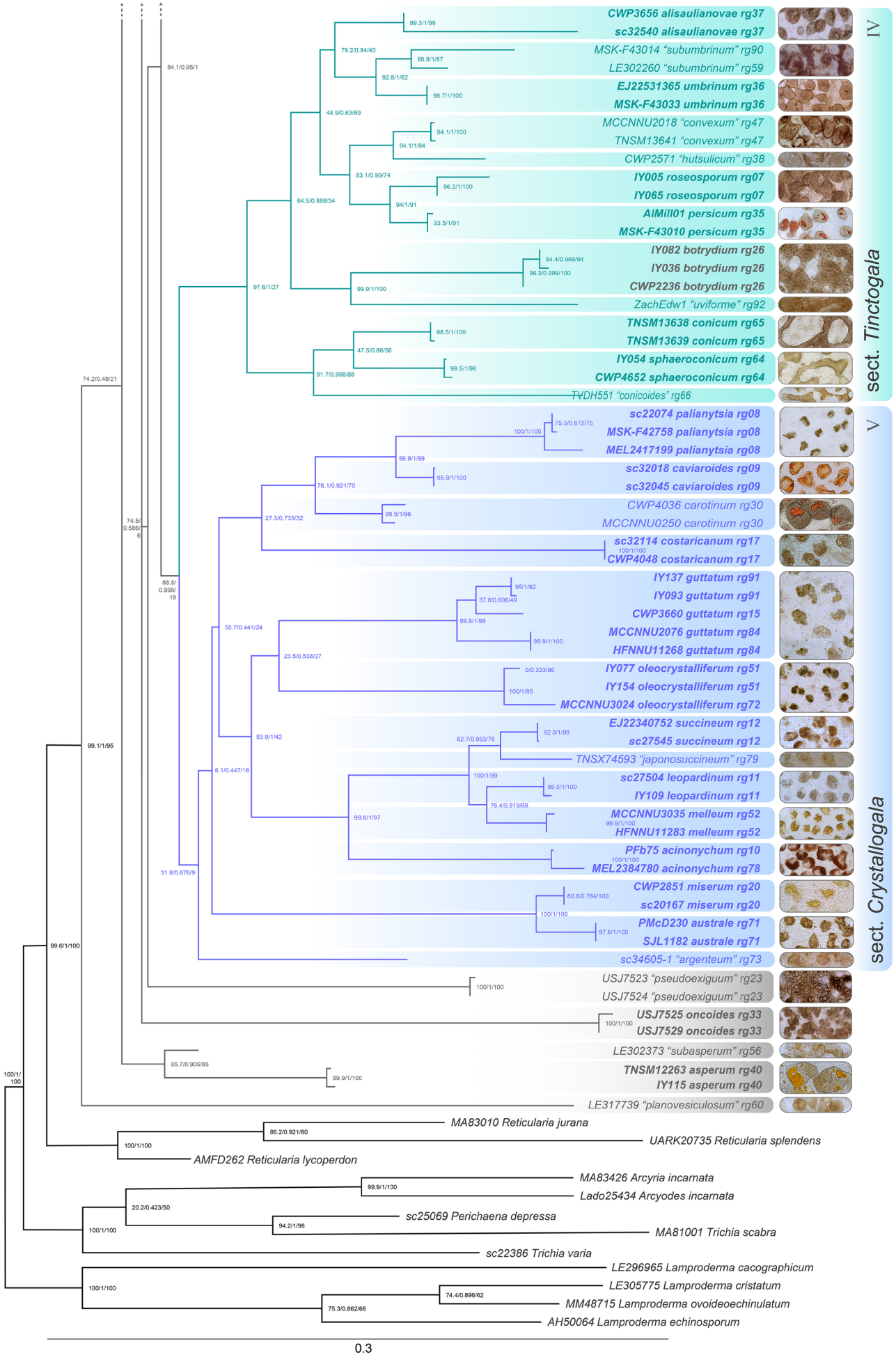

Fig. 3. (Continued).

© 2025 Westerdijk Fungal Biodiversity Institute

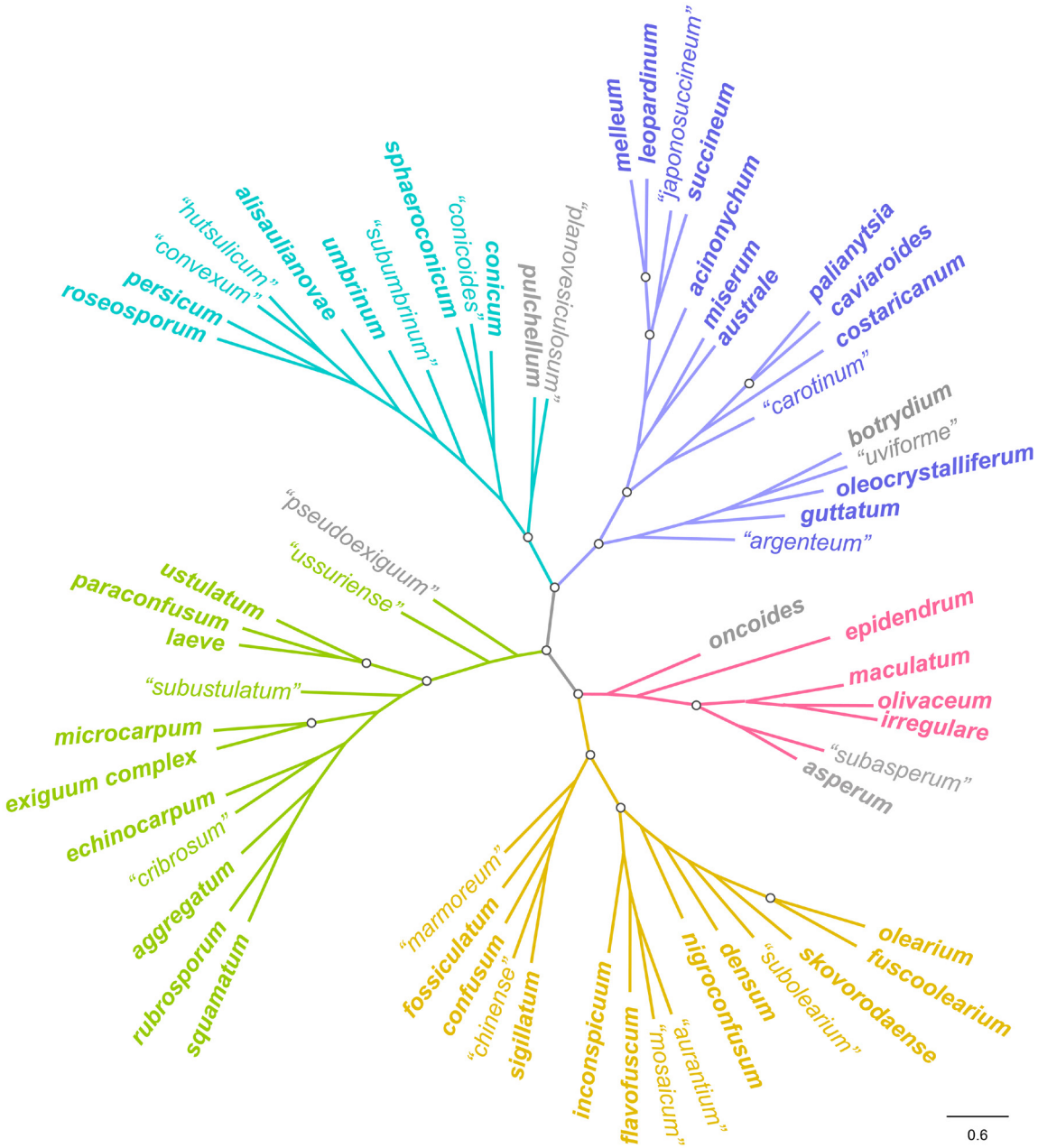

Fig. 4. Coalescent species tree based on three single-gene phylogenies built from 715 nucSSU, 278 mtSSU, and 130 *COI* sequences. Branch local posterior probabilities ≥ 0.8 are shown as hollow circles. Colours indicate the assignment of species to sections (the same as in Fig. 3); grey colour is used for species not assigned to any section.

Typus: Lycogala epidendrum (L.) Fr.

Species: *L. epidendrum*, *L. irregulare*, *L. maculatum*, *L. olivaceum.*

Lycogala* sect. *Oleogala Leontyev, Yatsiuk & Schnittler, ***sect. nov.*** MB 857822.

Etymology: *Oleum* (Latin), oil, and *gala* (Greek), milk, referring to the presence of oil in peridial vesicles and the attribution of the section to the genus *Lycogala*.

Diagnosis: Section unites species with peridial vesicles filled with considerable amount of oil.

Description: *Sporocarps* of different size, solitary or grouped, and in this case often deformed from mutual pressure. *Vesicle* pattern on the peridium distinct under RL, if not covered with patches of dried slime (*L. flavofuscum*); light or dark brown. Vesicles under TL densely distributed, solitary (*L. olearium*, *L. fuscoolearium*) or forming small compact rows and clusters with typically < 10 vesicles in one group. *Oil* in vesicles abundant, at least partially represented by conspicuous droplets, colourless, reddish or brownish. *Crystals* in vesicles absent or occasional (*L. fuscoolearium*). Rings or at least large, rounded pits present in ornamentation of *capillitium* and *peridium*. Fresh *spore mass* coloured in pale colours: beige, dull pinkish.

Typus: *Lycogala olearium* Leontyev, *et al.*

Species: *L. confusum*, *L. densum*, *L. flavofuscum*, *L. fossiculatum*, *L. fuscoolearium*, *L. inconspicuum*, *L. olearium*, *L. sigillatum*, *L. skovorodaense.*

© 2025 Westerdijk Fungal Biodiversity Institute

Lycogala* sect. *Tessellogala Leontyev, Yatsiuk & Schnittler, ***sect. nov.*** MB 857823.

Etymology: *Tesselatus* (Latin), decorated with a mosaic, and *gala* (Greek), milk, referring to the aggregated vesicles and the attribution of the section to the genus *Lycogala*.

Diagnosis: Section unites species with peridial vesicles forming large aggregates.

Description: *Sporocarps* small, scattered or grouped, more-or-less rounded in shape. *Vesicle* pattern on the peridium distinct, or faint (*L. laeve*) under RL, usually dark brown to black. Vesicles under TL densely distributed, forming large aggregates typically > 10 vesicles in one group; aggregates rounded, ovoid, rosette-shaped, papillate, or forming irregular reticulum. *Oil* in vesicles present, in form of granular material or droplets, colourless, brownish, or orange (*L. paraconfusum*, *L. rubrosporum*, *L. squamatum*). *Crystals* in vesicles absent or very scanty (*L. aggregantum*). *Capillitium* ornamented with small pits. Fresh *spore mass* beige, dull pinkish, or orange red (*L. rubrosporum*).

Typus: *Lycogala exiguum* Morgan

Species: *L. echinocarpum, L. exiguum, L. laeve, L. microcarpum, L. paraconfusum, L. rubrosporum, L. squamatum, L. ustulatum.*

Lycogala* sect. *Tinctogala Leontyev, Yatsiuk & Schnittler, ***sect. nov.*** MB 857824.

Etymology: *Tincto* (Latin), to dye, and *gala* (Greek), milk, referring to the bright pigmentation of sporocarps and spores, and the attribution of the section to the genus *Lycogala*.

Diagnosis: Section unites species with solitary or fused, but not aggregated peridial vesicles, and with bright pigmentation of immature fructification and spore mass.

Description: *Sporocarps* small or medium in size, scattered or grouped, rounded, egg-shaped, fusiform, conical. Pinkish, lilac or umber tint often present in the pigmentation of mature sporocarps. *Vesicles* under RL distinct, dark brown to black, with glossy or at least smooth surface. Vesicles in TL solitary, more-or-less uniform in size, isodiametric, or branched (*L. sphaeroconicum*) and even fused into the network (*L. conicium*). *Oil* in vesicles nearly absent, or present as inconspicuous granular matter, rarely in form of red droplets (*L. persicum*). *Crystals* in vesicles absent. *Capillitium* ornamented with small pits. Fresh *spore mass* saturated pink (*L. roseosporum*, *L. persicum*), blue, fading to green (*L. alisaulianovae*), beige (*L. umbrinum*).

Typus: Lycogala roseosporum Leontyev, *et al.*

Species: Includes *L. alisaulianovae*, *L. conicum*, *L. persicum*, *L. roseosporum, L. sphaeroconicum*, *L. umbrinum.*

Lycogala* sect. *Crystallogala Leontyev, Yatsiuk & Schnittler, ***sect. nov.*** MB 857825.

Etymology: *Crystallus* (Latin), crystal, and *gala* (Greek), milk, referring to the presence of crystals in peridial vesicles and the attribution of the section to the genus *Lycogala*.

Diagnosis: Section unites species with solitary peridial vesicles, regularly rounded in shape, uniform in size, evenly distributed, filled with crystals and/or yellow oily accumulations.

Description: *Sporocarps* medium in size to large, grouped, more-or-less rounded in shape. *Vesicles* under RL distinct, looking like dried droplets, evenly distributed, brown, honey yellow, orange or red. Vesicles under TL solitary, rounded or irregular (*L. australe*) in shape, filled with homogenous material. *Crystals* in vesicles present in considerable amount (visible under PL), rarely inconspicuous, and in this case yellow *oil* accumulations become visible (*L. australe, L. guttatum*, *L. melleum*, *L. miserum*). Orange *pigment*, not included in oil droplets, may be present in vesicles (*L. caviaroides*). *Capillitium* ornamented with bracelets. Fresh *spore mass* light-coloured: pinkish white, warm grey, beige.

Typus: *Lycogala leopardinum* Leontyev, *et al.*

Species: *L. acinonychum*, *L. australe*, *L. caviaroides*, *L. costaricanum*, *L. guttatum*, *L. leopardinum*, *L. melleum*, *L. miserum*, *L. oleocrystalliferum*, *L. palianytsia*, *L. succineum.*

***Lycogala* sect. incertae sedis:** *L. asperum*, *L. botrydium*, *L. oncoides*, *L. pulchellum.*

Lycogala persicum Leontyev, J. Kluša, E. Moroz, Millican & Ishchenko, ***sp. nov.*** MB 857826. Fig. 5.

Etymology: *Prunus persica* (Latin) peach, referring to the colour of the peridium.

Diagnosis: Similar to *L. roseosporum* but differs by much larger colonies, smaller sporocarps, sparser peridial vesicles, and red oil accumulations in vesicles.

Sporocarps in large, scattered groups, spherical to short horizontally ovoid, regular in shape, (0.5–)1–2.5(–3.5) mm diam. *Peridium* membranous, light reddish brown, covered by vesicles. *Peridial vesicles* (40–)90–150(–230) µm, in RL brown to black, solitary, convex, somewhat unevenly distributed, free or forming loose groups, in TL simple, ovoid or angular, brown. Vesicle walls light-brown, thin (1 µm), 1–2-layered. *Crystals* absent. *Oil* droplets numerous, from large to small, more-or-less rounded, saturated red. *Granular deposits*, if present, represented by small oil droplets. *Inner surface of the peridium* smooth or covered by rings 1–2 µm diam. *Capillitium* tubular, 4–9 µm diam., with smooth contour; surface fine pitted-warty. *Spore mass* bright pink. *Spores* (5.5–)6.5–7.5 µm diam., hyaline, reticulate, 6–8 meshes across diam., unornamented area occupies 1/4–1/5 of the spore surface. *Immature fructifications* bright pink, then light lilac.

Typus: **Latvia**, Pierīga, Jurmala, forest south of Kemeri, Kemeri National Park, (56.93383 23.49452), on a log of *Picea abies*, bare of bark, overgrown with moss, algae, and lichens, 1 Jul.

© 2025 Westerdijk Fungal Biodiversity Institute

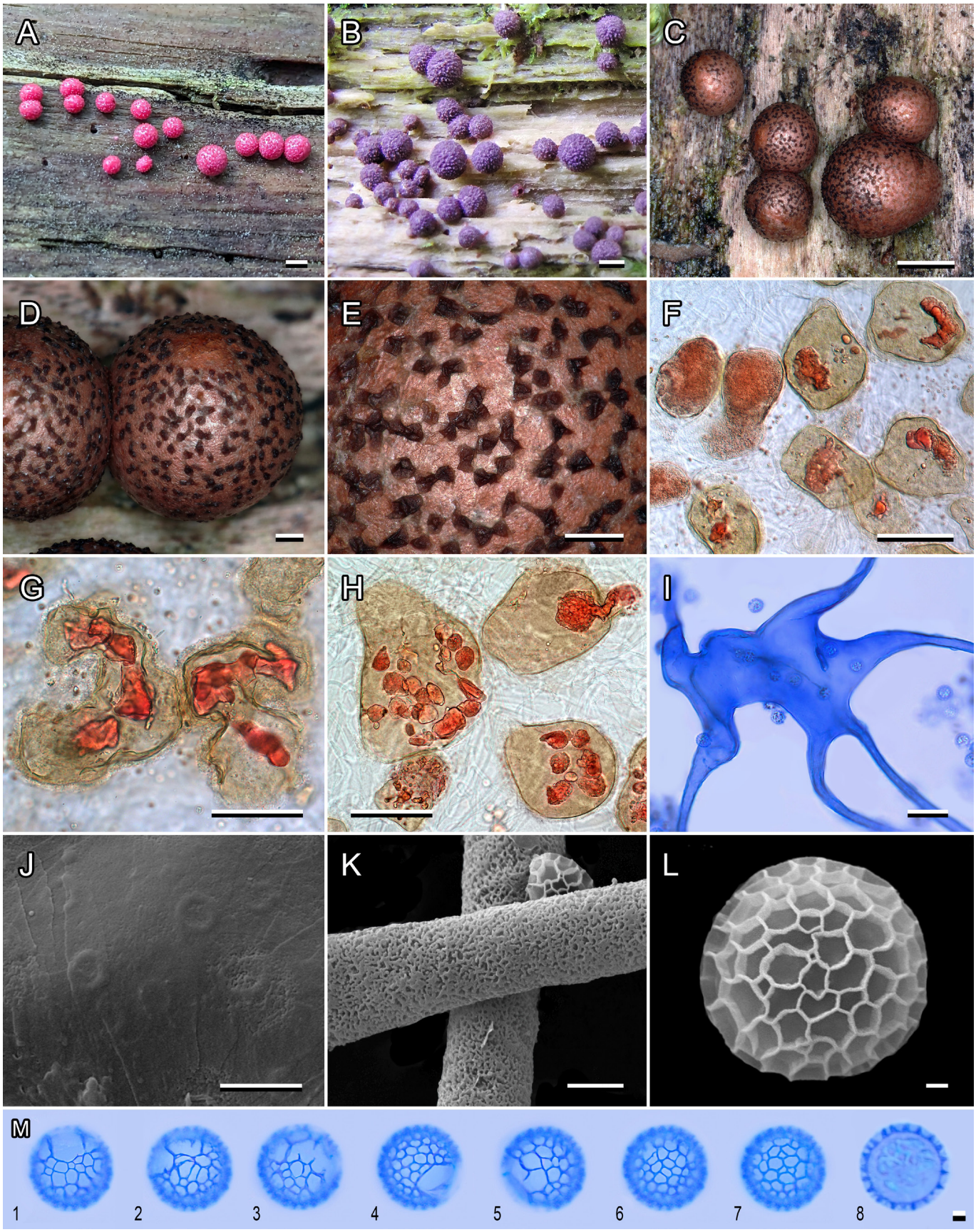

Fig. 5. *Lycogala persicum sp. nov.* [A, I, M. AlMill01; B. HollyJones01; C–H, J–L. JuKl01 (holotype)]. **A, B.** Immature fructifications (A – courtesy of A. Millican; B – courtesy of H. Jones). **C, D.** Sporocarps. **E.** Peridium in RL. **F–H.** Peridial vesicles in TL. **I.** Capillitium and spores, methyl blue in lactic acid. **J.** Inner surface of the peridium, SEM. **K.** Capillitial tubules, SEM. **L.** Spore, SEM. **M.** Spores, methyl blue in lactic acid. The last spore is shown in optical section. Scale bars: A–C = 1 mm; D, E = 250 µm; F–H = 100 µm; I = 20 µm; J, K = 5 µm; L = 0.5 µm; M = 1 µm.

© 2025 Westerdijk Fungal Biodiversity Institute

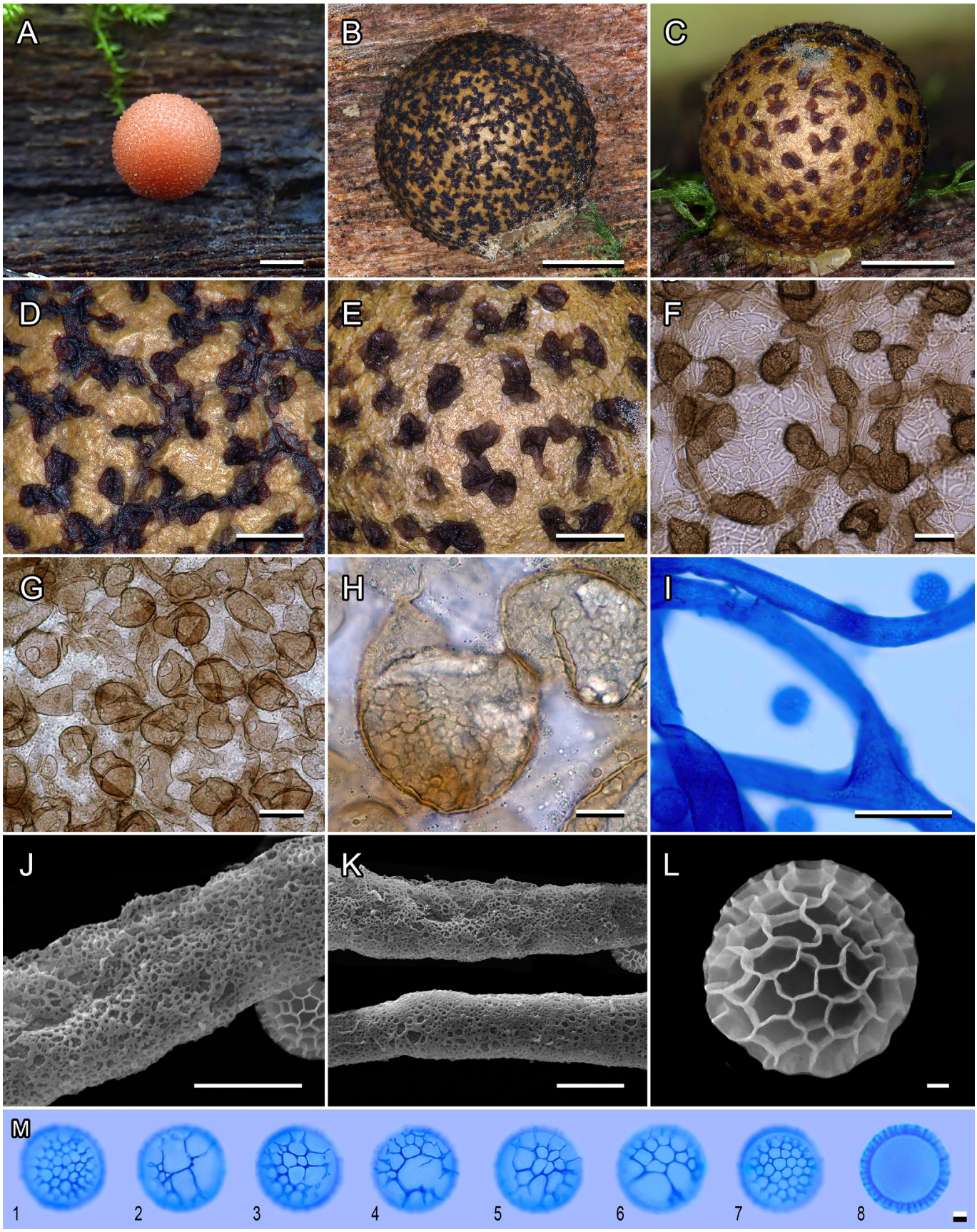

Fig. 6. *Lycogala pulchellum sp. nov.* [A, B, D, I–M. IY042; C, E, F. CWP2560 (holotype); G, H. MaIn224]. **A.** Immature fructification. **B, C.** Sporocarps. **D, E.** Peridium in RL. **F, G.** Peridial vesicles in TL. **H.** Peridium vesicles, covered by chain-mail ornamentation, TL. **I.** Capillitium and spores, methyl blue in lactic acid. **J, K.** Capillitial tubules, SEM. **L.** Spore, SEM. **M.** Spores, methyl blue in lactic acid. The last spore is shown in optical section. Scale bars: A–C = 1 mm; D, E = 250 µm; F, G = 100 µm; H, I = 20 µm; J, K = 5 µm; L = 0.5 µm; M = 1 µm.

© 2025 Westerdijk Fungal Biodiversity Institute

2023, *J. Kluša* (**holotype** GFW JuKl01). GenBank: nucSSU = PQ633803 (rg35).

Distribution: Europe (Belarus, Latvia, Russia), North America (Canada, USA). Hereinafter, refer to Table S1 for additional materials examined.

Notes: This beautiful myxomycete forms large colonies, which is quite unusual for *Lycogala* species with small (> 2 mm) sporocarps. In their young state, the sporocarps of *L. persicum* exhibit an exceptionally bright"chemical" pink colour, surpassing in intensity all other members of the genus. Based on the geographic distribution of records, the species seems to be associated with the boreal forest zone. From the related and similar *L. roseosporum*, *L. persicum* differs by the traits specified in the diagnosis.

Lycogala pulchellum Leontyev, Ishchenko, M. Inoue & V. Botyakov, ***sp. nov.*** MB 857827. Fig. 6.

Etymology: *Pulchellus* (Latin) pretty, charming.

Diagnosis: Differs from the rest of *Lycogala* species by small single light yellow sporocarps, densely covered with dark solitary peridial vesicles, the surface of which possesses the 'chain-mail' ornamentation.

Sporocarps solitary, spherical, regular in shape, 2–2.5 mm diam. *Peridium* membranous, yellowish brown, covered by vesicles. *Peridial vesicles* (60–)90−130(–180) µm, in RL dark brown, solitary, folded, free or forming loose groups, which sometimes merge into irregular network, in TL simple, ovoid or blot-shaped, brown. Vesicle walls brown, thin (1–2 µm), 1–layered, covered with 'chain-mail' ornamentation, which consists of densely arranged rings 5–10 µm diam. *Crystals* absent. *Oil* droplets sparse, from large to small, variable in shape, colourless. *Granular deposits* not observed. *Inner surface of the peridium* smooth. *Capillitium* tubular, 3–11 µm diam., with smooth or slightly uneven contour; surface fine pitted-warty, with occasional ring-shaped islets. *Spore mass* light beige to dirty white. *Spores* (5–)5.5–7.5 µm diam., hyaline, reticulate, 6–8 meshes across diam., unornamented area inconspicuous, represented by zone with larger meshes (2–4 across diam.). *Immature fructifications* light orange.

Typus: **Ukraine**, Ivano-Frankivsk Region, Halytskyi National Nature Park (49.0915 24.7175), on dead wood of *Fagus sylvatica*, 17 Aug 2010, *D. Leontyev* (**holotype** CWP2560). GenBank: nucSSU = OM423823 (rg34).

Distribution: Asia (Japan), Europe (Russia, Ukraine).

Notes: Species of the genus *Lycogala* with small solitary sporocarps are difficult to study: both their size and abundance present obvious challenges. However, among these species, *L. pulchellum* stands out for its unusual appearance and, when well-preserved, can be identified even without dissection. The contrast between the bright yellow peridium and large dark brown vesicles, along with the absence of coloured oil droplets and crystalline deposits, distinguishes *L. pulchellum* from *L. inconspicuum* and *L. asperum*. The presence of simple vesicles ornamented with a 'chain-mail' pattern differs it from *L. exiguum*, *L. rubrosporum*, and *L. microcarpum*.

Lycogala sphaeroconicum Leontyev, E. Moroz, Ishchenko, E. Johannesen, Schnittler, T. Kudryavtseva & Bortnikov, ***sp. nov.*** MB 857828. Fig. 7.

Etymology: *Sphaera* (Greek) ball, globe, and *conus* (Latin) cone, referring to the similarity to *L. conicum*, yet with more spherical sporocarps.

Diagnosis: Differs from *L. conicum* by egg-shaped, blunt spindle-shaped, to almost spherical sporocarps and by shorter peridial vesicles, which do not from a regular reticulum.

Sporocarps in large and rather dense groups, vertically elongated, ovoid, egg-shaped, fusiform, spherical, (1–)2–2.5 mm high, 1–1.5 mm diam. *Peridium* membranous, light greyish brown, densely covered by vesicles. *Peridial vesicles* (20–)50–80(–90) µm wide, (50–)100–300(–600) µm long, in RL glossy, black, brownish black, solitary, flattened, with thickened edges, forming a kind of labyrinth, in TL simple, elongate, worm-like, branched, often touching each other but not merging into regular reticulum, brown. Vesicle walls light brown, thin (1 µm), 1–2-layered. *Crystals* absent. *Oil* present in form of *granular deposits*, colourless. *Inner surface of the peridium* smooth. *Capillitium* tubular, 1–2(–3) µm diam., with smooth contour; surface fine pitted-warty or completely smooth, occasionally with large (2–4 µm) ring-shaped islets, which may exceed the diameter of the tube. *Spore mass* warm greyish. *Spores* 5.5–6(–7) µm diam., hyaline, reticulate, 7–9 meshes across diam., unornamented area occupies 1/4–1/5 of the spore surface. *Immature fructifications* bright red.

Typus: **Russia**, Moskovskaya Oblast: Dmitrov, Buharovo (56.08929 37.28996), on the fallen rotting tree trunk, 21 Jul. 2021, *T. Kudryavtseva* (**holotype** GFW IY054). GenBank: nucSSU = PQ633706 (rg64); mtSSU = PQ633457.

Distribution: Europe (Belarus, Germany, Norway, Russia).

Notes: This species is related to and similar to *L. conicum* (Fig. 8), sharing its highly elongated and branched peridial vesicles. However, in collections, it is often labelled as *L. exiguum* because of its nearly spherical sporocarps. The covering of the fruiting bodies with black, glossy spots further enhances its superficial resemblance to *L. exiguum*. However, these peridial spots are individual vesicles and not vesicle aggregates, as seen in *L. exiguum* and its related species.

Lycogala umbrinum Leontyev, P. Vetlesen, Schnittler, E. Moroz & E. Johannesen, ***sp. nov.*** MB 857829. Fig. 9.

Etymology: *Umbra* (Latin) shadow, referring to the colouration of sporocarps.

Diagnosis: Differs from *L. alisaulianovae* by the beige spore mass.

© 2025 Westerdijk Fungal Biodiversity Institute

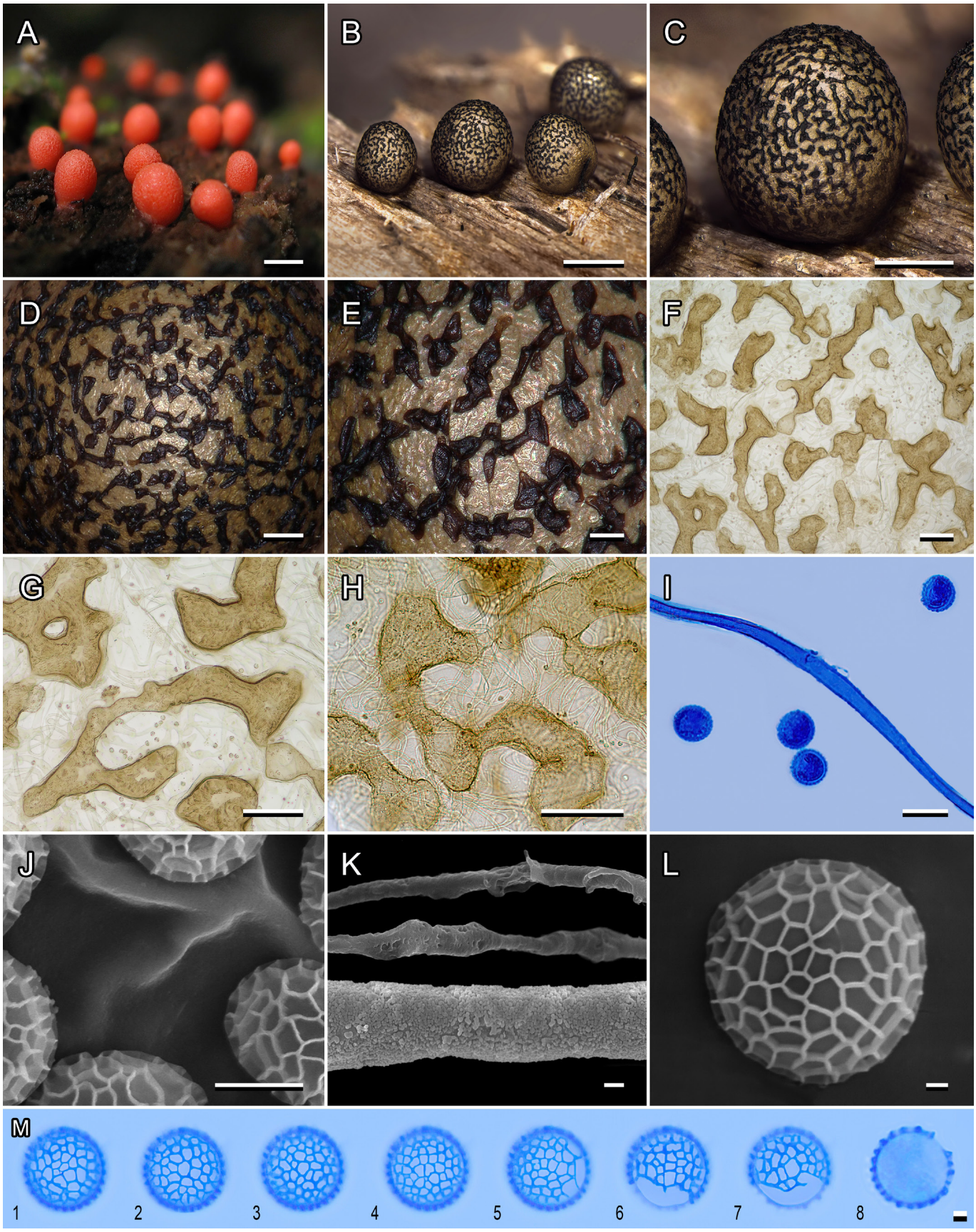

Fig. 7. *Lycogala sphaeroconicum sp. nov*. [A–G, I–M. IY054 (holotype); H. EJ18190388]. **A.** Immature fructifications. **B, C.** Sporocarps. **D, E.** Peridium in RL. **F–H.** Peridial vesicles in TL. **I.** Capillitium and spores, methyl blue in lactic acid. **J.** Inner surface of the peridium, spores, SEM. **K.** Capillitial tubules, SEM. **L.** Spore, SEM. **M.** Spores, methyl blue in lactic acid. The last spore is shown in optical section. Scale bars: A, B = 1 mm; C = 0.5 mm; D = 250 µm; E–H = 100 µm; I = 10 µm; J = 5 µm; K, M = 1 µm; L = 0.5 µm.

© 2025 Westerdijk Fungal Biodiversity Institute

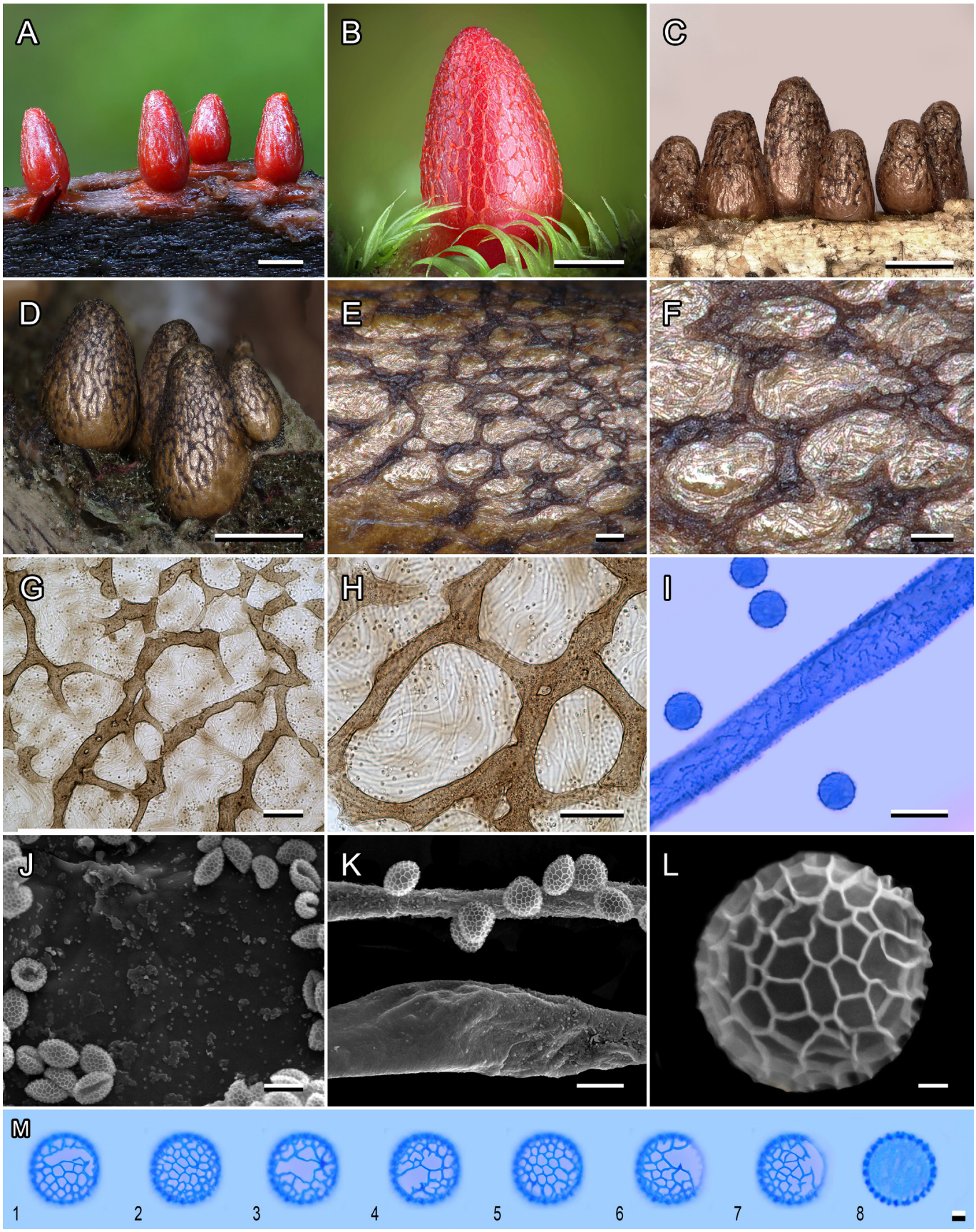

Fig. 8. *Lycogala conicum* (A, B. Not collected; C. TNSM13639; D–H, J–M. IY39; I. TNSM13638). **A, B.** Immature fructifications (A – courtesy of Michael Harz; B – courtesy of Karsten Buch). **C, D.** Sporocarps. **E, F.** Peridium in RL. **G, H.** Peridial vesicles in TL. **I.** Capillitium and spores, methyl blue in lactic acid. **J.** Inner surface of the peridium, SEM. **K.** Capillitial tubules, SEM. **L.** Spore, SEM. **M.** Spores, methyl blue in lactic acid. The last spore is shown in optical section. Scale bars: A–D = 1 mm; E–H = 100 µm; I = 10 µm; J, K = 5 µm; L = 0.5 µm; M = 1 µm.

© 2025 Westerdijk Fungal Biodiversity Institute

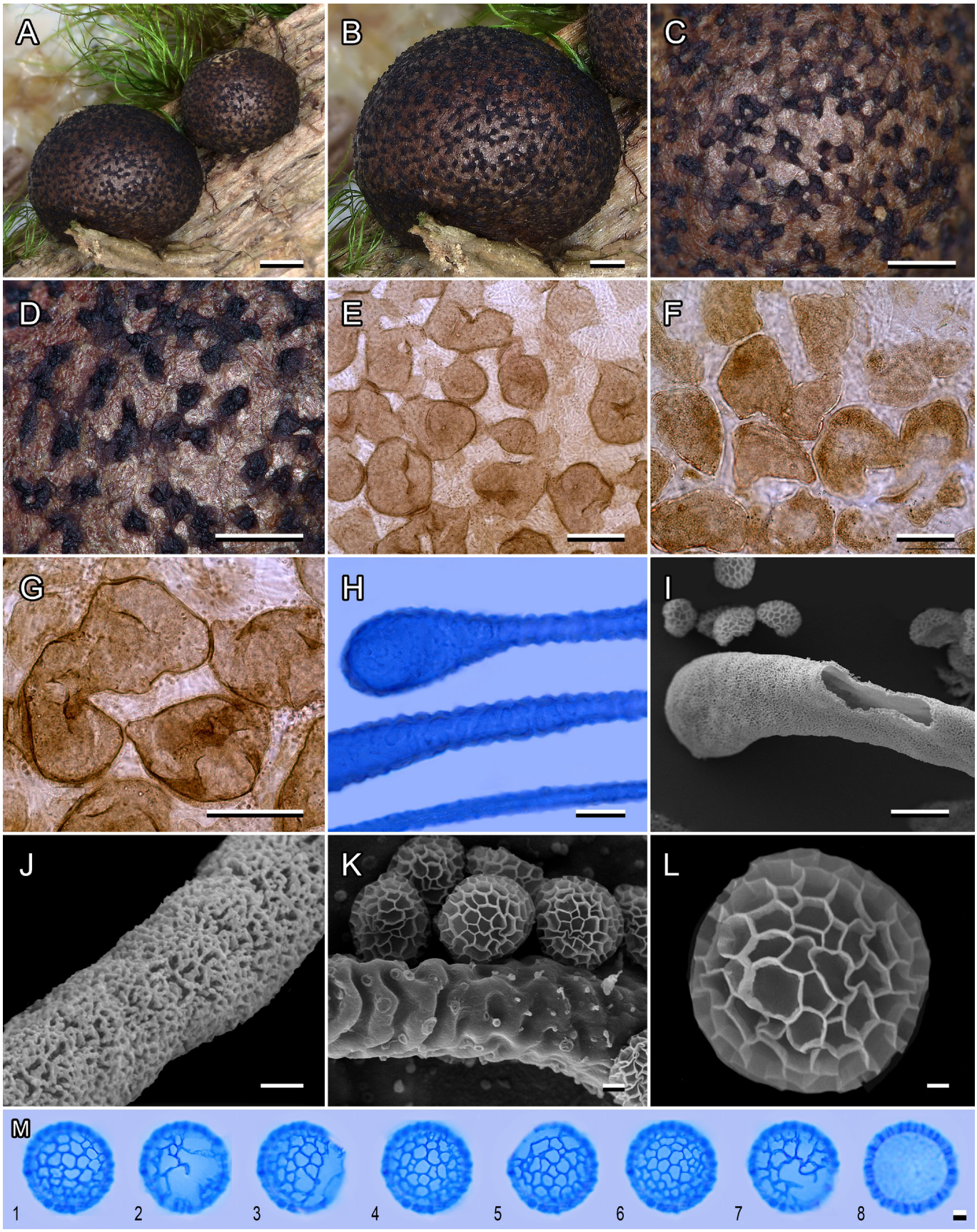

Fig. 9. *Lycogala umbrinum sp. nov*. [A–E, G, M. sc27827 (holotype); F. MSK-F43033; H–L. EJ22531365]. **A, B.** Sporocarps. **C, D.** Peridium in RL. **E–G.** Peridial vesicles in TL. **H.** Capillitium, methyl blue in lactic acid. **I–K.** Capillitial tubule, SEM. **L.** Spore, SEM. **M.** Spores, methyl blue in lactic acid. The last spore is shown in optical section. **Scale b**ars: A = 1 mm; B–D = 0.5 mm; E–G = 100 µm; H, I = 5 µm; J, K, M = 1 µm; L = 0.5 µm.

© 2025 Westerdijk Fungal Biodiversity Institute

Sporocarps in small dense groups, spherical to short horizontally ovoid, regular in shape or slightly deformed from mutual pressure, (1.5–)2.5–5(–6) mm diam. *Peridium* membranous, dark lilac-brown, umber-brown, dull brown, covered by vesicles. *Peridial vesicles* (60–)120–190(–230) µm, in RL dark brown to black, solitary, convex, forming loose groups, merging into very fragmented reticulum, in TL simple, ovoid or blot-shaped, brown. Vesicle walls mainly brown, of medium thickness (2 µm), 1–2-layered. *Crystals* absent. *Oil* present in form of *granular deposits*, brownish. *Inner surface of the peridium* smooth, covered by scattered warts or rings 0.5–1 µm diam. *Capillitium* tubular, 3–7 µm diam., with smooth contour and fine pitted-warty surface, or less regular, with wavy contour and smooth surface, covered with occasional warts and rings. *Spore mass* beige. *Spores* (6–)6.5–8(–8.5) µm diam., hyaline, reticulate, 6–8 meshes across diam., unornamented area occupies 1/3–1/4 of the spore surface. *Immature fructifications* unknown.

Typus: **Germany**, Bavaria, Bavarian Forest, Rachel, Transect 2, 6.9 km ESE to Frauenau (48.95264 13.37807), on strongly decayed and decorticated log of *Abies alba*, 3 Oct. 2013, *M. Schnittler* (**holotype** GFW sc27827). GenBank: nucSSU = OM424003 (rg36).

Distribution: Europe (Belarus, Germany, Norway).

Notes: A challenging species to identify, *L. umbrinum* resembles several taxa with solitary dark vesicles lacking crystals. The related species *L. alisaulianovae* differs from *L. umbrinum* by its bluish spore mass and looser arrangement of vesicles. The similar but unrelated *L. maculatum* is distinguished by its significantly darker, sometimes even black peridium without an umber hue and capillitium with pronounced warty bracelets. Another very similar species, *L. ustulatum*, has round thick-walled vesicles with a raised centre and flat periphery, and darker sporocarps without an umber hue.

Lycogala ustulatum Leontyev, Ishchenko & Schnittler, ***sp. nov.*** MB 857830. Fig. 10.

Etymology: *Ustulo* (Latin) to scorch, to burn slightly**,** referring to the colour of sporocarps.

Diagnosis: Differs from *L. umbrinum* by dark brown sporocarps densely covered with rounded, very thick-walled vesicles, that have a raised centre and a flat periphery, and by presence of small, aggregated vesicles, which surround bigger ones.

Sporocarps mainly solitary, spherical to short horizontally ovoid, more-or-less regular in shape, (2–)3.5–5(–7.5) mm diam. *Peridium* membranous, reddish brown, covered by vesicles so densely, that sporocarp looks dark brown. *Peridial vesicles* or two types, large and small. Large vesicles (70–)110–170(–230) µm, in RL deep brown, solitary, flattened, but with a convex centre, densely and evenly distributed, in TL simple, rounded, ovoid, blot-shaped, brown. Large vesicle walls brown, very thick (5–20 µm), 1–2-layered, with the granular outer layer. Small vesicles rather inconspicuous, (20–)30–50(–70) µm diam., in TL aggregated, angular, thin-walled (1–2 µm), forming spots or irregular network around large vesicles. *Crystals* absent. *Oil* in both types of vesicles represented by *granular deposits*, abundant, brown. *Inner surface of the peridium* smooth or covered by warts. *Capillitium* tubular, 2–6 µm diam., with wavy contour; surface fine pitted-warty, with ring-shaped islets. *Spore mass* pinkish grey. *Spores* (6.5–)7–8 µm diam., hyaline, reticulate, 5–7 meshes across diam., unornamented area occupies 1/3–1/4 of the spore surface. *Immature fructifications* orange pink.

Typus: **Russia**, Moskovskaya Oblast, Moscow, North-Eastern Administrative District, Severnyi (55.92853 37.5545), on rotting wooden building material (boards), 20 Jun. 2022, *Y. Ishchenko* (**holotype** GFW IY094). GenBank: nucSSU = PQ633746 (rg42); mtSSU = PQ633469; *COI* = PQ628478.

Distribution: Asia (Japan), Europe (Russia).

Notes: This species, apparently common in the boreal zone of Eurasia, is rather difficult to identify. As noted in the diagnosis, it is similar to *L. umbrinum*, which, however, has uniformly convex vesicles, and a lilac hue of the peridium under RL. Another similar species, *L. maculatum*, has the capillitium with pronounced warty bracelets, the dark pigmentation of peridium between the vesicles, and often forms rosette-like clusters of sporocarps. Thick-walled vesicles with a raised centre and flat periphery mentioned in the diagnosis appear to be a fairly stable characteristic of *L. ustulatum*.

Lycogala olivaceum Leontyev, Ishchenko & Gmoshinskiy, ***sp. nov.*** MB 857831. Fig. 11.

Etymology: *Oliva* (Latin) olive, referring to the colour of sporocarps.

Diagnosis: Differs from other *Lycogala* species by the greenish tint in the colouration of mature sporocarps and very large spores (8.5–9.5 µm diam.).

Sporocarps solitary or in small groups, spherical to horizontally ovoid, more-or-less regular in shape, (3–)3.5–5(–9.5) mm diam. *Peridium* membranous, light greenish or yellowish brown, covered by dark vesicles and abundant silvery patches of dried slime. *Peridial vesicles* (60–)80–120(–140) µm, in RL brown, solitary, folded, forming irregular chains, in TL simple, irregularly ovoid, light brown. Vesicle walls light-brownish, medium to thick (2–7 µm), 1–2-layered, with the granular outer layer. *Crystals* absent. *Oil* droplets scanty, *granular deposits* rather numerous, brownish. *Inner surface of the peridium* densely covered by warts. *Capillitium* tubular, 5–15 µm diam., with wavy contour; surface fine pitted-warty, with ring-shaped islets. *Spore mass* light pinkish. *Spores* (8–)8.5–9.5 µm diam., hyaline, reticulate, 5–7 meshes across diam., unornamented area indistinct, occupies 1/3–1/4 of the spore surface. *Immature fructifications* dull pink.

Typus: **Russia**, Moskovskaya Oblast, Gzhel, Kuzyaevo (55.62269 38.55919), on rotting trunk of *Picea abies*, on bare wood, on or near mosses, mainly *Ptilidium pulcherrimum* and *Lophocolea heterophylla*, as well as near lichens (*Cladonia* sp.), 13 Jul. 2020, *Y. Ishchenko* (**holotype** GFW IY043). GenBank: nucSSU = OM423951 (rg29).

© 2025 Westerdijk Fungal Biodiversity Institute

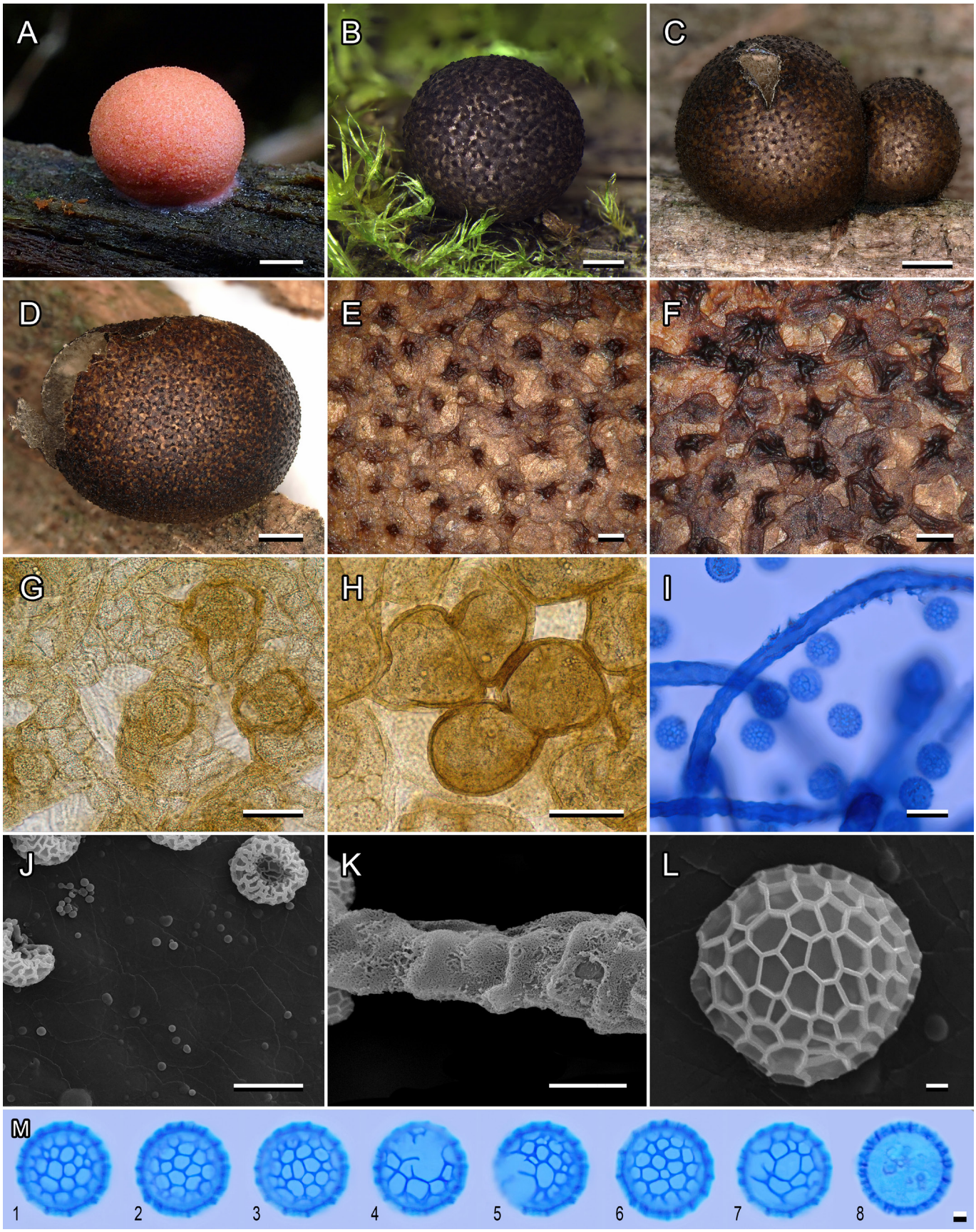

Fig. 10. *Lycogala ustulatum sp. nov*. [A. IY070; B, G. IY092; C, I–M. IY094 (**holotype**); D, F, H. IY096; E. IY048]. **A.** Immature fructifications. **B–D.** Sporocarps. **E, F.** Peridium in RL. **G, H.** Peridial vesicles in TL. **I.** Capillitium and spores, methyl blue in lactic acid. **J.** Inner surface of the peridium, SEM. **K.** Capillitial tubule, SEM. **L.** Spore, SEM. **M.** Spores, methyl blue in lactic acid. The last spore is shown in optical section. Scale bars: A–D = 1 mm; E–H = 100 µm; I = 10 µm; J, K = 5 µm; L = 0.5 µm; M = 1 µm.

© 2025 Westerdijk Fungal Biodiversity Institute

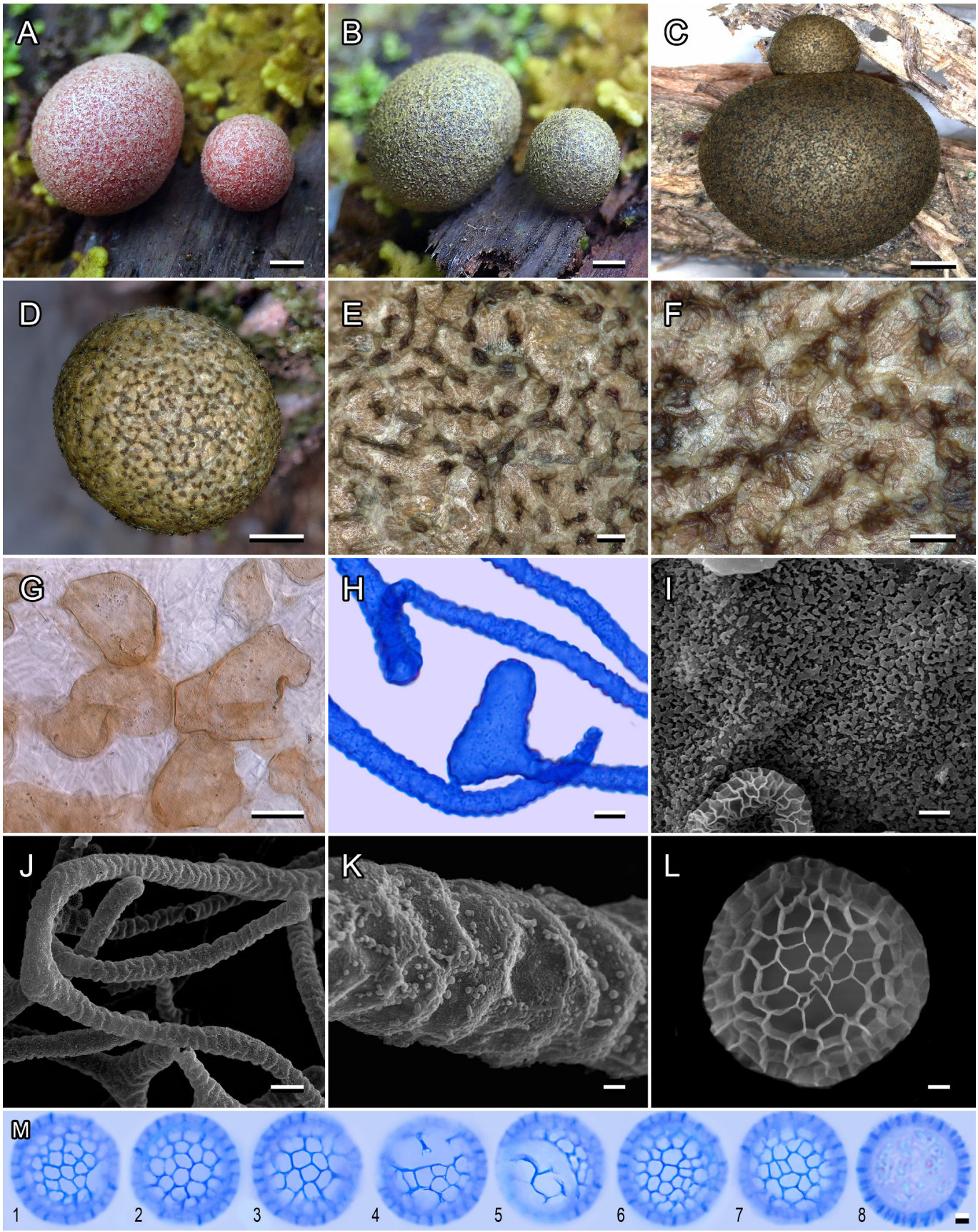

Fig. 11. *Lycogala olivaceum sp. nov*. [A–C, F–M. IY043 (holotype); D, E. MYX17468]. **A, B.** Immature fructifications. **C, D.** Sporocarps. **E, F.** Peridium in RL. **G.** Peridial vesicles in TL. **H.** Capillitium, methyl blue in lactic acid. **I.** Inner surface of the peridium, SEM. **J, K.** Capillitial tubule, SEM. **L.** Spore, SEM. **M.** Spores, methyl blue in lactic acid. The last spore is shown in optical section. Scale bars: A–D = 1 mm; E, F = 100 µm; G = 50 µm; H, J = 10 µm; I, K, M = 1 µm; L = 0.5 µm.

© 2025 Westerdijk Fungal Biodiversity Institute

Distribution: Europe (Russia).

Notes: The greenish colouration of the fruiting bodies fades with prolonged storage, complicating the identification of the species. Faded specimens, with their large size and peridium texture, resemble *L. epidendrum* s. str. Nonetheless, these two species can be distinguished by the texture of the capillitium: in *L. epidendrum*, the bracelets are densely ornamented with warty projections, whereas in *L. olivaceum*, warts are scanty. Additionally, the specimens of *L. olivaceum* we studied have very large spores (one of two biggest in the genus, together with *L. maculatum*), but more data are needed to evaluate the significance of this characteristic.

Lycogala laeve Leontyev, Schnittler & E. Johannesen, ***sp. nov.*** MB 857832. Fig. 12.

Etymology: *Laevis* (Latin) smooth, smoothed, referring to the appearance of sporocarps and capillitium.

Diagnosis: Differs from *L. epidendrum* by smooth capillitium tubes, bare of warts, and by clustered vesicles, filled with dense granular material.

Sporocarps in small tight groups, spherical to short horizontally ovoid, rather regular in shape, (2–)3–5.5(–8) mm diam. *Peridium* membranous, light greyish brown, covered by somewhat darker vesicles and silvery patches of dried slime. *Peridial vesicles* (20–)30–70(–110) µm, in RL dull brown, slightly convex to nearly smooth, forming vague marble-like or reticulate pattern, in TL loosely aggregated, with 2–3 vesicles across the group, rounded-angular from mutual pressure, light brownish. Vesicle walls light-brownish, medium to thick (2–8 µm), 1–2-layered, with the granular layer covering the whole group. *Crystals* absent. *Oil* present in form of *granular deposits*, brown, reddish brown. *Inner surface of the peridium* densely covered by warts. *Capillitium* tubular, 6–20 µm diam., with wavy contour and smooth surface, ornamented with only occasional warts or rings. *Spore mass* warm grey. *Spores* (6–)6.5–8.5 µm diam., hyaline, reticulate, 6–8 meshes across diam., unornamented area indistinct, 1/4–1/5 of the spore surface. *Immature fructifications* unknown.

Typus: **Germany**, Bavaria, lower montane forest near Garmisch-Partenkirchen, ca 600 m south of the Kainzenbad (47.47922 11.12411), on dead wood of *Picea abies*, ca 850 m a.s.l., 4 Jun. 2023, *D. Leontyev* (**holotype** CWP4644). GenBank: nucSSU = PQ633672 (rg43).

Distribution: Europe (Germany, Norway).

Notes: This species is a twin of *L. epidendrum*, sharing its large size, poorly defined texture, and silvery-brown colouration of sporocarps. The morphological distinction between *L. laeve* and *L. epidendrum* is rather problematic. However, as stated in the diagnosis, the new species has smooth capillitium tubes, almost devoid of warts (as observed under LM), whereas in *L. epidendrum* they are adorned with large warts. The peridial vesicles of *L. laeve* form a loose network of rows and clusters, while in *L. epidendrum*, they are barely grouped. *L. laeve* also appears less inclined to form large colonies, which is very typical of *L. epidendrum*. By its marble-like pattern, the peridium of *L. laeve* resembles that of *L. confusum*, but the latter lacks accumulations of dried slime and, as a result, does not exhibit a silvery hue. The new species seems to prefer cold habitats, as it has been found in Norway and the Bavarian Alps.

Lycogala paraconfusum Leontyev, Ishchenko & V. Dzizurova, ***sp. nov.*** MB 857833. Fig. 13.

Etymology: *Para* (Greek) near, beside, or *para* (Latin) protection against, and *confusus* (Latin) mixed, confused, referring to the similarity to *L. confusum*.

Diagnosis: Differs from *L. confusum* by the absence of marble-like reticulate pattern of the peridium and regular rounded shape of sporocarps.

Sporocarps in small tight groups and rows, spherical to short horizontally ovoid, often deformed from mutual pressure, (2.5–)4–5.5(–7.5) mm diam. *Peridium* membranous, light brown, covered by vesicles. *Peridial vesicles* (10–)30–60(–130) µm, in RL brown, folded, often with central depression, forming rather dense reticulate pattern, in TL aggregated, with 2–3 vesicles across the group, rounded-angular from mutual pressure, light brownish. Vesicle walls nearly colourless, multilayered, with the inner layer 1–3 µm thick, smooth, and rather indistinct outer layers 5–15 µm thick, granular, covering the whole group of vesicles. *Crystals* absent. *Oil* present in form of *granular deposits*, brown or orange red. *Inner surface of the peridium* covered by warts. *Capillitium* tubular, 3–10 µm diam., with smooth or wavy contour; surface fine pitted-warty, with occasional ring-shaped islets. *Spore mass* light pinkish. *Spores* 7–8.5(–9) µm diam., hyaline, reticulate, 5–8 meshes across diam., unornamented area indistinct, 1/4–1/5 of the spore surface. *Immature fructifications* pinkish orange.

Typus: **Russia**, Primorsky Krai, Ussuriysky State Reserve, Komarovka valley (43.64827 132.37017), on rotten wood, 18 Aug. 2022, *V. Dzizurova* (**holotype** GFW IY119). GenBank: nucSSU = PQ633772 (rg14); COI = PQ628497.

Distribution: Asia (Russia), Europe (Germany, Russia).

Notes: This species closely resembles *L. confusum* when examining the details of the peridium under RL and TL. This similarity is quite remarkable, considering that *L. confusum* and *L. paraconfusum* are not closely related. However, the overall appearance of the sporocarps allows these species to be distinguished even without dissection. *L. confusum* has irregularly shaped fruiting bodies, with vesicles on their surface forming a distinctive “marbled” pattern (Leontyev *et al.* 2023). In contrast, the sporocarps of *L. paraconfusum* are predominantly regular in shape, and their vesicles form a network of isolated spots. In *L. confusum*, we also observed pronounced differentiation in the ornamentation of the capillitium, with regularly spaced with ring-shaped islets, which are absent in *L. paraconfusum*. In *L. paraconfusum*, but not in *L. confusum*, oil accumulations in the peridium exhibit a reddish colouration. However, the last two traits require further study based upon a broader sampling.

© 2025 Westerdijk Fungal Biodiversity Institute

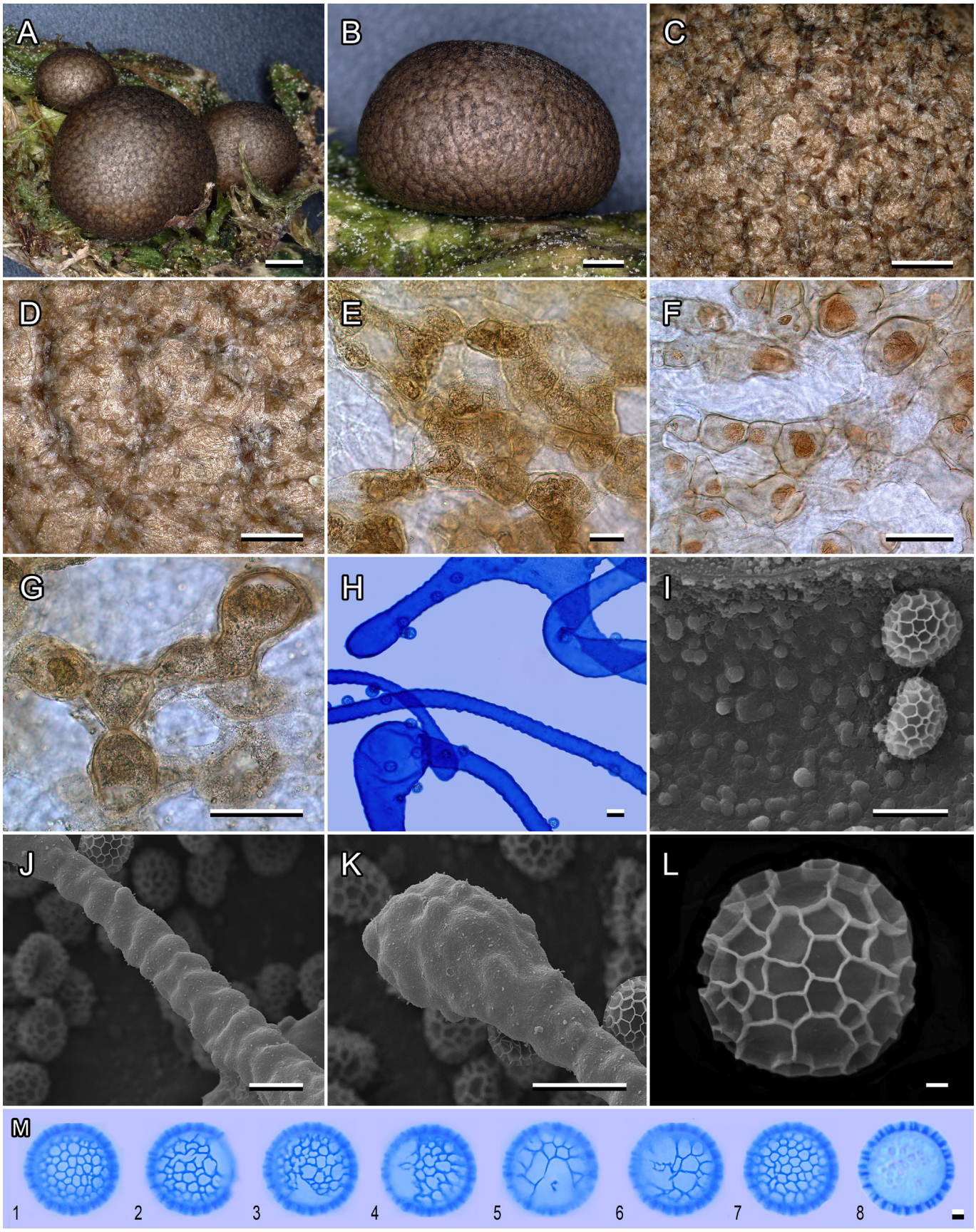

Fig. 12. *Lycogala laeve sp. nov.* [A–F, H–M. CWP4644 (holotype); G. MP1-030621]. **A, B.** Sporocarps. **C, D.** Peridium in RL. **E–G.** Peridial vesicles in TL. **H.** Capillitium and spores, methyl blue in lactic acid. **I.** Inner surface of the peridium, SEM. **J, K.** Capillitial tubules, SEM. **L.** Spore, SEM. **M.** Spores, methyl blue in lactic acid. The last spore is shown in optical section. Scale bars: A, B = 1 mm; C, D = 0.5 mm; E–G = 100 µm; H = 10 µm; I–K = 5 µm; L = 0.5 µm; M = 1 µm.

© 2025 Westerdijk Fungal Biodiversity Institute

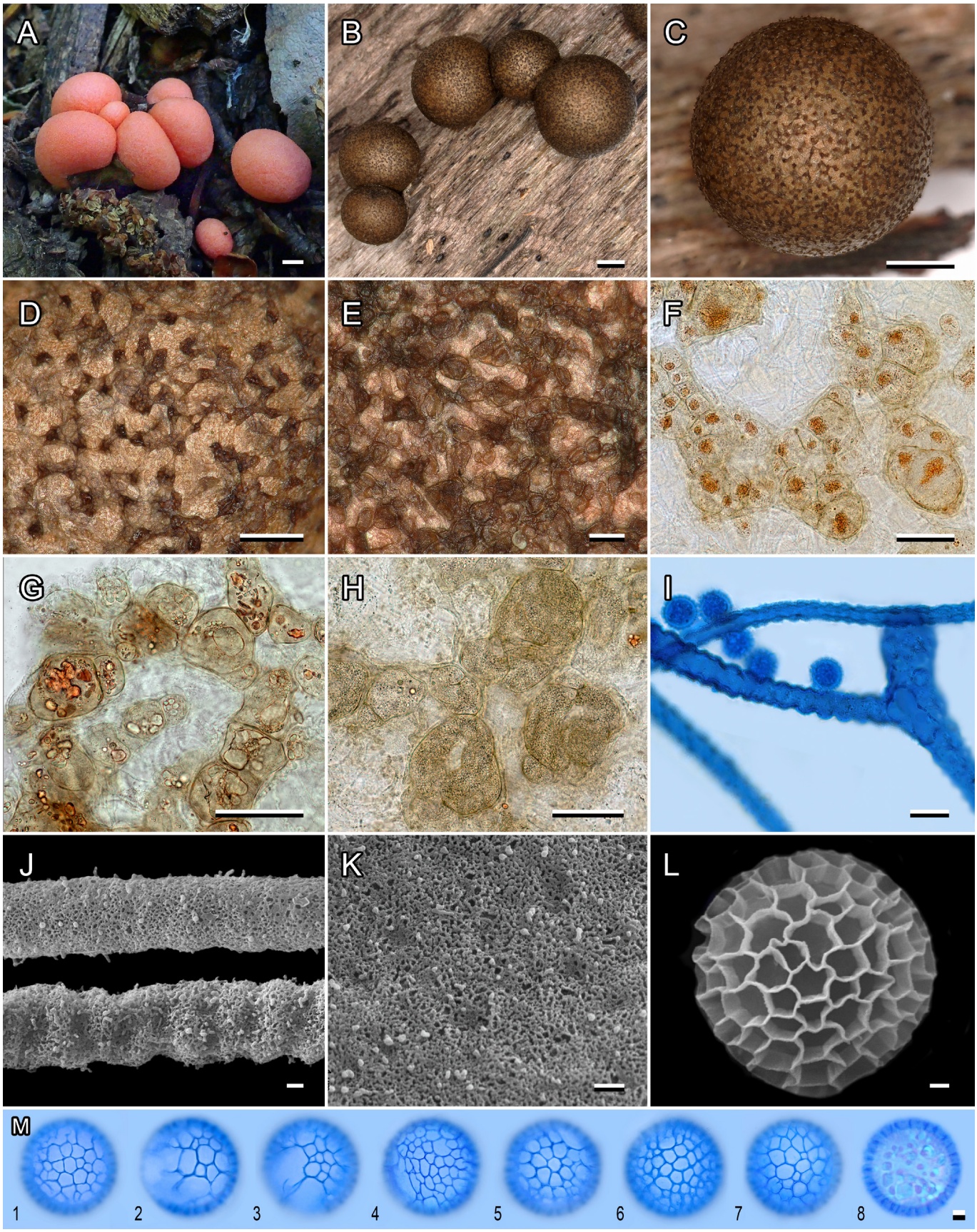

Fig. 13. *Lycogala paraconfusum sp. nov*. [A, E, G. IY055; B–D, F, I–K. IY119 (holotype); H. IY105; L, M. sc32076]. **A.** Immature fructifications. **B, C.** Sporocarps. **D, E.** Peridium in RL. **F–H.** Peridial vesicles in TL. **I.** Capillitium and spores, methyl blue in lactic acid. **J.** Capillitial tubule, SEM. **K.** Surface of wide capillitial tubule, SEM. **L.** Spore, SEM. **M.** Spores, methyl blue in lactic acid. The last spore is shown in optical section. Scale bars: A–C = 1 mm; D = 0.5 mm; E–H = 100 µm; I = 10 µm; J, K, M = 1 µm; L = 0.5 µm.

© 2025 Westerdijk Fungal Biodiversity Institute

Lycogala nigroconfusum Leontyev, W.-L. Song, Shuang L. Chen & S.L. Stephenson, ***sp. nov.*** MB 857834. Fig. 14.

Etymology: *Niger* (Latin) black, and *confusum* (Latin) confusing referring to the dark pigmentation of peridial vesicles and the similarity to *L. confusum* and *L. paraconfusum*.

Diagnosis: Differs from *L. confusum* and *L. paraconfusum* by the very dark peridial vesicles with multilayer walls.

Sporocarps solitary or in small groups, spherical to short horizontally ovoid, mostly regular in shape, (4–)4.5–6(–7.5) mm diam. *Peridium* membranous, light brown, covered by vesicles so densely, that sporocarp looks black. *Peridial* vesicles (10–)40–70(–80) µm, in RL black, forming dense reticulate pattern on the peridium, convex, matt, in TL aggregated in rows, rings or clusters, with 1–3 vesicles across the group, rounded or rounded-angular from mutual pressure, dark brown. Vesicle walls dark brown, multilayered, with the inner layer 2–3 µm thick, smooth, and the outer layers 5–20 µm thick, granular, covering the whole group of vesicles. *Crystals* absent. *Oil* droplets numerous, large, colourless (rg13) or orange red (rg45). *Inner surface of the peridium* smooth or covered by scanty warts and rings. *Capillitium* tubular, 4–10 µm diam., with wavy contour; surface fine pitted-warty, with ring-shaped islets. *Spore mass* beige. *Spores* (6–)6.5–7 µm diam., hyaline, reticulate, 5–6 meshes across diam., unornamented area occupies 1/4–1/5 of the spore surface. *Immature fructifications* unknown.

Typus: **USA**, Tennessee, Long Hunter State Park, cedar and hardwood forest (36.1173 -86.5660), on dead wood, 16 Aug. 2006, *W.C. Rosing* (**holotype** UARK36077). GenBank: nucSSU = OM424041 (rg13).

Distribution: Asia (China), North America (USA).

Notes: By the naked eye *L. nigroconfusum* resembles other species with nearly black fructifications (*L. maculatum* and *L. squamatum*) but differs from both by the mutual arrangement of peridial vesicles (which are free or clustered in rosettes, respectively, in two abovementioned species). A tendency to form rows of vesicles puts *L. nigroconfusum* together with *L. confusum*, *L. paraconfusum* and *L. fossiculatum*, but all these species have much lighter vesicle walls. Another similar species, *L. sigillatum* possesses vesicles resembling dried droplets, which, despite their dense arrangement, do not form a reticulum.

Lycogala inconspicuum Leontyev, Ishchenko, Schnittler & E. Johannesen, ***sp. nov.*** MB 857835. Fig. 15.

Etymology: *Inconspicuus* (Latin) invisible, indiscernible, referring to the small size and poor ornamentation of sporocarps.

Diagnosis: Differs from the rest of *Lycogala* species by the combination of small solitary sporocarps and small elongate peridial vesicles which form linear chains and contain reddish oil and scanty crystal druses.

Sporocarps solitary, spherical to short horizontally ovoid, often somewhat irregular in shape, (2–)2.5–3(–3.5) mm diam. *Peridium* membranous, light brown, covered by vesicles. *Peridial vesicles* (30–)50–90(–170) µm, in RL brown, dark brown, folded, forming loose reticulate pattern, in TL aggregated, with 1–2 vesicles across the group, elongate, with thinner "tails", often angular from mutual pressure, light brownish. Vesicle walls light-brownish, thin (1 µm), single-layered. *Crystals* present as small dense clusters, not filling the whole vesicle. *Oil* present in form of small droplets and *granular deposits*, brown or orange red. *Inner surface of the peridium* smooth or covered by warts. *Capillitium* tubular, 3–10 µm diam., with wavy contour; surface fine pitted-warty, with occasional ring-shaped islets. *Spore mass* beige. *Spores* (6–)6.5–7.5 µm diam., hyaline, reticulate, 7–9 meshes across diam., unornamented area 1/3–1/2 of the spore surface. *Immature fructifications* pink.

Typus: **Germany**, Mecklenburg-Vorpommern, Western Pomerania, Greifswald, small hedge around fields 1.5 km W Dersekow (54.04568 13.26444), on a strongly decayed log of *Fraxinus excelsior*, diam. 45 cm, 20 Jul. 2011, *M. Schnittler* (**holotype** GFW sc22097). GenBank: nucSSU = OM423968 (rg03); mtSSU = PQ633586.

Distribution: Europe (Germany, Norway, Russia).

Notes: Small solitary sporocarps with an indistinct vesicle pattern associate this species with *L. miserum* and *L. asperum*. Both of these differ from *L. inconspicuum* by their solitary vesicles, filled with yellow oil droplets, as well as by abundant crystalline deposits (*L. miserum*) and ring-like ornamentation of the peridium (*L. asperum*).

Lycogala echinocarpum Leontyev, Ishchenko & Bortnikov, ***sp. nov.*** MB 857836. Fig. 16.

Etymology: *Echinos* (Greek) sea urchin, and *carpon* (Greek) fruit, referring to the general appearance of sporocarps.

Diagnosis: Differs from the rest of *Lycogala* species by papillate projections on the sporocarp surface, formed by aggregated vesicles enclosed in thick covers.

Sporocarps in small groups, spherical to short horizontally ovoid, more-or-less regular in shape, (3–)4.5–5.5(–6.5) mm diam. *Peridium* membranous, light brown, covered by vesicles so densely, that sporocarp looks black. *Peridial vesicles* in aggregates that look like prominent papillate protrusions, giving the sporocarps a spiny appearance, black, glossy, forming dense, stellate or dotted pattern at the surface of sporocarp; in TL aggregates (80–)130–170(–220) µm diam. rounded, forming a dense network of moniliform rows, with 4–7 vesicles across the group. Individual vesicles (10–)20–40(–50) µm, angular from mutual pressure, dark brown. Vesicle walls brown, multi-layered, very thick-walled (12–25 µm), with the granular outer layer, covering the whole group. *Crystals* absent. *Oil* present in form of *granular deposits*, brown. *Inner surface of the peridium* smooth. *Capillitium* tubular, 8–20 µm diam., with wavy contour;

© 2025 Westerdijk Fungal Biodiversity Institute

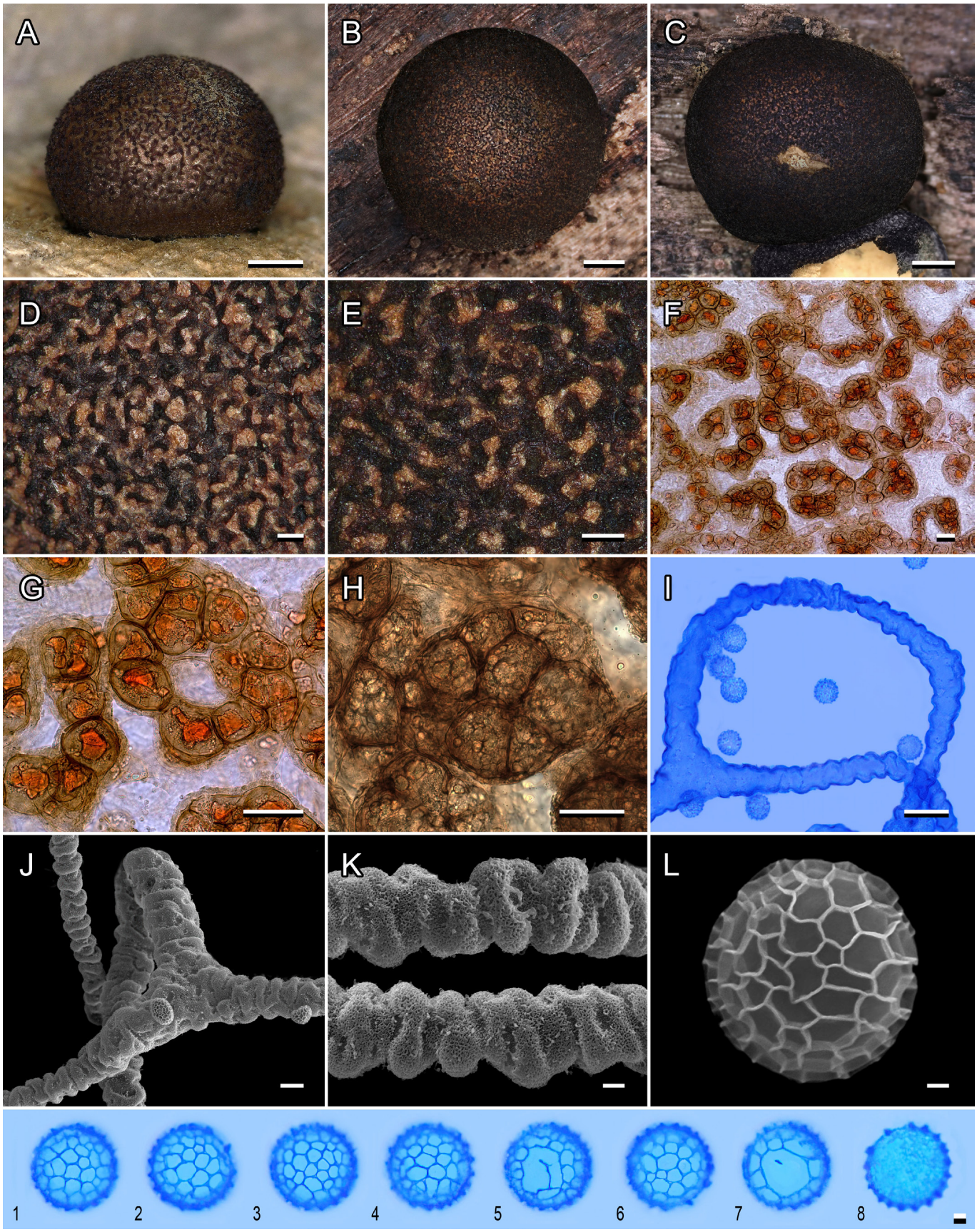

Fig. 14. *Lycogala nigroconfusum sp. nov*. [A, E, G. IY055; B–D, F, I–K. IY119 (holotype); H. IY105; L, M. sc32076]. **A–C.** Sporocarps. **D, E.** Peridium in RL. **F–H.** Peridial vesicles in TL. **I.** Capillitium and spores, methyl blue in lactic acid. **J, K.** Capillitial tubules, SEM. **L.** Spore, SEM. **M.** Spores, methyl blue in lactic acid. The last spore is shown in optical section. Scale bars: A–C = 1 mm; D, E = 0.1 mm; F–H = 50 µm; I = 10 µm; J = 5 µm; K, M = 1 µm; L = 0.5 µm.

© 2025 Westerdijk Fungal Biodiversity Institute

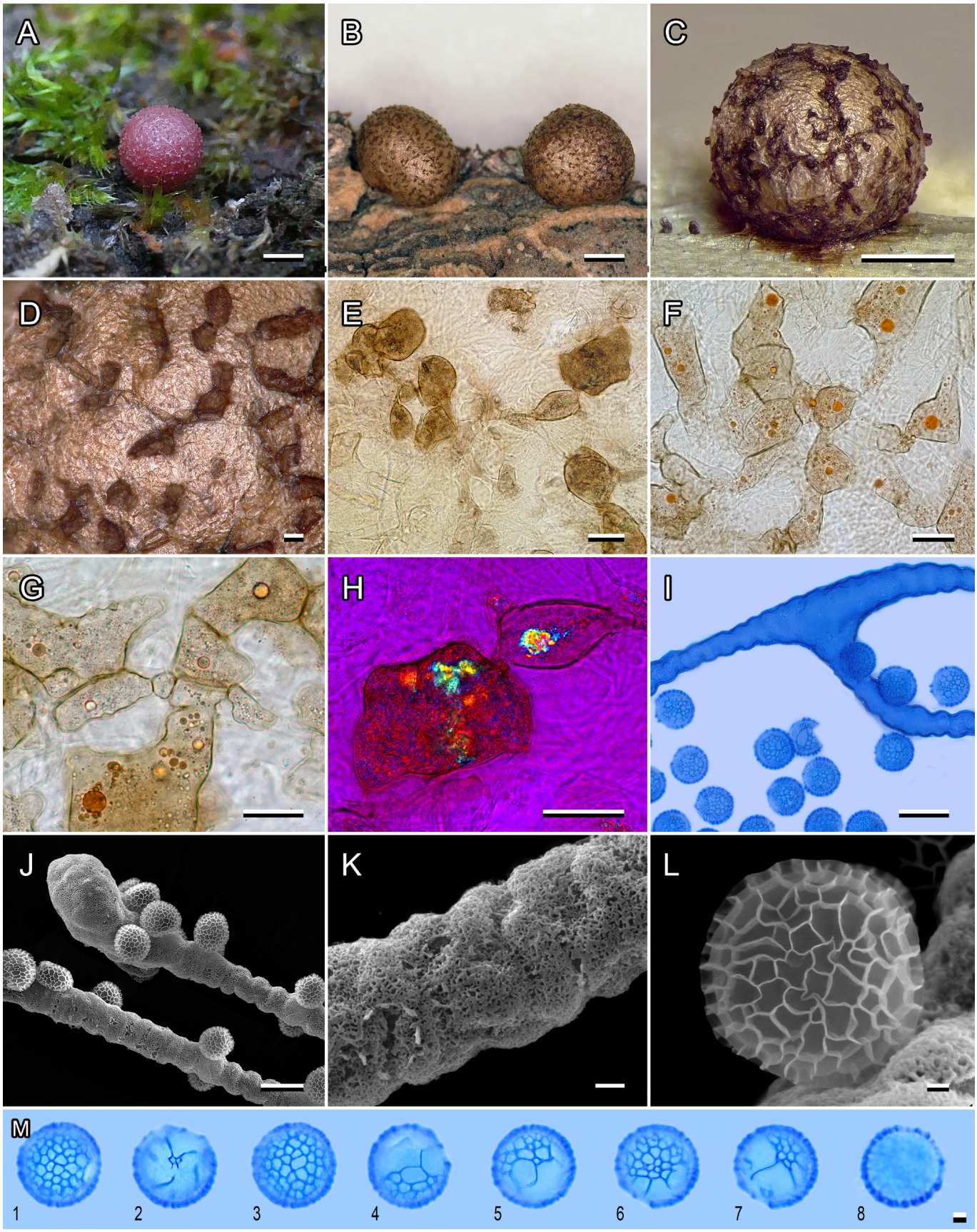

Fig. 15. *Lycogala inconspicuum sp. nov*. [A, F, G. MCCNNU1335 (rg45); B–E, H–M. UARK36077 (holotype)]. **A.** Immature fructifications. **B, C.** Sporocarps. **D.** Peridium in RL. **E–G.** Peridial vesicles in TL. **H.** Peridial vesicles in PL. **I.** Capillitium and spores, methyl blue in lactic acid. **J, K.** Capillitial tubules, SEM. **L.** Spore, SEM. **M.** Spores, methyl blue in lactic acid. The last spore is shown in optical section. Scale bars: A–C = 1 mm; D–H = 50 µm; I, J = 10 µm; K, M = 1 µm; L = 0.5 µm.

© 2025 Westerdijk Fungal Biodiversity Institute

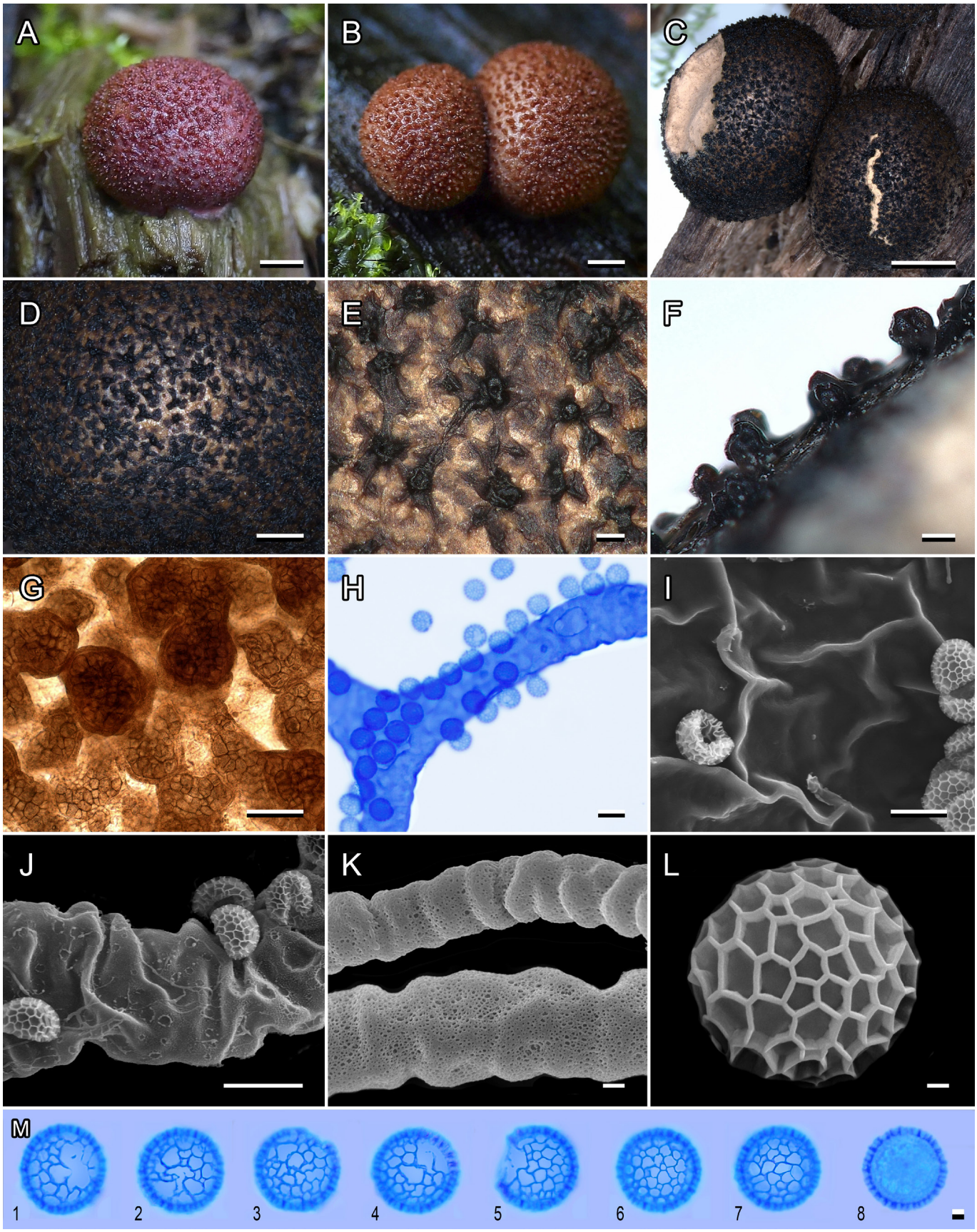

Fig. 16. *Lycogala echinocarpum sp. nov*. [A, B. IY025; C–M. IY038 (holotype)]. **A, B.** Immature fructifications. **C.** Sporocarps. **D.** Peridium in RL. **E.** Peridial vesicles in TL. **F.** Peridial vesicles, side view, TL. **G.** Peridial vesicles in PL. **H.** Capillitium and spores, methyl blue in lactic acid. **I.** Inner surface of the peridium, SEM. **J, K.** Capillitial tubules, SEM. **L.** Spore, SEM. **M.** Spores, methyl blue in lactic acid. The last spore is shown in optical section. Scale bars: A–C = 1 mm; D = 0.5 mm; E–G = 100 µm; H–J = 10 µm; K, M = 1 µm; L = 0.5 µm.

© 2025 Westerdijk Fungal Biodiversity Institute

surface fine pitted-warty or almost smooth, with occasional ring-shaped islets or rather well-developed rings. *Spore mass* beige. *Spores* (6–)6.5–7 µm diam., hyaline, reticulate, 7–9 meshes across diam., unornamented area indistinct, 1/4–1/5 of the spore surface. *Immature fructifications* pink, then reddish brown, with vesicles darker than the background.

Typus: **Russia**, Moskovskaya Oblast, Moscow, North-Eastern Administrative District, Severnyi (55.92839 37.55094), on deciduous tree logs, on bare wood, on and near the moss *Amblytegium* sp., 18 Jun. 2020, *Y. Ishchenko* (**holotype** GFW IY038). GenBank: nucSSU = OM423946 (rg25).

Distribution: Europe (Russia).

Notes: Noticeable papillate projections on the peridium, formed by aggregated vesicles, distinguish this species from any other *Lycogala*. Similar species with dark sporocarps (*L. maculatum*, *L. ustulatum*) have solitary and much flatter vesicles.

Lycogala rubrosporum Leontyev, W.-L. Song, Shuang L. Chen, Y. Yamamoto & Schnittler, ***sp. nov.*** MB 857837. Fig. 17.

Etymology: *Ruber* (Latin) red, and *spora* (Greek), seed, referring to the colour of the fresh spore mass.

Diagnosis: Differs from the rest of *Lycogala* species by combination of saturated brick red spore mass and rosette shape of vesicle aggregates.

Sporocarps scattered, spherical, regular in shape, 2–3.5(–4) mm diam. *Peridium* membranous, light reddish brown, covered by vesicles so densely, that sporocarp looks dark brown to black. *Peridial vesicles* in aggregates that look like black spots of rosette shape and pitted surface, separated from each other by a regular thin network of vesicle-lacking areas; in TL aggregates 220–300(–500) µm diam., dense, petaloid, with 5–7 vesicles across the group. Individual vesicles (30–)50–90(–130) µm, rounded, somewhat angular from mutual pressure, dark brown. Vesicle walls thin (1–2 µm), 1–2-layered, with inconspicuous outer layer covering the whole group. *Crystals* occasional or absent. *Oil* droplets numerous, from large to small, and in the form of *granular deposits*, orange-red, orange yellow, brownish. *Inner surface of the peridium* smooth or covered by scanty warts. *Capillitium* tubular, 2–10 µm diam., with wavy contour; surface fine pitted-warty, with ring-shaped islets. *Spore mass* bright orange red. *Spores* (5.5–)6–7 µm diam., hyaline, reticulate, 5–7 meshes across diam., unornamented area occupies 1/3–1/4 of the spore surface. *Immature fructifications* unknown.

Typus: **China**, Hubei Province, Houhe National Nature Reserve (47.757 133.695), on strongly decayed wood, 22 Jul. 2019, *M. Li, X. Tao & B. Li* (**holotype** MCCNNU3695). GenBank: nucSSU = ON920628 (rg53); mtSSU = PQ633513.

Distribution: Asia (China, Japan, South Korea, Vietnam).

Notes: This species is related to *L. aggregatum* and *L. squamatum*, sharing with them the rosette-shaped vesicle aggregates. However, the bright, brick-red colouration of the spore mass distinguishes *L. rubrosporum* not only from related taxa, but also from all other described species of the genus. When the spore mass of *L. rubrosporum* fades, it may resemble *L. squamatum*, but in the latter, the lines between the rosettes are usually darker in colour.

Lycogala squamatum Leontyev, Y. Bengus & Bortnikov, ***sp. nov.*** MB 857838. Fig. 18.

Etymology: *Squama* (Latin) scale, referring to the general appearance of sporocarps.

Diagnosis: Differs from *L. aggregatum* by darker and more regular lines between rosette-shaped vesicle aggregates, and by red oil droplets deposited in vesicles.

Sporocarps scattered, spherical to short horizontally ovoid, more-or-less regular in shape, (1.5–)2.5–3.3(–6.0) mm diam. *Peridium* membranous, dark brown, covered by vesicles so densely, that sporocarp looks entirely black. *Peridial vesicles* in aggregates that look like black spots of rosette shape and pitted surface, separated from each other by a regular thin network of vesicle-lacking areas; in TL aggregates (220–)250–310(–440) µm diam., dense, petaloid, with 2–7 vesicles across the group. Individual vesicles (40–)60–110(–160) µm, rounded, somewhat angular from mutual pressure, dark brown. Vesicle walls thin to medium (1–3 µm), 1–2-layered, with inconspicuous outer layer covering the whole group. *Crystals* occasional or absent. *Oil* droplets numerous, from large to small, and in the form of *granular deposits*, orange red. *Inner surface of the peridium* smooth or covered by warts and rings. *Capillitium* tubular, 3–10 µm diam., with wavy contour; surface fine pitted-warty, with ring-shaped islets or rather well-developed rings. *Spore mass* beige. *Spores* (5.5–)6–7 µm diam., hyaline, reticulate, 5–8 meshes across diam., unornamented area nearly absent or occupies 1/4–1/5 of the spore surface. *Immature fructifications* unknown.

Typus: **Ukraine**, Kharkiv Region, Kharkiv, Nova Bavaria (49.949313 36.18936), on the dead wood of *Acer negundo*, 4 Jul. 2020, *Y.V. Bengus* (**holotype** CWP4233). GenBank: nucSSU = OM423894 (rg31); *COI* = ON931560.

Distribution: Asia (Vietnam), Europe (Russia, Ukraine).

Notes: This taxon was described based on a complex of three phylogenetically close and morphologically similar putative biospecies (rg27, 31, 61); broader sampling in the future may allow these taxa to be separated. All members of the complex are characterized by dark fruiting bodies regularly paved with black spots, which represent rosette-like aggregates of vesicles. The dense arrangement of these aggregates gives the sporocarps a scaly appearance. Unlike *L. rubrosporum* and *L. aggregatum*, the spaces between the vesicles in *L. squamatum* are rather dark, and the vesicles themselves contain red oil droplets. The type specimen, representing rg31, is also distinguished by relatively large (up to 6 mm) and particularly darkly coloured fruiting bodies.

Lycogala microcarpum Leontyev, Ishchenko, W.-L. Song & Shuang L. Chen, ***sp. nov.*** MB 857839. Fig. 19.

© 2025 Westerdijk Fungal Biodiversity Institute

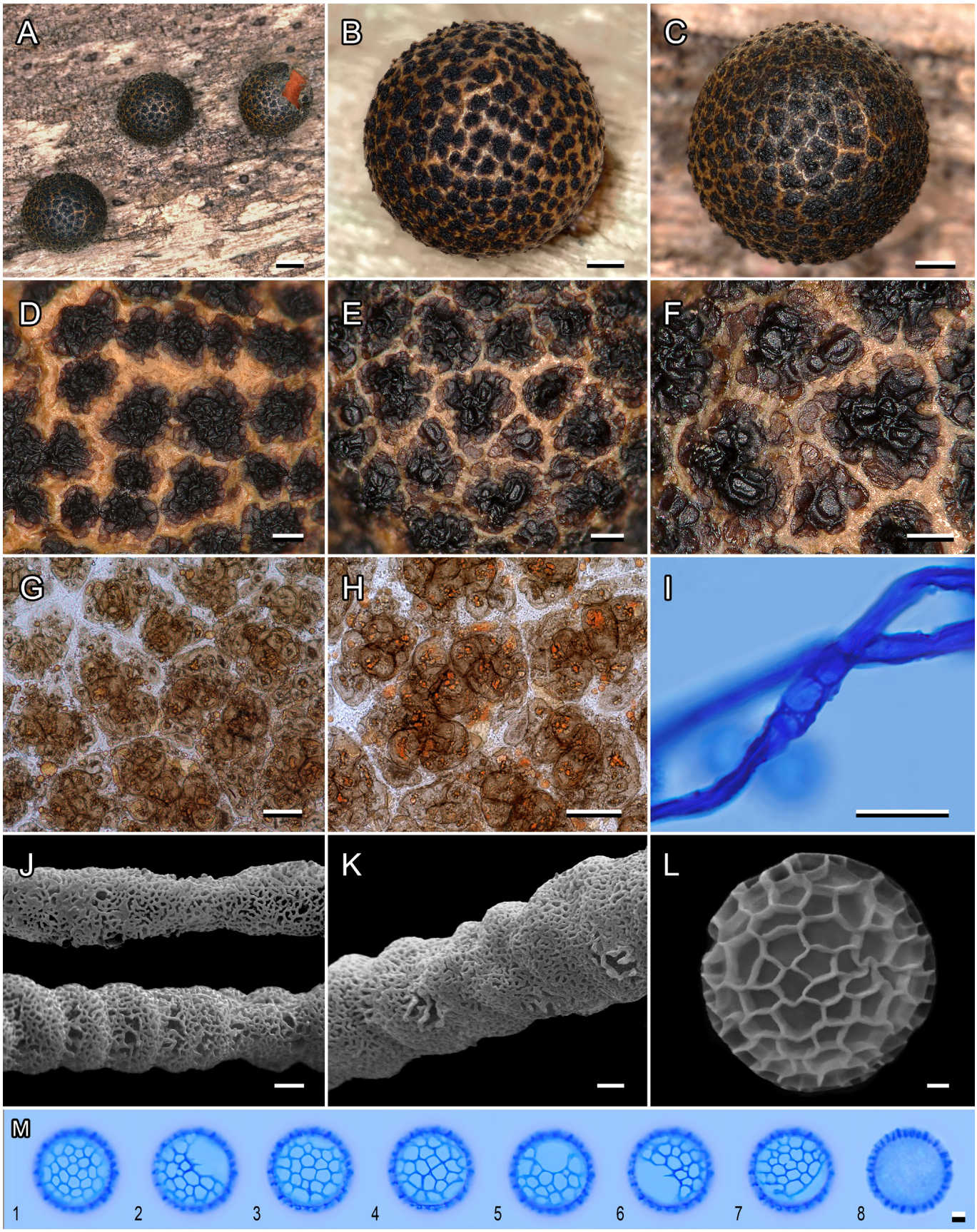

Fig. 17. *Lycogala rubrosporum sp. nov*. [A, C, E–M. MCCNNU3695 (holotype); B, D. MCCNNU3800]. **A–C.** Sporocarps. **D–F.** Peridium in RL. **G, H.** Peridial vesicles in TL. **I.** Capillitium, methyl blue in lactic acid. **J, K.** Capillitial tubules, SEM. **L.** Spore, SEM. **M.** Spores, methyl blue in lactic acid. The last spore is shown in optical section. Scale bars: A = 1 mm; B, C = 0.5 mm; D–H = 100 µm; I = 10 µm; J, K, M = 1 µm; L = 0.5 µm.

© 2025 Westerdijk Fungal Biodiversity Institute

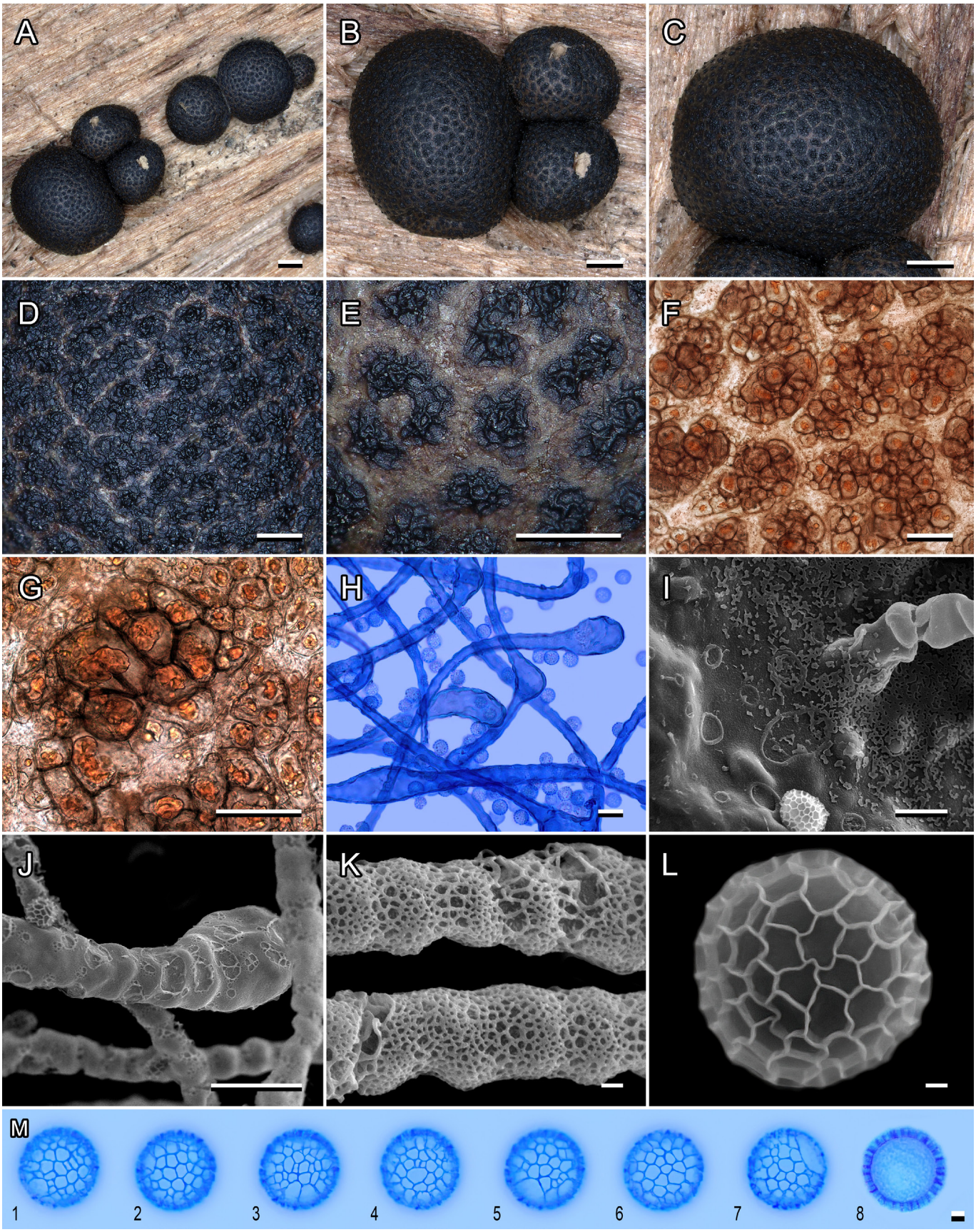

Fig. 18. *Lycogala squamatum sp. nov*. [CWP4233 (holotype)]. **A–C.** Sporocarps. **D, E.** Peridium in RL. **F, G.** Peridial vesicles in TL. **H.** Capillitium and spores, methyl blue in lactic acid. **I.** Inner surface of the peridium, SEM. **J, K.** Capillitial tubules, SEM. **L.** Spore, SEM. **M.** Spores, methyl blue in lactic acid. The last spore is shown in optical section. Scale bars: A–C = 1 mm; D, E = 0.5 mm; F, G = 100 µm; H–J = 10 µm; K, M = 1 µm; L = 0.5 µm.

© 2025 Westerdijk Fungal Biodiversity Institute

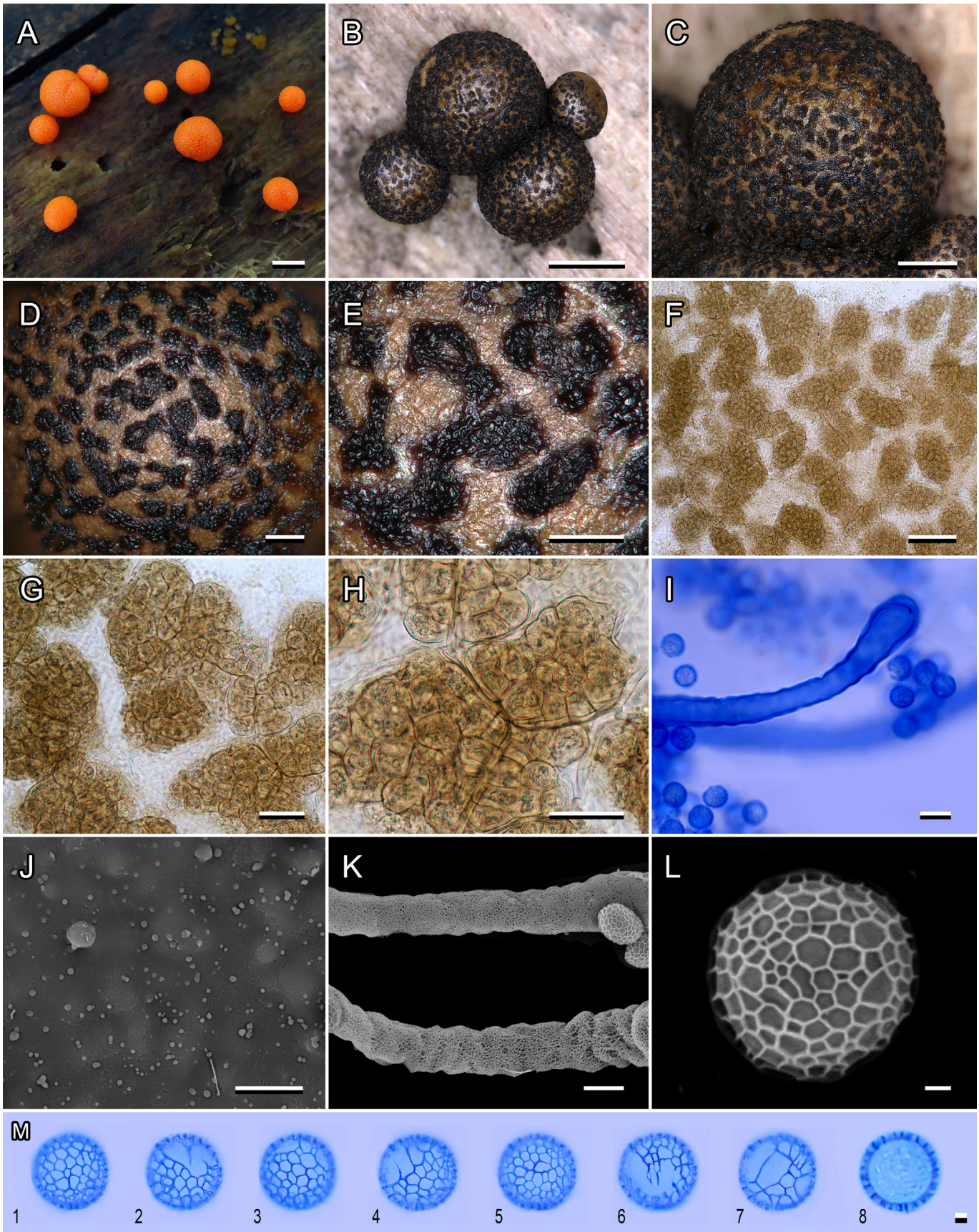

Fig. 19. *Lycogala microcarpum sp. nov*. [A–I, M. IY116 (holotype); J–L. HFNNU10824]. **A.** Immature fructifications. **B, C.** Sporocarps. **D, E.** Peridium in RL. **F–H.** Peridial vesicles in TL. **I.** Capillitium and spores, methyl blue in lactic acid. **J.** Inner surface of the peridium, SEM. **K.** Capillitial tubules, SEM. **L.** Spore, SEM. **M.** Spores, methyl blue in lactic acid. The last spore is shown in optical section. Scale bars: A, B = 1 mm; C = 0.5 mm; D–F = 100 µm; G, H = 50 µm; I = 10 µm; J, K = 5 µm; L = 0.5 µm; M = 1 µm.

© 2025 Westerdijk Fungal Biodiversity Institute

Etymology: *Micros* (Greek) small, and *carpon* (Greek) fruit, referring to the size of sporocarps.

Diagnosis: Differs from *L. exiguum* by the regular short ovoid shape of peridial vesicle aggregates, which do not form a unified network.

Sporocarps scattered, spherical, regular in shape, (0.5–)1–2.5(–3) mm diam. *Peridium* membranous, light reddish brown, covered by vesicles so densely, that sporocarp looks dark brown. *Peridial vesicles* in aggregates that look like dark brown to black spots of ovoid shape and pitted surface, separated from each other by a network of vesicle-lacking areas; in TL aggregates (20–)100–170(–220) µm diam., dense, ovoid, with 4–6 vesicles across the group. Individual vesicles (10–)30–40 µm, rounded, somewhat angular from mutual pressure, brown. Vesicle walls thin (1–2 µm), multi-layered, with smooth outer layer covering the whole group. *Crystals* absent. *Oil* droplets small or in the form of *granular deposits*, colourless or brownish. *Inner surface of the peridium* smooth or covered by scanty warts. *Capillitium* tubular, 2–10 µm diam., with slightly wavy contour; surface fine pitted-warty, with ring-shaped islets. *Spore mass* beige. *Spores* 5–6(–6.5) µm diam., hyaline, reticulate, 6–8 meshes across diam., unornamented area occupies 1/3–1/4 of the spore surface. *Immature fructifications* bright orange.

Typus: **Russia**, Primorsky Krai, Ussuriysky State Reserve (43.6525 132.46581), on the trunk of a rotting fallen tree, 17 Aug. 2022, *Y. Ishchenko* (**holotype** GFW IY116). GenBank: nucSSU = PQ633769 (rg50); mtSSU = PQ633476; *COI* = PQ628494.

Distribution: Asia (Vietnam), Europe (Russia, Ukraine).

Notes: This species belongs to the *L. exiguum* complex (Fig. 30, see below), which requires further studies, as it includes at least eight hard-to-distinguish putative biospecies. However, *L. microcarpum* can be reliably differentiated from the rest of the group, and particularly from the type material of *L. exiguum* (Leontyev & Schnittler 2023) by the regular ovoid shape of its vesicle aggregates, which do not form a network on the surface of the sporocarp. The appearance of the fruiting bodies in this species is distinctive enough to allow identification without dissection.

Lycogala sigillatum Leontyev, W.-L. Song & Shuang L. Chen. ***sp. nov.*** MB 857840. Fig. 20.

Etymology: *Sigillum* (Latin) stamp, referring to the similarity of peridial vesicles, as seen in RL, to the antique wax seal.

Diagnosis: Differs from *L. skovorodaense* by the light orange brown peridium, dark red brown vesicles and smooth capillitium threads.

Sporocarps solitary or in small groups, spherical to short horizontally ovoid, mostly regular in shape, (1.5–)2.5–5.5(–6.5) mm diam. *Peridium* membranous, light brown, densely covered by vesicles. *Peridial* vesicles (20–)40–80(–120) µm, in RL dark reddish brown, forming small irregular groups with pitted surface, in TL grouped in dense rounded clusters with 1–2 vesicles across the group, somewhat angular from mutual pressure, brown. Vesicle walls brown, thin to medium (1–2 µm), but looking thicker because the granular contents of the vesicle leave some free space around the wall; 1–2-layered. *Crystals* absent. *Oil* droplets numerous, small, variable in shape, colourless. *Inner surface of the peridium* smooth or covered by scanty warts and rings. *Capillitium* tubular, 2–15 µm diam., with wavy contour; surface fine pitted-warty, with ring-shaped islets. *Spore mass* beige. *Spores* (6–)6.5–7 µm diam., hyaline, reticulate, 5–6 meshes across diam., unornamented area occupies 1/3–1/4 of the spore surface. *Immature fructifications* unknown.

Typus: **China**, Guangdong Province, Dinghushan National Nature Reserve (23.1659 112.5409), on strongly decayed wood, 29 May 2014, *B. Wei & G. He* (**holotype** MCCNNU0796). GenBank: nucSSU = ON920615 (rg44).

Distribution: Asia (China).

Notes: This species resembles *L. skovorodaense*, although it is not closely related to it in terms of phylogeny. However, in the latter, the capillitium is covered with spine-like projections or at least with massive granulation, whereas in *L. sigillatum*, it is ornamented only with small pits and smooth bracelets. The new species also differs by pigmentation of the peridium and vesicles in RL: both structures are coloured in *L. sigillatum* much brighter, than in *L. skovorodaense*. From the superficially similar *L. ustulatum* and *L. maculatum* the new species differs by the grouping of vesicles into small, rounded aggregates.

Lycogala fuscoolearium Leontyev, Ishchenko, T. Kudryavtseva & R. Skrzypczak, ***sp. nov.*** MB 857841. Fig. 21.

Etymology: *Fuscus* (Latin) swarthy, dusky, and *olearius* (Latin), oily, referring to the similarity to *L. olearium*, but with darker oil accumulations.

Diagnosis: Differs from *L. olearium* by dark fuscous oil accumulations, more conspicuous peridial vesicles, occasional presence of crystals, and equal size of the meshes of spore ornamentation.

Sporocarps grouped, spherical to short horizontally ovoid, often deformed from mutual pressure, dull brown, (1–)4.5–7.5(–10) mm diam. *Peridium* membranous, light brown, dark brown, covered by vesicles. *Peridial vesicles* (80–)110–150(–210) µm, in RL light brown, amber yellow, light orange, convex, solitary or loosely grouped, in TL simple, ovoid or angular, brownish. Vesicle walls under TL hyaline, very thin (1 µm), inconspicuous. *Crystals* usually absent, if present – form small to rather large dense clusters. *Oil* droplets numerous, large (30–80 µm) and small, dull yellowish brown, orange brown, sometimes dark brown in mass, or only in the form or brownish *granular deposits*. *Inner surface of the peridium* smooth, sometimes pitted or covered by scattered warts or regular rings 1–2 µm diam. *Capillitium* tubular, 6–15 µm diam., with smooth or wavy contour, with two main types of ornamentation: by rings on the smooth surface or by regular warty bracelet-like thickenings. *Spore mass* light pinkish beige. *Spores* (6–)6.5–8 µm diam., hyaline, reticulate, 5–7

© 2025 Westerdijk Fungal Biodiversity Institute

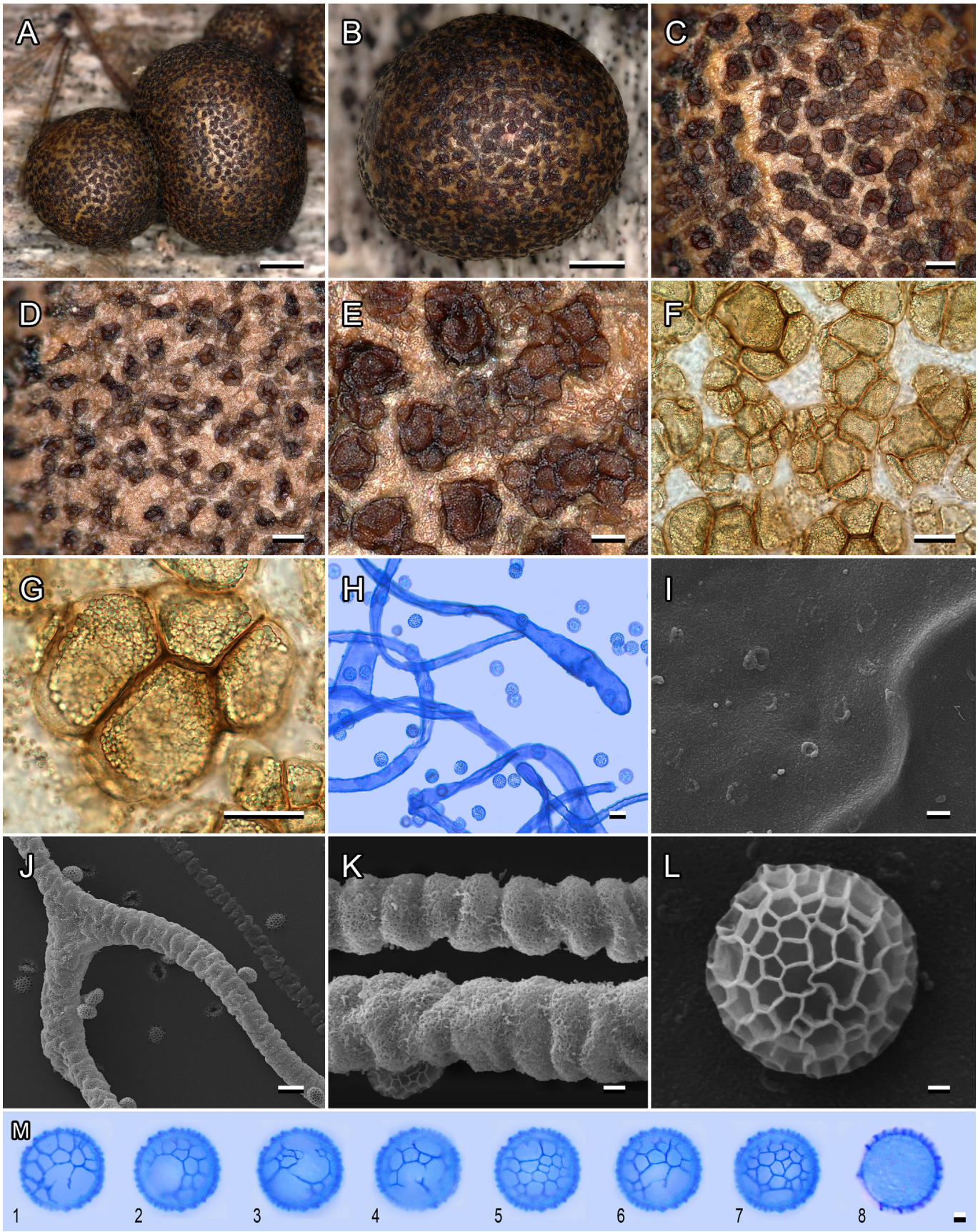

Fig. 20. *Lycogala sigillatum sp. nov*. [MCCNNU0796 (holotype)]. **A, B.** Sporocarps. **C–E.** Peridium in RL. **F, G.** Peridial vesicles in TL. **H.** Capillitium and spores, methyl blue in lactic acid. **I.** Inner surface of the peridium, SEM. **J, K.** Capillitial tubules, SEM. **L.** Spore, SEM. **M.** Spores, methyl blue in lactic acid. The last spore is shown in optical section. Scale bars: A, B = 1 mm; C, D = 100 µm; E–G = 50 µm; H, J = 10 µm; I, K, M = 1 µm; L = 0.5 µm.

© 2025 Westerdijk Fungal Biodiversity Institute

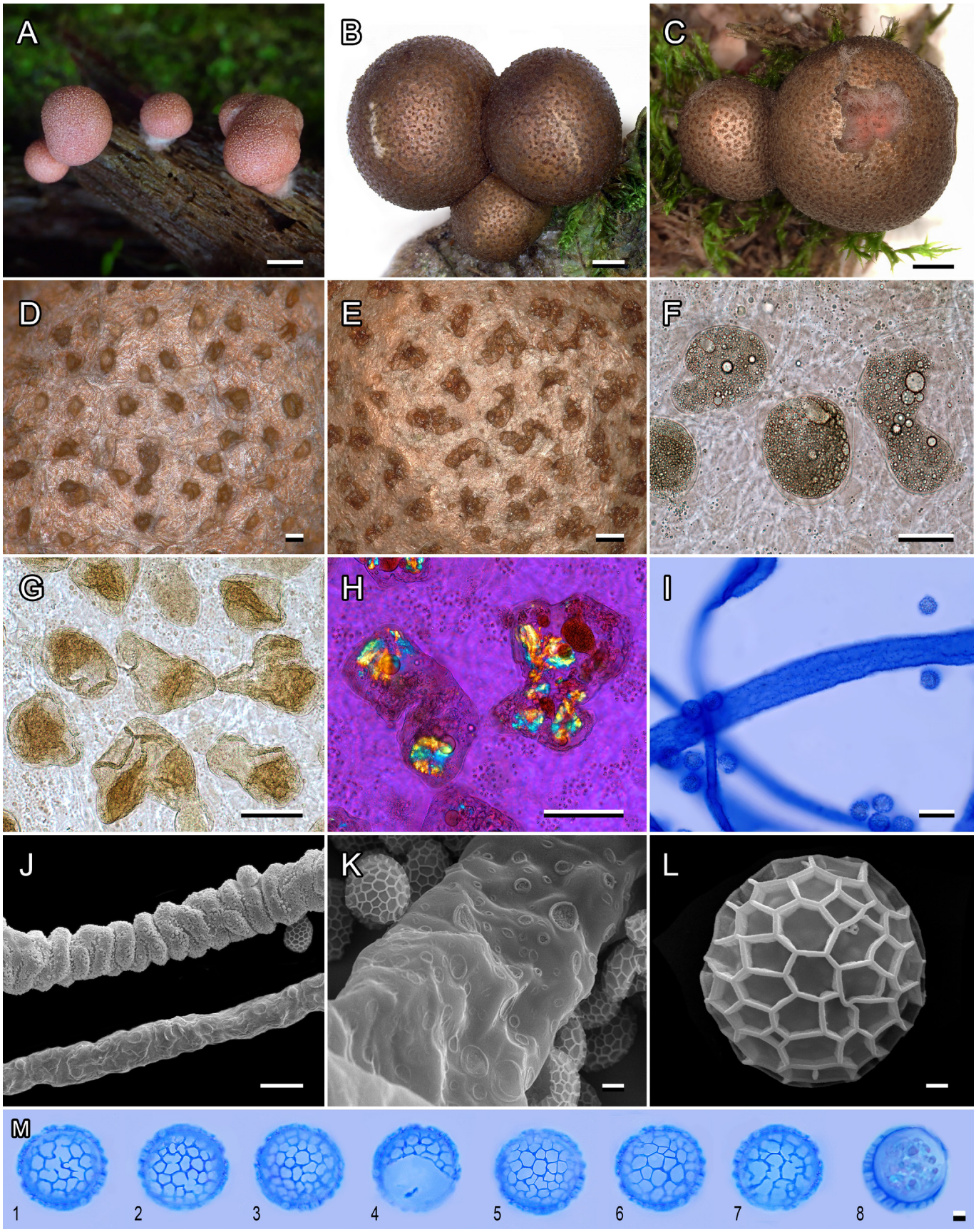

Fig. 21. *Lycogala fuscoolearium sp. nov.* [A, B, D, F, I, K–M. IY019 (holotype); C, E. IY056; G, H, J. IY053]. **A.** Immature fructifications. **B, C.** Sporocarps. **D, E.** Peridium in RL. **F, G.** Peridial vesicles in TL. **H.** Peridial vesicles in PL. **I.** Capillitium and spores, methyl blue in lactic acid. **J, K.** Capillitial tubules, SEM. **L.** Spore, SEM. **M.** Spores, methyl blue in lactic acid. The last spore is shown in optical section. Scale bars: A = 2 mm; B, C = 1 mm; D–H = 100 µm; I, J = 10 µm; K, M = 1 µm; L = 0.5 µm.

© 2025 Westerdijk Fungal Biodiversity Institute

meshes across diam., unornamented area occupies 1/2–1/3 of the spore surface. *Immature fructifications* light pinkish, with vesicles brighter than the background.

Typus: **Russia**, Moskovskaya Oblast, Volokolamsk, Litvinovo, Strizh (56.05156 36.19306), on decaying coniferous trunk, on rotten wood, on moss *Jochenia pallescens* and liverwort *Lophocolea heterophylla*, 12 Jun. 2020, *Y. Ishchenko* (**holotype** GFW IY019). GenBank: nucSSU = OM423930 (rg32); *COI* = ON931572.

Distribution: Europe (France, Russia).

Notes: This species is related to *L. olearium*, with which it shares many common features, including abundant oil accumulations in the peridial vesicles and ring-like ornamentation observed on the peridium and capillitium. The differences between these two species are specified in the diagnosis. Compared to another closely related species, *L. densum*, *L. fuscoolearium* differs by the sparser arrangement of vesicles and several other traits (see the diagnosis of *L. densum*). Due to its distinct vesicles, which may be yellowish or orange, *L. fuscoolearium* resembles 'crystalliferous' species, such as *L. leopardinum*, *L. succineum*, and *L. caviaroides*, but differs from them by the abundant presence of oil in the vesicles.

Lycogala densum Leontyev, M. Kobayashi, E. Moroz, T. van der Heul, Bortnikov, E. Johannesen & Schnittler, ***sp. nov.*** MB 857842. Fig. 22.

Etymology: *Densus* (Latin) dense, overgrown, tightly closed, referring to the dense cover of peridial vesicles.

Diagnosis: Differs from *L. fuscoolearium* by the dense arrangement of peridial vesicles, their orange-brown colouration and convex shape, as well as by the light yellowish oil accumulations, and bigger (6–8 µm) spores.

Sporocarps scattered, spherical to short horizontally ovoid, more-or-less regular in shape, (1.5–)3.5–6(–8) mm diam. *Peridium* membranous, light orange-brown, densely covered by vesicles. *Peridial vesicles* (30–)80–120(–160) µm, in RL look like dried droplets, as light as the peridium or somewhat darker, yellowish to orange-brown, solitary, convex, distant from each other on 0.5–1 of their diam., in TL simple, ovoid, light yellow. Vesicle walls light brownish, thin (1–2 µm), 1–2-layered, with the outer layers more-or-less smooth. *Crystals* absent. *Oil* droplets numerous, large (30–50 µm) or only small, more-or-less rounded, yellowish or light brown. *Inner surface of the peridium* smooth or covered by warts and inconspicuous rings. *Capillitium* tubular, 5–15 µm diam., with smooth or wavy contour, ornamented by clustered warts or nearly smooth. *Spore mass* pinkish beige. *Spores* (5–)6–8 µm diam., hyaline, reticulate, 5–7 meshes across diam., unornamented area indistinct, occupies 1/4–1/5 of the spore surface. *Immature fructifications* unknown.

Typus: **Japan**, Honshu, Nagano, Lake Matsubara, Koumi-Chom Minami Saku-Gun (36.054 138.456), on dead wood, 25 Jun. 2005, *M. Kobayashi & M. Kobayashi* (**holotype** TNSM12581). GenBank: nucSSU = PQ633916 (rg86).

Distribution: Asia (Japan), Australia, Europe (Belarus, Norway, Russia).

Notes: This taxon was described based on a complex of three phylogenetically close and morphologically similar biological species (rg28, 86, 87); broader sampling may allow to separate these biospecies in future. All members of the complex are characterized by densely arranged convex vesicles coloured in orange-brown tone and containing numerous yellowish or brownish oil droplets. Dense and convex vesicle patterns abovementioned traits distinguish *L. densum* from the related *L. fuscoolearium*. Additionally, although we observed ring-like ornamentation of the peridium in *L. densum*, it appears to be less developed than in other oil-containing species, such as *L. fuscoolearium* and *L. olearium*. By its distinct rounded vesicles, *L. densum* resembles 'crystalliferous' species, especially *L. acinonychum*, but differs from them by abundant oil accumulations.

Lycogala oleocrystalliferum Leontyev, Ishchenko, S.J. Lloyd ., W.-L. Song, Shuang L. Chen, Schnittler, V. Botyakov & E. Moroz, ***sp. nov.*** MB 857843. Fig. 23.

Etymology: *Olearius* (Latin), oily, and *crystallifer* (Latin), bearing crystals, referring to the presence of both oily and crystalline accumulations in peridial vesicles.

Diagnosis: Differs from *L. olearium* by more conspicuous peridial vesicles, often containing orange pigment, and from *L. caviaroides* by the presence of oil.

Sporocarps in tight groups, spherical to short horizontally ovoid, often deformed from mutual pressure, (1.5–)2.5–4(–6) mm diam. *Peridium* membranous, light orange-brown, covered by vesicles. *Peridial vesicles* (60–)80–120(–150) µm, in RL look like dried droplets, bright orange, orange-brown, brown, semitranslucent, solitary, convex or folded, evenly distributed, distant from each other on 0.5–2 of their diam., in TL simple, ovoid, brown. Vesicle walls colourless, thin (1 µm), single-layered. *Crystals* present, forming rounded aggregates, masked by the presence of oil. *Oil* in the form of *granular deposits*, brown, densely filling entire vesicle. Orange vesicles contain pigment accumulations of the same colour. *Inner surface of the peridium* smooth or covered by warts. *Capillitium* tubular, 3–15 µm diam., ornamented by regular warty bracelet-like thickenings; the depressions between the bracelets are ornamented with large ring-shaped pits. *Spore mass* light pinkish. *Spores* (6–)6.5–7.5 µm diam., hyaline, reticulate, 5–7 meshes across diam., unornamented area occupies 1/2–1/4 of the spore surface. *Immature fructifications* orange pink, with vesicles brighter than the background.

Typus: **Russia**, Moskovskaya Oblast, Moscow, North-Eastern Administrative District, Severnyi (55.92871 37.55439), on rotten wood, 3 Jul. 2023, *Y. Ishchenko* (**holotype** GFW IY154). GenBank: nucSSU = PQ633801 (rg51).

Distribution: Asia (China), Australia, Europe (Belarus, Russia).

Notes: This taxon was described based on a complex of three phylogenetically close and morphologically similar putative

© 2025 Westerdijk Fungal Biodiversity Institute

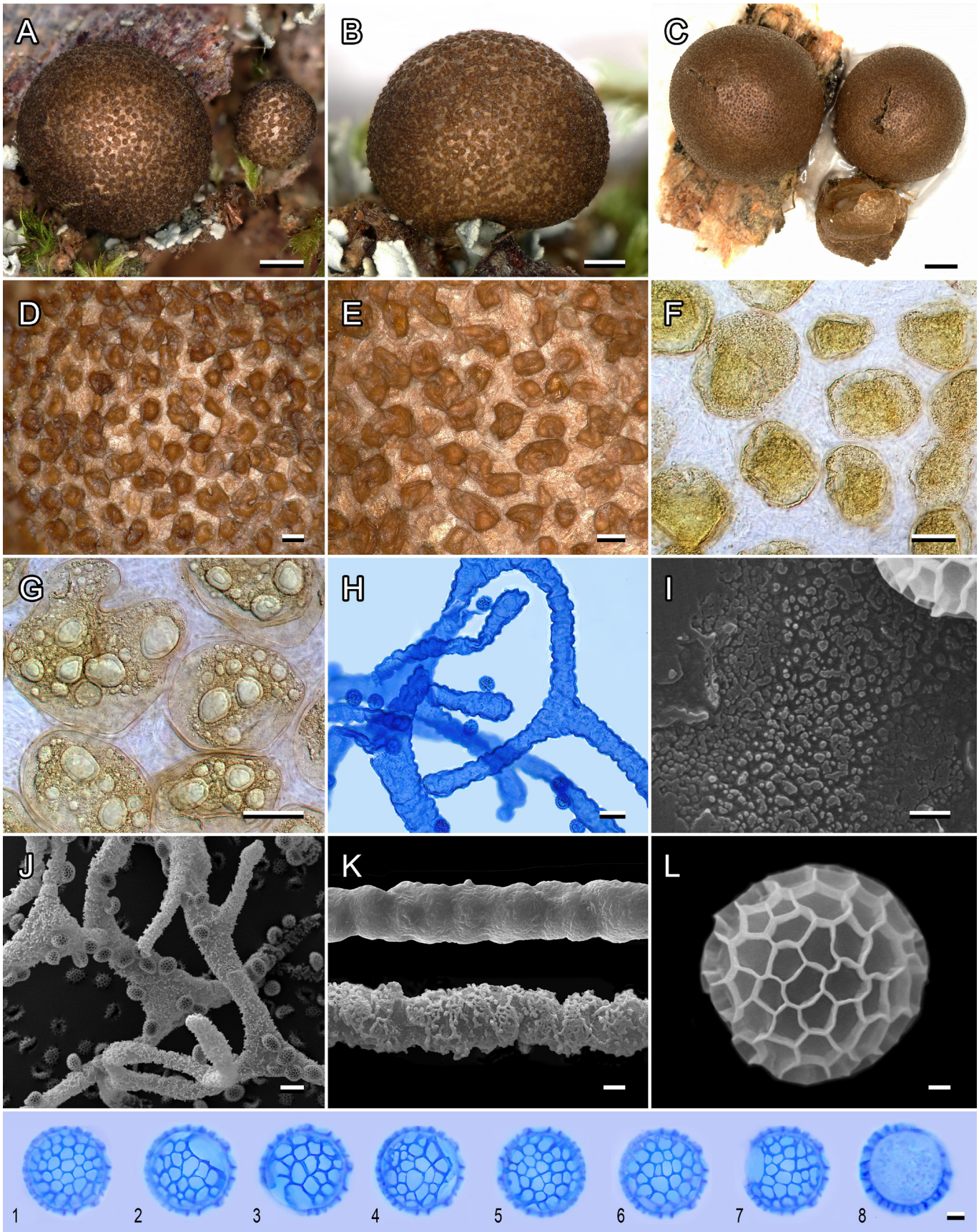

Fig. 22. *Lycogala densum sp. nov*. [A, B, D, F, G, I–M. TNSM12581 (holotype); C, H. MYX18345 (rg28); E. MSK43319 (rg87)]. **A–C.** Sporocarps. **D, E.** Peridium in RL. **F, G.** Peridial vesicles in TL. **H.** Capillitium and spores, methyl blue in lactic acid. **I.** Inner surface of the peridium, SEM. **J, K.** Capillitial tubules, SEM. **L.** Spore, SEM. **M.** Spores, methyl blue in lactic acid. The last spore is shown in optical section. Scale bars: A–C = 1 mm; D, E = 100 µm; E–G = 50 µm; H, J = 10 µm; I, K, M = 1 µm; L = 0.5 µm.

© 2025 Westerdijk Fungal Biodiversity Institute

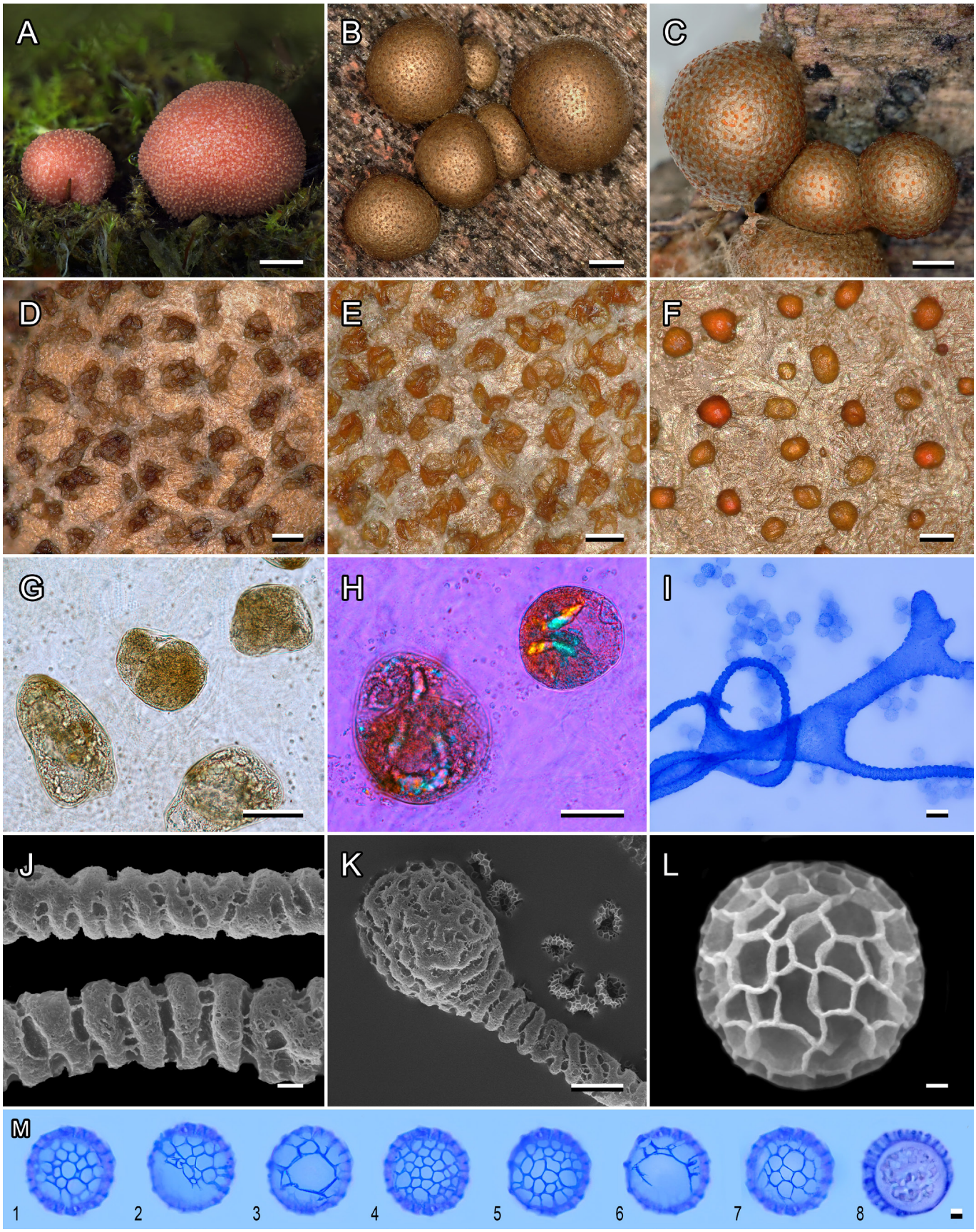

Fig. 23. *Lycogala oleocrystalliferum sp. nov.* [A, G, H. IY077; B, I–M. IY154 (holotype); C. MCCNNU3024 (rg72); D. IY139; E. sc34703 (rg74); F. MEL2533243 (rg74)]. **A.** Immature fructifications. **B, C.** Sporocarps. **D–F.** Peridium in RL. **G.** Peridial vesicles in TL. **H.** Peridial vesicles in PL. **I.** Capillitium and spores, methyl blue in lactic acid. **J, K.** Capillitial tubules, SEM. **L.** Spore, SEM. **M.** Spores, methyl blue in lactic acid. The last spore is shown in optical section. Scale bars: A–C = 1 mm; D–F = 100 µm; G, H = 50 µm; I, K = 10 µm; J, M = 1 µm; L = 0.5 µm.

© 2025 Westerdijk Fungal Biodiversity Institute

biological species (rg51, 72, 74); broader sampling may allow to separate these biospecies in future. All members of the complex are characterized by rounded solitary peridial vesicles, filled with brown granular oil and at the same time showing birefringence at polarized light, which indicates crystal accumulations. In RL the colour of these vesicles varies from bright orange to dull brown, resembling in the first case *L. caviaroides*, and in the second – *L. succineum*, *L. palyanytsia*, and *L. fuscoolearium.* Specimens with orange vesicles represent the only currently known "twin" species of *L. caviaroides.* Interestingly, *L. oleoctystalliferum* resembles this species also by the ornamentation of capillitium: the depressions between the bracelets are ornamented with large ring-shaped pits. This was observed in rg51, to which the species holotype belongs; in rg74 these structures are less prominent.

Lycogala guttatum Leontyev, W.-L. Song, Shuang L. Chen, Ishchenko, D. Panayotova & V. Botyakov, ***sp. nov.*** MB 857844. Fig. 24.

Etymology: *Gutta* (Latin) droplet, referring to the presence of large yellow oil droplets in peridial vesicles.

Diagnosis: Differs from *L. succineum* by the presence of yellowish oil droplets and absence of crystals in peridial vesicles.

Sporocarps grouped, spherical to short horizontally ovoid, often deformed from mutual pressure, (2.5–)4–5.5(–7.5) mm diam. *Peridium* membranous, light yellowish brown, covered by vesicles. *Peridial vesicles* (70–)100–140(–280) µm, in RL look like dried droplets, light brown, solitary, convex or depressed in the central part, evenly distributed, distant from each other on 1–3 of their diam., in TL simple, ovoid, nearly hyaline. Vesicle walls colourless, thin (1 µm), single-layered. *Crystals* absent. *Oil* droplets large [20–50(–120) µm] and small, bright warm-yellow, very conspicuous on the hyaline background. *Inner surface of the peridium* covered by warts and rings. *Capillitium* tubular, 2–10 µm diam., with smooth or wavy contour and two main types of ornamentation: by regular, bracelet-like thickenings and by rings and pits. *Spore mass* light pinkish. *Spores* (6–)6.5–8.5(–9.5) µm diam., hyaline, reticulate, 4–6 meshes across diam., unornamented area occupies 1/2–1/3 of the spore surface. *Immature fructifications* light to bright pinkish orange, with vesicles brighter than the background.

Typus: **USA**, California, Scotts Valley, Henry Cowell Redwoods State Park (37.028339 -122.04549), on dead wood, 14 Dec. 2019, *D. Panayotova* (**holotype** CWP3660). GenBank: nucSSU = OM423856 (rg15); mtSSU = PQ633412; *COI* = ON931546.

Distribution: Asia (China), Europe (Russia), North America (USA).

Notes: This taxon was described based on a complex of three phylogenetically close and morphologically similar biological species (rg15, 84, 91); broader sampling may allow to separate these biospecies in future. All members of the complex resemble *L. succineum* by their beige sporocarps, covered with accurate honey brown vesicles, rather distant from each other. Microscopic structures, like large oil droplets and ring ornamentation of capillitium, put *L. guttatum* together with oil-containing species, but the bright warm yellow pigmentation of oil distinguishes it from *L. olearium* and *L. fuscoolearium*. One more "oily" species, *L. densum*, has much denser and darker vesicles, and its oil pigmentation is only slightly yellowish. Two more species contain bright yellow oil: *L. miserum* and *L. asperum*, but both have small (3–3.5 and 2–3 mm, respectively) and solitary sporocarps. *L. miserum*, in addition, contains crystals, and *L. asperum* has convex dark brown vesicles, spiny capillitium and rings on peridium.

Lycogala melleum Leontyev, W.-L. Song, Shuang L. Chen & M. Shim, ***sp. nov.*** MB 857845. Fig. 25.

Etymology: *Mel* (Latin) honey, referring to the colour of the fresh peridial vesicles.

Diagnosis: Differs from *L. succineum* by yellow pigmentation of immature sporocarps and almost absent crystal accumulations in peridial vesicles.

Sporocarps in small groups, spherical to short horizontally ovoid, regular in shape, (1.5–)2.5–3(–4.5) mm diam. *Peridium* membranous, light orange brown, covered by vesicles. *Peridial vesicles* (100–)120–170(–270) µm, in RL look like dried droplets, dull orange, orange-brown, brown, semitranslucent, solitary, convex, evenly distributed, distant from each other on 0.5–1 of their diam., in TL simple, ovoid, yellowish to brown. Vesicle walls light brownish, thin (1 µm), single-layered. *Crystals* very rare, in form of small inclusions. *Oil* inconspicuous. Amorphous *pigment* accumulations of yellow or orange colour present in most of vesicles. *Inner surface of the peridium* covered by warts and rings. *Capillitium* tubular, 6–20 µm diam., with smooth or wavy contour and two main types of ornamentation: by regular, bracelet-like thickenings and by rings and pits. *Spore mass* light yellowish beige. *Spores* (5.5–)6–7 µm diam., hyaline, reticulate, 4–5 meshes across diam., unornamented area occupies 1/2–1/3 of the spore surface. *Immature fructifications* yellow.

Typus: **South Korea**, Ulsan, Nam-gu district, Ulsan Grand Park (35.527053 129.295456), on a cone of *Pinus densiflora*, 17 Jun. 2022, *K. Lee & M. Shim* (**holotype** GFW MiShim01). GenBank: nucSSU = ON920625 (rg52); mtSSU = PQ633510.

Distribution: Asia (China, South Korea).

Notes: The bright yellow colouration of the sporocarps distinguishes *L. melleum* from all other described members of the genus. However, the authors have seen photographs of orange yellow sporocarps in *L. epidendrum* s. str., which typically has pink colouration, thus revealing possible within-species polymorphism of this character (see www.naturephoto-cz.com, accession 17205) For this reason, the stability of the colour characteristic within *L. melleum* requires further study. This species, however, can as well be reliably identified in its fully mature state. It resembles the related *L. succineum*, but it has slightly smaller sporocarps

© 2025 Westerdijk Fungal Biodiversity Institute

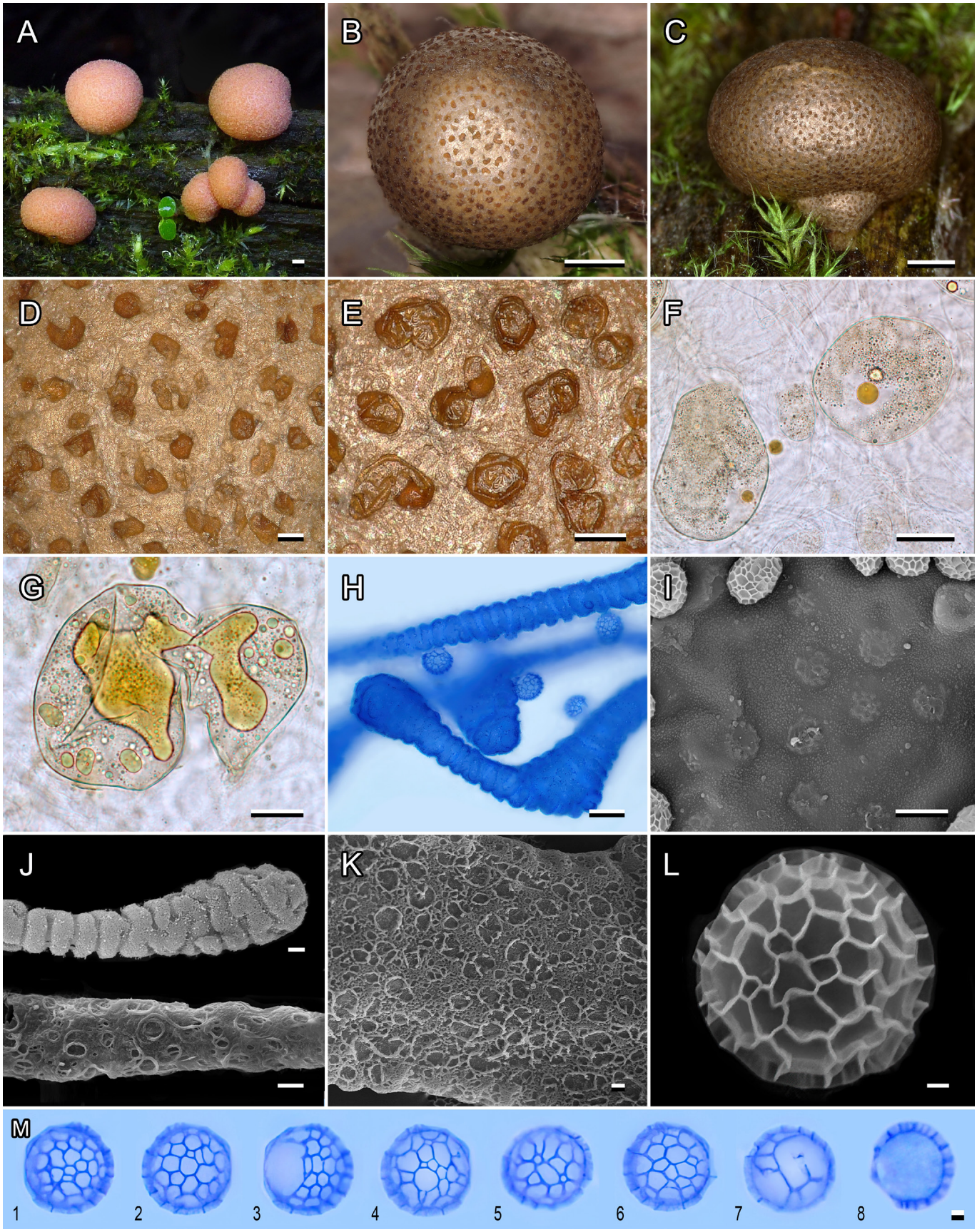

Fig. 24. *Lycogala guttatum sp. nov*. [A, C, F. IY099 (rg91); B, D, G. IY093 (rg91); E. MCCNNU2076 (rg84); H–M. CWP3660 (holotype)]. **A.** Immature fructifications. **B, C.** Sporocarps. **D, E.** Peridium in RL. **F, G.** Peridial vesicles in TL. **H.** Capillitium and spores, methyl blue in lactic acid. **I.** Inner surface of the peridium, SEM. **J.** Capillitial tubules, SEM. **K.** Surface of wide capillitial tubule, SEM. **L.** Spore, SEM. **M.** Spores, methyl blue in lactic acid. The last spore is shown in optical section. Scale bars: A–C = 1 mm; D, E = 100 µm; F, G = 50 µm; H, I = 10 µm; J, K, M = 1 µm; L = 0.5 µm.

© 2025 Westerdijk Fungal Biodiversity Institute

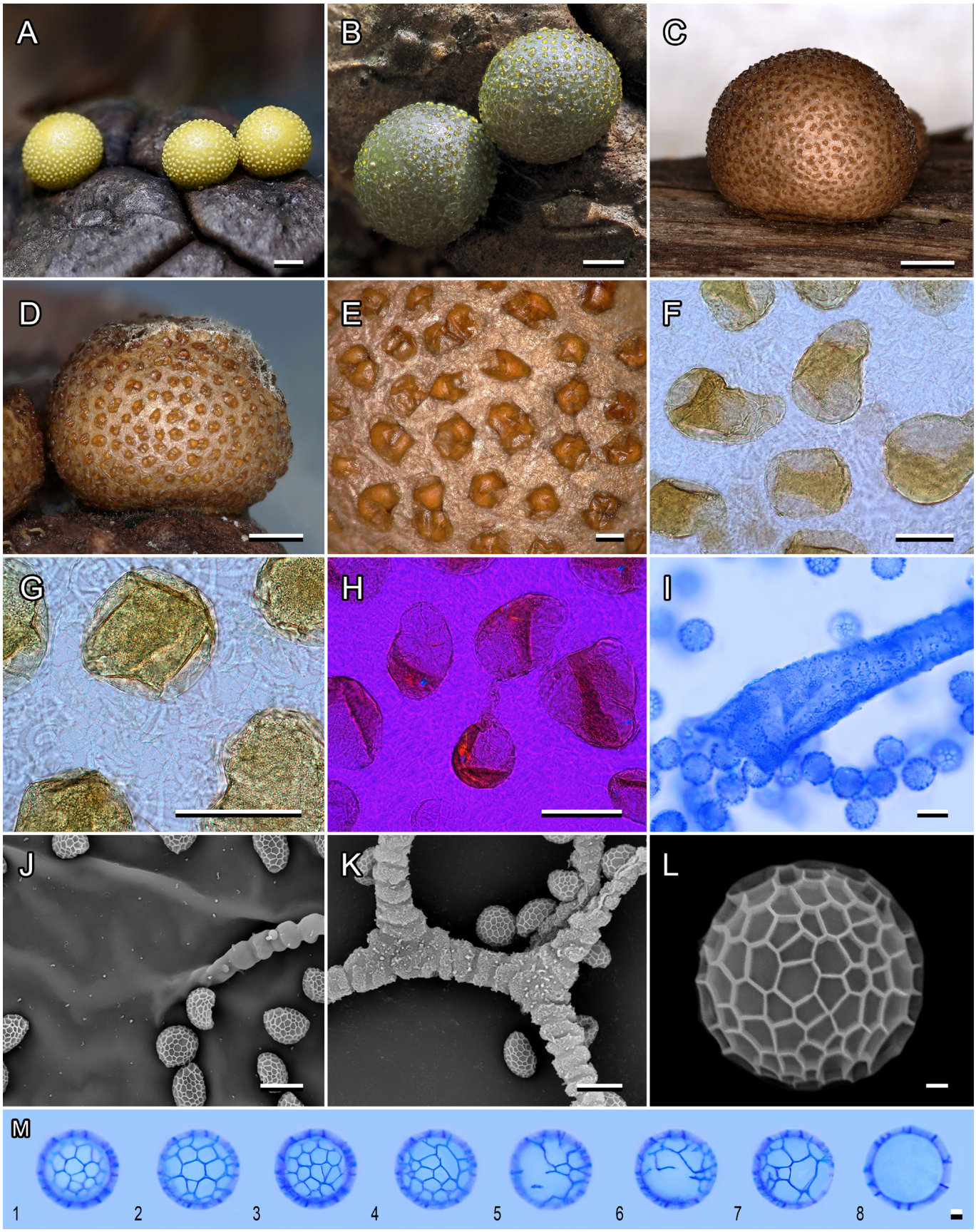

Fig. 25. *Lycogala melleum sp. nov*. [A, B, D–H, M. MiShim01 (holotype); C, I–L. MCCNNU3035]. **A, B.** Immature fructifications (courtesy of M. Shim). **C, D.** Sporocarps. **E.** Peridium in RL. **F, G.** Peridial vesicles in TL. **H.** Peridial vesicles in PL. **I.** Capillitium and spores, methyl blue in lactic acid. **J.** Inner surface of the peridium, SEM. **K.** Capillitial tubule, SEM. **L.** Spore, SEM. **M.** Spores, methyl blue in lactic acid. The last spore is shown in optical section. Scale bars: A–D = 1 mm; E–H = 100 µm; I–K = 10 µm; L = 0.5 µm; M = 1 µm.

© 2025 Westerdijk Fungal Biodiversity Institute

(2.5–3 mm) and, most important, its peridial vesicles contain virtually no crystals, whereas *L. succineum* is known for their abundant accumulation.

Lycogala costaricanum Leontyev, Schnittler & C. Rojas, ***sp. nov.*** MB 857846. Fig. 26.

Etymology: Costa Rica, referring to the type locality.

Diagnosis: Differs from other 'crystalliferous' species like *L. leopardinum* and *L. succineum* by the greyish colour of sporocarps, their smaller size (1.5–2.5 mm) and remarkably verrucose capillitium.

Sporocarps grouped, spherical to short horizontally ovoid, regular in shape, (0.5–)1.5–2.5(–3.5) mm diam. *Peridium* membranous, warm grey, covered by vesicles. *Peridial vesicles* (60–)90–120(–170) µm, in RL look like dried droplets, dull brownish, semitranslucent, solitary, convex or folded, evenly distributed, distant from each other on 0.5–1 of their diam., in TL simple, irregularly ovoid, light brownish. Vesicle walls hyaline, thin (1 µm), single-layered. *Crystals* numerous, forming irregular aggregates, often completely filling the inner space of the vesicle. *Oil* present in form of granular accumulations, brownish. *Inner surface of the peridium* smooth, with occasional warts. *Capillitium* tubular, 3–10 µm diam., with wavy contour, ornamented by regular, bracelet-like thickenings, which are covered by numerous large warts, clearly visible under TL. *Spore mass* light warm grey. *Spores* (5–)6–6.5 µm diam., hyaline, reticulate, 6–8 meshes across diam., unornamented area occupies 1/2–1/3 of the spore surface. *Immature fructifications* unknown.

Typus: **Costa Rica**, Cartago, Turrialba, FEIMA Experimental Forest, near village La Suiza (-83.63698 9.86589), on strongly decayed woody branch, 3 cm diam., 23 Feb. 2020, *M. Schnittler* (**holotype** GFW sc32114). GenBank: nucSSU = OM424026 (rg17); mtSSU = PQ633607; *COI* = ON931602.

Distribution: Central America (Costa Rica).

Notes: This is the only currently known representative of 'crystalliferous' *Lycogala* species in Central America. It differs quite sharply from other species of the group by the traits specified in the diagnosis, and its identification should not present any difficulties.

Lycogala australe Leontyev, S.J. Lloyd & P. McDonald, ***sp. nov.*** MB 857847. Fig. 27.

Etymology: *Australis* (Latin) southern, referring to the occurrences of the species in Southern Hemisphere.

Diagnosis: Differs from other 'crystalliferous' species like *L. leopardinum* and *L. succineum* by the irregular elongated shape of peridial vesicles, which tend to merge to each other, and by small [2–3(–4) mm], solitary sporocarps.

Sporocarps solitary, spherical to short horizontally ovoid, regular in shape, (1.5–)2–3.5(–4.5) mm diam. *Peridium* membranous, light orange brown, covered by vesicles. *Peridial vesicles* (60–)120–160(–240) µm, in RL look like dried droplets, orange-brown, brown, semitranslucent, solitary or forming loose groups, convex or folded, more-or-less evenly distributed, distant from each other on 1–2 of their diam., in TL simple or forming loose aggregates, ovoid to elongate, light brown. Vesicle walls light brownish, thin (1–2 µm), 1–2-layered with outer layer somewhat granular. *Crystals* numerous, in form of scattered inclusions. *Oil* present in form of occasional yellow droplets and abundant, brownish, *granular accumulations*. *Inner surface of the peridium* smooth or covered by warts. *Capillitium* tubular, 2–10 µm diam., with wavy contour, surface fine pitted, with occasional ring-shaped islets. *Spore mass* light pinkish beige. *Spores* (6–)6.5–8 µm diam., hyaline, reticulate, 6–8 meshes across diam., unornamented area occupies 1/2–1/3 of the spore surface. *Immature fructifications* unknown.

Typus: **Australia**, Tasmania, Mount Roland area, 2 km W of Sheffield (-41.3717 146.2841), on the bark of fallen stringy bark tree, 27 Oct. 2022, *P. McDonald* (**holotype** MEL PMcD230). GenBank: nucSSU = PQ633834 (rg71); mtSSU = PQ633575.

Distribution: Australia (Tasmania), South America (Argentina).

Notes: *Lycogala australe* is well distinguished from other members of the 'crystalliferous' group by the traits outlined in the diagnosis. However, there is a possibility of confusing it with the 'oily' species like *L. densum* and *L. guttatum*, especially since the former is found in Australia. However, both similar species have very abundant oil accumulations and lack crystals.

Lycogala miserum Leontyev & Schnittler, ***sp. nov.*** MB 857848. Fig. 28.

Etymology: *Miser* (Latin) wretched, miserable, referring to the poor development of sporocarps and indistinct diagnostic features.

Diagnosis: Differs from other 'crystalliferous' species like *L. palianytsia* by small irregular peridial vesicles filled with yellow oil accumulations, and by small (3–3.5 mm), solitary sporocarps.

Sporocarps solitary, spherical to short horizontally ovoid, regular in shape, (2.5–)3–3.5(–4) mm diam. *Peridium* membranous, light orange brown, covered by vesicles. *Peridial vesicles* (60–)100–150(–200) µm, in RL brown, solitary, folded, unevenly distributed, distant from each other on 2–4 of their diam., in TL simple, ovoid or angular, yellowish. Vesicle walls hyaline, thin (1 µm), single-layered. *Crystals* numerous, in form of scattered inclusions. *Oil* present in form of *granular accumulations*, brownish. *Inner surface of the peridium* smooth or covered by warts and rings. *Capillitium* tubular, 5–15 µm diam., with wavy contour, surface fine pitted, with occasional ring-shaped islets or more prominent rings. *Spore mass* warm grey. *Spores* (6–)6.5–8 µm diam., hyaline, reticulate, 5–7 meshes across diam., unornamented area indistinct, occupies 1/3–1/4 of the spore surface. *Immature fructifications* unknown.

© 2025 Westerdijk Fungal Biodiversity Institute

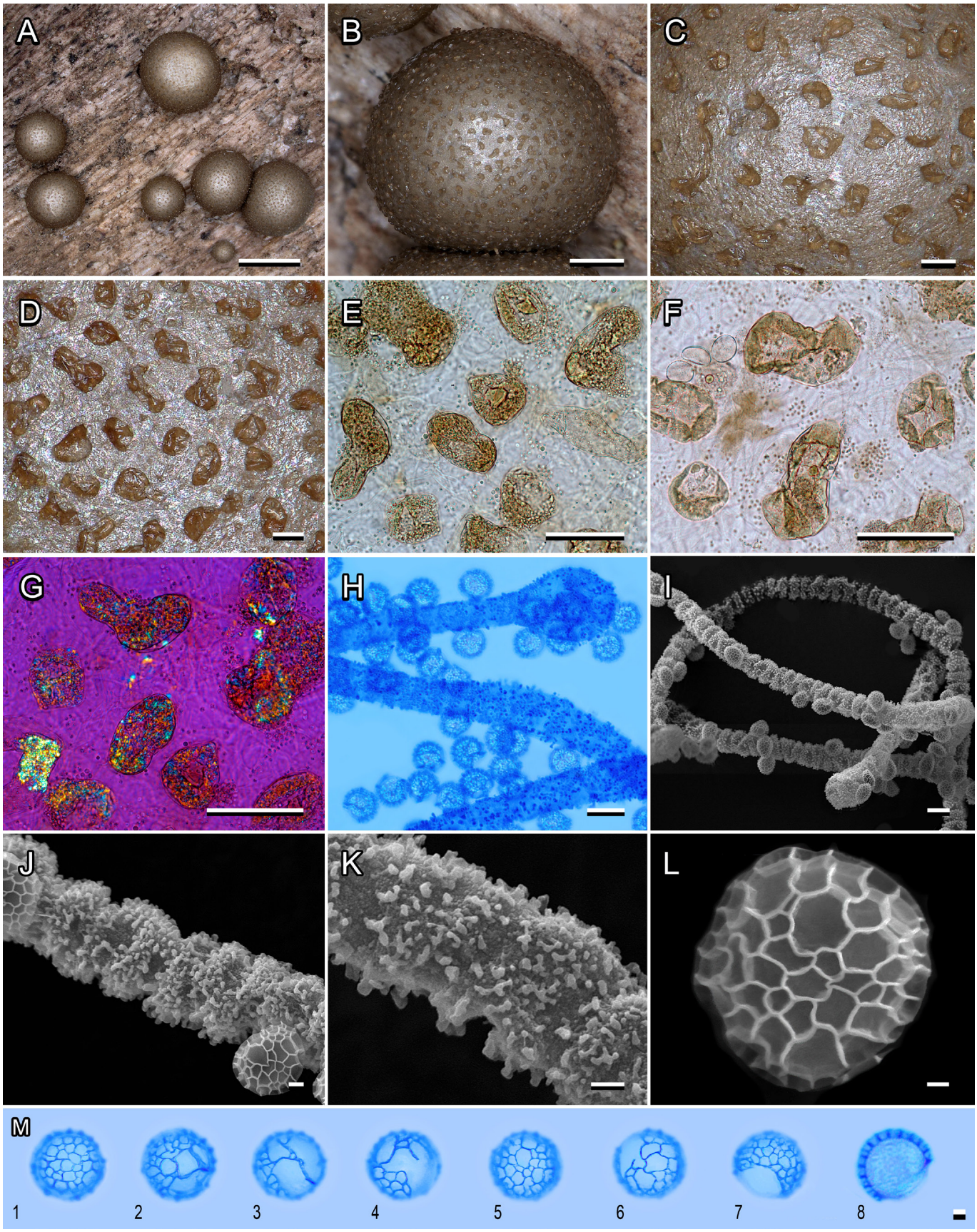

Fig. 26. *Lycogala costaricanum sp. nov*. [A, B, D, H, M. sc32114 (holotype); C, E–G, I–L. CWU4048]. **A, B.** Sporocarps. **C, D.** Peridium in RL. **E, F.** Peridial vesicles in TL. **G.** Peridial vesicles in PL. **H.** Capillitium and spores, methyl blue in lactic acid. **I–K.** Capillitial tubule, SEM. **L.** Spore, SEM. **M.** Spores, methyl blue in lactic acid. The last spore is shown in optical section. Scale bars: A = 2 mm; B = 0.5 mm; C–G = 100 µm; H, I = 10 µm; J, K, M = 1 µm; L = 0.5 µm.

© 2025 Westerdijk Fungal Biodiversity Institute

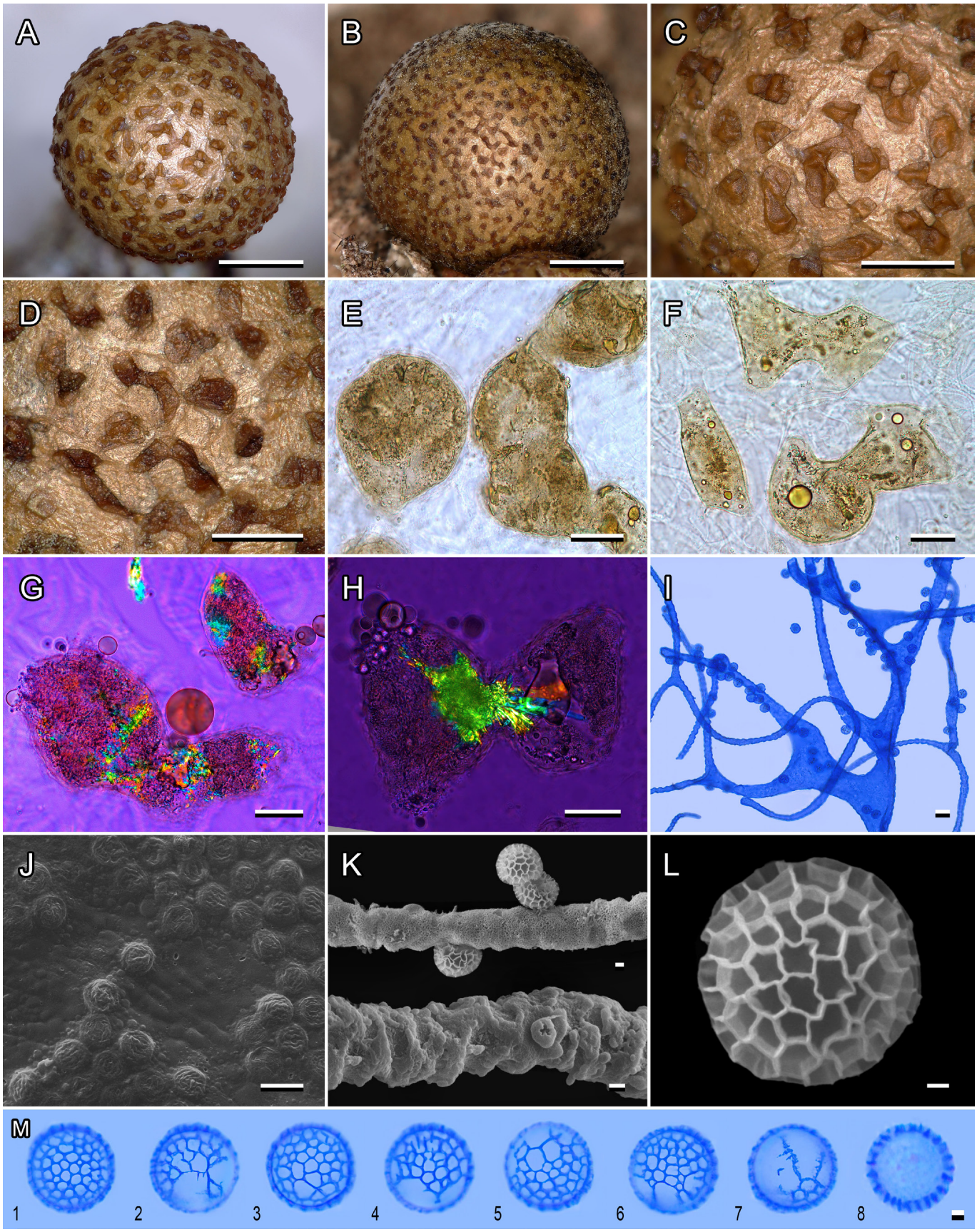

Fig. 27. *Lycogala australe sp. nov*. [A, C, F–M. PMcD230 (holotype); B, D, E. SJL1182]. **A, B.** Sporocarps. **C, D.** Peridium in RL. **E, F.** Peridial vesicles in TL. **G, H.** Peridial vesicles in PL. **I.** Capillitium and spores, methyl blue in lactic acid. **J.** Inner surface of the peridium, SEM. **K.** Capillitial tubules, SEM. **L.** Spore, SEM. **M.** Spores, methyl blue in lactic acid. The last spore is shown in optical section. Scale bars: A, B = 1 mm; C, D = 0.5 mm; E–H = 50 µm; I, J = 10 µm; K, M = 1 µm; L = 0.5 µm.

© 2025 Westerdijk Fungal Biodiversity Institute

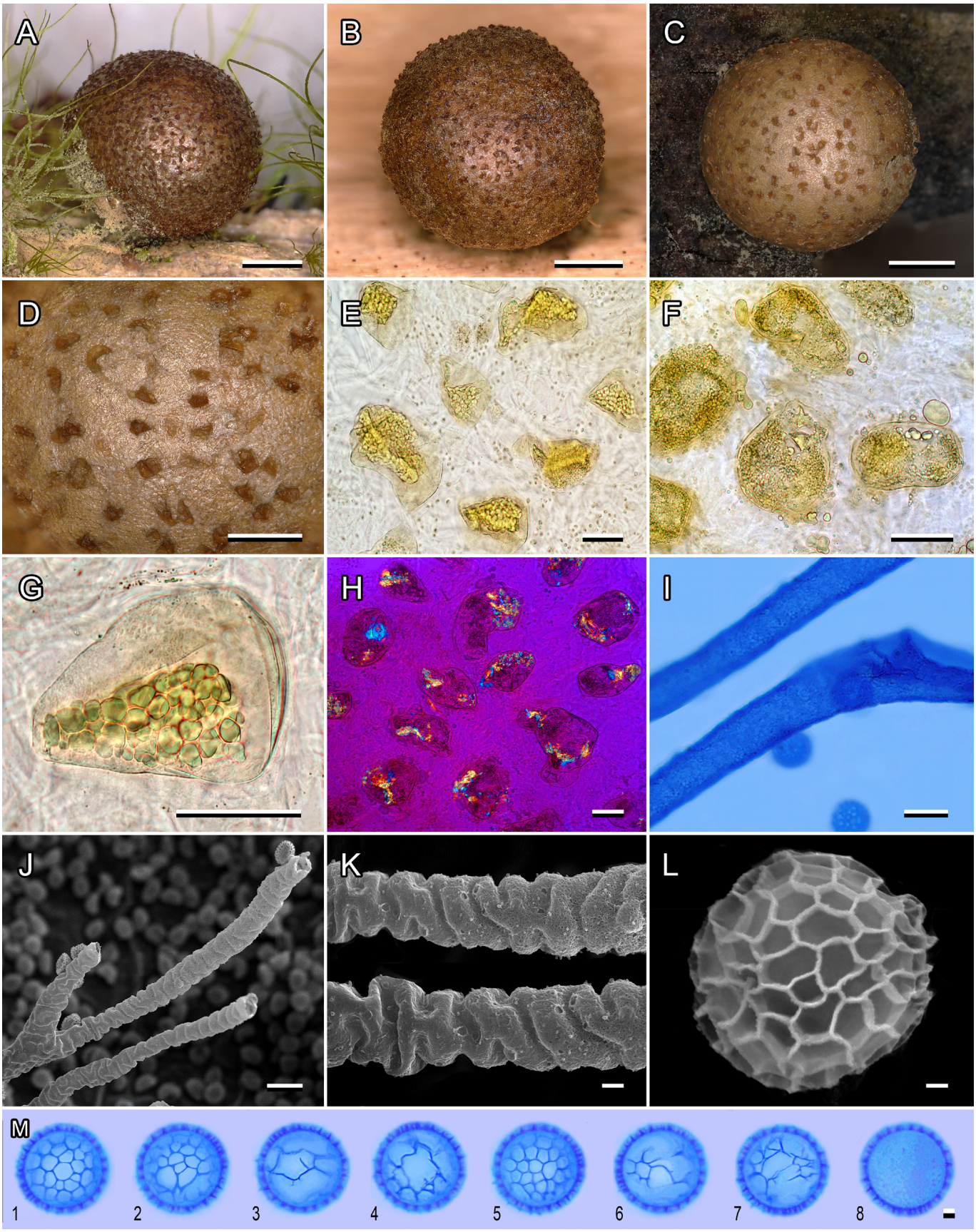

Fig. 28. *Lycogala miserum sp. nov*. [A, B, E, F, H–M. sc20167 (holotype); C, D, G. CWP2851]. **A–C.** Sporocarps. **D.** Peridium in RL. **E–G.** Peridial vesicles in TL. **H.** Peridial vesicles in PL. **I.** Capillitium and spores, methyl blue in lactic acid. **J, K.** Capillitial tubules, SEM. **L.** Spore, SEM. **M.** Spores, methyl blue in lactic acid. The last spore is shown in optical section. Scale bars: A–C = 1 mm; D = 0.5 mm; E–H = 50 µm; I, J = 10 µm; K, M = 1 µm; L = 0.5 µm.

© 2025 Westerdijk Fungal Biodiversity Institute

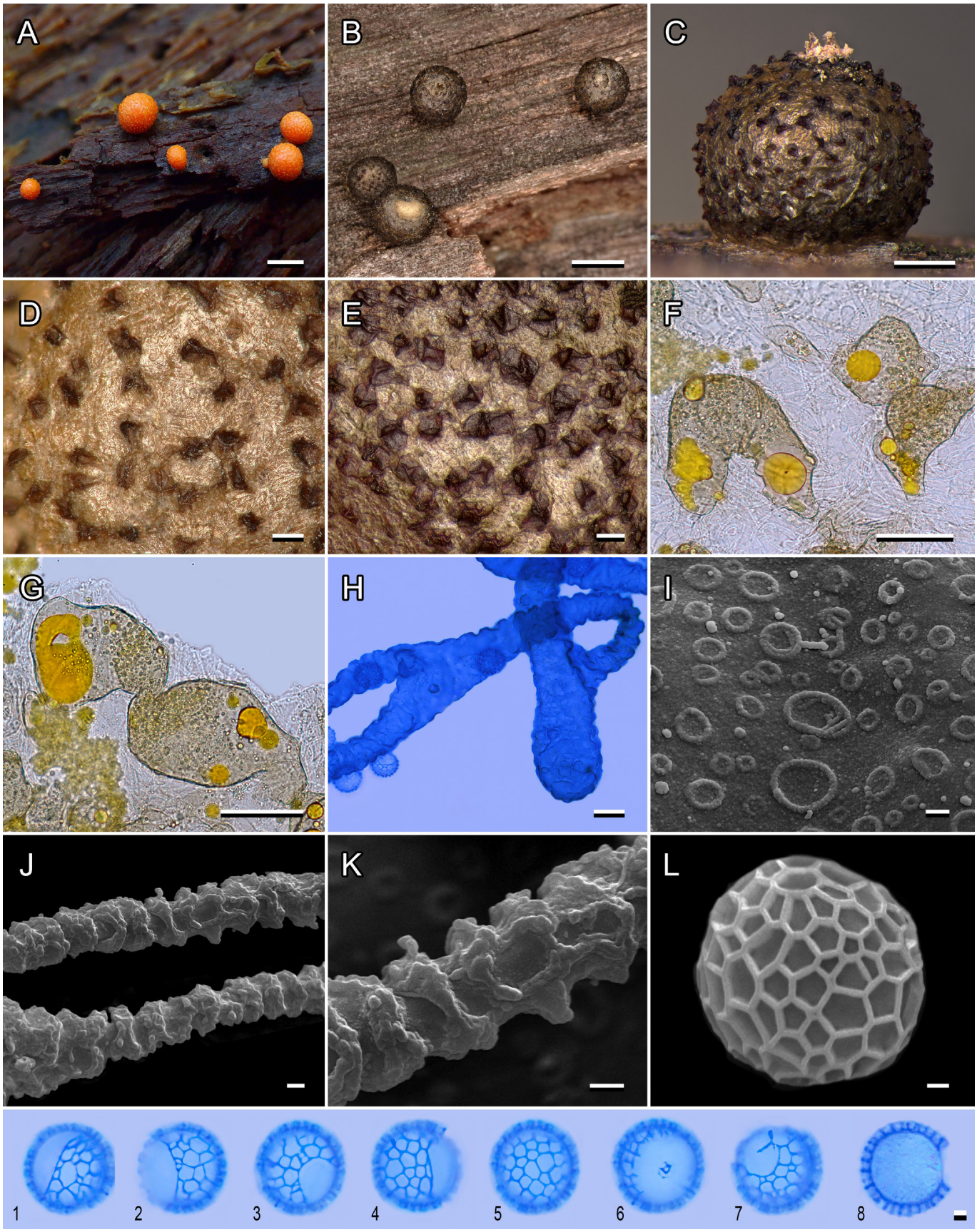

Fig. 29. *Lycogala asperum sp. nov.* [A–C, E–G, I–L. IY115 (holotype); D, H, M. TNSM12263]. **A.** Immature fructifications. **B, C.** Sporocarps. **D, E.** Peridium in RL. **F, G.** Peridial vesicles in TL. **H.** Capillitium and spores, methyl blue in lactic acid. **I.** Inner surface of the peridium, SEM. **J, K.** Capillitial tubules, SEM. **L.** Spore, SEM. **M.** Spores, methyl blue in lactic acid. The last spore is shown in optical section. Scale bars: A, B = 2 mm; C = 0.5 mm; D–G = 100 µm; H = 10 µm; I–K, M = 1 µm; L = 0.5 µm.

© 2025 Westerdijk Fungal Biodiversity Institute

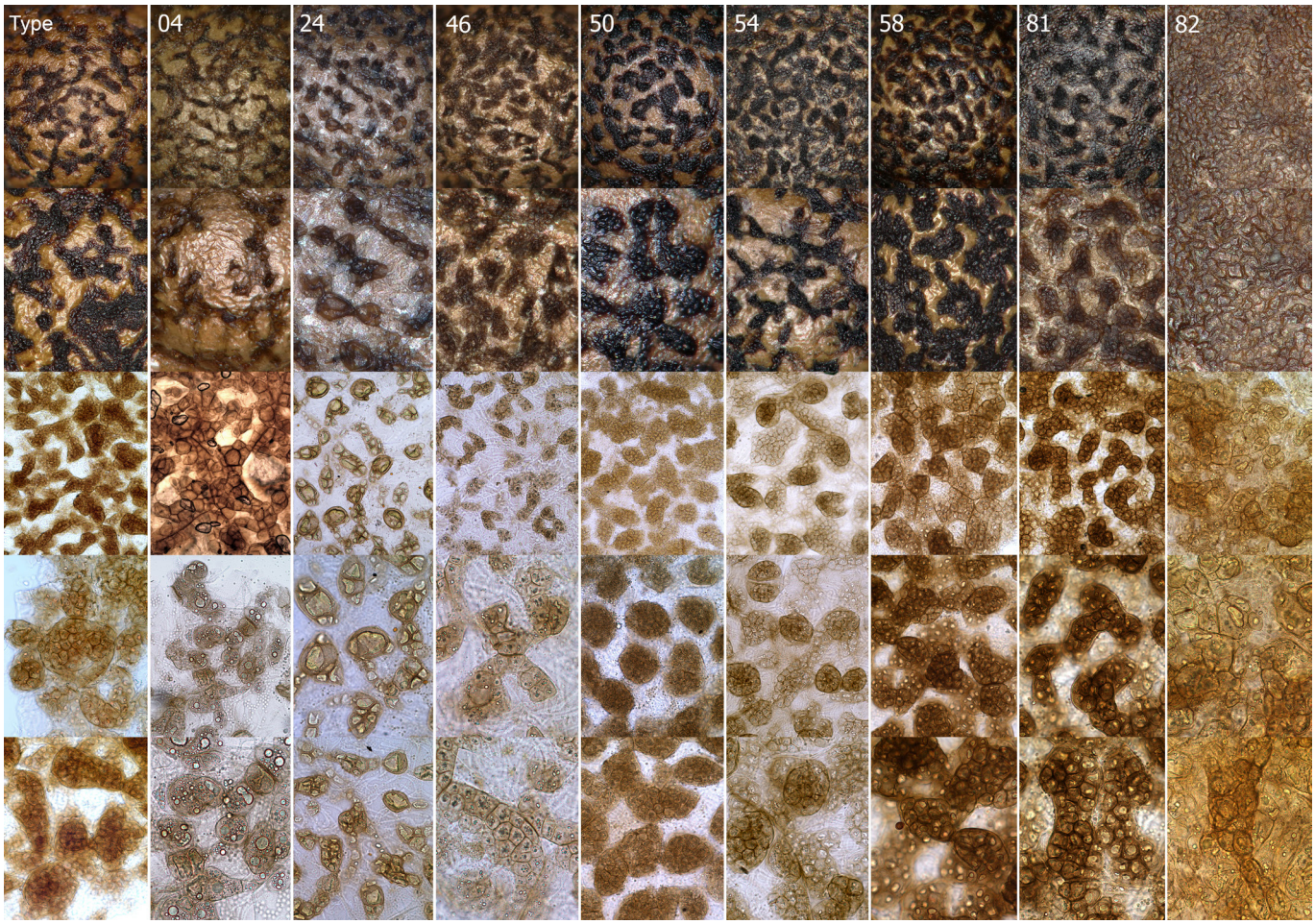

Fig. 30. Morphological variability of peridial structures within the *L. exiguum* complex, shown in RL and TL. Photographs from the same ribogroup are shown in columns. Numbers indicate ribogroups; "Type" corresponds to the isotype collection of the species.

Typus: **Germany**, Bavaria, Garmisch-Partenkirchen, northern Ammergauer Alps, near Brünstle Dienst-Hütte, gorge Sulzgraben (47.5195 11.0368), on dead wood, see Schnittler & Novozhilov (1998) for the detailed locality description, 1 Oct. 1997, *M. Schnittler* (**holotype** GFW sc20167). GenBank: nucSSU = OM423961 (rg20).

Distribution: Europe (Germany, Ukraine).

Notes: This is one of the most challenging species to identify. It closely resembles *L. succineum* and *L. palianytsia*, but these species are not prone to forming solitary sporocarps and are usually somewhat larger (up to 5 mm compared to the typical 3 mm for *L. miserum*). However, the oily accumulations, which are fairly abundant and have a yellowish hue, distinguish *L. miserum* among 'crystalliferous' species. Differentiating *L. miserum* from the 'oily' species, especially *L. fuscoolearium* and *L. guttatum*, is more complex. Nevertheless, these lack crystals and form groups of larger sporocarps.

Lycogala asperum Leontyev, Ishchenko, T. van der Heul & Schnittler, ***sp. nov.*** MB 857849. Fig. 29.

Etymology: *Asper* (Latin) rough, harsh, uneven, referring to the uneven surface of peridium and capillitium.

Diagnosis: Differs from the rest of *Lycogala* species by the combination of small (2–3 mm) grouped sporocarps, dark, simple, convex, peridial vesicles, which accumulate big droplets of orange-yellow oil.

Sporocarps scattered, spherical to short horizontally ovoid, regular in shape, (1.5–)2–3(–3.5) mm diam. *Peridium* membranous, light yellowish brown, covered by vesicles. *Peridial vesicles* (80–)100–130(–170) µm, in RL dark brown, solitary or forming loose groups, folded, with convex central part, more-or-less evenly distributed, distant from each other on 1–3 of their diam., in TL simple, ovoid, elongate or irregular, light brownish. Vesicle walls light brownish, thin (1 µm), single-layered. *Crystals* absent. *Oil* droplets large (20–60 µm) and small, bright warm-yellow, very conspicuous on the translucent background. *Inner surface of the peridium* covered by numerous rings 1–2 µm diam. *Capillitium* tubular, 4–15 µm diam., with wavy contour, ornamented by folds and bracelet-like thickenings, with no pits. *Spore mass* light pinkish. *Spores* (5.5–)6.5–8 µm diam., hyaline, reticulate, 6–7 meshes across diam., unornamented area occupies 1/2–1/3 of the spore surface. *Immature fructifications* bright orange.

Typus: **Russia**, Primorsky Krai, Ussuriysky State Reserve, Komarovka valley, Grabovaya hill (43.63899 132.34963), on the trunk of dead coniferous tree, 14 Aug. 2022, *Y. Ishchenko* (**holotype** GFW IY115). GenBank: nucSSU = PQ633768 (rg40); mtSSU = PQ633475; *COI* = PQ628493.

Distribution: Asia (Russia, Japan), Australia.

© 2025 Westerdijk Fungal Biodiversity Institute

Notes: The new species shows some affinity to *L. maculatum* and *L. irregulare*, sharing with them the presence of simple peridial vesicles. However, its small size, the accumulation of orange-yellow oil, the bright orange pigmentation of immature sporocarps and the ring ornamentation of the peridium allow to distinguish *L. asperum* from these species. Other taxa with yellow oils either contain crystals (*L. miserum*) or are larger in size and have lighter vesicles (*L. densum*, *L. guttatum*).

DISCUSSION

Ribogroups and species

The genus *Lycogala*, which until 2023 included only five widely recognized species (Poulain *et al.* 2011), now comprises at least 43 species. This is undoubtedly not the final count, as at least 18 morphologically distinct species identified in our study remain undescribed. In addition, some of the already described taxa encompass multiple ribogroups. Further investigation, incorporating larger datasets, may allow for the separation of these aggregates into multiple biospecies.

Despite the broad geographic coverage of the collections used in our study, molecular data on *Lycogala* remain completely or almost entirely absent for Africa, South America, Central Asia, and other regions with rich and distinct biotas. Therefore, even our predicted count of 183 ribogroups (putative biospecies) within the genus is likely an underestimate of the actual genetic diversity of *Lycogala*.

In some cases, we decided to describe complexes of multiple ribogroups as single morphological species (*L. densum*, *L. guttatum*, *L. squamatum*) or, at least, to associate singleton ribogroups with closely related biospecies (*L. pulchellum*, *L. rubrosporum*, *L. ustulatum*). All these morphology-based entities also appear as monophyletic groups in our nucSSU phylogeny (Fig. S6) and in the three-gene phylogeny with the exception of *L. squamatum* (Fig. 3). However, grouping several related biospecies into a single morphospecies is a temporary measure driven by data limitations. Our experience shows that when numerous and/or well-preserved specimens are available, even very closely related *Lycogala* species can be distinguished morphologically (*L. leopardinum* and *L. succineum*, *L. roseosporum* and *L. persicum*, *L. irregulare* and *L. epidendrum*). Therefore, we expect that the nine genetically heterogeneous species currently recognized in our study (see Results) will eventually be subdivided into reproductively isolated biospecies.

However, the existence of cryptic *Lycogala* species, for which no unique combination of morphological traits can be found, cannot be ruled out. Such cases are known in myxomycetes. For instance, three cryptic species have been identified within *Trichia varia* (Feng & Schnittler 2015), with no clear morphological differences among them. Similarly, when describing *Diacheopsis resinae*, an aggregate of three reproductively isolated units, the authors preferred to define only a single morphological species due to the absence of distinct differences between biospecies (Gøtzsche *et al.* 2024). Eighteen reproductively isolated lineages have been discovered within *Badhamia albescens*, with at least some of them lacking pronounced morphological features (Shchepin *et al.* 2021). Obviously, closely related species do not necessarily exhibit phenotypic differences, as this requires either (1) selection pressure on visually identifiable traits or (2) a 'fortunate' course of genetic drift leading to the random accumulation of distinct morphological characteristics. Thus, phenotypic distinctiveness does not necessarily evolve in parallel with genetic, ecological, or physiological divergence. This often leads to discrepancies between morphologically and genetically recognizable species (De Queiroz 2007). Currently, within the myxomycete research community, the prevailing view is that our knowledge remains insufficient to formally describe species for which morphological differences from other taxa are (yet) unknown (Schnittler *et al.* 2025). To date, no truly cryptic species of myxomycetes have been formally described, and we refrain from doing so as well. Therefore, the decision to describe several related but isolated lineages under a shared species name may be practically justified even in the long term.

A separate case concerns *L. exiguum*. The type specimen of this species was examined by us (Leontyev & Schnittler 2023), allowing comparisons with modern collections. As a result, we identified a large complex comprising ten ribogroups (rg04, 24, 46, 50, 54, 58, 75, 80–82), whose representatives exhibit substantial similarity to *L. exiguum*, with rg54 and rg58 displaying the highest resemblance (Fig. 30). Unfortunately, the type material of *L. exiguum* was collected in 1894 and cannot be barcoded using traditional methods. At the current state of art, we consider the group of species morphologically similar to *L. exiguum* as a single species complex. However, one lineage within this complex (rg50), which exhibits distinct differences from the type material of *L. exiguum*, has been formally described as a new species, *L. microcarpum* (Fig. 19).

Variability of *L. epidendrum* s. str.

The species *L. epidendrum* s. str. has recently been redefined with a narrow circumscription, corresponding to ribogroup rg01 (Leontyev *et al.* 2023b). It was found that this species is the most widespread representative of the genus, at least in temperate regions of the Northern Hemisphere. In our 2023 dataset, *L. epidendrum* s. str. accounted for 44.3 % of the specimens; in the expanded collection analysed in this study, it constituted 35.6 % (the decrease may be due to the intentional selection of non-*epidendrum* specimens by at least some collectors). Unlike most species of *Lycogala*, *L. epidendrum* s. str. appears to have a cosmopolitan distribution, occurring in Eurasia, North America, and Australia (we do not have barcoding data from Africa, and the only specimen from South America belongs to a different species). This cosmopolitan distribution is accompanied by an extraordinary genetic polymorphism: within rg01, we identified 29 subgroups (Fig. S6), denoted here by alphanumeric indices. Some of these subgroups have more restricted distributions than the species as a whole – for example, rg01f is found only in Australia, while rg01l occurs in Asia and North America (Table S1). The remaining groups, represented by 10 or more specimens, are widely distributed across Eurasia.

The genetic diversity of *L. epidendrum* s. str. raises the question of its taxonomic unity. The distance-based species delimitation (the ASAP method) suggests that *L. epidendrum* s. str. may comprise between five (nucSSU) and 16 (mtSSU)

© 2025 Westerdijk Fungal Biodiversity Institute

distinct species (see Fig. 2). However, only two of the five nucSSU-based groups form external branches in the tree of *L. epidendrum* s. str. The topologies of the nucSSU and mtSSU trees differ significantly, both in terms of group composition and relationships among them.

Recombination test indicates that most subgroups of *L. epidendrum* s. str. display no between-group recombination. The exception is three clusters of subgroups (b1+b2+h+v+w, c+p, d+i), between which occasional recombination was observed (Fig. S4). Importantly, the clusters do not necessarily unite closely related subgroups (Fig. S6). These data suggest that at least some degree of mixing between subgroups may occur within *L. epidendrum* s. str. An alternative hypothesis is that shared alleles across different subgroups may have been inherited from a common ancestor (incomplete lineage sorting) or resulted from introgression at early stages of speciation (Wei *et al.* 2016, Zhou *et al.* 2017).

The lack of cross-mating between most of the *L. epidendrum* ribogroups cannot be sufficiently explained by geographic isolation, since several large, isolated groups (a, e, l, o, x) co-occur in Europe and other regions. However, barriers between ribogroups may be based on ecological factors such as seasonality or trophic preferences, rather than cellular incompatibility.

In summary, the species-level distinctiveness of at least some lineages within *L. epidendrum* s. str. is supported by the reproductive isolation test and ASAP partitioning. Conversely, arguments against recognizing these lineages as distinct species include the disagreement between species delimitation based on two genetic markers, the cases of hybridization between unrelated subgroups, and the partial inconsistency between ASAP-based delimitation and nucSSU tree topology.

Delimitation of sections

The taxonomic significance of morphological traits in *Lycogala* has been discussed in our previous studies (Leontyev *et al.* 2022, 2023b). We concluded that the structure of the peridium is a character of major taxonomic importance in *Lycogala*, and that there are several morphotypes of peridium. These morphotypes differ in the presence or absence of oil and crystals, in the pigmentation of the wall and content of the vesicles, and in their aggregation into complex structures. In the present study, we demonstrate that these variants correspond to the main phylogenetic lineages of the genus (Fig. 3), allowing us to formally describe them as sections.

The assignment of species to sections, supported by three-gene phylogeny and CST (see Figs 1, 2), is generally well-supported by their morphology. For example, species of section *Crystallogala*, although not necessarily characterized by a high concentration of crystals in vesicles, exhibit a distinctive habit that allows identification even without microscopic preparation. The aggregates of vesicles typical of section *Tessellogala* are also highly recognizable, as are the dark, glossy vesicles characteristic of *Tinctogala*. However, some species exhibit an intermediate morphology that would not have allowed their assignment to a specific section without phylogenetic data. For example, *L. maculatum* from sect. *Lycogala* is morphologically similar to species of *Tinctogala*. *L. laeve, L. paraconfusum*, and *L. ustulatum* from *Tessellogala* possess light-coloured, oil-accumulating vesicles, resembling those of section *Oleogala*. Some species with uncertain position within phylogenies (section *incertae sedis*) may be assigned to sections based on their morphology: *L. pulchellum* fits well to *Tinctogala* (and branches within this group in CST), *L. oncoides* and *L. botrydium* are similar to the members of *Oleogala* (although do not branch with this group in any phylogeny), *L. asperum* shares yellow oil and solitary vesicles with *Crystallogala* (but also does not branch with this section).

It remains uncertain whether the counterintuitive placement of some species within sections is the result of parallel evolution or merely an artefact of phylogenetic analysis. Further studies are needed to resolve this issue.

Difficulties of species identification

The species within sections are differentiated by a number of characteristics, often rather subtle, including fine colour variations, details of the spatial arrangement of peridial vesicles, and differences in sporocarp and spore sizes. Additionally, some species exhibit unique traits that enable reliable identification, such as the blue colouration of the spore mass in *L. alisaulianovae* or the distinctive spore ornamentation in *L. olearium*.

With the addition of 24 species described in this study, some traits previously considered species-specific have been found in multiple species. For example, the intense pink spore mass, initially thought to be unique to *L. roseosporum*, was also observed in *L. persicum*. Large oil droplets in single vesicles, originally reported only in *L. olearium*, were also found in *L. densum*, *L. fuscoolearium*, and *L. oleocrystalliferum*. Similarly, the orange pigmentation of mature vesicles under reflected light, previously described only in *L. caviaroides*, was also observed in certain specimens of *L. olearium* and *L. oleocrystalliferum*.

Among the newly described species, several exhibit unique traits previously unknown in *Lycogala*. These include olive-coloured sporocarps in *L. olivaceum*, red-orange spore mass in *L. rubrosporum*, and a spiny peridium in *L. echinocarpum*. Distinctive new patterns of vesicular aggregation were observed in *L. microcarpum*, *L. rubrosporum*, and *L. squamatum*. Another newly identified trait – the accumulation of bright yellow oil within vesicles – was found in multiple species, including *L. asperum*, *L. guttatum*, and *L. miserum*. Interestingly, yellow oil appears to be characteristic of species in the section *Crystallogala* that contain few or no crystals within their vesicles, which may serve as an auxiliary diagnostic criterion.

All species described by us in 2023, as well as almost all species newly described in this study, belong to the *L. epidendrum* complex and were originally labelled as such in all studied collections. Specimens with small sporocarps and dark vesicles were sometimes identified as *L. exiguum*, making the only exception to this rule. However, in this study, we describe one species that was previously associated with another complex, *L. conicum*. This species aggregate is currently represented by three ribogroups, one of which (rg65) corresponds to the classical description of the species (Lister 1925), while another (rg64) is described here as a separate species, *L. sphaeroconicum*. Notably, due to its intermediate morphology, this newly described species was

© 2025 Westerdijk Fungal Biodiversity Institute

also occasionally labelled as *L. exiguum* in some collections. The third species in this complex, *L. 'conicoides' ad int.*, is represented by a single specimen from Australia and remains undescribed due to insufficient data.

Among the newly described species, as in the previous series of descriptions, some taxa are particularly challenging to identify. Major difficulties arise with morphologically similar species, such as *L. skovorodaense* – *L. sigillatum*, *L. olearium* – *L. fuscoolerium* – *L. oleocrystalliferum*, *L. guttatum* – *L. melleum* – *L. succineum*, and *L. umbrinum* – *L. ustulatum*. Further studies with a larger volume of field material may help determine the most reliable traits for distinguishing these species. However, it is important to emphasize that poor specimen condition, partial sclerotization or peridium damage, can make morphological identification impossible, especially in species with close morphological counterparts. A similar challenge arises with the fading of specimens preserved in herbaria for a long time (Leontyev *et al.* 2023b), which prevents the use of colour-based traits at both macroscopic and microscopic levels. In such cases, molecular barcoding remains the only reliable identification method. The importance of colour in a fresh state for identifying *Lycogala* once again underscores the value of this trait in myxomycetes (Yatsiuk *et al.* 2025) and highlights the need to document it when collecting specimens in the field or shortly thereafter (Schnittler *et al.* 2025).

To facilitate morphological species identification, we have developed a new identification key for the genus *Lycogala* (see below). The key excludes species that we consider dubious: *L. fuscoviolaceum*, *L. leiosporum*, and *L. heterospora*. It is based on qualitative macro- and micro-morphological traits that appear to be the most stable. Particular attention has been given to peridial structure, as it is species-specific in most cases. Quantitative traits are used only for distinguishing twin species.

Unexpectedly, *Lycogala* has proven to be a Klondike for taxonomists studying myxomycete species diversity. Research on this genus is only beginning and promises many future discoveries. Each of the species described in recent years must be further characterized in terms of its ecology, biology, distribution, and even biochemistry, as the diversity of colouration suggests potential interspecific differences in pigment composition. Everything previously known about the classical species *Lycogala epidendrum* sensu lato requires reassessment. A significant amount of work lies ahead, which can only be accomplished through consolidated efforts. We hope that our study will inspire colleagues to continue investigating one of the most well-known, and at the same time one of the least understood myxomycete.

Identification key to species of *Lycogala*

For recommendations on species identification, including the necessary tools and chemicals, see Leontyev *et al.* (2023b). Species described in this paper are marked in bold.

1a. Sporocarps taller than wide 2
1b. Sporocarps isodiametric or broader than tall 3

2a. Sporocarps conical, wide spindle-like, with blunt or relatively acute end; vesicles inconspicuous, from a regular reticulum ..... *L. conicum*
2b. Sporocarps egg-shaped, blunt spindle-shaped, to almost spherical; vesicles glossy, dark, do not from a regular reticulum ..... ***L. sphaeroconicum***

3a. Sporocarps 2–5 cm diam., silvery grey, usually on soft-wooded living trees well above ground ..... *L. flavofuscum*
3b. Sporocarps < 2 cm diam., brown, greyish brown, ochraceous yellow, black, on dead wood, wooden debris or moss 4

4a. Spots on the peridium simple, consisting of one vesicle (visible under transmitted light) 5
4b. Spots on the peridium compound, consisting of several to numerous tightly accreted vesicles forming aggregates (visible under transmitted light; in reflected light the spot may look pitted) 29

5a. Crystals inside vesicles absent or very scanty (check in PL). Vesicles of various types: rounded, spot-like, star-like, scattered or densely spaced at the peridium, coalescing to an irregular net 6
5b. Crystals inside vesicles numerous (visible in PL). Vesicles always rounded or short ovate, conspicuous, evenly distributed on the peridial surface, never forming a net 22

6a. Vesicles dark brown to black in RL, brown in TL 7
6b. Vesicles light brownish in RL, almost hyaline in TL 13

7a. Sporocarps pinkish, spore-mass bright pink 8
7b. Sporocarps not pinkish, spore mass of another colour 9

8a. Colonies small and compact; vesicles densely cover the upper part of the sporocarp; oily deposits inconspicuous, colourless ..... *L. roseosporum*
8b. Colonies vast and loose; vesicles more-or-less evenly distributed; oil droplets numerous, bright red ..... ***L. persicum***

© 2025 Westerdijk Fungal Biodiversity Institute

9a (7). Spore mass bluish grey, later greenish grey ..... *L. alisaulianovae*
9b. Spore mass beige, light grayish or pinkish 10

10a. Sporocarps solitary, small (≤ 2.5 mm) light yellow, densely covered with dark peridial vesicles, which give them a contrasting, spotty appearance ..... ***L. pulchellum***
(if vesicles are flat and glossy – check *L. sphaeroconicum*)
10b. Sporocarps in groups, medium-sized (2–5 mm diam.), in dark shades of brown; the contrast between vesicles and peridum less prominent 11

11a. Peridium background between vesicles dull ochraceous, dark grey brown, black ..... *L. maculatum*
11b. Peridium background between vesicles reddish or lilac brown 12

12a. Peridium dark lilac- to umber-brown; vesicles angular, convex, forming loose groups, that merge into very fragmented reticulum; vesicle walls 2 µm thick ..... ***L. umbrinum***
12b. Peridium reddish brown; vesicles rounded, with a raised centre and a flat periphery, densely and evenly distributed; vesicle walls 5–20 µm thick; small aggregated thin-walled vesicles may be present around central simple thick-walled vesicle ..... ***L. ustulatum***

13a (6). Oil deposits in vesicles scanty or absent 14
13b. Oil droplets and granular oily matter abundant 16

14a. Sporocarps somewhat olivaceous or greenish, or with faintest lemon yellow tint; the colour fades in old collections; spores 8.5–9.5 µm diam. ..... ***L. olivaceum***
14b. Sporocarps ochraceous- or greyish brown, with no green tint; spores 6.5–8.0 µm diam. 15

15a. Sporocarps up to 15 mm diam., rounded, wide- to narrow-ovoid from mutual pressure. Peridium covered with fine whitish strands of dried slime, which may cover and hide vesicles and make the peridium to look uniformly smooth ..... *L. epidendrum*
15b. Sporocarps up to 7 mm diam., rather irregular in shape even without mutual pressure. Strands of dried slime scanty, not hiding vesicles ..... *L. irregulare*
(if capillitium is smooth, and vesicles tend to form rows – check *L. laeve*)

16a (13). Spores with 3–7 meshes across diam., with small meshes tending to surround every large mesh ..... *L. olearium*
16b. Spores with 4–8 meshes across diam.; meshes are more-or-less similar in size 17

17a. Oil droplets colourless or dull yellowish or brownish; crystals may occur in vesicles 18
17b. Oil droplets bright yellow, orange yellow; crystals absent 21
(if the oil is red – check *L. persicum*; if vesicles contain crystals – check *L. miserum*)

18a. Vesicles distant from each other on 0.5–1 of their diam.; oil yellowish 19
18b. Vesicles distant from each other on 1–3 of their diam.; oil dull brownish 20

19a. Sporocarps 3.5–6(–8) mm diam., light pinkish (?) when immature; vesicles 80–120 µm diam., very densely distributed ..... ***L. densum***
19b. Sporocarps 2.5–3(–4.5) mm diam., yellow when immature; vesicles 120–180 µm diam., not that densely distributed ..... ***L. melleum***

20a (18). Sporocarps 2.5–4(–6) mm diam.; vesicles 80–120 µm diam., brown ..... ***L. fuscoolearium***
20b. Sporocarps 4.5–7.5(–10) mm diam.; vesicles 110–150 µm diam., orange, orange-brown or brown ..... ***L. oleocrystalliferum***
(if vesicles are orange or red, and filled with crystals – check *L. caviaroides*; if there are no crystals also check *L. olearium*, if there is no oil – check *L. leopardinum*)

21a (17). Sporocarps 4.0–5.5(–7.5) mm diam.; vesicles in RL light-brown, almost flat ..... ***L. guttatum***
21b. Sporocarps 2.0–3.0(–3.5) mm diam.; vesicles in RL very dark brown, convex to conical ..... ***L. asperum***

22a (5). Vesicles in RL orange red, dark red, looking like dried red caviar ..... *L. caviaroides*
(if vesicle contains oil droplets and/or granular deposits – check *L. olearium* and *L. oleocrystalliferum*)
22b. Vesicles in RL amber yellow or brown 23

23a. Sporocarps small (2–3 mm diam.), solitary; vesicles mostly merged into small blot-shaped groups; occurs in Southern Hemisphere ..... ***L. australe***
23b. Sporocarps small or large, in groups; vesicle free, evenly distributed; occurs in Northern Hemisphere 24

24a. Vesicles mostly elongate, distant from each other by distances equaling 1–2 times their diam. 25
24b. Vesicles mostly isodiametric, distances between them smaller than 1 times of their diam. 26

© 2025 Westerdijk Fungal Biodiversity Institute

25a. Sporocarps in groups, 2.5–5.5(–6.5) mm diam., vesicles do not contain oil ..... *L. palianytsia*
25b. Sporocarps solitary, 3–3.5(–4) mm diam.; vesicles contain yellowish oil droplets ..... ***L. miserum***

26a. Sporocarps 1.5–2.5(–3.5) mm diam., greyish; capillitium conspicuously verrucose; occurs in Neotropics ..... ***L. costaricanum***
26b. Sporocarps 2–5(–10) mm diam., of various tints of brown; capillitium slightly verrucose to almost smooth 27

27a. Vesicles amber yellow, light brown, distant from each other by 1 times of their diam ..... *L. succineum*
(if immature sporocarps are yellow, and crystals almost absent – check *L. melleum*)
27b. Vesicles dark brown, distant from each other by 1/3–1/2 times of their diam 28

28a. Sporocarps up to 10 mm diam., occurs in Holarctic ..... *L. leopardinum*
28b. Sporocarps up to 6 mm diam., occurs in Paleotropics ..... *L. acinonychum*

29a (4). Vesicle aggregates compact, with more-or-less smooth contour 30
29b. Vesicle aggregates loose, in form of branched rows, or aggregated vesicles covering entire surface of the peridium 39

30a. Aggregates of vesicles large, typically with > 8 vesicles in one group 31
30b. Aggregates of vesicles small, typically with < 8 vesicles in one group 37

31a. Aggregates look like prominent papillate protrusions, longer than wide, giving the sporocarps an obvious spiny appearance ..... ***L. echinocarpum***
31b. Aggregates less convex; sporocarps smooth or somewhat verrucose 32

32a. Aggregates in RL look like black spots of rosette shape with bigger vesicles grouped at the centre 33
32b. Aggregates in RL do not have a rosette shape 35

33a. Spore mass red, bright orangec red, occurs in Asia ..... ***L. rubrosporum***
33b. Spore-mass beige; other distribution 34

34a. Lines between rosette-shaped vesicle aggregates dark, regular; oil droplets in vesicles reddish; occurs in Holarctic ..... ***L. squamatum***
34b. Lines between rosette-shaped vesicle light, rather inconspicuous; oil droplets in vesicles colourless; occurs in Neotropics ..... *L. aggregatum*

35a (32). Aggregates in RL mat, angular, with amorphous surface; vesicle walls hardly visible in TL ..... *L. botrydium*
35b. Aggregates in RL glossy, with smooth contour and clearly pitted surface; vesicle walls well visible in TL 36

36a. Aggregates ovoid in shape, sometimes fused but not forming a reticulum ..... ***L. microcarpum***
36b. Aggregates blot-shaped, branched, forming a regular reticulum ..... *L. exiguum*

37a (30). Vesicles filled with dark brown oil material and contain crystals (see in PL) ..... *L. oncoides*
37b. Vesicles filled with distinguishable colourless oil droplets and do not contain crystals 38

38a. Peridium dull greyish, vesicles dull brown in RL; capillitium warty, sometimes spiny ..... *L. skovorodaense*
38b. Peridium light orange-brown, vesicles dark red brown in RL; capillitium looks smooth under LM ..... ***L. sigillatum***

39a (29). Sporocarps small (2–3 mm), solitary, loosely covered with branched rows of elongate vesicles ..... ***L. inconspicuum***
39b. Sporocarps larger (> 3 mm), grouped, densely covered by vesicles, which form a reticulum, irregular patches or spots 40

40a. Peridium with clear, contrast vesicle pattern in RL 41
40b. Peridium with blurred, indistinct vesicle pattern in RL 44

41a. Vesicles of two types, large solitary, with very thick brownish walls (5–20 µm), and small aggregated, thin-walled (1–2 µm), forming irregular network around large ones ..... *L. ustulatum* (see also paragraph 12)
41b. Vesicles only thin-walled, more-or-less uniform 42

42a. Vesicles nearly black in RL, dark brown in TL, with the thick, brownish outer layer ..... ***L. nigroconfusum***
42b. Vesicles brown in RL, light brownish in TL, with indistinct, colourless outer layer 43

43a. Sporocarps rather irregular in shape; vesicles 40–90 µm diam., forming a characteristic ‘marble’ pattern of large lighter and darker spots; oil droplets colourless; spores 5.5–8 µm ..... *L. confusum*
43b. Sporocarps regular in shape; vesicles 30–60 µm diam., evenly distributed with no marble pattern; oil droplets often reddish; spores 7–9 µm ..... ***L. paraconfusum***

© 2025 Westerdijk Fungal Biodiversity Institute

44s. Sporocarps dark brown to almost black; oil colourless; capillitium warty; spores 5.5–7.5 µm ..... *L. fossiculatum*
44b. Sporocarps light greyish brown; oil brownish or reddish; capillitium smooth; spores 6.5–8.5 µm..... ***L. laeve***

ACKNOWLEDGEMENTS

We first and foremost want to thank numerous ardent collectors: without their continued support and engagement a study like this would not have been possible. DL wishes to acknowledge the Humbold foundation (fellowship 2019–2023), and the DAAD program (fellowship 2024). Special gratitude is expressed to Dr. Rabea Schlüter (University of Greifswald) for the assistance during the SEM study. Molecular investigations were in part supported by grants of the DFG (RTG 2010 and SCHN1080/6-1) to MS.

Conflict of interest: The authors declare no conflicts of interest.

REFERENCES

Castresana J (2000). Selection of conserved blocks from multiple alignments for their use in phylogenetic analysis. *Molecular Biology and Evolution* **17**: 540–552. https://doi.org/10.1093/oxfordjournals.molbev.a026334

De Queiroz K (2007). Species concepts and species delimitation. *Systematic Biology* **56**: 879–886. https://doi.org/10.1080/10635150701701083

Feng Y, Schnittler M (2015). Sex or no sex? Group I introns and independent marker genes reveal the existence of three sexual but reproductively isolated biospecies in *Trichia varia* (*Myxomycetes*). *Organisms Diversity & Evolution* **15**: 631–650. https://doi.org/10.1007/s13127-015-0230-x

García-Cunchillos I, Zamora JC, Ryberg M, *et al.* (2022). Phylogeny and evolution of morphological structures in a highly diverse lineage of fruiting-body-forming amoebae, order *Trichiales* (*Myxomycetes*, *Amoebozoa*). *Molecular Phylogenetics and Evolution* **177**: 107609. https://doi.org/10.1016/j.ympev.2022.107609

Gøtzsche HF, Woerly B, Popa F, *et al.* (2024). A new species of *Diacheopsis* (*Myxomycetes*) and a new habitat for myxomycetes. *Mycologia*: 1–18. https://doi.org/10.1080/00275514.2024.2413343

Hall TA (1999). BioEdit: A user-friendly biological sequence alignment editor and analysis program for Windows 95/98/NT. *Nucleic Acids Symposium Series* **41**: 95–98.

Johannesen EW, Vetlesen P (2024). New and rare myxomycetes (*Mycetozoa, Myxogastria*) in Norway Part 2. *Agarica* **44**: 25–84. https://doi.org/10.5617/agarica.11615

Jones EP, Mahendran R, Spottswood MR, *et al.* (1990). Mitochondrial DNA of *Physarum polycephalum*: Physical mapping, cloning and transcription mapping. *Current Genetics* **17**: 331–337. https://doi.org/10.1007/BF00314881

Kalyaanamoorthy S, Minh BQ, Wong TKF, *et al.* (2017). ModelFinder: Fast model selection for accurate phylogenetic estimates. *Nature Methods* **14**: 587–589. https://doi.org/10.1038/nmeth.4285

Katoh K, Rozewicki J, Yamada KD (2019). MAFFT online service: Multiple sequence alignment, interactive sequence choice and visualization. *Briefings in Bioinformatics* **20**: 1160–1166. https://doi.org/10.1093/bib/bbx108

Lado C (2005–2025). An on-line nomenclatural information system of *Eumycetozoa*. http://www.eumycetozoa.com [accessed 13 Mar 2025]

Leontyev D, Buttgereit M, Kochergina A, *et al.* (2023a). Two independent genetic markers support separation of the myxomycete *Lycogala epidendrum* into numerous biological species. *Mycologia* **115**: 32–43. https://doi.org/10.1080/00275514.2022.2133526

Leontyev D, Ishchenko Y, Schnittler M (2023b). Fifteen new species from the myxomycete genus *Lycogala*. *Mycologia* **115**: 524–560. https://doi.org/10.1080/00275514.2023.2199109

Leontyev D, Moroz E, Schnittler M (2024). Molecular barcoding of herbarium collections reveals diversity of *Reticulariaceae* (*Myxomycetes*) in Belarus. *Nova Hedwigia* **119**: 369–386. https://doi.org/10.1127/nova_hedwigia/2024/1029

Leontyev D, Schnittler M (2017). The phylogeny of myxomycetes. In: *Myxomycetes: Biology, Systematics, Biogeography and Ecology* (Stephenson SL, Rojas C, eds). Press, Country: 83–106. https://doi.org/10.1016/B978-0-12-805089-7.00003-2

Leontyev D, Schnittler M (2022). The phylogeny and phylogenetically based classification of myxomycetes. In: *Myxomycetes* (Stephenson SL, Rojas C, eds). Elsevier: 97–124. https://doi.org/10.1016/B978-0-12-824281-0.00008-7

Leontyev D, Schnittler M (2023). What are *Lycogala confusum* and *L. exiguum*? Revising authentic collections of myxomycetes in the light of a molecular-aided species concept. *Nova Hedwigia* **116**: 403–416. https://doi.org/10.1127/nova_hedwigia/2023/0820

Leontyev D, Schnittler M, Ishchenko Y, *et al.* (2022). Another species complex in myxomycetes: Diversity of peridial structures in *Lycogala epidendrum*. *Nova Hedwigia* **114**: 413–434. https://doi.org/10.1127/nova_hedwigia/2022/0690

McHugh R, Reid C (2008). Aethalium cortex formation in the myxomycete *Lycogala terrestre*. *Revista Mexicana de Micología* **27**: 53–57.

Poulain M, Meyer M, Bozonnet J (2011). *Les Myxomycètes*. 1. Guide de Détermination. Fédération mycologique et botanique Dauphiné-Savoie, Sevrier.

Puillandre N, Brouillet S, Achaz G (2021). ASAP: Assemble species by automatic partitioning. *Molecular Ecology Resources* **21**: Article 2. https://doi.org/10.1111/1755-0998.13281

Rambaut A (2018). *FigTree*. Version 1.4.4. Institute of Evolutionary Biology, University of Edinburgh, Edinburgh.

Rambaut A, Drummond AJ, Xie D, *et al.* (2018). Posterior summarisation in Bayesian phylogenetics using Tracer 1.7. *Systematic Biology* **67**: 901–904. https://doi.org/10.1093/sysbio/syy032

Rannala B, Yang Z (2003). Bayes estimation of species divergence times and ancestral population sizes using DNA sequences from multiple loci. *Genetics* **164**: 1645–1656. https://doi.org/10.1093/genetics/164.4.1645

Riedel A, Sagata K, Suhardjono YR, *et al.* (2013). Integrative taxonomy on the fast track—Towards more sustainability in biodiversity research. *Frontiers in Zoology* **10**: 15. https://doi.org/10.1186/1742-9994-10-15

Ronquist F, Teslenko M, van der Mark P, *et al.* (2012). MrBayes 3.2: Efficient Bayesian phylogenetic inference and model choice

© 2025 Westerdijk Fungal Biodiversity Institute

across a large model space. *Systematic Biology* **61**: 539–542. https://doi.org/10.1093/sysbio/sys029

Sayyari E, Mirarab S (2016). Fast coalescent-based computation of local branch support from quartet frequencies. *Molecular Biology and Evolution* **33**: 1654–1668. https://doi.org/10.1093/molbev/msw079

Schnittler M, Leontyev D, Yatsiuk I, *et al.* (2025). Species descriptions in myxomycetes – can we settle on rules for good taxonomic practice? *IMA Fungus* **16**: e141199. https://doi.org/10.3897/imafungus.16.141199

Schnittler M, Novozhilov YK (1998). Late-autumn myxomycetes of the Northern Ammergauer Alps. *Nova Hedwigia* **66**: 205–222. https://doi.org/10.1127/nova.hedwigia/66/1998/205

Shchepin O, Novozhilov Y, Woyzichovski J, *et al.* (2021). Genetic structure of the protist *Physarum albescens* (*Amoebozoa*) revealed by multiple markers and genotyping by sequencing. *Molecular Ecology* **31**: 372–390. https://doi.org/10.1111/mec.16239

Song WL, Yan SZ, Chen SL (2024). Morphological and phylogenetic analyses reveal four species of myxomycetes new to China. *Archives of Microbiology* **206**: 364. https://doi.org/10.1007/s00203-024-04083-4

Tamura K, Stecher G, Kumar S (2021). MEGA11: Molecular evolutionary genetics analysis version 11. *Molecular Biology and Evolution* **38**: 3022–3027. https://doi.org/10.1093/molbev/msab120

Trifinopoulos J, Nguyen L-T, von Haeseler A, *et al.* (2016). W-IQ-TREE: A fast online phylogenetic tool for maximum likelihood analysis. *Nucleic Acids Research* **44**: W232–W235. https://doi.org/10.1093/nar/gkw256

Wei X, McCune B, Lumbsch HT, *et al.* (2016). Limitations of species delimitation based on phylogenetic analyses: A case study in the *Hypogymnia hypotrypa* group (*Parmeliaceae*, *Ascomycota*). *PLoS ONE* **11**: e0163664. https://doi.org/10.1371/journal.pone.0163664

Yatsiuk I, Leontyev D, Schnittler M, *et al.* (2025). *Arcyria* and allied genera: taxonomic backbone and character evolution. *Fungal Systematics and Evolution* **15**: 97–118. https://doi.org/10.3114/fuse.2025.15.04

Yatsiuk I, Leshchenko Y, Viunnyk V, *et al.* (2024). The comprehensive checklist of myxomycetes of Ukraine, based on extended occurrence and reference datasets. *Biodiversity Data Journal* **12**: e120891. https://doi.org/10.3897/BDJ.12.e120891

Zhang C, Mirarab S (2022). Weighting by gene tree uncertainty improves accuracy of quartet-based species trees. *Molecular Biology and Evolution* **39**: msac215. https://doi.org/10.1093/molbev/msac215

Zhou Y, Duvaux L, Ren G, *et al.* (2017). Importance of incomplete lineage sorting and introgression in the origin of shared genetic variation between two closely related pines with overlapping distributions. *Heredity* **118**: 211–220. https://doi.org/10.1038/hdy.2016.72

Supplementary Material: http://fuse-journal.org/

Fig. S1. Preliminary species delimitation based on ASAP analysis of the nucSSU alignment. The five best score partitions are shown.

Fig. S2. Preliminary species delimitation based on ASAP analysis of the mtSSU alignment. The five best score partitions are shown.

Fig. S3. Preliminary species delimitation based on ASAP analysis of the COI alignment. The five best score partitions are shown.

Fig. S4. Recombination test by LineChart for ribogroups of *Lycogala* spp. Ribogroups belonging to *L. epidendrum* are shown in red.

Fig. S5. Recombination test by LineChart for morphospecies of *Lycogala* spp.

Fig. S6. Maximum likelihood phylogeny of 706 nucSSU sequences of *Lycogala* spp. Branch support is shown as follows: Shimodara-Hasegawa SH-aLRT test / Approximate Bayes test / Ultrafast bootstrap (1000 true replicates). Colours indicate assignment of species to sections.

Fig. S7. Maximum likelihood phylogeny of 273 mtSSU sequences of *Lycogala* spp. Branch support is shown as follows: Shimodara-Hasegawa SH-aLRT test / Approximate Bayes test / Ultrafast bootstrap (1000 true replicates). Colours indicate assignment of species to sections.

Fig. S8. Maximum likelihood phylogeny of 130 *COI* sequences of *Lycogala* spp. Branch support is shown as follows: Shimodara-Hasegawa SH-aLRT test / Approximate Bayes test / Ultrafast bootstrap (1000 true replicates). Colours indicate assignment of species to sections.

Fig. S9. Three-gene Bayesian phylogeny based on concatenated three-gene dataset of 191 representative specimens of *Lycogala*, trimmed in GBlocks as described in Methods.

File S1. MAFFT alignment of partial nucSSU sequences of 706 specimens of *Lycogala* spp. (fasta file).

File S2. MAFFT alignment of partial mtSSU sequences of 273 specimens of *Lycogala* spp. (fasta file).

File S3. MAFFT alignment of partial *COI* sequences of 130 specimens of *Lycogala* spp. (fasta file).

Table S1. Collection and barcoding data for all studied specimens of *Lycogala*.

Table S2. Measurements of sporocarps, peridial vesicles, capillitium and spores (in separate sheets) for the species of *Lycogala* described in this study.

© 2025 Westerdijk Fungal Biodiversity Institute

FUSE

Fungal Systematics and Evolution

VOLUME 16
DECEMBER 2025
PAGES 147–153

doi.org/10.3114/fuse.2025.16.8

Hemileia ritscheliae, a new species of rust fungus on *Aristolochia* sp. collected from Uganda in 1943

J. Bailey[1*], S.T. Miller[2,3], L.A. Castlebury[2]

[1]NSW Department of Primary Industries, Plant Pathology and Mycology Herbarium, Orange Agricultural Institute, Orange, Australia
[2]United States Department of Agriculture, Agricultural Research Service, Mycology and Nematology Genetic Diversity and Biology Laboratory, Beltsville, MD, USA
[3]Oak Ridge Institute for Science and Education, ARS Research Participation Program, Oak Ridge, TN 37831, USA

*Corresponding author: jordan.bailey@dpi.nsw.gov.au

Key words:
Hemileia
LSU
new taxon
rust fungi
SSU
taxonomy

Abstract: The genus *Hemileia* was established in 1869 and made famous by *H. vastatrix*, the agent of coffee leaf rust. This group of obligate biotrophs has grown to include more than 42 species, infecting plant hosts from 43 genera across Africa and Asia. A specimen collected in 1943 in Uganda, on the host plant *Aristolochia,* was identified to *Hemileia* sp. (BPI019726). Species identification was historically inconclusive and subsequent examinations noted that the material was insufficient. In this study, the specimen was morphologically re-examined, and partial sequences of the small subunit (18S) and large subunit (28S) of the rDNA were obtained. It was found to be sufficiently different from other species in the genus, and here described as *Hemileia ritscheliae sp. nov.*, named for the work by Anja Ritschel in compiling the *Hemileia* monograph (Ritschel 2005), and whose research greatly assisted our work.

Citation: Bailey J, Miller ST, Castlebury LA (2025). *Hemileia ritscheliae*, a new species of rust fungus on *Aristolochia* sp. collected from Uganda in 1943. *Fungal Systematics and Evolution* **16**: 147–153. doi: 10.3114/fuse.2025.16.8.
Received: 26 May 2024; **Accepted:** 5 March 2025; **Effectively published online:** 16 July 2025
Corresponding editor: P.W. Crous

INTRODUCTION

Rust fungi (*Basidiomycota, Pucciniales*) are biotrophic plant pathogens that are widespread across all terrestrial ecosystems. Within natural plant communities, they play an important role in the overall framework of ecosystems promoting host genetic diversity, plant biodiversity, and successional processes of natural communities (Dobson & Crawley 1994, Gilbert 2002, Helfer 2014). However, species of rust fungi can greatly disturb natural and cultivated landscapes when introduced to non-native or agricultural systems. *Cronartium ribicola*, *Puccinia graminis*, and *Hemileia vastatrix* have historically caused significant disruptions to natural populations of pine, cultivated wheat/barley, and coffee, respectively (Kinloch & Bohun 2003, Leonard & Szabo 2005, Koutouleas *et al.* 2024). In fact, *H. vastatrix* is one the earliest and most significant examples of a rust pathogen causing an agricultural production shift for an entire region. During the mid-19th century coffee production surge in Sri Lanka, *H. vastatrix* was determined to be the causal agent of coffee leaf rust. The disease would eventually devastate the coffee industry forcing a complete shift to tea production for the region (Ritschel 2005, Koutouleas 2024). Reverend Berkeley and Broome identified the fungus and their description led to the typification of the genus in 1869 with *H. vastatrix* serving as the type species.

Species in the genus *Hemileia* produce uniquely shaped urediniospores, which have been described as hunchback. While most species have reniform urediniospores, some *Hemileia* species may have globose to ellipsoid urediniospores (Ritschel 2005, Wood & Aime 2024). The genus name, *Hemileia,* meaning half-smooth, alludes to the lack of echinulate ornamentation on the ventral side of the urediniospores, a feature true for most species in the genus, along with a suprastomatal habit (Ritschel 2005). The genus is currently placed in the *Zaghouaniaceae* lineage within the *Mikronegeriineae* radiation (*Pucciniales*, *Pucciniomycetes*, *Basidiomycota*) (Cummins & Hiratsuka 2003, Aime & McTaggart 2021). Since the discovery of *H. vastatrix*, more than 45 species of *Hemileia* have been placed in the genus. There are currently 69 described species records according to Index Fungorum (https://www.indexfungorum.org); Ritchsel recognized 42 species in the 2005 monograph on hosts from 43 genera and 12 families (five on unknown hosts).

As part of a preliminary phylogenetic analysis of *Hemileia*, an unidentified specimen of *Hemileia* on *Aristolochia* was examined. The specimen on *Aristolochia* sp., labelled as *A. dorsivenia*, (BPI 019726) is held at the U.S. National Fungus Collections (BPI) in Beltsville, Maryland, USA. It was collected in May 1943 from Entebbe Rd, in Uganda, by C.G. Hansford. Another specimen (PUR F19695) is held at the Arthur Fungarium (PUR), with matching collection data. Both the BPI and PUR specimens are in poor condition, with extensive overgrowth of hyphomycetous fungi. Earlier examinations by G.B. Cummins

Fungal Systematics and Evolution is licensed under a Creative Commons Attribution-NonCommercial-NoDerivatives 4.0 International License

© 2025 Westerdijk Fungal Biodiversity Institute

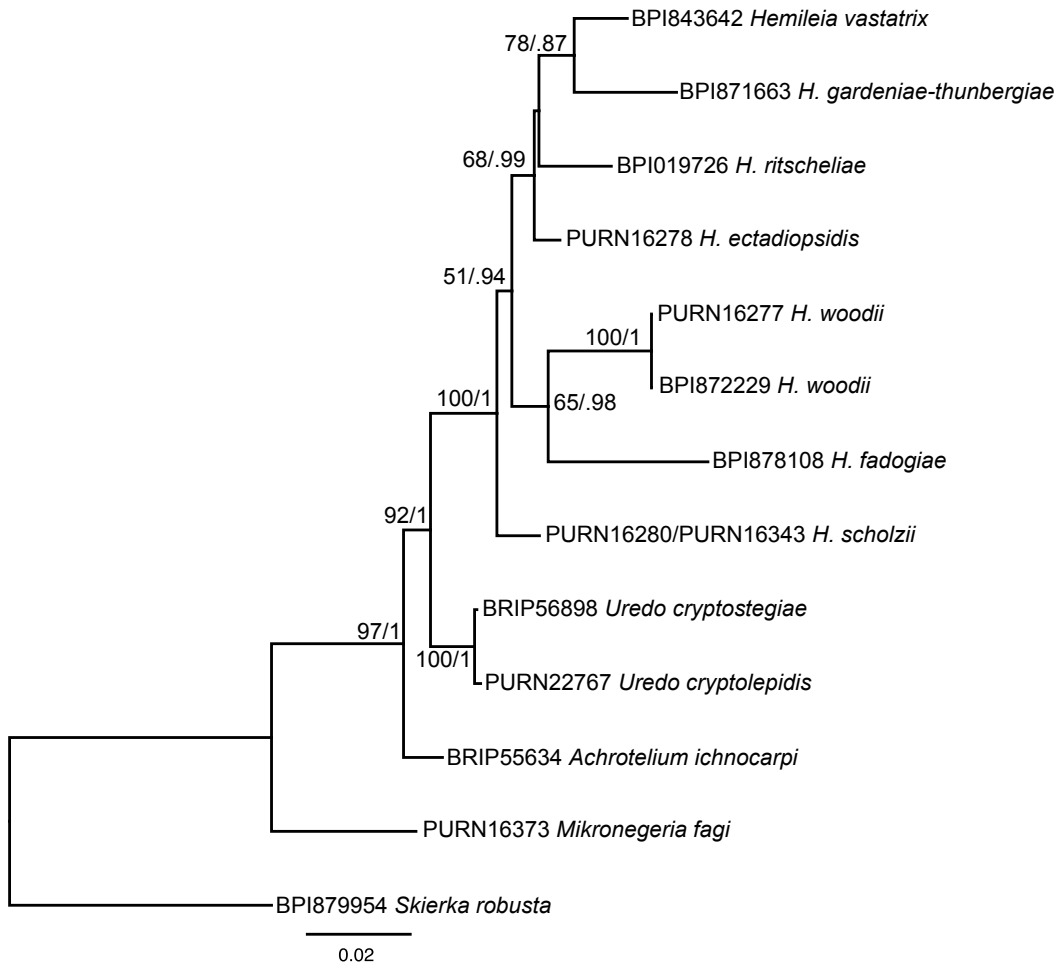

Fig. 1. Phylogenetic placement of *Hemileia ritscheliae* within the *Zaghouaniaceae* using maximum likelihood and Bayesian analysis of partial SSU and LSU gene sequences. Bootstrap support values ≥ 70 % and posterior probability values ≥ 0.95 are reported by each node (ML/BI). Sequence data is listed in Table 1 with corresponding gene identification numbers and/ or accession numbers.

and K.S. Gopalkrishan in 1949, and Ritschel in 2005, both concluded that the material was "too old" and, although clearly a species of *Hemileia*, an accurate description could not be formed (Ritschel 2005).

The objectives of this study were to identify and characterize the hemileia-like specimen through sequencing of the LSU and SSU region. Based on our phylogenetic and morphological observations, an identification for this 70-yr-old specimen was finally made and presented herein. We describe *Hemileia ritscheliae* as a novel species, named in honor of Anja Ritschel (2005) who compiled the *Hemileia* monograph, and whose work has greatly assisted our research.

MATERIALS AND METHODS

Primer design

Given the degraded nature of the samples being used, primers were designed for fragments of the SSU and LSU region using reference sequences of *Hemileia* and related species. The SSU and LSU regions were divided into four and three parts respectively and primers were designed to amplify targeted product in all available *Hemileia* species. See supplementary Table S1 for primer sequence details. Sequencing of the internal transcribed spacer regions was attempted but the resulting sequences were contaminated by other fungi.

DNA extraction and PCR amplification

A small section (< 5 mm^2) of infected leaf tissue was cut from the specimen using a new razor blade under a dissecting stereoscope. Only the area containing sori was sampled. The tissue was placed in a 2 mL micro-centrifuge tube and then cut further using sterilized dissecting scissors, 400 µL of lysis buffer was added, as per the instructions for the DNAeasy® plant DNA extraction kit (Qiagen, Hilden, Germany). Approximately 30micro-silica beads were added (800 µm; OPS Diagnostics, Lebanon, NJ, USA). The sample was hand ground using a micro-pestle and the sample was incubated at 55 °C overnight. The DNAeasy manufacturer's protocol was then followed with the exception that 50 µL of elution buffer was added in the final two steps rather than 100 µL, resulting in 100 µL of eluted DNA.

Polymerase chain reactions (PCRs) were performed in 15 µL reaction volumes with 7.5 µL KAPA 2G robust ready mix with dye (Kapa Biosystems, Inc., Wilmington, MA, USA), 0.75 µL each 10 µm primer, and 1–2 µL of diluted (10-fold) DNA template. Amplification of all regions was achieved using a 'touchdown' profile. An initial denaturation step of 5 min at 95 °C, 3 cycles of 30 s at 95 °C, 30 s at 65 °C, 45 s at 72 °C, 4 cycles of 30 s at 95 °C, 30 s at 64 °C, 45 s at 72 °C, 5 cycles of

© 2025 Westerdijk Fungal Biodiversity Institute

30 s at 95 °C, 30 s at 63 °C, 45 s at 72 °C, 6 cycles of 30 s at 95 °C, 30 s at 62 °C, 45 s at 72 °C, 30 cycles of 30 s at 95 °C, 30 s at 60 °C, 45 s at 72 °C, with a final extension of 10 min at 72 °C.

Sequencing and phylogenetic analyses

The PCR products were cleaned using ExoSAP-IT™ (Affymetrix, Santa Clara, CA, USA) at a rate of 2 µL to 5–10 µL of PCR product and incubated at 37 °C for 15 min followed by 80 °C for 1hr. Cleaned PCR products were sequenced with a BigDye® Terminator v. 3.1 cycle sequencing kit (Thermo Fisher Scientific, Waltham, MA, USA) using the following volumes: 1 µL BigDye®; 1 µL 1 µM primer, 2 µL 5× buffer, 2–6 µL cleaned PCR product (estimated as 20–30 ng) and ddH20 to 10 µL total reaction volume. Cycle sequencing profile consisted of an initial denaturation step of 1 min at 96 °C, followed by 35 cycles of 10 s at 96 °C, 5 s at 50 °C and 4 min at 60 °C. Sequencing reactions were cleaned by ethanol precipitation and sequenced on an ABI 3130xl Genetic Analyzer (Applied Biosystems, Waltham, MA, USA).

The resulting sequence fragments of *H. ritscheliae* were assembled in Geneious® v. 9.0.4 (Kearse *et al.* 2012) using the *H. vastatrix* sequences DQ354565 (SSU) & DQ354566 (LSU) as reference. The assembled sequences of the SSU and the LSU were concatenated and aligned with existing reference sequences, downloaded from GenBank (Table 1) using the MAFFT algorithm (Katoh *et al.* 2002) via the MAFFT plugin in Geneious® v. 9.0.4 (Kearse *et al.* 2012). The sequence alignment is available at TreeBase (study ID 32140).

Sequences for the phylogenetic analysis were selected based on recent literature within the *Zaghouaniaceae* and GenBank availability (Wood & Aime 2024). *Skierka robusta*, a member of the *Skierkaceae* family, was selected as the outgroup. The alignment was run as a partitioned dataset using both maximum likelihood and Bayesian analyses with GTRGAMMA as the model of evolution. The Bayesian analyses were carried out using MrBayes v. 2.24 (Drummond *et al.* 2012) whereas the maximum likelihood phylogenies were estimated using RAxML (Stamatakis 2014), implemented in Geneious Prime v. 9. For the Bayesian analysis, the Markov Chain Monte Carlo was performed with four heated chains for 1 M generations. Trees were sampled every 200th generation. For the maximum likelihood analysis, support for clades were evaluated using 1000 nonparametric bootstrap (BS) replicates. Trees were edited using Geneious Prime v.9 (https://www.geneious.com) and Adobe Illustrator CS v. 6 (Adobe Systems Inc., USA). The phylogenetic tree is available at TreeBase (study ID 32140).

Morphological observations

Uredinia were removed from the specimen leaves under dissecting stereoscope (Leica MZ APO, Leica Microsystems, Buffalo Grove, Illinois, USA), using a dissecting scalpel and forceps. The uredinia were mounted in 3 % potassium hydroxide, fixed with a coverslip, and allowed to soak for 5 min to rehydrate the specimen. Observations were made on a Zeiss AxioPlan 2 compound microscope at 40× and 63×. Digital images were captured using a Zeiss AxioCam HRc and measurements taken using AxioVision v. 4.9.1.0 (Carl Zeiss, Thornwood, New York, USA).

Spore length and width, spore wall thickness, aculei length and width at the base, and spacing between aculei were measured for 30 spores (five aculei were measured per spore, spacing was measured from one aculeus to five surrounding aculei).

Scanning electron microscopy photographs were taken using a variable pressure TM3030 Plus table-top scanning electron microscope (Hitachi, Dallas, TX) at the USDA-ARS electron and confocal microscopy unit, Beltsville, Maryland. An infected leaf was placed directly on a 25-mm-diam. black double-sided sticky tab (PELCO Carbon Conductive tabs, Ted Pella, Redding, CA) which was covering a 25-mm-diam. SEM stub (AMRAY aluminum stub, Ted Pella, Redding, CA) and photographed with the secondary electron detector set at charge-up reduction mode using the TM3030 Plus imaging software v. 02-02-01 (Hitachi). Samples did not require any treatment prior to imaging.

RESULTS

Phylogenetic analyses

Sequencing of products from designed primers was successful for one pair amplifying 18S (primers SSU_DF & SSU_DR) (372 bp; GenBank ID: MZ856324) and one pair amplifying 28S rDNA (primers LSU_AF & LSU_AR) (354 bp; GenBank ID: MZ856323), for *H. ritscheliae* herbarium specimen BPI019726. BLASTn searches returned *H. vastatrix* (97 % identity) and other closely related genera (92–96 % identity). The final alignment of *H. ritscheliae*, with reference sequences, contained 13 concatenated sequences. Maximum likelihood and Bayesian analyses yielded an identical topology and *H. ritscheliae* was found in a strongly supported clade containing all *Hemileia* species. (Fig. 1).

TAXONOMY

Hemileia ritscheliae J.Bailey & Castl., ***sp. nov*.** MB 849211. Figs 2, 3.

Etymology: Named in honor of Dr. Anja Ritschel author of the Monograph of the genus *Hemileia*.

Typus: **Uganda**, Entebbe Road, in follis *Aristolochia* (as *A. dorsivenia*), May 1943, leg. *C.G. Hansford* (**holotype** BPI 019726).

GenBank accession numbers: MZ856324 (SSU), MZ856323 (LSU).

Diagnosis: *Hemileia ritscheliae* has only been found on *Aristolochiaceae* and is the only known member of the genus reported from this host.

Description: *Leaf lesions* absent. *Uredinia* wholly abaxial, scattered across whole leaf, sporigenous cells fasciculate, originating from a substomatal primordium; *urediniospores* pale yellow (in preserved material), globose to obovoid, asymmetric, hilum displaced towards ventral side or centered on ventral side, spore length (22–)25–26.5–28(–30)

© 2025 Westerdijk Fungal Biodiversity Institute

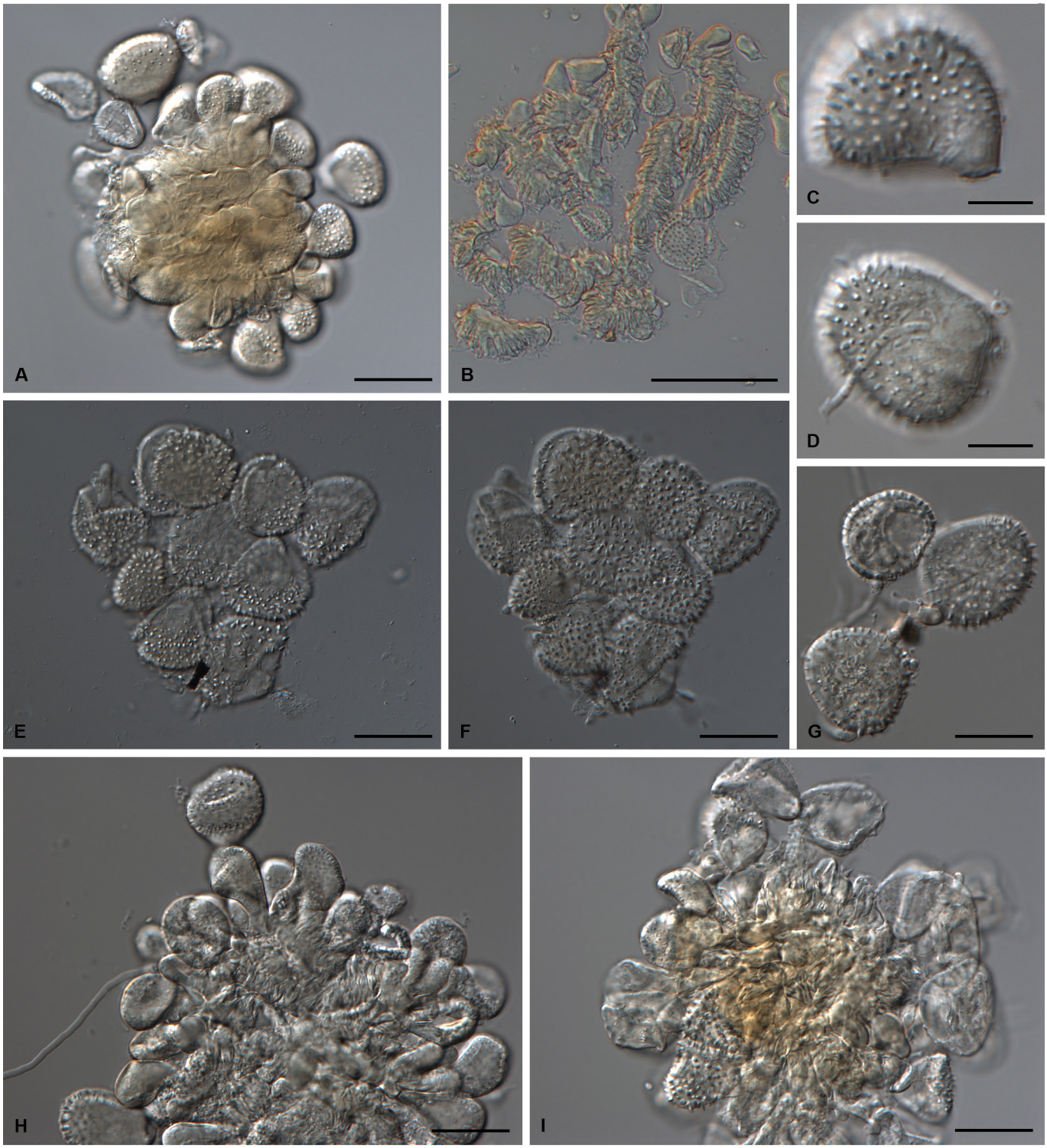

Fig. 2. *Hemileia ritscheliae* urediniospores. **A.** Upper view showing the sporigenous cells and urediniospores. **B.** Separated sporigenous cells and urediniospores, showing the fringed appearance of the pedicels. **C.** Urediniospore, side view. **D.** Urediniospore, showing the hilum **E.** Urediniospores, below median focus **F.** Urediniospores, above median focus. **G.** Urediniospores, below surface focus. **H.** Lower view showing immature urediniospores and fringed pedicels. **I**. Lower view showing malformed urediniospores. Scale bars: A, E–I = 20 µm; B = 50 µm; C, D = 10 µm.

µm, spore width (17–)20–22.5–25(–28) µm, smooth around the hilum and dorsally moderately finely echinulate, aculei irregularly spaced at 0.5–3(–3.5) µm, 1–2(–2.5) µm broad at the base and 1.5–3 µm long, germ pores not observed, pedicles hyaline, up to 12 µm long, spore wall 1.5–2(–2.4) µm; *teliospores* not observed.

Known distribution: Known only from the type locality (Uganda).

DISCUSSION

The authors were able to find sufficient uredinial material to describe the new species. The extraction of several uredinia containing whole mature urediniospores was fortunate, as the majority of the preserved specimen is in degraded condition and many uredinia had to be examined to find whole, mature spores. The asymmetrical urediniospores, with one flat, smooth side and an echinulate convex side,

© 2025 Westerdijk Fungal Biodiversity Institute

Table 1. Taxa used for phylogenetic analyses.

Genus	Fungarium Deposition ID	28S	18S	CO3	Host	Country, State	Source
Achrotelium ichnocarpi	BRIP55634	KT199393	KT199381	KT199404	*Apocynaceae; Ichnocarpus frutescens*	Australia, Queensland	McTaggart *et al.* (2016)
Hemileia ectadiopsidis	PURN16278 / PREM61406	OQ215021	OQ215133	—	*Apocynaceae; Cryptolepis oblongifolia*	South Africa, KwaZulu-Natal	Wood & Aime (2024)
Hemileia fadogiae	BPI878108 / PREM59124	OQ215022	—	—	*Rubiaceae; Pygmaeothamnus chamaedendrum*	South Africa, KwaZulu-Natal	Wood & Aime (2024)
Hemileia gardeniae-thunbergiae	BPI871663 / PREM58674	OQ215023	—	—	*Rubiaceae; Gardenia thunbergia*	South Africa, Mpumalanga	Wood & Aime (2024)
Hemileia ritcheliae	BPI019726	MZ856323	MZ856324	—	*Aristolochiaceae; Aristolochia* sp.	Uganda	This study
Hemileia scholzii	PURN16280 / PREM60938	OQ215024	—	—	*Lamiaceae; Clerodendrum glabrum*	South Africa, KwaZulu-Natal	Wood & Aime (2024)
	PURN16343	—	OQ215134	OR789147	*Lamiaceae; Clerodendrum glabrum*	South Africa, KwaZulu-Natal	Wood & Aime (2024)
Hemileia vastatrix	BPI843642	DQ354566	DQ354565	—	*Rubiaceae; Coffea arabica*	Mexico	Aime 2006
Hemileia woodii	BPI872229 / PREM59111	OQ215025	—	—	*Rubiaceae; Vangueria infausta*	South Africa, Mpumalanga	Wood & Aime (2024)
	PURN16277 / PREM60939	OQ215026	—	—	*Rubiaceae; Pachystigma latifolium*	South Africa, KwaZulu-Natal	Wood & Aime (2024)
Mikronegeria fagi	PURN16373	MW049267	MW049298	OR789149	*Nothofagaceae; Nothofagus obliqua*	Chile	Aime & McTaggart (2021), Wood & Aime (2024)
Uredo cryptolepidis	PURN22767 / PREM63123	OQ215086	OQ215142	OR789148	*Apocynaceae; Cryptolepis capensis*	South Africa, KwaZulu-Natal	Wood & Aime (2024)
Uredo cryptostegiae	BRIP56898	KT199401	KT199387	KT199412	*Apocynaceae; Cryptostegia grandiflora*	Australia, Queensland	McTaggart *et al*. (2016)
Skierka robusta	BPI879954 / PREM59047	MW049279	MW049305	—	*Vitaceae; Rhoicissus rhomboidea*	South Africa, KwaZulu-Natal	Aime & McTaggart (2021)

28S = LSU - Large subunit; 18S = SSU - small subunit; BPI = U.S. National Fungus Collections, Beltsville, MD, USA.

© 2025 Westerdijk Fungal Biodiversity Institute

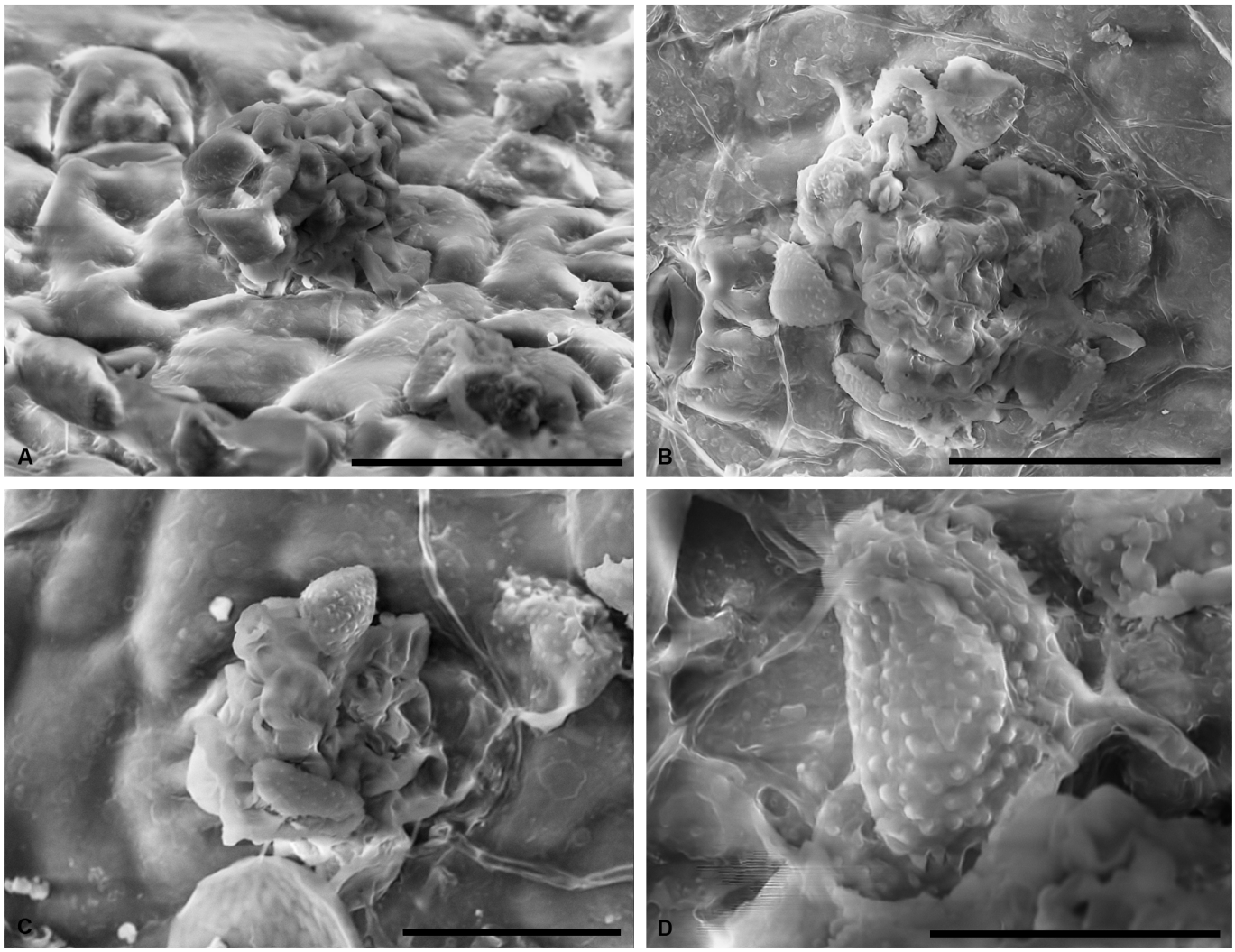

Fig. 3. *Hemileia ritscheliae* uredinia. **A.** Side view showing sporigenous cells and developing urediniospores emerging from the stomate. **B.** Upper view showing urediniospores with pedicel still attached. **C.** Upper view with guard cell. **D.** Urediniospore, side view showing echinulation. Scale bars: A, B = 50 µm; C = 30 µm; D = 20 µm.

make this species consistent with the current definition of the genus *Hemileia*. This was confirmed by DNA analyses using the SSU and LSU regions, which is sufficient for placing rust species (Kaishian *et al.* 2024).

Previously described *Hemileia* species are distinguished principally on host, and this is the only known member of this genus on a host in the *Aristolochiaceae*. Previously reported rusts on *Aristolochia* sp. have been collected in Europe, Asia-Pacific, The Middle East, Northern Africa and California (Farr & Rossman 2020), none of which are species of *Hemileia*. This is the first report of *Hemileia* on this host genus.

The original species identity of the host is problematic, *Aristolochia dorsivenia* appears to be an invalid name and is not listed at World Flora Online (World Flora Online 2025); it is mentioned only twice in relation to specimens of lichenicolous hyphomycetes, which were also collected by C.G. Hansford (Hawksworth 1979). Host DNA amplification of the rbc_LA region (Kress & Erickson 2007) a global plant DNA barcode system is evaluated by comparing universal application and degree of sequence divergence for nine putative barcode loci, including coding and non-coding regions, singly and in pairs across a phylogenetically diverse set of 48 genera two species per genus were obtained using the same DNA extracted for rust DNA amplification. BLASTn search returned several *Aristolochia* species with > 96 % identity, confirming the genus identification. The host species remains uncertain.

Museums rely upon collectors to submit specimens and carefully document their research, and these specimens form the foundation that future research is built on. Herbaria hold a wealth of undiscovered species and biological information. This study highlights the importance of herbarium and fungarium collections in documenting plant and fungal species in space and time and preserving scientific vouchers.

ACKNOWLEDGEMENTS

This project was supported by the Oak Ridge Institute for Science and Education through an interagency agreement between the U.S. Department of Energy and United States Department of Agriculture, Agricultural Research Service (USDA ARS) and USDA ARS National Programs 301 and 303, Projects 8042-22000-323-000D and 8042-22000-327-000D. The authors would like to thank G. Bauchan and the electron and confocal microscopy unit at USDA-ARS, Mehrdad Abbasi of the Purdue University Arthur Fungarium, J.D. Hall for confirming the negative ITS rDNA sequencing

© 2025 Westerdijk Fungal Biodiversity Institute

results and reviewing the manuscript, and S. Callaghan and B. Dominiak for review assistance. Mention of trade names or commercial products in this publication is solely for the purpose of providing specific information and does not imply recommendation or endorsement by the USDA; USDA is an equal opportunity provider and employer.

Conflict of interest: The authors declare that they have no conflict of interest.

REFERENCES

Aime MC (2006). Toward resolving family-level relationships in rust fungi (*Uredinales*). *Mycoscience* **47**: 112–122. https://doi.org/10.1007/S10267-006-0281-0

Aime MC, McTaggart AR (2021). A higher-rank classification for rust fungi, with notes on genera. *Fungal Systematics and Evolution* **7**: 21–47. https://doi.org/10.3114/fuse.2021.07.02

Berkeley MJ, Broome CE (1869). The Gardeners' Chronicle and Agricultural Gazette. *Gardener's Chronicle* **1157**.

Cummins GB, Hiratsuka Y (2003). *Illustrated genera of rust fungi*. 3rd ed. APS Press, USA.

Dobson A, Crawley M (1994). Pathogens and the structure of plant communities. *Trends in Ecology & Evolution* **9**: 393–398. https://doi.org/10.1016/0169-5347(94)90062-0

Drummond AJ, Suchard MA, Xie D, *et al.* (2012). Bayesian phylogenetics with BEAUti and the BEAST 1.7. *Molecular Biology and Evolution* **29**: 1969–1973. https://doi.org/10.1093/molbev/mss075

Farr DF, Rossman AY (2020). Fungal Databases, Systematic Mycology and Microbiology Laboratory, ARS, USDA. Retrieved 18 March 2020, from http://nt.ars-grin.gov/fungaldatabases/.

Gilbert GS (2002). Evolutionary ecology of plant diseases in natural ecosystems. *Annual Review of Phytopathology* **40**: 13–43. https://doi.org/10.1146/annurev.phyto.40.021202.110417

Hawksworth DL (1979). The Lichenicolous Hyphomycetes. *Bulletin of the British Museum* **6**: 224–227.

Helfer S (2014). Rust fungi and global change. *New Phytologist* **201**: 770–780. https://doi.org/10.1111/nph.12570

Huelsenbeck JP, Ronquist F (2001). MRBAYES: Bayesian inference of phylogeny. *Bioinformatics* **17**: 754–755. https://doi.org/10.1093/bioinformatics/17.8.754

Judith C, Rossman A (2014). Revised scientific names of the genus *Hemileia* (*Pucciniales*) based on the new ICN. *MycoKeys* **8**: 1–10. https://doi.org/10.3897/mycokeys.8.4040

Kaishain, P, Layug CRK, Anderson M, *et al.* (2024). Rust HUBB: DNA barcode-based identification of *Puccinales*. *IMA Fungus* **15**: 3. https://doi.org/10.1186/s43008-023-00132-7

Katoh K, Misawa K, Kuma K, *et al.* (2002). MAFFT: a novel method for rapid multiple sequence alignment based on fast Fourier transform. *Nucleic Acids Research* **30**: 3059–3066. https://doi.org/10.1093/nar/gkf436

Kearse M, Moir R, Wilson A, *et al.* (2012). Geneious Basic: an integrated and extendable desktop software platform for the organization and analysis of sequence data. *Bioinformatics* **28**: 1647–1649. https://doi.org/10.1093/bioinformatics/bts199

Kinloch Jr, Bohun B (2003). White pine blister rust in North America: past and prognosis. *Phytopathology* **93**: 1044–1047. https://doi.org/10.1094/PHYTO.2003.93.8.1044

Koutouleas A, Collinge DB, Boa E (2024). The coffee leaf rust pandemic: An ever-present danger to coffee production. *Plant Pathology* **73**: 522–534. https://doi.org/10.1111/ppa.13846

Kress, WJ., Erickson, DL (2007). A two-locus global DNA barcode for land plants: the coding rbcL gene complements the non-coding trnH-psbA spacer region. *PLoS ONE* **2**: e508. https://doi.org/10.1371/journal.pone.0000508

Leonard KJ, Szabo LJ (2005). Stem rust of small grains and grasses caused by *Puccinia graminis*. *Molecular Plant Pathology* **6**: 99–111. https://doi.org/10.1111/j.1364-3703.2005.00273.x

McTaggart AR, Shivas RG, Nest MA *et al.* (2016). Host jumps shaped the diversity of extant rust fungi (*Pucciniales*). *The New Phytologist* **209**: 1149–1158. https://doi.org/10.1111/nph.13686

Miller MA, Pfeiffer W, Schwartz T (2010). Creating the CIPRES Science Gateway for inference of large phylogenetic trees. *Gateway Computing Environments Workshop (GCE)*, USA. https://doi.org/10.1109/GCE.2010.5676129

Ritschel A (2005). Monograph of the genus *Hemileia* (*Uredinales*). *Bibliotheca Mycologica* **200**. J. Cramer Verlag, Germany.

Ronquist F, Huelsenbeck J (2003). MrBayes 3: Bayesian phylogenetic inference under mixed models. *Bioinformatics* **19**: 1572–1574. https://doi.org/10.1093/bioinformatics/btg180

Stamatakis A (2014). RAxML version 8: a tool for phylogenetic analysis and post-analysis of large phylogenies. *Bioinformatics* **30**: 1312–1313. https://doi.org/10.1093/bioinformatics/btu033

Wingfield BD, Ericson L, Szaro T, *et al.* (2004). Phylogenetic patterns in the *Uredinales*. *Australasian Plant Pathology* **33**: 327–335. https://doi.org/10.1071/AP04020

Wood AR, Aime MC (2024). Phylogenetics of the rust fungi (*Pucciniales*) of South Africa, with notes on their life histories and possible origins. *Mycologia* **116**: 509–535. https://doi.org/10.1080/00275514.2024.2334189

World Flora Online (2025). Published on the Internet; http://www.worldfloraonline.org. Accessed on 14 Apr. 2025.

Supplementary Material: http://fuse-journal.org/

Table S1. Primer sequence details.

© 2025 Westerdijk Fungal Biodiversity Institute

© 2025 Westerdijk Fungal Biodiversity Institute

FUSE

Fungal Systematics and Evolution

VOLUME 16
DECEMBER 2025
PAGES 155–180

doi.org/10.3114/fuse.2025.16.9

Diversity of fungicolous fungi associated with *Camarotella* spp. (*Phyllachorales*, *Sordariomycetes*) on *Cocos nucifera* in Brazil, including *Fusicolla parasitica sp. nov.* (*Nectriaceae*)

C.E.V.A. Sá[1*], C.M. Souza-Motta[1], P.V. Tiago[1], A.R. Machado[1,2]

[1]Departamento de Micologia, Universidade Federal de Pernambuco, Pernambuco, Brazil
[2]Departamento de Fitopatologia, Universidade Federal Rural de Pernambuco, Pernambuco, Brazil

[*]Corresponding author: camila.estelita@ufpe.br / camilavogeleysa@gmail.com

Key words:
coconut tree
Hypocreales
new taxon
phylogenetics
taxonomy

Abstract: *Camarotella torrendiella* and *Camarotella acrocomiae*, the causal agents of coconut black leaf spot, are of great economic importance to coconut cultivars. Species of hyperparasites have previously been reported in the stromata of these species, which delay and reduce the viability of the ascospores of these pathogens, demonstrating their bio-control potential. In order to identify and analyse the parasitic species affecting the pathogens that cause coconut black leaf spot, symptomatic leaflets exhibiting parasitized stromata of both *C. torrendiella* and *C. acrocomiae* were collected in the states of Pernambuco and Paraíba (Brazil) and the fungi present in the stromata were isolated. The hyperparasites were phylogenetically identified based on different gene regions according to genera and presented in this paper with a detailed taxonomic description as well as their abundance and constancy in the coconut grove. A new species of *Fusicolla* was described in this study as *Fusicolla parasitica sp. nov. Acremonium cavaraeanum* presented a new record for the states of Paraíba and Pernambuco*. Fusarium pseudocircinatum* and *Fusarium caatingaense* presented the first report of their fungicolous lifestyles, while *Purpureocillium lilacinum* was for the first time recorded hyperparasitizing a *Camarotella* spp. causing leaf lesions. This study shows *Fusicolla parasitica* and *Acremonium cavaraeanum* as constant and abundant species in the coconut grove, while *Fusarium pseudocircinatum* and *Purpureocillium lilacinum* are accessory and common; *Fusarium caatingaense* was considered rare and accidental.

Citation: Sá CEVA, Souza-Motta CM, Tiago PV, Machado AR (2025). Diversity of fungicolous fungi associated with *Camarotella* spp. (*Phyllachorales*, *Sordariomycetes*) on *Cocos nucifera* in Brazil, including *Fusicolla parasitica sp. nov.* (*Nectriaceae*). *Fungal Systematics and Evolution* **16**: 155–180. doi: 10.3114/fuse.2025.16.9
Received: 1 January 2025; **Accepted:** 5 March 2025; **Effectively published online:** 16 July 2025
Corresponding editor: P.W. Crous

INTRODUCTION

The coconut palm (*Cocos nucifera*) is considered one of the most widespread fruit trees in the world (Martins & Jesus Júnior 2011). Despite being typical in tropical climate regions, this species is of agronomic interest, and has acquired remarkable adaptability, allowing it to be cultivated in different regions and continents (Foale & Harries 2010, Martins & Jesus Júnior 2011). Coconut cultivation is extremely important for the economy of Brazil and the global market, and the global coconut industry is expected to exceed US $30 billion by 2026 (Johnson *et al.* 2024). Different parts of the plant, such as the dried coconuts, leaves and sheaths, are used in the agro, oleochemical and pharmaceutical industries, mainly as fertilizer, biofuel/biomass, cosmetics and others (Bonneau *et al.* 2010, Johnson *et al.* 2024). Over the years, coconut production for the food industry (coconut oil, coconut flour, coconut milk, among others) has been increasingly in demand, as has production for in natura consumption (Kaur *et al.* 2019). This palm species is affected by different types of pathogens. Among the most common leaf diseases, black leaf spot, caused by the fungi *Camarotella acrocomiae* and *C. torrendiella*, are responsible for up to 50 % of losses in coconut production (Vitória *et al.* 2008, Pinto *et al.* 2023).

The two etiological agents responsible for black leaf spot in coconut tree display distinct host colonization strategies. Araújo *et al.* (2017) delineated the colonization of *Camarotella torrendiella* into two distinct stages. In the first stage fungal hyphal growth is primarily restricted to the epidermal cells and the subjacent tissues beneath the adaxial epidermis. In the second stage, extensive cellular disorganization, characterized by the accumulation of highly pigmented material within the intercellular spaces and a significant increase in hyphal density results in the collapse of host tissues. However, *C. acrocomiae* follows a divergent colonization pattern, predominantly affecting the phloem cells within the vascular bundles adjacent to the stromata, without inducing tissue collapse (Araújo *et al.* 2017). The exact mechanisms by which these pathogens invade the epidermal and subepidermal tissues, as well as their ability to evade the host's defense mechanisms, remain unknown (Vitória *et al.* 2008).

The term hyperparasitism, when referring to fungi, refers

Fungal Systematics and Evolution is licensed under a Creative Commons Attribution-NonCommercial-NoDerivatives 4.0 International License

© 2025 Westerdijk Fungal Biodiversity Institute

to the phenomenon in which a fungus is able to parasitize another fungus. However, the term is only used when the host is also a parasite, differentiating it from the terms mycoparasitism and fungicolous fungi (Parratt & Laine 2016, Haelewaters *et al.* 2018, Bérmudez-Cova *et al.* 2022). Mycoparasitism is strictly defined as a trophic interaction in which a living fungal host serves as a direct nutrient source for another fungus, which does not need to be a parasite itself (Jeffries 1995). However, the concept is sometimes extended to include fungicolous associations, wherein fungi establish persistent yet ecologically diverse relationships with other fungi without confirmed nutrient transfer (Jeffries 1995, Gams *et al.* 2004, Sun *et al.* 2019). The complexity of these interactions often obscures the distinction between true parasitism and facultative or commensal associations, necessitating further investigation into their physiological and ecological mechanisms. Hyperparasitic fungi are present in different taxonomic groups, and among them the order *Hypocreales* (*Sordariomycetes*, *Ascomycota*) presents a rich diversity of hyperparasitic fungal species, comprising more than 320 genera, with *Trichoderma* spp. being the most well-known and currently most widely used in biological control (Bermúdez-Cova *et al.* 2023). Species belonging to *Acremonium* sp. and *Fusarium* sp. have already been reported as hyperparasites. *Acremonium implicatum* was originally characterized as a hyperparasite recorded on *Puccinia coronata*, the causal agent of oat crown rust (Leinhos & Buchenauer 1992). *Acremonium alternatum* was record as hyperparasite of *Sphaerotheca fuliginea* causing powdery mildew in cucurbits (Malathrakis 1985), while *A. strictum* has been documented parasitizing *Helminthosporium solani*, responsible for silver scurf of potato (Rivera-Varas *et al.* 2007).



Fig. 1. A. *Cocos nucifera* specimen at the Intituto de Pesquisa Agronômica (IPA) in Goiana (Pernambuco, Brazil). **B.** *Camarotella acrocomiae* stromata on a leaflet of *C. nucifera* hyperparasitised by *Acremonium cavaraeanum* under stereomicroscope. **C.** Cut leaflets of *C. nucifera* presenting hyperparasitised stromatas of *C. torrendiella* and *C. acrocromiae*.

© 2025 Westerdijk Fungal Biodiversity Institute

Fusarium merismoides has been reported as a hyperparasite of *Pythium ultimum*, causing root rot in different plant hosts (Hoch & Abawi 1979). Mower *et al.* (1975) and Hornok & Walc (1983) reported, respectively, *Fusarium roseum* and *F. heterosporum* as hyperparasites of *Claviceps purpurea*, the causal agent of ergot in wheat (medical importance due to ergotism). Recently, an unknown species of *Fusarium* was reported hyperparasitizing aecidia of *Puccinia coronata* (rust) on a leaf of *Rhamnus cathartica* (Bermúdez-Cova *et al.* 2023).

Knowledge about the diversity of hyperparasitic fungi present in *Camarotella* is still limited. Some species such as *Acremonium alternatum*, *A. cavareanum*, *Hansfordia pulvinata*, *Septofusidium elegantulum* and *Verruciconidia persicina* (Sudo 1989, Carvalho *et al.* 2003, Warwick 2007), have already been recorded based on morphological evidence, associated with black leaf spot on coconut trees. However, there is no record if these reports have been phylogenetically identified. The aim of this work is to present the first record of the diversity of fungicolous fungi associated with the etiological agents of leaf black spot of coconut trees based on molecular and phylogenetic evidence. For a better understanding of the diversity, distribution, biology and bio-control potential of fungicolous fungi, it is necessary to invest in new studies focusing on the ecology and taxonomy of these organisms.

MATERIALS AND METHODS

Isolates

Leaflets of coconut trees with hyperparasitic fungi present on the stromata of *Camarotella torrendiella* and *C. acrocomiae* were collected from five locations in northeast Brazil across different seasons. In Paraíba state, samples were collected in Aug. 2023 from a private property (6°38'29"S, 35°07'21.6"W, 105 m a.s.l.) in Camaratuba municipiality, while in Pernambuco state, collections were made at a private property (8°28'12"S, 35°43'44"W, 444 m a.s.l.) in Bonito (Feb. 2022), at the Universidade Federal Rural de Pernambuco (8°01'03"S, 34°57'05"W, 100 m a.s.l.) in Recife (Dec. 2022), at the Instituto de Pesquisa Agronômica (7°33'46"S, 35°00'47"W, 103 m a.s.l.) in Goiana (Jun. 2022), and at a private property (7°95'77"S, 35°10'68"W, 101 m a.s.l.) in Paudalho (Jun. 2023). In each location, leaflets were collected from 10 randomly selected coconut tree individuals, totalling 250 samples (five per plant). Samples were stored in sterile plastic bags and transported to the Laboratório de Micologia Ambiental, Departamento de Micologia, Universidade Federal de Pernambuco (Recife, Brazil) for analysis.

Three random black leaf spot stromata of *C. acrocomiae* and *C. torrendiella* containing visible hyperparasitic fungi were selected per leaf sample (Fig. 1). The fungal structures were collected from the selected stromata using a dissecting microscope and flamed needles and transferred to Petri dishes (9 cm diam.) containing Potato Dextrose Agar (PDA) medium and antibiotic [rifamycin SV sodium (10 mg/mL)], following the direct isolation technique proposed by Alfenas *et al.* (2016). The cultures were incubated at room temperature (25 to 27 °C) in darkness until the colonies grew, which was then plated onto Petri dishes containing PDA without antibiotic. Isolates with absent sporulation in PDA, like *Fusarium* and *Fusicolla*, were transferred to Spezieller Nährstoffarmer Agar (SNA) (Nirenberg 1976) in order to obtain conidia for morphological characterization. Ex-type cultures and other cultures studied were deposited in the Micoteca URM Culture Collection of the Departamento de Micologia of the Universidade Federal de Pernambuco, Recife, Pernambuco, Brazil.

Morphological characterization

Morphological characterization was based on cultures derived from hyphal fragments (Narayanasamy 2001). To determine radial mycelial growth, water agar blocks with the fungal isolate were transferred from 4-d-old cultures to the centre of Petri dishes containing PDA. Two replicate plates for each isolate were incubated at 27 °C in darkness. Colony diameters were measured after 7 d of growth. For characterization of conidia and conidiophores, *Fusarium* isolates were grown for 15 d on SNA at 27 °C, *Acremonium* and *Purpureocillium* isolates were grown for 7 d on PDA at 27 °C, while *Fusicolla* isolates were first grown in liquid ME (malt extract) medium for 7 d in darkness at 27 °C and then poured onto PDA plates which were grown for 7 d at same temperature (Costa *et al.* 2020).

Ecological data

The abundance (A) of each species was evaluated based on the ratio between number of specimens obtained and the total number of specimens of fungi (Sá *et al.* 2022). Schnittler & Stephenson (2000) classification was adopted: rare (< 1.5 %), occasional (1.5–3.5 %), common (3.5–6.5 %), and abundant (> 6.5 %). The constancy (C) of each species was assessed relating the total number of expeditions (P) and number of expeditions in which a fungal species was found (p) (C = p.100/P). The species were classified as constant (> 50 %), accessory (26 % to 50 %), or accidental (≤ 25 %) (Dajoz 1983, Sá *et al.* 2019, Barbosa *et al.* 2022).

In the commented list of species, for each taxon, in addition to the information requested, the following data are provided: number of specimens; abundance (A) and constancy (C) category.

DNA extraction, amplification and sequencing

Representative isolates of each genus were grown in PDA at 25 °C for 5 to 7 d. The mycelium was collected using a sterilized scalpel and placed in 2 mL microtubes containing four 3-mm-diam. glass beads. Genomic DNA was extracted from cultures that were 5-day-old (fast-growing isolates) or 7-d-old (slow-growing isolates) using the Wizard Genomic DNA Purification Kit (Promega Corporation, Brazil) following the manufacturer's instructions.

For isolates belonging to different genera, the most informative gene regions were selected for polymerase chain reactions (PCR's), following the most recent literature. Amplifications were performed using 6.25 µL GoTaq Master Mix polymerase buffer from Cellco®, 0.5 µL (10 mM concentration) of each forward and reverse primer, 4.25 µL of nuclease-free water and 1 µL of DNA sample for each

© 2025 Westerdijk Fungal Biodiversity Institute

Table. 1. Primer pairs, PCR amplification procedures and references used in this study. * = FFSC: *Fusarium fujikuroi* Species Complex; FIESC: *Fusarium incarnatum-equiseti* Species Complex.

Genus	Locus	Primers	PCR parameters	Reference
Acremonium	LSU	LR0R/LR5	94 °C 3 min; 35 cycles of 94 °C 35 s, 52 °C 60 s, 72 °C 90 s; 72 °C 10 min	Summerbell *et al.* (2011)
Fusarium FFSC* and FIESC*	*RPB2*	5F2/7cR	95 °C 5 min; 40 cycles of 94 °C 30 s, 51 °C 90 s, 68 °C 2 min; 68 °C 5 min	Liu *et al.* (1999), Sung *et al.* (2007)
	TEF1-α	EF1/EF2	95 °C 5 min; 35 cycles of 95°C 45 s, 52 °C 45 s, 72 °C 90 s; 72 °C 8 min	O'Donnell *et al.* (1998), Han *et al.* (2023)
Fusicolla	ITS	ITS5/ITS4	95 °C 5 min; 35 cycles of 95 °C 30 s, 52 °C 30 s, 72 °C 1 min; 72 °C 7 min	Bellemain *et al.* (2010), Gräfenhan *et al.* (2011)
	LSU	LR0R/LR5	94 °C 3 min; 35 cycles of 94 °C 35 s, 52 °C 1 min, 72 °C 90 s; 72 °C 10 min	Zeng & Zhuang (2023)
	RPB2	5F2/7cR	95 °C 5 min; 40 cycles of 94 °C 30 s, 51 °C 90 s, 68 °C 2 min; 68 °C 5 min	This study
	TUB2	T1/T222	95 °C 5 min; 35 cycles of 95 °C 45 s, 52 °C 45 s, 72 °C 90 s; 72 °C 8 min	Zeng & Zhuang (2023)
Purpureocillium	ITS	ITS5/ITS4	95 °C 5 min; 35 cycles of 95 °C 30 s, 52 °C 30 s, 72 °C 1 min; 72 °C 7 min	Bellemain *et al.* (2010)
	LSU	LR0R/LR5	94 °C 3 min; 35 cycles of 94 °C 35 s, 52 °C 1 min, 72 °C 90 s; 72 °C 10 min	Zeng & Zhuang (2023)
	TEF1-α	983F/2218R	95 °C 5 min; 35 cycles of 95 °C 45 s, 52 °C 45 s, 72 °C 90 s; 72 °C 8 min	Araújo *et al.* (2022)

reaction (20 ng of genomic DNA). For each genus in the study, the primer pairs, PCR amplification procedures and references used were compiled and listed in Table 1.

The PCR products were purified using the enzymes Exonuclease and Shrimp alkaline photosphatase [Exo + SAP (Cellco Biotech / Brazil)] and sequenced on the sequencing platform of the Departamento de Genética of the Centro de Biociências of the Universidade Federal de Pernambuco, Recife, Brazil. Sequence data were analysed and edited with DNA Baser v. 3.2.5 (Heracle BioSoft, Arges, Romania) to generate the consensus nucleotide sequences. The sequences were deposited in GenBank (http://www.ncbi.nlm.nih.gov; Tables 2–6).

Phylogenetic analyses

The sequences obtained were aligned with the type sequences of each species of the genera studied available in GenBank (http://www.ncbi.nlm.nih.gov) using the MUSCLE algorithm implemented in MEGA v. X (Kumar *et al.* 2018, Norphanphoun *et al.* 2019). The alignments were trimmed manually when necessary. For each genus, 1–2 outgroups were selected based on previous published phylogenetic analyses. To assemble the phylogenetic database, taxa belonging to the ex-type, holotypes and epitypes were selected from previous reference works (Xia *et al.* 2019, Calvillo-Medina *et al.* 2021, Yilmaz *et al.* 2021, Araújo *et al.* 2022, Bali *et al.* 2022, Crous *et al.* 2022, Li *et al.* 2022, Hou *et al.* 2023, Zeng & Zhuang 2023). Taxon information and GenBank accession numbers are provided in Tables 2–6. The sequences alignments generated in this study were deposited in Figshare (doi: 10.6084/m9.figshare.28629749). Phylogenetic analyses of individuals and concatenated datasets were performed using Bayesian Inference (BI) and Maximum Likelihood (ML). The BI analysis was performed using the Markov Chain Monte Carlo (MCMC) method. The nucleotide substitution models were selected using MrModeltest v. 2.3 (Posada & Buckley 2004) and estimated separately for each gene region according to the Akaike Information Criterion (AIC). The BI analysis was completed with MrBayes v. 3.1.1 (Ronquist & Huelsenbeck 2003) at 10 M generations with one tree sampled every 1000 generations, resulting in 10000 trees. The first 2500 trees were discarded from the analysis and the posterior probability (pp) values (Rannala & Yang 1996) were determined from the consensus tree using the remaining 7500 trees. A pp value ≥ 0.95 was considered significant. The ML analysis was performed using RAxML v. 8.2 (Stamatakis 2014), support for the internal branches was assessed by a search of 1000 bootstrapped sets of data (Sandoval-Denis *et al.* 2016). A bootstrap support (bs) of ≥ 70 % was considered significant. Phylogenetic trees were plotted using FigTree v. 1.4.4 (Rambaut 2018) and edited using InkScape v. 1.3.2. Sequences of different gene regions were concatenated using Mesquite v. 3.61 (Maddison & Maddison 2019) considering the Genealogical Concordance Phylogenetic Species Recognition (GCPSR) (Taylor *et al.* 2000).

RESULTS

In total, 70 specimens were obtained, representing five species and four genera of *Hypocreales* (order *Sordariomycetes*, *Ascomycota*). Of all specimens obtained, approximately 85.7 % belong to the *Niessliaceae* ("*Acremonium*"), 10 % to *Nectriaceae* (*Fusarium* and *Fusicolla*) and 4.3 % to *Ophiocordycipitaceae* (*Purpureocillium*). *Acremonium cavaraeanum* showed the highest constancy in the stromata of *Camarotella* spp. (C = 80 %) followed by *Fusicolla parasitica sp. nov.* (C = 60 %). The species *Purpureocillium lilacinum* and *Fusarium pseudocircinatum* obtained C = 40 %, while *Fusarium caatingaense* C = 20 %.

© 2025 Westerdijk Fungal Biodiversity Institute

Phylogenetic analysis of *Acremonium* was conducted using a single locus dataset (Table 1) which provided sufficient resolution for species identification when integrated with morphological characterization of the structures and colony. The final alignment included 30 sequences, representing 13 taxa, with *Nothoacremonium subcylindricum* (CBS 41668, ex-type) as the outgroup, and comprised 735 bp. For the *Fusarium fujikuroi* species complex (FFSC) and *Fusarium incarnatum-equiseti* species complex (FIESC), the concatenated analysis of two loci datasets (Table 1) enclosed, respectively, 221 / 123 sequences representing 63 / 40 taxa, including *Fusarium triceptatum* (CBS 25850, ex-type) and *Fusarium concolor* (IMI 296456, ex-type) as the outgroup, consisting of 1438 / 1544 bp (*TEF-1α* 617 / 653 bp and *RPB2* 821 / 891 bp). For *Fusicolla*, the final combined analysis of four mentioned loci datasets (Table 1) encompassed, respectively, 98 sequences representing 25 taxa, including *Macroconia leptosphaeriae* (CBS 100001) as the outgroup, and comprised 2590 bp (ITS 514 bp, LSU 736 bp, *RPB2* 779 bp and *TUB2* 561 bp). The final alignment, for *Purpureocillium*, included 32 sequences, representing six taxa and three loci (Table 1), with *Drechmeria zeospora* (CBS 33580, ex-type) as the outgroup, and comprised 2211 bp (*ITS* 497 bp, *LSU* 809 bp and *TEF-1α* 905 bp). The phylogenetic analysis revealed a taxonomic novelty for *Fusicolla*.

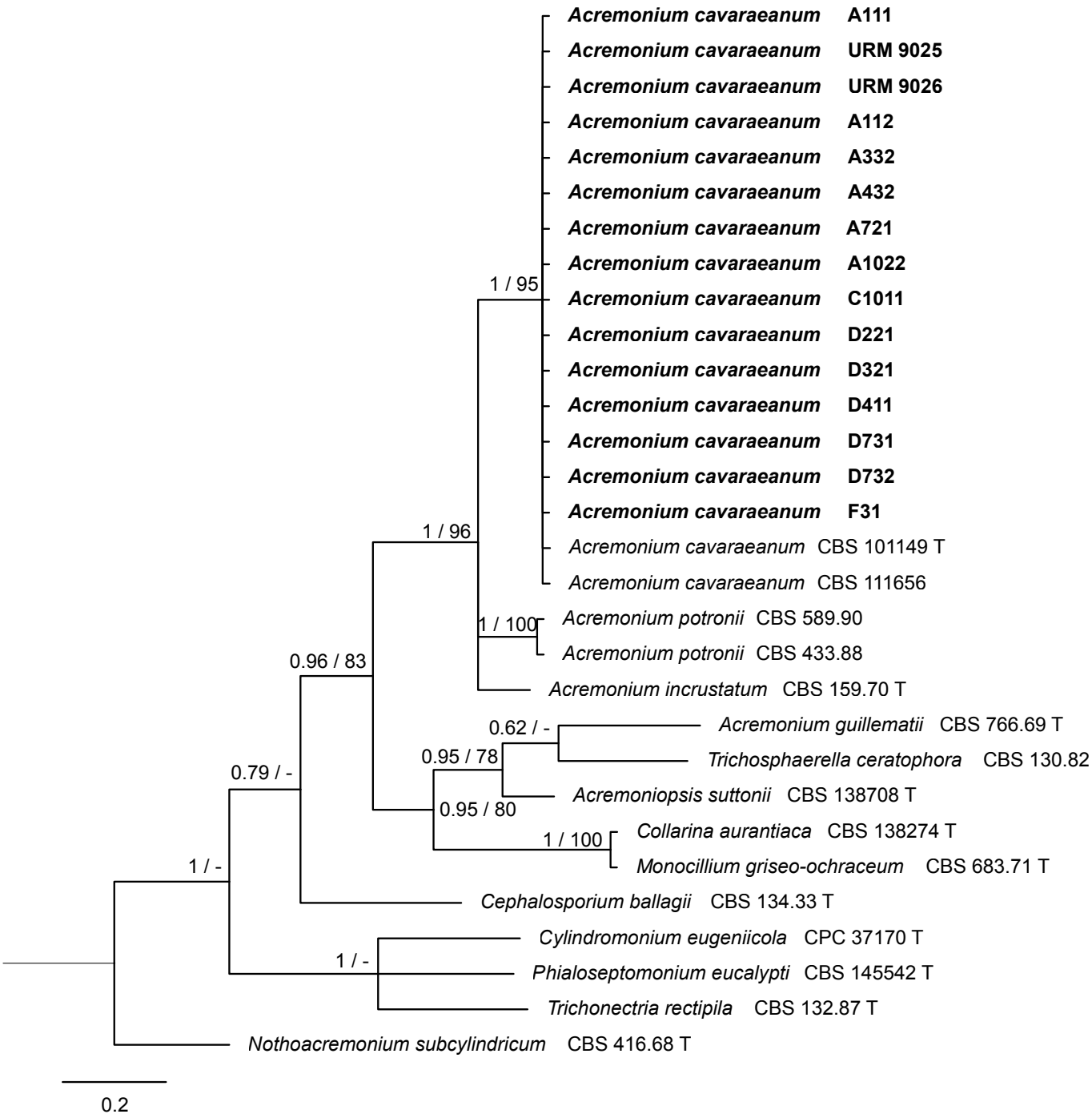

Fig. 2. Phylogenetic tree inferred from a Bayesian and Maximum Likelihood analysis based on alignment of LSU sequences. Posterior probabilities (pp) and bootstrap (bs) are given at the nodes (pp/bs). The scale bar represents the expected number of changes per site. Strains representing the ex-type was indicated with "T" after the accession number. Species in this study are highlighted in **bold**.

© 2025 Westerdijk Fungal Biodiversity Institute

Table. 2. List of *Fusarium fujikuroi* species complex species containing the culture accession code, GenBank accession number for the gene regions, hosts and countries. Isolates and sequences generated in this work are shown in **bold**. Ex-type cultures have been marked with a "T" in the culture accession code.

Species	Culture accession	Host/substrate	Country	Gene Region		Reference
				TEF	*RPB2*	
Fusarium acutatum	CBS 402.97 **T**	Environmental	India	MW402125	MW402768	Yilmaz *et al.* (2021)
	CBS 401.97	*Cajanus cajan*	India	MW402124	MW402813	Yilmaz *et al.* (2021)
Fusarium agapanthi	NRRL 54463 **T**	*Agapanthus* sp.	—	KU900630	KU900625	Yilmaz *et al.* (2021)
	CBS 100193	*Agapanthus praecox*	New Zeland	MW401959	MW402727	Yilmaz *et al.* (2021)
Fusarium ananatum	CBS 118516 **T**	*Ananas comosus*	Netherlands	LT996091	LT996137	Yilmaz *et al.* (2021)
	CBS 118517	*Ananas comosus*	South Africa	MN533988	MN534229	Yilmaz *et al.* (2021)
Fusarium andiyazi	CBS 119857 **T**	*Sorghum bicolor* soil debris	—	MN193854	LT996138	Yilmaz *et al.* (2021)
	CBS 119856	*Sorghum* grain	Ethiopia	MN533989	MN534286	Yilmaz *et al.* (2021)
Fusarium annulatum	CBS 258.54 **T**	*Oryza sativa*	Netherlands	MT010994	MT010983	Yilmaz *et al.* (2021)
	CBS 181.30	*Zea mays*	USA	MW402102	—	Yilmaz *et al.* (2021)
Fusarium anthophilum	CBS 222.76 **T**	*Euphorbia pulcherrima* stem	Germany	MW402114	MW402811	Yilmaz *et al.* (2021)
	CBS 737.97	*Hippeastrum* sp.	Germany	MN533992	MN534234	Yilmaz *et al.* (2021)
Fusarium awaxy	LGMF 1930 **T**	Rotten stalks of *Zea mays*	Brazil	MG839004	MK766941	Yilmaz *et al.* (2021)
	CBS 139380	Corn stalk	USA	MN534058	MN534238	Yilmaz *et al.* (2021)
Fusarium bactridioides	CBS 100057 **T**	*Cronartium conigenum*	USA	MN533993	MN534235	Yilmaz *et al.* (2021)
	NRRL 20476	*Cronartium conigenum*	—	AF160290	—	Yilmaz *et al.* (2021)
Fusarium begoniae	CBS 452.97 **T**	*Begonia elatior* hybrid	Germany	MN533994	MN534243	Yilmaz *et al.* (2021)
	CBS 403.97	*Begonia elatior* hybrid	—	MN193858	MN193886	Yilmaz *et al.* (2021)
Fusarium brevicatenulatum	CBS 404.97 **T**	*Striga asiatica*	Madagascar	MN533995	MN534295	Yilmaz *et al.* (2021)
	CBS 100196	*Striga asiatica*	—	MN193859	MN193887	Yilmaz *et al.* (2021)
Fusarium bulbicola	CBS 220.76 **T**	*Nerine bowdenii* bulb	—	KF466415	MW402767	Yilmaz *et al.* (2021)
Fusarium chinhoyiense	NRRL 25221 **T**	*Zea mays*	Zimbabwe	MN534050	MN534262	Yilmaz *et al.* (2021)
	NY 001B5	Soil	—	MN534051	MN534263	Yilmaz *et al.* (2021)
Fusarium circinatum	CBS 405.97 **T**	*Pinus radiata*	USA	MN533997	MN534252	Yilmaz *et al.* (2021)
	CBS 100197	*Pinus taeda*	Georgia	MW401960	—	Yilmaz *et al.* (2021)
	CBS 117843	*Pinus radiata*	Spain	MW401978	MW402786	Yilmaz *et al.* (2021)
Fusarium coicis	NRRL 66233 **T**	*Coix gasteenii*	—	KP083251	KP083274	Yilmaz *et al.* (2021)
Fusarium concentricum	CBS 450.97 **T**	*Musa fruit*	—	AF160282	JF741086	Yilmaz *et al.* (2021)
	CBS 453.97	*Musa sapientum*	Guatemala	MN533998	MN534264	Yilmaz *et al.* (2021)
Fusarium denticulatum	CBS 407.97 **T**	*Ipomoea batatas*	USA	MN534000	MN534274	Yilmaz *et al.* (2021)

© 2025 Westerdijk Fungal Biodiversity Institute

Table. 2. (Continued).

Species	Culture accession	Host/substrate	Country	Gene Region		Reference
				TEF	*RPB2*	
Fusarium dlaminii	CBS 119860 **T**	Plant debris in soil	South Africa	MW401995	KU171701	Yilmaz *et al.* (2021)
	CBS 175.88	*Zea mays* soil	South Africa	MN534002	MN534256	Yilmaz *et al.* (2021)
	CBS 671.94	Soil	South Africa	MN534004	MN534254	Yilmaz *et al.* (2021)
Fusarium echinatum	CBS 146497 **T**	Unidentified tree	South Africa	MW834273	MW834004	Yilmaz *et al.* (2021)
Fusarium elaeagni	LC13627 **T**	*Elaeagnus pungens*	China	MW580466	MW474412	Yilmaz *et al.* (2021)
Fusarium ficicrescens	CBS 125178 **T**	Environmental	—	—	KT154002	Yilmaz *et al.* (2021)
	CBS 125177	Environmental	Iran	MN534006	MN534281	Yilmaz *et al.* (2021)
Fusarium fractiflexum	NRRL 28852 **T**	*Cymbidium* sp.	—	AF160288	LT575064	Yilmaz *et al.* (2021)
Fusarium fredkrugeri	CBS 144209 **T**	*Melhania acuminata* rhizophere	—	LT996097	LT996147	Yilmaz *et al.* (2021)
	CBS 144495	*Melhania acuminata* rhizophere	—	LT996096	LT996146	Yilmaz *et al.* (2021)
Fusarium fujikuroi	CBS 221.76 **T**	*Oryza sativa* culm	Taiwan	MN534010	KU604255	Yilmaz *et al.* (2021)
	CBS 119855	Environmental	—	MW401994	MW402735	Yilmaz *et al.* (2021)
Fusarium globosum	CBS 428.97 **T**	*Zea mays* seed	—	KF466417	KF466406	Yilmaz *et al.* (2021)
	CBS 120992	*Maize kernels*	South Africa	MW401998	MW402788	Yilmaz *et al.* (2021)
Fusarium guttiforme	CBS 409.97 **T**	*Ananas comosus*	—	MT010999	MT010967	Yilmaz *et al.* (2021)
	NRRL 22945	*Ananas comosus*	—	AF160297	JX171618	Yilmaz *et al.* (2021)
Fusarium hechiense	LC13644	*Musa nana*	China	MW580494	MW474440	Yilmaz *et al.* (2021)
	LC13645	*Musa nana*	China	MW580495	MW474441	Yilmaz *et al.* (2021)
Fusarium konzum	CBS 119849 **T**	*Sorghastrum nuttans*	—	LT996098	MW402733	Yilmaz *et al.* (2021)
	CBS 139382	—	—	MW402071	MW402804	Yilmaz *et al.* (2021)
Fusarium lactis	CBS 411.97 **T**	*Ficus carica*	—	MN193862	MN534275	Yilmaz *et al.* (2021)
	CBS 420.97	*Ficus carica*	USA	MN534015	—	Yilmaz *et al.* (2021)
Fusarium madaense	CBS 146669 **T**	*Arachis hypogaea*	Nigeria	MW402098	MW402764	Yilmaz *et al.* (2021)
	CBS 146656	*Arachis hypogaea*	Nigeria	MW402097	MW402763	Yilmaz *et al.* (2021)
Fusarium mangiferae	CBS 120994 **T**	Mango with malformation disease	Israel	MN534017	MN534271	Yilmaz *et al.* (2021)
	NRRL 25226	*Mangifera indica*	—	AF160281	HM068353	Yilmaz *et al.* (2021)
Fusarium mexicanum	NRRL 53147 **T**	*Mangifera indica*	—	GU737282	MN724973	Yilmaz *et al.* (2021)
	NRRL 53571	*Mangifera indica*	—	GU737420	—	Yilmaz *et al.* (2021)
Fusarium mundagurra	RGB5717 **T**	Soil	—	KP083256	KP083276	Yilmaz *et al.* (2021)
Fusarium musae	CBS 624.87 **T**	*Musa sapientum* fruit	Honduras	FN552086	MW402772	Yilmaz *et al.* (2021)
	NRRL 28893	*Musa* sp.	Mexico	FN552092	FN552114	Yilmaz *et al.* (2021)

© 2025 Westerdijk Fungal Biodiversity Institute

Table. 2. (Continued).

Species	Culture accession	Host/substrate	Country	Gene Region		Reference
				TEF	*RPB2*	
Fusarium napiforme	CBS 748.97 **T**	*Pennisetum typhoides*	—	MN193863	MN534291	Yilmaz *et al.* (2021)
	CBS 135139	Keratitis	—	MN534019	MN534290	Yilmaz *et al.* (2021)
Fusarium nygamai	CBS 749.97 **T**	*Sorghum bicolor* necrotic root	Australia	MW402151	EF470114	Yilmaz *et al.* (2021)
	CBS 413.97	*Oryza sativa*	Morocco	MW402127	MW402815	Yilmaz *et al.* (2021)
Fusarium ophioides	CBS 118512 **T**	*Panicum maximum*	—	MN534022	MN534303	Yilmaz *et al.* (2021)
	CBS 118510	*Panicum maximum*	—	MN534020	MN534301	Yilmaz *et al.* (2021)
Fusarium panlongense	LC13656 **T**	*Musa nana*	China	MW580510	MW474456	Yilmaz *et al.* (2021)
Fusarium parvisorum	CMW 25267 **T**	*Pinus patula*	—	KJ541060	—	Yilmaz *et al.* (2021)
Fusarium phyllophilum	CBS 216.76 **T**	*Dracaena deremensis* leaf	—	MN193864	KF466410	Yilmaz *et al.* (2021)
	CBS 246.61	Leaf spot in *Sansevieria dooneri*	Germany	MW402118	—	Yilmaz *et al.* (2021)
Fusarium pilosicola	NRRL 29124 **T**	*Bidens pilosa*	USA	MN534054	MN534247	Yilmaz *et al.* (2021)
Fusarium proliferatum	CBS 480.96 **T**	Tropical rain forest soil	Papua New Guinea	MN534059	MN534272	Yilmaz *et al.* (2021)
Fusarium pseudoanthophilum	CBS 414.97 **T**	*Zea mays*	Zimbabwe	MW402128	—	Yilmaz *et al.* (2021)
	CBS 745.97	*Zea mays*	Zimbabwe	MW402148	MW402820	Yilmaz *et al.* (2021)
Fusarium pseudocircinatum	CBS 449.97 **T**	*Solanum* sp.	—	AF160271	MN534277	Yilmaz *et al.* (2021)
	NRRL 36939	Unknown	—	MN193866	MW402779	Yilmaz *et al.* (2021)
	CBS 455.97	*Heteropsylla incisa*	Papua New Guinea	MN534029	MN534276	Yilmaz *et al.* (2021)
	URM 9022	***Camarotella* sp.**	**Brazil**	**PQ208722**	**PQ246876**	This study
	URM 9021	***Camarotella* sp.**	**Brazil**	**PQ208723**	**PQ246877**	This study
	D621	***Camarotella* sp.**	**Brazil**	**PQ208724**	**PQ246878**	This study
Fusarium pseudonygamai	CBS 417.97 **T**	*Pennisetum typhoides*	—	AF160263	MN534285	Yilmaz *et al.* (2021)
	CBS 416.97	*Pennisetum typhoides*	Nigeria	MN534030	MN534283	Yilmaz *et al.* (2021)
Fusarium ramigenum	CBS 418.97 **T**	*Ficus carica*	—	KF466423	KF466412	Yilmaz *et al.* (2021)
	CBS 526.97	*Ficus carica*	USA	MN534032	MN534292	Yilmaz *et al.* (2021)
Fusarium sacchari	CBS 223.76 **T**	*Saccharum officinarum*	India	MW402115	JX171580	Yilmaz *et al.* (2021)
	CBS 121683	Human	India	MW402002	MW402789	Yilmaz *et al.* (2021)
Fusarium secorum	NRRL 62593 **T**	*Beta vulgaris*	—	KJ189225	—	Yilmaz *et al.* (2021)
	NRRL 62594	*Beta vulgaris*	—	KJ189228	—	Yilmaz *et al.* (2021)
Fusarium siculi	CBS 142222 **T** = NRRL 27188	*Citrus sinensis*	Italy	LT746214	LT746327	Yilmaz *et al.* (2021)
	CPC 27189	*Citrus sinensis*	Italy	LT746215	LT746328	Yilmaz *et al.* (2021)

© 2025 Westerdijk Fungal Biodiversity Institute

Table. 2. (Continued).

Species	Culture accession	Host/substrate	Country	Gene Region		Reference
				TEF	*RPB2*	
Fusarium sterilihyposum	NRRL 25623 **T**	Mango	—	MN193869	MN193897	Yilmaz *et al.* (2021)
	NRRL 53991	*Mangifera indica*	—	GU737413	—	Yilmaz *et al.* (2021)
Fusarium subglutinans	CBS 747.97 **T**	*Zea mays*	USA	MW402150	MW402773	Yilmaz *et al.* (2021)
	CBS 215.76	*Zea mays*	Germany	MN534061	MN534241	Yilmaz *et al.* (2021)
Fusarium succisae	CBS 219.76 **T**	*Succisa pratensis* flower	—	AF160291	MW402766	Yilmaz *et al.* (2021)
	CBS 187.34	*Zostera marina*	UK	MW402109	MW402810	Yilmaz *et al.* (2021)
Fusarium sudanense	CBS 454.97 **T**	*Striga hermonthica*	Sudan	MN534037	MN534278	Yilmaz *et al.* (2021)
	CBS 675.94	*Striga hermonthica*	Sudan	MN534038	MN534279	Yilmaz *et al.* (2021)
Fusarium temperatum	MUCL 52463 **T**	*Zea mays*	Belgium	—	MW402776	Yilmaz *et al.* (2021)
	CBS 135539	Pulmonary infection (Human)	Mexico	MN534040	MN534242	Yilmaz *et al.* (2021)
Fusarium terricola	CBS 483.94 **T**	Soil	Australia	MN534042	LT996156	Yilmaz *et al.* (2021)
	CBS 119850	Soil	Australia	MN534041	MN534280	Yilmaz *et al.* (2021)
Fusarium thapsinum	CBS 776.96 **T**	Unknown	—	MN534044	MN534289	Yilmaz *et al.* (2021)
	CBS 539.79	Man, white grained mycetoma	Italy	MW402140	MW402818	Yilmaz *et al.* (2021)
Fusarium tjaetaba	NRRL 66243 **T**	*Sorghum interjectum*	—	KP083263	KP083275	Yilmaz *et al.* (2021)
Fusarium triseptatum	CBS 258.50 **T**	*Ipomoea batatas*	USA	MH484964	MH484873	Yilmaz *et al.* (2021)
Fusarium tupiense	NRRL 53984 **T**	*Mangifera indica*	—	GU737404	LR792619	Yilmaz *et al.* (2021)
	NRRL 53996	*Mangifera indica*	Brazil	DQ452860	—	Yilmaz *et al.* (2021)
Fusarium udum	NRRL 25199 **T**	*Cajanus cajan*	—	KY498862	KY498875	Yilmaz *et al.* (2021)
	CBS 747.79	*Cajanus cajan*	—	MN193872	MN534258	Yilmaz *et al.* (2021)
Fusarium verticillioides	CBS 218.76 **T**	*Zea mays* stem	Germany	MW402113	—	Yilmaz *et al.* (2021)
	CBS 447.95	Asparagus	—	MW402133	MW402770	Yilmaz *et al.* (2021)
	CBS 531.95	*Zea mays*	—	MW402136	MW402771	Yilmaz *et al.* (2021)
Fusarium volatile	CBS 143874 **T**	Human bronchoalveolar lavage fluid	French Guiana	LR596007	LR596006	Yilmaz *et al.* (2021)
	NRRL 25615	*Oryza sativa* seed	—	AF160304	—	Yilmaz *et al.* (2021)
Fusarium werrikimbe	CBS 125535 **T**	*Sorghum leiocladum*	Australia	—	MN534304	Yilmaz *et al.* (2021)
Fusarium xyrophilum	NRRL 62721 **T**	*Xyris* spp.	—	MN193877	MN193905	Yilmaz *et al.* (2021)
	NRRL 66890	*Xyris* spp.	—	MN193876	MN193904	Yilmaz *et al.* (2021)

© 2025 Westerdijk Fungal Biodiversity Institute

Table. 3. List of *Acremonium* species containing the culture accession code, GenBank accession number for the gene regions, hosts and countries. Isolates and sequences generated in this work are shown in **bold**. Ex-type cultures have been marked with a "T" in the culture accession code.

Species	Culture accession	Host/substrate	Country	Gene Region	Reference
				LSU	
Acremoniopsis suttonii	CBS 138708 **T**	Forest soil	Spain	MH877666	Hou *et al.* (2023)
Acremonium cavaraeanum	CBS 101149 **T**	Outer wall of wooden house	Japan	HF680202	Li *et al.* (2022)
	CBS 111656	On lesions of "big verrucoses" (Lixa grande) disease caused by *Sphaerodothis acrocomiae*	Brazil	HF680203	Li *et al.* (2022)
	URM 9026	***Camarotella* sp.**	**Brazil**	**PQ196626**	This study
	URM 9025	***Camarotella* sp.**	**Brazil**	**PQ196625**	This study
	A111	***Camarotella* sp.**	**Brazil**	**PQ196624**	This study
	A112	***Camarotella* sp.**	**Brazil**	**PQ196627**	This study
	A332	***Camarotella* sp.**	**Brazil**	**PQ196628**	This study
	A432	***Camarotella* sp.**	**Brazil**	**PQ196629**	This study
	A721	***Camarotella* sp.**	**Brazil**	**PQ196630**	This study
	A1022	***Camarotella* sp.**	**Brazil**	**PQ196631**	This study
	C1011	***Camarotella* sp.**	**Brazil**	**PQ196632**	This study
	D221	***Camarotella* sp.**	**Brazil**	**PQ196633**	This study
	D321	***Camarotella* sp.**	**Brazil**	**PQ196634**	This study
	D411	***Camarotella* sp.**	**Brazil**	**PQ196635**	This study
	D731	***Camarotella* sp.**	**Brazil**	**PQ196636**	This study
	D732	***Camarotella* sp.**	**Brazil**	**PQ196637**	This study
	F31	***Camarotella* sp.**	**Brazil**	**PQ196638**	This study
Acremonium guillematii	CBS 766.69 **T**	Field soil	France	OQ055384	Hou *et al.* (2023)
Acremonium incrustatum	CBS 159.70 **T**	Rhizomorph of *Armillaria mellea*	Netherlands	OQ055385	Hou *et al.* (2023)
Acremonium potronii	CBS 589.90	Decaying wood	Germany	OQ055393	Hou *et al.* (2023)
	CBS 433.88	Gymnosperm forest soil	USA	HQ232098	Hou *et al.* (2023)
Cephalosporium ballagii	CBS 134.33 **T**	Nodular lymphangitis of man arm	—	OQ055427	Hou *et al.* (2023)
Collarina aurantiaca	CBS 138274 **T**	River sediments	Spain	OR052104	Hou *et al.* (2023)
Cylindromonium eugeniicola	CPC 37170 **T**	*Eugenia capensis*	South Africa	MN567649	Hou *et al.* (2023)
Monocillium griseo-ochraceum	CBS 683.71 **T**	Agricultural soil	Netherlands	MG826825	Hou *et al.* (2023)
Nothoacremonium subcylindricum	CBS 416.68 **T**	Skin and nail of man	Netherlands	OQ055648	Hou *et al.* (2023)
Phialoseptomonium eucalypti	CBS 145542 **T**	Leaves of *Eucalyptus grandis* x *camaldulensis* clone	Australia	NG_067890	Hou *et al.* (2023)
Trichonectria rectipila	CBS 132.87 **T**	*Sphaeriaceae*, on *Diatrype stigma*	USA	NG_064146	Hou *et al.* (2023)
Trichosphaerella ceratophora	CBS 130.82	*Carpinus betulus*	Switzerland	KM231727	Hou *et al.* (2023)

© 2025 Westerdijk Fungal Biodiversity Institute

Table. 4. List of *Fusicolla* species containing the culture accession code, GenBank accession number for the gene regions, hosts and countries. Isolates and sequences generated in this work are shown in **bold**. Ex-type cultures have been marked with a "T" in the culture accession code.

Species	Culture accession	Host/substrate	Country	Gene Region				Reference
				ITS	LSU	*RPB2*	*TUB2*	
Fusicolla acetilerea	BBA 63789 **T**	Polluted soil	Japan	HQ897790	U88108	HQ897701	—	Crous *et al.* (2022)
Fusicolla aeria	CGMCC 3.24908 **T**	Rotten twig	China	OQ128334	OQ128338	OQ134111	OQ134100	Zeng & Zhuang (2023)
Fusicolla aquaeductuum	CBS 837.85 **T**	Plug in water tap	Germany	KM231823	KM231699	HQ897744	KM232094	Craus *et al.* (2022), Zeng & Zhuang (2023)
	CBS 268.53	Rubber tubing	Netherlands	MH857190	MH868728	—	—	Crous *et al.* (2022)
Fusicolla betae	BBA 64317 **T**	*Triticum aestivum*	Germany	—	—	HQ897781	—	Crous *et al.* (2022)
Fusicolla bharatavarshae	NFCCI 4423 **T**	*Avicennia marina*	India	MK152510	MK152511	MK157022	MK376462	Crous *et al.* (2022)
Fusicolla cassiae-fistulae	MFLUCC 19-0318 **T**	*Cassia fistula*	Thailand	MT215497	MT215549	—	—	Crous *et al.* (2022)
Fusicolla coralloidea	CGMCC 3.24907 **T**	Twig associated with other fungi	China	OQ128333	OQ128337	OQ134110	OQ134099	Zeng & Zhuang (2023)
Fusicolla elongata	CBS 148934 **T**	Soil	Zimbabwe	ON763203	ON763200	ON759297	ON745628	Crous *et al.* (2022)
	CBS 148935	Soil	Zimbabwe	ON763204	ON763201	ON759298	ON745629	Crous *et al.* (2022)
Fusicolla epistroma	BBA 62201 **T**	*Diatrypella* sp., on *Betula* sp.	UK	—	AF228352	HQ897765	—	Crous *et al.* (2022)
Fusicolla filiformis	CGMCC 3.24910 **T**	Rotten twig	China	OQ128332	OQ128336	OQ134109	OQ134098	Zeng & Zhuang (2023)
Fusicolla gigantispora	MFLU 16-1206 **T**	*Avicennia marina*	Thailand	MN047104	MN017869	—	—	Zeng & Zhuang (2023)
	HKAS 101990	*Bruguiera* sp.	Thailand	MN047106	MN017870	—	—	Crous *et al.* (2022)
Fusicolla gigas	CGMCC 3.20680 **T**	Soil	China	OK465362	OK465449	—	—	Crous *et al.* (2022)
Fusicolla guangxiensis	CGMCC 3.20679 **T**	Rotten twig	China	OK465363	OK465450	—	—	Crous *et al.* (2022)
Fusicolla hughesii	NFCCI 4234 **T**	Air	India	MG779450	MG779452	—	—	Zeng & Zhuang (2023)
Fusicolla matuoi	CBS 581.78 **T**	*Albizzia julibrissin*	Japan	KM231822	KM231698	HQ897720	KM232093	Crous *et al.* (2022)
Fusicolla melogrammae	CBS 141092 **T**	*Melogramma campylosporum* on *Carpinus* sp.	UK	KX897140	KY092489	—	MW834305	Crous *et al.* (2022)
Fusicolla meniscoidea	CBS 110189 **T**	Soil	Australia	MW827613	MW827654	MW834010	MW834306	Crous *et al.* (2022)
Fusicolla merismoides	CBS 186.34 **T**	*Acer* sp.	Germany	MH855482	MH866963	—	—	Crous *et al.* (2022)
Fusicolla ossicola	CBS 140161 **T**	Bone of wild boar	Belgium	MF628022	MF628021	MW834011	MW834307	Crous *et al.* (2022)
Fusicolla parasitica sp.nov.	**URM 9019 T**	***Camarotella sp.***	**Brazil**	**PQ200508**	**PP971547**	**PQ208717**	**PQ246874**	This study
	URM 9018	***Camarotella sp.***	**Brazil**	**PQ200507**	**PP971546**	**PQ208716**	**PQ246873**	This study
	URM 9017	***Camarotella sp.***	**Brazil**	**PQ200509**	**PP971548**	**PQ208718**	**PQ246875**	This study
Fusicolla quarantenae	CBS 141541 **T**	*Melocactus zehntneri*	Brazil	MW553789	MW553788	MW556626	MW556624	Crous *et al.* (2022)
Fusicolla septimanifiniscientiae	CBS 144935 **T**	Soil	Netherlands	MK069422	MK069418	—	MK069408	Crous *et al.* (2022)

© 2025 Westerdijk Fungal Biodiversity Institute

Table. 4. (Continued).

Species	Culture accession	Host/substrate	Country	Gene Region				Reference
				ITS	LSU	*RPB2*	*TUB2*	
Fusicolla siamensi	MFLUCC 17-2577 **T**	*Cassia fistula*	Thailand	NR171300	NG073863	—	—	Zeng & Zhuang (2023)
Fusicolla sporellula	CBS 110191 **T**	Soil	South Africa	MW827614	MW827655	MW834012	MW834308	Crous *et al.* (2022)
Fusicolla violacea	CBS 634.76 **T**	*Quadraspidiotus perniciosus*	Iran	KM231824	KM231700	HQ897696	KM232095	Zeng & Zhuang (2023)
Macroconia leptosphaeriae	CBS 100001	*Leptosphaeria* sp.	Netherlands	HQ897810	KM231705	HQ728164	KM232097	Crous *et al.* (2022)

Table. 5. List of *Fusarium incarnatum-equiseti* species complex species containing the culture accession code, GenBank accession number for the gene regions, hosts and countries. Isolates and sequences generated in this work are shown in **bold**. Ex-type cultures have been marked with a "T" in the culture accession code.

Species	Culture accession	Host/substrate	Country	Gene Region		Reference
				TEF	*RPB2*	
Fusarium aberrans	CBS 131385 **T**	*Oryza australiensis*	*Australia*	MN170445	MN170378	Xia *et al.* (2019)
	CBS 131387	*Oryza australiensis*	Australia	MN170446	MN170379	Xia *et al.* (2019)
Fusarium brevicaudatum	NRRL 43638 **T**	*Trichechus* sp.	USA	GQ505665	GQ505843	Xia *et al.* (2019)
	NRRL 43694	Human eye	USA	GQ505668	GQ505846	Xia *et al.* (2019)
Fusarium bubalinum	NRRL 26918 **T**	Unknown	Australia	MN170448	MN170381	Xia *et al.* (2019)
Fusarium caatingaense	CBS 976.97	*Juniper chinensis*	USA	MN170449	MN170382	Xia *et al.* (2019)
	URM 9020	***Camarotella sp.***	**Brazil**	**PQ208725**	**PQ208726**	This study
Fusarium camptoceras	IMI 112500 **T**	*Theobroma cacao*	Costa Rica	MN170450	MN170383	Xia *et al.* (2019)
Fusarium cateniforme	ATCC 11853 **T**	Unknown	—	MN170451	MN170384	Xia *et al.* (2019)
Fusarium citri	CGMCC 3.19467 **T**	Unknown	China	MK289617	—	Tan & Shivas (2023)
	CBS 621.87	*Medicago sativa*	Denmark	MN170452	MN170385	Xia *et al.* (2019)
Fusarium clavum	CBS 126202 **T**	Soil	Namibia	MN170456	MN170389	Xia *et al.* (2019)
	CBS 131255	*Leucopoa sclerophylla*	Iran	MN170460	MN170393	Xia *et al.* (2019)
Fusarium coffeatum	CBS 635.76 **T**	*Cynodon lemfuensis*	South Africa	MN120755	MN120736	Xia *et al.* (2019)
	CBS 430.81	Grave stone	Romania	MN120756	MN120737	Xia *et al.* (2019)
Fusarium compactum	NRRL 36323 **T**	Cotton yarn	UK	GQ505648	GQ505826	Xia *et al.* (2019)
	CBS 185.31	Unknown	—	GQ505646	GQ505824	Xia *et al.* (2019)
Fusarium concolor	IMI 296456 **T**	Plant debris	South Africa	GQ505674	GQ505852	Xia *et al.* (2019)
Fusarium croceum	CBS 131777 **T**	*Triticum* sp.	Iran	MN170463	MN170396	Xia *et al.* (2019)

© 2025 Westerdijk Fungal Biodiversity Institute

Table. 5. (Continued).

Species	Culture accession	Host/substrate	Country	Gene Region		Reference
				TEF	*RPB2*	
	CBS 131788	*Triticum* sp.	Iran	MN170464	MN170397	Xia *et al.* (2019)
Fusarium duofalcatisporum	NRRL 36448 **T**	*Phaseolus vulgaris*	Sudan	GQ505652	GQ505830	Xia *et al.* (2019)
	CBS 264.50	*Gossypium hirsutum*	Mozambique	GQ505651	GQ505829	Xia *et al.* (2019)
Fusarium equiseti	CBS 307.94 **T**	Soil	Germany	GQ505599	GQ505777	Xia *et al.* (2019)
	CBS 185.34	Soil	Netherlands	MN170466	MN170399	Xia *et al.* (2019)
Fusarium fasciculatum	CBS 131382 **T**	*Oryza australiensis*	Australia	MN170473	MN170406	Xia *et al.* (2019)
	CBS 131383	*Oryza australiensis*	Australia	MN170474	MN170407	Xia *et al.* (2019)
Fusarium flagelliforme	NRRL 36269 **T**	*Pinus nigra*	Croatia	GQ505645	GQ505823	Xia *et al.* (2019)
	NRRL 31011	*Thuja* sp.	Germany	GQ505606	GQ505784	Xia *et al.* (2019)
Fusarium goeppertmayerae	BRIP 64547d **T**	Unknown	Australia	OQ626868	—	Tan & Shivas (2023)
Fusarium gracilipes	NRRL 43635 **T**	Horse	USA	GQ505662	GQ505840	Xia *et al.* (2019)
Fusarium guilinense	CGMCC 3.19495 **T**	*Musa nana*	China	MK289594	—	Tan & Shivas (2023)
	NRRL 13335	Alfalfa	Australia	GQ505590	GQ505768	Xia *et al.* (2019)
Fusarium humuli	CGMCC 3.19374 **T**	*Humulus scandens*	China	MK289570	—	Tan & Shivas (2023)
	LC 4490	*Osmanthus* sp.	China	MK289614	MK289767	Xia *et al.* (2019)
Fusarium incarnatum	NRRL 25478 **T**	*Trichosanthes dioica*	Malawi	MN170476	MN170409	Xia *et al.* (2019)
	CBS 132907	*Triticum* sp.	Iran	MN170477	MN170410	Xia *et al.* (2019)
Fusarium irregulare	CGMCC 3.19489 **T**	Unknown	China	MK289629	—	Tan & Shivas (2023)
	NRRL 32175	Human sputum	USA	GQ505609	GQ505787	Xia *et al.* (2019)
Fusarium lacertarum	IMI 300797 **T**	Lizard skin	India	GQ505593	GQ505771	Xia *et al.* (2019)
	CBS 102300	Unknown	—	GQ505643	GQ505821	Xia *et al.* (2019)
Fusarium longicaudatum	NRRL 25477 **T**	Unknown	Tanzania	MN170481	MN170414	Xia *et al.* (2019)
Fusarium luffae	CGMCC 3.19497 **T**	*Luffa aegyptiaca*	China	MK289601	—	Tan & Shivas (2023)
	CBS 131097	*Setaria verticilata*	Iran	MN170482	MN170415	Xia *et al.* (2019)
Fusarium makinsoniae	BRIP 64547a **T**	*Zea mays*	Australia	OQ626867	—	Tan & Shivas (2023)
	BRIP 64420g	*Vigna radiata*	Australia	OQ626866	—	Tan & Shivas (2023)
Fusarium mucidum	CBS 102395 **T**	*Anacardium occidentale*	El Salvador	MN170485	MN170418	Xia *et al.* (2019)
	CBS 102394	*Anacardium occidentale*	El Salvador	MN170484	MN170417	Xia *et al.* (2019)
Fusarium multiceps	NRRL 43639 **T**	*Trichechus* sp.	USA	GQ505666	GQ505844	Xia *et al.* (2019)

© 2025 Westerdijk Fungal Biodiversity Institute

Table. 5. (Continued).

Species	Culture accession	Host/substrate	Country	Gene Region		Reference
				TEF	***RPB2***	
Fusarium nanum	CGMCC 3.19498	*Musa nana*	China	MK289602	—	Tan & Shivas (2023)
	CBS 131781	*Triticum* sp.	Iran	MN170487	MN170420	Xia *et al.* (2019)
Fusarium neoscirpi	NRRL 26922 **T**	Soil	France	GQ505601	GQ505779	Xia *et al.* (2019)
Fusarium neosemitectum	CBS 189.60 **T**	*Musa sapientum*	Zaire	MN170489	MN170422	Xia *et al.* (2019)
	CBS 190.60	*Musa sapientum*	Democratic Republic of the Congo	MN170490	MN170423	Xia *et al.* (2019)
Fusarium pacificum	BRIP 60326a **T**	*Phormium tenax*	Australia	OQ626869	—	Tan & Shivas (2023)
Fusarium pernambucanum	CBS 791.70 **T**	*Musa sampientum*	—	MN170491	MN170424	Xia *et al.* (2019)
	CBS 132194	Human finger nail	Thailand	MN170492	MN170425	Xia *et al.* (2019)
Fusarium persicinum	CBS 479.83 **T**	Unknown	Iran	MN170496	MN170429	Xia *et al.* (2019)
	CBS 131780	*Triticum* sp.	Iran	MN170497	MN170430	Xia *et al.* (2019)
Fusarium ruthhalliae	BRIP 72406h **T**	*Sorghum* sp.	Australia	OP627085	—	Xia *et al.* (2019)
Fusarium scirpi	NRRL 36478 **T**	Pasture soil	Australia	GQ505654	GQ505832	Xia *et al.* (2019)
	CBS 448.84	Pasture soil	Australia	MN170498	MN170431	Xia *et al.* (2019)
Fusarium serpentinum	CBS 119880 **T**	Unknown	—	MN170499	MN170432	Xia *et al.* (2019)
Fusarium sulawesiense	NRRL 43730 **T**	Contact lens	USA	EF453042	GQ505847	Xia *et al.* (2019)
Fusarium tanahbumbuense	NRRL 34005 **T**	Human, intravitreal fluid of the eye	USA	GQ505629	GQ505807	Xia *et al.* (2019)
	CBS 131009	*Triticum* sp.	Iran	MN170506	MN170439	Xia *et al.* (2019)
Fusarium toxicum	NRRL 25796 **T**	Soil	Germany	MN170508	MN170441	Xia *et al.* (2019)
	CBS 130385	Dog	USA	MN170509	MN170442	Xia *et al.* (2019)

© 2025 Westerdijk Fungal Biodiversity Institute

Table. 6. List of *Purpureocillium* species containing the culture accession code, GenBank accession number for the gene regions, hosts and countries. Isolates and sequences generated in this work are shown in **bold**. Ex-type cultures have been marked with a "T" in the culture accession code.

Species	Culture accession	Host/substrate	Country	Gene Region			Reference
				ITS	*LSU*	*TEF-1α*	
Drechmeria zeospora	CBS 335.80 **T**	Nematode in soil	Iraq	NR_155046	NG_063928.1	EF469062	Araújo *et al.* (2022)
Purpureocillium atypicola	CBS 744.73	*Araneae*	Japan	GU980041	EF468841	EF468786	Araújo *et al.* (2022)
Purpureocillium lavendulum	FMR 10376 **T**	Soil	Venezuela	FR734106	FR775489	FR775516	Bali *et al.* (2022)
Purpureocillium lilacinum	CBS 284.36 **T**	Soil	USA	FR734101	FR775484	EF468792	Araújo *et al.* (2022), Sung *et al.* (2007)
	CBS 431.87	*Meloidogyne* sp., egg mass	Philippines	AY624188	EF468844	EF468791	Bali *et al.* (2022)
	URM 9023	***Camarotella sp.***	**Brazil**	**PQ200225**	**PQ200228**	**PQ208719**	This study
	URM 9024	***Camarotella sp.***	**Brazil**	**PQ200226**	**PQ200229**	**PQ208720**	This study
	D512	***Camarotella sp.***	**Brazil**	**PQ200227**	**PQ200230**	**PQ208721**	This study
Purpureocillium roseum	IOM 325363.1	Keratitis	Mexico	MT560195	MT560197	—	Calvillo-Medina *et al.* (2020)
Purpureocillium takamizusanense	NBRC 100742 **T**	*Hyalessa maculaticollis*	Japan	LC008197	—	LC008333	Araújo *et al.* (2022)
	TCTeb01	*Tessaratoma papillosa*	Taiwan	MK592777	MK598823	—	Araújo *et al.* (2022)

Taxonomy

Acremonium cavaraeanum (Jasevoli) W. Gams, *Cephalosporium-artige Schimmelpilze*: 65. 1971. Fig. 2 [60 specimens; A = 85 %; C = 80 %].
Basionym: *Fusidium cavaraeanum* Jasevoli, *Bull. Orto Bot. Regia Univ. Napoli*: 228. 1924.

Colonies on PDA showing radial mycelial growth of 1.5 cm in 7 d at 27 °C. Colony colouration ranging from pale yellow to pale purple and white to pale luteous at margin; pale orange-yellow exudation; reverse rosy vinaceous, with the pigment diffusing through the agar. *Aerial mycelium*, velvety, close to the medium, slow-growing and dense. *Hyphae* hyaline, thin walled, 2 µm wide. Abundant *sporulation*. *Phialides* orthotropic, solitary, straight, erect on the hyphae, (17.5–)18–30(–30.5) µm long. *Conidia* aseptate, cohering in long chains, fusiform to ellipsoid, smooth-walled, (3.2–)3.4–3.8(–4.0) × (1.2–)1.3–1.8(–1.9) µm.

Materials examined: **Brazil**, Pernambuco, Bonito, private property, 8°28'12"S, 35°43'44"W, 444 m asl., on *Camarotella torrendiella* and *C. acrocromiae* on living leaves of *Cocos nucifera*, 12 Feb. 2022, *C.E.V.A. Sá*, culture URM 9026; Pernambuco, Goiana, Intituto de Pesquisa Agronômica (IPA), 7°33'46"S, 35°00'47"O, 103 m a.s.l., on *C. torrendiella* and *C. acrocromiae* on living leaves of *C. nucifera*, 21 Jun. 2022, *C.E.V.A. Sá*, culture URM 9025; Pernambuco, Paudalho, private property, 7°95'77"S, 35°10'68"W, 101 m a.s.l., on *C. torrendiella* and *C. acrocromiae* on living leaves of *C. nucifera*, 10 Jun. 2023, *C.E.V.A. Sá*, culture C511; Paraíba, Camaratuba, private property, 6°38'29"S, 35°07'21.6"W, 105 m a.s.l., on *C. torrendiella* and *C. acrocromiae* on living leaves of *Cocos nucifera*, 27 Aug. 2023, *C.E.V.A. Sá*, culture D1011.

Notes: This species has previously been reported by Ito *et al.* (2000) on human sputum in the Netherlands and on an outer wall of a wooden house in Japan. In Brazil, this species was reported and classified by Warwick in 2007 as a hyperparasitic species of *Camarotella acrocomiae* on live coconut leaves. In 2013, Todaro *et al.* rediscovered the species in *Camarotella* sp. stromata on coconut palms, as well as reporting for the first time the antibacterial potential of the species.

Fusarium caatingaense A.C.S. Santos *et al.*, *Mycologia* **111**: 248. 2019. Fig. 3 [one specimen; A = 1.42 %; C = 20 %].

Colonies on PDA showing radial mycelial growth of 4.3 cm in 7 d at 27 °C in the dark. Well-defined colony margin, slightly undulated. Colony colouration ranging luteous white at middle and margin, buff to honey to cinnamon in the centre; reverse white to brownish. *Aerial mycelium*, fast-growing dense and sparse to abundant. Hyaline *hyphae*; no conidia or conidiophores present. On SNA: high intensity *sporulation*. Free *conidiophores* reduced to short conidiogenous cells, (6.0–)6.25–18.75(–19.0) µm tall, or long, branched sympodially, (80.0–)82.45–106.0(–106.25) µm. *Macroconidia* slightly curved to short-clavate, smooth-walled, 0–2-septate: (10.0–)12.5–15.62(–16.0) × (1.5–)1.8–2.5(–2.8) µm; obovoid conidia lacking septa, (5.6–)5.8–6.25(–6.87) × (1.8–)1.9–2.0(–2.5) µm.

© 2025 Westerdijk Fungal Biodiversity Institute

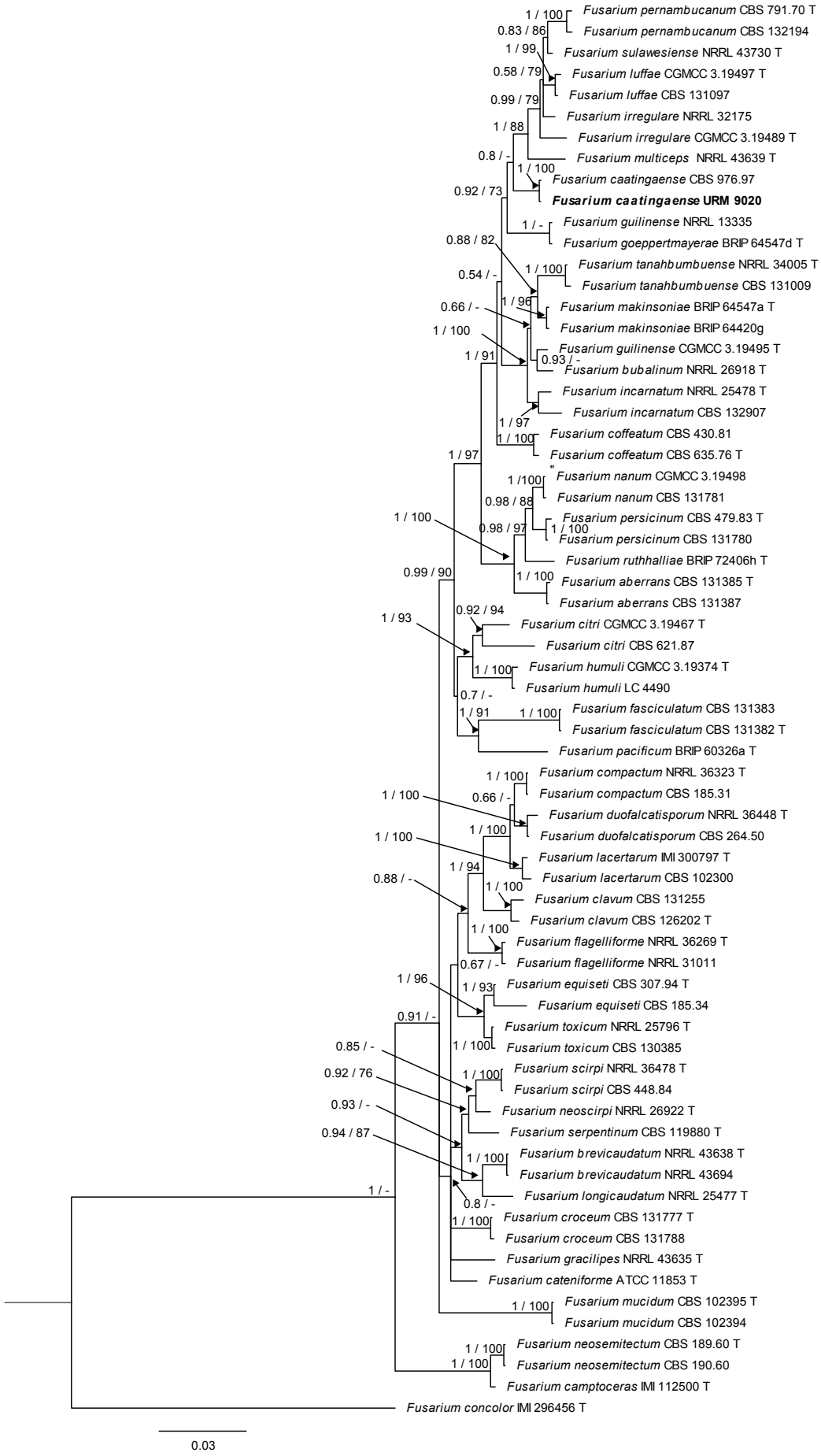

Fig. 3. Multilocus phylogenetic tree inferred from a Bayesian and Maximum Likelihood analysis based on a concatenated alignment of *RPB2* and *TEF-1α* sequences. Posterior probabilities (pp) and bootstrap (bs) are given at the nodes (pp/bs). The scale bar represents the expected number of changes per site Strains representing the ex-type was indicated with "T" after the accession number. Specimens in this study are highlighted in bold.

© 2025 Westerdijk Fungal Biodiversity Institute

Material examined: **Brazil**, Pernambuco, Bonito, private property, 8°28'12"S, 35°43'44"W, 444 m a.s.l., on *Camarotella torrendiella* and *C. acrocromiae* on living leaves of *Cocos nucifera*, 12 Feb. 2022, *C.E.V.A. Sá*, culture URM 9020.

Notes: Recorded in 2019 by Santos *et al.*, this species has a poorly known distribution, but has already been reported on *Dactylopius opuntiae* in Brazil (Santos *et al.* 2019, Diniz *et al.* 2020) and on *Ipomoea batatas* (sweet potato) in Brazil (Mello *et al.* 2024).

Fusarium pseudocircinatum O'Donnell & Nirenberg, *Mycologia* **90**: 448. 1998. Fig. 4. [three specimens; A = 4.28 %; C = 40 %].

Colonies on PDA showing radial mycelial growth of 4 cm in 7 d at 27 °C. Colony colouration ranging from pale orange to pale luteous with regular edge; reverse white. *Aerial mycelium*, sometimes producing orange pigments, floccose, fast-growing and dense. Hyaline *hyphae*; no conidiophores or conidia present. On SNA: low intensity *sporulation*. *Monophialides*, cylindrical, erect on the hyphae, 22 µm. *Macroconidia* slightly falcate, smooth-walled, 3–6-septate, (3.0–)3.2–3.4(–3.6) × (30–)31–32(–33) µm; oval *microconidia* produced in false heads on monophialides, (2.2–)2.4–3.0(–3.1) × (5.0–)5.1–5.6(–5.9) µm.

Materials examined: **Brazil**, Pernambuco, Paudalho, private property, 7°95'77"S, 35°10'68"W, 101 m a.s.l., on *Camarotella torrendiella* and *C. acrocromiae* on living leaves of *Cocos nucifera*, 10 Jun. 2023, *C.E.V.A. Sá*, culture URM 9022; Paraíba, Camaratuba, private property, 6°38'29"S, 35°07'21.6"W, 105 m a.s.l., on *C. torrendiella* and *C. acrocromiae* on living leaves of *C. nucifera*, 27 Aug. 2023, *C.E.V.A. Sá*, culture URM 9021.

Notes: Isolates of *F. pseudocircinatum* showed incongruence between the clades (Fig. 4). Considering the work of Taylor *et al.* (2000), a probable process of speciation of this species was noticeable. This species already have been recorded on different substrates as *Solanum* sp. in Ghana (Nirenberg & O'Donnell 1998), on *Pinus kesiya* (Khasia pine) in Philippines (Nirenberg & O'Donnell 1998), on textile and dead leaves in Panama (Nirenberg & O'Donnell 1998), on *Acacia koa* in Hawaii (Shiraishi *et al.* 2012), on *Mangifera indica* (mango) in Mexico (Freeman *et al.* 2014), Australia (Liew *et al.* 2016) and Dominican Republic (García-López *et al.* 2016), on *Swietenia macrophylla* (big-leaf mahogany) in Mexico (Santillán-Mendoza *et al.* 2018), on seeds of *Aspidosperma polyneuron* (pink peroba) in Brazil (Mazarotto *et al.* 2020), on *Tabebuia rosea* (rosy trumpet) in Mexico (Montoya-Martínez *et al.* 2021), on *Musa paradisiaca* (banana portalimón) in unspecified country (Calderón-Santoyo *et al.* 2022), on seeds of *Helianthus annuus* (sunflower) in Brazil (Farias *et al.* 2023).

Fusicolla parasitica C.E.V.A. Sá & A.R. Machado, ***sp. nov.*** MB 855456. Figs 5, 6. [three specimens; A = 4.28 %; C = 60 %].

Etymology: The specific epithet is derived from its parasitic habit, referring to the association between this fungus and *Camarotella* stromata.

Typus: **Brazil**, Pernambuco, Paudalho, isolated from *Camarotella torrendiella* and *C. acrocomiae* stromata in *Cocos nucifera*, Jun. 2023, *C.E.V.A. Sá* (**holotype** HURM 95613, **isotype** HURM 95614, ex-type living culture URM 9019). GenBank: ITS = PQ200508; LSU = PP971547; *RPB2* = PQ208717; *TUB2* = PQ246874.

Colonies on PDA showing radial mycelial growth of 2.5–2.6 cm in 7 d at 27 °C. Colony coloration ranging from luteous white to ochraceous with regular edge; reverse white to brownish. *Aerial mycelium*, sparce with slow-growing, sometimes producing pale orange pigments. Hyaline *hyphae*, thin-walled, 1.6–2.2 µm wide; no conidiophores or conidia present. On SNA: *sporulation* absent. On ME (liquid)+PDA: high intensity sporulation. *Sporodochia* with monophialides, cylindrical to conical, erect on the hyphae, 5–17 µm. *Macroconidia* slightly falcate to falcate, slightly hooked at one end, hyaline, smooth-walled,1–2-septate: (7.5–)12.0–22.0(–22.5) × 1–2 µm; 3–5-septate: 12.0–37.5(–40.0) × 1.0–3.0(–3.15) µm; 6–7-septate: (29.9–)30.0–37.5(–41.0) × 2.8–3.0 µm; *microconidia* absent. *Sexual morph* not observed.

Additional materials examined: **Brazil**, Pernambuco, Goiana, isolated from *C. torrendiella* and *C. acrocomiae* stromata in *C. nucifera*, Jun. 2022, *C.E.V.A. Sá*, culture URM 9017, GenBank: ITS = PQ200509; LSU = PP971548; *RPB2* = PQ208718; *TUB2* = PQ246875; Pernambuco, Recife municipality, isolated from *C. torrendiella* and *C. acrocomiae* stromata in *C. nucifera*, Dec. 2022, *C.E.V.A. Sá*, culture URM 9018, GenBank: ITS = PQ200507; LSU = PP971546; *RPB2* = PQ208716; *TUB2* = PQ246873.

Notes: Concatenated phylogenetic analyses of ITS, LSU, *RPB2* and *TUB2* sequences resolved *Fusicolla parasitica* as a new species, closely related to *F. gigantispora* (Fig. 6). Despite the low support (pp = 0.66, bs = 50) observed at the node separating these two clades, a clustering with high support between different isolates of the respective taxa was noted (*F. parasitica*, pp/bs = 0.97/85; *F. gingantispora*, pp/bs = 1/100), supporting the assertion of a phylogenetic difference between the two species. This was also confirmed in individual analyses of the ITS and LSU sequences (Fig. S1), since only these two gene regions were sequenced for existing isolates of *F. gigantispora*. The individual analysis of the ITS gene distinguished *F. parasitica* (pp = 0.83) from *F. gigantispora* (pp = 1). However, individual analysis of the LSU region revealed a similar pattern to the concatenated analysis, with a posterior probability (pp) of 0.54 at the node connecting the two species into distinct clades. The three isolates of *F. parasitica* formed a single clade with a high posterior probability (pp = 0.95), while *F. gigantispora* isolates clustered together, forming a distinct clade with pp = 0.83. Furthermore, pairwise comparisons distinguished *F. parasitica* from *F. gigantispora* MFLU 16-1206 by 20 (eight gaps, 97 % identity) and seven (99 %) nucleotides and from *F. gigantispora* HKAS 10-1990 by 19 (seven gaps, 96 %) and seven (99 %) nucleotides for ITS and LSU, respectively.

Considering that *F. gigantispora* has only sequence data from two non-protein-coding regions (ITS and LSU) available, we assume that the absence of the protein-coding genes (*RPB2* and *TUB2*) resulted in the low statistical

© 2025 Westerdijk Fungal Biodiversity Institute

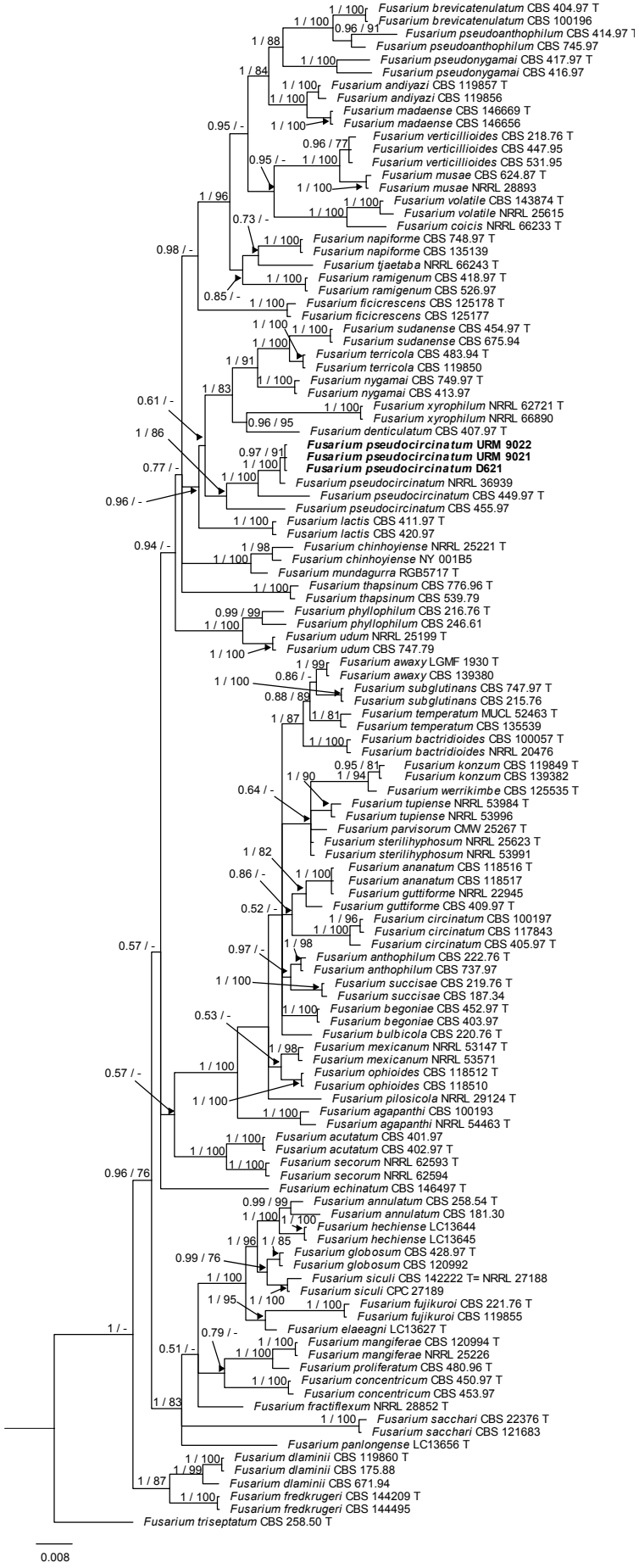

Fig. 4. Multilocus phylogenetic tree inferred from a Bayesian and Maximum Likelihood analysis based on a concatenated alignment of *RPB2* and *TEF-1α* sequences. Posterior probabilities (pp) and bootstrap (bs) are given at the nodes (pp/bs). The scale bar represents the expected number of changes per site. Strains representing the ex-type was indicated with "T" after the accession number. Species in this study are highlighted in bold.

© 2025 Westerdijk Fungal Biodiversity Institute

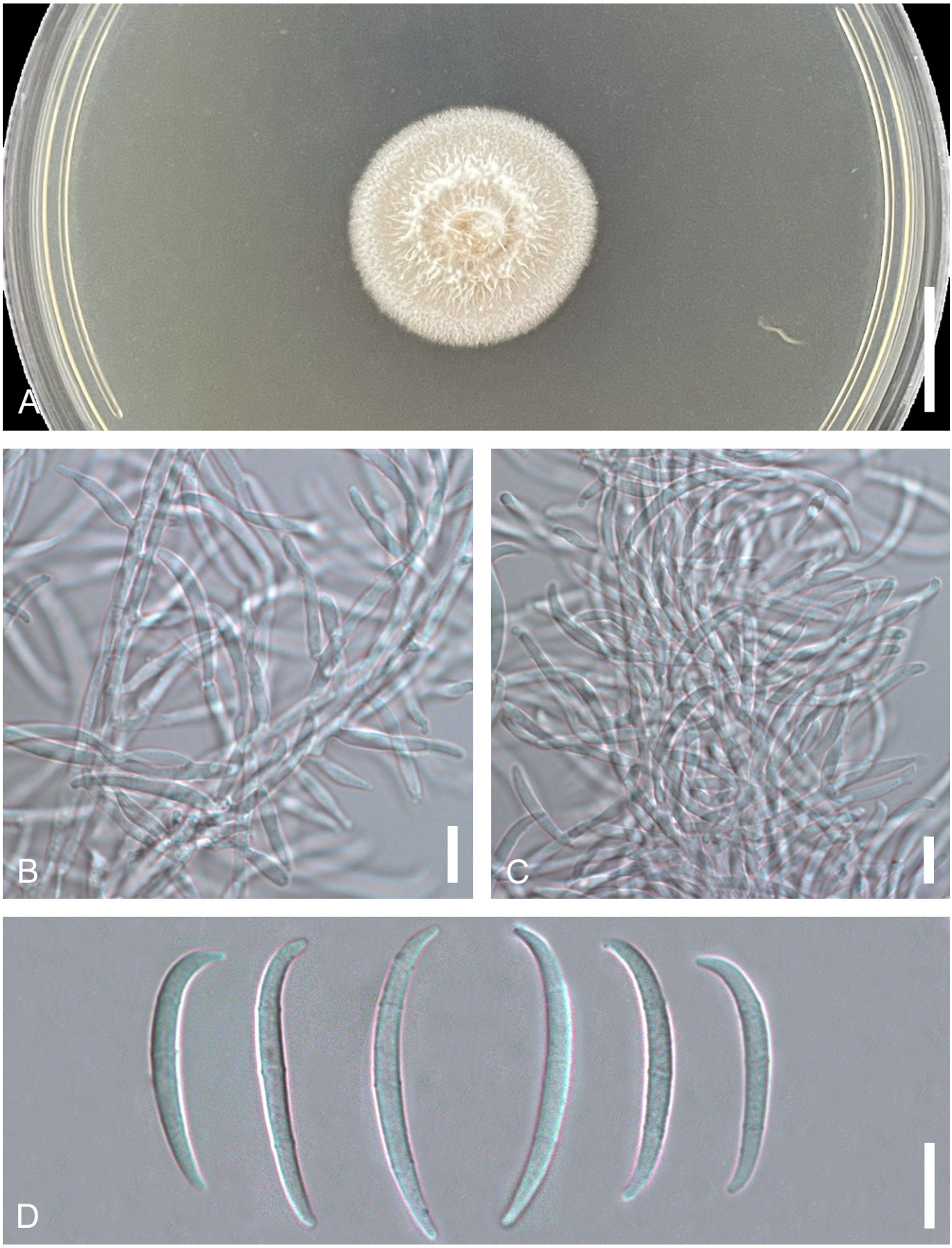

Fig. 5. Morphology of *Fusicolla parasitica* URM 9019 isolated from *Camarotella torrendiella* and *C. acrocomiae* in *Cocos nucifera,* Pernambuco, Brazil. **A.** Colony with 7-d-old growth at 27 °C on PDA medium (2.6 cm diam.). **B, C.** Conidiogenesis process; phialides and macroconidia formation. **D.** Morphological variation of conidia present in the species. Scale bars: A = 1.3 cm; B–D = 10 µm

© 2025 Westerdijk Fungal Biodiversity Institute

support present at the node linking the two clades (Fig. 6). A morphological comparison between *F. parasitica* and the phylogenetically closest species, *F. gigantispora*, was not possible as only the sexual morph of this species has been recorded (Dayarathne *et al.* 2020).

Purpureocillium lilacinum (Thom) Luangsa-ard *et al.*, *FEMS Microbiol. Lett*. **321**: 144. 2011. Fig. 7. [three specimens; A = 4.28 %; C = 40 %].
Basionym: *Penicillium lilacinum* Thom, *Bull. Bur. Anim. Ind. U.S. Dep. Agric.*: 73. 1910.
Synonyms: *Paecilomyces lilacinus* (Thom) Samson, *Stud. Mycol*. **6**: 58. 1974.
Spicaria rubidopurpurea Aoki, *Bull. Imp. Seri cult. Exp. Sta. Japan*: 440. 1941.

Colonies on PDA showing radial mycelial growth of 4 cm in 7 d at 27 °C. Colony colouration ranging from white to vinaceous with shades of purple in the centre and white to pale luteous at margin; sometimes presents yellow to honey mustard exudation; reverse white to brownish. *Aerial mycelium* floccose, fast-growing and dense. *Hyphae* hyaline, thick walled, 3–4 µm wide. Abundant *sporulation*. *Conidiophores* sub-merged from hyphae (3.5–)4.0–5.0(–5.5) µm consisting of verticillate branches with phialides. *Phialides* (6.5–)7.0–8.0(–8.5) µm long. *Conidia* aseptate, cohering in long chains, fusiform to ellipsoid, smooth-walled, (1.8–)2.0–3.25(–3.5) × 2.5–4.0(–4.5) µm.

Materials examined: **Brazil**, Paraíba, Camaratuba, private property, 6°38'29"S, 35°07'21.6"W, 105 m a.s.l., on *Camarotella torrendiella* and *C. acrocromiae* on living leaves of *Cocos nucifera*, 27 Aug. 2023, *C.E.V.A. Sá*, culture URM

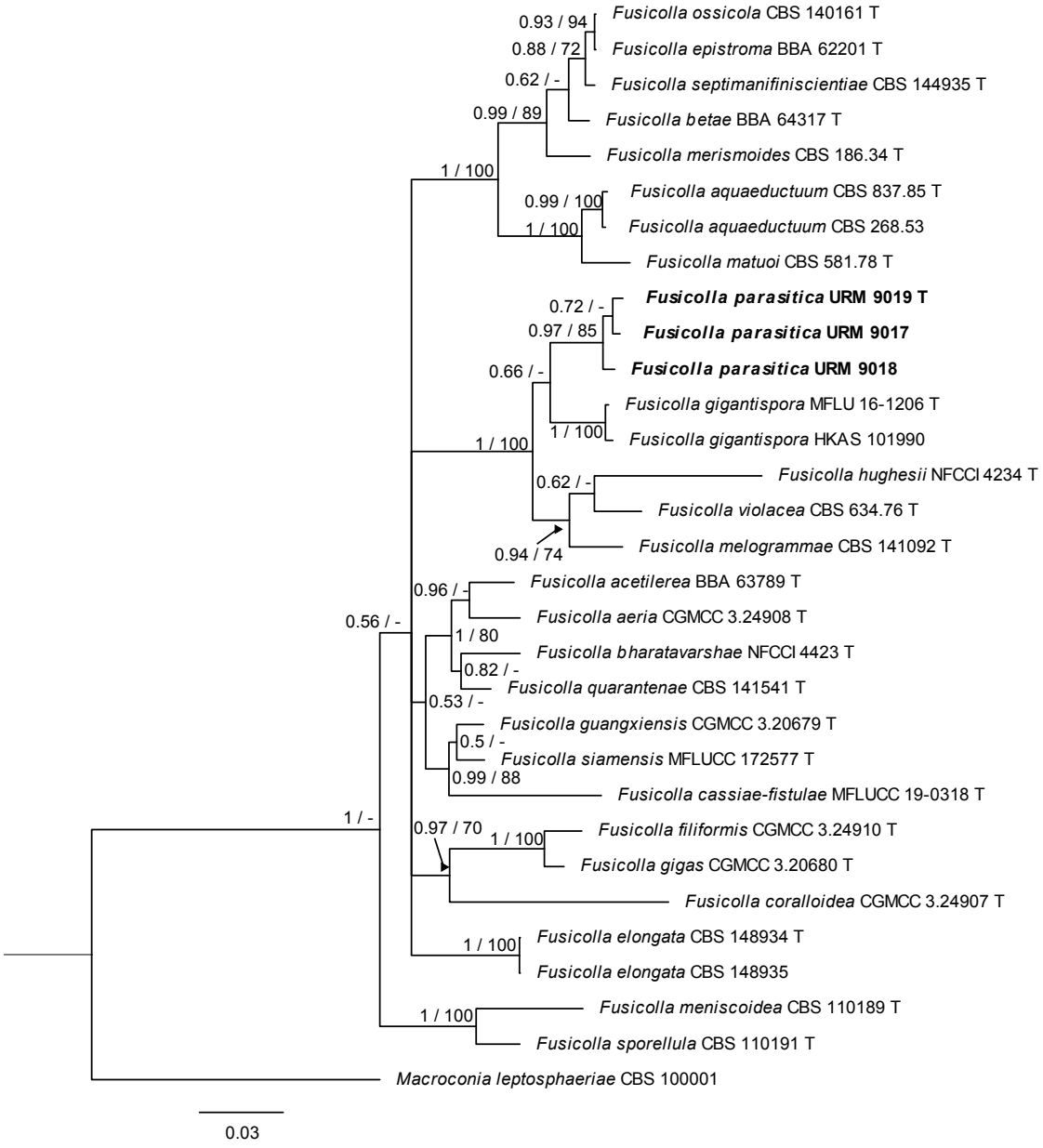

Fig. 6 Multilocus phylogenetic tree inferred from a Bayesian and Maximum Likelihood analysis based on a concatenated alignment of LSU, ITS, *RPB2* and *TUB2* sequences. Posterior probabilities (pp) and bootstrap (bs) are given at the nodes (pp/bs). The scale bar represents the expected number of changes per site. Strains representing the ex-type was indicated with "T" after the accession number. Species in this study are highlighted in bold.

© 2025 Westerdijk Fungal Biodiversity Institute

9024; Pernambuco, Goiana, Intituto de Pesquisa Agronômica (IPA), 7°33'46"S, 35°00'47"O, 103 m a.s.l., on *C. torrendiella* and *C. acrocromiae* on living leaves of *C. nucifera*, 21 Jun. 2022, *C.E.V.A. Sá*, culture URM 9023.

Notes: *Purpureocillium lilacinum* is considered a hyperparasitic nematophagous species with great bio-control potential of agricultural pests (Silva *et al.* 2017, Loureiro *et al.* 2020, Walia *et al.* 2021). This study presents the first record of hyperparasitism of this species on a leaf pathogen. This species have a wide distribution, already reported on *Theobroma cacao* in Ghana (Samson 1974), from a vaginal culture in the United States (Carey *et al.* 2003) on decayed grapes in Korea (Deng *et al.* 2012), on *Gossypium hirsutum* (Cotton) in the United States (Ek-Ramos *et al.* 2013), on human ocular tissues in Spain (López-Medrano *et al.* 2015), on deep-subseafloor sediments in New Zeland (Rédou *et al.* 2015), on *Meloidogyne incognita* (nematode) in Spain (Giné & Sorribas 2016), on eggs of *Meloidogyne enterolobii* (nematode) in Brazil (Silva *et al.* 2017), from soil in Egypt (Nawar *et al.* 2018), on contaminated soil in Algeria (Benguenab & Chibani 2021), from the eye of a child in Australia (Bennet & Shah 2022), on *Bemisia tabaci* (white fly) in Vietnam (Thi *et al.* 2023) and Malaysia (Sani *et al.* 2023), and from farmland soils in Taiwan (Tseng *et al.* 2023).

DISCUSSION

Hyperparasitic fungi have already been reported for *Camarotella*, a foliar pathogen that affects different botanical groups, in previous studies. In Lucena (Paraíba, Brazil), Sudo (1989) presented the world's first report of hyperparasitism on *C. acrocomiae* on coconut trees with *Acremonium alternatum* and *A. persicinum* (the latter also reported by

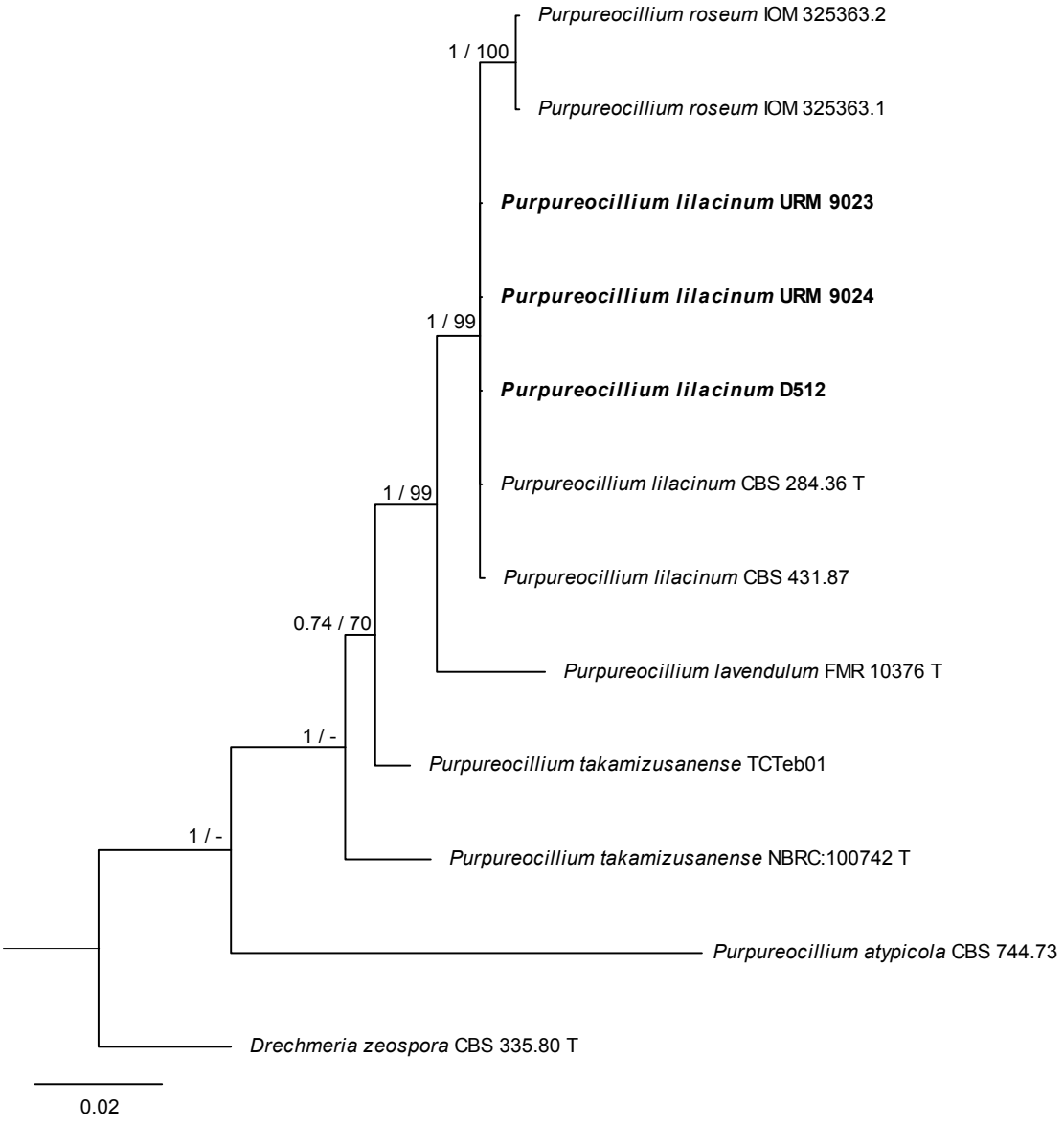

Fig. 7 Multilocus phylogenetic tree inferred from a Bayesian and Maximum Likelihood analysis based on a concatenated alignment of LSU, ITS, and *TEF-1α* sequences. Posterior probabilities (pp) and bootstrap (bs) are given at the nodes (pp/bs). The scale bar represents the expected number of changes per site. Strains representing the ex-type was indicated with "T" after the accession number. Species in this study are highlighted in bold.

© 2025 Westerdijk Fungal Biodiversity Institute

Warwick 2001), as well the first record of attempted biocontrol for this disease using hyperparasites. Eleven years after the first record in Brazil, Warwick (2000) reported *Septofusidium elegantulum* as a hyperparasite of *Camarotella torrendiella* on *Cocos nucifera*, as well as its biocontrol potential, which was later confirmed by Benassi *et al.* (2013). Afterwards, *Acremonium cavaraeanum* and *Hansfordia pulvinata* were reported in Brazil hyperparasitizing black leaf spot on *C. nucifera* (Warwick 2007, Benassi *et al.* 2013). Hofmann & Piepenbring (2014) reported *Asterolibertia licaniicola* hyperparasitizing *Camarotella* sp. on *Licania arborea* in Brazil. In the state of Rio de Janeiro (Brazil), *Acremonium* sp., *Cladosporium* sp., *Curvularia* sp., *Fusarium* sp., *Lasiodiplodia* sp., *Paecilomyces* sp., *Pestalotiopsis* sp. and *Trichoderma* sp. were reported present on *Camarotella* sp., which were associated with *Cocos nucifera* (Gonçalves 2020). Bermúdez-Cova *et al.* (2023) reported, for the first time, the presence of an unidentified hyphomycete on *Camarotella costaricensis* on *Acrocomia aculeata* leaves. With the exception of *Acremonium cavaraeanum* (considered a constant and abundant hyperparasite), all the species obtained in this study represent new hyperparasite reports of *Camarotella*. *Fusicolla parasitica* was considered constant and common in coconut groves; *Fusarium pseudocircinatum* and *Purpureocillium lilacinum* were considered accessory and common species associated with *Camarotella*, while *Fusarium caatingaense* was considered rare and accidental.

According to Carvalho *et al.* (2003), the incidence of hyperparasites on *Camarotella acrocomiae* on *Cocos nucifera* correlates positively and significantly with the climatic variables rainfall and relative humidity, and negatively with increasing temperature; it was also shown that successive increases in rainfall and relative humidity favoured the presence of hyperparasites, which decreased in incidence from August onwards (the beginning of the transition from the rainy to the dry season). Considering the species obtained in this study and the pluviometric data (Table 7) according to the "Agência Pernambucana de Água e Clima" (APAC-Government of Pernambuco) and the "Agência Executiva de Gestão das Águas" (AESA-Government of Paraíba), it was reported that the largest number of specimens were obtained in June during the rainy season (200.9 mm / 43 specimens) followed by August (94.5 mm / 23 specimens). In the transition period from a dry to a rainy season (February / 57.2 mm), four specimens were obtained. Only one isolate of *Fusicolla parasitica* was obtained in the dry season (December / 56.2 mm). The incidence of specimens obtained in this study corroborated the findings of Carvalho *et al.* (2003).

Considering the Genealogical Concordance Phylogenetic Species Recognition (GCPSR) (Taylor *et al.* 2000), which consists of comparing more than one gene genealogy for definition of the limit of phylogenetic species, *Fusicolla parasitica* strains grouped into a monophyletic clade (97 %) and were considered as a single species (Fig. 6).

In the redisposition of the order *Hypocreales* presented by Hou *et al.* (2023), *Acremonium cavareanum*, previously associated with the fusidioides clade within the family *Bionectriaceae* (Summerbell *et al.* 2011, Giraldo *et al.* 2014) was regrouped in the family *Niessliaceae*. However, the phylogeny in *Niessliaceae* is not well resolved and different genera remain polyphyletic, including the ex-type strain of *A. cavaraeanum* (CBS 101149). Further work is required to obtain a more accurate redisposition of these clades.

Despite the low support, the *Purpureocillium* isolates in this study morphologically resemble *P. lilacinum* (Fig. 7). It is assumed that the absence of the translation elongation factor *1-α* gene region (*TEF-1α*) from *P. roseum* implied a loss of phylogenetic support for the concise separation of the clade. This study reinforces the need for further work to add new gene regions for different genera, as well as the "conscious" publication of new species to contribute to more complete fungal databases.

In this study, *Acremonium cavaraeanum* was recorded as the first occurrence for the states of Paraíba and Pernambuco; *Purpureocillium lilacinum* was recorded for the first time as a hyperparasite of a leaf pathogen; new records of hyperparasitic habit were obtained for *Fusarium pseudocircinatum* and *F. caatingaense* known exclusively as phytopathogens and entomopathogens; and a new species of *Fusicolla*, a hyperparasite of *Camarotella* sp., is proposed.

Table. 7. List of fungal species collected on the stroma of *Camarotella* sp. on *Cocos nucifera*, in the states of Pernambuco and Paraíba (Brazil), with number of specimens, collection area, collection date and monthly rainfall.

Species	No. of specimens	Collection area (municipiality/state)	Collection date	Monthly rainfall (mm)
Acremonium cavaraeanum	3	Bonito/Pernambuco	2/12/2022	57.2
	26	Goiana/Pernambuco	6/21/2022	200.9
	13	Paudalho/Pernambuco	6/10/2023	200.9
	18	Camaratuba/Paraíba	8/27/2023	94.5
Fusarium caatingaense	1	Bonito/Pernambuco	2/12/2022	57.2
Fusarium pseudocircinatum	1	Paudalho/Pernambuco	6/10/2023	200.9
	2	Camaratuba/Paraíba	8/27/2023	94.5
Fusicolla parasitica	1	Goiana/Pernambuco	6/21/2022	200.9
	1	Recife/Pernambuco	12/15/2022	56.2
	1	Paudalho/Pernambuco	6/10/2023	200.9
Purpureocillium lilacinum	1	Goiana/Pernambuco	6/21/2022	200.9
	2	Camaratuba/Paraíba	8/27/2023	94.5

© 2025 Westerdijk Fungal Biodiversity Institute

ACKNOWLEDGEMENTS

This study was financed in part by the Coordenação de Aperfeiçoamento de Pessoal de Nível Superior - Brasil (CAPES) – Finance Code 001. We would like to thank the Conselho Nacional de Desenvolvimento Científico e Tecnológico (CNPq), which made it possible to carry out this work through research announcements. Also, we would like to thank the owners of the properties for allowing us to collect the material used in this study, as well the Micoteca URM of the Universidade Federal de Pernambuco for the assistance in the execution of this research.

Conflict of interest: The authors declare that they have no conflict of interest.

REFERENCES

Alfenas AC, Mafia RG (2016). *Métodos em Fitopatologia*. 1edn. UFV, Brazil.

Araújo JPM, Lebert BM, Vermeulen S, *et al.* (2022). Masters of the manipulator: two new hypocrealean genera, *Niveomyces* (*Cordycipitaceae*) and *Torrubiellomyces* (*Ophiocordycipitaceae*), parasitic on the zombie ant fungus *Ophiocordyceps camponoti-floridani*. *Persoonia* **49**: 171–194. https://doi.org/10.3767/persoonia.2022.49.05

Araújo KL, Silveira SF, Mussi-Dias V *et al.* (2017) Local infection associated with vascular bundles: the colonization of coconut palm leaflets by two *Camarotella* species. *European Journal of Plant Pathology* **148**: 413–422. https://doi.org/10.1007/s10658-016-1099-z

Bali GK, Singh SK, Maurya DK, *et al.* (2022). Morphological and molecular identification of the entomopathogenic fungus *Purpureocillium lilacinum* and its virulence against *Tuta absoluta* (Meyrick) (*Lepidoptera*: *Gelechiidae*) larvae and pupae. *Egyptian Journal of Biological Pest Control* **32**: 1–10. https://doi.org/10.1186/s41938-022-00582-y

Barbosa MA, Prazeres JFSA, Malosso E (2022). A higher altitude enclave of humid forest in the semi-arid of Brazil holds a diversity of conidial fungi on leaf-litter. *Acta Botanica Brasilica* **36**: 1–14. https://doi.org/10.1590/1677-941X-ABB-2022-0031

Bellemain E, Carlsen T, Brochmann C, *et al.* (2010). ITS as an environmental DNA barcode for fungi: an in silico approach reveals potential PCR biases. *BMC Microbiology* **10**: 1–9. https://doi.org/10.1186/1471-2180-10-189

Benassi AC, Fanton CJ, Santana EM (2013). *O cultivo do coqueiro-anão-verde: tecnologia de produção*. 227 edn., Incaper, Brazil.

Bennet HY, Shah SP (2022). A case of non-traumatic *Purpureocillium lilacinum* (*Paecilomyces lilacinus*) endophthalmitis in a child. *American Journal of Ophthalmology Case Reports* **26**: 1–3. https://doi.org/10.1016/j.ajoc.2022.101375

Benguenab A, Chibani A (2021). Biodegradation of petroleum hydrocarbons by filamentous fungi (*Aspergillus ustus* and *Purpureocillium lilacinum*) isolated from used engine oil contaminated soil. *Acta Ecologica Sinica* **41**: 416–423. https://doi.org/10.1016/j.chnaes.2020.10.008

Bermúdez-Cova MA, Cruz-Laufer AJ, Piepenbring M (2022). Hyperparasitic fungi on black mildews (*Meliolales*, *Ascomycota*): hidden fungal diversity in the tropics. *Frontiers in Fungal Biology* **3**: 1–13. https://doi.org/10.3389/ffunb.2022.885279

Bermúdez-Cova MA, Haelewaters D, De Bekker C, *et al.* (2023). Hyperparasitic fungi- definitions, diversity, ecology, and research. *Authorea* **2**: 1–33. https://doi.org/10.22541/au.168787020.07281183/v2

Bonneau X, Haryanto I, Karsiwan T (2010). Coconut husk ash as a fertilizer for coconut palms on peat. *Experimental Agriculture* **46**: 401–414. https://doi.org/10.1017/S0014479710000025

Calderón-Santoyo M, Iñiguez-Moreno M, Barros-Castillo JC, *et al.* (2022). Microencapsulation of citral with Arabic gum and sodium alginate for the control of *Fusarium pseudocircinatum* in bananas. *Iranian Polymer Journal* **31**: 665–676. https://doi.org/10.1007/s13726-022-01033-z

Calvillo-Medina RP, Ponce-Angulo DG, Raymundo T, *et al.* (2021). *Purpureocillium roseum sp. nov*. A new ocular pathogen for humans and mice resistant to antifungals. *Mycoses* **64**: 162–173. https://doi.org/10.1111/myc.13198

Carey J, D'Amico R, Sutton DA, *et al.* (2003). *Paecilomyces lilacinus* vaginitis in an immunocompetent patient. *Emerging Infectious Diseases* **9**: 1155–1158. https://doi.org/10.3201/eid0909.020654

Carvalho RAG, Araújo E, Barreto AF, *et al.* (2003) Severidade da lixa-grande do coqueiro anão e incidência de hiperparasitismo em Parnamirim, Rio Grande do Norte. *Revista Brasileira de Fruticultura* **25**: 546–548. https://doi.org/10.1590/S0100-29452003000300048

Costa GA, Freitas-Lopes RL, Lino JB, *et al.* (2020). An efficient method for inducing sporulation of cercosporoid fungal species causing leaf spots in cassava. *Journal of Plant Pathology* **102**: 201–204. https://doi.org/10.1007/s42161-019-00404-5

Crous PW, Sandoval-Denis M, Costa MM, *et al.* (2022). *Fusarium* and allied fusarioid taxa (FUSA). 1. *Fungal Systematics and Evolution* **9**: 161–200. https://doi.org/10.3114/fuse.2022.09.08

Dajoz R (1983). *Ecologia Geral*. Vozes, Brazil.

Dayarathne MC, Jones EBG, Maharachchikumbura SSN, *et al.* (2020). Morpho-molecular characterization of microfungi associated with marine based habitats. *Mycosphere* **11**: 1–188. https://doi.org/10.5943/mycosphere/11/1/1

Deng JX, Paul NC, Sang HK, *et al.* (2012). First report on isolation of *Penicillium adametzioides* and *Purpureocillium lilacinumfrom* decayed fruit of Cheongsoo grapes in Korea. *Mycobiology* **40**: 66–70. https://doi.org/10.5941/MYCO.2012.40.1.066

Diniz AG, Barbosa LFS, Santos ACS, *et al.* (2020). Bio-insecticide effect of isolates of *Fusarium caatingaense* (*Sordariomycetes*: *Hypocreales*) combined to botanical extracts against *Dactylopius opuntiae* (*Hemiptera*: *Dactylopiidae*). *Biocontrol Science and Technology* **30**: 384–395. https://doi.org/10.1080/09583157.2020.1720601

Ek-Ramos MJ, Zhou W, Valencia CU, *et al.* (2013). Spatial and temporal variation in fungal endophyte communities isolated from cultivated cotton (*Gossypium hirsutum*). *PLoS ONE* **8**: 1–13. https://doi.org/10.1371/journal.pone.0066049

Farias OR, Cruz JMFL, Veloso JS, *et al.* (2023). *Fusarium pseudocircinatum* causing stunting and malformation of sunflower plants in Brazil. *Plant Disease* **107**: 216. https://doi.org/10.1094/PDIS-01-22-0212-PDN

Foale M, Harries H (2010). Farm and forestry production and marketing profile for coconut (*Cocos nucifera*). In: *Elevitch CR Specialty Crops for Pacific Island Agroforestry*. Holualoa, Hawaii: 113–134.

Freeman S, Otero-Colina, Rodríguez-Alvarado G, *et al.* (2014). First report of mango malformation disease caused by *Fusarium pseudocircinatum* in Mexico. *Plant Disease* **98**: 1583–1583. https://doi.org/10.1094/PDIS-04-14-0375-PDN

© 2025 Westerdijk Fungal Biodiversity Institute

Gams W, Diederich P, Põldmaa K (2004). Fungicolous fungi. In: *Biodiversity of fungi: inventory and monitoring methods* (Mueller GM, Bills GF, Foster MS, eds). Academic Press, Amsterdam: 343–392.

García-López E, Mora-Aguilera A, Nava-Díaz C, *et al.* (2016). First report of *Fusarium pseudocircinatum* causing mango malformation disease in Dominican Republic. *Plant Disease* **100**: 1501. https://doi.org/10.1094/PDIS-12-15-1397-PDN

Giné A, Sorribas FJ (2017). Effect of plant resistance and BioAct WG (*Purpureocillium lilacinum* strain 251) on *Meloidogyne incognita* in a tomato–cucumber rotation in a greenhouse. *Pest Management Science* **73**: 880–887. https://doi.org/10.1002/ps.4357

Giraldo A, Gené J, Cano J (2014). *Acremonium* with catenate elongate conidia: phylogeny of *Acremonium fusidioides* and related species. *Mycologia* **106**: 328–338. https://doi.org/10.3852/13-158

Gonçalves JM (2020). *Fungos Associados as Lixas do Coqueiro (Cocos nucifera L.) e Potencial de Biocontrole*. MSc Dissertation. Departamento de Geografia, Universidade Estadual do Norte Fluminense Darcy Ribeiro, Brazil.

Gräfenhan T, Schroers HJ, Nirenberg HI, *et al.* (2011). An overview of the taxonomy, phylogeny, and typification of nectriaceous fungi in *Cosmospora*, *Acremonium*, *Fusarium*, *Stilbella*, and *Volutella*. *Studies in Mycology* **68**: 79–113. https://doi.org/10.3114/sim.2011.68.04

Haelewaters D, Hiller T, Dick CW (2018). Bats, bat flies, and fungi: A case of hyperparasitism. *Trends in Parasitology* **34**: 784–799. https://doi.org/10.1016/j.pt.2018.06.006

Han SL, Wang MM, Ma ZY, *et al.* (2023). *Fusarium* diversity associated with diseased cereals in China, with an updated phylogenomic assessment of the genus. *Studies in Mycology* **104**: 87–148. https://doi.org/10.3114/sim.2022.104.02

Hoch HC, Abawi GS (1979). Mycoparasitism of oospores of *Pythium ultimum* by *Fusarium merismoides*. *Mycologia* **71**: 621–625. https://doi.org/10.1080/00275514.1979.12021044

Hofmann TA, Piepenbring M (2014). New records of plant parasitic *Asterinaceae* (*Dothideomycetes*, *Ascomycota)* with intercalary appressoria from Central America and Panama. *Tropical Plant Pathology* **39**: 419–427. https://doi.org/10.1590/S1982-56762014000600001

Hornok L, Walcz I (1983). *Fusarium heterosporum*, a highly specialized hyperparasite of *Claviceps purpurea*. *Transactions of the British Mycological Society* **80**: 377–380. https://doi.org/10.1016/S0007-1536(83)80032-1

Hou LW, Giraldo A, Groenewald JZ, *et al.* (2023). Redisposition of acremonium-like fungi in *Hypocreales*. *Studies in Mycology* **105**: 23–203. https://doi.org/10.3114/sim.2023.105.02

Ito T, Okane I, Nakagiri A, *et al.* (2000). Two species of *Acremonium* section *Acremonium: A. borodinense sp.nov.* and *A. cavaraeanum* rediscovered. *Mycological Research* **104**: 77–80. https://doi.org/10.1017/S0953756299008977

Jeffries P (1995). Biology and ecology of mycoparasitism. *Canadian Journal of Botany* **73**: 1284–1290. https://doi.org/10.1139/b95-389

Johnson VB, Aguilar EA, Alouw J, *et al.* (2024). The future of coconut as an economic crop qorldwide. *The Coconut Botany, Production and Uses* **14**: 206–230. https://doi.org/10.1079/9781789249736.0014

Kaur K, Chhikara N, Sharma P, *et al.* (2019). Coconut meal: Nutraceutical importance and food industry application. *Food and Raw Materials* **7**: 419–427. http://doi.org/10.21603/2308-4057-2019-2-419-427

Kumar S, Stecher G, Li M, *et al.* (2018). MEGA X: Molecular evolutionary genetics analysis across computing platforms. *Molecular Biology and Evolution* **35**: 1647–1549. https://doi.org/10.1093/molbev/msy096

Leinhos GME, Buchenauer H (1992). Hyperparasitism of selected fungi on rust fungi of cereal. *Journal of Plant Disease and Protection* **99**: 482–498. https://www.jstor.org/stable/43386095

Li X, Zhang ZY, Ren YL, *et al.* (2022). Morphological characteristics and phylogenetic evidence reveal two new species of *Acremonium* (*Hypocreales*, *Sordariomycetes*). *MycoKeys* **91**: 85–96. https://doi.org/10.3897/mycokeys.91.86257

Liew ECY, Laurence MH, Pearce CA, *et al.* (2016). Review of *Fusarium* species isolated in association with mango malformation in Australia. *Australasian Plant Pathology* **45**: 547–559. https://doi.org/10.1007/s13313-016-0454-z

Liu YJ, Whelen S, Hall BD (1999). Phylogenetic relationships among ascomycetes: evidence from an RNA polymerse II subunit. *Molecular Biology and Evolution* **16**: 1799–1808. https://doi.org/10.1093/oxfordjournals.molbev.a026092

López-Medrano R, Madera AP, Foz CF (2015) Infecciones oculares por *Purpureocillium lilacinum*: presentación de un caso y revisión de la literatura. *Revista Iberoamericana de Micología* **32**: 111–114. https://doi.org/10.1016/j.riam.2013.11.004

Loureiro ES, Neto JAD, Pessoa LGA, *et al.* (2020). Management of *Pratylenchus brachyurus* with *Trichoderma harzianum* and *Purpureocillium lilacinum* in soybean. *Agrarian and Biological Sciences* **9**: 1–17. https://doi.org/10.33448/rsd-v9i7.3828

Maddison WP, Maddison DR (2019). Mesquite: a modular system for evolutionary analysis. Version 3.61. https://www.mesquiteproject.org.

Malathrakis NE (1985). The fungus *Acremonium alternatum* Line: Fr., a hyperparasite of the cucurbits powdery mildew pathogen *Sphaerotheca fuliginea*. *Journal of Plant Disease and Protection* **92**: 509–515. https://www.jstor.org/stable/43383066

Martins CR, Jesus Júnior LA (2011). Evolução da produção de coco no Brasil e o comércio internacional- Panorama 2010. *Embrapa Tabuleiros Costeiros* **164**: 1–28.

Mazarotto EJ, Poitevin CG, do Carmo ALM, *et al.* (2020). Pathogenic *Fusarium* species complexes associated to seeds of indigenous Brazilian forest tree *Aspidosperma polyneuron*. *European Journal of Plant Pathology* **158**: 849–857. https://doi.org/10.1007/s10658-020-02120-8

Mello JF, Santos ACS, Brito ACQ, *et al.* (2024). Species diversity of fusarioid genera associated with sweet potato in Brazil, including the description of a new species. *Plant Pathology* **73**: 975–990. https://doi.org/10.1111/ppa.13868

Montoya-Martínez AC, O'Donnell K, Busman M, *et al.* (2021). Malformation disease in *Tabebuia rosea* (rosy trumpet) caused by *Fusarium pseudocircinatum* in Mexico. *Plant Disease* **105**: 2822–2829. https://doi.org/10.1094/PDIS-09-20-1942-RE

Mower RL, Snyder WC, Hancock JG (1975). Biological control of ergot by *Fusarium*. *Phytopathology* **65**: 5–10. https://doi.org/10.1094/Phyto-65-5

Narayanasamy P (2001). *Plant Pathogen Detection and Disease Diagnosis*. 2 edn., CRC Press, USA.

Nirenberg HI (1976). Untersuchungen über die morphologische und biologische. Differenzierung in der *Fusarium*-Sektion *Liseola*. *Mitteilungen aus der Biologischen Bundesanstalt für Land- und Forstwirtschaft Berlin-Dahlem* **169**: 1–117. https://doi.

© 2025 Westerdijk Fungal Biodiversity Institute

org/10.5073/20210624-085725

Nawar MA, Abo-Elnasr AA, Kobisi ANA, *et al.* (2018). Evaluation of acaricidal activity of *Purpureocillium Lilacinum* isolated from Egyptian soil against *Tetranychus urticae*. *Egyptian Journal of Desert Research* **68**: 157–172. https://doi.org/10.21608/ejdr.2019.8033.1021

Nirenberg HI, O'Donnell K (1998). New *Fusarium* species and combinations within the *Gibberella fujikuroi* species complex. *Mycologia* **90**: 434–458. https://doi.org/10.1080/00275514.1998.12026929

Norphanphoun C, Jayawardena RS, Chen Y, *et al.* (2019). Morphological and phylogenetic characterization of novel pestalotioid species associated with mangroves in Thailand. *Mycosphere* **10**: 531–578. https://doi.org/10.5943/mycosphere/10/1/9

O'Donnell K, Kistler HC, Cigelnik E, *et al.* (1998). Multiple evolutionary origins of the fungus causing Panama disease of banana: concordant evidence from nuclear and mitochondrial gene genealogies. *Proceedings of the National Academy of Sciences of the United States of America* **95**: 2044–2049. https://doi.org/10.1073/pnas.95.5.2044

Parratt SR, Laine AL (2016). The role of hyperparasitism in microbial pathogen ecology and evolution. *The ISME Journal* **10**: 1815–1822. https://doi.org/10.1038/ismej.2015.247

Pinto JM, Silva MB, Arantes SD (2023). Controle da *Camarotella torrendiella* e *Camarotella acrocomiae* no cultivo do *Cocos nucifera* L. *Natural Resources* **13**: 1–26. https://doi.org/10.6008/CBPC2237-9290.2023.004.0001

Posada D, Buckley TR (2004). Model selection and model averaging in phylogenetics: Advantages of Akaike information criterion and Bayesian approaches over likelihood ratio tests. *Systematics Biology* **53**: 793–808. https://doi.org/10.1080/10635150490522304

Rambaut A (2018). FigTree. Version 1.4.4. http://tree.bio.ed.ac.uk/software/figtree

Rannala B, Yang Z (1996). Probability distribution of molecular evolutionary trees: a new method of phylogenetic inference. *Journal of Molecular Evolution* **43**: 304–311. https://doi.org/10.1007/BF02338839

Rédou V, Navarri M, Meslet-Cladière L, *et al.* (2015). Species richness and adaptation of marine fungi from deep-subseafloor sediments. *Applied and Environmental Microbiology* **81**: 3571–3582. https://doi.org/10.1128/AEM.04064

Rivera-Varas VV, Freeman TA, Gudmestad NC (2007). Mycoparasitism of *Helminthosporium solani* by *Acremonium strictum*. *Phytopathology* **9**: 1331–1337. https://doi.org/10.1094/PHYTO-97-10-1331

Ronquist F, Huelsenbeck JP (2003) MrBayes 3: Bayesian phylogenetics inference under mixed models. *Bioinformatics* **19**: 1572–1574. https://doi.org/10.1093/bioinformatics/btg180

Sá CEVA, Ferraz LGB, Cavalcanti LH (2019). *Mixomicetos* associados a coqueiro (*Cocos nucifera* L.) na Estação Experimental de Itapirema (Goiana, Pernambuco, Brasil). *Pesquisa Agropecuária Pernambucana* **24**: 1–7. https://doi.org/10.12661/pap.2019.007

Sá CEVA, Ferraz LGB, Cavalcanti LH (2022). Assemblages of *Myxomycetes* associated with *Cocos nucifera* L. trees. *Acta Brasiliensis* **6**: 35–42. https://doi.org/10.22571/2526-4338587

Samson RA (1974). *Paecilomyces* and some allied Hyphomycetes. *Studies in Mycology* **6**: 119.

Sandoval-Denis M, Gené J, Sutton DA *et al.* (2016). New species of *Cladosporium* associated with human and animal infections. *Persoonia* **36**: 281–298. http://dx.doi.org/10.3767/003158516X691951

Sani I, Jamian S, Saad N, *et al.* (2023). Identification and virulence of entomopathogenic fungi, *Isaria javanica* and *Purpureocillium lilacinum* isolated from the whitefly, *Bemisia tabaci* (Gennadius) (*Hemiptera*: *Aleyrodidae*) in Malaysia. *Egyptian Journal of Biological Pest Control* **33**: 1–12. https://doi.org/10.1186/s41938-023-00657-4

Santillán-Mendoza R, Fernández-Pavía SP, O'Donnell K, *et al.* (2018). A novel disease of big-leaf mahogany caused by two *Fusarium* species in Mexico. *Plant Disease* **102**: 1965–1972. https://doi.org/10.1094/PDIS-01-18-0060-RE

Santos ACS, Trindade JVC, Lima CS, *et al.* (2019). Morphology, phylogeny, and sexual stage of *Fusarium caatingaense* and *Fusarium pernambucanum*, new species of the *Fusarium incarnatum-equiseti* species complex associated with insects in Brazil. *Mycologia* **111**: 244–259. https://doi.org/10.1080/00275514.2019.1573047

Schnittler M, Stephenson SL (2000). Myxomycete biodiversity in four different forest types in Costa Rica. *Mycologia* **94**: 626–637. https://doi.org/10.1080/00275514.2000.12061203

Shiraishi A, Leslie JF, Zhong S, *et al.* (2012). AFLP, Pathogenicity, and VCG Analyses of *Fusarium oxysporum* and *Fusarium pseudocircinatum* from *Acacia koa*. *Plant Disease* **96**: 1111–1117. https://doi.org/10.1094/PDIS-06-11-0491

Silva SD, Carneiro RMDG, Faria M, *et al.* (2017). Evaluation of *Pochonia chlamydosporia* and *Purpureocillium lilacinum* for suppression of *Meloidogyne enterolobii* on tomato and banana. *Journal of Nematology* **49**: 77–85. https://doi.org/10.21307/jofnem-2017-047

Stamatakis A (2014). RAxML Version 8: a tool for phylogenetic analysis and post-analysis of large phylogenies. *Bioinformatics* **30**: 1312–1313. https://doi.org/10.1093/bioinformatics/btu033

Sudo S (1989). Biocontrole de *Catacauma torrendiella* e *Coccostroma palmicola*, agentes causadores da lixa preta do coqueiro. In: *Reunião brasileira sobre controle biológico de doenças de plantas. Piracicaba*. *Anais Piracicaba*: USP/EMBRAPA 57–59.

Summerbell RC, Gueidan C, Schroers HJ, *et al.* (2011). *Acremonium* phylogenetic overview and revision of *Gliomastix*, *Sarocladium*, and *Trichothecium*. *Studies in Mycology* **68**: 139–162. https://doi.org/10.3114/sim.2011.68.06

Sun JZ, Liu XZ, McKenzie EHC, *et al.* (2019). Fungicolous fungi: terminology, diversity, distribution, evolution, and species checklist. *Fungal Diversity* **95**: 337–430. https://doi.org/10.1007/s13225-019-00422-9

Sung GH, Sung JM, Hywel-Jones NL, *et al.* (2007). A multi-gene phylogeny of *Clavicipitaceae* (*Ascomycota*, *Fungi*): identification of localized incongruence using a combinational bootstrap approach. *Molecular Phylogenetics and Evolution* **44**: 1204–1223. https://doi.org/10.1016/j.ympev.2007.03.011

Tan YP, Shivas RG (2023). Nomenclatural novelties. *Index of Australian Fungi* **10**: 1–17. https://doi.org/10.13140/RG.2.2.16073.21600

Taylor JW, Jacobson DJ, Kroken S, *et al.* (2000) Phylogenetic species recognition and species concepts in *Fungi*. *Fungal Genetics and Biology* **31**: 21–32. https://doi.org/10.1006/fgbi.2000.1228

Thi HN, Le KYP, Thien NDT, *et al.* (2023). Insecticidal activity of isolated *Purpureocillium lilacinum* PL1 against whitefy, *Bemisia tabaci Gennadius* (*Hemiptera*: *Aleyrodidae*) on cassava plantations in southern Viet Nam. *Egyptian Journal of Biological Pest Control* **33**: 1–11. https://doi.org/10.1186/s41938-023-

© 2025 Westerdijk Fungal Biodiversity Institute

00691-2

Todaro AR, Nascimento VX, Souza NC, *et al.* (2013). Genetic variability in the ITS and IGS regions of the ribosomal DNA of *Acremonium cavaraeanum* exhibiting antimicrobial activity. *Genetics and Molecular Research* **12**: 6983–6995. http://dx.doi.org/10.4238/2013

Tseng WS, Lee MJ, Wu JA, *et al.* (2023). Poly (butylene adipate-co-terephthalate) biodegradation by *Purpureocillium lilacinum* strain BA1S. *Applied Microbial and Cell Physiology* **107**: 6057–6070. https://doi.org/10.1007/s00253-023-12704-z

Vitória NS, Bezerra JL, Gramacho KP, *et al.* (2008). *Camarotella torrendiella comb. nov*. e *C. acrocomiae*: agentes etiológicos das lixas do coqueiro. *Tropical Plant Pathology* **33**: 295–301. https://doi.org/10.1590/S1982-56762008000400006

Walia A, Putatunda C, Sharma R, *et al.* (2021). Biocontrol: A Sustainable Agricultural Solution for Management of Plant Diseases. In: *Microbial Biotechnology in Crop Protection* (Kaushal, M., Prasad, R. eds). Springer, Singapore.

Warwick DRN (2000). Influência dos fitopatógenos na cadeia produtiva do coqueiro. *Fitopatologia Brasileira* **25**: 296–302.

Warwick DRN (2001). Colonização de estromas de Sphaerodothis acrocomiae agente causal da lixa grande do coqueiro por *Acremonium persicinum*. *Fitopatologia Brasileira* **26**: 220. https://doi.org/10.1590/S0100-41582001000200020

Warwick DRN (2007). Índices de Parasitismo de Lixa-grande do coqueiro pelos fungos hiperparasitas: *Acremonium cavaraeanum* e *Dycima pulvinata*. *Boletim de pesquisa e Desenvolvimento / Embrapa Tabuleiros Costeiros* **25**: 678–1961. http://www.infoteca.cnptia.embrapa.br/infoteca/handle/doc/372211

Xia JW, Sandoval-Denis M, Crous PW, *et al.* (2019). Numbers to names - restyling the *Fusarium incarnatum-equiseti* species complex. *Persoonia* **43**: 186–221. https://doi.org/10.3767/persoonia.2019.43.05

Yilmaz N, Sandoval-Denis M, Lombard L, *et al.* (2021). Redefining species limits in the *Fusarium fujikuroi* species complex. *Persoonia* **46**: 129–162. https://doi.org/10.3767/persoonia.2021.46.05

Zeng ZQ, Zhuang WY (2023). Three new species of *Fusicolla* (*Hypocreales*) from China. *Journal of Fungi* **9**: 572. https://doi.org/10.3390/jof9050572

Supplementary Material: http://fuse-journal.org/

Fig. S1. Bayesian phylogenetic trees of *Fusicolla* based on individual ITS (Fig. S1.1) and LSU (Fig. S1.2) gene regions. Posterior probabilities (pp) are given at the nodes. The scale bar represents the expected number of changes per site. Strains representing the ex-type are indicated with "T" after the accession number. Species in this study are highlighted in **bold**.

© 2025 Westerdijk Fungal Biodiversity Institute

FUSE

Fungal Systematics and Evolution

VOLUME 16
DECEMBER 2025
PAGES 181–195

doi.org/10.3114/fuse.2025.16.10

Recent taxonomic discoveries suggest a host-symbiont co-migration of *Russula* subsect. *Castanopsidum* with *Fagaceae* in the Americas

C. Manz[1], A. Ortiz-Suárez[2], K. Adamčíková[3], B. Looney[4], C.R. Noffsinger[5], M. Caboň[6], F. Hampe[7], M. Piepenbring[1], T. Hofmann[8], B. Buyck[9], C.A. Parra-Aldana[2], S. Adamčík[6,10]*, A. Corrales[2,11]

[1]Mycology Working Group, Goethe University Frankfurt am Main, Biologicum, Max-von-Laue-Str. 13, 60438 Frankfurt am Main, Germany
[2]Centro de Investigaciones en Microbiología y Biotecnología-UR (CIMBIUR), Facultad de Ciencias Naturales, Universidad del Rosario, Bogotá, Colombia
[3]Department of Plant Pathology and Mycology, Institute of Forest Ecology, Slovak Academy of Sciences Zvolen, Akademická 2, 949 01 Nitra, Slovakia
[4]2104 Misty Glen, Columbia, MO 65203, USA
[5]Department of Ecology and Evolutionary Biology, University of Tennessee, 1416 Circle Drive, Knoxville, Tennessee 37996, USA
[6]Laboratory of Molecular Ecology and Mycology, Institute of Botany, Plant Science and Biodiversity Center, Slovak Academy of Sciences, Dúbravská cesta 9, 84523 Bratislava, Slovakia
[7]Wetzlarer Str. 1, 35510 Butzbach, Germany
[8]Vicerrectoría de Investigación y Posgrado (VIP), Centro de Investigaciones Micológicas (CIMi), Herbario UCH, Universidad Autónoma de Chiriquí, 0427, David, Panama
[9]Institut de Systématique, Evolution, Biodiversité (ISYEB), Muséum national d'Histoire naturelle, CNRS, Sorbonne Université, EPHE, Université des Antilles, case postale 39, 57 rue Cuvier, 75005 Paris, France
[10]Department of Botany, Faculty of Natural Sciences, Comenius University in Bratislava, Révová 39, 81102 Bratislava, Slovakia
[11]Society for the Protection of Underground Networks, SPUN, Dover, DE, USA

*Corresponding author: slavomir.adamcik@savba.sk

Key words:
Basidiomycota
ectomycorrhizal diversity
evolutionary history
neotropics
new taxa
Trigonobalanus excelsa

Abstract: Three members of ectomycorrhizal fungi belonging to *Russula* subsection *Castanopsidum* are described from neotropical montane forests dominated by species of *Fagaceae* in Panama and Colombia. *Russula esperanzae sp. nov*. from Colombia differs in the field from other members of the subsection by slender longitudinally striated red stipes as well as characteristics of spores and basidia. *Russula atroamethystina* subsp. *atroamethystina,* originally described from Costa Rica, is reported for the first time from Panama. Closely related and morphologically similar Colombian collections are described as *R. atroamethystina* subsp. *guacahayoensis subsp. nov*. and differ from the typical subspecies by longer hymenial cystidia as well as molecular sequence data. The distribution of this newly described subspecies is restricted to *Fagaceae* forests east of the Isthmus of Panama. This suggests an allopatric diversification, likely driven by the absence of *Fagaceae* in the tropical lowland forest of the Darién Gap. *Russula esperanzae* is exclusively associated with *Trigonobalanus excelsa*, a tree species of *Fagaceae* endemic to Colombia. The role of its association with this tree in the evolutionary history of the species is discussed. Based on molecular timing, species of the subsection *Castanopsidum* started to evolve approximately 15.1 M years ago (mya) and display an amphi-pacific disjunct distribution with an Asian clade that split from the American clade around 11 mya.

Citation: Manz C, Ortiz-Suárez A, Adamčíková K, Looney B, Noffsinger CR, Caboň M, Hampe F, Piepenbring M, Hofmann T, Buyck B, Parra-Aldana CA, Adamčík S, Corrales A (2025). Recent taxonomic discoveries suggest a host-symbiont co-migration of *Russula* subsect. *Castanopsidum* with *Fagaceae* in the Americas. *Fungal Systematics and Evolution* **16**: 181–195. doi: 10.3114/fuse.2025.16.10
Received: 17 January 2025; **Accepted:** 5 March 2025; **Effectively published online:** 25 July 2025
Corresponding editor: P.W. Crous

INTRODUCTION

The genus *Russula* is the second largest genus of ectomycorrhizal (ECM) fungi and is distributed worldwide. Based on recent analyses of fungal diversity in soils Tedersoo *et al.* (2022) concluded that *Russula* is one of the most species rich genera of soil fungi with an estimated molecular diversity of 20000 operational taxonomic units (OTUs) worldwide. In neotropical montane forests, the /russula-lactarius lineage is the most diverse and frequent ECM lineage (Corrales *et al.* 2022), but the diversity of *Russula* species is considerably underexplored in Central and South America (Manz *et al.* 2021). Until now, only 79 species of the genus were originally described from Central and South America in contrast to hundreds of species described and reported from Europe, North America and Asia (Buyck 2007, Adamčík *et al.* 2019, Vera *et al.* 2021, Miller *et al.* 2024).

Due to their obligate symbiotic lifestyle, the distribution of *Russula* species depends on the presence of suitable plant partners (Beenken 2004). Some species are generalists regarding their plant association (De Lange *et al.* 2023), others

Fungal Systematics and Evolution is licensed under a Creative Commons Attribution-NonCommercial-NoDerivatives 4.0 International License

© 2025 Westerdijk Fungal Biodiversity Institute

exhibit high specialisation, forming interactions exclusively with species of a single plant genus (Looney *et al.* 2016). Evolutionary processes shaping the diversity of strongly specialised ECM fungi are expected to be dependent from the factors influencing the migration of their associated ECM host plants such as their ecological preferences and dispersal abilities. On the other hand, successful colonization of new habitats by ECM plant hosts also depends on the presence of compatible ECM fungal partners or the ability of these fungal partners to co-migrate (Delavaux *et al.* 2019). As a result, some *Russula* species are intercontinentally distributed, others are endemic to a single region (Caboň *et al.* 2019, Noffsinger *et al.* 2024). It is well known that persistent reproductive isolation after migration leads to speciation of tree species, but the co-speciation of the equally isolated fungal symbionts is rarely considered.

The region of the Isthmus of Panama and adjacent regions are an ideal area to investigate a possible co-speciation of ECM fungi and their plant symbionts because the geological processes of the region are well understood. The closure of the Isthmus of Panama during the Pliocene and Pleistocene led to the Great American biotic interchange allowing a bidirectional migration of organisms between the Americas (Cody *et al.* 2010), during which *Quercus* species migrated from Central America to their current southern distribution limit in Colombia (Hooghiemstra 2006). In this region, *Russula* species are known to associate with tree species of *Fagaceae* (Vera *et al.* 2021, Buyck *et al.* 2022).

Today, tropical montane rainforests dominated by ECM *Fagaceae* trees harbour a unique diversity of *Russula* species (Gómez & Alfaro 1996, Manz *et al.* 2021). Tropical *Quercus* forests extend from Mexico to Colombia and 172 species of *Quercus* are known from Mexico alone (Cavender-Bares 2019). *Quercus* diversity decreases southwards: only nine species are present in Costa Rica (Hammel *et al.* 2010), nine in Panama (Mireya *et al.* 2004), and a single species, *Quercus humboldtii,* in Colombia. The only other species of *Fagaceae* present in this area is *Trigonobalanus excelsa*, which is endemic to Colombia (Vasco-Palacios *et al.* 2022). *Trigonobalanus* is a tree genus with a tropical amphi-pacific disjunct distribution comprising three species, the other two species are distributed in Southeast Asia (Melville 1982). The timespan and exact pathway of migration of the ancestor of *T. excelsa* from North America to Colombia is still unknown due to the lack of fossil data (Van der Hammen & Cleef 1983). It is likely, that some *Russula* species are strictly associated to *T. excelsa*, therefore we hypothesize that some *Russula* species migrated to Colombia together with *T. excelsa* and that their evolutionary history and current distribution differs from *Russula* species that migrated to Colombia together with *Quercus* species.

In the present study, we focus on *Russula* subsect. *Castanopsidum*, which is reported for the first time from *Fagaceae* forests of Central and South America. The subsection was recently described and is morphologically defined by a pseudoparenchymatic pileipellis forming a rapidly rupturing cuticle becoming granulose to areolate and a slender, frequently furfuraceous stipe that is longer than the pileus diameter (Rossi *et al.* 2020). So far, three formally described species from tropical areas of Southeast Asia (*R. castanopsidis, R. purpureogracilis*, *R. darjeelingensis*) and one undescribed species from North America were placed in subsect. *Castanopsidum* (Paloi *et al.* 2018, Adamčík *et al.* 2019, Rossi *et al.* 2020).

The present study forms part of a long term international scientific collaboration and is based on multiple field visits to Colombia and Panama. Our collections obtained from *Quercus* and *T. excelsa* forests in Colombia and Panama had purple or red pileus colours and resembled *R. purpureogracilis*. We recognized two distinct morphotypes in the field, one with a dark purple pileus colour and very strongly reddish-purple coloured stipes present only in *Trigonobalanus* forests in Colombia and another with paler purple pileus colours and white stipes with only a slight pinkish hue present in both Colombia and Panama. Our hypothesis is that these collections represent two distinct species of subsect. *Castanopsidum* with one of them potentially including two subspecies, which diversified recently along the Isthmus of Panama. We aim to understand the broader phylogenetic relationships, evolutionary history and morphological differences of *Castanopsidum* members in the area around the Isthmus of Panama.

MATERIALS AND METHODS

Sampling

Specimens were collected during field expeditions carried out in 2018 and 2022 in the provinces of Huila and Santander, Colombia and in 2018 in the Chiriquí province in Western Panama. All specimens were collected in premontane and montane tropical forests at elevations ranging between 1500 to 2200 m. In Colombia, all collecting sites were dominated by ECM species of *Fagaceae*, mainly *Q. humboldtii* and *T. excelsa*. In Panama, several species of *Quercus* were present, but *Q. humboldtii* was not. Colombian collections were deposited at the herbaria HUA, SAV and the recently created fungal collection hosted at the Universidad del Rosario (FUNGIUR). Panamanian collections were deposited at UCH (for acronyms see Index Herbariorum, Thiers, continuously updated). We searched the literature for morphologically similar species described from montane oak forests of Central America and Colombia and subsequently included the holotype specimen of *R. atroamethystina* as well as a collection labelled as "*R. epochnoa*" deposited at F in our analyses. Two recent collections of an undescribed *Russula* species from subsect. *Castanopsidum* from Florida, USA were also included in the molecular analysis.

Molecular analysis

Genomic DNA was extracted from fresh and dried basidiomata and stored in 2× cetyltrimethylammonium bromide (CTAB) following Gardes & Bruns (1993). DNA amplification was performed using 5× HOT FIREPol Blend Master Mix (Solis BioDyne, Tartu, Estonia) or *Taq* DNA Polymerase (VWR, Darmstadt, Germany) following the manufacturers' instructions. Six loci were amplified and sequenced: (i) nuc rDNA ITS1-5.8S-ITS2 (ITS); (ii) D1–D2 domains of nuc 28S rDNA (28S); (iii) and the largest subunit of RNA polymerase II, subunit 1 (*rpb1*); (iv) the region between domains 6 and 7 of the nuclear gene encoding the second largest subunit of RNA polymerase II (*rpb2*); (v)

© 2025 Westerdijk Fungal Biodiversity Institute

DNA replication licensing factor, MCM7 component (*mcm7*) and (vi) a portion of transcription elongation factor 1-alpha (*tef1*). The ITS region was amplified using the primer pair ITS5 and ITS4 or alternatively ITS5-ITS2 and ITS3-ITS4 (White *et al.* 1990, Gardes & Bruns 1993); 28S using LR0R (Cubeta *et al.* 1991) and LR5 (Vilgalys & Hester 1990); *rpb2* using bRPB2-6F and bRPB2-7.1R (Matheny 2005), or alternatively backwards primers 7cRruss1/7cRruss2 were used (Buyck *et al.* 2018); *rpb1* using fRPB1-Af (Stiller & Hall 1997) and fRPB1-Cr primers (Matheny *et al.* 2002); gene *mcm7* using *Mcm7*-709for and *Mcm7*-1348rev primers (Schmitt *et al.* 2009) and *tef1* using 983F and 2218R, or by additional internal primers 1567R and 1577F (Rehner & Buckley 2005). Polymerase chain reaction (PCR) cycling conditions for 28S, *rpb1*, and *rpb2* loci were the same as described in Buyck *et al.* (2020), for *mcm7* as described in Schmitt *et al.* (2010) and for *tef1* the touchdown PCR procedure was used as described in Don *et al.* (1991). Reaction conditions for ITS started with initial denaturation step at 95 °C for 15 min followed by 35 cycles each comprising of denaturation at 95 °C for 30 s, annealing at 56 °C for 30 s and elongation at 72 °C for 90 s. A final extension was carried out at 72 °C for 10 min. Amplicons were purified using ExoSap-IT (Thermo Fisher Scientific, Wilmington, Delaware) and sent to Seqme Company (Dobříš, Czech Republic), Macrogen Korea (Seoul, South Korea) or Microsynth Seqlab (Swiss) for Sanger sequencing.

Phylogenetic analysis and molecular timing

Sequences were edited in the BioEdit v. 7.2.5 sequence alignment editor (Hall 2013) and Geneious v. R10 (Kearse *et al.* 2012). Intraindividual polymorphic sites having more than one signal were marked with International Union of Pure and Applied Chemistry (IUPAC) ambiguity codes. We used sequence data published by Adamčík *et al.* (2019) and Rossi *et al.* (2020) for the phylogenetic placement of the studied species. We analysed publicly available ITS sequences retrieved by BLAST searches for estimating species diversity and distribution patterns of subsect. *Castanopsidum*. Each gene alignment was first automatically constructed using MAFFT v. 7.487 (Katoh & Standley 2013) with the E-INS-i strategy and manually edited in AliView v. 1.27 (Larsson 2014). A concatenated dataset partitioned by locus was automatically assembled by the program. We used complete sequences of all DNA regions. No sites were excluded. All sequences obtained in this study and their accession numbers are listed in suppl. Table S1 and the alignment is available from Figshare (doi: 10.6084/m9.figshare.29028260.v1).

The multilocus (ITS, 28S, *rpb1*, *rpb2*, *mcm7* and *tef1*) alignment of *Russula* subsect. *Castanopsidum* was supplemented by samples of a clade identified as sister by Rossi *et al.* (2020) as subsect. *Tricholomopsidum*. A time calibrated phylogeny was created in BEAST v. 2.7.6 (Bouckaert *et al.* 2019) using five secondary calibration estimates from Looney *et al.* (2016). The five nodes assigned age priors included the *Russula*/Crown Clade split at 25.96 [95 % posterior density (HPD) 19.36–33.72] M yr ago (mya), *R. lepida* Fr. split at 21.86 [15.88–28.5 HPD] mya, *R. romellii* split 18.95 [13.86–24.57 HPD] mya, *Lilaceinae* split at 15.81 [11.78–20.34] mya, and subsections *Lilaceinae*/*Roseinae* split at 14.04 [10.26–18.35 HPD] mya. The MCMC analysis was run three times for 50 M generations, storing every 10000 trees under the Yule model. The package bModelTest implemented in BEAST v. 2 was used to infer and marginalize site models (Bouckaert & Drummond 2017). Tracer v. 1.7.2 was used to summarize the posteriors and confirm that all MCMC chains reached convergence with ESS values > 200 (Rambaut *et al.* 2018). A concatenation of the resulting trees with a burn-in of 10 % was created using LogCombiner v. 2.6.3. A maximum clade credibility tree with mean node heights was summarized using TreeAnnotator v. 2.6.3. Phylogenetic informativeness of the genes used in the chronogram was assessed using PhyDesign (López-Giráldez & Townsend 2011, suppl. Fig. S1).

For the maximum likelihood (ML) analysis, a phylogeny was inferred using raxmlGUI v. 2.0.10 (Edler *et al.* 2021). To find an optimal site model for each locus ModelTest -NG v. 0.1.7 was used and the optimal model based on BIC was applied to each locus for the analysis (Darriba *et al.* 2020). The models applied were: HKY+G4 for ITS, K80+I for 28S, TrNef for *mcm7*, TrNef+G4 for *rpb1*, TPM2+G4 for *rpb2*, and K80+I for *tef1*. The analysis was run with rapid bootstrapping under the autoMRE function, which estimates an optimal number of bootstrap replications while reducing computational burden. *Russula betularum* Hora (BPL269), a member of the *Russula* core clade of subgenus *Russula*, was chosen as the outgroup following Looney *et al.* (2016).

An additional ITS data set was analysed on the CIPRES Science Gateway (Miller *et al.* 2010) as a partitioned data set to the ITS1, 5.8S, and ITS2 loci (as recommended by Petkovits *et al.* 2011) under the GTR+GAMMA model with 1000 bootstrap iterations (Stamatakis 2014).

Morphological analysis

Ephemerous morphological features were described based on fresh basidiomata in the field following Adamčík *et al.* (2019). All samples were processed as voucher herbarium specimens by dehydration on a food dryer at 40 °C for 24 h or were dried in plastic zip lock bags using silica gel. All micromorphological structures were observed following the standards proposed by Adamčík *et al.* (2019). Micromorphological characteristics were observed using an Olympus BX-43 microscope with an oil immersion lens at a magnification of 1000× (Tokyo, Japan). The structures were visualized and illustrated with a camera lucida using an Olympus U-DA drawing attachment at a projection scale of 2000×. The structures and contents of hymenial cystidia and pileocystidia were observed and measured in ammoniacal Congo red preparations from dried material. Basidiospores were observed on the surface of lamellae in Melzer's reagent and measured using Promicra camera (Prague, Czech Republic). All other microscopic observations were made in ammoniacal Congo red after a short treatment in an aqueous 10 % KOH solution to dissolve any gelatinous matrices and improve tissue dissociation. Additionally, all tissues were examined in Cresyl blue to detect the presence of ortho- or metachromatic reactions following Buyck (1989). Trama and cystidia were observed in a sulfovanillin solution (Caboň *et al.* 2017). To check for acid-resistant incrustations on pileipellis elements, tissues were stained with carbolfuchsin and observed in distilled water after incubation in a 10 % HCl solution (Romagnesi 1967). Colour codes follow (Kornerup & Wanscher 1978).

© 2025 Westerdijk Fungal Biodiversity Institute

RESULTS

Phylogenetic analysis

All collections of *Russula* from Panama, Colombia, and North America considered for the present analysis were placed in a strongly supported clade (ML = 98, BI = 1.0) corresponding to *Russula* subsect. *Castanopsidum* in the multilocus phylogenetic analysis (Fig. 1). All terminal clades corresponding to species or subspecies had strong support in both analyses (ML > 90, BI = 1.0). All American collections were placed in a strongly supported clade (ML = 96, BI = 1.0) that is sister to a clade formed by Asian species (ML = 96, BI = 1.0). The phylogeny supported four Asian species: *R. castanopsidis*, *R. darjeelingensis*, *R. purpureogracilis* and an undescribed species represented by a clade of Chinese samples sister to *R. castanopsidis*. Within the American clade, four strongly supported terminal clades were present. One of them included only samples from Florida, USA. All Colombian and Panamanian collections clustered together in a moderately supported clade (ML = 66, BI = 0.95). Within this clade, four collections from forests dominated by *T. excelsa* represent a species described here as *R. esperanzae sp. nov*. Sequences of the remaining collections from Colombia and Panama associated with *Quercus* form a clade that is sister to this new species. They are further separated into two strongly supported sister clades which are clearly grouped based on their geographical origin. Despite the strong support in the multilocus phylogeny, we decided to rank them at the subspecies level. This agrees with the approach previously applied by Vera *et al.* (2021) and Buyck *et al.* (2022) for closely related *Russula* taxa that diversified along the Isthmus of Panama. We managed to obtain partial ITS sequences of older collections (F1114464, F1037069) from Costa Rica and Colombia which were both placed inside of the sister clade to *R. esperanzae*. Panamanian *Castanopsidum* collections formed a strongly supported monophyletic clade (ML = 99, BI = 1.0) including the holotype of *R. atroamethystina*, which was collected in Costa Rica. Colombian collections are described as a new subspecies, namely *R. atroamethystina* subsp. *guacahayoensis subsp. nov*., and are placed as sister to the typical subspecies. The sample F1037069 labelled as "*R. epochnoa* nom. inval." from Colombia clustered within this new subspecies clade and represents the oldest sequenced collection of subsect. *Castanopsidum* deposited in herbaria globally (collected in 1968).

Molecular timing and phylogenetic informativeness

The stem age for *Castanopsidum* has a mean of 15.1 (12.5–17.8 HPD) M years with the American members splitting off from the Southeast Asian members 11.0 (8.0–14.1 HPD) mya. The Central and South American clades split from the North American clade 8.2 (5.3–11.4 HPD) mya. *Russula esperanzae* split from *R. atroamethystina* 6.4 (3.7–9.2 HPD) mya. The mean age of the *R. atroamethystina* clade is 2.9 (1.4–4.8 HPD) million years. According to the phylogenetic informativeness profile, *rpb2* is the best gene marker for resolving clades between the ages of about 1.5 and 27 million years and the second-best gene for resolving clades between the ages of 0 and 1.5 million years. ITS is the best gene marker for resolving clades between the ages of about 0 and 1.5 million years. *Tef1* was the second-best gene at resolving clades between the ages of 2.5 and 22 million years. *Rpb1* was the second-best gene at resolving clades between the ages 22 and 27 million years. 28S was the least phylogenetically informative gene marker across most ages (suppl. Fig. S1).

Morphology

The species of *Russula* subsect. *Castanopsidum* included in the present study are easy to distinguish from each other in the field. *Russula esperanzae* has smaller basidiomata than *R. atroamethystina* with stipe surfaces that are predominantly greyish red in colour. The basidiomata of *R. atroamethystina* usually have a completely white stipe or occasionally an indistinct pink hue. It is difficult to tell the two subspecies of *R. atroamethystina* apart in the field, but their areas of distribution are geographically separated by the Isthmus of Panama. In addition to macroscopic distinctive characteristics, *R. esperanzae* has larger spores and wider basidia than *R. atroamethystina*. *Russula atroamethystina* subsp. *guacahayoensis* differs by hymenial cystidia on average longer than 95 µm compared to the typical subspecies with hymenial cystidia on average shorter than 82 µm (suppl. Table S2). Three collections of subsp. *guacahayoensis* have very short terminal cells of hyphae near the pileus margin (on average up to 12 µm), but observations on one Colombian collection (Corrales861) overlap with values observed in subsp. *atroamethystina*. The microscopic differences between the two subspecies of *R. atroamethystina* observed on our recent material are consistent with our observations from the holotype of *R. atroamethystina* from Costa Rica and the collection of "*R. epochnoa* nom. inval." from Colombia.

TAXONOMY

Russula atroamethystina subsp. ***atroamethystina*** Alfaro *et al.*, *Revista de Biologia Tropical* **44** (Suppl. 4): 25. 1997. Figs 2A–D, 3–4.

Original description (Alfaro *et al.* 1997): *Pileus hemisphaericus umbilicus depressus lilaceo–amethystinus, in sicco violaceus, subvelutinus deinde rimulosus, semigranulosus, obtusus, marginibus laevibus, non viscidus, 29–39 mm latus. Lamellae albae, aequalis, raro furcatae et anastomosantes, adnexae–subliberae. Sporae Ia–Ib. Basidiis 33–45.8 × 13–13.8 µm, praecipue 4–sporis sed raro 2–sporis. Cystidiis 35–62 × 7.5–11 µm in sulphovanillinae non caerulascens apice dense hyalino–incrustatis, parietibus laevibus, fusoideis deinde acutae vel subacutis vel ampullaceis, numerosis. Sphaerocystidiis numerosis. Hyphae inamyloideae, fibulae nullae. Epicutis ca. 100 µm, intracellulis roseis, KOH evanescens. Dermatocystidiis: a) clavato–ventricosis 12–15–25 × 4–11 µm, b) subvesiculosis 20–26 × 10–17 µm, c) hymenocystidiis similis sed longitudine albescens (*fig. *1 a, b).*

Typus: **Costa Rica**, Provincia de Cartago, San Cristóbal Sur, alt. 1860 m, in a mixed stand of *Quercus*, 9 Jun. 1984, *R. Singer*, B14600A (**holotype** F1114464).

© 2025 Westerdijk Fungal Biodiversity Institute

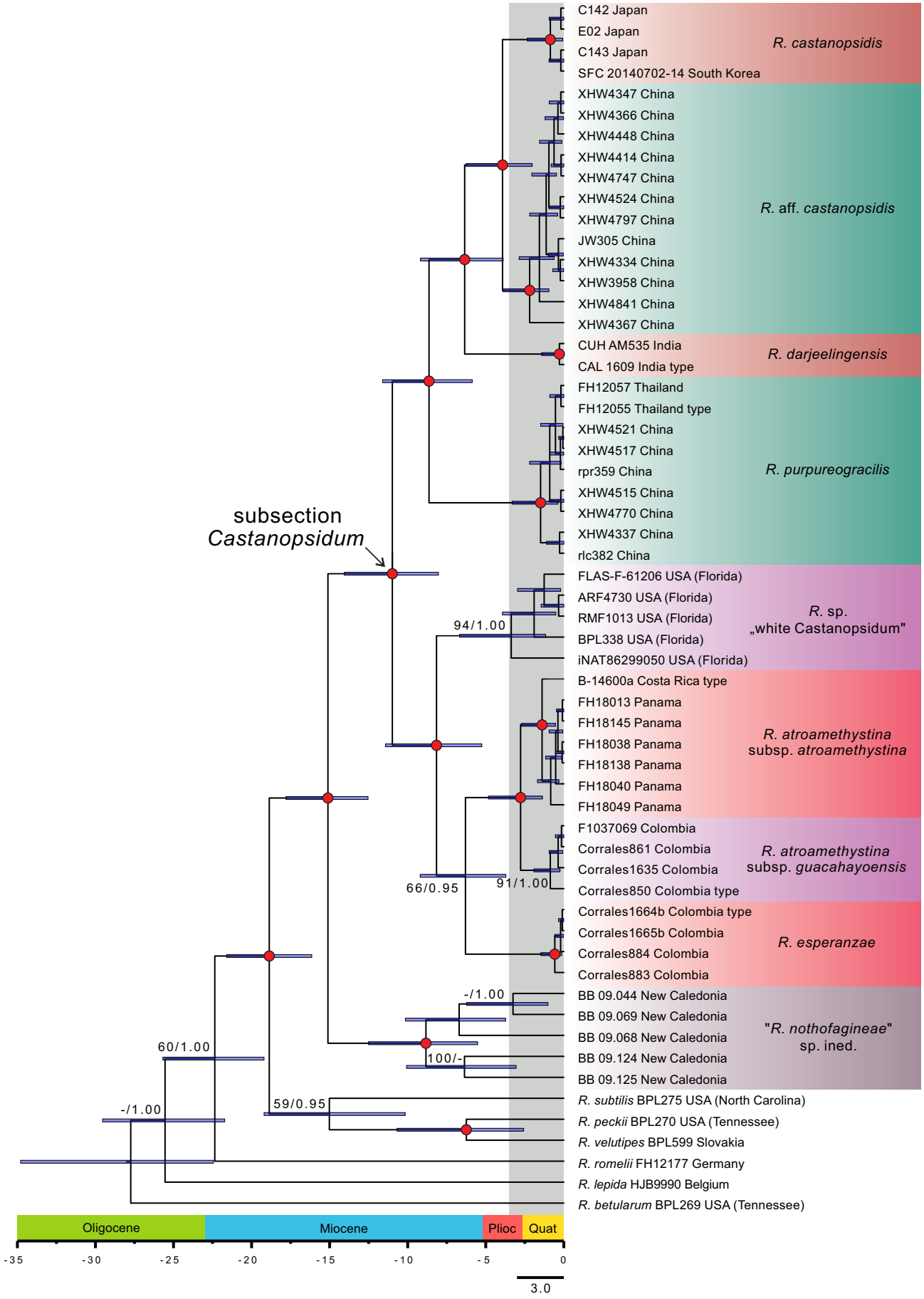

Fig. 1. The phylogeny of *Russula* subsection *Castanopsidium* from Bayesian and ML analyses. The main topology shown is a clock constrained tree constructed with BEAST using ITS, LSU, *mcm7*, *rpb1*, *rpb2* and *tef1* regions. Strongly supported nodes (BI = 1 and ML > 95) are labelled by a red circle. Bootstrap support values (ML) > 50 % and posterior probabilities (BI) > 0.95 are also provided for some nodes supported at least by one of the analyses. Vertical grey background indicates estimated evolutionary time of oak diversification (3.5 mya). The scale axis shows the estimated evolutionary time (in million years) computed under a lognormal relaxed molecular clock.

© 2025 Westerdijk Fungal Biodiversity Institute

Field description (field aspect based on recent Panamanian collections): Pileus medium sized, 12–45 mm (n = 21) in diam., when young convex to almost cylindrical with flattened top, then expanding first with incurved margin, later completely expanded with slightly depressed centre; margin with frequent radial crackings, mature striate up to 4 mm; cuticle dry, smooth, matt, finely pruinose at centre, towards the margin cracking into fine areolate patches, difficult to peel up to 1/3 of the radius, near the margin pinkish white (10A2), pale red (10A3), pastel red (10A4), old rose (10C5) or greyish ruby (12D3–4), towards the centre greyish red (10C–D4), old rose (10C5), but most frequently greyish magenta (13E3–4), sometimes with champagne (4A4), light orange (5A4) or salmon (6A4) discolorations. *Lamellae* 3–4 mm wide, thin, moderately distant, 8–9 in 1 cm near the pileus margin, adnexed, white to yellowish white, in old fruiting bodies cream, without furcations or anastomoses, lamellulae absent, edges entire and concolourous. *Stipe* 35–50 × 4–10 mm (n = 21), more or less cylindrical, but mostly narrowing towards the very base, white but sometimes with a very pale rose hue, smooth with very fine white floccules, medulla firm in young fruiting bodies, cottony stuffed with age. *Context* white, brittle to fragile, unchanging when damaged, 2–3 mm thick at half of pileus radius, *taste* mild,



Fig. 2. Basidiomata of studied specimens of *Russula* subsect. *Castanopsidum*. **A–D.** *Russula atroamethystina* subsp. *atroamethystina*. **A.** FH-18-145, bottom right corner: eosin red colour reaction with sulfovanillin. **B.** Dry material of the holotype collection (B-14600a). **C.** FH-18-138. **D.** FH-18-038. **E.** *Russula atroamethystina* subsp. *guacahayoensis* (Corrales850 HT). **F.** *Russula esperanzae* (Corrales883).

© 2025 Westerdijk Fungal Biodiversity Institute

but slightly bitter to astringent or like cedar wood after a few seconds, *odour* inconspicuous, *macrochemical reactions*: guaiac after 5 seconds negative on stipe and negative to weakly positive (+) on lamellae surfaces, FeSO4 pale orange, sulfovanillin eosin red. *Spore print* not observed, but probably white or cream. *Spores* (6.5–)7.2–7.8–8.4(–9.1) × (5.4–)6.0–6.5–7.0(–7.9) µm, subglobose to broadly ellipsoid, Q = (1.06–)1.14–1.20–1.26(–1.37), ornamentation of moderately large, narrowly conical, acute and moderately distant to dense [(3–)4–6(–11) in a 3 µm diam. circle] amyloid spines, 0.8–1.3 µm high, occasionally fused in pairs or small groups [0–2(–5) fusions in the circle], connected by dispersed to occasional, thin, short line connections [0–2(–5) in the circle], isolated spines occasional; suprahilar plage moderately large, amyloid, not descending onto hilum and covered by very low ornamentation. *Basidia* (15–)25–31.8–39(–49) × (5–)9–11–13(–14) µm, 4–spored, broadly clavate; basidiola cylindrical, ellipsoid or clavate, 6–11.5 µm wide. *Hymenial cystidia* dispersed, 350–450 per mm^2, (40–)61–76.2–91.5(–110) × (9–)10.5–12.9–15(–21) µm, very variable in size, some very large, originating in subhymenium and somewhat protruding over basidia, fusiform, apically acute, with or without 3–11(–18) µm long appendage, often distinctly thick-walled especially towards basal septum (up to 1 µm), contents usually consisting of refractive bodies at the apical part, often with some dispersed inclusions in central part, rarely also optically completely empty, in sulfovanillin not reacting but with pink incrustations; near lamellae edges abundant, smaller and narrower, measuring (20–)42–61.1–80.5(–108) × (5–)7–10.8–14(–19) µm, mainly fusiform or subulate, rarely subcylindrical, mainly acute, occasionally obtuse, often with 2–9(–12) µm long appendage. Lamellae edges sterile, *marginal cells* similar to basidiola but shorter, (7.5–)12–17.7–23(–36) × (4–)6–8.3–10(–12) µm, clavate, obpyriform or sphaeropedunculate, apically obtuse. *Pileipellis* orthochromatic in Cresyl blue, not sharply delimited from the underlying context, ca 30–60 µm deep; vaguely divided in 10–20 µm deep, not gelatinized suprapellis of erect or ascending, loose hyphae; and 25–40 µm deep subpellis of dense, subglobose, inflated, irregularly oriented, 4–13 µm wide hyphae. *Acid-resistant incrustations* on primordial hyphae present, especially abundant on basal parts and nearly absent at the terminal part. Hyphal terminations near the pileus margin composed of chains of 1–3(–4) unbranched, relatively short, ellipsoid or cylindrical cells, thin-walled, sometimes flexuous, terminal cells (6–)11–17.2–23(–51) × (3–)4–5.7–7.5(–15) µm, cylindrical, ellipsoid, clavate, sometimes slightly attenuated or pyriform, apically obtuse; subterminal cells branched or unbranched, usually inflated, sometimes cylindrical. Hyphal terminations near the pileus centre distinctly shorter and consisting of a single cell or a pair of unbranched cells, terminal cells (4.5–)7.5–11.7–16(–28) × (3–)5–6.7–8.5(–11) µm, ellipsoid to globose; subterminal cells and cells below inflated, mainly globose,

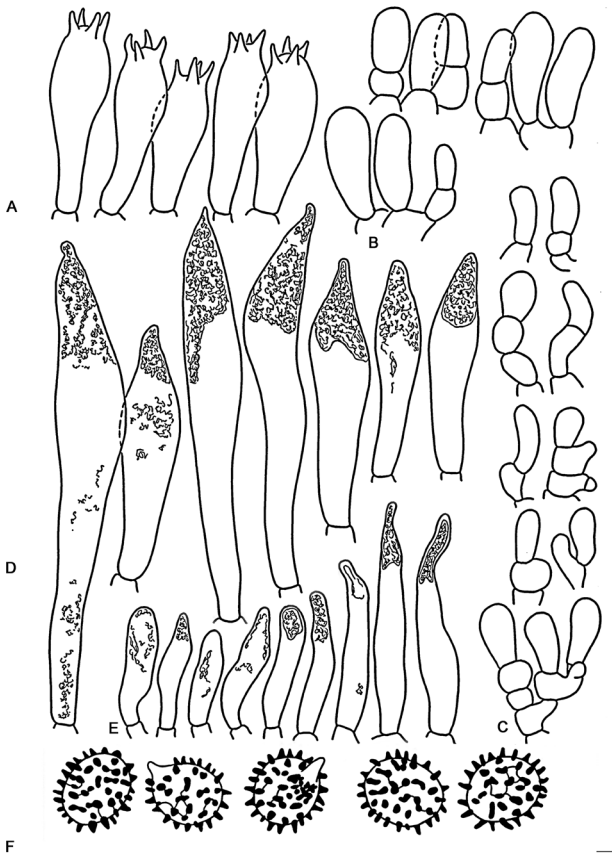

Fig. 3. Hymenial elements of *Russula atroamethystina* subsp. *atroamethystina* (B-14600a HT). **A.** Basidia. **B.** Basidiola. **C.** Marginal cells. **D.** Hymenial cystidia. **E.** Hymenial cystidia near the lamellae edges. **F.** Spores as seen in Melzer's reagent. Scale bar = 10 µm, but only 5 µm for spores.

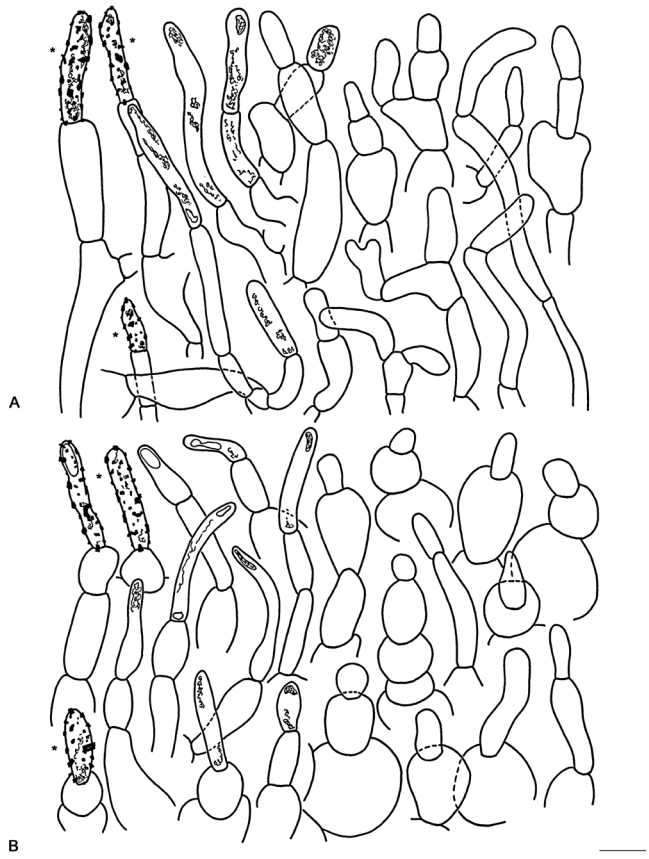

Fig. 4. Elements of the pileipellis of *Russula atroamethystina* subsp. *atroamethystina* (B-14600a HT). **A.** Hyphal terminations and primordial hyphae with contents near the pileus margin. **B.** Hyphal terminations and primordial hyphae with contents near the pileus centre. Asterisks (*) mark primordial hyphae observed after carbolfuchsin treatment with acid resistant incrustations. Scale bar = 10 µm.

© 2025 Westerdijk Fungal Biodiversity Institute

ca 10–13 µm wide, forming pseudoparenchymatic subpellis. *Primordial hyphae* near the pileus margin numerous and conspicuous, 1–3(–5)-celled, composed of cylindrical, straight or slightly curved cells, arising directly from inflated cells of subpellis, thin-walled, terminal cells (7–)14–27.4–40.5(–61) × (2–)3–4.7–6(–12) µm, cylindrical or subulate, occasionally also fusiform, apically obtuse or somewhat tapering; contents with dispersed refringent inclusions usually only in terminal cells, rarely also in subterminal cells. Primordial hyphae near the pileus centre smaller and less inconspicuous, usually 1–3-celled, terminal cells (9–)14–20.5–27(–45) × 3–4.9–6.5(–11) µm, cylindrical or subulate to lageniform, apically obtuse or somewhat tapering. *Cystidioid or oleiferous hyphae* absent, context turns purple in sulfovanillin, hyphae with strong purple incrustation in sulfovanillin present in pileus trama.

Additional specimens examined: **Panama**, Boquete, Finca Lerida, 08°49’10.25’’N, 82°29’09.22’’W, alt. 1820 m, on soil with *Quercus* sp., 13 Jun. 2018, *F. Hampe & C. Manz*, CM6560_FH18013 (UCH12211); ibid., 28 Jun. 2018, *F. Hampe & C. Manz* CM6662_FH18145 (UCH15967); ibid., Jaramillo Arriba, El Musgo, 08°47’26.9’’N, 82°24’34.4’’W, alt. 1670 m, on soil with *Quercus* sp., 15 Jun. 2018, *F. Hampe & C. Manz* CM6585_FH18038 (UCH12216); ibid., CM6587_FH18040 (UCH15966); *ibid.* CM6596_FH18049 (UCH12219); ibid., 24 Jun. 2018, *F. Hampe & C. Manz* CM6656_FH18138 (UCH12237).

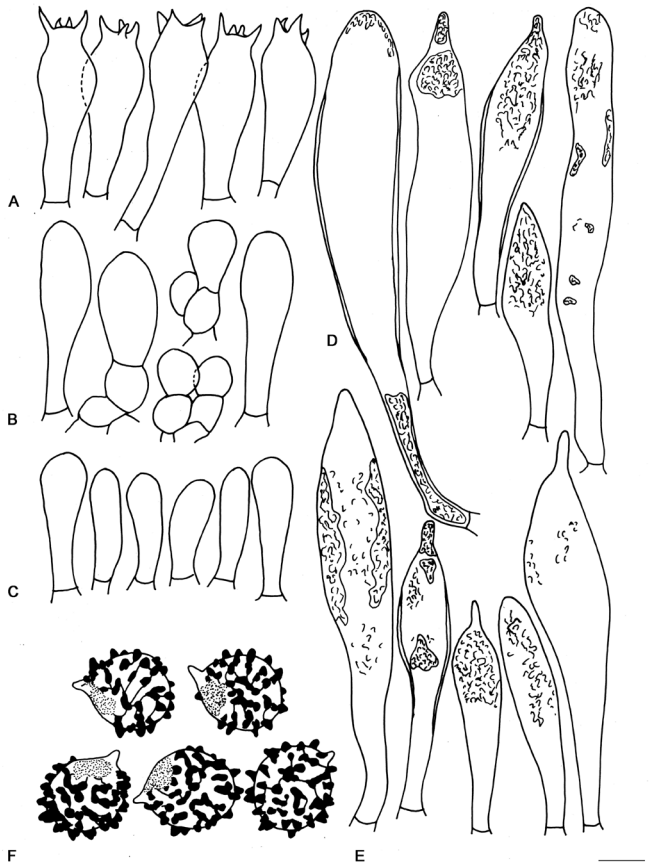

Fig. 5. Hymenial elements of *Russula atroamethystina* subsp. *guacahayoensis* (Corrales850 HT). **A.** Basidia. **B.** Basidiola. **C.** Marginal cells. **D.** Hymenial cystidia. **E.** Hymenial cystidia near the lamellae edges. **F.** Spores as seen in Melzer’s reagent. Scale bar = 10 µm, but only 5 µm for spores.

Russula atroamethystina subsp. ***guacahayoensis*** Corrales & Ortiz-Suarez, ***subsp. nov.*** MB 858787. Figs 2E, 5–6.

Etymology: “*guacahayo*” from Quechua language “Guaca–hayo” for Magdalena river which is the largest Colombian river situated in the basin where the type specimen was collected.

Typus: **Colombia**, Santander Province, Encino municipality, Cachalú Natural Reserve, 06°04’31.02’’ N, 7307’51.84’’ W, alt. 2120 m, on soil of *Quercus humboldtii* montane forest, 28 Jul. 2018, *A. Corrales & S. Adamčik*, Corrales850 (**holotype** SAV F-23335, **isotype** in HUA).

Short diagnosis: Differs from subsp. *atroamethystina* by its on average longer hymenial cystidia on lamellae sides and its occurrence on the other side of the Isthmus of Panama.

Description: *Pileus* medium sized, 40–48 mm in diam., young convex soon expanding plane with depressed centre, margin distinctly striated up to 5 mm, cuticle mat, dry and velvety, near margin soon cracking into small patches and becoming finely areolate, near centre rugulose and wrinkled, colour near margin pastel red (10A4), pale red (9A3, 10A3) or dull red (10B4) in old ones, near centre violet-brown (10E6, 10E7, 10F7). *Lamellae* narrow, 3.5–4 mm deep, moderately distant, 8–11 in 1 cm near the pileus margin, yellowish white (3A2–

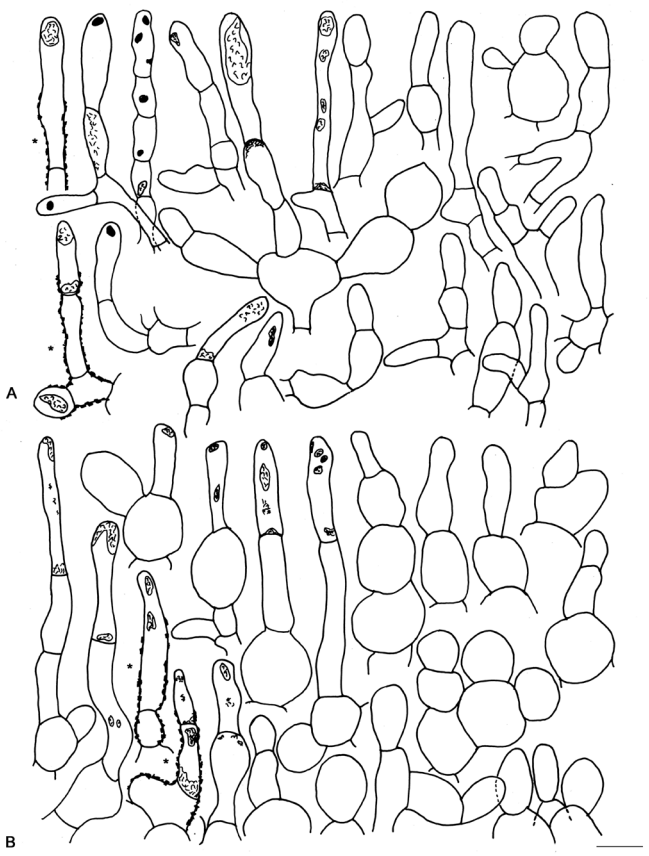

Fig. 6. Elements of the pileipellis of *Russula atroamethystina* subsp. *guacahayoensis* (Corrales850 HT). **A.** Hyphal terminations and primordial hyphae with contents near the pileus margin. **B.** Hyphal terminations and primordial hyphae with contents near the pileus centre. Asterisks (*) mark primordial hyphae observed after carbolfuchsin treatment with acid resistant incrustations. Scale bar = 10 µm.

© 2025 Westerdijk Fungal Biodiversity Institute

4A2); lamellulae absent, sometimes with furcations near the attachment to the stipe, edges entire and concolorous. *Stipe* 25–50 × 6–10 mm, cylindrical or clavate, white with greyish yellow spots near the base (4B3), surface strongly longitudinally striated. *Context* white, fragile in pileus, soft and flexible in stipe, unchanging when bruised, *taste* slightly bitter or acidic, *odour* fruity, pleasant, in stipe or when old like bleach or iodine, *macrochemical reactions*: eosin red with sulfovanillin. *Spore print* white. *Spores* (6.6–)7.4–8.0–8.6(–10.0) × (5.5–)6.3–6.8–7.3(–8.4) µm, subglobose to broadly ellipsoid, Q = (1.06–)1.11–1.18–1.24(–1.38); ornamentation of large, moderately distant to dense [(2–)4–7(–9) spines in a 3 µm circle], amyloid warts, (0.4–)0.8–1.2(–1.3) µm high; absent or frequently fused in pairs or short chains [0–3(–5) fusions in a 3 µm circle], connected by occasional fine line connections [(0–)1–2(–3) in a 3 µm circle], often forming branched structures but not reticulate, isolated elements rare; suprahilar plage large, amyloid. *Basidia* (8–)20.5–29.6–39(–66) × (5–)9–10.4–12(–14) µm, clavate, 4–spored; basidiola cylindrical or clavate, 6–12 µm wide. *Hymenial cystidia* widely dispersed to dispersed, ca 200–500/mm^2, (47.5–)70.5–99.7–129(–176) × (7–)10–13.5–17(–23) µm, mainly fusiform, occasionally clavate, pedunculate, apically mainly obtuse but occasionally acute, rarely with a 1–6(–21) µm long appendage, usually thick-walled (0.5–1 µm), contents with a large refractive body in the apical part, also with some dispersed inclusions in central part, no reaction in sulfovanillin but with faint purple incrustations; near lamellae edges smaller, (37–)55.5–76.2–97(–137) × (6–)8.5–11.5–14(–18) µm, fusiform or clavate, apically usually obtuse but occasionally acute, rarely with a 1–9(–16) µm long appendage, usually thick-walled, contents with a large refractive body in the apical or central part, sometimes with dispersed inclusions. Lamellae edges sterile, mainly composed of cystidia, *marginal cells* undifferentiated and similar to basidiola, (12–)14–19.5–24.5(–37) × (5–)7–8.7–10(–15) µm. *Pileipellis* orthochromatic in Cresyl Blue, gradually passing to the underlying context, 50–65 µm deep, vaguely divided into a 18–25 µm deep suprapellis of erect hyphal terminations forming an epithelium, and a pseudoparenchymatic, 30–50 µm deep subpellis of mainly inflated, densely arranged, ellipsoid to globose, 5–25 µm wide cells. *Acid-resistant incrustations* absent or weak on primordial hyphae, abundant in form of large droplets on hyphae in trama. Hyphal terminations near the pileus margin erect, 1–3 cells before they join inflated hyphae of subpellis, thin-walled, terminal cells (4–)7–11.7–17(–40) × (2–)4–5.7–8(–20) µm, mainly cylindrical or ellipsoid, occasionally pyriform or fusiform, apically obtuse; subterminal cells mainly branched, inflated, ellipsoid or subglobose, ca 5–12(–20) µm wide. Hyphal terminations near pileus centre composed of more inflated cells, maximum three originating from a single cell, terminal cells (5–)8–11.4–15(–26) × (2.5–)4.5–7.3–10(–16) µm, mainly subglobose or ellipsoid, rarely cylindrical or pyriform; subterminal and cells below in 2–4 ranks, inflated, ellipsoid or globose cells, ca 5–15(–25) µm wide. *Primordial hyphae* near the pileus margin inconspicuous, dispersed but also in small clusters, 1–3(–5)-celled, terminal cells (5–)10–18.4–26(–43) × (3–)3.5–4.6–6(–9) µm, usually cylindrical, apically obtuse; contents with few dispersed granulations or refringent patches usually only in terminal cell, but sometimes in subterminal or other cells below, no reaction in sulfovanillin, acid-resistant incrustations hardly visible, on basal cells only, in sulfovanillin with small, purple droplets only on subterminal or basal cells. Primordial hyphae near the pileus centre dispersed, often narrower and longer, 1–2(–4)-celled, terminal cells (5–)12–20.7–29(–44) × (2–)3–4.2–5(–8) µm, mainly cylindrical, apically obtuse. *Cystidioid or oleiferous hyphae* absent in the context, but hyphae with strong acid-resistant incrustations present.

Additional specimens examined: **Colombia**, Santander Province, Encino municipality, Cachalú Natural Reserve, 06°04’31.02’’N, 73°07’51.84’’W, alt. 2120 m, on soil of *Quercus humboldtii* montane forest, 29 Jul. 2018, *A. Corrales & S. Adamčík*, Corrales861 (SAV F-23336, duplicate in HUA); Huila Province, Acevedo municipality, La Palma protected forests of Serranía Peñas Blancas Reserve, 01°49’42.7’’N, 75°58’13.2’’W, alt. 1720 m, on soil of *Trigonobalanus excelsa* monodominant montane forest, 25 May 2022, *A. Corrales, A. Ortiz-Suarez, C. Parra & S. Adamčík*, Corrales1635 (SAV F-23319, duplicate in FUNGIUR); Cauca Province, 100 km from Cali, “Loz Araos”, 12 Apr. 1968, *R. Singer*, B6040 (F1037069), as “*R. epochnoa*” nom. inval.

Russula esperanzae Corrales & Ortiz-Suarez, ***sp. nov.*** MB 858786. Figs 2F, 7–8.

Etymology: In honour of Dr. Ana Esperanza Franco-Molano, mycologist, university professor, and pioneer of *Agaricales* studies in Colombia.

Typus: **Colombia**, Santander Province, Charalá municipality, in the protected forest of Finca El Roble property, 06°08’34.63’’N, 73°10’44.80’’ W, alt. 1660 m, on soil in *Trigonobalanus excelsa* montane forest, 31 May 2022, *A. Corrales, A. Ortiz-Suarez & S. Adamčík*, Corrales1664b (**holotype** SAV F-23326, **isotype** in FUNGIUR).

Short diagnosis: Differs from related American species *R. atroamethystina* in the greyish red coloured stipe, the distinctly larger spores with a much coarser ornamentation that is composed of more obtuse warts and short crests, as well as by its exclusive association with *Trigonobalanus*.

Description: *Pileus* small, 12–30 mm in diam., when young hemispherical, soon expanding plano-convex to plane with broadly depressed centre, margin strongly striate at 2–6 mm, when mature also crenulate, cuticle dry, distinctly granulose, towards centre also finely areolate, centre smooth, velvety, when wet shiny, colour when young and near margin when mature greyish ruby (12C7, 12D4) on white background, near centre dark ruby (12F5) with some reddish brown (8E4) small spots, peeling almost to centre. *Lamellae* 2–4 mm wide, moderately distant to distant, 7–18 in 1 cm near the pileus margin, white to yellowish white (3A1–3A2), lamellulae and furcations absent; edges entire or finely and irregularly serrulate, near pileus margin concolorous with pileus cuticle. *Stipe* 20–55 × 2.5–6 mm, cylindrical, flexuous, wider towards the base, surface strongly longitudinally striated and granulose, colour greyish red (9B6) or greyish ruby (12D6) on white surface, white at the base, with brownish yellow spots after handling or when bruised. *Context* white, soft and fragile in pileus, elastic in

© 2025 Westerdijk Fungal Biodiversity Institute

stipe, unchanging when bruised, *taste* slightly bitter, *odour* indistinct, *macrochemical reactions*: turning eosin red with sulfovanillin. *Spore print* white. *Spores* (7.9–)8.8–9.4–10.0(–10.9) × (6.5–)7.9–8.0–8.6(–9.3) µm, subglobose to ellipsoid, Q = (1.03–)1.12–1.18–1.25(–1.37); ornamentation of relatively large, moderately distant [(2–)3–6(–8) spines in a 3 µm circle] (0.7–)0.9–1.3(–1.7) µm high, amyloid warts or obtuse spines frequently fused in pairs or short chains or crests, [0–3(–5) fusions in a 3 µm circle], sometimes connected by fine line connections [0–3(–5) in a 3 µm circle]; suprahilar plage moderately large, amyloid. *Basidia* (12–)22–30.4–38.5(–52) × (7.5–)11–13.2–15.5(–20) µm, short, fusiform to clavate, 4-spored, basidiola cylindrical to clavate, ca 8–13 µm wide. *Hymenial cystidia* dispersed to moderately numerous, ca 350–870/mm^2, (55–)75–89.9–105(–122) × (9–)12.5–15.6–19(–23) µm, mainly fusiform, occasionally clavate, apically mainly obtuse, occasionally acute, rarely with a 1–8(–16) µm long appendage, thin-walled, occasionally with thickened walls (up to 1 µm), contents usually with a large refractive body in the apical part, sometimes with few more smaller spots in inflated central part, not reacting in sulfovanillin but with purple incrustations; near the lamellae edges (38–)55–74.4–94(–140) × (7–)10–13–16(–23) µm, mainly narrowly fusiform, occasionally clavate, apically usually obtuse, occasionally acute, rarely with 1–6(–11) µm long appendage, contents with single refractive body in apical part or sometimes with few dispersed inclusions or completely optically empty. Lamellae edges with dispersed basidia, *marginal cells* similar to basidiola on sides but often wider and shorter, (7–)12–17.6–23(–34) × (4.5–)7–9.2–12(–14) µm, clavate, subcylindrical or ellipsoid, apically obtuse. *Pileipellis* orthochromatic in Cresyl Blue, gradually passing to the underlying context, 55–65 µm deep, vaguely divided into a 25–30 µm deep suprapellis of erect hyphal terminations often clustered into small pyramidal structures, gradually passing to a pseudoparenchymatic, 25–35 µm deep subpellis of mainly inflated, densely arranged, ellipsoid to globose, 8–15 µm wide cells. *Acid-resistant incrustations* present, especially abundant on hyphae of subpellis. Hyphal terminations near the pileus margin erect, densely septate, and composed of 1–3(–5) cells before branching, thin-walled, terminal cells (6–)12.5–19.9–27.5(–50) × (3–)4–5.2–6.5(–11) µm, mainly cylindrical, occasionally clavate, rarely subulate, few nodulose, apically obtuse and often with glutinous coating not colouring in any reagent; subterminal cells and cells below mainly branched, few inflated, ellipsoid or cylindrical, originating from longer and narrower cells of subpellis, 2–10 µm wide. Hyphal terminations near the pileus centre forming a dense epithelium, always erect, formed by 1–2 cells before branching, terminal cells (7–)9.5–13.9–18.5(–32) × (2–)4.5–6.5–8.5(–16) µm, mainly ellipsoid or cylindrical, occasionally pyriform or clavate, subterminal cells in 1–3 ranks, inflated, ellipsoid or subglobose, 6–21 µm wide. *Primordial hyphae* near the pileus margin inconspicuous, dispersed but also in small fascicules, 1–4-celled, terminal cells (10–)13–21.2–29(–52.5) × (3–)4–5.2–6.5(–9) µm,

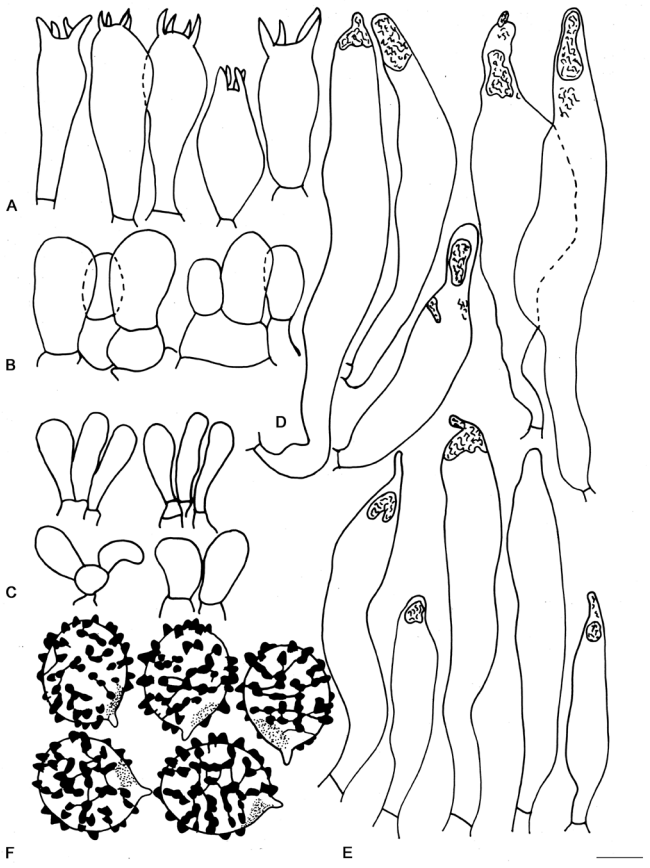

Fig. 7. Hymenial elements of *Russula esperanzae* (Corrales884). **A.** Basidia. **B.** Basidiola. **C.** Marginal cells. **D.** Hymenial cystidia. **E.** Hymenial cystidia near the lamellae edges. **F.** Spores as seen in Melzer's reagent. Scale bar = 10 µm, but only 5 µm for spores.

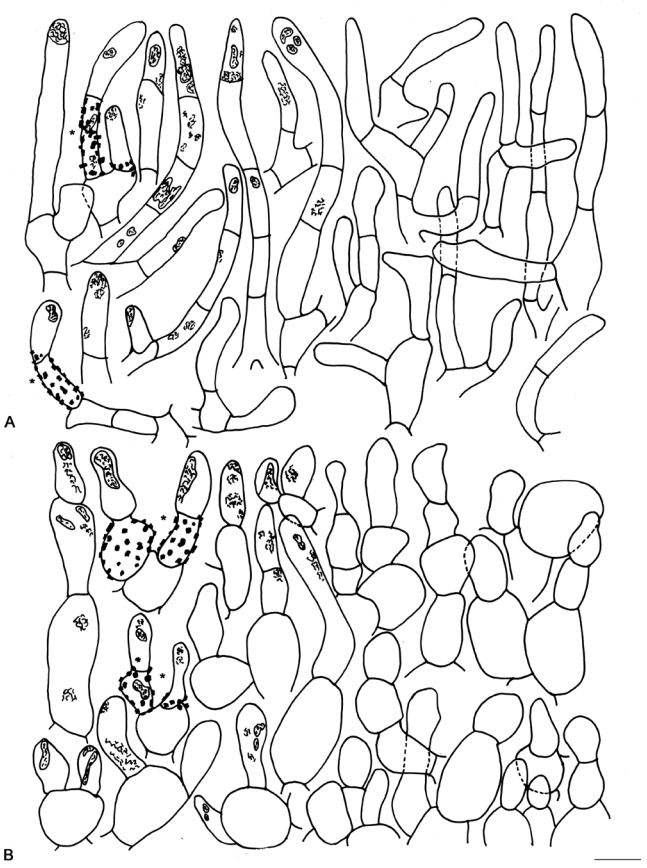

Fig. 8. Elements of the pileipellis of *Russula esperanzae* (Corrales884). **A.** Hyphal terminations and primordial hyphae with contents near the pileus margin. **B.** Hyphal terminations and primordial hyphae with contents near the pileus centre. Asterisks (*) mark primordial hyphae observed after carbolfuchsin treatment with acid resistant incrustations. Scale bar = 10 µm.

© 2025 Westerdijk Fungal Biodiversity Institute

cylindrical or clavate, apically obtuse, contents with few dispersed refringent patches or granulations usually only in terminal cells but sometimes also in subterminal cells, no reaction in sulfovanillin, with few large droplets of acid–resistant incrustations on subterminal cells and below but not present on terminal cells, in sulfovanillin with small, purple droplets that become bigger towards the subpellis. Primordial hyphae near the pileus centre dispersed, even less conspicuous, 1–3-celled, terminal cells (8–)10.5–16.7–22.5(–37) × (3–)4–5.3–6.5(–8) µm, ellipsoid or cylindrical, occasionally also clavate or pyriform, apically obtuse; contents and incrustations similar to pileus margin. *Cystidioid or oleiferous hyphae* in the context absent.

Additional specimens examined: **Colombia**, Huila Province, Pitalito municipality, Hiking trail connecting vereda Resinas and Charguacal, 01°44’29.6183”N, 76°02’31.6542”W, alt. 1700 m, on soil in *Trigonobalanus excelsa* montane forest, 25 Nov 2021, *A. Corrales, A. Ortiz, C. Parra, P. Velazco*, Corrales 1427 (FUNGIUR); Santander Province, Charalá municipality, protected forest of Finca El Roble, 06°08’34.63’’N, 73°10’44.80’’ W, alt. 1660 m, on soil in *T. excelsa* montane forest, 31 May 2022, *A. Corrales, A. Ortiz-Suarez & S. Adamčík,* Corrales 1665b (SAV F-23327, duplicate in FUNGIUR); ibid., forest near Cobaría stream, 06°09’05.9’’N, 73°10’36.11’’W, alt. 1540 m, on soil in *T. excelsa* montane forest, 31 Jul. 2018, *A. Corrales & S. Adamčík*, Corrales884 (SAV F-23339, duplicate in HUA); ibid., Corrales883 (SAV F-23338, duplicate in HUA).

DISCUSSION

The ECM dominated montane forests of Panama and Colombia are mycologically underexplored ecosystems with many undescribed fungal species (Piepenbring *et al.* 2012, Vargas & Restrepo 2020). From these ecosystems, we described *R. esperanzae* as new species and *R. atroamethystina* was reported for the first time for Panama and Colombia with the Colombian specimens described as a new subspecies. Our study is the most complete multilocus phylogenetic study on *Russula* subsect. *Castanopsidum* (Adamčík *et al.* 2019, Rossi *et al.* 2020), which contributes to a better understanding of *Russula* diversity and speciation in the studied area.

Taxonomic discoveries in *Russula* subsect. *Castanopsidum*

The specimens collected in Panama matched the morphology of the holotype of *R. atroamethystina* described from Costa Rica (Gómez & Alfaro 1997). Molecular sequence data of these specimens formed a strongly supported monophyletic clade with the holotype in our phylogeny.

We also discovered the earliest record of the subsect. *Castanopsidum* in the Americas, which was a specimen collected by Rolf Singer in 1968 from Colombia and deposited in the Field Museum of Natural History in Chicago, USA (as “*R. epochnoa*” nom inval.). Some of our recent collections from *Quercus humboltdtii* and *Trigonobalanus excelsa* forests in Colombia were identical to Singer’s collection and closely related to *R. atroamethystina*. Here we describe these collections as *R. atroamethystina* subsp. *guacahayoensis*. *Russula atroamethystina* appears to be a common element of ECM communities in the region because we were able to recollect multiple specimens of both subspecies during our visits to the area. Further Colombian collections of subsect. *Castanopsidum* found exclusively in *Trigonobalanus* forests did not correspond to any previously described species and are here described as the new species *R. esperanzae*.

Morphological differences among the three taxa described in the present study correspond to genetic distances (Fig. 1). *Russula esperanzae* is placed on a long branch sister to both subspecies of *R. atroamethystina* in the phylogenetic tree and is well defined by morphological characteristics. Both subspecies of *R. atroamethystina* share morphological similarities and an association with *Quercus*, showing only minor microscopic differences. *Castanopsidum* species can be distinguished from the majority of *Russula* species by a small pileus diameter compared to the length of the stipe, a pileus surface that cracks and becomes areolate, white spore print, mild taste of context, and eosin red reaction of context to sulfovanillin. However, distinguishing species of *Castanopsidum* from species belonging to some other groups of *Russula* may be challenging. Species of *Russula* subsect. *Roseinae* can be strikingly similar and have a similar reaction of the context to sulfovanillin. A notable example is *R. cynorhodon*, described from Panama, which shares similar colours, basidiomata shapes and micromorphological features with *R. atroamethystina* (Manz *et al.* 2021). Additionally, *R. rubellipes* described from eastern USA is similar in the field and has a similar pileipellis structure (Fatto 1998, Looney *et al.* 2022). For a preliminary identification of *Castanopsidum* species in the field, the granulose pileus surface that develops into an areolate structure is helpful, because this is rarely found in *Roseinae* species. Distinguishing these two groups by microscopy is even more challenging because they share a pseudoparenchymatic subpellis structure, presence of short primordial hyphae and red staining of context and incrustations in sulfovanillin (Caboň *et al.* 2017). Therefore, future keys for species identification should include members of both subsections.

Rossi *et al.* (2020) and Adamčík *et al.* (2019) reported the presence of only one type of hyphal endings in the pileipellis for *R. castanopsidis*, but additional incrusted primordial hyphae were reported for the Asian species *R. purpureogracilis* (Adamčík *et al.* 2019) and incrusted pileocystidia for *R. darjeelingensis* (Paloi *et al.* 2018). Our observations on all American *Castanopsidum* taxa confirmed the presence of primodial hyphae with red incrustations in sulfovanillin, similar to *R. purpureogracilis*. It seems that the compositions of the pileipellis elements are variable between *Castanopsidum* species. Presence of red staining incrustations in sulfovanillin (= presence of primodial hyphae) is a morphological trait that developed multiple times in the core clade of subgenus *Russula* and does not represent an apomorphy of any defined group (Caboň *et al.* 2017).

Biogeography of *Russula* subsect. *Castanopsidum*

According to our data in combination with publicly available sequence data in the UNITE database (https://unite.ut.ee/, accessed on 10 Nov 2024), subsect. *Castanopsidum* has a disjunct amphi-pacific distribution and occurs in Southeast Asia from India to Japan and in the Americas in the USA

© 2025 Westerdijk Fungal Biodiversity Institute

(Florida), Dominican Republic, Costa Rica, Panama and Colombia (suppl. Fig. S2). In the Americas, species of subsect. *Castanopsidum* are only reported from forests dominated by species of *Fagaceae*, but in Asia, *R. purpureogracilis* was reported from forests dominated by species of *Dipterocarpaceae* (Adamčík *et al.* 2019, Rossi *et al.* 2020).

The estimated diversification time of Asian and American *Castanopsidum* members is between 8–14.1 mya, which suggests that the group has a Northern Hemisphere boreotropical origin and their common ancestor migrated during mid-Miocene climatic optimum across the Bering land bridge (Jiang *et al.* 2019). The ancestors of the *Castanopsidum* species currently distributed in the Americas probably co-migrated southwards to Panama with species of Fagaceae. Intensified sampling of tropical forests dominated by species of *Fagaceae* from Mexico to Nicaragua might reveal the presence of *Castanopsidum* species on the American mainland between Florida and Costa Rica, which would support the co-migration hypothesis. However, since the current distribution pattern of *Castanopsidum* species in the Americas is dispersed with no record north of Florida and no fossil data available, long-distance spore dispersal cannot be excluded. Nevertheless, it is considered unlikely since ECM fungi are generally not cosmopolitan (Peay & Matheny 2017). The recent diversification of the two *R. atroamethystina* subspecies along the Isthmus of Panama was estimated at 2.9 mya which aligns with the migration of *Quercus* to Colombia and with the estimated diversification time of recent *Quercus* species around 3.5 mya (Hipp *et al.* 2020) adding strong evidence for a co-migration across the Isthmus of Panama. The co-migration hypothesis could further be tested by investigating ECM community compositions. It is to be expected that the overlap of ECM fungal taxa in *Fagaceae* forests decreases with increasing distance to the northernmost distribution site of *Castanopsidum* species in Florida. Similar observations supported the host-ECM fungi co-migration hypothesis from a common north temperate origin for *Alnus* species and their associated fungal partners in the Americas (Kennedy *et al.* 2011).

The current distribution of *Quercus* spp. around the Isthmus of Panama can be considered interrupted due to the absence of species of this genus at lower elevations of the Darién (Hooghiemstra 2006, Kappelle 2006). This interruption could be the cause of the recent diversification of *Russula* subspecies at opposing parts of the Isthmus in Colombia and Western Panama, similar to *R. floriformis* subsp. *floriformis* with its subsp. *symphoniae* (Vera *et al.* 2021) and *R. ferruginea* subsp. *ferruginea* with its subsp. *panamensis* (Buyck *et al.* 2022). Although the diversification of our two subspecies of *R. atroamethystina* does align with the migration time of *Quercus* to Colombia, the assessment of changes through time on phylogenies should be interpreted with caution. Using secondary time calibrations from Looney *et al.* (2016) may propagate errors in diversification time estimates within *Russula*. However, the alternative approach is to construct large, poorly sampled phylogenies to include limited fungal fossil data, which is susceptible to incorrect fossil calibration, uncertain branch placement, inflated clade diversity, and biased divergence estimates. While neither approach is perfect, investigating key diversification events between *Russula* and its plant hosts provides a valuable foundation for understanding the complex evolutionary histories of *Castanopsidum* species in the Americas and globally. Additionally, there is a great lack of information about the true diversity of *Russula* species in Colombia, Panama and Costa Rica. A more in-depth study of *Russula* species in the region will most likely allow further new species to be identified and contribute to a more complete knowledge to the biogeography and diversification of *Russula* species.

Our field observations suggest that the new Colombian species, *R. esperanzae*, is strictly associated with *T. excelsa*, a species of *Fagaceae* endemic to the Colombian Andes. The UNITE search did not reveal any closely related species and divergence from the closest related species, *R. atroamethystina*, is estimated around 6.4 mya. *Russula esperanzae* probably migrated from Central to South America along the Isthmus of Panama during the Great American Biotic Interchange (Cody *et al.* 2010). However, missing data about its relatives and ancestors raise additional questions. It is possible that more closely related species in Colombia or Central America are still undiscovered and may bring insight to the evolutionary history of this species.

Furthermore, we are not sure what role the association with *Trigonobalanus* plays in the evolutionary history of *R. esperanzae*. It is possible that the species evolved allopatrically by climatic disjunction at the Isthmus of Panama. Speciation may also have been driven by a host switch, which was shown to be an important factor in the evolution of *Russula* species by Looney *et al.* (2016). Expanded sampling from *Fagaceae*-dominated forests in undersurveyed regions such as Central American countries north of Costa Rica as well as root-associated fungal sequencing from *Trigonobalanus* and *Quercus* forests might add to an improved understanding of the factors that drove the speciation *R. esperanzae*.

There is no doubt that *T. excelsa* played an important role in shaping ECM diversity in the Colombian Andes. It has long been recognized as an ECM symbiont; however, there have only been a few isolated efforts to describe the associated fungi (Tulloss *et al.* 1992, Franco-Molano *et al.* 2022). The first and only previous record of an association of *Russula* with *T. excelsa* was made by Corner (1964) who observed a species similar to *Russula nigricans* in a *T. excelsa* stand. *Russula esperanzae* is the first species of *Russula* described with an apparently strict ECM association to *T. excelsa*. *Russula atroamethystina* subsp. *guacahayoensis* appears to be more generalist and forms ECM associations with *T. excelsa* and *Q. humboldtii*. Unfortunately, the evolutionary history of *T. excelsa* is poorly understood due to the lack of recent fossils. In the Tertiary, the genus *Trigonobalanus* was more or less continuously distributed in North America and Europe as part of the boreotropical flora and then became extinct in the majority of its former distribution area, except for two species in Southeast Asia and *T. excelsa* in Colombia (Manos & Standfort 2001). The most widely accepted theory for the occurrence of *T. excelsa* in Colombia is its recent migration during the Pleistocene, when the land bridge between the American subcontinents was established and a subsequent extinction of its ancestor in Central America (Nixon & Crepet 1989).

Species of *Trigonobalanus* and *Quercus* formed part of the tertiary boreotropical flora and migrated from Central to South America via the Panamanian Isthmus. *Trigonobalanus* species prefer warmer climates compared to *Quercus*

© 2025 Westerdijk Fungal Biodiversity Institute

species, which is reflected in the current distribution of *T. excelsa* is at the southern margin of *Quercus* distribution with populations of *T. excelsa* located at lower altitudes compared to *Q. humboltii* (Gentry 1993). Since the Andes were not yet uplifted at the time of the closing of the isthmus, species adapted to tropical climates were able to migrate earlier than those adapted to colder climates (Van der Hammen & Cleef 1983). Therefore, it is likely that the ancestor of *T. excelsa* migrated earlier across the isthmus compared to the *Q. humboldtii* ancestor. This hypothesis is further supported by the difference in the sizes of fruits, which are large and heavy in *Q. humboltii* limiting a fast dispersal, while the fruits of *T. excelsa* are smaller and lighter and thus more easily dispersed by birds (Lozano-C. *et al.* 1979, Orwa *et al.* 2009). Unfortunately, there are no fossil or pollen records to fix the extinction time of the ancestor of *T. excelsa* in Central America or to confirm its migration time to the South American continent. *Russula esperanzae* probably co-migrated earlier with *T. excelsa* than *R. atroamethystina* with *Quercus* species. This is one of several interesting hypotheses about the complex evolutionary history of members of *Russula* subsect. *Castanopsidum* that may foster further investigation.

ACKNOWLEDGEMENTS

The Panamanian Environmental Ministry (MiAmbiente) is thanked for issuing permits for collection (SE/PH-4-18, SE/P-39-11) and export (SEX/H-2-18, SEX/P-1-13) of fungi, Orlando Cáceres and Manlio Cuevas are thanked for logistic support in Panama. Colombian specimens were collected under ANLA collection permit Resolucion 530 from 2014 and ANLA export permit No. NO CITES 3400. We thank Pedro Velasco, Laura Quina, Juan David Rosales and Agrosolidaria members, and Sandra Galan from the Fundación Natura for their help during field work and Natalia Vargas Estupiñan for all her logistical help for exporting collections.

FUNDING

The work of S. Adamčík, M. Caboň and K. Adamčíková was supported by by Slovak Research and Development Agency project APVV-20-0257. C.R. Noffsinger was supported by the U.S. National Science Foundation (DEB-2030779). A. Corrales, C. Parra and A. Ortiz were funded by the Franklinia Fundation Project 2021-18 TR focusing on conservation of *Trigonobalanus excelsa* in Colombia.

Conflict of interest: The authors declare that they have no conflict of interest.

REFERENCES

Adamčík S, Looney B, Caboň M, *et al.* (2019). The quest for a globally comprehensible *Russula* language. *Fungal Diversity* **99**: 369–449. https://doi.org/10.1007/s13225-019-00437-2

Beenken L (2004). *Die Gattung Russula: Untersuchungen zu ihrer Systematik anhand von Ektomykorrhizen.* Ph.D. dissertation. Faculty of Biology, LMU Munich, Germany. 10.5282/edoc.3175

Bouckaert R, Vaughan TG, Barido-Sottani J, *et al.* (2019). BEAST 2.5: An advanced software platform for Bayesian evolutionary analysis. *PLoS Computational Biology* **15**: e1006650. https://doi.org/10.1371/journal.pcbi.1006650

Bouckaert R, Drummond AJ (2017). bModelTest: Bayesian phylogenetic site model averaging and model comparison. *BMC Evolutionary Biology* **17**: 1–11. https://doi.org/10.1186/s12862-017-0890-6

Buyck B (2007). An introduction to the study of *Russula* in the eastern United States. *Pagine di Micologia* **27**: 81–86.

Buyck B, Zoller S, Hofstetter V (2018). Walking the thin line… ten years later: the dilemma of above-versus below-ground features to support phylogenies in the *Russulaceae* (*Basidiomycota*). *Fungal Diversity* **89***:* 267–292. https://doi.org/10.1007/s13225-018-0397-5

Buyck B (1989). Valeur taxonomique du bleu de crésyl pour le genre *Russula*. *Bulletin de la Société Mycologique de France* **105**: 1–6.

Buyck B, Wang XH, Adamčíková K, *et al.* (2020). One step closer to unravelling the origin of *Russula*: subgenus *Glutinosae subg. nov*. *Mycosphere* **11**: 285–304. https://doi.org/10.5943/mycosphere/11/1/6

Buyck B, Eyssartier G, Armada F, *et al.* (2022). Fungal biodiversity profiles 111–120. *Cryptogamie, Mycologie* **43**: 23–61. https://doi.org/10.5252/cryptogamie-mycologie2022v43a2

Caboň M, Eberhardt U, Looney B, *et al.* (2017). New insights in *Russula* subsect. *Rubrinae*: phylogeny and the quest for synapomorphic characters. *Mycological Progress* **16**: 877–892. https://doi.org/10.1007/s11557-017-1322-0

Caboň M, Li GJ, Saba M, *et al.* (2019). Phylogenetic study documents different speciation mechanisms within the *Russula globispora* lineage in boreal and arctic environments of the Northern Hemisphere. *IMA Fungus* **10**: 1–16. https://doi.org/10.1186/s43008-019-0003-9

Cavender-Bares J (2019). Diversification, adaptation, and community assembly of the American oaks (*Quercus*), a model clade for integrating ecology and evolution. *New Phytologist* **221**: 669–692. https://doi.org/10.1111/nph.15450

Cody S, Richardson JE, Rull V, *et al.* (2010). The Great American Biotic Interchange revisited. *Ecography* **33**: 326–332. https://doi.org/10.1111/j.1600-0587.2010.06327.x

Corner EJH (1964). Royal Society Expedition to North Borneo 1961: Reports. *Proceedings Linnean Society London* **175**: 9–32. https://www.jstor.org/stable/42600854

Corrales A, Koch RA, Vasco–Palacios AM, *et al.* (2022). Diversity and distribution of tropical ectomycorrhizal fungi. *Mycologia* **114**: 919–933. https://doi.org/10.1080/00275514.2022.2115284

Cubeta MA, Echandi E, Abernethy T, *et al.* (1991). Characterization of anastomosis groups of binucleate *Rhizoctonia* species using restriction analysis of an amplified ribosomal RNA gene. *Phytopathology* **81**: 1395–1400. https://doi.org/10.1094/phyto-81-1395

Darriba D, Posada D, Kozlov AM, *et al.* (2020). ModelTest-NG: a new and scalable tool for the selection of DNA and protein evolutionary models. *Molecular Biology and Evolution* **37**: 291–294. https://doi.org/10.1093/molbev/msz189

De Lange R, Kleine J, Hampe F, *et al.* (2023). Stop black and white thinking: *Russula* subgenus *Compactae* (*Russulaceae*, *Russulales*) in Europe revised. *Persoonia* **51**: 152–193. https://doi.org/10.3767/persoonia.2023.51.04

Delavaux C, Weigelt P, Dawson W, *et al.* (2019). Mycorrhizal fungi influence global plant biogeography. *Nature Ecology & Evolution* **3**: 424–429. https://doi.org/10.1038/s41559-019-0823-4

Denk T, Grímsson F, Zetter R (2012). *Fagaceae* from the early

© 2025 Westerdijk Fungal Biodiversity Institute

Oligocene of Central Europe: persisting new world and emerging old world biogeographic links. *Review of Palaeobotany and Palynology* **169**: 7–20. https://doi.org/10.1016/j.revpalbo.2011.09.010

Don RH, Cox PT, Wainwright BJ, *et al.* (1991). 'Touchdown' PCR to circumvent spurious priming during gene amplification. *Nucleic Acids Research* **19**: 4008. https://doi.org/10.1093/nar/19.14.4008.

Edler D, Klein J, Antonelli A, *et al.* (2021). raxmlGUI 2.0: a graphical interface and toolkit for phylogenetic analyses using RAxML. *Methods in Ecology and Evolution* **12**: 373–377. https://doi.org/10.1111/2041-210X.13512

Fatto RM (1998). Notes on four little red Russulas. Mycotaxon 68: 193–204.

Franco-Molano AE, Palacio M, Gómez-Montoya N (2022). Diversity of *Basidiomycota* in Colombia. In: *Catalogue of Fungi of Colombia* (Lücking R, Diazgranados M, Vasco-Palacios AM, *et al.*, eds). Royal Botanic Gardens, Kew, UK: 59–65.

Gardes M, Bruns TD (1993). ITS primers with enhanced specificity for basidiomycetes-application to the identification of mycorrhizae and rusts. *Molecular Ecology* **2**: 113–118. https://doi.org/10.1111/j.1365-294X.1993.tb00005.x

Gentry AH (1993). *Woody plants of Northwest South America:(Colombia, Ecuador, Peru).* Conservation International, USA.

Gómez LD, Alfaro RM (1996). Basidiomicetes de Costa Rica. De Russulae novae. *Revista de Biologia Tropical* **44**: 25–37.

Hall T (2013). BioEdit, version 7.2.5. Ibis Biosciences, Carlsbad, CA, USA.

Hammel BE, Grayum MH, Herrera C, *et al.* (2010). Manual de plantas de Costa Rica. *Monographs in Systematic Botany from the Missouri Botanical Garden* **119**: 1–970.

Hipp AL, Manos PS, Hahn M, *et al.* (2020). Genomic landscape of the global oak phylogeny. *New Phytologist* **226**: 1198–1212. https://doi.org/10.1111/nph.16162

Hooghiemstra H (2006). Immigration of oak into northern South America: a paleo–ecological document. In: *Ecology and Conservation of Neotropical Montane Oak Forests* (Kappelle M, ed.) Springer, Germany: 17–28.

Jiang D, Klaus S, Zhang YP, *et al.* (2019). Asymmetric biotic interchange across the Bering land bridge between Eurasia and North America. *National Science Review* **6**: 739–745. https://doi.org/10.1093/nsr/nwz035

Kappelle M (2006). *Ecology and conservation of neotropical montane oak forests.* Springer, Germany. https://doi.org/10.1007/3-540-28909-7

Katoh K, Standley DM (2013). MAFFT multiple sequence alignment software version 7: improvements in performance and usability. *Molecular Biology and Evolution* **30**: 772–780. https://doi.org/10.1093/molbev/mst010

Kearse M, Moir R, Wilson A, *et al.* (2012). Geneious Basic: an integrated and extendable desktop software platform for the organization and analysis of sequence data. *Bioinformatics* **28**: 1647–1649. https://doi.org/10.1093/bioinformatics/bts199

Kennedy PG, Garibay-Orijel R, Higgins LM, *et al.* (2011). Ectomycorrhizal fungi in Mexican *Alnus* forests support the host co-migration hypothesis and continental-scale patterns in phylogeography. *Mycorrhiza* **21**: 559–568. https://doi.org/10.1007/s00572-011-0366-2

Kornerup A, Wanscher JH (1978). *Methuen Handbook of Colour*. 3rd edition. Eyre Methuen, London.

Larsson A (2014). Aliview: A Fast and Lightweight Alignment Viewer and Editor for Large Datasets. *Bioinformatics* **30**: 3276–3278. https://doi.org/10.1093/bioinformatics/btu531

Looney BP, Ryberg M, Hampe F, *et al.* (2016). Into and out of the tropics: global diversification patterns in a hyperdiverse clade of ectomycorrhizal fungi. *Molecular Ecology* **25**: 630–647. https://doi.org/10.1111/mec.13506

Looney BP, Manz C, Matheny PB, *et al.* (2022). Systematic revision of the *Roseinae* clade of *Russula*, with a focus on eastern North American taxa. *Mycologia* **114**: 270–302. https://doi.org/10.1080/00275514.2021.2018881

López-Giráldez F, Townsend JP (2011). PhyDesign: an online application for profiling phylogenetic informativeness. *BMC Evolutionary Biology* **11**: 152. https://doi.org/10.1186/1471-2148-11-152

Lozano-C G, Hernández-Camacho J, Henao-S JE, *et al.* (1979). Hallazgo del genero *Trigonobalanus* Forman, 1962 (*Fagaceae*) en el neotropico—I. *Caldasia* **12**: 517–537.

Manos PS, Stanford AM (2001). The historical biogeography of *Fagaceae*: tracking the tertiary history of temperate and subtropical forests of the Northern Hemisphere. *International Journal of Plant Sciences* **162**: 77–93. https://doi.org/10.1086/323280

Manz C, Adamčík S, Looney BP, *et al.* (2021). Four new species of *Russula* subsection *Roseinae* from tropical montane forests in western Panama. *PLoS ONE* **16**: e0257616. https://doi.org/10.1371/journal.pone.0257616

Matheny PB (2005). Improving phylogenetic inference of mushrooms with RPB1 and RPB2 nucleotide sequences (*Inocybe*; *Agaricales*). *Molecular Phylogenetics and Evolution* **35**: 1–20. https://doi.org/10.1016/j.ympev.2004.11.014

Matheny PB, Liu YJ, Ammirati JF, *et al.* (2002). Using RPB1 sequences to improve phylogenetic inference among mushrooms (*Inocybe*, *Agaricales*). *American Journal of Botany* **89**: 688–698. https://doi.org/10.3732/ajb.89.4.688

Melville RFLS (1982). The biogeography of *Nothofagus* and *Trigonobalanus* and the origin of the *Fagaceae*. *Botanical Journal of the Linnean Society* **85**: 75–88. https://doi.org/10.1111/j.1095-8339.1982.tb00586.x

Miller MA, Pfeiffer W, Schwartz T (2011). The CIPRES science gateway: a community resource for phylogenetic analyses. In: *Proceedings of the 2011 TeraGrid Conference: extreme digital discovery* (Towns J, ed.) Association for Computing Machinery, USA: 1–8. https://doi.org/10.1145/2016741.2016785

Miller SL, Aime MC, Henkel TW (2024). *Russulaceae* of the Pakaraima Mountains of Guyana 5. Two newly described diminutive species in a novel lineage of the crown clade of *Russula* (*Russulaceae*). *Phytotaxa* **668***:* 117–129. https://doi.org/10.11646/phytotaxa.668.2.1

Mireya D, Correa A, Galdames C, *et al.* (2004). *Catálogo de las Plantas Vasculares de Panamá.* Novo Art, Quebecor Bogotá:1–599.

Nixon KC, Crepet WL (1989). *Trigonobalanus* (*Fagaceae*): taxonomic status and phylogenetic relationships. *American Journal of Botany***76**:828–841.https://doi.org/10.1002/j.1537-2197.1989.tb15061.x

Noffsinger CR, Adamčíková K, Eberhardt U, *et al.* (2024). Three new species in *Russula* subsection *Xerampelinae* supported by genealogical and phenotypic coherence. *Mycologia* **116**: 322–349. https://doi.org/10.1080/00275514.2023.2295957

Orwa C, Mutua A, Kindt R, *et al.* (2009). Agroforestree Database: a tree reference and selection guide version 4.0. World Agroforestry Centre, Kenya. https://www.worldagroforestry.org/output/agroforestree-database accessed on 27 Nov2024.

© 2025 Westerdijk Fungal Biodiversity Institute

Paloi S, Das K, Acharya K (2018). *Russula darjeelingensis*, a new species from Eastern Himalaya, India. *Phytotaxa* **358**: 83–90. https://doi.org/10.11646/phytotaxa.358.1.6

Peay KG, Matheny PB (2017). The biogeography of ectomycorrhizal fungi–a history of life in the subterranean. *Molecular Mycorrhizal Symbiosis*: 341–361. https://doi.org/10.1002/9781118951446.ch19

Petkovits T, Nagy LG, Hoffmann K, *et al.* (2011). Data partitions, Bayesian analysis and phylogeny of the zygomycetous fungal family *Mortierellaceae*, inferred from nuclear ribosomal DNA sequences. *PLoS ONE* **6**: e27507. https://doi.org/10.1371/journal.pone.0027507

Piepenbring M, Hofmann TA, Unterseher M, *et al.* (2012). Species richness of plants and fungi in western Panama: towards a fungal inventory in the tropics. *Biodiversity and Conservation* **21**: 2181–2193. https://doi.org/10.1007/s10531-011-0213-y

Rambaut A, Drummond AJ, Xie D, *et al.* (2018). Posterior summarisation in Bayesian phylogenetics using Tracer 1.7. *Systematic Biology* **67**: 901–904. https://doi.org/10.1093/sysbio/syy032

Rehner SA, Buckley E (2005). A *Beauveria* phylogeny inferred from nuclear ITS and *EF1-α* sequences: evidence for cryptic diversification and links to *Cordyceps* teleomorphs. *Mycologia* **97**: 84–98. https://doi.org/10.1080/15572536.2006.11832842

Romagnesi H (1967). *Les Russules d'Europe et d'Afrique du Nord*. Bordas, France: 1–1030.

Rossi W, Das K, Hembrom ME, *et al.* (2020). Fungal biodiversity profiles 91-100. *Cryptogamie, Mycologie* **41**: 69–107. https://doi.org/10.5252/cryptogamie-mycologie2020v41a4

Schmitt I, Crespo A, Divakar PK, *et al.* (2009). New primers for promising single-copy genes in fungal phylogenetics and systematics. *Persoonia* **23**: 35–40. https://doi.org/10.3767/003158509X470602

Stamatakis A (2014). RAxML version 8: a tool for phylogenetic analysis and post-analysis of large phylogenies. *Bioinformatics* **30**: 1312–1313. https://doi.org/10.1093/bioinformatics/btu033

Stiller JW, Hall BD (1997). The origin of red algae: implications for plastid evolution. *Proceedings of the National Academy of Sciences, USA* **94**: 4520–4525. https://doi.org/10.1073/pnas.94.9.4520

Tedersoo L, Mikryukov V, Zizka A, *et al.* (2022). Global patterns in endemicity and vulnerability of soil fungi. *Global Change Biology* **28**: 6696–6710. https://doi.org/10.1111/gcb.16398

Thiers B (continuously updated). Index Herbariorum: a global directory of public herbaria and associated staff. New York Botanical Garden's Virtual Herbarium. http://sweetgum.nybg.org/science/ih/

Tulloss RE, Ovrebo CL, Halling RE (1992). Studies on *Amanita* (*Amanitaceae*) from Andean Colombia. *Memoirs of the New York Botanical Garden* **66**: 1–46.

Van der Hammen T, Cleef AM (1983). *Trigonobalanus* and the tropical amphi-pacific element in the North Andean forest. *Journal of Biogeography* **10**: 437–440. https://doi.org/10.2307/2844750

Vargas N, Restrepo S (2020). A checklist of ectomycorrhizal mushrooms associated with *Quercus humboldtii* in Colombia. In: *Mushrooms, Humans and Nature in a Changing World* (Pérez-Moreno J, Guerin-Laguette A, Flores Arzú R, *et al.*, eds). Springer, Germany: 425–450.

Vasco-Palacios AM, Lücking R, Moncada B, *et al.* (2022). A critical assessment of biogeographic distribution patterns of Colombian fungi. In: *Catalogue of Fungi of Colombia* (Lücking R, Diazgranados M, Vasco-Palacios AM, *et al.*, eds). Royal Botanic Gardens, Kew, UK: 121–136.

Vera M, Adamčík S, Adamčíková K, *et al.* (2021). Morphological and genetic diversification of *Russula floriformis*, *sp. nov.*, along the Isthmus of Panama. *Mycologia* **113**: 807–827. https://doi.org/10.1080/00275514.2021.1897377

Vilgalys R, Hester M (1990). Rapid genetic identification and mapping of enzymatically amplified ribosomal DNA from several *Cryptococcus* species. *Journal of Bacteriology* **172**: 4238–4246. https://doi.org/10.1128/jb.172.8.4238-4246.1990

White TJ, Bruns T, Lee S, *et al.* (1990). Amplification and direct sequencing of fungal ribosomal RNA genes for phylogenetics. In: *PCR protocols: a guide to methods and applications* (Innis MA, Gelfand DH, Sninsky JJ, *et al.*, eds) Academic Press, New York, USA: 315–322.

Supplementary Material: http://fuse-journal.org/

Fig. S1. Phylogenetic informativeness inferred in PhyDesign of the five nuclear markers used for inferring the phylogeny.

Fig. S2. Phylogram generated by Maximum Likelihood (RAxML) analysis based on the ITS region. Maximum likelihood bootstrap support values greater than 60 % are indicated above or below the nodes. The sampling is supplemented by massBLASTer search of UNITE database (https://unite.ut.ee/, accessed 10 Nov. 2024) and additional samples retrieved by this search are labelled by an asterisk (*).

Table S1. Samples of *Russula* spp. used in the multilocus phylogenetic analyses (Fig. 1).

Table S2. Microscopic characters observed on the studied material of *Russula esperanzae* & *Russula atroamethystina.*

© 2025 Westerdijk Fungal Biodiversity Institute

© 2025 Westerdijk Fungal Biodiversity Institute

FUSE

Fungal Systematics and Evolution

VOLUME 16
DECEMBER 2025
PAGES 197–214

doi.org/10.3114/fuse.2025.16.11

Uwebraunomyces, a novel genus of the family *Mycosphaerellaceae*

G. Singh[1], P. Kumari[2,3], S. Rajwar[2], S. Yadav[2], S. Mall[1], S. Kumar[4], R. Singh[2*]

[1]Department of Botany, DDU Gorakhpur University, Gorakhpur 273009, U.P., India
[2]Centre of Advanced Study in Botany, Institute of Science, Banaras Hindu University, Varanasi 221005, U.P., India
[3]School of Life Sciences, Jawaharlal Nehru University, New Delhi 110067, India
[4]Forest Pathology Department, KSCSTE-Kerala Forest Research Institute, Peechi, Thrissur 680653, Kerala, India

[*]Corresponding author: drsinghtaxon@gmail.com; singhr.bot@bhu.ac.in

Key words:
Dothideomycetes
Mycosphaerellales
new recombination
new taxon

Abstract: A hyaline to pale olivaceous brown hyphomycetous fungus was collected on living leaves of *Tinospora cordifolia* in India. Molecular phylogenetic analyses of several loci (LSU-*RPB2*-ITS) indicated a relationship with cercosporoid fungi (*Mycosphaerellaceae*). As no other known lineage shares similar morphology or DNA sequences, a new genus, *Uwebraunomyces*, is proposed, with *U. tinosporae comb. nov*. based on *Ramularia tinosporae* as the type species. Conidiophores are pale olivaceous to very pale brown in colour, typically unbranched, and subcylindrical to geniculate-sinuous at the tip. Conidia are solitary, obclavate to obpyriform, straight to curved, and few-septate. Additionally, the conidiogenous loci are characterized by a centrally located small papilla and a minute, distinct frill that is typically evident in older scars. These characteristics distinguish *Uwebraunomyces* from other closely related members of the ramularioid complex. Additionally, *Cercosporella bundelkhandae* is recognized as a new synonym as it shares nearly identical morphological features with *U. tinosporae*. At the ultrastructural level, *Uwebraunomyces* is further characterized by conidiogenous loci that bulge outward, forming convex or truncated cone shapes, with wall thickening extending beyond the area originally occupied by the base of the conidium. Older scars display a minute papilla or small, somewhat conical protuberant like structure in the centre of their apical depression, often accompanied by a minute, distinct frill. The conidial base is obconically truncate, featuring a basal depression with a centrally located, slightly protuberant structure. These distinct ultrastructural features set *Uwebraunomyces* apart from other members of the ramularioid complex, underscoring its taxonomic significance within the *Mycosphaerellaceae*.

Citation: Singh G, Kumari P, Rajwar S, Yadav S, Mall S, Kumar S, Singh R (2025). *Uwebraunomyces*, a novel genus of the family *Mycosphaerellaceae*. *Fungal Systematics and Evolution* **16**: 197–214. doi: 10.3114/fuse.2025.16.11
Received: 12 January 2025; **Accepted:** 15 May 2025; **Effectively published online:** 25 July 2025
Corresponding editor: P.W. Crous

INTRODUCTION

The genus *Cercosporella* is characterized by its distinctive morphological features. Its hyphae are hyaline to faintly pigmented, with stromata composed of aggregated, hyaline to olivaceous, swollen hyphal cells. Conidiophores emerge either through stomata or are erumpent through the cuticle; they are straight, subcylindrical to geniculate-sinuous, hyaline, and occasionally faintly pigmented near the base or exhibiting faint greenish, yellowish, or reddish tinges. Conidiogenous cells are integrated, terminal, polyblastic, sympodial, and mostly conspicuously geniculate. The old conidial scars are thickened, hyaline, refractive, and raised in the shape of a truncated cone (ultrastructure). Conidia are formed singly, hyaline, occasionally faintly greenish, obclavate, and sometimes broadly fusoid. They are euseptate, thin-walled, with an obtuse apex and a base that is either somewhat narrowed, rounded, or truncate. The hilum is slightly thickened and convex (Braun 1995, Kirschner 2009).

The taxonomic distinction between *Cercosporella* and *Ramularia* has been clarified through morphological and molecular studies (Braun 1995, 1998, Kirschner 2009, Videira *et al.* 2016). Phylogenetic analyses using LSU and *rpb2* sequences demonstrate that these two genera cluster separately, confirming their distinct evolutionary relationships (Kirschner 2009, Videira *et al.* 2016). Morphologically, *Cercosporella* is differentiated from *Ramularia* by its formation of an appressorium structure for plant cell adhesion and its unique conidiogenous scars, which are flat and cone-shaped (Kirschner 2009). In *Ramularia*, the scar of the conidiogenous locus is of the *Cladosporium*-type, characterized by a raised periclinal rim, a central dome, and a crater situated between the rim and dome. The central dome is typically elevated above the rim's surface, forming a distinctive morphological feature. This structure is key in identifying *Ramularia* and distinguishing it from related fungal genera based on conidiogenous characteristics (Kirschner 2009).

Several studies have explored the diversity of phytopathogenic fungi in India related to *Mycosphaerellaceae* (Singh *et al.* 2011, 2012, 2013, 2014a, b, 2020a, 2022, Kamal

Fungal Systematics and Evolution is licensed under a Creative Commons Attribution-NonCommercial-NoDerivatives 4.0 International License

© 2025 Westerdijk Fungal Biodiversity Institute

2010, Kharwar *et al.* 2015, Kumar & Singh 2015, 2016, Kushwaha *et al.* 2020). However, these studies have primarily relied on morphological data, with limited inclusion of cultural data. Only a few studies have provided molecular support for species identification (Singh *et al.* 2020b, Verma *et al.* 2021a, b, Yadav *et al.* 2021, 2022, 2023).

During a survey of foliicolous fungi in Kusumhi Forest, Gorakhpur, Uttar Pradesh, India, in September 2021, a hyaline to pale olivaceous brown hyphomycetous fungus was found on leaves of *Tinospora cordifolia*. This fungus was originally collected in Patna, Bihar (India), in 1950 and described as *Ramularia tinosporae* (Thirumalachar & Lacy 1951). However, the true generic placement of *R. tinosporae* remained unresolved due to the absence of DNA phylogenetic data. Given the limitations of morphological traits for determining generic relationships, phylogenetic studies revealed that this fungus does not align with any existing genus in the *Mycosphaerellaceae*. Consequently, a new genus, *Uwebraunomyces*, is proposed to accommodate this fungus. This proposal is supported by comprehensive phylogenetic evidence and the ultrastructure of conidiogenous loci and hila, which highlight this distinct evolutionary lineage.

MATERIALS AND METHODS

Fungal isolation and morphology

Infected leaves were collected in sterilized polyethylene bags and placed in dry paper envelopes for transport to the laboratory. Close-up photographs of the infected plant parts were captured under a dissecting microscope (Magnus: MSZ-TR) with an attached CatCam 300EF camera. For light microscopy, fungal structures from the infected leaves were transferred to glass slides and mounted in both clear glycerine as well as lactophenol cotton-blue mixture. These fungal propagules were then photographed using an Olympus compound microscope (BX53) with a DP28 camera.

Scanning Electron Microscopy (SEM) was performed using a Field Emission Scanning Electron Microscope (FEI Nova Nano SEM-450). Detailed morphological observations were made at various magnifications, including light microscopy at 450× and 1000×, and SEM at up to ~20 K× magnification. For SEM analysis, specimens were coated with a gold-palladium mixture using a POLARON Sputter Coater (180 s, nitrogen atmosphere, 20 mA, 30 mm electrode distance), and examined with a LEO-430 scanning electron microscope.

Morphological feature sizes were derived from at least 25 measurements, with 95 % confidence intervals calculated, and extreme values were recorded. The examined reference specimens are deposited in the fungarium of Ajrekar Mycological Herbarium (AMH) at Agharkar Research Institute (ARI), Pune, India, while duplicates material are retained in the Mycological Herbarium of the Department of Botany at Banaras Hindu University, Varanasi, U.P., India (MH-BHU).

Conidia of *Uwebraunomyces* AMH 10705 and AMH 10734 were transferred to Petri dishes with potato dextrose agar (PDA). The dishes were incubated at room temperature (25 ± 5 °C) under diffuse daylight. A purified ex-type culture was deposited in the National Fungal Culture Collection of India (NFCCI), Pune, India. Growth rates and colony characteristics were observed on PDA after 14 d of incubation.

DNA extraction, polymerase chain reaction (PCR) and sequencing

Genomic DNA was extracted from mycelia and spores scraped from PDA plates using a sterile scalpel blade. Approximately 200 mg of the wet-weight sample was transferred to 2 mL microcentrifuge tubes, which were kept in liquid nitrogen for two min, then grinded into a fine powder using a pestle and mortar. The DNA extraction was performed using the Himedia DNA Isolation Kit (HiPurA™ Fungal DNA Purification Kit) following the manufacturer's protocol.

The quality of the isolated DNA was assessed by electrophoresis in a 1 % agarose gel (w/v) stained with ethidium bromide under a Gel Documentation system (Bio-Rad Universal Hood II). The DNA concentration was quantified using a NanoDrop microvolume spectrophotometer (Thermo Scientific™ NanoDrop™ One/OneC Microvolume UV-Vis Spectrophotometer with Wi-Fi).

For sequencing, three regions of the fungal genome were targeted: the Internal Transcribed Spacer (ITS) region, the large subunit nuclear ribosomal DNA (LSU), and a partial fragment of the DNA-directed RNA polymerase II subunit (*RPB2*). To amplify these regions, the following primers were used: ITS1/ITS4 (White *et al.* 1990) for the ITS region, LROR/LR7 (Vilgalys & Hester 1990, Rehner & Samuels 1994) for LSU, and RPB2-5F/RPB2-7cR (Liu *et al.* 1999, Sung *et al.* 2007) for the *RPB2* gene. The amplification mixture (50 µL total volume) contained 5 µL of template DNA, 5 µL of PCR buffer with $MgCl_2$, 1.5 µL of each primer (10 pmol), 1 µL of dNTP mix (10 mM), 0.3 µL of *Taq* DNA polymerase (HiMedia: 5 Units/µL), and 35.7 µL of milli-Q water. The amplification was carried out in a Bio-Rad T100™ thermal cycler with the following conditions: an initial denaturation at 95 °C for 5 min, followed by 35 cycles of denaturation at 94 °C for 1 min, annealing at 55 °C, 52 °C, and 54 °C for 1 min (for ITS, LSU, and *RPB2*, respectively), and extension at 72 °C for 1 min. The final extension was performed at 72 °C for 8 min. The PCR products were analysed by electrophoresis on a 1.2 % agarose gel and visualized using a Bio-Rad Universal Hood II Gel Documentation system for the product size and purity.

The amplicons were purified using the FavorPrep™ PCR Purification Kit. The DNA sequencing was performed by Eurofins Genomics India Pvt. Ltd., Bengaluru using the Sanger sequencing method, employing the same primers used in PCR amplification. Sequencing was carried out using the BigDye® Terminator v. 3.1 Cycle Sequencing Kit and ABI 3100 DNA Analyzer.

Sequence alignment and phylogenetic analysis

In this study, gene sequences were assembled and edited using Chromas v. 2.6.6 (https://technelysium.com.au/wp/chromas/). The manually edited sequences were submitted to NCBI GenBank (Table 1) and subjected to a megablast search to retrieve related sequences from the NCBI GenBank nucleotide database. Additional reference sequences were selected from literature (Table 1). Sequence alignments were performed using MAFFT v. 7 (Katoh *et al.* 2019), followed by manual refinement and concatenation using BioEdit v. 7.0.9 (Hall 2007) and MEGA-X v. 10.1.8 (Kumar *et al.* 2018). The final aligned sequences were deposited in TreeBASE (study number 31915).

© 2025 Westerdijk Fungal Biodiversity Institute

Table 1. Taxa included in the molecular phylogenetic analyses with their GenBank accession numbers. Newly generated sequences are in **bold**.

Taxons	Host	Locality	Isolate / Voucher ID	GenBank Accession No.			References
				ITS	LSU	*RPB2*	
Acervuloseptoria ziziphicola	*Ziziphus mucronata*	South Africa	CBS 138009 / CPC 23707	KJ869164	KJ869221	MF951425	Corus *et al.* (2014), Videira *et al.* (2017)
Amycosphaerella africana	*Eucalyptus viminalis*	South Africa	CBS 116154 / CPC 794	KF901700	GU214433	KF902224	Quaedvlieg *et al.* (2014), Crous *et al.* (2009a)
Caryophylloseptoria pseudolychnidis	*Lychnis cognata*	North Korea	CBS 128630	KF251291	KF251795	KF252297	Verkley *et al.* (2013)
Caryophylloseptoria spergulae	*Spergula morisonii*	Netherlands	CBS 109010	KF251294	KF251798	KF252300	Verkley *et al.* (2013)
Cercospora apii	—	Fiji	CBS 118712	KF251296	GQ852583	KT216554	Crous *et al.* (2009b), Verkley *et al.* (2013), Ismail *et al.* (2016)
Cercospora asparagi	*Asparagus officinalis*	USA	AS16-02	KY549098	KY549100	—	Videira *et al.* (2017)
Cercospora beticola	*Beta vulgaris*	Italy	CBS 116456 / CPC 11557	NR_121315	NG_068999	KT216555	Crous *et al.* (2009a), Groenewald *et al.* (2005)
Cercospora capsici	*Capsicum annuum*	South Korea	CPC 12307	GU214654	GU214654	—	Crous *et al.* (2009a),
	Capsicum annuum	Republic of Korea	CBS 132622 / CPC 14520	JX143568	MF951136	MF951456	Videira *et al.* (2017)
Cercospora coniogrammes	*Coniogramme japonica* var. *gracilis*	Australia	CBS 132634	JX143583	—	—	Groenewald *et al.* (2013)
Cercospora rodmanii	*Pontederia crassipes*	Maxico	5H-GTOX	GQ884184	GQ884186	—	Montenegro-Calderón *et al.* (2011)
Cercospora sojina	*Glycine soja*	South Korea	CPC 12322	GU214655	GU214655	—	Crous *et al.* (2009a)
Cercospora zebrina	*Trifolium subterraneum*	Australia	CBS 118789	GU214656	GU214656	—	Crous *et al.* (2009a)
Cercospora zebrina	*Trifolium subterraneum*	Australia	CBS 118790	GU214657	GU214657	KF252156	Crous *et al.* (2009a), Quaedvlieg *et al.* (2013)
Cercosporella pfaffiae	*Pfaffia glomerata*	Brazil	Vic31849	JQ990331	JQ990330	—	Machado *et al.* (2012)
Cercosporella virgaureae	*Erigeron annuus*	South Korea	CBS 113304	GU214658	GQ852585	KX348051	Crous *et al.* (2009b), Videira *et al.* (2016)
	Erigeron annuus	South Korea	CPC 11461	KX287284	KX286977	KX288427	Videira *et al.* (2016)
	Erigeron annuus	South Korea	CPC 11456	MF951303	KX286974	KX348050	Videira *et al.* (2016, 2017)
	Conyza canadensis	Brazil	CPC 19492	KX287288	KX286981	KX288431	Videira *et al.* (2016)
	Erigeron annuus	South Korea	CPC 10287	KX287286	KX286979	KX288429	Videira *et al.* (2016)
	Erigeron annuus	South Korea	CPC 10286	KX287285	KX286978	KX288428	Videira *et al.* (2016)
	Erigeron annuus	South Korea	CPC 10288	KX287287	KX286980	KX288430	Videira *et al.* (2016)
	Erigeron annuus	South Korea	CPC 11460	KX287283	KX286976	KX288426	Videira *et al.* (2016)
	Erigeron annuus	South Korea	CPC 11457	KX287282	KX286975	KX288425	Videira *et al.* (2016)
Cladocillium musae	*Musa itinerans*	Taiwan	CCH05A / BCRC FU30634	MT460404	MT460396	LC546944	Chen *et al.* (2020)
Clypeosphaerella calotropidis	*Calotropis procera*	Egypt	CBS 129.30	MF951308	MF951153	MF951477	Videira *et al.* (2017)
Clypeosphaerella quasiparkii	*Eucalyptus* sp.	Thailand	CBS 123243	MH863287	MH874811	KF902219	Quaedvlieg *et al.* (2014), Vu *et al.* (2019)
Coremiopassalora eucalypti	*Eucalyptus saligna*	Brazil	CBS 111306 / CPC 1455 / CMW 14907	NR_165597	NG_058736	MF951481	Hunter *et al.* (2006), Videira *et al.* (2017), Crous *et al.* (2019a)

© 2025 Westerdijk Fungal Biodiversity Institute

Table 1. (Continued).

Taxons	Host	Locality	Isolate / Voucher ID	GenBank Accession No.			References
				ITS	LSU	*RPB2*	
Devonomyces endophyticus	*Eucalyptus* sp.	South Africa	CBS 114662 / CPC 1193	KF901713	GU214435	MF951590	Crous *et al.* (2009a), Quaedvlieg *et al.* (2014), Videira *et al.* (2017)
Distocercospora pachyderma	*Dioscorea* sp.	Japan	CBS 138247	NR_156369	MH877655	MF951486	Videira *et al.* (2017), Vu *et al.* (2019)
Epicoleosporium ramularioides	*Phellodendron amurense*	South Korea	CPC 10672	GU214688	GU214688	KX288433	Crous *et al.* (2009a), Videira *et al.* (2016)
Exutisphaerella laricina	*Larix decidua*	Switzerland	CBS 326.52	GU269643	GU253693	MF951496	Crous *et al.* (2013a), Videira *et al.* (2017)
Graminopassalora geissorhizae	*Geissorhiza splendidissima*	South Africa	CBS 146788 / CPC 38623	MW175336	MW175376	MW173111	Crous *et al.* (2020b)
Graminopassalora graminis	*Alopecurus aequalis* var. *amurensis*	South Korea	CBS 113303	GU214666	GQ852621	MF951502	Crous *et al.* (2009a, b), Videira *et al.* (2017)
Hippopotamyces phragmitis	*Phragmites australis*	South Africa	CBS 146086 / CPC 36385	MN562122	MN567630	MN556803	Crous *et al.* (2019b)
Hyalozasmidium aerohyalinosporum	*Eucalyptus tectifica*	Australia	CBS 125011 / CPC 14636	GQ852839	KF901930	KF902509	Crous *et al.* (2009d), Quaedvlieg *et al.* (2014)
Juncomyces patwiniorum	*Juncus effusus*	USA	CBS 146798 / CPC 37991	MW175337	MW175377	MW173112	Crous *et al.* (2020b),
Madagascaromyces intermedius	*Eucalyptus camaldulensis*	Madagascar	CBS 124154 / CPC 15745	FJ790267	FJ790297	MF951511	Videira *et al.* (2017), Crous *et al.* (2009c)
Mycosphaerelloides madeirae	*Eucalyptus globulus*	Portugal	CBS 112895	KF901675	DQ204756	KF902214	Hunter *et al.* (2006), Quaedvlieg *et al.* (2014)
Neoacervuloseptoria fraxini	*Fraxinus* sp.	Russia	CBS 145992 / CPC 36558	MT223773	MT223870	MT223673	Yadav *et al.* (2023)
Neocercosporella peristrophes	*Peristrophe bicalyculata*	India	AMH 9671	MZ311866	MZ311874	OL773683	Yadav *et al.* (2023)
	Peristrophe bicalyculata	India	AMH 10363	ON310831	ON310846	ON376994	Yadav *et al.* (2023)
Neodeightoniella phragmiticola	*Phragmites australis*	South Africa	CBS 136418 / CPC 22059	KF777171	KF777224	MF951543	Crous *et al.* (2013b), Videira *et al.* (2017)
Neokamalomyces indicus	*Ficus benghalensis*	India	NFCCI 4870	MT731962	MT731328	OL773682	Yadav *et al.* (2022)
Neokirramyces syzygii	*Syzygium* sp.	South Africa	CPC 36122	MN562115	MN567623	—	Crous *et al.* (2019b)
Neopseudocercosporella brassicae	*Brassica oleracea*	Denmark	CBS 228.32	MH855297	KF251808	KX348058	Vu *et al.* (2019)
	—	—	CBS 163.26	MH854876	MF951192	MF951548	Vu *et al.* (2019)
Neopseudocercosporella capsellae	*Capsella bursa-pastoris*	South Korea	CPC 12519	KX287296	KX286995	KX288452	Videira *et al.* (2016)
	Capsella bursa-pastoris	South Korea	CPC 12518	KX287295	KX286994	KX288451	Videira *et al.* (2016)
Neoramulariopsis catenulata	*Phaseolus vulgaris*	Rwanda	CBS 355.73	KX287281	KX286973	KX288424	Yadav *et al.* (2023)
Neoramulariopsis dolichandrae	*Dolichandra unguis-cati*	South Africa	CBS 138101 / CPC 22948	KJ869140	KJ869197	KX288423	Yadav *et al.* (2023)
Neosonderhenia eucalypti	*Eucalyptus costata*	Australia	CBS 145081 / CPC 34405	MN161927	MN162191	MN162578	Crous *et al.* (2019a)
Nothophaeocryptopus gaeumannii	—	Austria	CBS 244.38	MF951336	MF951191	GU371740	Schoch *et al.* (2009), Videira *et al.* (2017)
Nothoseptoria caraganae	*Caragana arborescens*	Russia	CPC 36565	MT223826	MT223918	MT223694	Crous *et al.* (2020a)
Pallidocercospora heimii	*Eucalyptus* sp.	Madagascar	CBS 110682 / CPC 760	KF901671	GQ852604	MF951554	Crous *et al.* (2009b), Quaedvlieg *et al.* (2014), Videira *et al.* (2017)
Parapallidocercospora colombiensis	*Eucalyptus urophylla*	Colombia	CBS 110968 / CPC 1105	AY752148	KF901969	MF951581	Crous *et al.* (2004), Quaedvlieg *et al.* (2014), Videira *et al.* (2017)

© 2025 Westerdijk Fungal Biodiversity Institute

Table 1. (Continued).

Taxons	Host	Locality	Isolate / Voucher ID	GenBank Accession No.			References
				ITS	LSU	*RPB2*	
Passalora bacilligera	*Alnus glutinosa*	Poland	CBS 131547 / CPC 19944	MF951356	MF951210	MF951585	Videira *et al*. (2017)
Pedrocrousiella pongamiae	*Pongamia pinnata*	India	NFCCI 4881	MW327548	MW327593	MW363496	Rajeshkumar *et al*. (2021)
Phloeospora ulmi	*Ulmus* sp.	Austria	CBS 613.81	GU269825	GU253842	MF951601	Videira *et al*. (2017)
Pleuropassalora armatae	*Dalbergia armata*	South Africa	CBS 125420	MH863597	MH875073	MF951609	Vu *et al*. (2019), Videira *et al*. (2017)
Pseudocercospora angolensis	*Citrus sinensis*	Angola	CBS 149.53	MH857140	GU214471	JX902004	Vu *et al*. (2019), Crous *et al*. (2009a), Quaedvlieg *et al*. (2012)
Pseudocercospora assamensis	*Musa* sp.	India	CBS 122467 / X988	GU269656	GU253705	JX902005	Crous *et al*. (2013a), Quaedvlieg *et al*. (2012)
Pseudocercospora corylopsidis	*Corylopsis spicata*	Japan	MUCC 908 / MAFF 237795	GU269684	GU253727	KX462621	Crous *et al*. (2013a), Nakashima *et al*. (2016)
Pseudocercospora ershadii	*Diospyros lotus*	Iran	CBS 136114 / CCTU 1206	KM452867	KP717032	MN786459	Bakhshi *et al*. (2014), Braun *et al*. (2020)
Pseudocercospora eupatoriella	*Chromolaena odorata*	Jamaica	CBS 113372	GU269704	GU253743	PP404447	Crous *et al*. (2013a)
Pseudocercospora flavomarginata	*Eucalyptus* sp.	China	CBS 126001 / CPC 14142	GU269804	GU253822	LC599604	Crous *et al*. (2013a), Chen *et al*. (2022)
Pseudocercospora fukuokaensis	*Styrax japonica*	Japan	MUCC 887 / MAFF 237768	GU269714	GU253751	KX462632	Crous *et al*. (2013a), Nakashima *et al*. (2016)
Pseudocercospora haiweiensis	*Eucalyptus* sp.	China	CBS 131584 / CPC 14084	GU269803	GU253821	KX462634	Crous *et al*. (2013a), Nakashima *et al*. (2016)
Pseudocercospora heteropyxidicola	*Heteropyxis* sp.	South Africa	CPC 31359	PP387190	—	PP404493	Crous *et al*. (2019b)
Pseudocercospora humuli	*Humulus lupulus*	Japan	MUCC 742	GU269725	GU253758	KX462637	Crous *et al*. (2013a), Nakashima *et al*. (2016)
Pseudocercospora ixorana	*Ixora chinensis*	Malaysia	MUCC 2608	LC599350	—	LC599610	Chen *et al*. (2022)
Pseudocercospora kobayashiana	*Diospyros kaki*	Japan	MAFF 236999	LC511998	—	LC515791	Braun *et al*. (2020)
Pseudocercospora ocimicola	*Ocimum basilicum*	Mexico	CPC 10283	GU214678	GU214678	—	Crous *et al*. (2009a)
Pseudocercospora robusta	*Angophora robur*	Malaysia	CBS 111175 / CMW 5151 / CPC 1269	KF901678	DQ204767	KX348075	Hunter *et al*. (2006), Quaedvlieg *et al*. (2014), Videira *et al*. (2016)
Pseudocercospora stephanandrae	*Neillia incisa*	Japan	MUCC 914	GU269814	GU253831	KX462658	Crous *et al*. (2013a), Nakashima *et al*. (2016)
Pseudocercospora tabernaemontanae	*Tabernaemontana pandacaqui*	Laos	CPC 19198	LC599363	—	LC599625	Chen *et al*. (2022)
Pseudocercospora tereticornis	*Eucalyptus tereticornis*	Australia	CBS 125214 / CPC 13299	KF901532	KF901854	KX462659	Quaedvlieg *et al*. (2014), Nakashima *et al*. (2016)
Pseudocercospora vitis	*Vitis vinifera*	South Korea	CBS 132012 / CPC 11595	DQ073923	GU214483	KX348076	Ayala-Escobar *et al*. (2006), Crous *et al*. (2009a), Videira *et al*. (2016)
Pseudophaeophleospora atkinsonii	*Hebe*sp.	New Zealand	CBS 124565 / ICMP 17860	GU214643	MF951236	MF951635	Crous *et al*. (2009a), Videira *et al*. (2017)
Pseudophaeophleospora stonei	*Eucalyptus* sp.	Australia	CBS 120830 / CPC 13330	EF394856	FJ493210	MF951636	Videira *et al*. (2017)
Pteridopassaloranephrolepidicola	*Nephrolepis falcata*	Australia	CBS 128211 / CPC 17049	HQ599590	HQ599591	KX462646	Crous *et al*. (2010), Nakashima *et al*. (2016)
Ramularia acroptili	*Rhaponticum repens*	Turkey	CBS 120252	GU214689	GU214689	KX288472	Crous *et al*. (2009a), Videira *et al*. (2016)
Ramularia beticola	*Beta vulgaris*	France	CPC 30066	KX287338	KX287038	KX288497	Videira *et al*. (2016)

© 2025 Westerdijk Fungal Biodiversity Institute

Table 1. (Continued).

Taxons	Host	Locality	Isolate / Voucher ID	GenBank Accession No.			References
				ITS	LSU	*RPB2*	
Ramularia stellariicola	*Myosoton aquaticum*	South Korea	CBS 130592 / CPC 11297 / KACC 42363	GU214693	GU214693	KX288675	Crous *et al.* (2009a), Videira *et al.* (2016)
Ramulariopsis gossypii	*Gossypium* sp.	Brazil	CPC 25909	KX287540	KX287243	KX288702	Videira *et al.* (2016)
Ramulariopsis pseudoglycines	*Gossypium* sp.	Brazil	CPC 18242	KX287543	KX287246	KX288705	Videira *et al.* (2016)
Scirrhia brasiliensis	—	Brazil	CBS 129061	MH865161	MH876602	—	Vu *et al.* (2019)
	Pteridium aquilinum	Brazil	CPC 18733	JN197292	JN197293	—	Crous *et al.* (2011b)
Scolecostigmina mangiferae	*Mangifera indica*	Australia	CBS 125467	MH863595	GU253877	MF951660	Crous *et al.* (2013a), Videira *et al.* (2017), Vu *et al.* (2019)
Septoria convolvuli	*Calystegia sepium*	Netherlands	CBS 102325	GU214697	GU214697	KF252388	Crous *et al.* (2009a), Verkley *et al.* (2013)
Septoria dysentericae	*Daucus carota*	Brazil	CBS 131892 / CPC 12328	GU269854	GU214699	KF252406	Crous *et al.* (2013a), Verkley *et al.* (2013)
Septoria leucanthemi	*Leucanthemum vulgare*	Austria	CBS 109090	KF251455	GQ852677	KF252452	Crous *et al.* (2009b), Verkley *et al.* (2013)
Septoria obesa	*Chrysanthemum indicum*	Germany	CBS 354.58	KF251483	GU214493	KF252479	Crous *et al.* (2009a), Verkley *et al.* (2013)
Septoria senecionis	*Senecio fluviatilis*	Netherlands	CBS 102366	KF251544	GU214498	KF252538	Crous *et al.* (2009a), Verkley *et al.* (2013)
Septoria sonchi	*Sonchus asper*	Korea	CBS 128757	MH865131	MH876570	KF252546	Vu *et al.* (2019)
Septoria stachydicola	*Stachys riederi*	Korea	CBS 128662	MH865109	MH876549	KF252559	Vu *et al.* (2019)
Sonderhenia eucalypticola	*Eucalyptus* sp.	Spain	CBS 112502 / CPC 3749	KF901677	KF902019	MF951672	Quaedvlieg *et al.* (2014), Videira *et al.* (2017)
Sonderhenia eucalyptorum	*Eucalyptus coccifera*	Australia	CBS 120220	KF901505	KF901822	MF951673	Quaedvlieg *et al.* (2014), Videira *et al.* (2017)
Sphaerulina menispermi	*Menispermum dauricum*	Korea	CBS 128666	MH865112	KF252122	KF252609	Vu *et al.* (2019)
Sphaerulina myriadea	*Quercus dentata*	Japan	CBS 124646	JF770455	JF770468	KF252256	Crous *et al.* (2011a), Quaedvlieg *et al.* (2013)
Trochophora fasciculata	*Daphniphyllum macropodum*	South Korea	CBS 124744 / SMKC 21713	GU269872	GU253880	MF951684	Videira *et al.* (2017)
Uwebraunomyces tinosporae	***Tinospora cordifolia***	**India**	**NFCCI 5662**	**PQ811838**	**OR346329**	**PQ861960**	**This study**
	Tinospora cordifolia	**India**	**NFCCI 6083**	**PQ810989**	**PQ810990**	**PQ861961**	**This study**
Uwemyces elaeidis	*Elaeis oleifera*	Colombia	CPUwZC-01	KX228299	KX228356	KX228371	Crous *et al.* (2013b)
Xenoramularia neerlandica	*Iris pseudacorus*	Netherlands	CPC 18377	KX287554	KX287260	KX288722	Videira *et al.* (2016)
Xenosonderhenia eucalypti	*Eucalyptus urophylla*	Mozambique	CBS 138858 / CPC 24247	KP004457	KP004485	MF951688	Videira *et al.* (2017)
Zasmidium arcuatum	*Ischyrolepis subverticillata*	South Africa	CBS 113477	EU041779	EU041836	MF951692	Arzanlou *et al.* (2007), Videira *et al.* (2017)
Zasmidium cellare	Wall in wine cellar	Germany	CBS 892.85	MF951397	MF951262	KT356875	Videira *et al.* (2017)
Outgroup							
Ramichloridium apiculatum	Forest soil	USA	CBS 156.59	EU041791	EU041848	GU371770	Arzanlou *et al.* (2007), Schoch *et al.* (2009)
Uwebraunia australiensis	*Eucalyptus platyphylla*	Australia	CBS 120729 / CPC 13282	KF442513	KF442553	KX348105	Videira *et al.* (2016)

© 2025 Westerdijk Fungal Biodiversity Institute

Two phylogenetic datasets were analysed: dataset 1 (LSU-*RPB2*) and dataset 2 (LSU-*RPB2*-ITS), representing 50 genera of the family *Mycosphaerellaceae* as different combinations of genes may result in alternative phylogenetic hypotheses as described by Videira *et al.* (2017). Bayesian inference (BI) and maximum likelihood (ML) methods were used to generate phylogenetic trees. The BI analysis was conducted using MrBayes v. 3.2.7 (Ronquist *et al.* 2012) with the GTR+I+G model and a Markov chain Monte Carlo (MCMC) algorithm (Rannala & Yang 1996). The analysis was run until the standard deviation of split frequency was below 0.01. A burn-in phase (first 25 % of trees) was discarded, and posterior probabilities were calculated from the remaining trees to generate a majority rule consensus tree. The ML analysis was conducted with RAxML v. 8.2.10 (Stamatakis 2014), using a GTR model with GAMMA and a proportion of invariant sites (Stamatakis 2014), and evaluated with 1000 bootstrap replicates. Both analyses included 110 strains.

The final alignment of the dataset contained 1983 characters, divided into three partitions: 720 (LSU), 828 (*RPB2*), and 435 (ITS), including alignment gaps. Both analyses were rooted with *Ramichloridium apiculatum* (CBS 156.59) and *Uwebraunia australiensis* (CBS 120729). Tree reconstruction, visualization, and editing were performed using FigTree v. 1.4.4 (https://tree.bio.ed.ac.uk/software/figtree/) and TreeGraph v. 2.15.0 (Stöver & Müller 2010).

Genealogical concordance phylogenetic species recognition analysis

The Genealogical Concordance Phylogenetic Species Recognition (GCPSR) model (as described by Taylor *et al.* 2000) was used to clarify species boundaries among closely related and potentially ambiguous taxa by using pairwise homoplasy index (Φw) test, a statistical test to evaluate genetic data. GCPSR is valued for its ability to synthesize information from multiple genes, evaluate gene flow, operate within an evolutionary timescale, and provide practical insights into species delimitation. It underscores the complexity

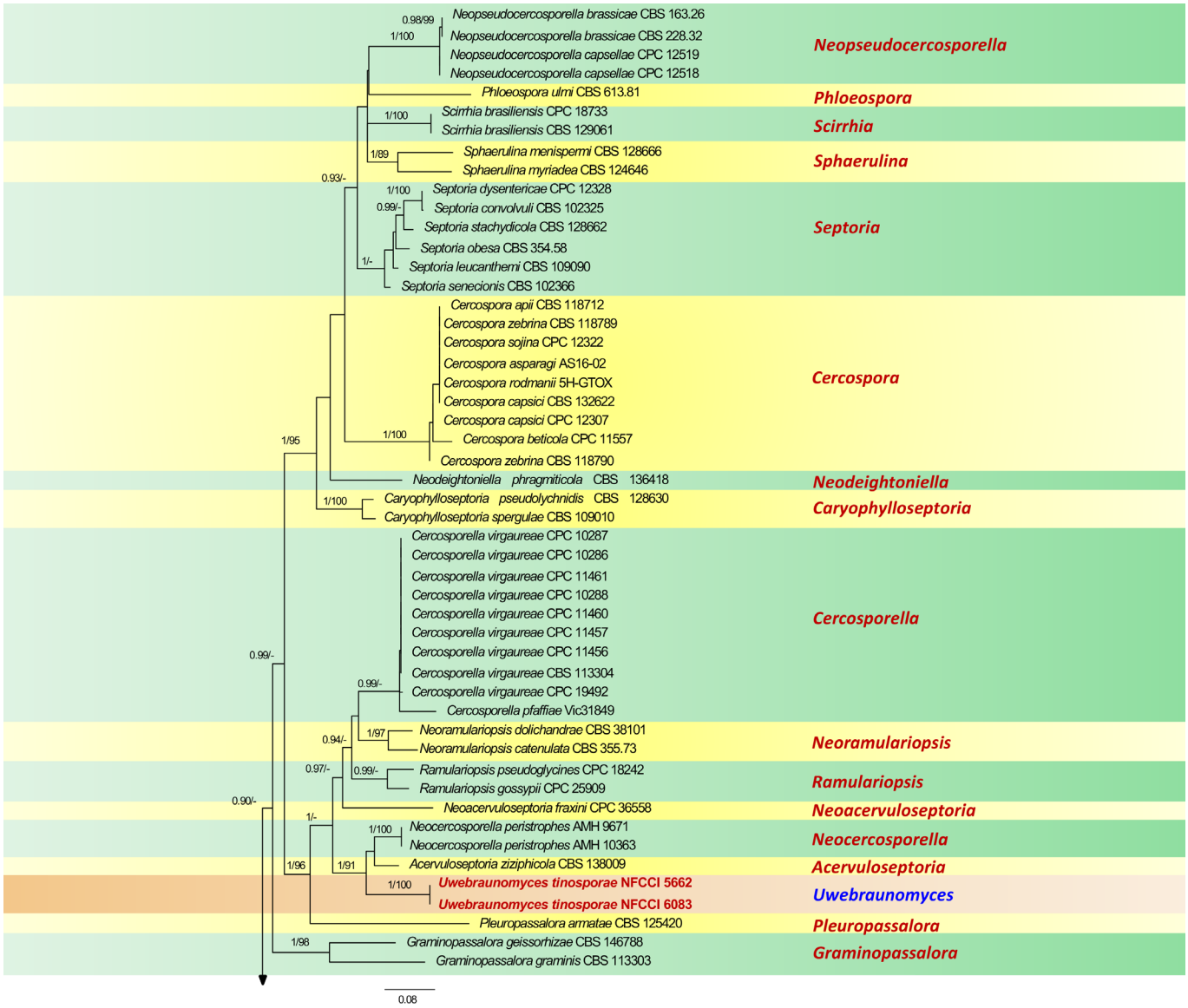

Fig. 1. Phylogenetic tree resulting from a RAxML analysis of the combined LSU/*RPB2* sequence alignment (dataset 1). The Bayesian posterior probabilities (≥ 0.90; BI-PP) and maximum likelihood bootstrap support values (≥ 85 %; ML-BS) are given at the nodes (BI-PP/ML-BS). The newly introduced lineage is represented in **bold** and novel genus denoted in blue. The tree is rooted to *Ramichloridium apiculatum* (CBS 156.59) and *Uwebraunia australiensis* (CBS 120729).

© 2025 Westerdijk Fungal Biodiversity Institute

of species boundaries and offers a robust framework for understanding evolutionary relationships among organisms (Koufopanou *et al.* 1997, Geiser *et al.* 1998, Taylor *et al.* 2000, Starkey *et al.* 2007). A pairwise homoplasy index (PHI) test (Philippe & Bryant 2006) was performed in SplitsTree4 (Huson 1998, Huson & Bryant 2006) in order to determine the recombination level within phylogenetically closely related species using a three-locus concatenated dataset of closely related species. If the pairwise homoplasy index (PHI) value exceeds the threshold of 0.05 (Φw ≥ 0.05), it signifies the absence of significant recombination in the dataset. The relationships between these three, closely related, genus groups were visualized by constructing splits graphs (Fig. 3) from the three-locus concatenated datasets, using both the Log-Det transformation and splits decomposition options.

RESULTS

Taxonomy

Uwebraunomyces Gargee Singh & Raghv. Singh, ***gen. nov.*** MB 857059.

Etymology: Latin, *Uwebraunomyces* derived from the name of Prof. dr Uwe Braun (Martin-Luther-Universität, Germany), a globally renowned mycologist.

Type species: *Uwebraunomyces tinosporae* (Lacy &Thirum.) Gargee Singh & Raghv. Singh (≡ *Ramularia tinosporae* Lacy & Thirum.)

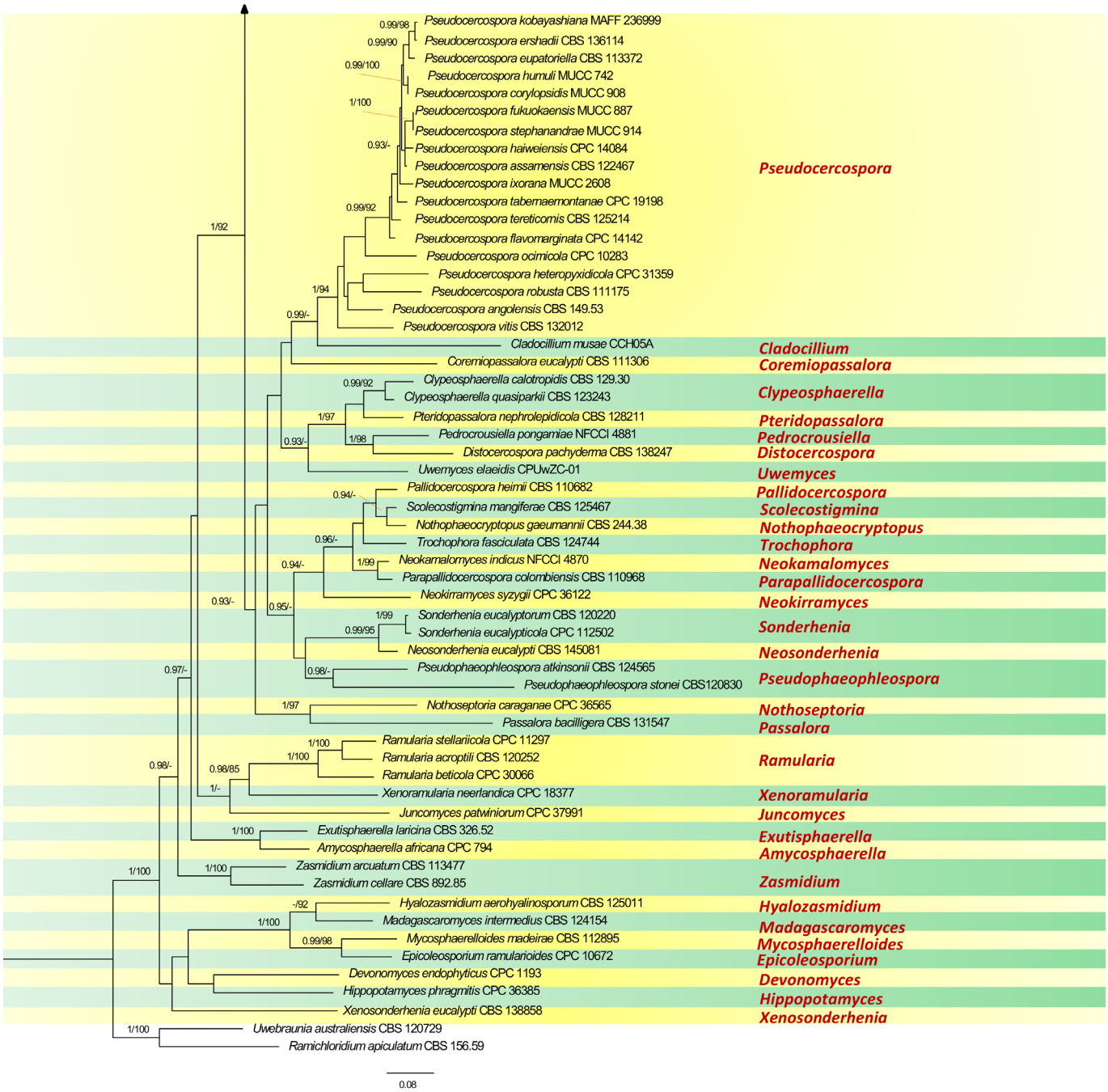

Fig. 1. (Continued).

© 2025 Westerdijk Fungal Biodiversity Institute

Diagnosis: Differs from *Neocercosporella* by its protuberant loci, which bulge outward to form a convex or truncated cone with an apical depression, a small papilla or conical protuberant structure at the centre, and with a minute frill, usually in older scars (ultrastructure). It produces solitary conidia that are obpyriform, oval, or obclavate with obconically truncated bases with a basal depression having a centrally located, somewhat protuberant structure (ultrastructure), and somewhat thickened, darkened hila. In contrast, *Neocercosporella* has conical loci with small rim-like depressions on the top encircling a small, flat and protuberant-like structure (ultrastructure). *Neocercosporella* produces weak catenation with obclavate to obclavate-cylindrical conidia, a truncate base (ultrastructure), and unthickened or slightly thickened, darkened hila. Additionally, *Uwebraunomyces* is hyphomycetous, unlike the coelomycetous *Acervuloseptoria*.

Description: *Infection spots* amphigenous, initial discolouration angular to vein-limited, white, later centre white surrounded by brown to dark blackish brown, coalescing to cover entire leaf surface, necrotic. *Colonies* hypogenous, white, punctiform to dense velvety. *Mycelium* internal. *Stromata* present, globose to sub-globose, sub-stomatal, pale brown to dark brown. *Conidiophores* macronematous, densely fasciculate, arising from stromata, initially erumpent through stomata, later by rupturing epidermis, erect to procumbent, pale olivaceous to very pale brown, slightly roughened, thin- to thick-walled, mostly unbranched, rarely branched, subcylindrical to geniculate-sinuous at the tip, septate. *Conidiogenous cells* integrated, terminal, polyblastic, cylindrical, conidiogenous loci prominently protuberant, thickened and darkened, extended beyond the area originally occupied by the base of the conidium, loci bulge outward, forming a convex or truncated cone with apical depression having centrally located a small papilla or somewhat conical protuberant like structure and with minute distinct frill usually in old scar (ultrastructure). *Conidia* solitary, obpyriform, oval to obclavate, sometimes slightly curved, mostly pale olivaceous to very pale brown, sometimes hyaline, dry, smooth, thin-walled, septate, base obconically truncated, with a basal depression having a centrally located, somewhat protuberant structure (ultrastructure), tip attenuated, hila somewhat thickened and darkened.

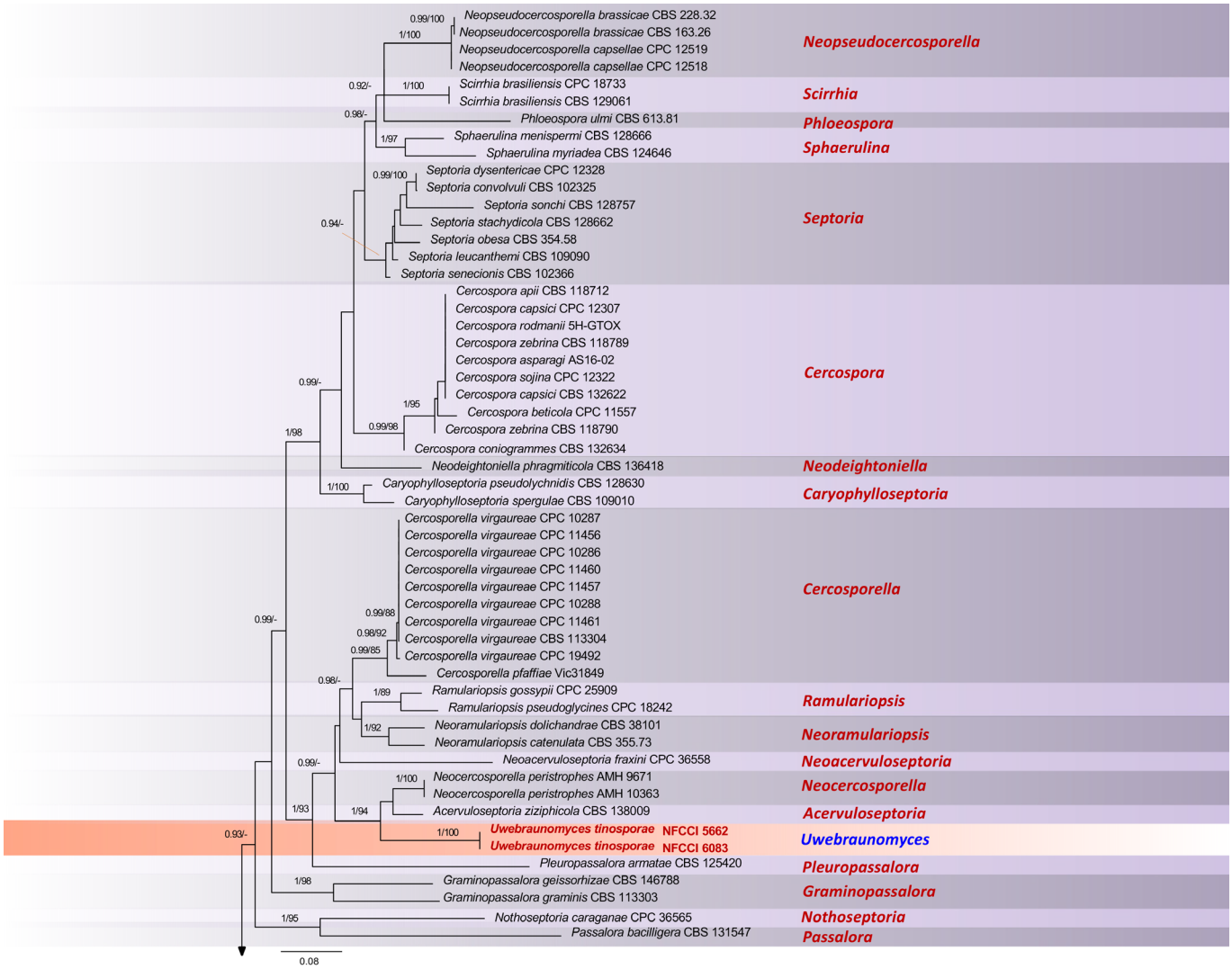

Fig. 2. Phylogenetic tree resulting from a RAxML analysis of the combined LSU/*RPB2*/ITS sequence alignment (dataset 2). The Bayesian posterior probabilities (≥ 0.90; BI-PP) and maximum likelihood bootstrap support values (≥ 85 %; ML-BS) are given at the nodes (BI-PP/ML-BS). The newly introduced lineage is represented in **bold** and novel genus denoted in blue. The tree is rooted to *Ramichloridium apiculatum* (CBS 156.59) and *Uwebraunia australiensis* (CBS 120729).

© 2025 Westerdijk Fungal Biodiversity Institute

Uwebraunomyces tinosporae (Lacy & Thirum.) Gargee Singh & Raghv. Singh, ***comb. nov.*** MB 857060. Figs 4–6.
Basionym: *Ramularia tinosporae* Lacy & Thirum., *Sydowia* **5**: 126. 1951.
Synonyms: *Cercosporella tinosporae* (Lacy & Thirum.) Deighton, *Mycol. Pap*. **133**: 35. 1973.
Cercosporidium tinosporae A.K. Kar & J.B. Ray, *Indian Phytopathol*. **38**: 180. 1985.
Passalora tinosporae (A.K. Kar & J.B. Ray) Poonam Srivast., *J. Liv. World* **1**: 118. 1994.
Pseudocercosporella bundelkhandae S. Shrivast. *et al.*, *J. Mycol. Pl. Pathol*. **39**: 305. 2009.
Cercosporella bundelkhandae (S. Shrivast. *et al.*) Raghv. Singh *et al. Mycotaxon* **135**: 317. 2020.

Typus: **India**, Patna, Bihar, on leaves of *Tinospora cordifolia* (*Menispermaceae*), 28 Aug. 1950, coll. *R.C. Lacy* (**holotype** not seen!); [**Lectotype** designated here, MBT 10026489: Pl. V, fig. 2, Thirum. & Lacy (1951), *Sydowia* **5**: 126]; Uttar Pradesh, Gorakhpur, Kusumhi Forest, 26.7407N, 83.36065E, on living leaves of *T. cordifolia*, 2 Sep. 2021, coll. *G. Singh*, MH-BHU 93 (**epitype** designated here AMH 10705, MBT 10026339), ex-epitype culture NFCCI 5662, GenBank: PQ811838 (ITS), OR346329 (LSU), PQ861960 (*RPB2*).

Additional specimens examined: **India**, Uttar Pradesh, Jhansi, on living leaves of *T. cordifolia*, Dec. 2010, coll. *S. Jain* (HCIO 44091); Uttar Pradesh, Varanasi, BHU Campus, 25.2678N, 82.9904E, on living leaves of *T. cordifolia*, 9 Oct. 2023, coll. *P. Kumari*, MH-BHU 122 (AMH 10734), culture NFCCI 6083, GenBank: PQ810989 (ITS), PQ810990 (LSU), PQ861961 (*RPB2*).

Infection spots amphigenous, initially discolourations, angular to vein-limited, 2–14 mm diam., white, later centre white surrounded by brown to dark blackish brown region, coalescing to cover entire leaf surface, necrotic. *Colonies* hypogenous, white, punctiform to dense velvety. *Mycelium* internal. *Stromata* present, globose to sub-globose, sub-stomatal, light brown to dark brown, (20–)25–30(–35) × (10–)20–30(–35) µm. *Conidiophores* macronematous, densely fasciculate, arising from stromata, initially erumpent through stomata, later by rupturing epidermis, erect to procumbent, light olivaceous to very light brown, slightly roughened, thin-walled to thick-walled, mostly unbranched, rarely branched, subcylindrical to geniculate-sinuous at the tip, 0–3-euseptate, (15–)25–85(–95) × (2–)2.5–5(–6.5) µm. *Conidiogenous cells* integrated, terminal, polyblastic, cylindrical, conidiogenous loci prominently protuberant,

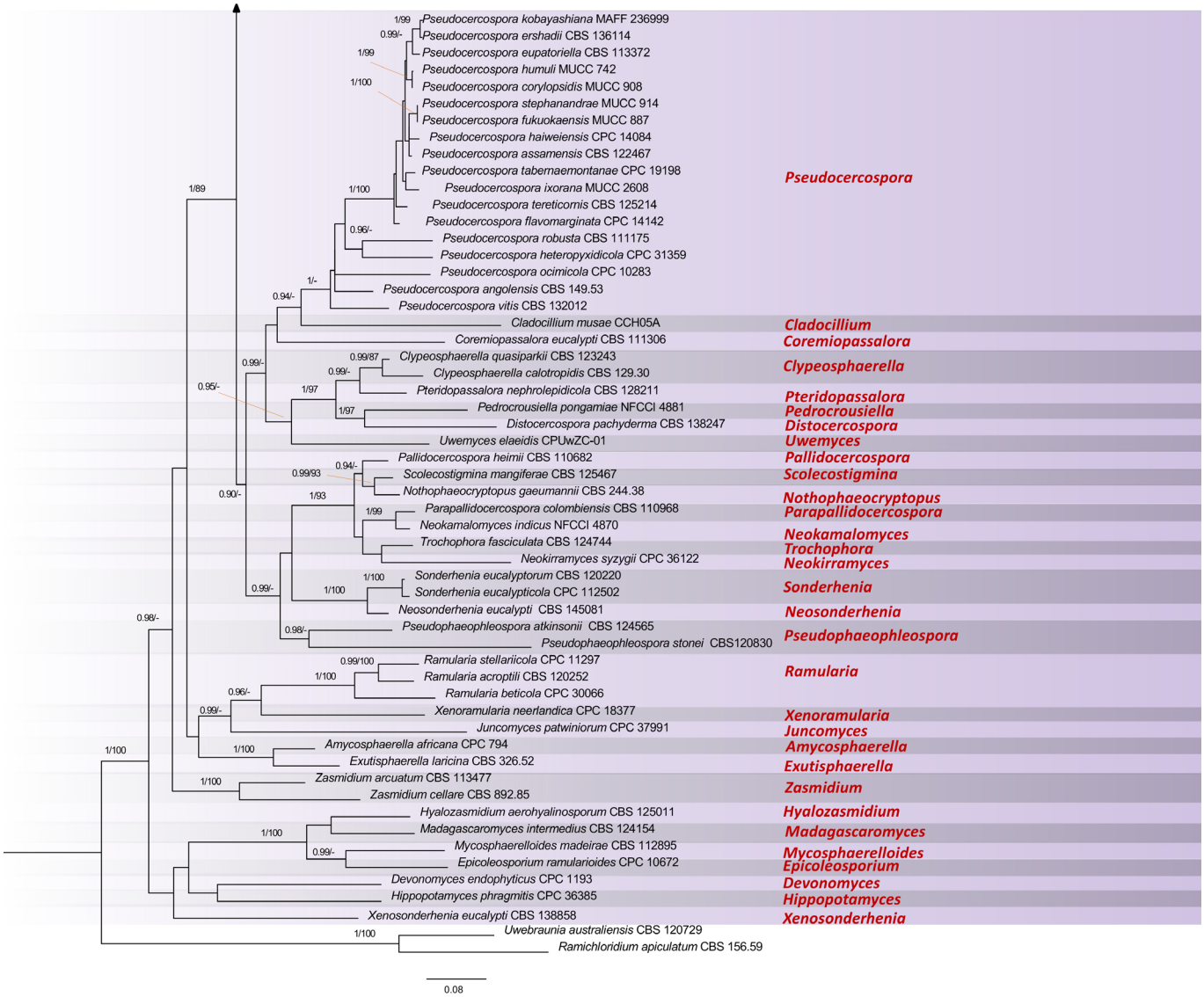

Fig. 2. (Continued).

© 2025 Westerdijk Fungal Biodiversity Institute

thickened and darkened, (2.5–)3–4(–4.5) µm wide, extended beyond the area originally occupied by the base of the conidium, loci bulge outward, forming a convex or truncated cone with apical depression having centrally located a small papilla or somewhat conical protuberant like structure and with minute distinct frill usually in old scar (ultrastructure), frill 1.5–2 diam. *Conidia* solitary, obpyriform, oval to obclavate, sometimes slightly curved, mostly light olivaceous to very light brown, sometimes hyaline, dry, smooth, thin-walled, 0–4-euseptate, base obconically truncated, with a basal depression having a centrally located, somewhat protuberant structure (ultrastructure), tip attenuated, (15–)25–50(–60) × (6.5–)7.5–9(–11) µm, hila somewhat thickened and darkened, (1–)2.5–2.8 µm wide.

Culture characteristics (*25 °C, 2 wk*): Very slow growing, reaching up to 5–6 mm diam. on PDA after 2 wk. Top colour cottony whitish and reverse dark blackish brown, surface raised, margin almost circular to sub-circular. *Hyphae* branched, septate, smooth, thin-walled, hyaline to pale olivaceous brown and 2–4.5 µm diam. Fertile. *Conidiophores* develop on terminal as well as lateral branches of hyphae. *Conidiogenous cells* integrated, terminal, cylindrical, thin-walled, smooth, (20–)23–31(–37) × (4–)4.5–4.7(–5.5) µm, loci indistinct. *Conidia* solitary, obpyriform, oval to obclavate, sometimes slightly curved, hyaline to mostly very pale olivaceous brown, dry, smooth, thin-walled, 0–2-euseptate, base obconically truncated, tip attenuated, (22–)25–35(–40) × (6–)6.5–8.5(–10) µm, hila somewhat thickened and darkened, 1.5–2.5 µm wide.

Blast results and Phylogeny

Based on a megablast search of NCBI's GenBank nucleotide database, the closest hits using the **ITS** sequence had highest similarity to *Neocercosporella peristrophes* [strain AMH 9671, GenBank MZ311866; Identities = 358/390 (92 %), 13 gaps (3 %)], *Neocercosporella peristrophes* [strain AMH 10363, GenBank ON310831; 358/390 (92 %), 13 gaps (3 %)], and *Acervuloseptoria ziziphicola* [strain CBS 138009, GenBank NR_156287; Identities = 354/389 (91 %), 10 gaps (2 %)]. Closest hits using the **LSU** sequence are *Cercosporella virgaureae* [strain CBS 113304, GenBank GU214658; Identities = 1123/1165 (96 %), no gaps], *Septoria obesa* [strain CBS 354.58, GenBank GU214493; Identities = 1122/1165 (96 %), no gaps], and *Septoria dysentericae* [strain CBS 12328, GenBank GU214699; Identities = 1121/1165 (96 %), no gaps]. Closest hits using the ***RPB2*** sequence had highest similarity to *Acervuloseptoria ziziphicola* [strain CBS 138009, GenBank MF951425; Identities = 691/787 (88 %), no gaps], *Neocercosporella peristrophes* [strain AMH 10363, GenBank ON376994; Identities = 690/790 (87 %), no gaps], and *Neocercosporella peristrophes* [strain AMH 9671, GenBank OL773683; Identities = 690/790 (87 %), no gaps].

The sequences from specimens NFCCI 5662 and NFCCI 6083 were 100 % identical in each region. Phylogenetic trees generated from Bayesian inference (BI) and maximum likelihood (ML) analyses showed almost similar topologies. The best-scoring RAxML tree is presented in Figs 1 and 2. Analysis of dataset 1 fully supported the results from dataset 2 analysis.

Based on both datasets, *Uwebraunomyces* belongs to the *Mycosphaerellaceae* (Figs 1, 2). However, both strains (NFCCI 5662 and NFCCI 6083) cluster together with strong statistical support (BI-PP/ML-BS: 1/100) and formed a well-defined clade close to *Acervuloseptoria* and *Neocercosporella* with strong statistical support in both datasets (BI-PP/ML-BS: 1/91 in dataset 1 and 1/94 in dataset 2). This confirmed that *Acervuloseptoria*, *Neocercosporella*, and *Uwebraunomyces* represent separate clades within a statistically supported monophyletic group (Figs 1, 2).

Phylogenetically, *Acervuloseptoria* forms a single-strain lineage and differs from *Uwebraunomyces* in morphology. *Acervuloseptoria* has black, subepidermal, erumpent, multilocular conidiomata with an upper layer breaking open irregularly, forming an acervular appearance. Its conidiophores are pale brown and verruculose, and its conidia are narrowly obclavate to subcylindrical and guttulate (Crous *et al.* 2014). These differences in morphology are significant enough for retaining *Uwebraunomyces* (a hyphomycete) as distinct from *Acervuloseptoria* (a coelomycete).

Uwebraunomyces and *Neocercosporella* can be easily distinguished based on the ultrastructure of their conidiogenous loci. *Neocercosporella* has conical loci with

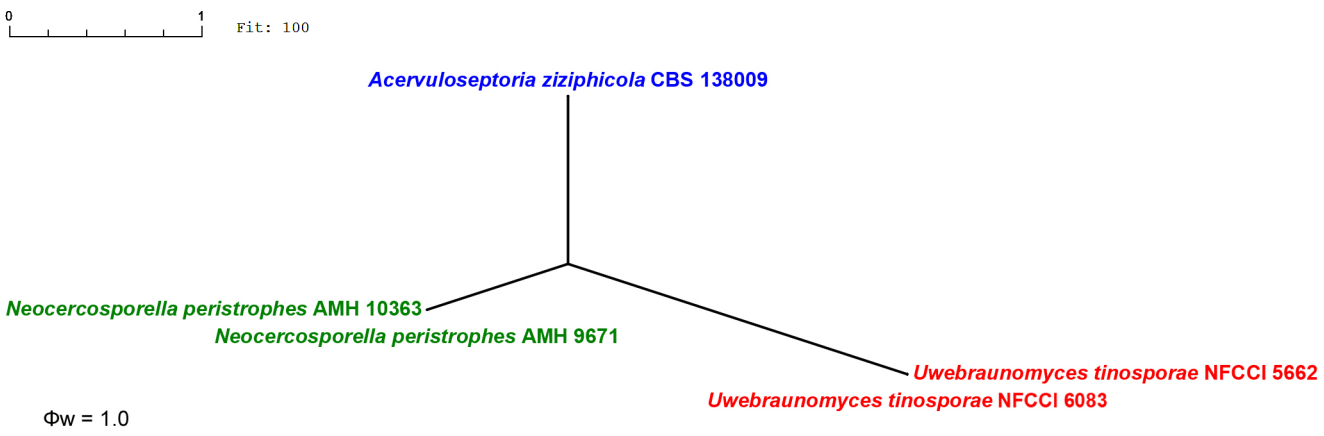

Fig. 3 Split graph showing the results of the pairwise homoplasy index (PHI) test of closely related genera using both LogDet transformation and splits decomposition. The PHI test results (Φw) ≤ 0.05 from the PHI test denotes the presence of significant recombination within the dataset. The newly identified taxon is shown in red.

© 2025 Westerdijk Fungal Biodiversity Institute

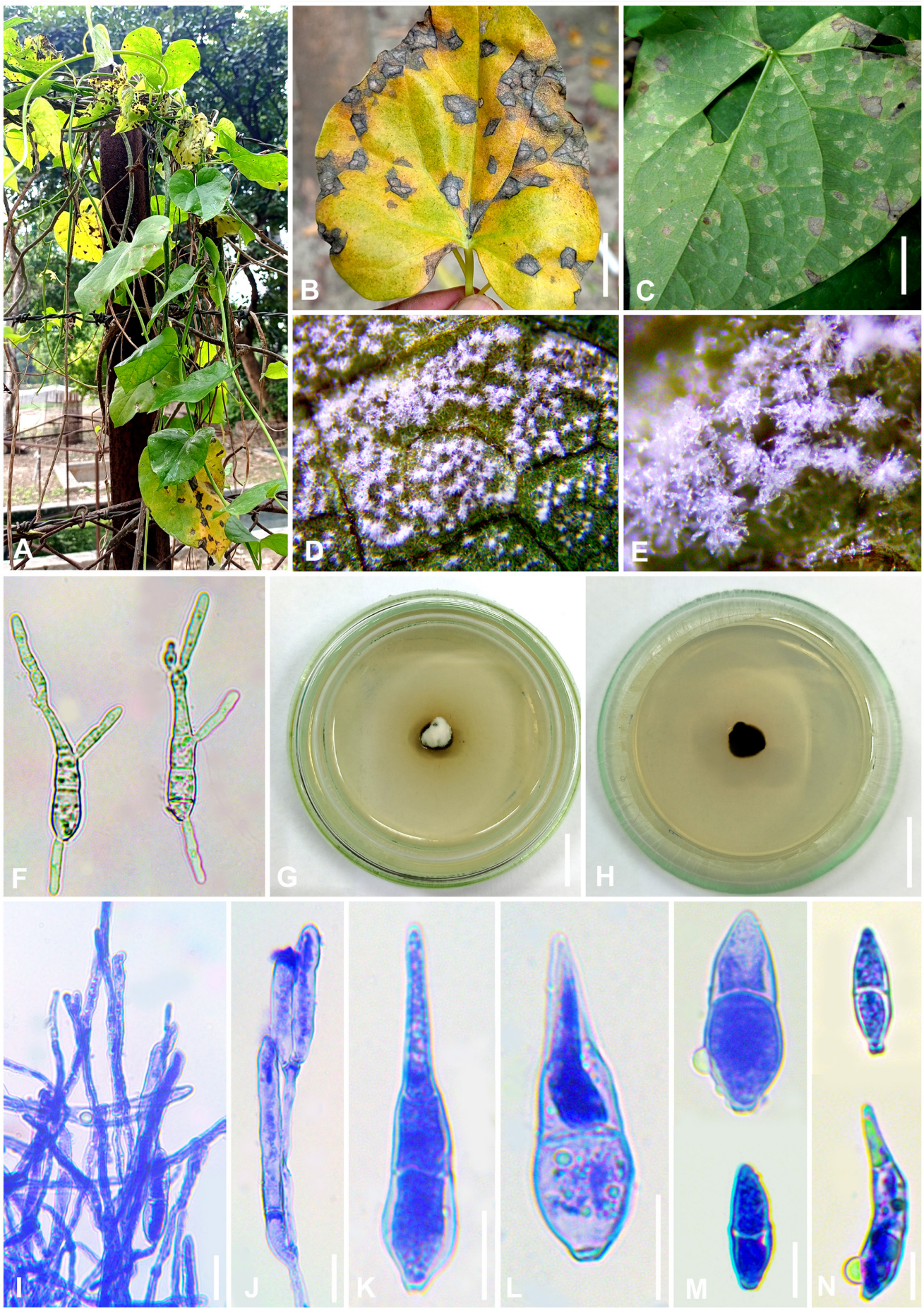

Fig. 4. Symptoms of infection of *Uwebraunomyces tinosporae* on *Tinospora cordifolia*. **A.** *Tinospora cordifolia* in natural habitat. **B.** Symptom on upper leaf surface. **C.** Symptom on lower leaf surface. **D, E.** Close-up of leaf surface showing fructification. **F.** Germinating conidia. **G.** Top view of culture on PDA. **H.** Reverse view of culture on PDA. **I, J.** Mycelia from culture showing fructification. **K–N.** Conidia from culture. Scale bars: B, C = 20 mm; G, H = 10 mm; I–N = 10 µm.

© 2025 Westerdijk Fungal Biodiversity Institute

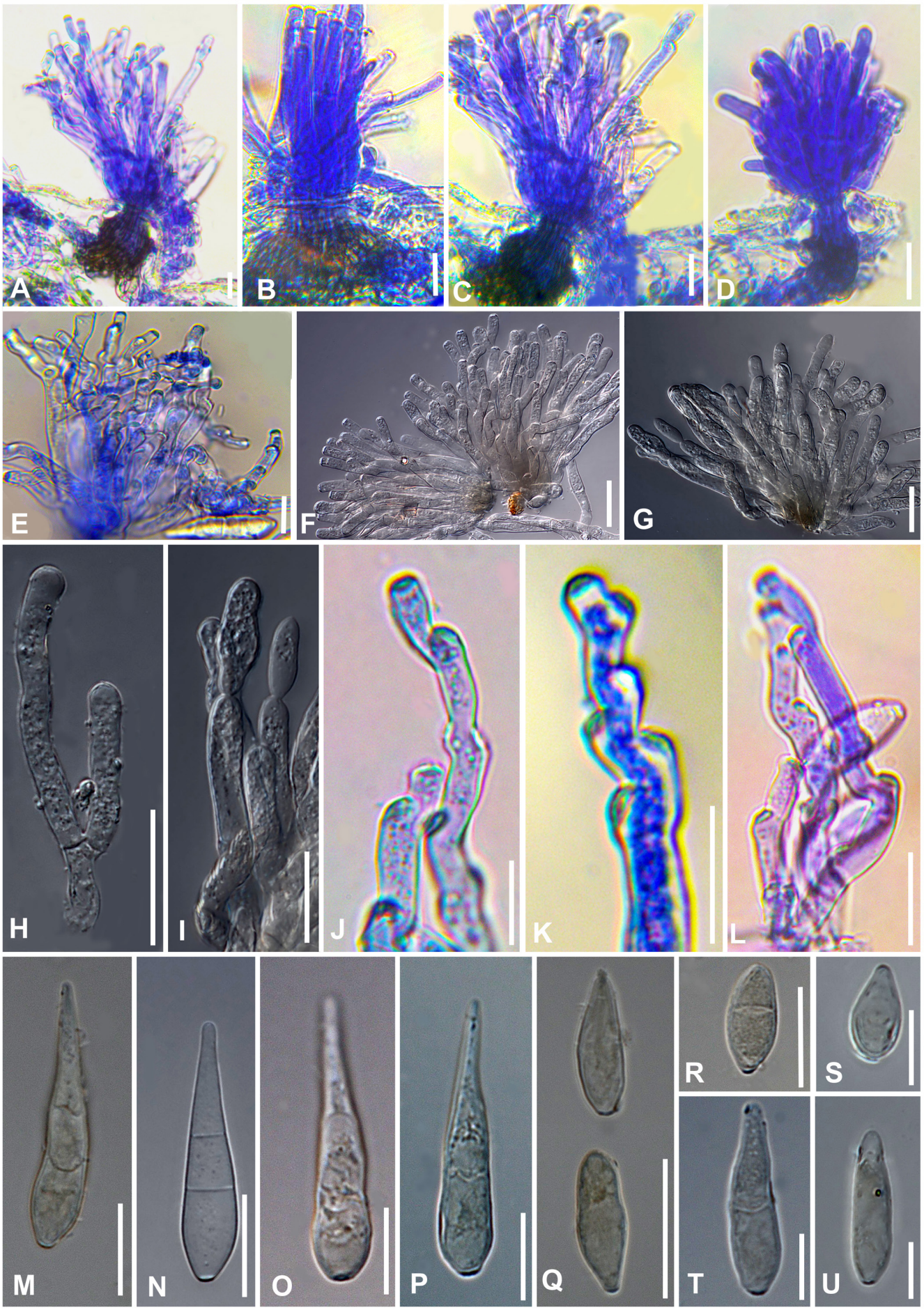

Fig. 5. *Uwebraunomyces tinosporae* (AMH 10705). **A–D.** Fascicles of conidiophores develop from sub-stomatal stromata. **E–G.** Fascicles of conidiophores. **H.** Branched conidiophore. **I.** Conidia with conidiophores. **J–L.** Conidiogenous cells with protuberant, thickened and darkened loci. **M–U.** Conidia. Scale bars: A–E, J–L, S–U = 10 µm; F–I, M–R = 20 µm.

© 2025 Westerdijk Fungal Biodiversity Institute

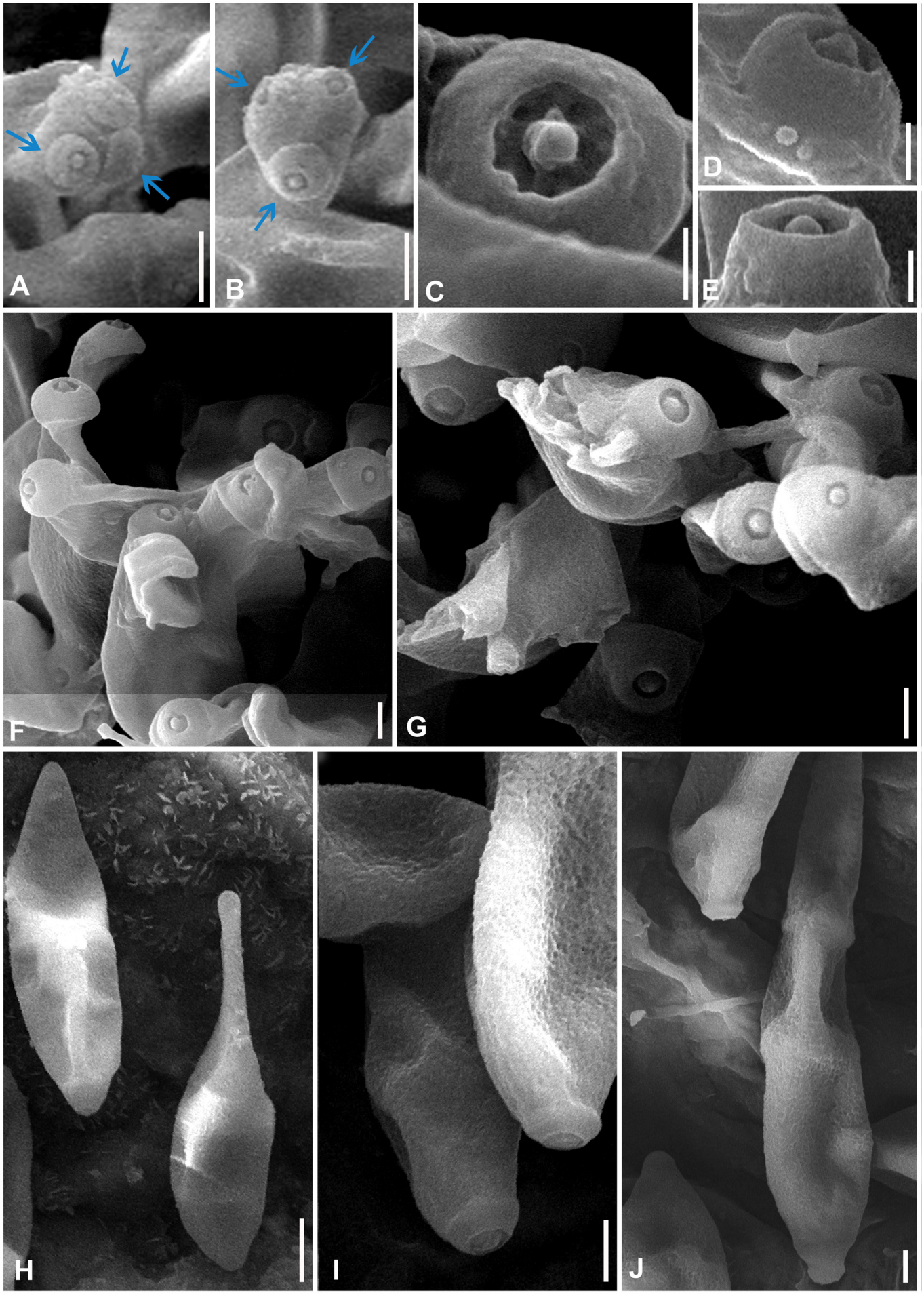

Fig. 6. Scanning electron microphotographs of *Uwebraunomyces tinosporae* (AMH 10705). **A, B.** Polyblastic conidiogenous cells (blue arrows). **C–G.** Top and lateral view of conidiogenous loci. **H.** Conidia. **I, J.** Top and lateral view of conidial hila. Scale bars: A, B, H = 5 µm; C–E = 1 µm; F, G, I, J = 2 µm.

© 2025 Westerdijk Fungal Biodiversity Institute

very small rim-like depressions on the top encircling a small, flat and protuberant-like structure (Yadav *et al.* 2023), whereas *Uwebraunomyces* has prominently protuberant loci, extended beyond the area originally occupied by the base of the conidium, loci bulge outward, forming a convex or truncated cone with apical depression having centrally located a small papilla or conical protuberant structure and with minute distinct frill usually in old scar. *Neocercosporella* produces weak catenation with obclavate to obclavate-cylindrical conidia, a truncate base (ultrastructure), unthickened or slightly thickened and darkened hila. In contrast, *Uwebraunomyces* produces solitary, obpyriform, oval, or obclavate conidia with the base obconically truncated, with a basal depression having a centrally located, somewhat protuberant structure (ultrastructure), and somewhat thickened and darkened hila.

Based on the morphological and molecular data, the separation of *Uwebraunomyces* from *Acervuloseptoria*, *Neocercosporella*, and potentially other cercosporella-like genera is strongly supported, highlighting its distinct characteristics and phylogenetic placement.

Genealogical concordance phylogenetic species recognition analysis

The PHI tests were carried out to calculate the recombination level within three phylogenetically closely related genera. The PHI tests showed that there is no significant recombination (Φw = 1.0) between *Uwebraunomyces* strains and their closely related taxa viz., *Acervuloseptoria* and *Neocercosporella* (Fig. 3).

DISCUSSION

Only three species of *Cercosporella* are so far reported on *Tinospora* spp. viz., *Cercosporella bundelkhandae*, *Cercosporella dioscoreophylli* (≡ *Cercospora dioscoreophylli*) and *Cercosporella tinosporae* (≡ *Ramularia tinosporae*) (Thirumalachar & Lacy 1951, Deighton 1973, Braun 1995, Singh *et al.* 2020a).

Cercosporella tinosporae was originally described as *Ramularia tinosporae*. The true generic affinity of *R. tinosporae* was unclear due to the lack of molecular sequence data and ultrastructural analysis, hence, its classification was relying solely on morphological features (Thirumalachar & Lacy 1951). Consequently, it was placed in *Ramularia*. However, Deighton (1973) transferred it to *Cercosporella tinosporae* based on the morphological features described by Thirumalachar & Lacy (1951), including 1–2 septate conidia with an obpyriform shape.

Cercosporella bundelkhandae (Singh *et al.* 2020a), *C. tinosporae* (Deighton 1937), and *Uwebraunomyces tinosporae* share nearly identical morphological features, supporting their taxonomic synonymy. All three produce similar infection spots and whitish colonies, with stromata developing beneath the stomata. Their conidiophores are likewise comparable — arising in fascicles from stromata, typically unbranched, subcylindrical to geniculate-sinuous at the apex, few-septate, and pale olivaceous to very pale brown in colour. The conidiogenous loci are thickened, darkened, and outwardly bulging, bearing a centrally located small papilla and a minute, distinct frill that becomes especially noticeable in older scars. Their conidia are also similar: hyaline, solitary, obpyriform to obclavate, straight to curved, and few-septate, with somewhat thickened and darkened hila.

Based on both datasets, *Uwebraunomyces tinosporae* is phylogenetically distinct from the *Cercosporella s. str.* clade, supporting its exclusion from *Cercosporella*. The DNA sequence analysis of strains NFCCI 5662 and NFCCI 6083 reveals that they are identical, cluster together with strong statistical support (BI-PP/ML-BS: 1/100), and do not fit into any of the known *Mycosphaerellaceae* genera (Figs 1, 2). This analysis supports the establishment of the new monotypic genus, *Uwebraunomyces*, to accommodate this distinct lineage, highlighting its unique evolutionary placement. Consequently, *C. bundelkhandae* and *C. tinosporae* are synonymized under *Uwebraunomyces,* with *Ramularia tinosporae* designated as its type species.

Morphologically, *Uwebraunomyces* can be distinguished from *Cercosporella* by differences in their conidiogenous scars. *Cercosporella* has unique flat, cone-shaped conidiogenous scars, as described by Kirschner (2009), while *Uwebraunomyces* features scars that bulge outward, forming a convex or truncated cone. These scars have a thickening extending beyond the area originally occupied by the base of the conidium. Additionally, *Uwebraunomyces* displays a minute papilla or small somewhat conical protuberant-like structure in the centre of the apical depression of older scars, while a minute frill is commonly observed at the apex.

Uwebraunomyces tinosporae is distinct from *C. dioscoreophylli* due to its wider, commonly obpyriform, oval to obclavate conidia, which are typically 0–4-septate. Additionally, its conidiophores are rarely branched and less septate, distinguishing it morphologically (Deighton 1973, Braun 1995).

Some other cercosporoid species reported on *Tinospora* spp. are *Cercospora madhauliensis* (Kamal *et al*. 1987), *Passalora menispermi* (Crous & Braun 2003), *Pseudocercospora cocculi* (Deighton 1976), *P. madhauliensis* (Kamal *et al.* 1991), *P. tinosporae* (Rai & Kamal 1989), *P. tinosporicola* (Bagyanarayana & Braun 1992) and *P. tinosporigena* (Braun & Crous 2005).

Cercospora madhauliensis differs from *U. tinosporae* in having completely hyaline, acicular, and highly septate conidia with thickened, darkened, rim-like hila, as well as rim-like, thickened, and darkened conidiogenous loci. *Passalora menispermi* differs in having multiseptate, olivaceous brown to dark brown conidia and conidiophores. *Uwebraunomyces tinosporae* differs from all the *Pseudocercospora* spp. in that the *Pseudocercospora* spp. produce pigmented conidia and conidiophores without having thickened and darkened loci and hila.

ACKNOWLEDGEMENTS

The authors are indebted to anonymous reviewers for helpful comments and the curator of AMH and NFCCI for accepting material and providing an accession number. We are also thankful to the Head, CAS in Botany, Banaras Hindu University, Varanasi for instrumental facilities. RS thanks the Science & Engineering Research Board (SERB), Department

© 2025 Westerdijk Fungal Biodiversity Institute

of Science & Technology (DST), Govt. of India (Scheme No. CRG/2020/006053), Institution of Eminence (R/Dev./D/IoE/Incentive/2021-22/32387), BHU, Varanasi, Bridge Grant (No. SRICC/Bridge Grant/2024-25/3151), BHU, Varanasi and SY acknowledge the Raja Jwala Prasad Post-Doctoral Fellowship (No. SRICC/RJP-PDF/2023-24/6158) under Institution of Eminence, BHU, Varanasi for providing financial support.

Conflict of interest: The authors declare that there is no conflict of interest.

REFERENCES

Arzanlou M, Groenewald JZ, Gams W, *et al.* (2007). Phylogenetic and morphotaxonomic revision of *Ramichloridium* and allied genera. *Studies in Mycology* **58**: 57–93. https://doi.org/10.3114/sim.2007.58.03

Ayala-Escobar V, Yánez-Morales de Jesùs M, Braun U, *et al.* (2006). *Pseudocercospora opuntiae sp. nov*., the causal organism of cactus leaf spot in Mexico. *Fungal Diversity* **21**: 1–9

Bagyanarayana G, Braun U (1992). Notes on Indian *Cercosporae* and allied genera (I). *International Journal of Mycology and Lichenology* **5**: 165–174.

Bakhshi M, Arzanlou M, Babai-Ahari A, *et al.* (2014). Multi-gene analysis of *Pseudocercospora* spp. from Iran. *Phytotaxa* **184**: 245–264. https://doi.org/10.11646/phytotaxa.184.5.1

Braun U (1995). *A monograph of Cercosporella, Ramularia and allied genera (phytopathogenic hyphomycetes): Vol. 1*. IHW-Verlag, Eching, Munich, Germany.

Braun U (1998). *A monograph of Cercosporella, Ramularia and allied genera (phytopathogenic hyphomycetes): Vol. 2*. IHW-Verlag, Eching, Munich, Germany.

Braun U, Crous PW (2005). Additions and corrections to names published in *Cercospora* and *Passalora*. *Mycotaxon* **92**: 395–416.

Braun U, Nakashima C, Bakhshi M, *et al.* (2020). Taxonomy and phylogeny of cercosporoid ascomycetes on *Diospyros* spp. with special emphasis on *Pseudocercospora* spp. *Fungal Systematics and Evolution* **6**: 95–127. https://doi.org/10.3114/fuse.2020.06.06

Chen CH, Hsieh SY, Yeh YH, *et al.* (2020). *Cladocillium musae*, a new genus and species of cercosporoid fungi (*Mycosphaerellaceae*) on wild banana in Taiwan. *Mycological Progress* **19**: 837–843. https://doi.org/10.1007/s11557-020-01595-3

Chen Q, Bakhshi M, Balci Y, *et al.* (2022). Genera of phytopathogenic fungi: GOPHY 4. *Studies in Mycology* **101**: 417. https://doi.org/10.3114/sim.2022.101.06

Crous PW, Braun U (2003). *Mycosphaerella* and its anamorphs: 1. Names published in *Cercospora* and *Passalora*. *CBS Biodiversity Series* **1**. Westerdijk Fungal Biodiversity Institute, Utrecht, the Netherlands.

Crous PW, Braun U, Hunter GC, *et al.* (2013a). Phylogenetic lineages in *Pseudocercospora*. *Studies in Mycology* **75**: 37–114. https://doi.org/10.3114/sim0005

Crous PW, Cowan DA, Maggs-Kölling G, *et al.* (2020b) Fungal Planet description sheets: 1112–1181. *Persoonia* **45**: 251–409. https://doi.org/10.3767/persoonia.2020.45.10

Crous PW, Groenewald JZ, Pongpanich K, *et al.* (2004). Cryptic speciation and host specificity among *Mycosphaerella* spp. occurring on Australian *Acacia* species grown as exotics in the tropics. *Studies in Mycology* **50**: 457–469.

Crous PW, Groenewald JZ, Shivas RG (2010). *Pseudocercospora nephrolepidicola*.: Fungal Planet 59. *Persoonia* **25**: 138–139.

Crous PW, Minnis AM, Pereira OL, *et al.* (2011b). What is *Scirrhia*? *IMA Fungus* **2**: 127–133. https://doi.org/10.5598/imafungus.2011.02.02.03

Crous PW, Schoch CL, Hyde KD, *et al.* (2009a). Phylogenetic lineages in the *Capnodiales*. *Studies in Mycology* **64**: 17–47. https://doi.org/10.3114/sim.2009.64.02

Crous PW, Shivas RG, Quaedvlieg W, *et al.* (2014). Fungal Planet description sheets: 214–280. *Persoonia* **32**: 184–306. https://doi.org/10.3767/003158514X682395

Crous PW, Summerell BA, Carnegie AJ, *et al.* (2009b). Unravelling *Mycosphaerella*: do you believe in genera? *Persoonia* **23**: 99–118. https://doi.org/10.3767/003158509X479487

Crous PW, Summerell BA, Carnegie AJ, *et al.* (2009d). Novel species of *Mycosphaerellaceae* and *Teratosphaeriaceae*. *Persoonia* **23**: 119–146. https://doi.org/10.3767/003158509X479531

Crous PW, Tanaka K, Summerell BA, *et al.* (2011a). Additions to the *Mycosphaerella* complex. *IMA Fungus* **2**: 49–64. https://doi.org/10.5598/imafungus.2011.02.01.08

Crous PW, Wingfield MJ, Cheewangkoon R, *et al.* (2019a). Foliar pathogens of eucalypts. *Studies in Mycology* **94**: 125–298. https://doi.org/10.1016/j.simyco.2019.08.001

Crous PW, Wingfield MJ, Groenewald JZ (2009c). Niche sharing reflects a poorly understood biodiversity phenomenon. *Persoonia* **22**: 83–94. https://doi.org/10.3767/003158509X439364

Crous PW, Wingfield MJ, Guarro J, *et al.* (2013b). Fungal Planet description sheets: 154–213. *Persoonia* **31**: 188–296. https://doi.org/10.3767/003158513X675925

Crous PW, Wingfield MJ, Lombard L, *et al.* (2019b). Fungal Planet description sheets: 951–1041. *Persoonia* **43**: 223–425. https://doi.org/10.3767/persoonia.2019.43.06

Crous PW, Wingfield MJ, Schumacher RK, *et al.* (2020a). New and Interesting Fungi 3. *Fungal Systematics and Evolution* **6**: 157–231. https://doi.org/10.3114/fuse.2020.06.09

Deighton FC (1973). Studies on *Cercospora* and allied genera. IV. *Cercosporella* Sacc., *Pseudocercosporella gen. nov*. and *Pseudocercosporidium gen. nov*. *Mycological Papers* **133**: 1–62.

Deighton FC (1976). Studies on *Cercospora* and allied genera. VI. *Pseudocercospora* Speg., *Pantospora* Cif., and *Cercoseptoria* Petr. *Mycological Papers* **140**: 1–168.

Geiser DM, Pitt JI, Taylor JW (1998). Cryptic speciation and recombination in the aflatoxin-producing fungus *Aspergillus flavus*. *Proceedings of the National Academy of Sciences of the USA* **95**: 388–393. https://doi.org/10.1073/pnas.95.1.388

Groenewald JZ, Nakashima C, Nishikawa J *et al.* (2013). Species concepts in *Cercospora:* spotting the weeds among the roses. *Studies in Mycology* **75**: 115–170. https://doi.org/10.3114/sim0012

Groenewald M, Groenewald JZ, Crous PW (2005). Distinct species exist within the *Cercospora apii* morphotype. *Phytopathology* **95**: 951–959. https://doi.org/10.1094/PHYTO-95-0951

Hall T (2007). *Bioedit*, Version 7.0.9. [Online]. Ibis Biosciences, Carlsbad, 1997–2007.

Hunter GC, Wingfield BD, Crous PW, *et al.* (2006). A multi-gene phylogeny for species of *Mycosphaerella* occurring on *Eucalyptus* leaves. *Studies in Mycology* **55**: 147–61. https://doi.org/10.3114/sim.55.1.147

Huson DH (1998). SplitsTree: analyzing and visualizing evolutionary data. *Bioinformatics* **14**: 68–73. https://doi.org/10.1093/bioinformatics/14.1.68

Huson DH, Bryant D (2006). Application of phylogenetic networks

© 2025 Westerdijk Fungal Biodiversity Institute

in evolutionary studies. *Molecular Biology and Evolution* **23**: 254–267. https://doi.org/10.1093/molbev/msj030

Ismail SI, Batzer JC, Harrington TC, *et al.* (2016). Ancestral state reconstruction infers phytopathogenic origins of sooty blotch and flyspeck fungi on apple. *Mycologia* **108**: 292–302. https://doi.org/10.3852/15-036

Kamal (2010). *Cercosporoid fungi of India*. Bishen Singh Mahendra Pal Singh, Dehra Dun., India.

Kamal, Gupta BK, Verma RK (1987). New species of *Cercospora* and *Cercosporidium* from Uttar Pradesh, India. *Canadian Journal of Botany* **65**: 1259–1261. https://doi.org/10.1139/b87-175

Kamal, Rai AN, Rai AN, *et al.* (1991). Some new species and a new combination in *Pseudocercospora* from India. *Mycological Research* **95**: 401–404. https://doi.org/10.1016/S0953-7562(09)80836-8

Katoh K, Rozewicki J, Yamada KD (2019). MAFFT online service: multiple sequence alignment, interactive sequence choice and visualization. *Briefings in Bioinformatics* **20**: 1160–1166. https://doi.org/10.1093/bib/bbx108

Kharwar RN, Singh A, Singh R *et al.* (2015). Two new species of *Zasmidium* from Nepal. *Mycotaxon* **130**: 241–246. https://doi.org/10.5248/130.241

Kirschner R (2009). *Cercosporella* and *Ramularia*. *Mycologia* **101**: 110–119. https://doi.org/10.3852/07-038

Koufopanou V, Burt A, Taylor JW (1997). Concordance of gene genealogies reveals reproductive isolation in the pathogenic fungus *Coccidioides immitis*. *Proceedings of the National Academy of Sciences of USA* **94**: 5478–5482. https://doi.org/10.1073/pnas.94.10.5478

Kumar S, Singh R (2015). *Passalora musicola, sp. nov*. – a new Indian hyphomycete. *Sydowia* **67**: 21–23.

Kumar S, Singh R (2016). *Passalora caesalpiniicola sp. nov*. from India on *Caesalpinia bonduc. Mycotaxon* **131**: 25–30. https://doi.org/10.5248/131.25

Kumar S, Stecher G, Li M, *et al.* (2018). MEGA X: Molecular Evolutionary Genetics Analysis across computing platforms. *Molecular Biology and Evolution* **35**: 1547–1549. https://doi.org/10.1093/molbev/msy096

Kushwaha P, Singh R, Chaurasia B (2020). *Ramularia titarpaniensis* – a new species of ramularioid complex from central India. *Phytotaxa* **429**: 274–280. https://doi.org/10.11646/phytotaxa.429.4.3

Liu YJ, Whelen S, Hall BD (1999). Phylogenetic relationships among ascomycetes: evidence from an RNA polymerse II subunit. *Molecular Biology and Evolution* **16**: 1799–1808. https://doi.org/10.1093/oxfordjournals.molbev.a026092

Machado AR, Pinh DB, Silva M, *et al.* (2012). First report of leaf spot disease caused by *Cercosporella pfaffiae* on Brazilian ginseng (*Pfaffia glomerata*) in Brazil. *Plant Disease* **96**: 1702–1702. https://doi.org/10.1094/PDIS-06-12-0614-PDN

Montenegro-Calderón JG, Martínez-Álvarez JA, Vieyra-Hernández MT, *et al.* (2011). Molecular identification of two strains of *Cercospora rodmanii* isolated from water hyacinth present in Yuriria lagoon, Guanajuato, Mexico and identification of new hosts for several other strains. *Fungal Biology* **115**: 1151–1162. https://doi.org/10.1016/j.funbio.2011.08.001

Nakashima C, Motohashi K, Chen CY, *et al.* (2016). Species diversity of *Pseudocercospora* from far East Asia. *Mycological Progress* **15**: 1093–1117. https://doi.org/10.1007/s11557-016-1231-7

Philippe H, Bryant D (2006). A simple and robust statistical test for detecting the presence of recombination. *Genetics* **172**: 2665–2681. https://doi.org/10.1534/genetics.105.048975

Quaedvlieg W, Binder M, Groenewald JZ, *et al.* (2014). Introducing the Consolidated Species Concept to resolve species in the *Teratosphaeriaceae*. *Persoonia* **33**: 1–40. https://doi.org/10.3767/003158514X681981

Quaedvlieg W, Groenewald JZ, de Jesús Yáñez-Morales M, *et al.* (2012). DNA barcoding of *Mycosphaerella* species of quarantine importance to Europe. *Persoonia* **29**: 101–115. https://doi.org/10.3767/003158512X661282

Quaedvlieg W, Verkley GJM, Shin HD, *et al.* (2013). Sizing up *Septoria*. *Studies in Mycology* **75**: 307–390. https://doi.org/10.3114/sim0017

Rai AN, Kamal (1989). Two new species of *Pseudocercospora* from India. *Current Science* **58**: 1327-1330.

Rajeshkumar KC, Braun U, Groenewald JZ, *et al.* (2021). Phylogenetic placement and reassessment of *Asperisporium pongamiae* as *Pedrocrousiella pongamiae gen. et comb. nov*. (*Mycosphaerellaceae*). *Fungal Systematics and Evolution* **7**: 165–176. https://doi.org/10.3114/fuse.2021.07.08

Rannala B, Yang Z (1996). Probability distribution of molecular evolutionary trees: a new method of phylogenetic inference. *Journal of Molecular Evolution* **43**: 304–311. https://doi.org/10.1007/PL00006090

Rehner SA, Samuels GJ (1994). Taxonomy and phylogeny of *Gliocladium* analysed from nuclear large subunit ribosomal DNA sequences. *Mycological Research* **98**: 625–634. https://doi.org/10.1016/S0953-7562(09)80409-7

Ronquist F, Teslenko M, van der Mark P, *et al.* (2012). MrBayes 3.2: Effcient Bayesian phylogenetic inference and model choice across a large model space. *Systematic Biology* **61**: 539–542. https://doi.org/10.1093/sysbio/sys029

Schoch CL, Crous PW, Groenewald JZ, *et al.* (2009). A class-wide phylogenetic assessment of *Dothideomycetes*. *Studies in Mycology* **64**: 1–15. https://doi.org/10.1016/S0166-0616(14)60093-2

Singh A, Kharwar RN, Singh R, *et al.* (2014a). A new species of *Zasmidium* (*Mycosphaerellaceae*) from India. *Sydowia* **66**: 309–312

Singh G, Yadav S, Singh R, *et al.*(2022). *Passalora golaghati comb. nov*. from India. *Mycotaxon* **137**: 89–94. https://doi.org/10.5248/137.89

Singh R, Chaurasia B, Shukla K, *et al.* (2012). *Passalora aseptata*, a new cercosporoid fungus from northeastern Uttar Pradesh, India. *Mycotaxon* **120**: 461–463. https://doi.org/10.5248/120.461

Singh R, Kumar S, Kamal (2011). Two new species of *Passalora* and *Pseudocercospora* from northeastern Uttar Pradesh, India. *Mycotaxon* **117**: 137–143. https://doi.org/10.5248/117.137

Singh R, Kumar S, Saini DC, *et al.* (2013). Diversity of *Passalora* on *Ficus*. *Mycological Progress* **12**: 637–643. https://doi.org/10.1007/s11557-012-0870-6

Singh R, Singh A, Kumar S, *et al.* (2014b). Two new species of *Zasmidium* from northeastern Uttar Pradesh, India. *Nova Hedwigia* **98**: 257–263. https://doi.org/10.1127/0029-5035/2013/0137

Singh R, Verma SK, Yadav S, *et al.* (2020a). *Cercosporella bundelkhandae comb. nov*. from India. *Mycotaxon* **135**: 315–320. https://doi.org/10.5248/135.315

Singh R, Verma SK, Yadav S, *et al.* (2020b). Morphology and phylogeny of *Pseudocercospora hamiltoniani* – A new species comparable to *Sirosporium* from Uttarakhand, India. *Phytotaxa* **458**: 281–293. https://doi.org/10.11646/phytotaxa.458.4.4

Stamatakis A (2014). RAxML version 8: a tool for phylogenetic analysis and post-analysis of large phylogenies. *Bioinformatics*

© 2025 Westerdijk Fungal Biodiversity Institute

30: 1312–1313. https://doi.org/10.1093/bioinformatics/btu033

Starkey DE, Ward TJ, Aoki T *et al.* (2007). Global molecular surveillance reveals novel Fusarium head blight species and trichothecene toxin diversity. *Fungal Genetics and Biology* **44**: 1191–1204. https://doi.org/10.1016/j.fgb.2007.03.001

Stöver BC, Müller KF (2010), TreeGraph 2: Combining and visualizing evidence from different phylogenetic analyses. *BMC Bioinformatics* **11**: 7. https://doi.org/10.1186/1471-2105-11-7

Sung G-H, Sung J-M, Hywel-Jones NL, *et al.* (2007). A multigene phylogeny of *Clavicipitaceae* (*Ascomycota*, *Fungi*): identification of localized incongruence using a combinational bootstrap approach. *Molecular Phylogenetics and Evolution* **44**: 1204–1223. https://doi.org/10.1016/j.ympev.2007.03.011

Taylor JW, Jacobson DJ, Kroken S *et al.* (2000). Phylogenetic species recognition and species concepts in fungi. *Fungal Genetics and Biology* **31**: 21–32. https://doi.org/10.1006/fgbi.2000.1228

Thirumalachar MJ, Lacy RC (1951). Notes on some Indian fungi. I. *Sydowia* **5**: 124–128.

Verkley GJM, Quaedvlieg W, Shin H-D, *et al.* (2013). A new approach to species delimitation in *Septoria*. *Studies in Mycology* **75**: 213–305. https://doi.org/10.3114/sim0018

Verma SK, Kushwaha P, Yadav S, *et al.* (2021a). Morphology and phylogeny of *Teratoramularia rumicis* – a new foliar pathogen of *Rumex crispus* from India and diversity of ramularioid complex on *Rumex* spp. *Phytotaxa* **523**: 208–228. https://doi.org/10.11646/phytotaxa.523.3.2

Verma SK, Yadav S, Singh G, *et al.* (2021b). *Pseudocercospora cappadocici*, a new Stigmina-like *Pseudocercospora* species on *Acer cappadocicum* from India. *Sydowia* **74**: 79–91

Videira SIR, Groenewald JZ, Braun U, *et al.* (2016). All that glitters is not *Ramularia*. *Studies in Mycology* **83**: 49–163. https://doi.org/10.1016/j.simyco.2016.06.001

Videira SIR, Groenewald JZ, Nakashima C, *et al.* (2017). *Mycosphaerellaceae* – chaos or clarity? *Studies in Mycology* **87**: 257–421. https://doi.org/10.1016/j.simyco.2017.09.003

Vilgalys R, Hester M (1990). Rapid genetic identification and mapping of enzymatically amplified ribosomal DNA from several *Cryptococcus* species. *Journal of Bacteriology* **172**: 4238–4246. https://doi.org/10.1128/jb.172.8.4238-4246.1990

Vu D, Groenewald M, De Vries M, *et al.* (2019). Large-scale generation and analysis of filamentous fungal DNA barcodes boosts coverage for kingdom fungi and reveals thresholds for fungal species and higher taxon delimitation. *Studies in Mycology* **92**: 135–154. https://doi.org/10.1016/j.simyco.2018.05.001

White TJ, Bruns T, Taylor J (1990). Amplification and direct sequencing of fungal ribosomal RNA genes for phylogenetics. In: *A guide to molecular methods and applications* (Innis MA, Gelfand DH, Sninsky JJ, *et al.*, eds). Academic Press, New York: 315–322. https://doi.org/10.1016/B978-0-12-372180-8.50042-1

Yadav S, Singh R, Verma SK, *et al.* (2023). Addition of three new lineages in *Mycosphaerellaceae*: *Neoacervuloseptoria gen. nov.*, *Neocercosporella gen. nov*. and *Neoramulariopsis gen. nov*. *Mycological Progress* **22**: 26. https://doi.org/10.1007/s11557-023-01871-y

Yadav S, Verma SK, Singh R, *et al.* (2022). *Neokamalomyces indicus gen. nov., sp. nov.* (*Mycosphaerellaceae*) — a *Septoria*-like genus from India. *Phytotaxa* **571**:141–168. https://doi.org/10.11646/phytotaxa.571.2.3

Yadav S, Verma SK, Singh VK, *et al.* (2021). Morphology and phylogeny of a new species, *Pseudocercospora haldinae* (*Mycosphaerellaceae*) on *Haldina cordifolia* from India. *Phytotaxa* **501**: 281–292. https://doi.org/10.11646/phytotaxa.501.2.3

© 2025 Westerdijk Fungal Biodiversity Institute

FUSE

Fungal Systematics and Evolution

VOLUME 16
DECEMBER 2025
PAGES 215–231

doi.org/10.3114/fuse.2025.16.12

Integrative taxonomy and genus delimitation in the *Rhizocarpaceae* (lichenized *Ascomycota*)

E.J. Möller[1*], E. Timdal[1], R. Haugan[1], M. Bendiksby[1]

[1]Natural History Museum, University of Oslo, Oslo, Norway

[*]Corresponding author: e.j.moller@nhm.uio.no

Key words:
Catolechia
Epilichen
Haugania
Lecanoromycetes
molecular phylogeny
new taxa
Poeltinula
Rehmia
Rhizocarpon

Abstract: The *Rhizocarpaceae*, a family of lichenized fungi within the *Ascomycota*, comprises approximately 160 species within five genera: *Catolechia*, *Epilichen*, *Haugania*, *Poeltinula*, and *Rhizocarpon*. *Rhizocarpon* is the most species-rich, with about 150 species predominantly inhabiting siliceous rock in boreal and arctic-alpine environments. Molecular phylogenetic studies have revealed that current taxonomy, heavily reliant on morphology, chemistry, and life strategies, renders *Rhizocarpon* paraphyletic. This study aims to elucidate the phylogenetic relationships and clarify genus delimitation within the *Rhizocarpaceae* using an integrative taxonomic approach that combines three genetic markers and a diversity of taxa covering the morphological, chemical, and ecological spectrum of the family. Our comprehensive sampling includes 50 species across the *Rhizocarpaceae* collected from diverse geographical locations and ecological settings. Our phylogenetic hypothesis is based on a concatenated dataset of two nuclear (ITS and MCM7) and one mitochondrial (mtSSU) genetic marker. Ascospore characteristics and thallus pigmentation alongside secondary metabolite profiles were mapped onto this DNA-based evolutionary framework. Our results underscore significant refinements in the classification of the *Rhizocarpaceae*, highlighting the inadequacy of traditional taxonomic markers alone to infer robust phylogenetic affiliations. We advocate for new circumscriptions of *Catolechia*, *Poeltinula*, and *Rhizocarpon* based on the molecular phylogeny and propose synonymizing *Epilichen* with *Catolechia*, the transfer of the species in the *R. hochstetteri* complex to *Poeltinula*, and the resurrection of *Rehmia*. We hence propose 24 new combinations and three typifications. Collectively, this study sets the groundwork for future research and stability in the systematics of the *Rhizocarpaceae*, augmenting our understanding of their diversity and evolutionary dynamics.

Citation: Möller EJ, Timdal E, Haugan R, Bendiksby M (2025). Integrative taxonomy and genus delimitation in the *Rhizocarpaceae* (lichenized *Ascomycota*). *Fungal Systematics and Evolution* **16**: 215–231. doi: 10.3114/fuse.2025.16.12
Received: 13 March 2025; **Accepted:** 16 June 2025; **Effectively published online:** 25 July 2025
Corresponding editor: P.W. Crous

INTRODUCTION

The *Rhizocarpaceae* (*Ascomycota*: *Lecanoromycetes*: *Lecanoromycetidae*: *Rhizocarpales*) is a family of lichenized fungi that consists of ca 160 currently accepted species unevenly distributed across five genera: *Catolechia* (one species), *Epilichen* (three species), *Haugania* (two species), *Poeltinula* (three species), and *Rhizocarpon* (ca 150 species) (Fryday *et al.* 2024). In addition, Hafellner (1984) lists nine generic names as synonyms of these (*Catillariopsis*, *Catocarpus*, *Dimaura*, *Diphaeis*, *Diphanis*, *Lepidoma*, *Phalodictyum*, *Rehmia*, and *Siegertia*). The current generic circumscriptions are based mainly on thallus morphology and ecology, and some phylogenies render *Rhizocarpon* paraphyletic, suggesting that the current taxonomy needs revision (Ihlen & Ekman 2002, Miadlikowska 2014). In this study we include three genetic markers and a broad taxonomic sampling to investigate this suspected paraphyly.

The family is characterized by having a crustose thallus (lobate in one species) or lacking a thallus in some lichenicolous species; green, unicellular photobionts (very rarely also cyanobacteria in cephalodia); lecideine apothecia (i.e., having a proper exciple without a thalline margin); richly branched, anastomosing, and strongly conglutinated paraphyses; and asci with a moderately amyloid tholus with an internal, apical, and deeper pigmented amyloid cap (a small structure at the apex of the ascus; Honegger 1980, Hafellner 1984). The ascospores, usually eight per ascus (sometimes a reduced number), are 1-septate to eumuriform, hyaline to green or dark brown, and often surrounded by a gelatinous perispore.

Of the five genera in the *Rhizocarpaceae*, ***Rhizocarpon*** is by far the most speciose with ca 150 species. They grow mainly on rocks in the boreal and arctic-alpine regions, but the genus also occurs throughout the temperate, subtropical, and even tropical regions (GBIF 2025). The type species, *R. geographicum* was first described by Linnaeus (1753) as *Lichen geographicus*. The species is both abundant and globally distributed, sometimes completely dominating alpine rock surface ecosystems. The species is, however, very diverse and poorly understood and must be considered a species complex (Roca-Valiente *et al.* 2016).

Rhizocarpon was described by De Candolle in Lamarck & De Candolle (1805) and represents one of the earliest described lichen genera. The species in the genus grow mainly on siliceous rock. Although most species are autonomous

Fungal Systematics and Evolution is licensed under a Creative Commons Attribution-NonCommercial-NoDerivatives 4.0 International License

© 2025 Westerdijk Fungal Biodiversity Institute

lichens from the start, some start their lives growing on other lichens (lichenicolous) and carry on autonomously after consuming their host, and some species are persistent obligately lichenicolous on other crustose lichens (Holtan-Hartwig & Timdal 1987, Timdal & Holtan-Hartwig 1988, Poelt 1990). A typical lichenized *Rhizocarpon* thallus is areolate (or sometimes more continuous and cracked) with a conspicuous, usually black hypothallus from which the areolae and apothecia originate. A few species are mainly sterile and propagate vegetatively by isidia or soredia. The number of species in the genus is difficult to estimate accurately as many areas of the world lack lichen checklists and those that exist have a partly incompatible taxonomy for *Rhizocarpon*. We estimate roughly 150 species, although Lücking *et al.* (2017) indicates there may be as many as 225 species and MycoBank (2025) lists 258 accepted species names out of 361 legitimate names.

Catolechia is currently a monotypic genus. This narrow circumscription was established by Koerber (1855) after exclusion of some additional species placed in the genus by Flotow (1850; the protologue) and Massalongo (1852). *Catolechia wahlenbergii* was first described as *Lecidea wahlenbergii* and moved to *Catolechia* by Koerber in 1855. *Catolechia* was placed in the *Rhizocarpaceae* by Hafellner (1984) based primarily on ascus type. It can be found growing on soil and moss-carpets in shaded crevices of humid rock walls in boreal and arctic-alpine habitats. According to GBIF (2025), the species is found mainly in the Northern Hemisphere, with some outliers in the tropics that may need confirmation.

The three species of ***Epilichen*** are all small and lichenicolous on crustose lichens. The genus was described by Clements (1909) and placed in the *Rhizocarpaceae* by Hafellner (1984), also based mainly on ascus type. The type species, *E. scabrosus*, and *E. glauconigellus* grow on terricolous *Baeomyces* spp. (Ihlen 1997). The former is known from throughout the Northern Hemisphere, southernmost South America and New Zealand, while the latter is only registered from Europe and Greenland (Fryday 2019, GBIF 2025). The third species, *E. stellatus*, parasitizes *Lecidea tessellata* and is reported from the type locality in the Russian Far East and from North America (Triebel 1989, Triebel *et al.* 1991).

The *Catolechia* and *Epilichen* species lack a perispore around their ascospores. Otherwise, the two genera are anatomically similar to the rest of the family by having *Rhizocarpon*-type asci and brown, 1-septate ascospores. Both *C. wahlenbergii* and *E. scabrosus* contain two yellow pigments, apparently pulvinic acid derivatives, but not the common yellow pigment of *Rhizocarpon*, rhizocarpic acid. In addition to their different ecologies, Hafellner (1979) notes that the two species mainly differ in thallus thickness and apothecial ontogeny. There is also a significant size difference between the two species. While *C. wahlenbergii* is one of the larger species in the family, with thalli often reaching 5–10 cm or more in diameter, *Epilichen* species rarely grow larger than a centimetre in diameter.

Haugania was described as a segregate of *Rhizocarpon* in Fryday *et al.* (2024), based on its phylogenetic position (to be presented here), the rusty thallus colour, and metallophilic habitat preference. The genus was established for two species, *H. oederi* and *H. pycnocarpoides*, both of which grow on heavy metal rock-substrates, often in abandoned mining areas. Both species have halonate, hyaline ascospores; *H. oederi* having three-septate to submuriform ascospores and *H. pycnocarpoides* having sub- to eumuriform ascospores.

Poeltinula was introduced as a new name for *Melanospora* Mudd (nom. illeg.) and originally included only a single species, *P. cerebrina* (Hafellner 1984). Later, three more species have been included in the genus, *P. cacuminum*, *P. cerebrinella*, and *P. interjecta*. The latter species is currently included in *Melaspilea* (e.g., by BLS 2025), a view we follow here although its generic position is not supported by any public DNA sequence. None of the *Poeltinula* species make conspicuous thalli, but are instead endolithic and appear only as small, black apothecia with furrows of sterile tissue on calcareous rock. The species all have 1-septate, halonate *Rhizocarpon*-type ascospores; those of *P. cerebrina* and *P. cacuminum* soon becoming green. *Poeltinula* was placed in the *Rhizocarpaceae* by Hafellner (1984) based mainly on ascus type. According to GBIF (2025), the type species, *P. cerebrina*, occurs in the Alps and the British Isles, while *P. cacuminum* occurs only in the Alps. The third species, *P. cerebrinella*, is known only from the type locality on Kerguelen and from the Marion Island in the Antarctic Sea and must be considered poorly understood.

Even though the *Rhizocarpaceae*, especially *Rhizocarpon*, is both widespread and abundant, there is no comprehensive molecular phylogenetic study focusing on the genus or family level relationships. Most published *Rhizocarpon* sequences were provided for phylum and class level phylogenetics (e.g., Lutzoni *et al.* 2001, Miadlikowska *et al.* 2014, Kraichak *et al.* 2018) or, alternatively, for studies focusing on some other lichen family (e.g. Buschbom & Mueller 2004). At the other end of the scale, molecular phylogenies have been provided in support of descriptions of new species (McCune *et al.* 2016, Davydov & Yakovchenko 2017, Halici *et al.* 2022, Timdal *et al.* 2024).

The only study known to us that addresses inter-genus relations and character evolution in the *Rhizocarpaceae* is Ihlen & Ekman (2002), which presented a phylogeny based on ITS and mtSSU sequences of 15 species of *Rhizocarpon*, *Catolechia* and *Poeltinula*. In their study, *R. hochstetteri* is the phylogenetic sister to *P. cerebrina*. These two species do not resemble each other morphologically (Fig. 1), although they do share one key character: sharply delimited pigmented apical caps on the otherwise hyaline paraphyses (Fryday 2002, Möller 2021), a character state that is mostly lacking in the rest of the *Rhizocarpaceae*. Pigmented paraphysis caps, albeit not as swollen and less sharply delimited, are also reported in some yellow species of *Rhizocarpon* (Runemark 1956). In the study by Ihlen & Ekman (2002), the *Poeltinula-R. hochstetteri*-clade was either sister to the rest of the family or sister to the rest of *Rhizocarpon*, with *Catolechia* recovered as sister to the rest of the family. In the large phylogeny of the *Lecanoromycetes* by Miadlikowska *et al.* (2014), *Poeltinula* is not included, but the *R. hochstetteri* group is phylogenetic sister to *Catolechia*, and *H. oederi* (as *R. oederi*) is sister to the rest of the family [with the exception of an accession of *R. geographicum* (AFTOL-ID 2067) that appears to be based on two specimens, from which one of the three markers, nucSSU GenBank AF088246, seems to be a contamination].

The position of the *Rhizocarpaceae* in the *Lecanoromycetidae* is still not resolved. Some studies

© 2025 Westerdijk Fungal Biodiversity Institute

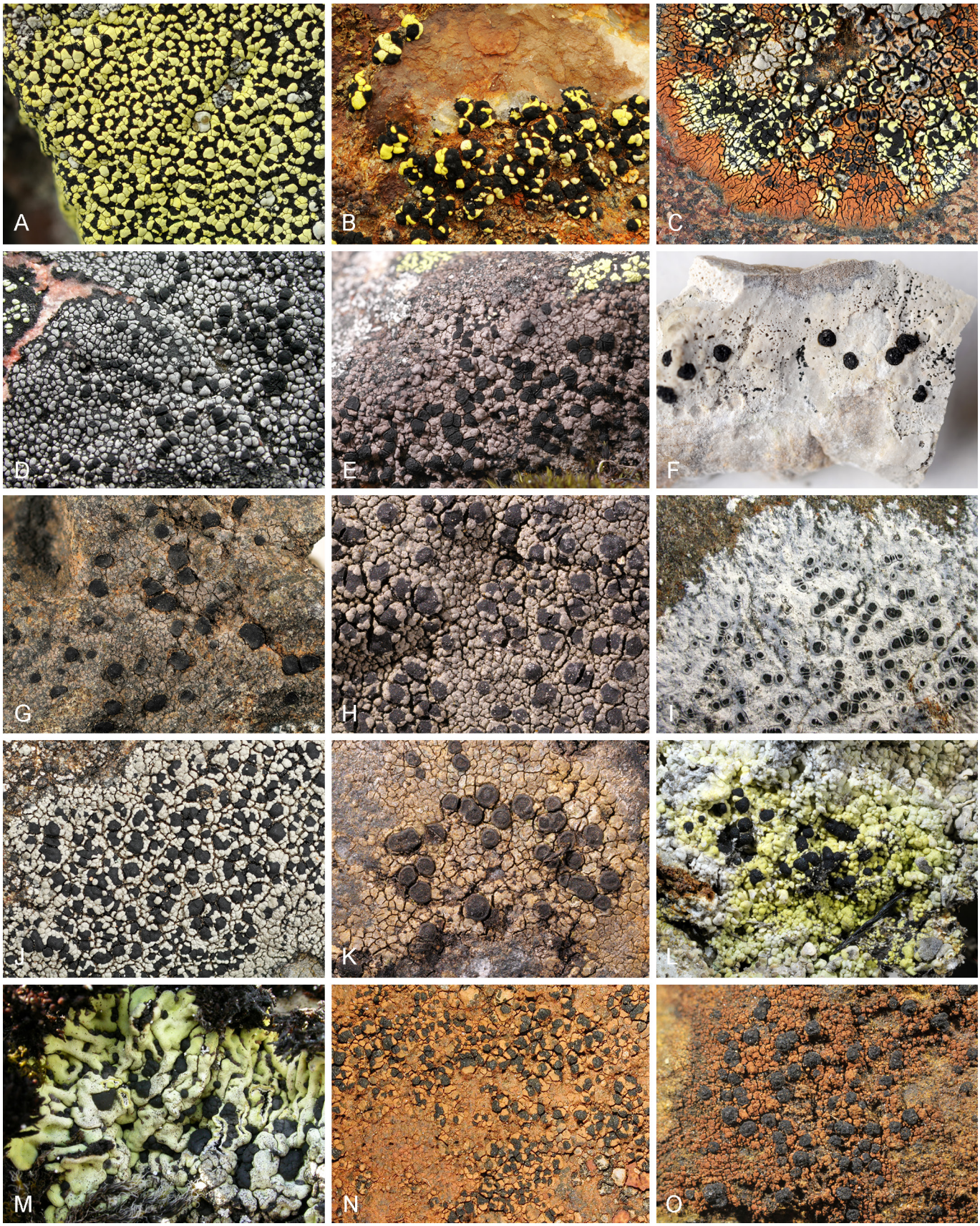

Fig. 1. Habitus photographs of selected species of the *Rhizocarpaceae*. **A.** *Rhizocarpon geographicum*, Norway, O-L-161808. **B.** *R. norvegicum*, Norway, O-L-163568. **C.** *R. parvum*, Norway, O-L-225584. **D.** *R. eupetraeum*, Greenland, O-L-139134. **E.** *R. hochstetteri*, Norway, O-L-149415. **F.** *Poeltinula cacuminum*, Austria, Hafellner 63791, GZU. **G.** *R. caesium*, Iceland, O-L-160733. **H.** *R. amphibium*, Norway, O-L-169822. **I.** *R. umbilicatum*, Norway, O-L-123119. **J.** *R. cinereovirens*, Norway, O-L-163425. **K.** *R. lavatum*, Norway, O-L-169833. **L.** *Epilichen scabrosus*, Norway, O-L-164936. **M.** *Catolechia wahlenbergii*, Norway, not collected. **N.** *Haugania oederi*, Norway, O-L-51867. **O.** *H. pycnocarpoides*, Norway, O-L-184267. Photo credits: E. Timdal.

© 2025 Westerdijk Fungal Biodiversity Institute

have placed the family as the phylogenetic sister to the *Sporastatiaceae* and the *Rhizocarpaceae* + *Sporastatiaceae* as sister to the rest of the *Lecanoromycetidae* (Miadlikowska *et al.* 2014, Kraichak *et al.* 2018). Others placed the *Sporastatiaceae* as sister to the *Rhizocarpaceae* + the rest of the *Lecanoromycetidae* (e.g., Bendiksby & Timdal 2013). Whichever of these two topologies is correct, the long genetic distance between the *Rhizocarpaceae* and its nearest neighbour makes investigations of the deep topology and selection of a suitable outgroup for the family challenging. This was also highlighted by Ihlen & Ekman (2002).

According to the molecular phylogenetic hypotheses by Ihlen & Ekman (2002) and Miadlikowska *et al.* (2014), *Rhizocarpon* is, as currently circumscribed, paraphyletic. In both studies, the *R. hochstetteri* complex seems to be more closely related to one of the smaller genera, either *Poeltinula* or *Catolechia*, than to *Rhizocarpon*.

In this study, we aim to discover, understand, delimit, and circumscribe the genera of the *Rhizocarpaceae*, reveal their phylogenetic interrelations, and identify informative diagnostic characters at genus level. To reach that goal, we include a set of species that covers most of the anatomical, morphological, chemical and ecological variation of the family. We study these features integratively within the framework of a phylogenetic hypothesis based on three genetic markers to conclude meaningful taxon limits.

MATERIAL AND METHODS

Taxon sampling

In this study, we have included 87 specimens representing 50 species of the *Rhizocarpaceae*, both freshly collected from field work in Norway during the summers of 2019 and 2020 and as dried specimens from various fungaria (BG, E, GZU, MSC, O, OSC, hb Wheeler; Table 1). The fungarium material includes specimens from Austria, Canada, Iceland, Japan, Norway, Russia, Sweden, UK and USA. Specimens were selected to represent most of the breadth of variation in ascospore morphology (i.e., septation, pigmentation, and number of spores per ascus), chemistry, and ecology in the *Rhizocarpaceae*. *Lecanora cavicola* and *L. coronulans* were used as outgroup taxa, as they are phylogenetically far from the *Rhizocarpaceae* and had all the included markers available in GenBank.

Ascospore characters, thallus colour, and secondary metabolites

The morphology in the group has been studied for decades, including by co-authors of this study, and the microscopical characters and secondary metabolites for the species concepts are documented by, e.g., Timdal (1986), Holtan-Hartwig & Timdal (1987), Timdal & Holtan-Hartwig (1988), Purvis *et al.* (1992), Fryday (2002), Feuerer & Timdal (2004), Ihlen (2004), McCune *et al.* (2016), Halici *et al.* (2022), Fryday *et al.* (2024), and Timdal *et al.* (2024). In this study, the material sequenced by us was identified by microscopical and chemical methods described by Timdal *et al.* (2024). The photographs of ascospores and microtome cross-sections of apothecia were made by a Nikon Z 6II camera attached to a Leitz Aristoplan compound microscope. Ascospore characters (i.e., pigmentation, septation, and number of septa), thallus colour, amyloidity in the medulla, and presence of secondary metabolites were mapped onto the phylogeny using ggtree (Yu *et al.* 2017).

DNA extraction and amplification

Total genomic DNA was extracted from 1–5 apothecia per specimen or a small thallus piece if apothecia were scarce or missing. We used two different extraction protocols: (1) the E.Z.N.A.® SP Plant DNA Kit (Omega Bio-Tek, Georgia, U.S.A) following a modified protocol (Bendiksby & Timdal 2013) and (2) the Chelex 100 protocol (Bio-Rad, Hercules, CA, USA) according to Ferencova *et al.* (2017); the latter selected for speed in the second period of the project. For each accession, we sequenced up to three genetic markers: the nuclear ribosomal internal transcribed spacer (ITS), the Minichromosome Maintenance Complex Component 7 (MCM7), and the mitochondrial ribosomal small subunit (mtSSU). For the amplification reactions, the Illustra™ PuReTaq Ready-To-Go™ PCR Beads (GE Healthcare, Buckinghamshire, UK) were used to amplify the markers, following the manufacturer's protocol, except for using half reactions (i.e., 9.95 uL water, 1.25 µL MgCl2, 0.3 µL of each primer, 0.7 µL template DNA = 12.5 µL per reaction). The ITS and MCM7 loci were mainly amplified as single fragments using the primer pairs ITS1F/ITS4 (White *et al.* 1990, Gardes & Bruns 1993) and MCM7-709for/MCM7-1348rev (Schmitt *et al.* 2009), respectively. In some cases, the ITS locus was amplified as two shorter fragments using the primer pairs ITS1F/ITS2 and ITS3/ITS4 (White *et al.* 1990). The mtSSU locus was mostly amplified in two fragments using the primer pairs mtSSU1/mtSSU-RhiR (Zoller *et al.* 1999; this study: 5'-AAT AAC ATA CTT CAC TAC TGG T-3', respectively) and mtSSU-RhiF/mtSSU3R (this study: 5'-ACC AGT AGT GA A GTA TGT TAT T-3'; Zoller *et al.* 1999, respectively).

DNA sequence analysis

The ITS and mtSSU markers were aligned using PASTA (Mirarab *et al.* 2014), as it performs well for variable markers and in cases where many gaps can be expected. The more conserved, protein coding MCM7 marker was aligned using MAFFT (algorithm E-INS-i) (Katoh *et al.* 2019). For both alignment methods, the same settings were used as in Svensson & Fryday (2022). For viewing the alignments, AliView was used (Larsson 2014). Parsimony informative sites were inspected in MEGA v. 11 (Tamura *et al.* 2021). Gene trees were inferred for all markers using RAxML-NG-MPI v. 1.0.2. (Stamatakis 2006, Kozlov *et al.* 2019) with 1000 bootstrap repeats (Felsenstein 1985). The three markers were also concatenated, and the concatenated alignment was used for both Bayesian inference (BI) using MrBayes v. 3.2.7a (Ronquist *et al.* 2012), and Maximum Likelihood (ML) using RAxML-NG-MPI v. 1.0.2. with 1000 bootstrap repeats. The MrBayes analysis ran until the average standard deviation of split frequencies (ASDSF) reached below 0.01, with four runs, four chains, and a relative burn-in of 25 %. Effective sample sizes (ESS) were examined in Tracer v. 1.7.1 (Rambaut *et al.* 2018). The resulting phylogenies were edited in ggtree and Inkscape (Inkscape 2023).

© 2025 Westerdijk Fungal Biodiversity Institute

Table 1. Voucher specimen table. Current name, previous name, voucher ID, country, GenBank accession numbers for the ITS, mtSSU, and MCM7 markers (sequences produced for this study are in **bold**), and references for existing sequences are provided. Taxonomic novelties are highlighted in **bold** text in the first column.

Current name	Previous name	Voucher	Country	ITS	mtSSU	MCM7	Reference
Catolechia glauconigella	*Epilichen glauconigellus*	O-L-141634	Norway	MK811705	—	—	Marthinsen *et al.* (2019)
		O-L-179907	Norway	MK812566	—	—	Marthinsen *et al*. (2019)
		O-L-239178	Norway	**PV665039**	—	—	This study
Catolechia scabrosa	*Epilichen scabrosus*	O-L-164936	Norway	MK812386	**PV661952**	**PV738713**	Marthinsen *et al*. (2019)
		O-L-179955	Norway	MK812558	—	—	Marthinsen *et al*. (2019)
		O-L-225908	Norway	—	**PV661953**	—	This study
		O-L-227683	Norway	**PV665040**	—	**PV738714**	This study
Catolechia wahlenbergii		O-L-226116	Norway	**PV665035**	**PV661948**	**PV738709**	This study
		O-L-226139	Norway	**PV665036**	**PV661949**	**PV738710**	This study
		O-L-227703	Norway	**PV665037**	**PV661950**	**PV738711**	This study
		O-L-227789	Norway	**PV665038**	**PV661951**	**PV738712**	This study
Haugania oederi		O-L-151401	Norway	**PV665041**	**PV661954**	—	This study
		O-L-28978	Norway	AF483612	AF483180	—	Ihlen & Ekman (2002)
		Spribille 36629 (MSC)	USA, Alaska	MN437622	MN508296	MN437622	Spribille *et al.* (2020)
Haugania pycnocarpoides		O-L-179560	Norway	KR780753	**PV661955**	—	Westberg *et al.*(2015)
Lecanora cavicola		Flakus29582	Bolivia	OL604041	OL604121	OK665503	Medeiros *et al.* (2021)
Lecanora coronulans		Flakus29260	Bolivia	OL604008	OL604090	OK665498	Medeiros *et al.* (2021)
Poeltinula cacuminum		Hafellner 63781 (GZU)	Austria	**PV665042**	—	—	This study
		Hafellner 63791 (GZU)	Austria	**PV665043**	—	—	This study
Poeltinula caesia	*Rhizocarpon caesium*	E-456329 (Holotype)	Great Britain	**PV665049**	—	—	This study
		O-L-160733	Iceland	**PV665050**	**PV661959**	—	This study
Poeltinula cerebrina		Mayrhofer et al. 12838 (GZU)	Austria	AF483173	AF483606	—	Ihlen & Ekman (2002)
Poeltinula hensenniae	*Rhizocarpon hensenniae*	O-L-209863	Japan	**PV665058**	**PV661967**	**PV738719**	This study
		O-L-209874	Japan	—	**PV661968**	**PV738720**	This study
Poeltinula hochstetteri	*Rhizocarpon hochstetteri*	O-L-222653	Norway	**PV665059**	**PV661969**	**PV738721**	This study
		O-L-225971	Norway	**PV665060**	**PV661970**	**PV738722**	This study
		O-L-227846	Norway	**PV665061**	—	—	This study
		O-L-227912	Norway	**PV665062**	**PV661971**	**PV738723**	This study
Poeltinula infernula	*Rhizocarpon infernulum*	McCune 32921 (OSU)	USA, Alaska	—	**PV661972**	—	This study
Poeltinula sylvatica	*Rhizocarpon infernulum f. sylvaticum*	O-L-119602	Norway	AF483607	—	—	Ihlen & Ekman (2002)
		O-L-228034	Norway	**PV665063**	—	**PV738724**	This study

© 2025 Westerdijk Fungal Biodiversity Institute

Table 1. (Continued).

Current name	Previous name	Voucher	Country	ITS	mtSSU	MCM7	Reference
Rehmia amphibia	*Rhizocarpon amphibium*	BG-L-68527	Sweden	AF483611	AF483179	—	Ihlen & Ekman (2002)
		O-L-163528	Norway	**PV665045**	**PV661957**	—	This study
Rehmia caeruleoalba	*Rhizocarpon caeruleoalbum*	9.8.1987 Poelt (GZU)	Austria	**PV665046**	—	—	This study
		hb Wheeler 5259	USA, Alaska	**PV665047**	—	—	This study
		UPS-L-67821	Norway	**PV665048**	—	—	This study
Rehmia chionea	*Rhizocarpon chioneum*	O-L-175723	Norway	**PV665051**	**PV661960**	—	This study
		O-L-195535	Norway	KY266951	—	—	Westberg *et al*. (2015)
Rehmia cinereovirens	*Rhizocarpon cinereovirens*	O-L-174113	Norway	—	**PV661961**	—	This study
Rehmia furfurosa	*Rhizocarpon furfurosum*	O-L-169766	Norway	**PV665056**	**PV661963**	—	This study
Rehmia haidensis	*Rhizocarpon haidense*	Fryday 10680 (MSC)	USA, Alaska	MN483143	MN508295	—	Spribille *et al.* (2020)
Rehmia lavata	*Rhizocarpon lavatum*	O-L-228204	Norway	**PV665066**	—	—	This study
		O-L-28923	Norway	AF483610	AF483178	—	Ihlen & Ekman (2002)
Rehmia petraea	*Rhizocarpon petraeum*	O-L-169123	Norway	**PV665072**	**PV661979**	—	This study
		O-L-225882	Norway	**PV665073**	**PV661980**	**PV738725**	This study
		O-L-29039	Norway	AF483609	AF483177	—	Ihlen & Ekman (2002)
Rehmia reducta	*Rhizocarpon reductum*	McCune 36587 (OSU)	USA, Oregon	**PV665077**	**PV661985**	**PV738729**	This study
Rehmia roridula	*Rhizocarpon roridulum*	O-L-201497	Norway	**PV665079**	**PV661986**	—	This study
Rehmia rubescens	*Rhizocarpon rubescens*	UPS-L-131191	Sweden	**PV665080**	—	—	This study
Rehmia tetramera	*Rhizocarpon tetramerum*	O-L-29034	Norway	**PV665083**	—	—	This study
Rehmia timdalii	*Rhizocarpon timdalii*	O-L-71409	Norway	**PV665084**	**PV661989**	—	This study
		UPS-L-160175	Sweden	**PV665085**	—	—	This study
Rehmia umbilicata	*Rhizocarpon umbilicatum*	O-L-163744	Norway	**PV665086**	—	—	This study
		O-L-163789	Norway	**PV665087**	—	—	This study
		O-L-184352	Norway	**PV665088**	—	—	This study
Rhizocarpon alpicola		O-L-170541	Norway	**PV665044**	**PV661956**	—	This study
		O-L-223755	Canada, British Columbia	ON332060	ON324015	—	Halici *et al. (*2022)
Rhizocarpon atroflavescens		O-L-228046	Norway	—	**PV661958**	—	This study
Rhizocarpon dinothetes		O-L-184631	Norway	**PV665052**	—	—	This study
Rhizocarpon distinctum		O-L-28901	Norway	AF483615	—	—	Ihlen & Ekman (2002)
Rhizocarpon effiguratum		O-L-223731	Canada, Alberta	PQ219499	ON324016	**PV738715**	ITS: Timdal & Rui (2024) | mtSSU: Halici *et al.* (2022)
Rhizocarpon eupetraeum		O-L-163557	Norway	**PV665053**	—	—	This study

© 2025 Westerdijk Fungal Biodiversity Institute

Table 1. (Continued).

Current name	Previous name	Voucher	Country	ITS	mtSSU	MCM7	Reference
		O-L-165382	Norway	**PV665054**	—	**PV738716**	This study
Rhizocarpon ferax		O-L-175699	Norway	**PV665055**	**PV661962**	—	This study
Rhizocarpon geographicum		O-L-175717	Norway	**PV665057**	**PV661964**	—	This study
		O-L-223664	Canada, Alberta	PQ219488	**PV661965**	**PV738717**	Timdal & Rui (2024)
		O-L-223711	Canada, Alberta	PQ219494	**PV661966**	**PV738718**	Timdal & Rui (2024)
Rhizocarpon intermediellum		O-L-149126	Norway	**PV665064**	**PV661973**	—	This study
Rhizocarpon intersitum		O-L-227971	Norway	**PV665065**	**PV661974**	—	This study
Rhizocarpon lecanorinum		McCune 36309 (OSU)	USA, Alaska	**PV665067**	**PV661975**	—	This study
		O-L-169130	Norway	**PV665068**	**PV661976**	—	This study
Rhizocarpon macrosporum		McCune 32022 (OSU)	USA, Montana	**PV665069**	**PV661977**	—	This study
Rhizocarpon norvegicum		O-L-163568	Norway	**PV665070**	**PV661978**	—	This study
Rhizocarpon parvum		O-L-225584	Norway	**PV665071**	—	—	This study
Rhizocarpon polycarpum		McCune 36183 (OSU)	USA, Alaska	**PV665074**	**PV661981**	**PV738726**	This study
		O-L-175739	Norway	**PV665075**	**PV661982**	—	This study
		O-L-227898	Norway	**PV665076**	**PV661983**	**PV738727**	This study
Rhizocarpon pusillum		O-L-223718	Canada	PQ219496	**PV661984**	**PV738728**	Timdal & Rui (2024)
Rhizocarpon richardii		O-L-145354	Norway	**PV665078**	—	—	This study
Rhizocarpon saurinum		hb Wheeler 6026 p.p	USA, Montana	**PV665081**	**PV661987**	—	This study
Rhizocarpon subgeminatum		O-L-165477	Norway	KU687452	—	—	McCune *et al.* (2016)
		O-L-166501	Norway	KU687457	—	—	McCune *et al.* (2016)
Rhizocarpon suomiense		O-L-169818	Norway	**PV665082**	**PV661988**	—	This study
		O-L-19770	Norway	AF483613	AF483181	—	Ihlen & Ekman (2002)
Rhizocarpon viridiatrum		McCune 34748 (OSU)	USA, Oregon	**PV665089**	**PV661990**	—	This study
		O-L-160701	Iceland	**PV665090**	—	—	This study
		O-L-183807	Norway	**PV665091**	—	—	This study
Rhizocarpon vorax		O-L-20249	Norway	**PV665092**	**PV661991**	—	This study

© 2025 Westerdijk Fungal Biodiversity Institute

RESULTS

Microscopic characters and chemistry

Ascospore morphology, thallus colour and secondary metabolites are shown in the character matrix in Fig. 2. The character states shown represent what is known for the species concepts, not necessarily the individual accessions [e.g., *R. hochstetteri* does not always contain stictic acid, but it is the only secondary metabolite that has been detected in this species (Fryday *et al.* 2024)].

Molecular phylogeny

The ITS alignment of the 83 accessions was 717 base pairs (bp) long. Of the 357 variable sites in the ingroup 315 were parsimony informative. The MCM7 alignment was 609 bp long with 24 accessions and the ingroup contained 188 parsimony informative sites. The mtSSU alignment was 901 bp long with 56 accessions and the ingroup contained 126 parsimony informative sites. As there were no supported incongruences [a branch is here considered supported in the BI analysis if the posterior probability (PP) exceeds 0.95 and in the ML analysis if the bootstrap support (BS) exceeds 70] between the gene trees (supplementary material), ML and BI phylogenies were inferred for a concatenated alignment (2227 bp long with 88 accessions). The BI analysis converged after 2.2 million generations and all ESS values exceeded 200. All alignments and phylogenies are deposited at Figshare [doi (alignments and trees, respectively): 10.6084/m9.figshare.28596479.v2 and 10.6084/m9.figshare.28596530.v2; Möller *et al.* 2025a, b].

The two analyses showed no supported incongruences and display five distinct, highly supported major clades (Fig. 2): (1) *Catolechia* (three species), (2) *Haugania* (two species), (3) *Poeltinula* (seven species), (4) *Rehmia* (14 species; named so because the generic name is available for the clade), and (5) *Rhizocarpon* s. str. (20 species). *Catolechia* and *Poeltinula* are supported as sisters in the BI analysis (PP = 0.98). This relation is not significantly supported in the ML analysis (BS = 60). Four accessions, representing two species of *Rhizocarpon*, are not assigned to any of the above listed five major clades and are hereafter referred to as *Rhizocarpon* rest group.

***Catolechia* (PP = 1 / BS = 97):** *Catolechia wahlenbergii* and the two *Epilichen* species form a highly supported clade, with *E. glauconigellus* as sister to a genetically uniform clade consisting of *C. wahlenbergii* and *E. scabrosus.*

***Haugania* (PP = 1 / BS = 100):** The two species *H. oederi* and *H. pycnocarpoides* form a fully supported clade.

***Poeltinula* (PP = 1 / BS = 99):** The five species/taxa in the *Rhizocarpon hochstetteri* complex (*R. caesium*, *R. hensseniae*, *R. hochstetteri*, *R. infernulum*, and *R. infernulum f. sylvaticum*) and the two *Poeltinula* species (*P. cacuminum* and *P. cerebrina*) form a fully supported clade.

***Rehmia* (PP = 1 / BS = 89):** The 14 species *Rhizocarpon amphibium*, *R. caeruleoalbum*, *R. chioneum*, *R. cinereovirens*, *R. furfurosum*, *R. haidense*, *R. lavatum*, *R. tetramerum*, *R. timdalii*, *R. petraeum*, *R. umbilicatum*, *R. reductum*, *R. roridulum*, and *R. rubescens*, form a highly supported clade.

***Rhizocarpon* s. str. (PP = 1 / BS = 100):** The 20 species *R. alpicola*, *R. atroflavescens*, *R. eupetraeum*, *R. dinothetes*, *R. distinctum*, *R. effiguratum*, *R. ferax*, *R. geographicum*, *R. intermediellum*, *R. lecanorinum*, *R. macrosporum*, *R. norvegicum*, *R. parvum*, *R. polycarpum*, *R. pusillum*, *R. richardii*, *R. saurinum*, *R. viridiatrum* and *R. vorax* form a fully supported clade.

***Rhizocarpon* rest group (PP = 1 / BS = 94):** The two species *R. subgeminatum* and *R. suomiense* are not assigned to any of the major clades, but form a highly supported clade which is sister to *Rhizocarpon* s. str. with PP = 0.94 / BS = 64.

Taxonomy

The following names include all accepted genera (including synonyms) of the *Rhizocarpaceae* and all accepted species (excluding synonyms) with the exception of the numerous species of *Rhizocarpon*.

Catolechia Flot., *Bot. Zeitung (Berlin)* **8**: 367. 1850.
Typification: *Lecidea wahlenbergii* Ach., designated by Koerber, *Systema Lichenum Germaniae* (2): 181. 1854–1855.
Synonyms: *Dimaura* Norman, *Conatus praemissus redactionis novae generum nonnullorum lichenum*: 23. 1852.
Typification: *Lecidea wahlenbergii* Ach., designated by Hafellner, *Beiheft zur Nova Hedwigia* **79**: 330. 1984.
Xanthopsis Acloque, *Les Lichens*: 346. 1893.
Typification: *Lecidea wahlenbergii* Ach.
Epilichen Clem., *The Genera of Fungi:* 69, 174. 1909.
Typification: *Lecidea scabrosa* Ach.

Catolechia glauconigella (Nyl.) E.J. Möller, Timdal, Haugan & Bendiksby, ***comb. nov.*** MB 859240.
Basionym: *Lecidea glauconigella* Nyl., *Lichenes Scandinaviae*: 238. 1861.

Catolechia scabrosa (Ach.) E.J. Möller, Timdal, Haugan & Bendiksby, ***comb. nov.*** MB 859241.
Basionym: *Lecidea scabrosa* Ach., *Methodus*: 48. 1803.

Catolechia stellata (Triebel) E.J. Möller, Timdal, Haugan & Bendiksby, ***comb. nov.*** MB 859242.
Basionym: *Epilichen stellatus* Triebel, *Biblioth. Lichenol.* **35**: 136. 1989.

Catolechia wahlenbergii (Ach.) Körb., *Systema Lichenum Germaniae* (2): 181. 1854–1855.
Basionym: *Lecidea wahlenbergii* Ach., *Methodus*: 81. 1803
Typification: «Lapponia» H9510095 (H-ACH 219D, **lectotype designated here**) MBT 10026483.

Haugania E.J. Möller & Timdal in Fryday *et al.*, *Revisions of British and Irish Lichens* **41**: 27. 2024.
Typification: *Lecidea oederi* Ach.

Haugania oederi (Ach.) E.J. Möller & Timdal in Fryday *et al.*, *Revisions of British and Irish Lichens* **41**: 27. 2024.
Basionym: *Lecidea oederi* Ach., *Methodus*: 49. 1803 (nom. cons.).

© 2025 Westerdijk Fungal Biodiversity Institute

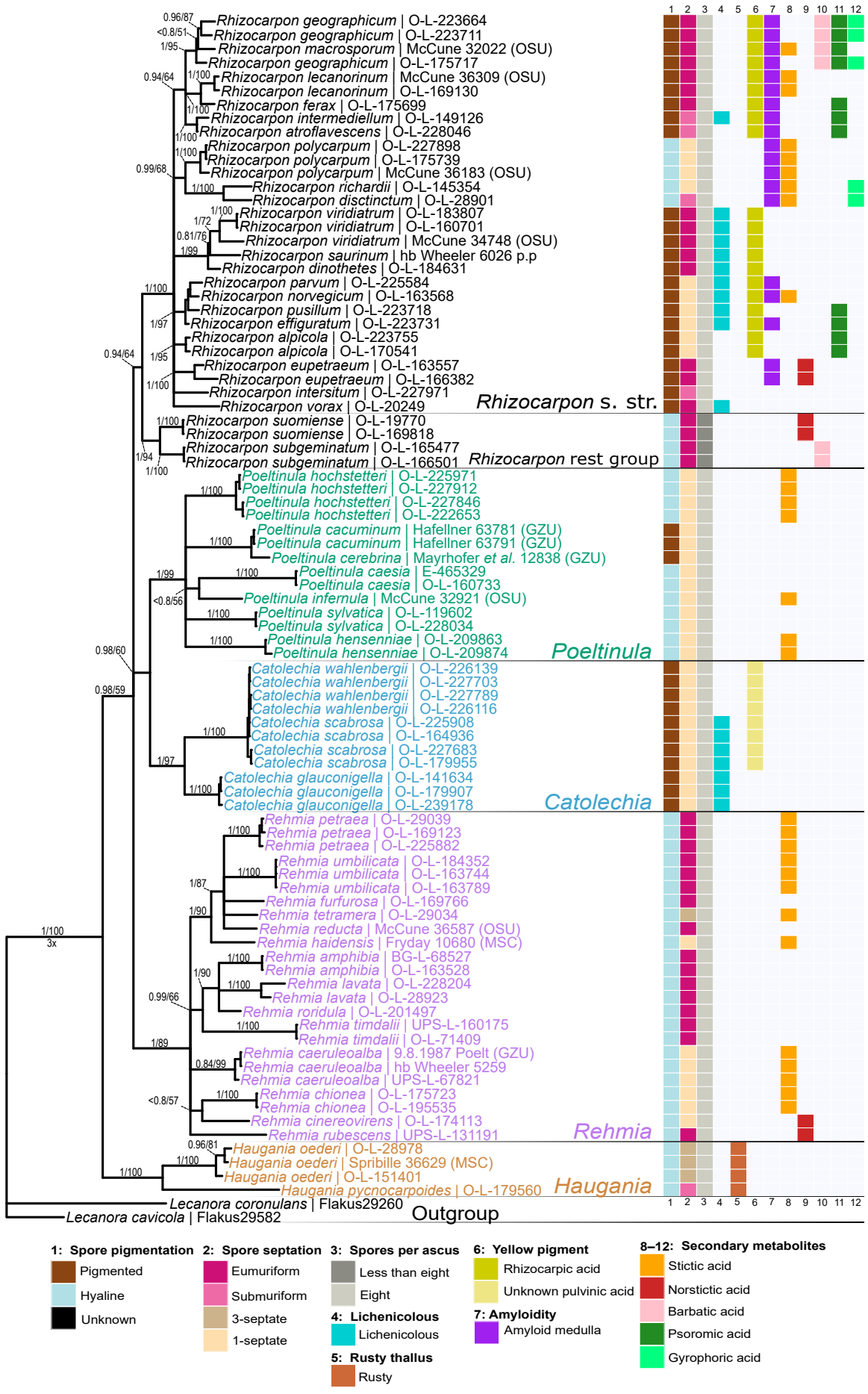

Fig. 2. Best tree from the ML analysis of the concatenated alignment, branches with BS < 50 % are collapsed. Numbers above branches indicate PP/BS support from the BI/ML analyses. The character matrix shows character states known for the species concepts (not necessarily the specimen): 1: ascospore pigmentation; 2: ascospore septation; 3: ascospores per ascus; 4: lichenicolous lifestyle; 5: rusty thallus; 6: yellow pigment; 7: thallus amyloidity; 8–13: secondary metabolites known to occur in the species.

© 2025 Westerdijk Fungal Biodiversity Institute

Haugania pycnocarpoides (Eitner) E.J. Möller & Timdal in Fryday *et al.*, *Revisions of British and Irish Lichens* **41**: 27. 2024.
Basionym: *Rhizocarpon pycnocarpoides* ["*pycnocappoides*"] Eitner, *Jahresber. Schles. Ges. Vaterl. Cult.* **88**: 46. 1911.

Poeltinula Hafellner, *Nova Hedwigia Beih.* **79**: 330. 1984**.**
Basionym: *Melanospora* Mudd, *A Manual of British Lichens*: 226. 1861 (nom. illegit., Art. 53.1), non *Melanospora* Corda, *Icones Fungorum* Tomus 1: 24. 1837.
Typification: *Opegrapha cerebrina* DC.

Poeltinula cacuminum (Asta, Clauzade & Cl.Roux) Clauzade & Cl. Roux, *Bull. Soc. Bot. Centre-Ouest.* **7**: 827. 1985
Basionym: *Encephalographa cerebrina* subsp. *cacuminum* Asta, Clauzade & Cl.Roux, *Bull. Soc. Linn. Provence* **30**: 11. 1977.

Poeltinula caesia (Fryday) E.J. Möller, Timdal, Haugan & Bendiksby, ***comb. nov.*** MB 859243.
Basionym: *Rhizocarpon caesium* Fryday, *Lichenologist* **34**: 458. 2002.

Poeltinula cerebrina (DC.) Hafellner, *Nova Hedwigia Beih.* **79**: 330. 1984.
Basionym: *Opegrapha cerebrina* DC. in Lamarck & de Candolle, *Flore Française*. ed. 3, 2: 312. 1805.

Poeltinula cerebrinella (Nyl.) Øvstedal, *S. African J. Bot.* **67**: 563. 2001.
Basionym: *Lecidea cerebrinella* Nyl., *J. Bot.* **14**: 22. 1876.

Poeltinula hensseniae (Brodo) E.J. Möller, Timdal, Haugan & Bendiksby, ***comb. nov.*** MB 859244.
Basionym: *Rhizocarpon hensseniae* Brodo, *Biblioth. Lichenol.* **38**: 32. 1990.

Poeltinula hochstetteri (Körb.) E.J. Möller, Timdal, Haugan & Bendiksby, ***comb. nov.*** MB 859245.
Basionym: *Catillaria hochstetteri* Körb., *Parerga Lichenologica*: 195. 1861.

Poeltinula infernula (Nyl.) E.J. Möller, Timdal, Haugan & Bendiksby, ***comb. nov.*** MB 859246.
Basionym: *Lecidea infernula* Nyl., *Flora* **68**: 440. 1885.

Poeltinula sylvatica (Fryday) E.J. Möller, Timdal, Haugan & Bendiksby, ***comb. et stat. nov.*** MB 859247.
Basionym: *Rhizocarpon infernulum f. sylvaticum* Fryday, *Lichenologist* **34**: 468. 2002.

Rehmia Kremp., *Denkschr. Königl.-Baier. Bot. Ges. Regensburg* **4, 2**: 211. 1861.
Typification: *Rehmia caeruleoalba* Kremp.

Rehmia amphibia (Fr.) E.J. Möller, Timdal, Haugan & Bendiksby, ***comb. nov.*** MB 859248.
Basionym: *Lecidea amphibia* Fr., *Kongl. Vetensk. Acad. Handl.* **1822**: 262. 1822.

Rehmia anapera (Vain.) E.J. Möller, Timdal, Haugan & Bendiksby, ***comb. nov.*** MB 859249.
Basionym: *Lecidea anapera* Vain., *Meddeland. Soc. Fauna Fl. Fenn.* **10**: 141. 1883.

Rehmia caeruleoalba Kremp., *Denkschr. Königl.-Baier. Bot. Ges. Regensburg* **4, 2**: 211. 1861.

Rehmia chionea (Norman) E.J. Möller, Timdal, Haugan & Bendiksby, ***comb. nov.*** MB 859250.
Basionym: *Catillaria chionea* Norman, *Kongel. Norske Videnskabers Selsk. Skr. 19de Aarhundr.* **5**: 355. 1868.

Rehmia cinereovirens (Müll. Arg.) E.J. Möller, Timdal, Haugan & Bendiksby, ***comb. nov.*** MB 859251.
Basionym: *Patellaria cinereovirens* Müll. Arg., *Flora* **51**: 49. 1868.

Rehmia furfurosa (H. Magn. & Poelt) E.J. Möller, Timdal, Haugan & Bendiksby, ***comb. nov.*** MB 859252.
Basionym: *Rhizocarpon furfurosum* H. Magn. & Poelt, *Verh. Zool.-Bot. Ges. Wien* **95**: 110. 1955.

Rehmia haidensis (Brodo & Fryday) E.J. Möller, Timdal, Haugan & Bendiksby, ***comb. nov.*** MB 859253.
Basionym: *Rhizocarpon haidense* Brodo & Fryday, *Lichenologist* **52**: 116. 2020.

Rehmia lavata (Fr.) E.J. Möller, Timdal, Haugan & Bendiksby, ***comb. nov.*** MB 859254.
Basionym: *Lecidea atroalba* var. *lavata* Fr., *Nova Schedulae Criticae de Lichenius Suecanis*: 18. 1827.
Synonym: *Lecidea lavata* (Fr.) Nyl., *Flora* **56**: 23. 1873.

Rehmia petraea (Wulfen) E.J. Möller, Timdal, Haugan & Bendiksby, ***comb. nov.*** MB 859255.
Basionym: *Lichen petraeus* Wulfen, *Schriften Ges. Naturf. Freunde Berlin* **8**: 89. 1787.

Rehmia postuma (Nyl.) E.J. Möller, Timdal, Haugan & Bendiksby, ***comb. nov.*** MB 859256.
Basionym: *Lecidea postuma* Nyl., *Flora* **51**: 345. 1868.

Rehmia reducta (Th. Fr.) E.J. Möller, Timdal, Haugan & Bendiksby, ***comb. nov.*** MB 859257.
Basionym: *Rhizocarpon reductum* Th. Fr., *Lichenographia Scandinavica* Pars prima (2): 633. 1874.

Rehmia roridula (Th. Fr.) E.J. Möller, Timdal, Haugan & Bendiksby, ***comb. nov.*** MB 859258.
Basionym: *Rhizocarpon obscuratum* ssp. *roridulum* Th. Fr., *Lichenographia Scandinavica* Pars prima (2): 629. 1874.
Synonym: *Lecidea roridula* (Th. Fr.) Stizenb., *Ber. Thätigk. St. Gallischen Naturwiss. Ges.* **1874–1875**: 235. 1876.

Rehmia rubescens (Th. Fr.) E.J. Möller, Timdal, Haugan & Bendiksby, ***comb. nov.*** MB 859259.
Basionym: *Rhizocarpon rubescens* Th. Fr., *Lichenographia Scandinavica* Pars prima (2): 631. 1874.
Typification: **Sweden**, Uppland, Lyran prope Stockholm, 1870, *S. Almquist* (UPS L-107090, **lectotype designated here**) MBT 10026484.

© 2025 Westerdijk Fungal Biodiversity Institute

Rehmia subpostuma (Arnold) E.J. Möller, Timdal, Haugan & Bendiksby, ***comb. nov.*** MB 859260.
Basionym: *Rhizocarpon subpostumum* Arnold, *Verh. K. K. Zool.-Bot. Ges. Wien.* **27**: 554. 1877.

Rehmia tetramera (Vain.) E.J. Möller, Timdal, Haugan & Bendiksby, ***comb. nov.*** MB 859261.
Basionym: *Lecidea postuma* var. *tetramera* Vain., *Meddeland. Soc. Fauna Fl. Fenn.* **10**: 141. 1883.
Synonym: *Rhizocarpon tetramerum* (Vain.) Vain., *Acta Soc. Fauna Fl. Fenn.* **51, 1**: 316. 1922.

Rehmia timdalii (Ihlen & Fryday) E.J. Möller, Timdal, Haugan & Bendiksby, ***comb. nov.*** MB 859262.
Basionym: *Rhizocarpon timdalii* Ihlen & Fryday, *Lichenologist* **34**: 96. 2002.

Rehmia umbilicata (Ramond) E.J. Möller, Timdal, Haugan & Bendiksby, ***comb. nov.*** MB 859263.
Basionym: *Lecidea umbilicata* Ramond, *Mém. Acad. Sci. Inst. France* **6**: 128. 1827.

Rhizocarpon Ramond ex DC., *Flore française*, Ed. 3, **2**: 365. 1805.
Typification: *Lichen geographicus* L., designated by Fink, *Contr. U. S. Natl. Herb.* **14**: 97. 1910.

Lepidoma Link, *Neues J. Bot.* **3**: 5. 1809.
Typification: *Lichen geographicus* L.

Catocarpus (Körb.) Arnold, *Flora (Regensburg)* **54**: 147. 1871.
Basionym: *Buellia* sect. *Catocarpus* Koerb. *Systema Lichenum Germaniae*: 223. 1855.
Typification: *Lecidea badioatra* Flörke ex Schaer. (**type designated here**, MBT 10026487).

Notes: The genus is currently regarded as typified by Dodge (1973: 88). Dodge (1973), however, merely states (erroneously) that the genus was based on *Lecidea badioatra* Flörke. There are four species in the protologue (*Buellia badioatra* "Flörke", *B. ocellata* "Flörke", *B. coracina* "Hoffm." and *Catolechia lactea* A. Massal.), and we designate the first as the type in accordance with how the name is usually applied. The typification of *Lecidea badioatra* Flörke ex Schaer. [i.e., the name that we think is the basionym of *Buellia badioatra* "Flörke"] was treated in Timdal *et al.* (2024).

Diphaeis Clem., *The Genera of Fungi*: 77, 174. 1909.
Typification: *Lecidea badioatra* Flörke ex Schaer.

Diphanis Clem., *The Genera of Fungi*: 77, 174. 1909.
Typification: *Lecidea confervoides* var. *polycarpa* Hepp.

Catillariopsis (Stein) M. Choisy, *Bull. Mens. Soc. Linn. Lyon.* **19**: 158. 1950.
Basionym: *Catocarpus* sect. *Catillariopsis* Stein, *Kryptogamen-Flora von Schlesien* Zweiter Band, zweite Häfte, Flechten: 225. 1879.
Typification: *Lecidea confervoides* var. *polycarpa* Hepp, designated by Hafellner, *Beiheft zur Nova Hedwigia* **79**: 329. 1984.

Rhizocarponomyces Cif. & Tomas., *Atti Ist. Bot. Lab. Crittog. Univ. Pavia* **10**: 38, 65. 1953 (nom. illegit., Art. 52.1).
Typification: The type of *Rhizocarpon* DC. (Art. 7.5).

Excluded genera

The following genera are listed as synonyms of *Rhizocarpon* in MycoBank (2025), but are here excluded from the *Rhizocarpaceae*.

Cormothecium A. Massal., *Geneacaena Lichenum noviter proposita ac descripta*: 8. 1854.
Typification: *Lecidea duebenii* Fr.

Note: *Lecidea duebenii* is currently regarded as a synonym of *Monerolechia badia* (Fr.) Kalb (*Caliciaceae*) [e.g., Nimis *et al.* 2018, as *Buellia duebenii* (Fr.) Hellb.]. *Cormothecium* actually predates *Monerolechia* Trev. (priority 1857).

Phalodictyum Clem., *The Genera of Fungi*: 77, 174. 1909.
Typification: *Lecidea petraea* var. *obscurata* Ach.

Note: The type [syn. *Rhizocarpon obscuratum* (Ach.) A. Massal.] is a synonym of *Fuscidea lygaea* (W. Mann) V. Wirth & Vězda (*Fusideaceae*) (lectotypified by Ihlen 2004: 556). *Phalodictyum* actually predates *Fuscidea* V. Wirth & Vězda (priority 1972).

Siegertia Körb., *Parerga Lichenologica* (2): 180. 1860.
Typification: *Lichen calcareus* L.

Notes: Although the protologue apparently describes the genus here named *Rehmia*, the only included species was named "*S. calcarea* (Weis) Kbr." with reference to the species described in Koerber (1855: 220) as "*Diplotomma calcarea* Weis". This can only be *Lichen calcarius* in Weis (1770) which refers (indirectly, through phrase name) to *Lichen calcareus* L. That name is the basionym of the species currently named *Circinaria calcarea* (L.) A. Nordin, Savić & Tibell (*Megasporaceae*). *Siegertia* antedates *Circinaria* Link (priority 1809).

DISCUSSION

Our phylogenetic results show that *Rhizocarpon*, as currently circumscribed, is paraphyletic with *Catolechia*, *Epilichen*, and *Poeltinula* nested within it, corroborating the findings of prior studies with a more limited taxon sampling (Ihlen & Ekman 2002, Miadlikowska *et al.* 2014). Our integrated assessment of molecular, anatomical and chemical evidence in a molecular phylogenetic framework suggests that the family consists of at least five major lineages. These five clades do not reflect current generic circumscriptions.

One solution is to synonymize *Catolechia*, *Epilichen*, *Poeltinula*, and *Haugania* with *Rhizocarpon*. However, this would have rendered *Rhizocarpon* an even larger genus with few unifying characters and the only genus in the *Rhizocarpales*. Under the current classification, *Rhizocarpon* species are characterized by being saxicolous and having a crustose thallus with apothecia originating from the hypothallus, in addition to having 1- to pluriseptate

© 2025 Westerdijk Fungal Biodiversity Institute

ascospores with perispores. *Catolechia* and *Epilichen* species are terricolous or lichenicolous on terricolous lichens and do not have perispores. *Poeltinula* species barely form visible thalli. Synonymizing all these genera with *Rhizocarpon* would result in a quite large genus (150–200 species) being the single genus in the family or, possibly, order. The only common character would be the ascus anatomy (Hafellner 1984).

Here, we propose to instead accept the five major genetic lineages as distinct genera (*Catolechia*, *Haugania*, *Poeltinula*, *Rehmia*, and *Rhizocarpon*), distinguishable by sets of traits (i.e., septation and pigmentation of ascospores, number of ascospores per ascus, hymenial characters, thallus colour, amyloidity, chemistry and ecology). In the following discussion we refer to the species under the old generic names, even though the new combinations were already made above.

***Catolechia*:** Morphologically and ecologically, *C. wahlenbergii* and the two *Epilichen* species are quite different: *C. wahlenbergii* is autonomous, up to 10 cm in diameter, and grows almost exclusively in shaded crevices in more or less humid, rock walls, while the *Epilichen* species are obligate parasites on other lichens, rarely more than 1 cm in diameter. However, species in this clade are similar in microscopic characters, unique in the family, by having ascospores without a gelatinous perispore. *Catolechia wahlenbergii* and *E. scabrosus* are both yellow due to two yellow pigments, apparently pulvinic acid derivatives that are not rhizocarpic acid. Also, the clade is unique in the family in being terricolous or lichenicolous on other terricolous lichens.

We include sequences from four specimens of *C. wahlenbergii* (all three markers for all four specimens) and four specimens of *E. scabrosus* (three ITS sequences, two MCM7 sequences, and two mtSSU sequences). Curiously, *C. wahlenbergii* and *E. scabrosus* are nested with each other on all three markers (see gene trees, supplementary material), and consequently in the species tree. Normally, the microscopical, chemical and genetic evidence provided here would merit synonymization. Due to the large morphological and ecological differences, the lack of intermediates, and the fact that we use only three markers, we do not synonymize the two species here. Further investigations are needed to confidently revise this species complex. Regardless of whether the two species are conspecific, there is no doubt that *Epilichen* should be synonymized with *Catolechia*.

***Haugania*:** *Haugania oederi* and *H. pycnocarpoides* form a fully supported clade. The species are similar in having eight, halonate, hyaline ascospores, rust red thalli, and by growing exclusively on heavy metal rich rocks. These characters are admittedly not unique within the family and hardly of high taxonomic value, but, as a combination, a key character for the genus. *Haugania* is here accepted based on the phylogenetic reconstruction.

***Poeltinula*:** The species in the *R. hochstetteri* complex are characterized by being crustose, non-yellow, having a distinct apothecial margin, a non-amyloid medulla, swollen and sharply delimited paraphysis caps, and 1-septate, halonate, hyaline ascospores (Fig. 3). Together with the two included *Poeltinula* species, which have an endolithic thallus, furrowed apothecia, green, 1-septate ascospores, and pigmented, albeit substantially smaller, paraphysis caps, the complex constitutes a fully supported clade. Species in the clade either have stictic acid or no secondary metabolites.

Runemark (1956) reports observing pigmented paraphysis caps in some yellow species, but his description of the caps differs from the ones observed in *Poeltinula* and the *R. hochstetteri* complex by being more diffuse and not as sharply delimited. Furthermore, hyaline, 1-septate ascospores also occur in *R. polycarpum* and *R. richardii*, but those species have a strongly amyloid medulla. *Rehmia caeruleoalba*, *R. chionea*, *R. cinereovirens* and *R. haidensis*, also have similar ascospores, but lack the distinct apothecial margin and the swollen pigmented paraphysis caps.

Poeltinula is the only available genus name for this group, and we propose to include *Rhizocarpon hochstetteri*, *R. caesium*, *R. infernulum* and *R. hensseniae* in that genus. Additionally, we accept *R. infernulum f. sylvaticum* as a distinct species, since the branch lengths in all gene trees are equivalent to the accepted species in the group.

***Rehmia*:** The 14 species that constitute the *Rehmia* clade are similar in having a non-amyloid medulla and halonate, hyaline, mainly muriform ascospores (some have 1-septate ascospores and those of *Rhizocarpon tetramerum* are 3-septate ascospores) (Fig. 4). The four species that have 1-septate ascospores can be distinguished from *Poeltinula* by lacking an apothecial margin and swollen paraphysis caps. In addition, *R. caeruleoalbum* and *R. chioneum* have white thalli similar to *R. umbilicatum*. Hyaline, muriform ascospores also occur in species outside of *Rehmia*: *Rhizocarpon subgeminatum* and *R. suomiense* both have less than eight ascospores per ascus, whereas all *Rehmia* species have eight, and *Rhizocarpon distinctum*, which is retained in *Rhizocarpon,* has a strongly amyloid medulla, whereas all *Rehmia* species have a non-amyloid medulla.

The clade here named *Rehmia* largely corresponds to the so-called *Rhizocarpon obscuratum* group (i.e., non-yellow species with hyaline, muriform ascospores) studied by Ihlen (2004). Of the 16 species placed in the group by Ihlen (2004), we include 12 in *Rehmia* (nine from molecular evidence, three from morphology) and exclude four (three from molecular evidence, i.e., *Rhizocarpon distinctum*, *R. subgeminatum*, and *R. suomiense*) and one from preliminary, incomplete molecular data indicating distant relationship (*R. sublavatum*; Möller 2021). Our molecular evidence clearly shows that ascospore morphology alone is not diagnostic for the circumscription of *Rehmia*, but that amyloidity and number of ascospores per ascus must also be taken into account. This is emphasized by the fact that *Rhizocarpon caeruleoalbum*, *R. cinereovirens*, *R. chioneum* and *R. haidense*, all with 1-septate ascospores and hence not included in the *R. obscuratum* group, belong in the *Rehmia* clade.

The clade is phylogenetically well separated from the rest of the family, and is anatomically distinguishable by the traits mentioned above. We propose accepting it as a distinct genus and resurrect the name *Rehmia*. The type species of *Rehmia* is *Rhizocarpon caeruleoalbum*, in our tree represented by three specimens collected in North America, Norway and Austria. In addition to the fourteen species in the *Rehmia* clade, we also transfer three non-sequenced species to *Rehmia* based on the morphological features given above.

***Rhizocarpon* s. str.:** The clade that contains the type species of the genus (*Rhizocarpn geographicum*) is a diverse

© 2025 Westerdijk Fungal Biodiversity Institute

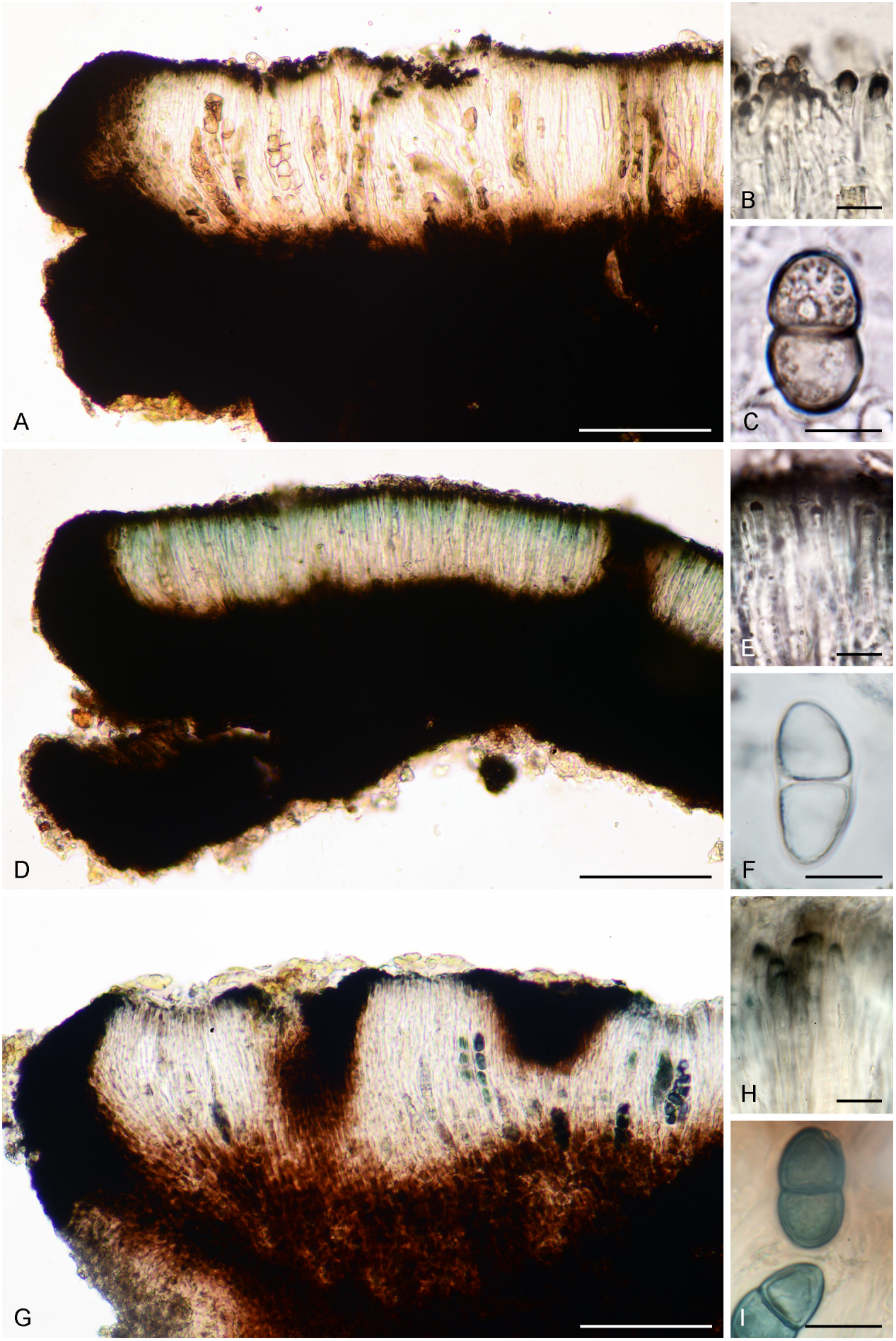

Fig. 3. *Poeltinula* anatomy: Transverse sections through apothecia (A, D, G), tip of paraphyses (B, E, H), and ascospores (C, F, I). **A–C**. *Rhizocarpon hochstetteri*, Norway, O-L-227846. **D–F.** *R. infernulum* f. *sylvatica*, Norway, O-L-228034. **G–I.** *P. cacuminum*, Austria, Wilfling & Möslinger 569, GZU. Photo credits: E. Timdal. Scale bars: A, D, G = 100 µm; B, C, E, F, H, I = 10 µm.

© 2025 Westerdijk Fungal Biodiversity Institute

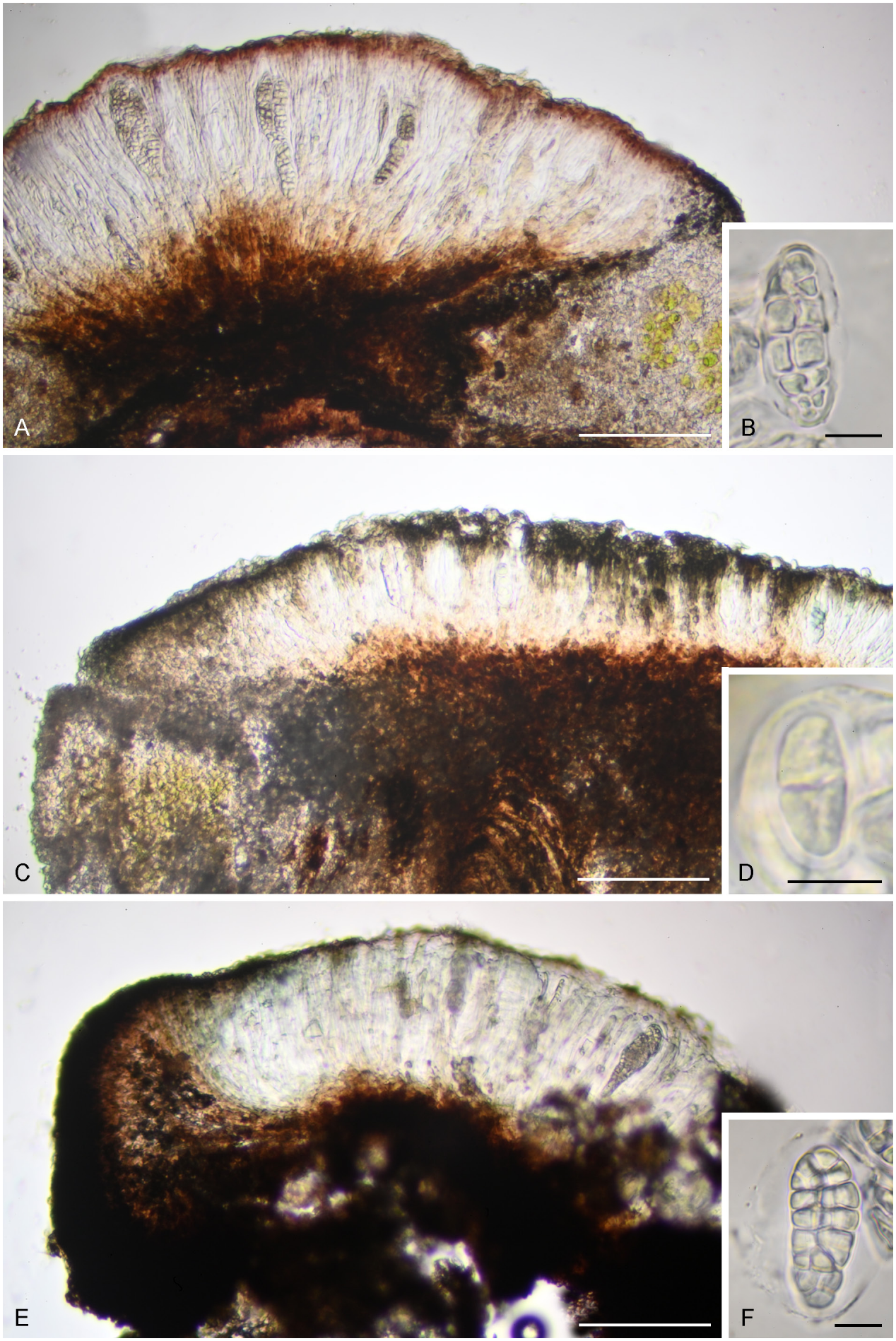

Fig. 4. *Rehmia* anatomy: Transverse sections through apothecia (A, C, E) and ascospores (B, D, F). **A, B.** *Rhizocarpon amphibium*, Norway, O-L-163528. **C, D.** *R. caeruleoalbum*, Norway, UPS L-67821. **E, F.** *R. lavatum*, Norway, O-L-28923. Photo credits: E. Timdal. Scale bars: A, C, E = 100 µm; B, D, F = 10 µm.

© 2025 Westerdijk Fungal Biodiversity Institute

group and has few traits that unite them. However, there are trends, albeit with many exceptions. All the species of the *Rhizocarpaceae* with an amyloid medulla belong here, as do all the species with secondary compounds other than barbatic, stictic, and norstictic acids (i.e. confriesiic, diffractaic, gyrophoric, psoromic, and rhizocarpic acids). The only *Rhizocarpaceae* species in our phylogeny known to contain barbatic acid outside *Rhizocarpon* s. str. is *R. subgeminatum* of the *Rhizocarpon* rest group. Most of the species have pigmented ascospores, but they vary in number of septa. All of the lichenicolous species except the two *Epilichen* species also belong here. It is likely that the group is even more diverse than shown here, since this study did not include all known *Rhizocarpon* species.

***Rhizocarpon* rest group:** *Rhizocarpon subgeminatum* and *R. suomiense* are morphologically and anatomically similar to *Rehmia* species, but are easily distinguishable by the number of ascospores per ascus (all *Rehmia* species have eight ascospores per ascus, while *Rhizocarpon subgeminatum* and *R. suomiense* have two). They were included in the study because they have hyaline ascospores, and could therefore be suspected to belong to either the *Rehmia* or the *Poeltinula* clade. Here, we show that they do not appear in either of those clades, but rather form a well-supported, distinct clade with uncertain placement in the presented phylogeny. We do not formally describe the clade as a genus because we do not consider evidence from so few markers for only four accessions (ITS and mtSSU for *R. suomiense* and only ITS for *R. subgeminatum*) to be sufficient for describing these two species as a distinct genus. We know from preliminary analyses that the group adjacent to what we here refer to as *Rhizocarpon* s. str. requires more data to be properly treated.. We have ITS sequences for ca 80 accepted species of *Rhizocarpon*, but here we excluded many species and groups that we know from preliminary analyses do not belong to any of the groups we treat taxonomically. These species include putatively monophyletic groups, like the *R. geminatum* complex (i.e. *R. geminatum*, *R. disporum*, and *R. sulphurosum*) and the *R. badioatrum* complex (Timdal *et al.* 2024), and several more species that so far form a polytomy close to *Rhizocarpon* s. str. (e.g. *R. inarense*, *R. jemtlandicum*, *R. leptolepis*, and *R. superficiale*) (Möller 2021). To our best knowledge, we included all accepted species that do not belong in or are closely related to *Rhizocarpon* s. str., with the exception of *R. sublavatum*, which has an uncertain placement based on preliminary studies (Möller 2021). All of these species would be interesting to analyse further with a more complete dataset.

Outgroup: In the previous genus level study of the *Rhizocarpaceae*, the authors disclose that finding a suitable outgroup for the family is challenging due the uncertain placement of the *Rhizocarpaceae* (Ihlen & Ekman 2002). At the time, the family was hypothesized to belong to the *Lecanorales*, but has since been described as an order itself, possibly together with the *Sportastatiaceae* (e.g. Bendiksby & Timdal 2013, Miadlikowska *et al.* 2014, Kraichak *et al.* 2018). In this study, we had similar issues with outgroup selection as Ihlen & Ekman (2002). In the end, *Lecanora cavicola* and *L. coronulans* were selected as an outgroup based on having all the three markers publicly available for both accessions. It should be noted that we analysed the dataset multiple times with different outgroups, or without outgroups, and the same five major clades appear. For future studies that intend to investigate the deep topology of the family, we recommend acquiring additional conserved markers for e.g. the *Sporastatiaceae*. With the advent of phylogenomics, the answer to the placement of the *Rhizocarpaceae* within the *Lecanoromycetes* may be closer.

CONCLUSION

The molecular results clearly show that the taxonomy of the *Rhizocarpaceae* needs revision. The current circumscription is largely based on morphology and life-strategy, and renders *Rhizocarpon* paraphyletic. Our phylogeny indicates that microscopical traits (e.g. spore morphology and hymenial characters) are more informative.

We have presented evidence for making nomenclatural changes in the clades *Catolechia*, *Poeltinula* and *Rehmia*: specifically, we propose to synonymize *Epilichen* with *Catolechia*, to move the species in the *Rhizocarpon hochstetteri* complex to *Poeltinula*, and to resurrect the genus *Rehmia* for a set of species previously placed in *Rhizocarpon*.

ACKNOWLEDGEMENTS

This study was part of EM's master thesis, which was supervised by the co-authors ET, RH and MB. We are grateful to the fungarium curators at E, GZU, MSC, O, and OSC for lending us specimens used for the present study. Siri Rui is thanked for her invaluable technical support with regard to handling loans and curating specimens in the O lichen collection. L. Thorbeck and A. Schrøder Nilsen at the NHM molecular laboratory are cordially thanked for their help with some of the molecular data production, and support and training during EM's master thesis. We acknowledge generous financial support (project Nos. 70184216, 70184227) from the Norwegian Taxonomy Initiative (Norske Artsprosjektet) administered by The Norwegian Biodiversity Information Centre (Artsdatabanken). The Norwegian Barcode of Life (NorBOL) funded the sequencing at the Canadian Centre for DNA Barcoding. We also thank B. McCune and T. Wheeler for loan of material, and S.D. Kistenich for work at the DNA laboratory at Natural History Museum in Oslo. M. Naranjo-Ortiz and A. Simon are thanked for valuable discussions. M. Svensson is thanked for advice and guidance.

Conflict of Interest: The authors declare no conflicts of interest.

REFERENCES

Bendiksby M, Timdal E (2013). Molecular phylogenetics and taxonomy of *Hypocenomyce* sensu lato (*Ascomycota*: *Lecanoromycetes*): extreme polyphyly and morphological/ecological convergence. *Taxon* **62**: 940–956. https://doi.org/10.12705/625.18

BLS (2025). The British Lichen Society: Lichen Taxon Dictionary. <https://britishlichensociety.org.uk/resources/lichen-taxon-database> Accessed on 15 May 2025.

Buschbom J, Mueller G (2004). Resolving evolutionary relationships

© 2025 Westerdijk Fungal Biodiversity Institute

in the lichen-forming genus *Porpidia* and related allies (*Porpidiaceae*, *Ascomycota*). *Molecular Phylogenetics and Evolution* **32**: 66–82. https://doi.org/10.1016/j.ympev.2003.11.012

Clements FE (1909). *The Genera of Fungi*. The H. W. Wilson Company, U.S.A.

Davydov EA, Yakovchenko LS (2017). *Rhizocarpon smaragdulum* a new monosporic yellow-thalline species and some additional species of the genus *Rhizocarpon* from the Altai Mountains (Siberia). *The Lichenologist* **49**: 457–466. https://doi.org/10.1017/s0024282917000469

Dodge CW (1973). *Lichen flora of the Antarctic Continent and adjacent islands*. Phoenix Publishing Co., U.S.A.

Felsenstein J (1985). Confidence limits on phylogenies: an approach using the bootstrap. *Evolution* **39**: 783–791. https://doi.org/10.2307/2408678

Ferencova Z, Rico VJ, Hawksworth DL (2017). Extraction of DNA from lichen-forming and lichenicolous fungi: a low-cost fast protocol using Chelex. *The Lichenologist* **49**: 521–525. https://doi.org/10.1017/s0024282917000329

Feuerer T, Timdal E (2004). *Rhizocarpon*. In: *Lichen flora of the greater Sonoran Desert region* 2nd vol. (Nash TH III, Ryan BD, Diederich P, *et al.*, eds). Lichens Unlimited, Arizona State University, USA: 456–466.

Flotow J von (1850). Mikroskopische Flechtenstudien. *Botanische Zeitung (Berlin)* **8**: 361–369, 377–382.

Fryday AM (2002). A revision of the species of the *Rhizocarpon hochstetteri* group occurring in the British Isles. *The Lichenologist* **34**: 451–477. https://doi.org/10.1006/lich.2002.0416

Fryday AM (2019). Corrections to reports of buellioid lichens from New Zealand'ssubantarctic islands, including *Sclerococcum thelotrematicola comb. nov*. and *Epilichen scabrosus* new to the Southern Hemisphere. *Australasian Lichenology* **84**: 26–32.

Fryday A, Möller EJ, Timdal E, *et al.* (2024). *Rhizocarpales*, including *Catolechia*, *Epilichen*, *Haugania*, *Poeltinula* and *Rhizocarpon* (*Rhizocarpaceae*), and *Sporastatia* and *Toensbergia* (*Sporastatiaceae*). *Revisions of British and Irish Lichens* **41**: 1–30. https://britishlichensociety.org.uk/sites/default/files/Rhizocarpales.pdf

Gardes M, Bruns TD (1993). ITS primers with enhanced specificity for basidiomycetes-application to the identification of mycorrhizae and rusts. *Molecular Ecology* **2**: 113–118. https://doi.org/10.1111/j.1365-294x.1993.tb00005.x

GBIF (2025). Global Biodiversity Information Facility: Occurrences. <https://www.gbif.org/occurrence/search> Accessed on 7 March 2025.

Hafellner J (1979). *Catolechia* Flotow ex Massalongo emend. Körber und *Epilichen* Clements ex Hafellner - zwei nahe verwandte Flechtengattungen. *Nova Hedwigia* **30**: 673–696. https://doi.org/10.1127/nova.hedwigia/30/1979/673

Hafellner J (1984). Studien in Richtung einer natürlichen Gliederung der Sammelfamilien *Lecanoraceae* und *Lecideaceae*. *Beiheft zur Nova Hedwigia* **79**: 241–371.

Halici MG, Möller E, Timdal E, *et al.* (2022). *Rhizocarpon ozsoyae sp. nova* (*Rhizocarpaceae*, lichenized Ascomycetes) from James Ross Island (Antarctic Peninsula). *Herzogia* **35**: 105–114. https://doi.org/10.13158/heia.35.1.2022.105

Holtan-Hartwig J, Timdal E (1987). Notes on some parasitic *Rhizocarpon* species. *The Lichenologist* **19**: 335–338. https://doi.org/10.1017/s002428298700029x

Honegger R (1980). The ascus apex in lichenized fungi II. The *Rhizocarpon*-type. *The Lichenologist* **12**: 157–172. https://doi.org/10.1017/s002428298000014x

Ihlen PG (1997). The lichen genus *Baeomyces* (*Leotiales*, *Ascomycotina*) in Norway. *Nova Hedwigia* **64**: 137–146. https://doi.org/10.1127/nova.hedwigia/64/1997/137

Ihlen PG (2004). Taxonomy of the non-yellow species of *Rhizocarpon* (*Rhizocarpaceae*, lichenized *Ascomycota*) in the Nordic countries, with hyaline and muriform ascospores. *Mycological Research* **108**: 533–570. https://doi.org/10.1017/s0953756204009803

Ihlen PG, Ekman S (2002). Outline of phylogeny and character evolution in *Rhizocarpon* (*Rhizocarpaceae*, lichenized *Ascomycota*) based on nuclear ITS and mitochondrial SSU ribosomal DNA sequences. *Biological Journal of the Linnean Society* **77**: 535–546. https://doi.org/10.1046/j.1095-8312.2002.00127.x

Inkscape home page (2023). <www.inkscape.org>

Katoh K, Rozewicki J, Yamada KD (2019). MAFFT online service: multiple sequence alignment, interactive sequence choice and visualization. *Briefings in Bioinformatics* **20**: 1160–1166. https://doi.org/10.1093/bib/bbx108

Kozlov AM, Darriba D, Flouri T, *et al.* (2019). RAxML-NG: a fast, scalable and user-friendly tool for maximum likelihood phylogenetic inference. *Bioinformatics* **35**: 4453–4455. https://doi.org/10.1093/bioinformatics/btz305

Kraichak E, Huang JP, Nelsen M, *et al.* (2018). A revised classification of orders and families in the two major subclasses of *Lecanoromycetes* (*Ascomycota*) based on a temporal approach. *Botanical Journal of the Linnean Society* **188**: 233–249. https://doi.org/10.1093/botlinnean/boy060

Koerber GW (1855). *Systema Lichenum Germaniae*. Von Trewendt & Granier, Germany.

Lamarck J-B, De Candolle AP (1805). *Flore française* 3rd edn, 2nd vol. Desray, France.

Larsson A (2014). AliView: a fast and lightweight alignment viewer and editor for large data sets. *Bioinformatics* **30**: 3276–3278. https://doi.org/10.1093/bioinformatics/btu531

Linnaeus C (1753). *Species plantarum* 2nd vol. L Salvius, Sweden.

Lücking R, Hodkinson BP, Leavitt SD (2017). The 2016 classification of lichenized fungi in the *Ascomycota* and *Basidiomycota*–Approaching one thousand genera. *The Bryologist* **119**: 361–416. https://doi.org/10.1639/0007-2745-119.4.361

Lutzoni F, Pagel M, Reeb V (2001). Major fungal lineages are derived from lichen symbiotic ancestors. *Nature* **411**: 937–940. https://doi.org/10.1038/35082053

Marthinsen G, Rui S, Timdal E (2019). OLICH: A reference library of DNA barcodes for Nordic lichens. *Biodiversity Data Journal* **7**: e36252. https://doi.org/10.3897/bdj.7.e36252

Massalongo AB (1852). *Ricerche sull'autonomia dei licheni crostosi*. A Frizerio, Italy.

McCune B, Timdal E, Bendiksby M (2016). *Rhizocarpon quinonum*, a new anthraquinone-containing species from the Alaska Peninsula. *The Lichenologist* **48**: 367–375. https://doi.org/10.1017/s0024282916000347

Medeiros ID, Mazur E, Miadlikowska J (2021). Turnover of lecanoroid mycobionts and their *Trebouxia* photobionts along an elevation gradient in Bolivia highlights the role of environment in structuring the lichen symbiosis. *Frontiers in Microbiology* **12**: 774839. https://doi.org/10.3389/fmicb.2021.774839

Miadlikowska J, Kauff F, Högnabba F, *et al.* (2014). A multigene phylogenetic synthesis for the class *Lecanoromycetes* (*Ascomycota*): 1307 fungi representing 1139 infrageneric taxa, 317 genera and 66 families. *Molecular Phylogenetics*

© 2025 Westerdijk Fungal Biodiversity Institute

and Evolution **79**: 132–168. https://doi.org/10.1016/j.ympev.2014.04.003

Mirarab S, Nguyen N, Warnow T (2014). PASTA: ultra-large multiple sequence alignment. *Journal of Computational Biology* **22**: 377–386. https://doi.org/10.1007/978-3-319-05269-4_15

Möller EJ (2021). Molecular phylogenetics and genus delimitation in the *Rhizocarpaceae* (lichenized ascomycetes) with focus on the *Rhizocarpon hochstetteri*-complex. MSc thesis. Natural History Museum, University of Oslo, Norway. https://www.duo.uio.no/bitstream/handle/10852/89898/11/ErikMoller_thesis_fixed3.pdf

Möller EJ, Timdal E, Haugan R, Bendiksby M (2025a). Alignments. figshare. Dataset. https://doi.org/10.6084/m9.figshare.28596479.v2

Möller EJ, Timdal E, Haugan R, Bendiksby M (2025b). Trees. figshare. Dataset. https://doi.org/10.6084/m9.figshare.28596530.v2

MycoBank (2025). Fungal Databases, Nomenclature & Species Banks. <www.mycobank.org> Accessed on 7 March 2025.

Nimis PL, Hafellner J, Roux C, *et al.* (2018). The lichens of the Alps - An annotated checklist. *MycoKeys* **31**: 1–634. https://doi.org/10.3897/mycokeys.31.23568

Poelt J **(**1990). Parasitische Arten der Flechtengattung *Rhizocarpon*: eine weitere Übersicht. *Mitteilungen der Botanische Staatssammlung* München **29**: 515–538.

Purvis OW, Halls C (1996). A review of lichens in metal-enriched environments. *The Lichenologist* **28**: 571–601. https://doi.org/10.1006/lich.1996.0052

Rambaut A, Drummond AJ, Xie D, *et al.* (2018). Posterior summarisation in Bayesian phylogenetics using Tracer 1.7. *Systematic Biology* **67**: 901–904. https://doi.org/10.1093/sysbio/syy032

Roca-Valiente B, Hawksworth DL, Pérez-Ortega S, *et al.* (2016). Type studies in the *Rhizocarpon geographicum* group (*Rhizocarpaceae*, lichenized *Ascomycota*). *The Lichenologist* **48**: 97–110. https://doi.org/10.1017/s002428291500050x

Ronquist F, Teslenko M, Van Der Mark P, *et al.* (2012). MrBayes 3.2: efficient Bayesian phylogenetic inference and model choice across a large model space. *Systematic Biology* **61**: 539–542. https://doi.org/10.1093/sysbio/sys029

Runemark H (1956). Studies in *Rhizocarpon*. I. Taxonomy of the yellow species in Europe. *Opera Botanica* **2**: 1–152.

Schmitt I, Crespo A, Divakar PK, *et al.* (2009). New primers for promising single-copy genes in fungal phylogenetics and systematics. *Persoonia* **23**: 35–40. https://doi.org/10.3767/003158509x470602

Spribille T, Fryday AM, Pérez-Ortega S, *et al.* (2020). Lichens and associated fungi from Glacier Bay National Park, Alaska. *The Lichenologist* **52**: 61–181. https://doi.org/10.1017/s0024282920000079

Stamatakis A (2006). RAxML-VI-HPC: maximum likelihood-based phylogenetic analyses with thousands of taxa and mixed models. *Bioinformatics* **22**: 2688–2690. https://doi.org/10.1093/bioinformatics/btl446

Svensson M, Fryday AM (2022). *Gilbertaria*, a first crustose genus in the *Sphaerophoraceae* (*Lecanoromycetes*, *Ascomycota*) for *Catillaria contristans*, *Toninia squalescens* and related species. *Mycological Progress* **21**: 90. https://doi.org/10.1007/s11557-022-01838-5

Tamura K, Stecher G, Kumar S (2021). MEGA 11: Molecular Evolutionary Genetics Analysis Version 11. *Molecular Biology and Evolution* **38**: 3022–3027. https://doi.org/10.1093/molbev/msab120

Timdal E, Holtan-Hartwig J (1988). A preliminary key to *Rhizocarpon* in Scandinavia. *Graphis Scripta* **2**: 41–54.

Timdal E (1986). *Rhizocarpon santessonii*, a new parasitic lichen from Norway. *The Lichenologist* **18**: 317–320. https://doi.org/10.1017/s0024282986000506

Timdal E, Möller EJ, Bendiksby M (2024). *Rhizocarpon vulgare*, a new species in the *R. badioatrum* species complex. *Graphis Scripta* **36**: 89–105. https://www.duo.uio.no/handle/10852/111388

Timdal E, Rui S (2024). Contributions to the lichen flora of the province of Alberta, Canada, with the description of two new species and revised status for the subspecies of *Toninia tristis*. *Opuscula Philolichenum* **23**: 33–81.

Triebel D (1989). Lecideicole Ascomyceten. Eine Revision der obligat lichenicolen Ascomyceten auf lecideoiden Flechten. *Bibliotheca Lichenologica* **35**: 1–278.

Triebel D, Rambold G, Nash TH III (1991). On lichenicolous fungi from continental North America. *Mycotaxon* **42**: 263–296.

Westberg M, Timdal E, Asplund J, *et al.* (2015). New records of lichenized and lichenicolous fungi in Scandinavia. *MycoKeys* **11**: 33–61. https://doi.org/10.3897/mycokeys.11.6670

White TJ, Bruns T, Lee S, *et al.* (1990). Amplification and direct sequencing of fungal ribosomal RNA genes for phylogenetics. In: *PCR protocols: a guide to methods and applications* (Innis MA, Gelfand DH, Sninsky JJ, *et al.*, eds). Academic Press, Inc., New York, USA: 315–322. https://doi.org/10.1016/B978-0-12-372180-8.50042-1

Yu G, Smith DK, Zhu H, *et al.* (2017). ggtree: an R package for visualization and annotation of phylogenetic trees with their covariates and other associated data. *Methods in Ecology and Evolution* **8**: 28–36. https://doi.org/10.1111/2041-210x.12628

Zoller S, Scheidegger C, Sperisen C (1999). PCR primers for the amplification of mitochondrial small subunit ribosomal DNA of lichen-forming ascomycetes. *The Lichenologist* **31**: 511–516. https://doi.org/10.1006/lich.1999.0220

Supplementary Material: http://fuse-journal.org

Fig. S1. Best tree from the ML analysis of the ITS alignment, branches with BS < 50 % are collapsed. Numbers above branches indicate BS support.

Fig. S2. Best tree from the ML analysis of the mtSSU alignment, branches with BS < 50 % are collapsed. Numbers above branches indicate BS support.

Fig. S3. Best tree from the ML analysis of the *MCM7* alignment, branches with BS < 50 % are collapsed. Numbers above branches indicate BS support.

© 2025 Westerdijk Fungal Biodiversity Institute

© 2025 Westerdijk Fungal Biodiversity Institute

FUSE

Fungal Systematics and Evolution

VOLUME 16
DECEMBER 2025
PAGES 233–242

doi.org/10.3114/fuse.2025.16.13

Phylogeny and taxonomy of *Cercospora malkoffii* (*Mycosphaerellaceae*)

L.-S. Kreth[1], J.Z. Groenewald[2], U. Braun[3*], M. Götz[1]

[1]Institute for Plant Protection in Horticulture and Urban Green, Julius Kühn-Institute (JKI) – Federal Research Centre for Cultivated Plants, Braunschweig, Germany
[2]Westerdijk Fungal Biodiversity Institute, Uppsalalaan 8, 3584 CT Utrecht, The Netherlands
[3]Herbarium, Department of Geobotany and Botanical Garden, Institute of Biology, Martin Luther University, Kirchtor 3, 06099 Halle (Saale), Germany

*Corresponding author: uwe.braun@botanik.uni-halle.de

Abstract: The phylogeny and taxonomy of *Cercospora malkoffii*, an anamorphic ascomycete (*Mycosphaerellaceae*) causing a phytopathologically relevant leaf-spot disease on anise (*Pimpinella anisum*), are examined and clarified. This species is currently treated as belonging to the genus *Passalora*, based on a morphological species concept. However, genera of the *Mycosphaerellaceae* in general and particularly *Passalora s. lat*. underwent significant taxonomic changes in the past decades owing to comprehensive molecular phylogenetic revisions of cercosporoid fungi. *Cercospora malkoffii* has recently been repeatedly observed in commercial fields of *P. anisum* and has been isolated and cultivated in this study. Based on these cultures, ITS, LSU, *CaM*, *tef1*, *tub2*, and *rpb2* sequences were retrieved and phylogenetic analyses were performed. These analyses revealed that *C. malkoffii* pertains to the genus *Fusoidiella* that currently comprises two former *Passalora* species on apiaceous hosts. Accordingly, the new combination *Fusoidiella malkoffii* is introduced. In addition, an epitype is designated here for *C. malkoffii*, and a pathogenicity test has been successfully carried out to fulfil Koch's postulates.

Key words:
Ascomycota
cercosporoid fungi
epitypification
Mycosphaerellales
new combination
Passalora malkoffii
systematics

Citation: Kreth L-S, Groenewald JZ, Braun U, Götz M (2025). Phylogeny and taxonomy of *Cercospora malkoffii* (*Mycosphaerellaceae*). *Fungal Systematics and Evolution* **16**: 233–242. doi: 10.3114/fuse.2025.16.13
Received: 14 March 2025; **Accepted:** 22 June 2025; **Effectively published online:** 1 August 2025
Corresponding editor: P.W. Crous

INTRODUCTION

Anise (*Pimpinella anisum*, *Apiaceae*) is a widely cultivated and used spice and flavour herb, native to the Mediterranean region and Southwest Asia, utilized for culinary and pharmaceutical purposes, manufacturing alcoholic drinks and in the traditional medicine (Peter 2004, Sun *et al*. 2019; http://gernot-katzers-spice-pages.com/engl/Pimp_ani.html, last visited 11/06/2024). Amongst diverse plant pathogenic fungi reported to occur on anise, *Cercospora malkoffii* is a leaf-spotting, anamorphic ascomycete, described by Bubák (1906) from Bulgaria. Over a long period, this species had been recognized as a member of *Cercospora* s. lat. (Chupp 1954). Based on a revised concept of cercosporoid genera and a re-examination of the type material of *C. malkoffii*, Braun, in Braun & Mel'nik (1997), reallocated this species to *Passalora*. The new, revised morphological circumscription of *Passalora* was discussed and outlined in detail by Crous & Braun (2003). Therefore, it is not surprising that the name *Passalora malkoffii* for this anise disease has prevailed to date. However, results of broad-scale phylogenetic analyses of cercosporoid ascomycetes revealed that the genus *Passalora* is confined to its type species and probably a few closely allied taxa (Videira *et al*. 2017). The whole genus *Passalora* s. lat. proved to be a complex of numerous genera (Videira *et al*. 2017). More than 3000 names have been assigned to *Cercospora* in its previous wide circumscription, and only 659 species were recognized by Crous & Braun (2003), and about 550 names, previously described under *Cercospora* s. lat., *Mycovellosiella*, *Phaeoramularia*, etc., were reallocated to *Passalora* emend. Crous & Braun (2003) recognized in that time with a broad, morphology-based circumscription. However, although Videira *et al*. (2017) introduced numerous new genera for cercosporoid fungi of the former *Passalora* complex, only few species previously assigned to *Passalora* have been phylogenetically examined and taxonomically reassessed. *Cercospora malkoffii* (≡ *Passalora malkoffii*) is one of the numerous species concerned that are still unrevised. Recently, successfully performed attempts to cultivate the latter species (present study) provided the basis for sequence analyses, which led to the clarification of its phylogenetic affinity and a taxonomic reassessment.

MATERIALS AND METHODS

Sample collection and isolation

Symptomatic plants of *P. anisum* were collected from eight commercial fields in Austria in 2022 and 2024 and one experimental plot in Germany in 2023 (Table 1). Stems, leaves, and seeds were inspected macroscopically and microscopically

Fungal Systematics and Evolution is licensed under a Creative Commons Attribution-NonCommercial-NoDerivatives 4.0 International License

© 2025 Westerdijk Fungal Biodiversity Institute

(VHX-7100 Digital Microscope with fully-integrated head, equipped with lenses VHX-E20, VHX-E100, VHX-E500, Keyence Deutschland GmbH, Germany), and conidia of the pathogen were transferred to potato dextrose agar (PDA; Becton Dickinson, USA) amended with antibiotics [100 mg/L penicillin G sodium salt (PEN−NA, Merck, Germany), 10 mg/L chlortetracycline hydrochloride (C4881, Merck, Germany), and 50 mg/L streptomycin sulphate salt (S6501, Merck, Germany)] with an inoculation loop. Plates were incubated at room temperature under daylight conditions. After one day, cultures were inspected using an inverted microscope (PrimoVert, Zeiss, Germany) and germinated conidia were cut with a lancet and transferred to new PDA plates amended with antibiotics. Cultures were incubated at 25 °C in the dark and inspected regularly for contaminations. After 2 wk, isolates were transferred to new PDA without antibiotics.

For long-term storage in the institute´s culture collection, the strains were grown on PDA supplemented with 5 % (v/v) glycerol (Carl Roth, Germany) at 25 °C in the dark for 2 wk. Mycelial plugs were cut from the border of the growing colonies, transferred to Nalgene® cryotubes (Thermo Scientific, Germany) containing potato dextrose broth (Becton Dickinson, USA) amended with 15 % (v/v) glycerol and frozen at -70 °C in Nalgene® Mr. Frosty® freezing containers (Thermo Scientific, Germany).

Four voucher herbarium specimens of the collection used for isolation of fungi have been deposited at the Herbarium of the Martin Luther University, Halle (Saale), Germany (HAL 3774 F, HAL 3793 F, HAL 3794 F, HAL 3795 F), and living cultures are preserved at the Leibniz Institute − German Collection of Microorganisms and Cell Cultures GmbH, Germany (DSMZ; DSM 116561, DSM 116562) and the culture collection of the Westerdijk Fungal Biodiversity Institute, The Netherlands (CBS 153212, CBS 153213).

Morphology

Fungal hyphae and conidia of the strain JKI-GP-22-021 (= DSM 116561, = CBS 153212) and conidia of the herbarium specimen voucher HAL 1750 F were mounted in distilled water, lactic acid, and aniline blue (cotton blue) and examined by light microscopy (Olympus BS50, Olympus, Germany, and Axio Imager.A1 equipped with an AxioCam MRc5 camera, Zeiss, Germany). Measurements were made (conidia: n = 50 for JKI-GP-22-021, n = 30 for HAL 1750 F) and images were taken with the calibrated ZEN Blue Edition software v. 3.0 (Zeiss, Germany).

Growth in vitro

The growth rates of two representative strains (JKI-GP-22-021, JKI-GP-23-022) were determined on four culture media at temperatures from 5–35 °C at 5 °C intervals in the dark. Agar discs (7-mm-diam.) were cut from the edge of 14-d-old cultures on PDA and placed in the centre of plates of PDA, oatmeal agar (OA; 40 g/L wholemeal oat flour, 15 g/L Difco™ agar, Becton Dickinson, USA), malt extract peptone yeast extract agar (MPY; Carl Roth, Germany), and synthetic nutrient-poor agar (SNA; Nirenberg 1976). As the radial growth of the fungus was almost uniform, the colony diameters were measured using crosses at the bottom of the Petri dishes. After fungal establishment on the medium, the weekly colony growth was measured along the four axes of the crosses over a period of 4 wk and the arithmetic mean was determined (n = 3). Colony colours were described following Rayner (1970).

Pathogenicity tests

To fulfil Koch's postulates, pathogenicity tests were performed with the strains JKI-GP-22-021 (= DSM 116561, = CBS 153212), JKI-GP-22-028, JKI-GP-22-029, JKI-GP-22-030, JKI-GP-23-022 (= DSM 116562, = CBS 153213) and 4-wk-old anise plantlets. As the fungus sporulated sparsely on all artificial media and under all cultivation conditions tested (data not shown), suspensions of conidia and mycelium in sterile deionised water were prepared by scraping spores and mycelium from 4-wk-old cultures on PDA. The conidial concentration was determined using a Neubauer improved counting chamber (Assistent, Karl Hecht GmbH and Co KG, Germany) and adjusted to 1×10^4 conidia/mL. Anise plants were inoculated by spraying the leaves dripping wet with a manual DC Chromatography Sprayer (n = 6). Plants sprayed with sterile deionized water served as non-inoculated control plants (n = 6). Sprayed plants were incubated in a humid chamber at 25 °C ± 1 °C and photoperiod of 14 h and were inspected for symptoms regularly. Re-isolation of the inoculated pathogen was done from symptomatic plant tissue as described above. The re-isolated fungi were identified based on the morphology of their colonies and conidia. The experiment was repeated twice.

DNA extraction, amplification, sequencing

Total genomic DNA was extracted from mycelia grown on PDA using the DNeasy Plant Mini Kit (Qiagen GmbH, Germany) according to the manufacturer's protocol. For each strain, up to five loci were amplified and sequenced. The internal transcribed spacer (ITS) regions including 5.8S nrDNA and a partial sequence of the large subunit (LSU; 28S), nrDNA were amplified using the primer pair V9G and LR5 (de Hoog & Gerrits van den Ende 1998, Vilgalys & Hester 1990). The partial DNA-directed RNA polymerase II second largest subunit (*rpb2*) gene was amplified with the primer pair RPB2-5f2 and fRPB2-7cR (Liu *et al.* 1999, Sung *et al.* 2007). The partial translation elongation factor 1-α (*tef1*) gene was amplified with the primer pair EF1-728F and EF2 (O'Donnell *et al.* 1998, Carbone & Kohn 1999). The partial β-tubulin (*tub2*) gene was amplified with the primer pair T1 and beta-Sandy-R (O'Donnell & Cigelnik 1997, Stukenbrock *et al.* 2012). The partial calmodulin (*CaM*) gene was amplified with the primer pair CAL-228F and CAL-737R (Carbone & Kohn 1999). The reaction mixture for ITS-LSU, *tef1*, *tub2* and *CaM* contained 25 µL of 2× MyFi™ Mix (Meridian Bioscience, USA), 3 µL of forward and reverse primers (10 µM each), 5 µL of genomic DNA, and was filled up to a total volume of 50 µL with PCR-grade water. The PCR was performed in a Tone cycler (Analytik Jena, Germany) with an initial denaturation step at 95 °C for 3 min, followed by 35 cycles of 30 s at 94 °C for denaturation, primer annealing (ITS/LSU: 1 min at 52 °C / *tef1*: 30 s at 54 °C / *tub2*: 30 s at 52 °C / *CaM*: 30 s at 58 °C), extension at 72 °C for 1 min, and a final extension at 72 °C for 10 min. The reaction mixture for *rpb2* contained 25 µL of 2× MangoMix™ (Meridian Bioscience, USA), 2 µL of bovine

© 2025 Westerdijk Fungal Biodiversity Institute

serum albumine (20 mg/mL, Carl Roth, Germany), 5 µL of each primer (10 µM), 5 µL of genomic DNA, and was filled up to a total volume of 50 µL with PCR-grade water. The PCR was performed in a ProFlex PCR System (ThermoFisher Scientific, Germany) with an initial denaturation step at 95 °C for 15 min, followed by 30 cycles of denaturation for 1 min at 95 °C, annealing starting at 55 °C for 5 s with increments of 1 °C for 5 s each to 72 °C, and extension at 72 °C for 2 min, and a final extension at 72 °C for 10 min.

Amplicons were purified using the MSB® Spin PCRapace Kit (INVITEK diagnostics, Germany) and sequenced in both directions (Microsynth Seqlab GmbH, Germany). Contigs were generated and edited using CLC Main Workbench v. 23.0.1 (Qiagen, Germany) following the EPPO recommendations for sequence analysis (OEPP/EPPO 2021). Consensus sequences were deposited in GenBank. The accession numbers are listed in Table 1.

Phylogenetic analysis

The LSU and *rpb2* sequences obtained in this study, as well as additional sequences retrieved from GenBank that were not included in the previous study, were manually added to the concatenated matrix by Videira *et al.* (2017) downloaded from TreeBASE (Study 21537; see Supplementary Table S1 of this study). An initial tree (data not shown) was calculated from this alignment and used as a basis for the reduced set tree shown in this study. The most likely tree was calculated using a Maximum likelihood (ML) analysis in IQ-TREE v. 2.1.3 (Nguyen *et al.* 2015). The maximum likelihood branch support values (ML-bs) were obtained from 1000 non-parametric bootstrap replicates as implemented in IQ-TREE v. 2.1.3 and a SH-aLRT combination test based on 1000 replicates was included in the same analysis; optimal partition models were selected using the TESTNEW

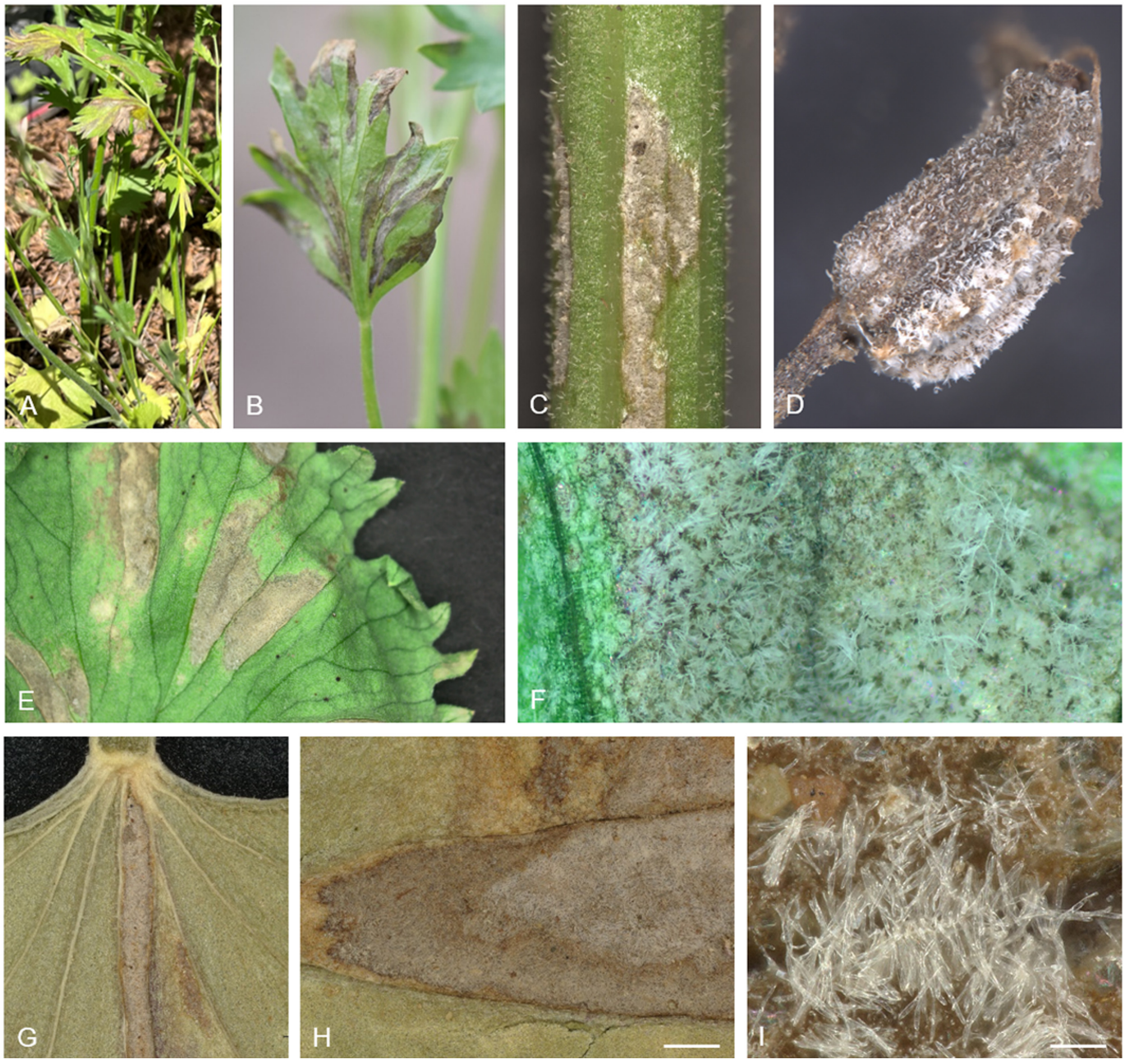

Fig. 1. *Pimpinella anisum* after infection with *Cercospora malkoffii*. **A–D.** Symptoms after natural infection. **E, F.** Symptoms 3 wk after inoculation with strain JKI-GP-23-022 (= DSM 116562, CBS 153212). **G–I.** Herbarium specimen voucher HAL 1750 F. Scale bars: H = 500 µm; I = 50 µm.

© 2025 Westerdijk Fungal Biodiversity Institute

Table 1. Collection details and GenBank accession numbers of *Fusoidiella malkoffii* strains used in this study.

Voucher or culture accession number(s)[1]	Host	Country	Coordinates	Collector, Collection date	GenBank Accession[2]				
					ITS-LSU	*CaM*	*rpb2*	*tef1*	*tub2*
HAL 1750 F	*Pimpinella anisum*	Turkey	—	S. Maden, 25. Jul. 2005	PQ963374	n/d	n/d	n/d	n/d
JKI-GP-22-021 = DSM 116561 = CBS 153212, ex-epitype culture	*Pimpinella anisum*	Austria	48.331433, 16.800549	E. Stopper, 30 May 2022	PQ963365	PV056161	PV056167	PV056163	PV056165
JKI-GP-23-022 = DSM 116562 = CBS 153213	*Pimpinella anisum*	Austria	48.169262, 16.776616	E. Stopper, 2 Aug. 2022	PQ963369	PV056162	PV056171	PV056164	PV056166
JKI-GP-22-028	*Pimpinella anisum*	Austria	48.224805, 16.755208	E. Stopper, 2 Aug. 2022	PQ963366	n/d	PV056168	n/d	n/d
JKI-GP-22-029	*Pimpinella anisum*	Austria	48.336134, 16.500727	E. Stopper, 2 Aug. 2022	PQ963367	n/d	PV056169	n/d	n/d
JKI-GP-22-030	*Pimpinella anisum*	Austria	48.350620, 16.745179	E. Stopper, 2 Aug. 2022	PQ963368	n/d	PV056170	n/d	n/d
JKI-GP-23-047	*Pimpinella anisum*	Germany	52.276313, 10.564507	L.-S. Kreth, 24 Jul. 2023	PQ963370	n/d	PV056172	n/d	n/d
JKI-GP-24-007	*Pimpinella anisum*	Austria	48.35795, 16.53939	L.-S. Kreth, 2 Jul. 2024	PQ963371	n/d	PV056173	n/d	n/d
JKI-GP-24-008	*Pimpinella anisum*	Austria	48.31617, 16.81324	L.-S. Kreth, 2 Jul. 2024	PQ963372	n/d	PV056174	n/d	n/d
JKI-GP-24-009	*Pimpinella anisum*	Austria	48.19372, 16.83925	L.-S. Kreth, 2 Jul. 2024	PQ963373	n/d	PV056175	n/d	n/d

[1] DSM: Leibniz Institute – German Collection of Microorganisms and Cell Cultures GmbH, Germany; JKI: Julius Kühn-Institute – Federal Research Centre for Cultivated Plants, Braunschweig, Germany.

[2] ITS: internal transcribed spacers and intervening 5.8S nrDNA; LSU: large subunit (28S) of the nrRNA gene operon; *CaM*: partial calmodulin gene; *rpb2*: partial DNA-directed RNA polymerase II second largest subunit gene; *tef1*: partial translation elongation factor 1-alpha gene; *tub2*: partial beta-tubulin gene. n/d: not determined.

parameter. The Bayesian posterior probability analysis was performed using MrBayes v. 3.2.7a (Ronquist *et al.* 2012), using the parameter settings of two parallel runs of four chains each, run for 100 M generations but with the stop value set at 0.01, the temperature set at 0.35 and the sample frequency every 100th generation. The model identified in Videira *et al.* (2017) as the best model for both partitions was also used in this study (dirichlet base frequencies and the GTR+I+G model). The 50 % majority rule consensus tree was created after the first 25 % of saved trees were discarded as burn-in. The alignment is deposited in Figshare (doi 10.6084/m9.figshare.28296056).

RESULTS

Sample collection, fungal cultivation, and pathogenicity

In the field, all above-ground parts of the plants can be infected. First symptoms appeared on leaves as small chlorotic and waterlogged spots, especially on the margins, which developed into segment-shaped necroses as the season progressed (Fig. 1). The pathogen develops lots of conidia, especially on the lower surface of the leaves, which let appear the lesions silvery. Infected seeds show dark brown discolouration due to fungal stroma and silvery white areas due to massive conidial development (Fig. **1**). Isolates could be obtained by streaking conidia on artificial media. From each location, one representative single conidial isolate was selected and used for further molecular and morphological analyses (Table 1).

Inoculation onto anise plants was performed to confirm Koch's postulates. Symptoms were found 3 wk after inoculation on some plants inoculated with the strains JKI-GP-22-030 and JKI- GP-23-022 (Fig. 1E, F). Symptoms were identical to those observed in the field (Fig. 1A–D) and masses of conidia of the inoculated fungus were observed. From all symptomatic tissues, *C. malkoffii* could be re-isolated. Non-inoculated control plants showed no symptoms during the whole observation period.

Phylogenetic position of *Cercospora malkoffii* (≡ *Passalora malkoffii*)

The final concatenated matrix comprised a total of 1453 characters (including all alignment gaps) for 101 OTUs (including the outgroup sequence). For the Maximum Likelihood analysis, 668 distinct patterns, 537 parsimony-informative, 88 singleton sites, and 828 constant sites were observed. The best-fit models identified in IQ-TREE using the TESTNEW option were GTR+F+I+G4 for *rpb2* and TIM+F+R3 for LSU. The optimal log likelihood for the best ML tree shown in Fig. 2 is -27305.473. For the Bayesian analysis, the data partitions contained 201 and 469 unique site patterns for LSU and *rpb2*, respectively. The analysis ran for 2740000 generations after which it stopped as the average standard deviation of split frequencies reached 0.009982. In total, 54802 trees were saved after which 41102 were sampled to calculate the posterior probability (PP) values and the 50 % majority rule consensus tree (PP values plotted on Fig. 2).

© 2025 Westerdijk Fungal Biodiversity Institute

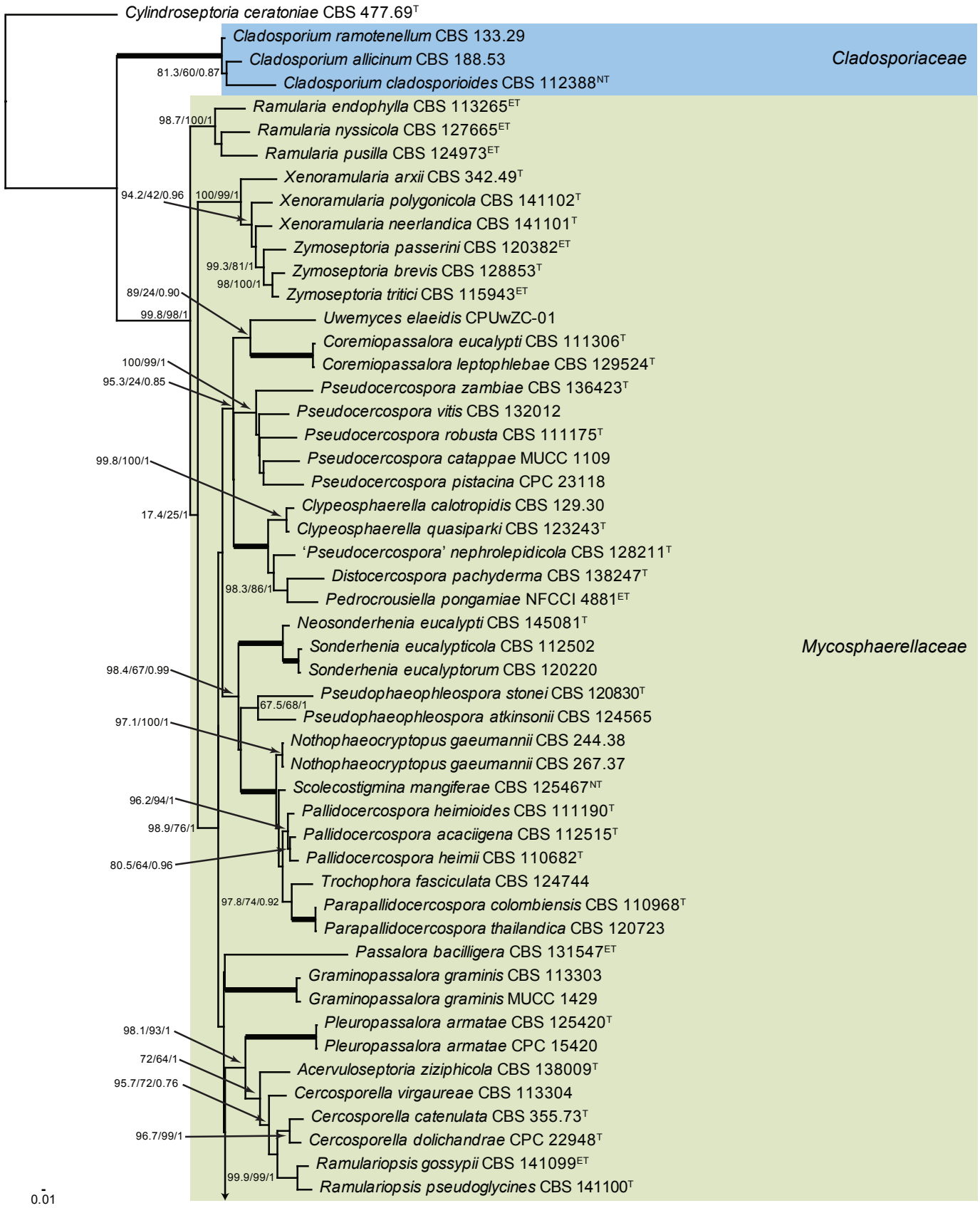

Fig. 2. Most likely phylogram obtained from the maximum likelihood (ML) analysis with IQ-TREE v. 2.1.3 of the combined LSU-*rpb2* nucleotide alignment. The Shimodaira–Hasegawa approximate likelihood ratio test (SH-aLRT; first value) value, the ML bootstrap support value from 1000 non-parametric bootstrap replicates (ML-bs; middle value) and the Bayesian posterior probability value (PP; third value) are shown at the nodes (values at the nodes are only shown if either the ML-bs is > 74 % or the PP > 0.74; branches with ML-bs = 100 % and PP = 1 are thickened). Culture collection or specimen voucher numbers and type status (superscript, see Table S1) are indicated for all species. The tree was rooted to *Cylindroseptoria ceratoniae* (CBS 477.69) and the novelty described here is highlighted with a blue colored block and **bold** font. The families are shown to the right of the tree in colored blocks.

© 2025 Westerdijk Fungal Biodiversity Institute

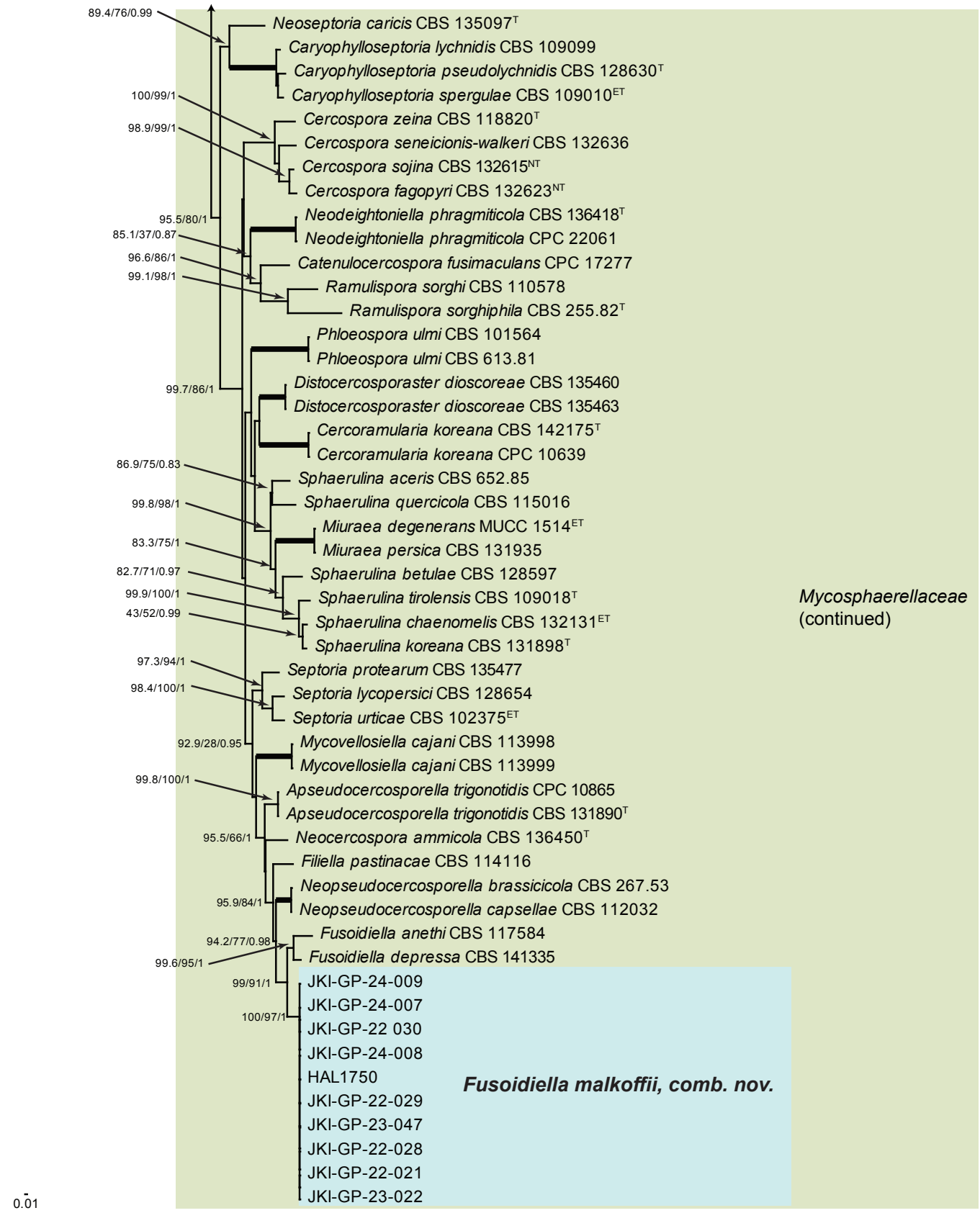

Fig. 2. (Continued).

© 2025 Westerdijk Fungal Biodiversity Institute

All strains of *Cercospora malkoffii* clustered together with high support (SH-aLRT = 100 % / ML-bs = 97 % / PP = 1). The clade has a highly supported sister relationship with two species of *Fusoidiella* in both the ML and Bayesian analyses (SH-aLRT = 99 % / ML-bs = 91 % / PP = 1) and a new combination is therefore proposed below.

Taxonomy

Fusoidiella malkoffii (Bubák) L.-S. Kreth & M. Götz, ***comb. nov.*** MB 857637. Figs 1, 3.
Basionym: *Cercospora malkoffii* Bubák, *Ann. Mycol*. **4**(2): 121. 1906.
Synonym: *Passalora malkoffii* (Bubák) U. Braun, *Trudy Bot. Inst. V.L. Komarova* **20**: 71. 1997.

Illustrations: Braun & Mel'nik (1997: fig. 41, based on type material), Erzurum *et al.* (2005: 264, fig. 1).

Description in vivo: *Disease* affecting all above-ground parts of the plants, including stems, leaves, inflorescences and even seeds. *Leaf spots* amphigenous, variable in shape and size, subcircular, angular-irregular to oblong, later expanded or confluent, pale grey to dark brown, brownish green, sometimes darker, looking like water-soaked, finally greyish white by abundant sporulation, margin indefinite. *Mycelium* internal. *Caespituli* amphigenous, punctiform, scattered to confluent and dense, whitish to greyish white. *Stromata* well-developed, arrangement often in lines, substomatal, subglobose to somewhat irregular in shape, 10–80 µm diam., yellowish brown to brown, composed of swollen hyphal cells or only of the somewhat swollen bases of the conidiophores, 3–8 µm diam. *Conidiomata* sporodochial, composed of well-developed stromata and numerous, short, densely arranged conidiophores, arising from the stromata. *Conidiophores* erect, straight to slightly curved, subcylindrical to usually conical, unbranched, 5–20 × 3–6 µm, aseptate, i.e., conidiophores reduced to conidiogenous cells, proliferation sympodial, subhyaline to pale olivaceous throughout or pale olivaceous below and paler (subhyaline) towards the tip, thin-walled, smooth, with a single or two conspicuous conidiogenous loci, barely or slightly thickened and somewhat darkened-refractive, 1.5–2 µm wide. *Conidia* formed singly, fusiform, subcylindrical-obclavate, (36–)40–53(–56) × 2–3 µm, (0–)1–2-septate, not constricted at the septa, hyaline, subhyaline to pale yellowish green or very

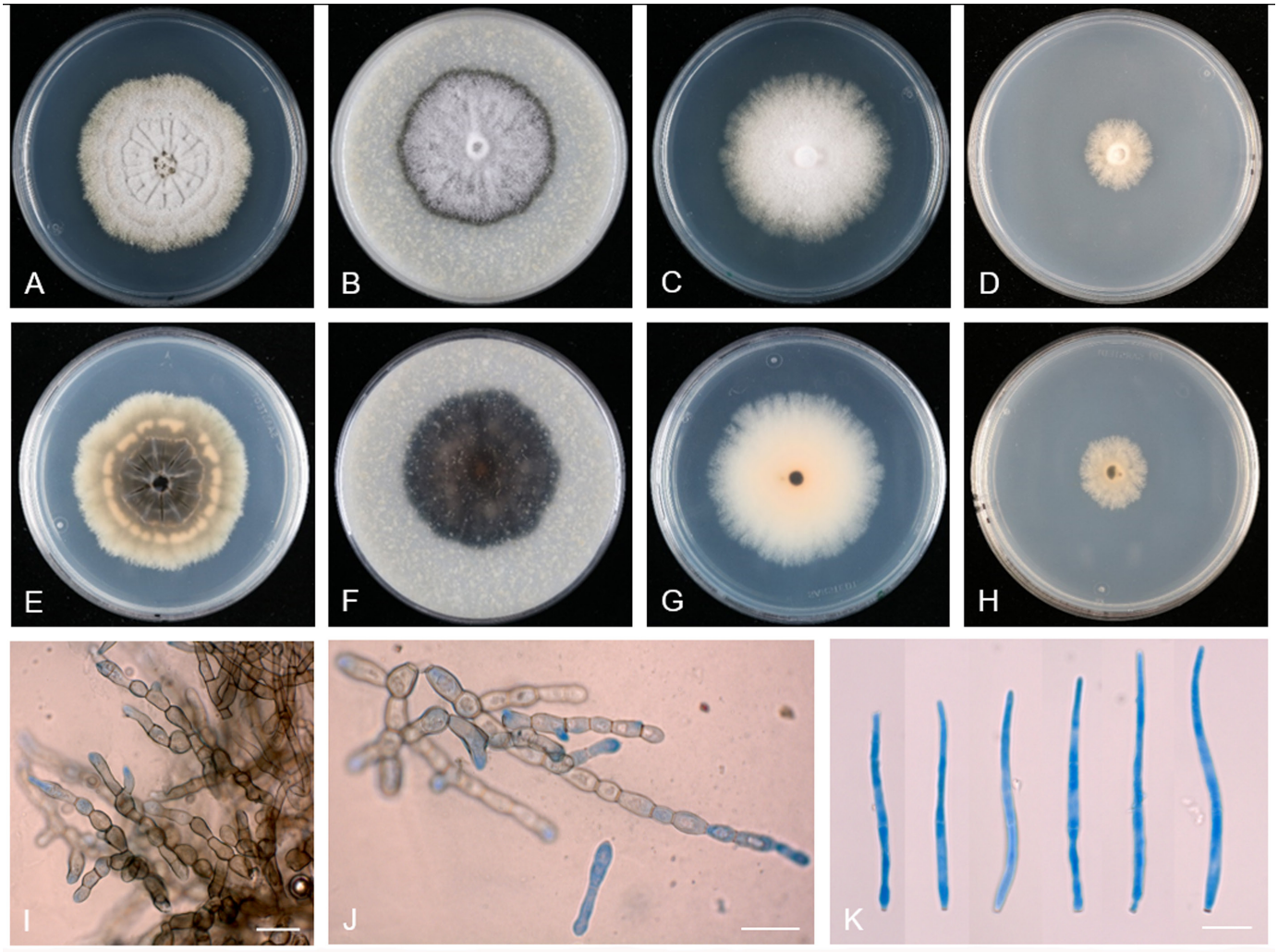

Fig. 3. *Fusoidiella malkoffii* from *Pimpinella anisum*, strain JKI-GP-23-022 (= DSM 116562, CBS 153213). Colony characteristics after incubation at 25 °C in the dark for 28 d. **A.** Obverse on PDA. **B.** Obverse on OA. **C.** Obverse on MPY. **D.** Obverse on SNA. **E.** Reverse on PDA. **F.** Reverse on OA. **G.** Reverse on MPY. **H.** Reverse on SNA. **I, J.** Mycelium after 2 wk on PDA. **K.** Conidia from herbarium specimen voucher HAL 1750 F. Scale bars: I, K = 10 µm; J = 20 µm.

© 2025 Westerdijk Fungal Biodiversity Institute

pale olivaceous, thin-walled, smooth, apex obtuse, rounded, base short obconically truncate, basal hilum barely or slightly thickened and somewhat darkened-refractive.

Description in vitro: Colonies slow-growing, at 20 °C on PDA reaching 4.1 cm diam. in 28 d; optimum temperature for growth 25 °C on PDA reaching 5.7 cm after 28 d; at 5 °C on PDA reaching 1.1 cm after 28 d; no growth observed at 35 °C; optimum temperature for growth on other examined cultural media after 28 d at 25 °C: 5.3 cm (OA), 5.7 cm (MPY), 2.7 cm (SNA).

Culture characteristics: Colony obverse on PDA compact, almost circular, margin slightly undulate, slightly raised, wrinkled in the centre, whitish to very pale mouse grey (Fig. 3); colony reverse greyish sepia in the centre to rosy buff and buff at the farther outboard. Colony characteristics on other media are depicted in Fig. 3. *Vegetative hyphae* filiform, branched, 4–9 µm wide, septate, with constrictions at the septa and swollen cells (monilioid), colourless to brown, smooth. *Conidia* formed singly, subcylindrical-obclavate, fusiform, (24–)35–58(–85) × 2–4(–6) µm, (0–)1–2-septate, not constricted at the septa, hyaline, subhyaline to pale yellowish green or very pale olivaceous, thin-walled, rounded at the apex and slightly tapered at the base, occasionally with a minute collar-like remnant, very rarely on the media tested. *Sexual morph* not observed.

Typus (examined): **Bulgaria**, Sadovo [near Plovdiv], on *Pimpinella anisum*, collection date unknown, *Malkoff* (**lectotype**, designated by Braun & Mel'nik 1997, BPI 438167); **isolectotype** B 70 0100768); **epitype** (designated here, MycoBank MBT 10027037): **Austria**, Weikendorf, on *Pimpinella anisum*, 30 Aug. 2022, *E. Stopper* (HAL 3774 F); ex-epitype culture: DSM 116561 (= JKI-GP-22-021, = CBS 153212); ex-epitype sequences: PQ963365 (ITS+LSU), PV056167 (*rpb2*), PV056161 (*CaM*), PV056163 (*tef1*), PV056165 (*tub2*).

Additional specimens examined: **Austria**, Pillichsdorf, on *Pimpinella anisum*, 2 Jul. 2024, *L.-S. Kreth* (HAL 3793 F); culture: JKI-GP-24-007; sequences: PQ963371 (ITS+LSU), PV056173 (*rpb2*). **Austria**, Weiden an der March, on *Pimpinella anisum*, 2 Jul. 2024, *L.-S. Kreth* (HAL 3794 F); culture: JKI-GP-24-008; sequences: PQ963372 (ITS+LSU), PV056174 (*rpb2*). **Austria**, Lassee, on *Pimpinella anisum*, 2 Jul. 2024, *L.-S. Kreth* (HAL 3795 F); culture: JKI-GP-24-009, sequences: PQ963373 (ITS+LSU), PV056175 (*rpb2*). **Turkey**, without special locality, on *Pimpinella anisum*, c. 2004, *S. Maden* (HAL 1750 F); sequence: PQ963374 (ITS+LSU). **USA**, Virginia, Fairfax County, Wakefield, on *Pimpinella anisum*, 4 Sep. 1909, *C.L. Shear* (BPI 438166).

Host range and distribution: On *Pimpinella anisum*, **Asia**: India [Avan 2021, Ghosh & Gupta 2024], Syria [Youssef *et al.* 2024], Tadzhikistan [Crous & Braun 2003], Turkey [Erzurum *et al.* 2005]; **Europe**: Austria [present work], Bulgaria [Chupp 1954: 576, Bakalova & Borisova 2010], Czech Republic [Picbauer 1942, Ondřej 1984], Germany [Oberwinkler 2000; Ullah *et al.* 2013, 2014], Greece [Świderska-Burek 2015], Poland [Świderska-Burek 2007, 2015], Romania [Bontea 1985], Russia (Voronesh Oblast) [Ryakhovsky 1931, Vasil'evskij & Karakulin 1937, Braun & Mel'nik 1997]; **North America**: Canada [Howard *et al.* 1994], USA [Virginia, Crous & Braun 2003]; West Indies: Cuba [Fornet *et al.* 1990]. On *P. wallichiana* (= *P. monoica*), Asia: India (M.S.) [Kamal 2010]. On *P. puberula*, **Asia**: Tadzhikistan [Braun & Mel'nik 1997]. On *P. saxifraga*, **Europe**: Estonia [Põldmaa 1966, Braun & Mel'nik 1997, Kalamees 2000], Romania [Bontea 1985], Russia (Orel Oblast) [Braun & Mel'nik 1997]. A record from Armenia, Caucasus, on *Astrodaucus orientalis* (Braun & Mel'nik 1997, with question mark) is doubtful and requires confirmation. A further report of '*Cercospora malkoffii*' from Georgia (Caucasus) on *Torilis japonica* [= *Caucalis anthriscus*] (Vasil'evskij & Karakulin 1937: 355, Chupp 1954: 576) pertains undoubtedly to *Passalora scandicearum* (Magnus) U. Braun & Crous.

Notes: The association of this species with the genus *Fusoidiella* is best done based on phylogenetic or blast inference of especially *rpb2* sequence data. Based on a megablast search of NCBI's GenBank nucleotide database, the closest hits using the **ITS** sequence of DSM 116561 had highest similarity to *Cercospora* sp. [strain CBS 112737, GenBank GU214684.1; Identities = 601/612 (98 %), one gap (0 %)], *Pseudocercosporella* sp. [strain CPC 4008, GenBank GU214686.1; Identities = 600/612 (98 %), one gap (0 %)], *Cercospora canescens* [strain Cer 04-18, GenBank MW430675.1; Identities = 598/611 (98 %), one gap (0 %)], *Ramulispora sorghi* [strain CBS 478.92, GenBank KX287278.1; Identities = 598/612 (98 %), two gaps (0 %)], and *Sphaerulina rhododendricola* [strain CPC 21813, GenBank KF777187.1; Identities = 597/611 (98 %), one gap (0 %)]. Closest hits using the **LSU** sequence of DSM 116561 are *Pseudocercosporella* sp. [strain CPC 4008, GenBank GU214686.1; Identities = 873/878 (99 %), no gaps], *Septoria leucanthemi* [strain CBS 109090, GenBank GQ852677.1; Identities = 873/878 (99 %), no gaps], *Cercospora* sp. [strain CBS 112737, GenBank GU214684.1; Identities = 873/878 (99 %), no gaps], *Septoria leucanthemi* [strain CBS 109090, GenBank GU214492.1; Identities = 873/878 (99 %), no gaps], and *Apseudocercosporella trigonotidis* [strain CBS 131890, GenBank JQ324972.1; Identities = 865/870 (99 %), no gaps]. Closest hits using the ***CaM*** sequence of DSM 116561 had highest similarity to *Neocercospora carotae* [strain CBS 101.65, GenBank MT586452.1; Identities = 146/154 (95 %), no gaps], *Fusoidiella depressa* [as *Passalora depressa*; strain CPC 14915, GenBank KF253972.1; Identities = 157/172 (91 %), two gaps (1 %)], *Septoria carvi* [strain KML93, GenBank KX822095.1; Identities = 149/160 (93 %), no gaps], and *Septoria paridis* [strain CBS 109111, GenBank KF254142.1; Identities = 144/152 (95 %), no gaps]. Closest hits using the ***rpb2*** sequence of DSM 116561 had highest similarity to *Fusoidiella anethi* [strain CBS 117584, GenBank MF951500.1; Identities = 760/843 (90 %), no gaps], *Fusoidiella depressa* [strain CPC 14915, GenBank KX348055.1; Identities = 698/765 (91 %), no gaps], *Fusoidiella anethi* [strain CBS 296.32, GenBank MF951499.1; Identities = 694/766 (91 %), no gaps], *Neopseudocercosporella brassicae* [strain CBS 267.53, GenBank KX348059.1; Identities = 736/830 (89 %), no gaps], and *Neopseudocercosporella capsellae* [strain MAFF 237605, GenBank MF951550.1; Identities = 718/809 (89 %), no gaps]. Closest hits using the ***tef1*** sequence of DSM 116561 had highest similarity

© 2025 Westerdijk Fungal Biodiversity Institute

to *Apseudocercosporella trigonotidis* [strain CBS 131890, GenBank GU384569.1; Identities = 225/288 (78 %), 11 gaps (3 %)], *Septoria passiflorae* [strain CBS 102701, GenBank KF253442.1; Identities = 200/262 (76 %), 13 gaps (4 %)], and *Neopseudocercosporella capsellae* [strain CBS 135464, GenBank KX287858.1; Identities = 191/249 (77 %), 11 gaps (4 %)]. The *tef1* sequence of *Fusoidiella depressa* (as *Passalora depressa*; strain CPC 14915, GenBank KF253256.1) is 76 % (189/249, including 10 gaps) similar. Closest hits using the ***tub2*** sequence of DSM 116561 had highest similarity to *Fusoidiella depressa* [as *Passalora depressa*; strain CPC 14915, GenBank KF252788.1; Identities = 252/301 (84 %), five gaps (1 %)], *Neopseudocercosporella capsellae* [as *Pseudocercosporella capsellae*; strain CBS 112033, GenBank KF252785.1; Identities = 207/241 (86 %), one gap (0 %)], and *Septoria pileicola* [strain GUCC 2131.4, GenBank MT984354.1; Identities = 311/392 (79 %), 23 gaps (5 %)].

DISCUSSION

Anise is a widely cultivated spice and flavour herb (Peter 2004, Sun *et al*. 2019). A common anise blight is caused by an asexual ascomycete that is currently usually referred to as *Passalora malkoffii*. In recent decades, this anise disease attracted the attention of applied phytopathologists, including various biological and plant pathogenic aspects, such as adjusted cultural managements, transmission, control, and fungicide treatments (Maden *et al*. 2001, Erzurum *et al*. 2005, Ullah *et al*. 2013, 2014, Sun *et al*. 2019). However, the true phylogenetic affinity of this species and resulting taxonomic consequences remained in the dark, above all in the light of the strongly altered concepts of cercosporoid genera in recent years (Videira *et al*. 2017). Successful recent attempts to cultivate this cercosporoid fungus enabled phylogenetic analyses based on ITS+LSU nrDNA and *rpb2* sequences, which helped to clarify the phylogenetic affinity and genuine generic affiliation of this species. Our analyses revealed that sequences retrieved from *C. malkoffii* cluster within the *Fusoidiella* clade (see Fig. 2), together with sequences of *F. anethi* and *F. depressa*, two species on apiaceous hosts, which have previously also been treated as *Passalora* spp. (Crous & Braun 2003). This result agrees with previous outcomes of phylogenetic analyses which have shown that modern phylogenetic genus concepts in cercosporoid ascomycetes in general and in the *Passalora* complex in particular are not in line with formerly applied morphological concepts and generic circumscriptions (Bakhshi *et al*. 2015, 2021, Videira *et al*. 2017, Rajeshkumar 2021). Most characteristics of the conidiomata, conidiophores and conidia are not diagnostic for individual cercosporoid genera and occur in varying combinations in different genera. It is even possible that cercosporoid species with typical *Cercospora* (s. str.) morphology may pertain to other genera, which has been strikingly demonstrated by Bakhshi *et al*. (2015) and Bakhshi & Braun (2022) who introduced the new cercospora-like genera *Neocercospora* on *Ammi majus* (*Apiaceae*) and *Acericercospora* on *Acer velutinum* (*Sapindaceae*), respectively. In the case of *Cercospora malkoffii*, the generic affinity to *Fusoidiella* (Videira *et al*. 2016) seem to reflect the co-evolution of this genus with hosts of the family *Apiaceae*.

ACKNOWLEDGEMENTS

We are obliged to the curators of the herbaria BPI and B for previous possibilities to examine specimens in their keeping and our partners for providing infected plant material. This study was carried out in the project Junior Research Group Medicinal Plants (NWG-Arzneipflanzen) and was supported by the Agency of Renewable Resources (FNR) of the Federal Ministry of Food and Agriculture (BMEL) (project code 22002818). We thank F. Marthe (Institute for Breeding Research on Horticultural Crops, JKI, Germany) for project organization; A.-C. Leiendorf for excellent technical assistance; and E. Jeworutzki for growing and maintaining the experimental plants.

Conflict of interest: The authors declare that there is no conflict of interest.

REFERENCES

Avan M (2021). Important fungal diseases in medicinal and aromatic plants and their control. *Turkish Journal of Agricultural Engineering Research* **2**: 239–259. https://dergipark.org.tr/en/pub/turkager

Bakalova GG, Borisova TI (2010). *Cercosporoid hyphomycetous fungi*. [*Fungi of Bulgaria* Vol. 7]. Institut of Botany, Bulgarian Academy of Sciences, Sofia.

Bakhshi M, Arzanlou M, Babai-Ahari A, *et al.* (2015). Is morphology in *Cercospora* a reliable reflection of generic affinity? *Phytotaxa* **213**: 22–34. http://dx.doi.org/10.11646/phytotaxa.213.1.2

Bakhshi M, Braun U (2022). *Acericercospora hyrcanica gen. et sp. nov*. (*Mycosphaerellaceae*) and *Paramycocentrospora acericola gen. et sp. nov*. (*Dothidotthiaceae*) on maple trees in Hyrcanian forests. *Mycological Progress* **21**: 1–15.

Bakhshi M, Zare R, Braun U, *et al.* (2021). Polyphasic taxonomy of four passaloralike taxa occurring on fruit and forest trees. *Mycological Progress* **20**: 1157–1173. https://doi.org/10.1007/s11557-021-01725-5

Bontea V (1985). *Ciuperci parasite si saprofite din România, Volumul I*. Editura Academiei Republicii Socialiste România, Bucureşti.

Braun U, Melnik VA (1997). Cercosporoid fungi from Russia and adjacent countries. *Trudy Botanicheskogo Instituta Imeni V.L. Komarova, Rossijskaya Akademiya Nauk St. Petersburg* **20**: 1–130.

Carbone I, Kohn LM (1999). A method for designing primer sets for speciation studies in filamentous ascomycetes. *Mycologia* **91**: 553–556. https://doi.org/10.1080/00275514.1999.12061051

Chupp C (1954). *A monograph of the fungus genus Cercospora*. Ithaca, NY, Published by the author.

Crous PW, Braun U (2003). *Mycosphaerella* and its anamorphs: 1. Names published in *Cercospora* and *Passalora*. CBS Biodiversity Series **1**: 1–569.

De Hoog GS, Gerrits van den Ende AHG (1998). Molecular diagnostics of clinical strains of filamentous Basidiomycetes. Mycoses **41**: 183–189. https://doi.org/10.1111/j.1439-0507.1998.tb00321.x

Erzurum K, Demirci F, Karakaya A, *et al.* (2005). Passalora blight of anise (*Pimpinella anisum*) and its control in Turkey. *Phytoparasitica* **33**: 261–266.

Fornet E, Gutiérrez CE, Kindelán A, *et al.* (1990). *Relación de Hongos Patógenos de Plantas Medicinales en Cuba*. Centro de Información y Documentación Agropecuario, Cuba, Ciudad de

© 2025 Westerdijk Fungal Biodiversity Institute

La Habana.
Ghosh P, Gupta SK (2024). Diseases of medicinal plants in India: A review. *Journal of Medicinal Plants Journal* **12**: 19–34.
Howard RJ, Garland JA, Seaman WL (1994). *Diseases and pests of vege*table *crops in Canada: an illustrated compendium*. The Canadian Phytopathological Society. Printed in Canada.
Kalamees K (2000). *Eesti seenestik*. EPMÜ, Tartu, Estonia.
Kamal (2010). *Cercosporoid fungi of India*. Bishen Singh Mahendra Pal Singh, Dehra Dun, India.
Liu YJ, Whelen S, Hall BD (1999). Phylogenetic relationships among ascomycetes: evidence from an RNA polymerse II subunit. *Molecular Biology and Evolution* **16**: 1799–1808. Doi: https://doi.org/10.1093/oxfordjournals.molbev.a026092
Maden S, Erzurum K, Demirci F, *et al.* (2001). Studies on the blight disease occurring at Antalya, Burdur and Denizli anise growing areas. *Proceedings IX, Turkish Phytopathology Congress (Terkirdağ, Turkey)*: 317–323.
Nguyen L-T, Schmidt HA von Haeseler A, *et al.* (2015). IQ-TREE: A fast and effective stochastic algorithm for estimating maximum likelihood phylogenies. *Molecular Biology and Evolution* **32**: 268–274. https://doi.org/10.1093/molbev/msu300
Nirenberg H (1976). Untersuchungen über die morphologische und biologische Differenzierung in der *Fusarium*-Sektion Liseola. *Mitteilungen aus der Biologischen Bundesanstalt für Land- und Forstwirtschaft. Vol.* **169**. Kommissionsverlag Paul Parey, Berlin, Germany.
Oberwinkler F (2000). Samenpflanzen und Farne und mit ihnen vergesellschaftete Pilze. Korrekturversion einer Flora von Oberjoch. https://dr-franz.oberwinkler.de/wp-content/uploads/Oberjochflora-2000.pdf
O'Donnell K, Cigelnik E (1997). Two divergent intragenomic rDNA ITS2 types within a monophyletic lineage of the fungus *Fusarium* are nonorthologous. *Molecular Phylogenetics and Evolution* **7**: 103–116. https://doi.org/10.1006/mpev.1996.0376
O'Donnell K, Kistler HC, Cigelnik E, *et al.* (1998). Multiple evolutionary origins of the fungus causing Panama disease of banana: Concordant evidence from nuclear and mitochondrial gene genealogies. *Proceedings of the National Academy of Sciences USA* **95**: 2044–2049. https://doi.org/10.1073/pnas.95.5.2044
OEPP/EPPO (2021). PM 7/129 (2) DNA barcoding as an identification tool for a number of regulated pests. *EPPO Bulletin* **51**: 100–143. https://doi.org/10.1111/epp.12724
Ondřej M (1984). Funde von parasitischen imperfekten Pilzen *Cercospora* Fres. aus der Tschechoslowakei (Teil III.). *Česká Mykologie* **38**: 230–234. http://www.czechmycology.org/_cm/CM384.pdf
Peter KV (2004) *Handbook of herbs and spices*. Volume 2. Woodhead Publishing Limited, Cambridge.
Picbauer R (1942) Beitrag zur Pilzflora von Böhmen, Mähren und der Slowakei. *Verhandlungen des Naturforschenden Vereines in Brünn* **73**: 177–203.
Põldmaa P (1967). *Fitopatogennye mikromicety severnoj Estonii*. Izdatel'svo 'Valgus', Tallin, Estland.
Rajeshkumar KC, Braun U, Groenewald JZ, *et al.* (2021). Phylogenetic placement and reassessment of *Asperisporium pongamiae* as *Pedrocrousiella pongamiae gen. et comb. nov.* (*Mycosphaerellaceae*). *Fungal Systematics and Evolution* **7**: 165–176. https://doi.org/10.3114/fuse.2021.07.08
Rayner RW (1970). *A mycological colour chart*. Commonwealth Mycological Institute and British Mycological Society, Kew, U.K.
Ronquist F, Teslenko M, van der Mark P, *et al.* (2012). MrBayes 3.2: efficient Bayesian phylogenetic inference and model choice across a large model space. *Systematic Biology* **61**: 539–542. https://doi.org/10.1093/sysbio/sys029
Ryakhovsky N (1931). Key to the fungal diseases of Anise and Coriander. *Zashchita Rastenii (Leningrad)* **8**: 185–186.
Stukenbrock EH, Quaedvlieg W, Javan-Nikhah M, *et al.* (2012). *Zymoseptoria ardabiliae* and *Z. pseudotritici*, two progenitor species of the septoria tritici leaf blotch fungus *Z. tritici* (synonym: *Mycosphaerella graminicola*). *Mycologia* **104**: 1397–1407. https://doi.org/10.3852/11-374
Sun W, Shahrajabian MH, Cheng Q (2019). Anise (*Pimpinella anisum* L.), a dominant spice and traditional medicinal herb for both food and medicinal purposes. *Cogent Biology* **5**: 167368. https://doi.org/10.1080/23312025.2019.1673688
Sung G-H, Sung J-M, Hywel-Jones NL, *et al.* (2007). A multi-gene phylogeny of *Clavicipitaceae* (*Ascomycota*, *Fungi*): Identification of localized incongruence using a combinational bootstrap approach. *Molecular Phylogenetics and Evolution* **44**: 1204–1223. https://doi.org/10.1016/j.ympev.2007.03.011
Świderska-Burek U (2007). Preliminary list of cercosporoid fungi from Poland. *Mycotaxon* **102**: 5–8.
Świderska-Burek U (2015). Cercosporoid fungi of Poland. *Monographiae Botanicae* **105**: 1–166.
Ullah H, Mahmood A, Honermeier B (2013). Effects of different fungicides on the infection by *Passalora malkoffii* with respect to the fruit yield and quality of aniseed (*Pimpinella anisum* L.) in Germany. *Journal of Medicinal and Spice Plants* **18**: 89–98.
Ullah H, Mahmood A, Honermeier B (2014). Essential oil and composition of anise (*Pimpinella anisum* L.) with varying seed rates and row spacing. *Pakistan Journal of Botany* **46**: 1859–1864.
Vasil'evskij NI, Karakulin BP (1937). *Parazitnye nesovershennye griby.* Chast' 1, Gifomicety. Isdatel'stvo Akademii Nauk SSSR, Moskva, Leningrad.
Videira SIR, Groenewald JZ, Braun U, *et al.* (2016). All that glitters is not *Ramularia*. *Studies in Mycology* **83**: 49–163. https://doi.org/10.1016/j.simyco.2016.06.001
Videira SIR, Groenewald JZ, Nakashima C, *et al.* (2017). *Mycosphaerellaceae* – chaos or clarity? *Studies in Mycology* **87**: 257–421. https://doi.org/10.1016/j.simyco.2017.09.003
Vilgalys R, Hester M (1990). Rapid genetic identification and mapping of enzymatically amplified ribosomal DNA from several *Cryptococcus* species. *Journal of Bacteriology* **172**: 4238–4246. https://doi.org/10.1128/jb.172.8.4238-4246.1990
Youssef RN, Khalil HA, Bdour NA, *et al.* (2024). First record of Passalora blight caused by *Passalora malkoffii* on anise crop in Syria. *Arab Journal of Plant Protection* **42**: 9–14. https://doi.org/10.22268/AJPP-001207

Supplementary Material: http://fuse-journal.org/

Table S1. Collection details and GenBank accession numbers of isolates included in the phylogenetic analyses. Cultures with a type status are indicated in **bold** text. See Table 1 for the GenBank accession numbers of the novelty described in this study.

© 2025 Westerdijk Fungal Biodiversity Institute

FUSE

Fungal Systematics and Evolution

VOLUME 16
DECEMBER 2025
PAGES 243–264

doi.org/10.3114/fuse.2025.16.14

There is gold in the graveyard: a new lineage of zombie-ant fungi in the genus *Ophiocordyceps* (*Ophiocordycipitaceae*: *Hypocreales*) from Minas Gerais, Brazil

S.J. Lima-Santos[1*], J.P.M. Araújo[2], R.M. Feitosa[3], T. Mendes-Pereira[1], S.L. Elliot[1*], H.C. Evans[4]

[1]Laboratory of Insect-Microbe Interactions, Departamento de Entomologia, Universidade Federal de Viçosa, Viçosa, 36570-900, MG, Brazil
[2]Natural History Museum of Denmark, University of Copenhagen, Copenhagen 1350, Denmark
[3]Programa de Pós-Graduação em Entomologia, Departamento de Zoologia, Universidade Federal do Paraná, 82590-300, Curitiba, Brazil
[4]CAB International, UK Centre, Egham, Surrey TW20 9TY, UK

[*]Corresponding authors: samuel.j.santos@ufv.br; selliot@ufv.br

Key words:
Acanthoponera
Atlantic rainforest-Cerrado ecotone
Heteroponerini
host manipulation
new taxon
systematics

Abstract: *Ophiocordyceps* serves as a key model for studying cryptic fungal diversity and behavioural manipulation of hymenopterous insects. Here, we describe *Ophiocordyceps acanthoponerae*, a newly discovered species infecting *Acanthoponera mucronata* (*Heteroponerini*: *Formicidae*) in a Brazilian Atlantic rainforest-Cerrado ecotone. Morphological analyses revealed mixed traits characteristic of *Ophiocordyceps* lineages associated with ants and wasps, including leaf biting behaviour manipulation, dark brown ascostromata covering 360º of the stalk, ascospores producing capilliconidia and hirsutelloid asexual morphs. Phylogenetic analyses based on four genomic regions (SSU, LSU, *TEF* and *RPB1*) placed this species outside the traditional myrmecophilous hirsutelloid clades *O. unilateralis* and *O. kniphofioides*, and within a novel clade closely related to the wasp pathogen *O. humbertii*. This discovery represents the first record of *Ophiocordyceps* infecting *Heteroponerini* and highlights an unexplored lineage of manipulative fungi. Our findings expand the known host range for myrmecophilous *Ophiocordyceps* and underscore the importance of studying fungal diversity in under-sampled ecological niches.

Citation: Lima-Santos SJ, Araújo JPM, Feitosa RM, Mendes-Pereira T, Elliot SL, Evans HC (2025). There is gold in the graveyard: a new lineage of zombie-ant fungi in the genus *Ophiocordyceps* (*Ophiocordycipitaceae*: *Hypocreales*) from Minas Gerais, Brazil. *Fungal Systematics and Evolution* **16**: 243–264. doi: 10.3114/fuse.2025.16.14
Received: 26 February 2025; **Accepted:** 30 June 2025; **Effectively published online:** 8 August 2025
Corresponding editor: P.W. Crous

INTRODUCTION

The order *Hypocreales* (*Ascomycota*) comprises most of the fungal species that are known as insect pathogens, or entomopathogenic fungi distributed predominantly across three families: *Clavicipitaceae*, *Cordycipitaceae* and *Ophiocordycipitaceae* (Sung *et al.* 2007, 2008). The ancestral trait of the order is an association with plants (decomposers, phytopathogens, epiphytes and endophytes), with the insect-associated lineages arising around 160 million years ago (Sung *et al.* 2008). The evolution of hypocrealean entomopathogens probably occurred via the process of inter-kingdom host-jumping (or host-switching), in which closely-related fungi are able to exploit nutritional resources from even distantly related host taxa (e.g. animals, plants and other fungi) that share the same habitat or niche (Spatafora *et al.* 2007, Sung *et al.* 2008, Yu *et al.* 2021, Wei *et al.* 2022). This phenomenon is considered to be a major driver of diversity, lifestyle differentiation and speciation for the entomopathogenic fungi (Thines 2019, Wei *et al.* 2022).

Ophiocordyceps (*Ophiocordycipitaceae*: *Hypocreales*) is a flagship genus for the study of cryptic fungal diversity, particularly in tropical forests (Evans *et al.* 2011a). Current hypotheses suggest that *Ophiocordyceps* arose nearly 100 million years ago (Sung *et al.* 2008) and is almost exclusively comprised of pathogens of insects (nine insect orders) with approximately 350 legitimate species described (Sung *et al.* 2007, Quandt *et al.* 2014, Araújo & Hughes 2019, MycoBank 2025). The diversification process of *Ophiocordyceps* might have been favoured by successive and independent host-jumps from the ancestral host-association with *Coleoptera* larvae to other orders of insects and also between taxa within these orders (Araújo & Hughes 2019). A characteristic of the genus is firm, mostly darkly pigmented stromata, in contrast to the fleshy and brightly pigmented stromata of *Cordyceps* (Sung *et al.* 2007). The most widely known species is the lepidopteran pathogen *O. sinensis*, which has been studied extensively because of its pharmaceutical applications, especially in traditional Chinese medicine (Shrestha & Bawa 2013, Baral 2017). Within the genus, *O. unilateralis* s. l. — the so-called "zombie-ant fungus" — has also been a subject of interest to scientists and the general public alike because of its behavioural manipulation of the ant host. This has inspired successful video games and television series, as well as number of books (Andersen *et al.* 2009, Araújo & Hughes 2016, Hughes *et al.* 2016, Araújo *et al.* 2018).

Fungal Systematics and Evolution is licensed under a Creative Commons Attribution-NonCommercial-NoDerivatives 4.0 International License

© 2025 Westerdijk Fungal Biodiversity Institute

Following infection by *O. unilateralis* and related taxa, the ant climbs to an elevated position in the forest understorey where it bites into the plant stem or leaf (the so-called death-grip; Hughes *et al.* 2011); dying attached to the vegetation and locked into it by its mandibles (Evans 1982, Evans & Samson 1982, Andersen *et al.* 2009). This manipulation strategy allows the fungus to optimise spore release from an elevated position onto the forest floor where foraging hosts are found (Andersen *et al.* 2009, Hughes *et al.* 2016). Dead ants are commonly found aggregated at high densities — especially, in tropical forests — forming "graveyards" or "cemeteries", which can persist in the same location for months or even years (Evans & Samson 1982, Pontoppidan *et al.* 2009, Loreto *et al.* 2014, Neto *et al.* 2019, Will *et al.* 2023). These aggregations are constantly resupplied with new infected hosts, revealing the chronic or enzootic nature of *Ophiocordyceps*-ant interactions at the colony level, rather than epizootic events (Andersen *et al.* 2012, Loreto *et al.* 2014).

Evans *et al.* (2011b) determined that the fungus previously identified as *O. unilateralis* was, in fact, a complex of species strictly associated with ants of the tribe *Camponotini* (*Formicinae*: *Formicidae*). Evans *et al.* (2011a, b) also hypothesized that species within the complex were each restricted to one species of host and, therefore, that on a global scale, tens or hundreds of species would eventually be delimited within this complex. If the one-species-one-fungus hypothesis holds, then the cosmopolitan nature of the *Camponitini* across the tropics — with almost 2,500 described species with a wide range of habitats (Feitosa & Dias 2024, Bolton 2025) — seems to make this conjecture feasible. Since 2011, new fungal species strictly associated with a particular *Camponotini* host are constantly being discovered and described worldwide, increasing the support for this hypothesis (Kepler *et al.* 2011, Luangsa-ard *et al.* 2011, Kobmoo *et al.* 2012, 2015, Sanjuan *et al.* 2015, Araújo *et al.* 2015, 2018). A recent study, however, has shown that this interaction might not be as strict or host-specific as previously thought (Tang *et al.* 2023) and more research is needed to determine the level or levels of host specificity.

These new myrmecophilous species associated with *Camponotini* are currently inserted in what is now recognized as the *O. unilateralis* clade (Kepler *et al.* 2011, Luangsa-ard *et al.* 2011, Kobmoo *et al.* 2012, 2015, Sanjuan *et al.* 2015, Araújo *et al.* 2015, 2018, Tang *et al.* 2023). This considers their phylogenetic proximity and shared morphological traits, especially ascospore morphology and their *Hirsutella*-like (or hirsutelloid) asexual morphs, but also host specificity (Araújo & Hughes 2017, Araújo *et al.* 2018). Among all *Ophiocordyceps* lineages that infect ants, the *O. unilateralis* core clade and the *O. kniphofioides* sub-clade are, to date, the only hirsutelloid lineages that induce 'death-grip' manipulation in their hosts (Araújo & Hughes 2017, Araújo *et al.* 2018, 2020). The *O. unilateralis* core clade exclusively infects *Camponotini* and can be recognized by the brown or black fertile region (or ascoma) that forms laterally on the stalk (or stroma) (Evans & Samson 1984, Araújo & Hughes 2017, Araújo *et al.* 2018). The *O. kniphofioides* sub-clade comprises five known species and infects other ant tribes (*Cephalotini*, *Dacetini*, *Dolichoderini* and *Paraponerini*) and produces a single ascoma that grows laterally from the host's thorax, with the fertile portion covering all sides of the stalk (Evans & Samson 1982, Araújo & Hughes 2017, Araújo *et al.* 2018).

The myrmecophilous and manipulative *Ophiocordyceps* (*O. unilateralis* core clade and *O. kniphofioides* sub-clade) are closely related to another hirsutelloid lineage, composed of *O. humbertii*, which infects and induces behavioural manipulation in social wasps similar to that seen in *O. unilateralis* infections (Petch 1935, Araújo & Hughes 2019, Somavilla *et al.* 2020, Sobczak *et al.* 2020, Barbosa & Somavilla 2022). It is considered that behavioural manipulation might have occurred first in social wasps, rather than in ants, during the evolution of manipulative *Ophiocordyceps* (Araújo & Hughes 2019). All hymenopterans descend from a common ancestor, so it is possible that the morpho-physiological similarities between them follows their co-existence in the same habitat (host-habitat hypothesis) which could have facilitated host-jumps during the evolution of *Ophiocordyceps* (Branstetter *et al.* 2017, Huber *et al.* 2017, Araújo & Hughes 2019). It is also possible that the evolution of manipulative *Ophiocordyceps* was favoured by the social behaviour exhibited by the hosts, given that behavioural manipulation is considered to be a parasite strategy that helps to cope with social immunity inside colonies (Loreto *et al.* 2014, Araújo & Hughes 2019). To address these questions, it is important to expand our knowledge of *Ophiocordyceps*-infecting social hymenopterans and, in particular, those where there are features in common or in closely-related lineages with a scarcity of taxon sampling.

Here, we describe a new species of *Ophiocordyceps* infecting *Acanthoponera mucronata* (*Heteroponerini*: *Ectatomminae*: *Formicidae*) in Brazil: an ant species for which life-history and ecological data are scarce. This species has morphological traits similar to known myrmecophilous *Ophiocordyceps* species but also to the wasp-parasitic species *O. humbertii*. Our phylogenetic analyses have revealed that this new taxon also represents a new origin of myrmecophily and of host-manipulative *Ophiocordyceps* species, closely-related to the wasp pathogen, *O. humbertii*. This is also the first record of ants belonging to the *Heteroponerini* tribe being infected by *Ophiocordyceps*, expanding the host range for the genus.

MATERIALS AND METHODS

In this study, we combined morphological, ecological and molecular data for the description of the new species. Our methodologies for collection, field observations, morphological characterisation and molecular analyses are based on previous studies with other myrmecophilous *Ophiocordyceps* species (Araújo *et al.* 2015, 2018, 2020, Evans *et al.* 2011b, 2018).

Field collections

Collection of specimens was concentrated at the Estação Ecológica do Tripuí (EET), Ouro Preto municipality, Minas Gerais, Brazil (BR 356, km 90, R. Nossa Senhora, da Conceição, 375, 20°23'5"S, 43°32'34.8"W) (Fig. 1). The forest reserve covers approximately 392 ha, with altitudes varying between 1,180 and 1,300 m.a.s.l., and is located in the transition (or ecotone) between Atlantic Forest and Cerrado biomes,

© 2025 Westerdijk Fungal Biodiversity Institute

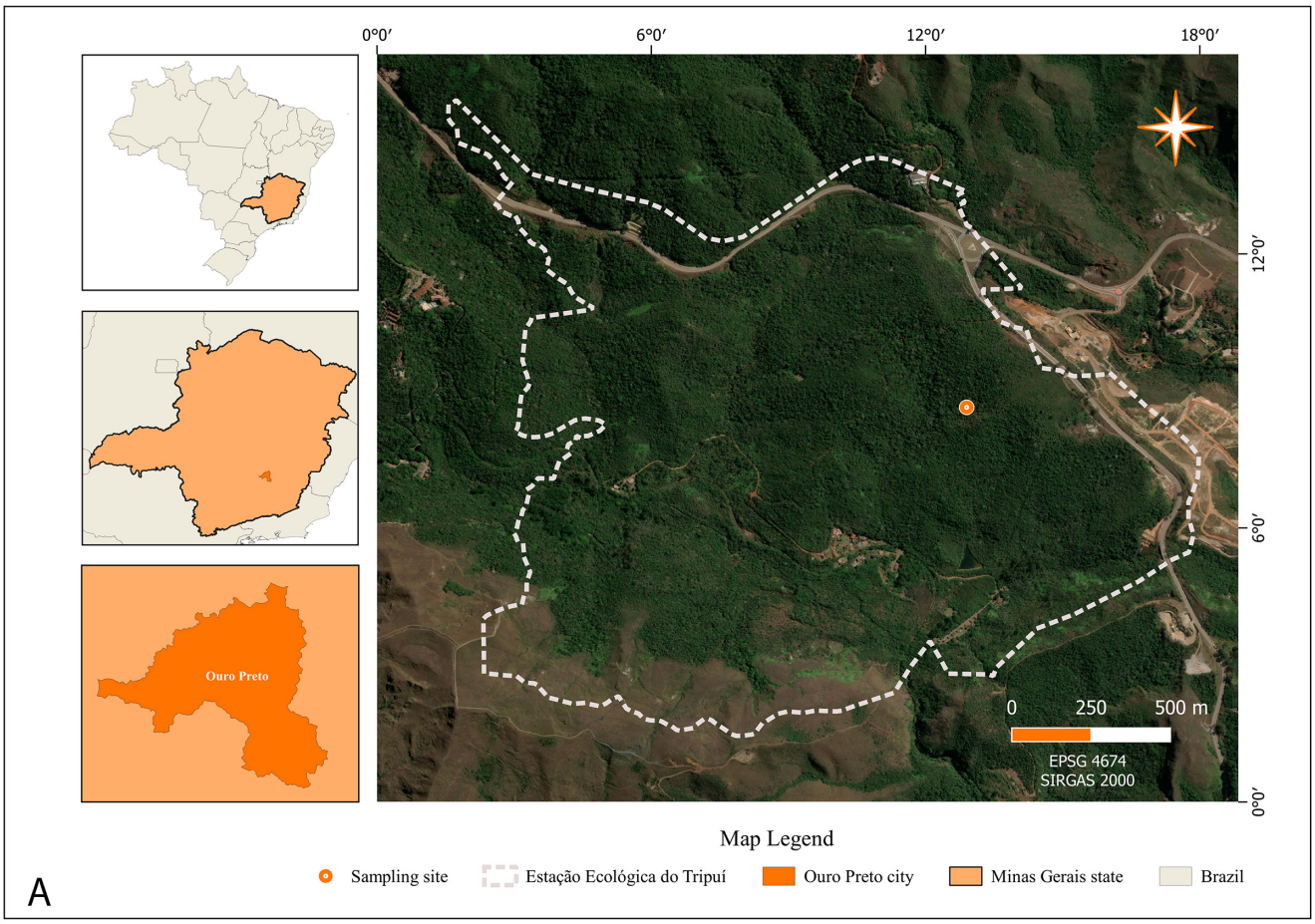







Fig. 1. Sampling site in Ouro Preto, Minas Gerais, Brazil. **A.** Map with an overview of the forest reserve, Estação Ecológica do Tripuí. **B, D.** Sampling sites at the higher and drier elevations showing the relatively open canopy and the understorey dominated by tree ferns (*Cyathea* spp.), where ant graveyards predominantly occurred. **C.** Lower, wetter parts of the trail being invaded by exotic wild ginger (*Hedychium coronarium*).

© 2025 Westerdijk Fungal Biodiversity Institute

with a mixed vegetation belonging to both; including semi-deciduous mesophytic forests, Cerrado and permanent swamps (FEAM 1995, Pedralli *et al.* 1997, Werneck *et al.* 2001). The forest reserve is also hyperdiverse in arthropods, especially *Coleoptera* (Gatti & Carneiro 2019). Surveys were conducted along the "Trilha da Guarita" trail (Fig. 1) in July and October 2023, March and November 2024 and February 2025. Collections were concentrated at the same spot (20°22'48"S, 43°32'24"W) (Fig. 1) where the infected ants formed a major graveyard. These collections consisted of careful examination of the vegetation (mainly understory shrubs), from ground level up to ca 2 m in height. Infected ants attached to the substratum (leaves and twigs) were then transferred to sterile containers and taken to the Laboratory of Insect-Microbe Interactions at the Universidade Federal de Viçosa (LIIM-UFV) for morphological and molecular analyses. Permits for collection and transport were provided by SISBIO (No. 86685–4) and the Instituto Estadual de Florestas (IEF; No. 037/2023). Images of the specimens were taken in situ and their positions on the vegetation were noted.

The ant hosts were identified by RMF, specialist in the taxonomy of *Heteroponerini*. Voucher specimens of *O. acanthoponerae* (holotype and paratypes) were deposited at the VIC Fungarium, located at UFV, at Royal Botanic Gardens Kew Fungarium (K-M: IMI) and at the Natural History Museum of Denmark, University of Copenhagen (NHMD). The remaining specimens are conserved at LIIM-UFV and at the Entomological Collection Padre Jesus Santiago Moure at the Universidade Federal do Paraná (DZUP-UFPR).

DNA extraction, amplification and sequencing

For molecular identification, DNA was extracted from ascostromata (ascoma + stroma) and synnemata which had been excised from the host and macerated in microtubes and then placed in liquid nitrogen. The DNA extraction was performed using the Wizard™ Genomic DNA Purification Kit (Promega™, Madison, USA), following the manufacturer's recommendations. The final concentrations of the DNA extractions were determined by NanoDrop™ spectrophotometry (Thermo Scientific™, Waltham, USA).

In total, four genomic regions were amplified using polymerase chain reaction (PCR): i) the nuclear ribosomal small subunit (SSU), ii) the nuclear ribosomal large subunit (LSU), iii) the translation elongation factor 1-α (*TEF*), and iv) RNA polymerase II largest subunit (*RPB1*). Primers used for each region were: (SSU) NS1 (5'-GTAGTCATATGCTTGTCTC-3') and NS4 (5'-CTTCCGTCAATTCCTTTAAG-3') (White *et al.* 1990), (LSU) LR0R (5'-ACCCGCTGAAC-TTAAGC-3') and LR5 (5'-TCCTGAGGGAAACTTCG-3') (Vilgalys & Sun 1994), (*TEF*) 983F (5'-GCYCCYGGHCAYCGTGAYTTYAT-3') and 2218R (5'-ATGACACCRACRGCRACRGTYTG-3') (Rehner & Buckley 2005), (*RPB1*) RPB1-Ac: (5'-GARTGYCCDGGDCAYTTYGG-3') and RPB1-Cr (5'- CCNGCDATNTCRTTRTCCATRTA-3') (Murata *et al.* 2014).

Each 25 µL PCR amplification reaction contained 12.5 µL KAPA *Taq* ReadyMix (KAPA Biosystems™), 1 µL of each forward and reverse primers (10 pmol/µL), 5 µL of DNA template, and 5.5 µL of DNAse/RNAse Free Water (ZymoBIOMICS™). The amplification reactions were placed in an Eppendorf™ thermocycler under the following conditions: for SSU and LSU, 2 min at 95 °C, 4 cycles of denaturation at 94 °C for 30 s, annealing at 55 °C for 30 s, and extension at 72 °C for 2 min, followed by 35 cycles of denaturation at 94 °C for 30 s, annealing at 50.5 °C for 1 min, and extension at 72 °C for 2 min and final extension at 5 min at 72 °C. For *TEF*, 2 min at 94 °C, 10 cycles of denaturation at 94 °C for 30 s, annealing at 64 °C for 1 min, and extension at 72 °C for 1 min, followed by 35 cycles of denaturation at 94 °C for 30 s, annealing at 54 °C for 1 min, extension at 72 °C for 1 min and final extension at 3 min at 72 °C. For *RPB1*, 2 min at 95 °C, 10 cycles of denaturation at 95 °C for 30 s, annealing at 66 °C for 1 min, and extension at 72 °C for 1 min, followed by 35 cycles of denaturation at 95 °C for 30 s, annealing at 56.6 °C for 1 min, extension at 72 °C for 1 min and final extension at 3 min at 72 °C. After amplification, PCR products were purified and sequenced by Macrogen™ (Seoul, South Korea).

Phylogenetic analyses

The obtained contigs were compared to sequences of related species deposited in the NCBI (https://www.ncbi.nlm.nih.gov/) nucleotide database using BLASTn at Geneious Prime™ 2025.0.3 (Kearse *et al.* 2012) to confirm that they belonged to the genus *Ophiocordyceps*. We aligned the *O. acanthoponerae* to a database with 530 OTUs from species (Table S1) that broadly represent the order *Hypocreales*. The final database consisted of 323 SSU, 479 LSU, 360 *TEF* and 444 *RBP1* sequences.

We generated, improved (excluding gaps and removing ambiguously aligned regions) and combined individual gene alignments with Geneious Prime v. 2025.0.3. The final alignment length was 3972 bp with 1242 bp for SSU, 999 bp for LSU, 1006 bp for *TEF* and 725 bp for *RBP1*. We used the ModelTest-NG v. 0.1.7 (Darriba *et al.* 2020) on CIPRES Science Gateway v. 3.3 (Miller *et al.* 2012) for selecting the nucleotide substitution models, considering the lowest Akaike Information Criterion (AIC). The final dataset consisted of eight data partitions (one for SSU, one for LSU, three for *TEF* and three for *RBP1*).

Concatenated phylogenetic trees for all four genes were reconstructed performing Maximum Likelihood analysis using IQ-TREE v. 2.2.2.7, based on the fit-model for each region (GTR+I+G4) and generated 1000 bootstrap replicates, (Nguyen *et al.* 2015, Chernomor *et al*. 2016, Kalyaanamoorthy *et al*. 2017, Hoang et al. 2018, Minh *et al*. 2020) on the CIPRES webserver. The species *Verticillium dahliae* (ATCC 16535) was used as the outgroup. The resulting consensus phylogenetic tree was visualized in FigTree v. 1.4.4 (Rambaut 2017) and edited in Adobe Illustrator™.

Morphological characterisation

The samples were examined and photographed under a stereomicroscope Zeiss Discovery V20™ with an attached camera (AxioCam MRc). The photos were processed with the AxionVisionSE64™ software. Characteristics such as the host's position and attachment to the plant substrate, shape, colour and size of the sexual and asexual structures were considered for macro-morphological characterisation.

For micro-morphological characterisation, ascostromata and synnemata were removed from hosts and were hand-sectioned using a single-sided razor blade and placed on slides with lacto-glycerol (20 mL lactic acid in 40 mL glycerol and 20

© 2025 Westerdijk Fungal Biodiversity Institute

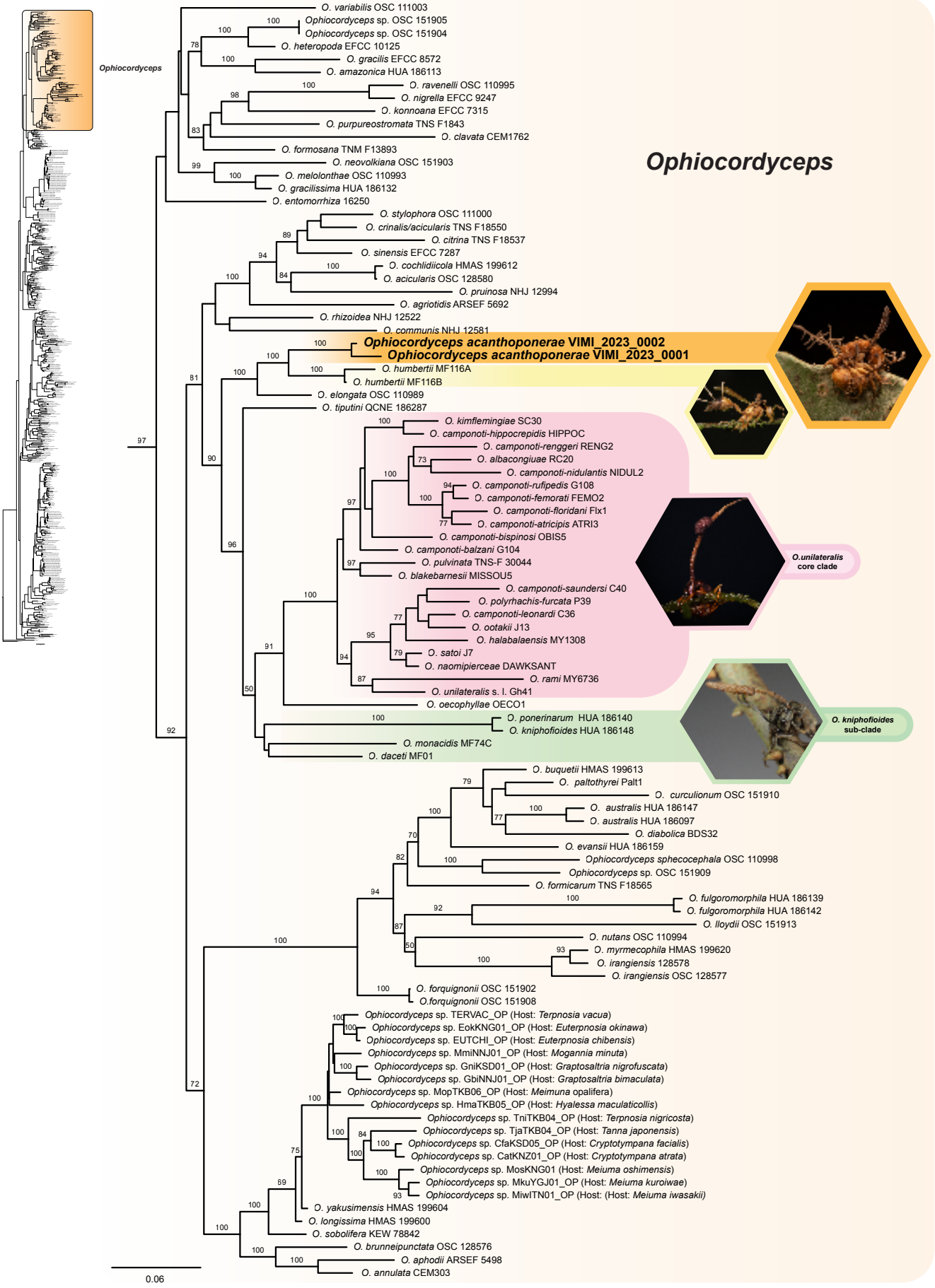

Fig. 2. Maximum likelihood tree of *Ophiocordyceps* obtained with a concatenated dataset of SSU, LSU, *TEF* and *RPB1*. Numbers on nodes represent bootstrap values > 70 %. *Ophiocordyceps acanthoponerae sp. nov.* is indicated in **bold** font and highlighted in orange. The wasp-parasitic species, *O. humbertii* (yellow), and the myrmecophilous clades, *O. unilateralis* core clade (pink) and O. *kniphofioides* sub-clade (green), are also highlighted in the tree. The whole analysis tree of the order *Hypocreales* is depicted in the top-left corner, with the position of *Ophiocordyceps* highlighted in orange.

© 2025 Westerdijk Fungal Biodiversity Institute

mL distilled water) or lacto-fuchsin 1 % (0.1 g acid fuchsin in 100 mL lactic acid). Specimens were examined under an Olympus™ BX53 light photomicroscope with an attached digital camera (Olympus Q-Color 3). The microphotographs were processed with the cellSens Dimensions™ software.

To obtain mature ascospores and to follow the germination process, specimens bearing ascostromata were taped to the lids of 9-cm-diam. Petri dish and suspended with Vaseline above the dish containing a thin layer of distilled water agar (DWA) and kept in an incubator in the dark at 20 °C, to await the release of ascospores (Evans *et al.* 2011b). Specimens were examined daily under a dissecting microscope to check for spore discharge and germination. A minimum of 50 discharged (mature) ascospores were examined and measured for comparative morphology.

RESULTS

Phylogenetic analyses

Sequences of the genomic regions SSU (= 2), LSU (= 2), *TEF* (= 2) and *RPB1* (= 1) (Table 1) from infected *Acanthoponera* samples clustered together with strong bootstrap support value (BS = 100 %) (Fig. 2). Single-locus phylogenies for *TEF* and *RPB1* also supported the new species (Figs S1, S2). *Ophiocordyceps acanthoponerae* was placed in a strongly supported clade (BS = 100 %) alongside the wasp pathogen *O. humbertii* and the lepidopteran pathogen *O. elongata* (Fig. 2). This clade clustered as a sister group of the clade *O. unilateralis* (BS = 90 %). Building on the previous work by Araújo *et al.* (2018), *O. acanthoponerae* was positioned outside the two traditional clades of hirsutelloid *Ophiocordyceps* associated with ants, the *O. unilateralis* core clade, *O. kniphofioides* sub-clade and *O. oecophyllae*. The *O. unilateralis* core clade included 22 combined sequences of different species and was strongly supported (BS = 100 %) (Fig. 2; Table 1). *Ophiocordyceps oecophyllae* clustered as a sister-group of *O. unilateralis* core clade (BS = 91 %). The sub-clade *O. kniphofioides* was placed as a sister group of the *O. unilateralis* core clade together with *O. oecophyllae*, but this relationship had no support.

Taxonomy

Based on morphology, and supported by the molecular data, a new species in the genus *Ophiocordyceps* is proposed:

Ophiocordyceps acanthoponerae S.J. Lima-Santos, H.C. Evans & J.P.M. Araújo, ***sp. nov.*** MB 859808. Figs 3–7.

Etymology: Named after the host ant genus *Acanthoponera* (*Heteroponerini*: *Formicidae*).

Typus: **Brazil**, Minas Gerais state, Ouro Preto municipality, Estação Ecológica do Tripuí (20°22’48”S, 43°32’24”W), on *Acanthoponera mucronata*, in forest understorey, 23 Nov. 2024, *S.J. Lima-Santos, B.L. Clemente, N.L.S. Lima & T. Mendes-Pereira* (**holotype** VIC 49609). **Paratypes**: All from **Brazil**, Minas Gerais state, Ouro Preto municipality, Estação Ecológica do Tripuí (20°22’48”S, 43°32’24”W), on *Acanthoponera mucronata*, in forest understorey, 12 Oct. 2023, *S.J. Lima-Santos, G.S. de Paula, M.C. Castro, M.M. Moreira & R.C. Silva*, VIC 49613; ibid., 11 Mar. 2024, *S.J. Lima-Santos, L.C. dos Reis, S.L. Elliot & H.C. Evans*, VIC 49614; ibid., 23 Nov. 2024, *B.L. Clemente, N.L.S. Lima & T. Mendes-Pereira*, VIC 49610, VIC 49611, VIC 49612 VIC 49615, NHMD001788818, NHMD001788819, NHMD001788820; ibid., 19 Feb. 2025, *S.J. Lima-Santos*, *B.L. Clemente, G.S. de Paula & H.C. Evans*, IMI 507615.

Additional specimens examined: In total 75 infected *Acanthoponera mucronata* ants were collected at different stages of infection. All of them were used to conduct fungus diagnosis. Specimens that are not deposited can be located at LIIM-UFV and in the Entomological Collection Padre Jesus Santiago Moure at the Universidade Federal do Paraná (DZUP-UFPR).

Description: *External mycelium* white in early stages, becoming light brown with age, emerging from all host orifices and sutures. *Sexual morph* (Fig. 3): One or up to three stromata produced from dorsal pronotum, simple or branched, clavate to cylindrical, 2.8–4 mm in length, 0.2–0.3 mm thick, pale brown, clavate; fertile region consisting of a dark brown ascoma, covering 360° and mostly not reaching the tip of the stalk, averaging 1.6 × 0.5 mm (Fig. 3A–C). *Perithecia* immersed to partially erumpent, flask-shaped, (209–)247(–289) × (103–)134(–179) µm (Fig. 3D–E). *Asci* with 8 intertwined spores, cylindrical, hyaline, (131–)150(–175) × (6.0–)7.4(–9.0) µm; with a prominent apical cap with a narrow pore, (2.0–)4.9(–6.0) × (4.5–)5.2(–6.0) µm (Fig. 3F). *Ascospores* vermiform, hyaline, (94–)126(–152) × (2.0–)2.6(–3.0) µm, 7–septate, slightly curved, tapering towards the apices (Fig. 3G–H). *Asexual morph* (Fig. 4): *Hirsutella*-like phialides produced along the stromatal stalk and on synnemata emerging from sutures and joints. *Synnemata* pale brown or tan-coloured, single or branched, usually with secondary smaller and delicate branches produced particularly near the base; main stalks often subcapitate, produced from the dorsal pronotum, the leg joints, thorax and abdominal sutures; averaging 2.5 mm in length (Fig. 4A, B). *Phialides* lageniform, guttulate, hyaline, (10.0–)13.7(–16.5) × (3.0–)4.5(–6.5) µm, tapering to a short neck, (4.5–)8.3(–10.5) × (0.5–)1.2(–2.0) µm (Fig. 4C, D); occasionally with much longer, needle-like neck, especially on the ascostromata, up to 60 µm in length; *conidia* aseptate, tear-shaped, smooth, guttulate, hyaline, (7.5–)8.6(–10.0) × (2.0–)2.2(–2.5) µm (Fig. 4E). *Hyphal bodies* ovoid to pyriform, swollen, aseptate to septate, guttulate, hyaline, (16.0–)29.8(–58) × (8.0–)11.5(–14) µm, excised from abdomen, glistening white en masse (Fig. 4F).

Germination process: Ascospores, ejected onto DWA, germinated within 24–48 h, often accompanied by spore swelling, to produce up to four straight capilliconidiophores, averaging 17.3 × 1.3 µm (Fig. 3I); each bearing a single, terminal, fusiform capilliconidium (Fig. 3J), averaging 8.4 × 1.6 µm. Germ-tubes were not produced and no further growth was observed.

Habitat: Semi-deciduous, mesophytic forest in a transition area between Atlantic rainforest and Cerrado in the municipality of Ouro Preto, Minas Gerais, Brazil. Ouro Preto

© 2025 Westerdijk Fungal Biodiversity Institute

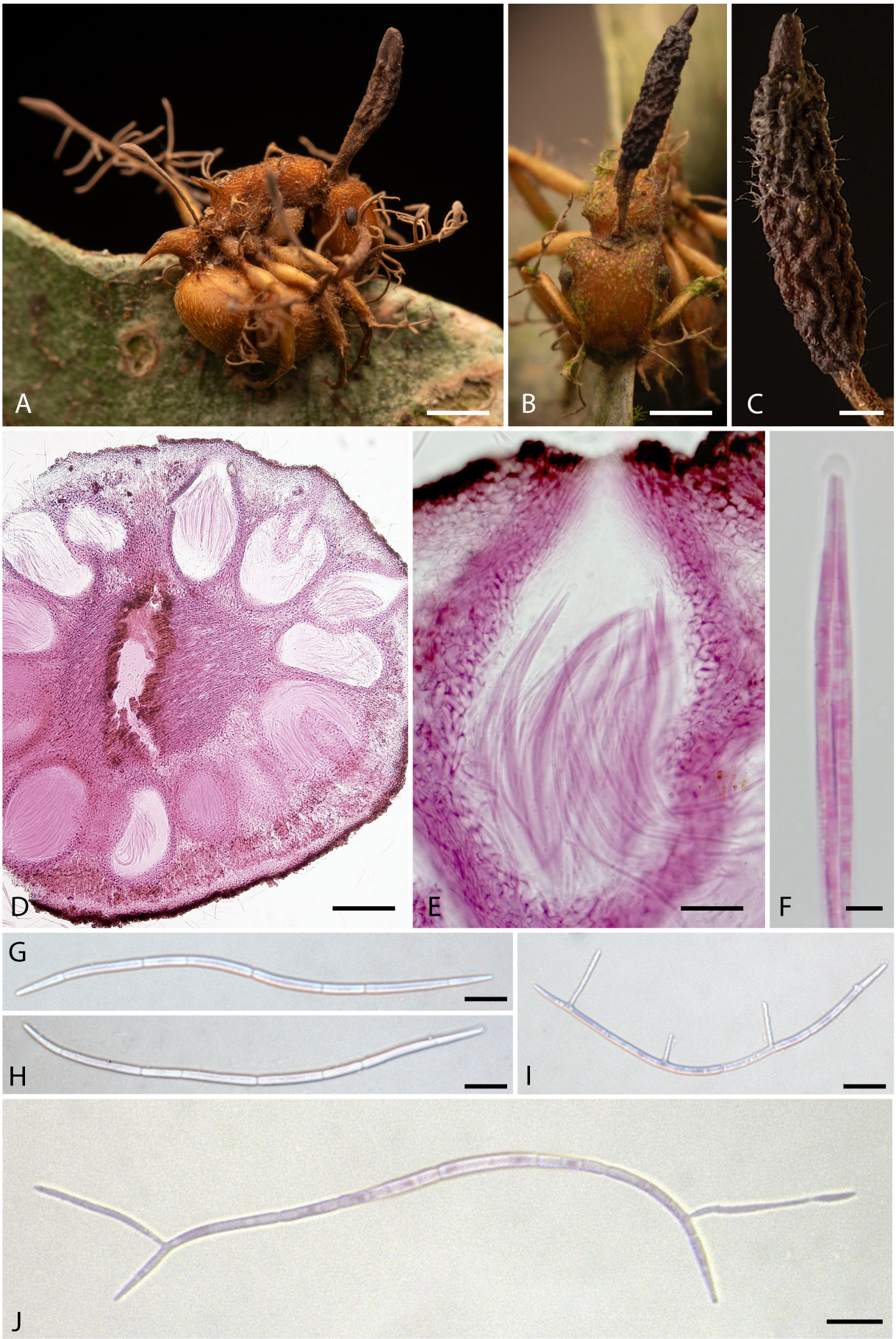

Fig. 3. *Ophiocordyceps acanthoponerae*. **A.** Holomorph with mature sexual and asexual morphs. **B, C.** Ascostromata produced from the dorsal neck region, dark brown, non-fleshy. **D.** Transversal section of the fertile part showing the buried perithecia. **E.** Perithecium with asci. **F.** Ascus, 8–spored with an apical cap. **G, H.** 7-septate ascospores. **I.** Germinated ascospore with three capilliconidiophores. **J.** Germinated ascospore bearing a capilliconidium on the right corner. Images A–C by Frederico Salles. Scale bars: A = 1 mm; B = 0.5 mm; C = 50 µm; D = 30 µm; E = 0.2 µm; F = 10 µm; G–J = 10 µm.

© 2025 Westerdijk Fungal Biodiversity Institute

Table 1. List of *Ophiocordyceps* species, vouchers, GenBank accession numbers and host associations. *Ophiocordyceps acanthoponerae sp. nov.* is highlighted in **bold** font.

Species	Voucher	nSSU rDNA	nLSU rDNA	*TEF*	*RPB1*	Host	Reference
Ophiocordyceps acanthoponerae	**VIMI_2023_0001**	**PV283217**	**PV283219**	**PV356076**	**PV356074**	***Acanthoponera mucronata***	**This study**
	VIMI_2023_0002	**PV283216**	**PV283218**	**PV356075**	—	***Acanthoponera mucronata***	**This study**
Ophiocordyceps acicularis	OSC 128580	DQ522543	DQ518757	DQ522326	DQ522371	*Coleoptera*	Quandt *et al.* (2014)
Ophiocordyceps agriotidis	ARSEF 5692	DQ522540	DQ518754	DQ522322	DQ522368	*Coleoptera*	Quandt *et al.* (2014)
Ophiocordyceps albacongiuae	RC20	KX713633	—	KX713670	—	*Hymenoptera*	Araújo *et al.* (2019)
Ophiocordyceps amazonica	HUA 186113	KJ917566	KJ917571	—	KP212903	*Orthoptera*	Sanjuan et al. (2015)
Ophiocordyceps annulata	CEM303	KJ878915	KJ878881	KJ878962	KJ878995	*Coleoptera*	Quandt *et al.* (2014)
Ophiocordyceps aphodii	ARSEF 5498	DQ522541	DQ518755	DQ522323	—	*Coleoptera*	Quandt *et al.* (2014)
Ophiocordyceps australis	HUA 186097	KC610786	KC610765	KC610735	KF658662	*Hymenoptera*	Sanjuan et al. (2015)
	HUA 186147	KC610784	KC610764	KC610734	KF658678	*Hymenoptera*	Quandt *et al.* (2014)
Ophiocordyceps blakebarnesii	MISSOU5	KX713641	KX713610	KX713688	KX713716	*Hymenoptera*	Araújo *et al.* (2018)
Ophiocordyceps brunneipunctata	OSC 128576	DQ522542	DQ518756	DQ522324	DQ522369	*Coleoptera*	Quandt *et al.* (2014)
Ophiocordyceps buquetii	HMAS_199613	KJ878939	KJ878904	KJ878984	KJ879019	*Hymenoptera*	Araújo *et al.* (2018)
Ophiocordyceps camponoti-atricipis	A25	KX713666	—	KX713677	—	*Hymenoptera*	Araújo *et al.* (2018)
Ophiocordyceps camponoti-balzani	G104	KX713660	KX713593	KX713689	KX713703	*Hymenoptera*	Araújo *et al.* (2018)
Ophiocordyceps camponoti-bispinosi	OBIS5	KX713636	KX713616	KX713693	KX713721	*Hymenoptera*	Araújo *et al.* (2018)
Ophiocordyceps camponoti-femorati	FEMO2	KX713663	KX713590	KX713678	KX713702	*Hymenoptera*	Araújo *et al.* (2018)
Ophiocordyceps camponoti-floridani	Flx1	KX713661	—	—	—	*Hymenoptera*	Araújo *et al.* (2018)
Ophiocordyceps camponoti-hippocrepidis	HIPPOC	KX713655	KX713597	KX713673	KX713707	*Hymenoptera*	Araújo *et al.* (2018)
Ophiocordyceps camponoti-leonardi	C36	KJ201512	—	JN819013	—	*Hymenoptera*	Kobmoo *et al.* (2018)
Ophiocordyceps camponoti-nidulantis	NIDUL2	KX713640	KX713611	KX713669	KX713717	*Hymenoptera*	Araújo *et al.* (2018)
Ophiocordyceps camponoti-renggeri	RENG2	KX713632	—	KX713672	—	*Hymenoptera*	Araújo *et al.* (2018)
Ophiocordyceps camponoti-rufipedis	G108	KX713659	KX713594	KX713679	KX713704	*Hymenoptera*	Araújo *et al.* (2018)
Ophiocordyceps camponoti-saundersi	C40	KJ201519	—	JN819012	—	*Hymenoptera*	Araújo *et al.* (2018)
Ophiocordyceps citrina	TNS F18537	—	KJ878903	KJ878983	—	*Hemiptera*	Quandt *et al.* (2014)
Ophiocordyceps clavata	CEM1762	KJ878916	KJ878882	KJ878963	KJ878996	*Coleoptera*	Quandt *et al.* (2014)
Ophiocordyceps cochlidiicola	HMAS_199612	KJ878917	KJ878884	KJ878965	KJ878998	*Lepidoptera*	Quandt *et al.* (2014)
Ophiocordyceps communis	NHJ 12581	EF468973	EF468831	EF468775	—	*Coleoptera*	Quandt *et al.* (2014)

© 2025 Westerdijk Fungal Biodiversity Institute

Table 1. (Continued).

Species	Voucher	nSSU rDNA	nLSU rDNA	*TEF*	*RPB1*	Host	Reference
Ophiocordyceps curculionum	OSC 151910	KJ878918	KJ878885	—	KJ878999	*Coleoptera*	Quandt *et al.* (2014)
Ophiocordyceps daceti	MF01	—	KX713604	KX713667	—	*Hymenoptera*	Araújo *et al.* (2018)
Ophiocordyceps diabolica	BDS 32	MK393830	MK393322	—	—	*Hymenoptera*	Araújo *et al.* (2018)
Ophiocordyceps dipterigena	OSC 151912	KJ878920	KJ878887	KJ878967	KJ879001	*Diptera*	Quandt *et al.* (2014)
Ophiocordyceps elongata	OSC 110989	—	EF468808	EF468748	EF468856	*Lepidoptera*	Quandt *et al.* (2014)
Ophiocordyceps entomorrhiza	16250	KJ878942	—	KJ878987	KJ879021	*Coleoptera*	Quandt *et al.* (2014)
Ophiocordyceps evansii	HUA 186159	KC610796	KC610770	KC610736	KP212916	*Hymenoptera*	Sanjuan *et al.* (2015)
Ophiocordyceps formicarum	TNS F18565	KJ878921	KJ878888	KJ878968	KJ879002	*Hymenoptera*	Quandt *et al.* (2014)
Ophiocordyceps formosana	TNM F13893	KJ878908	—	KJ878956	KJ878988	*Coleoptera*	Quandt *et al.* (2014)
Ophiocordyceps forquignonii	OSC 151902	KJ878912	KJ878876	—	KJ878991	*Diptera*	Quandt *et al.* (2014)
	OSC 151908	KJ878922	KJ878889	—	KJ879003	*Diptera*	Quandt *et al.* (2014)
Ophiocordyceps fulgoromorphila	HUA 186139	KC610794	KC610760	KC610729	KF658676	*Hemiptera*	Sanjuan *et al.* (2015)
	HUA 186142	KC610795	KC610761	KC610730	KF658677	*Hemiptera*	Sanjuan *et al.* (2015)
Ophiocordyceps gracilis	EFCC 8572	EF468956	EF468811	EF468751	EF468859	*Lepidoptera*	Quandt *et al.* (2014)
Ophiocordyceps gracillisima	HUA 186132	—	KC610768	KC610744	KF658666	*Coleoptera*	Sanjuan et al. (2015)
Ophiocordyceps halabalaensis	MY1308	KM655825	—	GU797109	—	*Hymenoptera*	Luangsa-ard *et al.* (2011)
Ophiocordyceps heteropoda	EFCC 10125	EF468957	EF468812	EF468752	EF468860	*Hemiptera*	Quandt *et al.* (2014)
Ophiocordyceps humbertii	MF116A	MK874747	MK875537	—	MK863828	*Hymenoptera*	Araújo *et al.* (2019)
	MF116B	MK874748	MK875536	—	MK863829	*Hymenoptera*	Araújo *et al.* (2019)
Ophiocordyceps irangiensis	128578	DQ522556	DQ518770	DQ522345	DQ522391	*Hymenoptera*	Quandt *et al.* (2014)
	OSC 128577	DQ522546	DQ518760	DQ522329	DQ522374	*Hymenoptera*	Sanjuan *et al.* (2015)
Ophiocordyceps kimflemingiae	SC30	KX713629	KX713622	KX713699	KX713727	*Hymenoptera*	Araújo *et al.* (2019)
Ophiocordyceps kniphofioides	HUA 186148	KC610790	KF658679	KC610739	KF658667	*Hymenoptera*	Sanjuan et al. (2015)
Ophiocordyceps konnoana	EFCC 7315	EF468959	—	EF468753	EF468861	*Coleoptera*	Quandt *et al.* (2014)
Ophiocordyceps lloydii	OSC 151913	KJ878924	KJ878891	KJ878970	KJ879004	*Hymenoptera*	Quandt *et al.* (2014)
Ophiocordyceps longissima	HMAS_199600	KJ878926	—	KJ878972	KJ879006	*Hemiptera*	Quandt *et al.* (2014)
Ophiocordyceps melolonthae	OSC 110993	DQ522548	DQ518762	DQ522331	DQ522376	*Coleoptera*	Quandt *et al.* (2014)
Ophiocordyceps monacidis	MF74	KX713646	KX713606	—	—	*Hymenoptera*	Araújo *et al.* (2018)
Ophiocordyceps myrmecophila	HMAS_199620	KJ878927	KJ878893	KJ878973	KJ879007	*Hymenoptera*	Quandt *et al.* (2014)

© 2025 Westerdijk Fungal Biodiversity Institute

Table 1. (Continued).

Species	Voucher	nSSU rDNA	nLSU rDNA	*TEF*	*RPB1*	Host	Reference
Ophiocordyceops naomipierceae	DAWKSANT	KX713664	KX713589	—	KX713701	*Hymenoptera*	Araújo et al (2018)
Ophiocordyceps neovolkiana	OSC 151903	KJ878930	KJ878896	KJ878976	KJ879010	*Coleoptera*	Quandt *et al.* (2014)
Ophiocordyceps nigrella	EFCC 9247	EF468963	EF468818	EF468758	EF468866	*Coleoptera*	Quandt *et al.* (2014)
Ophiocordyceps nutans	OSC 110994	DQ522549	DQ518763	DQ522333	DQ522378	*Hemiptera*	Quandt *et al.* (2014)
Ophiocordyceps oecophyllae	OECO1	KX713635	—	—	—	*Hymenoptera*	Araújo *et al.* (2018)
Ophiocordyceps ootakii	J13	KX713652	KX713600	KX713681	KX713708	*Hymenoptera*	Araújo *et al.* (2018)
Ophiocordyceps palthothyreum	Palt1	MK393848	MK393345	—	—	*Hymenoptera*	Araújo *et al.* (2019)
Ophiocordyceps polyrhachis-furcata	P39	KJ201504	—	JN819003	—	*Hymenoptera*	Kobmoo *et al.* (2015)
Ophiocordyceps ponerinarum	HUA 186140	KC610789	KC610767	KC610740	KF658668	*Hymenoptera*	Sanjuan *et al.* (2015)
Ophiocordyceps pruinosa	NHJ 12994	EU369106	EU369041	EU369024	EU369063	*Lepidoptera*	Quandt *et al.* (2014)
Ophiocordyceps pulvinata	TNS-F 30044	GU904208	—	GU904209	GU904210	*Hymenoptera*	Kepler *et al.* (2011)
Ophiocordyceps purpureostromata	TNS F1843	KJ878931	KJ878897	KJ878977	KJ879011	*Coleoptera*	Quandt *et al.* (2014)
Ophiocordyceps rami	MY6736	KM655823	—	KJ201532	—	*Hymenoptera*	Kobmoo *et al.* (2015)
Ophiocordyceps ravenelii	OSC 110995	DQ522550	DQ518764	DQ522334	DQ522379	*Coleoptera*	Quandt *et al.* (2014)
Ophiocordyceps rhizoidea	NHJ 12522	EF468970	EF468825	EF468764	EF468873	*Coleoptera*	Quandt *et al.* (2014)
Ophiocordyceps satoi	J7	KX713653	KX713599	KX713683	KX713711	*Hymenoptera*	Araújo *et al.* (2018)
Ophiocordyceps sinensis	EFCC 7287	EF468971	EF468827	EF468767	EF468874	*Lepidoptera*	Quandt *et al.* (2014)
Ophiocordyceps sobolifera	KEW 78842	EF468972	EF468828	—	EF468875	*Hemiptera*	Quandt *et al.* (2014)
Ophiocordyceps sp.	TNS F18495	KJ878937	KJ878901	—	KJ879017	*Coleoptera*	Quandt *et al.* (2014)
	OSC 151904	KJ878934	KJ878899	KJ878980	KJ879014	*Hemiptera*	Quandt *et al.* (2014)
	OSC 151905	KJ878935	—	KJ878981	KJ879015	*Hemiptera*	Quandt *et al.* (2014)
	CatKNZ01_OP	LC370816	LC370818	LC370821	LC370819	*Hemiptera* (Symbiont)	Matsuura *et al.* (2018)
	CfaKSD05_OP	LC370788	LC370790	LC370801	LC370791	*Hemiptera* (Symbiont)	Matsuura *et al.* (2018)
	EUTCHI_OP	LC370888	LC370890	LC370893	LC370891	*Hemiptera* (Symbiont)	Matsuura *et al.* (2018)
	EokKNG01_OP	LC370894	LC370896	LC370899	LC370897	*Hemiptera* (Symbiont)	Matsuura *et al.* (2018)
	GbiNNJ01_OP	LC370850	LC370852	LC370855	LC370853	*Hemiptera* (Symbiont)	Matsuura *et al.* (2018)
	GniKSD01_OP	LC370844	LC370846	LC370849	LC370847	*Hemiptera* (Symbiont)	Matsuura *et al.* (2018)
	HmaTKB05_OP	LC370983	LC370985	LC370988	LC370986	*Hemiptera* (Symbiont)	Matsuura *et al.* (2018)
	MiwITN01_OP	LC370967	LC370969	LC370972	LC370970	*Hemiptera* (Symbiont)	Matsuura *et al.* (2018)
	MkuYGJ01_OP	LC370960	LC370962	LC370965	LC370963	*Hemiptera* (Symbiont)	Matsuura *et al.* (2018)

© 2025 Westerdijk Fungal Biodiversity Institute

Table 1. (Continued).

Species	Voucher	nSSU rDNA	nLSU rDNA	*TEF*	*RPB1*	Host	Reference
	MopTKB06_OP	LC370921	LC370923	LC370926	LC370924	*Hemiptera* (Symbiont)	Matsuura *et al.* (2018)
	MosKNG01	LC370940	LC370942	LC370945	LC370943	*Hemiptera* (Symbiont)	Matsuura *et al.* (2018)
	MmiNNJ01_OP	LC370999	LC371001	LC371004	LC371002	*Hemiptera* (Symbiont)	Matsuura *et al.* (2018)
	TERVAC_OP	LC370866	LC370868	LC370871	LC370869	*Hemiptera* (Symbiont)	Matsuura *et al.* (2018)
	TjaTKB04_OP	LC370902	LC370904	LC370907	LC370905	*Hemiptera* (Symbiont)	Matsuura *et al.* (2018)
	MopTKB01_01	LC371006	LC371008	LC371011	LC371009	*Hemiptera* (Symbiont)	Matsuura *et al.* (2018)
	TniTKB04_OP	LC370872	LC370874	LC370877	LC370875	*Hemiptera* (Symbiont)	Matsuura *et al.* (2018)
	Gh41	KX713656	—	KX713668	KX713706	*Hymenoptera*	Araújo *et al.* (2019)
	OSC 151909	KJ878936	KJ878900	KJ878982	KJ879016	*Hymenoptera*	Quandt *et al.* (2014)
Ophiocordyceps sphecocephala	OSC 110998	DQ522551	DQ518765	DQ522336	DQ522381	*Hymenoptera*	Quandt *et al.* (2014)
Ophiocordyceps stylophora	OSC 111000	DQ522552	DQ518766	DQ522337	DQ522382	*Coleoptera*	Quandt *et al.* (2014)
Ophiocordyceps tiputini	QCNE 186287	KC610792	KC610773	KC610745	KF658671	*Megaloptera*	Sanjuan *et al.* (2015)
Ophiocordyceps variabilis	OSC 111003	EF468985	EF468839	EF468779	EF468885	*Coleoptera*	Quandt *et al.* (2014)
Ophiocordyceps yakusimensis	HMAS_199604	KJ878938	KJ878902	—	KJ879018	*Hemiptera*	Quandt *et al.* (2014)

— so-named because of the dark layer of iron oxide covering the gold — was the centre of a gold rush in the 18th century; becoming famous for its many Baroque-style churches, often adorned with gold leaf: hence, the gold reference in the title of this article. Also refers to the golden colour of the workers of *A. mucronata*.

Notes: Infected ants were found biting mostly on the edges of leaves — but also on the abaxial side, typically on the midrib — as well as clinging and biting onto twigs and side branches, at heights ranging from 0.5 up to 2 m above ground level. All the infected ants were found in the same location, forming one major graveyard at a specific spot along the Trilha da Guarita trail (20°22'48"S, 43°32'24"W). All specimens (n = 75) of *A. mucronata* infected by *O. acanthoponerae* were found consistently attached to the vegetation with their mandibles embedded in the substratum, often with evidence of scarring; a characteristic of the so-called zombie ants, as typified by species of the *O. unilateralis* complex attacking formicine ants of the tribe *Camponotini*.

DISCUSSION

The unusual morphologies of both the asexual and sexual morphs of *O. acanthoponerae* were the first indication that this could represent a new hirsutelloid species within *Ophiocordyceps* (Table 2). Myrmecophilous hirsutelloid *Ophiocordyceps* can be divided into two clades: *O. unilateralis* core clade and *O. kniphofioides* sub-clade (Fig. 2). The *O. unilateralis* core clade usually produces brown or black cushion-like fertile regions (single or multiple) that emerge unilaterally on the stalk, hence the name *O. unilateralis*, with ascospores that germinate via capilliconidiophores (Evans & Samson 1984, Evans *et al.* 2011b, Araújo *et al.* 2015, 2018). In comparison, the *O. kniphofioides* sub-clade typically produces a single ascostroma, covering 360° of the stalk, with ascospores that do not germinate (at least in vitro) via capilliconidiophores (Evans & Samson 1982, Sanjuan *et al.* 2015, Araújo *et al.* 2018). We have shown that *O. acanthoponerae* shares mixed traits with both clades, such as the dark brown ascostromata covering 360° of the stalk and ascospores producing capilliconidiophores and capilliconidia (Fig. 3I, J). Whilst in the asexual morph, the pale-coloured, multi-branched synnemata producing tear-shaped conidia (Fig. 4E) readily distinguish this species from other myrmecophilous hirsutelloid species described thus far.

The Maximum Likelihood phylogenetic analysis confirmed this novelty. Surprisingly, *O. acanthoponerae* clustered in a strongly supported clade (BS = 100 %) outside of the traditional hirsutelloid myrmecophilous clade (*O. unilateralis* core clade + *O. oecophyllae* + *O. kniphofioides* sub-clade) (Fig. 2). This unexpected phylogenetic position corroborates the existence of a novel lineage of myrmecophilous and hirsutelloid *Ophiocordyceps*.

It is important to compare the current host association, death position and mechanisms of infection of *O. acanthoponerae*, with the two traditional clades of manipulative *Ophiocordyceps*; firstly, with the *O. unilateralis* core clade, whose species exclusively infect ants of the tribe *Camponotini* (Evans *et al.* 2011b). Their hosts are

© 2025 Westerdijk Fungal Biodiversity Institute

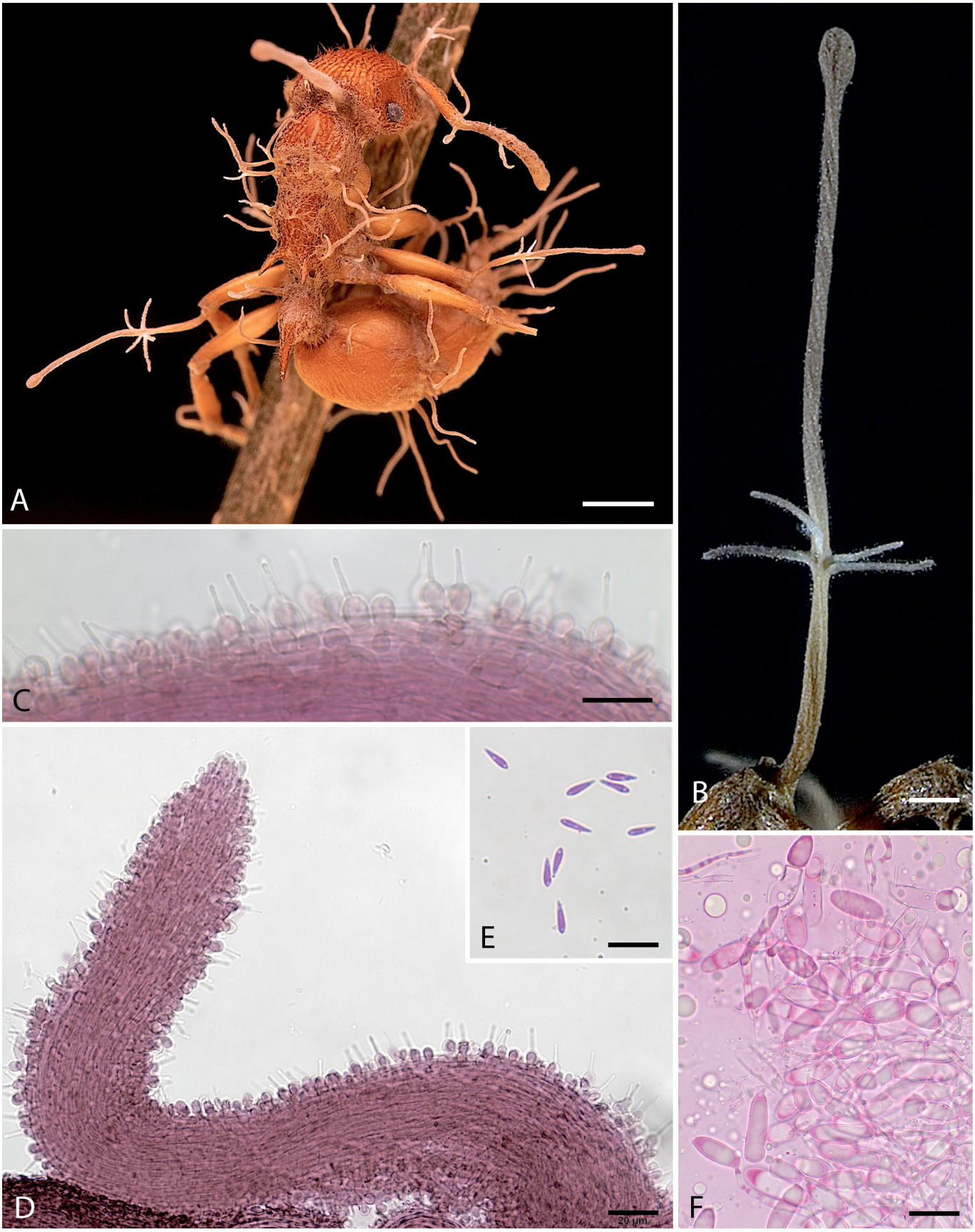

Fig. 4. *Ophiocordyceps acanthoponerae* asexual morph. **A, B.** Clavate and cylindrical branched synnemata, pale or tan-coloured arising from sutures on the body and appendages. **C, D.** Phialides along the synnemata. **E.** Tear-shaped conidia. **F.** Chains of hyphal bodies located internally in the host's abdomen. Image A by Frederico Salles. Scale bars: A = 1 mm; B = 0.2 mm; C–F = 10 µm; F = 20 µm.

© 2025 Westerdijk Fungal Biodiversity Institute

Table 2. Comparison of host, death position (first part of table), ascospore morphology and geographic allocation (second part of table) of hirsutelloid species of *Ophiocordyceps*. *Ophiocordyceps acanthoponerae sp. nov.* is highlighted in **bold** font.

Species Complex and Species	Host	Death position	Stromata	Fertile region	Source
Unnamed lineages					
Ophiocordyceps acanthoponerae sp. nov.	***Acanthoponera mucronata***	**biting the edges of leaves, abaxial faces of leaves and twigs**	**1–3 stromata, simple or branched, produced from dorsal pronotum**	**Dark brown, covering 360° and mostly not reaching the tip of the stalk**	**This study**
O. elongata	*Apatela americana* (*Lepidoptera*) larva and pupa	—	1–3 stromata, arising from each host	Pale yellow, cylindric, terete, equal	Petch (1937)
O. humbertii	*Hymenoptera*	biting leaf	Two stromata produced from points of insertion of the wings on each side	Dark brown, covering 360° and not reaching the tip of the stalk	Petch (1935)
O. tiputini	*Megaloptera*	leaf litter	Single, simple or branched, capitate, slender	Dark orange to deep orange, having a central core and sterile acuminate tip	Sanjuan *et al.* (2015)
***O. unilateralis* s. l.**					
O. unilateralis (Epitype)	*Camponotus sericeiventris*	biting leaf	Solitary, arising from the dorsal pronotum	Dark brown, hemisphaerical produced unilaterally	Evans *et al.* (2018)
O. camponoti-atricipis	*Camponotus atriceps*	biting leaf	Single, produced from dorsal pronotum	Chocolate brown, 1–2 lateral cushions, hemispherical	Araújo *et al.* (2015)
O. camponoti-balzani	*Camponotus balzani*	biting leaf	Single, produced from dorsal pronotum	Brown to black, lateral cushions, disc-shaped to hemisphaerical	Evans *et al.* (2011b)
O. camponoti-bispinosi	*Camponotus bispinosus*	biting spines	Single, produced anterior to pronotum	Dark brown becoming black with age, lateral globose cushion	Araújo *et al.* (2015)
O. camponoti-chartificis	*Camponotus chartifex*	biting leaf	Single, produced from dorsal pronotum	Chocolate brown, 1–2 lateral cushions	Araújo *et al.* (2018)
O. camponoti-femorati	*Camponotus femoratus*	biting leaf/spines	Single, produced from dorsal pronotum	Chestnut-brown, terminal of 1–3 lateral cushions, disc-shaped to hemispherical	Araújo *et al.* (2018)
O. camponoti-hippocrepidis	*Camponotus hippocrepidis*	biting spines	Single, produced from dorsal pronotum	Chestnut-brown, circular, produced at the middle part of stroma, laterally attached	Araújo *et al.* (2018)
O. camponoti-indiani	*Camponotus indianus*	biting leaf	Multiple, arising from right and left sides of pronotum, and leg joints	Chocolate to dark brown with age, 1–4 lateral cushions, hemispherical	Araújo *et al.* (2015)
O. camponoti-melanotici	*Camponotus melanoticus*	biting leaf	Single, produced from dorsal pronotum	Dark brown to black, 1–2 lateral cushions, hemispherical	Evans *et al.* (2011b)
O. camponoti-nidulantis	*Camponotus nidulans*	biting saplings	Single, produced from dorsal pronotum	Light brown, 1–2 lateral cushions, disc-shaped to hemispherical	Araújo *et al.* (2018)

© 2025 Westerdijk Fungal Biodiversity Institute

Table 2. (Continued).

Species Complex and Species	Host	Death position	Stromata	Fertile region	Source
O. camponoti-novogranadensis	*Camponotus novogranadensis*	biting epiphytes	Single, produced from dorsal pronotum	Brown, 1–2 lateral cushions, disc-shaped to hemisphaerical	Evans *et al.* (2011b)
O. camponoti-renggeri	*Camponotus renggeri*	biting leaf/moss	Single, rarely branched, produced from dorsal pronotum	Dark-brown to black, 1–2 lateral cushions, hemispherical to globose	Araújo *et al.* (2018)
O. camponoti-rufipedis	*Camponotus rufipes*	biting leaf	Single, produced from dorsal pronotum	Pale to chestnut-brown, 1–3 lateral cushions, disc-shaped to hemisphaerical	Evans *et al.* (2011b)
O. camponoti-sexguttati	*Camponotus sexguttatus*	biting leaf	Single, arising from the dorsal pronotum, never branching	Chestnut-brown, single lateral cushion, disc-shaped	Araújo *et al.* (2018)
***O. kniphofioides* s. l.**					
O. monacidis	*Dolichoderus bispinosus*	base of trunk (moss)	Single, emerges laterally from the pronotum, rarely from the gaster	Dark orange, terminal	Evans *et al.* (1982); Araújo *et al.* (2018)
O. daceti	*Daceton armigerum*	leaf (not biting)	Arising from the dorsal pronotum	—	Araújo *et al.* (2018)
O. kniphofioides	*Cephalotes atratus*	base of trunk	Simple or branched, arising laterally from neck or upper thorax (pronotum), occasionally dorsally	Light to deep orange, terminal, clavate to conical	Evans *et al.* (1982)
O. ponerinarum	*Paraponera clavata*	base of trunk	Simple or branched, emerging laterally from the pronotum	Acuminate	Evans *et al.* (1982)

Table 2. (Part 2).

Species Complex and Species	Ascospores					Distribution
	Shape	Size (µm)	Septation	Capilliconidiophore	Capilliconidia	
Unnamed lineages						
Ophiocordyceps acanthoponerae sp. nov.	**vermiform**	**(94–)126(–152) × (1.9–)2.6(–3.2)**	**7**	**straight, averaging 17.3 × 1.3 µm**	**fusiform, averaging 8.4 × 1.6 µm**	**Brazilian Atlantic Forest-Cerrado ecotone**
O. elongata	cylindrical	—	—	—	—	USA
O. humbertii	narrow-fusoid	75 × 2.5	at intervals of 6 to 16 µm	—	—	Sarawak, Malaysia
O. tiputini	elongate-fusiform	120–180 × 1.5–1.5	—	—	—	Amazon region, Ecuador and Bolivia
***O. unilateralis* s. l.**						
O. unilateralis (Epitype)	filiform	(70–)75–85 × 2–2.5	4–5	—	—	Brazilian Atlantic Forest
O. camponoti-atricipis	vermiform	(75–)80–85(–100) × (2–)3(–3.5)	5	straight, thread-like structures, 55 µm in length	allantoid, 10–11 × 2–2.5 µm	Brazilian Central Amazon
O. camponoti-balzani	cylindrical	(120–)135–175 × 4–5	14–22(–27)	—	—	Brazilian Atlantic Forest

© 2025 Westerdijk Fungal Biodiversity Institute

Table 2. (Part2. Continued).

Species Complex and Species	Ascospores					Distribution
	Shape	Size (µm)	Septation	Capilliconidiophore	Capilliconidia	
O. camponoti-bispinosi	cylindrical	(60–)70–75(–80) × 4.5–5(–6)	4–5	straight, (50–)65(–80) µm	slightly truncate at the base, 10–11 × 3–4 µm	Brazilian Central Amazon
O. camponoti-chartificis	vermiform	75–85 × 5	9–13	long and extremely narrow hair-like, (65–)75–90(–95) µm	fusoid	Brazilian Central Amazon
O. camponoti-femorati	sinuous to curved	75–90 × 3	5	narrow, 35–40 µm long	clavate, 9 × 3 µm	Brazilian Central Amazon
O. camponoti-hippocrepidis	cylindrical	75–85 × 4–5	5	straight, 45–50 µm long	truncate at base, narrowing apically, 10–11 × 4 µm	Brazilian Central Amazon
O. camponoti-indiani	cylindrical	(60–)75(–80) × (3.5–)4.5(–5)	5	hair-like, 120–130 µm in length	fusoid, 13–14 µm	Brazilian Central Amazon
O. camponoti-melanotici	cylindrical	170–210 × 4–5	27–35	—	—	Brazilian Atlantic Forest
O. camponoti-nidulantis	vermiform	90–105(–115) × 3–4	5	straight, extremely narrow hair-like, 50–60 µm	clavate, 9 × 2 µm	Brazilian Central Amazon
O. camponoti-novogranadensis	filiform	75–95 × 2.5–3.5	5–10	20–25 × 0.2–0.4 µm	reniform, (5–)7–8 × 2.5–3.0 µm	Brazilian Atlantic Forest
O. camponoti-renggeri	vermiform	90–120 × 4	5–8	—	—	Brazilian Central Amazon
O. camponoti-rufipedis	vermiform	(75–)80–95(–115) × 2–3	4–7	extremely narrow hair-like structures, (45–)60–70(–80) µm	clavate, (7–)9–11 × 1.5–2.5 µm	Brazilian Atlantic Forest
O. camponoti-sexguttati	cylindrical	120–140 × 3	7	straight, 25–30 µm	narrowing apically, 5–9 × 2 µm	Brazilian Central Amazon
***O. kniphofioides* s. l.**						
O. monacidis	—	(80–)95–110(–120)	3–4	—	—	Brazilian Amazon
O. daceti	—	—	—	—	—	Brazilian Central Amazon
O. kniphofioides	filiform	110–150 × 1.5–3.0	3–5	—	—	Brazilian Amazon, Colombia
O. ponerinarum	—	—	—	—	—	Brazilian Amazon, Colombia

© 2025 Westerdijk Fungal Biodiversity Institute

commonly found biting on leaves — the so-called death grip (Hughes *et al.* 2011) — usually at the edges or tips, but also can occur attached to palm spines, epiphytes and mosses (in tropical forests), and twigs (in temperate forests) (Table 2), with heights varying up to 2 m (Evans *et al.* 2011b, Hughes *et al.* 2016, Araújo *et al.* 2018, Loreto *et al.* 2018, van Roosmalen & de Bekker 2024). It is posited that ants are infected on or near their foraging trails when coming into contact with sticky capilliconidia, a secondary and infective spore produced on hirsutelloid conidiogenous cells (capilliconidiophores) arising from germinating ascospores that have been ejected from ascostromata on infected ants in the forest understorey (Evans *et al.* 2011a, b). This infection process has been likened, somewhat fancifully, to "a delayed-action landmine" (Evans & Boddy 2010), and the germination of the ascospores, essential for the infection process, can be simulated in vitro, following the protocol described previously in the Materials and Methods (Evans *et al.* 2011b). The morphology of the ascus, with its thickened apical cap and a narrow pore — diagnostic of the genus (Petch 1931) — is crucial for the explosive release of the ascospores and the purported infection cycle with ascospores raining on and 'contaminating' the ant trails. As graphically shown in Figs 5 & 6, the death positions and the biting strategy of *Acanthoponera* ants infected with *O. acanthoponerae* replicate the behaviours of *Camponotini* ants infected with *O. unilateralis* sensu lato. This evidence of fungal manipulation, with the ants positioned in the lower understorey above the nests and the trails emanating from them on the forest floor, justifies the classification of *O. acanthoponerae* within the zombie-ant fungi.

Species of the *O. kniphofioides* sub-clade infect ant hosts belonging to the distantly related genera *Cephalotes*, *Daceton*, *Dolichoderus* and *Paraponera*. The most studied interaction involves *O. kniphofioides* sensu stricto and *Cephalotes atratus* — an arboreal myrmicine ant highly adapted to living in the forest canopy where it nests and forages on pollen and homopteran exudates with the aid of adhesive tarsal pads (Stark & Yanoviak 2018)— where infected ants aggregate on tree trunks (Table 2) (Evans & Samson 1982, Sanjuan *et al.* 2015, Araújo *et al.* 2018, Imirzian *et al.* 2020). Healthy workers scavenge on the trees attempting to remove infected cadavers and it is most probable that these become infected when encountering the mucilaginous conidia produced on hirsutelloid, rhizoid-like synnemata that radiate out on the tree bark from the ant host (Evans & Samson 1982, Araújo *et al.* 2018).

A closely-related species within the *O. kniphofioides* complex is *O. monacidis* on the myrmicine ant *Dolichoderus* (*Monacis*) *bispinosus* (Araújo *et al.* 2018): a strictly arboreal ant with similar foraging habits to *C. atratus* (Mackay 1993). As with diseased *C. atratus* ants, infected *D. bispinosus* ants descend from their arboreal habitats and die amongst clumps of moss on the buttress roots of upperstorey trees, where the dark-orange, poker-like ascostromata of *O. monacidis* mimick the moss sporophores (Araújo *et al.* 2018). If, as the evidence suggests (Mackay 1993), *D. bispinosus* is an arboreal ant — foraging and nesting in the canopy — with only occasional sorties to the forest floor, it is difficult to determine how the ascospores reach their target hosts and function in the infection cycle. Rather than being manipulated by the fungus, infected ants would appear to be moving away from their arboreal habitats and actively hiding within the moss substrate, which could be interpreted to be altruistic by avoiding infection of the nests and trails in the canopy. Such an interpretation has been posited regarding both *C. atratus* and *D. bispinosus* infected by another *Ophiocordyceps* species complex, *O. cucumispora* sensu lato, where both hosts when infected descend from the forest upperstorey and die hidden within the litter layer (Evans 1982, 1988, Evans & Samson 1982). The ascospores readily break into highly-distinct, cucumber-like, longitudinally-ridged and echinulate part-spores. The form and function of these unusual spores is unknown, as is how they reach their arboreal targets, although the striation and echinulation indicates the likely involvement of phoresy on a vector.

In the phylogenetic analyses, *O. acanthoponerae* clustered in a clade (BS = 100 %) with sequences obtained for the wasp pathogen *O. humbertii* and the lepidopteran pathogen *O. elongata* (Fig. 2). We were able to identify shared traits between the taxa associated with hymenopteran insects. Both taxa, *O. acanthoponerae* and *O. humbertii*, have conspicuous hirsutelloid asexual morphs, dark brown ascostromata covering 360° of the stalk and vermiform (or narrow-fusoid) ascospores (Table 2) (Petch 1935, Somavilla *et al.* 2020, Sobczak *et al.* 2020, Barbosa & Somavilla, 2022). Wasps are also manipulated by *O. humbertii* and are mostly found biting on the border of leaves (Somavilla *et al.* 2020, Sobczak *et al.* 2020, Barbosa & Somavilla 2022), in a similar way to *O. acanthoponerae*. An analysis by Araújo & Hughes (2019) placed *O. humbertii* as a sister group of *O. unilateralis* clade (BS = 100 %) and it was hypothesized that an intermediate step might have occurred via social wasps, in the sense that an ancient *Ophiocordyceps* lineage jumped from wasps to ants, during the evolution of the myrmecophilous clade. Our new findings could represent such a missing link between manipulative ant- and wasp-associated *Ophiocordyceps*. Currently, studies are under way to provide a more robust phylogenetic framework for wasp-associated species, in the *O. humbertii* clade or complex, with the objective of elucidating the origins and evolution of manipulative *Ophiocordyceps* lineages.

This study is also the first record of ants belonging to the genus *Acanthoponera* (*Heteroponerini*: *Ectatomminae*: *Formicidae*) being infected by *Ophiocordyceps*. The genus *Acanthoponera* is restricted to the Neotropics and these relatively-large, golden-coloured ponerines are characterized by their prominent spines, the well-developed eyes and their long palps (Feitosa 2015, Camacho *et al.* 2022). They represent a lineage of nocturnal ants which forage exclusively on arboreal substrates, mostly in humid forests (Feitosa 2015, Feitosa & Prada-Achiardi 2019, Camacho *et al.* 2022). Workers are usually found foraging alone on the vegetation searching for small arthropods (Feitosa 2015, Feitosa & Prada-Achiardi 2019). It is thought that their colonies may harbour dozens to a few hundred individuals but data on nest structure and colony size are lacking (Feitosa 2015, and pers. obs.). The species *A. mucronata* has the largest distribution of the genus and is found in all Brazilian regions (Feitosa 2015, Feitosa & Prada-Achiardi 2019). This raises the questions of whether *O. acanthoponerae* is to be found across its host's range and whether other *Ophiocordyceps* species exist that parasitize the rarer members of the genus. *Acanthoponera mucronata* shares arboreal nesting and foraging habits with

© 2025 Westerdijk Fungal Biodiversity Institute



Fig. 5. Sequence of events following infection of *Acanthoponera mucronata* by *Ophiocordyceps acanthoponerae*: development of asexual morph. **A.** Recently dead ant biting into leaf midrib with no external evidence of infection. **B–D.** White silky hyphae emerging from sutures on body and appendages, including the antennae, on ants clinging to leaf margins. **E, F.** Developing synnemata, pale-coloured emerging from body and appendages. Scale bars: A–E = 1.5 mm; F = 2.5 mm.

© 2025 Westerdijk Fungal Biodiversity Institute

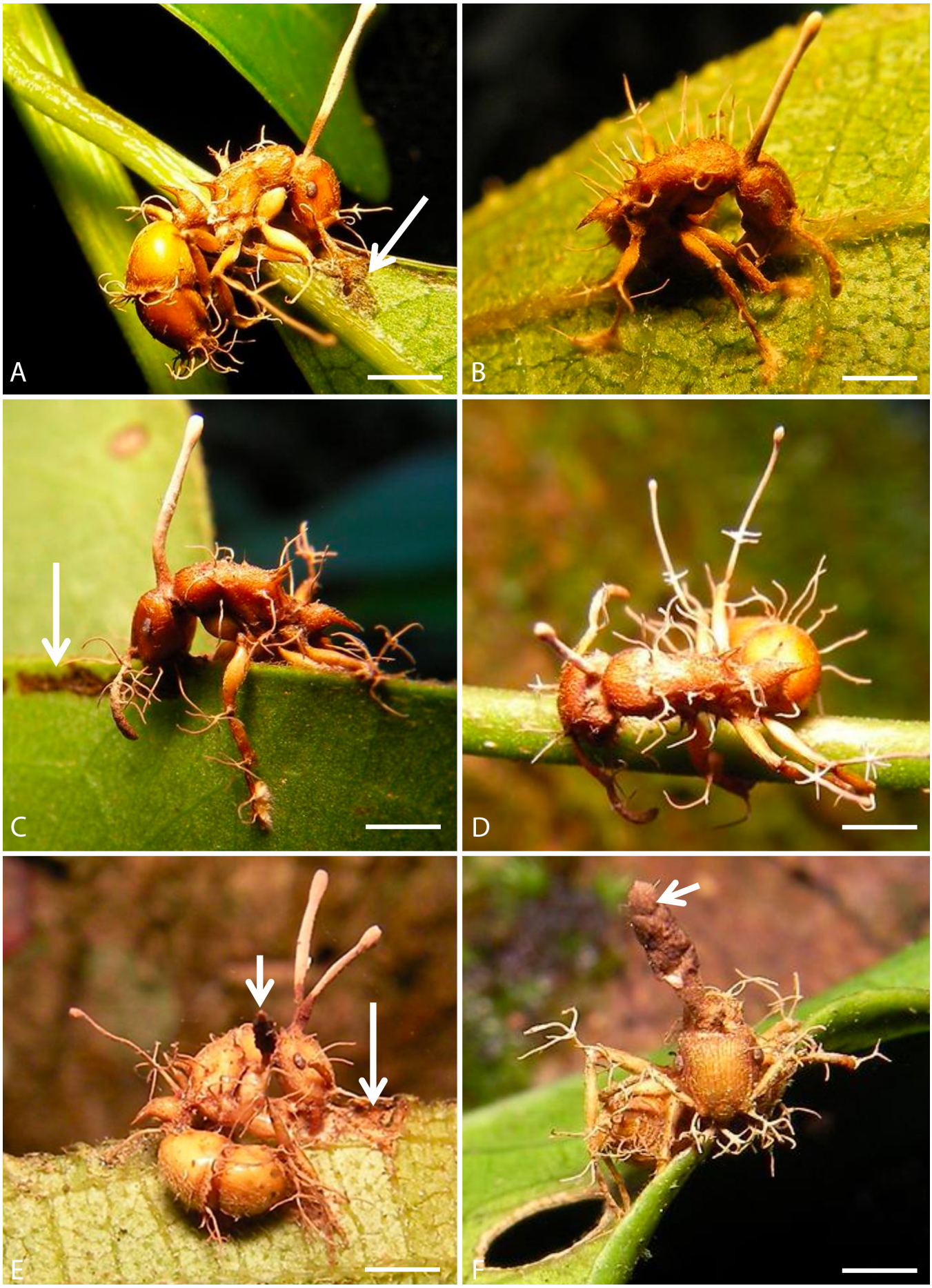

Fig. 6. Sequence of events following infection of *Acanthoponera mucronata* by *Ophiocordyceps acanthoponerae*: development of sexual morph. **A–D.** Single immature, pale-coloured ascostroma emerging from dorsal pronotum of each ant, dying in various positions biting into leaf margins, midribs and small branches. **E, F.** Mature, dark brown ascostromata (short arrows); atypically, in **E**, it is emerging from the lateral thorax. Note the leaf scars in **A**, **C** and **E** (long arrows), caused by repetitive biting prior to death. Scale bars = 2.5 mm.

© 2025 Westerdijk Fungal Biodiversity Institute

other genera of ants commonly infected by manipulative *Ophiocordyceps* (i.e., *Camponotus*, *Cephalotes*, *Daceton*, *Paraponera* and *Polyrhachis*) (Feitosa & Dias 2024). This life-history trait might have favoured infection and ultimately host-switching by *Ophiocordyceps* between hosts sharing the same ecological niche or habitat (Sanjuan *et al.* 2015, Araújo & Hughes 2019). The fact that workers forage alone rather than in collective trails is likely to influence how *O. acanthoponerae* infects and manipulates them. Their colony size, with fewer individuals, might also indicate host-parasite dynamics different from that described for *O. unilateralis* sensu lato on *Camponotini* (Andersen *et al.* 2012, Loreto *et al.* 2014).

In their recent review of behavioural manipulation, van Roosmalen & de Bekker (2024) stressed that more studies are needed to fully elucidate the infection biology of *Ophiocordyceps*. There is accumulating evidence which indicates "that the secretion of parasite proteins and light-driven biological rhythms are likely involved in the infection and manipulation biology" (van Roosmalen & de Bekker 2024). In particular, it is posited that *Ophiocordyceps* turn their ant hosts into light seekers (Andriolli *et al.* 2019). How this would relate to a nocturnal ant species, such as *A. mucronata*, would be worthy of further investigation.

CONCLUSIONS

The morphological and phylogenetic analyses confirm *O. acanthoponerae* as a new species within the genus *Ophiocordyceps*. The fungus presents mixed morphological traits related to the myrmecophilous and manipulative clade *O. unilateralis* (*O. unilateralis* core clade and *O. kniphofioides* sub-clade) and shows similarities with the wasp-parasitic fungus, *O. humbertii*. Significantly, the phylogenetic reconstruction showed that *O. acanthoponerae* falls outside of these 'traditional' clades and indicates the existence of a new lineage of myrmecophilous and manipulative fungi within the genus *Ophiocordyceps.* This is also the first record of *Heteroponerini* ants being infected by *Ophiocordyceps*, which expands our knowledge of the host range for these fungi. More work is needed, especially on the little-researched ant-host species, to further elucidate the biological and ecological factors that may influence this host-parasite interaction.

ACKNOWLEDGEMENTS

We would like to thank A. Chavier, S. Pontes Ribeiro, B. Clemente, G. de Paula, L. Viana, L. Reis, M. Moreira, M. Castro, N. Lima and R. Cardoso for logistical support during the field and laboratory analyses. We are grateful to R.W. Barreto and K. Yotoko for providing laboratory support. Special thanks go to J. Basílio, EET manager, for providing access and facilities during collections, to A. Lalas for constructing the map of the reserve and to F. Salles for photographic assistance. The Conselho Nacional de Desenvolvimento Científico e Tecnológico (CNPq) provided the doctorate scholarship (160886/2021-0) for SJLS. We are also grateful for additional financial support from the Coordenação de Aperfeiçoamento de Pessoal de Nível Superior - Brasil (CAPES) - Finance Code 001 and the Grant CNPq/INCT - Innovative Bioinputs (406803/2022-6). SLE and RMF were supported by CNPq Productivity Grants 315590/2021-1 and 304012/2023-8, respectively.

DATA AVAILABILITY

The sequences generated in this study are deposited with NCBI GenBank (Table 1) and the alignment and phylogenetic trees in Zenodo (doi: 10.5281/zenodo.16687083).

Conflict of Interest: The authors declare that they have no conflicts of interest.

REFERENCES

Andersen SB, Gerritsma S, Yusah KM, *et al.* (2009). The life of a dead ant: the expression of an adaptive extended phenotype. *The American Naturalist* **174**: 424–433. https://doi.org/10.1086/603640

Andersen SB, Ferrari M, Evans HC, *et al.* (2012). Disease dynamics in a specialized parasite of ant societies. *PLoS ONE* **7**: e36352. https://doi.org/10.1371/journal.pone.0036352

Andriolli FS, Ishikawa NK, Vargas-Isla R, *et al.* (2019). Do zombie ant fungi turn their hosts into light seekers? *Behavioural Ecology* **30**: 609–616. https://doi.org/10.1093/beheco/ary198

Araújo JPM, Evans HC, Geiser DM, *et al.* (2015). Unravelling the diversity behind the *Ophiocordyceps unilateralis* (*Ophiocordycipitaceae*) complex: Three new species of zombie-ant fungi from the Brazilian Amazon. *Phytotaxa* **220**: 224–238. https://doi.org/10.11646/phytotaxa.220.3.2

Araújo JPM, Hughes DP (2016). Diversity of entomopathogenic fungi: which groups conquered the insect body? *Advances in Genetics* **94**: 1–39. https://doi.org/10.1016/bs.adgen.2016.01.001

Araújo JPM, Hughes DP (2017). The fungal spore: myrmecophilous *Ophiocordyceps* as a case study. In: *The Fungal Community: Its Organization and Role in the Ecosystem* (Dighton J, White JF, eds). CRC Press, USA: 359–367.

Araújo JPM, Evans HC, Kepler R, *et al.* (2018). Zombie-ant fungi across continents: 15 new species and new combinations within *Ophiocordyceps*. I. Myrmecophilous hirsutelloid species. *Studies in Mycology* **90**: 119–160. https://doi.org/10.1016/j.simyco.2017.12.002

Araújo JPM, Hughes DP (2019). Zombie-ant fungi emerged from non-manipulating, beetle-infecting ancestors. *Current Biology* **29**: 3735–3738. https://doi.org/10.1016/j.cub.2019.09.004

Araújo JPM, Evans HC, Fernandes IO, *et al.* (2020). Zombie-ant fungi cross continents: II. Myrmecophilous hymenostilboid species and a novel zombie lineage. *Mycologia* **112**: 1138–1170. https://doi.org/10.1080/00275514.2020.1822093

Araújo JPM, Lebert BM, Vermeulen S, *et al.* (2022). Masters of the manipulator: two new hypocrealean genera, *Niveomyces* (*Cordycipitaceae*) and *Torrubiellomyces* (*Ophiocordycipitaceae*), parasitic on the zombie-ant fungus *Ophiocordyceps camponoti-floridani*. *Persoonia* **49**: 171–194. https://doi.org/10.3767/persoonia.2022.49.05

Baral B (2017). Entomopathogenicity and biological attributes of Himalayan treasured fungus *Ophiocordyceps sinensis* (Yarsagumba). *Journal of Fungi* **3**: 4. https://doi.org/10.3390/jof3010004

© 2025 Westerdijk Fungal Biodiversity Institute

Barbosa BC, Somavilla A (2022). New manipulation records of social wasps (*Hymenoptera*: *Vespidae*) behavior by the entomopathogenic *Ophiocordyceps* Petch (*Hypocreales*: *Ophiocordycipitaceae*) fungus. *Studies on Neotropical Fauna and Environment* **59**: 119–122. https://doi.org/10.1080/01650521.2022.2062184

Bolton B (2025). An online catalogue of the ants of the world. https://antcat.org. Accessed on 26 February 2025.

Branstetter MG, Danforth BN, Pitts JP, *et al.* (2017). Phylogenomic insights into the evolution of stinging wasps and the origins of ants and bees. *Current Biology* **27**: 1019–1025. https://doi.org/10.1016/j.cub.2017.03.027

Camacho GP, Franco W, Branstetter MG, *et al.* (2022). UCE phylogenomics resolves major relationships among ectaheteromorph ants (*Hymenoptera*: *Formicidae*: *Ectatomminae*, Heteroponerinae): a new classification for the subfamilies and the description of a new genus. *Insect Systematics and Diversity* **6**: 5. https://doi.org/10.1093/isd/ixab026

Chernomor O, von Haeseler A, Minh BQ. (2016). Terrace aware data structure for phylogenomic inference from supermatrices. *Systematic Biology* **65**: 997–1008. https://doi.org/10.1093/sysbio/syw037

Darriba D, Posada D, Kozlov, AM, *et al.* (2020). ModelTest-NG: a new and scalable tool for the selection of DNA and protein evolutionary models. *Molecular Biology and Evolution* **37**: 291–294. https://doi.org/10.1093/molbev/msz189

Evans HC (1982). Entomogenous fungi in tropical forest ecosystems: an appraisal. *Ecological Entomology* **7**: 47–60. https://doi.org/10.1111/j.1365-2311.1982.tb00643.x

Evans HC (1988). Coevolution of entomogenous fungi and their insect hosts. In: *Coevolution of Fungi with Plants and Animals* (Pirozynski KA & Hawksworth DL, eds). Academic Press: London: 149–171.

Evans HC, Samson RA (1982). *Cordyceps* species and their anamorphs pathogenic on ants (*Formicidae*) in tropical forest ecosystems I. The *Cephalotes* (*Myrmicinae*) complex. *Transactions of the British Mycological Society* **79**: 431–453. https://doi.org/10.1016/S0007-1536(82)80037-5

Evans HC, Samson RA (1984). *Cordyceps* species and their anamorphs pathogenic on ants (*Formicidae*) in tropical forest ecosystems II. The *Camponotus* (*Formicinae*) complex. *Transactions of the British Mycological Society* **82**: 127–150. https://doi.org/10.1016/S0007-1536(84)80219-3

Evans HC & Boddy L (2010). Animal slayers, saviours and socialists. In: *From Another Kingdom* (Boddy L, Coleman M, eds.). Royal Botanic Garden Edinburgh, Edinburgh: 68–81.

Evans HC, Elliot SL, Hughes DP (2011a). *Ophiocordyceps unilateralis*: A keystone species for unraveling ecosystem functioning and biodiversity of fungi in tropical forests? *Communicative & Integrative Biology* **4**: 598–602. https://doi.org/10.4161/cib.4.5.16721

Evans HC, Elliot SL, Hughes DP (2011b). Hidden diversity behind the zombie-ant fungus *Ophiocordyceps unilateralis*: four new species described from carpenter ants in Minas Gerais, Brazil. *PLoS ONE* **6**: e17024. https://doi.org/10.1371/journal.pone.0017024

Evans HC, Araújo JPM, Halfeld VR, *et al.* (2018). Epitypification and re-description of the zombie-ant fungus, *Ophiocordyceps unilateralis* (*Ophiocordycipitaceae*). *Fungal Systematics and Evolution* **1**: 13–22. https://doi.org/10.3114/fuse.2018.01.02

FEAM (1995). Fundação Estadual do Meio Ambiente. *Plano de Manejo da Estação Ecológica do Tripuí*, Ouro Preto, MG. Belo Horizonte: 1995. v. 1. https://ief.mg.gov.br/w/plano-de-manejo-estacao-ecologico-do-tripui

Feitosa RM (2015). Estado da arte sobre a taxonomia e filogenia de *Heteroponerinae*. In: *As formigas Poneromorfas do Brasil* (Delabie JHC, Feitosa RM, Serrão JE, Mariano CSF, Majer JD, eds). Editus, Brazil: 33–41. https://doi.org/10.7476/9788574554419

Feitosa RM, Dias AM (2024). An illustrated guide for the identification of ant subfamilies and genera in Brazil. *Insect Systematics & Evolution* **55**: 451–571. https://doi.org/10.1163/1876312X-bja10062

Feitosa RM, Prada-Achiardi FC (2019) Subfamilia *Ectatomminae*. In: *Hormigas de Colombia* (Fernandez F, Guerrero RJ, Delsinne T, eds). Universidad Nacional de Colombia, Colombia: 659–679.

Gatti FD, Carneiro MAA (2019). Estimation of the species richness of hyperdiverse beetles (*Coleoptera*: *Cerambycidae*) in an area of Atlantic Forest, Minas Gerais, southeastern Brazil. *Neotropical Biology and Conservation* **14**: 489–498. https://doi.org/10.3897/neotropical.14.e49026

Hoang DT, Chernomor O, von Haeseler A, *et al*. (2018). UFBoot2: Improving the ultrafast bootstrap approximation. *Molecular Biology and Evolution* **35**(2): 518-522. https://doi.org/10.1093/molbev/msx281

Huber JT (2017). Biodiversity of *Hymenoptera*. In: *Insect biodiversity: Science and Society* (Foottit RG, Adler PH, eds). John Wiley & Sons, USA: 419–461. https://doi.org/10.1002/9781118945568.ch12

Hughes DP, Wappler T, Labandeira CC (2011). Ancient death-grip leaf scars reveal ant–fungal parasitism. *Biology Letters* **7**: 67–70. https://doi.org/10.1098/rsbl.2010.0521

Hughes DP, Andersen S, Hywel-Jones NL, *et al.* (2011). Behavioral mechanisms and morphological symptoms of zombie ants dying from fungal infection. *BMC Ecology* **11**: 13. https://doi.org/10.1186/1472-6785-11-13

Hughes DP, Araújo JPM, Loreto RG, *et al.* (2016). From so simple a beginning: the evolution of behavioral manipulation by fungi. *Advances in Genetics* **94**: 437–469. https://doi.org/10.1016/bs.adgen.2016.01.004

Imirzian N, Araújo JPM, Hughes DP (2020). A new zombie ant behavior unraveled: Aggregating on tree trunks. *Journal of Invertebrate Pathology* **177**: 107499. https://doi.org/10.1016/j.jip.2020.107499

Kalyaanamoorthy S, Minh B, Wong T, *et al.* (2017). ModelFinder: fast model selection for accurate phylogenetic estimates. *Nature Methods* **14**: 587–589. doi: https://doi.org/10.1038/nmeth.4285

Kearse M, Moir R, Wilson A, *et al.* (2012). Geneious basic: an integrated and extendable desktop software platform for the organization and analysis of sequence data. *Bioinformatics* **28**: 1647–1649. https://doi.org/10.1093/bioinformatics/bts199

Kepler RM, Kaitsu Y, Tanaka E, *et al.* (2011). *Ophiocordyceps pulvinata sp. nov.*, a pathogen with a reduced stroma. *Mycoscience* **52**: 39–47. https://doi.org/10.1007/S10267-010-0072-5

Kepler RM, Luangsa-Ard JJ, Hywel-Jones NL, *et al.* (2017). A phylogenetically-based nomenclature for *Cordycipitaceae* (*Hypocreales*). *IMA Fungus* **8**: 335–353.

Kobmoo N, Mongkolsamrit S, Tasanathai K, *et al.* (2012). Molecular phylogenies reveal host-specific divergence *of Ophiocordyceps unilateralis sensu lato* following its host ants. *Molecular Ecology* **21**: 3022–3031. https://doi.org/10.1111/j.1365-294x.2012.05574.x

Kobmoo N, Mongkolsamrit S, Wutikhun T, *et al.* (2015). New

© 2025 Westerdijk Fungal Biodiversity Institute

species of *Ophiocordyceps unilateralis*, an ubiquitous pathogen of ants from Thailand. *Fungal Biology* **119**: 44–52. https://doi.org/10.1016/j.funbio.2014.10.008

Kobmoo N, Wichadakul D, Arnamnart N, *et al.* (2018). A genome scan of di versifying selection in *Ophiocordyceps* zombie-ant fungi suggests a role for enterotoxins in co-evolution and host specificity. *Molecular Ecology* **27**: 3582–3598. https://doi.org/10.1111/mec.14813

Loreto RG, Elliot SL, Freitas ML, *et al.* (2014). Long-term disease dynamics for a specialized parasite of ant societies: a field study. *PLoS ONE* **9**: e103516. https://doi.org/10.1371/journal.pone.0103516

Loreto RG, Araújo JPM, Kepler RM, *et al.* (2018). Evidence for convergent evolution of host parasitic manipulation in response to environmental conditions. *Evolution* **72**: 2144–2155. https://doi.org/10.1111/evo.13489

Luangsa-Ard JJ, Ridkaew R, Tasanathai K, *et al.* (2011). *Ophiocordyceps halabalaensis*: a new species of *Ophiocordyceps* pathogenic to *Camponotus gigas* in Hala Bala Wildlife Sanctuary, Southern Thailand. *Fungal Biology* **115**: 608–614. https://doi.org/10.1016/j.funbio.2011.03.002

MacKay WP (1993). A review of the New World ants of the genus *Dolichoderus* (*Hymenoptera*: *Formicidae*). *Sociobiology* **22**: 1–147.

Matsuura Y, Moriyama M, Łukasik P, *et al.* (2018). Recurrent symbiont recruitment from fungal parasites in cicadas. *Proceedings of National Academy of Sciences* USA **115**: 5970–5979. https://doi.org/10.1073/pnas.1803245115

Miller MA, Pfeiffer W, Schwartz T (2012). The CIPRES science gateway: Enabling high-impact science for phylogenetics researchers with limited resources. *ACM International Conference Proceedings* **39**: 1–8. https://doi.org/10.1145/2335755.2335836

Minh BQ, Schmidt HA, Chernomor O, *et al*. (2020). IQ-TREE 2: new models and efficient methods for phylogenetic inference in the genomic era. *Molecular Biology and Evolution* **37**: 1530–1534. https://doi.org/10.1093/molbev/msaa015

Murata N, Aoki T, Kusaba M, *et al.* (2014). Various species of *Pyricularia* constitute a robust clade distinct from *Magnaporthe salvinii* and its relatives in *Magnaporthaceae*. *Journal of General Plant Pathology* **80**: 66–72. https://doi.org/10.1007/s10327-013-0477-z

MycoBank (2025). MycoBank – an online database of fungal names and associated data. https://www.mycobank.org. Accessed on 26 February 2025.

Neto JAC, Leal LC, Baccaro FB (2019). Temporal and spatial gradients of humidity shape the occurrence and the behavioral manipulation of ants infected by entomopathogenic fungi in Central Amazon. *Fungal Ecology* **42**: 100871. https://doi.org/10.1016/j.funeco.2019.100871

Nguyen LT, Schmidt HA, Von Haeseler *et al.* (2015). IQ-TREE: a fast and effective stochastic algorithm for estimating maximum-likelihood phylogenies. *Molecular Biology and Evolution* **32**: 268–274. https://doi.org/10.1093/molbev/msu300

Pedralli G, Freitas VLO, Meyer ST, *et al.* (1997). Levantamento florístico na Estação Ecológica do Tripuí, Ouro Preto, MG. *Acta Botanica Brasilica* **11**: 191–213. https://doi.org/10.1590/S0102-33061997000200009

Petch T (1931). Notes on entomogenous fungi. *Transactions of the British Mycological Society*, **16**: 55–75. https://doi.org/10.1016/S0007-1536(31)80006-3

Petch T (1935). Notes on entomogenous fungi. *Transactions of the British Mycological Society*, **19**: 161–194. https://doi.org/10.1016/S0007-1536(35)80008-9

Petch T (1937). Notes on entomogenous fungi. *Transactions of the British Mycological Society*, **21**: 34–67. https://doi.org/10.1016/S0007-1536(37)80005-4

Pontoppidan MB, Himaman W, Hywel-Jones NL, *et al.* (2009). Graveyards on the move: the spatio-temporal distribution of dead *Ophiocordyceps*-infected ants. *PLoS ONE* **4**: e4835. https://doi.org/10.1371/journal.pone.0004835

Quandt CA, Kepler RM, Gams W, *et al.* (2014). Phylogenetic-based nomenclatural proposals for *Ophiocordycipitaceae* (*Hypocreales*) with new combinations in *Tolypocladium*. *IMA Fungus* **5**: 121–134. https://doi.org/10.5598/imafungus.2014.05.01.12

Rambaut A (2017). FigTree: tree figure drawing tool version 1.4.4. 2009. http://tree.bio.ed.ac.uk/software/figtree/

Rehner SA, Buckley E (2005). A *Beauveria* phylogeny inferred from nuclear ITS and EF1-α sequences: evidence for cryptic diversification and links to *Cordyceps* teleomorphs. *Mycologia* **97**: 84–98. https://doi.org/10.1080/15572536.2006.11832842

Sanjuan TI, Franco-Molano AE, Kepler RM, *et al.* (2015). Five new species of entomopathogenic fungi from the Amazon and evolution of neotropical *Ophiocordyceps*. *Fungal Biology* **119**: 901–916. https://doi.org/10.1016/j.funbio.2015.06.010

Shrestha UB, Bawa KS (2013). Trade, harvest, and conservation of caterpillar fungus (*Ophiocordyceps sinensis*) in the Himalayas. *Biological Conservation* **159**: 514–520. https://doi.org/10.1016/j.biocon.2012.10.032

Sobczak JF, Arruda IDP, Fonseca EO, *et al.* (2020). Manipulation of wasp (*Hymenoptera*: *Vespidae*) behavior by the entomopathogenic fungus *Ophiocordyceps humbertii* in the Atlantic forest in Ceará, Brazil. *Entomological News* **129**: 98–104. https://doi.org/10.3157/021.129.0115

Somavilla A, Barbosa BC, Prezoto F, *et al.* (2020). Infection and behavior manipulation of social wasps (*Vespidae*: *Polistinae*) by *Ophiocordyceps humbertii* in Neotropical forests: new records of wasp-zombification by a fungus. *Studies on Neotropical Fauna and Environment* **55**: 23–28. https://doi.org/10.1080/01650521.2019.1691908

Spatafora JW, Sung GH, Sung JM, *et al.* (2007). Phylogenetic evidence for an animal pathogen origin of ergot and the grass endophytes. *Molecular Ecology* **16**: 1701–1711. https://doi.org/10.1111/j.1365-294x.2007.03225.x

Stark AY, Yanoviak SP (2018). Adhesion and running speed of a tropical arboreal ant (*Cephalotes atratus*) on wet substrates. *Royal Society Open Science* **5**: 181540. https://doi.org/10.1098/rsos.181540

Sung GH, Hywel-Jones NL, Sung JM, *et al.* (2007). Phylogenetic classification of *Cordyceps* and the clavicipitaceous fungi. *Studies in Mycology* **57**: 5–59. https://doi.org/10.3114/sim.2007.57.01

Sung GH, Poinar Jr GO, Spatafora JW (2008). The oldest fossil evidence of animal parasitism by fungi supports a Cretaceous diversification of fungal–arthropod symbioses. *Molecular Phylogenetics and Evolution* **49**: 495–502. https://doi.org/10.1016/j.ympev.2008.08.028

Tang D, Huang O, Zou W. *et al.* (2023). Six new species of zombie-ant fungi from Yunnan in China. *IMA Fungus* **14**: 9. https://doi.org/10.1186/s43008-023-00114-9

Thines M (2019). An evolutionary framework for host shifts–jumping ships for survival. *New Phytologist* **224**: 605–617. https://doi.org/10.1111/nph.16092

van Roosmalen E, de Bekker C. (2024). Mechanisms underlying

© 2025 Westerdijk Fungal Biodiversity Institute

Ophiocordyceps infection and behavioral manipulation of ants: Unique or ubiquitous?. *Annual Review of Microbiology* **78**: 575–593. https://doi.org/10.1146/annurev-micro-041522-092522

Vilgalys R, Sun BL (1994). Ancient and recent patterns of geographic speciation in the oyster mushroom *Pleurotus* revealed by phylogenetic analysis of ribosomal DNA sequences. *Proceedings of the National Academy of Sciences USA* **91**: 4599–4603. https://doi.org/10.1073/pnas.91.16.7832

Wei DP, Gentekaki E, Wanasinghe DN, *et al.* (2022). Diversity, molecular dating and ancestral characters state reconstruction of entomopathogenic fungi in *Hypocreales*. *Mycosphere* **13**: 281–351. https://doi.org/10.5943/mycosphere/si/1f/8

Werneck MS, Pedralli G, Gieseke LF (2001), Produção de serapilheira em três trechos de uma floresta semidecídua com diferentes graus de perturbação na Estação Ecológica do Tripuí, Ouro Preto, MG. *Revista Brasileira Botânica* **24**: 185–198. https://doi.org/10.1590/S0100-84042001000200009

White TJ, Bruns T, Lee SJWT, *et al.* (1990). Amplification and direct sequencing of fungal ribosomal RNA genes for phylogenetics. In: *PCR Protocols: A Guide to Methods and Applications* (Innis MA, Gelfand DH, Sninsky JJ, White TJ, eds). Academic Press, USA: 315–322. https://doi.org/10.1016/B978-0-12-372180-8.50042-1

Will I, Linehan S, Jenkins DG, *et al.* (2023). Natural history and ecological effects on the establishment and fate of Florida carpenter ant cadavers infected by the parasitic manipulator *Ophiocordyceps camponoti-floridani*. *Functional Ecology* **37**: 886–899. https://doi.org/10.1111/1365-2435.14224

Yu FM, Thilini Chethana KW, Wei DP, *et al.* (2021). Comprehensive review of *Tolypocladium* and description of a novel lineage from Southwest China. *Pathogens* **10**: 1389. https://doi.org/10.3390/pathogens10111389

Supplementary Material: http://fuse-journal.org/

Fig. S1. Single-locus Maximum likelihood tree of *Ophiocordyceps* for the translation elongation factor 1-α (*TEF*) genomic region. Numbers on nodes represent bootstrap values > 70 %. *Ophiocordyceps acanthoponerae sp. nov*. is indicated in **bold** font. The whole analysis tree of the order *Hypocreales* is depicted in the top-left corner, with the position of the clade containing *O. acanthoponerae* highlighted in orange.

Fig. S2. Single-locus Maximum likelihood tree of *Ophiocordyceps* for the RNA polymerase II largest subunit (*RPB1*) genomic region. Numbers on nodes represent bootstrap values > 70 %. *Ophiocordyceps acanthoponerae sp. nov*. is indicated in **bold** font. The whole analysis tree of the order *Hypocreales* is depicted in the top-left corner, with the position of the clade containing *O. acanthoponerae* highlighted in orange.

Table S1. List of species from the order *Hypocreales*, vouchers, GenBank accession numbers and host associations, with exception of *Ophiocordyceps* which is in Table 1.

© 2025 Westerdijk Fungal Biodiversity Institute

FUSE

Fungal Systematics and Evolution

VOLUME 16
DECEMBER 2025
PAGES 265–281

doi.org/10.3114/fuse.2025.16.15

Two novel species of *Pestalotiopsis* on *Picea* and *Tsuga* from temperate forests in the United States

S.T. Miller[1,2], C. Salgado-Salazar[1*], I. Munck[3], L.A. Castlebury[1]

[1]Mycology and Nematology Genetic Diversity and Biology Laboratory, U.S. Department of Agriculture, Agriculture Research Service (USDA-ARS), Beltsville, MD 20705, USA
[2]Oak Ridge Institute for Science and Education, ARS Research Participation Program, Oak Ridge, TN 37831, USA
[3]Eastern Region State, Private and Tribal Forestry, U.S. Department of Agriculture, U.S. Forest Service, 271 Mast Rd., Durham, NH 03824, USA

*Corresponding author: catalina.salgado@usda.gov

Key words:
Ascomycota
conifer
hemlock
new taxa
Sporocadaceae
spruce

Abstract: In a 2023 survey evaluating conifers with *Rosellinia* infections, five *Pestalotiopsis* fungal strains were isolated from plant samples obtained from Maine, New Hampshire, and Ohio. Based on a multi locus phylogenetic analysis (ITS, *TUB*, *TEF*), species-specific base pair substitutions, and morphological characterization, the five isolates were determined to constitute two novel species within the genus *Pestalotiopsis*. These two new species are introduced here as *Pestalotiopsis maineana* and *Pestalotiopsis neohantoniensis*. *Pestalotiopsis maineana* shares close phylogenetic affinity to *P. fusiformis*, *P. brachiata*, and *P. hispanica,* while *P. neohantoniensis* shares affinity with *P. daliensis*, *P. chamaeropis,* and *P. hainanensis.* Both new species described herein differ from close relatives based on various morphological characters including the number of basal appendages of the conidia. Further, species-specific base pair substitutions are provided for the *TEF* locus which had the most resolution when compared to the ITS and *TUB* loci. To our knowledge, *P. maineana* is the first species of *Pestalotiopsis* to be isolated and reported from white spruce (*Picea glauca*) while *P. neohantoniensis* is the first species to be isolated and reported from Serbian spruce (*Picea omorika*) and eastern hemlock (*Tsuga canadensis*). Overall, this study provides insight into the microfungi associated with conifers in the United States.

Citation: Miller ST, Salgado-Salazar CS, Munck I, Castlebury LA (2025). Two novel species of *Pestalotiopsis* on *Picea* and *Tsuga* from temperate forests in the United States. *Fungal Systematics and Evolution* **16**: 265–281. doi: 10.3114/fuse.2025.16.15
Received: 27 March 2025; **Accepted:** 27 June 2025; **Effectively published online:** 8 August 2025
Corresponding editor: P.W. Crous

INTRODUCTION

In the United States (US) forests are economically and ecologically important systems covering approximately 38 % of the land in the country, estimated to be 8 % of the world's total forest area (Renwick 2023). Maine (ME) and New Hampshire (NH) are the two most heavily wooded states in the US with 89 and 83 % forest coverage, respectively (USDA FS 2022a, USDA FS 2022b). The most common type of forest in ME and NH is the maple/beech/birch forest; whereas spruce/fir and white/red pine are the most common softwood forests (Butler 2017, Morin & Lombard 2017). While there are various threats to forests in North America, emerging or re-emerging diseases remain a concern as they can significantly alter existing ecosystem diversity (Guegan *et al.* 2023). Historically, there has been concern for the spread of *Rosellinia* species from nursery planted to naturally regenerative conifers (Shea 1964, Francis 1986). The shift in community diversity caused by host mortality from emerging diseases directly affects forest ecosystems; thus, in 2023 concern for the spread of Rosellinia needle blight between conifer species prompted creation of a surveillance program and the collection of symptomatic plant tissue. The collected plant samples usually yield isolates of *Pestalotiopsis*-like fungi, as well as the target pathogen *Rosellinia*.

The genus *Pestalotiopsis* consists of asexual species with appendage-bearing conidia (Stayaert 1949). The genus is currently placed in the family *Sporocadaceae*, order *Amphisphaeriales*, class *Sordariomycetes*, in the *Ascomycota* (Wijayawardene *et al.* 2020). *Pestalotiopsis* was segregated from *Pestalotia* by Stayaert (1949) based on conidium cell number. More recently, Jaklitsch *et al.* (2016) synonymized *Bartaliniaceae*, *Discosiaceae*, *Pestalotiopsidaceae*, and *Robillardaceae* with *Sporocadaceae* and placed the family within the order *Xylariales*. However, *Amphisphaeriales* was later resurrected over *Xylariales* for the placement of *Sporocadaceae* (Hyde *et al.* 2020, Wijayawardene *et al.* 2020). To date, 445 species of *Pestalotiopsis* have been described (https://www.indexfungorum.org 2025). Species of *Pestalotiopsis* are usually described based on conidial morphology (i.e. apical and basal appendages) paired with gene sequence data. The length, number, position, and branching pattern of the apical or basal appendages are often utilized to differentiate between closely related species (Crous *et al.* 2012, Maharachchikumbura *et al.* 2012). When discerning between species of *Pestalotiopsis* through phylogenetic analyses, current studies use the ITS, *TUB*, and *TEF* gene regions as these have been reported as the most effective in resolving species within

Fungal Systematics and Evolution is licensed under a Creative Commons Attribution-NonCommercial-NoDerivatives 4.0 International License

© 2025 Westerdijk Fungal Biodiversity Institute

the genus. Maharachchikumbura *et al.* (2012) evaluated 10 loci including ACT, *TUB*, CAL, GPDH, GS, ITS, LSU, RPB 1, SSU and *TEF*; they reported ITS, *TUB*, and *TEF* as providing the most resolution with *TEF* being the most informative locus.

Species of *Pestalotiopsis* vary in lifestyle and host specificity. They have been reported as saprophytes, endophytes, plant pathogens, animal/human pathogens, and as parasymbionts (Maharachchikumbura *et al.* 2011, Li *et al.* 2024, Luo *et al.* 2024). Although historically reported as endophytic and weak/ opportunistic pathogens, some studies have shown some species can be aggressive plant pathogens in various agricultural and horticultural systems, including but not limited to tea (*Camellia sinensis*), coconut (*Cocos nucifera*), pine (*Pinus massoniana*) and hardy ornamentals such as *Calluna vulgaris*, *Erica carnea*, and *Rhododendron* spp. (Hopkins & McQuilken 2000, Sanjay *et al.* 2008, Maharachchikumbura *et al.* 2013, Chen *et al.* 2018, Bhuiyan *et al.* 2021, Li *et al.* 2024). Some species, such as *P. microspora*, have been observed to switch between being endophytic and pathogenic depending on physiological and environmental factors (Lee 1995, Maharachchikumbura *et al.* 2011).

The objectives of this study were to identify and characterize *Pestalotiopsis* species isolated from conifer samples affected by Rosellinia needle blight. Based on a multi locus phylogenetic analysis, species-specific base pair substitutions, and spore morphology, we introduce here two novel species of *Pestalotiopsis* from conifers in the US.

MATERIALS AND METHODS

Sampling, isolation, and morphological characterization

Trees displaying signs and symptoms of Rosellinia needle blight were targeted for collection. Branches were collected from eastern hemlock trees (*Tsuga canadensis*) in Hillsborough County, New Hampshire and Hocking County, Ohio in December of 2023. Branches from white spruce (*Picea glauca*) and Serbian spruce (*Picea omorika*) were collected in Hancock County, Maine in November of 2023. Eleven collected samples were mailed to the Mycology and Nematology Genetic Diversity and Biology Laboratory, U.S. Department of Agriculture, Agricultural Research Service in Beltsville, Maryland, USA, for analysis. Segments of plant tissue no larger than 2 cm^3 adjacent to *Rosellinia* perithecia, were removed from branches and sterilized with 10 % sodium hypochlorite (Clorox™; Oakland, CA, USA) for 3 min and rinsed with sterile distilled water before being air dried. The cut segments included the margin between the plant tissue showing *Rosellinia* symptoms and the adjacent asymptomatic plant tissue. Cut segments were then placed on P4083 Penicillin – Streptomycin – Neomycin antibiotic microbial solution (Sigma-Aldrich; St. Louis, Missouri, USA) supplemented corn meal agar (CMA) (BD Difco; Franklin Lakes, NJ, USA) and incubated at 21–25 °C under an alternating 12-h light and 12-h dark schedule. Following growth of fungi, hyphal tips were transferred to potato dextrose agar (PDA) (BD Difco; Franklin Lakes, NJ, USA) and incubated at 21–25 °C under the same light regimen. Once pure cultures were obtained, agar plugs of isolates were transferred to cryogenic tubes with sterile 20 % MB grade glycerol (USB Corporation; Cleveland, OH, USA) diluted with ultrapure water, for long-term storage. Living cultures were deposited at the Westedijk Fungal Biodiversity Institute culture collection (CBS), while dried specimens were deposited at the US National Fungus Collection (BPI) (Table 1).

For morphological observations, the *Pestalotiopsis* cultures were grown for 21 d on PDA and synthetic nutrient poor agar (SNA; Nirenberg 1981) at 25 °C with 12 h of light and 12 h of darkness. Growth rates and morphological characteristics of colonies were evaluated every 7 d for 3 wk. Colour of the colonies were determined using the Rayner (1970) colour chart. Photographs of colonies on agar plates were taken with a Canon EOS 5D Mark III digital camera (Canon; Tokyo, Japan) in a lighting booth (MK Digital Direct). To induce conidiomatal development, twice autoclaved pine needles were placed on SNA as described by Maharachchikumbura *et al.* (2014). Morphological structures were evaluated on 85 % lactic acid slides after incubation on a warming plate at 50 °C for a minimum of 30 min prior to examination with a Zeiss Axio Imager M2 compound microscope (Zeiss, Jena, Germany). At least 30 measurements were taken for each reported structure. Descriptive statistics are presented and include minimum-maximum, mean, and standard deviation.

DNA extraction, PCR amplification, sequencing

In preparation for extraction of DNA, single hyphal-tipped isolates were grown on full strength PDA plates for 4 wk at 25 °C with alternating 12 h of light and 12 h of darkness. The hyphal mat was then scraped, and mycelia were transferred to 2 mL polypropylene tubes with 500 µm garnet beads and a 6-mm-diam. zirconium bead (OPS Diagnostics, Lebanon, NJ, USA). The tissue was lysed with a Precellys® Evolution homogenizer (Bertin instruments, France). After lysis, DNA was extracted using the E.Z.N.A. HP Plant & Fungal DNA Kit (OMEGA® Bio-Tek, Norcross, GA, USA) following manufacturer's protocol.

Three loci were amplified, including the internal transcribed spacer (ITS: ITS5/ITS4) (White *et al.*1990), partial beta-tubulin gene (*TUB*: T1/Bt-2b) (Glass & Donaldson 1995, O'Donnell & Cigelnik 1997), and partial translation elongation factor 1-alpha gene (*TEF*: EF1-728/ EF-2) (O'Donnell *et al.* 1998, Carbone & Kohn 1999). Amplification reactions were conducted in 25 µL volumes with 12.5 µL of KAPA2G Robust Hotstart® (Kapa Biosystems, Inc., Wilmington, MA, USA), 1.25 µL of the forward and reverse primers at 10 µM, 1–1.75 µL of DNA at 10–20 ng, and 8 µL of molecular grade H2O. Amplifications were performed following the protocol described by Maharachchikumbura *et al.* (2014) in a C1000 Touch PCR Thermal Cycler (Bio-Rad, Hercules, CA). The PCR products were analysed through capillary electrophoresis using the QIAxcel Advanced System instrument and the QIAxcel ScreenGel software (Qiagen, Hilden, Germany). The PCR products were then purified using ExoSAP-IT Cleanup (Affymetrix, Santa Clara, CA) following the manufacturer's protocol. The BigDye™ v. 3.1 Terminator Cycle sequencing kit was used to sequence amplicons bi-directionally with the Applied Biosystems SeqStudio Genetic Analyzer (Thermo Fisher Scientific, Waltham, MA, USA).

© 2025 Westerdijk Fungal Biodiversity Institute

Table 1. Taxa used for phylogenetics analyses.

Species	Strain Number	Type	*Host*	Location	GenBank Accession			Reference
					ITS	*TUB*	*TEF*	
Neopestalotiopsis saprophytica	MFLUCC 12-0282	**T**	*Magnolia* sp. (*Magnoliaceae*)	China	JX398982	JX399017	JX399048	Maharachchikumbura *et al.* (2014)
Pestalotiopsis abietis	*CFCC 53011*	**T**	*Abies fargesii* (*Pinaceae*)	China	*MK397013*	*MK622280*	*MK622277*	Gu *et al.* (2021)
P. abietis	*CFCC 53012*		*Abies fargesii* (*Pinaceae*)	China	*MK397014*	*MK622281*	*MK622278*	Gu *et al.* (2021)
P. americana	CBS 111576	**T**	*Leucospermum cunei* × *conocarpodendron* (*Proteaceae*)	USA	MH553961	MH554620	MH554379	Liu *et al.* (2019)
P. anhuiensis	*CFCC 54791*	**T**	*Cyclobalanopsis glauca* (*Fagaceae*)	China	*ON007028*	*ON005056*	*ON005045*	Jiang *et al.* (2022)
P. appendiculata	CGMCC 3.23550	**T**	*Rhododendron decorum* (*Ericaceae*)	China	OP082431	OP185516	OP185509.1	Gu *et al.* (2022)
P. australasiae	*CBS 114126*	**T**	*Knightia* sp. (*Proteaceae*)	New Zealand	*KM199297*	*KM199409*	KM199499	Maharachchikumbura *et al.* (2014)
P. australis	CBS 114193; STE-U 3011	**T**	*Grevillea* sp. (*Proteaceae*)	Australia	KM199332	KM199383	KM199475	Maharachchikumbura *et al.* (2014)
	CBS 111503; STE-U 1770		*Protea neriifoliax susannae* cv. "Pink Ice" (*Proteaceae*)	South Africa	KM199331	KM199382	KM199557	Maharachchikumbura *et al.* (2014)
	CBS 114474; STE-U 1769		*Protea neriifoliax susannae* cv. "Pink Ice" (*Proteaceae*)	South Africa	KM199334	KM199385	KM199477	Maharachchikumbura *et al.* (2014)
	CBS 119350; CMW 20013		*Brabejum stellatifolium* (*Proteaceae*)	South Africa	KM199333	KM199384	KM199476	Maharachchikumbura *et al.* (2014)
P. biciliata	CBS 124463	**T**	*Platanus hispanic* (*Platanaceae*)	Slovakia	KM199308	KM199399	KM199505	Maharachchikumbura *et al.* (2014)
	CBS 236.38		*Paeonia* sp. (*Paeoniaceae*)	Italy	KM199309	KM199401	KM199506	Maharachchikumbura *et al.* (2014)
P. brachiata	LC2988	**T**	*Camellia* sp. (*Theaceae*)	China	NR_175047.1	KX895265.1	KX895150.1	Liu *et al.* (2017)
	LC8188		*Camellia* sp. (*Theaceae*)	China	KY464142.1	KY464162.1	KY464152.1	Liu *et al.* (2017)
	LC8189		*Camellia* sp. (*Theaceae*)	China	KY464143.1	KY464163.1	KY464153.1	Liu *et al.* (2017)
P. brassicae	CBS 170.26	**T**	*Brassica napus* (*Brassicaceae*)	New Zealand	KM199379	—	KM199558	Maharachchikumbura *et al.* (2014)
P. camelliae-oleiferae	CSUFTCC08	**T**	*Camellia oleifera* (*Theaceae*)	China	OK493593	OK562368	OK507963	Li *et al.* (2021)
	CSUFTCC09		*Camellia oleifera* (*Theaceae*)	China	OK493594	OK562369	OK507964	Li *et al.* (2021)
P. chamaeropis	CBS 186.71	**T**	*Chamaerops humilis* (*Arecaceae*)	Italy	KM199326	KM199391	KM199473	Maharachchikumbura *et al.* (2014)
	CBS 113604; STE-U 3078		n/a	n/a	KM199323	KM199389	KM199471	Maharachchikumbura *et al.* (2014)
	CBS 113607; STE-U 3080		n/a	n/a	KM199325	KM199390	KM199472	Maharachchikumbura *et al.* (2014)

© 2025 Westerdijk Fungal Biodiversity Institute

Table 1. (Continued).

Species	Strain Number	Type	*Host*	Location	GenBank Accession			Reference
					ITS	*TUB*	*TEF*	
P. chamaeropis	CBS 237.38		n/a	n/a	KM199324	KM199392	KM199474	Maharachchikumbura *et al.* (2014)
P. chinensis	*MFLUCC 12–0273*	**T**	n/a	*China*	JX398995	—	—	Maharachchikumbura *et al.* (2012)
P. clavata	MFLUCC 12-0268; NN0471340	**T**	*Buxus* sp. (*Buxaceae*)	China	JX398990	JX399025	JX399056	Maharachchikumbura *et al.* (2012)
	MFLUCC 12–0268	**T**	*Buxus* sp. (*Buxaceae*)	China	*JX398990*	*JX399025*	JX399056	Maharachchikumbura *et al.* (2012)
P. daliensis	CGMCC 3.23548 = KUNCC 22-12403	**T**	*Rhododendron decorum* (*Ericaceae*)	China	OP082429	OP185518	OP185511	Gu *et al.* (2022)
P. digitalis	*MFLU 14-0208*	**T**	*Digitalis purpurea* (*Plantaginaceae*)	*New Zealand*	*KP781879*	KP781883	—	Liu *et al.* (2015)
P. disseminata	CBS 143904		*Persea americana* (*Lauraceae*)	New Zealand	MH554152.1	MH554825.1	MH554587.1	Liu *et al.* (2019)
P. endophytica	MFLUCC 18-0932	**T**	*Magnolia garrettii* (*Magnoliaceae*)	Thailand	PQ129358.1	—	MW417119.1	De Silva *et al.* (2021)
P. exudata	*CGMCC 3.23488*	**T**	*Aucuba japonica* (*Garryaceae*)	China	*OR247985*	*OR381060*	*OR361460*	Razaghi *et al.* (2024)
	LC15850		*Aucuba japonica* (*Garryaceae*)	China	*OR247986*	*OR381061*	OR361461	Razaghi *et al.* (2024)
P. ficicrescens	GUCC21556	**T**	*Ficus tikoua* (*Moraceae*)	China	MZ477311	MZ868301	MZ868328	Hyde *et al.* (2023)
	LC12337; CGMCC3.23471		*Oleaceae*	China	OR247980	OR381055	OR361455	Razaghi *et al.* (2024)
	LC2960		*Cleyera japonica* (*Theaceae*)	China	OR247983	OR381058	OR361458	Razaghi *et al.* (2024)
P. fusiformis	LC4365; CGMCC3.23495	**T**	*Rhododendron* sp. (*Ericaceae*)	China	OR247995	OR381070	OR361470	Razaghi *et al.* (2024)
	LC15852		*Rhododendron* sp. (*Ericaceae*)	China	OR247996	OR381071	OR361471	Razaghi *et al.* (2024)
P. fusoidea	*CGMCC 3.23545*	**T**	*Rhododendron delavayi* (*Ericaceae*)	China	*OP082427*	OP185519	OP185512	Gu *et al.* (2022)
P. ganzhouensis	*CGMCC 3.23489*	**T**	*Cinnamomum camphora* (*Lauraceae*)	China	*OR247987*	*OR381062*	*OR361462*	Razaghi *et al.* (2024)
	LC5089		*Cinnamomum camphora* (*Lauraceae*)	China	*OR247998*	*OR381073*	*OR361473*	Razaghi *et al.* (2024)
P. grandis-urophylla	*E72-04*		*Eucalyptus grandis* (*Myrtaceae*)	Brazil	*KU926710*	*KU926718*	KU926714	Carvalho *et al.* (2019)
P. grevilleae	CBS 114127; STE-U 2919	**T**	*Grevilleae* sp. (*Proteaceae*)	Australia	KM199300	KM199407	KM199504	Maharachchikumbura *et al.* (2014)
P. guangxiensis	CFCC 54308	**T**	*Quercus griffithii* (*Fagaceae*)	China	*OK339737*	OK358513	*OK358498*	Jiang *et al.* (2022)
P. guiyangensis	*CFCC 70626*		*Eriobotrya japonicac* (*Rosaceae*)	China	PP784740	PP842617	*PP842629*	Zhang *et al.* (2013)
	CFCC 70630		*Rohdea japonica* (*Asparagaceae*)	China	*PP784741*	PP842618	*PP842630*	Zhang *et al.* (2013)
P. hainanensis	PSHI2004Endo166	**T**	*Podocarpus macrophyllus* (*Podocarpaceae*)	China	DQ334863	DQ137861	—	Liu *et al.* (2007)
	GUCC 23-0314		n/a	n/a	PQ129355.1	PQ148940.1	PQ140990.1	Unpublished (Genbank)
P. hederae	HJAUP C1638.221	**T**	*Hedera helix* (*Araliaceae*)	China	*PP962270*	*PP952234*	*PP952252*	Luo *et al.* (2024)

© 2025 Westerdijk Fungal Biodiversity Institute

Table 1. (Continued).

Species	Strain Number	Type	*Host*	Location	GenBank Accession			Reference
					ITS	*TUB*	*TEF*	
P. hederae	*HJAUP C1638.222*		*Hedera helix* (*Araliaceae*)	China	*PP962271*	*PP952216*		Luo *et al.* (2024)
P. heterocornis	PSHI2002Endo303		*C. japonica* (*Theaceae*)	n/a	AY687874.1	DQ137867.1	—	Liu *et al.* (2007)
P. hispanica	CBS 115391 = CPC5193	**T**	*Protea* cv. 'Susara' (*Proteaceae*)	Spain	MH553981	MH554640	MH554399	Liu *et al.* (2019)
P. hollandica	CBS 265.33	**T**	*Sciadopitys verticillata* (*Sciadopityaceae*)	Netherlands	KM199328	KM199388	KM199481	Maharachchikumbura *et al.* (2014)
P. hydei	*MFLUCC 20–0135*	**T**	*Litsea elliptica* (*Lauraceae*)	Thailand	*MW266063*	MW251112	*MW251113*	Huanaluek *et al.* (2021)
P. iberica	*CAA 1004*	**T**	*Pinus radiata* (*Pinaceae*)	Spain	MW732248	MW759035	MW759038	Monteiro *et al.* (2022)
P. intermedia	MFLUCC 12-0259; NN0476420	**T**	Unidentified tree	China	JX398993	JX399028	JX399059	Maharachchikumbura *et al.* (2012)
P. italiana	MFLUCC12-0657	**T**	*Cupressus glabra* (*Cupressaceae*)	Italy	KP781878	KP781882	KP781881	Liu *et al.* (2015)
P. jiangxiensis	LC4399	**T**	*Camellia* sp. *(Theaceae*)	China	KX895009	KX895341	KX895227	Liu *et al.* (2017)
	LC4242		*Eurya* sp. *(Pentaphylacaceae*)	China	KX895035	KX895327	KX895213	Liu *et al.* (2017)
P. kaki	*KNU–PT–1804*	**T**	*Diospyros kaki* (*Ebenaceae*)	Korea	*LC552953*	*LC552954*	LC553555	Das *et al.* (2021)
P. kenyana	*CBS 442.67*	**T**	*Coffea* sp. *(Rubiaceae*)	Kenya	*KM199302*	*KM199395*	*KM199502*	Maharachchikumbura *et al.* (2014)
P. knightiae	CBS 114138; STE-U 2906	**T**	*Knightia* sp. (*Proteaceae*)	New Zealand	KM199310	KM199408	KM199497	Maharachchikumbura *et al.* (2014)
	CBS 111963; STE-U 2905		*Knightia* sp. (*Proteaceae*)	New Zealand	KM199311	KM199406	KM199495	Maharachchikumbura *et al.* (2014)
P. lawsoniae	PSH2000I-057		*Pinus massoniana* (*Pinaceae*)	n/a	AY687871	DQ333577	—	Liu *et al.* (2007)
P. lespedezae	*SY16E*		*Pinus armandii* (*Pinaceae*)	China	*EF055205*	—	*EF055242*	Hu *et al.* 2007
P. leucadendri	CBS 121417	**T**	*Leucadendron* sp. (*Proteaceae*)	South Africa	MH553987	MH554654	MH554412	Liu *et al.* (2019)
P. linearis	MFLUCC 12-0271; NN0471900	**T**	*Trachelospermum* sp. (*Apocynaceae*) & *Tsuga* sp. *(Pinaceae*)	China	JX398992	JX399027	JX399058	Maharachchikumbura *et al.* (2012)
P. lobata	*CGMCC 3.23467 T*	**T**	*Lithocarpus glaber* (*Fagaceae*)	China	*OR247976*	*OR381051*	*OR361451*	Razaghi *et al.* (2024)
	LC15843		*Lithocarpus glaber* (*Fagaceae*)	*China*	OR247977	OR381052	OR361452	Razaghi *et al.* (2024)
P. lushanensis	*LC4344*	**T**	*Camellia* sp. *(Theaceae*)	China	*KX895005*	*KX895337*	*KX895223*	Liu *et al.* (2017)
P. macadamiae	*BRIP 63738b*	**T**	*Macadamia integrifolia* (*Proteaceae*)	Australia	*KX186588*	*KX186680*	*KX186621*	Akinsanmi *et al.* (2017)
P. machiliana	*HJAUP C1790.221*	**T**	*Machilus pauhoi* (*Lauraceae*)	China	*PP962355*	PP952214	PP952253	Luo *et al.* (2024)
	HJAUP C1790.222		*Machilus pauhoi* (*Lauraceae*)	China	*PP962356*	PP952215	PP952254	Luo *et al.* (2024)
P. mainena	CBS 153151	**T**	*Picea glauca* (*Pinaceae*)	United States	PQ568305	PQ573018	PQ573023	This Study
	CBS 153150		*Picea glauca* (*Pinaceae*)	United States	PQ568304	PQ573017	PQ573022	This Study
P. mangifolia	PSHI2002Endo672		*Cameillia sasanqua* (*Theaceae*)	n/a	AY687307.1	DQ333578	—	Liu *et al.* (2007)

© 2025 Westerdijk Fungal Biodiversity Institute

Table 1. (Continued).

Species	Strain Number	Type	*Host*	Location	GenBank Accession			Reference
					ITS	*TUB*	*TEF*	
P. menhaiensis	*YN3A1*	**T**	*Camellia sinensis* (*Theaceae*)	China	*KU252272*	*KU252488*	KU252401	Wang *et al.* (2019)
P. microspora	*SS1-033I*		*Cornus canadensis* (*Cornaceae*)	Canada	*MT644300*	—	—	Unpublished (Genbank)
P. monochaeta	CBS 144.97	**T**	*Quercus robur* (*Fagaceae*)	Netherlands	KM199327	KM199386	KM199479	Maharachchikumbura *et al.* (2014)
	CBS 440.83; IFO 32686		*Taxus baccata* (*Taxaceae*)	Netherlands	KM199329	KM199387	KM199480	Maharachchikumbura *et al.* (2014)
P. multicolor	CFCC59981	**T**	*Taxus chinensis* (*Taxaceae*)	China	OQ626676	OQ714336	OQ714341	Wang *et al.* (2024)
	CFCC59982		*Taxus chinensis* (*Taxaceae*)	China	OQ771896	OQ779488	OQ779483	Wang *et al.* (2024)
	LC3616; CGMCC 3.23171		*Camellia* sp. (*Theaceae*)	China	KX894990	KX895321	KX895207	Liu *et al.* (2017)
P. neohantoniensis	CBS 153149	**T**	*Tsuga canadensis* (*Pinaceae*)	United States	PQ568303	PQ573016	PQ573021	This study
	CBS 153152		*Picea omrorika* (*Pinaceae*)	United States	PQ568306	PQ573019	PQ573024	This study
	CBS 153153		*Tsuga canadensis* (*Pinaceae*)	United States	PQ568307	PQ573020	PQ573025	This study
P. olivacea	PSHI2002Endo696		*Cameillia sasanqua* (*Theaceae*)	n/a	AY687883	DQ333580	—	Liu *et al.* (2007)
P. oryzae	*CBS 353.69*	**T**	*Oryza sativa* (*Poaceae*)	Denmark	*KM199299*	KM199398	*KM199496*	Maharachchikumbura *et al.* (2014)
P. parva	CBS 278.35	**T**	*Leucothose fontanesiana* (*Ericaceae*)	n/a	KM199313	KM199405	KM199509	Maharachchikumbura *et al.* (2014)
	CBS 265.37; BBA 2820		*Delonix regia* (*Fabaceae*)	n/a	KM199312	KM199404	KM199508	Maharachchikumbura *et al.* (2014)
P. phoebes	*SAUCC230093*	**T**	*Phoebe zhennan* (*Lauraceae*)	China	*OQ692028*	*OQ718803*	*OQ718745*	Zhang *et al.* (2023)
P. pini	*MEAN 1092*	**T**	*Pinus pinea* (*Pinaceae*)	Portugal	*MT374680*	*MT374705*	*MT374693*	Silva *et al.* (2020)
P. piraubensis	*COAD 2165*	**T**	*Psidium guajava* (*Myrtaceae*)	Brazil	*MH627381*	MH643773	*MH643774*	Jayawardena *et al.* (2022)
P. pruni	*CGMCC 3.23507*	**T**	*Prunus cerasoides* (*Rosaceae*)	China	*OR248001*	*OR381076*	OR361476	Razaghi *et al.* (2024)
P. rhododendri	IFRDCC 2399	**T**	*Rhododendron sinogrande* (*Ericaceae*)	China	KC537804	KC537818	KC537811	Zhang *et al.* (2013)
P. rosarioides	CGMCC 3.23549	**T**	*Rhododendron decorum* (*Ericaceae*)	China	OP082430	OP185520	OP185513	Gu *et al.* (2022)
P. rosea	MFLUCC 12-0258; NN0471350	**T**	*Pinus* sp. (*Pinaceae*)	China	JX399005	JX399036	JX399069	Maharachchikumbura *et al.* (2012)
P. rubrae	LC4567; CGMCC 3.23499	**T**	*Quercus rubra* (*Fagaceae*)	China	OR247997	OR381072	OR361472	Razaghi *et al.* (2024)
P. rubrae	LC8233		*Plagiogyria glauca* (*Plagiogyriaceae*)	China	OR248000	OR381075	OR361475	Razaghi *et al.* (2024)
P. scoparia	CBS 176.25	**T**	*Chamaecyparis* sp. (*Cupressaceae*)	n/a	KM199330	KM199393	KM199478	Maharachchikumbura *et al.* (2014)
	CBS296.58		*Picea* rootstock (*Pinaceae*)	Netherlands	MH554026	MH554703	MH554461	Liu *et al.* (2019)
P. sequoia	*MFLUCC 13–0399*	**T**	*Sequoia sempervirens* (*Cupressaceae*)	Italy	*KX572339*	—	—	Hyde *et al.* (2016)

© 2025 Westerdijk Fungal Biodiversity Institute

Table 1. (Continued).

Species	Strain Number	Type	*Host*	Location	GenBank Accession			Reference
					ITS	*TUB*	*TEF*	
P. shaanxiensis	*CFCC 54958*	**T**	*Quercus variabilis* (*Fagaceae*)	China	ON007026	ON005054	ON005043	Jiang *et al.* (2022)
P. shandogensis	*JZB340038*	**T**	*Robinia pseudoacacia* (*Fabaceae*)	China	MN625275	*MN626729*	*MN626740*	Unpublished (Genbank)
P. taxicola	CFCC59976	**T**	*Taxus chinensis* (*Taxaceae*)	China	OQ626673	OQ714333	OQ714338	Wang *et al.* (2024)
	CFCC59978		*Taxus chinensis* (*Taxaceae*)	China	OQ771893	OQ779485	OQ779480	Wang *et al.* (2024)
P. telopeae	*CBS 114161*	**T**	*Telopea* sp. (*Proteaceae*)	*Australia*	*KM199296*	*KM199403*	KM199500	Maharachchikumbura *et al.* (2014)
P. terricola	*CBS 141.69*	**T**	Soil	Pacific Islands	MH554004	MH554680	MH554438	Liu *et al.* (2019)
P. trachycarpicola	OP068	**T**	*Trachycarpus fortunei* (*Arecaceae*)	China	*JQ845947*	*JQ845945*	JQ845946	Zhang *et al.* (2012)
P. tumida	CFCC55158	**T**	*Rosa chinensis* (*Rosaceae*)	China	OK560610	OM158174	OL814524	Peng *et al.* (2022)
	CFCC55159		*Rosa chinensis* (*Rosaceae*)	China	OK560613	OM158177	OL814527	Peng *et al.* (2022)
	LC6057; CGMCC 3.23502		n/a	China	OR247999	OR381074	OR361474	Razaghi *et al.* (2024)
P. unicolor	MFLUCC 12-0276; NN0469740	**T**	*Rhododendron* sp. (*Ericaceae*)	China	JX398999	JX399030	—	Maharachchikumbura *et al.* (2012)
	MFLUCC 12-0275; NN0473080		Unidentified tree	China	JX398998	JX399029	JX399063	Maharachchikumbura *et al.* (2012)
P. verruculosa	MFLUCC 12-0274; NN0473090	**T**	*Rhododendron* sp. (*Ericaceae*)	China	JX398996	—	JX399061	Maharachchikumbura *et al.* (2012)
P. yunnanensis	*HMAS 96359*	**T**	*Podocarpus macrophyllus* (*Podocarpaceae*)	China	AY373375	—	—	Wei *et al.* (2013)
P. cangshanensis	*CGMCC 3.23544*	**T**	*Rhododendron delavayi* (*Ericaceae*)	China	OP082426	OP185517	OP185510	Gu *et al.* (2022)

© 2025 Westerdijk Fungal Biodiversity Institute

Alignment and phylogenetic analyses

Electropherograms from forward and reverse reads were analysed, edited, and combined with Geneious Prime v. 9 (https://www.geneious.com). Trimmed sequences were aligned with reference sequences obtained from GenBank after using the NCBI BLAST search engine and reviewing relevant literature (Table 1). MAFFT v. 7.490 (Katoh *et al.* 2002, Katoh & Standley 2013) was used to generate alignments for each locus. Alignments for the comparative analysis of species-specific base pair substitutions were deposited in National Agricultural Library AgData Commons (https://doi.org/10.15482/USDA.ADC/28263920) (Tables 2, 3). The nucleotide substitution model for each alignment was estimated using ModelTest-NG (Darriba *et al.* 2019) as implemented by RAxML GUI v. 2.0.10 (Edler *et al.* 2021) based on the Akaike Information Criterion (AICc; Burnham & Anderson 2002). For ITS, *TUB*, *TEF* the best fit models were TPM3uf+I+G4, TrN+I+G4, and TIM2+I+G4, respectively. Maximum likelihood (ML) and Bayesian inference (BI) analyses were generated from the individual and combined data sets. *Neopestalotiopsis saprophytica* (MFLUCC12-0282) was chosen as the outgroup taxa for all analyses. The BI phylogenies were conducted with MrBayes v. 2.24 (Drummond *et al.* 2012) utilizing the GTR GAMMA I (GTR+I+G) model. The ML phylogenies were generated using RAxML (Stamatakis 2014) as implemented by Geneious Prime v. 9. For the BI analysis, the Markov Chain Monte Carlo (BMCMC) was performed with four heated chains for 1000000 generations with trees being sampled every 200th generation. Convergence for each partition was assessed in Geneious Prime v. 9; all parameters had effective sample sizes (ESS) greater than 200. For the ML trees, support for clades were assessed using 1000 nonparametric bootstrap (BS) replicates. Phylogenetic trees were edited using Geneious Prime v.9 (https://www.geneious.com) and Adobe Illustrator CS v.6 (Adobe Systems Inc., USA).

RESULTS

Sampling and fungal isolation

Five *Pestalotiopsis*-like strains were isolated from the 11 conifer plant samples; each strain originating from different trees within the United States. Strains C5 (CBS 153149) and C10 (CBS 153153) were isolated from two different eastern hemlock trees in Hillsborough County, New Hampshire and Hocking County, Ohio, respectively. Strain C9 (CBS 153152) was isolated from a Serbian spruce tree in Hancock County, Maine. Lastly, strains C7 (CBS 153150) and C8 (CBS 153151) were obtained from two different white spruce trees located at separate sites in Hancock County, Maine.

Phylogenetic analyses

The nucleotide sequences generated in this study were deposited in GenBank (Table 1). Alignment data sets were generated for ITS, *TUB*, *TEF*, and a concatenation of the three. The ITS alignment contained 116 taxa and consisted of 534 characters, of which 441 were conserved, 91 variable, and 24 parsimony informative. The *TUB* alignment contained 109 taxa, consisting of 785 characters with 545 being conserved, 205 variable, and 117 parsimony informative. The *TEF* alignment contained 102 taxa and consisted of 925 characters of which 680 were conserved, 221 variable, and 137 parsimony informative. For the ITS single gene phylogenetic analysis, species of *Pestalotiopsis* do not resolve into the currently recognized species. The *TUB* single gene tree provides more resolution when compared to the ITS tree, however various species remain unresolved. Comparatively, the *TEF* single gene tree provides the most resolution and is most concordant with the multi-gene phylogenetic analysis. The concatenated phylogenetic reconstruction using both ML and BI analyses indicated that our five isolates belong to two significatively supported

Table 2. *TEF* species-specific base pair substitutions between *Pestalotiopsis maineana sp. nov.* and closely related species.

	Nucleotide position											
Species	24	31	32	33	39	40	55	56	57	61	65	68
P. maineana (CBS153150)	A	—	—	—	C	T	C	C	T	A	G	G
P. maineana (CBS153151)	A	—	—	—	C	T	C	C	T	A	G	G
P. brachiata (LC2988)	A	—	—	—	C	T	C	C	T	A	G	G
P. hispanica (CBS115391)	A	T	C	A	A	T	C	C	T	A	G	G
P. fusiformis (LC4365)	T	—	—	—	T	C	—	—	—	C	A	T

	Nucleotide position											
Species	71	73	80	167	168	236	243	401	421	422	432	440
P. maineana (CBS153150)	A	A	C	A	T	C	A	C	A	T	T	C
P. maineana (CBS153151)	A	A	C	A	T	C	A	C	A	T	T	C
P. brachiata (LC2988)	A	A	G	A	T	C	A	T	T	C	G	T
P. hispanica (CBS115391)	A	A	C	A	T	C	A	T	T	C	G	T
P. fusiformis (LC4365)	T	C	T	G	C	—	G	C	A	T	T	C

© 2025 Westerdijk Fungal Biodiversity Institute

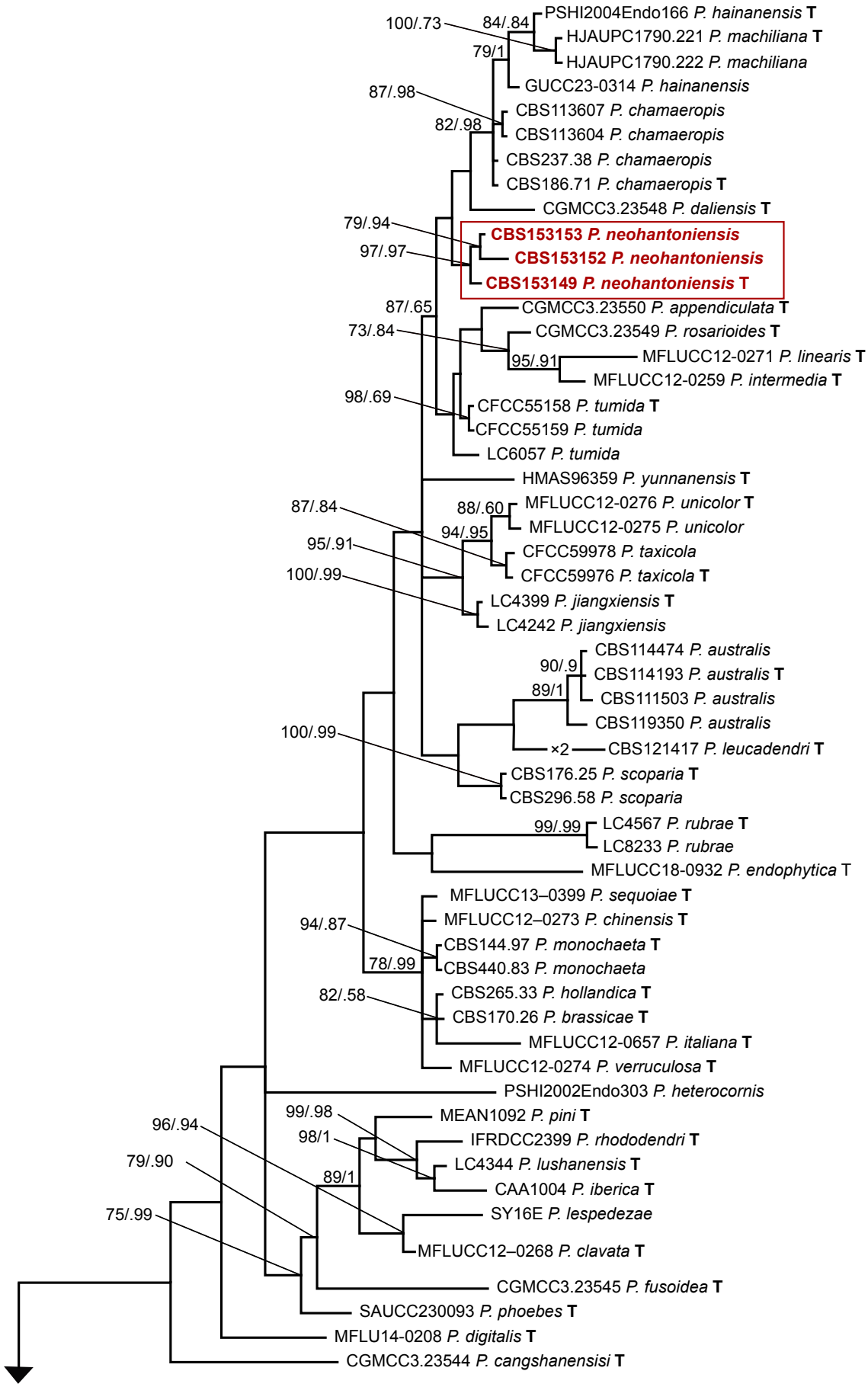

Fig. 1. Phylogenetic tree (ML and BI) based on concatenated sequences of the internal transcribed spacer (ITS), partial beta-tubulin gene (*TUB*), and partial translation elongation factor 1-alpha gene (*TEF*). Bootstrap support values ≥ 70 % and posterior probability values ≥ 0.95 are presented above each node (ML/BI). The two new species reported in this study are in red and "T" indicates the type specimen. *Neopestalotiopsis saprophytica* was used as the outgroup. All isolates are listed in Table 1 with corresponding gene identification numbers and / or accession numbers.

© 2025 Westerdijk Fungal Biodiversity Institute

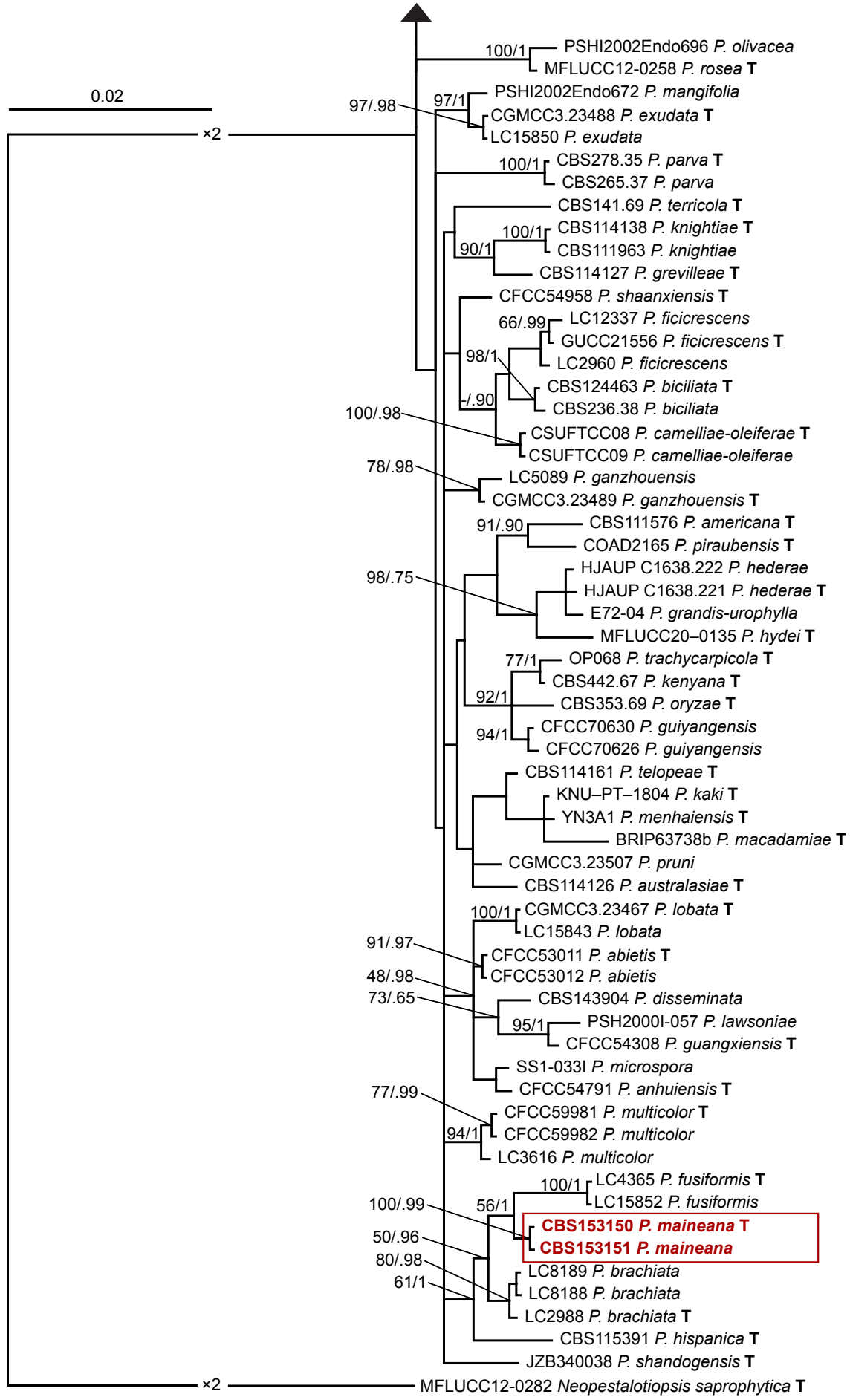

Fig. 1. (Continued).

© 2025 Westerdijk Fungal Biodiversity Institute

subclades within the genus of *Pestalotiopsis* (Fig. 1) and are here recognized as *Pestalotiopsis maineana sp. nov*. and *P. neohantoniensis sp. nov. Pestalotiopsis maineana* shares close affinity to *P. fusiformis*, *P. brachiata*, and *P. hispanica*. *Pestalotiopsis neohantoniensis* shares affinity with *P. daliensis*, *P. chamaeropis*, *P. machiliana*, and *P. hainanensis*. Species descriptions, genetic identification, and a comparative morphological analysis of closely related species are presented in the taxonomy section.

TAXONOMY

Pestalotiopsis maineana S.T. Miller & C. Salgado, ***sp. nov.*** MB 857038. Fig. 2.

Etymology: Named after the location where the fungus was collected, Maine, United States of America.

Diagnosis: *Pestalotiopsis maineana* can be diagnosed from the closely related species *P. brachiata*, *P. hispanica*, *P. fusiformis* by nucleotide characters in the *TEF* locus (Table 2). *Pestalotiopsis maineana* can be distinguished from *P. brachiata* by positions 80 (C:G), 401 (C:T), 421 (A:T), 422 (T:C), 432 (T:G), 440 (C:T). From *P. hispanica* by positions 31–33 (- - -:TCA), 401 (C:T), 421 (A:T), 422 (T:C), 432 (T:G), 440 (C:T). From *P. fusiformis* by positions 24 (A:T), 39 (C:T), 40 (T:C), 55–57 (CCT:- - -), 61 (A:C), 65 (G:A), 68 (G:T), 71 (A:T), 73(A:C), 80 (C:T), 167 (A:G), 168 (T:C), 236 (C:-), 243 (A:G).

Description: *Sexual morph*: Undetermined. *Asexual morph*: Conidiomata forming on pine needles or PDA, globose to clavate, scattered or gregarious, exuding black conidial masses. *Conidiophores* indistinct, often reduced to conidiogenous cells. *Conidiogenous cells* discrete, cylindrical or subcylindrical, ampulliform, flask shaped, hyaline, thin-walled, 5.1–18 × 2.1–4.9 µm (av. 10.5 ± 3.69 × 3.1 ± 0.81 µm). *Conidia* fusoid, straight to slightly curved, 4-septate and usually constricted, 21.8–27.9 × 5.4–7.0 µm (av. 25 ± 1.45 × 6.3 ± 0.41 µm); basal cell conic with a truncate base, hyaline, and thin-walled, 4.0–6.4 µm long (av. 5.1 ± 0.69 µm); three median cells doliiform, 14.3–18.4 µm long (av. 15.9 ± 1.08 µm), concolourous, olivaceous to greenish olivaceous with dark septa dividing the cells; apical cell 3.4–6.0 µm long (av. 4.6 ± 0.58 µm), hyaline, subcylindrical with truncate base, thin-walled; with 2–3 tubular apical appendages, arising from the apical or subapical crest, unbranched, filiform, flexuous, 12.4–25.6 µm long (av. 16.4 ± 3.88 µm); basal appendage single, tubular, unbranched 4.4–9.8 µm long (av. 6.4 ± 1.23 µm) (Fig. 2; Table 4).



Fig. 2. *Pestalotiopsis maineana* (ex-holotype culture CBS 153151). **A–D.** Upper and reverse PDA (**A, B**) and SNA (**C, D**) cultures after 7 d of growth. **E.** Conidiomata on SNA. **F.** Conidiomata on PDA. **G–J.** Conidiogenous cells and conidia. **K–N.** Conidia. Scale bars: E = 1 mm; F = 500 µm; G–N = 10 µm.

© 2025 Westerdijk Fungal Biodiversity Institute

Culture characteristics: Colonies on PDA flat, entire at the edge, white with flocculent arial mycelia, underside pale luteous in the centre transitioning to white along the margin; after 7 d at 25 °C colonies reach a diameter of 73–80 mm on PDA and 61 mm on SNA. Colonies on SNA flat and colourless (Fig. 2).

Typus: **USA**, Maine, Hancock County, on *Picea glauca* (*Pinaceae*), 20 Nov. 2023, *A. Bergdahl* (**holotype** BPI 977274, culture ex-type CBS 153151; GenBank accession numbers PQ568305, PQ573018, PQ573023).

Notes: *Pestalotiopsis maineana* shares close affinity to *Pestalotiopsis fusiformis*, *P. brachiata*, and *P. hispanica*; however, *P. maineana* differs from *P. fusiformis* and *P. brachiata* based on the number of basal appendages (1 vs 1–2 vs 1–4, respectively) and is somewhat similar to *P. hispanica* in basal appendage number (1 vs 0–1, respectively). *Pestalotiopsis fusiformis* has up to five apical appendages while *P. maineana* has up to three. *Pestalotiopsis mainenana* differs from *P. hispanica* based on the length of the basal appendage (4.4–9.8 µm vs 1.4–4.5 µm), the apical appendage number (2–3 vs 2–4) and length (12.4–25.6 µm vs 2–14 µm), and the width of conidia (5.4–7.0 µm vs 6–9.5 µm) (Table 4).

Pestalotiopsis neohantoniensis S.T. Miller & C. Salgado, ***sp. nov.*** MB 857039. Fig. 3.

Etymology: Named after the location where the fungus was collected, New Hampshire, United States of America.

Diagnosis: *Pestalotiopsis neohantoniensis* can be diagnosed from the closely related species *P. daliensis*, *P. hainanensis*, *P. machiliana*, *P. chamaeropis* by nucleotide characters in the *TEF* locus (Table 3). *Pestalotiopsis neohantoniensis* can be distinguished from *P. daliensis* by positions 11 (G:A), 16 (T:-), 31 (T:C), 33 (C:T), 40–42 (- - -: TCA), 96 (C:T), 205 (T:C), 224 (A:T), 418 (-:C), 478 (T:G). From *P. hainanensis* by positions 16 (T:C), 40–42 (- - -: TCA), 96 (C:T), 154 (T:A), 205 (T:C), 224 (A:T), 411 (C:T), 418 (-:C). From *P. machiliana* by positions 16 (T:C), 40–42 (- - -: TCA), 96 (C:T), 154 (T:A), 205 (T:C), 224 (A:T), 262 (A:T). From *P. chamaeropis* by positions 40–42 (- - -:TCA), 96 (C:T), 154 (T:A), 205 (T:C), 224 (A:T), 411 (C:T), 418 (-:C).

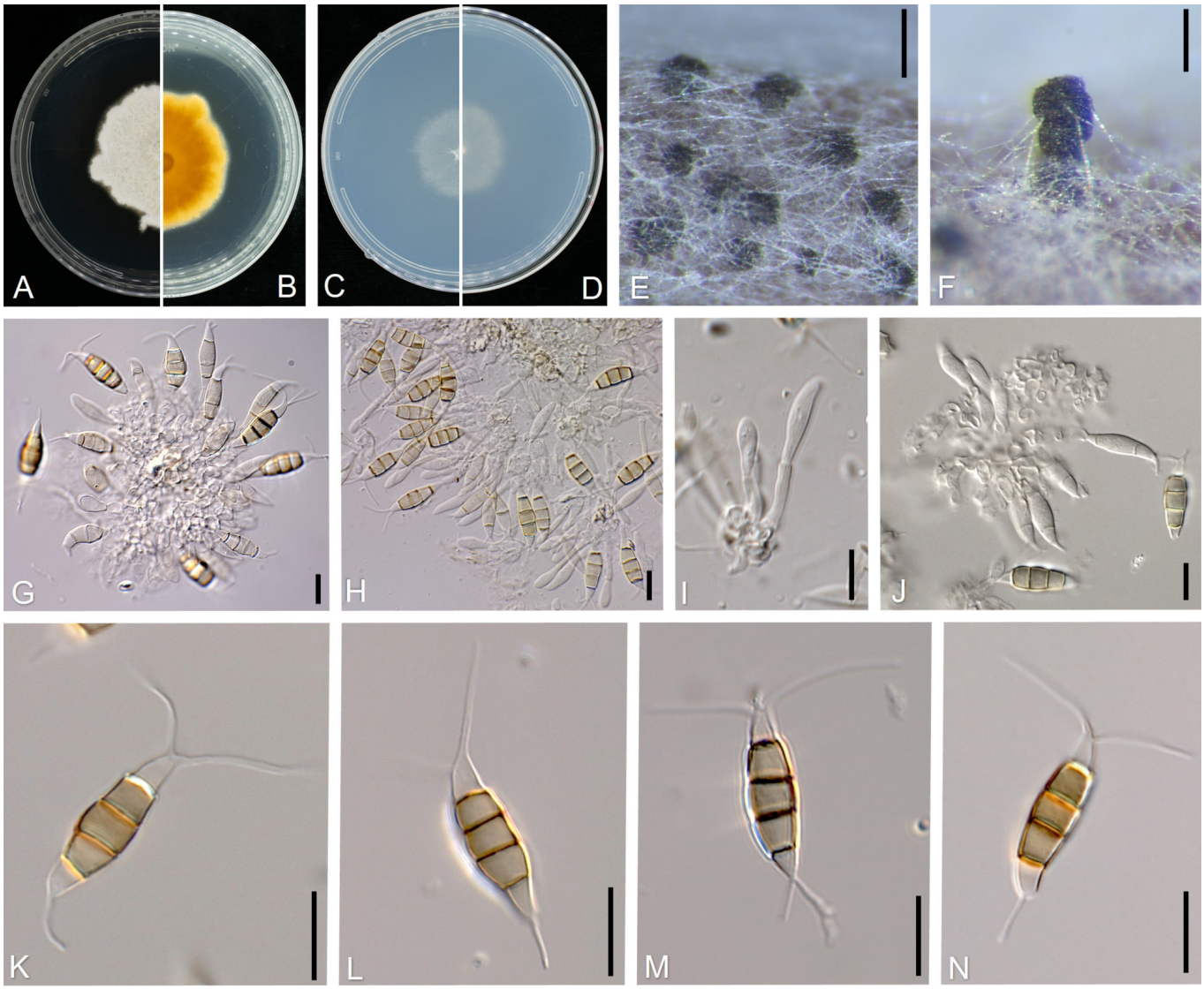

Fig. 3. *Pestalotiopsis neohantoniensis* (ex-holotype culture CBS 153149). **A–D.** Upper and reverse PDA (**A, B**) and SNA (**C, D**) cultures after 7 d of growth. **E, F.** Conidiomata on pine needle. **G–J.** Conidiogenous cells and conidia. **K–N.** Conidia. Scale bars: E = 200 µm; F = 100 µm; G–N = 10 µm.

© 2025 Westerdijk Fungal Biodiversity Institute

Description: *Sexual morph*: Undetermined. *Asexual morph*: *Conidiomata* forming on pine needles, globose to clavate, scattered or gregarious, covered by aerial mycelia, exuding dark black conidial masses. *Conidiophores* indistinct, often reduced to conidiogenous cells. *Conidiogenous cells* discrete, cylindrical or subcylindrical, ampulliform, hyaline, 6.2–20 × 1.9–5.8 µm (av. 12.9 ± 3.470 × 3.71 ± 1.2 µm). *Conidia* fusoid, ellipsoid, usually straight but sometimes curved, 4-septate, usually constricted at septa, 19.2–25.5 × 5.1–7.6 µm (av. 22.2 ± 1.43 × 6.6 ± 0.54 µm); basal cell conic with a truncate base, hyaline, and thin-walled, 3.1–6.6 µm long (av. 4.2 ± 0.64 µm); three median cells doliiform, 12–15.9 µm long (av. 14.1 ± 0.91 µm), concolourous, olivaceous to olivaceous buff with dark septa dividing the cells; apical cell 3.3–6.0 µm long (av. 4.6 ± 0.62 µm) hyaline, subcylindrical with truncate base, thin-walled; with 1–4 (usually 1–3) tubular apical appendages, arising from the apical or subapical crest, unbranched (occasionally branched), filiform, flexuous, 10.9–26 µm long (av. 17.9 ± 3.9 µm); basal appendage 1–2 (usually 1), tubular, centric, unbranched (occasionally branched), 3.8–13.2 µm long (av. 7.4 ± 2.4 µm) (Fig. 3; Table 4).

Culture characteristics: Colonies on PDA are flat with round edges; white with flocculent aerial mycelia, underside luteous to amber with a pure yellow margin on day 7, and after 14 d the centre darkens while the outer mycelia remain pure yellow with a white margin. Colonies reach a diameter of 35 mm after 7 d and 50 mm after 14 d on PDA at 25 °C; on SNA colonies are flat and colourless reaching 32 mm after 7d and 55.8 mm after 14 d at 25 °C (Fig. 3).

Typus: **USA**, New Hampshire, Hillsborough County, on *Tsuga canadensis* (*Pinaceae*), 12 Dec. 2023, *W. Davidson* (**holotype** BPI 911275, culture ex-type CBS 153149; GenBank accession numbers PQ568303, PQ573016, PQ573021).

Notes: *Pestalotiopsis neohantoniensis* shares close affinity to *Pestalotiopsis daliensis*, *P. hainanensis*, *P. machiliana*, and *P. chamaeropis*; however, *P. neohantoniensis* is the only species that has up to 2 basal appendages (usually 1) and up to 4 apical appendages (usually 1–3) when compared to *P. daliensis*, *P. hainanensis*, *P. machiliana* and *P. chamaeropis* (Table 4). *Pestalotiopsis neohantoniensis* exhibited two basal appendages in 7.5 % of observed spores (n = 40) (Fig. 3M). *Pestalotiopsis neohantoniensis* differs from *P. daliensis* and *P. hainanensis* based on the length of the basal appendage (3.8–13.2 µm vs 10–16 µm vs absent, respectively). *Pestalotiopsis neohantoniensis* has wider conidia cells when compared to *P. daliensis* (5.1–7.6 µm vs 4–5 µm). Further, *P. neohantoniensis* has longer apical appendages when compared to *P. hainanensis* (10.9–26 µm vs 1–10 µm) (Table 4).

DISCUSSION

Historically, species of *Pestalotiopsis* were often named based on the host from which they were isolated; however, host association is unreliable for delimiting species of *Pestalotiopsis* when compared to DNA sequence-based analyses and morphological characterization (Jeewon *et al.* 2004, Crous *et al.* 2012, Maharachchikumbura *et al.* 2012). When analysing the ITS, *TUB*, and *TEF* sequence data individually, *TEF* was the most effective for species delimitation within our analysis while ITS and *TUB* did not resolve all the known taxonomic relationships of species. Maharachchikumbura *et al.* (2012) reported *TEF* and *TUB* to be the most favourable markers when comparing 10 loci, including *ACT*, *TUB*, *CAL*, *GPDH, GS*, ITS, LSU, *RPB1*, SSU and *TEF.* The concatenated phylogenetic analysis indicates that our five isolates belong to two well supported subclades within *Pestalotiopsis*. Considering morphological characteristics, we found the appendages of the conidia to be helpful for discerning between closely related species, as has been reported in previous studies (Crous *et al.* 2012, Maharachchikumbura *et al.* 2012).

When comparing *Pestalotiopsis* species which have historically been reported on spruce or hemlock trees, the two new species described herein differ morphologically and on DNA sequence data (where available). *Pestalotiopsis stevensonii*, *P. gravesii,* and *P. heterocornis* have all been reported from either Norway spruce (*Picea abies*), red spruce (*Picea rubens*), or dragon spruce (*Picea asperata*)

Table 3. *TEF* species-specific base pair substitutions between *Pestalotiopsis neohantoniensis sp. nov.* and closely related species.

	Nucleotide position														
Species	11	16	31	33	40	41	42	96	154	205	224	262	411	418	478
P. neohantoniensis (CBS153149)	G	T	T	C	—	—	—	C	T	T	A	A	C	—	T
P. neohantoniensis (CBS153152)	G	T	T	C	—	—	—	C	T	T	A	A	C	—	T
P. neohantoniensis (CBS153153)	G	T	T	C	—	—	—	C	T	T	A	A	C	—	T
P. daliensis[a]	A	—	C	T	T	C	A	T	T	C	T	A	C	C	G
P. hainanensis (PSHI2004Endo166)	G	C	T	C	T	C	A	T	A	C	T	A	T	C	T
P. machiliana (HJAUPC1790.221)	G	C	T	C	T	C	A	T	A	C	T	T	N/A	N/A	N/A
P. chamaeropis (CBS186.71)	G	C	T	C	T	C	A	T	A	C	T	A	T	C	T

[a] CGMCC3.23548 = KUNCC22-12403

© 2025 Westerdijk Fungal Biodiversity Institute

while *P. linearis* was described from *Tsuga* sp. (Nag Raj 1993, Kobayashi 2007, Ge *et al.* 2009, Chandelier *et al.* 2010, Maharachikumbura *et al.* 2012). There is no sequence data available for *P. stevensonii* and *P. gravesii*; however, morphological differences are prominent. In fact, *P. stevensonii* likely does not belong to the *Pestalotiopsis* genus. As discussed by Maharachchikumbura *et al.* (2014), Nag Raj (1993) grouped *P. stevensonii* within *Pestalotiopsis* due to his broad concept of the genus which included 3-septate, and 2-central celled conidial forms; therefore, *P. stevensonii* likely belongs in the genus *Truncatella* (Adrianova & Minter 2012). *Pestalotiopsis gravesii* has been documented as having 3–4 apical appendages with one located at the apical cell apex and the other 2–3 appendages located on the basal part of the apical cell pointing horizontally/backwards towards the basal cell (Kobayashi 1974). Comparatively, both *P. maineana* and *P. neohantoniensis* have apical appendages which arise from the apical or subapical crest and not on the lower portion of the apical cell. Furthermore, the apical appendages for *P. maineana* and *P. neohantoniensis* do not point towards the basal cell. Sequence data is available for *P. heterocornis* and *P. linearis* and based on the multi-gene phylogeny, both belong to subclades separate from *P. maineana* and *P. neohantoniensis* within *Pestalotiopsis*.

The host specificity of *P. maineana* and *P. neohantoniensis* is unclear. If they are specific to conifers or if they occur on other hosts is not yet known. To our knowledge, *P. maineana* is the first species to be found associated with white spruce (*Picea glauca*) while *P. neohantoniensis* is the first species of *Pestalotiopsis* found associated with Serbian spruce (*Picea omorika*) and eastern hemlock (*Tsuga canadensis*). As discussed by Razaghi *et al.* (2024), it is common for very closely related species of *Pestalotiopsis* to differ in host specificity; one species may have a broad host range while a close relative can remain specialized. The species closely related to *P. maineana* include *P. fusiformis*, *P. brachiata*, and *P. hispanica. Pestalotiopsis fusiformis* and *P. brachiata* have only been reported on one host thus far, *Rhododendron* sp. and *Camellia* sp., respectively, whereas *P. hispanica* has been reported on *Protea* sp., *Dianthus caryophyllus*, *Peristrophe japonica*, and *Cryptomeria japonica* (Liu *et al.* 2017, Liu *et al.* 2019, Fan 2023, Sun 2023, Hsu *et al.* 2024, Razaghi *et al.* 2024). Comparatively, of the species closely related to *P. neohantoniensis,* two (*P. daliensis* and *P. hainanensis*) have only been reported on one host, *Rhododendron decorum* and *Podocarpus macrophyllus* var. *maki*, respectively (Liu *et al.* 2007, Gu *et al.* 2022). The other closely related species, *P. chamaeropis*, has been reported on over eight hosts including *Chamaerops humilis*, *Camellia sinensis*, *Eurya nitida*, *Prostanthera rotundifolia*, *Vaccinium corymbosum*, *Vandopsis gigantea*, *Dianthus caryophyllus,* and *Vitis vinifera* (Maharachchikumbura *et al.* 2014, Moslemi & Taylor 2015, Ran *et al.* 2017, Jayawardena *et al.* 2018, Chen *et al.* 2021, Qiu *et al.* 2022, Santos *et al.* 2022, Hsu *et al.* 2024). It is important to note that the plant samples collected in this study, from which the two new species were isolated, were collected from conifers with Rosellinia needle blight, which may have biased these results. It is uncertain if *P. maineana* and *P. neohantoniensis* are generalists or specialists; however, previous studies have reported that species of *Pestalotiopsis* are usually not specific to one host plant (Liu *et al.* 2007).

Table 4. Comparison of conidia spores from *Pestalotiopsis* species which are closely related to the two species described in this study.

Species	Conidia Size (µm)	Length			Apical appendages		Basal appendages		References
		Apical cell (µm)	Median cells (µm)	Basal cell (µm)	Number	Length (µm)	Number	Length (µm)	
P. maineana (CBS153151) Type	21.8–27.9 × 5.4–7.0	3.4–6.0	14.3–18.4	4.0–6.4	2–3	12.4– 25.6	1	4.4–9.8	This study
P. fusiformis[a]	18–25 × 5.5–8	3–5.5	12–15	3.5–7	2–5	13–25	1–2	3–11	Razaghi *et al.* (2024)
P. brachiata[b]	23.5–25 × 6.5–8	3.5–6	14–16.5	4–6.5	2–3	16–28.5	1–4	5.5–9.5	Liu *et al.* (2017)
P. hispanica[c]	16.5–29 × 6–9.5	2–4.5	14–18.5	3–5	2–4	2–14	0–1	1.4–4.5	Liu *et al.* (2019)
P. neohantoniensis (CBS153149) Type	19.2–25.5 × 5.1–7.6	3.3–6.0	12.0–15.9	3.1–6.6	1–4	10.9–26	1–2	3.8–13.2	This Study
P. daliensis[d]	23–26 × 4–5	4–6	13–16	4–6	2–3	13–22	1	10–16	Gu *et al.* (2022)
P. hainanensis[e]	19–22 × 5–6	n/d	13–15	n/d	1–3	1–10	absent	absent	Liu *et al.* (2007)
P. machiliana[f]	18.6–27.2 × 5.6–7.4	3–4.8	12.5–17.3	3–5.2	2–3	12.9–22.5	1	4.5–10.2	Luo *et al.* (2024)
P. chamaeropis[g]	21–28 × 6–9.5	4–6	15–18.5	5–6.5	2–3	13–24	1	4–8.5	Maharachchikumbura *et al.* (2014)

[a] CGMCC3.23495 = LC4365
[b] CGMCC3.18151 = LC2988
[c] CBS115391 = CPC5193
[d] CGMCC3.23548 = KUNCC22-12403
[e] PSHI2004Endo166
[f] HJAUPC1790.221
[g] CBS186.71

© 2025 Westerdijk Fungal Biodiversity Institute

Pestalotiopsis maineana and *P. neohantoniensis* were asymptomatic when discovered and if they are endophytes or if they cause disease is not known. They may be pathogenic depending on physiological and environmental triggers like *P. microspora* who Lee *et al.* (1995) reported as being able to switch between endophytic and pathogenic lifestyles (Maharachchikumbura *et al.* 2011). Inoculation assays in future studies are needed to help clarify if they pose a threat to conifer species. Furthermore, surveys investigating the microfungi of different tree species within temperate forests of the US would help explain host specificity, distribution, and disease severity/ incidence (if any) of the newly described species.

ACKNOWLEDGEMENTS

We thank A. Smart, A. Bergdahl, T. Macy, K. Sturgeon, F. Millett, W. Davidson, B. Guess, E. Linquist, M. Heydt, and L. Godfrey for their assistance in coordinating sample collections. This work was supported by funds from USDA-ARS project 8042-22000-323-000-D. Mention of trade names or commercial products in this publication is solely for the purpose of providing specific information and does not imply recommendation or endorsement by the USDA. The USDA is an equal opportunity provider and employer.

Conflict of Interest: The authors declare no conflicts of interest.

REFERENCES

Akinsanmi OA, Nisa S, Jeff-Ego OS, *et al.* (2017). Dry flower disease of Macadamia in Australia caused by *Neopestalotiopsis macadamiae sp. nov*. and *Pestalotiopsis macadamiae sp. nov*. *Plant Disease* **101**: 45–53. https://doi.org/10.1094/PDIS-05-16-0630-RE

Allen BP, Seaboyer IV (2017). Fifty-six years of forest development following the 1938 hurricane in Hillsborough, New Hampshire, USA. *Forests* **8**: 225. https://doi.org/10.3390/f8070225

Andrianova TV, Minter DW (2012). *Pestalotiopsis stevensonii*. *IMI Descriptions of Fungi and Bacteria* **194**: No.1937. https://doi.org/10.1079/DFB/20123409302

Bhuiyan AB, Sultana N, Mahmud NU, *et al.* (2021). Characterization of *Pestalotiopsis* sp. causing gray leaf spot in coconut (*Cocos nucifera* L.) in Bangladesh. *Journal of Basic Microbiology* **61**: 1085–1097. https://doi.org/10.1002/jobm.202100253

Burnham KP, Anderson D (2002). *Model Selection and Multi-Model Inference*. New York, NY: Springer-Verlag.

Butler BJ (2017). *Forests of Maine, 2016. Resource Update FS-128*. Newtown Square, PA: U.S. Department of Agriculture, Forest Service, Northern Research Station. https://doi.org/10.2737/FS-RU-128

Cale JA, McNulty SA, Teale SA, *et al.* (2013). The impact of beech thickets on biodiversity. *Biological Invasions* **15**: 699–706. https://doi.org/10.1007/s10530-012-0319-5

Carvalho DD, Oliveira RM, Marques MG, *et al.* (2019). Molecular, morphophysiological and pathogenic characterization of eucalypt *Pestalotiopsis grandis-urophylla* isolates, a new species. *Tropical Plant Pathology* **44**: 132–139. https://doi.org/10.1007/s40858-019-00277-0

Carbone I, Kohn LM (1999). A method for designing primer sets for speciation studies in filamentous ascomycetes. *Mycologia* **91**: 553–556. https://doi.org/10.1080/00275514.1999.12061051

Chandelier A, Andre F, Laurent F (2010). Detection of *Chalara fraxinea* in common ash (*Fraxinus excelsior*) using real time PCR. *Forest Pathology* **40**: 87–95. https://doi.org/10.1111/j.1439-0329.2009.00610.x

Chen Y, Wan Y, Zeng L, *et al.* (2021). Characterization of *Pestalotiopsis chamaeropis* causing gray blight disease on tea leaves (*Camellia sinensis*) in Chongqing, China. *Canadian Journal of Plant Pathology* **43**: 413–420. https://doi.org/10.1080/07060661.2020.1816582

Chen Y, Zeng L, Shu N, *et al.* (2018). *Pestalotiopsis*-like species causing gray blight disease on *Camellia sinensis* in China. *Plant Disease* **102**: 98–106. https://doi.org/10.1094/PDIS-05-17-0642-RE

Crous PW, Verkley GJM, Christensen M, *et al.* (2012). How important are conidial appendages? *Persoonia* **28**: 126–137. https://doi.org/10.3767/003158512X652624

Darriba D, Posada D, Kozlov A M, *et al.* (2019). ModelTest-NG: A new and scalable tool for the selection of DNA and protein evolutionary models. *Molecular Biology and Evolution* **37**: 291–294. https://doi.org/10.1093/molbev/msz189

Das K, Lee SY, Jung HY (2021). *Pestalotiopsis kaki sp. nov*., a novel species isolated from persimmon tree (*Diospyros kaki*) bark in Korea. *Mycobiology* **49**: 54–60. https://doi.org/10.1080/12298093.2020.1852703

de Silva NI, Maharachchikumbura SSN, Thambugala KM, *et al.* (2021). Morpho-molecular taxonomic studies reveal a high number of endophytic fungi from *Magnolia candolli* and *M. garrettii* in China and Thailand. *Mycosphere* **12**: 163–237. https://doi.org/10.5943/mycosphere/12/1/3

Drummond AJ, Suchard MA, Xie D, *et al.* (2012). Bayesian phylogenetics with BEAUti and the BEAST 1.7. *Molecular Biology and Evolution* **29**: 1969–1973. https://doi.org/10.1093/molbev/mss075

Edler D, Klein J, Antonelli A, *et al.* (2021). raxmlGUI 2.0: a graphical interface and toolkit for phylogenetic analyses using RAxML. *Methods in Ecology and Evolution* **12**: 373–377. https://doi.org/10.1111/2041-210X.13512

Fan S, Liu X, Su J, *et al.* (2023). *Pestalotiopsis hispanica*, a new pathogenic fungus responsible for Cryptomeria japonica red blight. *Acta Phytopathologica Sinica* **53**: 321–325. https://doi.org/10.13926/j.cnki.apps.000815

Ford CR, Elliott KJ, Clinton BD, *et al.* (2012) Forest dynamics following eastern hemlock mortality in the southern Appalachians. *Oikos* **121**: 523–536. https://doi.org/10.1111/j.1600-0706.2011.19622.x

Francis SM (1986). Needle blights of conifers. *Transactions of the British Mycological Society* **87**: 397–400. https://doi.org/10.1016/S0007-1536(86)80215-7

Ge Q, Chen Y, Xu T (2009). *Flora Fungorum Sinicorum. Vol. 38. Pestalotiopsis redactores principales*. Science Press, New York.

Glass NL, Donaldson GC (1995). Development of primer sets designed for use with the PCR to amplify conserved genes from filamentous ascomycetes. *Applied and Environmental Microbiology* **61**: 1323–1330. https://doi.org/10.1128/aem.61.4.1323-1330.1995

Gu MO, Hu DW, Han Bing, *et al.* (2021). *Pestalotiopsis abietis sp. nov*. from *Abies fargesii* in China. *Phytotaxa* **509**: 93–105. https://doi.org/10.11646/phytotaxa.509.1.4

Gu R, Bao DF, Shen HW, *et al.* (2022). Endophytic *Pestalotiopsis*

© 2025 Westerdijk Fungal Biodiversity Institute

species associated with *Rhododendron* in Cangshan Mountain, Yunnan Province, China. *Frontiers in Microbiology* **13**: 1016782. https://doi.org/10.3389/fmicb.2022.1016782

Guegan JF, de Thoisy B, Gómez-Gallego M, *et al.* (2023). World forests, global change, and emerging pests and pathogens. *Current Opinion in Environmental Sustainability* **61**: 101266. https://doi.org/10.1016/j.cosust.2023.101266

Hopkins KE, McQuilken MP (2000). Characteristics of *Pestalotiopsis* associated with hardy ornamental plants in the UK. *European Journal of Plant Pathology* **106**: 77–85. https://doi.org/10.1023/A:1008776611306

Hsu SY, Xu YC, Lin YC, *et al.* (2024). Hidden diversity of *Pestalotiopsis* and *Neopestalotiopsis* (*Amphisphaeriales*, *Sporocadaceae*) species allied with the stromata of entomopathogenic fungi in Taiwan. *MycoKeys* **101**: 275. https://doi.org/10.3897/mycokeys.101.113090

Hu H, Jeewon R, Zhou D, *et al.* (2007). Phylogenetic diversity of endophytic *Pestalotiopsis* species in *Pinus armandii* and *Ribes* spp.: evidence from rDNA and β-tubulin gene phylogenies. *Fungal Diversity* **24:** 1–22.

Huanaluek N, Jayawardena RS, Maharachchikumbura SS, *et al.* (2021). Additions to pestalotioid fungi in Thailand: *Neopestalotiopsis hydeana sp. nov*. and Pestalotiopsis hydei *sp. nov*. *Phytotaxa* **479**: 23–43. https://doi.org/10.11646/phytotaxa.479.1.2

Hyde KD, Hongsanan S, Jeewon R, *et al.* (2016). Fungal diversity notes 367–490: taxonomic and phylogenetic contributions to fungal taxa. *Fungal Diversity* **80**: 1–270. https://doi.org/10.1007/s13225-016-0373-x

Hyde KD, Norphanphoun C, Maharachchikumbura SSN, *et al.* (2020). Refined families of *Sordariomycetes*. *Mycosphere* **11**: 305–1059. https://doi.org/10.5943/mycosphere/11/1/7

Hyde KD, Norphanphoun C, Ma J, *et al.* (2023). Mycosphere notes 387–412 - novel species of fungal taxa from around the world. *Mycosphere* **14**: 663744. https://doi.org/10.5943/mycosphere/14/1/8

Jaklitsch WM, Gardiennet A, Voglmayr H (2016). Resolution of morphology-based taxonomic delusions: *Acrocordiella*, *Basiseptospora*, *Blogiascospora*, *Clypeosphaeria*, *Hymenopleella*, *Lepteutypa*, *Pseudapiospora*, *Requienella*, *Seiridium* and *Strickeria*. *Persoonia* **37**: 82–105. https://doi.org/10.3767/003158516X690475

Jayawardena RS, Hyde KD, Chethana KWT, *et al.* (2018). Mycosphere Notes 102–168: saprotrophic fungi on *Vitis* in China, Italy, Russia and Thailand. *Mycosphere* **9**: 1–114. https://doi.org/10.5943/mycosphere/9/1/1

Jayawardena RS, Hyde KD, Wang S, *et al.* (2022). Fungal diversity notes 1512–1610: taxonomic and phylogenetic contributions on genera and species of fungal taxa. *Fungal Diversity* **117**: 1–272. https://doi.org/10.1007/s13225-022-00513-0

Jeewon R, Liew ECY, Hyde KD (2004). Phylogenetic evaluation of species nomenclature of *Pestalotiopsis* in relation to host association. *Fungal Diversity* **17**: 39–55.

Jiang N, Voglmayr H, Xue H, *et al.* (2022). Morphology and phylogeny of *Pestalotiopsis* (*Sporocadaceae*, *Amphisphaeriales*) from *Fagaceae* leaves in China. *Microbiology Spectrum* **10**: e03272–22. https://doi.org/10.1128/spectrum.03272-22

Katoh K, Misawa K, Kuma KI, *et al.* (2002). MAFFT: a novel method for rapid multiple sequence alignment based on fast Fourier transform. *Nucleic Acids Research* **30**: 3059–3066. https://doi.org/10.1093/nar/gkf436

Katoh K, Standley DM (2013). MAFFT multiple sequence alignment software version 7: improvements in performance and usability. *Molecular Biology and Evolution* **30**: 772–780. https://doi.org/10.1093/molbev/mst010

Kobayashi T (1974). Notes on new or little-known fungi inhabiting woody plants in Japan VI. *Transactions of the Mycological Society Japan* **15**: 382.

Kobayashi T (2007). *Index of fungi inhabiting woody plants in Japan. Host, Distribution and Literature*. Zenkoku-Noson-Kyoiku Kyokai Publishing Co. Ltd: 1227.

Lee JC, Yang X, Schwartz M, *et al.* (1995). The relationship between an endangered North American tree and an endophytic fungus. *Chemistry & Biology* **2**: 721–727. https://doi.org/10.1016/1074-5521(95)90100-0

Li H, Peng BY, Xie JY, *et al.* (2024). *Pestalotiopsis jiangsuensis sp. nov.* causing needle blight on *Pinus massoniana* in China. *Journal of Fungi* **10**: 230. https://doi.org/10.3390/jof10030230

Li L, Yang Q, Li H (2021). Morphology, phylogeny, and pathogenicity of pestalotioid species on *Camellia oleifera* in China. *Journal of Fungi* **7**: 1080. https://doi.org/10.3390/jof7121080

Liu AR, Xu T, Guo LD (2007). Molecular and morphological description of *Pestalotiopsis hainanensis sp. nov*., a new endophyte from a tropical region of China. *Fungal Diversity* **24**: 23–36.

Liu F, Bonthond G, Groenewald JZ, *et al.* (2019). *Sporocadaceae*, a family of coelomycetous fungi with appendage-bearing conidia. *Studies in Mycology* **92**: 287– 415. https://doi.org/10.1016/j.simyco.2018.11.001

Liu F, Hou L, Raza M, *et al.* (2017). *Pestalotiopsis* and allied genera from *Camellia*, with description of 11 new species from China. *Scientific Reports* **7**: 1–19. https://doi.org/10.1038/s41598-017-00972-5

Liu JK, Hyde KD, Jones EBG, *et al.* (2015). Fungal diversity notes 1–110: taxonomic and phylogenetic contributions to fungal species. *Fungal Diversity* **72**: 1–197. https://doi.org/10.1007/s13225-015-0324-y

Luo XX, Liao MG, Zhang K, *et al.* (2024). Morphological and phylogenetic analyses reveal eight novel species of *Pestalotiopsis* (*Sporocadaceae*, *Amphisphaeriales*) from southern China. *MycoKeys* **109**: 207. https://doi.org/10.3897/mycokeys.109.131000

Maharachchikumbura SS, Chukeatirote E, Guo LD, *et al.* (2013). *Pestalotiopsis* species associated with *Camellia sinensis* (tea). *Mycotaxon* **123**: 47–61. https://doi.org/10.5248/123.47

Maharachchikumbura SS, Guo LD, Cai L, *et al.* (2012). A multi-locus backbone tree for *Pestalotiopsis*, with a polyphasic characterization of 14 new species. *Fungal Diversity* **56**: 95–129. https://doi.org/10.1007/s13225-012-0198-1

Maharachchikumbura SS, Guo LD, Chukeatirote E, *et al.* (2011). *Pestalotiopsis* morphology, phylogeny, biochemistry and diversity. *Fungal Diversity* **50**: 167–187. https://doi.org/10.1007/s13225-011-0125-x

Maharachchikumbura SS, Hyde KD, Groenewald JZ, *et al.* (2014). *Pestalotiopsis* revisited. *Studies in Mycology* **79**: 121–186. https://doi.org/10.1016/j.simyco.2014.09.005

Morin RS, Lombard K (2017). *Forests of New Hampshire, 2016. Resource Update FS-124*. Newtown Square, PA: U.S. Department of Agriculture, Forest Service, Northern Research Station. https://doi.org/10.2737/FS-RU-124

Monteiro P, Gonçalves MF, Pinto G, *et al.* (2022). Three novel species of fungi associated with pine species showing needle blight-like disease symptoms. *European Journal of Plant Pathology* **1**: 1–20. https://doi.org/10.1007/s10658-021-02395-5

Moslemi A, Taylor PW (2015). *Pestalotiopsis chamaeropis* causing

© 2025 Westerdijk Fungal Biodiversity Institute

leaf spot disease of round leaf mint-bush (*Prostanthera rotundifolia*) in Australia. *Australasian Plant Disease Notes* **10**: 1–5. https://doi.org/10.1007/s13314-015-0179-9

Nag Raj TN (1993). *Coelomycetous anamorphs with appendage-bearing conidia*. Mycologue Publications, Waterloo, Ontario.

Nirenberg HI (1981). A simplified method for identifying *Fusarium* spp. occurring on wheat. *Canadian Journal of Botany* **59**: 1599–1609. https://doi.org/10.1139/b81-217

O'Donnell K, Cigelnik E (1997). Two divergent intragenomic rDNA ITS2 types within a monophyletic lineage of the fungus *Fusarium* are nonorthologous. *Molecular Phylogenetics and Evolution* **7**: 103–116. https://doi.org/10.1006/mpev.1996.0376

O'Donnell K, Kistler HC, Cigelnik E, *et al.* (1998). Multiple evolutionary origins of the fungus causing Panama disease of banana: concordant evidence from nuclear and mitochondrial gene genealogies. *Proceedings of the National Academy of Sciences* **95**: 2044–2049. https://doi.org/10.1073/pnas.95.5.2044

Peng C, Crous PW, Jiang N, *et al.* (2022). Diversity of *Sporocadaceae* (pestalotioid fungi) from *Rosa* in China. *Persoonia* **49**: 201–260. https://doi.org/10.3767/persoonia.2022.49.07

Qiu L, Liu J, Kuang W, *et al.* (2022). First report of *Pestalotiopsis chamaeropis* causing leaf spot on *Eurya nitida* in China. *Plant Disease* **106**: 329. https://doi.org/10.1094/PDIS-06-21-1170-PDN

Ran SF, Maharachchikumbura SSN, Ren YL, *et al.* (2017). Two new records in *Pestalotiopsidaceae* associated with *Orchidaceae* disease in Guangxi Province, China. *Mycosphere* **8**: 121–130. https://doi.org/10.5943/mycosphere/8/1/11

Rayner RW (1970). *A mycological colour chart*. CMI and British Mycological Society, Kew, Surrey, UK.

Razaghi P, Raza M, Han SL, *et al.* (2024). *Sporocadaceae* revisited. *Studies in Mycology* **79**: 121–186. https://doi.org/10.3114/sim.2024.109.03

Renwick K (2023). *Forest Inventory and Analysis Fiscal Year 2022 Business Report. FS-1230*. United States Department of Agriculture, Forest Service. Available at: https://research.fs.usda.gov/understory/2022-forest-inventory-and-analysis-business-report

Sanjay R, Ponmurugan P, Baby UI (2008). Evaluation of fungicides and biocontrol agents against grey blight disease of tea in the field. *Crop Protection* **27**: 689–694. https://doi.org/10.1016/j.cropro.2007.09.014

Santos J, Hilário S, Pinto G, *et al.* (2022). Diversity and pathogenicity of pestalotioid fungi associated with blueberry plants in Portugal, with description of three novel species of *Neopestalotiopsis*. *European Journal of Plant Pathology* **162**: 539–555. https://doi.org/10.1007/s10658-021-02419-0

Shea KR (1964). *Rosellinia herpotrichoides* in Sitka Spruce seedlings in Washington. *Plant Disease Reporter* **48**: 512–513.

Silva AC, Diogo E, Henriques J, *et al.* (2020). *Pestalotiopsis pini sp. nov*., an emerging pathogen on stone pine (*Pinus pinea* L.). *Forests* **11**: 805. https://doi.org/10.3390/f11080805

Steyaert RL (1949). Contribution a l'etude monographique de *Pestalotia* de Not. et *Monochaetia* Sacc. (*Truncatella gen. nov. et Pestalotiopsis gen. nov*.). *Bulletin du Jardin botanique de l'etat Bruxelles* **19**: 285–354. https://doi.org/10.2307/3666710

Stamatakis A (2014). RAxML version 8: a tool for phylogenetic analysis and post-analysis of large phylogenies. *Bioinformatics* **30**: 1312–1313. https://doi.org/10.1093/bioinformatics/btu033

Sun YR, Jayawardena RS, Sun JE, *et al.* (2023). Pestalotioid species associated with medicinal plants in southwest China and Thailand. *Microbiology Spectrum* **11**: e03987–22. https://doi.org/10.1128/spectrum.03987-22

Tomback DF, Achuff P (2010). Blister rust and western forest biodiversity: ecology, values and outlook for white pines. *Forest Pathology* **40**: 186–225. https://doi.org/10.1111/j.1439-0329.2010.00655.x

United States Department of Agriculture (USDA), Forest Service (FS) (2022a). *Forests of Maine, 2021. Resource Update FS-366*. Madison, WI: U.S. Department of Agriculture, Forest Service, Northern Research Station. https://doi.org/10.2737/FS-RU-366

United States Department of Agriculture (USDA), Forest Service (FS) (2022b) *Forests of New Hampshire, 2021. Resource Update FS-495*. Madison, WI: U.S. Department of Agriculture, Forest Service, Northern Research Station. https://doi.org/10.2737/FS-RU-371

Wang YF, Tsui KM, Chen SM, *et al.* (2024). Diversity, pathogenicity and two new species of pestalotioid fungi (*Amphisphaeriales*) associated with Chinese Yew in Guangxi, China. *MycoKeys* **102**: 201224. https://doi.org/10.3897/mycokeys.102.113696

Wang Y, Xiong F, Lu Q, *et al.* (2019). Diversity of Pestalotiopsis-like species causing gray blight disease of tea plants (*Camellia sinensis*) in China, including two novel *Pestalotiopsis* species, and analysis of their pathogenicity. *Plant Disease* **103**: 2548–2558. https://doi.org/10.1094/PDIS-02-19-0264-RE

Wei JG, Phan CK, Wang L, *et al.* (2013). *Pestalotiopsis yunnanensis sp. nov*., an endophyte from *Podocarpus macrophyllus* (*Podocarpaceae*) based on morphology and ITS sequence data. *Mycological Progress* **12**: 563–568. https://doi.org/10.1007/s11557-012-0863-5

White TJ, Bruns T, Lee S, *et al.* (1990). Amplification and direct sequencing of fungal ribosomal RNA genes for phylogenetics. In: *PCR protocols: a guide to methods and applications* (Innis MA, Gelfand DH, Sninsky JJ, *et al.*, eds). Academic Press, Inc., New York, USA: 315–322. https://doi.org/10.1016/B978-0-12-372180-8.50042-1

Wijayawardene NN, Hyde KD, Al-Ani LKT, *et al.* (2020). Outline of *Fungi* and fungus-like taxa. *Mycosphere* **11**: 1060–1456. https://doi.org/10.5943/mycosphere/11/1/8

Zhang Y, Maharachchikumbura SS, Mckenzie EH, *et al* (2012). A novel species of *Pestalotiopsis* causing leaf spots of *Trachycarpus fortunei*. *Cryptogamie, Mycologie* **33**: 311–318. https://doi.org/10.7872/crym.v33.iss3.2012.311

Zhang Y, Maharachchikumbura SS, Tian Q, *et al.* (2013). *Pestalotiopsis* species on ornamental plants in Yunnan Province, China. *Sydowia* **65**: 113–128.

Zhang Z, Zhang J, Li D, *et al.* (2023). Morphological and phylogenetic analyses reveal three new species of *Pestalotiopsis* (*Sporocadaceae*, *Amphisphaeriales*) from Hainan, China. *Microorganisms* **11**: 1627. https://doi.org/10.3390/microorganisms11071627

© 2025 Westerdijk Fungal Biodiversity Institute

© 2025 Westerdijk Fungal Biodiversity Institute

FUSE

Fungal Systematics and Evolution

VOLUME 16
DECEMBER 2025
PAGES 283–305

doi.org/10.3114/fuse.2025.16.16

Purple Pinwheel and more: The *Marasmius haematocephalus* complex (*Marasmiaceae*) in Australia

F.E. Guard[1*], J. Dearnaley[1], T. Lebel[2]

[1]University of Southern Queensland, Toowoomba, QLD, Australia
[2]Botanic Gardens & State Herbarium of South Australia, Hackney Road, Adelaide, SA, Australia

*Corresponding author: franguard@icloud.com

Key words:
Australian fungi
colour forms
cryptic species
distribution
long-term studies
new taxa
taxonomy

Abstract: *Marasmius haematocephalus* forms a distinctive pan-tropical species complex. While it has been confirmed that *M. haematocephalus* s. s. occurs only in the neotropics, morphologically similar taxa across the world continue to be attributed to this species. Phylogenies utilising nrITS, nrLSU and *TEF1*, were constructed to identify relationships within the complex, and morphological data used to document and explore the taxa endemic to Australia and those which co-occur in Asia, Madagascar and the USA. Seven new species found in Australia are described and illustrated — *M. campaniformis sp. nov.*, *M. pervagatus sp. nov.*, *M. porphyrocephalus sp. nov.*, *M. purpureospadiceus sp. nov.*, *M. vinaceus sp. nov.*, *M. wianwian sp. nov*. and *M. wunga sp. nov.* A key to Australian species of the *M. haematocephalus* complex is provided. Historic records and observational data (iNaturalist and Atlas of Living Australia) were used to indicate potential distributions of all species within the complex that occur in Australia and explore biogeographic relationships more broadly.

Citation: Guard FE, Dearnaley J, Lebel T (2025). Purple Pinwheel and more: The *Marasmius haematocephalus* complex (*Marasmiaceae*) in Australia. *Fungal Systematics and Evolution* **16**: 283–305. doi: 10.3114/fuse.2025.16.16
Received: 17 February 2025; **Accepted:** 13 June 2025; **Effectively published online:** 8 August 2025
Corresponding editor: P.W. Crous

INTRODUCTION

Marasmius is the type genus for the family *Marasmiaceae* (Kühner 1980). Recently both genus and family have been extensively revised by Oliveira *et al.* (2024b), using morphological and multigene phylogenetic data. The genus *Marasmius* contains approximately 700 species worldwide (Bhunjun *et al.* 2022). While the majority of species are forest floor leaf litter saprotrophs, some form aerial leaf litter traps (Guard *et al.* 2024, Oliveira *et al.* 2024a) and a few occur in grasslands (Antonin & Noordeloos 2010, Crous *et al.* 2020). Rarely they are plant pathogens and possible endophytes (Amoako-Attah *et al.* 2020, Huamán-Pilco *et al.* 2023). As in many diverse basidiomycete lineages, while there are unique morphologically distinctive taxa, there are also many species complexes. Historical separation of species and varieties based on morphological variations (*e.g*. colour morphs), cultural or functional roles is not always maintained when data from new geographic regions is incorporated or molecular data investigated.

The purple pinwheel, *Marasmius haematocephalus* is a distinctive species in the genus *Marasmius.* Its blood red basidiome was first described from Brazil by Montagne in 1837 as *Agaricus haematocephalus* and placed in *Marasmius* by Fries (1838). It was considered pan-tropical and sub-tropical by subsequent mycologists examining the species in tropical Africa, East Africa, Cameroon, Papua New Guinea, Madagascar, Indonesia, Central America and southern Asia (Singer 1976, Pegler 1977, Pegler 1986, Desjardin & Horak 1997, Desjardin *et al.* 2000, Mossebo & Antonin 2004, Antonín & Buyck 2006, Antonin 2007, Tan *et al.* 2009, Wannathes *et al.* 2009). Even though colour and size variations, and spore and cystidia differences suggested that all collections were possibly not one species, these morphological variations were considered to be varieties (Singer 1976), forms (Wannathes *et al.* 2009) or of little taxonomic significance (Desjardin & Horak 1997). Singer (1976) listed nine varieties of *M. haematocephalus* in the neotropics, mainly on colour differences, of which only one, *M. rubicundus*, has been recognised at species level (Oliveira *et al.* 2022). Subsequently, Wannathes *et al.* (2009) reported six forms of *M. haematocephalus* based on variations in colour, pileal dimensions, spore size and substrate, in their study of Thai *Marasmius*. The characters of some Thai forms were similar to those of Singer's varieties, e.g. f. "*violaceus*" appeared to be the same as var. *atroviolaceus*, f. "*luteocephalus"* bore some resemblance to var. *leucophyllus* and f. "*robustus*" shared characters with var. *macrocephalus,* though the substrates differed. Wannathes *et al.* (2009) were unwilling to equate these forms with Singer's varieties, given their vast geographic separation and the lack of molecular data from the neotropical populations.

The addition of molecular data (nrITS only) revealed that all the forms of *M. haematocephalus* in the Thai study grouped in a well-supported clade, and some of them clustered in subclades with good support, while others were unresolved (Wannathes *et al.* 2009). Shay *et al.* (2017) in a study of *Marasmius* in Madagascar simply noted that it "probably represents a complex

Fungal Systematics and Evolution is licensed under a Creative Commons Attribution-NonCommercial-NoDerivatives 4.0 International License

© 2025 Westerdijk Fungal Biodiversity Institute

of species". Oliveira *et al.* (2022) completed the essential critical evaluation of type material of many Brazilian species, epitypified *M. haematocephalus*, and described four new cryptic species in the *M. haematocephalus* complex. That study concluded that *M. haematocephalus* s. s. is a neotropical species, restricted at most to Central and South America. However, it forms a well-supported monophyletic clade with closely related species in tropical Africa and Indo-Malaysia. The sequences from the Thai (Wannathes *et al.* 2009), Malaysian (Tan *et al.* 2009) and Madagascan (Shay *et al.* 2017) specimens were included in the analysis and appeared to resolve into several distinct species level clades. The recent revision of the genus *Marasmius* by Oliveira *et al.* (2024b) has placed the species complex in the newly created subgen. *Globulares*, sect. *Sicci*, emend. J.S. Oliveira & Moncalvo, series *Haematocephali*, emend. J.S. Oliveira & Moncalvo. This revision divides the awkwardly combined *Globulares* - '*globulares/sicci'* section (Antonin & Noordeloos 2010) into two separate sections (*Globulares* and *Sicci*) within the upgraded *Globulares* subgenus. Section *Sicci* forms a monophyletic divergent lineage including the characters of small, parasol-like, sulcate, marasmioid basidiomata, with filiform stipes and scant basal mycelium, well-developed pleurocystidia and elongate basidiospores (Oliveira *et al.* 2024b). No Australian sequences or collections were available at the time for inclusion in the analysis of the *M. haematocephalus* complex (Oliveira *et al.* 2022) and few in the broader revision of the genus *Marasmius* (Oliveira *et al.* 2024b).

Eastern Australian tropical and subtropical habitats are rich in species that appear to be part of the broader *Marasmius haematocephalus* complex. Specimens identified as *M. haematocephalus* have been collected in Australia from as early as 1887, though some were misidentifications. The majority of records in the Atlas of Living Australia are from after 2010, when observational records were included. As little was known about the *M. haematocephalus* complex in Australia, collections in Australian fungaria were listed under this name rather than using Singer's (1976) nine varieties or Wannathes' (2009) six 'forms'. Few collections are held in the southern Australian fungaria [MEL (2), CANB (1), AD (0), NSW (0)], which is logical given the subtropical to tropical distribution of all known species in the complex. Only 6 of the 50 collections in the Queensland herbarium (BRI) were made prior to this study.

Collection of substantial new material of *Marasmius* from tropical and subtropical eastern Australia in the last four years, enabled us to document and explore phylogenetic and biogeographic relationships of Australian endemic taxa, and distinguish and describe seven new species in the *M. haematocephalus* complex. The question of colour as a distinguishing character for species was also investigated.

MATERIALS AND METHODS

Collections and observational records

Fresh collections examined in this study were principally made from 2014 to 2024 in the wet season (December to May) on regular surveys within Dilkusha Nature Refuge in southeast Queensland (SEQ), far north Queensland (FNQ) (Feb. 2021 and Feb. 2023) and northern New South Wales (NSW) (Feb. 2022). These were supplemented by collections from the Queensland Mycological Society (QMS) field trips to Linda Garrett National Park (NP), Mt Cordeaux section of Main Range NP, Springbrook NP, Murrumba Downs Reserve and Bornhoffen Campsite in Numinbah Valley. All collections identified as *Marasmius haematocephalus* and held in the Queensland Herbarium (BRI) were examined. The Atlas of Living Australia records were examined for distributional data and records of historic collections in other Australian Herbaria. The iNaturalist citizen science database of observational records was also examined.

All collections in Queensland were made under the Permits Nos. WITK18734918-1 to 2021 and P-PTUKI-100021825 to 2023 (FNQ) and WITK18760918 and WIF418760818 to 2021 and P-PTUKI-100091861-1 to 2024 (SEQ) and with permission from private landowners. The surveys and collections in NSW were made with permission of the relevant local National Parks Rangers.

Fresh collections were photographed in situ, described and samples taken for DNA analysis (desiccated in silica gel in 1.5 mL tubes). Collections were then dried in an *Ezidri* Snackmaker FD500 (Hydraflow Industries Ltd, Upper Hutt, NZ) food dehydrator at lowest setting for at least 12 h before packeting and storing for submission to BRI fungarium.

Morphology

Basidiomata characters were described from fresh material where possible. These included *pileus* diameter range in millimetres, colour using the Flora of British Fungi Colour Identification Chart (Royal Botanic Garden Edinburgh 1969), shape from juvenile to mature; *lamellae* (L) number range for up to 10 basidiomata, *lamellulae* (l) number of tiers where present, colour and whether marginate, attachment to stipe; *stipe* length and diameter range in millimetres, colour from base to apex, surface texture and insertion into substrate. *Substrate, habitat* and number of basidiomata were also noted. *Spore prints* were obtained whenever possible.

Dried specimens were examined microscopically using a Leica dissecting microscope for hand-cutting sections, and a Prism Optical (Model EX-30T) compound microscope with Tucsen GT12 camera (Tucsen Photonics Co., China) with a 100× objective, for examination of hand cut sections, rehydrated in 5 % potassium hydroxide. Microscopic details were recorded with Mosaic v. 2.0 software (http:// www.tucsen.com). Ammoniacal Congo Red stain and Melzer's reagent were used respectively for recording and measuring details of the pileipellis, cheilocystidia, pleurocystidia, stipe, lamellar and pileal trama and spore length and width and for the amyloid/dextrinoid reaction. Spore measurements were made from fresh spore prints within 12–24 h, or from dried spore prints or herbarium material for a minimum of 10 basidiospores per specimen, and up to 50 basidiospores from each of 2–11 basidiomata for new taxa, where possible, obtaining range of length × width in micrometres, mean length [± standard deviation SD], × width [± SD], with Q (Quotient of length/width) measurements for mean (Qm) [± SD], minimum and maximum; N = number of basidiospores measured.

© 2025 Westerdijk Fungal Biodiversity Institute

Molecular sampling and analysis

Samples were first ground with two 3-mm-diam. tungsten carbide balls at high speed for 20 s, twice in a bead mill (Fast Prep-24™ 5G, MP Biomedicals, CA, USA). The DNA extraction was performed using the Omega Bio-tek Inc. Norcross, GA, USA, EZNA Forensic Kit following the prescribed protocols for hair, nails & feathers, apart from substituting 0.8 µL b-mercaptoethanol for 20 µL 1 M DTT and using 50 µL elution buffer twice instead of 100 µL, for a more concentrated extract. The internal transcribed spacer region (ITS1-5.8S-ITS2; nrITS) rDNA, was amplified using primers ITS1-F (Gardes & Bruns 1993) and ITS4 (White *et al.* 1990) and the large subunit (nrLSU) with primers LR7 & LROR (Vilgalys & Hester 1990) in a reaction mixture of 1 µL of each primer, 12.5 µL MyTaq Red Mix (Bioline, NSW, Australia), 0.8 µL 10 % bovine serum albumin (BSA) and 7.7 µL sterile water. The thermal cycling conditions included 35 cycles of 95 °C for 60 s, 51 °C for 60 s and 72 °C for 60 s, with a final extension step of 72 °C for 10 min for the nrITS, and 95 °C for 60 s, 48 °C for 60 s, 72 °C for 60 s, with a final extension step of 72 °C for 10 min for nrLSU. In addition, the translation elongation factor (*TEF1*) region, using primers EF1-983F and EF1-1567R (Rehner & Buckley 2005), was amplified from representatives of each group in the complex. The thermocycling conditions used were an initial denaturation for 15 min at 95 °C, followed by 10 cycles of 94 °C for 30 s, 65 °C for 60 s (decreasing by 1 °C per cycle) and 72 °C for 90 s; then 30 cycles of 94 °C for 45 s, 55 °C for 60 s, 72 °C for 70 s (extending 1 s per cycle); with a final elongation step of 72 °C for 5 min. Samples were sent to Macrogen, Seoul, Korea, for purification and Sanger sequencing.

Sequences generated for this project were manually edited using Geneious Prime 3 v. 2023.2.1. (https://www.geneious.com). BLAST searches were conducted in the GenBank NCBI database (http://www.ncbi.nlm.nih.gov/) to recover sequences of conspecific or close species. Initial alignments of nrITS, nrLSU and *TEF1* were constructed using MAFFT (Katoh & Standley 2013). All sequences in GenBank labelled *Marasmius haematocephalus* or aff. *haematocephalus* were also downloaded and included in an initial phylogenetic tree for the nrITS gene region. Subsequent alignments included only those sequences that were good quality and relevant for this study. i.e. exemplars from sect. *Sicci*, ser. *Haematocephali*. Following Oliveira *et al.* (2024b), *Marasmius recreigardneri* in the closely related ser. *Ferruginei*, was used as the outgroup. Table S1 (Supplementary material) lists all sequences used in the phylogenetic analyses of this study, with newly generated sequences in **bold** and those from the holotypes in red. Names of species from sequences downloaded from GenBank are as they appear in GenBank.

Phylogenetic analyses were conducted for each gene region separately using Bayesian and Maximum Likelihood. Maximum likelihood (ML) analyses were conducted using RAxML v. 8.2.11 (Stamatakis 2014) with the GTR+GAMMA+I model using default parameters for 1500 rapid bootstrap (BS) replicates. Bayesian analysis was performed with MrBayes v. 3.2.6 (Huelsenbeck & Ronquist 2001) using the substitution model GTR and Metropolis Coupled (MCMCMC) settings, for 1 M iterations. Here we present the Bayesian phylogenetic tree of the nrITS data with maximum likelihood values shown (BS/PP) at nodes with support =/> 70/0.9 (Fig. 1), and the *TEF1* tree (Fig. 2) in the same way. The nrLSU and concatenated nrITS+nrLSU+*TEF1* alignments are included in Supplementary material (Figs S1, S2). Newly generated sequences were registered with GenBank and new taxa with MycoBank.

RESULTS

DNA sequencing

Approximately 60 fresh collections, supplemented by herbarium specimens, were examined in this study and 52 of them successfully sequenced with nrITS and nrLSU primers. The translation-elongation factor 1-alpha (*TEF1*) region was also sequenced for 31 collections. The Bayesian and Maximum likelihood analyses of all three gene regions gave congruent results in supporting broader clades and grouping of species. While *TEF1* was a much reduced dataset, it was useful in disentangling relationships within some apparent species complexes not clearly resolved by the nrITS alone. The final nrITS alignment included a total of 33 sequences generated for Australian taxa and 50 of several geographic origins from GenBank representing the *M. haematocephalus* complex. The final *TEF1* alignment includes 42 sequences.

A monophyletic clade of the broader *haematocephali* complex (ser. *Haematocephali)* is strongly supported (ITS 100/1), and most species also have strong support with lower support for some relationships between taxa (Fig. 1). Within the complex are four major clades and several geographic subclades, annotated on the nrITS phylogeny as *e.g*. 3A, 3B, etc.

Marasmius wianwian sp. nov. (clade 1A), one of the red-pileate species, is strongly supported (100/1) across all gene regions, as a distinct taxon, sister to all other species in the complex (Figs 1, 2). It appears to be an Australian endemic species with a highly restricted distribution in northern New South Wales and southeast Queensland.

The remainder of the complex then divides into two clades. Clade 2A contains three closely related Australian endemic species (*M. vinaceus*, *M. purpureospadiceus* and *M. campaniformis),* and a single sequence representing a species from Hainan, China. This clade has moderately high support for both nrITS (79/0.99) and *TEF1* (100/1). The sequences are up to 98.2 % identical for the nrITS across the four species in this clade but for the *TEF1* region, they are only 93 to 95.4 % identical between the four species. The Chinese sequence is most similar to that of *M. vinaceus sp. nov.*, with 98.2 % similarity for the nrITS. No morphological information was accessible for the Chinese collection. Morphological differences among the three new Australian species also support their delineation as distinct taxa — *M. vinaceus sp. nov.*, *M. purpureospadiceus sp. nov*. and *M. campaniformis sp. nov.* Interestingly, *M. campaniformis* basidiomata are trimorphic, with the colour variants — cinnamon, lilac and pink showing no significant molecular variation in all three gene regions (99.3 to 100 % identical).

Clade 2B includes all other currently known members of the *M. haematocephalus* complex worldwide with strong support for the nrITS (96/1) (Fig. 1) and moderate to strong support for the *TEF1* (78/0.98) (Fig. 2), in three distinct

© 2025 Westerdijk Fungal Biodiversity Institute

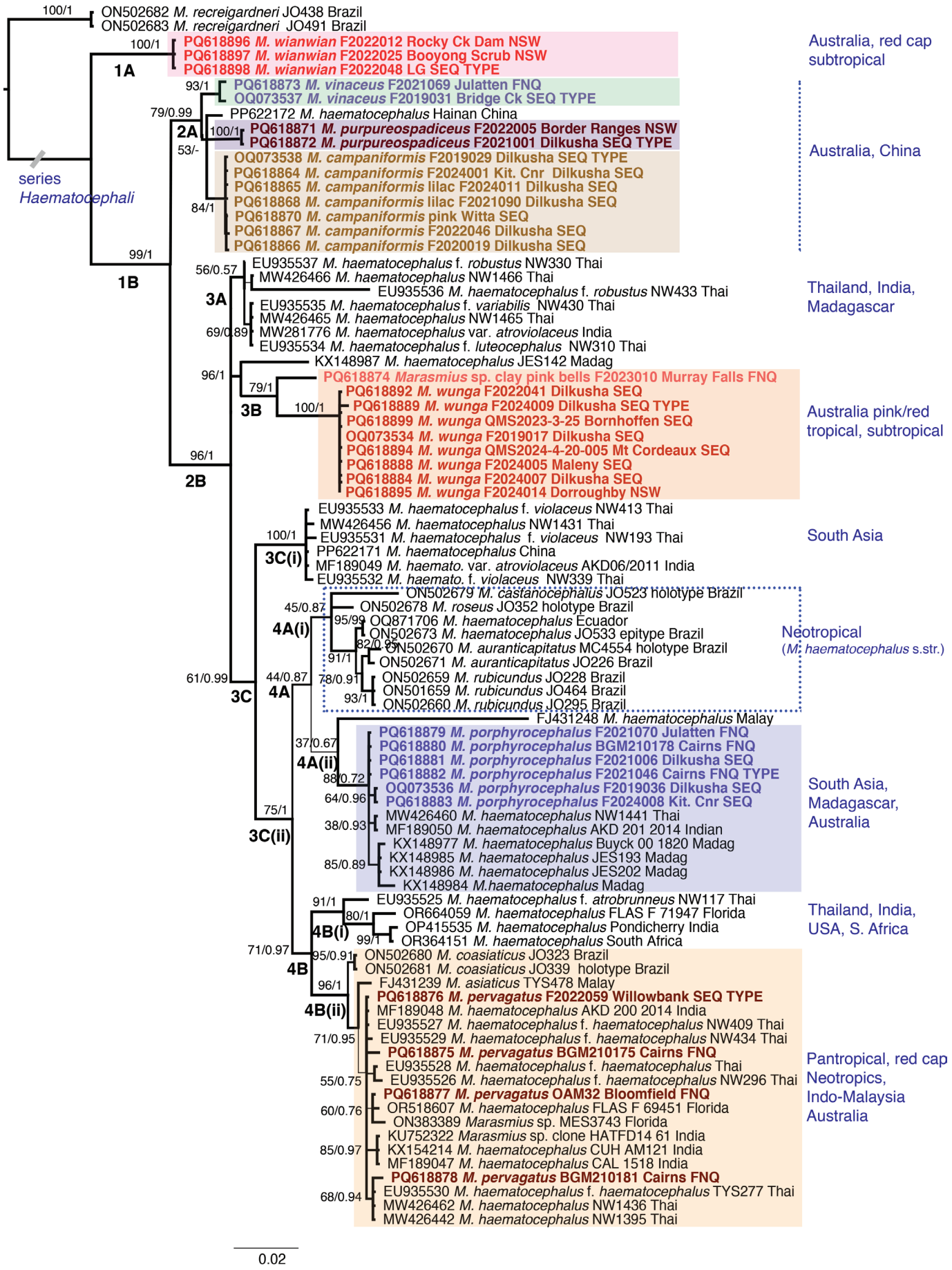

Fig. 1. Phylogenetic analysis of the *Haematocephali* complex in sect. *Sicci*, ser. *Haematocephali* inferred from Bayesian and Maximum Likelihood analysis of the nrITS region with *M. recreigardneri,* subsect. *Ferruginei,* as outgroup, showing the geographic distribution of the complex, with coloured blocks indicating species that occur in Australia. All coloured sequences have been produced in this study.

© 2025 Westerdijk Fungal Biodiversity Institute

groupings. With weak support for the nrITS (56/0.57), subclade 3A consists of taxa from Thailand-India-Madagascar and includes four of the six Thai colour variants noted by Wannathes *et al.* (2009) (*M. haematocephalus* f. *robustus*, var. *atroviolaceus*, f. *luteocephalus* and f. *variabilis*) and a single sequence from Madagascar (JES142). JES142 was also noted to be on a long branch from other Madagascan '*haematocephalus*' sequences by Shay *et al.* (2017). With the addition of more sequences from Brazil, the Indian subcontinent and Australia, it remains on a separate branch, distant from the other Madagascan *M.* '*haematocephalus*' complex species. This whole subclade requires analysis of other gene regions for further clarification of the status of these taxa.

The moderately to strongly supported (nrITS 79/1) subclade 3B consists of two Australian species, *Marasmius* sp. 'buff pink bells' represented by a single specimen from north Queensland and *Marasmius wunga sp. nov.* (100/1), which has a limited distribution in south-east Queensland and northern New South Wales. *Marasmius wunga sp. nov*. is the second red-pileate species in Australia. Subclade 3C is weakly to strongly supported (61/0.99) and contains a diverse mix of species, including *M. haematocephalus* s. s. from Brazil, and more Australian, southeast Asian, Madagascan and pan-tropical subclades. The support for this subclade with the *TEF1* region is strong (98/1). Subclade 3C(i) appears to equate with *M. haematocephalus* f. *violaceus,* sensu Wannathes *et al.* (2009). A sequence labelled as *M. haematocephalus* var. *atroviolaceus* from India (AKD06/2011) is 99.4 % similar to the Thai sequences. The recent addition of a sequence from the tropical Chinese island of Hainan, makes this a south Asian species clade.

The moderately well supported subclade 3C(ii) (75/1.0) contains the poorly supported subclade 4A (44/0.87) with a

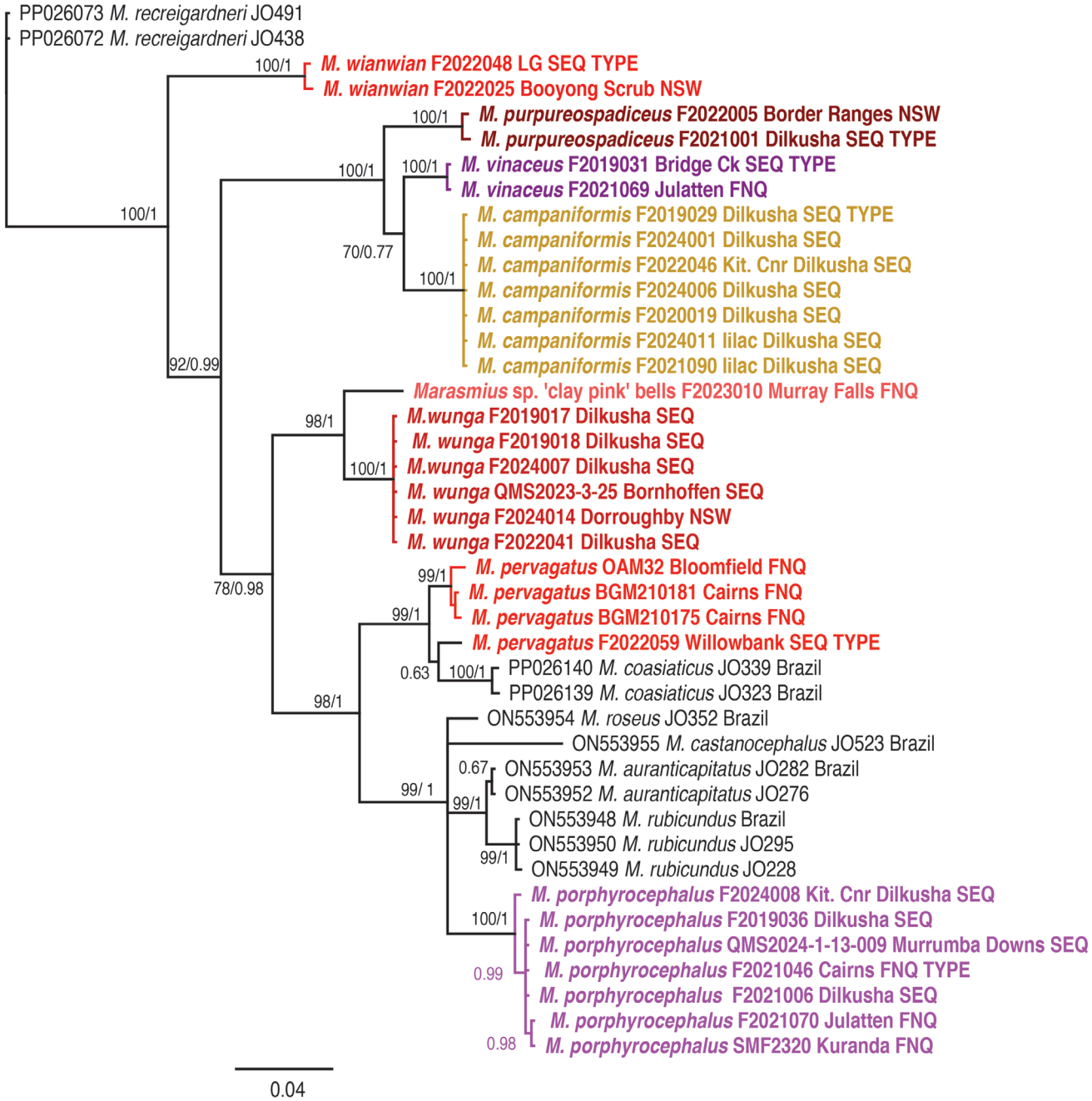

Fig. 2. *TEF1* analysis with Bayesian & RAxML; BS/PP and bolded lines for well-supported nodes. All coloured sequences have been produced in this study.

© 2025 Westerdijk Fungal Biodiversity Institute

neotropical group of species 4A(i), and a mixed Australian, Madagascan and south Asian group of species 4A(ii). The neotropical endemic clade from Brazil and surrounds includes *M. haematocephalus* s. s., several recently described species from Brazil — *M. roseus*, *M. castanocephalus*, *M. auranticapitatus* and *M. rubicundus* (was var. *rubicundus* Singer) (Oliveira *et al.* 2022). The clade has low support (45/0.87) with the nrITS. Oliveira *et al.* (2022) used other gene regions (*TEF1* and *RPB2*), together with morphological differences, to separate the closely related, cryptic species in this clade (Fig. 2).

Subclade 4A(ii) includes the Malaysian TYS523 '*M. haematocephalus*' (sequence FJ431248) as sister species on a long branch to the moderately supported (88/0.72) *M. porphyrocephalus sp. nov.*, which includes sequences from Thailand, India and Madagascar. The Australian sequences are 99.1–99.9 % identical for the nrITS, with slightly less support for the Thai-Indian pair (MW426460 and MF189050) and the Madagascan sequences. However, as with the neotropical Brazilian clade 4A(i), further analysis of other gene regions (*TEF1* and *RPB2*) and morphological data are needed to confirm whether non-Australian material represent additional cryptic species.

The final subclade 4B, with moderate to strong support (71/0.97), includes specimens from across the world including Thailand, India, South Africa, Brazil, Malaysia, Queensland (Australia) and Florida (USA). Subclade 4B(i) with strong support (91/1.0), contains a single specimen each from Thailand (f. *atrobrunneus* Wannathes *et al.* 2009), USA (Florida), India and South Africa. More data are required to elucidate this group.

The strongly supported (96/1.0) subclade 4B(ii) includes *Marasmius coasiaticus* from Brazil and *M. asiaticus* from Malaysia. *Marasmius asiaticus* is moderately to strongly supported (71/0.95) as sister species to the final pantropical species, *M. pervagatus sp. nov.*, which shows some molecular (nrITS) and geographic variation. Four Australian specimens (F2022059, OAM32, BGM210175 & BGM210181), and multiple Indian, Thai and USA (Florida) specimens are included in this complex clade. Most of the Thai sequences are from the *M. haematocephalus* form *'haematocephalus'* sensu Wannathes *et al.* (2009). Morphologically they closely resemble *M. pervagatus sp. nov.* Analysis of the *TEF1* data groups three of the Australian sequences (OAM32, BGM210175 & BGM210181) in a clade with strong support (99/1.0) and F2022059 remains on a separate branch with low support (Fig. 2), distinct from *M. coasiaticus*. At this point we prefer not to describe multiple single collection taxa within this complex, even though *TEF1* does suggest that F2022059 is likely a different species. Instead, we describe a single species, *M. pervagatus* to provide a point of reference for international researchers to utilise. Further work is needed on this group, with more collections, morphological data and using more gene regions to resolve these potentially cryptic taxa.

Taxonomy

Marasmius campaniformis F.E. Guard, T. Lebel, Dearnaley, ***sp. nov.*** MB 857168. Figs 3, 4.

Etymology: The epithet is from the Latin '*campaniformis*' meaning bell-shaped, referring to the shape of mature caps of this species.

Typus: **Australia**, Queensland, Balmoral Ridge, Dilkusha Nature Refuge, Kitchen Corner, S26°44'19.9", E152°53'39.9", 335 m.a.s.l., on road verge in *Allocasuarina* needles and regenerating subtropical rainforest leaf litter, 26 Apr. 2019, *F.E. Guard*, F2019029 (cinnamon form) (**holotype** BRI AQ1007372, **isotype** MEL2469586); GenBank numbers nrITS OQ073538, nrLSU OQ073543, *TEF1* PV151757.

Description: *Basidiomata* small marasmioid. *Pileus* 10–20 mm diam., three colour forms: (i) common, sienna (11) to cinnamon (10), smooth central disc with buff (52) outer

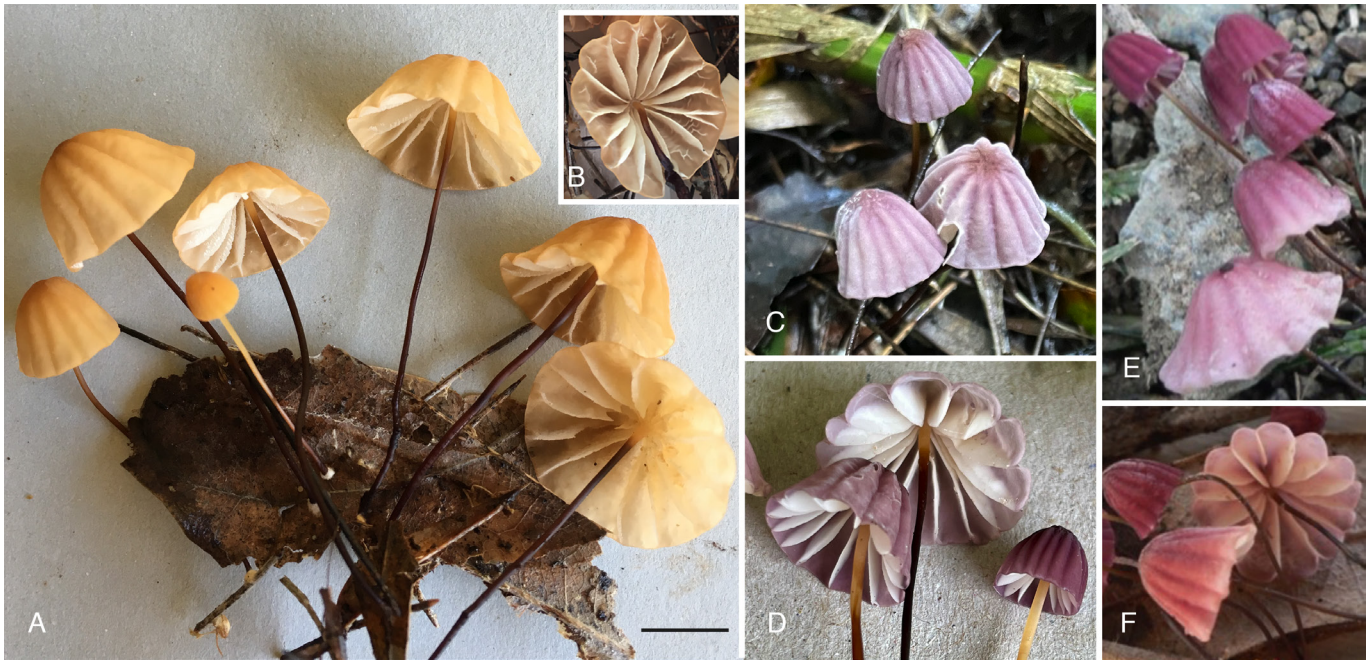

Fig. 3. *Marasmius campaniformis.* **A.** Cinnamon colour variant. **B.** Inset showing lamellae attachment. **C, D.** Lilac to vinaceous-grey. **E, F.** Pink con-specific forms. Scale bar = 10 mm. Images by F.E. Guard.

© 2025 Westerdijk Fungal Biodiversity Institute

two-thirds, (ii) uncommon lilac (79) central disc with pale lilac to lavender (81) outer two-thirds, juveniles vinaceous grey (80) and (iii) rare dusty rose (39) with paler margin and maroon juveniles; deeply sulcate-striate, broadly parabolic to campanulate, surface dry. *Lamellae* free, distant, 12–16, cream-buff to pale pink, non-marginate, with low inter-venations or uncommon bifurcations in mature pilei. *Lamellulae* rare to absent. *Stipe* 30–45(–60) × 0.5–1 mm, filiform, central, base black, mid-shaft dark brown to chestnut (23), apex buff, juvenile stipes more reddish with pale pink apex, smooth, glossy, twisted, hollow, non-insititious insertion with small off-white basal mycelial pad. *Spore print* white. *Basidiospores* (14–)17.5–21 × 4–4.5 µm, mean 19 [± 1.09 SD] × 4 [± 0.21 SD] µm, *Q* = 4.43–5.36, *Qm* = 4.73 [± 0.28 SD], N = 20, narrow, clavate, slightly curved, thin-walled, smooth, inamyloid. *Basidia* not found, *Basidioles* clavate, fusoid 19–28 × 5.5–7.5 µm. *Cheilocystidia* of two types in equal proportions – (i) *Siccus*-type cells, narrow to broadly clavate, cylindrical, sub-globose, main body 9–16 × 6.5–13 µm, with crowded to sparse apical setulae 2–5 × 0.5–1 µm and (ii) smooth cells similar to the pleurocystidia, capitate, utriform, lageniform, lecythiform, 21–43 × 6.5–9.5 µm. *Pleurocystidia* common, mostly capitate, occasionally strangulate, fusoid, lageniform, rarely bifid, 31–50 × (6–)7–11 µm. *Lamellar trama* mildly dextrinoid, hyphae thin-walled 6.5–7.5 µm diam. *Pileal trama* hyphae 5.5–8 µm diam. *Pileipellis* a hymeniderm of *Siccus*-type cells, main body clavate, cylindrical, sub-globose 6–16 × 5.5–10 µm, with usually crowded (rarely sparse) thick-walled apical setulae, 3–5 × 0.5–1 µm. *Stipe* hyphae parallel, those in cortex 5–6 µm diam., those in medulla 4–7 µm diam., inamyloid. *Caulocystidia* absent. *Clamp connections* present in all tissues.

Other collections examined: **Australia,** Queensland, Balmoral Ridge, Dilkusha Nature Refuge, road verge Elsie's Grove, in *Allocasuarina* needles and twigs (cinnamon form), 29 Jan. 2020, *F.E. Guard*, F2020019 (BRI AQ1017487; GenBank numbers nrITS PQ618866, nrLSU PQ618826, *TEF1* PV151733); Kitchen Corner in *Allocasuarina* litter (cinnamon form), 5 Mar. 2022, *F.E. Guard*, F2022046, (BRI AQ1041084; GenBank numbers nrITS PQ618867, nrLSU PQ618867, *TEF1* PV151744); towards Kitchen Corner in leaf litter under regenerating subtropical rainforest (cinnamon form), 5 Jan. 2024, *F.E. Guard*, F2024001 (BRI AQ1045954; GenBank numbers nrITS PQ618864, nrLSU PQ618840, *TEF1* PV151749); Hilary's Corner, in road verge litter under regenerating subtropical rainforest (cinnamon form), 9 Jan. 2024, *F.E. Guard*, F2024006 (BRI AQ1045958; GenBank numbers nrITS PQ618869, nrLSU PQ618869, *TEF1* PV151750); above Lot 3, in road verge litter, (lilac form), 19 Mar. 2021, *F.E. Guard*, F2021090 (BRI AQ1034086; GenBank numbers nrITS PQ618868, nrLSU PQ618827, *TEF1* PV151731); above Lot 1 in road verge litter (lilac form), 19 Jan. 2024, *F.E. Guard*, F2024011 (BRI AQ1045963; GenBank numbers nrITS PQ618865, nrLSU PQ618841, *TEF1* PV151753); Witta, Schultz Rd, private garden leaf litter (pink form), 4 Feb. 2009, *F.E. Guard*, FG0036 (BRI AQ1004887; GenBank number nrITS PQ618870).

Habit, habitat and distribution: *Marasmius campaniformis sp. nov.* occurs regularly in scattered groups among leaf litter from *Allocasuarina* needles and pioneer species of regenerating subtropical rainforest, on damp roadside verges in Dilkusha Nature Refuge, Blackall Range, SEQ. Regular observation of fungi in the Refuge, has shown *M. campaniformis* to produce basidiomata in wet seasons from January to April. No basidiomata were produced in the drought year of 2023. On one occasion (2009) the pink form was collected from mulch under regenerating rainforest on private land in Witta, approximately 12 km from Dilkusha.

Notes: Dilkusha Nature Refuge was originally covered by subtropical rainforest, but was cleared in the 1940s and used as a dairy farm until the early 1980s. It has been actively revegetated with native plants since 1990 and was gazetted a Nature Refuge in 1993. In 30 years (1990–2020), the rainforest has become well established, though it will be decades before 'old growth' status is achieved. This transitional phase, as pioneer tree species are gradually replaced by climax species, appears to suit many saprotrophic fungal species, including *M. campaniformis*, which are not found in neighbouring reserves of old growth rainforest. Apart from their colour, the cinnamon, lilac and pink forms are identical morphologically and molecularly. *Marasmius campaniformis* differs from *M. haematocephalus* s. s. in its colour (all forms), pileal size (10–20 mm c.f. 2.5–16 mm), number of lamellae (12–16 c.f. 7–10) and shorter, sturdier stipe (30–40 × 0.5–1 mm c.f. 22–62 × 0.2–0.5 mm) and also the dimorphic cheilocystidia (Oliveira *et al.* 2022). *Marasmius campaniformis* (Fig. 3) in its lilac form resembles the Thai *M. haematocephalus* f. '*robustus*' with its pileal colour and robust stature, though the basidiospores are slightly shorter (mean 19 c.f. 20 µm) and lamellae more numerous (12–16 c.f. 9–15); both have similar dimorphic cheilocystidia (Wannathes *et al.* 2009). However, molecular analysis places them in two widely separated and distinct clades (Fig. 1). *Marasmius campaniformis* in its cinnamon

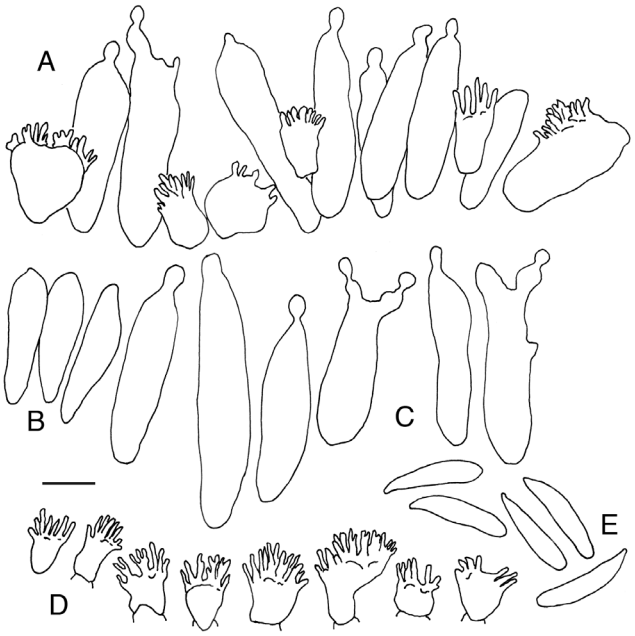

Fig. 4. *Marasmius campaniformis* (F2024001). **A.** Cheilocystidia *Siccus*-type cells and pleurocystidia-type cells. **B.** Basidioles. **C.** Pleurocystidia. **D.** Pileipellis *Siccus*-type cells. **E.** Basidiospores. Scale bar = 10 µm. Illustrated by F.E. Guard.

© 2025 Westerdijk Fungal Biodiversity Institute

form resembles *M. lebeliae* (Crous *et al.* 2019) which occurs in the same habitat. However, *M. lebeliae* is more brownish, has smaller pilei (5–12 c.f. 10–20 mm), fewer lamellae (7–11 c.f. 12–16), longer stipes (35–60 c.f. 30–40 mm) and much larger basidiospores (mean 32 × 5 µm). *Marasmius lebeliae* is in the recently established sect. *Globulares*, subsect. *Atrorubentes* (Oliveira *et al.* 2024), ser. *Crinipes* (Oliveira *et al.* 2020). *Marasmius vinaceus sp. nov.* is difficult to distinguish macroscopically from the lilac form (though slightly more pinkish in colour and with smaller pilei on longer stipes), but microscopically the basidiospores are shorter (mean 17.5 c.f. 19 µm); the pleurocystidia are mostly longer and simpler in form and the cheilocystidia are monomorphic, *Siccus*-type cells only, while *M. campaniformis* has both *Siccus*-type and pleurocystidia-type cheilocystidia cells. *Marasmius purpureospadiceus sp. nov.* is similar in colour and pileal size, but has more lamellae (16–18 c.f. 12–16) and longer, more robust stipes (45–60 × 1 mm c.f. 30–40 × 0.5–1 mm). All three species form a strongly supported clade Fig. 1 (79/0.99), Fig. 2 (100/1) with their sister species from China (GenBank nrITS PP622172) in the nrITS tree.

Marasmius pervagatus F.E. Guard, T. Lebel, J. Dearnaley, ***sp. nov.*** MB 857172. Figs 5, 6.

Etymology: The epithet *pervagatus* is Latin for widespread and common, and refers to its pan-tropical distribution.

Typus: **Australia**, Queensland, Brisbane, Willowbank, Champions Way, S 27°41’31.31”, E152°39’55.13”, 56 m.a.s.l., in leaf litter on urban road verge with *Eucalyptus*, *Acacia* and *Alphitonia* sp. trees, 6 Jun. 2022, *N.A. Fechner*, F2022059 (**holotype** BRI AQ1043697); GenBank numbers nrITS PQ618876, nrLSU PQ618876, *TEF1* PV151737.

Description: *Basidiomata* small, marasmioid. *Pileus* 5–10 mm diam., blood red (41), red (42) or coral (44), broadly convex, parabolic to campanulate, sulcate-striate, central disc smooth, dry glabrous. Figure 5 illustrates the colour variations of this species. *Lamellae* distant, 8–13, occasionally bifurcate, free, pale pink (39) with margin concolourous with the pileus. *Lamellulae* sparse, 1–2 tiers. *Stipe* 15–50 × 0.1–0.5 mm, central, filiform, smooth, hollow, dark brown base grading to buff apex, non-insititious, with small off-white basal mycelial disc. *Basidiospores* (15–)16–19.5 × 4–5 µm, mean 17.5 [±0.82 SD] × 4 [± 0.26 SD] µm, Q = 3.78–5.57, Qm = 4.51 [± 0.35 SD], N = 50 from type collection, narrow, clavate, slightly curved, thin-walled, smooth, inamyloid. *Basidia* 4-spored. *Basidioles* fusoid to clavate, 19–25 × 6–7 µm. *Cheilocystidia* dimorphic with (i) common *Siccus*-type cells, cylindrical, clavate, sub-globose, main body 9–20 × 6.5–9 µm, apical setulae thick-walled, refractile, occasionally in bunches, (2–)3–6 × 1–1.5 µm and (ii) less common smooth cells similar to the *pleurocystidia* 29–38 × 7–11.5 µm. *Pleurocystidia* large smooth cells, thin-walled, inamyloid, capitate, with 1–3



Fig. 5. *Marasmius pervagatus* basidiomata. **A–C.** Holotype collection BRI AQ1043697 (images by F.E. Guard). **D, E.** BGM210175 & BGM210181 (images by B.G. Muir). **F.** OAM32 (image by O. Albert-Mitchell). Scale bars = 10 mm.

© 2025 Westerdijk Fungal Biodiversity Institute

constrictions, occasionally branched, lageniform, hyphoid or utriform, 24–49 × 5.5–14 µm. *Lamellar trama* dextrinoid, hyphae 3.5–5 µm diam. *Pileipellis* mottled, consisting of a hymeniderm of *Siccus*-type cells, clavate, broadly clavate, sub-globose, pyriform, sometimes bifid, main body 6–22 × 6–10 µm, usually thin-walled, occasionally thick-walled, with multiple thick-walled refractile apical setulae, occasionally bifid, 2–5 × 0.5–1(–2) µm. *Pileal trama* weakly dextrinoid, hyphae 4–6 µm diam. *Stipe* hyphae parallel, cortex 3.5–5.5 µm diam., medulla 5–6 µm diam., inamyloid. *Caulocystidia* absent. *Clamp connections* present in all tissues.

Other collections examined: **Australia**, Queensland, Bloomfield, in wet tropical rainforest, on leaf litter, 10 Jan. 2020, *O. Albert-Mitchell*, OAM32 (envt; GenBank numbers nrITS PQ618877, nrLSU PQ618863, *TEF1* PV151713); Cairns, Flecker Botanic Gardens, in mulched garden bed, 19 Jan. 2021, *B.G. Muir*, BGM210175 (BRI AQ1034090; GenBank numbers nrITS PQ618875, nrLSU PQ618831, *TEF1* PV151728) and BGM210181 (BRI AQ1041070; GenBank numbers nrITS PQ618878, nrLSU PQ618832, *TEF1* PV151738).

Habit, habitat and distribution: Basidiomata of *Marasmius pervagatus* are gregarious, often with 20–30 basidiomata in a group. It has been found in north Queensland (FNQ) and also in Brisbane (SEQ). Basidiomata production may occur from summer through to winter. The habitat is often disturbed vegetation, e.g. mulched garden beds, but may also be undisturbed rainforest.

Notes: *Marasmius pervagatus sp. nov.* is one of the blood red species of the *M. haematocephalus* complex found in Australia. It differs from *M. haematocephalus* s. s. in having overlapping but usually more lamellae (8–13 c.f. 7–10), shorter basidiospores (mean 17.5 µm c.f. 20 µm) and two types of cheilocystidia, both *Siccus*-type cells and pleurocystidia-type cells c.f. *Siccus*-type only. It is morphologically very similar to *M. wianwian sp. nov.,* though the cheilocystidia of *M. wianwian* are mono-morphic; also *M. wunga sp. nov.* which has more lamellae (12–16 c.f. 8–13), larger basidiospores (mean 21 × 4.5 µm) and longer stipes (30–60 mm c.f. 15–50 mm).

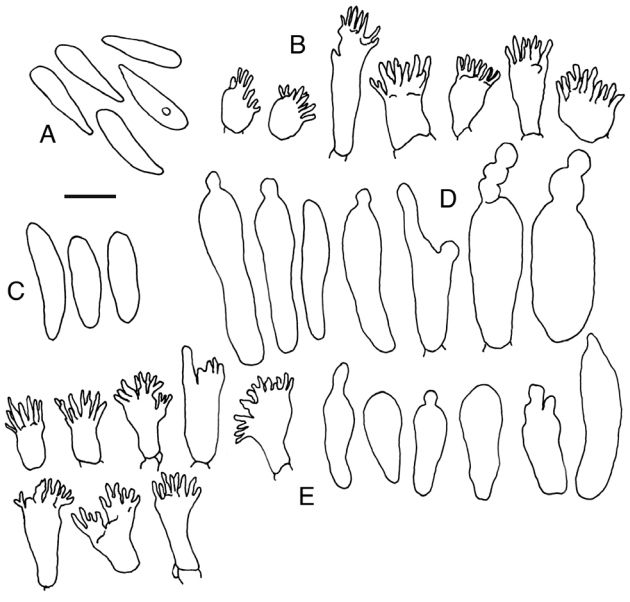

Fig. 6. *Marasmius pervagatus* (BRI AQ1043697). **A.** Basidiospores. **B.** Pileipellis *Siccus*-type cells. **C.** Basidioles. **D.** Pleurocystidia. **E.** Cheilocystidia *Siccus*-type cells and smooth cells. Scale bar = 10 µm. Illustrated by F.E. Guard.

Phylogenetic analysis resulted in the three red-pileate species of the complex occurring in Australia placed in widely separated clades. *Marasmius pervagatus sp. nov.* is closely related to both *M. asiaticus* described from Malaysia (Tan *et al.* 2009) and *M. coasiaticus* described from Brazil (Oliveira *et al.* 2022). It differs in the pileus size, being bigger than that in *M. asiaticus* (5–10 mm pileal diam. c.f. 2–8 mm), with more lamellae (8–13 c.f. 7–8) and longer stipe (15–50 mm c.f. 11–22 mm). The basidiospores are smaller on average (18.5 × 4 µm c.f. 21.5 × 4 µm) and the cheilocystidia are dimorphic, whereas in *M. asiaticus* they are *Siccus*-type cells only. *Marasmius coasiaticus* differs in colour being brownish red to brownish pink, with lamellae that are adnate, cream, non-marginate and no lamellulae, whereas *M. pervagatus sp. nov.* produces purple to blood red pilei, with free to adnexed, pink, marginate lamellae and 1–2 tiers of sparse lamellulae.

Morphologically the Australian specimens are variable in pileal diameter and colour, stipe dimensions and substrate. Specimen OAM32 is at the smaller end of the range for all macro-morphological parameters. However, based on the nrITS (Fig. 1), they form a single clade with low to moderate support (55/0.75) and the *TEF1* tree (Fig. 2) has the three north Queensland collections in a well-supported clade (99/1.0) and the south-east Queensland collection on a separate branch with low support (Fig. 2). No nrLSU or *TEF1* sequences of the Thai collections are available for comparison. In Thailand this species has been called *M. haematocephalus* f. '*haematocephalus*', one of the six morphological forms described by Wannathes *et al.* (2009). Macro- and micro-morphology of these collections match *M. pervagatus sp. nov.*, except for the non-marginate lamellae in the Thai forms. The Indian and Florida, USA specimens are almost identical in the nrITS data, but these collections have not been compared morphologically or using other gene regions.

Although *M. pervagatus sp. nov*. has been found in widely separated locations in Queensland, it does not appear to be as common as *M. porphyrocephalus* and more search effort is required to determine its full distribution and whether there are cryptic species hidden in this clade.

Marasmius porphyrocephalus F.E. Guard, T. Lebel, Dearnaley, ***sp. nov.*** MB 857173. Figs 7, 8.

Etymology: The epithet is from the Greek '*porphyro*' meaning purple, referring to the colour of the pileus of this species and '*cephalus*' is Greek for head.

Typus: **Australia**, Queensland, Cairns Botanical Gardens, S16°53'58.4", E145°44'51.2", in garden mulch, 11 Feb. 2021, *F.E. Guard* & *T. Lebel,* F2021046 (**holotype** BRI AQ1034084); GenBank numbers nrITS PQ618882, nrLSU PQ618852, *TEF1* PV151740.

Description: *Basidiomata* small, marasmioid. *Pileus* (3–)5–14(–20) mm diam., colours varying from candy pink, pinkish-purple (40) to vinaceous (76), with blood red (41) to livid vinaceous (77) central disc and radiating sulci, colour fading

© 2025 Westerdijk Fungal Biodiversity Institute

with age, broadly parabolic to almost applanate with wavy margins at maturity, and a slightly depressed darker central disc, surface dry, glabrous. *Lamellae* free to adnexed, distant, 12–16, with occasional irregular lamellulae and bifurcations, pale rose (39) to pale vinaceous (76), ± margin faintly concolourous with pileus. *Stipe* (15–)30–45(–60) × 0.2–0.5 mm, blackish-brown base, purplish chestnut (21) trunk, rose pink (39) to purple (40) apex, glabrous, hollow, filiform, non-insititious with tiny basal disc of off-white mycelium. *Spore print* white. *Basidiospores* (15.5–)16.5–19.5(–23) × 4–4.5 µm, mean 17.5 [± 0.99 SD] × 4 [± 0.20 SD] µm, Q = 3.56–4.76, Qm = 4.13 [± 0.32 SD], N = 20, narrow, elongate, clavate, thin-walled, smooth, inamyloid. *Basidia* 4-spored, 20–24 × 7–8.5 µm. *Basidioles* 20–23 × 6–8.5 µm, fusoid to clavate. *Cheilocystidia* (i) *Siccus*-type cells forming a sterile edge, cylindrical, broadly clavate, sub-globose, occasionally bifid, main body 10–22 × 7.5–10 µm with multiple apical thick-walled setulae 2–5 × 1–1.5 µm; (ii) rare smooth, irregular, clavate to bifid cells 12–38 × 10–17 µm. *Pleurocystidia* moderately common 22–54 × 5–13 µm, simple cylindrical with obtuse apex, lageniform, capitate occasionally strangulate, thin-walled, hyaline. *Lamellar trama* hyphae 3.5–5 µm diam. *Pileal trama* dextrinoid, hyphae thin-walled, 5–5.5 µm diam. *Pileipellis* a hymeniderm of *Siccus*-type cells, similar to cheilocystidia type (i), cylindrical, clavate, spathulate, sub-globose, main body 7.5–14.5 × 5.5–9 µm with multiple thick-walled refractile apical setulae 2–6 × 1–2 µm. Stipe hyphae parallel, cortex with hyphae 5–6 µm diam., slightly dextrinoid, medullary hyphae 5–7 µm diam., slightly dextrinoid. *Caulocystidia* absent. *Clamp connections* present in all tissues.

Other collections examined: **Australia**, Queensland, Balmoral Ridge, Dilkusha Nature Refuge, road verge near creek, in subtropical rainforest understorey, 1 May 2019, *F.E. Guard*, F2019036 (BRI AQ1007378; GenBank numbers nrITS OQ073536, nrLSU OQ073539, *TEF1* PV151763); on road verge in leaf litter, 29 Jan. 2020, *F.E. Guard*, F2020021 (BRI AQ1017489; GenBank number nrLSU PQ618834); in subtropical riparian rainforest, on mossy bark, 20 Jan. 2021, *F.E. Guard*, F2021006 (BRI AQ1021681; GenBank numbers nrITS PQ618881, nrLSU PQ618853, *TEF1* PV151741); and on road verge among *Allocasuarina* sp. needles, 9 Jan. 2024, *F.E. Guard*, F2024008 (BRI AQ1045960; GenBank numbers nrITS PQ618883, nrLSU PQ618851, *TEF1* PV151752); Cairns, Edge Hill, Flecker Botanic Gardens, Collins Avenue, in garden bed mulch, 19 Jan. 2021, *B.G. Muir*, BGM210178 (BRI AQ1041069; GenBank numbers nrITS PQ618880, nrLSU PQ618838); Eudlo, 56 Eudlo School Rd, in garden mulch, 14 Feb. 2024, *J. Rodwell*, JR001 (BRI AQ1052603; GenBank number nrLSU PQ618835); Julatten, Clacherty Road, on road verge in leaf litter, 17 Feb. 2021, *F.E. Guard*, F2021070 (BRI AQ1034085; GenBank numbers nrITS PQ618879, nrLSU PQ618833, *TEF1* PV151730); Kuranda, Russett Park, Jeffrey Rd, 300 m from Barron River bridge, in rainforest litter, 22 Jan. 2006, *S.J.M. McMullan-Fisher*, SMF2320 (MEL2297133; GenBank number *TEF1* PV151759); Murrumba Downs, John Oxley Reserve, in wet sclerophyll forest among leaf litter, 13 Jan. 2024, *W.G. Boatwright*, QMS2024-01-13-009 (BRI AQ1045965; GenBank numbers nrLSU PQ618837, *TEF1* PV151754).

Habit, habitat & distribution: This species occurs in leaf litter in natural and disturbed areas, including mulched garden beds and road verges in tropical and subtropical areas of Queensland and northern NSW. The litter is usually thick, consisting of *Allocasuarina* needles, regenerating rainforest tree leaves or artificially mulched garden beds with native or exotic species. At times it occurs on the bark of living trees in a vertical position. It is gregarious and may produce basidiomata in abundance (hundreds).



Fig. 7. *Marasmius porphyrocephalus* holotype collection BRI AQ1034084 and other collections to illustrate variations in colour and form **A.** Campanulate pilei. **B, C.** Applanate pilei. **D.** Lamellae. **E.** Dusty vinaceous (76) colour form. Scale bar = 10 mm. Images by F.E. Guard.

© 2025 Westerdijk Fungal Biodiversity Institute

Notes: *Marasmius porphyrocephalus sp. nov.* is a morphologically distinct species. Its candy pink pilei with blood red central disc and radiating striations, habit of opening to almost applanate, the pale pink lamellae — not or only faintly marginate, with short bifurcations and irregular lamellulae make it usually recognisable macroscopically and different from other rust red, blood red and wine red members of the complex in Australia. *Marasmius porphyrocephalus sp. nov.* is by far the most widespread and common with over 150 observational records in the Atlas of Living Australia to 23 May 2024, from Cape York Peninsula, QLD to northern NSW with a few from the Northern Territory. Molecular analysis of the nrITS gene region shows that it forms a well-supported (88/0.72) clade with close relatives from Thailand, India and Madagascar, but is not closely related to other (probably endemic) members of the complex in Australia (Fig. 1).

It differs macroscopically from *M. haematocephalus* s. s. in pileal colour, being more pinkish-purple; with more lamellae (12–16 c.f. 7–10) that are pinkish coloured; in having generally shorter stipes (30–45 c.f. 22.5–62 mm); and in having basidiospores shorter than *M. haematocephalus*, mean 17.5 × 4 µm c.f. 20.5 × 4 µm (Oliveira *et al.* 2022). '*Marasmius haematocephalus*' sensu Desjardin & Horak (1997) from Papua New Guinea is a very good match morphologically, but molecular study is required to confirm. '*Marasmius haematocephalus' sensu* Desjardin, Retnowati & Horak (2000) from Java & Bali has a more reddish-brown pileus, fewer lamellae (9–12), longer basidiospores (mean 20.5 × 4 µm) and more common and larger pleurocystidia with more apical constrictions (no molecular data available). '*Marasmius haematocephalus*' sensu Tan *et al.* (2009) from Malaysia is also similar, but has smaller pilei (2–7 mm diam.) which are darker violet, and also has shorter thicker stipes (8–23 × 0.5–1 mm) and marginally longer basidiospores (mean 18.2 µm c.f. 17.5 µm). Molecular study of the nrITS region suggests this is sister to *M. porphyrocephalus*, with low support [subclade 4A(ii)]. *Marasmius asiaticus* (Mešić & Tkalčec 2010), described by Tan *et al.* (2009) as *M. distantifolius* (nom. illeg.) is more similar in colour, but has fewer lamellae (7–8), no lamellulae, short stipe (11–22 × 0.1–0.2 mm) and longer basidiospores (mean 21.5 × 4 µm). Molecularly this species is distant from *M. porphyrocephalus sp. nov.* and is closer to the neotropical *M. coasiaticus* and *M. pervagatus sp. nov*. Of the six forms of '*M. haematocephalus*' *sensu* Wannathes *et al.* (2009) in Thailand, form '*violaceous*' is the closest in colour to *M. porphyrocephalus,* but the basidiospores are longer (21.5 µm c.f. 17.5 µm). Phylogenetic analysis shows most specimens of *M. haematocephalus* f. 'violaceous', together with var. *atroviolaceus* (India) and a specimen of '*M. haematocephalus*' (China) form a distinct and separate southern Asian clade not close to *M. porphyrocephalus* [subclade 3C(i) in Fig. 1]. '*Marasmius haematocephalus* f.1' (AKD 201 2014) *sensu* Dutta from India (2017) is morphologically quite distinct with its small pileal size (5–6 mm), non-marginate cream lamellae with no lamellulae, short stipe (11–18 mm) and very small basidiospores (14–15 × 3.5–5 µm). However, phylogenetic analysis of the nrITS region shows it to be 100 % similar to a specimen of '*M. haematocephalus*' from Thailand (GenBank nrITS MW426460, voucher NW1441) and both are within the *M. porphyrocephalus* clade. Pairwise analysis of the nrITS region of *'M. haematocephalus' sensu* Shay *et al.* (2017) from Madagascar shows the Madagascan species to be 99.3 to 99.7 % identical with *M. porphyrocephalus.* It is morphologically similar but differs in the shape of mature pilei (convex to campanulate and umbilicate with age), fewer lamellae (10–12), no lamellulae, shorter stipe (12–25 mm) and wider range of basidiospore lengths (13.5–22 µm). As well, one conspecific collection from Madagascar has cream coloured pilei (JES193, image on iNaturalist7000636). Further collections and analysis of other gene regions are necessary to confirm the morphological distinction of these species. The neotropical species *M. rubicundus* in its ruby pink form is similar, but has fewer lamellae (7–12). With current data, *M. porphyrocephalus* appears to be a widespread and variable species. However, examination of further gene regions may help to resolve taxon boundaries in this group.

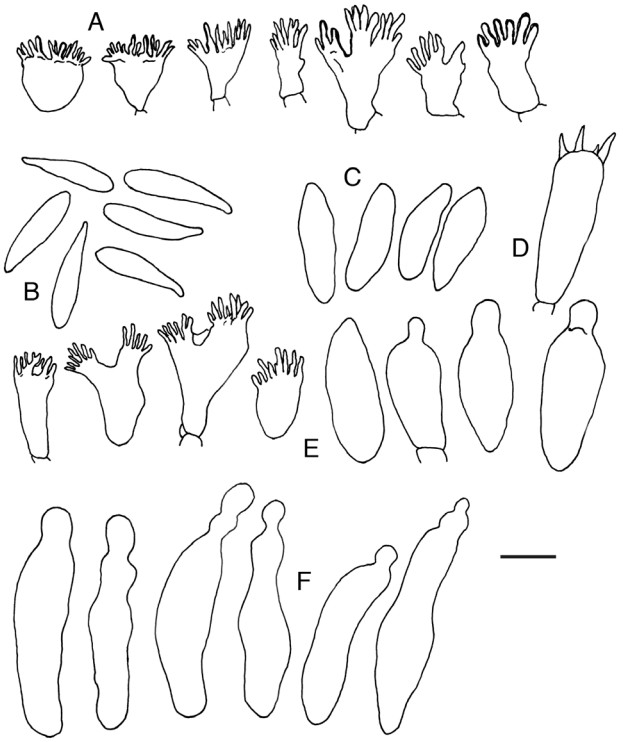

Fig. 8. *Marasmius porphyrocephalus* (F2024008). **A.** Pileipellis *Siccus*-type cells. **B.** Basidiospores. **C.** Basidioles. **D.** Basidium. **E.** Cheilocystidia *Siccus*-type cells and smooth cells. **F.** Pleurocystidia. Scale bar = 10 µm. Illustration by F.E. Guard.

Marasmius purpureospadiceus F.E. Guard, T. Lebel, Dearnaley, ***sp. nov.*** MB 857174. Figs 9, 10.

Etymology: The epithet is a combination of the Latin words "*purpureo*" meaning purplish and "*spadiceus*" meaning date-coloured to describe the purple-brown colour of the pileus.

Typus: **Australia**, Queensland, Balmoral Ridge, Dilkusha Nature Refuge, road verge above Lot 3, in leaf litter, S26°44'24.5", E152°53'36.4", 374 m.a.s.l., 10 Jan. 2021, *F.E. Guard*, F2021001 (**holotype** BRI AQ1021678); GenBank numbers nrITS PQ618872, nrLSU PQ6188622, *TEF1* PV151739.

Basidiomata small to medium-sized, marasmioid. *Pileus* 10–20 mm diam., juvenile: purplish chestnut (21) with paler margins, mature: very distinct, slightly raised, purplish date

© 2025 Westerdijk Fungal Biodiversity Institute

(22) central disc, then fawn (29), grading to clay pink (23) outer half with fawn sulci, parabolic to broadly convex, surface dry. *Lamellae* moderately close, 16–18, with occasional lamellulae, free, pale clay pink (23), ± faintly darker margin. *Stipe* 45–60 × 1 mm, central, filiform, blackish base, purplish chestnut (21) upper trunk and clay pink (30) apex, smooth, hollow, non-insititious basal attachment with small buff mycelial pad and moderate cream mycelial mat on surrounding substrate. *Spore print* white. *Basidiospores* 16.5–19.5 × 3.5–4.5 µm, mean 18.0 [± 0.75 SD] × 4.0 [± 0.21 SD] µm, Q = 4.12–4.68, Qm = 4.42 [± 0.17 SD], N = 20, elongate, clavate, with blunt narrow ends, thin-walled, inamyloid. *Basidia* only one seen, 2-spored, 29 × 6.5 µm. *Basidioles* bluntly fusoid, clavate, oblong 19–27 × 5–9 µm. *Cheilocystidia Siccus*-type cells forming a sterile edge variable in shape, clavate, sub-globose, bifid, at times irregular, main body 8–22 × 5–8 µm, with thick-walled, refractile setulae 2.5–5 × 0.5–1.5 µm. *Pleurocystidia* in moderate numbers, smooth walled, utriform, lageniform, occasionally capitate, 30–42 × 6–8 µm. *Lamellar trama* faintly dextrinoid, hyphae 3–4 µm diam. *Pileal trama* dextrinoid, hyphae 4–5 µm diam. *Pileipellis* a hymeniderm of *Siccus*-type cells, narrow to broadly clavate, cylindrical, sub-globose, main body 5–16 × 5–8 µm, setulae, thick-walled, refractile 2–6 × 0.5–1 µm. *Stipe* consists of parallel hyphae 5–5.5 µm diam., cortex dextrinoid. *Caulocystidia* absent. *Clamp connections* present in all tissues.

Other collection examined: **Australia**, NSW, Border Ranges National Park, Helmholtzia Loop, S 28°22'40.5", E153°04'07.7", 839 m.a.s.l., 18 Feb. 2022, *F.E. Guard*, F2022005 (BRI AQ1034087; GenBank numbers nrITS PQ618871, nrLSU PQ618839, *TEF1* PV151720).

Habit, habitat and distribution: *Marasmius purpureospadiceus* has only been collected twice, with sparse basidiomata, once in disturbed road verge habitat and once in old growth subtropical rainforest. Its distribution currently appears restricted to SE QLD and northern NSW.

Notes: The medium-sized basidiomata of *Marasmius purpureospadiceus sp. nov.* with purplish-brown pilei and sturdy filiform, non-insititious stipes make it morphologically similar to *M. brunneolorobustus* (Tan *et al.* 2022) which occurs in similar habitat and locations. However, basidiomata of the latter have more lamellae (20–30 c.f. 16–18) and have no pleurocystidia. Molecularly, *M. brunneolorobustus* is in sect. *Globulares,* possibly subsect. *Fusicystides* (Oliveira *et al.* 2024) though this is not yet confirmed, and therefore is not closely related to *M. purpureospadiceus sp. nov. Marasmius haematocephalus* f. *robustus* from Thailand (Wannathes *et al.* 2009) is similar in size and colour, but has fewer lamellae (9–15) and longer basidiospores (mean 20 µm c.f. 18 µm). *Marasmius vinaceus sp. nov.* is also similar, but is generally



Fig. 9. *Marasmius purpureospadiceus* holotype collection BRI AQ1021678. **A.** Lamellae detail. **B.** Basidiomata in situ. **C.** Pilei purplish chestnut (21) central discs. **D.** Stipes. Scale bar = 10 mm. Images by F.E. Guard.

© 2025 Westerdijk Fungal Biodiversity Institute

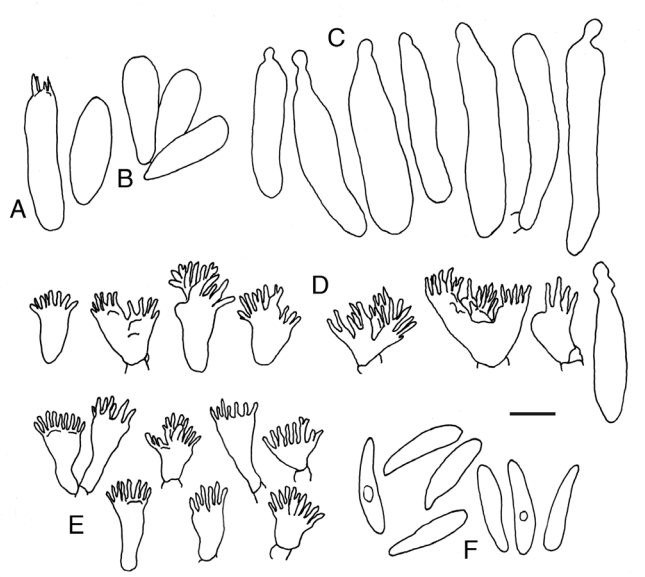

Fig. 10. *Marasmius purpureospadiceus.* **A.** Basidium. **B.** Basidioles. **C.** Pleurocystidia. **D.** Cheilocystidia *Siccus*-type cells and smooth cell. **E.** Pileipellis *Siccus*-type cells. **F.** Basidiospores. Scale bar = 10 µm. Illustrated by F.E. Guard.

less robust and differs in colour (more pinkish grey), in pileal size (6–15 mm diam.) and in fewer lamellae (13–16 c.f. 16–18). They are closely related molecularly being 97.6 to 98.1 % identical on the nrITS, though only 93.6 to 94.2 % identical on *TEF1* pairwise analysis. The lilac colour variant of *M. campaniformis sp. nov.* has a more deeply sulcate, bell-shaped pileus, more purplish colour and fewer lamellae (12–16). *Marasmius purpureospadiceus sp. nov.*, *M. campaniformis sp. nov.* and *M. vinaceus sp. nov*. together with '*M. haematocephalus*' from Hainan, China (GenBank nrITS PP622172) form a monophyletic group based on phylogenetic analysis of the nrITS (Fig. 1). The analysis of the *TEF1* region also supports these three new species in a strongly supported clade wherein *M. purpureospadiceus* is rather sister to *M. vinaceus* (Fig. 2).

Marasmius vinaceus F.E. Guard, T. Lebel, Dearnaley, ***sp. nov.*** MB 857175. Figs 11, 12.

Etymology: The epithet is the Latin word for vinaceous (wine-coloured) or greyish-pink and applies to the pileus colour, as illustrated in Flora of British Fungi Colour Identification Chart.

Typus: **Australia**, Queensland, Maleny, Bridge Creek, Wells Rd S26°43'46.7", E152°50'51.5", 333 m.a.s.l., in regenerating wet sclerophyll forest understorey, 27 Apr. 2019, *F.E. Guard*, F2019031 (**holotype** BRI AQ1007374, **isotype** MEL2469588); GenBank numbers nrITS OQ073537, nrLSU OQ073542, *TEF1* PV151757.

Description: *Basidiomata* small, marasmioid. *Pileus* 6–15 mm diam., livid vinaceous (77) central disc, vinaceous (76) remainder of the pileus with a paler margin, sulci darker especially in juveniles, convex to broadly conical, deeply sulcate-striate producing a scalloped margin, surface dry, glabrous. *Lamellae* free, distant, 13–16, with only occasional lamellulae, pale pinkish-cream, non-marginate. *Stipe* 35–70 × 0.5–1 mm, purplish-chestnut (21) base, reddish-brown mid-shaft and buff (52) to pale pink upper end, juveniles reddish-



Fig. 11. *Marasmius vinaceus* holotype collection BRI AQ1007374. **A.** Central disc detail. **B.** Basidiomata collection. **C.** Lamellae detail. **D.** Basal mycelial disc details. Scale bar = 10 mm. Images by F.E. Guard.

© 2025 Westerdijk Fungal Biodiversity Institute

brown throughout the length, central, smooth, hollow, non-insititious with small basal off-white mycelial pad. *Spore print* white. *Basidiospores* 16.5–19.5 × 4–5.5 µm, mean 17.5 [± 0.63 SD] × 4.5 [± 0.35 SD] µm, Q = 3.51–4.62, Qm = 3.97 [± 0.27 SD], N = 20, narrow, elongate, clavate, thin-walled, inamyloid. *Basidia* 3- to 4-spored, 10–25 × 7–8 µm. *Basidioles* 20–26 × 6–9 µm, fusoid to clavate. *Cheilocystidia* common, forming sterile edge, *Siccus*-type cells, cylindrical, clavate, sub-globose, main body thin-walled 6–18 × 5.5–8.5 µm, setulae thin to thick-walled and refractile 3–5 × 1–1.5 µm. *Pleurocystidia* common, capitate, utriform, occasionally strangulate 36–52 × 7–12(–14) µm. *Lamellar trama* dextrinoid, hyphae 3–4 µm diam., occasionally inflated hyphae to 12 µm diam. *Pileal trama* dextrinoid, hyphae 3.5–8 µm diam. *Pileipellis* a hymeniderm of *Siccus*-type cells, main body cylindrical, clavate, sub-globose, 6–17 × 4.5–9 µm with multiple apical setulae, thick-walled and refractile 2–6 × 0.5–1 µm. *Stipe* hyphae parallel, those of the cortex 4–5 µm diam., inamyloid, those of the medulla 5–8 µm diam., inamyloid. *Caulocystidia* absent. *Clamp connections* present in all tissues.

Other collections examined: **Australia**, Queensland, Julatten, Clacherty Road, 16 Feb. 2021, *T. Lebel & J. Dearnaley*, F2021069 (BRI AQ1034085; GenBank numbers nrITS PQ618873, nrLSU PQ618829, *TEF1* PV151729) and Mapleton, Linda Garrett National Park, among leaf litter in wet sclerophyll forest, 13 Mar. 2016, *F.E. Guard & QMS members*, QMS LG55 (envt.).

Habit, habitat and distribution: *Marasmius vinaceus sp. nov.* forms gregarious basidiomata, but has only been collected three times, in widely separated locations in subtropical SEQ and tropical FNQ. All collections were made in disturbed habitat among leaf litter by road verges in subtropical or tropical rainforest and wet sclerophyll forest.

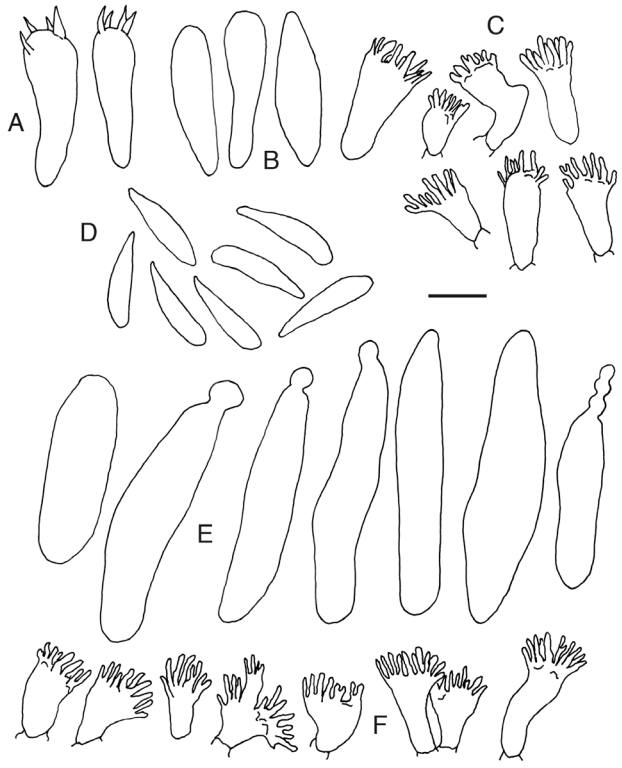

Fig. 12. *Marasmius vinaceus* (BRI AQ1007374). **A.** Basidia. **B.** Basidioles. **C.** Pileipellis *Siccus*-type cells. **D.** Basidiospores. **E.** Pleurocystidia. **F.** Cheilocystidia *Siccus*-type cells. Scale bar = 10 µm. Illustrated by F.E. Guard.

Notes: *Marasmius vinaceus sp. nov.* is very similar to the lilac form of *M. campaniformis sp. nov*., but basidiospores are slightly shorter (17.5 µm c.f. 19 µm), the stipe is often longer (35–70 mm c.f. 30–45 mm), and the pileal size while overlapping is generally smaller (6–15 mm c.f. 10–20 mm). It is also to be noted that, while the basidiospores of the holotype and the Linda Garrett specimen (not sequenced) were identical in size, the Julatten specimen had a greater range in spore size (17–21 × 4–5 µm, mean 19 [± 1.13 SD] × 4.5 [± 0.29 SD] µm, Q = 3.82–5.04, Qm = 4.35 [± 0.31 SD], N = 20). Phylogenetic analyses of the nrITS and *TEF1* regions place *M. vinaceus* as sister with strong support (79/0.99) and (100/1.0) respectively to *M. purpureospadiceus* and *M. campaniformis.* (Figs 1, 2).

Marasmius wianwian F.E. Guard, T. Lebel, Dearnaley, ***sp. nov.*** MB 857176. Figs 13, 14.

Etymology: The epithet *wianwian* (pronounced *"wee-un-wee-un"*) is derived from the local first nation's name for a special place, in the area known by Europeans as The Big Scrub in northern NSW, where the species was first identified. It is a noun in apposition.

Typus: **Australia**, Queensland, Linda Garrett National Park, S26°37'07.35", E152°51'02.6", in leaf litter, 5 Mar. 2022, *W.G. Boatwright*, QMS2022-03-05-013 (**holotype** BRI AQ1041081); GenBank numbers nrITS PQ618898, nrLSU PQ618857, *TEF1* PV151742.

Description: *Basidiomata* small, marasmioid. *Pileus* 4–9 mm diam., colours between blood red (41), rust (13) and dark brick (20), convex to parabolic, sulcate-striate with darker smooth central disc, surface dry, glabrous. *Lamellae* free to adnexed, distant, 11–14, off-white to pale pink with margins concolorous with pileus, *lamellulae* occasional, short. *Stipe* 25–40 × 0.2–0.3 mm, central, filiform, black base, brown mid-stipe, pale apex, glabrous, hollow, non-insititious, with tiny off-white basal mycelial disc. *Spore print* white. *Basidiospores* 16–18 × 3.5–4 µm, mean 17 [± 0.49 SD] × 4 [± 0.19 SD] µm, Q = 3.94–4.79, Qm = 4.46 [± 0.25 SD], N = 20, narrow, clavate, thin-walled, smooth, inamyloid. *Basidia* 4-spored, 19–25 × 7–9 µm, with occasional larger 2-spored basidia. *Basidioles* clavate to fusoid, 22–25 × 5.5–10 µm. *Cheilocystidia Siccus*-type cells, cylindrical, clavate, occasionally bifid or branched, main body 12–26 × 6–10 µm, multiple apical setulae, thick-walled, refractile 3–6(–9) × 0.5–1 µm. *Pleurocystidia* moderately common, smooth cells, 30–50(–62) × 8–11 µm, usually capitate, utriform, thin-walled, hyaline. *Lamellar trama* weakly dextrinoid, hyphae 4.5–7.5 µm diam. *Pileal trama* dextrinoid, hyphae 3–6 µm diam. *Pileipellis* a hymeniderm of *Siccus*-type cells similar to cheilocystidia, cylindrical, clavate, occasionally bifid or elongate, main body 9–24 × 5.5–8 µm with multiple thick-walled, refractile apical setulae 3–6 × 0.5–1 µm. *Stipe* hyphae parallel, those of the cortex 3.5–6 µm diam., weakly dextrinoid, medullary hyphae 6–8 µm, inamyloid. *Caulocystidia* absent. *Clamp connections* present in all tissues.

© 2025 Westerdijk Fungal Biodiversity Institute



Fig. 13. *Marasmius wianwian.* **A.** Holotype collection BRI AQ1041081. **B.** Lamellae detail. **C–G.** Collections showing colour variations. C–E. F2022025. F, G. F2022012. Scale bars: A–F = 10 mm; G = 5 mm. Images by F.E. Guard.

Other collections examined: **Australia**, New South Wales, Booyong Scrub Reserve, on fallen leaves in subtropical rainforest, 21 Feb. 2022, *F.E. Guard*, F2022025 (BRI AQ1034089; GenBank numbers nrITS PQ618897, nrLSU PQ618860, *TEF1* PV151732); Rocky Creek Dam, Big Scrub Loop, on leaf litter in subtropical rainforest, 20 Feb. 2022, *F.E. Guard*, F2022012 (BRI AQ1034088; GenBank numbers nrITS PQ618896, nrLSU PQ618859).

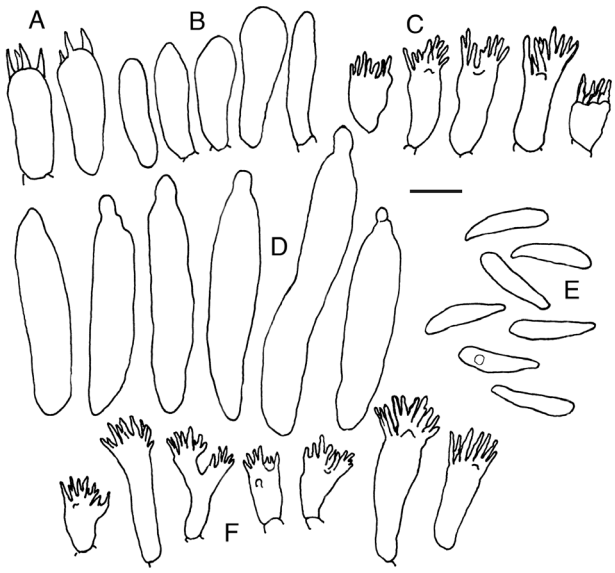

Fig. 14. *Marasmius wianwian* (BRI AQ1041081). **A.** Basidia. **B.** Basidioles. **C.** Cheilocystidia *Siccus*-type cells. **D.** Pleurocystidia. **E.** Basidiospores. **F.** Pileipellis *Siccus*-type cells. Scale bar = 10 µm. Illustrated by F.E. Guard.

Habit, habitat and distribution: Basidiomata of this Australian endemic, *Marasmius wianwian sp. nov.,* occur in small groups, on deep leaf litter, and have to date been found in moderately undisturbed subtropical old growth rainforest, or mixed wet sclerophyll and palm forest. It has been collected from three locations — two remnants of the 'Big Scrub' in northern New South Wales and one National Park in the Sunshine Coast hinterland, Queensland.

Notes: *Marasmius wianwian sp. nov.* is not easily distinguished in the field from the other blood, brick or rust species of the complex in Australia, *M. wunga sp. nov.* and *M. pervagatus sp. nov.* All three species show colour variations. Microscopically, it has shorter basidiospores than *M. wunga* (17 µm c.f. 21 µm) and marginally shorter than *M. pervagatus* (17 µm c.f. 17.5 µm). The smooth pleurocystidia in *M. wianwian sp. nov.* are simpler in form than *M. pervagatus* and smaller in size than *M. wunga. Marasmius haematocephalus* s. s. is similar, but may be bigger in pileal diam. (2.5–16 mm c.f. 4–9 mm), with longer stipes (to 62 mm c.f. 45 mm), fewer lamellae (7–10, non-marginate c.f. 11–14, marginate) and basidiospores that are longer (mean 20 µm c.f. 17 µm). Phylogenetic analysis of the nrITS region shows this well supported (100/1.0) clade to be quite distant from and basal to all others in the broad *haematocephalus* clade, including the epitype from Brazil in the neotropics (Figs 1, 2). Closest to *Marasmius wianwian sp. nov.* molecularly is a well-supported clade of four species, three of which appear to be restricted in distribution to Australia, with a fourth from tropical China (Hainan).

Marasmius wunga F.E. Guard, T. Lebel, Dearnaley, ***sp. nov.*** MB 857177. Figs 15, 16.

© 2025 Westerdijk Fungal Biodiversity Institute

Etymology: The epithet '*wunga*' is the name for a fungus in the Dungidau dialect of the Yinibara people on whose land it was first identified. The term '*wunga*' is a noun in apposition.

Typus: **Australia**, Queensland, Balmoral Ridge, Dilkusha Nature Refuge, above Lot 3, S26°44'24.5", E152°53'36.4", 374 m.a.s.l., on road verge in leaf litter in regenerating subtropical rainforest, 13 Jan. 2024, *F.E. Guard*, F2024009 (**holotype** BRI AQ1045961); GenBank numbers nrITS PQ618889, nrLSU PQ618848.

Description: *Basidiomata* small, marasmioid. *Pileus* (3–)5–9(–13) mm diam., from scarlet (43) to coral (44), red (42) to blood red (41), occasionally purple (40) with darker, smooth central disc, sulcate-striate, parabolic to campanulate with everted margins, surface dry, glabrous. *Lamellae* usually free, distant, 12–16, with occasional *lamellulae* and rare bifurcations, pale pink to pale salmon (45), margins usually concolorous with the pileus, occasionally non-marginate. *Stipe* 30–60(–80) × 0.2–0.5 mm, central, filiform, black to purplish-chestnut (21) base, bay (19) to blood red (41) mid-stipe, pink to salmon (45) apex, glabrous, hollow, non-insititious with small off-white basal mycelial disc. *Spore print* white. *Basidiospores* 18.5–22.5(–24) × 4–5 µm, mean 21 [± 0.98 SD] × 4.5 [± 0.24 SD] µm, Q = 4.17–5.14, Qm = 4.78 [± 0.25 SD], N = 20, narrow, clavate, slightly curved, thin-walled, smooth, inamyloid. *Basidia* 4-spored, rare, 30–42 × 8.5–10 µm, sterigmata up to 5 µm long. *Basidioles* clavate to fusoid, 22–28 × 6.5–9.5 µm. *Cheilocystidia* (i) common *Siccus*-type cells, forming a sterile edge, main body sub-globose, clavate, narrow clavate, cylindrical, occasionally bifid, or irregular, 9–20(–25) × 5.5–9 µm, with multiple thick-walled, apical setulae 2.5–5 × 0.5–1(–2.5) µm, (ii) uncommon irregular smooth cells 17–20(–28) × 6–12 µm and (iii) rare intermediate cells, bifid with one branch



Fig. 15. *Marasmius wunga* holotype collection BRI AQ1045961. **A–C.** Basidiomata in situ, showing pilei, lamellae and substrate detail. **D–H.** Collections showing colour variations. D. F2024004. E. F2024005. F. 2024007. G. F2020047. H. F2014148. Scale bar = 10 mm. Images by F.E. Guard.

© 2025 Westerdijk Fungal Biodiversity Institute

smooth and one branch digitate. *Pleurocystidia* common, (35–)42–76 × 7.5–12 µm, thin-walled, simple cylindrical, lageniform, capitate, occasionally strangulate. *Lamellar trama* weakly dextrinoid, hyphae 7–9 µm diam. *Pileal trama* dextrinoid, hyphae 4–6 µm diam. *Pileipellis* a hymeniderm of *Siccus*-type cells, cylindrical, spathulate, narrow to broadly clavate, occasionally branched, main body 9–16 × 6–10 µm, with multiple apical, thick-walled, refractile setulae 3–6 × 0.5–1.5 µm. *Stipe* hyphae parallel, cortex dextrinoid, hyphae 5–6 µm diam., medulla inamyloid, hyphae 5–9 µm diam. *Caulocystidia* absent. *Clamp connections* present in all tissues.

Other collections examined: **Australia**, Queensland, Balmoral Ridge, Dilkusha Nature Refuge, in regenerating rainforest, near creek, on well-rotted wood, 12 Dec. 2014, *F.E. Guard*, F2014148 (BRI AQ1001910; GenBank number nrITS PQ618887); road verge near entry, in leaf litter under regenerating subtropical rainforest, 22 Apr. 2019, *F.E. Guard*, F2019017 (BRI AQ1007367, MEL2469581; GenBank numbers nrITS OQ073534, nrLSU OQ073540, *TEF1* PV151760); Wren Gully, in leaf litter under regenerating subtropical rainforest, 22 Apr. 2019, *F.E. Guard*, F2019018 (BRI AQ1007368, MEL2469582; GenBank numbers nrITS OQ073535, nrLSU OQ073541, *TEF1* PV151762); road verge leaf litter, 19 Mar. 2021, *F.E. Guard*, F2021091 (envt, GenBank numbers nrITS PQ61889, nrLSU PQ618842); road verge above Lot 3 in leaf litter, 4 Mar. 2022, *F.E. Guard*, F2022041 (BRI AQ1041091; GenBank numbers nrITS PQ618892, nrLSU PQ618861, *TEF1* PV151745); road verge near bunya tree above Lot 3, 8 Jan. 2024, *F.E. Guard*, F2024004 (BRI AQ1045956; GenBank numbers nrITS PQ618893, nrLSU PQ618844); road verge needle-litter under *Allocasuarina* sp., 9 Jan. 2024, *F.E. Guard*, F2024007 (BRI AQ1045959; GenBank numbers nrITS PQ618884, nrLSU PQ618843, *TEF1* PV151751); Maleny, Maleny Precinct, in leaf litter under mixed native and exotic trees, 8 Jan. 2024, *W. Nash* & *F.E. Guard*, F2024005 (BRI AQ1045957; GenBank numbers nrITS PQ618888, nrLSU PQ618850); Mount Cordeaux, Main Range National Park, wet sclerophyll forest in leaf litter, 20 Apr. 2024, *W.G. Boatwright*, QMS2024-4-20-005 (BRI AQ104807; GenBank numbers nrITS PQ618894, nrLSU PQ618846); Numinbah Valley, Bornhoffen Camp, in leaf litter under lantana shrubs, 25 Mar. 2023, *F.E. Guard*, QMS2023-3-25 (BRI AQ1040807; GenBank numbers nrITS PQ618899, nrLSU PQ618849, *TEF1* PV151755); Springbrook, Best of All Lookouts, on leaf litter in roadside grass, 12 Feb. 2015, *J.C. Peuchmarin*, Peuchmarin#1 (BRI AQ1019380; GenBank number nrITS PV016896); New South Wales: Dorroughby, road verge in leaf litter, 15 Jan. 2024, *C. Marciniak*, F2024014, iNaturalist200315251 (BRI AQ1046796; GenBank numbers nrITS PQ618895, nrLSU PQ618845, *TEF1* PV151756).

Habit, habitat and distribution: This species produces gregarious basidiomata that often occur in large numbers, most commonly in disturbed areas including road verges and mulched gardens in subtropical vegetation, growing in deep leaf litter. However, it appears to be a species endemic to Australia, with the current distribution restricted to south east Queensland and northern New South Wales.

Notes: *Marasmius wunga sp. nov.* is one of three red-pileate Australian species (*M. pervagatus sp. nov.*, *M. wianwian sp. nov.* and *M. wunga sp. nov.*) in the broader *M. haematocephalus* complex. *M. wunga* occurs in numerous shades of red and occasionally it is purplish, but usually lacks the pinkish-purple tones of *M. porphyrocephalus*. The red-pileate species can be difficult to differentiate in the field. All three occur in southeast QLD, but only *M. pervagatus sp. nov.* in FNQ. Microscopically, *M. wunga sp. nov.* has the biggest basidiospores (mean 21 × 4.5 µm, c.f. 17.5 × 4 µm in *M. pervagatus* and 17 × 4 µm in *M. wianwian*). Cheilocystidia vary from monomorphic (*M. wianwian*), to dimorphic (*M. pervagatus*) and trimorphic (*M. wunga*), and *M. wunga* has the largest pleurocystidia. These three red-pileate species fall into distantly related clades in analyses of the nrITS and *TEF1* trees (Figs 1, 2).

It differs from *M. haematocephalus* s. s. in its generally smaller pileus (5–9 mm, c.f. 2.5–16 mm), with more

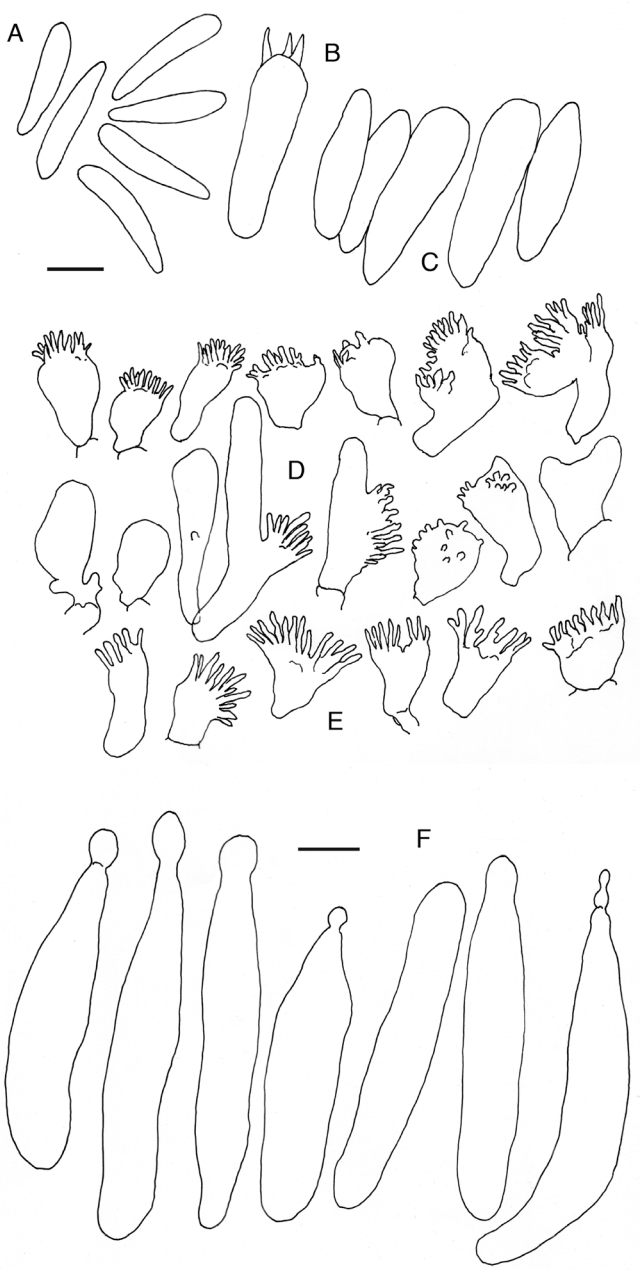

Fig. 16. *Marasmius wunga* (BRI AQ1045961). **A.** Basidiospores. **B.** Basidium. **C.** Basidioles. **D.** Cheilocystidia *Siccus*-type cells, intermediate cells and smooth cells. **E.** Pileipellis *Siccus*-type cells. **F.** Pleurocystidia. Scale bars = 10 µm. Illustrated by F.E. Guard.

© 2025 Westerdijk Fungal Biodiversity Institute

numerous (12–16 c.f. 7–10) and marginate lamellae and slightly larger basidiospores (mean 21 × 4.5 µm, c.f. 20 × 4 µm). Despite the morphological similarities, it is molecularly only distantly related to *M. haematocephalus* s. s. (Fig. 1). Its sister species with strong support (79/1.0) is an unnamed Australian taxon, *Marasmius* sp. 'clay-pink bells', from FNQ (F2023010), for which there is only one collection to date.

Key to the species of the *Marasmius haematocephalus* complex occurring in Australia

(The following key was prepared for field mycologists. See list below the key for definition of colours used.)

1a. Pileus **cinnamon** 2
1b. Pileus another colour 3

2a. Basidiospores mean 32 × 5 µm, monomorphic cheilocystidia ..... *M. lebeliae*
2b. Basidiospores mean 19 × 4 µm, dimorphic cheilocystidia ..... *M. campaniformis* (cinnamon form)

3a. Pileus **lilac to vinaceous grey** 4
3b. Pileus another colour 5

4a. Basidiospores mean 19 × 4 µm, dimorphic cheilocystidia ..... *M. campaniformis* (lilac form)
4b. Basidiospores mean 17.5 × 4.5 µm, monomorphic cheilocystidia ..... *M. vinaceus*

5a. Pileus **purplish-date** ..... *M. purpureospadiceus*
5b. Pileus another colour 6

6a. Pileus **pale pink** 7
6b. Pileus another colour 8

7a. Pileus **pale rose pink**, basidiospores mean 19 × 4 µm, dimorphic cheilocystidia ..... *M. campaniformis* (pink form)
7b. Pileus **clay pink**, basidiospores mean 21 × 3.5 µm, monomorphic cheilocystidia ..... *Marasmius* sp. "clay-pink"

8a. Pileus **candy pink** with **darker red** disc and sulci ..... *M. porphyrocephalus*
8b. Pileus another colour 9

9. Pileus **red – (dark brick, rust red, blood red, wine red, scarlet, coral**) 10

10a. Basidiospores mean 17 × 4 µm, monomorphic cheilocystidia ..... *M. wianwian*
10b. Basidiospores mean 17.5 × 4 µm, dimorphic cheilocystidia ..... *M. pervagatus*
10c. Basidiospores mean 21 × 4.5 µm, trimorphic cheilocystidia ..... *M. wunga*

Colours from Flora of British Fungi Colour Identification Chart, Royal Botanic Garden, Edinburgh 1969 where possible.

"blood red" = blood red (41)
"candy pink" = strong pink with purple tones, not illustrated (Google)
"cinnamon" = cinnamon (10) to 'ochre' (9H)
"clay pink" = clay pink (30)
"coral" = coral (44) which has apricot tones
"dark brick red" = close to dark brick (20) with brownish tones
"lilac" = lilac (79), matures to vinaceous grey (80)
"pink" = rose (39)
"purplish date" = purplish date (22) has brown tones
"rust red" = close to rust (13)
"scarlet" = scarlet (43) red with orange tones
"vinaceous grey" = vinaceous grey (80) has violet tones
"wine red" not illustrated, darker than blood red. (Google)

© 2025 Westerdijk Fungal Biodiversity Institute

DISCUSSION

Colour is often used to aid field-identification and in naming of fungal species. The name *"haematocephalus"* means 'blood-red head'. Curiously, the common name for *M. haematocephalus* is 'purple pinwheel', yet the etymology suggests it should be 'blood red pinwheel'. Other species in the complex have been named to emphasise specific colours (e.g. *rubicundus*, *roseus*, *auranticapitatus* and *castanocephalus* in Oliveira *et al.* (2022) and *porphyrocephalus*, *vinaceus* and *purpureospadiceus* (in this study). When *M. haematocephalus* sensu lato was considered to be a single species, Singer (1976) described nine variants in the neotropics based mainly on the colour of the pileus. Wannathes *et al.* (2009) described six forms in Thailand based on the pileal colour and size, two of which, f. *haematocephalus* and f. *violaceus*, did form separate subclades with strong support, and f. *luteocephalus* (with cream pileus) and f. *variabilis* (with greyish-brown pileus) fell in the same subclade. However, none of the forms correlated fully to Singer's varieties. With the larger dataset available for this current study, f. *violaceus* (with its pinkish-purple pileus very similar to *M. porphyrocephalus sp. nov.*) remains in a well-supported clade distant from *M. porphyrocephalus*; f. *haematocephalus* (with its brick red pileus) appears conspecific with *M. pervagatus*; and the cream f. *luteocephalus*, vinaceous f. *robustus* and grey-brown f. *variabilis* remain together in another poorly supported clade.

Madagascan collections studied by Shay *et al.* (2017) show that three collections (JES110, JES202, Buyck_00_1820) have purple pilei and one collection (JES193) has a cream pileus (images on iNaturalist7000636). They are con-specific, not closely related to the f. *luteocephalus* from Thailand, but are part of the *M. porphyrocephalus sp. nov.* clade [4A(ii), Fig. 1]. Oliveira *et al.* (2022) in their study of *M. haematocephalus* s. s. and related cryptic species from Brazil illustrated the colour variations in *M. rubicundus* (from pale pink to purple and salmon peach). In this study, *M. campaniformis* occurs in three colour forms — cinnamon (common), lilac (uncommon) and pink (rare). Morphologically, apart from the pileus colour, they are identical and molecularly they are con-specific across nrITS, nrLSU and *TEF1*. Red-pileate species are difficult to differentiate morphologically and there are three distinct subclades of these in Australia, two endemic and one globally widespread. Colour photography has enhanced our ability to identify species, but has its own biases. Red is a particularly difficult colour to render accurately (pers. comm. Steven Axford, Fungal Photographer). Ambient light, background colours and the camera settings used can all influence the colour outcomes. Our conclusion is that while colour is an important character for identifying species of *Marasmius*, it has limited value for separating some of the species in ser.



Fig. 17. Atlas of Living Australia data: 164 observational records with historic collections from Victoria & southern NSW 1887 (misidentified), Solomon Islands 1972 & Norfolk Is 1995 (within the complex). Of those with images, over 90 % are pinkish-purple and appear to be *Marasmius porphyrocephalus.* Image from *Atlas of Living Australia* accessed 18 Nov. 2024.

© 2025 Westerdijk Fungal Biodiversity Institute

Haematocephali and must be used in conjunction with other characters and with caution.

Distribution and phenology

All of the Australian collections investigated have been identified as seven unique species within the broader *M. haematocephalus* clade. They are all tropical or subtropical in origin. No herbarium material studied from locations in temperate Australia appear to be members of the *M. haematocephalus* complex and there are no iNaturalist observational records from the southern Australian states, while there are 225 from QLD, 12 from NSW (Sydney being the most southerly) and 4 from NT (see Fig. 17 and ALA records below). While the type species appears to have a restricted distribution in the neotropics — Brazil and Ecuador (Oliveira *et al.* 2022) and (GenBank nrITS OQ871706), further molecular data from GenBank and analyses in this study have expanded the complex and show there to be at least one taxon that is probably pan tropical (*M. pervagatus sp. nov.*) potentially including cryptic species and another to be Afrotropical, Indo-Malaysian and Australasian (*M. porphyrocephalus sp. nov.*). As well, there are centres of high diversity in the sub-tropical forests of southeast Queensland and northern New South Wales, where morphologically similar species can be separated by multilocus phylogenetic analysis.

Examination of Atlas of Living Australia (ALA) data (accessed on 18 Nov. 2024) records of *Marasmius 'haematocephalus'* in Australia show the species complex to be a tropical/subtropical group, with few outliers (Fig. 17). The ALA contains 164 observational records of the *M. haematocephalus* complex and 43 preserved specimens held in various herbaria. Three records are likely to be misidentifications, but the remainder appear to be within the complex. Of the records with images, over 90 % appear to be *Marasmius porphyrocephalus sp. nov.* The concentration of records in the wet tropics (centred on Cairns) and the subtropics of southeast QLD and northern NSW (centred on Brisbane) may reveal biodiversity hotspots, or perhaps population centres with concentrations of search effort. The citizen science observations on iNaturalist of this eye-catching group of species support the suggestion of biodiversity hotspots, with additional sporadic occurrences in other, generally drier parts of QLD. All species in the *haematocephalus* complex produce basidiomata after rain, usually in the summer through autumn months (December to May). If significant rain occurs early or late, they may rarely appear in November or June (one record of each on ALA). The year 2022 was a year of record rainfall in SEQ and observations were made of *M. porphyrocephalus* basidiomata in unusual numbers and in unusual places. The central QLD occurrences were in normally dry habitats which had received unusually high rainfall. They are 450–700 km from the nearest areas of regular occurrence. Its usual habitat is variable, ranging from rainforest, wet sclerophyll forest to parks, gardens and road verges under native or exotic trees. The substrate is deep leaf litter and twigs, garden mulch and occasionally mossy bark on living trees (four ALA records). *Marasmius porphyrocephalus* is widespread and is probably present throughout tropical-subtropical Australasia (including Papua New Guinea), south Asia and at least as far as Madagascar. It is not currently threatened. Of the remaining ALA records with images, ca 8 % (15) are red-pileate species, which cannot be further identified. Two other records from north QLD appear to be *Marasmius vinaceus sp. nov*. (Reinhold 2022; iNaturalist 109522131 and 109594364).

The distribution of fresh collections of taxa (2014–2024) in the *M. haematocephalus* complex, with concentrations in the wet tropics and the subtropics, is shown in Fig. 18. The FNQ and NSW collections were from short, targeted forays in the wet season of three consecutive years (2021 FNQ, 2022 NSW and 2023 FNQ). Additionally, a long-term study of *Marasmius* at Dilkusha Nature Refuge SEQ, over more than ten years of daily observations, collections, records of changing habitat and rainfall, has contributed significantly to our knowledge of species diversity and phenology, including five of the new species in this study [*M. campaniformis* (two of the three colour forms), *M. porphyrocephalus*, *M. purpureospadiceus*, *M. vinaceus* and *M. wunga*]. Stallman *et al.* (2024) have analysed the value of long-term studies of fungi in Guyana over and beyond short sporadic forays, in previously understudied tropical areas, for their important contribution to capturing the extent of species diversity. Straatsma, Ayer & Egli (2001) in a weekly survey during the fungal fruiting season in Switzerland over 21 yr came to the same conclusion. Our study has shown the same importance in subtropical areas of Australia.

Of the red-pileate species, *Marasmius wianwian sp. nov*. is endemic to remnant rainforest of the formerly large subtropical lowland rainforest (termed 'Big Scrub') of

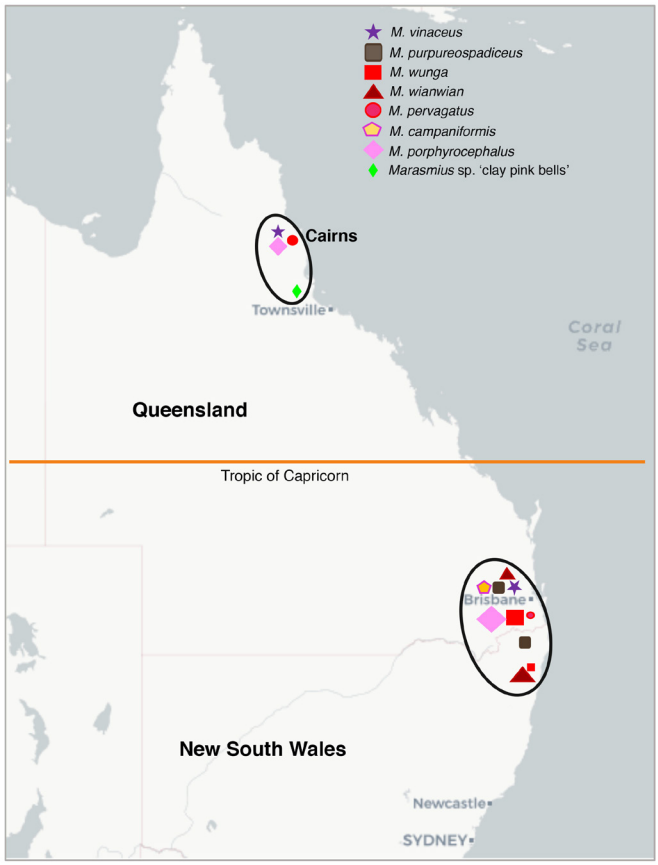

Fig. 18. Map of Queensland and New South Wales illustrating the distribution of the 40 fresh specimens collected and sequenced for this study. Biodiversity hotspots appear to be centred in the wet tropics and in the subtropics of SEQ and northern NSW shown by black ovals.

© 2025 Westerdijk Fungal Biodiversity Institute

northern NSW and one small national park in SEQ. Only 1 % of the original 75 000 ha of Big Scrub remains, in fragmented patches of rainforest. *Marasmius wianwian* has only been found three times, always in rainforest habitat, on leaf litter, in February and March of the extremely wet year 2022. Given its limited distribution, in natural forest habitat, areas which are under threat from weed incursion, human activities, drought and fire due to climate change, this species may be threatened and should be considered for conservation protection.

The second red-pileate species, *Marasmius wunga sp. nov.,* is also endemic to southeast QLD and northern NSW. It has been collected in eight sites with multiple collections over ten years (2014–2024) in the months of December to April, with a peak of collections in January. It is much less particular in its habitat requirements than *M. wianwian*. The most common habitat is in leaf litter on road verges and walking tracks in regenerating subtropical rainforest mixed with exotic weeds such as *Lantana camara.* This species occurs with large numbers of basidiomata at times. There is one collection from northern NSW, made on a road verge. Despite its small geographic distribution to date, *M. wunga* does not currently appear to be threatened.

The third red-pileate species, *Marasmius pervagatus sp. nov.*, is not endemic and has been found in Brisbane, Cairns Botanic Gardens (twice) and Bloomfield on Cape York Peninsula. The habitat is garden beds, road verge and disturbed areas, growing on mulch and twigs with native and exotic vegetation. On the nrITS tree (Fig. 1), it forms a clade together with sequences from Thailand, India and Florida. The Bloomfield and Florida sequences have high similarity (99.1–99.5 % identical for the nrITS). Examination of more specimens using other gene regions may help to resolve any cryptic geographically delimited species in this group, and perhaps determine whether the Floridian cluster of specimens are an indication of an exotic introduction to Queensland or vice versa.

CONCLUSION

Marasmius haematocephalus, commonly known in Australia as the 'purple pin-wheel', has been shown in our study to be a much broader complex of taxa, that includes pileal colours ranging from pink to purple, scarlet to coral, blood red to wine red and cinnamon to lavender with many variations in form. The addition of eight novel species adds significantly to our understanding of the global diversity, distribution and relationships of the species complex. Certainly there are more species awaiting discovery, including the undescribed species in this study. Six of the species found in Australia appear to be endemic to highly restricted areas and habitats, which has serious implications for conservation. The two more widespread taxa have more variability both morphologically and molecularly and are probably hiding a number of cryptic species. The nrITS gene region is useful for delimiting most of the species, but the use of *TEF1* gene region together with detailed morphological examination has been important in separating some of the more cryptic species complexes. Further investigation of both *M. porphyrocephalus* and *M. pervagatus* would be useful in studying potential geographic variants and possible dispersal of the species to and from Australia. While this study raises more questions particularly in regard to the relationships between Australian and Asian species, it also contributes significantly to our understanding of the complex across the world.

ACKNOWLEDGEMENTS

Our thanks go to the Queensland Herbarium (BRI) for assistance with collections and permission to examine and undertake DNA analysis on historic collections in the Herbarium. Also we thank the National Herbarium of Victoria (MEL) and particularly G. Holmes who undertook DNA extraction and sequencing of a number of specimens used in this study. We sincerely thank G. Laurie of the Wiyebal jagun naa Nation in northern New South Wales for a conversation about naming one of the new species to honour the first Nations people of the "Big Scrub" region, and his suggestion that we use "wianwian" meaning "a special place" in the local language. We also wish to thank members of the Yinibara Aboriginal Corporation for conversations regarding use of a name in their language for the *Marasmius* first found on their country, and B.J. Murphy, a Yinibara/KabiKabi man, who gave permission for use of the word "wunga" for that species. Thanks to Queensland Mycological Society (QMS) members who made collections and contributed photographs which have significantly assisted this project. Thanks to P. Bostock for help with Latin names. Thanks to S. Axford, professional fungal photographer, for his comments on the challenges of photographing red fungi. Sincere thanks to M. Barrett (JCU) for assistance with submission of *TEF1* sequences to GenBank. We are grateful for financial assistance through a Hansjörg Eichler Australian Systematic Botany Society (ASBS) grant for fieldwork for F.E. Guard.

Conflict of Interest: The authors declare no conflicts of interest.

REFERENCES

Amoako-Attah I, Akrofi AY, Hakeem R, *et al.* (2016). White thread blight disease caused by *Marasmiellus scandens* (Massee) Dennis & Reid on cocoa and its control in Ghana. *African Journal of Agricultural Research* **11**: 5064–5070. https://doi.org/10.5897/AJAR2016.11681

Antonín V, Buyck B (2006). *Marasmius* (*Basidiomycota*, *Marasmiaceae*) in Madagascar and the Mascarenes. *Fungal Diversity* **23**: 17–50. https://www.fungaldiversity.org/fdp/sfdp/23-2.pdf

Antonin V (2007). Monograph of *Marasmius*, *Gloiocephala*, *Palaeocephala* and *Setulipes* in Tropical Africa. *Fungus Flora of Tropical Africa* **1**: 1–200. https://www.ffta-online.org/ffta1/

Antonin V, Noordeloos M (2010). *A monograph of marasmioid and collybioid fungi in Europe* IHW-Verlag, Eching, Germany.

Bhunjun CS, Niskanen T, Suwannarach N *et al.* (2022). The numbers of fungi: are the most speciose genera truly diverse? *Fungal Diversity* **114**(1): 387–462. https://doi.org/10.1007/s13225-022-00501-4

Crous PW, Carnegie A, Wingfield M, *et al.* (2019). Fungal Planet description sheets: 868–950. *Persoonia* **42**: 291–473. https://doi.org/10.3767/persoonia.2019.42.11

© 2025 Westerdijk Fungal Biodiversity Institute

Crous PW, Wingfield M, Chooi Y-H, *et al.* (2020). Fungal Planet description sheets: 1042–1111. *Persoonia* **44**: 301–459. https://doi.org/10.3767/persoonia.2020.44.11

Desjardin D, Retnowati A, Horak E (2000). *Agaricales* of Indonesia. 2. A preliminary monograph of *Marasmius* from Java and Bali. *Sydow* **52**(2): 92–193.

Desjardin DE, Horak E (1997). *Marasmius and Gloiocephala in the south Pacific region: Papua New Guinea, New Caledonia and New Zealand* **Vol 2**. Cramer J, Berlin.

Dutta AK (2017). *Taxonomic study on marasmioid and gymnopoid fungi of West Bengal based on morphological and molecular features.* Thesis submitted for the degree of Doctor of Philosophy (Science) in Botany, University of Calcutta, India.

Fries EM (1836–1838). *Epicrisis systematis mycologici seu synopsis Hymenomycetum* Upsaliae.

Gardes M, Bruns T (1993). ITS primers with enhanced specificity for basidiomycetes - application to the identification of mycorrhizae and rusts. *Molecular Ecology* **2**(2): 113–118. https://doi.org/10.1111/j.1365-294X.1993.tb00005.x

Guard FE, Dearnaley J, May TW *et al.* (2024). Untangling horsehair fungi in Australia: *Marasmius crinis-equi* (*Marasmiaceae*) and related taxa. *Mycological Progress* **23**: 1–27. https://doi.org/10.1007/s11557-024-01995-9

Huamán-Pilco AF, Ramos-Carrasco TA, Franco MEE *et al.* (2023). Morphological, phylogenetic and genomic evidence reveals the causal agent of thread blight disease of cacao in Peru is a new species of *Marasmius* in the section *Neosessiles*, *Marasmius infestans sp. nov*. *F1000Research* **12**: 1327. https://doi.org/10.12688/f1000research.140405.2

Huelsenbeck JP, Ronquist F (2001). MRBAYES: Bayesian inference of phylogenetic trees. *Bioinformatics* **17**(8): 754–755. https://doi.org/10.1093/bioinformatics/17.8.754

Katoh K, Standley DM (2013). MAFFT Multiple Sequence Alignment Software Version 7: Improvements in Performance and Usability. *Molecular Biology and Evolution* **30**(4): 772–780. https://doi.org/10.1093/molbev/mst010

Kühner R (1980). Les Hyménomycètes agaricoides (*Agaricales*, *Tricholomatales*, *Pluteales*, *Russulales*). Étude générale et classification. Numéro spécial *Bulletin de la Société Linnéenne de Lyon* **49**: 76–184.

Mešić A, Tkalčec Z (2010). New names in the genus *Marasmius*. *Mycotaxon* **113**(1): 283. https://doi.org/10.5248/113.283

Mossebo DC, Antonin V (2004). *Marasmius* species (*Tricholomataceae*) found in man-influenced habitats in the vicinity of Yaoundé, Cameroon. *Czech Mycology* **56** (1/2): 85–112. https://czechmycology.org/article/56107

Oliveira JJS, Moncalvo JM, Margaritescu S *et al.* (2020). A morphological and phylogenetic evaluation of *Marasmius* sect. *Globulares* (*Globulares-Sicci* complex) with nine new taxa from the Neotropical Atlantic Forest. *Persoonia* **44**: 240–277. https://doi.org/10.3767/persoonia.2020.44.09

Oliveira JJ, Capelari M, Margaritescu S (2022). Disentangling cryptic species in the *Marasmius haematocephalus* (Mont.) Fr. and *M. siccus* (Schwein.) Fr. species complexes (*Agaricales*, *Basidiomycota*). *Cryptogamie, Mycologie* **43**(5): 91–137. https://doi.org/10.5252/cryptogamie-mycologie2022v43a5

Oliveira JJS, Vargas-Isla R, Cabral TS *et al.* (2024a). Spider fungi: new species of *Marasmius* and *Pusillomyces* in the aerial rhizomorph web-making guild in Amazonia. *Fungal Systematics and Evolution* **14**: 35–55. https://doi.org/10.3114/fuse.2024.14.03

Oliveira J, Desjardin D, Jenkinson T, *et al.* (2024b). Taxonomic revision of *Marasmius* Fr. and *Marasmiaceae* Roze *ex* Kühner based on multigene phylogenetics and morphological evidence. *Fungal Diversity* **127**: 1–54. https://doi.org/10.1007/s13225-024-00534-x

Pegler DN (1977). A preliminary agaric flora of East Africa. *Kew Bull Addit Ser* **6**:1–615.

Pegler D (1986). Agaric flora of Sri Lanka. *Kew Bull Addit Ser* **12**: 1–519.

Rehner SA, Buckley E (2005). A *Beauveria* phylogeny inferred from nuclear ITS and *EF1-α* sequences: evidence for cryptic diversification and links to *Cordyceps* teleomorphs. *Mycologia* **97**(1): 84–98. https://doi.org/10.3852/mycologia.97.1.84

Reinhold L (2022). iNaturalist: https://www.inaturalist.org/observations/109522131 Accessed on 25 Oct. 2024.

Royal Botanic Garden Edinburgh (1969). *Flora of British fungi Colour Identification Chart*. Her Majesty's Stationery Office, Edinburgh.

Shay JE, Desjardin DE, Perry BA, *et al.* (2017). Biodiversity and phylogeny of *Marasmius* (*Agaricales*, *Basidiomycota*) from Madagascar. *Phytotaxa* **292**: 101–149. https://doi.org/10.11646/phytotaxa.292.2.1

Singer R (1976). Marasmieae (*Basidiomycetes-Tricholomataceae*). *Flora Neotropica* **17**: 1–347.

Stallman JK, Haelewaters D, *et al.* (2024). The contribution of tropical long-term studies to mycology. *IMA Fungus* **15**: 1–18. https://doi.org/10.1186/s43008-024-00166-5

Stamatakis A (2014). RAxML version 8: a tool for phylogenetic analysis and post-analysis of large phylogenies. *Bioinformatics* **30**(9): 1312–1313. https://doi.org/10.1093/bioinformatics/btu033

Straatsma G, Ayer F, Egli S (2001). Species richness, abundance and phenology of fungal fruit bodies over 21 years in a Swiss forest plot. *Mycological Research* **105**(5): 515–523. https://doi.org10.1017/S0953756201004154

Tan Y-P, Bishop-Hurley SL, Shivas RG, *et al* (2022). Fungal planet description sheets: 1436–1477. *Persoonia* **49**: 261–350. https://doi.org/10.3767/persoonia.2022.49.08

Tan Y-S, Desjardin D, Perry B, *et al.* (2009). *Marasmius* sensu stricto in peninsular Malaysia. *Fungal Diversity* **37**: 9–100.

Vilgalys R, Hester M (1990). Rapid genetic identification and mapping of enzymatically amplified ribosomal DNA from several *Cryptococcus* species. *Journal of Bacteriology* **172**(8): 4238–4246. https://doi.org/10.1128/jb.172.8.4238-4246.1990

Wannathes N, Desjardin D, Hyde K, *et al.* (2009). A monograph of *Marasmius* (*Basidiomycota*) from northern Thailand based on morphological and molecular (ITS sequences) data. *Fungal Diversity* **37**: 209–306.

White TJ, Bruns T, Lee S, *et al.* (1990). Amplification and direct sequencing of fungal ribosomal RNA genes for phylogenetics. In: *PCR protocols: a guide to methods and applications* (Innis MA, Gelfand DH, Sninsky JJ, *et al.*, eds). *Academic Press, Inc.*, New York, USA: 315–322. https://doi.org/10.1016/B978-0-12-372180-8.50042-1

Supplementary Material: http://fuse-journal.org/

Fig. S1. Phylogenetic analysis of the *Haematocephali* complex in sect. *Sicci*, ser. *Haematocephali* inferred from Bayesian and Maximum Likelihood analysis of the nrLSU region with *M. recreigardneri,* subsect. *Ferruginei,* as outgroup. BS/PP and bolded lines for well supported nodes. All coloured sequences have been produced in this study, except the epitype, *M. haematocephalus* (blue).

Fig. S2. *Marasmius haematocephalus* complex phylogenetic tree

© 2025 Westerdijk Fungal Biodiversity Institute

using concatenated nrITS, nrLSU and *TEF1* sequences with Bayesian analysis. All coloured sequences have been produced in this study, except the type sequences of *M. haematocephalus* in blue (only the neotropical and Australian sequences have all three gene regions.)

Table S1. Table of all sequences used in this study of the *Marasmius haematocephalus* complex, including GenBank numbers for nrITS, nrLSU and *TEF1* and Herbarium numbers of the Australian collections. Species in **bold** are new collections and /or sequences produced in this study and those in red are holotypes. Not determined = n/d.

© 2025 Westerdijk Fungal Biodiversity Institute

© 2025 Westerdijk Fungal Biodiversity Institute

FUSE

Fungal Systematics and Evolution

VOLUME 16
DECEMBER 2025
PAGES 307–316

doi.org/10.3114/fuse.2025.16.17

The sexual morph of *Hohenbuehelia subreniformis* (*Pleurotaceae*) discovered in Finland

R.G. Thorn[1*], G. Consiglio[2], L. Setti[3], T. Kekki[4], B.C. Daigneault[1], E.S.T. O'Neill[1]

[1]Department of Biology, University of Western Ontario, London, ON, N6A 5B7, Canada
[2]Via C. Ronzani 61, I-40033 Casalecchio di Reno (Bologna), Italy
[3]Via C. Pavese 1, I-46029 Suzzara (Mantova), Italy
[4]Department of Ecology and Genetics, P.O. Box 3000, University of Oulu, Oulu, FI-90014, Finland

[*]Corresponding author: rgthorn@uwo.ca

Key words:
asexual-sexual connections
nematophagous fungi

Abstract: A fresh collection of a *Hohenbuehelia* from Turku, Finland was determined through phylogenetic analyses of sequences of the nuclear ribosomal internal transcribed spacer (ITS) region, large ribosomal subunit (nLSU), translation elongation factor 1-alpha (*TEF-1α*), and RNA polymerase II second largest subunit (*RPB2*) genes to be conspecific with ex-type cultures of *Hohenbuehelia subreniformis*, originally described from Ontario, Canada. No sexual morph was known; it is a member of the broad *H. atrocoerulea* clade. We provide a detailed description of the macro- and micromorphology of this species, which resembles pale forms of *H. grisea* but differs in having a more spathulate pileus and broader spores. Of the fifteen valid species formerly classified in the anamorph genus *Nematoctonus*, all but three are now linked to conspecific or closely related sexual morphs in *Hohenbuehelia*.

Citation: Thorn RG, Consiglio G, Setti L, Kekki T, Daigneault BC, O'Neill EST (2025). The sexual morph of *Hohenbuehelia subreniformis* (*Pleurotaceae*) discovered in Finland. *Fungal Systematics and Evolution* **16**: 307–316. doi: 10.3114/fuse.2025.16.17
Received: 18 February 2025; **Accepted:** 30 June 2025; **Effectively published online:** 8 August 2025
Corresponding editor: P.W. Crous

INTRODUCTION

Hohenbuehelia (Schulzer *et al*. 1866; *Basidiomycota*: *Agaricales*, *Pleurotaceae*) is a genus of agarics with pleurotoid basidiocarps and a nematophagous lifestyle during the mycelial assimilative phase (Thorn & Barron 1986). All species that have been studied in culture produce holoblastic conidia that, previous to 2012 (Taylor 2011), would have been referred to the asexual genus *Nematoctonus* (Drechsler 1941), which is now considered a synonym of *Hohenbuehelia* (Thorn 2013). Ten of the 15 validly described species originally placed in *Nematoctonus* were first described as predators or parasitoids of nematodes, with no associated sexual basidiocarps (Drechsler 1941, 1943, 1946, 1949, 1954, Jones 1964, Giuma & Cooke 1972, Thorn & Barron 1986). A strain of one of these, identified as *N. robustus*, formed a basidiocarp initially identified as *Hohenbuehelia atrocoerulea* in pure culture (now identified as *H. grisea*), making the first recognized connection between the asexual and sexual morphs (anamorph-teleomorph) (Barron 1977, Barron & Dierkes 1977). Subsequently, five species placed in *Nematoctonus* were isolated from basidiocarps of named *Hohenbuehelia* (Thorn & Barron 1986) but complicating the asexual-sexual connections is the fact that single form-species of *Nematoctonus,* having fewer morphological features than the sexual morph, were often associated with multiple species of *Hohenbuehelia*. In addition, the correct species identity of the sexual morphs of the ex-type strains of *Nematoctonus cylindrosporus*, *N. geogenius*, and *N. hamatus* was not realized at the time of their publication (Thorn & Barron 1986). Molecular phylogenetic analyses within the genus *Hohenbuehelia* and, particularly, the fixing of species concepts by designation of neotypes or epitypes of older species names (Consiglio 2016, 2017a, b, Consiglio & Setti 2017, 2018), have resolved the historically controversial applications of many names in this group, and provided finer species resolution where morphology had previously led to multiple species being treated under a broad species concept (Pilát 1935, Coker 1944, Miller 1986, Thorn & Barron 1986, Elborne 1995). In addition, phylogenetic studies have revealed previously unrecognized asexual-sexual connections in this group (Consiglio & Setti 2018), as in other groups of fungi (e.g., Rehner & Buckley 2005, Wingfield *et al*. 2012).

Hohenbuehelia subreniformis is one species for which no sexual morph is known. It was first described as a nematode-attacking fungus, isolated from humic-rotted hardwood in Algonquin Provincial Park, Ontario, Canada (Thorn & Barron 1986). Sequences of the nuclear ribosomal internal transcribed spacer (ITS) region and adjacent 5'-end of the large ribosomal subunit (nLSU) of the ex-holotype and one paratype strain were obtained by Koziak *et al*. (2007b) and remained in an isolated position in phylogenetic trees at that time and since (Consiglio *et al*. 2018, Consiglio & Setti 2018). This report describes a sexual (teleomorphic) specimen recently collected in Finland whose ITS sequences clustered with those of *H. subreniformis* and provides additional sequences of the translation elongation factor 1-alpha (*TEF-1α*), and RNA polymerase II second largest subunit (*RPB2*) genes of Ontario and Finnish materials to test

Fungal Systematics and Evolution is licensed under a Creative Commons Attribution-NonCommercial-NoDerivatives 4.0 International License

© 2025 Westerdijk Fungal Biodiversity Institute

the proposed asexual-sexual connection. Additionally, we present an updated list of asexual-sexual connections for all described *Nematoctonus* species.

MATERIALS AND METHODS

Morphological methods

The macroscopic description was derived from a photograph of the dried specimen. Microscopic structures were observed with a Zeiss Axioscope 40, in bright field, in phase contrast and in interferential contrast, by using 10×, 20×, 40×, and 63× and 100× oil immersion objectives. Gill fragments, transverse sections and edges as well as pileipellis radial sections were mounted in L4 (Clémençon 1972) and stained in Congo red (1 % aqueous). Melzer's reagent (Melzer 1924) was used to determine amyloidity and cresyl blue (Clémençon 1972) was used to assess metachromatism. Spore measurements were made by photographing all the spores (taken from the hymenophore of mature specimens) occurring in the field of view and then using Mycomètre software (Fannechère 2011). Spore dimensions with exclusion of the hilar appendix are given as: average minus standard deviation–average plus standard deviation of length × average minus standard deviation–average plus standard deviation of width; Q = average minus standard deviation–average plus standard deviation of ratio length/width; Qm = average of ratio length/width; Vm = average of the volume (in µm^3). The approximate spore volume was calculated as that of an ellipsoid (Gross 1972, Meerts 1999). Photomicrographs were taken with a Canon PowerShot A640 digital camera.

DNA extraction, amplification and sequencing

Genomic DNA was extracted and amplified from dry specimens employing the methods reported in Alvarado *et al*. (2010, 2012). The PCR amplifications were performed with the primers ITSF1 and ITSF4 for the ITS region (White *et al*. 1990, Gardes & Bruns 1993); while LR0R and LR3 or LR5 (Vilgalys & Hester 1990, Cubeta *et al*. 1991) were used to amplify the nLSU rDNA region; EF1-728F, EF1-983F and EF1-1567R (Carbone & Kohn 1999, Rehner & Buckley 2005) for the partial translation elongation factor 1-*α* (*TEF-1α*) gene, and bRPB2-6F2 (reverse of bRPB2-6R2), bRPB2-7.1R2 and bRPB2-7R2 for the RNA polymerase II second largest subunit (*RPB2*) gene (Liu *et al*. 1999, Matheny *et al*. 2007).

The sequences obtained were assembled and checked for possible read errors with MEGA v. 6.0 (Tamura *et al*. 2013), aligned with its MUSCLE application and then manually corrected. The ITS, nLSU, *RPB2* and *TEF-1α* alignments were carried out separately, with the 18S region trimmed from the ITS alignment.

Phylogenetic analyses

The ITS matrix had 349 variable sites in 727 bases, the nLSU matrix 153 in 944, the *RPB2* matrix 376 in 768, and the *TEF-1α* matrix 142 in 430. The data matrices of ITS, nLSU, *RPB2* and *TEF-1α* were combined into a single multilocus matrix. This matrix (2869 alignment positions), which covered a total of 236 sequences for four markers (234 ITS, 123 nLSU, 56 *RPB2* and 56 *TEF-1α*), was analysed with Bayesian Inference (BI) and the Maximum Likelihood (ML) criteria using MrBayes v. 3.2.7a (Ronquist & Huelsenbeck 2003) and RAxML (Stamatakis 2014), respectively. Bayesian analysis was performed through the CIPRES Science Gateway v. 3.3 (Miller *et al*. 2010) with the GTR+G+I evolutionary model for all partitions. The analysis was run for 3410000 generations, with 2 simultaneous runs, 6 chains, temperature set at 0.2, sampling every 1000 generations, and the first 25 % of the trees discarded. Maximum likelihood analysis was conducted in RAxML (Stamatakis 2014) using the standard search algorithm with 1000 bootstrap cycles and the GTR+G model, with *Pleurotus ostreatus* as outgroup. The trees in .tre format were read with the software SEAVIEW v. 4 (Gouy *et al*. 2010) and saved in a vector format for printing. Figure 1 shows the BI tree with the maximum likelihood bootstrap values (MLB) and Bayesian posterior probabilities (BPP). Newly derived sequences (shown in **bold**) and reference sequences from GenBank are listed in Table S1. Fungarium acronyms follow Thiers (2020). Nomenclature and author citations follow Index Fungorum (http://www.indexfungorum.org/authorsoffungalnames.htm).

RESULTS

Phylogenetic results

MrBayes and RAxML did not produce the same topology. This being the case, we decided to adopt the MrBayes phylogram as the basic phylogram and use the MLB values from RAxML only where the topology was the same.

The phylogenetic analysis showed that, apart from two minor groupings (*H. pinacearum-H. unguicularis* and *H. algonquinensis-H. boullardii*), the ingroup is divided in two main strongly supported clades (Fig. 1), i.e., clade A (1.0 BPP) with the species *H. mastrucata*, *H. valesiaca*, *H. pachyspora*, *H. tylospora*, *H. faerberioides*, *H. pseudofaerberioides*, *H. leptospora*, *H. auriscalpium*, *H. bonii*, *H. leiospora*, *H. petaloides*, *H. pseudopetaloides*, *H. longipes*, *H. tremula*, *H. thornii*, *H. wilhelmii* and *H. angustata*, and clade B (0.95 BPP) with the species *H. carlothornii*, *H. grisea*, *H. tristis*, *H. subreniformis*, *H. mustialensis*, *H. leightonii*, *H. nimueae*, *H. cyphelliformis*, *H. pseudocyphelliformis*, *H. ilerdensis*, *H. culmicola*, *H. josserandii*, *H. fluxilis*, *H. atrocoerulea*, *H. canadensis* and *H. portegna*. Within these two large clades are the following species groups, all with 1.0 BPP: a) *H. pachyspora* with *H. mastrucata* and *H. valesiaca*; b) *H. faerberioides* and *H. pseudofaerberioides* with *H. tylospora*; c) *H. bonii* with *H. leiospora*; d) *H. petaloides* with *H. pseudopetaloides*; e) *H. longipes* with *H. tremula*; f) *H. thornii*, *H. wilhelmii* and *H. angustata*; g) *H. grisea*, *H. carlothornii*, *H. tristis* and *H. portegna*; h) *H. cyphelliformis* with *H. pseudocyphelliformis*; i) *H. ilerdensis*, *H. culmicola*, *H. josserandii*, *H. fluxilis*, *H. atrocoerulea*, and *H. canadensis*, and j) *H. atrocoerulea* with *H. canadensis*. Some of these groups correspond with what were formerly treated as form-species of *Nematoctonus*, such as *N. angustatus* (*H. angustata – H. wilhelmii*), *N. hamatus* (*H. mastrucata – H. valesiaca*), *N. leiosporus* (*H. leiospora – H. boniii*), *N. robustus* (*H. carlothornii – H. grisea – H. tristis*; but also applied to asexual morphs of *H. pseudocyphelliformis*; Thorn & Barron

© 2025 Westerdijk Fungal Biodiversity Institute

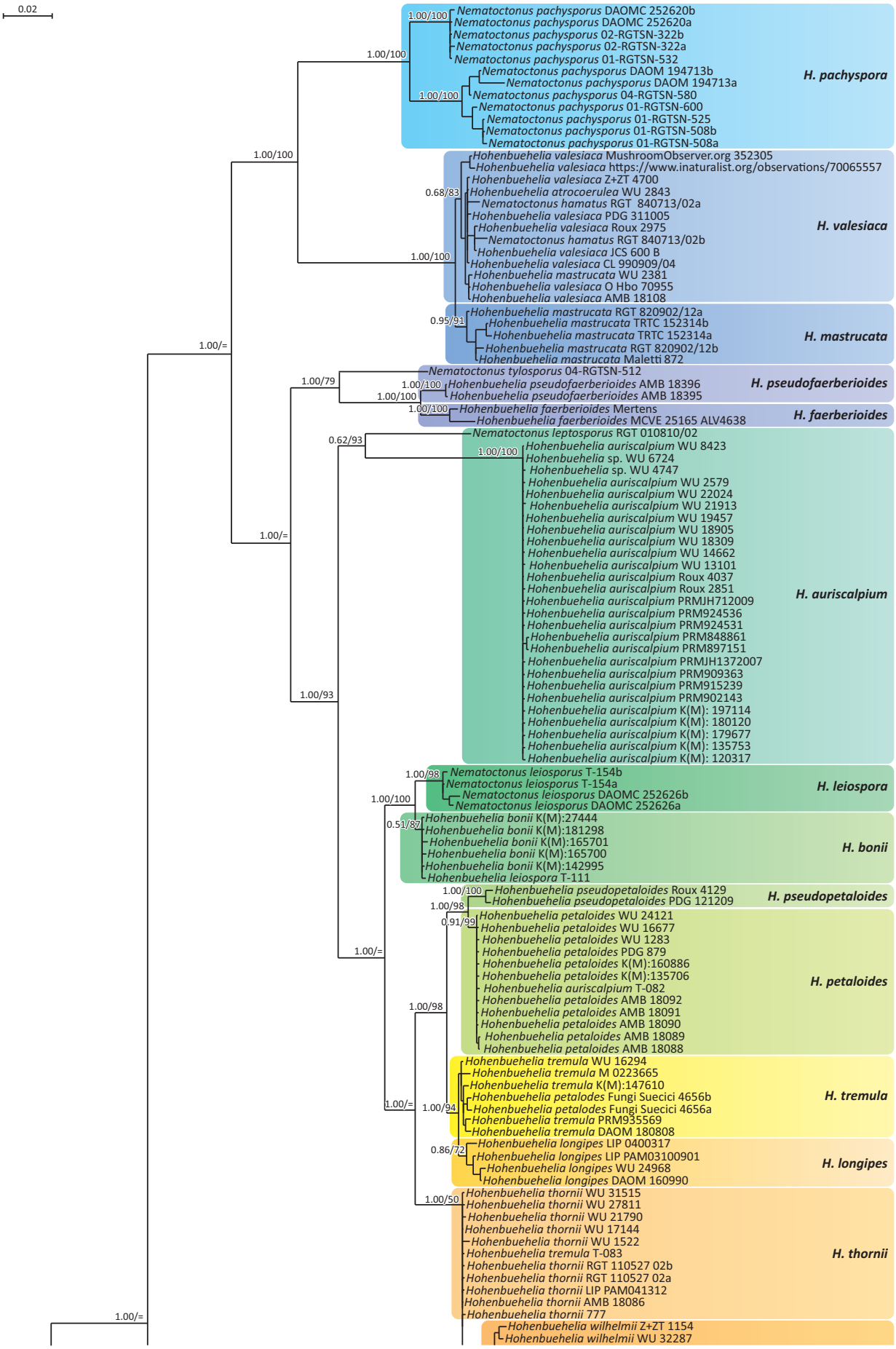

Fig. 1. Bayesian inference phylogram built with nucleotide sequence data of four loci (ITS, nLSU, *RPB2*-exons and *TEF1*-exons) of selected members of *Hohenbuehelia* rooted with *Pleurotus ostreatus*. Bayesian posterior probability values and Maximum Likelihood bootstrap values are shown on the branches. For each taxon, voucher number and original determination are given. The relevant GenBank accession numbers are shown in Table S1.

© 2025 Westerdijk Fungal Biodiversity Institute

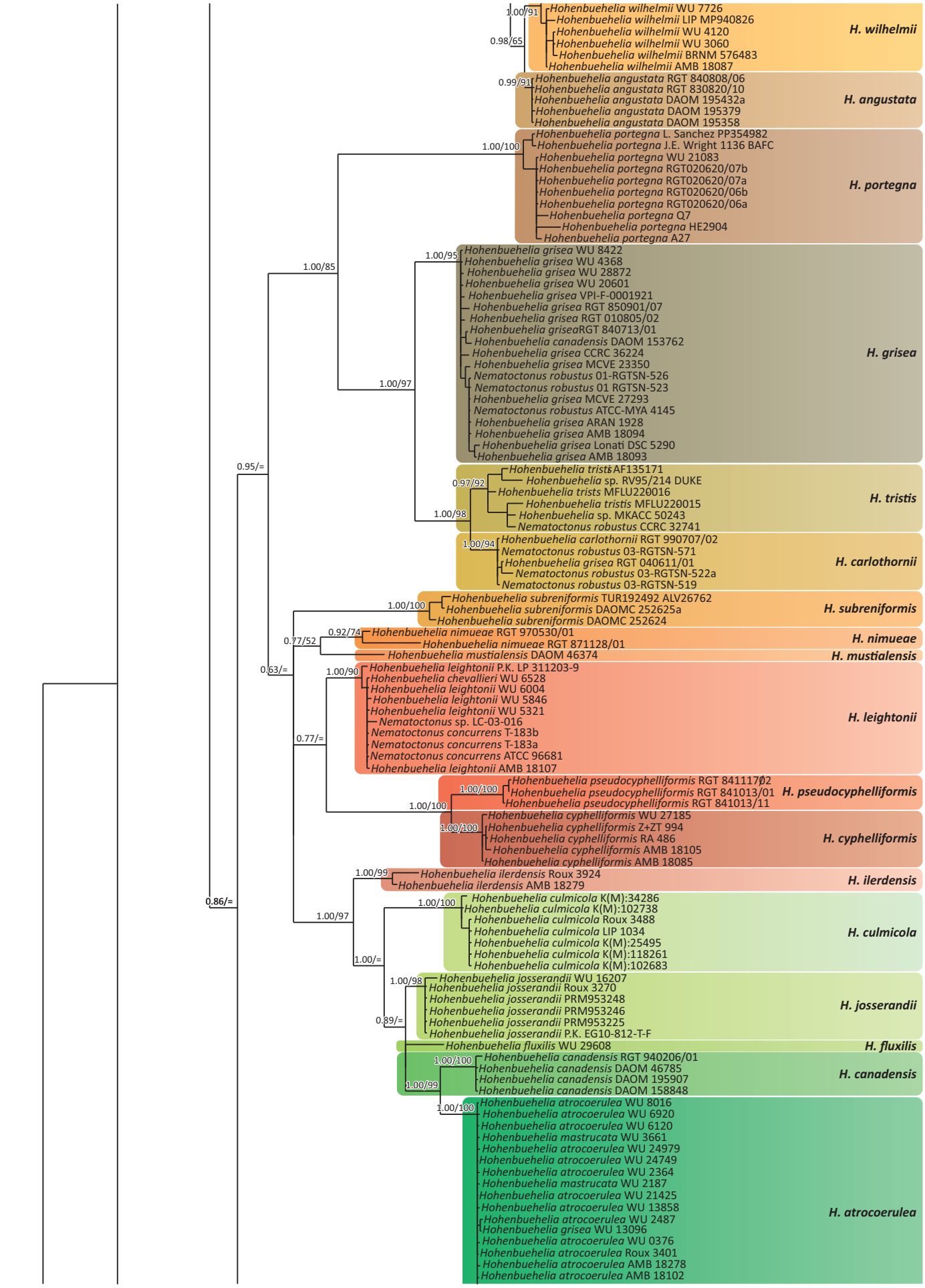

Fig. 1. (Continued).

© 2025 Westerdijk Fungal Biodiversity Institute

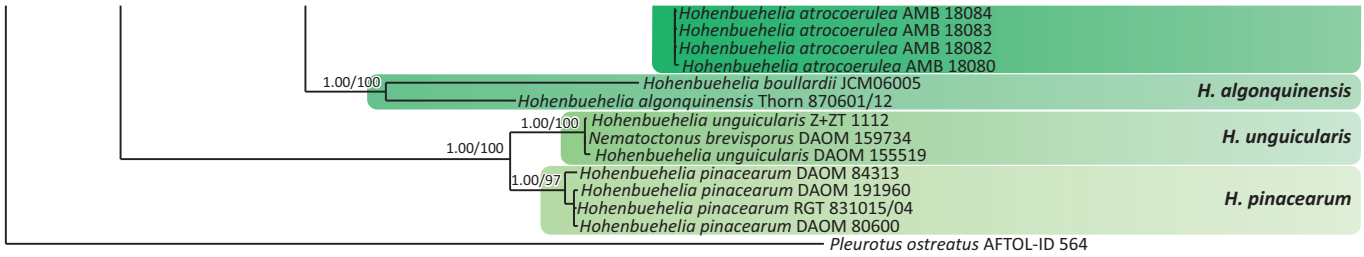

Fig. 1. (Continued).

1986), and *N. brevisporus* (*H. pinacearum – H. unguicularis*), whereas other former species of *Nematoctonus* formed isolated clades or single branches, such as *N. pachysporus* (*H. pachyspora*), *N. tylosporus* (*H. tylospora*), *N. leptosporus* (*H. leptospora*), *N. campylosporus* (*H. portegna*), *N. subreniformis* (*H. subreniformis*), and *N. concurrens* (*H. leightonii*).

A sexual collection of *Hohenbuehelia subreniformis*

Hohenbuehelia subreniformis (Thorn & G.L. Barron) Thorn, *Index Fungorum* **16**: 1. 2013. MB 550131. Fig. 2.
Basionym: *Nematoctonus subreniformis* Thorn & G.L. Barron, *Mycotaxon* **25**: 364. 1986.

Typus: **Canada**, Ontario, Algonquin Provincial Park, near the West Gate, approximately 45.44°N, 78.82°W, 440 m.a.s.l., in mature hardwood forest dominated by sugar maple (*Acer saccharum*) with American beech (*Fagus grandifolia*), yellow birch (*Betula alleghaniensis*), ironwood (*Ostrya virginiana*) and blue-beech (*Carpinus caroliniana*), 18 May 1984, *R.G. Thorn*, N84-240 (**holotype** DAOM 193363, a permanent slide derived from ex-type culture T-137, the latter deposited as ATCC 60607).

Description: *Basidiocarps* (macroscopic description from photograph of dried specimen). *Pileus* spathulate-orbicular, approximately 2.5 cm long and 2 cm broad, pale creamy beige overlain with whitish to pale greyish yellow tomentum from base almost to margin, margin narrowly acute, decurved and wavy. *Lamellae* close, narrow (approximately 1 mm deep as dried), decurrent onto pseudostipe, whitish to pale yellow, seriate. *Pseudostipe* underside off-white, tomentose, with raised lines extending from base of lamellae and forming a loose reticulum, arising from well-rotted wood without visible rhizomorphs or mycelial cords. *Odour* and *taste* not recorded. *Basidiospores* (Fig. 2A) hyaline, inamyloid, smooth, ellipsoid to broadly ellipsoid, 7.1–8.4 × 4.9–5.9 µm (on average 7.7 × 5.4) (n = 32), Q = 1.31–1.54 (on average 1.43), Vm =121 µm^3, with dull, granular content or with one or more oily drops. *Basidia* 22–26 × 7–8 µm, tetrasporic, clavate, with sterigmata up to 4 µm long. *Hymenophoral trama* irregular, made up of hyphae up to 8 µm broad, hyaline in L4, yellow in Melzer's. *Cheilometuloids* (Fig. 2D) in groups along the lamellar edge, subfusoid, generally with a narrow base, mostly with a lanceolate apical part and partly covered with refringent, yellow or whitish, crystalline granules, 17–33 × 7–9 µm. Mounted in Melzer's (Fig. 2F, G) they react pale reddish (dextrinoid reaction), while in cresyl blue (Fig. 2E) the wall stains vinaceous red (metachromatic reaction). *Cheilocystidia* (Fig. 2D, E) (leptocystidia) of the gloeosphex type (Thorn & Barron 1986), 10–17 × 5 µm, plus a neck and capitulum of 6–12 × 1.5–2 µm, often capped with a tiny, vanishing drop of mucus. *Pleurometuloids* similar to cheilometuloids, 40–60 × 8–10 µm. *Pileipellis* near margin (Fig. 2B) consisting of an ixocutis of variously intertwined, gelatinized, filamentous, smooth hyphae, 6–8 µm wide, yellow in Melzer's, with an intracellular yellowish pigment; halfway from the point of attachment (Fig. 2C) with a trichoderm of often tufted hairs. *Clamp connections* ubiquitous in all tissues.

Habitat and distribution: Originally described from well-decayed hardwood in Ontario, Canada (Barron & Thorn 1986; see *Isolates studied*, below), and found on a rotten branch in a mixed forest in southwest Finland. A search of globalfungi.com (Větrovský *et al*. 2020), a fungal environmental DNA (eDNA) database, yielded only a single full matching ITS1 sequence from a Swedish air sample (SH0815783.10FU) and no exact ITS2 matches (17 Jul. 2025).

Specimen examined: **Finland**, Southwest Finland region, Turku, Ruissalo, Kuuva, east side of the road Kuuvannokantie, in rich mixed forest near field, approximately 60.4109°N, 22.1175°E, 3 m.a.s.l., on fallen rotten branch beside *Alnus glutinosa*, near *Betula* and *Quercus robur*, 6 Aug. 2007, *K. Kokkonen*, 189/07 (TUR 192492, as *Hohenbuehelia mastrucata*?).

Isolates studied: **Canada**, Ontario, Algonquin Provincial Park, near the West Gate, approximately 45.44°N, 78.82°W, 440 m.a.s.l., in mature hardwood forest dominated by sugar maple (*Acer saccharum*) with American beech (*Fagus grandifolia*), yellow birch (*Betula alleghaniensis*), ironwood (*Ostrya virginiana*) and blue-beech (*Carpinus caroliniana*); recovered using the centrifuge plate technique, infecting unknown rhabditid nematodes (Thorn & Barron 1986) from three samples of well-decayed hardwood, 14 Oct. 1983, *R.G. Thorn*, N83-147 (source of culture T-108 = CBS 858.85); idem., 18 May 1984, *R.G. Thorn*, N84-240 (source of culture T-137 = ATCC 60607, source of holotype specimen, DAOM 193363); idem., N84-243 (source of cultures T-138, T-139 and T-140).

Notes: The basidiocarp of *H. subreniformis* resembles pale versions of *H. grisea* or *H. auriscalpium*, differing from the former by its spathulate, rather than dimidiate, shape and from both by the broad basidiospores, averaging 5.4 µm compared to less than 4 µm broad (Consiglio & Setti 2018). The hardwood (angiosperm) substrate also differs from the gymnosperm (conifer) substrate of *H. auriscalpium* (Consiglio & Setti 2018).

© 2025 Westerdijk Fungal Biodiversity Institute

DISCUSSION

It is difficult to know, with just two published observations, whether this species is truly rare or is rarely encountered. Rabinowitz (1981), referring to vascular plants, identified three axes of rarity: small geographic range – related to endemism; high habitat specificity – in fungi, related to a specialized nutritional mode or substrate; and small local population size, or few individuals – which, for fungi and other microbes, is perilously difficult to establish (Burnett

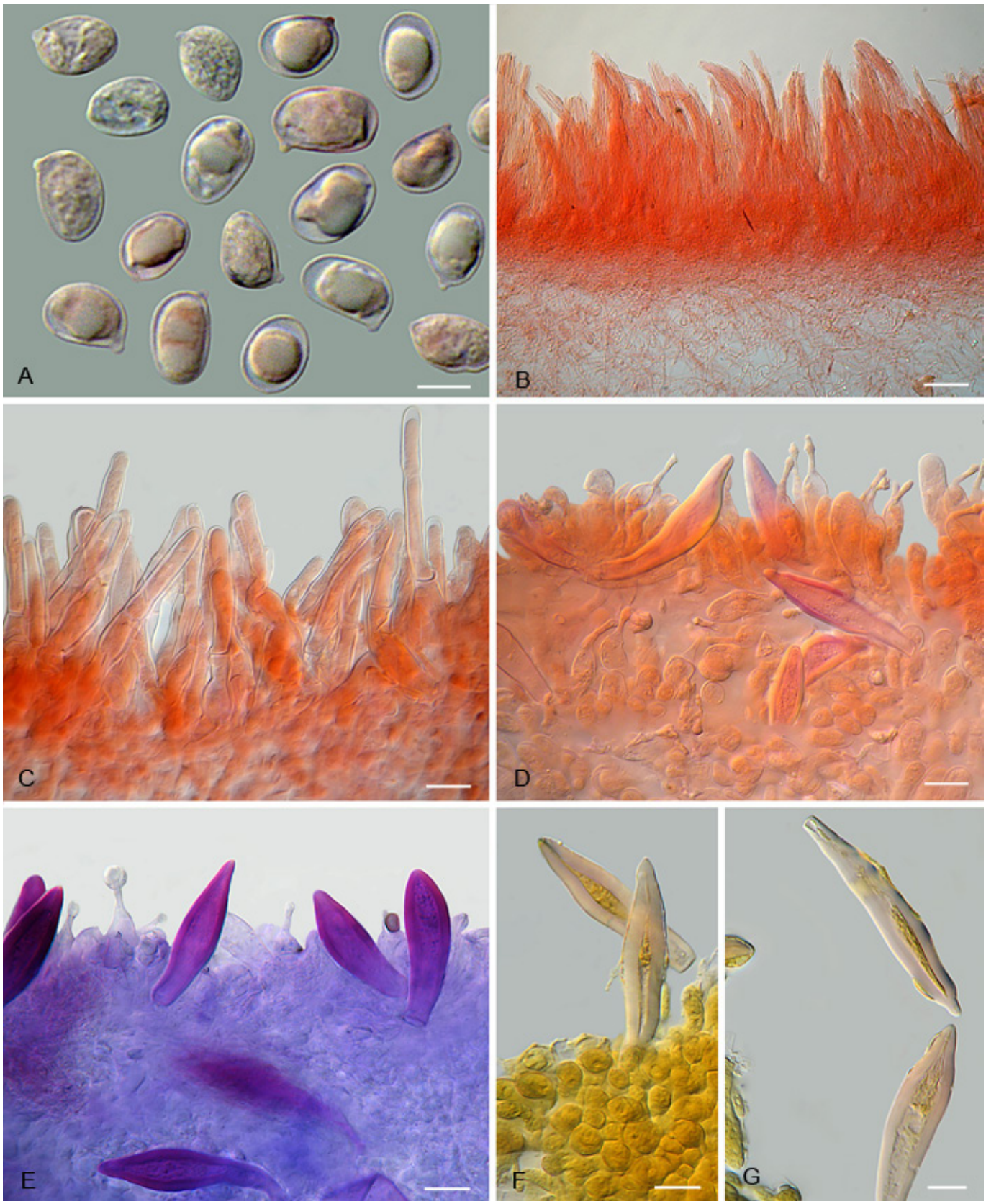

Fig. 2. Photomicrographs of K. Kokkonen 189/07 (TUR *192492*). **A.** Basidiospores. **B.** Pileipellis near pileus margin. **C.** Pileipellis halfway between margin and base. **D.** Gill edge showing cheilometuloids and gloeosphex-type leptocystidia stained with Congo Red. **E.** Gill edge showing metachromatic cheilometuloids and gloeosphex-type leptocystidia stained with cresyl blue. **F, G.** Faintly dextrinoid metuloid cystidia in Melzer's reagent. Scale bars: A = 5 µm; B = 50 µm; C–G = 10 µm.

© 2025 Westerdijk Fungal Biodiversity Institute

2003). Adding to these is a low likelihood of encounter; unlike many birds, mammals and vascular plants, fungi and other inconspicuous organisms may be rarely detected without being rare (Kijpornyongpan & Aime 2016). In the case of *H. subreniformis*, it was first encountered in three samples of humic, well-rotted hardwood, the first collected in 1983, followed by two other samples collected in 1984 (Thorn & Barron 1986). The fungus was isolated five times from water agar plates inoculated with fine organic material and baited with rhabditid nematodes (Thorn & Barron 1986) but no inter-compatibility tests or fine-scale sequencing data are available to determine if each isolate was a separate genetic individual (genet), or if all were derived from propagules (infective conidia) of the same one. Many fungal individuals are perennial (Burnett 2003, Zotti *et al*. 2025), so the 1984 isolates could have been of the same individual that persisted since it was first detected in 1983. The most that can be said is that the same taxon was not encountered in any of more than 700 other samples of soil and rotted wood from across Ontario in the same study (Thorn & Barron 1986), and that it has not been reported in other studies of nematophagous fungi worldwide before or since (reviewed in Berhanu *et al*. 2024). With a range spanning over 6000 km, with three detection points, *H. subreniformis* is clearly not "rare and local" or endemic, a pattern also seen in rare wood-inhabiting fungi in New Zealand (Dickie *et al*, 2020). However, its ecological specialization suggests that it may have very spotty distribution at low densities across a circumpolar range and is unlikely to be detected by standardized surveys of basidiocarps or environmental DNAs. There is much work to be done to learn the true abundance and distributions of fungi, even in parts of the world that have been extensively investigated.

The discovery of the sexual morph of *H. subreniformis* marks another connection between the asexual forms previously classified in *Nematoctonus* and named species of *Hohenbuehelia*, first hinted by Drechsler (1941) and established by Barron & Dierkes (1977). Altogether, 15 species have been validly described in *Nematoctonus*, for which the correct names in *Hohenbuehelia* are not readily discoverable in Index Fungorum (https://indexfungorum.org/names/Names.asp). For this reason, we provide here a synopsis of known asexual-sexual connections and the correct names for each species.

Asexual-sexual connections for the 15 species described in *Nematoctonus*

1) *Nematoctonus angustatus* Thorn & Barron, *Mycotaxon* **25**: 333. 1986 (Ontario, Canada) is a synonym of ***Hohenbuehelia angustata*** (Berk.) Singer. The **holotype** of *N. angustatus*, DAOM 193369, is a permanent slide prepared from culture T-91, isolated from a basidiocarp of *H. angustata* (RGT 830820/10; ITS-LSU sequence EF409718), whose sequence is conspecific with the **epitype** of *Panus angustatus* Berk., DAOM 195358 (Consiglio & Setti 2017, 2018).

2) *Nematoctonus brevisporus* Thorn & Barron, *Mycotaxon* **25**: 337, 1986 (Ontario, Canada) is a synonym of ***Hohenbuehelia unguicularis*** (Fr.) Singer. The **holotype** of *N. brevisporus*, DAOM 193368, is a permanent slide prepared from culture T-47, isolated from a basidiocarp of *H. unguicularis* (DAOM 159734; ITS-LSU sequences EF409721, MH861918 and MH873607). These sequences are conspecific with that of the **neotype** of *Agaricus unguicularis* Fr., Z+ZT 1112 (Consiglio 2016, Consiglio & Setti 2018). The asexual morph of *H. pinacearum* Thorn (Thorn 1986) is morphologically identical, so the asexual morph description in Thorn & Barron (1986) includes both species, which are closely related in molecular phylogenies (Fig. 1).

3) *Nematoctonus campylosporus* Drechsler, *J. Wash. Acad. Sci.* **44**: 82, 1954 (Louisiana, U.S.A.; no type was designated and there is no living or preserved original material) is a synonym of ***Hohenbuehelia portegna*** (Speg.) Singer, as fixed by the epitypification below. **Lectotype** for *N. campylosporus*, here designated (MBT 10017554): Drechsler's original illustrations, figs 1–6 (J. Wash. Acad. Sci. 44: 83, 1954). For both *N. campylosporus* and *H. portegna*, the **epitype**, here designated (MBT 10017555 and MBT 10017556, respectively): **Argentina**, Buenos Aires, Llavallol, Santa Catalina, 3 Nov. 1968, *J.E. Wright* 1136, (specimen BAFC 29143; culture T-007 = ATCC 60630 = BAFC 280; ITS-LSU sequence AF139959.2), which cements the synonymy of the two species.

4) *Nematoctonus concurrens* Drechsler, *Mycologia* **41**: 382, 1949 (Oregon, U.S.A.; no type was designated and there is no living or preserved original material) is a synonym of ***Hohenbuehelia leightonii*** (Berk.) Watling ex Courtec. & P. Roux. **Lectotype** for *N. concurrens*, here designated (MBT 10017557): Drechsler's original illustrations, figs 1–4 (Mycologia 41: 371, 374, 378, 381, 1949, all illustrating the same mycelial individual). **Epitype** for *N. concurrens*, here designated (MBT 10017558): **USA**, California, Bodega Bay, 5 Dec. 1994, *B.A. Jaffee* (culture ATCC 96681; preserved in a metabolically inactive state; ITS-LSU sequence EF546658). This species is a synonym of *H. leightonii*, based on apparent conspecificity of sequences of the epitype, designated above, and that of the **epitype** of *Agaricus leightonii* Berk., AMB 18107 (Consiglio 2016, Consiglio & Setti 2018).

5) *Nematoctonus cylindrosporus* Thorn & Barron, *Mycotaxon* **25**: 344, 1986 (Oxford, England) is a synonym of ***Hohenbuehelia petaloides*** (Bull.) Schulzer. The **holotype** of *N. cylindrosporus*, DAOM 193366, is a permanent slide prepared from culture T-82 (= CBS 102.82 and CSAV 373; E. Jones), isolated from a basidiocarp of *H. petaloides*. This identification is based on apparent conspecificity of the sequences of this strain with those of the **epitype** of *Agaricus petaloides* Bull., AMB 18091 (Consiglio 2016, Consiglio & Setti 2018). Thorn (2013) incorrectly indicated the sexual morph to be *H. auriscalpium*.

6) *Nematoctonus geogenius* Thorn & Barron, *Mycotaxon* **25**: 348, 1986 (California, USA). The correct name in *Hohenbuehelia* is unresolved. The **holotype** of *N. geogenius*, DAOM 193365, is a permanent slide prepared from culture T-180, isolated from a basidiocarp of what was probably *Hohenbuehelia thornii* Consiglio & Setti, but there are no sequence data for this collection (BL Thompson 411, HSC), and the ex-type culture is lost. The species *H. thornii* is often found growing from soil of potted house plants and horticultural beds (e.g., https://inaturalist.ca/observations/63193326

© 2025 Westerdijk Fungal Biodiversity Institute

and https://inaturalist.ca/observations/63193323), as was BL Thompson 411. The epithet *geogenius* is not available for transfer from *Nematoctonus* to *Hohenbuehelia* because of the prior existence of *H. geogenia* (DC.) Singer (1951) so, if *N. geogenius* and *H. thornii* are synonymous, the correct name for this species would be *H. thornii*. Consiglio & Setti (2018) showed that sequences identified as *N. geogenius* fall in four separate clades of *Hohenbuehelia*, a situation requiring further study. **Epitype** for *N. geogenius*, here designated (MBT 10017559): **USA**, California, Sacramento, growing from soil of a potted house plant, 22 Aug. 1984, *B.L. Thompson*, 411 (the portion of the sexual morph, BL Thompson 411, preserved as DAOM 195416).

7) *Nematoctonus hamatus* Thorn & Barron, *Mycotaxon* **25**: 351, 1986 (Ontario, Canada) is a synonym of ***Hohenbuehelia valesiaca*** (Ces. ex Sacc.) Singer. The **holotype** of *N. hamatus*, DAOM 193364, is a permanent slide prepared from culture T-23, isolated from soil nematodes; the sequences of this strain are conspecific with those of the **epitype** of *H. valesiaca* (F. Fouchier, FF13115a), fide Consiglio & Setti (2018). The asexual morph of *H. mastrucata* (Fr.) Singer is morphologically identical, so the asexual morph description in Thorn & Barron (1986) includes both species, which are closely related in molecular phylogenies (Fig. 1).

8) *Nematoctonus haptocladus* Drechsler, *Mycologia* **38**: 19, 1946 (Colorado, U.S.A.; no type was designated and there is no living or preserved original material) is a synonym of ***Hohenbuehelia haptoclada*** (Drechsler) Thorn (2013), but no sexual morph or sequence data are known. **Lectotype** for *N. haptocladus*, here designated (MBT 10017560): Drechsler's original illustrations, figs 1–7 (Mycologia 38: 3, 5, 7, 11, 13, 14, 15, 1946). Designation of an epitype awaits living material that is geographically and morphologically appropriate.

9) *Nematoctonus leiosporus* Drechsler, *Phytopathology* **31**: 779, 1941 (Wisconsin, U.S.A.; no type was designated and there is no living or preserved original material) is a synonym of ***Hohenbuehelia leiospora*** (Drechsler) Thorn (2013). **Lectotype** for *N. leiosporus*, here designated (MBT 10017561): Drechsler's original illustration, fig. 2A–K (Phytopathology 31: 776, 1941). **Epitype** for *N. leiosporus*, here designated (MBT 10017562): **Canada**, Ontario, London, isolated from infected nematodes from soil in urban lawn, 13 Jun. 1984, *R.G. Thorn*, subculture of culture T-148 (DAOMC-252626, a culture preserved in metabolically inactive state). No sexual morph is known. A closely related sequence of one isolate previously identified as this species, but with shorter-than-average conidia (T-111 = ATCC 60605, from Morriston, Ontario, Canada; Thorn & Barron 1986, Koziak *et al*. 2007b) has been found to be conspecific with a sequence of the **holotype** of *Hohenbuehelia bonii* A.M. Ainsw., K(M) 165701, fide Consiglio & Setti (2018). *Hohenbuehelia bonii* and *H. leiospora* are seen as sister species in molecular phylogenies (Fig. 1).

10) *Nematoctonus leptosporus* Drechsler, *J. Wash. Acad. Sci*. **33**: 188, 1943 (Maryland, U.S.A.; no type was designated and there is no living or preserved original material) is a synonym of ***Hohenbuehelia leptospora*** (Drechsler) Thorn (2013). **Lectotype** for *N. leptosporus*, here designated (MBT 10017590): Drechsler's original illustration, fig. 2 (J. Wash. Acad. Sci. 33: 186, 1943). Designation of an epitype awaits living material that is geographically and morphologically appropriate. A culture identified as *N. leptospora* (Koziak *et al*. 2007a) was isolated from a basidiocarp of a *Hohenbuehelia* [RGT 010810/02 (UWO), La Selva, Costa Rica 10 Aug. 2001 (culture since lost; ITS-LSU sequence EF409743; Koziak *et al*. 2007b)], but description of the sexual morph awaits better material.

11) *Nematoctonus pachysporus* Drechsler, *J. Wash. Acad. Sci*. **33**: 185, 1943 (Maryland, U.S.A.). **Lectotype** for *N. pachysporus*, here designated (MBT 10017591): Drechsler's original illustration, fig. 1 (J. Wash. Acad. Sci. 33: 184, 1943) is a synonym of ***Hohenbuehelia pachyspora*** (Drechsler) Thorn, ***comb. nov.*** (MB 851648; basionym *Nematoctonus pachysporus* Drechsler, *J. Wash. Acad. Sci.* **33**: 185, 1943). Thorn (2013) reported that a culture matching this asexual morph description had been isolated from a basidiocarp identified as *Hohenbuehelia izonetae* Singer and that *N. pachysporus* may represent an earlier name for *H. izonetae*. However, sequences of cultures identified by this name form two or three separate clades (Koziak *et al*. 2007b, Fig. 1), so designation of an epitype and clarification of possible synonymy awaits studies to determine which clade best fits Drechsler's original species.

12) *Nematoctonus robustus* F.R. Jones, *Trans. Brit. Mycol. Soc*. **47**: 57, 1964 (Ghana, **holotype** IMI 102541) is a synonym of ***Hohenbuehelia robusta*** (F.R. Jones) Thorn (2013). Previously regarded as a synonym of *H. atrocoerulea* (Barron & Dierkes 1977) or *H. grisea* (Thorn & Barron 1986), but likely an independent species. Unfortunately, the ex-type culture has been lost and no similar cultures from the same geographic region are known.

13) *Nematoctonus subreniformis* Thorn & Barron, *Mycotaxon* **25**: 364, 1986 (Ontario, Canada, holotype DAOM 193363) is a synonym of ***Hohenbuehelia subreniformis*** (Thorn & Barron) Thorn (2013) and herein connected with its sexual morph.

14) *Nematoctonus tripolitanius* Giuma & Cooke, *Trans. Brit. Mycol. Soc*. **59**: 215, 1972 (Libya, holotype IMI 162669) is a synonym of ***Hohenbuehelia tripolitania*** (Giuma & Cooke) Thorn (2013). No sexual morph or sequences are known, and the ex-type culture has apparently been lost. The culture IMI 162669, as received, was morphologically identical to CBS 129.68(*Nematoctonus concurrens*, also from R.C. Cooke); that is, it did not conform to the original description of the species and had identical ITS-LSU sequence to CBS 129.68 (R.G. Thorn, unpubl. data).

15) *Nematoctonus tylosporus* Drechsler, *Phytopathology* **31**: 779, 1941 (Maryland, District of Columbia, and Virginia, U.S.A.; no type was designated and there is no living or preserved original material) is a synonym of ***Hohenbuehelia tylospora*** (Drechsler) Thorn (2013). **Lectotype** for *N. tylosporus*, here designated (MBT 10017592): Drechsler's original illustration, fig. 1 (Phytopathology 31: 774, 1941). Designation of an epitype awaits geographically and morphologically suitable living material. The culture 04-RGTSN-512, isolated from infected nematodes from Costa Rica, 1 Jun. 2004, has been

© 2025 Westerdijk Fungal Biodiversity Institute

identified as this species (Koziak *et al*. 2007a) and has ITS-LSU sequence EF409766 (Koziak *et al*. 2007b), but no sexual morph is known.

ACKNOWLEDGEMENTS

We thank K. Kokkonen, E. Brugaletta and L. Sanchez for making their collections and sequences available, and M. Phonemany and P.W. Crous for improvements to the manuscript.

Conflict of Interest: The authors declare no conflicts of interest.

REFERENCES

Alvarado P, Manjón JL, Matheny P.B. *et al*. (2010). *Tubariomyces*, a new genus of *Inocybaceae* from the Mediterranean region. *Mycologia* **102**: 1389–1397. https://doi.org/10.3852/10-041

Alvarado P, Moreno G, Manjón JL (2012). Comparison between *Tuber gennadii* and *T. oligospermum* lineages reveals the existence of the new species *T. cistophilum* (*Tuberaceae*, *Pezizales*). *Mycologia* **104**: 894–910. https://doi.org/10.3852/11-254

Barron GL (1977). *The nematode-destroying fungi*. Canadian Biological Publications, Guelph, Canada.

Barron GL, Dierkes Y (1977). Nematophagous fungi: *Hohenbuehelia*, the perfect state of *Nematoctonus*. *Canadian Journal of Botany* **55**: 3045–3062. https://doi.org/10.1139/b77-345

Berhanu M, Gebeyaw DT, Kefale D et al. (2024). Overview of nematophagous fungi, isolation techniques, and their role in biological control of helminthic parasites: A literature review. *Acta Entomology and Zoology* **5**(1): 133–143. https://doi.org/10.33545/27080013.2024.v5.i1b.133

Burnett J (2003). Defining fungal individuals: ecological, biological and genetical aspects. In: *Fungal populations and species* (Burnett J). Oxford Academic, Oxford, UK: 65–79. https://doi.org/10.1093/oso/9780198515524.003.0005

Carbone I, Kohn LM (1999). A method for designing primer sets for speciation studies in filamentous ascomycetes. *Mycologia* **91**: 553–556. https://doi.org/10.1080/00275514.1999.12061051

Clémençon H (1972). Zwei verbesserte Präparierlösungen für die microskopische Untersuchung von Pilze. *Zeitschrift für Pilzkunde* **38**: 49–53.

Coker WC (1944). The smaller species of *Pleurotus* in North Carolina. *Journal of the Elisha Mitchell Society* **60**: 71–95, pl. 40–52.

Consiglio G (2016). Nomenclatural novelties. *Index Fungorum* **292**: 1–2.

Consiglio G (2017a). Nomenclatural novelties. *Index Fungorum* **326**: 1.

Consiglio G (2017b). Nomenclatural novelties. *Index Fungorum* **327**: 1.

Consiglio G, Setti L (2017). Novitates nei Generi *Hohenbuehelia* e *Resupinatus*. *Rivista di Micologia* **60**(1): 19–22.

Consiglio G, Setti L (2018). *I generi* Hohenbuehelia *e* Resupinatus *in Europa*. Associazione Micologica Bresadola, Trento, Italy.

Consiglio G, Setti L, Thorn RG (2018). New species of *Hohenbuehelia*, with comments on the *Hohenbuehelia atrocoerulea* – *Nematoctonus robustus* species complex. *Persoonia* **41**: 201–212. https://doi.org/10.3767/persoonia.2018.41.10

Cubeta MA, Echandi E, Abernethy T, *et al*. (1991). Characterization of anastomosis groups of binucleate *Rhizoctonia* species using restriction analysis of an amplified ribosomal RNA gene. *Phytopathology* **81**: 1395–1400.

Dickie IA, Wakelin A, Richardson SJ (2020). Rare species of wood-inhabiting fungi are not local. *Ecological Applications* **30**: e02156. https://doi.org/10.1002/eap.2156

Drechsler C (1941). Some hyphomycetes parasitic on free-living terricolous nematodes. *Phytopathology* **31**: 773–801.

Drechsler C (1943). Two new basidiomycetous fungi parasitic on nematodes. *Journal of the Washington Academy of Science* **33**: 183–189.

Drechsler C (1946). A clamp-bearing fungus parasitic and predaceous on nematodes. *Mycologia* **38**: 1–23. https://doi.org/10.2307/3755043

Drechsler C (1949). A nematode-capturing fungus with anastomosing clamp-bearing hyphae. *Mycologia* **41**: 369–387. https://doi.org/10.2307/3755230

Drechsler C (1954). A nematode-capturing fungi with clamp connections and curved conidia. *Journal of the Washington Academy of Science* **44**: 82–85.

Elborne S (1995). *Hohenbuehelia*. In: *Flora Agaricina Neerlandica*, vol. 3 (Bas C, Kuyper TW, Noordeloos ME, *et al*., eds). Balkema, Rotterdam, Netherlands: 158–166.

Fannechère G (2011). Mycomètre, logiciel d'aide à la mesure et de traitement statistique. http://mycolim.free.fr/DOC_SML/mycm202/Charg_Mycm202.htm

Gardes M, Bruns TD (1993). ITS primers with enhanced specificity for *Basidiomycetes*—application to the identification of mycorrhizae and rusts. *Molecular Ecology* **2**: 113–118. https://doi.org/10.1111/j.1365-294x.1993.tb00005.x

Giuma AY, Cooke RC (1972). Some endozoic fungi parasitic on soil nematodes. *Transactions of the British Mycological Society* **59**: 213–218. https://doi.org/10.1016/S0007-1536(72)80004-4

Gouy M, Guindon S, Gascuel O (2010). SeaView version 4: A multiplatform graphical userinterface for sequence alignment and phylogenetic tree building. *Molecular Biology and Evolution* **27**(2): 221–224. https://doi.org/10.1093/molbev/msp259

Gross G (1972). Kernzahl und sporenvolumen bei einigen Hymenogasterarten. *Zeitschrift für Pilzkunde* **38**: 109–158.

Jones FR (1964). *Nematoctonus robustus sp. nov. Transactions of the British Mycological Society* **47**: 57–60. https://doi.org/10.1016/S0007-1536(64)80080-2

Kijpornyongpan T, Aime MC (2016). Rare or rarely detected? *Ceraceosorus guamensis sp. nov.*: a second described species of *Ceraceosorales* and the potential for under detection of rare lineages with common sampling techniques. *Antonie van Leeuwenhoek* **109**: 1127–1139. https://doi.org/10.1007/s10482-016-0715-4

Koziak ATE, Chavarria Diaz F, Diaz J, *et al*. (2007a). Costa Rican species of *Nematoctonus* (anamorphic *Pleurotaceae*). *Canadian Journal of Botany* **85**(8): 749–761. https://doi.org/10.1139/B07-049

Koziak ATE, Cheng KC, Thorn RG (2007b). Phylogenetic analyses of *Nematoctonus* and *Hohenbuehelia* (*Pleurotaceae*). *Canadian Journal of Botany* **85**: 762–773. https://doi.org/10.1139/B07-083

Liu YJ, Whelen S, Hall BD (1999). Phylogenetic relationships among *Ascomycetes*: evidence from an RNA polymerse II subunit. *Molecular Biology and Evolution* **16**: 1799–1808. https://doi.org/10.1093/oxfordjournals.molbev.a026092

Matheny PB, Wang Z, Binder M, *et al*. (2007). Contributions of *rpb2* and *tef1* to the phylogeny of mushrooms and allies (*Basidiomycota*, *Fungi*). *Molecular Phylogenetics and Evolution*

© 2025 Westerdijk Fungal Biodiversity Institute

43: 430–451. https://doi.org/10.1016/j.ympev.2006.08.024

Meerts P (1999). The evolution of spores in Agarics: do big mushrooms have big spores? *Journal of Evolutionary Biology* **12**: 161–165. https://doi.org/10.1046/j.1420-9101.1999.00020.x

Melzer, V (1924). L'ornementation des spores de Russules. *Bulletin de la Société Mycologique de France* **40**: 78–81.

Miller MA, Pfeiffer W, Schwartz T (2010). Creating the CIPRES science gateway for inference of large phylogenetic trees. In: *Proceedings of the Gateway Computing Environments workshop (GCE)*, 14 November 2010. New Orleans, LA, USA: 1–8. https://doi.org/10.1109/GCE.2010.5676129

Miller OK Jr (1986). Pleurotoid fungi in the *Hohenbuehelia – Resupinatus* complex in North America. In: *La famiglia delle Tricholomataceae* (Borghi E, ed.). Centro Studi per la Flora Mediterranea, Borgo Val di Taro, Italy: 111–144.

Pilát A (1935). *Pleurotus* Fries. In: *Atlas des champignons de l'Europe*, vol. 2, fasc. 6–16 (Kavina C, Pilát A, eds). Chez les éditeurs, Prague, Czechoslovakia: 1–193, pl. 1–80.

Rabinowitz D (1981). Seven forms of rarity. In: *The biological aspects of rare plant conservation* (Synge H, ed.). John Wiley and Sons, New York: 205–217.

Rehner SA, Buckley E (2005). A *Beauveria* phylogeny inferred from nuclear ITS and EF1-a sequences: evidence for cryptic diversification and links to *Cordyceps* teleomorphs. *Mycologia* **97**: 84–98. https://doi.org/10.3852/mycologia.97.1.84

Ronquist F, Huelsenbeck JP (2003). MrBayes 3: Bayesian phylogenetic inference under mixed models. *Bioinformatics* **19**(12): 1572–1574. https://doi.org/10.1093/bioinformatics/btg180

Schulzer S von Müggenberg, Kanitz A, Knapp JA (1866). Die bisher bekannten Pflanzen Slavoniens. *Verhandlungen der Zoologisch-Botanischen Gesellschaft in Wien* **16**: 1–172.

Stamatakis A (2014). RAxML version 8: a tool for phylogenetic analysis and post-analysis of large phylogenies. *Bioinformatics* **30**: 1312–1313. https://doi.org/10.1093/bioinformatics/btu033

Tamura K, Stecher G, Peterson D, *et al*. (2013). MEGA6: molecular evolutionary genetics analysis version 6.0. *Molecular Biology and Evolution* **30**: 2725–2729. https://doi.org/10.1093/molbev/mst197

Taylor JW (2011). One fungus = one name: DNA and fungal nomenclature twenty years after PCR. *IMA Fungus* **2**(2): 113–120. https://doi.org/10.5598/imafungus.2011.02.02.01

Thiers B (2020). [continuously updated] Index Herbariorum: A global directory of public herbaria and associated staff. New York Botanical Garden's Virtual Herbarium. http:// sweetgum.nybg.org/ih/

Thorn RG (2013). Nomenclatural novelties. *Index Fungorum* 16: 1.

Thorn RG, Barron GL (1986). *Nematoctonus* and the tribe *Resupinateae* in Ontario, Canada. *Mycotaxon* **25**: 321–453. https://www.biodiversitylibrary.org/part/417083

Větrovský T, Morais D, Kohout P, et al. (2020). GlobalFungi, a global database of fungal occurrences from high-throughput-sequencing metabarcoding studies. *Scientific Data* **7**: 228.

Vilgalys R, Hester M (1990). Rapid genetic identification and mapping of enzymatically amplified ribosomal DNA from several *Cryptococcus* species. *Journal of Bacteriology* **172**: 4238–4246. https://doi.org/10.1128/jb.172.8.4238-4246.1990

White TJ, Bruns T, Lee S, *et al*. (1990). Amplification and direct sequencing of fungal ribosomal RNA genes for phylogenetics. In: *PCR protocols: a guide to methods and applications* (Innis MA, Gelfand DH, Sninsky JJ, *et al*., eds). Academic Press, New York, USA: 315–322. http://dx.doi.org/10.1016/B978-0-12-372180-8.50042-1

Wingfield MJ, De Beer ZW, Slippers B, *et al*. (2012). One fungus, one name promotes progressive plant pathology. *Molecular Plant Pathology* **13**: 604–613. https://doi.org/10.1111/j.1364-3703.2011.00768.x

Zotti M, Bonanomi G, Mazzoleni S (2025). Fungal fairy rings: history, ecology, dynamics and engineering functions. *IMA Fungus* **16**: e138320. https://doi.org/10.3897/imafungus.16.138320.

Supplementary Material: http://fuse-journal.org/

Table S1. Sequences used and generated in this study. Newly sequenced collections are **in bold.** Two-letter province codes are added for Canada and the U.S.A. An emdash (—) indicates data lacking.

© 2025 Westerdijk Fungal Biodiversity Institute

Fungal Systematics and Evolution (ISSN: 2589-3823, E-ISSN: 2589-3831)

About Fungal Systematics and Evolution

Fungal Systematics and Evolution has an OPEN ACCESS publishing policy. All manuscripts will undergo peer review before acceptance, and will be published as quickly as possible following acceptance. There are no page charges or length restrictions, or fees for colour plates. The official journal language is English. All content submitted to Fungal Systematics and Evolution is checked for plagiarism.

Fungal Systematics and Evolution is licensed under a Creative Commons Attribution-NonCommercial-ShareAlike 4.0 International License

For more information and ordering of other books and publications, see www.fuse-journal.org and www.wi.knaw.nl.

About the Westerdijk Fungal Biodiversity Institute

The Westerdijk Fungal Biodiversity Institute is the largest expertise centre for microfungi in the world. Our renowned researchers dedicate themselves to enriching and expanding our Fungal Biobank. We explore the fungal kingdom to gain a better understanding of their fungal characteristics and their potential applications, especially in the fields of industry, agriculture and healthcare.

The Westerdijk Fungal Biodiversity Institute is part of the Royal Netherlands Academy of Arts and Sciences (KNAW).

Explore - study - preserve - apply

WESTERDIJK
FUNGALBIO
DIVERSITY
INSTITUTE